Marko Milosevic Author

TU Delft

Master Thesis

The Zwartewaterbrug project



Structural Health Monitoring of the Zwartewaterbrug Bridge

By

Marko Milosevic

in partial fulfilment of the requirements for the degree of

Master of Science
in Civil Engineering

at the Delft University of Technology,
to be defended publicly on Monday July 30, 2018 at 2:00 PM.

Supervisor:	Prof. dr. E. Lourens	TU Delft
Thesis committee:	Prof. dr. A. Metrikine	TU Delft
	Prof. dr. M. Pavlovic	TU Delft
	phd cand. D. Fallais	TU Delft

This thesis is confidential and cannot be made public until July 30, 2018.

An electronic version of this thesis is available at http://repository.tudelft.nl/.

TU Delft

Abstract

Vibration-based structural health monitoring of civil engineering structures is receiving increasing attention in recent years. This is due to the development of more robust system identification techniques as well as improvements with regard to the practicality of installing the necessary instrumentation. Health monitoring systems are more often replacing static deflection tests and detailed visual inspections, where continuous monitoring of vibration data aims for early damage detection.
This thesis can be summarized as the development of a structural health monitoring method for bridges. It forms a part of the Zwartewaterbrug project, related to the Zwartewater bridge located in the city of Hasselt, in the Dutch province of Overijssel. The Zwartewater bridge served as a case study for validation of the proposed early damage detection algorithm.
The wider purpose of this work was to address the problem of having a large number of bridges in Europe that are facing the end of their service life and should either be retrofitted or decommissioned.. The chosen approach consisted of a low-cost vibration monitoring method, that is suitable for continuous structural health monitoring.
The initial challenge was to introduce a small change to the structure, representative of early damage, without actually damaging the structure. For this an added mass approach was taken, where weights of respectively 25, 50, 75, and 100 kg were added below the bridge deck. The vibration data (accelerations) measured on the "damaged" structure were then used to solve an inverse problem where the aim was to detect the induced damage without closing the bridge to traffic.
Since the data was gathered with only ambient excitation by wind and traffic, a new challenge arose, which is considered to be the core of this thesis. The structural differences between vibration measurements related to the "healthy" and "damaged" structure were concluded to be smaller than the structural changes due to the differences in unknown traffic loading. The traffic loads were namely varying from 200kg motorcycles to 50t trucks.
In this thesis the method of Probabilistic Filtering was developed to face the aforementioned challenge. The method involves mainly a data pre-processing step, and the probabilistically filtered signals are subsequently processed with two output-only identification methods: Frequency Domain Decomposition and data-driven Stochastic Subspace Identification. The full process was integrated into an automatic analysis algorithm, performed in MatLab.
It was concluded that both detection and localization of the induced damage is possible with the proposed methodology. Further work was then performed to quantify the detected added mass in terms of structural damage. A quantitative finite element analysis was performed with the substructure approach (super-element, static boundary conditions to the substructure of interest). The given analysis concluded that the developed structural health monitoring method is able to detect anomalies comparable to a 35cm crack in the welds securing the longitudinal stiffeners to the tranverse beams.
Finally, recommendations were made regarding an expansion of the method to structure service life predictions and more computationally efficient calculation set-ups.

For answering any possible question to a possible reader of this thesis, I could be contacted on email markomilosevic021@gmail.com.

Acknowledgments

When you come to Delft

When you come to Delft,
you will meet the one you had to meet,
on the path you had to take.

The path that does not exist,
but echoes with you,
and the one that you cannot see.

The one that is on that path,
in a place where a clock does not work,
as long as you did not look.

But exactly there, will you find the TU Delft,
and it will show you to the unknown one,
that is your Future Self.

Marko Milosevic

Maybe I should have put the poem into the abstract section, but to be short I feel that TU Delft strongly impacts your future. That is something I am glad off, and for that, I have to thank the grandfathers and the grand grand... fathers of my Dutch colleagues who built this University. Especially that they built it in a place where Vermeer lived, so dankjewel.

What I conclude, without a doubt, that TU Delft has the most powerful curriculum for Structural Dynamics for Civil Engineers in the World. The person behind that power is professor Andrei Metrikine, who holds a cult status among the students. So what an immense pleasure for me is that professor Andrei Metrikine is the Chairman of my Master Thesis committee.

The most important person of this Master Thesis for me is my mentor professor Eliz-Mari Lourens, who gave the job, and the knowledge, to me. My brother says that luck is a marriage between opportunity and preparedness to take that opportunity (wise basketball player), but I was really lucky to get this project. For the given opportunity, and the given knowledge I loudly thank professor Eliz-Mari Lourens.

The person that was tieing the ropes to set the sails of this Thesis is my daily supervisor, Dominik Fallais. Not just that he did that job good, he also provided the necessary wind when there was none. After every meeting, I was supplied with proper guidance, motivation, and wreckage of awe I had for some topics. I conclude exceptional sailing maneuvering skills, and thank him for that.

The fourth member of my Master Thesis committee is professor Marko Pavlovic. It is also an honor to have somebody with such a great reputation amongst students, for a committee member. I thank him for constructive comments he had for my work.

The people I respect very much, that built foundation for my knowledge building, belong to Statics team of Faculty of Technical Science of the University of Novi Sad, Serbia, my bachelor University. They are Prof. dr Djordje Ladjinovic, Doc.dr Andrija Raseta, Doc. dr Aleksandra Radujkovic and Asistent-master Igor Dzolev. It is an honor for me that they were members of my Bachelor Thesis committee.

The most important person in my life is my brother Strahinja, to him, to my father Dusan, my mother Gordana and my grandmother Jelena, I thank the most. My family is the only supporter of my education and that is the biggest honor I can have. Also, I thank my friends, for being my friends.

Nomenclature

Mathematical tools

Φ	Mode shape vector
$\Phi_{[A,B]}$	Covariance between matrix A and B
Σ	Matrix of singular values
$\mathbf{E}_j$	Expectation operator
$\widehat{E}_t$	Estimated error at time t
$\widehat{X}_t$	Estimation of a measurement value at time t
E_t	Measurement error at time t
KG_t	Kalman gain at time t
U	Matrix of left singular vectors
V	Matrix of right singular vectors
X_t	Measurement value at time t
MAC	Modal assurance criterion

Output only identification methods

$\boldsymbol{\omega}_k$	White noise sequence vector k
$\boldsymbol{\upsilon}_k$	White noise sequence vector k
$\boldsymbol{E}$	Expectation operator
$\boldsymbol{u}(t)$	Time domain input vector function
$\boldsymbol{x}(t)$	Time domain state space vector function
$\boldsymbol{y}(t)$	Time domain output vector function
$\dagger$	Moore−Penrose pseudo inverse operation
Δt	Measurements time sample
$\Delta_{[1,2i]}$	Reversed extended controllability matrix
$\Gamma_{[1,2i]}$	Extended ($i > n$) observability matrix
$\hat{\boldsymbol{x}}_k$	Kalman filter state estimate vector
$\hat{\Gamma}_i$	Observability matrix estimate

$\hat{X}_i$	Kalman filter state sequence matrix
Λ_i	Output covariance matrix
λ_i	Continuous time poles
μ_i	Discrete time poles
ω_i	Systems circular eigenfrequencies
Φ	Vibration mode shape
$\Phi_{[Y_{i\|i,1\|1]}}$	Output covariance matrix estimation
Ψ	Eigenvector
Σ_s	State covariance matrix
Σ_s^f	Forward innovation model state covariance matrix
$\sim$	Variable in frequency domain
$\mathbf{u}_k$	Input sequence vector k
$\mathbf{x}_k^f$	Forward innovation model state space sequence vector k
$\mathbf{x}_k$	State space sequence vector k
$\mathbf{y}_k$	Output sequence vector k
$\widetilde{\boldsymbol{f}}(\omega)$	Input force vector in frequency domain
$\widetilde{\boldsymbol{y}}(\omega)$	Output displacement vector in frequency domain
$\widetilde{H}(\omega)$	Transfer function matrix in frequency domain
$\widetilde{S}_{ff}(\omega)$	Input spectral density matrix
$\widetilde{S}_{yy}(\omega)$	Output spectral density matrix
ξ_i	Systems damping coefficients
A_c	State space continuous system matrix
A_d	State space discrete system matrix
C_i	Block Toeplitz matrix
D	Damping matrix
f_i	Systems frequencies
$H_{[1,2i]}$	Lower block triangular Toeplitz matrix
K	Stiffness matrix
K^f	Forward Kalman gain
L_i	Block Toeplitz matrix
M	Mass matrix
O_i	Projection matrix

U_F	Input future block Hankel matrix
U_P	Input past block Hankel matrix
$U_{2i\|j}$	Input block Hankel matrix of 2i rows and j columns
W_1	Weighting matrix
W_P	Vertical stack matrix of the past input and output Hankel matrices
X_i	State sequence matrix
Y_F	Output future block Hankel matrix
Y_P	Output past block Hankel matrix
$Y_{2i\|j}$	Output block Hankel matrix of 2i rows and j columns
A	System matrix of state space system
B	System matrix of state space system
C	System matrix of state space system
D	System matrix of state space system
T	Some invertible matrix T

Probabilistic filtering

$\boldsymbol{f}(t)$	Vector of input force
$\boldsymbol{y}_i(t)$	Vector of output measurements (i^{th} measurement)
$\bullet$	Tensor scalar product (summation of element wise multiplication, result is scalar)
$\ast_{i=1}^{n}$	Multiple convolution operation (between functions from i to n)
$\cdot\ast$	Element wise product of tensors
$\mathcal{F}$	Fourier transform operator
$\prod_{i=1}^{n}$	Multiple product operation(between functions from i to n)
$\prod_{i=1}^{n}$	Multiple element wise product operation(between tensors from i to n)
$\bigtimes^{n}_{i=2}$	Dimensional expansion of tensor, with vectors (from vector 2 to vector n)
$\square^{n}_{\boldsymbol{f}_i}$	Tensor of order n, of expanded vector functions $\boldsymbol{f}_i$ (i to n)
$\square^{n}_{\boldsymbol{h}_p}$	Tensor of order n, of expanded vector function $\boldsymbol{h}_p$
$\square^{n}_{I}$	Unit tensor of order n
$\widetilde{f}(\omega)$	Force function frequency domain
$\widetilde{h}(\omega)$	Transfer function
$\widetilde{y}(\omega)$	Output displacement function frequency domain
$\widetilde{y}_{ip}(\omega)$	i^{th} output measurement at spatial node p, in frequency domain

$f(t)$	Force function
$H(t)$	Impulse response function matrix
$h(t)$	Impulse response function
i	Subscript i, measurement number (i^{th} measurement)
p	Subscript p, spatial position of function
$y(t)$	Output displacement function

Contents

Abstract **i**

Acknowledgments **iii**
When you come to Delft . . . iii

Nomenclature **v**

1 Introduction **4**
1.1 Research context . . . 4
1.2 Research project and thesis assignment . . . 5
1.3 Thesis outline . . . 6

Level 0

2 Introduction to Structural health monitoring **8**
2.1 Vibration-based structural health monitoring . . . 8
2.2 Multidisciplinary nature . . . 8
2.3 Damage detection . . . 9
2.4 Damage identification levels . . . 10
2.5 Application . . . 10

3 The Zwartewaterbrug project **11**
3.1 Structure description . . . 12
3.2 The measurement campaign . . . 14
3.2.1 The sensor network . . . 14
3.2.2 Installation of the measuring system . . . 14
3.2.3 The measurement campaign . . . 15
3.3 Project goals . . . 18
3.4 Data classification . . . 18
3.4.1 Excitation characteristics . . . 18
3.4.2 Classification characteristics . . . 18
3.4.3 Environmental conditions . . . 21

Theory

4 Mathematical tools **26**
4.1 Geometrical projections in statistical framework . . . 26
4.2 Singular value decomposition . . . 29
4.3 Modal assurance criterion . . . 30
4.4 1D Kalman filter . . . 31

5 Output only identification methods **32**
5.1 Frequency domain decomposition . . . 32
5.2 Stochastic subspace identification . . . 34
5.2.1 Deterministic subspace identification . . . 34
5.2.2 Data driven stochastic subspace identification . . . 38
5.2.3 Implementation of the data driven stochastic subspace identification . . . 43

6 Probabilistic filtering **49**
6.1 Convolution properties . . . 50
6.2 Structural system . . . 51
6.3 White noise . . . 52
6.4 Multi-degree of freedom system . . . 56
6.5 Notation . . . 60
6.6 Reducing the order of the transfer function . . . 61
6.7 Conclusion . . . 63

Level 1

7 The Zwartewaterbrug data analysis **65**
7.1 Analysis goals . . . 65
7.2 Frequency content . . . 66
7.3 Analysis algorithm composition . . . 71
7.4 Analysis output . . . 74
7.4.1 Unreduced order probabilistic filtering output . . . 74
7.4.2 Unreduced order probabilistic filtering result . . . 79
7.4.3 Reduced order probabilistic filtering output . . . 81
7.4.4 Reduced order probabilistic filtering result . . . 86

Level 2

8 Health monitoring algorithm calibration **89**
8.1 Analysis concept . . . 89
8.2 Damage localisation results . . . 90
8.2.1 Unreduced order probabilistic filtering results . . . 90
8.2.2 Reduced order probabilistic filtering results . . . 93
8.3 GPU optimization . . . 96
8.4 Analysis algorithm calibration . . . 97

Level 3

9 Finite element model **99**
9.1 Global model . . . 99
9.1.1 Analysis set-up . . . 99
9.1.2 Results . . . 101
9.2 Local model 1 . . . 103
9.2.1 Analysis set-up . . . 104
9.2.2 Results . . . 106
9.3 Local model 2 . . . 109
9.3.1 Analysis set-up . . . 110

9.3.2 Results 112
9.4 Conclusion 117

10 Conclusions and recommendations **118**
10.1 Conclusions 118
10.2 Recommendations 119
10.2.1 Level 4 119
10.2.2 Analysis set-up improvements 120

List of Figures **121**

List of Tables **124**

Bibliography **125**

Appendix A1 **126**

Appendix A2 **186**

Appendix A3 **246**

Appendix A4 **366**

Appendix F1 **486**

Appendix F2 **508**

Appendix F3 **573**

Chapter 1

Introduction

The aim of this chapter is to answer questions "Why?", "What?" and "How?", related to work done for this thesis. The chapter is divided into three sections, answering the aforementioned questions.

Before going into the chapter, the highest level of the question "What?", has to be introduced. What this thesis is about is: "Vibration-based structural health monitoring".

1.1 Research context

Before answering this question some facts need to be introduced, but it would be assumed that the answer would be in the financial domain.

Referring to the fact that in the Netherlands and in Europe, a large number of bridges was built in the period between 1950 and 1970, and that today they still present key nodes in transportation networks, the question is raised what is the optimal way to keep those structures alive.

▼ **Main issues that occur with those bridges:**

- Present time traffic load requirements
- Structural deficiency according to Eurocode (EN 1992-2) and NEN-Norm (NEN 8702)
- End of the design life

With the evolution of traffic systems, it is reasonable to raise a question whether old bridges are sufficient to satisfy present time traffic load requirements. Forwarding issues to design norms structural deficiency occurs. The recalculated design checks do not necessarily correspond to the actual structural behavior, which gives the opportunity to evaluate possible benefits of investing in knowledge about the actual structural state. When it comes to the optimal method of determining the actual structural state of the bridge, vibration-based structural health monitoring is the leading option. With the use of the knowledge about the actual state of the structure, required structural interventions can be optimally planned.

▼ **Benefits of vibration based structural health monitoring:**

- Reduction in intervention costs
- Reduction in traffic disturbance
- Knowledge about the risk of failure
- Beautiful jobs for structural engineers

So, we do not trust the design norms(1) and we would like to preserve the aforementioned structures with a minimum amount of structural interventions(2), based on the data generated with vibration-based structural health monitoring methods(3). Arguments for answering the question "Why?" on the three stated facts in the previous question, are briefly described in this section. The universal answer to all three is that our intention is to create benefits in financial and time-consuming terms, related to the given problem. Stating again that the main identified problem is the structural deficiency of structures that present the key nodes in the transportation networks.

1.2 Research project and thesis assignment

As mentioned in the introduction of this chapter, the highest level of the answer to the question "What?", is: "Vibration-based structural health monitoring".

What needs to be done is to measure vibration data of the structure, and based on the measured data estimate the state of the structure.

▼ **Challenges that are being faced:**

- Generate vibration data of a damaged structure without damaging it
- Develop an early damage detection algorithm (presence of small damage)
- Develop reliability test for damage detection algorithm
- Calibrate reliable damage detection algorithm with numerically simulated damage scenarios
- Estimate possibilities of predicting service life of the structure based on the vibration-based structural health monitoring
- Automatise the process

What needs to be done is highly ambitious. Produce anomaly in the structure that can be interpreted as a small damage and detect it. Raise the reliability of detection method and generate numerical data with realistic damage scenarios, with the support of the real measurements.

It is obvious that the question of structure service life prediction cannot be answered just with vibration-based structural health monitoring. Detail inspections of the structure need to be performed, with load-deflection tests for calibration of new design model, so present time load requirements can be tested for the redesigned structure. Additionally, it is to estimate whether at that point vibration-based structural health monitoring can continue predicting the service life of the structure.

The first "How?" question is related to the introduction of damage to the structure, without damaging it. The real damage present in terms of cracks, fatigue... will produce a reduction of the structure's stiffness. The reduced stiffness will generally result in "lover" eigenfrequencies. To reproduce similar effects, the added mass will be introduced to the healthy structure, with intentions of lowering the eigenfrequencies. It is questionable formulating added mass as damage, more proper term would be an anomaly to the healthy structure.

As it is necessary to develop early damage detection algorithm, the low value of added mass will be introduced in the measurement campaign. The advantage of this method is that performance of installed Vibration based structural health monitoring method could be easily checked for performance with tests by introducing the low value of added mass to the structure. With an easy way to check the performance of the method, reliability of given method can be concluded.

As mentioned, added mass cannot be thought of as damage. It is intended to perform FEM model update based on real measurements, and with the given model generate numerical data with realistic damage scenarios for calibrating the algorithm for vibration-based structural health monitoring. The method is intended to be developed to work with ambient excitation, opening the opportunity to be fully automatic.

What is left as an open question, is what is necessary to perform so vibration-based structural health monitoring method can predict the service life of the structure?

1.3 Thesis outline

The workflow of this thesis is based on the classification of levels of the structural health monitoring [9]. Additionally, level 0 is added, presenting the preparation for the analysis.

▼ **Workflow levels:**

- Level 0, preparation for the analysis
- Level 1, damage detection
- Level 2, damage localization
- Level 3, damage quantification

The description of the workflow regarding the particular level is presented in form of the flowchart, following ISO 1028:1973. The given flowcharts are set at the beginning of the chapters that summarize the particular level.

▼ **Flowcharts of the workflow:**

- Level 0, figure L.0 on the following page
- Level 1, figure L.1 on page 64
- Level 2, figure L.2 on page 88
- Level 3, figure L.3 on page 98

Level 0

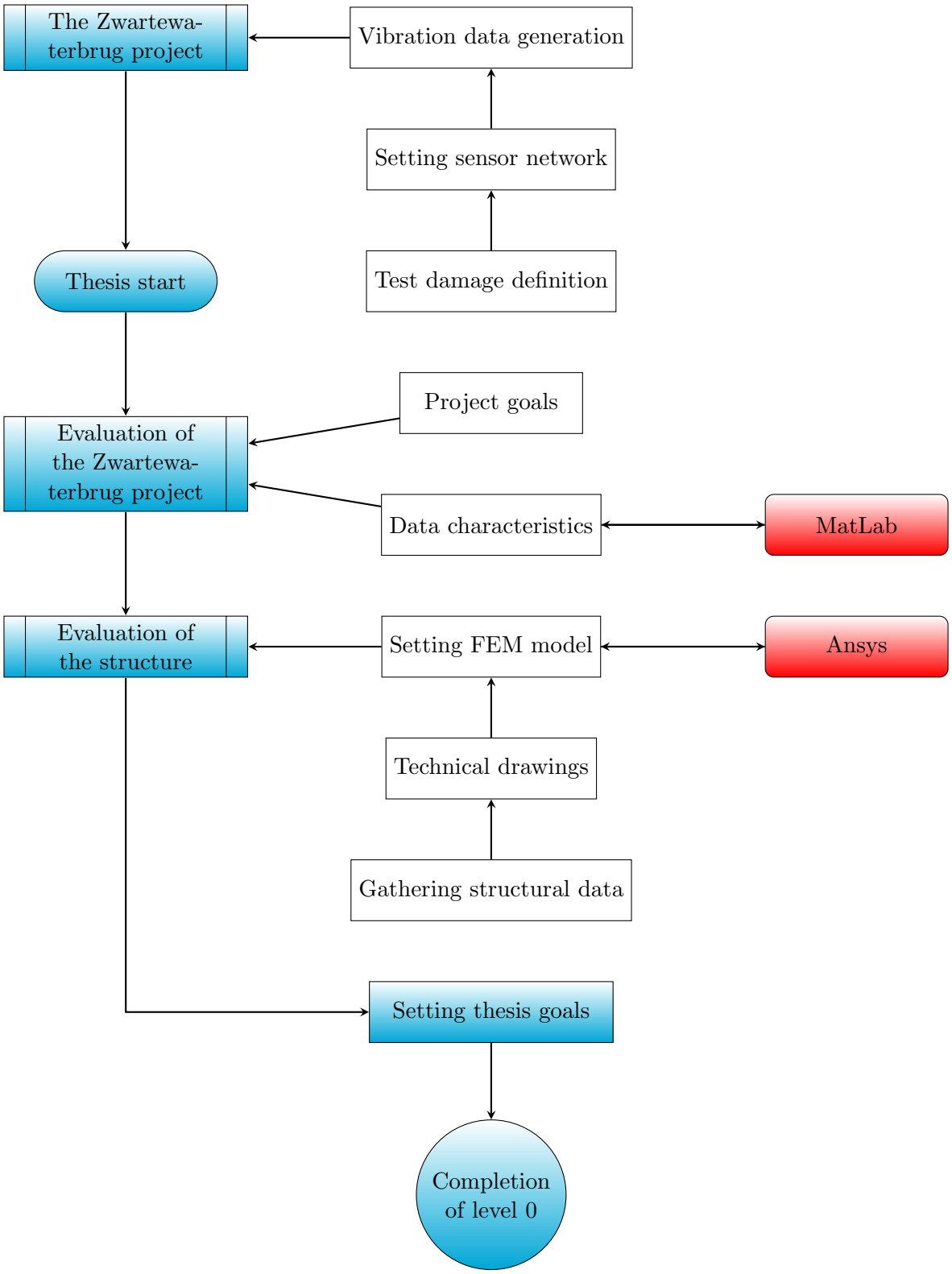


Figure L.0: Workflow of level 0

Chapter 2

Introduction to Structural health monitoring

Intentions of this chapter is to introduce concepts and terminology of structural health monitoring.

Emphasis will be set on damage identification levels, which conceptually guide work flow of this thesis.

▼ **Terminology that focus is put on in this chapter:**

- System identification
- Operational modal analysis
- Vibration based structural health monitoring
- Damage detection

2.1 Vibration-based structural health monitoring

Structural health monitoring is an objective, non-destructive, structural evaluation method, based on physical measurements and computer calculations. To be on the target, it is important to introduce an initial classification of structural health monitoring.

▼ **Approach to structural health monitoring:**

- Local structural health monitoring
- Global structural health monitoring

Local structural health monitoring approach relies on radiography, x-rays, acoustics... where global approach concentrates on static or dynamic large-scale structure tests. The interest of this work is laid down in semi-global structural dynamics, evaluating the health of the structure based on vibration data generated on a segment of the structure. Using the appropriate terminology, the focus of this work is vibration-based structural health monitoring.

2.2 Multidisciplinary nature

Engineering attractiveness of vibration-based structural health monitoring lies in multidisciplinary nature, connecting electrical engineering, mechanical engineering, and civil engineering.

Vibration based structural health monitoring is connected to electrical engineering physically trough sensors and acquisition systems, and theoretically trough control theory and system identification. Mechanical engineering comes to the story with experimental modal analysis, proceeding to operational modal analysis, structural analysis, with finalization in built environment and civil engineering.

Not to go deep at this level, details introduced would be kept short. Starting with electrical engineering, the sensor network is to be set, vibration data generated and processing of generated signals starts. The important part is system identification, which determines the experimental model that represents information of generated vibration data. Talking about system identification and experimental model, when the environment is structural, we come to the field of mechanical engineering called experimental modal analysis. The experimental modal analysis determines a main dynamic characteristic of the structure, eigenfrequencies, and eigenmodes.

▼ **With difference of structures vibration test set-up, distinguish is made with:**

- Experimental modal analysis (EMA)
- Operational modal analysis (OMA)

When the excitation of the structure is known, we are talking about experimental modal analysis, or in other words when the model is determined based on known input and output data. With operational modal analysis input, being the excitation is unknown. It is based only on output vibration data, the measured vibration response of the structure.
With smaller scale structures, mainly in mechanical engineering, EMA is used. When it comes to civil structures, EMA is either expensive or not possible, and more challenging OMA steps in to deal with structures of larger scale. Finally, what vibration-based structural health monitoring aims is an evaluation of the health of the structure, based on the analysis of vibration response of the structure only.

Conceptually, all of the aforementioned engineering disciplines develop tools for purposes inside the discipline, with optimality staying inside the discipline. For successful handling of multidisciplinary nature of vibration based health monitoring, a deeper understanding of subjects belonging to different engineering disciplines is necessary.

2.3 Damage detection

Vibration-based structural health monitoring is damage detection tool. Damage can be represented as degradation of material properties, failure of structural elements... but mainly it leads to a reduction of stiffness. Reduction of stiffness leads to change in the eigenstructure. The aim of vibration-based structural health monitoring is to capture the change of the eigenstructure and evaluate it in terms of damage.

▼ **Damage detection scale:**

- Local damage effect
- Global damage effect

Detecting damage that has a global effect on the structure, requires larger and more expensive sensor network but simpler damage identification method, than damage with a local effect. The main question raised is whether it is late for structural interventions if damage progressed to have a global effect on the structure.
It is reasonable to have intentions to detect damage on smaller, local scale, creating an opportunity to react with less expensive, smaller structural interventions. Detecting small changes in

the structure also leaves enough time to properly plan the future required interventions.

With the prediction of damage scenarios, the sensor network is set on a segment of the structure, aiming to detect local damage. The challenge that is being faced is to find a reliable local damage identification method. The smaller the size of detected damage, the more successful detection method is.

2.4 Damage identification levels

As very important terminology that conceptually forms this thesis, damage identification levels are put in the separate section of this chapter. Given classification is adopted from [9], with modification regarding level 0.

▼ **Damage identification levels:**

- Level 0,
- Level 1, detection
- Level 2, localization
- Level 3, quantification
- Level 4, structures service life prediction

It would be concluded that successful application of structural health monitoring is one that can go up to level 4 damage identification, with detecting damage on a local scale.

2.5 Application

Initial classification of vibration-based structural health monitoring in the domain of application relies on vibration measurement duration.

▼ **Structures monitoring duration:**

- Temporary (temporary placement of sensors and acquisition systems)
- Continuous (embedded sensors and acquisition systems)

This work is based on real-life data, generated on temporary placed accelerometers and acquisition system. The aim of successful vibration-based structural health monitoring method is to be set as continuous monitoring system with embedded sensors and acquisition systems.

Application of vibration-based structural health monitoring is related to structures prone to fatigue due to dominant dynamic loads.

▼ **Vibration based structural health monitoring finds application with:**

- Bridge structures
- High rise buildings
- Wind turbines
- Offshore structures
- Other structures with dominant dynamic load

Chapter 3

The Zwartewaterbrug project

Under a collaboration between the University of Twente and TU Delft, the project called: "SHM2.0 – Smart monitoring of bridge performance", has been created. The projected tangible result of the project is a prototype of a SHM2.0 system for bridges that demonstrates (i) the applicability of a low-cost sensor network for acquiring sufficient data (quality) on the dynamic behaviour of bridges, and (ii) the validated estimation of the change in structural response of a bridge - implying real structural changes, which allows for the prediction of structural damages. This estimation only requires an easy-to-use structural model and the application of a novel damage detection algorithm.The Zwartewaterbrug project is a part of the SHM2.0 project.

The Zwartewaterbrug project is related to vibration assessment of steel arched bridge, located in the city of Hasselt, in the Dutch province of Overijssel. Data containing dynamic behavior of aforementioned bridge is base of this thesis.



Figure 3.1: Hasselt, Overijssel, Bridge over river Zwarte Water

3.1 Structure description

The structure that is being analyzed is steel arched bridge, built in 1969. The bridge is located in the city of Hasselt, in the Dutch province of Overijssel, crossing river Zwarte Water with a span of 104 meters. In figure 3.1 the bridge can be seen.

▼ **Structural characteristics of the bridge:**

- Span of 104 meters
- Steel arch with vertical hangers
- Steel deck
- Asphalt cover
- Concrete foundations
- Design load unknown

The sensor network is set on a segment of the bridge deck. Location of the segment can be seen in figure 3.2. Dominant load of the bridge is traffic load.
Traffic load is transferred to deck steel plate through asphalt cover and passes to main longitudinal beams through deck girder system. Main longitudinal beams together with a system of the arch and vertical hangers, transfer traffic load to foundations. Additional technical drawing of the bridge can be seen in figure 3.3.

▼ **Structural characteristics of a segment of the bridge equipped with sensors:**

- I shape main longitudinal steel beams
- I shape transverse steel beams
- U shape longitudinal span steel stiffeners
- Steel plate welded to deck girder system
- Asphalt cover

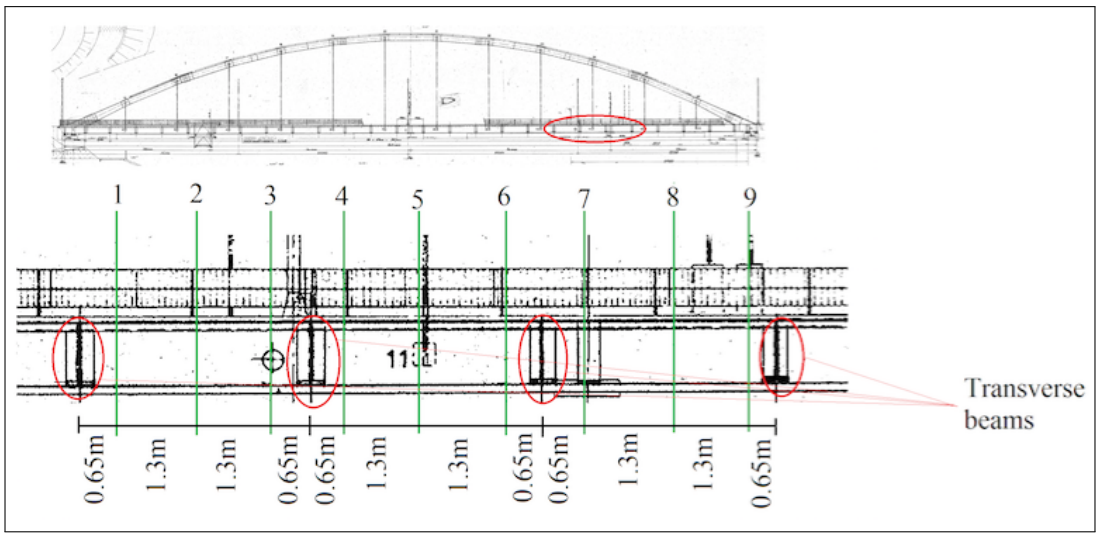


Figure 3.2: Deck segment equipped with sensors

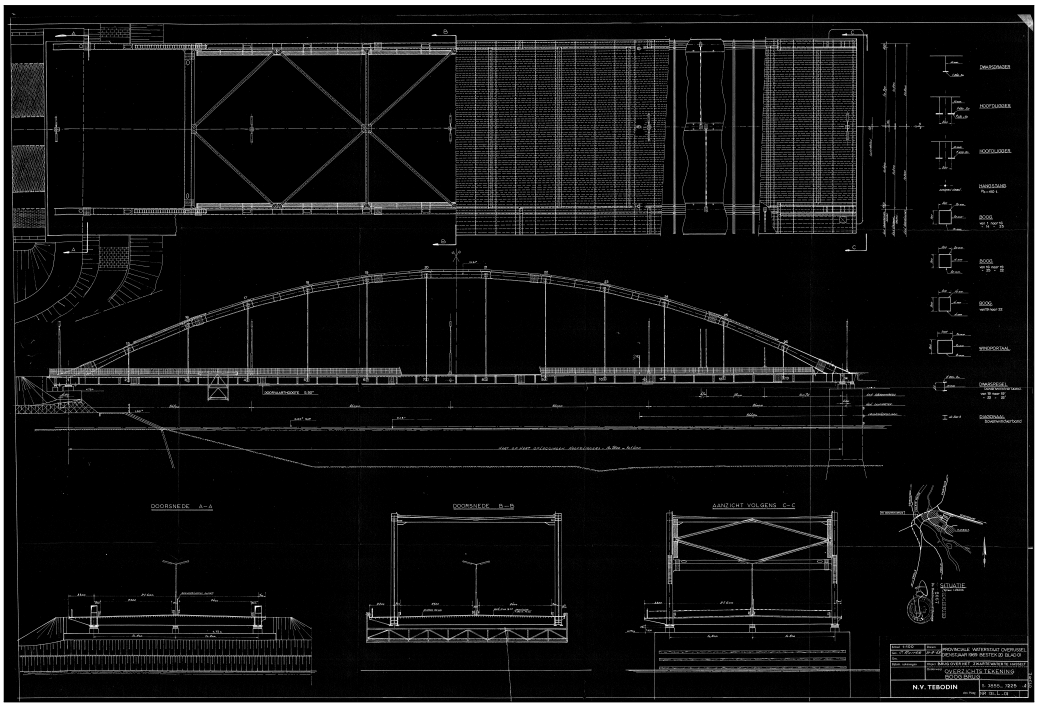


Figure 3.3: Technical drawing of the bridge

Based on the obtained technical drawings FEM geometry is designed, observe figure (3.4). Further discussion on the FEM parameters will be presented in the analysis section.

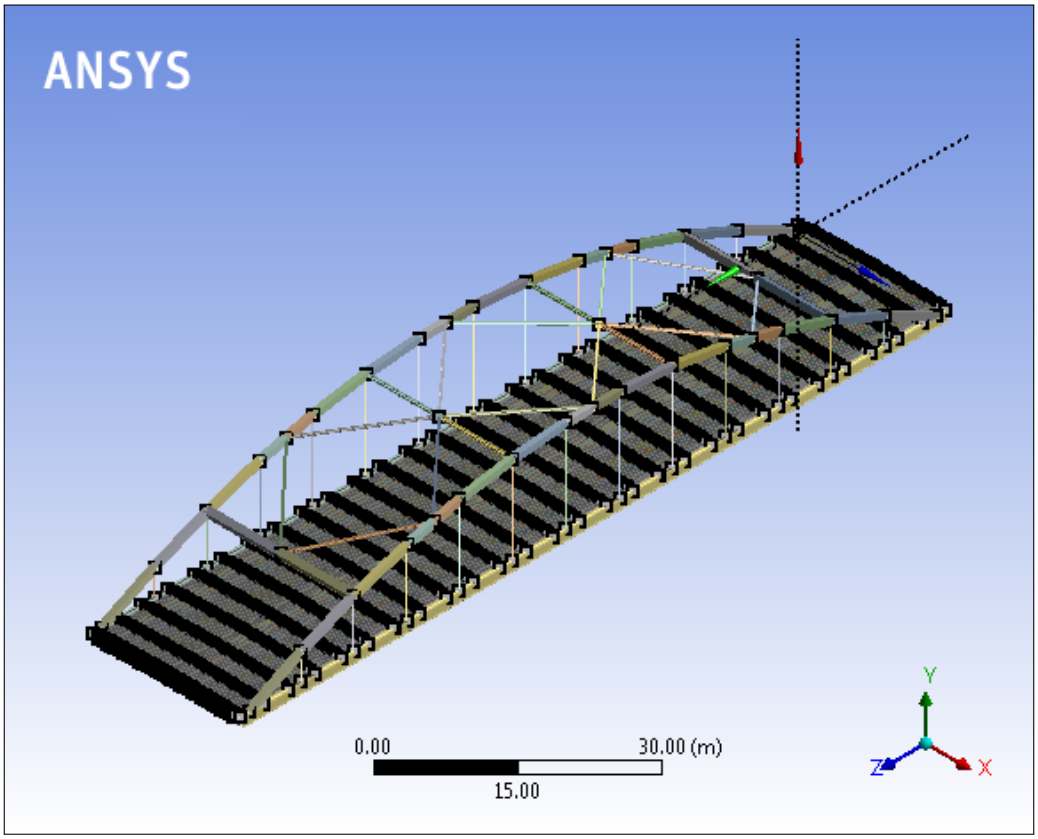


Figure 3.4: FEM geometry

3.2 The measurement campaign

The main idea behind the Zwartewaterbrug project was to generate vibrational data with healthy structure, and structure with the presence of small damage. As mentioned in the previous chapter, damage usually presents itself in terms of reduced stiffness.
The reduction of stiffness has an influence on the reduction on eigenfrequencies, and reduction of eigenfrequencies can also be caused by an increase in mass.

The Zwartewaterbrug project is based on measurement campaign with a variety of small added masses that are considered as presence of small damage.
Development of vibration-based health monitoring system for early detection of damage is based on data generated during the Zwartewaterbrug project.

▼ **This section presents:**

- The sensor network
- Installation of the measuring system
- The measurement campaign

3.2.1 The sensor network

Location of the bridge segment that is equipped with accelerometers is shown in figure 3.2. The sensor network contains a total of 32 accelerometers. Spatial positioning of accelerometers is presented in figure 3.5.

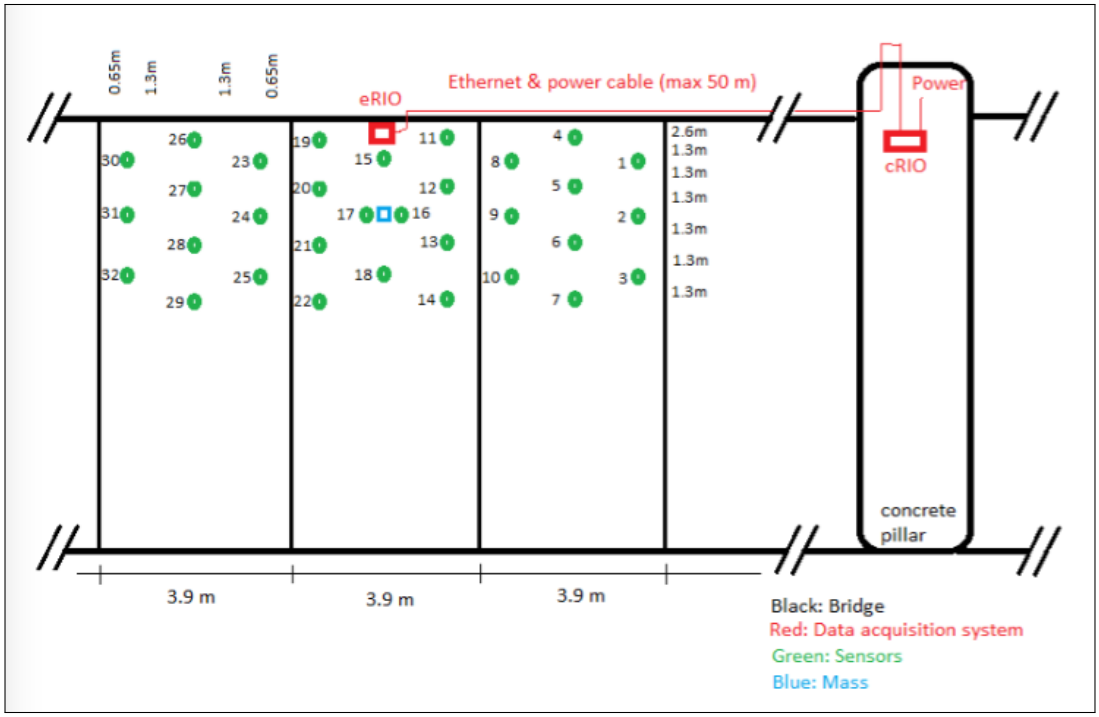


Figure 3.5: Spatial resolution of sensor network

3.2.2 Installation of the measuring system

The construction used for installing the measuring system can be seen in figure 3.6. During installation of the measuring system, the passage for ships under the bridge was closed in con-

nection with the use of the maintenance trolley, to accommodate the different parts of the measuring system. The maintenance trolley is served by a county employee.



Figure 3.6: The construction used for installing the measuring system

3.2.3 The measurement campaign

▼ **To perform the measurements, a number of steps were taken:**

1 Installation of the measuring system
2 Testing function of the measuring system
3 Applying added mass
4 Setting measurement-specific variables (weight)

Testing functionality:
The system's functionality was tested to verify whether all sensors are active, all cables properly connected. Given the differences in the expected response per location, it was difficult to verify the sensors in absolute terms.

Applying added mass:
The added mass that represents the presence of a damage is attached to the bridge with use of a magnet, as shown in figure 3.7.

Setting measurement-specific variables (weight)
Sand was used to manipulate the amount of added mass. Measurements were performed in steps of 25kg. The maximum total mass is 100 kg, with the magnet's own weight of 25 kg. In figure 3.8 applied added mass can be observed.



(a) (b)

Figure 3.7: System for attaching added mass



Figure 3.8: Added mass system

In table 3.1 test matrix of the Zwartewaterbrug project is presented.

▼ **Recived data for analysis-added mass/date of test**

- 23.03.2016 (0kg,50kg,100kg)
- 28.03.2016 (25kg,50kg)
- 31.03.2016 (75kg)

Table 3.1: Test matrix for the measurements on the Zwartewaterbrug

ID	Afk.	Description	Duration
Day 1			
1	INS	Installation	4 hours
2	INIT	Initialization test, no weight at bridge	1 hour
3	T1-0	Test 1: Reference, no weight at bridge	2 hours
4	T2-0	Test 2: Weight 25kg at bridge	2 hours
Day 2			
5	T3-0	Test 3: Weight 50kg at bridge	2 hours
6	T4-0	Test 4: Weight 75kg at bridge	2 hours
7	T5-0	Test 5: Weight 100kg at bridge	2 hours
8	T1-1	Test 1: Reference, no weight at bridge	2 hours
Day 3			
9	T2-1	Test 2: Weight 25kg at bridge	2 hours
10	T3-1	Test 3: Weight 50kg at bridge	2 hours
11	T4-1	Test 4: Weight 75kg at bridge	2 hours
12	T5-1	Test 5: Weight 100kg at bridge	2 hours
Prolonged testing			
13	T6-0	Test 6: No weight, traffic tax measurement longer duration	1 week

▼ Comments

In figure 3.8 it can be observed that added mass is attached to bridge with a flexible connection. The used connection does not have compression stiffness and it would be assumed that presence of added mass has a non-linear effect. Additionally, wind of different direction and intensity could interfere with hanging added mass system.
Having in mind that magnet is used for attachment of added mass, an additional issue is raised following that electrical current is generated in the conductor that moves in the magnetic field. The weight of the bridge segment with sensor network has approximately 40 tons. The added mass of 25kg is 0.0625% of bridge segment equipped with sensors.
Question is also raised whether attachment of magnet could increase local stiffness as small changes are of interest in the analysis.

Data that is received for the analysis doesn't follow received test matrix presented in table 3.1.

▼ Valuable information for further analysis:

- Non-linear effect of added mass
- Interference of magnet with close accelerometers
- The percentage of added mass with respect to weight of the bridge segment equipped with sensors
- Interference of attaching system with local stiffness

3.3 Project goals

▼ **The goal for prototype of an SHM2.0 system**

- Prove applicability of a low-cost sensor network for acquiring sufficient data quality on the dynamic behavior of bridges
- Estimation of the change in structural response of a bridge - implying real structural changes, which allows for the prediction of structural damages

▼ **The goal of the Zwartewaterbrug project**

- Development of damage identification method sensitive to small changes
- Coming up to level 4 damage identification

3.4 Data classification

In this chapter, classification of the Zwartewaterbrug project data is presented. Classification is formed for the purpose of supporting further analysis.

▼ **Main characteristics that are presented in this chapter:**

- Excitation types
- Measurement duration
- Measurement intensity
- Frequency content
- Environmental conditions

3.4.1 Excitation characteristics

Data is generated without information about excitation. Data processing will be based on the output only algorithms.

▼ **Excitation types:**

- Traffic load and wind load (ambient excitation)
- Hammer impact tests

3.4.2 Classification characteristics

Data classification is made upon same characteristics count. It is assumed that classification information would be beneficial in the initial analysis, to reduce possible dissipation of results due to the difference in data type. Information about classified data count is presented in tables 3.2 on the following page, to 3.7 on page 20.

▼ **Time domain data characteristics are related to:**

- Long: $40s$ <duration< $60s$
- Medium: $20s$ <duration< $40s$
- Short: duration< $20s$
- High intensity: maximum acceleration> $0.5\frac{m}{s^2}$
- Medium intensity: $0.5\frac{m}{s^2}$ >maximum acceleration> $0.1\frac{m}{s^2}$
- Low intensity: maximum acceleration< $0.1\frac{m}{s^2}$

Table 3.2: 0kg added mass stable mode count

Stable frequency content	0 to 10Hz	10 to 20Hz	20 to 35Hz	35 to 50Hz	50 to 75Hz	75 to 100Hz	100 to 200Hz	200 to 300Hz	300 to 400Hz	400 to 500Hz
Duration	High intensity									
Long (2)	2	2	1	1	2	2	2	2	1	1
Medium (8)	8	8	5	0	3	3	6	6	2	2
Short (0)	0	0	0	0	0	0	0	0	0	0
Duration	Medium intensity									
Long (28)	28	27	13	11	22	20	12	9	7	5
Medium (91)	91	77	36	38	59	43	25	28	24	27
Short (20)	20	4	2	0	5	2	1	0	0	1
Duration	Low intensity									
Long (0)	0	0	0	0	0	0	0	0	0	0
Medium (3)	3	0	0	0	1	0	0	0	0	0
Short (16)	16	0	0	0	2	1	0	0	0	0
Total	168 measurements performed									

Table 3.3: 25kg added mass stable mode count

Stable frequency content	0 to 10Hz	10 to 20Hz	20 to 35Hz	35 to 50Hz	50 to 75Hz	75 to 100Hz	100 to 200Hz	200 to 300Hz	300 to 400Hz	400 to 500Hz
Duration	High intensity									
Long (0)	0	0	0	0	0	0	0	0	0	0
Medium (2)	2	2	1	0	2	1	1	1	0	0
Short (0)	0	0	0	0	0	0	0	0	0	0
Duration	Medium intensity									
Long (7)	7	7	5	7	6	6	3	1	2	0
Medium (65)	65	49	29	25	37	31	17	22	11	23
Short (14)	14	4	0	1	6	2	0	0	1	0
Duration	Low intensity									
Long (0)	0	0	0	0	0	0	0	0	0	0
Medium (5)	5	3	0	1	3	1	0	0	0	0
Short (18)	18	4	2	0	0	0	0	0	0	0
Total	111 measurements performed									

Table 3.4: 50kg added mass stable mode count

Stable frequency content	0 to 10Hz	10 to 20Hz	20 to 35Hz	35 to 50Hz	50 to 75Hz	75 to 100Hz	100 to 200Hz	200 to 300Hz	300 to 400Hz	400 to 500Hz
Duration	High intensity									
Long (3)	3	3	2	1	2	2	2	3	0	1
Medium (14)	14	12	3	4	7	8	8	10	6	8
Short (0)	0	0	0	0	0	0	0	0	0	0
Duration	Medium intensity									
Long (17)	17	17	11	7	14	15	9	5	7	5
Medium (125)	125	89	36	54	79	65	35	35	30	31
Short (25)	25	5	0	2	3	1	0	0	0	1
Duration	Low intensity									
Long (0)	0	0	0	0	0	0	0	0	0	0
Medium (5)	5	3	0	2	2	1	0	0	0	0
Short (20)	20	2	0	2	0	1	0	0	0	0
Total	209 measurements performed									

Table 3.5: 75kg added mass stable mode count

Stable frequency content	0 to 10Hz	10 to 20Hz	20 to 35Hz	35 to 50Hz	50 to 75Hz	75 to 100Hz	100 to 200Hz	200 to 300Hz	300 to 400Hz	400 to 500Hz
Duration	High intensity									
Long (3)	3	3	3	2	3	3	3	1	1	1
Medium (8)	8	7	6	4	4	6	3	4	3	2
Short (0)	0	0	0	0	0	0	0	0	0	0
Duration	Medium intensity									
Long (16)	16	16	13	9	13	13	9	6	5	8
Medium (62)	62	50	23	28	42	33	23	24	14	13
Short (9)	9	3	1	0	3	1	0	0	1	1
Duration	Low intensity									
Long (0)	0	0	0	0	0	0	0	0	0	0
Medium (7)	7	3	1	1	2	1	1	0	0	0
Short (22)	22	2	1	2	4	1	0	1	0	0
Total	127 measurements performed									

Table 3.6: 100kg added mass stable mode count

Stable frequency content	0 to 10Hz	10 to 20Hz	20 to 35Hz	35 to 50Hz	50 to 75Hz	75 to 100Hz	100 to 200Hz	200 to 300Hz	300 to 400Hz	400 to 500Hz
Duration	High intensity									
Long (1)	1	1	1	1	1	1	1	1	1	0
Medium (6)	6	5	4	3	2	1	4	3	2	2
Short (0)	0	0	0	0	0	0	0	0	0	0
Duration	Medium intensity									
Long (15)	15	15	14	9	11	9	5	4	5	5
Medium (76)	76	60	30	37	56	39	20	23	11	19
Short (22)	22	7	0	1	5	3	0	0	1	1
Duration	Low intensity									
Long (0)	0	0	0	0	0	0	0	0	0	0
Medium (3)	3	0	1	0	2	1	0	0	0	0
Short (28)	28	9	3	4	5	1	0	0	0	0
Total	151 measurement performed									

Table 3.7: Hammer test stable mode count

Stable frequency content	0 to 10Hz	10 to 20Hz	20 to 35Hz	35 to 50Hz	50 to 75Hz	75 to 100Hz	100 to 200Hz	200 to 300Hz	300 to 400Hz	400 to 500Hz
Duration	High intensity									
Long (6)	6	6	4	3	2	2	2	5	5	4
Medium (0)	0	0	0	0	0	0	0	0	0	0
Short (0)	0	0	0	0	0	0	0	0	0	0
Duration	Medium intensity									
Long (0)	0	0	0	0	0	0	0	0	0	0
Medium (0)	0	0	0	0	0	0	0	0	0	0
Short (0)	0	0	0	0	0	0	0	0	0	0
Duration	Low intensity									
Long (0)	0	0	0	0	0	0	0	0	0	0
Medium (0)	0	0	0	0	0	0	0	0	0	0
Short (0)	0	0	0	0	0	0	0	0	0	0
Total	6 measurements performed									

▼ **Comments**

In tables 3.2 to 3.7, it can be seen that majority of measurements are characterized by medium duration (around 60%). Data considered as a low-quality (short duration and low intensity) is present in the amount of 10-20%.

Additionally, in aforementioned tables, information of the frequency content is presented. Frequency content information is based on the Frequency domain decomposition with stabilization diagram (further discussed in the theory section). Result of the given procedure is identified mode count for the particular frequency region. At this point, no additional comments are going to be made on the frequency content.

3.4.3 Environmental conditions

Environmental condition data is based on information from Netherlands Historical Weather Almanac [7] and temperature data generated during tests.

Environmental data obtained from Netherlands Historical Weather Almanac [7] can be observed in figure 3.9 on the following page to figure 3.11 on page 23. Temperature data obtained during live measurements is presented in figure 3.12 on page 23 to figure 3.16 on page 24.

▼ **Important information from Netherlands Historical Weather Almanac**

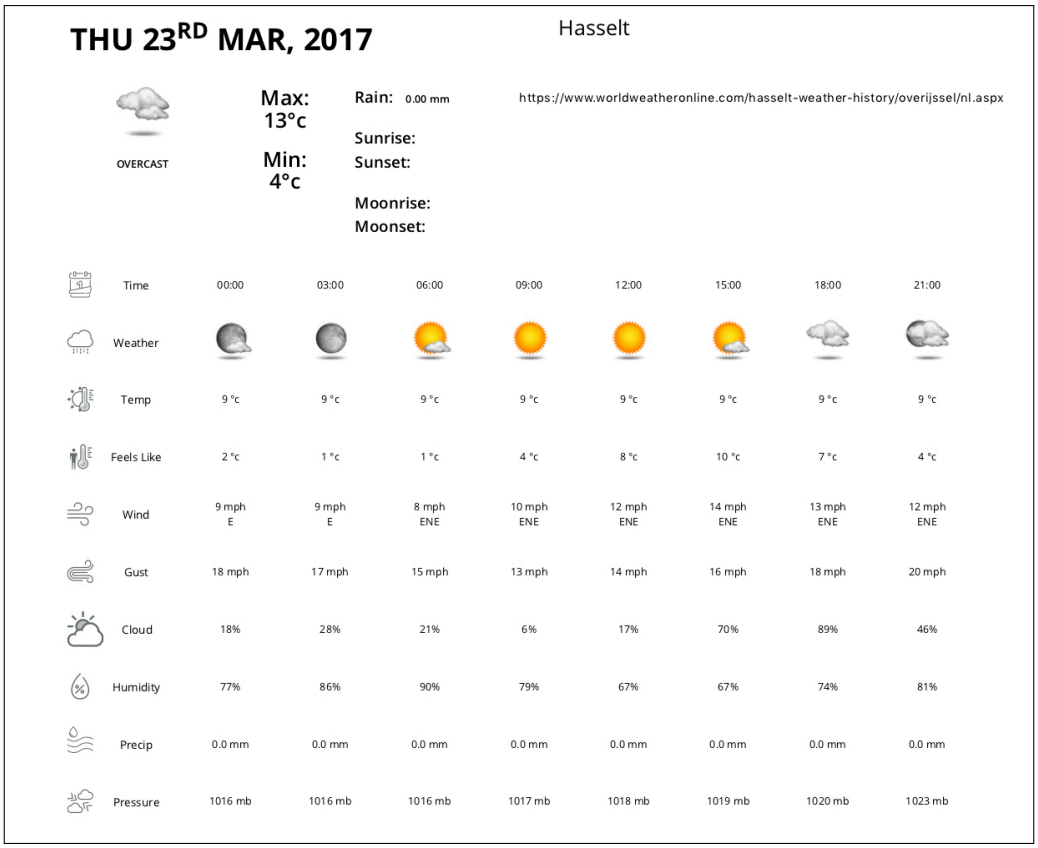
- Temperature
- Amount of rain
- Wind speed
- Gust speed
- Wind direction

As main goal of this work is to develop damage detection algorithm sensitive to small changes, environmental conditions are considered as possible factor for deviation of results.

▼ **Comments**

Used data is generated on the 23rd, 28th and 31st of March 2017. Measurements on the 31st of March were completed by 15 : 00 hrs, before the rain started (figure 3.11 on page 23). In 3.14 on page 24, part of the measurements related to the 28th of March show slightly higher temperatures than other measurements, also on that date measurements with 25kg are performed and in 3.13 on page 23 larger deviations of the temperature are observed.

It is concluded that not enough measurements are performed to include impact of environmental conditions in the development of the Structural health monitoring algorithm.



THU 23RD MAR, 2017 — Hasselt

OVERCAST

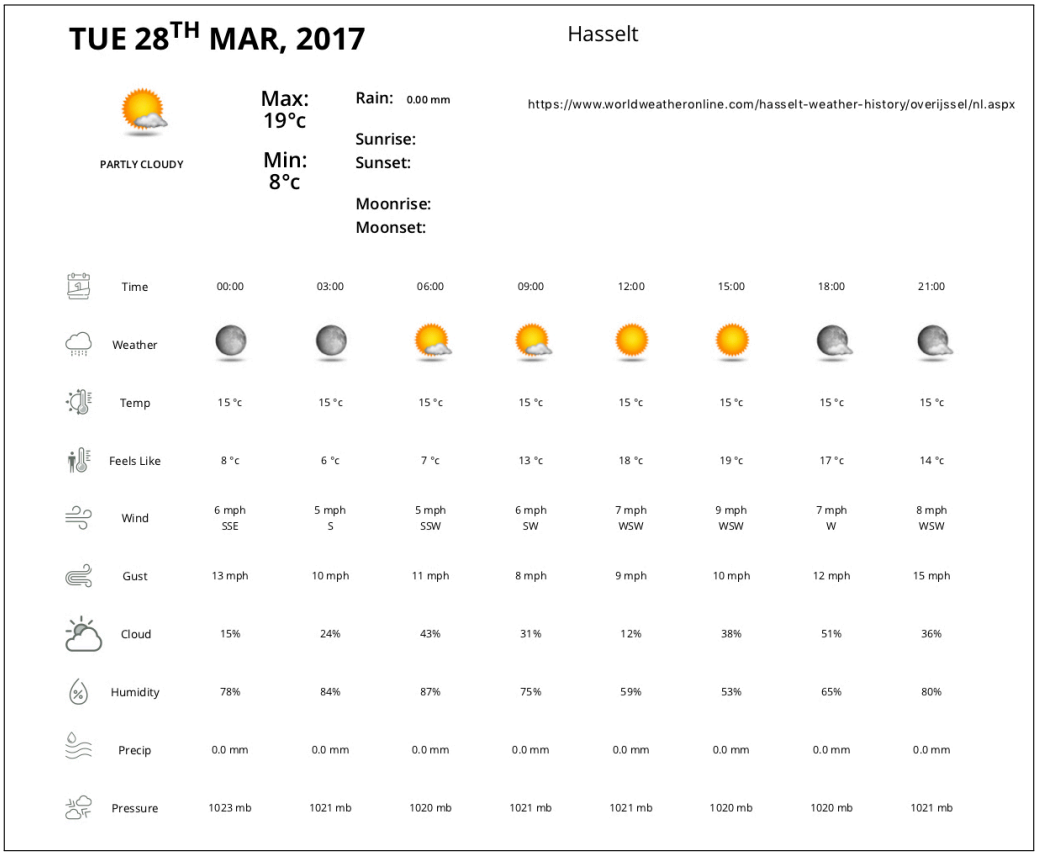
Max: 13°c
Min: 4°c

Rain: 0.00 mm
Sunrise:
Sunset:
Moonrise:
Moonset:

https://www.worldweatheronline.com/hasselt-weather-history/overijssel/nl.aspx

	00:00	03:00	06:00	09:00	12:00	15:00	18:00	21:00
Time								
Weather								
Temp	9 °c	9 °c	9 °c	9 °c	9 °c	9 °c	9 °c	9 °c
Feels Like	2 °c	1 °c	1 °c	4 °c	8 °c	10 °c	7 °c	4 °c
Wind	9 mph E	9 mph E	8 mph ENE	10 mph ENE	12 mph ENE	14 mph ENE	13 mph ENE	12 mph ENE
Gust	18 mph	17 mph	15 mph	13 mph	14 mph	16 mph	18 mph	20 mph
Cloud	18%	28%	21%	6%	17%	70%	89%	46%
Humidity	77%	86%	90%	79%	67%	67%	74%	81%
Precip	0.0 mm	0.0 mm	0.0 mm	0.0 mm	0.0 mm	0.0 mm	0.0 mm	0.0 mm
Pressure	1016 mb	1016 mb	1016 mb	1017 mb	1018 mb	1019 mb	1020 mb	1023 mb

Figure 3.9: Hasselt, Overijssel, Netherlands Historical Weather Almanac 3/23/2017



TUE 28TH MAR, 2017 — Hasselt

PARTLY CLOUDY

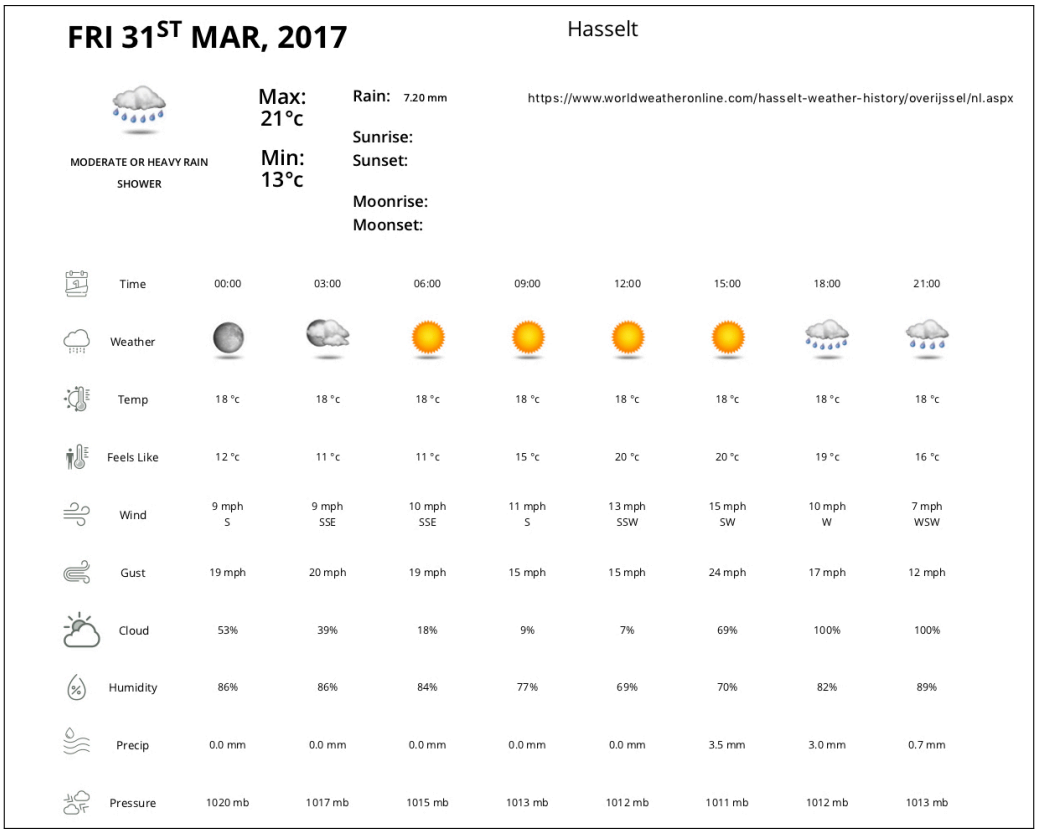
Max: 19°c
Min: 8°c

Rain: 0.00 mm
Sunrise:
Sunset:
Moonrise:
Moonset:

https://www.worldweatheronline.com/hasselt-weather-history/overijssel/nl.aspx

	00:00	03:00	06:00	09:00	12:00	15:00	18:00	21:00
Time								
Weather								
Temp	15 °c	15 °c	15 °c	15 °c	15 °c	15 °c	15 °c	15 °c
Feels Like	8 °c	6 °c	7 °c	13 °c	18 °c	19 °c	17 °c	14 °c
Wind	6 mph SSE	5 mph S	5 mph SSW	6 mph SW	7 mph WSW	9 mph WSW	7 mph W	8 mph WSW
Gust	13 mph	10 mph	11 mph	8 mph	9 mph	10 mph	12 mph	15 mph
Cloud	15%	24%	43%	31%	12%	38%	51%	36%
Humidity	78%	84%	87%	75%	59%	53%	65%	80%
Precip	0.0 mm	0.0 mm	0.0 mm	0.0 mm	0.0 mm	0.0 mm	0.0 mm	0.0 mm
Pressure	1023 mb	1021 mb	1020 mb	1021 mb	1021 mb	1020 mb	1020 mb	1021 mb

Figure 3.10: Hasselt, Overijssel, Netherlands Historical Weather Almanac 3/28/2017



FRI 31ST MAR, 2017 — Hasselt

MODERATE OR HEAVY RAIN SHOWER

Max: 21°c
Min: 13°c

Rain: 7.20 mm
Sunrise:
Sunset:
Moonrise:
Moonset:

https://www.worldweatheronline.com/hasselt-weather-history/overijssel/nl.aspx

	00:00	03:00	06:00	09:00	12:00	15:00	18:00	21:00
Time								
Weather								
Temp	18 °c	18 °c	18 °c	18 °c	18 °c	18 °c	18 °c	18 °c
Feels Like	12 °c	11 °c	11 °c	15 °c	20 °c	20 °c	19 °c	16 °c
Wind	9 mph S	9 mph SSE	10 mph SSE	11 mph S	13 mph SSW	15 mph SW	10 mph W	7 mph WSW
Gust	19 mph	20 mph	19 mph	15 mph	15 mph	24 mph	17 mph	12 mph
Cloud	53%	39%	18%	9%	7%	69%	100%	100%
Humidity	86%	86%	84%	77%	69%	70%	82%	89%
Precip	0.0 mm	0.0 mm	0.0 mm	0.0 mm	0.0 mm	3.5 mm	3.0 mm	0.7 mm
Pressure	1020 mb	1017 mb	1015 mb	1013 mb	1012 mb	1011 mb	1012 mb	1013 mb

Figure 3.11: Hasselt, Overijssel, Netherlands Historical Weather Almanac 3/31/2017

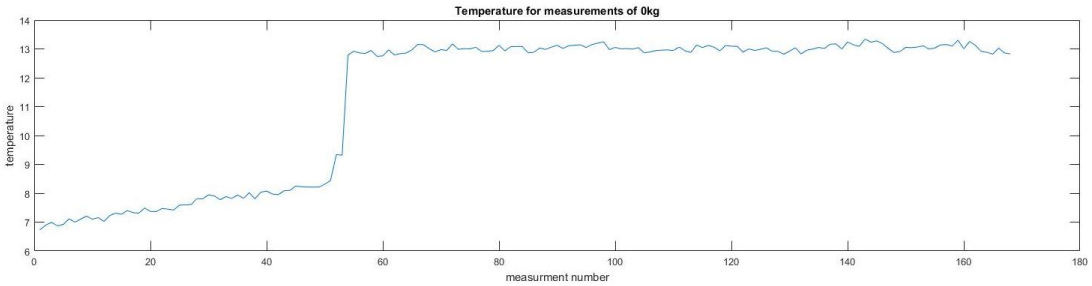


Figure 3.12: Recorded temperature for measurements performed with 0kg

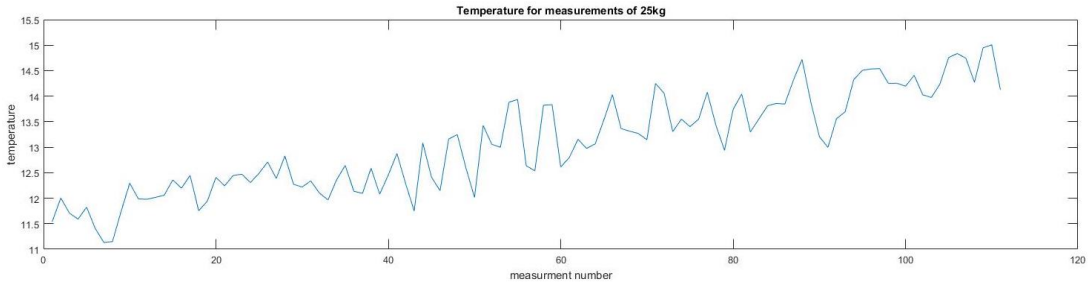


Figure 3.13: Recorded temperature for measurements performed with 25kg

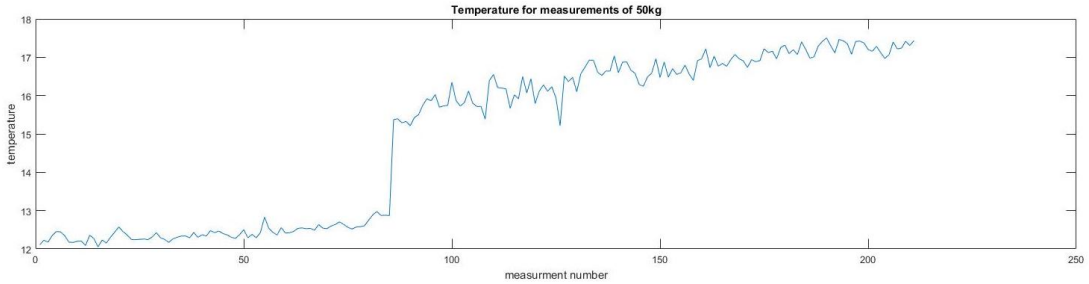


Figure 3.14: Recorded temperature for measurements performed with 50kg

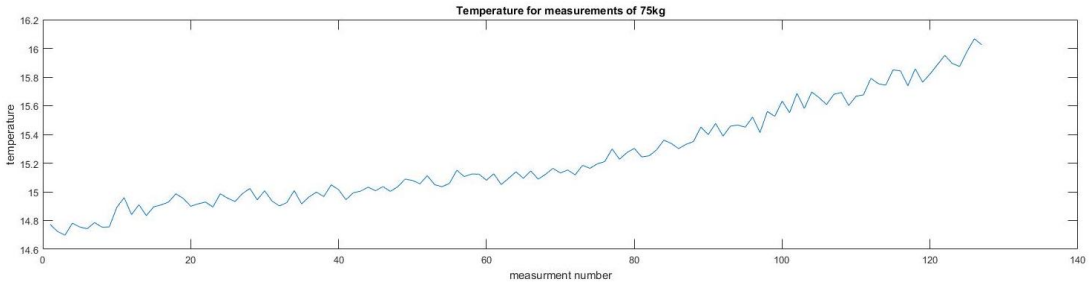


Figure 3.15: Recorded temperature for measurements performed with 75kg

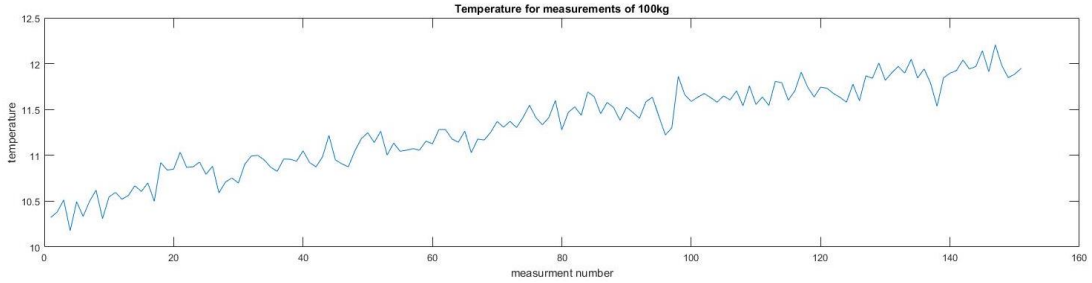


Figure 3.16: Recorded temperature for measurements performed with 100kg

Theory

Chapter 4

Mathematical tools

Intentions of this chapter are to introduce mathematical tools that are important for understanding output only identification methods and development of identification concepts for further analysis. The provided mathematical notation will be kept through the work.

Style of presenting given mathematical tools refers to a style I would prefer if I was reading the subject for the first time. Initially answering the question "Why?", that is related to further work, followed by description and simple example. The aim is that possible awe for the subject is avoided with good perspective for easy implementation.

4.1 Geometrical projections in statistical framework

Geometrical tools

Geometrical projections are introduced as they play important role in data-driven stochastic subspace identification. In figure 4.1 geometrical projection of 2D vectors is presented. Based on the 2D example, the concept is expanded to geometrical projections of matrices.

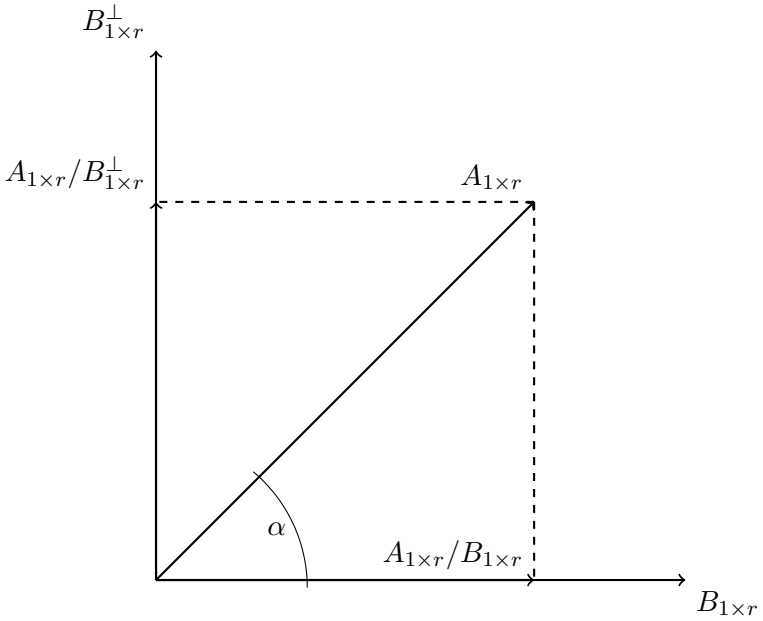


Figure 4.1: Geometrical projection of 2D vectors

In equation (4.1), projection of vector $A_{1\times r}$ to vector $B_{1\times r}$ is presented. Vector $A_{1\times r}/B_{1\times r}$ is lying down in space of vector $B_{1\times r}$. Following simple derivations, main relation is derived and

presented in equation (4.4). As geometrical projections in stochastic subspace identification are used to project rows of one matrix onto rows of another matrix, row vector of a matrix is used in derivations.

$$A_{1\times r}/B_{1\times r} = |A_{1\times r}|\cos(\alpha)\frac{B_{1\times r}}{|B_{1\times r}|} \tag{4.1}$$

$$\cos(\alpha) = \frac{A_{1\times r}B_{1\times r}^T}{|A_{1\times r}||B_{1\times r}|} \tag{4.2}$$

$$A_{1\times r}/B_{1\times r} = |A_{1\times r}|\frac{A_{1\times r}B_{1\times r}^T}{|A_{1\times r}||B_{1\times r}|}\frac{B_{1\times r}}{|B_{1\times r}|} \tag{4.3}$$

$$A_{1\times r}/B_{1\times r} = A_{1\times r}B_{1\times r}^T(B_{1\times r}B_{1\times r}^T)^{-1}B_{1\times r} \tag{4.4}$$

For sake of simplicity, the projection of vector to the vector of perpendicular space is presented on 2D example, observe (4.5). It is clear that cosine between them is zero.

$$B_{1\times r}/B_{1\times r}^{\perp} = 0 \tag{4.5}$$

Expanding provided concept to matrices, for projecting rows of matrix A onto rows of matrix B, relation (4.6) is presented.

$$A/B = AB^T(BB^T)^{-1}B \tag{4.6}$$

$$B/B^{\perp} = 0 \tag{4.7}$$

Statistical tools

For subspace identification relation between geometrical and statistical tools plays major role. Before introducing their relation, statistical tools that would be used, are presented.

Consider two row sequences $\boldsymbol{\omega}_k \in \mathbb{R}^{j\times 1}$ and $\boldsymbol{\upsilon}_k \in \mathbb{R}^{j\times 1}$, $k = 1...j$. In subspace identification, it is assumed that data contains long time series ($j \to \infty$), and that data is ergodic. Due to ergodicity and "infinite" number of data, expectation operator $\mathbf{E}$ is replaced with operator $\mathbf{E}_j$. Observe defined relations in (4.8).

$$\begin{aligned}\mathbf{E}\left[\boldsymbol{\omega}_k\boldsymbol{\upsilon}_k^T\right] &= \lim_{j\to\infty}\left(\frac{1}{j}\sum_{i=1}^{j}\boldsymbol{\omega}_i\boldsymbol{\upsilon}_i^T\right)\\ &= \mathbf{E}_j\left(\sum_{i=1}^{j}\boldsymbol{\omega}_i\boldsymbol{\upsilon}_i^T\right)\end{aligned} \tag{4.8}$$

$$\mathbf{E}_j[...] \overset{\text{def}}{=} \lim_{j\to\infty}\frac{1}{j}[...] \tag{4.9}$$

Considering aforementioned assumptions, for the case where $\boldsymbol{\omega}_k$ and $\boldsymbol{\upsilon}_k$ are independent, we obtain (4.10).

$$\mathbf{E}_j\left(\sum_{i=1}^{j}\boldsymbol{\omega}_i\boldsymbol{\upsilon}_i^T\right) = 0 \tag{4.10}$$

Putting data in row matrices, $\boldsymbol{\omega} = [\boldsymbol{\omega}_1\ \boldsymbol{\omega}_2\ ...\ \boldsymbol{\omega}_j]$ and $\boldsymbol{\upsilon} = [\boldsymbol{\upsilon}_1\ \boldsymbol{\upsilon}_2\ ...\ \boldsymbol{\upsilon}_j]$, relation (4.11) is obtained. which implies that vector $\boldsymbol{\omega}$ is perpendicular to vector $\boldsymbol{\upsilon}$.

$$\mathbf{E}_j\left[\boldsymbol{\omega}\boldsymbol{\upsilon}^T\right] = 0 \tag{4.11}$$

Geometrical projections in statistical framework

For the statistical framework, covariance $\Phi_{[A,B]}$ between two matrices, $A \in \mathbb{R}^{m\times j}$ and $B \in \mathbb{R}^{n\times j}$, is defined (4.12).

$$\Phi_{[A,B]} \stackrel{\text{def}}{=} \mathbf{E}_j \left[AB^T\right] \tag{4.12}$$

Now geometric framework can be related to the statistical framework.

$$\Phi_{[A,B]} \to AB^T \tag{4.13}$$

Moore−Penrose pseudo inverse is introduced with "†" symbol.

$$\begin{aligned} A/B &= AB^T(BB^T)^{-1}B \\ &= \Phi_{[A,B]}\Phi^{\dagger}_{[B,B]}B \end{aligned} \tag{4.14}$$

When we implement the algorithms, number of measurements is finite ($j \neq \infty$), so covariance $\Phi_{[A,B]}$ is approximated (4.15).

$$\Phi_{[A,B]} \simeq \frac{1}{j}AB^T \tag{4.15}$$

Although an approximation of covariance is introduced, the relation between geometrical and statistical tools remain the same (4.16)

$$\begin{aligned} A/B &= \Phi_{[A,B]}\Phi^{\dagger}_{[B,B]}B \\ &= \left[\frac{1}{j}AB^T\right]\left[\frac{1}{j}BB^T\right]^{\dagger}B \\ &= \left[AB^T\right]\left[BB^T\right]^{\dagger}B \end{aligned} \tag{4.16}$$

4.2 Singular value decomposition

Singular value decomposition comes in the end stage of both, frequency domain decomposition and stochastic subspace identification.

Singular value decomposition of matrix C consist of left singular vector matrix U, singular values Σ and right singular vector matrix V, observe (4.17).

$$C = U\Sigma V^T \tag{4.17}$$

Matrix of left singular vectors U is orthonormal (4.19). From the orthonormal property, relation (4.18) is obtained.

$$C^T C = V\Sigma^T \Sigma V^T \tag{4.18}$$

$$U^T U = I \tag{4.19}$$

$$V^T V = 1 \tag{4.20}$$

$$CV = U\Sigma \tag{4.21}$$

From relation (4.18), it can be seen that singular value matrix is obtained as square root of $C^T C$ eigenvalues, see (equation (4.22) and (4.23)).

$$det(C^T C - \lambda I) = 0 \tag{4.22}$$

$$\Sigma^2 = \begin{bmatrix} \lambda_i & & \\ & \ddots & \\ & & \lambda_n \end{bmatrix} \tag{4.23}$$

From kernel (right nullspace) of matrix A_i (4.24), columns of right singular vector matrix is obtained (equation (4.25) and (4.26)). Solution for right singular vectors is not unique.

$$C^T C - \lambda_i I = A_i \tag{4.24}$$

$$A_i \mathbf{v}_i = \mathbf{0}_{n\times 1} \tag{4.25}$$

$$V = \begin{bmatrix} \mathbf{v}_i & \dots & \mathbf{v}_n \end{bmatrix} \tag{4.26}$$

With obtained singular value matrix and right singular vectors, left singular vectors can be obtained (4.27).

$$U = CV\Sigma^{-1} \tag{4.27}$$

4.3 Modal assurance criterion

In this section, the Modal Assurance Criterion is introduced (MAC). An additional recommendation is to read a paper, with an interesting title, *"The Modal Assurance Criterion-Twenty Years of Use and Abuse"* [1]. In the given paper, multiple assurance criterion models are summarized and explained.

Purpose of introduction and use of MAC is to set quality assurance indicator for identified experimental modal vectors from measured data. MAC is a scalar value, defining the degree of consistency between reference modal vector and another modal vector. The relation for obtaining MAC is presented in equation (4.28).

$$\mathrm{MAC} = \frac{\boldsymbol{\Phi}_n^H \boldsymbol{\Phi}_r \boldsymbol{\Phi}_r^H \boldsymbol{\Phi}_n}{\boldsymbol{\Phi}_n^H \boldsymbol{\Phi}_n \boldsymbol{\Phi}_r^H \boldsymbol{\Phi}_r} \tag{4.28}$$

MAC takes values from zero (no consistent correspondence) to one (consistent correspondence). It is important to take results critically, reasons are provided bellow.

▼ Possible reasons for zero MAC (no consistent correspondence):

- Non-stationary system (non-linearity with respect to time or excitation)
- Noise on reference modal vector
- Modal parameter estimation is invalid
- Modal vectors are from linearly unrelated mode shape vectors

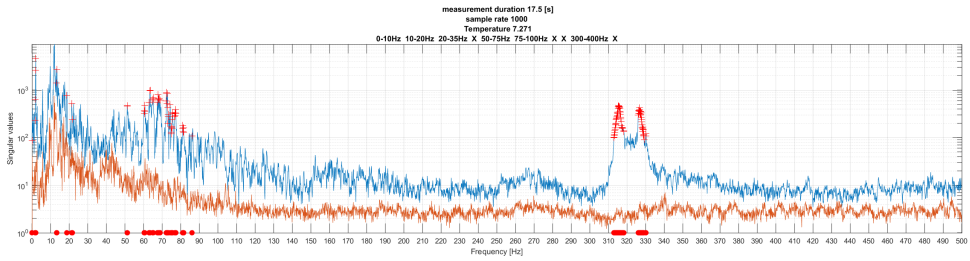
▼ Possible reasons for unity MAC (consistent correspondence):

- Incomplete measurements of modal vectors
- The modal vectors are the result of forced excitation
- The modal vectors are dominantly coherent noise
- The modal vectors represent the same vector with different scaling

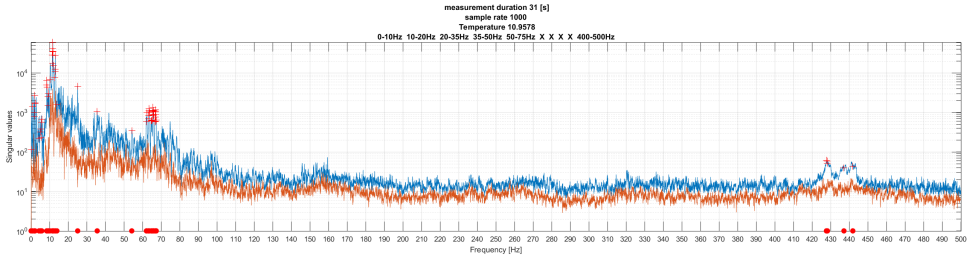
Stabilisation diagram example

The MAC in this work is used to form stabilization diagrams for the FDD plot figure 4.2. In the given figures red crosses represent regions with stable mode shapes.

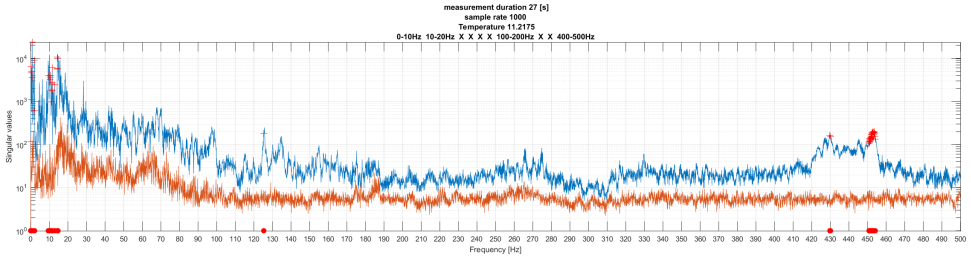
One red cross is plotted at a frequency where in the neighborhood of one frequency sample MAC value between left singular vectors of FDD (mode shapes) holds MAC larger than 0.97.



(a) Example of stabilisation diagram 1



(b) Example of stabilisation diagram 2



(c) Example of stabilisation diagram 3

Figure 4.2: Use of MAC for stabilisation diagram

4.4 1D Kalman filter

The 1D Kalman filter is presented in equation (4.29). Hat symbol in $\widehat{X}_t$ represents estimation of the measurement X_t.

$$\widehat{X}_t = \widehat{X}_{t-1} + KG_t(X_t - \widehat{X}_{t-1}) \tag{4.29}$$

Relation for Kalman gain KG_t is presented in equation (4.30). It is based on a ratio between estimated error $\widehat{E}_t$ and measurement error E_t. Kalman gain introduces weight between measurement and previous measurement estimate. When Kalman gain is close to 1 large weight is set on real measurement, and when Kalman gain is close to 0 large weight is set on previous measurement estimate.

$$KG_t = \frac{\widehat{E}_t}{\widehat{E}_t + E_t} \qquad 0 \leq KG_t \leq 1 \tag{4.30}$$

Estimated measurement error is based on previous estimated error $\widehat{E}_{t-1}$ and current measurement error $\widehat{E}_t$ (4.31).

$$\begin{aligned} \widehat{E}_t &= \frac{\widehat{E}_{t-1}E_t}{\widehat{E}_{t-1} + E_t} \\ &= (1 - KG_{t-1})\widehat{E}_{t-1} \end{aligned} \tag{4.31}$$

Through an iterative algorithm, 1D Kalman filter is used to estimate measurement value.

Chapter 5

Output only identification methods

In this chapter theoretical background of the Frequency domain decomposition (FDD) and the Stochastic subspace identification (SSI) is presented. A larger weight is put on the SSI, as it was a part of the literature study for this thesis. Additionally, implementation of the SSI will be described.

5.1 Frequency domain decomposition

The frequency domain decomposition (FDD) is an output-only system identification method. The system realization is based on the frequency response of the output data. In the following section, the FDD concept is just briefly described.

Before describing the FDD, let's revise that vectors are represented with small bold letters, matrices with large letters, and that frequency dependent variables are represented with tilde hat.

The steady-state solution in the frequency domain of the linear Mdof structural system is presented in equation (5.1). The output displacement vector in the frequency domain is represented with $\widetilde{\boldsymbol{y}}(\omega)$. $\widetilde{H}(\omega)$ represents matrix of transfer function and $\widetilde{\boldsymbol{f}}(\omega)$ represents force vector.

$$\widetilde{\boldsymbol{y}}(\omega) = \widetilde{H}(\omega)\widetilde{\boldsymbol{f}}(\omega) \tag{5.1}$$

Post-multiplying equation (5.1) by its Hermitian (conjugate transpose) (5.2), equation (5.3) is obtained.

$$\widetilde{\boldsymbol{y}}^H(\omega) = \widetilde{\boldsymbol{f}}^H(\omega)\widetilde{H}^H(\omega) \tag{5.2}$$

$$\widetilde{\boldsymbol{y}}(\omega)\widetilde{\boldsymbol{y}}^H(\omega) = \widetilde{H}(\omega)\widetilde{\boldsymbol{f}}(\omega)\widetilde{\boldsymbol{f}}^H(\omega)\widetilde{H}^H(\omega) \tag{5.3}$$

Introducing input ($\widetilde{S}_{ff}(\omega)$) and output ($\widetilde{S}_{yy}(\omega)$) spectral density matrices, the relation (5.4) is obtained:

$$\widetilde{S}_{yy}(\omega) = \widetilde{H}(\omega)\widetilde{S}_{ff}(\omega)\widetilde{H}^H(\omega) \tag{5.4}$$

Before going to the key step of the FDD, assumptions on the input forces are introduced. It is considered very important to go back to the assumptions when the analysis under-perform.

▼ **Assumptions on the input forces:**

- Broadband and smooth spectra, acting over the entire structure (all modes excited)
- Uncorrelated (off-diagonal terms of the input spectral density matrix $\widetilde{S}_{ff}(\omega)$ are zero)
- Similar amplitudes (diagonal terms of the input spectral density matrix $\widetilde{S}_{ff}(\omega)$ are constant)

From the given assumptions relation (5.5) is obtained:

$$\widetilde{S}_{ff}(\omega) = \widetilde{\boldsymbol{f}}(\omega)\widetilde{\boldsymbol{f}}^{H}(\omega) \propto I \tag{5.5}$$

Following that the input spectral density matrix ($\widetilde{S}_{ff}(\omega)$) is assumed to be proportional (approximate) to identity matrix, relation (5.6) follows:

$$\widetilde{S}_{yy}(\omega) \propto \widetilde{H}(\omega)\widetilde{H}^{H}(\omega) \tag{5.6}$$

Using the SVD of the output spectral density matrix $\widetilde{S}_{yy}(\omega)$, relation (5.7) is obtained:

$$\widetilde{S}_{yy}(\omega) = U\Sigma V^{T} \tag{5.7}$$

From the peaks of the plot of singular values Σ, modes are obtained. The mode shapes are recovered from the left singular vectors U of the chosen peaks.

5.2 Stochastic subspace identification

The aim of this section is to form the foundation for an understanding of the stochastic subspace identification methods used. The intention is to present section pragmatically, in the tunneled path, with aim of effective implementation and application. For going deeper into the understanding of presented theory (mainly mathematical proofs), reference to appropriate literature is made.

For effective implementation, it is considered that inappropriate awe should be eliminated. The main goal is to achieve effective analysis, built on foundations that give an opportunity for quality decisions that can lead to the fast identification of possible problems.

Simple steps are made with derivations, with complex proofs being referenced. Theory and derivations are based on [12], with adaptation for structural engineering use.

5.2.1 Deterministic subspace identification

Before going to stochastic subspace identification, it is important to introduce deterministic subspace identification.

Deterministic subspace identification refers to computing state space models from known input-output data. Contrary to the term deterministic, stochastic subspace identification refers to unknown input and known output.

Problem statement:

State space system presented in equations (5.8) and (5.9), of unknown order n, is to be determined with s measurements of input $\mathbf{u}_k \in \mathbb{R}^{m\times 1}$ and output $\mathbf{y}_k \in \mathbb{R}^{l\times 1}$. Small bold letters represent column vectors of measurements, where data in rows refers to the different spatial position of measurements, and index k is related to the position in time.

$$\mathbf{x}_{k+1} = A\mathbf{x}_k + B\mathbf{u}_k \tag{5.8}$$

$$\mathbf{y}_k = C\mathbf{x}_k + D\mathbf{u}_k \tag{5.9}$$

$$A \in \mathbb{R}^{n\times n},\ B \in \mathbb{R}^{n\times m},\ C \in \mathbb{R}^{l\times n},\ D \in \mathbb{R}^{l\times n}.$$

In equation (5.10) state space system is represented in a matrix form and multiplied with some invertible matrix T.

$$\begin{bmatrix} \mathbf{x}_2 & \mathbf{x}_3 & \dots & \mathbf{x}_{p+1} \\ \mathbf{y}_1 & \mathbf{y}_2 & \dots & \mathbf{y}_p \end{bmatrix} = \begin{bmatrix} A & B \\ C & D \end{bmatrix} \begin{bmatrix} \mathbf{x}_1 & \mathbf{x}_2 & \dots & \mathbf{x}_p \\ \mathbf{u}_1 & \mathbf{u}_2 & \dots & \mathbf{u}_p \end{bmatrix} \quad \left\{ \times \begin{bmatrix} T & 0 \\ 0 & I \end{bmatrix} \right. \tag{5.10}$$

The intention of presenting equation (5.10) and equation (5.11) is to show that for same inputs and same outputs, different system matrices are present (ABCD), concluding that solution of state space system is not unique. The term subspace is related to the fact that subspace identification determines one of those solutions.

$$\begin{aligned} \begin{bmatrix} T\mathbf{x}_2 & T\mathbf{x}_3 & \dots & T\mathbf{x}_{p+1} \\ \mathbf{y}_1 & \mathbf{y}_2 & \dots & \mathbf{y}_p \end{bmatrix} &= \begin{bmatrix} TA & TB \\ C & D \end{bmatrix} \begin{bmatrix} \mathbf{x}_1 & \mathbf{x}_2 & \dots & \mathbf{x}_p \\ \mathbf{u}_1 & \mathbf{u}_2 & \dots & \mathbf{u}_p \end{bmatrix} \\ &= \begin{bmatrix} TA & TB \\ C & D \end{bmatrix} \begin{bmatrix} T & 0 \\ 0 & I \end{bmatrix}^{-1} \begin{bmatrix} T & 0 \\ 0 & I \end{bmatrix} \begin{bmatrix} \mathbf{x}_1 & \mathbf{x}_2 & \dots & \mathbf{x}_p \\ \mathbf{u}_1 & \mathbf{u}_2 & \dots & \mathbf{u}_p \end{bmatrix} \\ &= \begin{bmatrix} TAT^{-1} & TB \\ CT^{-1} & D \end{bmatrix} \begin{bmatrix} T\mathbf{x}_1 & T\mathbf{x}_2 & \dots & T\mathbf{x}_p \\ \mathbf{u}_1 & \mathbf{u}_2 & \dots & \mathbf{u}_p \end{bmatrix} \end{aligned} \tag{5.11}$$

The notation

Important step in notation is to introduce block Hankel matrices of output (5.12) and input data (5.13). The aforementioned matrices are made from 2i block rows. Let's remind that small bold letters present column vectors ($r \times 1$). One row block refers to a row vector of input/output data, spreading with subscript index in time. Finally, observe that the Hankel matrix expands with equal anti-diagonal elements (main characteristic).

2i row block notation is introduced, as Hankel matrix is vertically unstacked (split) into two Hankel matrices of 1i block rows. Notation of subscript "P" refers to "Past" and "F" to "Future", although "Past" and "Future" matrices overlap on the majority of the time domain (row length j, $overlap = j - i$, with $j >> i$). Picking the proper values for i and j would be introduced in the analysis section.
The subscript in square brackets refers to domain of row/columns: "[1,i]=[from 1,to i]".

$$Y_{2i|j} = \begin{bmatrix} \mathbf{y}_1 & \mathbf{y}_2 & \cdots & \mathbf{y}_j \\ \mathbf{y}_2 & \mathbf{y}_3 & \cdots & \mathbf{y}_{j+1} \\ \vdots & \vdots & \iddots & \vdots \\ \mathbf{y}_i & \mathbf{y}_{i+1} & \cdots & \mathbf{y}_{j+i-1} \\ \updownarrow & \updownarrow & \updownarrow & \updownarrow \\ \mathbf{y}_{i+1} & \mathbf{y}_{i+2} & \cdots & \mathbf{y}_{j+i} \\ \vdots & \vdots & \iddots & \vdots \\ \mathbf{y}_{2i} & \mathbf{y}_{2i+1} & \cdots & \mathbf{y}_{2i+j-1} \end{bmatrix} = \begin{bmatrix} Y_{[1,i]|j} \\ Y_{[i+1,2i]|j} \end{bmatrix} = \begin{bmatrix} Y_P \\ Y_F \end{bmatrix} \tag{5.12}$$

$$U_{2i|j} = \begin{bmatrix} \mathbf{u}_1 & \mathbf{u}_2 & \cdots & \mathbf{u}_j \\ \mathbf{u}_2 & \mathbf{u}_3 & \cdots & \mathbf{u}_{j+1} \\ \vdots & \vdots & \iddots & \vdots \\ \mathbf{u}_i & \mathbf{u}_{i+1} & \cdots & \mathbf{u}_{j+i-1} \\ \updownarrow & \updownarrow & \updownarrow & \updownarrow \\ \mathbf{u}_{i+1} & \mathbf{u}_{i+2} & \cdots & \mathbf{u}_{j+i} \\ \vdots & \vdots & \iddots & \vdots \\ \mathbf{u}_{2i} & \mathbf{u}_{2i+1} & \cdots & \mathbf{u}_{2i+j-1} \end{bmatrix} = \begin{bmatrix} U_{[1,i]|j} \\ U_{[i+1,2i]|j} \end{bmatrix} = \begin{bmatrix} U_P \\ U_F \end{bmatrix} \tag{5.13}$$

In the equation (5.14) state sequence matrix X_i is introduced:

$$X_i = \begin{bmatrix} \mathbf{x}_i & \cdots & \mathbf{x}_{j+i-1} \end{bmatrix} \tag{5.14}$$

$$X_1 = \begin{bmatrix} \mathbf{x}_1 & \cdots & \mathbf{x}_j \end{bmatrix} \tag{5.15}$$

Referring to the equation (5.8), time wise analogy is introduced in equations (5.16) and (5.17), for the purpose of introduction of the reversed extended controllability matrix $\Delta_{[1,2i]}$ (5.18).

$$\mathbf{x}_2 = A\mathbf{x}_1 + B\mathbf{u}_1 \tag{5.16}$$

$$\mathbf{x}_3 = A\mathbf{x}_2 + B\mathbf{u}_2 = A^2\mathbf{x}_1 + AB\mathbf{u}_1 + B\mathbf{u}_2 \tag{5.17}$$

$$\Delta_{[1,2i]} = \begin{bmatrix} A^{2i-1}B & A^{2i-2}B & \cdots & B \end{bmatrix} \qquad \in \mathbb{R}^{n \times 2im} \tag{5.18}$$

Referring to the equation (5.9), time wise analogy is introduced in equations from (5.19) to (5.22), for the purpose of introduction of the extended ($i > n$) observability matrix $\Gamma_{[1,2i]}$ (5.23), and the lower block triangular Toeplitz matrix $H_{[1,2i]}$ (5.24).

$$\mathbf{y}_1 = C\mathbf{x}_1 + D\mathbf{u}_1 \tag{5.19}$$

$$\mathbf{y}_2 = C\mathbf{x}_2 + D\mathbf{u}_2 = CA\mathbf{x}_1 + CB\mathbf{u}_1 + D\mathbf{u}_2 \tag{5.20}$$

$$\mathbf{y}_3 = CA\mathbf{x}_2 + CB\mathbf{u}_2 + D\mathbf{u}_3 = CA^2\mathbf{x}_1 + CAB\mathbf{u}_1 + CB\mathbf{u}_2 + D\mathbf{u}_3 \tag{5.21}$$

$$Y_{3|1} = \begin{bmatrix} \mathbf{y}_1 \\ \mathbf{y}_2 \\ \mathbf{y}_3 \end{bmatrix} = \begin{bmatrix} C\mathbf{x}_1 \\ CA\mathbf{x}_1 \\ CA^2\mathbf{x}_1 \end{bmatrix} + \begin{bmatrix} D\mathbf{u}_1 \\ CB\mathbf{u}_1 + D\mathbf{u}_2 \\ CAB\mathbf{u}_1 + CB\mathbf{u}_2 + D\mathbf{u}_3 \end{bmatrix} \tag{5.22}$$

$$\Gamma_{[1,2i]} = \begin{bmatrix} C \\ CA \\ \vdots \\ CA^{2i-1} \end{bmatrix} \qquad \in \mathbb{R}^{2il \times n} \tag{5.23}$$

$$H_{[1,2i]} = \begin{bmatrix} D & 0 & 0 & 0 & \cdots & 0 \\ CB & D & 0 & 0 & \cdots & 0 \\ CAB & CB & D & 0 & \cdots & 0 \\ CA^2B & CAB & CB & D & \cdots & 0 \\ \vdots & \ddots & \ddots & \ddots & \ddots & 0 \\ CA^{2i-2}B & CA^{2i-3}B & CA^{2i-4}B & \cdots & CA^{2i-2i}B & D \end{bmatrix} \qquad \in \mathbb{R}^{2il \times 2im} \tag{5.24}$$

From this point, with given notation, the equation representing the main problem for solving (5.36) can be formed. Starting with the equation (5.25), output block Hankel matrix can be explicitly written in the given terms. Same analogy follows equation (5.26) and equation (5.27).

$$Y_{2i|j} = \Gamma_{[1,2i]}X_1 + H_{[1,2i]}U_{2i|j} \tag{5.25}$$

$$Y_P = \Gamma_{[1,i]}X_1 + H_{[1,i]}U_P \tag{5.26}$$

$$Y_F = \Gamma_{[i+1,2i]}X_1 + H_{[i+1,2i]}U_F = \Gamma_{[1,i]}X_{i+1} + H_{[i+1,2i]}U_F \tag{5.27}$$

Referring to the equation (5.26), state space sequence X_1 is presented (5.28). Symbol "†" refers to the Moore−Penrose pseudo inverse operation.

$$X_1 = \Gamma^{\dagger}_{[1,i]}Y_P - \Gamma^{\dagger}_{[1,i]}H_{[1,i]}U_P \tag{5.28}$$

Based on the equation (5.8), in state sequence form, equation (5.29) is formed. Generally, notation becomes more complex, but it follows simple derivations. With writing down simple example of smaller size (i=1-2,...,j=2-3), notation becomes perfectly clear.

$$X_{2i+1} = A^{2i}X_1 + \Delta_{[1,2i]}U_{2i|j} \tag{5.29}$$

$$X_{i+1} = A^{i}X_1 + \Delta_{[1,i]}U_P \tag{5.30}$$

$$\rightarrow (5.28), (5.30) \rightarrow \qquad X_{i+1} = (\Delta_{[1,i]} - A^i\Gamma^{\dagger}_{[1,i]}H_{[1,i]})U_P + (A^i\Gamma^{\dagger}_{[1,i]})Y_P \tag{5.31}$$

With the vertical stack of the past input and output Hankel matrices, the matrix W_P is formed (5.32).

$$W_P = \begin{bmatrix} U_P \\ Y_P \end{bmatrix} \tag{5.32}$$

Observing equation (5.31) the analogy for forming matrix $L_{[1,i]}$ can be seen, and further used for the equation (5.34).

$$L_{[1,i]} = \begin{bmatrix} \Delta_{[1,i]} - A^i\Gamma^{\dagger}_{[1,i]}H_{[1,i]} & A^i\Gamma^{\dagger}_{[1,i]} \end{bmatrix} \tag{5.33}$$

For the simplicity reasons, state sequence X_{i+1} is written as (5.34):

$$X_{i+1} = L_{[1,i]} W_P \tag{5.34}$$

Finally, the equation (5.35) presents main problem statement:

$$Y_F = \Gamma_{[1,i]} X_{i+1} + H_{[i+1,2i]} U_F \tag{5.35}$$

Important terminology and notation are introduced, so the main step is to be performed. Referring back to equation (5.9), we can conclude that: **"If we are able to do something to the output $\mathbf{y}_k$ to eliminate the input part $\mathbf{u}_k$, we would obtain the system that is proportional to the hidden state $\mathbf{x}_k$"**.

$$\mathbf{y}_k = C\mathbf{x}_k + D\mathbf{u}_k \tag{5.9 revisited}$$

With the projection (see 4.1) of equation (5.36) to the space that is perpendicular to space of the future input Hankel matrix U_F, the aforementioned idea is achieved. It can be concluded that determined solution is lying down in the subspace that is proportional to the hidden states $\mathbf{x}_k$.

$$Y_F = \Gamma_{[1,i]} L_{[1,i]} W_P + H_{[i+1,2i]} U_F \quad \Big\{ \times / U_F^{\perp} \tag{5.36}$$

$$Y_F / U_F^{\perp} = \Gamma_{[1,i]} L_{[1,i]} W_P / U_F^{\perp} + \cancelto{0}{H_{[i+1,2i]} U_F / U_F^{\perp}} \Big\{ \times W_P \tag{5.37}$$

$$\Gamma_{[1,i]} L_{[1,i]} W_P = Y_F / U_F^{\perp} (W_P / U_F^{\perp})^{\dagger} W_P \tag{5.38}$$

$$\rightarrow (5.34) \rightarrow \qquad \Gamma_{[1,i]} X_{i+1} = Y_F / U_F^{\perp} (W_P / U_F^{\perp})^{\dagger} W_P \tag{5.39}$$

Projection matrix O_i is presented in the equation (5.40):

$$O_i = Y_F / U_F^{\perp} (W_P / U_F^{\perp})^{\dagger} W_P \tag{5.40}$$

The final step is to perform singular value decomposition (sometimes referred as a "trick") of the projection matrix O_i, equation (5.42). The solution obtains observability matrix $\Gamma_{[1,i]}$ (5.43), and the state sequence matrix X_{i+1} (5.44).

$$\Gamma_{[1,i]} X_{i+1} = O_i \tag{5.41}$$

$$U \Sigma V^T = Y_F / U_F^{\perp} (W_P / U_F^{\perp})^{\dagger} W_P \tag{5.42}$$

$$\Gamma_{[1,i]} = U \Sigma^{1/2} \tag{5.43}$$

$$X_{i+1} = \Sigma^{1/2} V^T \tag{5.44}$$

The weighting algorithms for the singular value decomposition are not introduced as deterministic subspace identification is introduced to form the basic understanding and notation for the further stochastic subspace identification.

5.2.2 Data driven stochastic subspace identification

In this section, data-driven stochastic subspace identification is presented. Given derivations are based on [12]. The notation is based on provided notation used for describing deterministic subspace identification.

Intentions of this sections are to form the foundation for the understanding of identification methods used in the further analysis. Keeping the focus on data analysis and implementation, the theory will be presented in the path that leads to the forward innovation model of data-driven stochastic subspace identification, with the unweighed principal component algorithm.

Let's remind that initial difference between deterministic and stochastic subspace identification starts with input (the excitation) being unknown in the stochastic model (input sequence in state space model).

▼ **Concepts described in this subsection:**

- Forward model
- Forward innovation model
- Kalman filter states
- Unweighed principal component algorithm

Forward model

Problem statement:

Stochastic system presented in equation (5.45) and equation (5.46), holds assumption for the input related sequences $\boldsymbol{\omega}_k$ and $\boldsymbol{\upsilon}_k$ as zero mean white noise sequences. Covariance matrix, of the "input", is presented in the equation (5.47). The given system is assumed to be stochastic stationary process (5.48) with the state covariance matrix Σ_s being independent of time k (5.49).

$$\mathbf{x}_{k+1} = A\mathbf{x}_k + \boldsymbol{\omega}_k \tag{5.45}$$

$$\mathbf{y}_k = C\mathbf{x}_k + \boldsymbol{\upsilon}_k \tag{5.46}$$

$$\mathbf{E}\left[\begin{bmatrix}\boldsymbol{\omega}_k \\ \boldsymbol{\upsilon}_k\end{bmatrix}\begin{bmatrix}\boldsymbol{\omega}_k^T & \boldsymbol{\upsilon}_k^T\end{bmatrix}\right] = \begin{bmatrix}Q & S \\ S^T & R\end{bmatrix}\delta_{pq} \tag{5.47}$$

$$\mathbf{E}\left[\mathbf{x}_k\right] = 0 \tag{5.48}$$

$$\mathbf{E}\left[\mathbf{x}_k\mathbf{x}_k^T\right] \overset{\text{def}}{=} \Sigma_s \tag{5.49}$$

As $\boldsymbol{\omega}_k$ and $\boldsymbol{\upsilon}_k$ are white noise vector sequences, independent of $\mathbf{x}_k$, equation (5.50) and equation (5.51) hold relation:

$$\mathbf{E}\left[\mathbf{x}_k\boldsymbol{\upsilon}_k^T\right] = 0 \tag{5.50}$$

$$\mathbf{E}\left[\mathbf{x}_k\boldsymbol{\omega}_k^T\right] = 0 \tag{5.51}$$

In the equation (5.52) Lyapunov relation for the state covariance matrix Σ_s is presented:

$$\begin{aligned}
\Sigma_s &= \mathbf{E}\left[\mathbf{x}_{k+1}\mathbf{x}_{k+1}^T\right] \\
\rightarrow (5.45) \rightarrow \quad &= \mathbf{E}\left[(A\mathbf{x}_k + \boldsymbol{\omega}_k)(A\mathbf{x}_k + \boldsymbol{\omega}_k)^T\right] \\
&= A\mathbf{E}\left[\mathbf{x}_k\mathbf{x}_k^T\right]A^T + \mathbf{E}\left[\boldsymbol{\omega}_k\boldsymbol{x}_k^T\right]A^T + A\mathbf{E}\left[\mathbf{x}_k\boldsymbol{\omega}_k^T\right] + \\
&+ \mathbf{E}\left[\boldsymbol{\omega}_k\boldsymbol{\omega}_k^T\right] \\
\rightarrow (5.49), (5.51), (5.47) \rightarrow \quad &= A\Sigma_s A^T + Q
\end{aligned} \tag{5.52}$$

Output covariance matrix Λ_i is defined in the equation (5.53) and Λ_0 in the equation (5.54):

$$\Lambda_i = \mathbf{E}\left[\mathbf{y}_{k+1}\mathbf{y}_k^T\right] \tag{5.53}$$

$$\begin{aligned}
\Lambda_0 &= \mathbf{E}\left[\mathbf{y}_k\mathbf{y}_k^T\right] \\
\rightarrow (5.46) \rightarrow \quad &= \mathbf{E}\left[(C\mathbf{x}_k + \boldsymbol{\upsilon}_k)(C\mathbf{x}_k + \boldsymbol{\upsilon}_k)^T\right] \\
&= C\mathbf{E}\left[\mathbf{x}_k\mathbf{x}_k^T\right]C^T + \cancelto{0}{\mathbf{E}\left[\boldsymbol{\upsilon}_k\mathbf{x}_k^T\right]C^T} + \cancelto{0}{C\mathbf{E}\left[\mathbf{x}_k\boldsymbol{\upsilon}_k^T\right]} + \\
&+ \mathbf{E}\left[\boldsymbol{\upsilon}_k\boldsymbol{\upsilon}_k^T\right] \\
\rightarrow (5.49), (5.50), (5.47) \rightarrow \quad &= C\Sigma_s C^T + S
\end{aligned} \tag{5.54}$$

$$\begin{aligned}
G &\overset{\text{def}}{=} \mathbf{E}\left[\mathbf{x}_{k+1}\mathbf{y}_k^T\right] \\
\rightarrow (5.45), (5.46) \rightarrow \quad &= \mathbf{E}\left[(A\mathbf{x}_k + \boldsymbol{\omega}_k)(C\mathbf{x}_k + \boldsymbol{\upsilon}_k)^T\right] \\
&= A\mathbf{E}\left[\mathbf{x}_k\mathbf{x}_k^T\right]C^T + \cancelto{0}{\mathbf{E}\left[\boldsymbol{\omega}_k\mathbf{x}_k^T\right]C^T} + \cancelto{0}{A\mathbf{E}\left[\mathbf{x}_k\boldsymbol{\upsilon}_k^T\right]} + \\
&+ \mathbf{E}\left[\boldsymbol{\omega}_k\boldsymbol{\upsilon}_k^T\right] \\
\rightarrow (5.49), (5.50), (5.51), (5.47) \rightarrow \quad &= A\Sigma_s C^T + S
\end{aligned} \tag{5.55}$$

In the equation (5.56) and equation (5.57) observation is made that output covariances can be considered as Markov parameters of the deterministic linear time-invariant systems A, G, C,Λ_0:

$$\Lambda_i = CA^{i-1}G \tag{5.56}$$

$$\Lambda_{-i} = G^T(A^{i-1})^T C^T \tag{5.57}$$

Forward innovation model

Problem statement:

The forward innovation model is obtained by applying a Kalman filter to the forward model, equation (5.45) and equation (5.46). In equation (5.58) and equation (5.59) the problem statement of the forward innovation model is presented.

$$\mathbf{x}_{k+1}^f = A\mathbf{x}_k^f + K^f\mathbf{e}_k^f \tag{5.58}$$

$$\mathbf{y}_k = C\mathbf{x}_k^f + \mathbf{e}_k^f \tag{5.59}$$

$$\mathbf{E}\left[\mathbf{x}_k^f\mathbf{x}_k^{f\,T}\right] \overset{\text{def}}{=} \Sigma_s^f \tag{5.60}$$

$$
\begin{aligned}
\rightarrow (5.59) \rightarrow \quad \mathbf{E}\left[\mathbf{e}_k^f \mathbf{e}_k^{f\,T}\right] &= \mathbf{E}\left[(\mathbf{y}_k - C\mathbf{x}_k^f)(\mathbf{y}_k - C\mathbf{x}_k^f)^T\right] \\
&= \mathbf{E}\left[\mathbf{y}_k \mathbf{y}_\mathbf{k}^T\right] - 2\mathbf{E}\left[\mathbf{y}_k \mathbf{x}_\mathbf{k}^{f\,T}\right] C^T + C\mathbf{E}\left[\mathbf{x}_k^f \mathbf{x}_k^{f\,T}\right] C^T \\
\rightarrow (5.54), (5.60) \rightarrow \quad &= \Lambda_0 - C\Sigma_s^f C^T
\end{aligned} \tag{5.61}
$$

In the equation (5.62) the forward Kalman gain is presented:

$$
K^f = (G - A\Sigma_s^f C^T)(\Lambda_0 - C\Sigma_s^f C^T)^{-1} \tag{5.62}
$$

The forward innovation state covariance matrix Σ_s^f can be obtained as the stabilizing solution of the forward Riccati equation (5.63). Detailed solution of the aforementioned equation is based on the Schur decomposition, that can be seen in [6].

$$
\Sigma_s^f = (A\Sigma_s^f A^T) + (G - A\Sigma_s^f C^T)(\Lambda_0 - C\Sigma_s^f C^T)^{-1}(G - A\Sigma_s^f C^T)^T \tag{5.63}
$$

System related matrices

Before proceeding to the realization, notation of the system related matrices needs to be introduced. The reversed extended stochastic controllability matrix Δ_i^f is presented in the equation (5.64):

$$
\Delta_i^f \stackrel{\text{def}}{=} \begin{bmatrix} A^{i-1}G & A^{i-2}G & \cdots & AG & G \end{bmatrix} \qquad \in \mathbb{R}^{n \times li} \tag{5.64}
$$

From output covariance matrices the block Toeplitz matrices C_i and L_i are constructed, follow (5.65 and 5.66):

$$
C_i \stackrel{\text{def}}{=} \begin{bmatrix} \Lambda_i & \Lambda_{i-1} & \cdots & \Lambda_2 & \Lambda_1 \\ \Lambda_{i+1} & \Lambda_i & \cdots & \Lambda_3 & \Lambda_2 \\ \Lambda_{i+2} & \Lambda_{i+1} & \cdots & \Lambda_4 & \Lambda_3 \\ \cdots & \cdots & \cdots & \cdots & \cdots \\ \Lambda_{2i-1} & \Lambda_{2i-2} & \cdots & \Lambda_{i+1} & \Lambda_i \end{bmatrix} \qquad \in \mathbb{R}^{li \times li} \tag{5.65}
$$

$$
L_i \stackrel{\text{def}}{=} \begin{bmatrix} \Lambda_0 & \Lambda_{-1} & \cdots & \Lambda_{2-i} & \Lambda_{1-i} \\ \Lambda_1 & \Lambda_0 & \cdots & \Lambda_{3-i} & \Lambda_{2-i} \\ \Lambda_2 & \Lambda_1 & \cdots & \Lambda_{4-i} & \Lambda_{3-i} \\ \cdots & \cdots & \cdots & \cdots & \cdots \\ \Lambda_{i-1} & \Lambda_{i-2} & \cdots & \Lambda_1 & \Lambda_0 \end{bmatrix} \qquad \in \mathbb{R}^{li \times li} \tag{5.66}
$$

Output covariance matrices are estimated as (see Subsection 4.1 for definition of $\mathbf{E}_j$ and $\Phi_{[A,B]}$):

$$
\begin{aligned}
\Lambda_i &= \mathbf{E}_j \left[\sum_{k=1}^{j} \mathbf{y}_{k+1} \mathbf{y}_k^T\right] \\
&= \Phi_{[Y_{i|i}, Y_{1|1}]}
\end{aligned} \tag{5.67}
$$

The covariance sequence Λ_k should be a positive real sequence. With several equivalent statement tests, the positive realness of sequence is checked. The statements and tests can be seen in [4].

From equation (5.67) it follows (additionally see [11]):

$$
C_i = \Phi_{[Y_f, Y_p]} \tag{5.68}
$$

$$
\begin{aligned}
L_i &= \Phi_{[Y_p, Y_p]} \\
&= \Phi_{[Y_f, Y_f]}
\end{aligned} \tag{5.69}
$$

Kalman filter states

In this subsection, the "forward Kalman filter state estimate" is introduced. The intention is to indicate how to recover the state sequence directly from the output data $\mathbf{y}_k$. State estimates are represented with addition of hat symbol, $\hat{\mathbf{x}}_k$.

Forward Kalman filter:

▼ **Given:**

- The initial state estimate: $\hat{\mathbf{x}}_0 = 0$
- The initial covariance of the state estimate: $\Sigma_0^f = \mathbf{E}[\hat{\mathbf{x}}_0\hat{\mathbf{x}}_0] = 0$
- The output measurements: $\mathbf{y}_0, \mathbf{y}_1, ..., \mathbf{y}_{k-1}$

The Kalman filter state estimate $\hat{\mathbf{x}}_k$ is defined by following recursive formulas (preceded by the forward innovation model):

$$\hat{\mathbf{x}}_\mathbf{k} = A\hat{\mathbf{x}}_{k-1} + K_{k-1}(\mathbf{y}_{k-1} - C\hat{\mathbf{x}}_{k-1}) \tag{5.70}$$

$$K_{k-1} = (G - A\Sigma_{k-1}^f C^T)(\Lambda_0 - C\Sigma_{k-1}^f C^T)^{-1} \tag{5.71}$$

$$\Sigma_k^f = (A\Sigma_{k-1}^f A^T) + (G - A\Sigma_{k-1}^f C^T)(\Lambda_0 - C\Sigma_{k-1}^f C^T)^{-1}(G - A\Sigma_{k-1}^f C^T)^T \tag{5.72}$$

From defined system related matrices (5.64 and 5.65) and equations 5.70, 5.71 and 5.72, state estimate can be explicitly written as (5.73):

$$\hat{\mathbf{x}}_k = \Delta_k^f L_k^{-1} \begin{bmatrix} \mathbf{y}_0 \\ \mathbf{y}_1 \\ \vdots \\ \mathbf{y}_{k-1} \end{bmatrix} \tag{5.73}$$

The explicit solution to the covariance matrix Σ_k^f is equal to (5.74):

$$\Sigma_k^f = \Delta_k^f L_k^{-1} (\Delta_k^f)^T \tag{5.74}$$

The proof can be seen in Appendix A.2 of [12]. Appendix A.3 of [12] contains notes regarding equations (5.70)-(5.72).

From equation (5.73), the forward Kalman filter state sequence is formed (5.75):

$$\begin{aligned} \hat{X}_i &= (\hat{\mathbf{x}}_i \;\; \hat{\mathbf{x}}_{i+1} \;\; ... \;\; \hat{\mathbf{x}}_{i+j-1}) \\ &= \Delta_k^f L_k^{-1} Y_p \end{aligned} \tag{5.75}$$

The state sequence $\hat{X}_i$ is generated by a bank of Kalman filters applied in parallel to each column of block Hankel matrix Y_p (runs in the vertical direction over columns).

With multiplication of equation (5.75) with extended observability matrix Γ_i, equation (5.76) is obtained.

$$\Gamma_i \hat{X}_i = \Gamma_i \Delta_k^f L_k^{-1} Y_p \tag{5.76}$$

Important observations:

$$\left.\begin{aligned}
&\rightarrow (5.23) \rightarrow \quad \Gamma_i = \begin{bmatrix} C \\ CA \\ \vdots \\ CA^{i-1} \end{bmatrix} \\
&\rightarrow (5.64) \rightarrow \quad \Delta_i^f \overset{\text{def}}{=} \begin{bmatrix} A^{i-1}G & A^{i-2}G & \cdots & AG & G \end{bmatrix} \\
&\rightarrow (5.56) \rightarrow \quad \Lambda_i = CA^{i-1}G \\
&\rightarrow 5.65 \rightarrow \quad C_i \overset{\text{def}}{=} \begin{bmatrix} \Lambda_i & \Lambda_{i-1} & \cdots & \Lambda_2 & \Lambda_1 \\ \Lambda_{i+1} & \Lambda_i & \cdots & \Lambda_3 & \Lambda_2 \\ \Lambda_{i+2} & \Lambda_{i+1} & \cdots & \Lambda_4 & \Lambda_3 \\ \cdots & \cdots & \cdots & \cdots & \cdots \\ \Lambda_{2i-1} & \Lambda_{2i-2} & \cdots & \Lambda_{i+1} & \Lambda_i \end{bmatrix} \\
&\rightarrow 5.68 \rightarrow \quad C_i = \Phi_{[Y_f, Y_p]}
\end{aligned}\right\} \quad C_i = \Gamma_i \Delta_k^f \tag{5.77}$$

From the important observations above, the equation (5.78) is formed:

$$\begin{aligned}
&\rightarrow (5.76), (5.77) \rightarrow \qquad \Gamma_i \hat{X}_i = C_i L_k^{-1} Y_p \\
&\rightarrow (5.68), (5.69) \rightarrow \qquad\quad = \Phi_{[Y_f, Y_p]} \Phi_{[Y_p, Y_p]}^{-1} Y_p
\end{aligned} \tag{5.78}$$

Projection matrix O_i is presented in the equation (5.79):

$$O_i = \Gamma_i \hat{X}_i \tag{5.79}$$

Using formulations from the section "Geometrical projections in statistical framework" (see section 4.1), formulation for the problem statement is formed (5.81).

$$A/B = \Phi_{[Y_A, Y_B]} \Phi_{[Y_B, Y_B]}^{\dagger} B = AB^T [BB^T]^{\dagger} B \tag{5.80}$$

Projection matrix of the data driven stochastic subspace identification:

$$O_i = Y_F / Y_P \tag{5.81}$$

The final step is to perform singular value decomposition of the projection matrix O_i, equation (5.81).

In the literature, multiple weighting algorithms for the singular value decomposition can be found. As the aim of further analysis is to recover the system matrices, not state sequences, the unweighted principal component algorithm is used [12]. The unweighed principal component algorithm uses identity matrix for "weighting".

$$\begin{aligned}
W_1 O_i W_2 &= \begin{bmatrix} U_1 & U_2 \end{bmatrix} \begin{bmatrix} \Sigma_1 & 0 \\ 0 & 0 \end{bmatrix} \begin{bmatrix} V_1^T \\ V_2^T \end{bmatrix} \\
&= U_1 \Sigma_1 V_1^T
\end{aligned} \tag{5.82}$$

$$\begin{aligned}
\rightarrow (W_1 = I_{li},\ W_2 = I_j), (5.82) \rightarrow \qquad U_1 \Sigma_1 V_1^T &= Y_F / Y_P \\
&= Y_F Y_P^T [Y_P Y_P^T]^{\dagger} Y_P
\end{aligned} \tag{5.83}$$

The solution obtains the observability matrix Γ_i (5.81) and the state sequence matrix X_{i+1} (5.82).

$$\Gamma_i = U_1 \Sigma_1^{1/2} \tag{5.84}$$

$$X_i = \Sigma_1^{1/2} V_1^T \tag{5.85}$$

In the next section dynamical system will be introduced and implementation of the stochastic subspace identification, for solving the given system will be provided.

5.2.3 Implementation of the data driven stochastic subspace identification

Dynamical system

The implementation of the stochastic subspace identification, regarding the further analysis of this thesis, is aimed towards determination of the eigenfrequencies and the eigenvectors for the presented dynamical system (5.86). The dynamical system is multi-degree of freedom structural system, with matrices M, C, K representing mass, damping, and stiffness. The force vector is represented with $\mathbf{u}(t)$.

$$M\ddot{\mathbf{y}}(t) + D\dot{\mathbf{y}}(t) + K\mathbf{y}(t) = \mathbf{u}(t) \tag{5.86}$$

The first step is to present given dynamical system in the state space formulation. Observe equations (5.87) and (5.88).

$$\mathbf{x}(t) = \begin{bmatrix} \mathbf{y}(t) \\ \dot{\mathbf{y}}(t) \end{bmatrix} \qquad \dot{\mathbf{x}}(t) = \begin{bmatrix} \dot{\mathbf{y}}(t) \\ \ddot{\mathbf{y}}(t) \end{bmatrix} \tag{5.87}$$

$$\begin{aligned} \dot{\mathbf{x}}(t) &= A_c\mathbf{x}(t) + B\mathbf{u}(t) \\ \mathbf{y}(t) &= C\mathbf{x}(t) + D\mathbf{u}(t) \end{aligned} \tag{5.88}$$

The state space system matrices are presented in continuous time and can be observed in (5.89).

$$A_c = \begin{bmatrix} 0 & I \\ -M^{-1}K & -M^{-1}D \end{bmatrix} \qquad B = \begin{bmatrix} 0 \\ M^{-1} \end{bmatrix} \qquad C = \begin{bmatrix} 1 & 0 \end{bmatrix} \qquad D = \begin{bmatrix} 0 \end{bmatrix} \tag{5.89}$$

General solution for the state $\mathbf{x}(t)$ is presented in equation (5.90), see [5]. The exponent operation is element-wise.

$$\mathbf{x}(t) = \exp(A_c t)\mathbf{x}(0) + \int_0^t \exp\left(A_c(t-\tau)\right) B\mathbf{u}(\tau)d\tau \tag{5.90}$$

To go to the next step, time discretization needs to be performed. Time discretization is introduced with the time sample Δt and position in time k, with $t = k\Delta t$, and $k = 0...N$.

From the literature confusion can be made related to the continuation to the subspace identification problem statement, regarding equation (5.88) and equation (5.90). With introduction of the discrete time matrix A_d (5.91), formulation of the problem statement can be formed, observe equation (5.92).

$$A_d^k = \exp(A_c k\Delta t) \qquad A_d = \exp(A_c \Delta t) \tag{5.91}$$

$$\mathbf{x}_1 = A_d\mathbf{x}_0 + \int_0^{\Delta t} \exp\left(A_c(t-\tau)\right) B\mathbf{u}(\tau)d\tau \tag{5.92}$$

Assuming zero order hold for the discretized input $\mathbf{u}(t)$, on the time segment Δt, input $\mathbf{u}_k$ is constant. With the given assumption equation (5.92) becomes equation (5.93).

$$\mathbf{x}_1 = A_d\mathbf{x}_0 + \underbrace{\left(\int_0^{\Delta t} \exp\left(A_c(t-\tau)\right)(\tau)d\tau\right) B\mathbf{u}_0}_{\text{white noise related in SSI}} \tag{5.93}$$

The integral part of equation (5.93) will not be further discussed, as the intention is related towards stochastic subspace identification where the input is assumed to be unknown.

With the forward innovation model (5.58 revisited), the Kalman filter state estimate (5.70 revisited), and previous derivations (5.90) to (5.93), it can be concluded that Kalman state estimate $\hat{\mathbf{x}}_{k-1}$ presents initial conditions for the Kalman state estimate $\hat{\mathbf{x}}_\mathbf{k}$. In other words, the system that will be identified uses current state estimate and noise excitation to estimate next time step state.

Although the Kalman states are sometimes referred as "mysterious", see [2], some physical sense was attempted to be brought on how system matrices operate in the Kalman filter state estimate of the forward innovation model.

$$\mathbf{x}_{k+1}^f = A\mathbf{x}_k^f + K^f\mathbf{e}_k^f \tag{5.58 revisited}$$

$$\hat{\mathbf{x}}_\mathbf{k} = A\hat{\mathbf{x}}_{k-1} + K_{k-1}(\mathbf{y}_{k-1} - C\hat{\mathbf{x}}_{k-1}) \tag{5.70 revisited}$$

System properties

Referring back to the data driven stochastic subspace identification, observability matrix estimate, $\hat{\Gamma}_i$, for the structural dynamic system (5.86) is formed (5.23 modified).

$$\hat{\Gamma}_i = \begin{bmatrix} C \\ C\hat{A}_d \\ \vdots \\ C\hat{A}_d^{i-1} \end{bmatrix} \tag{5.23 modified}$$

Observability matrix estimate $\hat{\Gamma}_i$ is determined through singular value decomposition of the projection matrix. The unweighed principal component algorithm is used, as the system properties are aimed to be identified (not states). Let's remind that Y_P and Y_F represent past and future Hankel matrices of the output measurements. Determination of the appropriate block size and length of the given Hankel matrices will be further discussed in the analysis example.

$$O_i = \hat{\Gamma}_i\hat{X}_i \tag{5.79 revisited}$$

$$\begin{aligned} O_i &= Y_F/Y_P \\ &= Y_F Y_P^T[Y_P Y_P^T]^\dagger Y_P \end{aligned} \tag{5.81 revisited}$$

$$\text{SVD} \rightarrow U_1\Sigma_1 V_1^T$$

$$\hat{\Gamma}_i = U_1\Sigma_1^{1/2} \tag{5.84 revisited}$$

$$\hat{X}_i = \Sigma_1^{1/2}V_1^T \tag{5.85 revisited}$$

System matrix estimate $\hat{A}_d$ and $\hat{C}$ are obtained from the observability matrix estimate $\hat{\Gamma}_i$ (5.95). From the identified observability matrix estimate $\hat{\Gamma}_i$, one row block i is eliminated from the bottom and top, see (5.94).

$$\hat{\Gamma}_{[1:i-1]}\hat{A}_d = \hat{\Gamma}_{[2:i]} \;\rightarrow\; \begin{bmatrix} \hat{C} \\ \hat{C}\hat{A}_d \\ \vdots \\ \hat{C}\hat{A}_d^{i-2} \end{bmatrix} \hat{A}_d = \begin{bmatrix} \hat{C}\hat{A}_d \\ \hat{C}\hat{A}_d^{2} \\ \vdots \\ \hat{C}\hat{A}_d^{i-1} \end{bmatrix} \tag{5.94}$$

$$\hat{A}_d = \hat{\Gamma}^{\dagger}_{[1:i-1]}\hat{\Gamma}_{[2:i]} \qquad \hat{C} = \hat{\Gamma}_{[1:1]} \tag{5.95}$$

Finally, common structural vibration relations can be obtained. The eigenvalue decomposition of matrix $\hat{A}_d$ is performed (5.96).

$$\Psi\hat{A}_d = [\mu_i]\Psi \tag{5.96}$$

Continuous time poles λ_i (system eigenfrequencies) and discrete time poles μ_i are related by (5.97). Note that the time sample Δt (measurements time sample), has a role in the relation. The given relation is based on (5.91).

$$\mu_i = \exp(\lambda_i \Delta t) \tag{5.97}$$

The output measurements are related to the states through the system matrix estimate $\hat{C}$, see (5.88) and (5.89). With the given analogy and identified properties, vibration mode shapes are related to the identified eigenvectors through the system matrix estimate $\hat{C}$, see (5.102).

DETERMINED SYSTEM PROPERTIES

Continuous time poles: $$\lambda_i = \frac{\ln(\mu_i)}{\Delta t} \tag{5.98}$$

Systems circular eigenfrequencies: $$\omega_i = |\lambda_i| \quad \left[\frac{\text{rad}}{s}\right] \tag{5.99}$$

Systems eigenfrequencies: $$f_i = \frac{\omega_i}{2\pi} \quad [\text{Hz}] \tag{5.100}$$

Systems damping coeficients: $$\xi_i = -\frac{Re(\lambda_i)}{\omega_i} \tag{5.101}$$

Systems mode shapes: $$\Phi = \hat{C}\Psi \tag{5.102}$$

Analysis example

Through the analysis example, it will be shown how to implement presented theory with emphasis on the block Hankel matrix and the stabilization diagram.

In the expression (5.103) output block Hankel matrix, of the acceleration measurements is presented. Theoretically, number of block rows i should fit the order of the system, which cannot be satisfied as realistic system holds infinite order.

CHOOSING THE NUMBER OF BLOCK ROWS OF THE OUTPUT HANKEL MATRIX

As this analysis example is set to operate in the targeted frequency region, block rows i are chosen to fit an estimated number of modes in the given region. For the analysis result that will be presented, 4 block rows are chosen ($i = 4$). To be more precise data is filtered, and it could be interpreted as the system is filtered, and that the filtered system holds the finite order for the preserved frequency region.

$$\ddot{Y}_{2i|j}(t) = \begin{bmatrix} \ddot{\mathbf{y}}_1(t) & \ddot{\mathbf{y}}_2(t) & \cdots & \ddot{\mathbf{y}}_j(t) \\ \ddot{\mathbf{y}}_2(t) & \ddot{\mathbf{y}}_3(t) & \cdots & \ddot{\mathbf{y}}_{j+1}(t) \\ \vdots & \vdots & \ddots & \vdots \\ \ddot{\mathbf{y}}_i(t) & \ddot{\mathbf{y}}_{i+1}(t) & \cdots & \ddot{\mathbf{y}}_{j+i-1}(t) \\ \updownarrow & \updownarrow & \updownarrow & \updownarrow \\ \ddot{\mathbf{y}}_{i+1}(t) & \ddot{\mathbf{y}}_{i+2}(t) & \cdots & \ddot{\mathbf{y}}_{j+i}(t) \\ \vdots & \vdots & \ddots & \vdots \\ \ddot{\mathbf{y}}_{2i}(t) & \ddot{\mathbf{y}}_{2i+1}(t) & \cdots & \ddot{\mathbf{y}}_{2i+j-1}(t) \end{bmatrix} = \begin{bmatrix} \ddot{Y}_{[1,i]|j}(t) \\ \ddot{Y}_{[i+1,2i]|j}(t) \end{bmatrix} = \begin{bmatrix} \ddot{Y}_P(t) \\ \ddot{Y}_F(t) \end{bmatrix} \tag{5.103}$$

The next step is to obtain singular value decomposition of the projection matrix (5.104).

$$\text{SVD}\{O_i = Y_F/Y_P\} \rightarrow = U_1 \Sigma_1 V_1^T \tag{5.104}$$

As the aim of the analysis is to recover system properties (modes) only observability matrix estimate $\hat{\Gamma}_i$ is recovered (5.84 revisited).

$$\hat{\Gamma}_i = U_1 \Sigma_1^{1/2} \tag{5.84 revisited}$$

With the observability matrix estimate, $\hat{\Gamma}_i$, modes are recovered. The issue that occurs at the given step is that not all recovered modes are physical modes. What is also being obtained are mathematical modes that are the product of the numerical aspect of the analysis. The given numerical anomaly is solved with the stabilization diagram. Before describing the procedure of the used stabilization diagram, relations for obtaining system properties are revisited.

$$\hat{A}_d = \hat{\Gamma}^{\dagger}_{[1:i-1]} \hat{\Gamma}_{[2:i]} \qquad \hat{C} = \hat{\Gamma}_{[1:1]} \tag{5.95 revisited}$$

$$\Psi \hat{A}_d = [\mu_i] \Psi \tag{5.96 revisited}$$

Continuous time poles: $$\lambda_i = \frac{\ln(\mu_i)}{\Delta t} \tag{5.98 revisited}$$

Systems circular eigenfrequencies: $$\omega_i = |\lambda_i| \quad \left[\frac{\text{rad}}{s}\right] \tag{5.99 revisited}$$

Systems eigenfrequencies: $$f_i = \frac{\omega_i}{2\pi} \quad [\text{Hz}] \tag{5.100 revisited}$$

Systems damping coeficients: $$\xi_i = -\frac{Re(\lambda_i)}{\omega_i} \tag{5.101 revisited}$$

Systems mode shapes: $$\Phi = \hat{C}\Psi \tag{5.102 revisited}$$

From the previously revisited relations, it can be seen that system properties $\{f_i, \xi_i, \Phi\}$ are dependant on the observability matrix estimate $\hat{\Gamma}_i$, which is dependant on SVD values $U\Sigma^{1/2}$.

Finally, the stabilization diagram is formed by variation of the number of chosen SVD values, $U\Sigma^{1/2}$, for computing the observability matrix estimate $\hat{\Gamma}_i$. The initial size of $[U\Sigma^{1/2}]$ is the number of spatial outputs n in vector $\ddot{\mathbf{y}}_i(t)$, times the number of block rows i.

The concept of the stabilization diagram is presented in the figure 5.1. Between the two consecutive observability matrix estimates $\hat{\Gamma}_i$, system properties $\{f_i, \xi_i, \Phi\}$ are compared. The used comparison holds three criteria, MAC larger than 0.97, frequency difference smaller than 1%, and damping difference smaller than 5%. The given criterion is assumed to filter out mathematical modes (spurious modes). The identified modes, presented as stable poles, satisfy all three criteria.

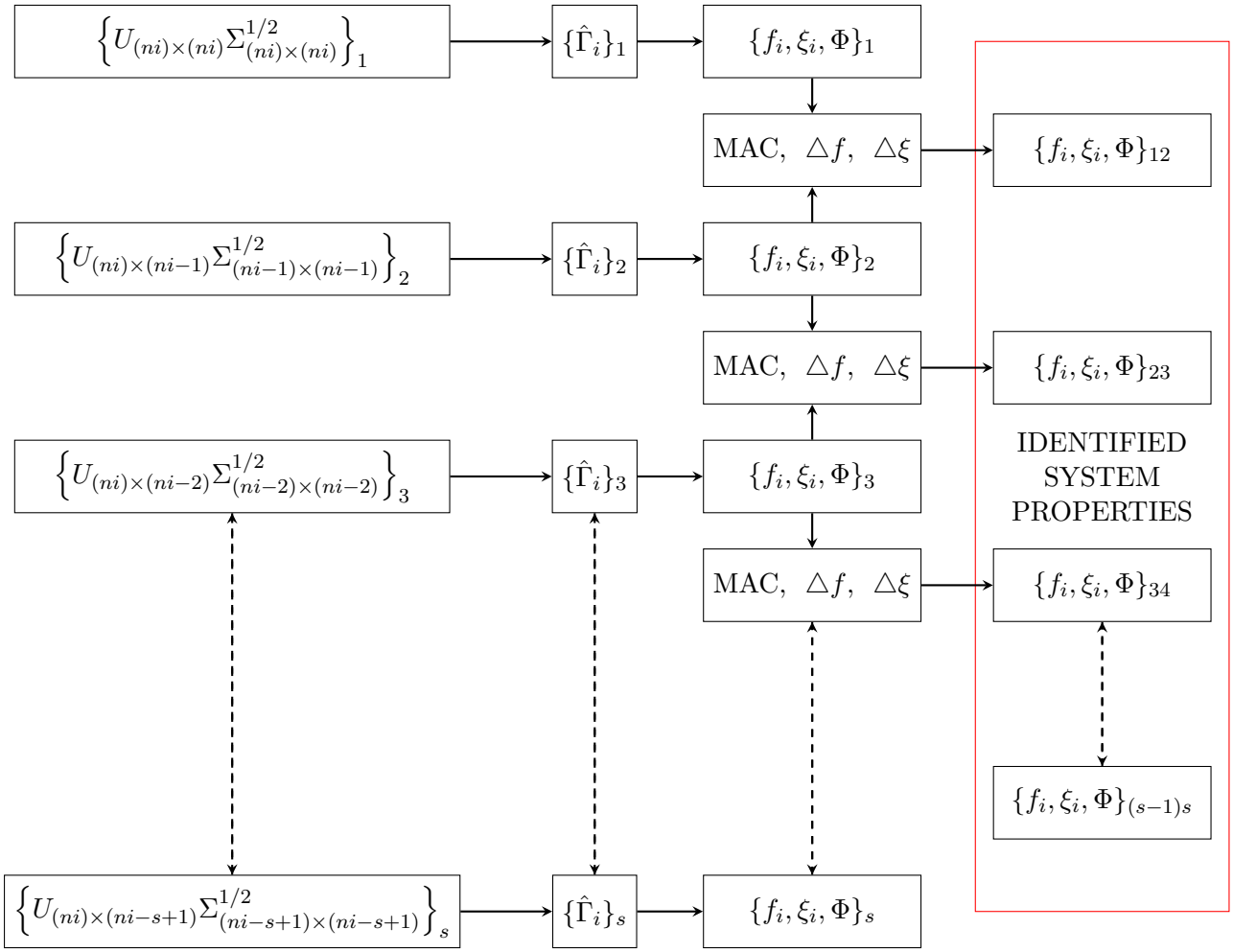


Figure 5.1: Stabilization diagram concept

The stabilization diagram is formed as a plot of the identified eigenfrequencies for chosen variation of sizes of $U\Sigma^{1/2}$. Regarding figure 5.1, results that will be provided consist of stabilisation diagram of size 6 ($s = 6$).

Finally, analysis example of the FDD singular value plot with SSI stabilization diagram poles (black dots) is presented in figure 5.2. The used data in the given example is preprocessed with

probabilistic filtering and a bandpass filter between 50Hz and 75Hz.

The given example is chosen as it shows high-quality stabilization diagram, as criteria that are used is high (compared with the results found in the literature).

Additionally, red crosses that are observed are not a part of the SSI stabilization diagram. The red crosses are related with searching for the modes of interest for solving the presented problem of this thesis (dominant movement of spatial position related to added mass).

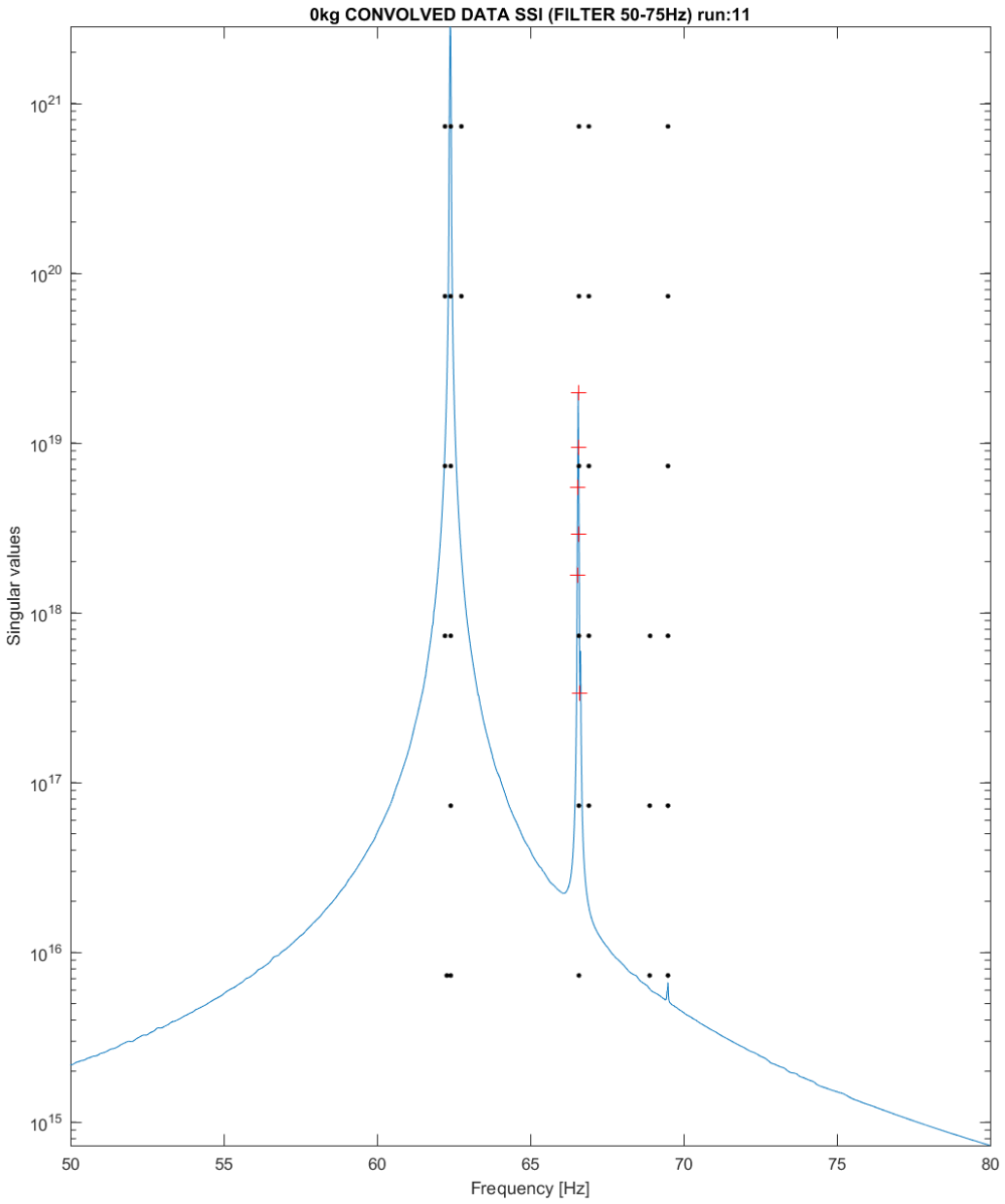


Figure 5.2: FDD singular value plot with SSI stabilization diagram

Chapter 6

Probabilistic filtering

The Zwartewaterbrug project (see Chapters 2. and 3.) brought big challenge: "Detect via vibrations 25kg on 800t bridge". For the aforementioned challenge, a method of probabilistic filtering is developed. Before going into details, some characteristics of the Zwartewaterbrug project are emphasized in order to present the reason and the logic behind probabilistic filtering method.

Measured vibrations of the bridge are generated by unknown traffic load. That unknown traffic load consist of moving vehicles of unknown speed and mass range from 200kg to 50t.

The goal of the Zwartewaterbrug project is to detect changes in vibration data of the bridge for 0kg added mass with respect to situations where added masses of 25kg, 50kg, 75kg, and 100kg are present.
As the bridge is excited by the unknown traffic load with much larger variations in vehicle mass than variation in test set-up added masses, which are to be detected, engineering smile was raised and the great challenge faced.

After multiple unsuccessful attempts to solve the problem, the important conclusion was made: ***"Between different vibration data samples, of same added mass set-up, what is physically different is the mass of vehicles that are exciting the bridge, and what is physically similar is the present test set-up added mass"***.

The aforementioned conclusion leads to the idea that filtering out the differences between signals with preservation of the similarities, would lead to the solution of the wide range of problems that are being faced. The concept of such filtering is based on the convolution properties, the central probabilistic theory, with the further considerations of the main assumptions of the FDD and the SSI.

▼ **Path to understanding probabilistic filtering consists of:**

- Convolution properties
- Structural system
- Random signal/White noise
- Non-LTI system behavior
- Multi-degree of freedom system
- Reducing order of the transfer function

6.1 Convolution properties

In this section algebraic properties of the convolution are emphasized. The notation used for convolution operation is introduced in equation (6.1).

$$\begin{aligned} f(t) * h(t) &\overset{\text{def}}{=} \int_{-\infty}^{\infty} f(\tau) g(t-\tau) d\tau \\ &= \int_{-\infty}^{\infty} f(t-\tau) g(\tau) d\tau \end{aligned} \tag{6.1}$$

Algebraic properties

Given algebraic properties present commutative algebra without identity [10].

Commutativity:

$$f(t) * h(t) = h(t) * f(t) \tag{6.2}$$

Associativity:

$$f(t) * (h(t) * g(t)) = (f(t) * h(t)) * g(t) \tag{6.3}$$

Observe now function $y(t)$ as output of the convolution of functions $h(t)$ and $f(t)$ (6.4):

$$y(t) = h(t) * f(t) \tag{6.4}$$

Convolution between multiple output functions is presented in (6.5), as it will play a major role in probabilistic filtering.

$$y_1(t) * y_2(t) * ... * y_n(t) = (h_1(t) * f_1(t)) * (h_2(t) * f_2(t)) * ... * (h_n(t) * f_n(t)) \tag{6.5}$$

Based on Commutativity and Associativity equation (6.6) is formed:

$$y_1(t) * y_2(t) * ... * y_n(t) = (h_1(t) * h_2(t) * ... * h_n(t)) * (f_1(t) * f_2(t) * ... f_n(t)) \tag{6.6}$$

Notation for the convolution of multiple functions is presented in equation (6.7):

$$\overset{n}{\underset{i=1}{\ast}} y_i(t) = \left(\overset{n}{\underset{i=1}{\ast}} h_i(t) \right) * \left(\overset{n}{\underset{i=1}{\ast}} f_i(t) \right) \tag{6.7}$$

Convolution theorem

The convolution theorem states (6.4), where $\mathcal{F}\{f(t)\}$ denotes Fourier transform of $f(t)$, and k is a constant dependant on normalization of Fourier transform.

Fourier transform:

$$\mathcal{F}\{f(t) * h(t)\} = k \; \mathcal{F}\{f(t)\} \; \mathcal{F}\{h(t)\} \tag{6.8}$$

6.2 Structural system

To introduce the relation between convolution properties and the structural system of interest, single degree of freedom linear structural dynamics system is introduced in equation (6.9) (it's assumed no further comments are needed on SDOF dynamic system).

$$m\ddot{y}(t) + c\dot{y}(t) + ky(t) = f(t) \tag{6.9}$$

Notation of the Fourier transforms is represented by the tilde on the top of the symbol, with dependence on frequency ω (6.10).

$$\mathcal{F}\{y(t)\} = \widetilde{y}(\omega) \tag{6.10}$$

Without derivations, the steady-state solution of the given system can be represented in the time domain as (6.11) and in the frequency domain as (6.12). For further derivations, it is important to emphasize that convolution in time domain equals multiplication in the frequency domain.

$$y(t) = h(t) * f(t) \tag{6.11}$$

$$\widetilde{y}(\omega) = \widetilde{h}(\omega)\widetilde{f}(\omega) \tag{6.12}$$

Functions $h(t)$ and $\widetilde{h}(\omega)$ are transfer functions (in time and frequency domain). A solution of the transfer function that relates displacements and excitation is presented in equation (6.13).

$$\widetilde{h}(\omega) = (-\omega^2 m + i\omega c + k)^{-1} \tag{6.13}$$

Before going a step deeper in the concept of probabilistic filtering, convolution properties presented in the previous section are used for representing the solution of SDOF system. Observe that probabilistic filtering is based on convolving multiple measured vibration outputs y_i with each other (one output denoted with subscript i). Equation (6.11) under convolution operation (6.7) is presented in equation (6.14).

$$\begin{aligned} \overset{n}{\underset{i=1}{\ast}} y_i(t) &= \overset{n}{\underset{i=1}{\ast}} (h_i(t) * f_i(t)) \\ &= \left(\overset{n}{\underset{i=1}{\ast}} h_i(t) \right) * \left(\overset{n}{\underset{i=1}{\ast}} f_i(t) \right) \end{aligned} \tag{6.14}$$

The same relation in the frequency domain (obtained with Fourier transform) is presented in equation (6.15). With the assumption that the dynamical system stays the same and force that excites the system is changing for different outputs y_i, we observe that transfer function in the frequency domain is being raised to the order that is same as the number of used outputs.

$$\begin{aligned} \prod_{i=1}^{n} \widetilde{y}_i(\omega) &= \left(\prod_{i=1}^{n} \widetilde{h}_i(\omega) \right) \cdot \left(\prod_{i=1}^{n} \widetilde{f}_i(\omega) \right) \\ &= \widetilde{h}^n(\omega) \cdot \left(\prod_{i=1}^{n} \widetilde{f}_i(\omega) \right) \end{aligned} \tag{6.15}$$

Further discussion on multi-degree of freedom system will be presented after the introduction of the white noise approximations. Next step in the development of probabilistic filtering method is to observe the result of the convolution of the excitation term ($\overset{n}{\underset{i=1}{\ast}} f_i(t)$).

6.3 White noise

White noise is a random signal with constant intensity in the frequency domain. The same terminology is used in many scientific and technical disciplines, generally with similar meanings. The aim of introducing the term in this work is for the use of the flat power spectral density concept.

What is the aim of this section is to show that by performing convolution of random independent signals, the product of those convolutions improves the approximation of the white noise. Or in other words, the more the random independent signals are convolved the better its product approximates the white noise.

For the output only identification methods, excitation is unknown and assumed random. Referring back to equation (6.15) in the situation of unknown random excitation, it is assumed (to be proven) that by multiple convolution of output measurements y_i part related to random excitation $\left(\prod_{i=1}^{n} \widetilde{f}_i(\omega)\right)$ tends to approximate white noise (6.16). If so, the product of multiple convolutions of y_i becomes proportional to transfer function raised to order n $\widetilde{h}^n(\omega)$ (6.17).

$$\widetilde{h}^n(\omega) \cdot \underbrace{\left(\prod_{i=1}^{n} \widetilde{f}_i(\omega)\right)}_{\textbf{white noise}} = \prod_{i=1}^{n} \widetilde{y}_i(\omega) \tag{6.16}$$

$$\widetilde{h}^n(\omega) \cdot const = \prod_{i=1}^{n} \widetilde{y}_i(\omega) \tag{6.17}$$

In the probabilistic theory, randomness is approached in form of the distribution functions of random variables. Direct analytical representation of a random function is not possible and the proofs for the above assumptions would be presented in the form of numerical examples.

With the use of MatLab random signal is generated (200Hz sample rate). In the figure 6.1 time and frequency domain of one random signal are presented. It is concluded that given random signal does not represent white noise. Additionally, observe spectrogram of generated signal in the figure 6.2.

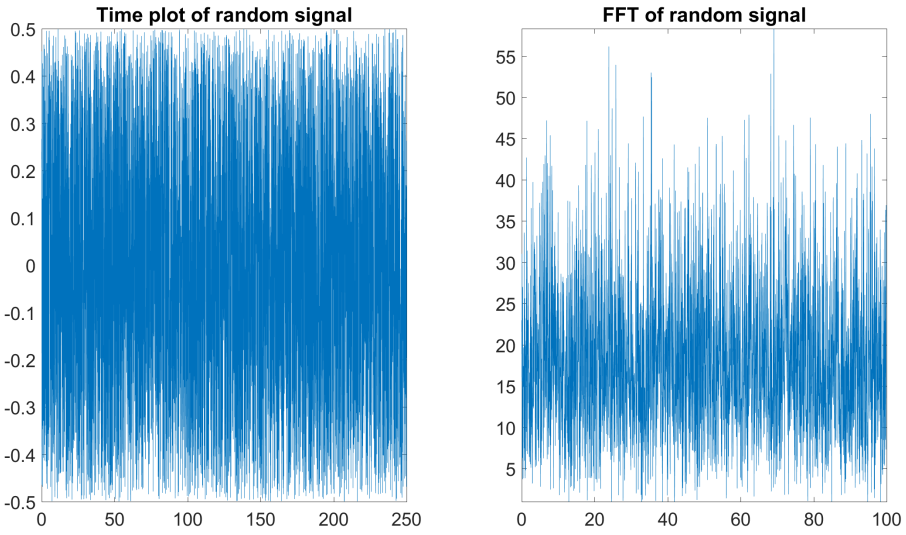


Figure 6.1: Random signal (time and frequency domain)

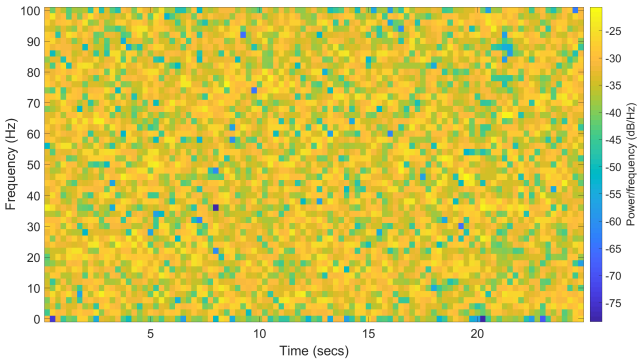
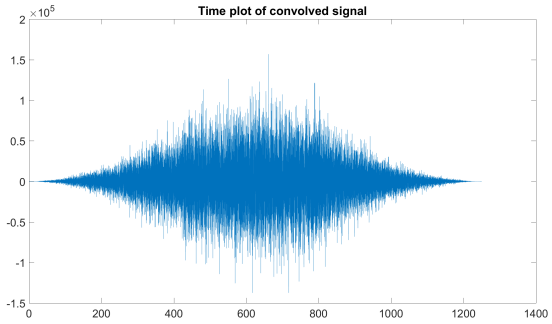
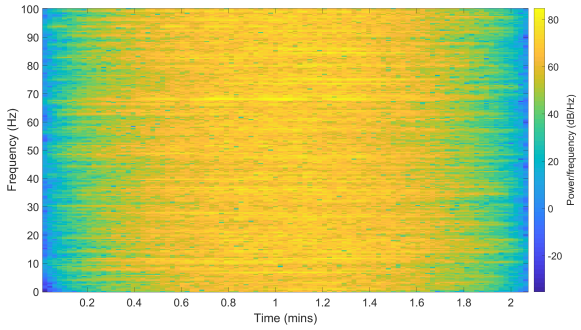


Figure 6.2: Spectrogram of random signal

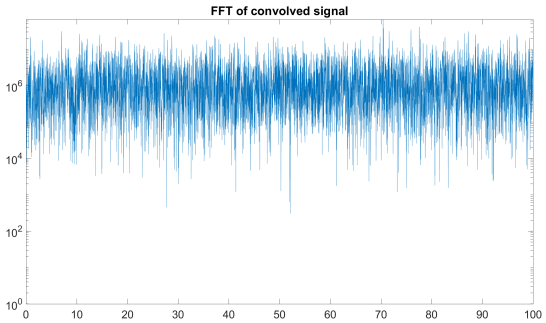
In the figure 6.3 result of the convolution of 5 random signals is presented. Observe the level of approximation of white noise, for the convolved signal in the figure 6.3c.



(a) Time plot of 5 convolved random signals



(b) Spectrogram of 5 convolved random signals

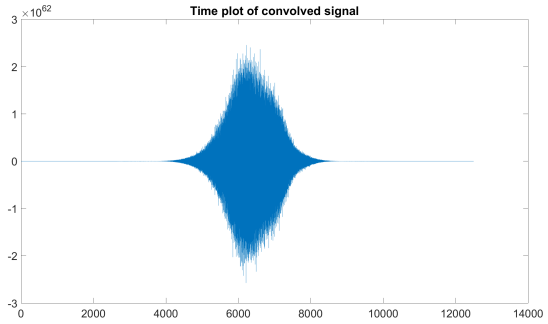


(c) FFT of 5 convolved random signals

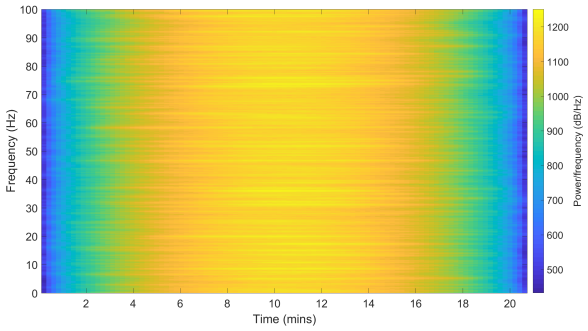
Figure 6.3: 5 convolved random signals

In the figure 6.4 convolution of 50 random signals is presented. It can be observed that with an increase in the number of the convolved random signals higher approximation of white noise is achieved.

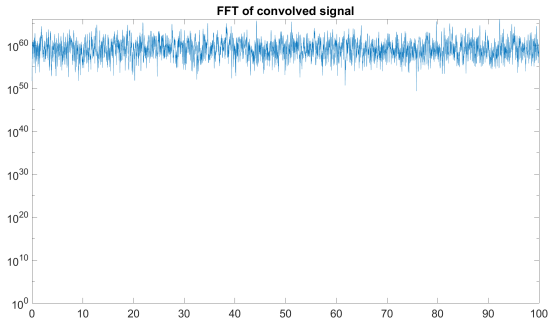
What is in the interest for the analysis is to cut segment of time signal in the region of constant power spectral density. Segment of interest is observed with spectrogram figure 6.4b, generally it is centred in time domain.



(a) Time plot of 50 convolved random signals



(b) Spectrogram of 50 convolved random signals

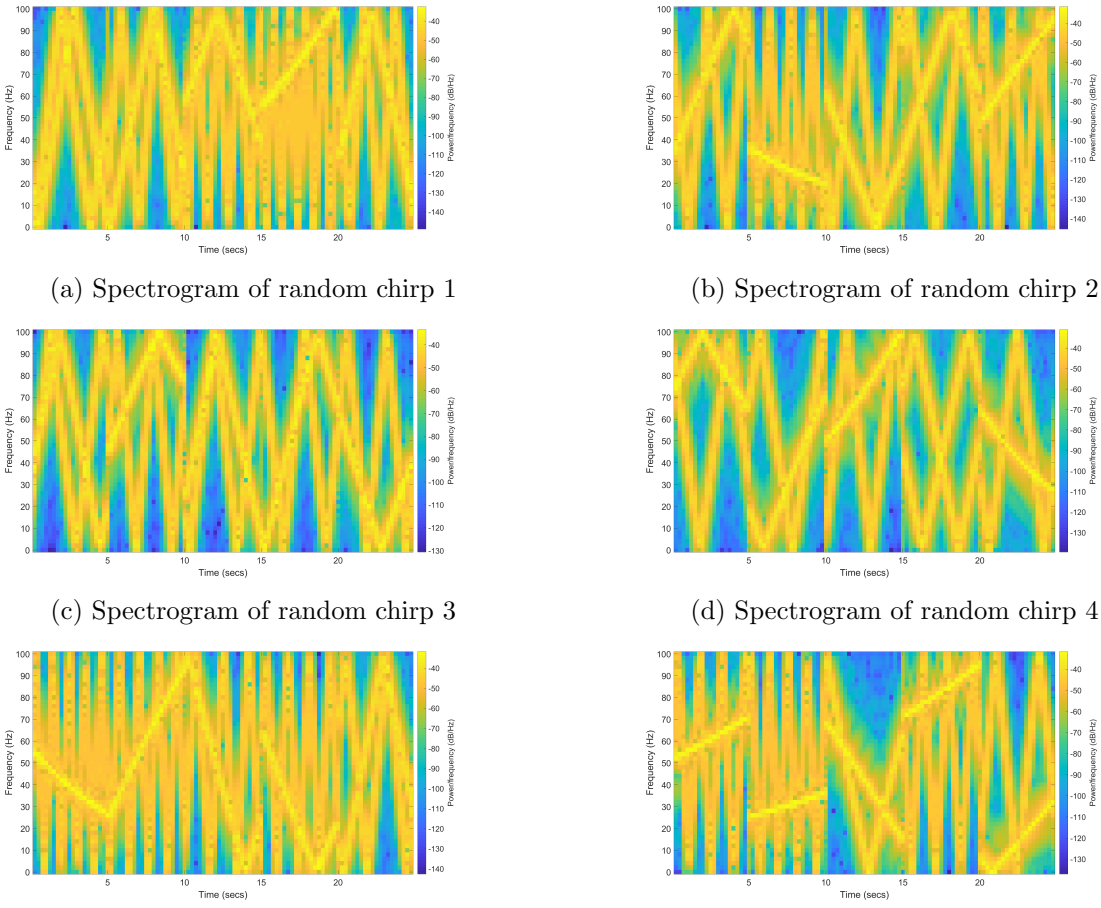


(c) FFT of 50 convolved random signals

Figure 6.4: 50 convolved random signals

As convolution will increase similarities in the signals and damp differences, an additional example for time variant signals is presented. The aim is to show how non-linearities are damped out. Spectrograms of generated signals through the time variant chirp systems are presented in figure 6.5.

The result of the convolution of 100 random time variant signals is presented in the figure 6.6. From spectrogram in figure 6.6c, it can be observed that systems non-linearities are dampened out. Observe in the figure 6.6d that product of performed convolution has a high approximation of the white noise.



(a) Spectrogram of random chirp 1

(b) Spectrogram of random chirp 2

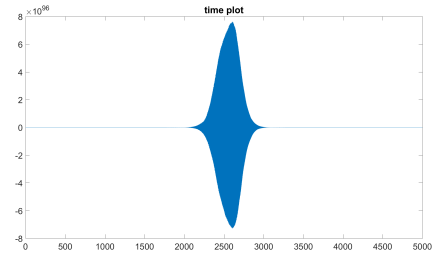
(c) Spectrogram of random chirp 3

(d) Spectrogram of random chirp 4

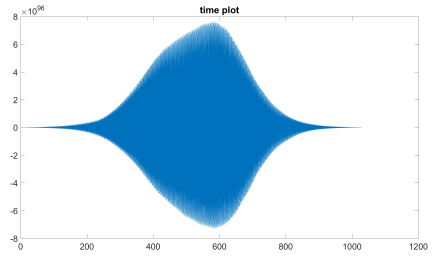
(e) Spectrogram of random chirp 5

(f) Spectrogram of random chirp 6

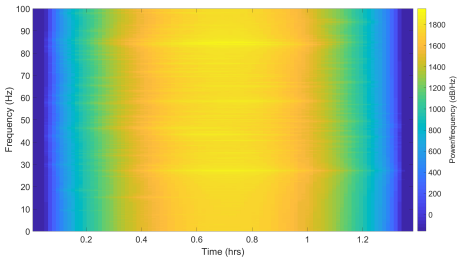
Figure 6.5: Example of used time variant signals



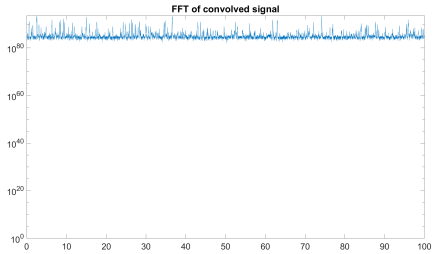
(a) Convolved signal



(b) Centered signal for analysis



(c) Spectrogram of convolved signal



(d) FFT of centered signal

Figure 6.6: Analysis of convolved signal

As stated previously, the aim was to show that multiple convolutions of random signals increases the approximation of white noise. For the dynamical Sdof system with unknown excitation, with the process of multiple convolutions relation (6.18) is achieved ($\widetilde{c}$ presenting constant).

$$\widetilde{h}^n(\omega) \ \cdot \ const = \prod_{i=1}^{n} \widetilde{y}_i(\omega) \tag{6.18}$$

The next step in probabilistic filter development is to extend the above-mentioned concept to multi-degree of freedom structural system.

6.4 Multi-degree of freedom system

In the previous sections, foundation idea of probabilistic filtering was shown. Mathematically, relation between the dynamical system and multiple convolution of output signals becomes more complex for multi degree of freedom systems. As high dimension tensor algebra will be introduced, slow pace of providing information will be taken.

By extending the model of Sdof system that was introduced in the section (6.2), multi degree of freedom (Mdof) system is introduced in equation (6.19).

$$M\ddot{\boldsymbol{y}}(t) + C\dot{\boldsymbol{y}}(t) + K\boldsymbol{y}(t) = \boldsymbol{f}(t) \tag{6.19}$$

The steady state solution of the given system can be represented in the time domain as (6.20) and in the frequency domain as (6.21).

$$\boldsymbol{y}(t) = H(t) * \boldsymbol{f}(t) \tag{6.20}$$

$$\widetilde{\boldsymbol{y}}(\omega) = \widetilde{H}(\omega)\widetilde{\boldsymbol{f}}(\omega) \tag{6.21}$$

Matrices $H(t)$ and $H(\omega)$ are impulse response and transfer function. Solution of the transfer function that relates displacements and excitation in frequency domain is presented in equation equation (6.22).

$$\widetilde{H}(\omega) = (-\omega^2 M + i\omega C + K)^{-1} \tag{6.22}$$

With application of row wise multiple output vector $\boldsymbol{y}_i(t)$ convolution, relation (6.23) is obtained.

$$\overset{n}{\underset{i=1}{\ast}} \boldsymbol{y}_i(t) = \overset{n}{\underset{i=1}{\ast}} (H(t) * \boldsymbol{f}_i(t)) \tag{6.23}$$

Observe that impulse response function $H(t)$ is a matrix, and convolution relation $H(t) * \boldsymbol{f}_i(t)$ follows analogy with matrix vector product. The complex tensor notation needs to be introduced, as commutativity relation does not hold (6.24).

$$H(t) * \boldsymbol{f}_i(t) \neq \boldsymbol{f}_i(t) * H(t) \tag{6.24}$$

For the Sdof system commutative property was used to isolate excitation and obtain white noise. For Mdof system commutative analogy does not hold (6.25).

$$\overset{n}{\underset{i=1}{\ast}} (H(t) * \boldsymbol{f}_i(t)) \neq (\overset{n}{\underset{i=1}{\ast}} H(t)) * (\overset{n}{\underset{i=1}{\ast}} \boldsymbol{f}_i(t)) \tag{6.25}$$

Concept of isolation of transfer function term $H(t)$ and excitation term $\boldsymbol{f}_i(t)$, is achieved through tensor notation. Derivation of aforementioned concept will be guided with 2dof example in frequency domain.

Starting with equation (6.26), follow further derivations. In the equations, functions with two subscripts are related to measurement number i and spatial node position of that measurement p, $\widetilde{y}_{ip}(\omega)$. So, for an example $\widetilde{y}_{47}(\omega)$ is the 4^{th} measurement at node position 7. As convolution operation operates between different measurements, it is related to subscript i.

$$\overset{2}{\underset{i=1}{\ast}} (\boldsymbol{y}_i(t)) = (\overset{2}{\underset{i=1}{\ast}} H(t)) * (\overset{2}{\underset{i=1}{\ast}} \boldsymbol{f}_i(t)) \tag{6.26}$$

Note that $\prod_{i=1}^{n}$ operation holds for multiple element-wise product of vectors from i to n, and that $.*$ is single element-wise product operation.

$$\prod_{i=1}^{2} \widetilde{\boldsymbol{y}}_i(\omega) = \left(\prod_{i=1}^{2} \left(\widetilde{H}(\omega) \widetilde{\boldsymbol{f}}_i(\omega) \right) \right) \tag{6.27}$$

$$\begin{bmatrix} \widetilde{y}_{11}(\omega) \\ \widetilde{y}_{12}(\omega) \end{bmatrix} .* \begin{bmatrix} \widetilde{y}_{21}(\omega) \\ \widetilde{y}_{22}(\omega) \end{bmatrix} = \left(\begin{bmatrix} \widetilde{h}_{11}(\omega) & \widetilde{h}_{12}(\omega) \\ \widetilde{h}_{21}(\omega) & \widetilde{h}_{22}(\omega) \end{bmatrix} \begin{bmatrix} \widetilde{f}_{11}(\omega) \\ \widetilde{f}_{12}(\omega) \end{bmatrix} \right) .* \left(\begin{bmatrix} \widetilde{h}_{11}(\omega) & \widetilde{h}_{12}(\omega) \\ \widetilde{h}_{21}(\omega) & \widetilde{h}_{22}(\omega) \end{bmatrix} \begin{bmatrix} \widetilde{f}_{21}(\omega) \\ \widetilde{f}_{22}(\omega) \end{bmatrix} \right) \tag{6.28}$$

For simplicity of presenting derivation one output point of the 2dof system would be taken for observation (6.29).

$$\begin{aligned} \widetilde{y}_{11}(\omega)\widetilde{y}_{21}(\omega) &= \left(\begin{bmatrix} \widetilde{h}_{11}(\omega) & \widetilde{h}_{12}(\omega) \end{bmatrix} \begin{bmatrix} \widetilde{f}_{11}(\omega) \\ \widetilde{f}_{12}(\omega) \end{bmatrix} \right) \cdot \left(\begin{bmatrix} \widetilde{h}_{11}(\omega) & \widetilde{h}_{12}(\omega) \end{bmatrix} \begin{bmatrix} \widetilde{f}_{21}(\omega) \\ \widetilde{f}_{22}(\omega) \end{bmatrix} \right) \\ &= (\widetilde{h}_{11}\widetilde{f}_{11}(\omega) + \widetilde{h}_{12}\widetilde{f}_{12}(\omega))(\widetilde{h}_{11}f_{21}(\omega) + \widetilde{h}_{12}\widetilde{f}_{22}(\omega)) \\ &= \widetilde{h}_{11}^2\widetilde{f}_{11}\widetilde{f}_{21}(\omega) + \widetilde{h}_{11}\widetilde{h}_{12}\widetilde{f}_{11}\widetilde{f}_{22}(\omega) + \widetilde{h}_{12}\widetilde{h}_{11}\widetilde{f}_{12}\widetilde{f}_{21}(\omega) + \widetilde{h}_{12}^2\widetilde{f}_{12}\widetilde{f}_{22}(\omega) \end{aligned} \tag{6.29}$$

The mathematical challenge that is being faced is to isolate transfer function terms $\widetilde{h}(\omega)$ from excitation terms $\widetilde{f}(\omega)$, in order to formulate relation analog with Sdof system. The wanted relation is obtained by extending vectors to Scalar product (noted as Tensor scalar product $\bullet$)

of higher dimension tensors (6.30). For this initial example, tensor terminology refers to vectors as thefirst order tensors, and matrices as the second order tensors.

$$\widetilde{y}_{11}(\omega)\widetilde{y}_{21}(\omega) = \left(\begin{bmatrix} \widetilde{h}_{11}(\omega) \\ \widetilde{h}_{12}(\omega) \end{bmatrix}_{2\times 1} \begin{bmatrix} \widetilde{h}_{11}(\omega) & \widetilde{h}_{12}(\omega) \end{bmatrix}_{1\times 2} \right) \bullet \left(\begin{bmatrix} \widetilde{f}_{11}(\omega) \\ \widetilde{f}_{12}(\omega) \end{bmatrix}_{2\times 1} \begin{bmatrix} \widetilde{f}_{21}(\omega) & \widetilde{f}_{22}(\omega) \end{bmatrix}_{1\times 2} \right) \tag{6.30}$$

We observe that given concept of Scalar product of vectors extended dimensionally to matrices holds same solution as initial relation, observe results of (6.29) and (6.31).

$$\begin{aligned} \widetilde{y}_{11}(\omega)\widetilde{y}_{21}(\omega) &= \begin{bmatrix} \widetilde{h}_{11}^2(\omega) & \widetilde{h}_{11}\widetilde{h}_{12}(\omega) \\ \widetilde{h}_{12}\widetilde{h}_{11}(\omega) & \widetilde{h}_{12}^2(\omega) \end{bmatrix}_{2\times 2} \bullet \begin{bmatrix} \widetilde{f}_{11}\widetilde{f}_{21}(\omega) & \widetilde{f}_{11}\widetilde{f}_{22}(\omega) \\ \widetilde{f}_{12}\widetilde{f}_{21}(\omega) & \widetilde{f}_{12}\widetilde{f}_{22}(\omega) \end{bmatrix}_{2\times 2} \\ &= \widetilde{h}_{11}^2\widetilde{f}_{11}\widetilde{f}_{21}(\omega) + \widetilde{h}_{11}\widetilde{h}_{12}\widetilde{f}_{11}\widetilde{f}_{22}(\omega) + \widetilde{h}_{12}\widetilde{h}_{11}\widetilde{f}_{12}\widetilde{f}_{21}(\omega) + \widetilde{h}_{12}^2\widetilde{f}_{12}\widetilde{f}_{22}(\omega) \end{aligned} \tag{6.31}$$

Expanding relation to 3 convolutions of output $\widetilde{y}_{i1}(\omega)$ equation (6.32) is obtained:

$$\begin{aligned} \widetilde{y}_{11}(\omega)\widetilde{y}_{21}(\omega)\widetilde{y}_{31}(\omega) &= \begin{bmatrix} \widetilde{h}_{11}(\omega) & \widetilde{h}_{12}(\omega) \end{bmatrix} \begin{bmatrix} \widetilde{f}_{11}(\omega) \\ \widetilde{f}_{12}(\omega) \end{bmatrix} \begin{bmatrix} \widetilde{h}_{11}(\omega) & \widetilde{h}_{12}(\omega) \end{bmatrix} \begin{bmatrix} \widetilde{f}_{21}(\omega) \\ \widetilde{f}_{22}(\omega) \end{bmatrix} \begin{bmatrix} \widetilde{h}_{11}(\omega) & \widetilde{h}_{12}(\omega) \end{bmatrix} \begin{bmatrix} \widetilde{f}_{31}(\omega) \\ \widetilde{f}_{32}(\omega) \end{bmatrix} \\ &= \widetilde{h}_{11}^3\widetilde{f}_{11}\widetilde{f}_{21}\widetilde{f}_{31}(\omega) + \widetilde{h}_{11}^2\widetilde{h}_{12}\widetilde{f}_{11}\widetilde{f}_{21}\widetilde{f}_{32}(\omega) + \widetilde{h}_{11}^2\widetilde{h}_{12}\widetilde{f}_{11}\widetilde{f}_{22}\widetilde{f}_{31}(\omega) + \widetilde{h}_{11}\widetilde{h}_{12}^2\widetilde{f}_{11}\widetilde{f}_{22}\widetilde{f}_{32}(\omega) + \\ &+ \widetilde{h}_{12}\widetilde{h}_{11}^2\widetilde{f}_{12}\widetilde{f}_{21}\widetilde{f}_{31}(\omega) + \widetilde{h}_{12}^2\widetilde{h}_{11}\widetilde{f}_{12}\widetilde{f}_{21}\widetilde{f}_{32}(\omega) + \widetilde{h}_{12}^2\widetilde{h}_{11}\widetilde{f}_{12}\widetilde{f}_{22}\widetilde{f}_{31}(\omega) + \widetilde{h}_{12}^3\widetilde{f}_{12}\widetilde{f}_{22}\widetilde{f}_{32}(\omega) \end{aligned} \tag{6.32}$$

Relation for 3 convolutions of output $\widetilde{y}_{i1}(\omega)$ in tensor notation holds (6.33):

$$\begin{aligned} \widetilde{y}_{11}(\omega)\widetilde{y}_{21}(\omega)\widetilde{y}_{31}(\omega) = &\left(\begin{bmatrix} \widetilde{h}_{11}^2(\omega) & \widetilde{h}_{11}\widetilde{h}_{12}(\omega) \\ \widetilde{h}_{12}\widetilde{h}_{11}(\omega) & \widetilde{h}_{12}^2(\omega) \end{bmatrix}_{2\times 2\times 1} \begin{bmatrix} \widetilde{h}_{11}(\omega) & \widetilde{h}_{12}(\omega) \end{bmatrix}_{1\times 2} \right) \bullet \\ &\bullet \left(\begin{bmatrix} \widetilde{f}_{11}\widetilde{f}_{21}(\omega) & \widetilde{f}_{11}\widetilde{f}_{22}(\omega) \\ \widetilde{f}_{12}\widetilde{f}_{21}(\omega) & \widetilde{f}_{12}\widetilde{f}_{22}(\omega) \end{bmatrix}_{2\times 2\times 1} \begin{bmatrix} \widetilde{f}_{31}(\omega) & \widetilde{f}_{32}(\omega) \end{bmatrix}_{1\times 2} \right) \end{aligned} \tag{6.33}$$

Graphical illustration of equation (6.33) is presented in figure 6.7. It can be observed that Tensor scalar product of dimensionally expanded vectors to 3^{rd} order tensor ("cube") of transfer function and excitation holds the same solution as (6.32).

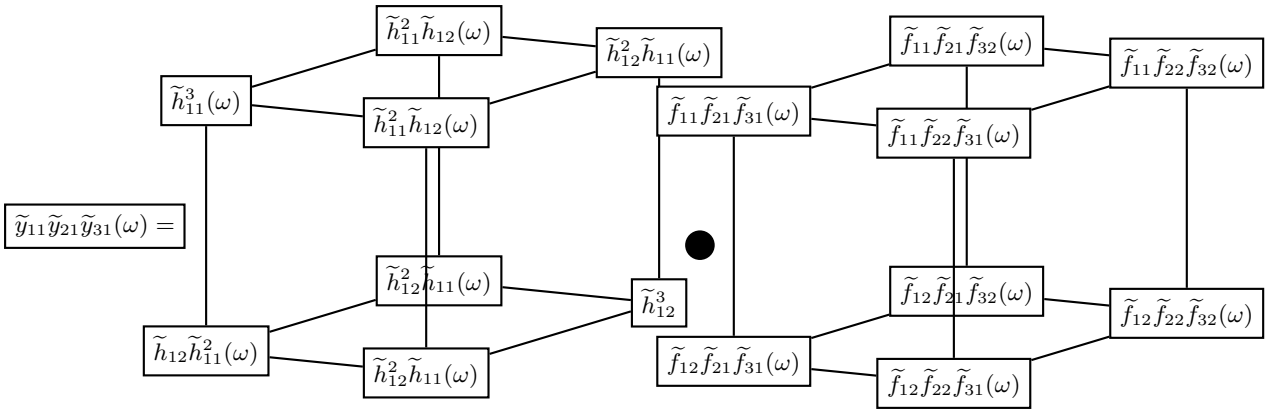


Figure 6.7: 3D illustration of 3 convolutions of Mdof system

For the Sdof system, commutativity was applied to separate transfer functions from excitation functions. For the Mdof system, commutativity relation does not hold. It is concluded that Tensor scalar product of dimensionally expanded transfer function vector and excitation vector achieves intended separation. Concept is proven on 2 and 3 convolution example.

The next step is to show the behavior of the excitation tensor assuming system is excited by unknown random excitation. A numerical example representing 2dof system is observed. The figure 6.8 shows 100 elements of excitation tensor of order 100. It can be observed that excitation tensor elements tend to approximate white noise, with a small difference between them. Further, it will be assumed that raising the order of excitation tensor its elements tend to have a better approximation of white noise with a small difference between them. The given excitation tensor will be approximated (and represented) as a unit a tensor multiplied by a constant.

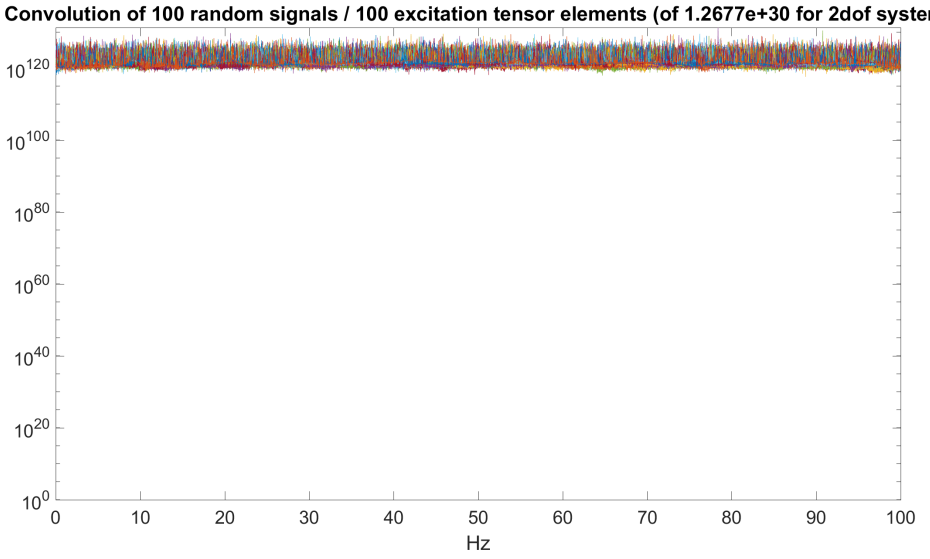


Figure 6.8: FFT for 100 elements of 100 order excitation tensor

6.5 Notation

Observing Mdof system of order m, output displacement $\widetilde{y}_{1p}(\omega)$ is represented with equation (6.34). The subscript p denotes the spatial position of the given displacement output, and subscript 1 represents signal (measurement) number. Revise that column vectors are presented with small bold letters and scalars with normal small letters.

The subscript notation "$row : p$" in $\widetilde{\boldsymbol{h}}_{row:p}$ is used to emphasise that the vector of transfer function is composed out of the p^{th} row of the transfer function matrix.

$$\widetilde{y}_{1p}(\omega) = \left[\widetilde{h}_{p1}(\omega) \;\; \widetilde{h}_{p2}(\omega) \;\; ... \;\; \widetilde{h}_{pm}(\omega)\right]_{1\times m} \begin{bmatrix} \widetilde{f}_{11}(\omega) \\ \widetilde{f}_{12}(\omega) \\ \vdots \\ \widetilde{f}_{1m}(\omega) \end{bmatrix}_{m\times 1} \tag{6.34}$$

$$= \widetilde{\boldsymbol{h}}^{T}_{row:p}(\omega)\widetilde{\boldsymbol{f}}_1(\omega)$$

Tensor expansion product $\bigtimes_{i=2}^{n}$ is described on example of 3 convolutions ($n = 3$) for the Mdof system, observe equation (6.35). In equation (6.37) the final product of the given tensor expansion is presented. Notation $\square^{3}_{\widetilde{\boldsymbol{h}}_{row:p}}$ represents tensor of order 3, for the expanded transfer function vector $\widetilde{\boldsymbol{h}}_{row:p}$.

$$\begin{bmatrix} \widetilde{h}_{p1}(\omega) \\ \widetilde{h}_{p2}(\omega) \\ \vdots \\ \widetilde{h}_{pm}(\omega) \end{bmatrix}_{m\times 1} \bigtimes_{i=2}^{n} \left[\widetilde{h}_{p1}(\omega) \;\; \widetilde{h}_{p2}(\omega) \;\; ... \;\; \widetilde{h}_{pm}(\omega)\right]_{1\times m} = \tag{6.35}$$

$$= \left[\begin{bmatrix} \widetilde{h}_{p1}(\omega) \\ \widetilde{h}_{p2}(\omega) \\ \vdots \\ \widetilde{h}_{pm}(\omega) \end{bmatrix}_{m\times 1} \cdot \left[\widetilde{h}_{p1}(\omega) \;\; \widetilde{h}_{p2}(\omega) \;\; ... \;\; \widetilde{h}_{pm}(\omega)\right]_{1\times m} \right]_{m\times m\times 1} \cdot \left[\widetilde{h}_{p1}(\omega) \;\; \widetilde{h}_{p2}(\omega) \;\; ... \;\; \widetilde{h}_{pm}(\omega)\right]_{1\times m} = \tag{6.36}$$

$$= \begin{bmatrix} \overset{3}{\square} \\ \widetilde{\boldsymbol{h}}_{row:p} \end{bmatrix}_{m\times m\times m} \tag{6.37}$$

For the n convolutions of output signal $y_{ip}(t)$ notation represented in equation (6.38) is used. The symbol $\square^{n}_{\widetilde{\boldsymbol{h}}_{row:p}}$ represents the tensor of order n of the transfer function $\widetilde{\boldsymbol{h}}_{row:p}$, and $\square^{n}_{\widetilde{\boldsymbol{f}}_i}$ is the tensor of order n for the excitation function.

$$\prod_{i=1}^{n} \widetilde{y}_{ip}(\omega) = \left([\widetilde{\boldsymbol{h}}_{row:p}]_{m\times 1} \bigtimes_{i=2}^{n} [\widetilde{\boldsymbol{h}}^{T}_{row:p}]_{1\times m}\right) \bullet \left([\widetilde{\boldsymbol{f}}_1]_{m\times 1} \bigtimes_{i=2}^{n} [\widetilde{\boldsymbol{f}}_i^{T}]_{1\times m}\right) \tag{6.38}$$

$$= \overset{n}{\underset{\widetilde{\boldsymbol{h}}_{row:p}}{\square}} \bullet \overset{n}{\underset{\widetilde{\boldsymbol{f}}_i}{\square}}$$

As it was shown, when raising the order of excitation tensor, it's elements tend to have a better approximation of white noise, with a small difference between them. The given excitation tensor

will be approximated as unit tensor $\square_I^n$ of order n, multiplied by a constant (6.39).

$$\prod_{i=1}^{n} \widetilde{y}_{ip}(\omega) = \underset{\widetilde{\boldsymbol{h}}_{row:p}}{\overset{n}{\square}} \bullet const \cdot \overset{n}{\underset{I}{\square}} \tag{6.39}$$

Note that with changing spatial position of output signal $y_{ip}(t)$ excitation function tensor remains exactly the same , only transfer function tensor changes (6.40).

$$\begin{aligned} \prod_{i=1}^{n} \widetilde{y}_{i1}(\omega) &= \underset{\widetilde{\boldsymbol{h}}_{row:1}}{\overset{n}{\square}} \bullet const \cdot \overset{n}{\underset{I}{\square}} \\ \prod_{i=1}^{n} \widetilde{y}_{i2}(\omega) &= \underset{\widetilde{\boldsymbol{h}}_{row:2}}{\overset{n}{\square}} \bullet const \cdot \overset{n}{\underset{I}{\square}} \end{aligned} \tag{6.40}$$

6.6 Reducing the order of the transfer function

From the previous sections regarding Sdof system, it can be concluded that process of multiple convolutions obtains the product that is proportional to the transfer function (6.18 revisited). The process of reducing the order of the transfer function is based on n^{th} root of the convolution product in the frequency domain (6.41).

$$\widetilde{h}^n(\omega) \ \cdot \ const = \prod_{i=1}^{n} \widetilde{y}_i(\omega) \tag{6.18 revisited}$$

$$\widetilde{h}(\omega) \ \cdot \ (const)^{\frac{1}{n}} = \left(\prod_{i=1}^{n} \widetilde{y}_i(\omega) \right)^{\frac{1}{n}} \tag{6.41}$$

The case with Mdof system is more complex. Purpose of reducing the order of the transfer function is to obtain mode shapes related to the spatial coordinates of convolved signals. Based on the fact that for all spatial coordinates of the convolved signals transfer function tensor is excited with exactly the same excitation tensor (6.42) same analogy with Sdof system is applied.

$$\begin{aligned} \prod_{i=1}^{n} \widetilde{y}_{i1}(\omega) &= \underset{\widetilde{\boldsymbol{h}}_{row:1}}{\overset{n}{\square}} \bullet const \cdot \overset{n}{\underset{I}{\square}} \\ \prod_{i=1}^{n} \widetilde{y}_{i2}(\omega) &= \underset{\widetilde{\boldsymbol{h}}_{row:2}}{\overset{n}{\square}} \bullet const \cdot \overset{n}{\underset{I}{\square}} \\ &\vdots \\ \prod_{i=1}^{n} \widetilde{y}_{im}(\omega) &= \underset{\widetilde{\boldsymbol{h}}_{row:m}}{\overset{n}{\square}} \bullet const \cdot \overset{n}{\underset{I}{\square}} \end{aligned} \tag{6.42}$$

The n^{th} root of the convolution product in the frequency domain is assumed to approximate information of the row of the transfer function matrix related to the spatial position of the signal, excited by white noise (6.43).

$$\left(\prod_{i=1}^{n} \widetilde{y}_{ip}(\omega) \right)^{\frac{1}{n}} \approx \left[\widetilde{h_{p1}}(\omega) \ \widetilde{h_{p2}}(\omega) \ \cdots \ \widetilde{h_{pm}}(\omega) \right]_{1\times m} const^{\frac{1}{n}} \begin{bmatrix} 1 \\ 1 \\ \vdots \\ 1 \end{bmatrix}_{m\times 1} \tag{6.43}$$

In the figure 6.9 FFT for the n^{th} root ($n = 100$) of the 100 convolved random signals is presented (analogue to figure 6.8). It is observed that through the process of convolution and reducing the

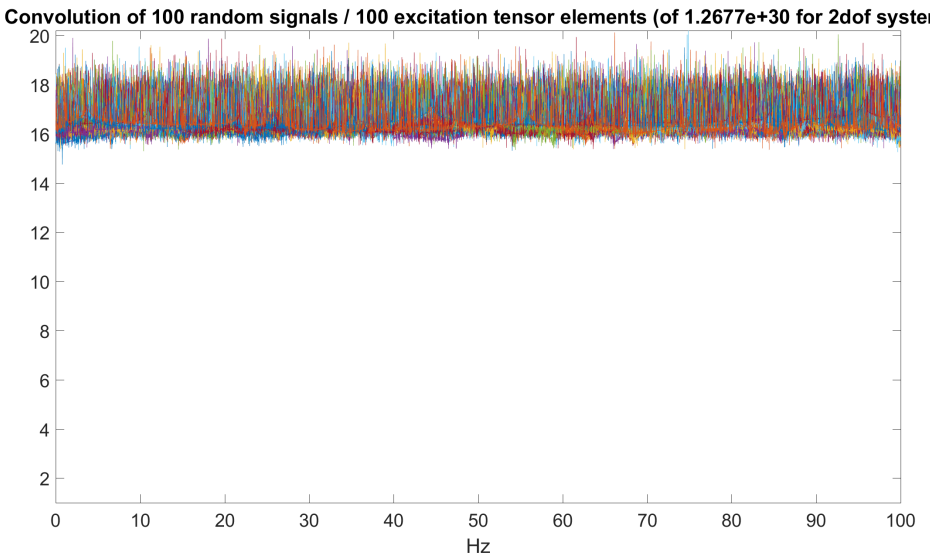


Figure 6.9: FFT for 100 elements of 100 order excitation tensor reduced with root of 100

order in the frequency domain, output of the PF of the random signals shows good approximation of the white noise in non-logarithmic scale.

The described process is named Probabilistic Filtering considering its physical interpretation. The given filter is used as preprocessing step for the FDD and SSI analysis.

This chapter intention was to provide the mathematical background for the idea behind probabilistic filtering. As the transfer function holds only information of the excited modes, physical interpretation regards that most probable modes will survive the process of multiple convolutions between different signals of the same system and different excitation.

It will be left as an open question to develop a more sophisticated process of reducing the order of the transfer function. The idea of consecutive convolution and deconvolution is to be explored.

6.7 Conclusion

Let's revise the statement from the introduction: ***"Between different vibration data samples of same added mass test set-up, what is physically different is the mass of vehicles that are exciting the bridge, and what is physically similar is the present test set-up added mass"***.

It is concluded that Probabilistic Filtering is sufficient tool to overcome the problem of differences between the unknown excitation being larger than the differences between the added masses that are used in tests.

Stating in simple words, convolution raises the similarities and dampens the differences between signals. Traffic vehicle weight ranges from 200kg (KTM 990 adventure) to 50t (heavy truck). Between the vibration measurements, for example of 50kg tests, what is physically different is the fact that one vibration measurement could be generated by a passing motorcycle and others by cars or large trucks. But what is physically similar between the given measurements is the presence of the 50kg added mass in all. What is to be done in the further analysis is to damp out the excitation differences with the probabilistic filtering and compare measurements for the 0kg-25kg-50kg-75kg-100kg added mass test set-up.

Level 1

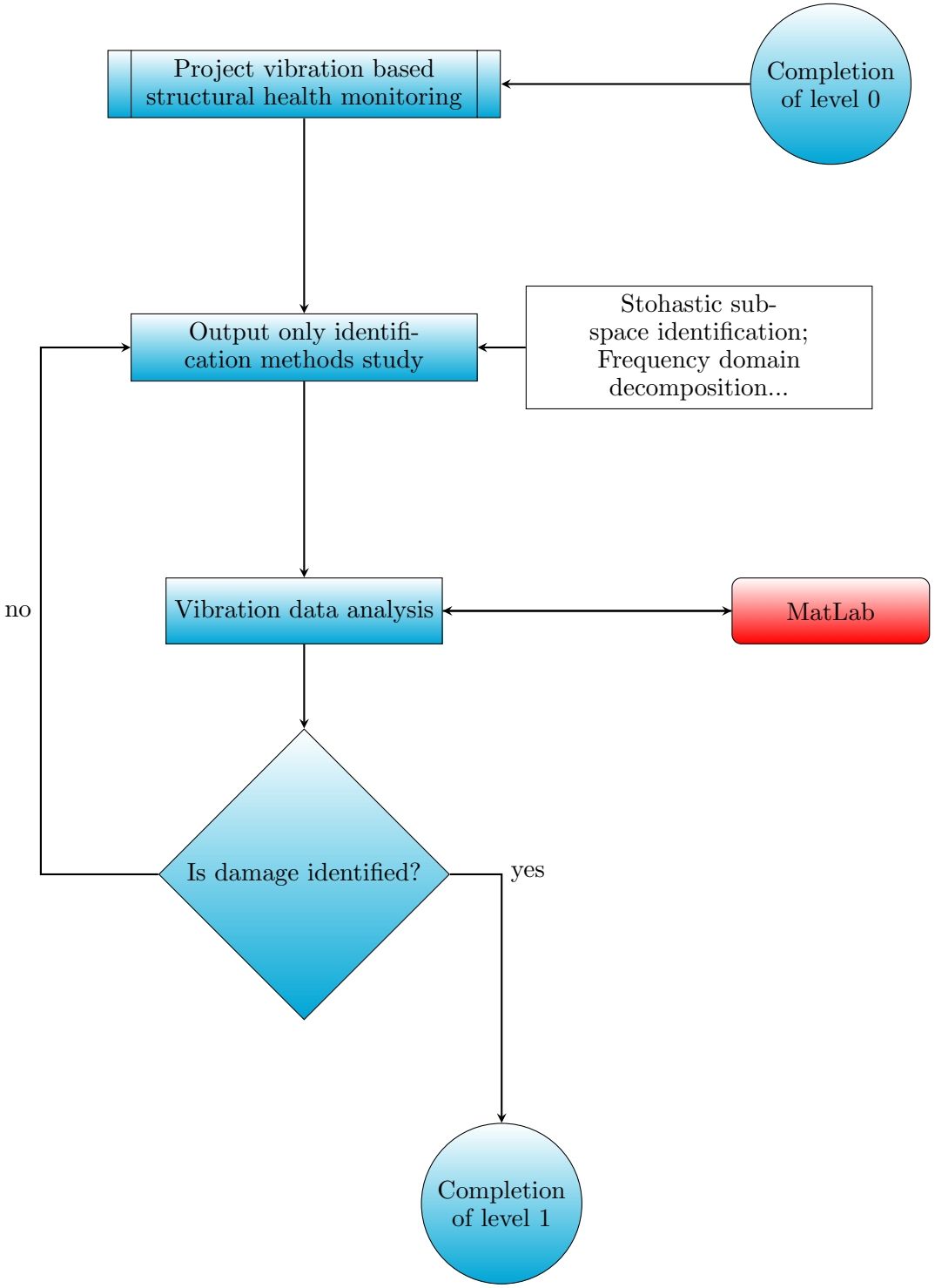


Figure L.1: Workflow of level 1

Chapter 7

The Zwartewaterbrug data analysis

This chapter provides SHM level 1 analysis. The final results of the chapter are related to the damage identification.

7.1 Analysis goals

The main goal of the analysis presented in this chapter is the added mass identification in the data of the Zwartewaterbrug project. The Zwartewaterbrug project is described in detail in the chapter 3. of this thesis.

At this point what is important to emphasise is that intentions of the analysis are to detect the added masses of 25kg-50kg-75kg-100kg, that are set on the 800t Zwartewaterbrug bridge.

It is clear that the added masses present very small structural changes compared to the mass of the bridge, and also, compared to the vehicle masses that present the excitation of the measured vibrations.

What needs to be done is to determine the reliable high frequency region in the data, for the analysis. The higher the frequency region, the more it will be sensitive to small changes.

After establishing the targeted frequency region, methods to overcome the aspect of the unknown traffic load will be brought to the analysis.

Finally, the algorithm for the added mass identification is to be composed.

▼ **Analysis goals**

- Determine the reliable high frequency region
- Compose the mass identification algorithm
- Detect the added masses

7.2 Frequency content

Initial data classification is presented in the chapter 3. of this thesis. The aim of this section is to determine the reliable high frequency region.

Based on the Frequency Domain Decomposition (FDD) and Modal Assurance Criterion (MAC), frequency regions with stable modes are determined.

Ten examples of the FDD singular value plot with MAC stabilization diagram are provided in figure 7.1 on the next page, and figure 7.2 on page 68. From the given figures, it can be observed that deviation in the frequency content is high. Red crosses that are observed in the given figures, present stable mode points.

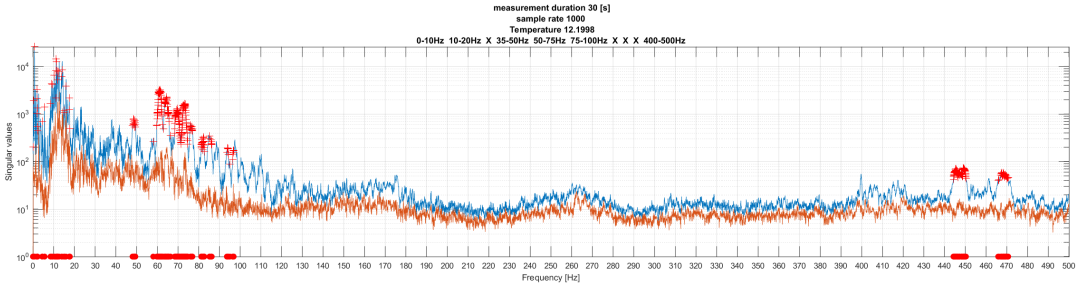
The total number of the preformed vibration measurements is 774. The FDD singular value plots with MAC stabilization diagram are used to form histograms of the stable mode count. Based on all 774 measurements separated by the added mass value, histograms are formed, observe figure 7.3 on page 69 and figure 7.4 on page 70.

Conclusion

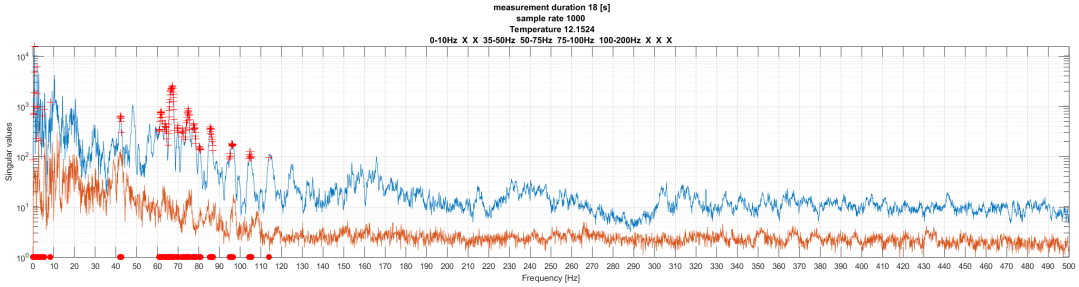
From figure 7.3 and figure 7.4 it can be concluded that region of 60-80Hz has a large number of the stable modes. It is assumed that aforementioned frequency region corresponds to the local modes related to the spatial size of the sensor network. Hammer impact test are considered not beneficial to this work as they are not performed with a variety of added masses.

Additionally, revise the tables 3.2 on page 19, to 3.7 on page 20. In the given tables, it can be observed what amount of data contains the stable modes in the region of 50-75Hz. The given frequency region is active in the amount of $50 - 60\%$ with respect to the amount of performed measurements.

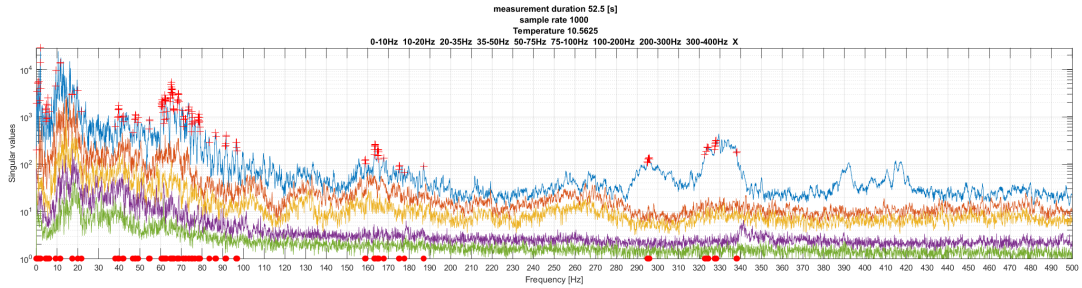
Based on the provided analysis concept, it is concluded that optimal frequency region for achieving specified analysis goals is 60-75Hz. Additionally, a bandpass filter will be designed to operate in the given frequency region.



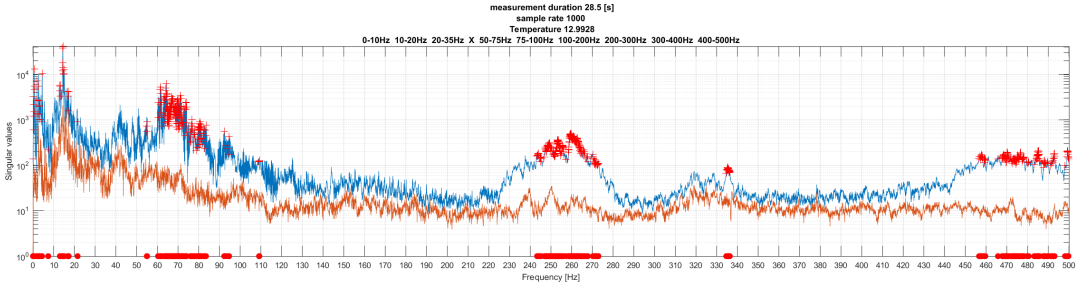
(a) Example 1



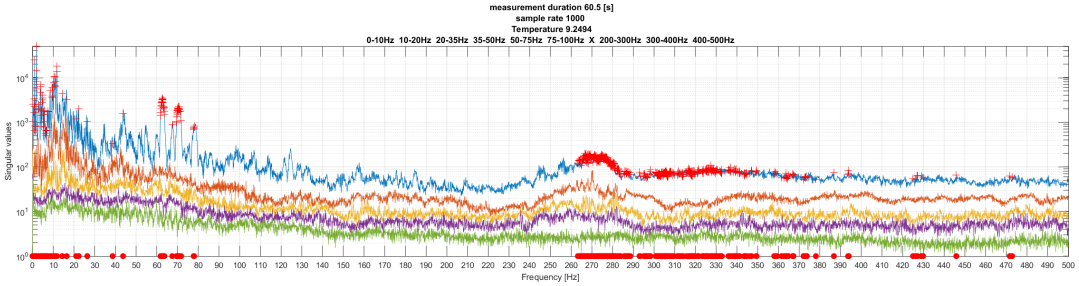
(b) Example 2



(c) Example 3

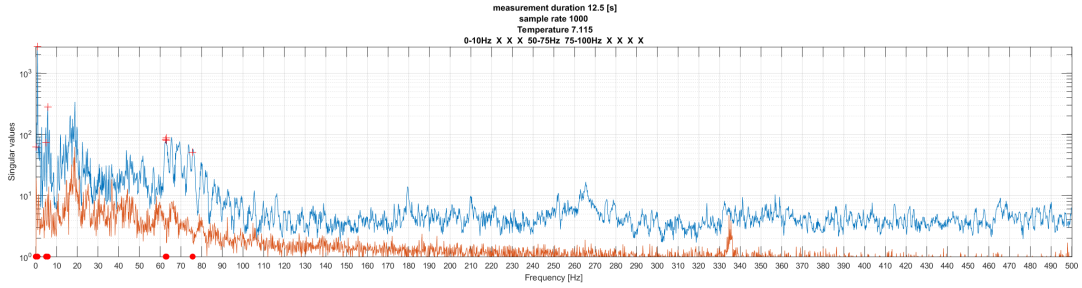


(d) Example 4

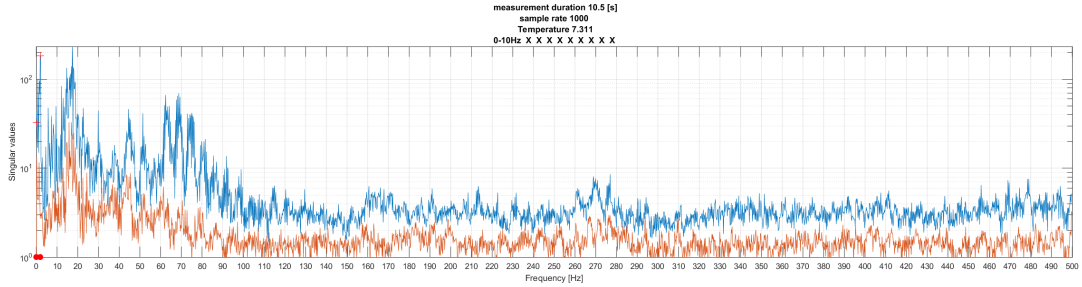


(e) Example 5

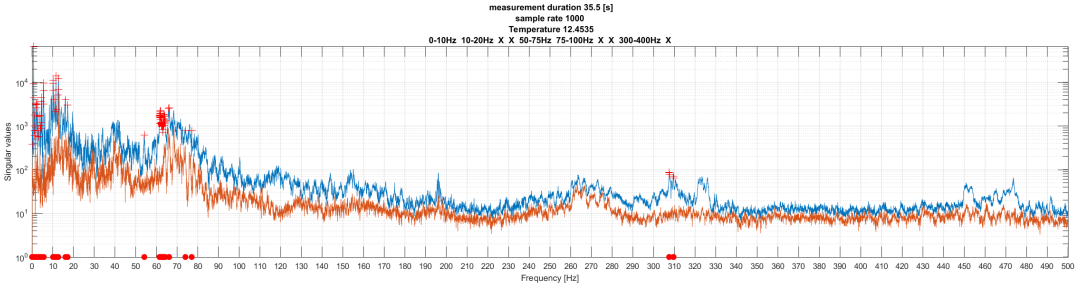
Figure 7.1: FDD plot with stabilization diagram



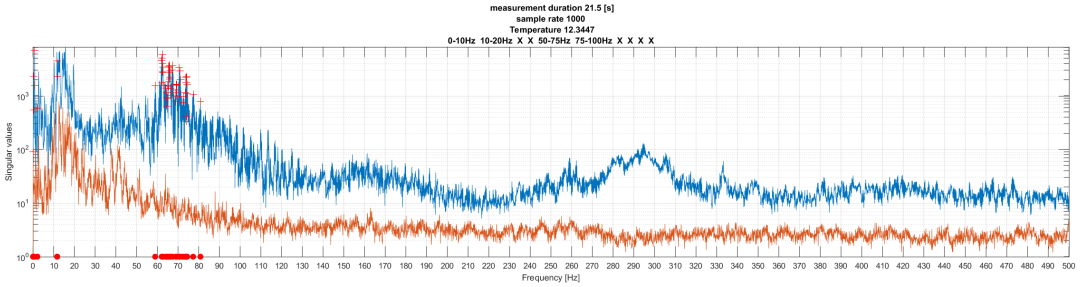
(a) Example 6



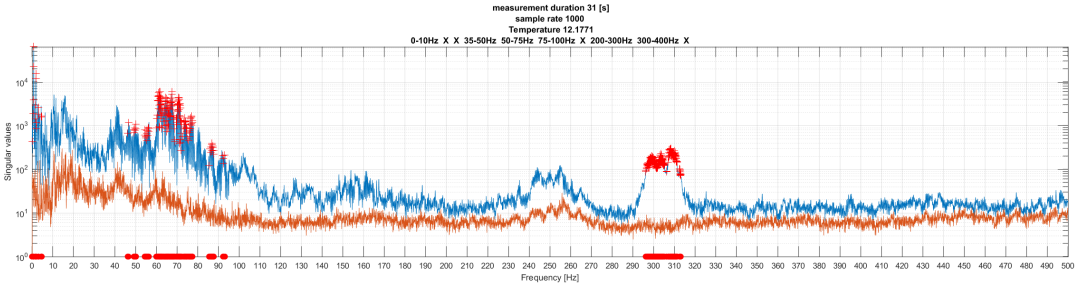
(b) Example 7



(c) Example 8

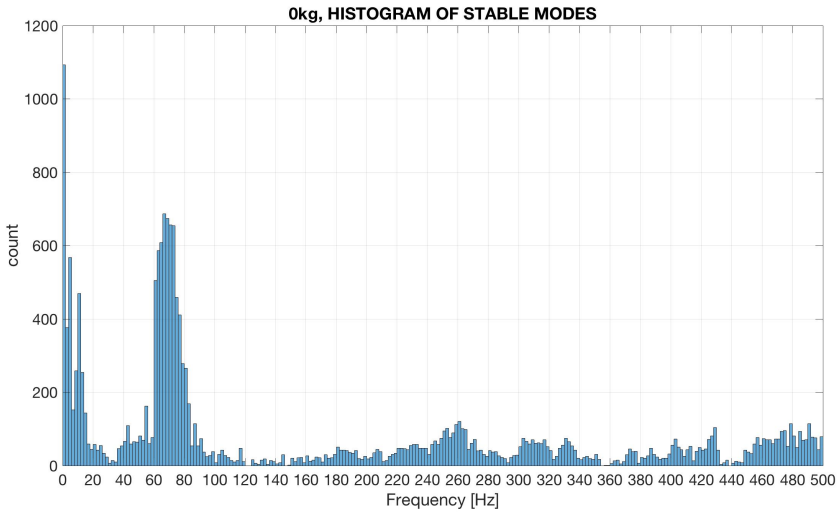


(d) Example 9

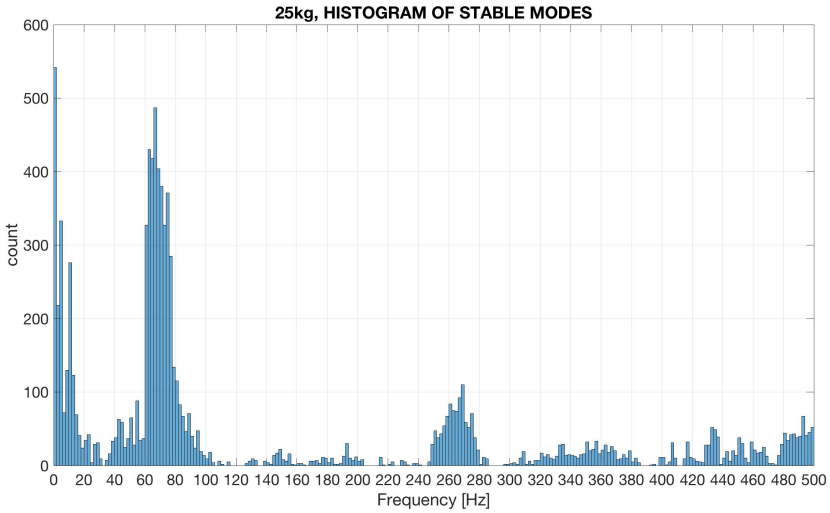


(e) Example 10

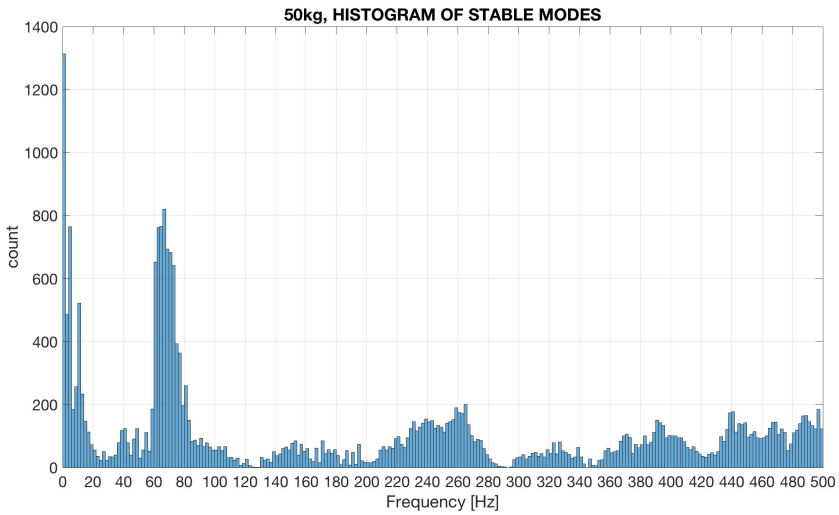
Figure 7.2: FDD plot with stabilization diagram



(a) Measurements performed with 0kg

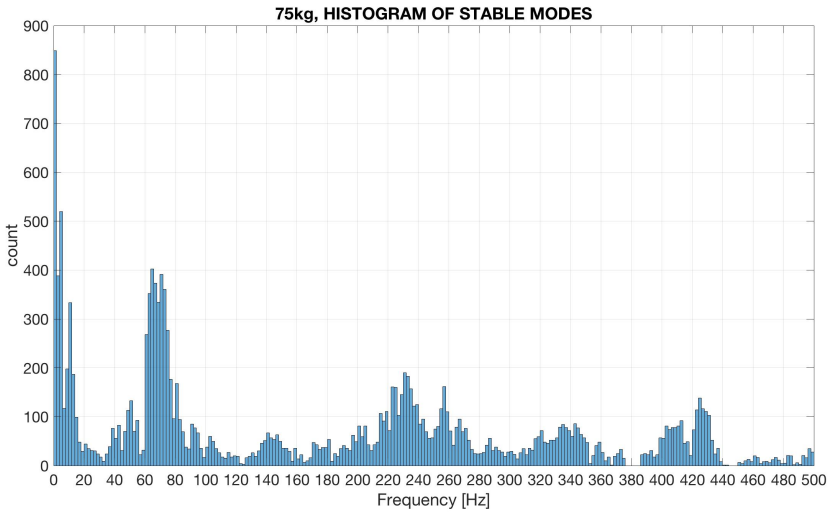


(b) Measurements performed with 25kg

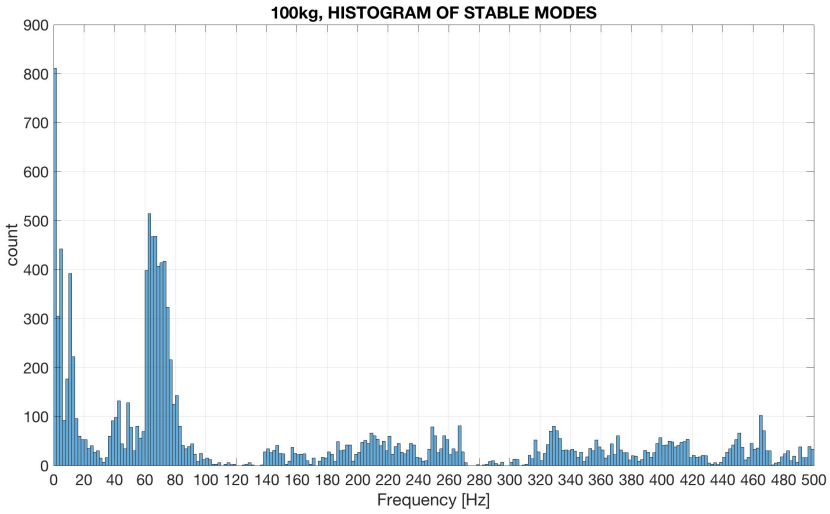


(c) Measurements performed with 50kg

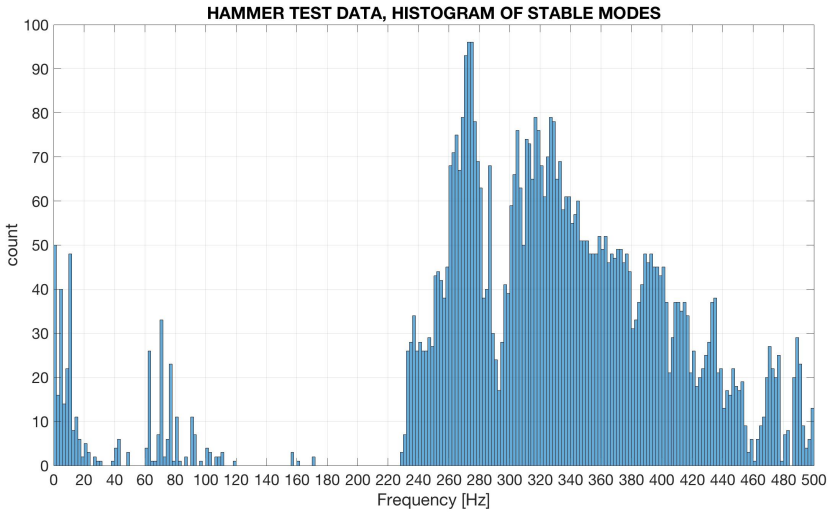
Figure 7.3: Histograms of stable mode count



(a) Measurements performed with 75kg



(b) Measurements performed with 100kg



(c) Measurements performed with impact hammer

Figure 7.4: Histograms of stable mode count

7.3 Analysis algorithm composition

This section presents the composition for the analysis algorithm. To increase the influence of the added mass with respect to spatial size of the sensor network mid 12 sensors are chosen for the analysis, see figure 9.6.

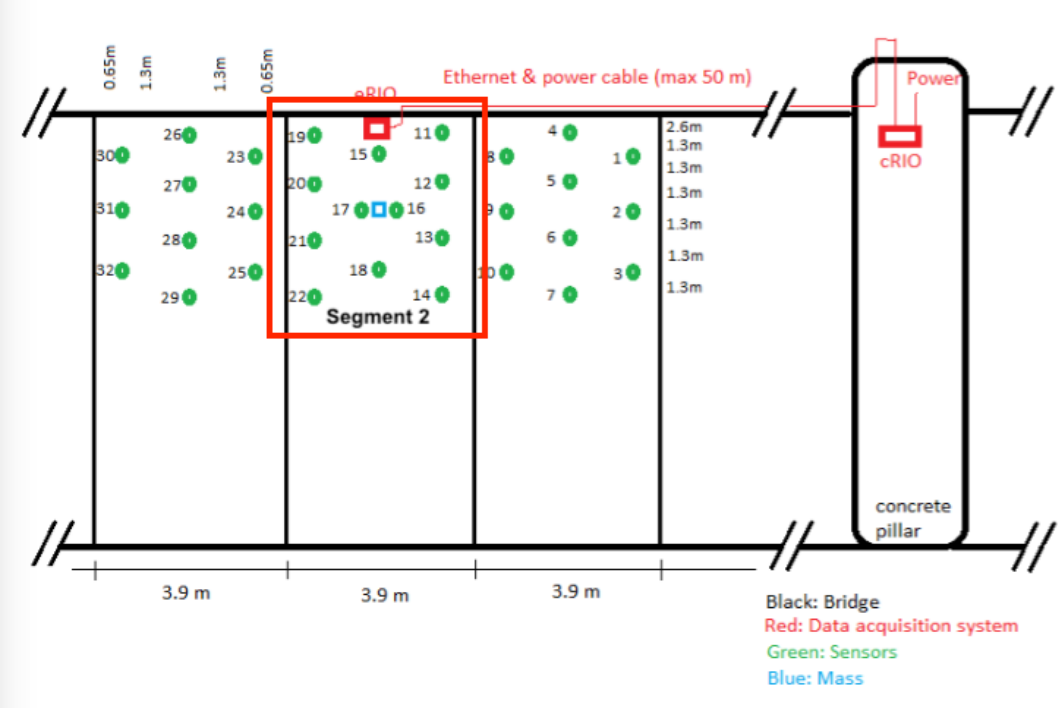


Figure 7.5: Sensors chosen for the level 1 analysis

Analysis algorithm is based on the Monte Carlo algorithm. For the specified added mass data storage (0kg-25kg-50kg-75kg-100kg), measurements samples are randomly taken and proceeded to the identification analysis. The given step completes one run of the algorithm.

The algorithm loop is based on the repetition of randomly picking data samples that will be proceeded to the identification analysis. The given algorithm concept was tested for optimality, and the 25 runs per added mass group showed sufficient results. Generally, the algorithm was tested for up to 200 runs, which results show greater stability, but are much more computationally expensive.

Data preprocessing:
1. For 1 run inside the algorithm, data samples are randomly picked in the amount that exceeds 500s of vibration measurements (data samples together).
2. To the chosen data samples, a bandpass filter of 60-75Hz is applied. The given frequency region was previously determined as a reliable high-frequency region.
3. Considering the established frequency region (high) for the analysis, data is segmented to the sample size of 5s. The given step is a preprocessing step for the probabilistic filtering.
4. In total 100 data samples (5s in length) are proceeded to the probabilistic filtering. The probabilistic filtering is applied in two schemes, with and without the order reduction. The reasons for the given double scheme will be further discussed in the results section.
5. Finally, the data is preprocessed and proceeded to the identification analysis. The product of the preprocessing step is one signal per sensor. For the 12 chosen sensors, signals are submitted to the identification analysis.

Identification analysis:
The identification analysis are based on the FDD and the data driven SSI. The output of the FDD and SSI is stored, and 1 run of the algorithm is done.

Algorithm loop:
The given run is performed 25 times per added mass group. After the algorithm is done, the outputs are post-processed with 1D Kalman filter.

Two groups of data are made, 0kg-50kg-75kg-100kg and 25kg-50kg. The data group of 25kg-50kg is generated on 28th of March, and it is separated from the group 0kg-50kg-75kg-100kg as analysis showed unstable behaviour (disagreement) between FDD and SSI identification for that data group. Initial conclusion for such a behaviour were related to the environmental conditions, but not enough information is gathered to make a valid arguments.

Detailed flowchart of the analysis algorithm is presented in figure 7.6 on the next page.

▼ **Reasons for the given analysis concept**

- Added mass 25kg presents 0.003125% with respect to 800t bridge
- Added mass 25kg presents 0.19% with respect to 13t sensor segment 2
- Goal is to detect 0.19% of structural change
- The load is unknown
- The variation in added mass is 25kg, the variation in mass of the unknown load ranges from 200kg motorcycle to 15t trucks
- Low literature support on the behaviour of the bridge structures in "high" frequency

Post-processing parameters:
The stored data of the 25 run algorithm is post-processed with 1D Kalman filter (see Chapter Mathematical tools). The input parameter for a given statistical post-processing method is measurement error. The measurement error was calibrated through variation of values from 0 to 2Hz, and observation of the results. The final measurement error value was established from Level 2 analysis results, see figure 8.3 on page 91, as a value of 0.6Hz. The purpose of such a post-processing method is to follow stability of analysis algorithm with respect to a number of the performed runs.

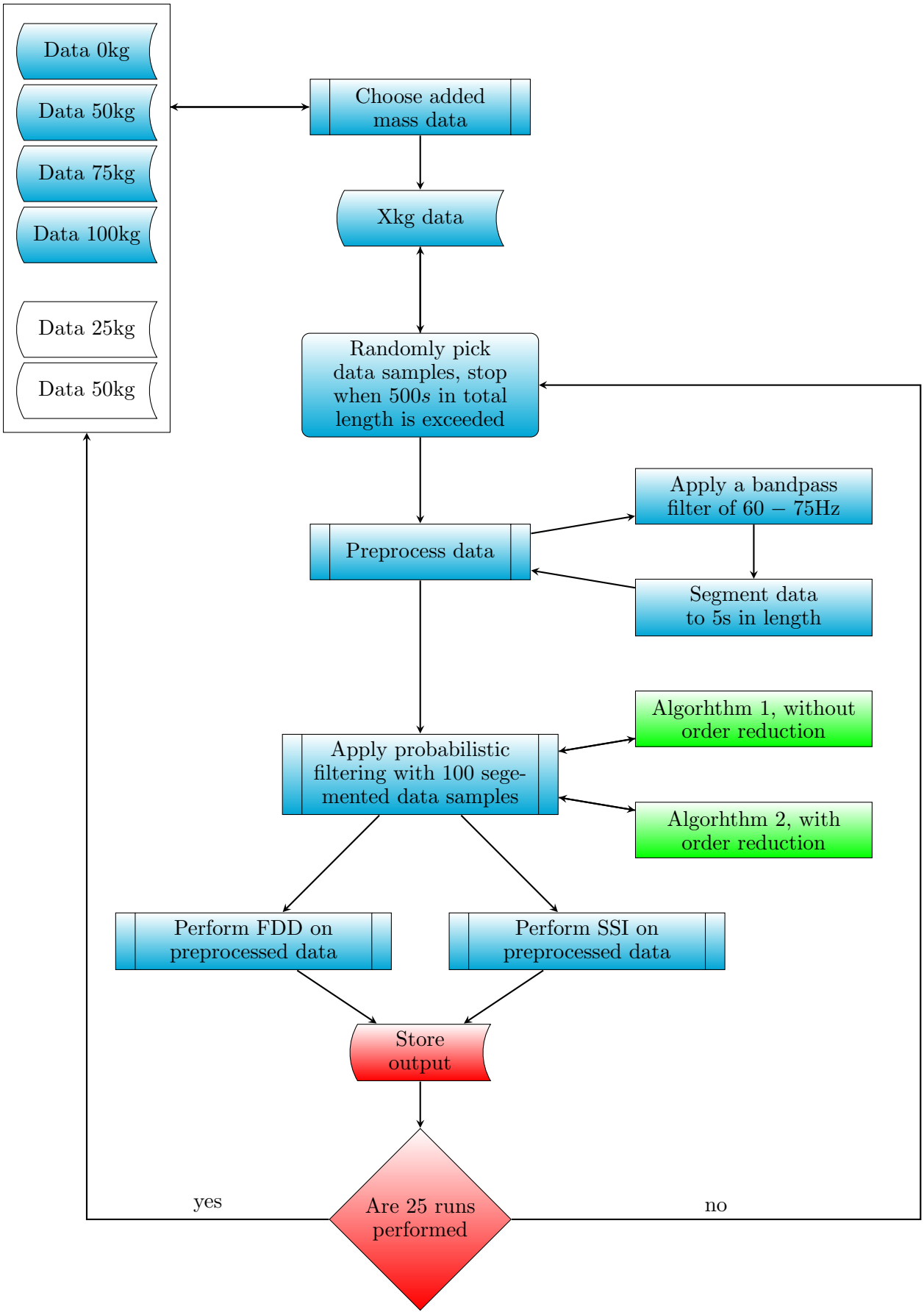


Figure 7.6: Analysis algorithm composition

7.4 Analysis output

In this section the results of the previously described analysis will be presented. As an unanswered question, reason for double scheme regarding the probabilistic filtering (PF) was left. The PF assumes that the system (transfer function) generating the output accelerations is constant for variation of the excitation. The targeted frequency region showed high sensitivity, which was concluded as systems changes due to variation of the excitation mass (the unknown traffic load), violating the constant transfer function assumption.

From the given analysis the most probable mode is determined, which is clearly observed from the FDD first singular value plots.

The assumption was that PF will damp out possible structural changes due to variation of the vehicle added mass. The given assumption holds, but the damped behaviour can be observed.

From the FDD second singular value plot variation of the structural behaviour is observed for different algorithm runs. The given behaviour is concluded as structural sensitivity to variation in the excitation mass, which is more expressed for the reduced order probabilistic filtering.

The SSI shows ability to detect the damped modes, in agreement with the FDD second singular value plot. The end result of both reduced and unreduced probabilistic filtering is in agreement. Both schemes are applied, as the unreduced method showed smoother detection of the most probable mode and the reduced order method is necessary to conclude the identified mode shapes.

7.4.1 Unreduced order probabilistic filtering output

The analysis are performed with the algorithm concept as presented in the figure 7.6 on the previous page. Results for the data group 0kg-50kg-75kg-100kg are presented in this section. Results for the data group, 25kg-50kg are provided in appendix A1, as mentioned this data group is separated as results show disagreement of FDD and SSI. Mainly FDD singular values are low with addition of SSI not being able to detect modes. Additional analysis are required to identify the reason of the corruption of this data group. Initial assumption was made towards environmental conditions which did not hold. Additional comments are left for the Conclusion and Recommendations chapter.

The full output of the 25 runs, for the described analysis algorithm is presented in the appendix A1. In this subsection examples of the outputs will be presented, ending with the post-processing of the results. Example of the PF signal is presented in the figure 7.7 on the following page. Examples of the FDD and the SSI output can be seen in figures 7.9 on page 76, and 7.10 on page 77.

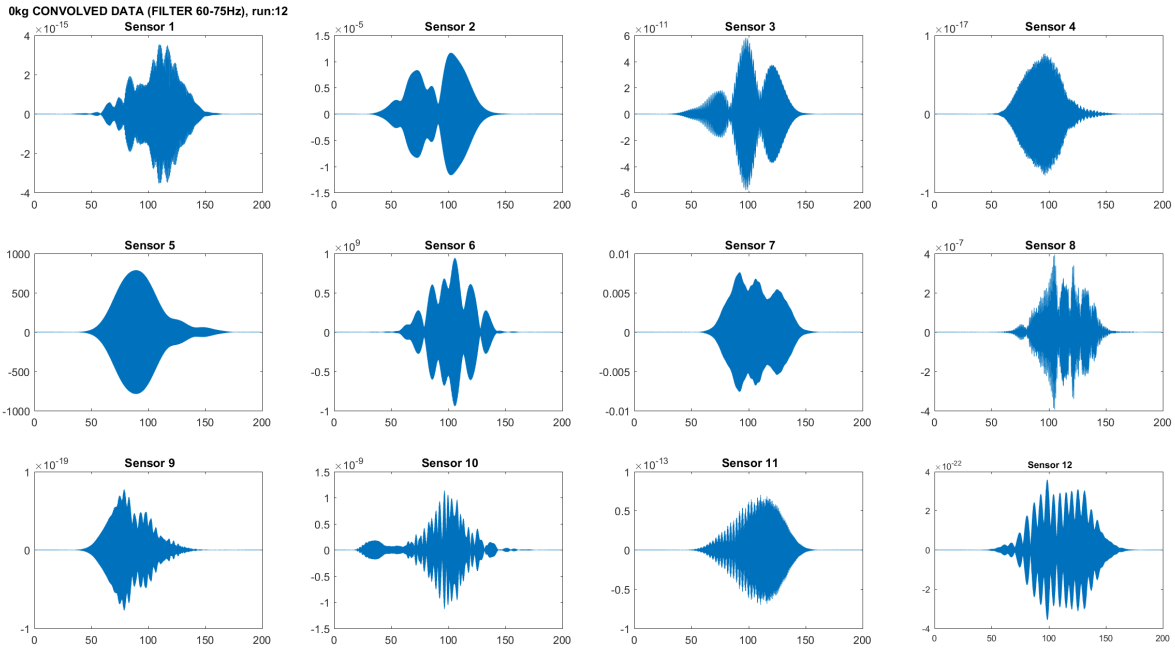


Figure 7.7: Example of the unreduced order PF signal

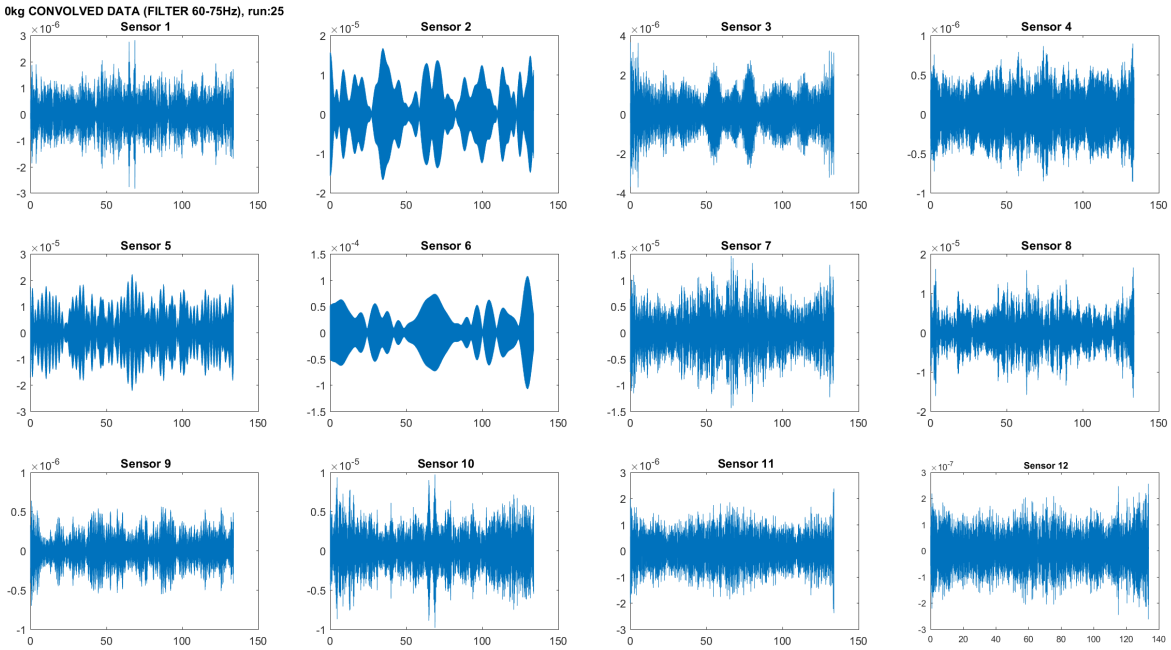
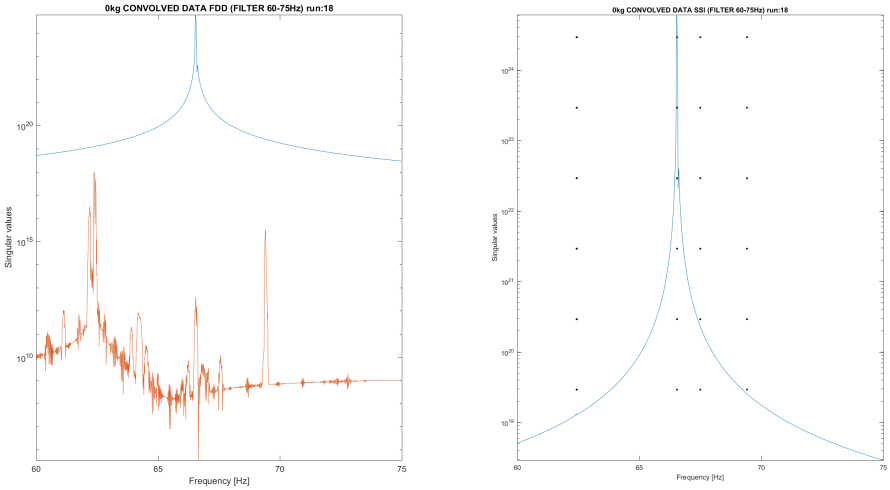
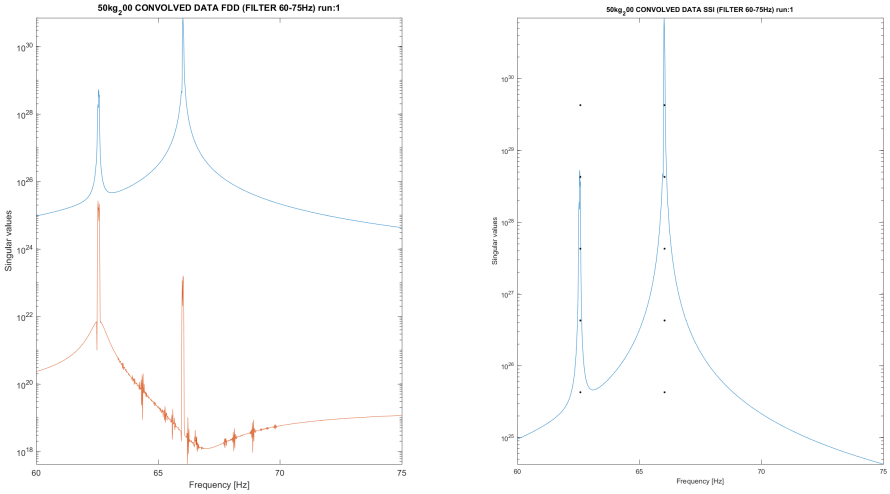


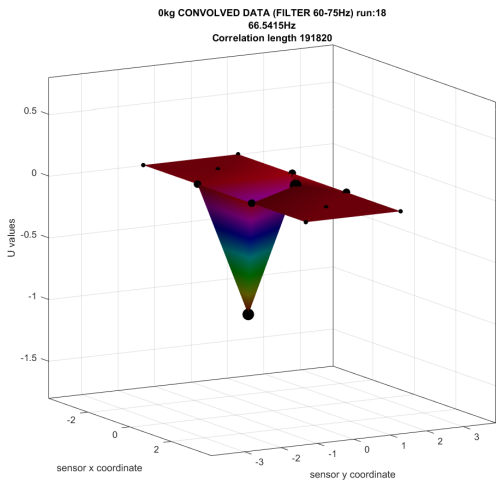
Figure 7.8: Example of the reduced order PF signal



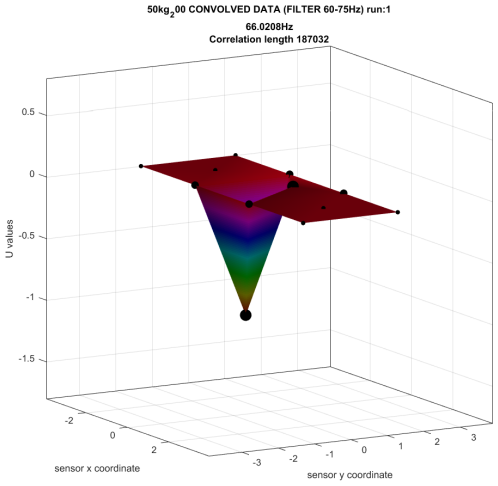
(a) Example of FDD and SSI output for 0kg data



(b) Example of FDD and SSI output for 50kg data

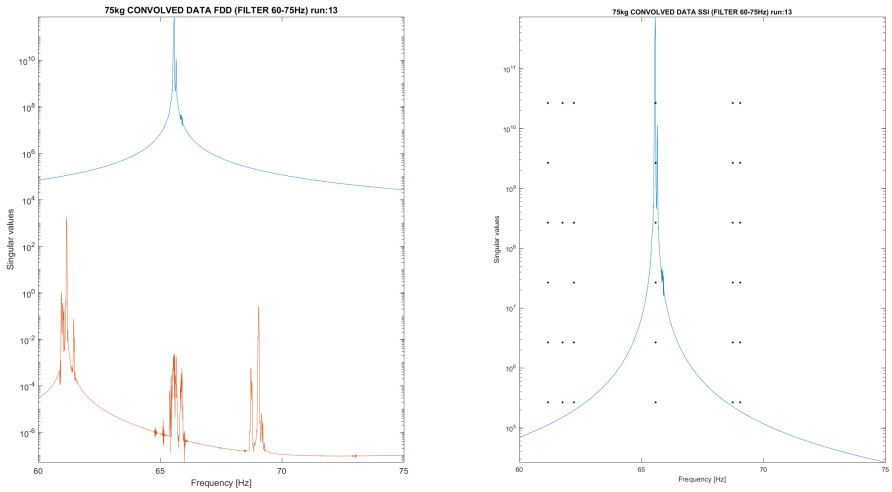


(c) Related identified mode shape 0kg

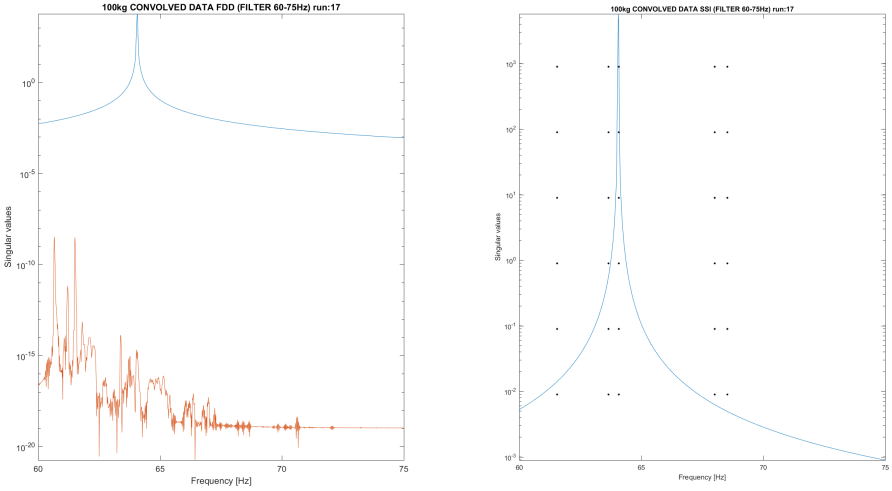


(d) Related identified mode shape 50kg

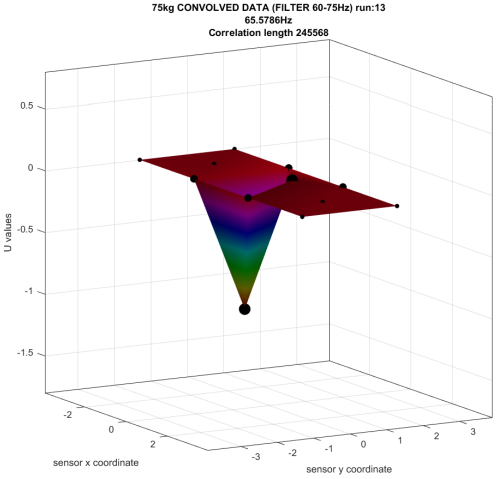
Figure 7.9: Example of FDD and SSI output for 0kg and 50kg



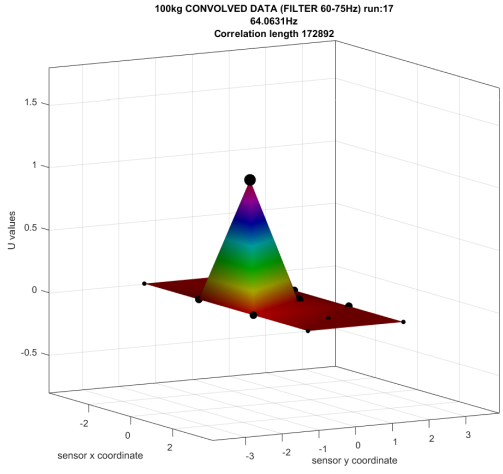
(a) Example of FDD and SSI output for 75kg data



(b) Example of FDD and SSI output for 100kg data



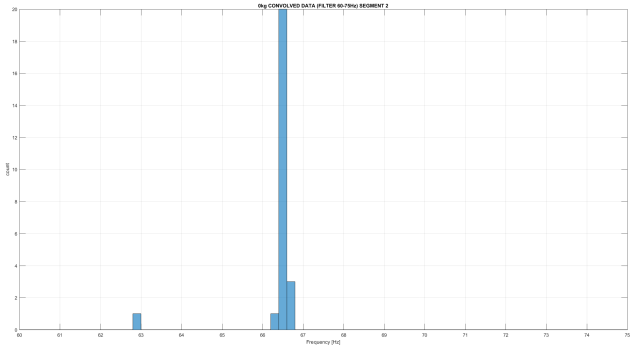
(c) Related identified mode shape 75kg



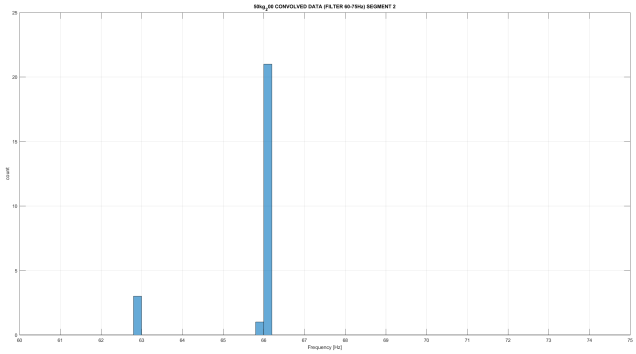
(d) Related identified mode shape 100kg

Figure 7.10: Example of FDD and SSI output for 75kg and 100kg

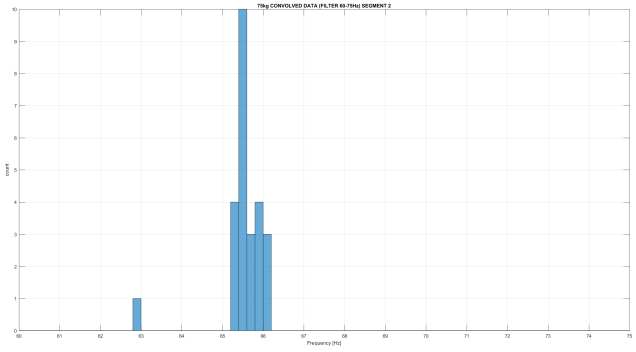
Based on the 25 runs, histograms of the identified most dominant modes, from the FDD first singular value plot are formed, observe figure 7.11.



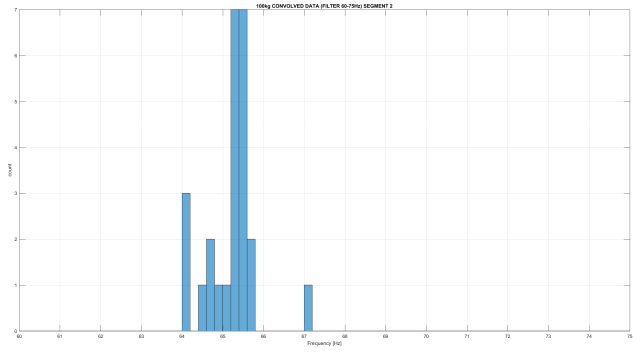
(a) Histogram for 0kg data



(b) Histogram for 50kg data



(c) Histogram for 75kg data



(d) Histogram for 100kg data

Figure 7.11: Histograms of identified FDD modes

7.4.2 Unreduced order probabilistic filtering result

From the output examples of the FDD and the SSI, revise figures 7.9 on page 76, and 7.10 on page 77, it can be seen that the most probable mode has a smooth identification. Additionally, from the SSI stable poles it is observed that deviations in the transfer functions are identified.

Based on the output of the 25 runs, 1D Kalman filter is used to statistically post-process the FDD obtained results, observe figure 7.12. From the given figure, the distinction between data with 0kg-50kg-75kg-100kg is observed.

Conclusion:
It is concluded that the unreduced order PF algorithm identifies the added masses with relation to the most probable FDD identified mode. With the values 0kg-66.5Hz, 50kg-66.1Hz, 75kg-65.6Hz and 100kg-65.2Hz.

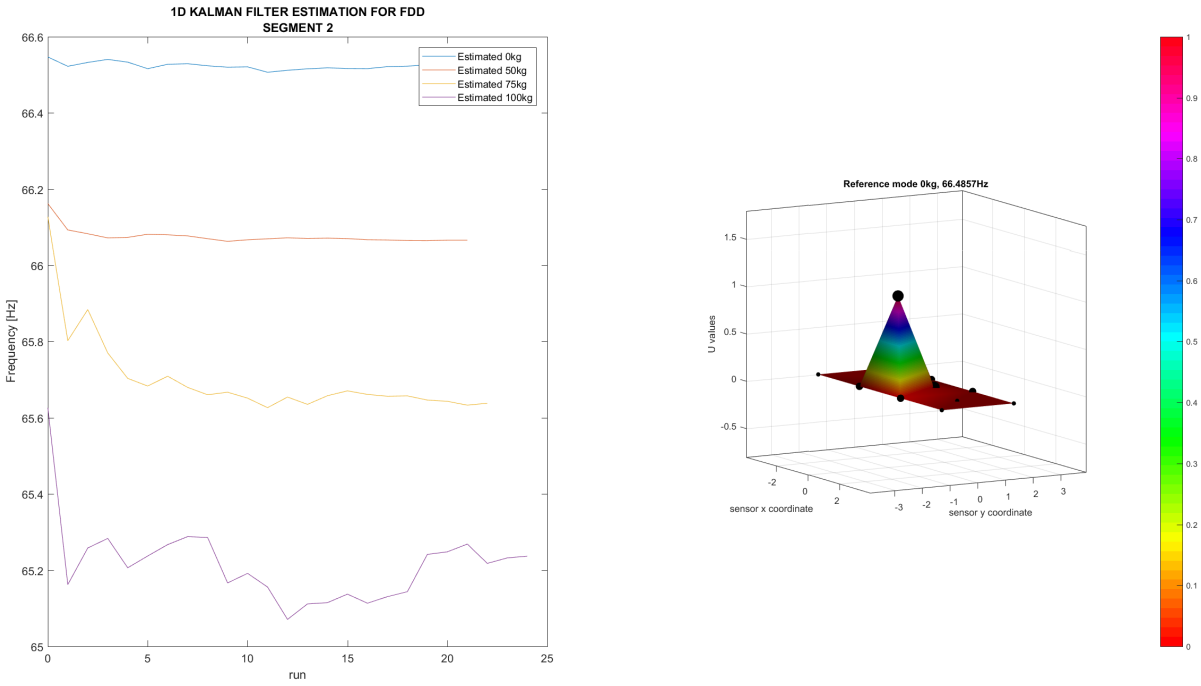
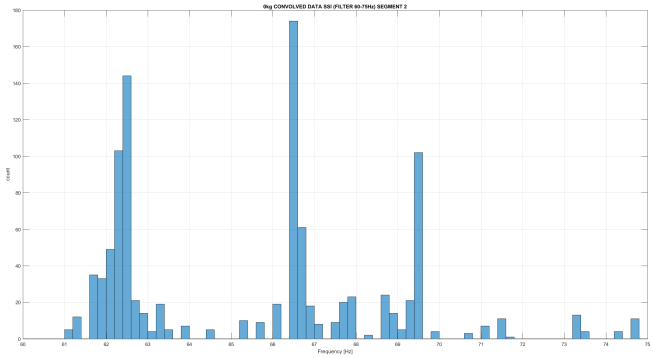
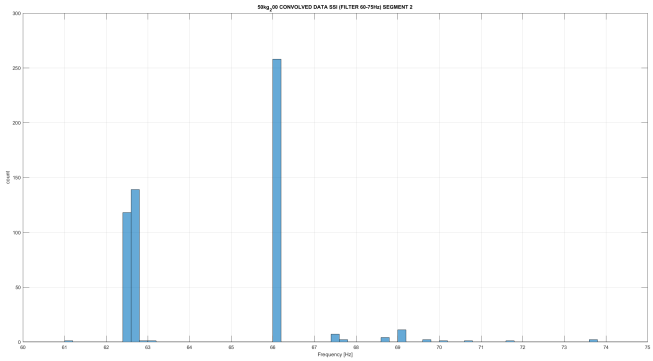


Figure 7.12: 1D Kalman filter of the obtained FDD results

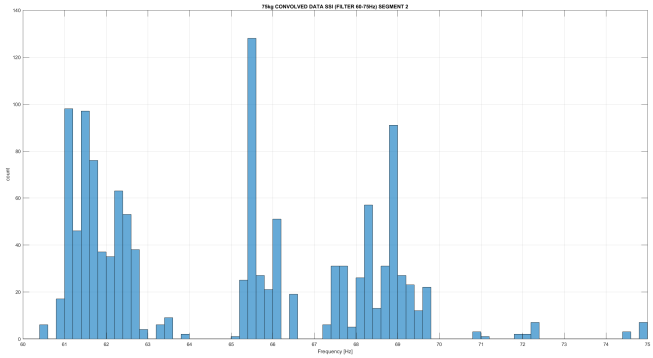
The histograms of the identified SSI modes (with respect to frequency) are presented in figure 7.13 on the next page. It is observed that SSI identifies the damped transfer functions. For the 0kg-50kg-75kg data, the modes with the highest count are in agreement with 1D Kalman filter estimation. For the 100kg data, larger deviations in the identified eigen-structure are present.



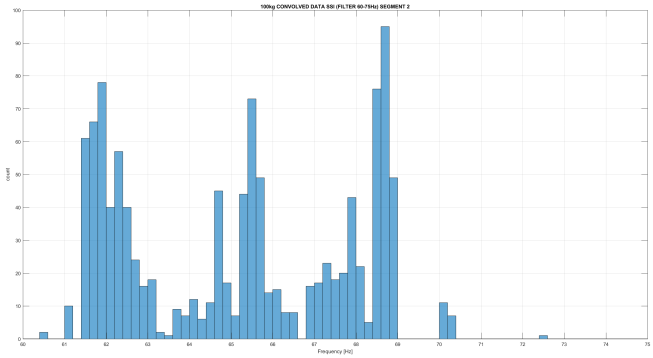
(a) Histogram for 0kg data



(b) Histogram for 50kg data



(c) Histogram for 75kg data



(d) Histogram for 100kg data

Figure 7.13: Histograms of identified SSI modes

7.4.3 Reduced order probabilistic filtering output

In this subsection the output of the reduced order probabilistic filtering algorithm is presented.

In theory, averaging was related to number of performed convolutions n, see equation (6.43 revisited).

$$\left(\prod_{i=1}^{n} \widetilde{y}_{ip}(\omega)\right)^{\frac{1}{n}} \approx \left[\widetilde{h_{p1}}(\omega)\ \widetilde{h_{p2}}(\omega)\ \cdots\ \widetilde{h_{pm}}(\omega)\right]_{1\times m} const^{\frac{1}{n}} \begin{bmatrix} 1 \\ 1 \\ \vdots \\ 1 \end{bmatrix}_{m\times 1} \qquad \text{(6.43 revisited)}$$

Focusing on physical and numerical aspect of the analysis we need to consider variation of transfer function (not constant due to structural changes) and signal samples with no activity. From data characterisation tables we observe that frequency content of interest (60-75Hz) for the analysis is not excited in every measurement. The intention is to detect structural changes, so transfer function is not constant. Analysis are performed with 100 convolutions of 5s signal samples. When time domain of signals is observed, it is concluded that some number of 5s samples will contain no information as there was no recorded excitation. In conclusion, what needs to be performed is estimation of order reduction, which will be smaller than number of convolutions, to recover the most probable mode and it's shape.

We came to the initial question of the reduced order probabilistic filtering, the choice of the reduction order. With revision of the tables 3.2 on page 19, to 3.7 on page 20, it can be observed what amount of the data contains the stable modes in the region of 50-75Hz. The given frequency region is active in the amount of $50-60\%$ with respect to the amount of the performed measurements. Additional important consideration is that the data is segmented to 5s samples. Observe figures 7.14 to 7.16 on the next page, where the examples of the acceleration time domain plots with relation to the FDD plots are presented (raw data).

Considering the amount of data with activity in the targeted frequency region, the activity in the 5s segmented samples, the 100 samples submitted to PF , and the possible deviations in the transfer functions, it is concluded as optimal to use the order reduction of 10 (the root of 10).

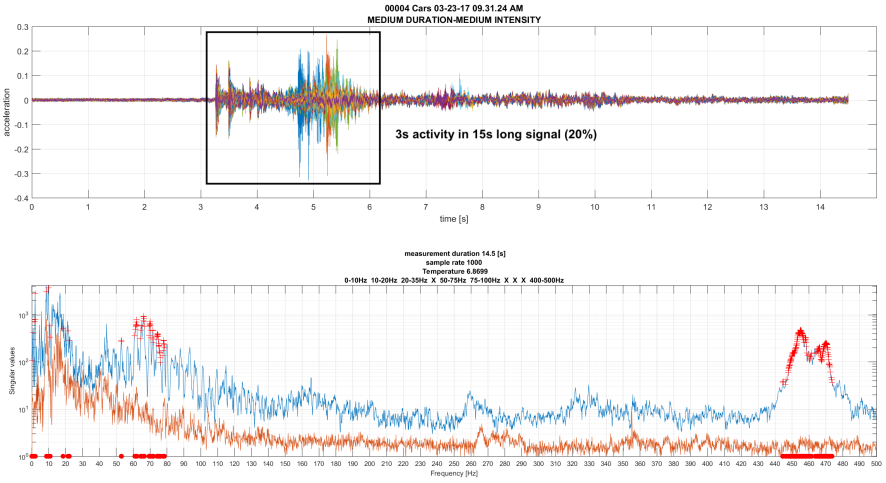


Figure 7.14: Example 1 of the time domain plot and the related FDD plot

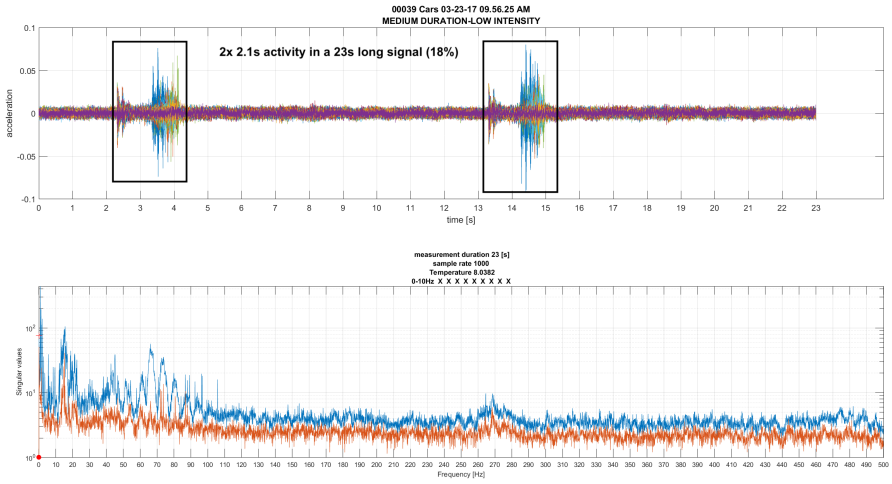


Figure 7.15: Example 2 of the time domain plot and the related FDD plot

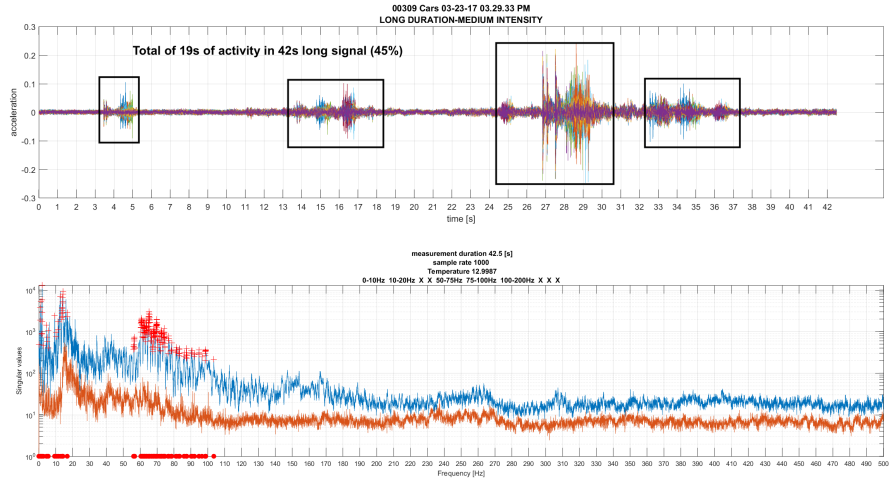
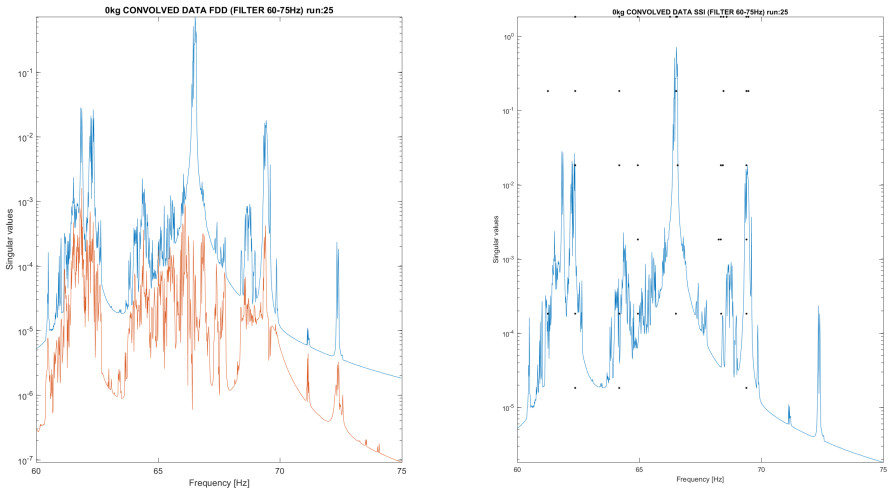


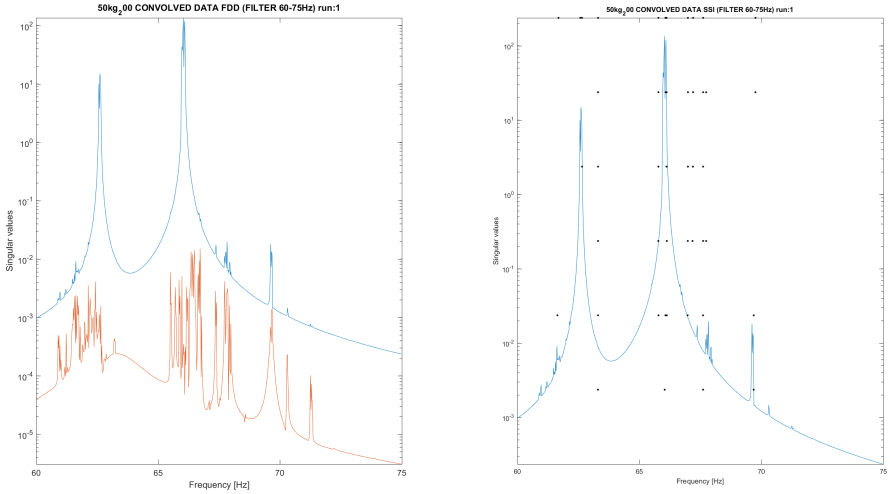
Figure 7.16: Example 3 of the time domain plot and the related FDD plot

The analysis are performed with the algorithm concept as presented in the figure 7.6 on page 73. Results for the data group 0kg-50kg-75kg-100kg are presented in this section. Results for the data group, 25kg-50kg are provided in appendix A2, as mentioned this data group is separated as results show disagreement of FDD and SSI. Mainly FDD singular values are low with addition of SSI not being able to detect modes. Additional analysis are required to identify the reason of the corruption of this data group. Initial assumption was made towards environmental conditions which did not hold. Additional comments are left for the Conclusion and Recommendations chapter.

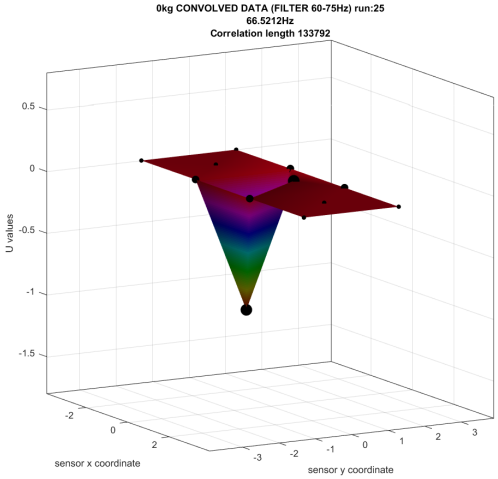
The full output of the 25 runs, for the described analysis algorithm is presented in the appendix A2. In this subsection examples of the outputs will be presented, ending with the post-processing of the results. Example of the reduced order PF signal is presented in the figure 7.8 on page 75. Examples of the FDD and the SSI output can be seen in figures 7.17 on the following page, and 7.18 on page 84.



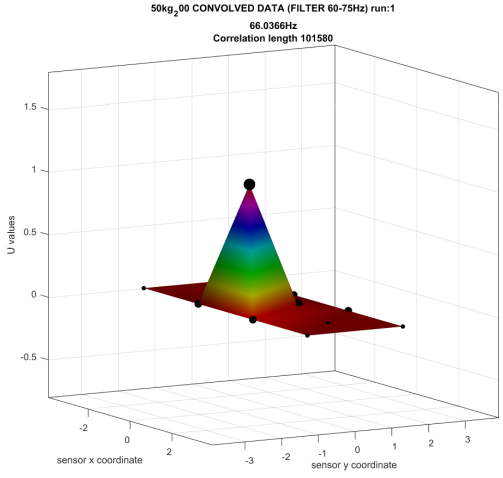
(a) Example of FDD and SSI output for 0kg data



(b) Example of FDD and SSI output for 50kg data

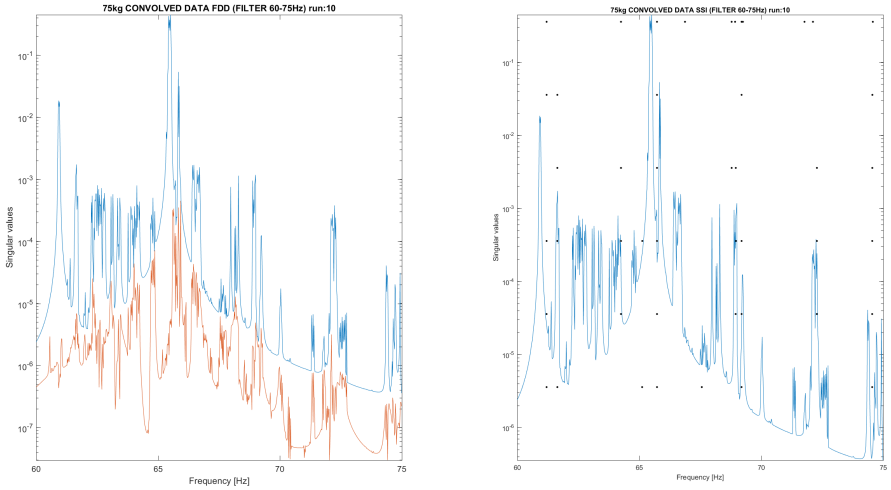


(c) Related identified mode shape 0kg

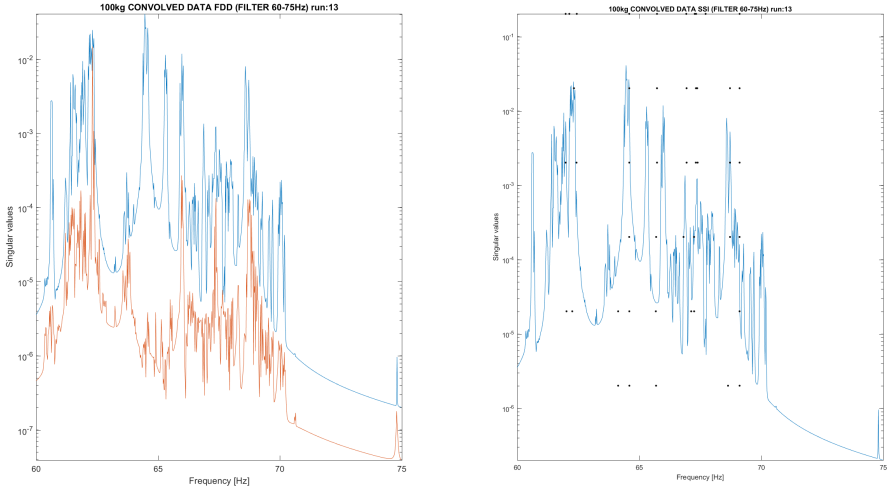


(d) Related identified mode shape 50kg

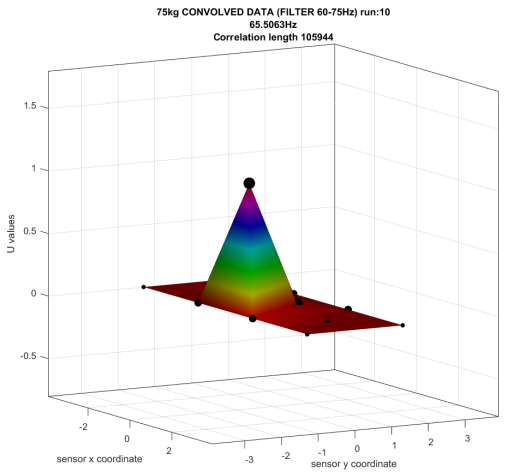
Figure 7.17: Example of FDD and SSI output for 0kg and 50kg



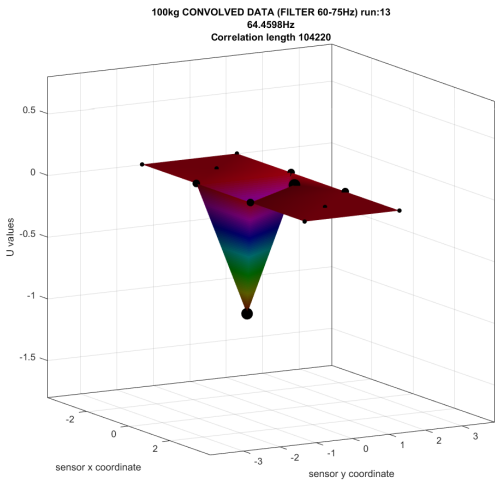
(a) Example of FDD and SSI output for 75kg data



(b) Example of FDD and SSI output for 100kg data



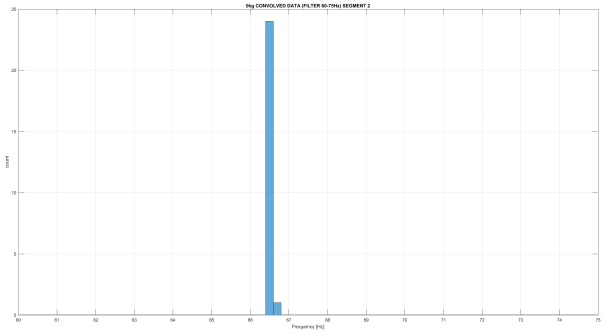
(c) Related identified mode shape 75kg



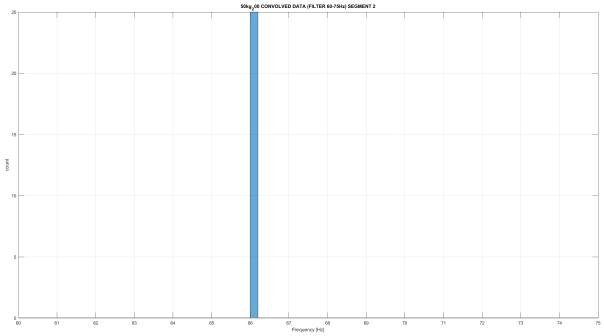
(d) Related identified mode shape 100kg

Figure 7.18: Example of FDD and SSI output for 75kg and 100kg

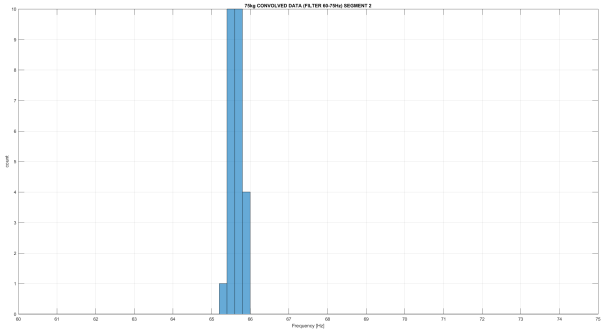
Based on the 25 runs, histograms of the identified most dominant modes, from the FDD first singular value plot are formed, observe figure 7.19.



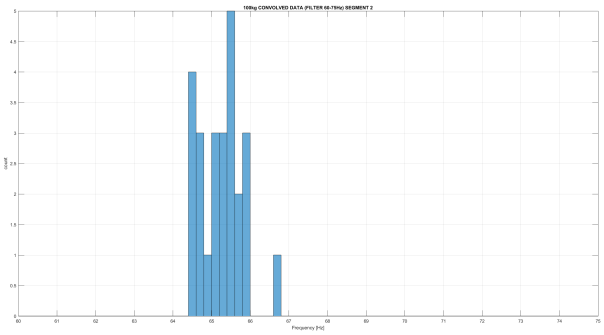
(a) Histogram for 0kg data



(b) Histogram for 50kg data



(c) Histogram for 75kg data



(d) Histogram for 100kg data

Figure 7.19: Histograms of identified FDD modes

7.4.4 Reduced order probabilistic filtering result

From the output examples of the FDD and the SSI, revise figures 7.17 on page 83, and 7.18 on page 84, it can be concluded that the most probable identified mode does not have a smooth identification, as for the unreduced order PF. Additionally, from the SSI stable poles it is observed that deviations in the transfer functions are larger, than for results of the unreduced order PF. The identified mode shapes of the reduced order PF show similar shapes as the identified mode shapes of the unreduced order PF (revise figures 7.9c on page 76, 7.9d on page 76, 7.10c on page 77, 7.10d on page 77, and figures 7.17c on page 83, 7.17d on page 83, 7.18c on page 84, 7.18d on page 84). It is considered that the identified modes present local modes of small area influence.

Based on the output of the 25 runs, 1D Kalman filter is used to statistically post-process the FDD obtained results, observe figure 7.20. From the given figure, the distinction between data with 0kg-50kg-75kg-100kg is observed, with an agreement to unreduced order PF results.

Conclusion:
It is concluded that the reduced order PF algorithm identifies the added masses with relation to the most probable FDD identified mode. With the values 0kg-66.5Hz, 50kg-66.1Hz, 75kg-65.6Hz and 100kg-65.2Hz.

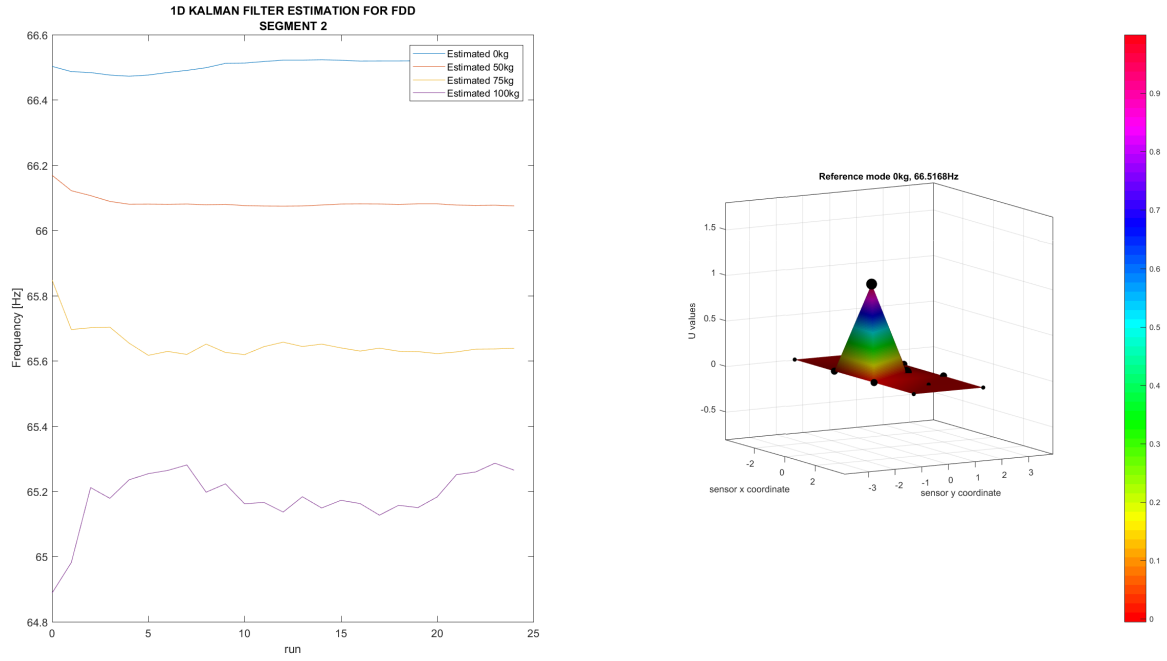
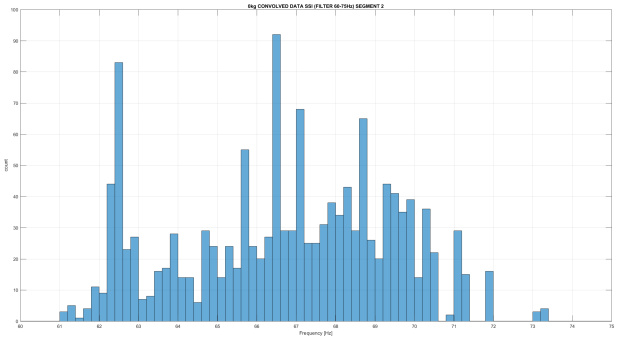
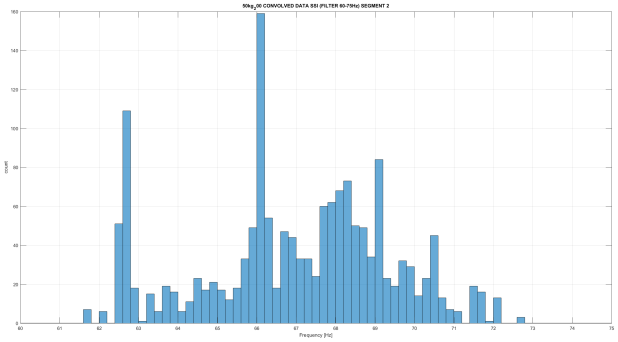


Figure 7.20: 1D Kalman filter of the obtained FDD results

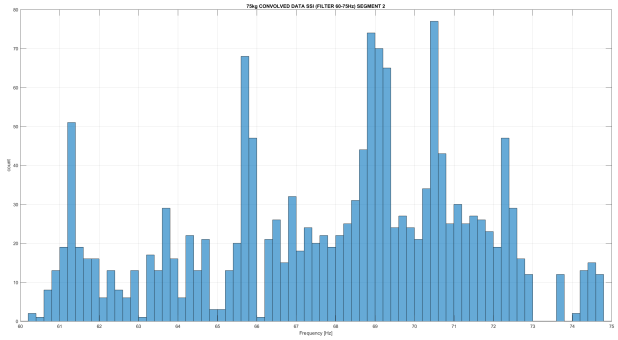
The histograms of the identified SSI modes (with respect to frequency) are presented in figure 7.21 on the following page. It is observed that SSI identifies the damped transfer functions. For the 0kg-50kg data, the modes with the highest count are in agreement with 1D Kalman filter estimation. For the 75kg-100kg data, larger deviations in the identified eigen-structure are present. For the all 4 groups of data, larger deviations are present than for the unreduced order PF.



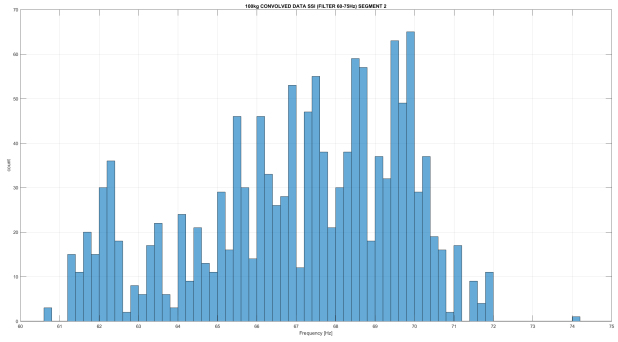
(a) Histogram for 0kg data



(b) Histogram for 50kg data



(c) Histogram for 75kg data



(d) Histogram for 100kg data

Figure 7.21: Histograms of identified SSI modes

Level 2

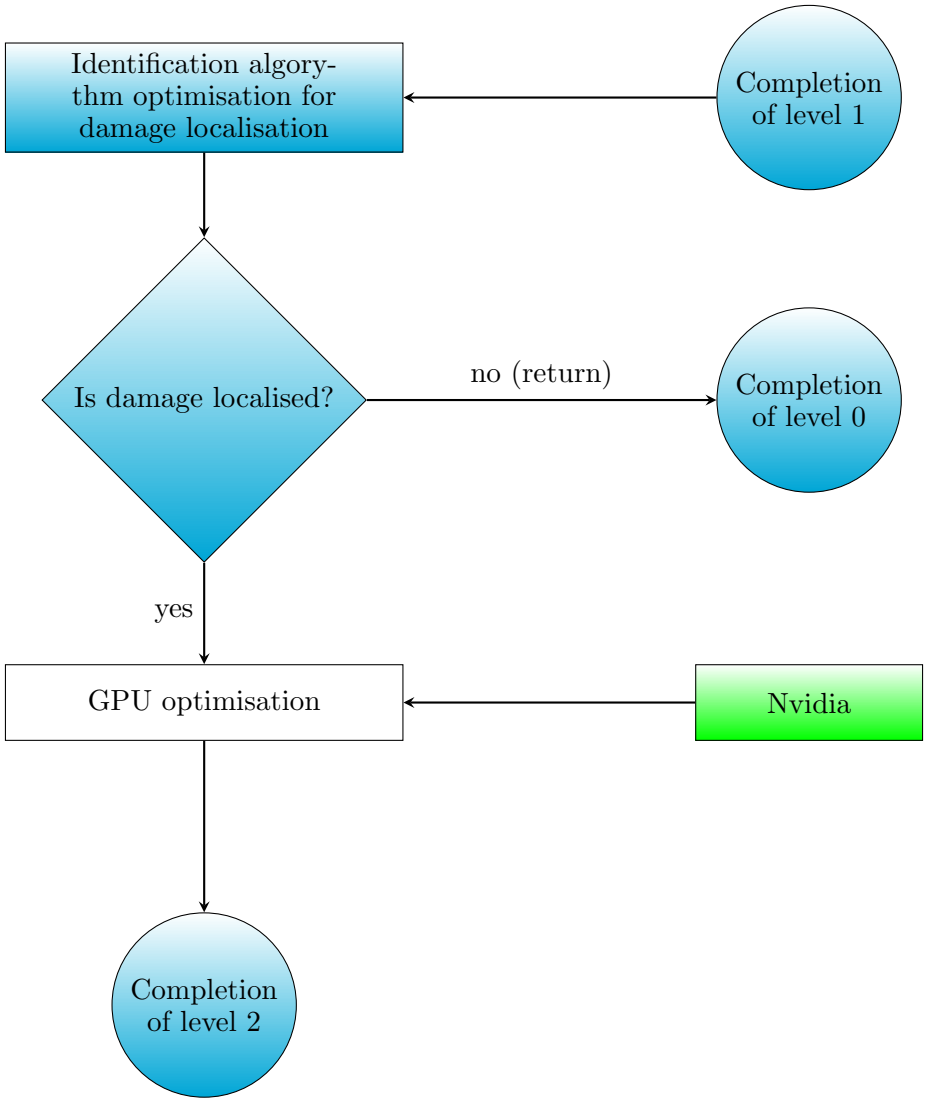


Figure L.2: Workflow of level 2

Chapter 8

Health monitoring algorithm calibration

This chapter provides SHM level 2 analysis with calibration to level 1 analysis. The final results of the chapter are related to the localisation identification.

8.1 Analysis concept

The analysis concept of the damage localisation is based on the assumption that the added mass will not influence the behaviour of the segment 1 and the segment 3 of the sensor network, see figure 8.1.

The vibration measurements generated on the segment 1 and the segment 3 are submitted to the algorithm that was presented in previous chapter, see figure 7.6 on page 73.

The goal of the analysis is to conclude whether added masses influence the behaviour of the segment 1 and the segment 3.

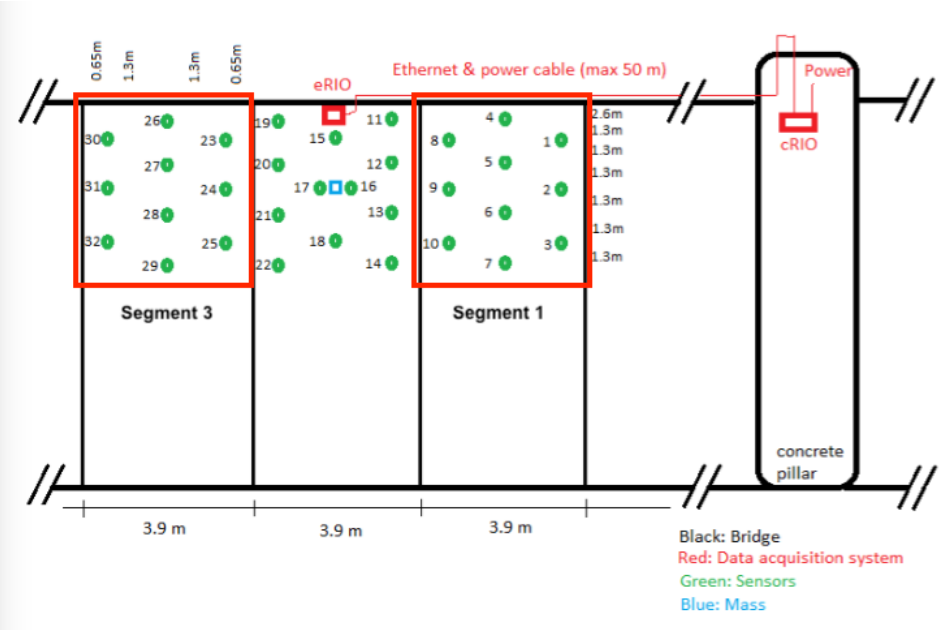


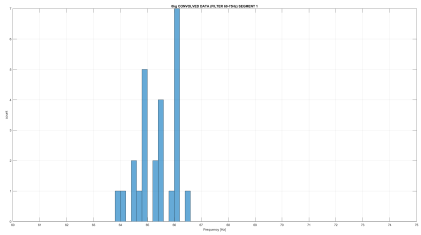
Figure 8.1: Segment 1 and Segment 3 of the sensor network

8.2 Damage localisation results

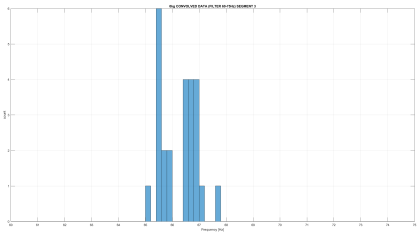
In this section, the results of the level 2 analysis are presented. Analysis are performed with the two PF schemes, the unreduced order PF and the reduced order PF. The presented results are related to the data group of 0kg-50kg-75kg-100kg. Results for the data group, 25kg-50kg are provided in appendix A3, this data group is separated as results show disagreement of FDD and SSI. Additional analysis are required to identify the reason of the corruption of this data group. Initial assumption was made towards environmental conditions which did not hold. Additional comments are left for the Conclusion and Recommendations chapter.

8.2.1 Unreduced order probabilistic filtering results

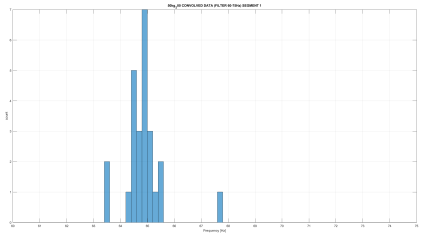
As output of the analysis algorithm was described in detail in previous chapter, full 25 runs of the algorithm will be presented in appendix A3. In the figure 8.2 histograms of the FDD most dominant mode count, for the segment 1 and segment 3, are presented.



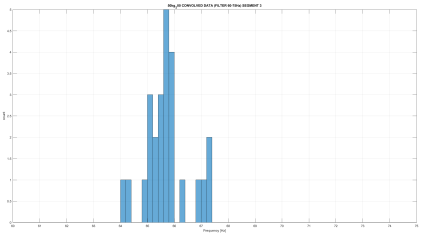
(a) Segment 1, 0kg



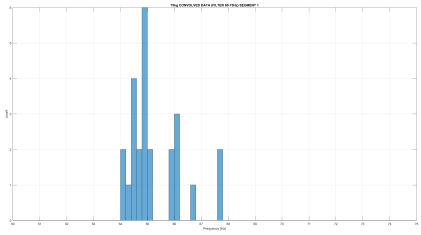
(b) Segment 3, 0kg



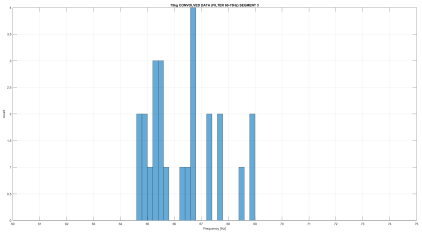
(c) Segment 1, 50kg



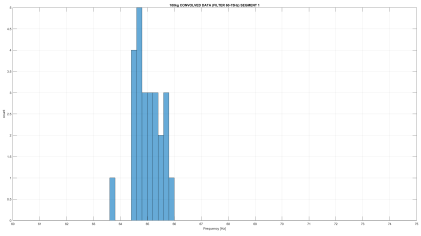
(d) Segment 3, 50kg



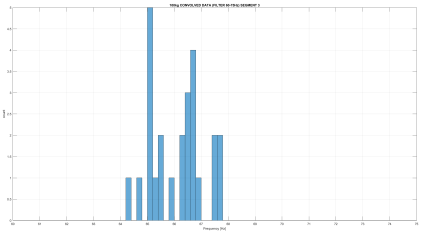
(e) Segment 1, 75kg



(f) Segment 3, 75kg



(g) Segment 1, 100kg

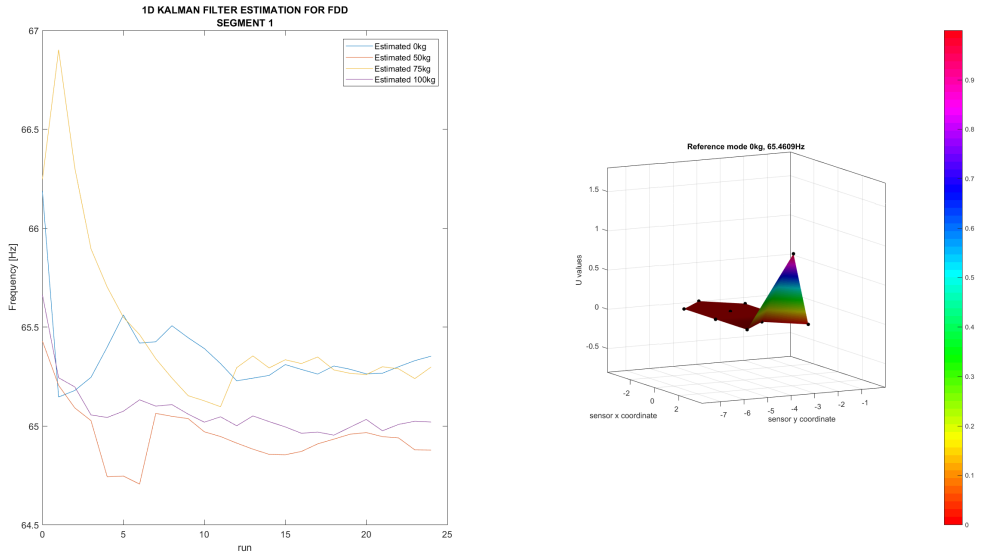


(h) Segment 3, 100kg

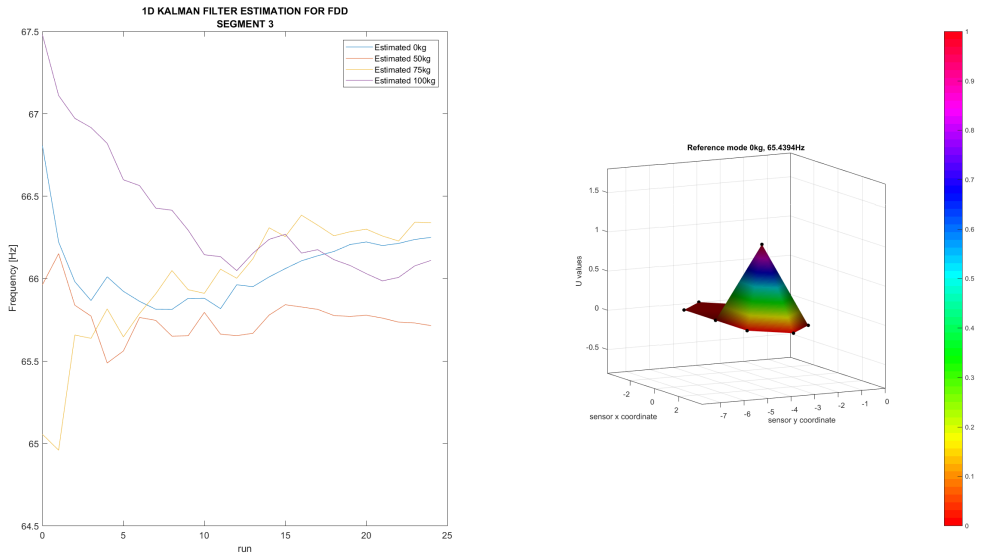
Figure 8.2: Histograms of identified FDD modes

From the figure 8.2 on the previous page, it is observed that the deviation in the identified modes is higher than ones obtained for the segment 2, see figure 7.11 on page 78.

Based on the output of the 25 runs, 1D Kalman filter is used to statistically post-process the FDD obtained results, observe figure 8.3. From the given figure, the distinction between data is not related to the added mass value. The relation of the identified frequency to added mass, for segment 1 is 0kg-65.35Hz, 50kg-64.9Hz, 75kg-65.3Hz, 100kg-65Hz, and for the segment 3 0kg-66.25Hz, 50kg-65.7Hz, 75kg-66.4Hz, 100kg-66.1Hz.



(a) Segment 1



(b) Segment 3

Figure 8.3: 1D Kalman filter estimation of the FDD most dominant mode

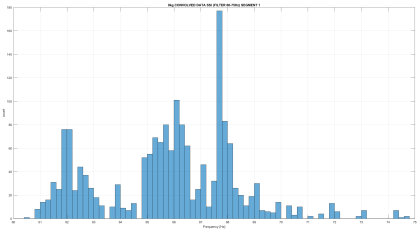
The histograms of the identified SSI modes are presented in the figure 8.4 on the following page. From the given figure, it can be clearly observed that the mode with the highest count, for the segment 1, has a value of 67.7Hz for all the added mass data. Similar distinction cannot be made for the segment 3.

Conclusion:
From the obtained results it is observed that no particular frequency is dominating in the FDD plots.

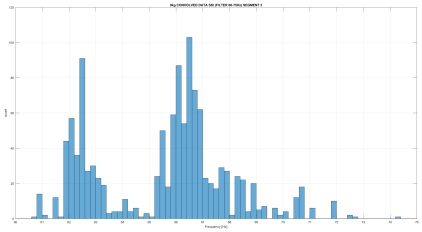
The segment 1 and the segment 3 have different spatial sensor formation from the segment 2, where obtained results showed higher stability. To be more confident in the conclusions it would be recommended that the resolution of the sensor network is higher.

It is observed that the unreduced order PF algorithm does not detect the distinction between data in relation to the added mass value. It is assumed that the segment 1 and the segment 3 behaviour is not influenced by the variation of the added masses.

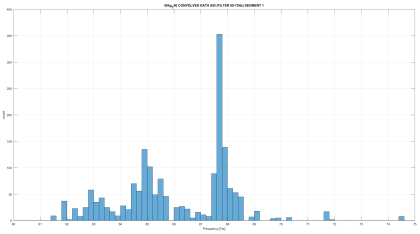
The main conclusion is that the localisation of the added mass can be related to the segment 2, as the added masses did not influence the behaviour of the segment 1 and the segment 3.



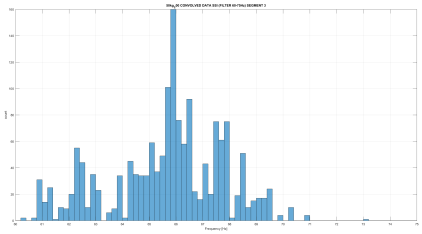
(a) Segment 1, 0kg



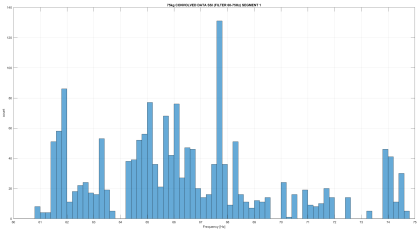
(b) Segment 3, 0kg



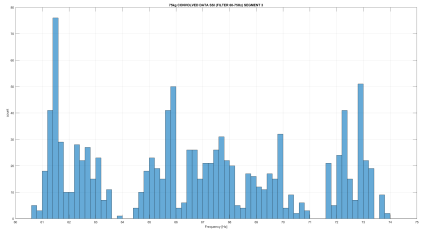
(c) Segment 1, 50kg



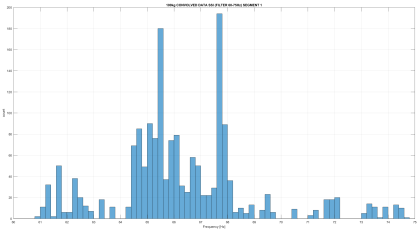
(d) Segment 3, 50kg



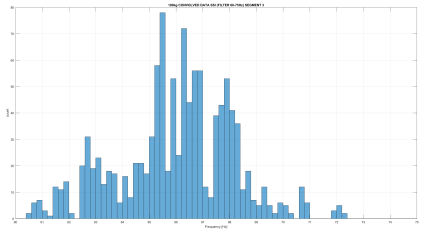
(e) Segment 1, 75kg



(f) Segment 3, 75kg



(g) Segment 1, 100kg



(h) Segment 3, 100kg

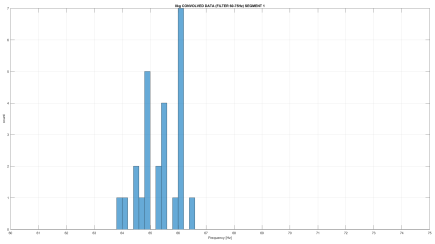
Figure 8.4: Histograms of identified SSI modes

8.2.2 Reduced order probabilistic filtering results

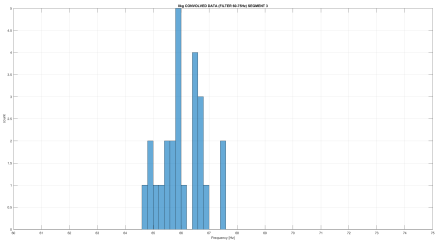
Analogue to the analysis of level 1, level 2 analysis are performed. The order of the reduction of the probabilistic filter is 10 (the root of 10).

As output of the analysis algorithm was described in detail in previous chapter, full 25 runs of the algorithm are be presented in appendix A4.

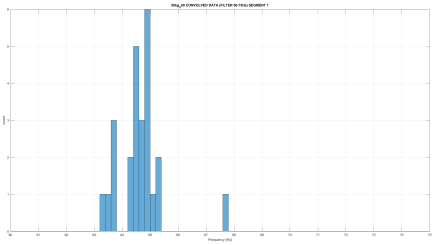
In the figure 8.5 histograms of the FDD most dominant mode count, for the segment 1 and segment 3, are presented.



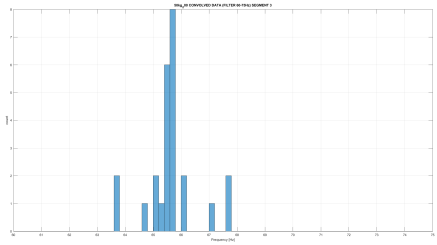
(a) Segment 1, 0kg



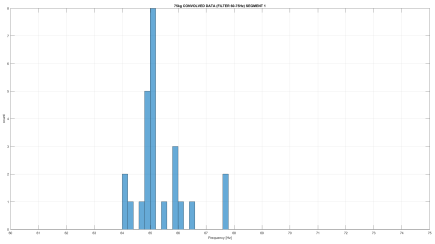
(b) Segment 3, 0kg



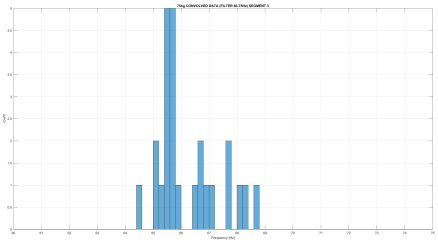
(c) Segment 1, 50kg



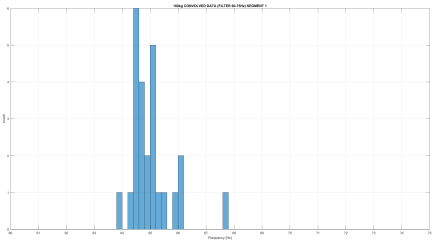
(d) Segment 3, 50kg



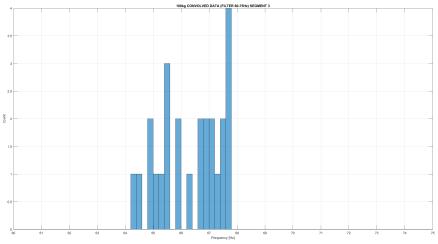
(e) Segment 1, 75kg



(f) Segment 3, 75kg



(g) Segment 1, 100kg

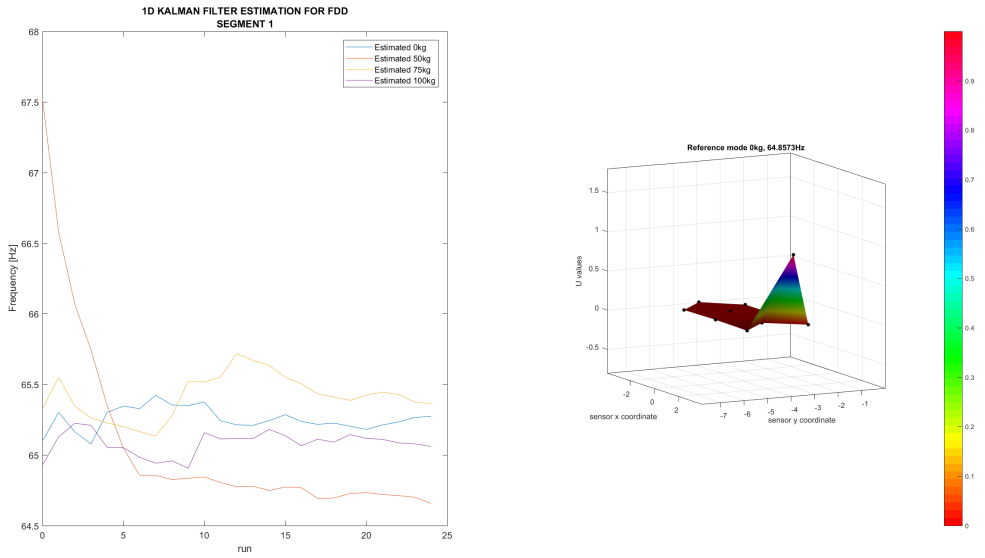


(h) Segment 3, 100kg

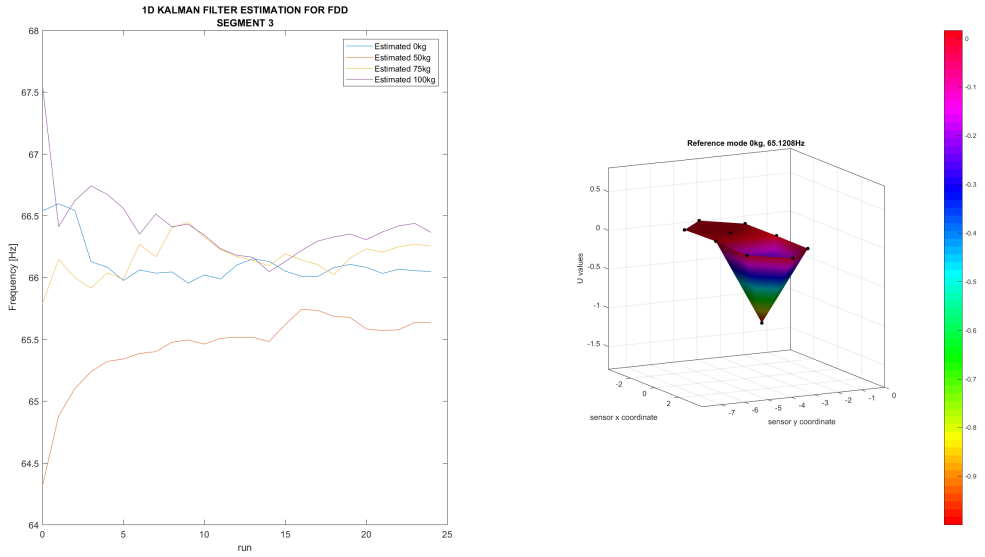
Figure 8.5: Histograms of identified FDD modes

From the figure 8.5 on the preceding page, it is observed that the deviation in the identified modes is higher than ones obtained for the segment 2, see figure 7.19 on page 85.

Based on the output of the 25 runs, 1D Kalman filter is used to statistically post-process the FDD obtained results, observe figure 8.6. From the given figure, the distinction between data is not related to the added mass value. The relation of the identified frequency to added mass, for segment 1 is 0kg-65.3Hz, 50kg-64.7Hz, 75kg-65.4Hz, 100kg-65.05Hz, and for the segment 3 0kg-66.05Hz, 50kg-65.65Hz, 75kg-66.25Hz, 100kg-66.35Hz.



(a) Segment 1



(b) Segment 3

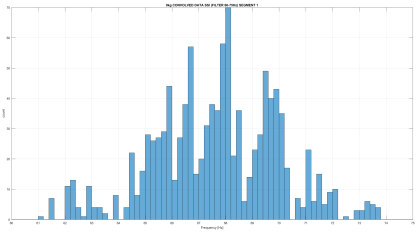
Figure 8.6: 1D Kalman filter estimation of the FDD most dominant mode

The histograms of the identified SSI modes are presented in the figure 8.7 on the next page. It is observed that SSI is recovering the damped transfer functions.

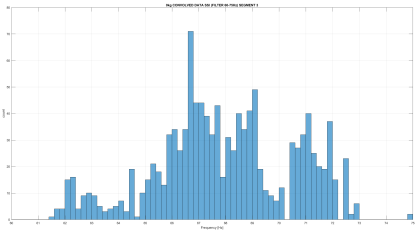
Conclusion:
The results of the reduced order PF and the unreduced order PF are in agreement. The 50kg data shows lower value trend than rest, for both algorithms. It can be concluded that frequency region of the analysis is very sensitive to the structural changes, which can be related to the variation of the excitation masses, with no transfer function dominance. The given observation can also be related to the spatial formation of the sensor network (different from the segment 2).

It is observed that the reduced order PF algorithm does not detect the distinction between data in relation to the added mass value. It is assumed that the segment 1 and the segment 3 behaviour is not influenced by the variation of the added masses.

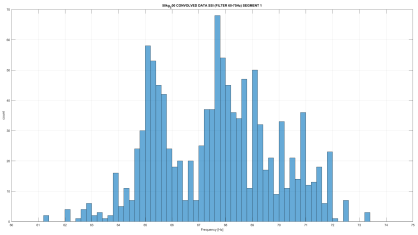
The main conclusion is that the localisation of the added mass can be related to the segment 2, as the added masses did not influence the behaviour of the segment 1 and the segment 3.



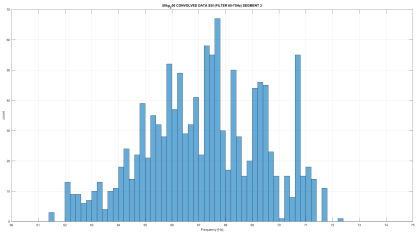
(a) Segment 1, 0kg



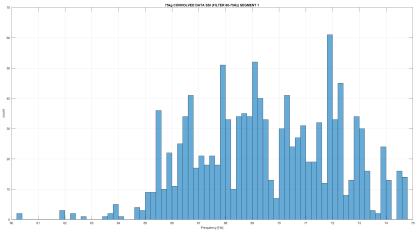
(b) Segment 3, 0kg



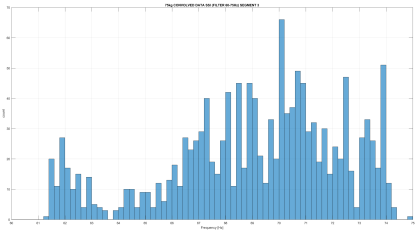
(c) Segment 1, 50kg



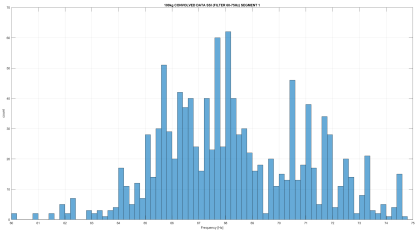
(d) Segment 3, 50kg



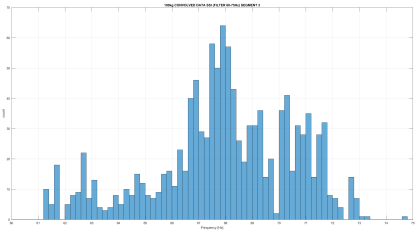
(e) Segment 1, 75kg



(f) Segment 3, 75kg



(g) Segment 1, 100kg



(h) Segment 3, 100kg

Figure 8.7: Histograms of identified SSI modes

8.3 GPU optimization

Probabilistic filtering is the most CPU expensive part of the level 1 and the level 2 analysis. As the PF is suitable for parallel optimization, this section provides proposal for the use of the general purpose graphics processing unit acceleration (GPGPU/GPU).

As I find highly attractive turning a laptop to a mini-supercomputer with the use of tunderbolt cable, see 8.8b, simple scheme for the acceleration of the PF computation with the use of one GPU is composed.



GPU	1 NVIDIA Pascal GPU
CUDA Cores	3,840
Memory Size	24 GB GDDR5
H.264 1080p30 streams	24
Max vGPU instances	24 (1 GB Profile)
vGPU Profiles	1 GB, 2 GB, 3 GB, 4 GB, 6 GB, 8 GB, 12 GB, 24 GB
Form Factor	PCIe 3.0 Dual Slot (rack servers)
Power	250 W
Thermal	Passive

(a) Nvidia Tesla P40 [3]



(b) External GPU acceleration [8]

Figure 8.8: General purpose graphics processing unit

In the figure 8.9, PF scheme for the 128 signal samples is presented. For applying PF on a sensor network with 60 sensors in total, 3840 operations are needed to be performed in the first step of the parallel algorithm. The Nvidia Tesla P40, figure 8.8a, has 3840 cuda cores with 24GB of physical memory, making it very suitable for the PF computational acceleration.

The given example is provided as a possible argument for the more efficient use of the PF method.

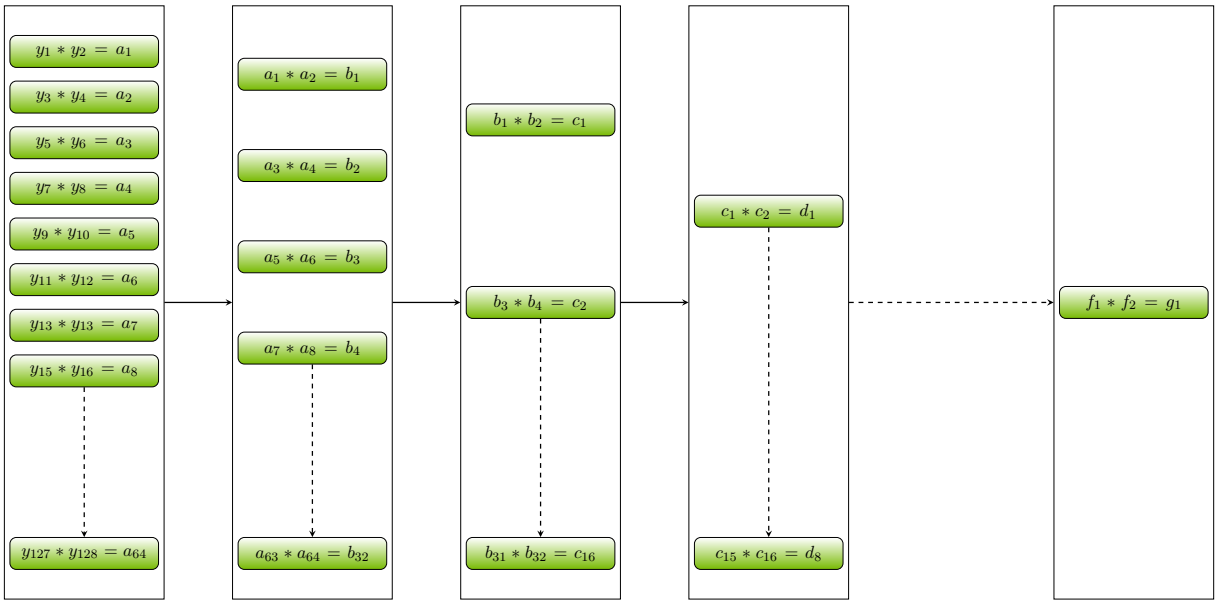


Figure 8.9: Parallel algorithm scheme

8.4 Analysis algorithm calibration

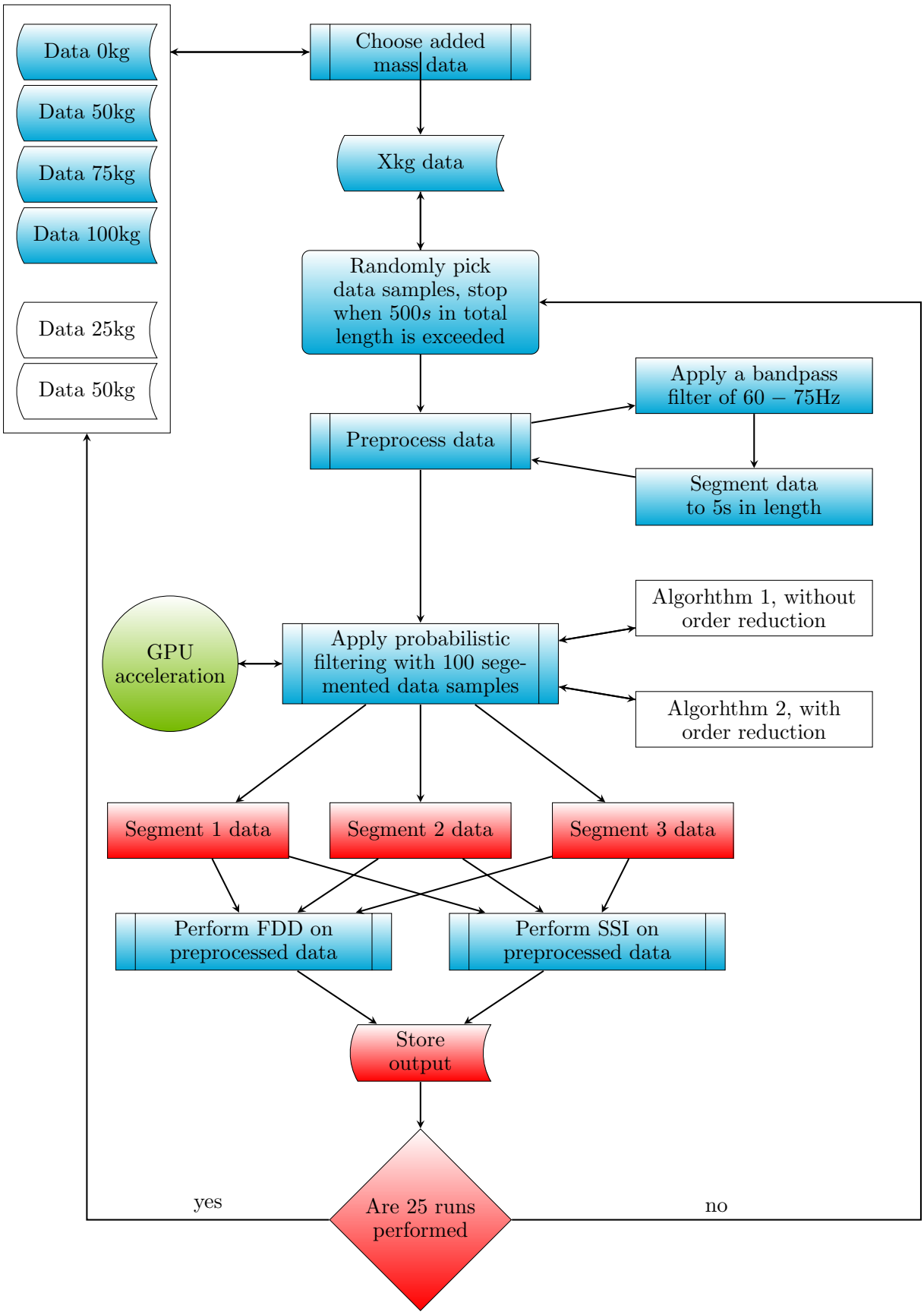


Figure 8.10: Analysis algorithm calibration with level 1 and level 2

Level 3

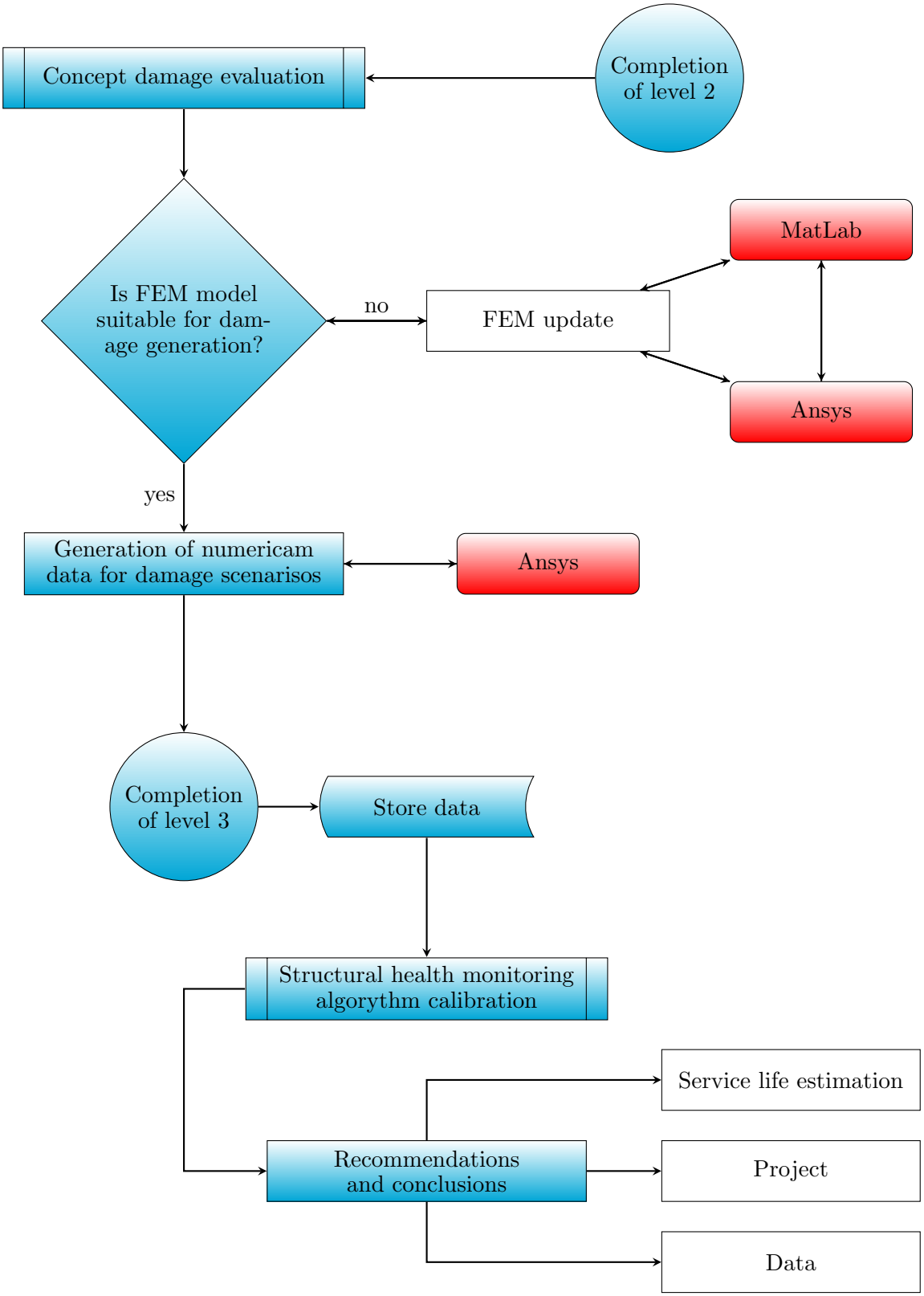


Figure L.3: Workflow of level 3

Chapter 9

Finite element model

This chapter presents the results of the Finite element method analysis (FEM). FEM was used to achieve level 3 of the Structural health monitoring, the damage quantification.

For purpose of damage quantification, 3 models of the bridge were designed. Firstly, simplified global model of the bridge was set. Conclusions from the global model led to design of the two local models with different approaches to the boundary conditions.

Quantitative studies were performed with comparison of FEM results between the models designed with the deck segment added mass (as in real measurements) and the models designed with the realistic damage.

For the analysis Ansys software package was used (17.2 Academic), program Modal analysis.

9.1 Global model

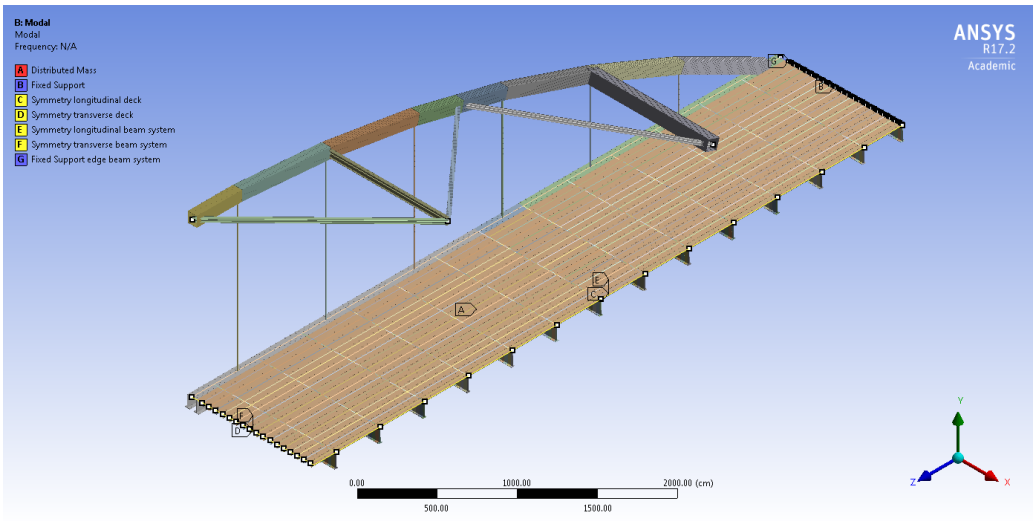
In this section global FEM model set-up and the main results are presented. The full FEM analysis and parameters of this model are presented in appendix F1.

For the global FEM model transverse and longitudinal symmetry was used, and only the one fourth of the structure is modelled. The model is simplified and consist of 1D beam elements and 2D plate elements. Purpose of such analysis was initial insight in the behaviour of the bridge.

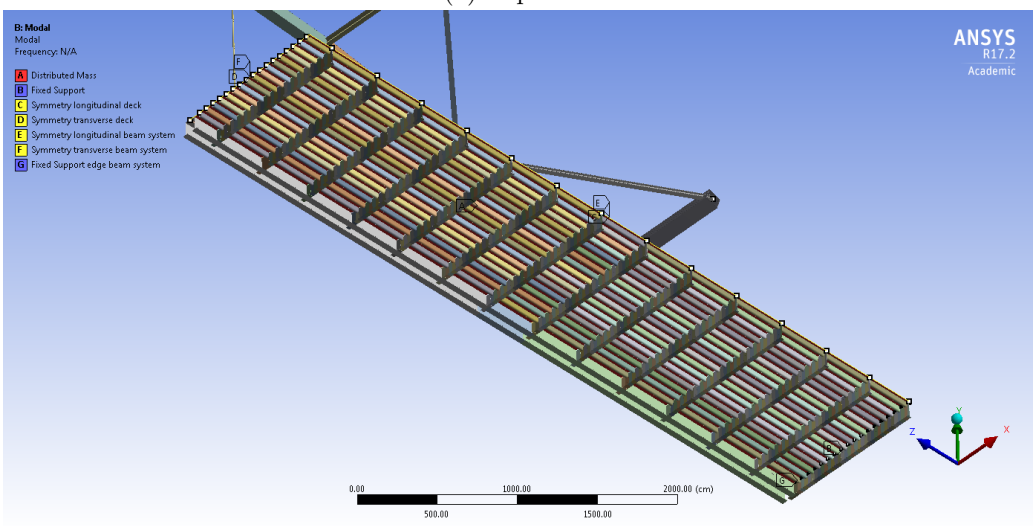
9.1.1 Analysis set-up

Geometry and Boundary conditions can be seen in figure 9.1 on the next page and mesh in figure 9.2 on the following page. Symmetry Boundary conditions are modelled with restrains of rotation of the plane of symmetry and it's translation in perpendicular direction.

Modal analysis of the first 500 modes are performed. Model is meshed with 82555 elements. Results are shown in next subsection.



(a) Top view



(b) Bottom view

Figure 9.1: Geometry and Boundary conditions

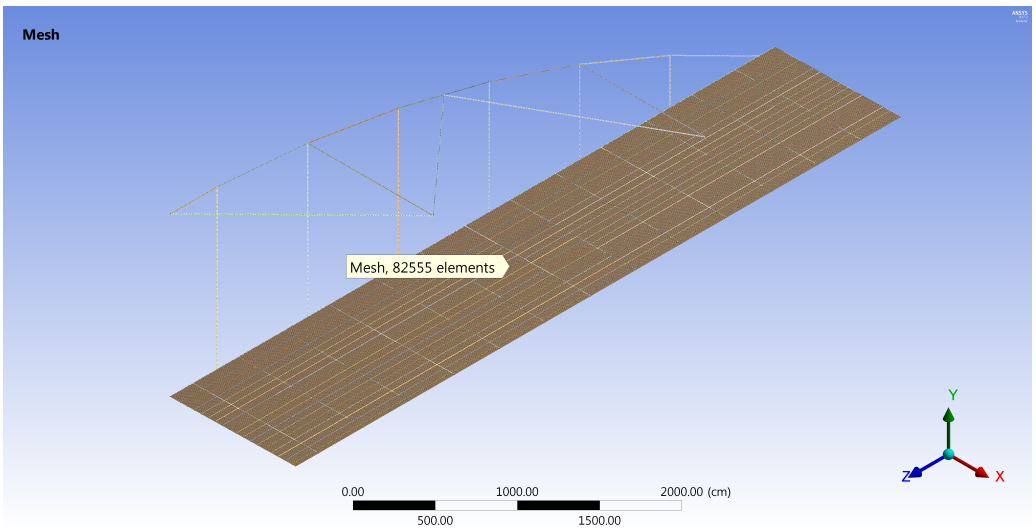


Figure 9.2: Mesh of the global FEM model

9.1.2 Results

In this subsection main results are shown. Graph of the first 500 modes with respect to frequency is presented in figure 9.3. In figure 9.4 the first two mode shapes are shown. In figure 9.5 on the next page 3 examples of mode shapes in the frequency region of interest are presented.

For further analysis it is important to state that those high modes have high sensitivity and low ability to approximate "realistic" behaviour. Small changes will make big contributions, and generally bridge was designed with simplified model, so that behaviour it describes. Additionally, modes are very densely spread, about 150 modes in frequency region of interest. Post-processing of results in case damage and added mass was modelled would be quite hard to obtain in a conclusive manner. With a complex global model of the bridge, the first 500 modes were under 16Hz.

Conclusion was made to proceed to quantitative analysis related to the isolated segment of the bridge. Results of the global FEM model are considered valuable in terms of the chosen frequency region of the analysis for the measured vibrations.

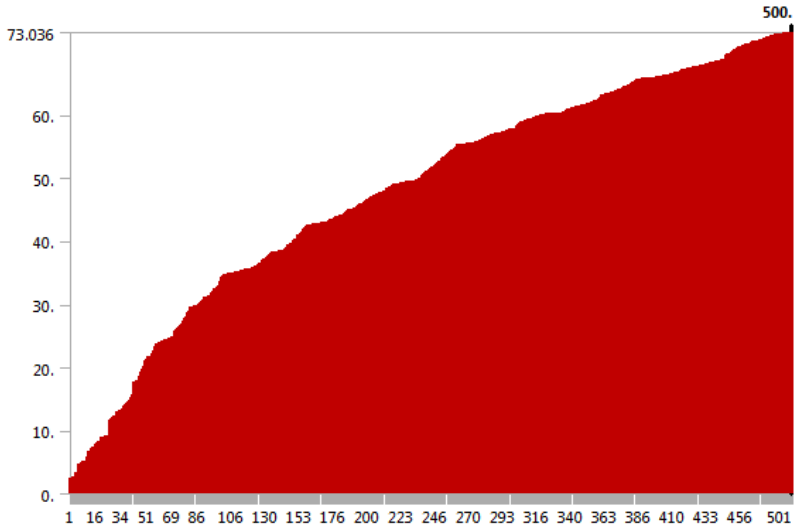
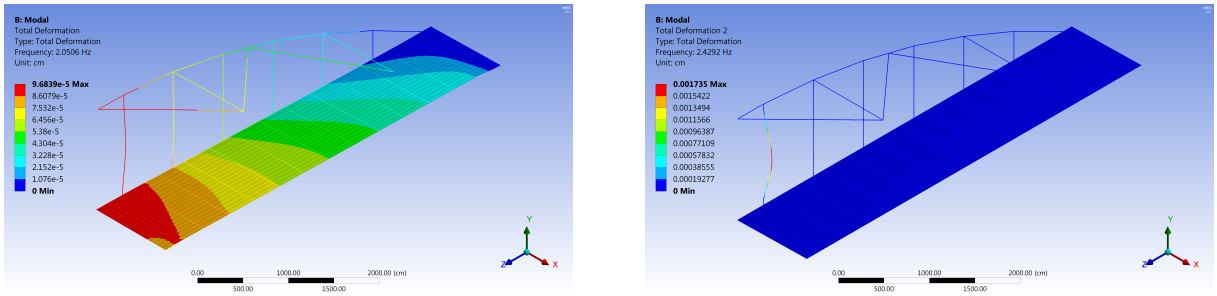


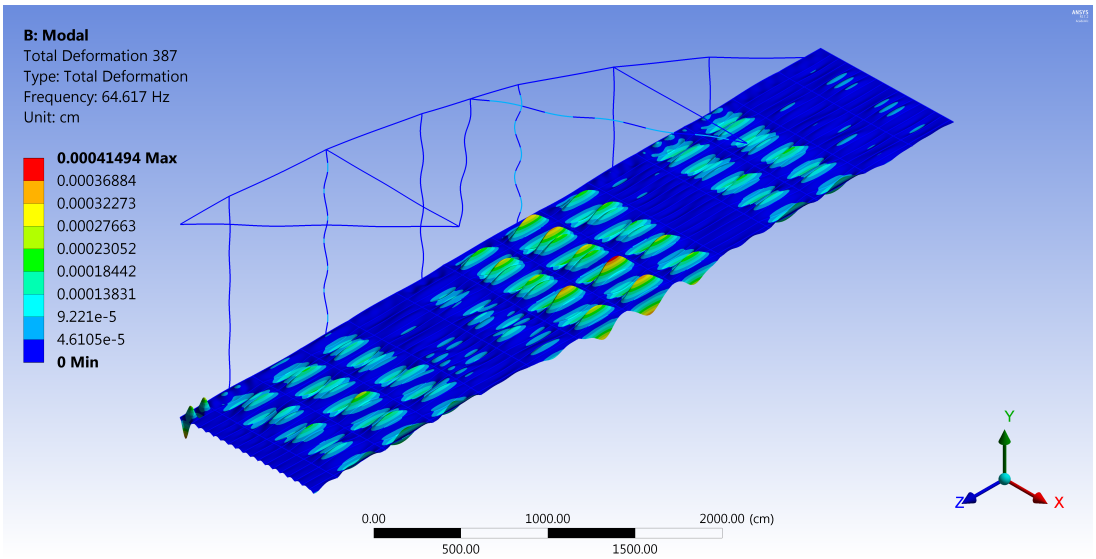
Figure 9.3: The first 500 modes of global FEM analysis



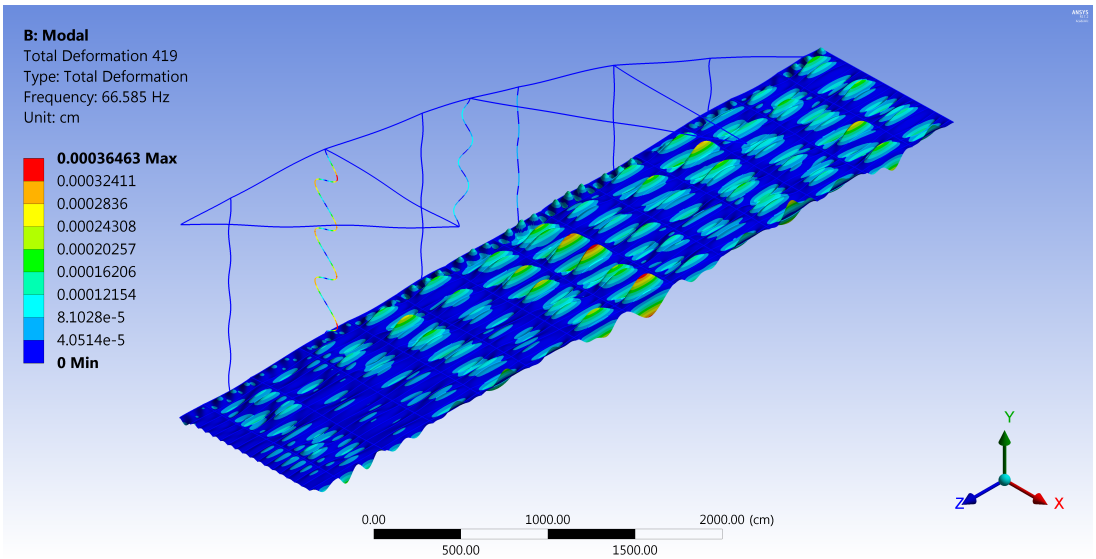
(a) Mode 1, 2.0506Hz

(b) Mode 2, 2.4292Hz

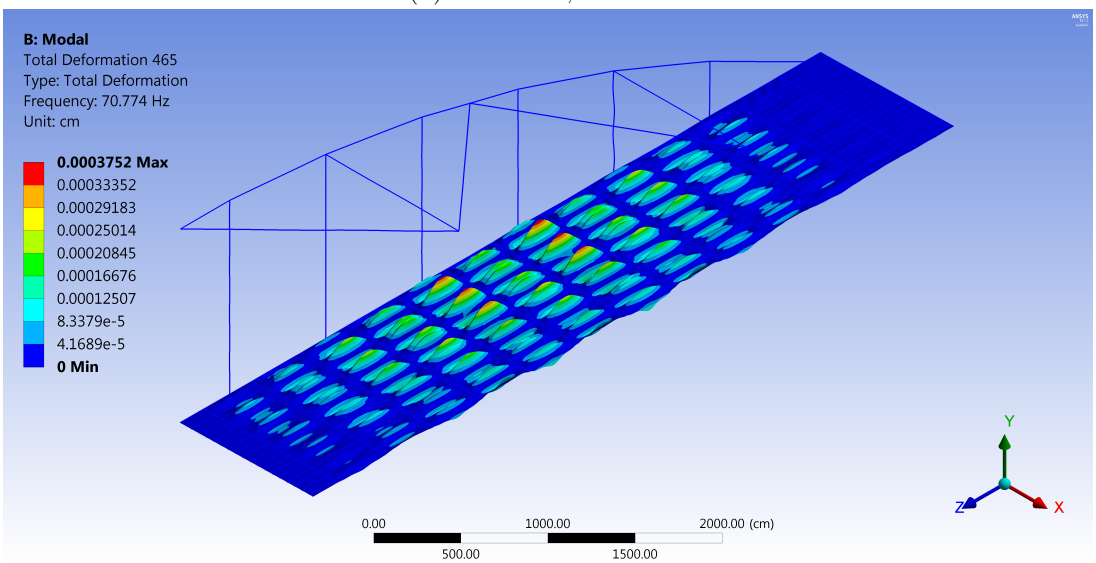
Figure 9.4: Mode shapes, total deformation



(a) Mode 387, 64.617Hz



(b) Mode 419, 66.585Hz



(c) Mode 465, 70.774Hz

Figure 9.5: Mode shapes, total deformation

9.2 Local model 1

In this section reasoning for local FEM model, analysis set-up and the main results are presented. The full FEM analysis and parameters of this model are presented in appendix F2.

For the local model 1 analysis, only segment 2 of the bridge structure is modelled figure 9.6. As seen in the global analysis, modes are densely spread. The interest of analysis is investigation of the dynamical behaviour of the segment 2 of the bridge structure. Analysis purpose is relation to the level 1 SHM analysis of real measured data.

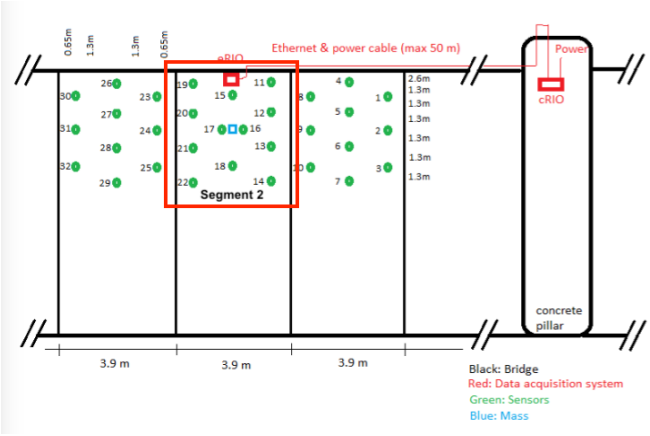


Figure 9.6: Segment 2 of the bridge structure

The given structure segment is modelled with fixed Boundary conditions. The logic behind doing so is found in the sub-structuring concept, observe figure 9.7.

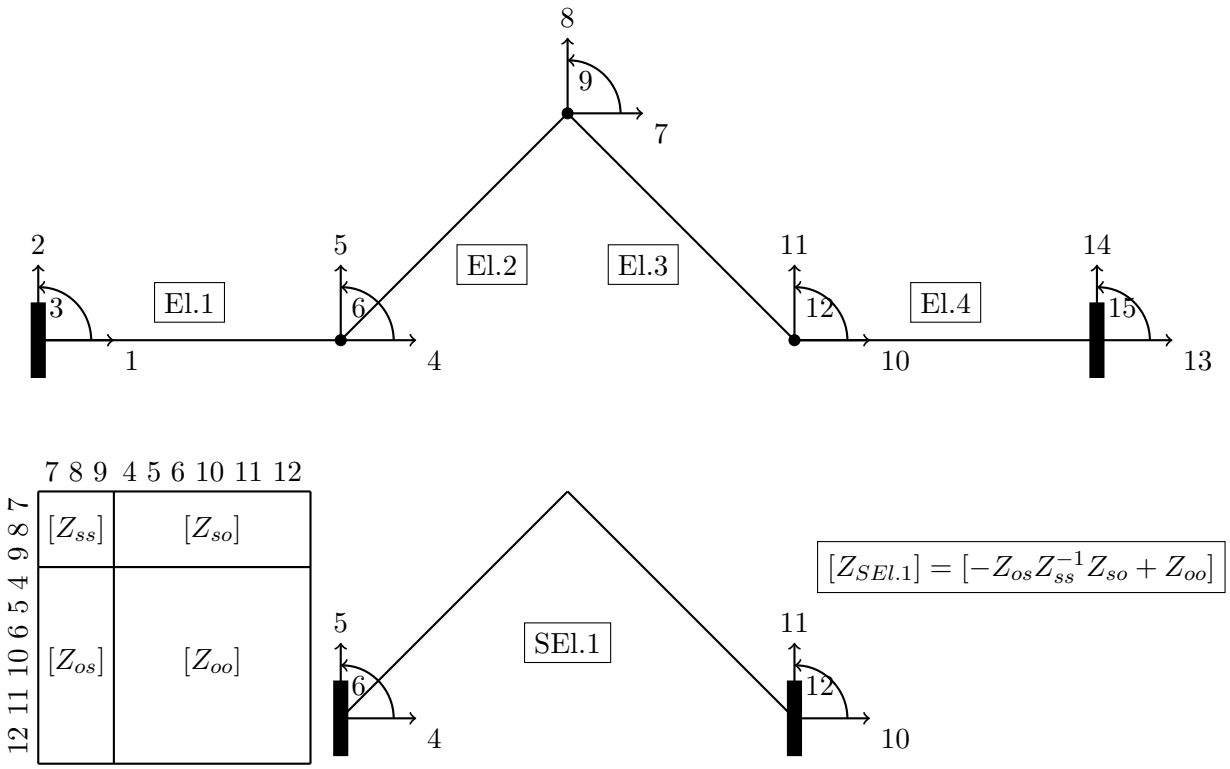


Figure 9.7: Sub-structuring of system with element SEl.1 instead of elements El.2 and El.3

When we perform sub-structuring, the sub-structure elements are isolated and fixed supports are set on the boundaries. For that isolated structure Impedance matrix is derived, and it joins with superposition the global impedance matrix. Further, modes are recovered through global impedance matrix inverse.

So, for the local mode behaviour related to the segment of the structure, it is assumed that it's properties dominant in the global Impedance matrix. As we are interested in local mode behaviour of the structures segment, the following analysis are performed with analogy of observing the given segment as a super-element of the sub-structured analysis.

9.2.1 Analysis set-up

Geometry and Boundary conditions can be seen in figure 9.8 and mesh in figure 9.9. 3D solids are used for U stiffeners, 2D plate for rhe road deck and 1D beam for the edge longitudinal beam. Mesh size was set close to Ansys Academic licence limit of 256.000 nodes.

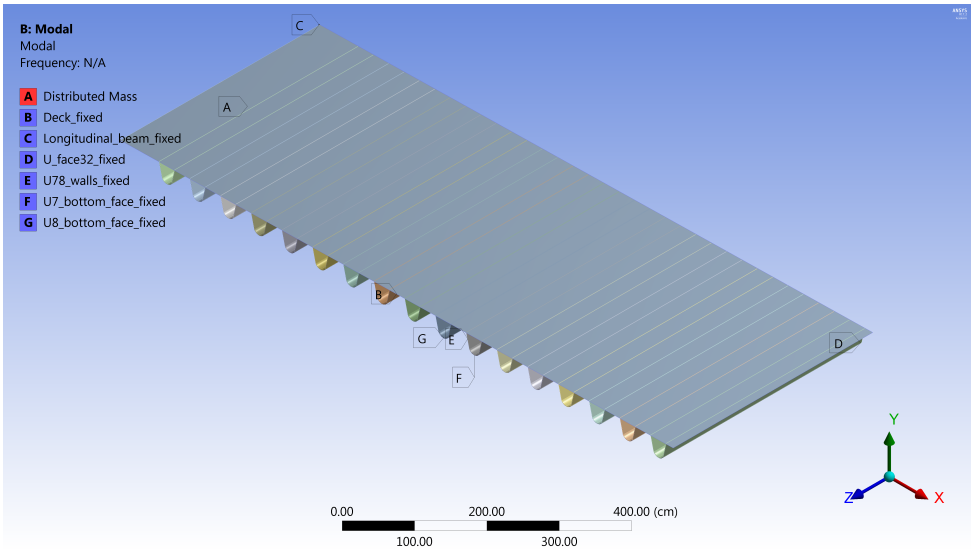


Figure 9.8: Geometry and Boundary conditions of the model

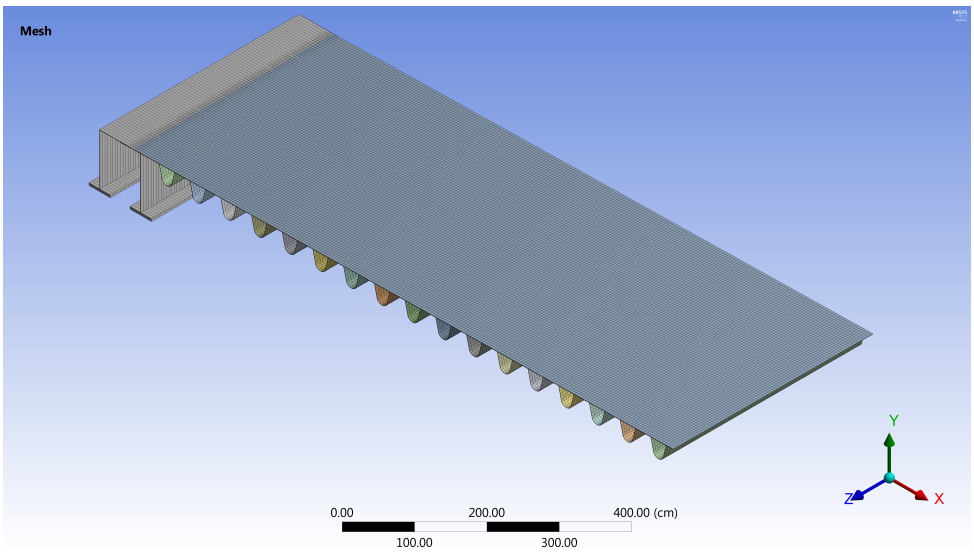


Figure 9.9: Mesh of the model

The quantitative studies are based on the comparison of models with 0kg-50kg-75kg-100kg added masses and the scenarios with realistic damage model. For the design of the realistic damage, static analysis are performed, and it is concluded that the largest stresses occur at the connection of the U shape stiffeners to the transverse beams (supports) in the bottom of U section region.

Three scenarios for realistic damage model are designed. The first scenario is the 35cm long bottom U section crack, figure 9.10. The second scenario is 35cm long bottom crack at two neighbour U sections, figure 9.11. The third scenario is 2 full U section cracks, figure 9.12.

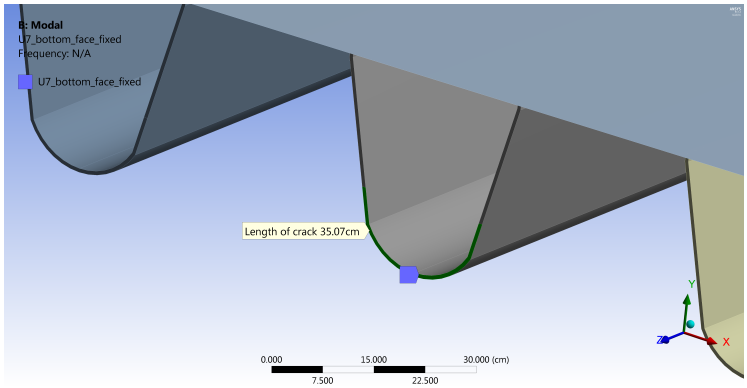


Figure 9.10: The first damage scenario

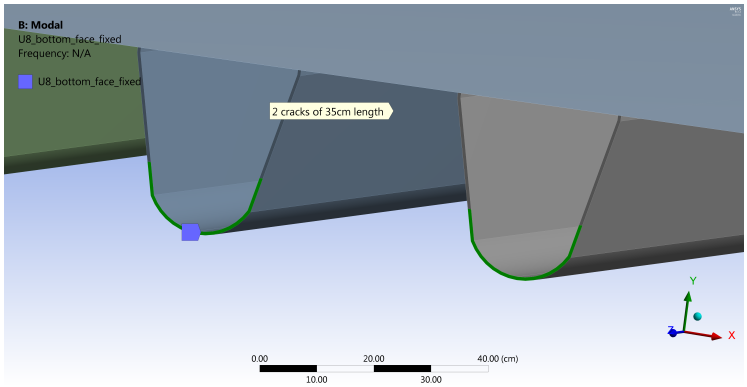


Figure 9.11: The second damage scenario

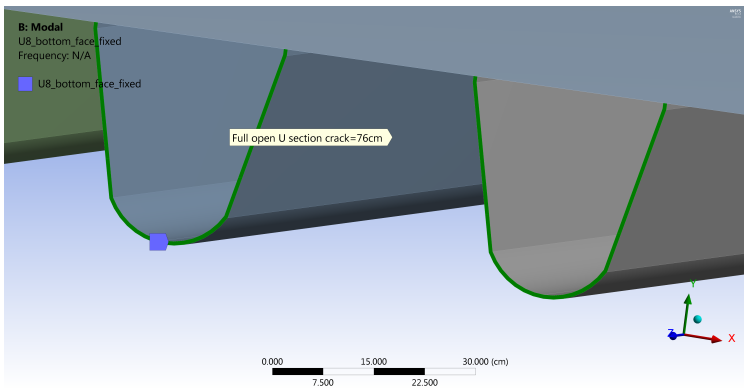


Figure 9.12: The third damage scenario

9.2.2 Results

In this subsection main results are shown. Analysis are performed for the first 20 modes of the healthy structure and 6 "damage" scenarios (50kg-75kg-100kg, 35cm-crack, 2x35cm-cracks, and 2 full U section cracks).

Results of the mode shape of interest are presented in figure 9.13 to figure 9.19 on page 108. For the level 1 analysis of real data, frequency range from 0kg to 100kg was 1.4Hz. For the given FEM analysis frequency range from 0kg to 100kg is 2.5Hz. It is observed that results of the model with 100kg added mass are comparable to 35cm long U section crack, 63.121Hz and 63.193Hz. As the level 1 analysis showed ability to detect 50kg added mass, it is assumed that the model could detect smaller crack than 35cm. Further conclusions will be made after the results of the Local model 2 analysis.

The given results of FEM analysis provide support to the chosen frequency range for the level 1 analysis. The full FEM analysis report, as mentioned, can be seen in appendix F2.

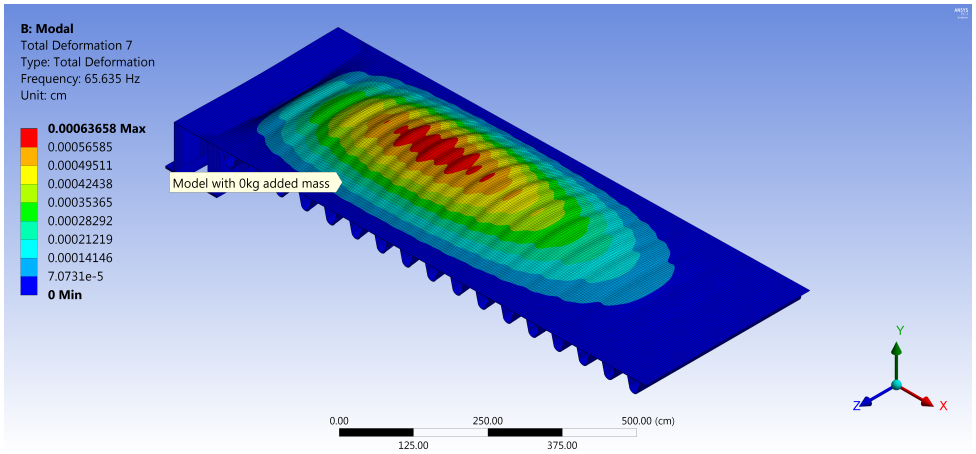


Figure 9.13: Mode 7, 0kg model, 65.635Hz

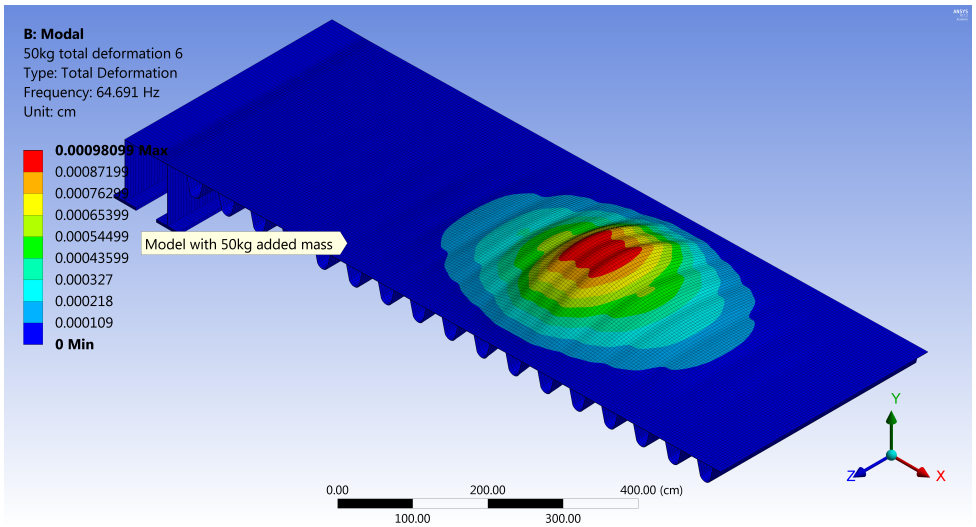


Figure 9.14: Mode 6, 50kg model, 64.691Hz

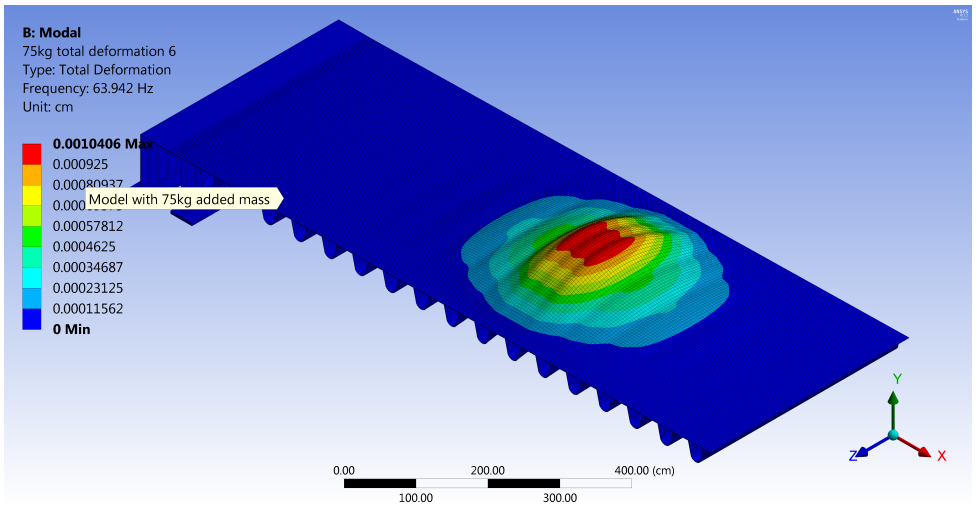


Figure 9.15: Mode 6, 75kg model, 63.942Hz

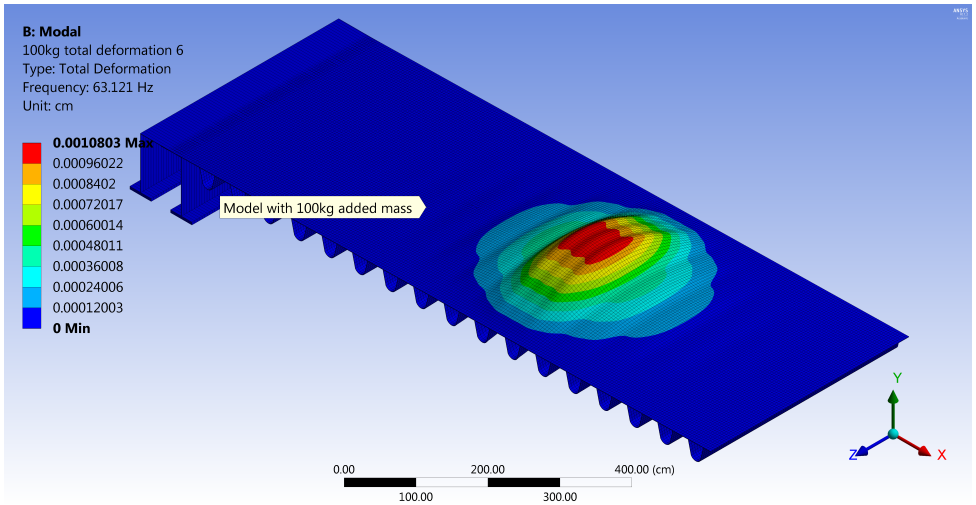


Figure 9.16: Mode 6, 100kg model, 63.121Hz

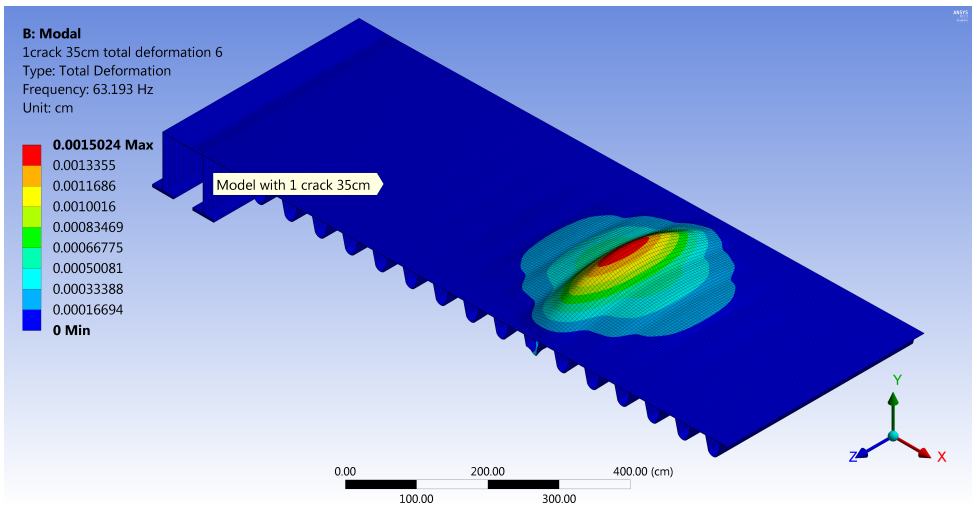


Figure 9.17: Mode 6, 35cm crack model, 63.193Hz

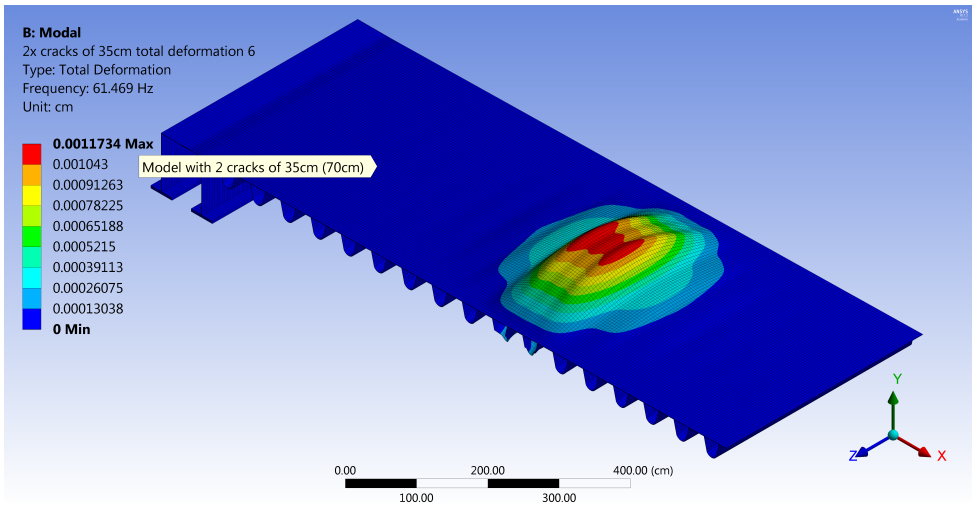


Figure 9.18: Mode 6, 2 times 35cm crack model, 61.469Hz

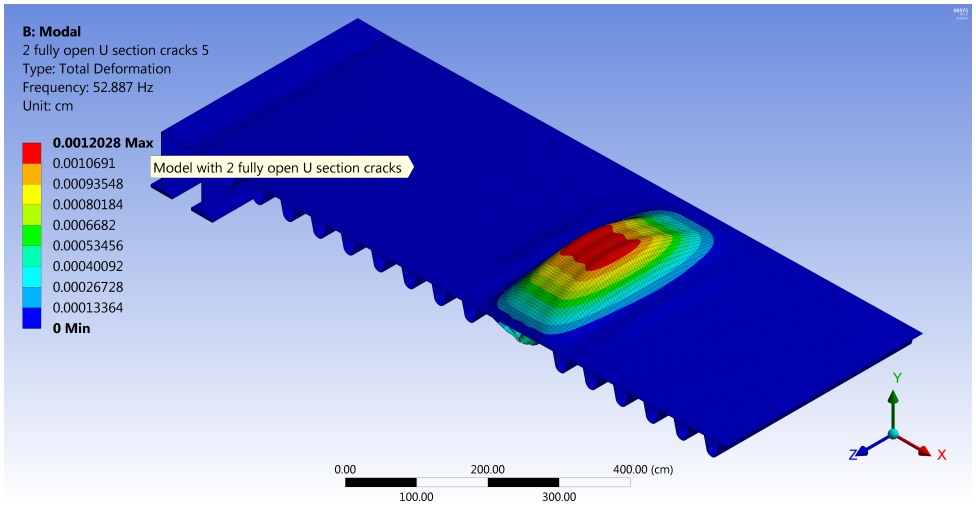


Figure 9.19: Mode 5, full two U section cracks, 52.887Hz

9.3 Local model 2

In this section reasoning for local FEM model, analysis set-up and the main results are presented. The full FEM analysis and parameters of this model are presented in appendix F3.

For the local model 2 analysis, concept of local model 1 is extended to more realistic Boundary conditions (compared to the fixed case). Concept of calculating individual static spring stiffness's is considered.

It should be mentioned that modelling dynamic springs was avoided as it is approximation of the sub-structuring concept, which would recover full global modes, and the intention is to observe local modes related to the isolated segment of the bridge.

The concept of applying static springs as Boundary conditions introduces decoupling of the transverse and flexural stiffness, at the given node. The given problem is solved by taking the full global model of the bridge, and assigning zero mass to the elements outside of the segment of interest, observe illustration in figure 9.20.

In conclusion, the isolated segment of the bridge is bounded by simplified full bridge elements of zero mass. It is assumed that modes related to the zero mass elements will tend to high frequencies, and the fundamental modes of the analysis will be related to the local behaviour of the isolated segment.

The interest of the analysis is investigation of the dynamical behaviour of the "segment 2" of the bridge structure. Analysis purpose is relation to the level 1 SHM analysis of the real measured data.

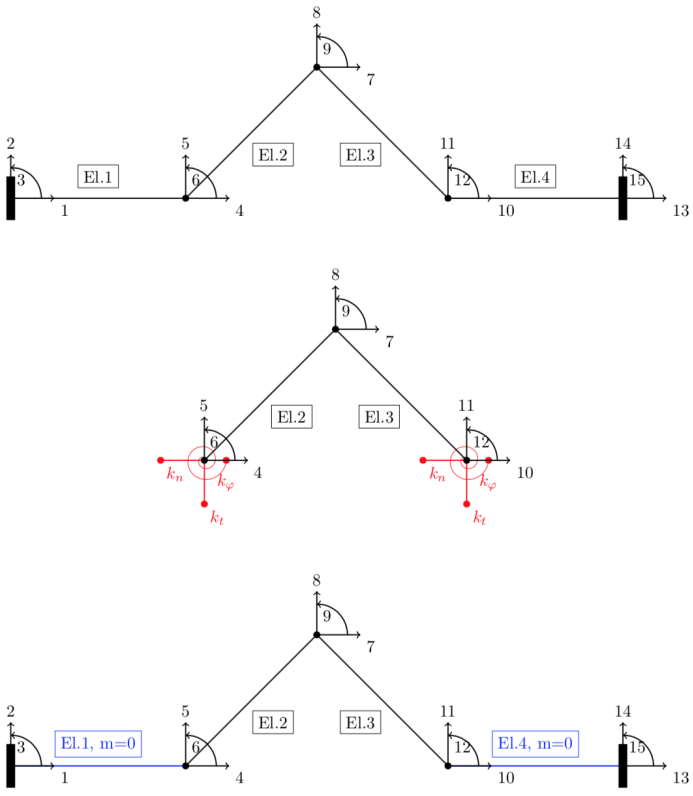


Figure 9.20: Local model 2 Boundary condition concept illustration

9.3.1 Analysis set-up

Geometry and Boundary conditions can be seen in figure 9.21. Model is based on bounding "segment 2" of the bridge with massless full bridge model, observe figure 9.22. For the "segment 2" 3D solids are used for U stiffeners, 2D plates for the road deck and 1D beam for the edge longitudinal beam, to this elements mass is applied. The elements that are bounding the "segment 2" consist of 2D plates and 1D beams, with no mass applied. Mesh size was set close to Ansys Academic licence limit of 256.000 nodes, observe figures 9.23 on the following page and 9.24 on the next page.

In the figure 9.25 on the following page isolated "segment 2" that is subject of the quantitative analysis is presented (segment with mass). The quantitative studies are based on the comparison of models with 0kg-50kg-75kg-100kg added masses and the scenarios with realistic damage model. The realistic damage model is the same as in Local model 1 analysis. Three scenarios for realistic damage model are designed. The first scenario is the 35cm long bottom U section crack, revise figure 9.10 on page 105. The second scenario is 35cm long bottom crack at two neighbour U sections, revise figure 9.11 on page 105. The third scenario is 2 full U section cracks, revise figure 9.12 on page 105.

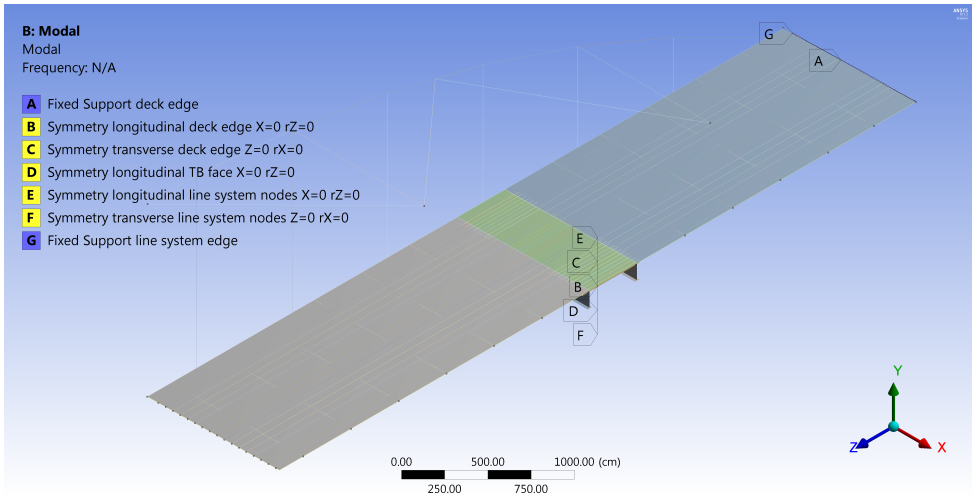


Figure 9.21: Geometry and Boundary conditions of the model

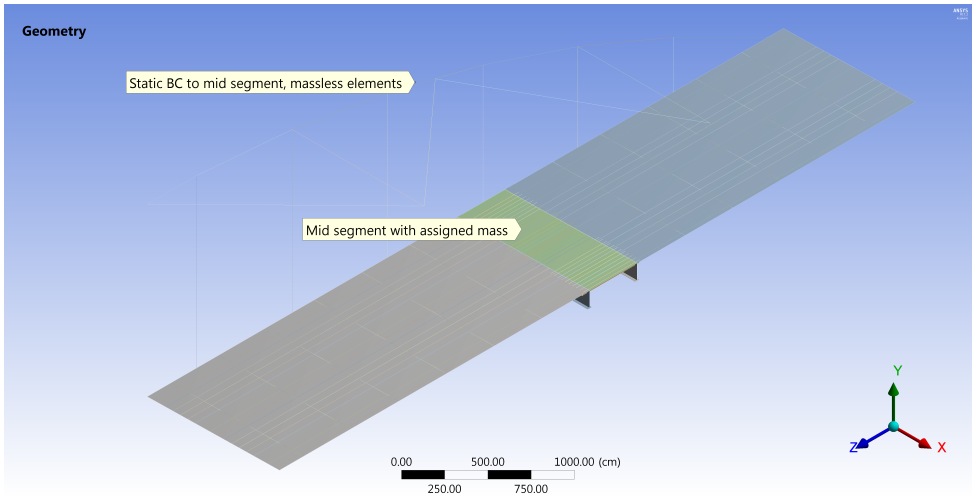


Figure 9.22: Geometry and applied mass

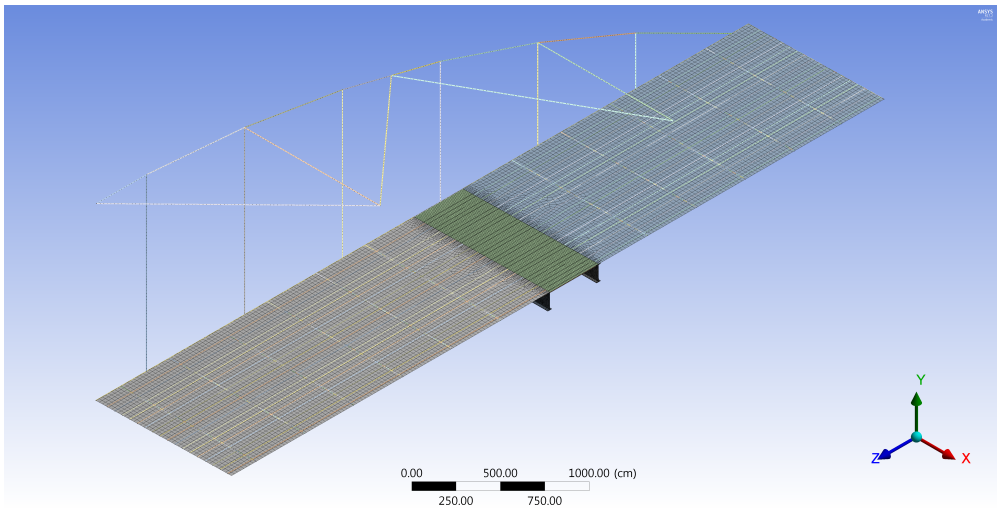


Figure 9.23: Mesh of the structure, global

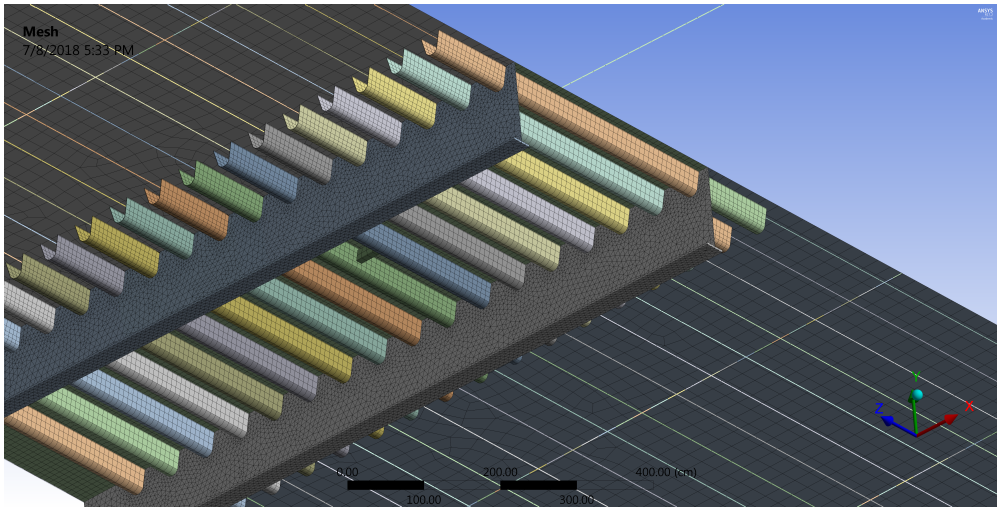


Figure 9.24: Mesh of the structure, bottom view

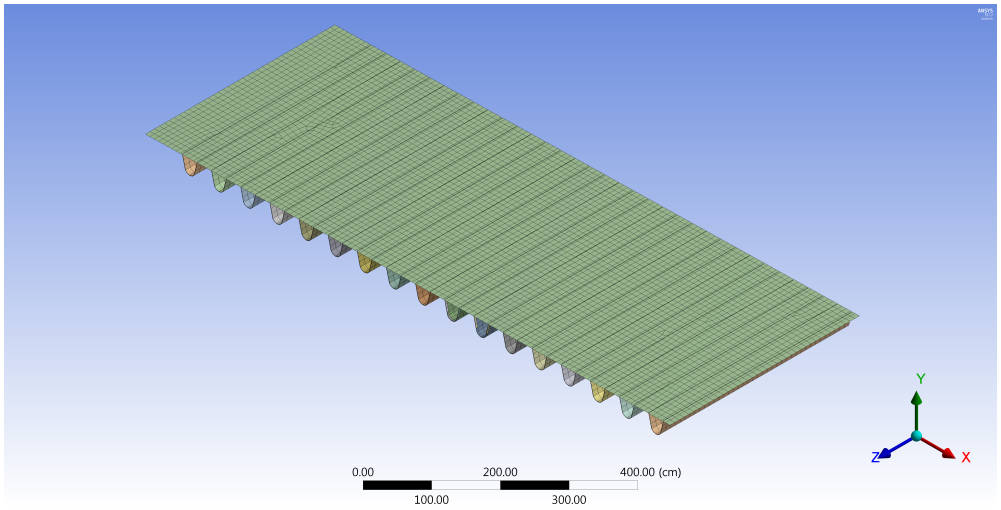
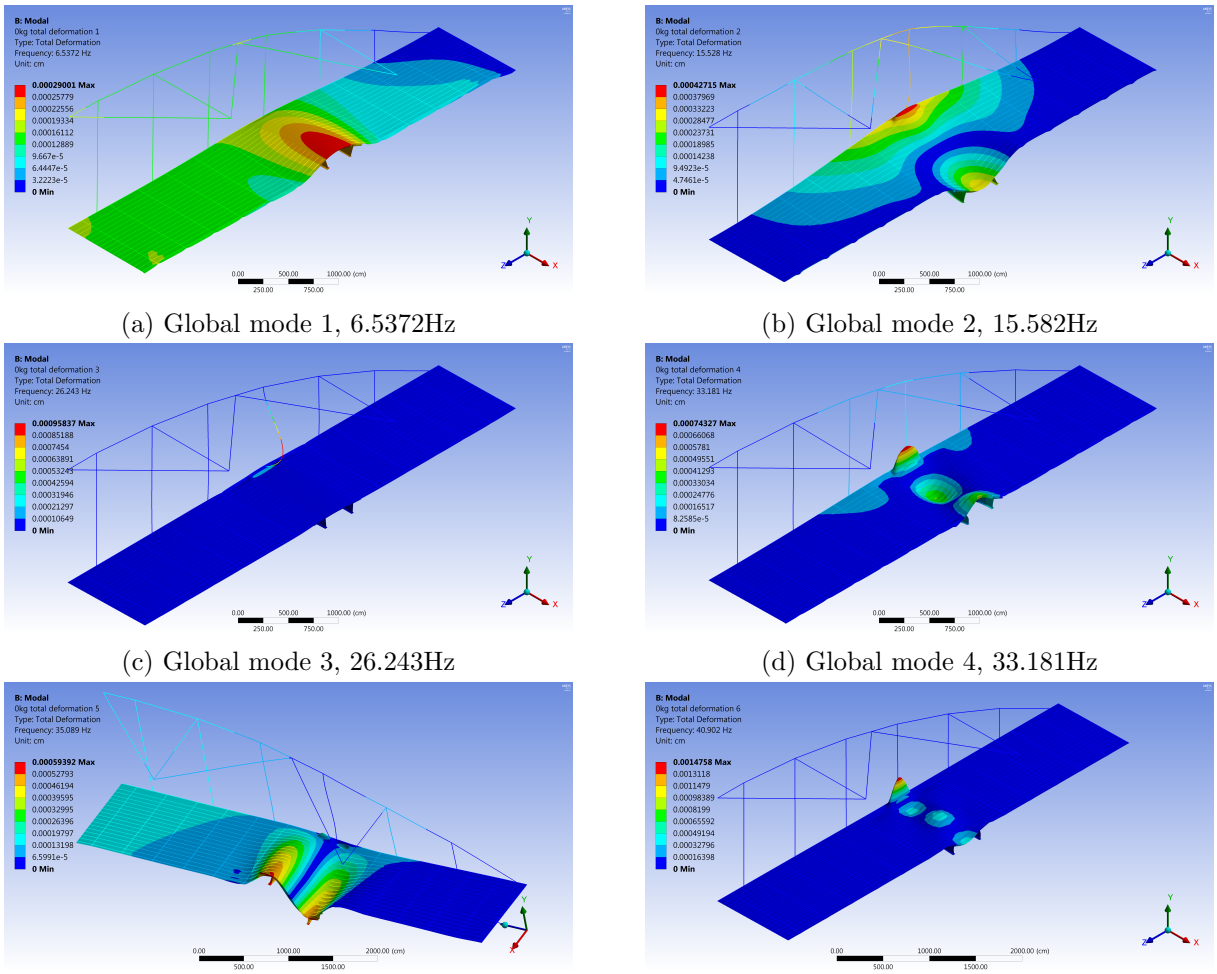


Figure 9.25: Mesh of the "segment 2" (segment with mass)

9.3.2 Results

In this subsection main results are shown. Analysis are performed for the first 30 modes of the healthy structure and 6 "damage" scenarios (50kg-75kg-100kg, 35cm-crack, 2x35cm-cracks, and 2 full U section cracks).

Results that show global behaviour of the first 6 modes, for the 0kg case, are presented in figure 9.26. Intention is to show that dynamical behaviour is localised to the "segment 2".



(a) Global mode 1, 6.5372Hz

(b) Global mode 2, 15.582Hz

(c) Global mode 3, 26.243Hz

(d) Global mode 4, 33.181Hz

(e) Global mode 5, 35.089Hz

(f) Global mode 6, 40.902Hz

Figure 9.26: The first 6 modes, global representation

Results of the mode shape of interest are presented in figure 9.27 on the next page to figure 9.33 on page 115. For the level 1 analysis of real data, frequency range from 0kg to 100kg was 1.4Hz. For the given FEM analysis frequency range from 0kg to 100kg is 0.413Hz. It is observed that results of the model with 50kg added mass are comparable to 35cm long U section crack, 54.936Hz and 54.919Hz. As the level 1 analysis showed ability to detect 50kg added mass, it is assumed that the model could detect crack of 35cm. In the conclusion section, further discussion on the identified frequency differences range will be raised. The full FEM analysis report, as mentioned, can be seen in appendix F3.

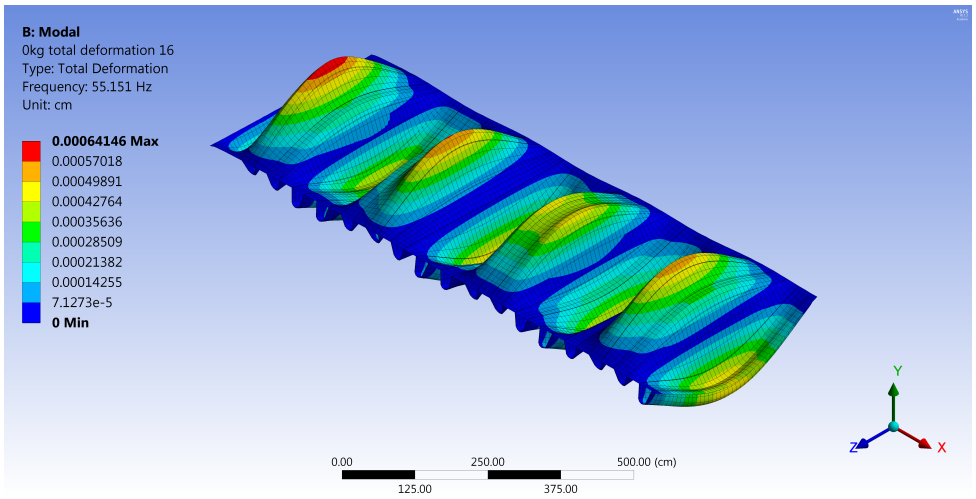


Figure 9.27: Mode 16, 0kg model, 55.151Hz

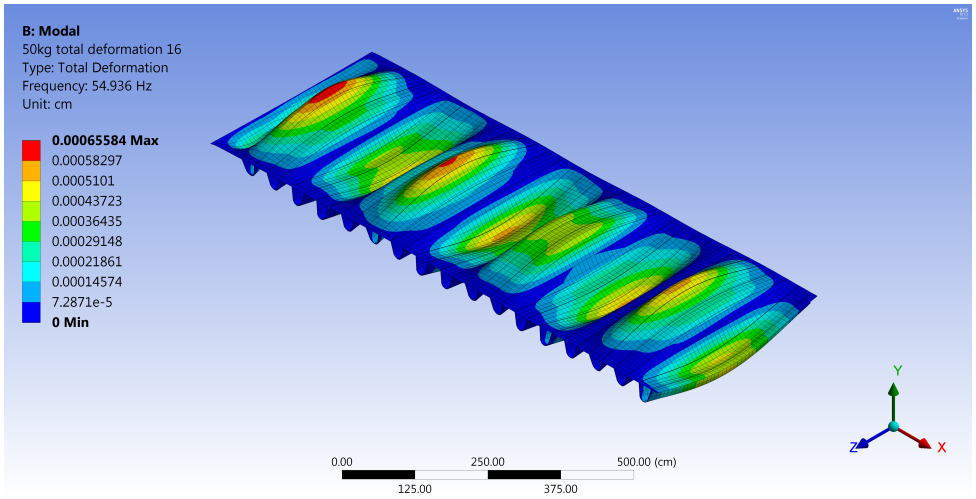


Figure 9.28: Mode 16, 50kg model, 54.936Hz ($\Delta f = 0.215$Hz)

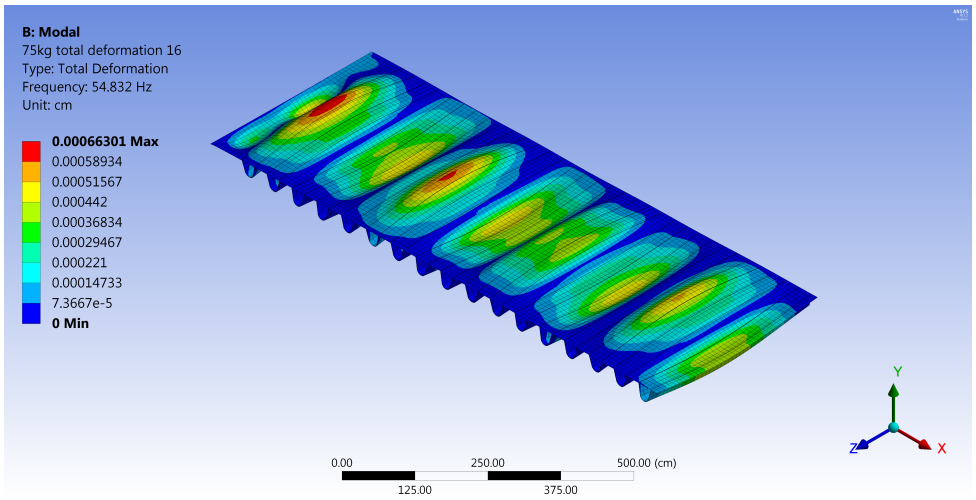


Figure 9.29: Mode 16, 75kg model, 54.832Hz ($\Delta f = 0.319$Hz)

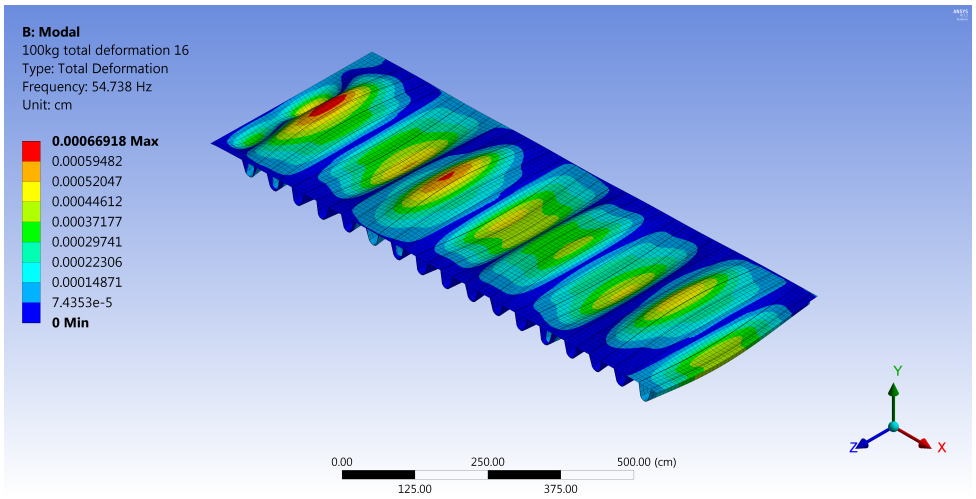


Figure 9.30: Mode 16, 100kg model, 54.738Hz ($\Delta f = 0.413$Hz)

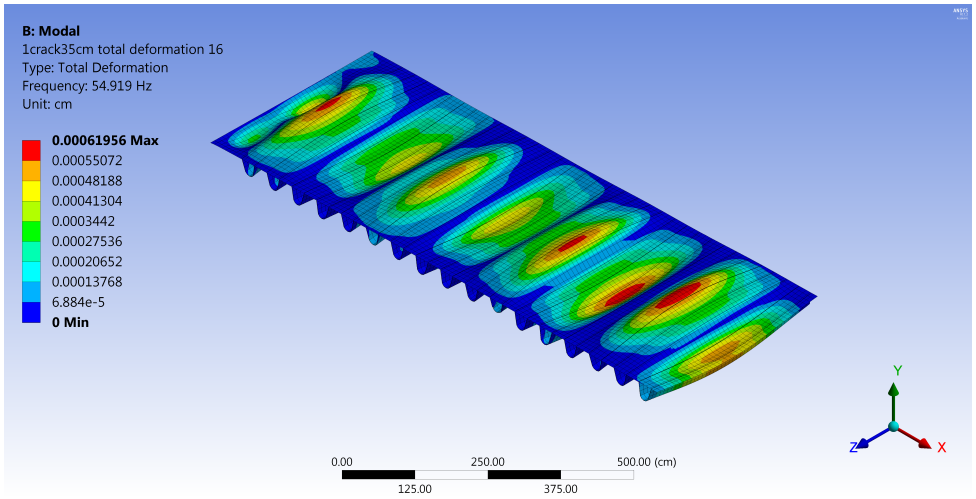


Figure 9.31: Mode 16, 35cm crack model, 54.919Hz ($\Delta f = 0.232$Hz)

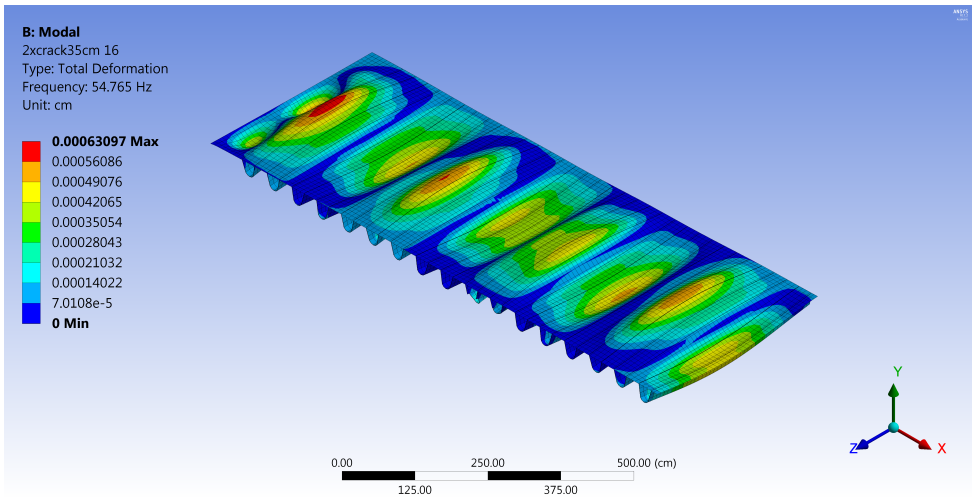
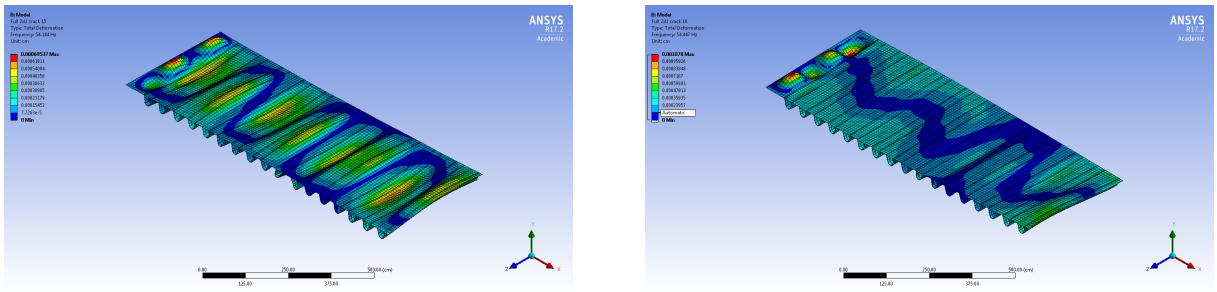


Figure 9.32: Mode 16, 2 times 35cm crack model, 54.765Hz ($\Delta f = 0.386$Hz)



(a) Mode 15, 54.144Hz ($\Delta f = 1.007$Hz) (b) Mode 16

Figure 9.33: Mode 15 and 16 for the 2 full U section cracks

Results for the mode shape that was identified only in added mass cases (50kg, 75kg, 100kg) is presented in figures 9.34 to 9.36 on the following page. The given mode shows local behaviour of the "segment 2" that is comparable to the Local model 1 case. The differences between added mass step of 25kg, is 0.6Hz as in the Local model 1 case. The given mode shape was not comparable to identified modes of 0kg model and models with presence of realistic damage. Main conclusions will be presented in the conclusion section.

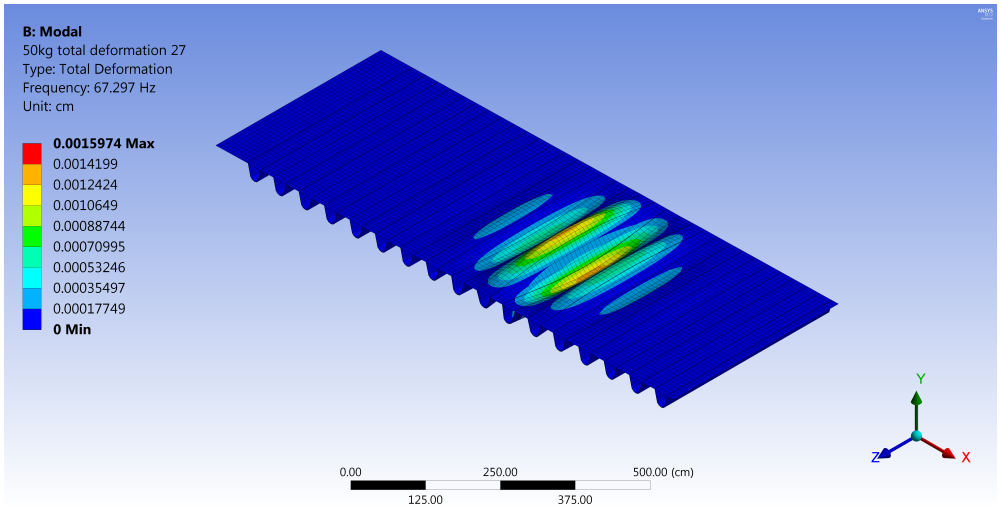


Figure 9.34: Mode 27, 50kg model, 67.297Hz

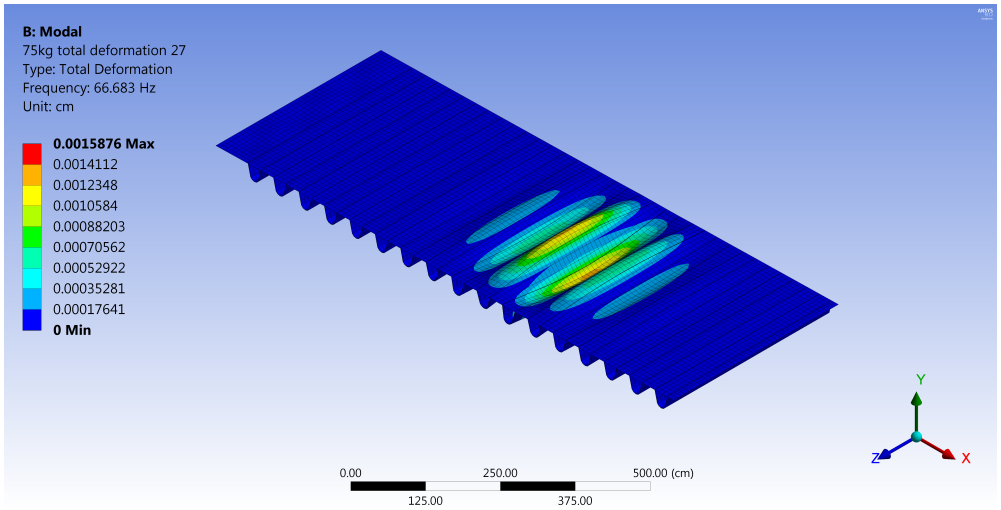


Figure 9.35: Mode 27, 75kg model, 66.683Hz ($\Delta f = 0.614$Hz from 50kg)

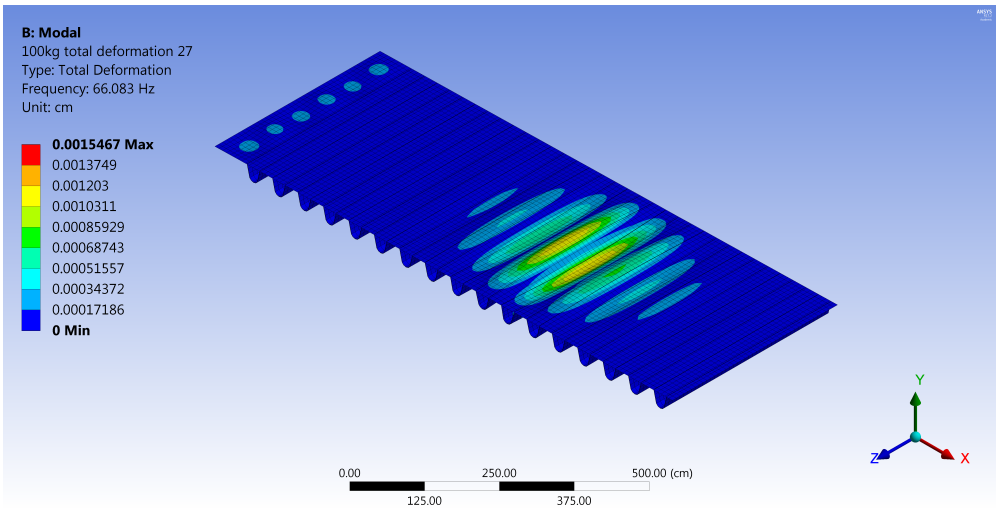


Figure 9.36: Mode 27, 100kg model, 66.083Hz ($\Delta f = 0.6$Hz from 75kg)

Additionally, it is worth observing figure 9.37, where frequencies of the first ten modes of Local model 2 FEM analysis are presented. It can be observed that for frequencies up to 50Hz differences between the "healthy" structure and the "damaged" structure are very small. This observation provides support for the chosen frequency range for the level 1 SHM analysis. The full mode shapes of the first 30 modes can be observed in Appendix F3.

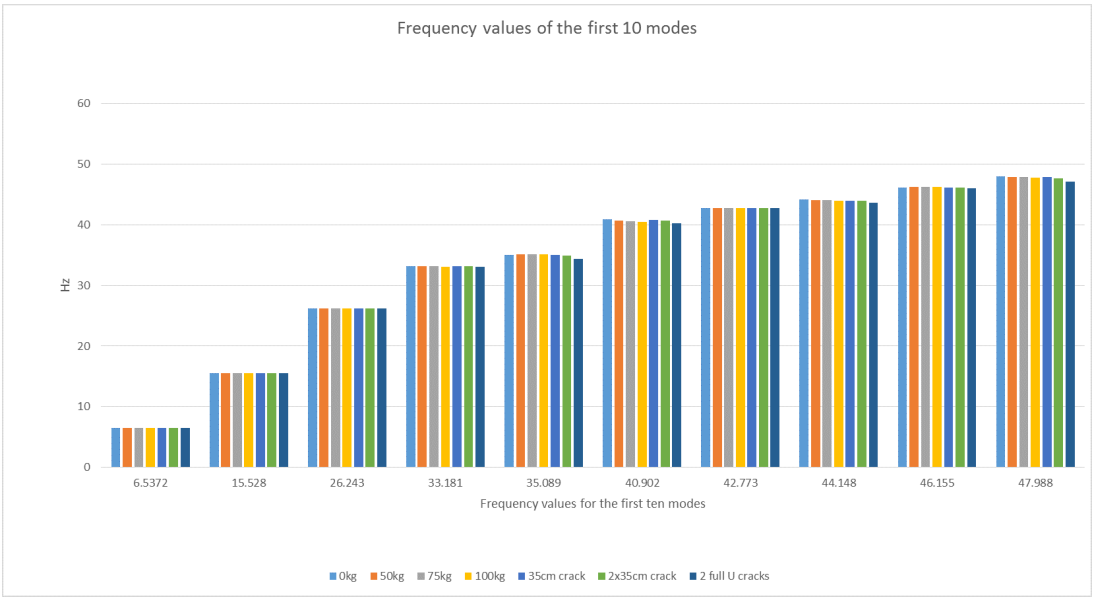


Figure 9.37: The first ten modes of Local model 2 FEM analysis

9.4 Conclusion

The global model, the Local model 1 and the Local model 2 show support to the chosen region of the analysis frequencies for the Level 1 SHM analysis.

For the level 1 analysis of real data, quantitative frequency range from 0kg to 100kg was 1.4Hz.

For the Local model 1 FEM analysis quantitative frequency range from 0kg to 100kg is 2.5Hz. It is observed that results of the Local model 1 with 100kg added mass are comparable to 35cm long U section crack, 63.121Hz and 63.193Hz.

For the Local model 2 FEM analysis quantitative frequency range from 0kg to 100kg is 0.413Hz. It is observed that results of the model with 50kg added mass are comparable to 35cm long U section crack, 54.936Hz and 54.919Hz.

The quantitative frequency difference per 25kg added mass for the FEM Local model 1 is 0.6Hz, for the FEM Local model 2 is 0.1Hz, and for the real data 0.35Hz. It is obvious that the FEM Local model 1 (fixed supports) is a stiffer model than Local model 2 (static bounds), and the structural changes in that model had bigger impact (0.6Hz to 0.1Hz quantitative values). Additionally, Local model 2 identified local mode (mode 27) where quantitative differences between added masses (50kg-75kg-100kg) was in analogy with the Local model 1 with value of 0.6Hz, but that mode could not be compared in shape to 0kg case and realistic damage models.

What was not considered in the given models is the influence of the vehicle friction force through wheels that is pre-stressing the bridge deck and could have impact in the given high frequency region on the increase of stiffness. The real data has that information, and that could be one of the reasons why the real measurement quantitative frequency differences for the added masses is between those two FEM models (0.1Hz<0.35Hz<0.6Hz).

The FEM Local models provided valuable knowledge. The Local model 1 is set as upper bound model with ability to detect crack of 35cm with quantitative frequency value comparable to 100kg case. The Local model 2 is set as lower bound model with ability to detect crack of 35cm with quantitative frequency value comparable to 50kg case.

The case with real measurements is found in between those two bounds, linearly concluding that quantitative frequency value of 75kg case can be observed as indicator of anomaly of size of 35cm crack in the bottom of U section (in connection to the transverse beam).

Chapter 10

Conclusions and recommendations

10.1 Conclusions

This thesis started with receiving the data from the Zwartewaterbrug project. The goal was set to detect the added masses of 0kg-25kg-50kg-75kg-100kg that were attached to the deck of the bridge. Initial observed challenge was to detect the difference of 25kg of attached added mass on 800t bridge, via vibrations. Vibrations were generated with the unknown traffic load that has the difference in vehicle masses between 200kg and 50t. Additionally, considering the frequency region that was chosen for the analysis, friction force of the vehicles was considered as a possible pre-stressing force that could impact the dynamical behaviour of the bridge deck. The problem was approached with the search of the reliable high frequency region for the analysis,for that the MAC stabilisation diagram was established. Analysis were proceeded with the development of the Probabilistic filtering method and Monte-Carlo based algorithm that uses PF, FDD and SSI. The purpose was overcoming the larger differences between the unknown traffic load and the introduced structural anomalies. Level 1 of the analysis was closed, added mass was identified.

The same analysis algorithm is set to operate on three different segments. The added mass was located in the segment 2 of the measurement system, and the level 2 of the analysis was closed, added mass was localised.

Level 3 of the analysis was approached with two local FEM models, with the concept of quantitative analysis. The two models were set as Upper bound and Lower bound models. The added mass of the real measurements was quantified in terms of the realistic damage case scenario that fitted between the Upper and Lower bound. Conclusion was made that identified results for the real measurements of the 75kg added mass could indicate the presence of anomaly of size of 35cm long crack at the bottom of the U section longitudinal stiffener, in the region of connection to the transverse beam. With that conclusion, level 3 of the analysis was closed, damage was quantified.

What is left to do is to give recommendations for the possible approach to the level 4 analysis that were not able to be conducted, and further improvements of the analysis set-up for the purpose of the more efficient level 1 to level 3 analysis.

10.2 Recommendations

Recommendations are made with relation to achieving Level 4 of the Structural health monitoring and further improvements of the analysis set-up.

10.2.1 Level 4

The Level 4 of SHM is related to the structures service life prediction. In the fulfilment of the Service limit state for the bridges, requirement is set for the maximum mid span deflection u_{SLS}. Based on that, recommendation is set for estimation of the return period of exceeding the u_{SLS}. The u_{SLS} is not calculated, it is set by code (example $u_{SLS} = Lspan/400$).

To obtain the return period of exceeding the u_{SLS}, mid span deflections should be included in the measurement network. The deflections should be monitored continuously.

Assuming that the given measured signal is Gaussian stationary process, relation for the return period will be derived. Relation for exceedance probability of deflection with relation to u_{sls} in period $[0, T]$ is given in equation (10.1).

$$P\{u(t) > u_{sls}\ in\ [0,T]\} = P\{u_1 > u_{sls}\ or\ u_2 > u_{sls}\ or\ ...\ u_n > u_{sls}\} \tag{10.1}$$

Elementary probability calculus holds, (10.2):

$$P\{A\ or\ B\} = P\{A\} + P\{B\} - P\{A\ and\ B\} \tag{10.2}$$

Taking a conservative approach, variable independence is introduced, and relation (10.5) is obtained.

$$P\{A\} + P\{B\} \geq P\{A\ or\ B\} \tag{10.3}$$

$$\sum_{i=1}^{n} P\{u_i > u_{sls}\} \geq P\{u(t) > u_{sls}\ in\ [0,T]\} \tag{10.4}$$

$$\sum_{i=1}^{n} P\{u_i > u_{sls}\} \approx P\{u(t) > u_{sls}\ in\ [0,T]\} \tag{10.5}$$

From the assumption of the stationary process, relation (10.6) is obtained.

$$P\{u(t) > u_{sls}\ in\ [0,T]\} \approx n * P\{u_i > u_{sls}\} \tag{10.6}$$

For the Gaussian narrow-band process, peaks u_i have a Rayleigh distribution. With the given assumption, relation (10.7) is obtained, that proceeds to relation (10.8).

$$P\{u_i > u_{sls}\} = exp\left(-\frac{(u_{sls} - \mu_u)^2}{2\sigma_u^2}\right) \tag{10.7}$$

$$P\{u(t) > u_{sls}\ in\ [0,T]\} \approx n * exp\left(-\frac{(u_{sls} - \mu_u)^2}{2\sigma_u^2}\right) \tag{10.8}$$

From the relation for the n samples in period T, and probability of exceedance equal to 1, final approximation for the period T of the service life is obtained (10.10).

$$n = T * F_s \tag{10.9}$$

$$T \approx \frac{1}{F_s * exp\left(-\frac{(u_{sls}-\mu_u)^2}{2\sigma_u^2}\right)} \tag{10.10}$$

Additional suggestion is made that this approximation should be used only on a structures with proven announced failure. Which additionally requires FEM non-linear analysis of the failure behaviour.

10.2.2 Analysis set-up improvements

For the more efficient measurement analysis, sensor network repositioning is suggested. The recommended measurement network can be seen in figure 10.1. It is based on the placement of the sensors below the wheel lines of the traffic vehicles. It is assumed that the friction force from the wheels of the vehicles will enhance the local mode behaviour in the surrounding region. The given enhancement will provide more stable results of local mode identification.

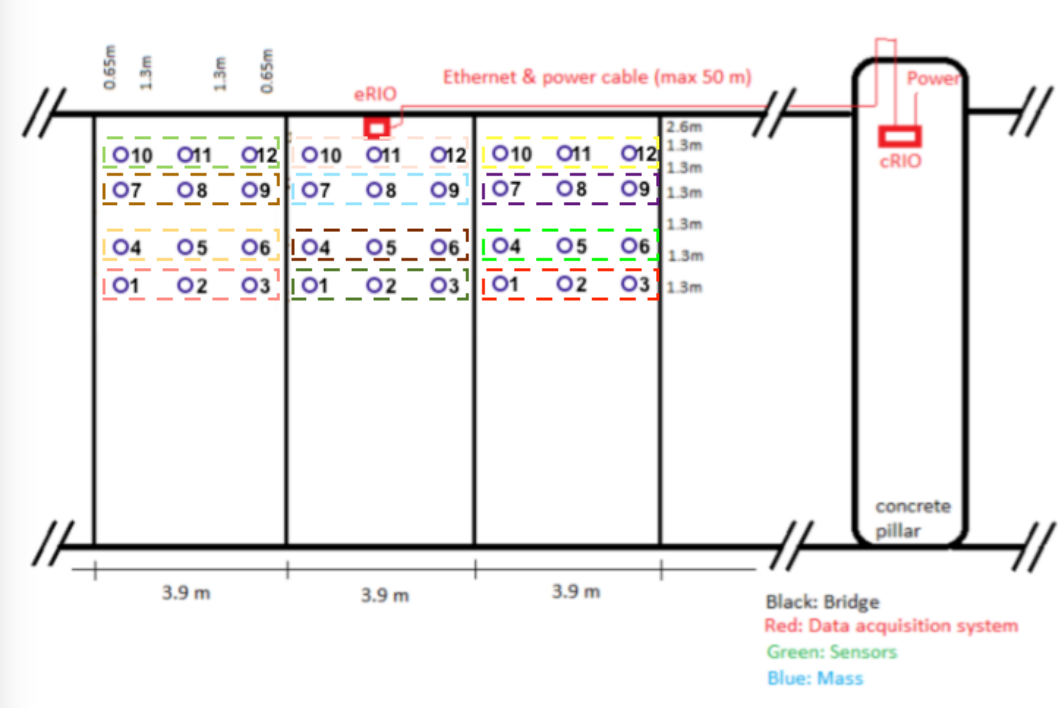


Figure 10.1: Recommended measurement network

To take the environmental conditions into account, long time algorithm calibration could be made (in various environmental conditions) or larger scale damages could be targeted for detection (that are larger than environmental impact).

Additionally idea is suggested, related to figure 10.1, dotted rectangles present suggestion for sensor bundles for the analysis (total of 12 separated segments). To take environmental conditions into account, assumption could be made that the environmental conditions could impact the behaviour of those segments equally. Proceeding to continuous monitoring, trend related to different environmental conditions could be followed. Referring back to the assumption that environmental conditions would impact all segments equally, segment that shows different environmental trend from the other segments could be identified as segment with the anomaly.

List of Figures

L.0 Workflow of level 0 . . . 7

3.1 Hasselt, Overijssel, Bridge over river Zwarte Water . . . 11
3.2 Deck segment equipped with sensors . . . 12
3.3 Technical drawing of the bridge . . . 13
3.4 FEM geometry . . . 13
3.5 Spatial resolution of sensor network . . . 14
3.6 The construction used for installing the measuring system . . . 15
3.7 System for attaching added mass . . . 16
3.8 Added mass system . . . 16
3.9 Hasselt, Overijssel, Netherlands Historical Weather Almanac 3/23/2017 . . . 22
3.10 Hasselt, Overijssel, Netherlands Historical Weather Almanac 3/28/2017 . . . 22
3.11 Hasselt, Overijssel, Netherlands Historical Weather Almanac 3/31/2017 . . . 23
3.12 Recorded temperature for measurements performed with 0kg . . . 23
3.13 Recorded temperature for measurements performed with 25kg . . . 23
3.14 Recorded temperature for measurements performed with 50kg . . . 24
3.15 Recorded temperature for measurements performed with 75kg . . . 24
3.16 Recorded temperature for measurements performed with 100kg . . . 24

4.1 Geometrical projection of 2D vectors . . . 26
4.2 Use of MAC for stabilisation diagram . . . 31

5.1 Stabilization diagram concept . . . 47
5.2 FDD singular value plot with SSI stabilization diagram . . . 48

6.1 Random signal (time and frequency domain) . . . 52
6.2 Spectrogram of random signal . . . 53
6.3 5 convolved random signals . . . 53
6.4 50 convolved random signals . . . 54
6.5 Example of used time variant signals . . . 55
6.6 Analysis of convolved signal . . . 56
6.7 3D illustration of 3 convolutions of Mdof system . . . 59
6.8 FFT for 100 elements of 100 order excitation tensor . . . 59
6.9 FFT for 100 elements of 100 order excitation tensor reduced with root of 100 . . . 62
L.1 Workflow of level 1 . . . 64

7.1 FDD plot with stabilization diagram . . . 67
7.2 FDD plot with stabilization diagram . . . 68
7.3 Histograms of stable mode count . . . 69
7.4 Histograms of stable mode count . . . 70
7.5 Sensors chosen for the level 1 analysis . . . 71
7.6 Analysis algorithm composition . . . 73
7.7 Example of the unreduced order PF signal . . . 75

7.8 Example of the reduced order PF signal . . . 75
7.9 Example of FDD and SSI output for 0kg and 50kg . . . 76
7.10 Example of FDD and SSI output for 75kg and 100kg . . . 77
7.11 Histograms of identified FDD modes . . . 78
7.12 1D Kalman filter of the obtained FDD results . . . 79
7.13 Histograms of identified SSI modes . . . 80
7.14 Example 1 of the time domain plot and the related FDD plot . . . 81
7.15 Example 2 of the time domain plot and the related FDD plot . . . 82
7.16 Example 3 of the time domain plot and the related FDD plot . . . 82
7.17 Example of FDD and SSI output for 0kg and 50kg . . . 83
7.18 Example of FDD and SSI output for 75kg and 100kg . . . 84
7.19 Histograms of identified FDD modes . . . 85
7.20 1D Kalman filter of the obtained FDD results . . . 86
7.21 Histograms of identified SSI modes . . . 87
L.2 Workflow of level 2 . . . 88

8.1 Segment 1 and Segment 3 of the sensor network . . . 89
8.2 Histograms of identified FDD modes . . . 90
8.3 1D Kalman filter estimation of the FDD most dominant mode . . . 91
8.4 Histograms of identified SSI modes . . . 92
8.5 Histograms of identified FDD modes . . . 93
8.6 1D Kalman filter estimation of the FDD most dominant mode . . . 94
8.7 Histograms of identified SSI modes . . . 95
8.8 General purpose graphics processing unit . . . 96
8.9 Parallel algorithm scheme . . . 96
8.10 Analysis algorithm calibration with level 1 and level 2 . . . 97
L.3 Workflow of level 3 . . . 98

9.1 Geometry and Boundary conditions . . . 100
9.2 Mesh of the global FEM model . . . 100
9.3 The first 500 modes of global FEM analysis . . . 101
9.4 Mode shapes, total deformation . . . 101
9.5 Mode shapes, total deformation . . . 102
9.6 Segment 2 of the bridge structure . . . 103
9.7 Sub-structuring of system with element SEl.1 instead of elements El.2 and El.3 . . . 103
9.8 Geometry and Boundary conditions of the model . . . 104
9.9 Mesh of the model . . . 104
9.10 The first damage scenario . . . 105
9.11 The second damage scenario . . . 105
9.12 The third damage scenario . . . 105
9.13 Mode 7, 0kg model, 65.635Hz . . . 106
9.14 Mode 6, 50kg model, 64.691Hz . . . 106
9.15 Mode 6, 75kg model, 63.942Hz . . . 107
9.16 Mode 6, 100kg model, 63.121Hz . . . 107
9.17 Mode 6, 35cm crack model, 63.193Hz . . . 107
9.18 Mode 6, 2 times 35cm crack model, 61.469Hz . . . 108
9.19 Mode 5, full two U section cracks, 52.887Hz . . . 108
9.20 Local model 2 Boundary condition concept illustration . . . 109
9.21 Geometry and Boundary conditions of the model . . . 110
9.22 Geometry and applied mass . . . 110
9.23 Mesh of the structure, global . . . 111
9.24 Mesh of the structure, bottom view . . . 111

9.25 Mesh of the "segment 2" (segment with mass) . . . 111
9.26 The first 6 modes, global representation . . . 112
9.27 Mode 16, 0kg model, 55.151Hz . . . 113
9.28 Mode 16, 50kg model, 54.936Hz ($\Delta f = 0.215$Hz) . . . 113
9.29 Mode 16, 75kg model, 54.832Hz ($\Delta f = 0.319$Hz) . . . 113
9.30 Mode 16, 100kg model, 54.738Hz ($\Delta f = 0.413$Hz) . . . 114
9.31 Mode 16, 35cm crack model, 54.919Hz ($\Delta f = 0.232$Hz) . . . 114
9.32 Mode 16, 2 times 35cm crack model, 54.765Hz ($\Delta f = 0.386$Hz) . . . 114
9.33 Mode 15 and 16 for the 2 full U section cracks . . . 115
9.34 Mode 27, 50kg model, 67.297Hz . . . 115
9.35 Mode 27, 75kg model, 66.683Hz ($\Delta f = 0.614$Hz from 50kg) . . . 115
9.36 Mode 27, 100kg model, 66.083Hz ($\Delta f = 0.6$Hz from 75kg) . . . 116
9.37 The first ten modes of Local model 2 FEM analysis . . . 116

10.1 Recommended measurement network . . . 120

List of Tables

3.1 Test matrix for the measurements on the Zwartewaterbrug 17
3.2 0kg added mass stable mode count 19
3.3 25kg added mass stable mode count 19
3.4 50kg added mass stable mode count 19
3.5 75kg added mass stable mode count 20
3.6 100kg added mass stable mode count 20
3.7 Hammer test stable mode count 20

Bibliography

[1] Randall J Allemang. The modal assurance criterion–twenty years of use and abuse. *Sound and vibration*, 37(8):14–23, 2003.

[2] Rune Brincker and Palle Andersen. Understanding stochastic subspace identification. *Proceedings of the 24th IMAC, St. Louis, Missouri*, pages 279–311, 2006.

[3] NVIDIA Corporation. Nvidia tesla p40 gpu accelerator, 2017.

[4] P Faure. Stochastic realization algorithms. system identification: Advances and case studies. eds. mehra r. and lainiotis d, 1976.

[5] Thomas Kailath. *Linear systems*, volume 156. Prentice-Hall Englewood Cliffs, NJ, 1980.

[6] Alan Laub. A schur method for solving algebraic riccati equations. *IEEE Transactions on automatic control*, 24(6):913–921, 1979.

[7] World Weather Online. Netherlands historical weather almanac, 2016.

[8] Daniel Puschina. Test razer core v2 + blade stealth (i7-8550u), 2017.

[9] Anders Rytter. *Vibrational based inspection of civil engineering structures*. PhD thesis, Dept. of Building Technology and Structural Engineering, Aalborg University, 1993.

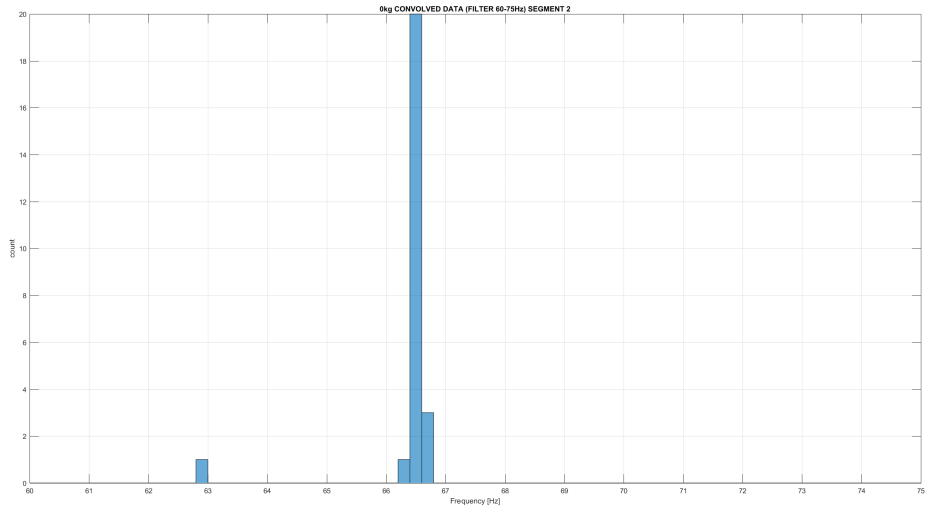
[10] Robert S Strichartz. *A guide to distribution theory and Fourier transforms*. World Scientific Publishing Company, 2003.

[11] Peter Van Overschee and Bart De Moor. N4sid: Subspace algorithms for the identification of combined deterministic-stochastic systems. *Automatica*, 30(1):75–93, 1994.

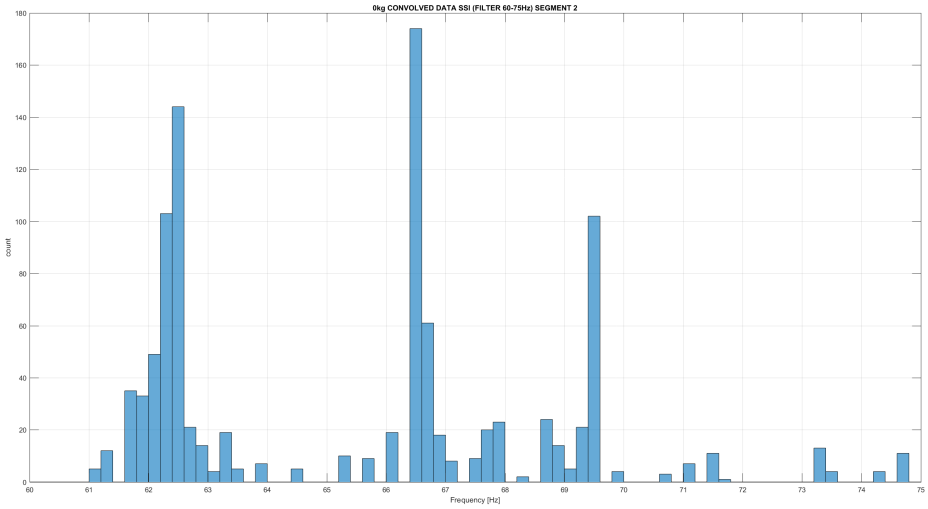
[12] Peter Van Overschee and BL De Moor. *Subspace identification for linear systems: Theory-Implementation-Applications*. Springer Science & Business Media, 2012.

Appendix A1

Data 0kg-50kg-75kg-100kg segment 2 (Unreduced order PF)

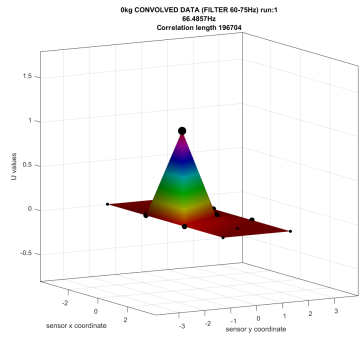


(a) 0kg FDD histogram

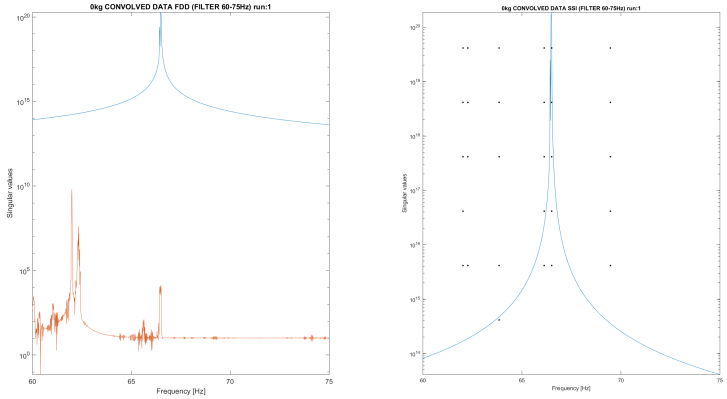


(b) 0kg SSI histogram

Figure A1.0kg: Histograms of identified modes, 0kg data

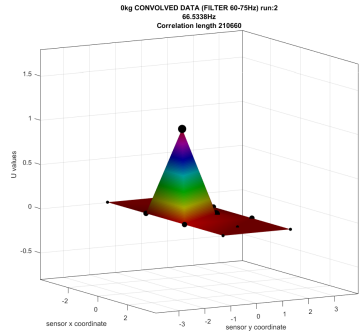


(a) 0kg mode shape, run 1

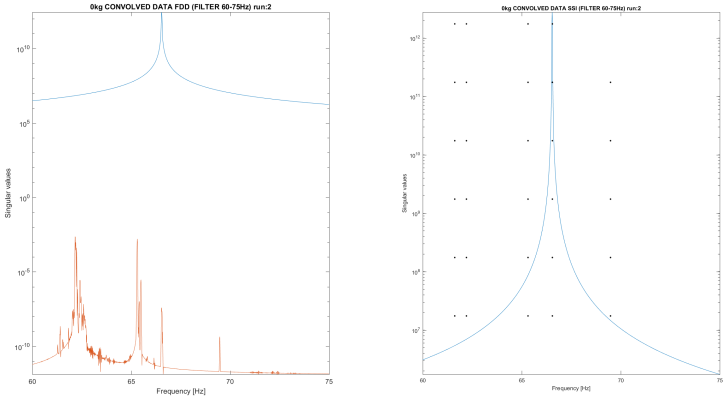


(b) 0kg FDD SSI output, run 1

Figure A1.0kg: Run 1

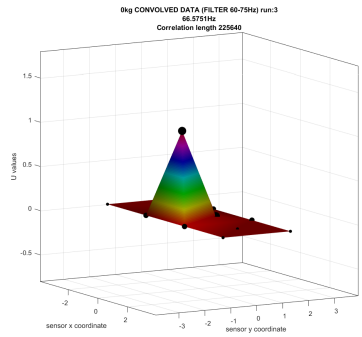


(a) 0kg mode shape, run 2

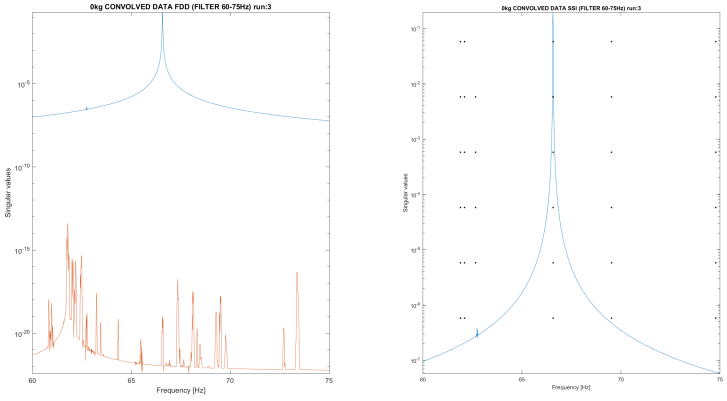


(b) 0kg FDD SSI output, run 2

Figure A1.0kg: Run 2

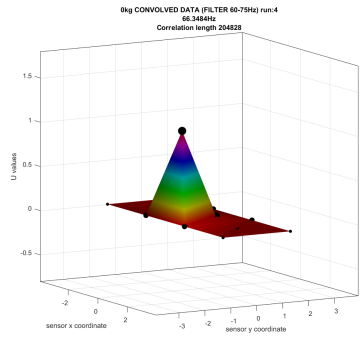


(a) 0kg mode shape, run 3

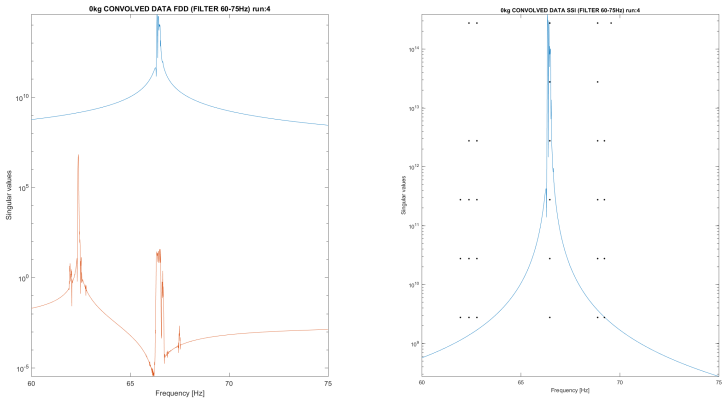


(b) 0kg FDD SSI output, run 3

Figure A1.0kg: Run 3

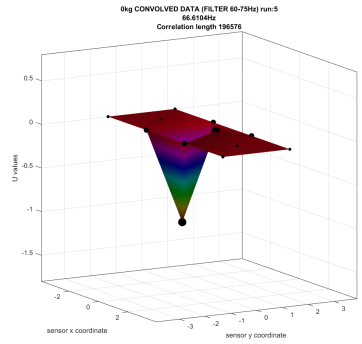


(a) 0kg mode shape, run 4

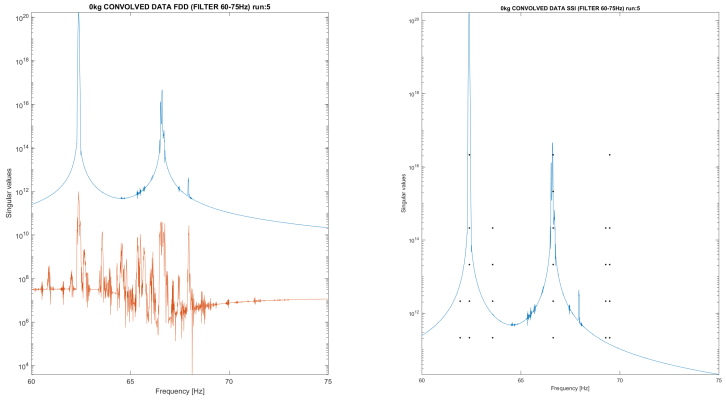


(b) 0kg FDD SSI output, run 4

Figure A1.0kg: Run 4

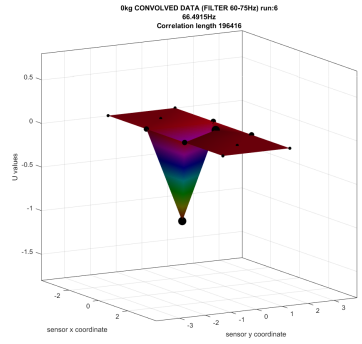


(a) 0kg mode shape, run 5

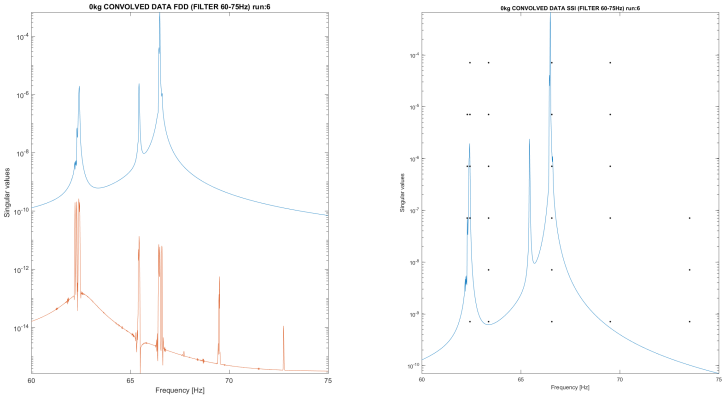


(b) 0kg FDD SSI output, run 5

Figure A1.0kg: Run 5

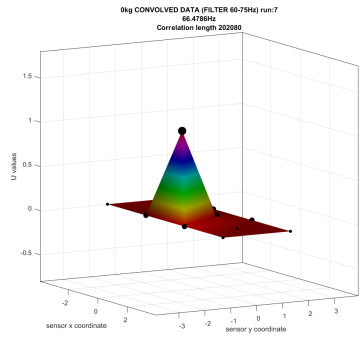


(a) 0kg mode shape, run 6

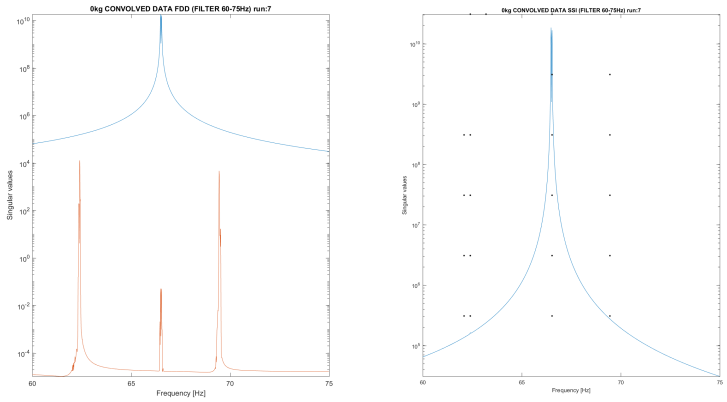


(b) 0kg FDD SSI output, run 6

Figure A1.0kg: Run 6

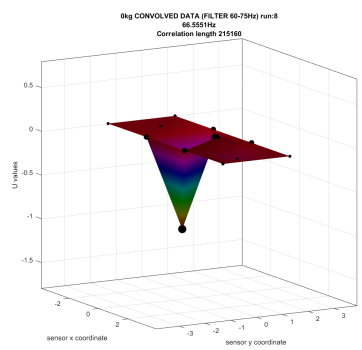


(a) 0kg mode shape, run 7

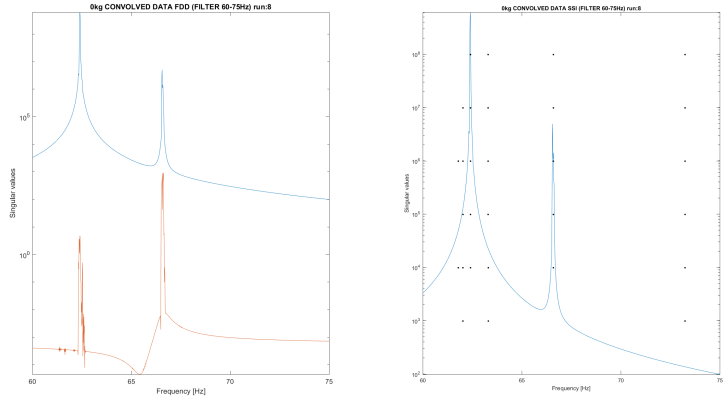


(b) 0kg FDD SSI output, run 7

Figure A1.0kg: Run 7

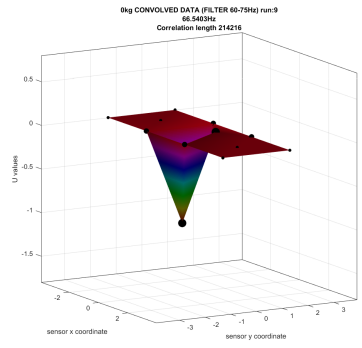


(a) 0kg mode shape, run 8

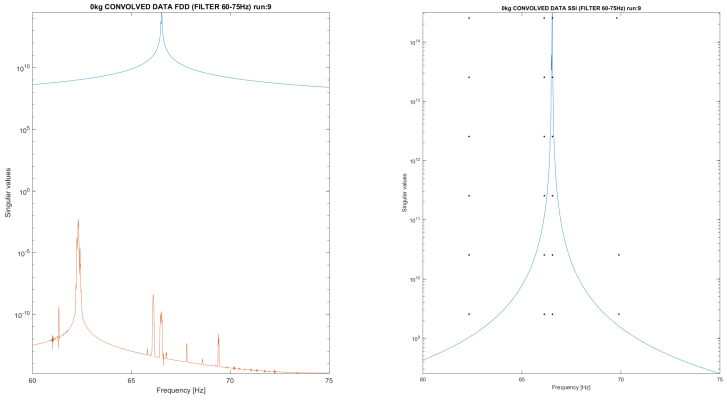


(b) 0kg FDD SSI output, run 8

Figure A1.0kg: Run 8

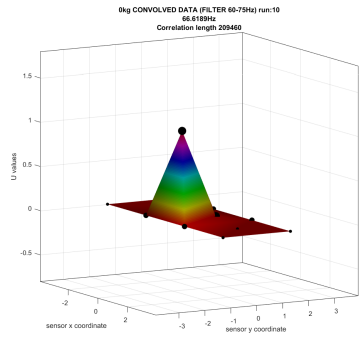


(a) 0kg mode shape, run 9

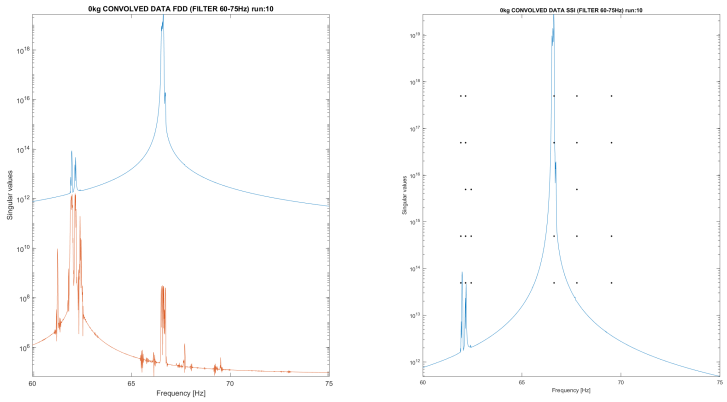


(b) 0kg FDD SSI output, run 9

Figure A1.0kg: Run 9

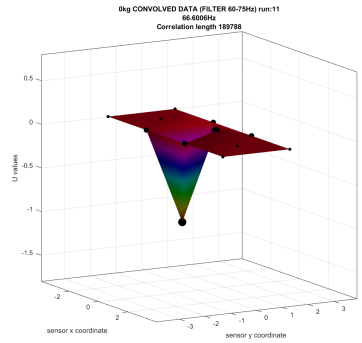


(a) 0kg mode shape, run 10

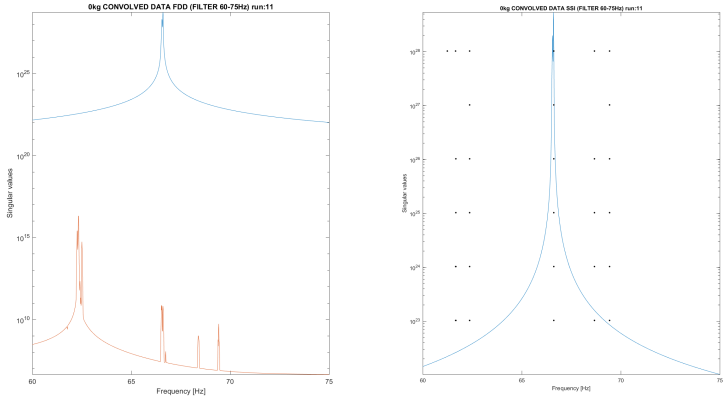


(b) 0kg FDD SSI output, run 10

Figure A1.0kg: Run 10

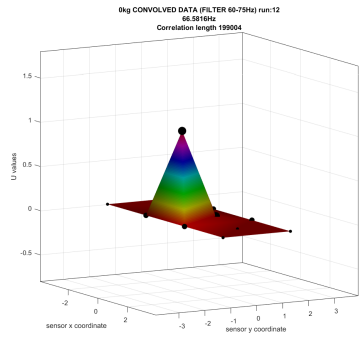


(a) 0kg mode shape, run 11

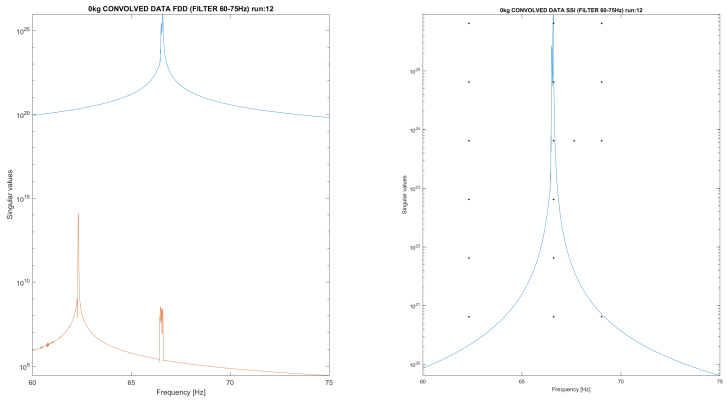


(b) 0kg FDD SSI output, run 11

Figure A1.0kg: Run 11

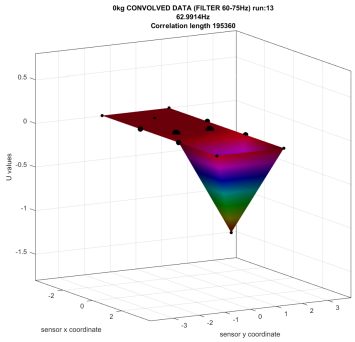


(a) 0kg mode shape, run 12

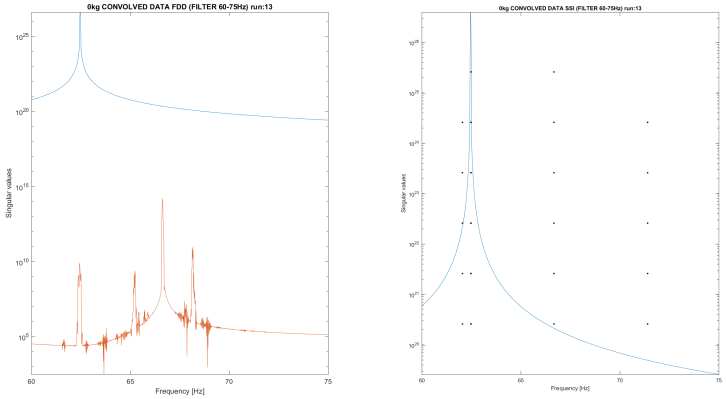


(b) 0kg FDD SSI output, run 12

Figure A1.0kg: Run 12

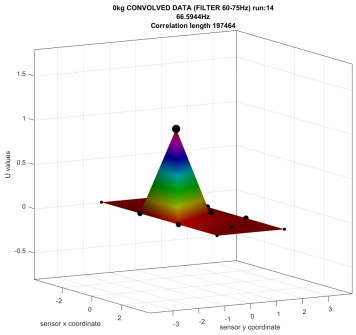


(a) 0kg mode shape, run 13

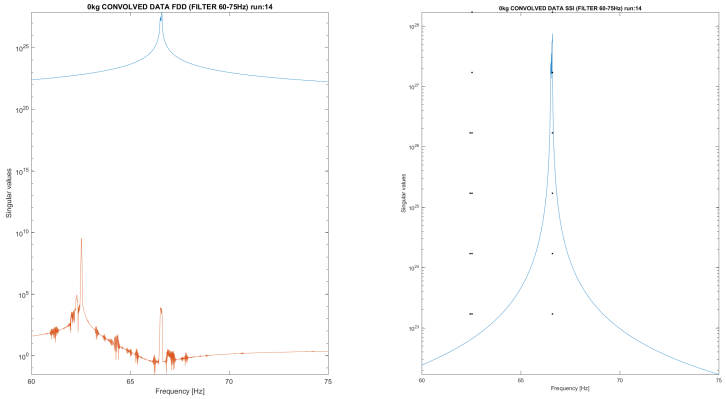


(b) 0kg FDD SSI output, run 13

Figure A1.0kg: Run 13

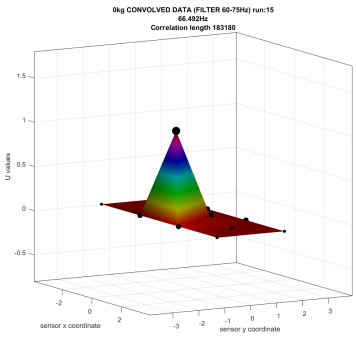


(a) 0kg mode shape, run 14

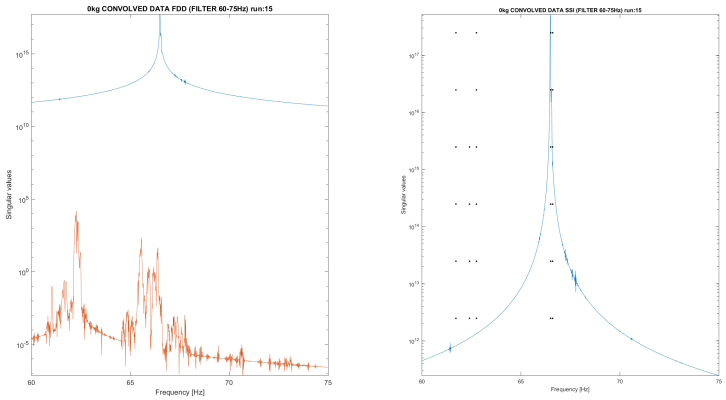


(b) 0kg FDD SSI output, run 14

Figure A1.0kg: Run 14

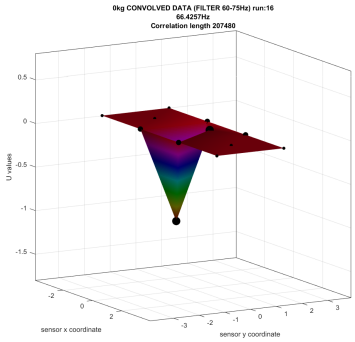


(a) 0kg mode shape, run 15

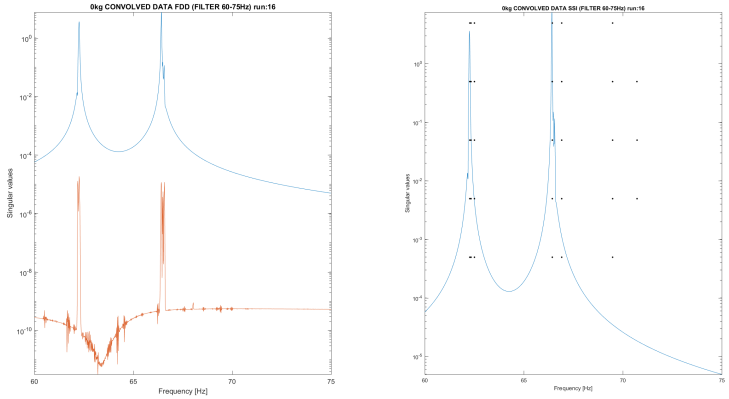


(b) 0kg FDD SSI output, run 15

Figure A1.0kg: Run 15

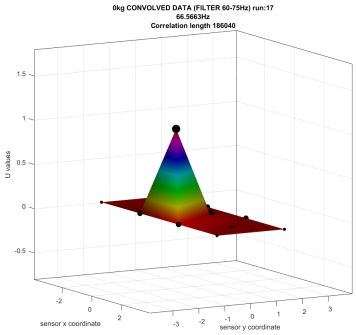


(a) 0kg mode shape, run 16

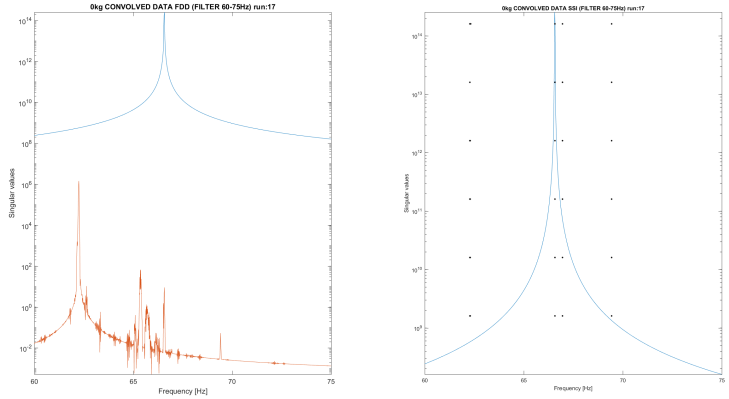


(b) 0kg FDD SSI output, run 16

Figure A1.0kg: Run 16

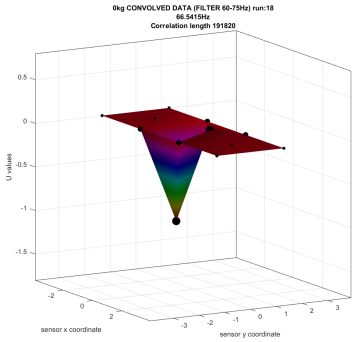


(a) 0kg mode shape, run 17

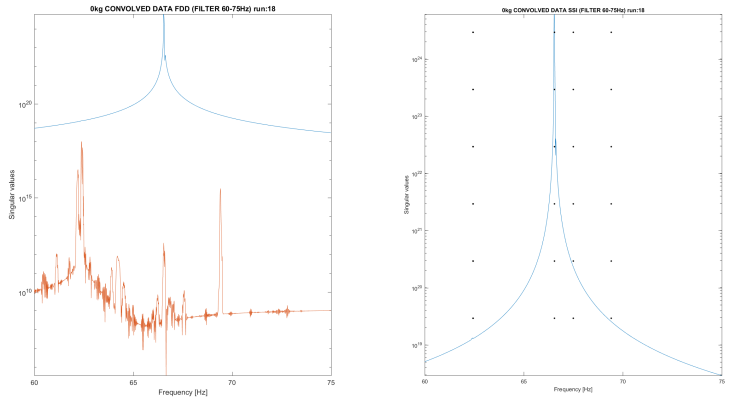


(b) 0kg FDD SSI output, run 17

Figure A1.0kg: Run 17

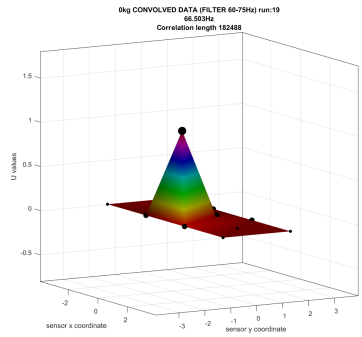


(a) 0kg mode shape, run 18

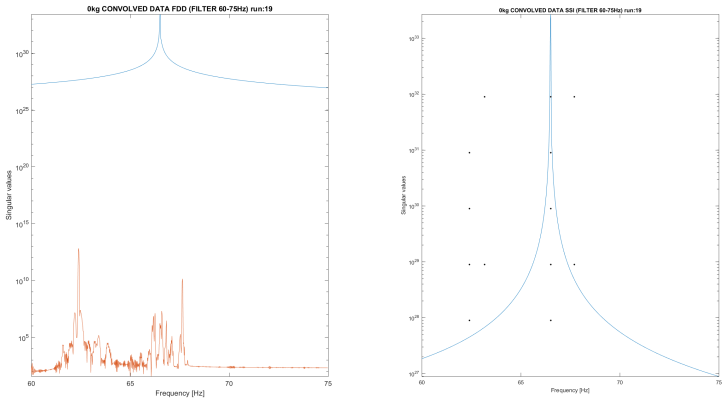


(b) 0kg FDD SSI output, run 18

Figure A1.0kg: Run 18

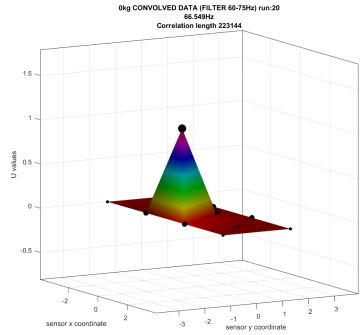


(a) 0kg mode shape, run 19

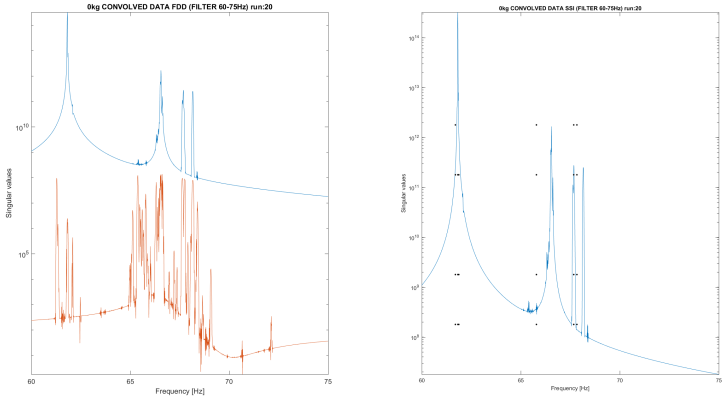


(b) 0kg FDD SSI output, run 19

Figure A1.0kg: Run 19

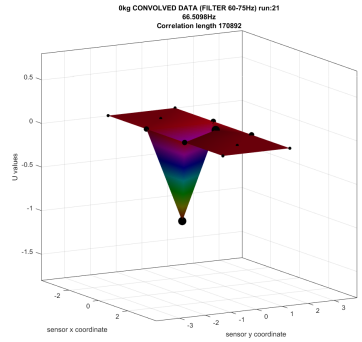


(a) 0kg mode shape, run 20

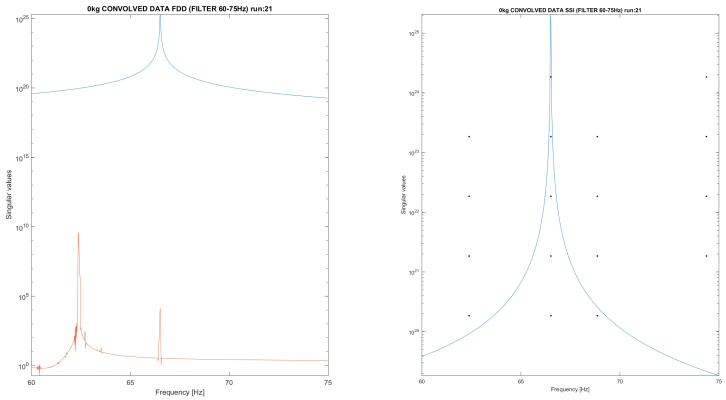


(b) 0kg FDD SSI output, run 20

Figure A1.0kg: Run 20

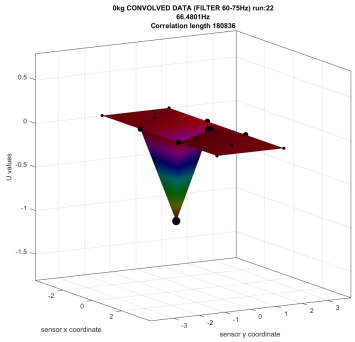


(a) 0kg mode shape, run 21

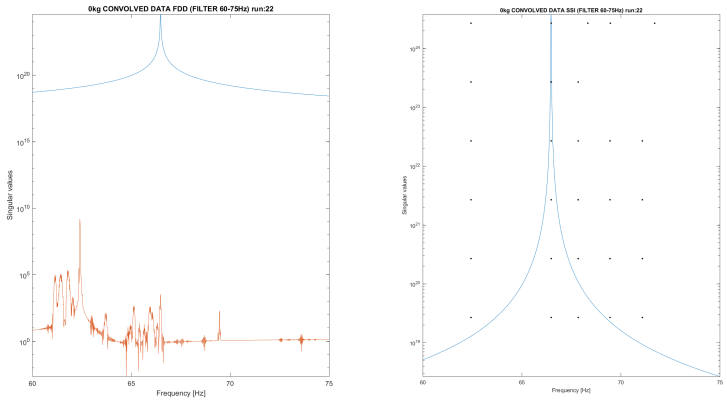


(b) 0kg FDD SSI output, run 21

Figure A1.0kg: Run 21

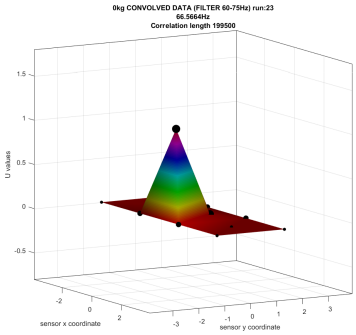


(a) 0kg mode shape, run 22

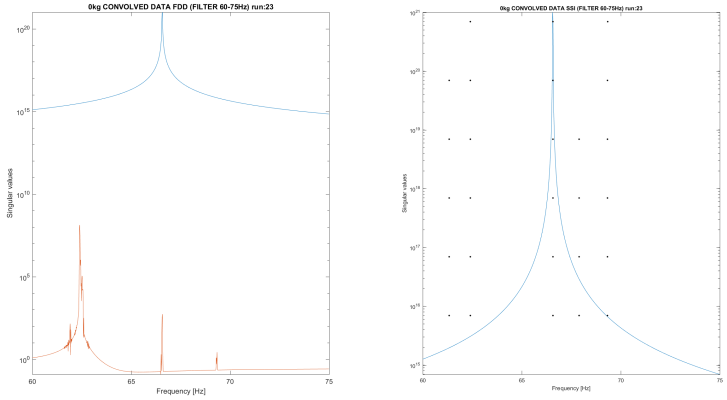


(b) 0kg FDD SSI output, run 22

Figure A1.0kg: Run 22

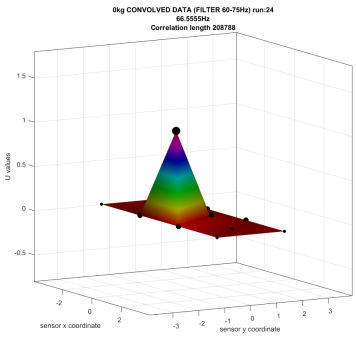


(a) 0kg mode shape, run 23

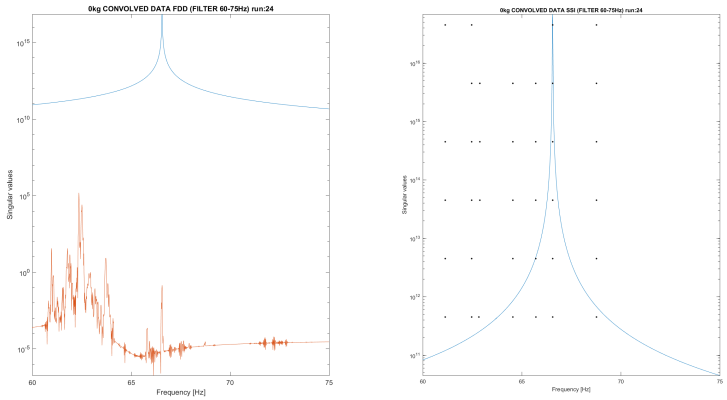


(b) 0kg FDD SSI output, run 23

Figure A1.0kg: Run 23

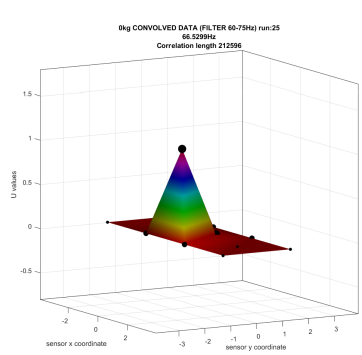


(a) 0kg mode shape, run 24

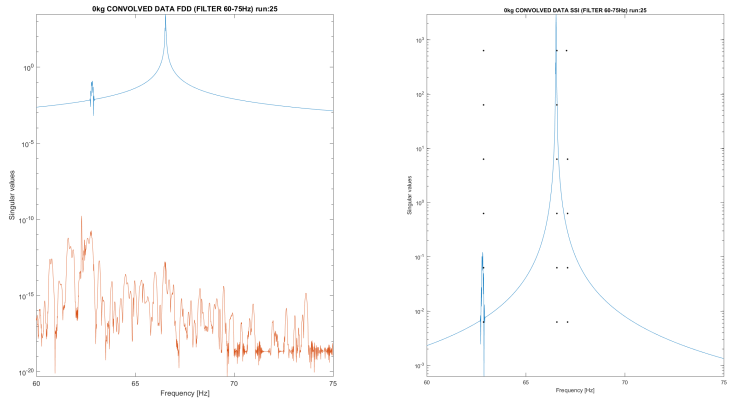


(b) 0kg FDD SSI output, run 24

Figure A1.0kg: Run 24



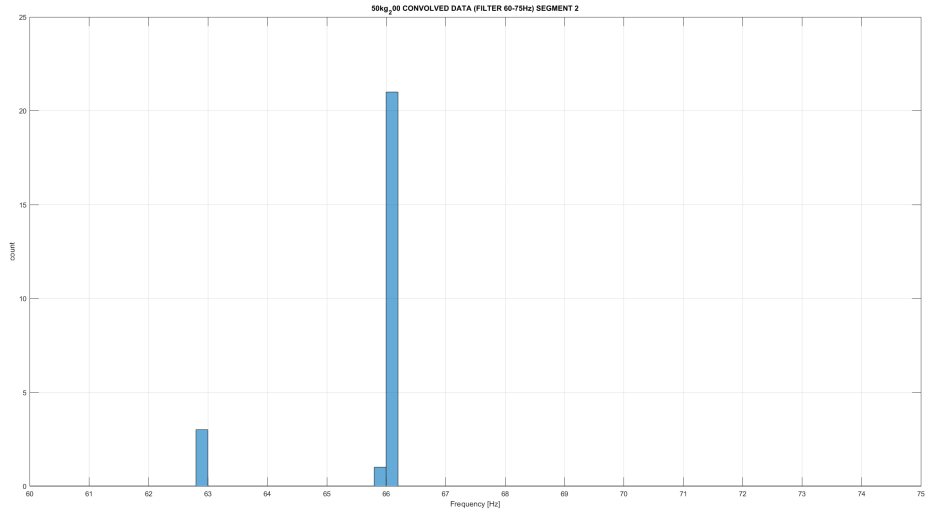
(a) 0kg mode shape, run 25



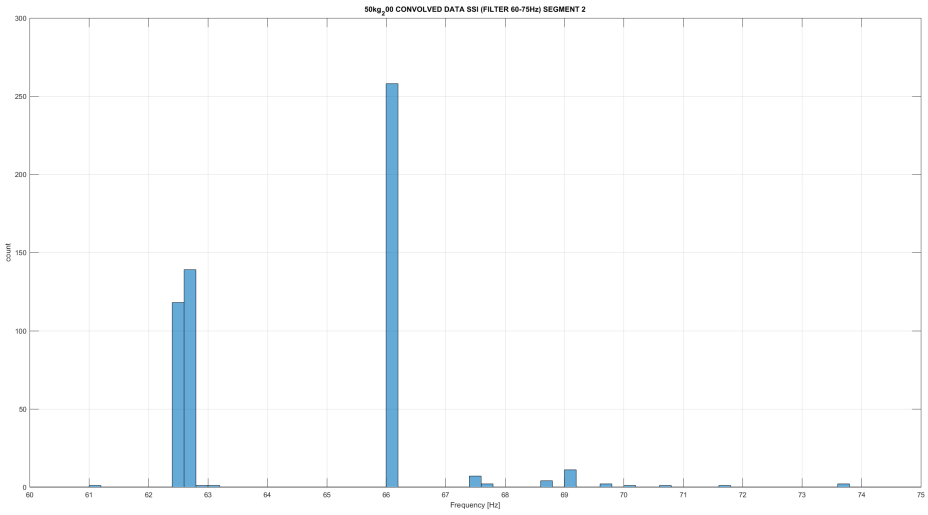
(b) 0kg FDD SSI output, run 25

Figure A1.0kg: Run 25

50kg data segment 2

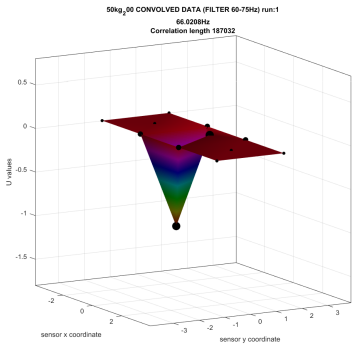


(a) 50kg FDD histogram

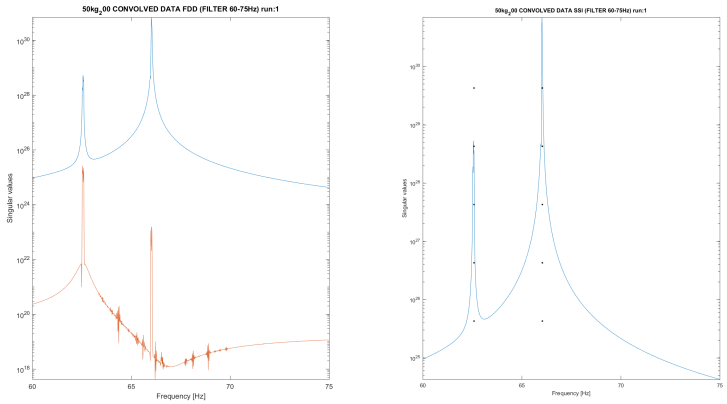


(b) 50kg SSI histogram

Figure A1.50kg: Histograms of identified modes, 50kg data

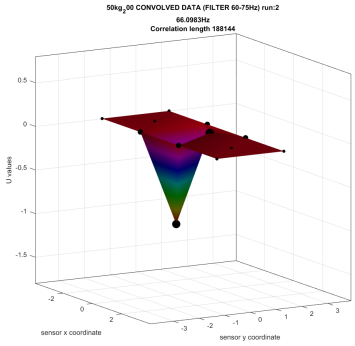


(a) 50kg mode shape, run 1

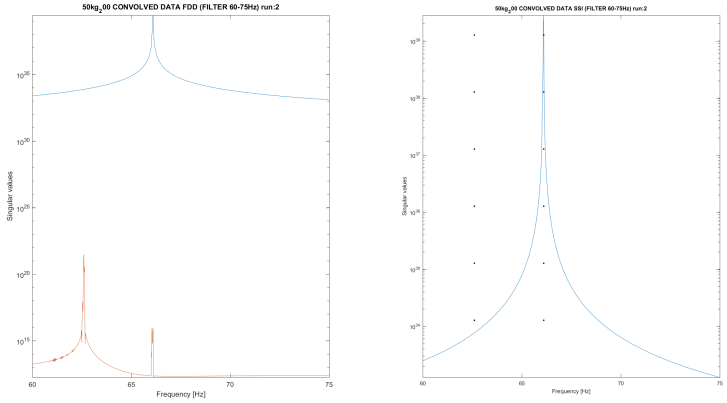


(b) 50kg FDD SSI output, run 1

Figure A1.50kg: Run 1

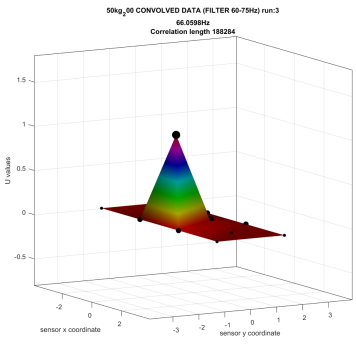


(a) 50kg mode shape, run 2

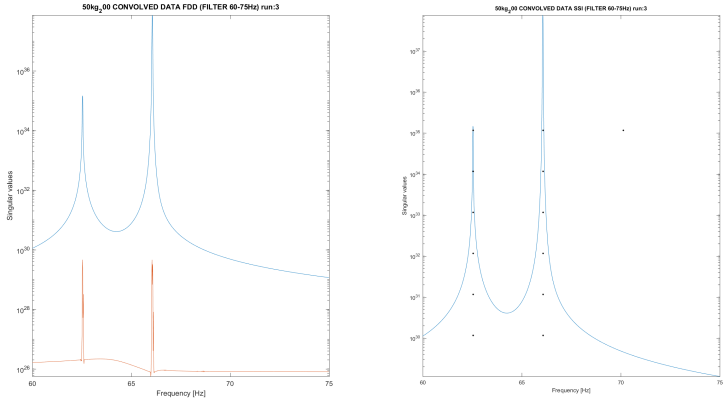


(b) 50kg FDD SSI output, run 2

Figure A1.50kg: Run 2

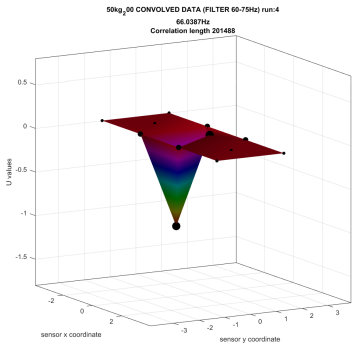


(a) 50kg mode shape, run 3

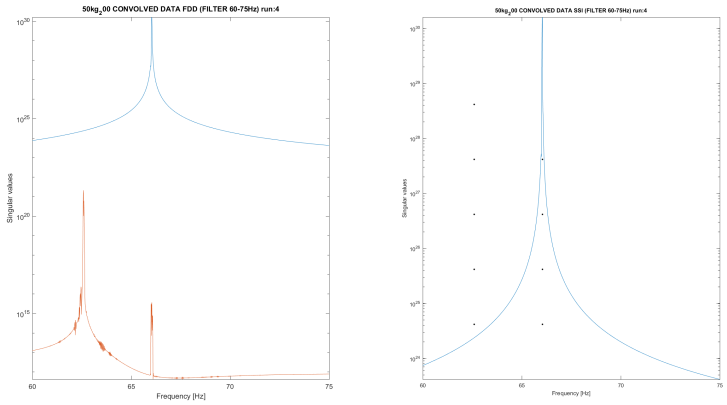


(b) 50kg FDD SSI output, run 3

Figure A1.50kg: Run 3

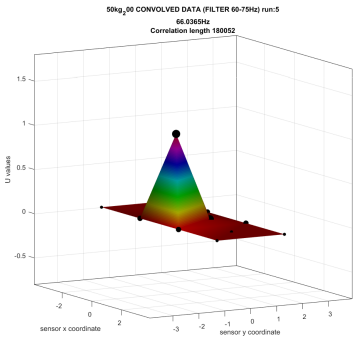


(a) 50kg mode shape, run 4

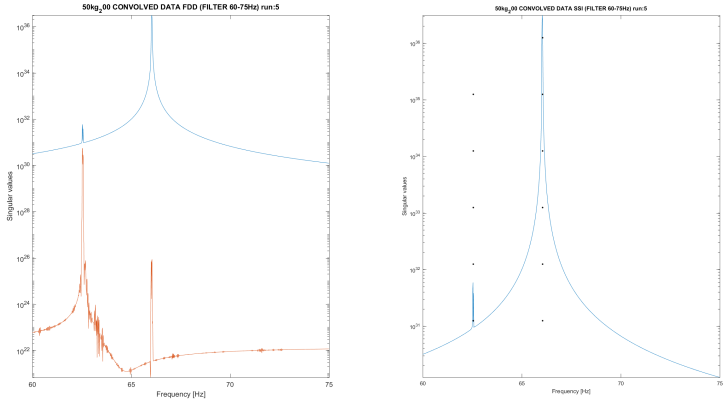


(b) 50kg FDD SSI output, run 4

Figure A1.50kg: Run 4

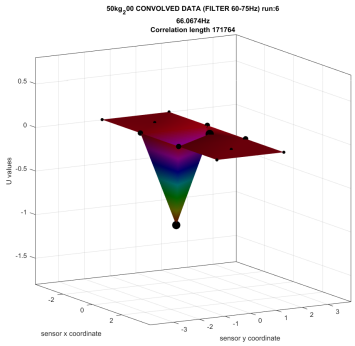


(a) 50kg mode shape, run 5

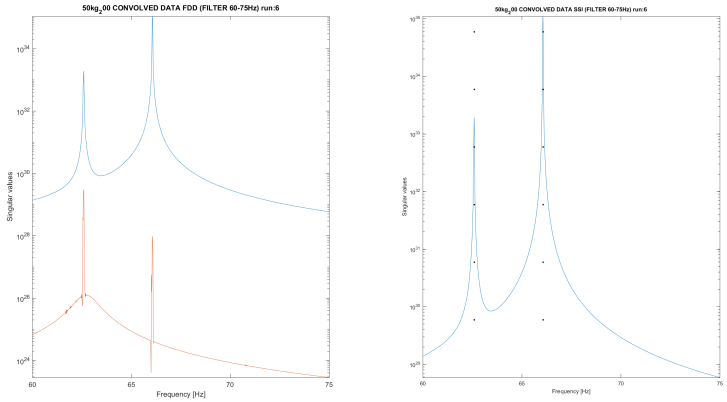


(b) 50kg FDD SSI output, run 5

Figure A1.50kg: Run 5

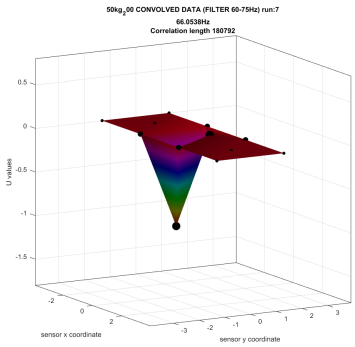


(a) 50kg mode shape, run 6

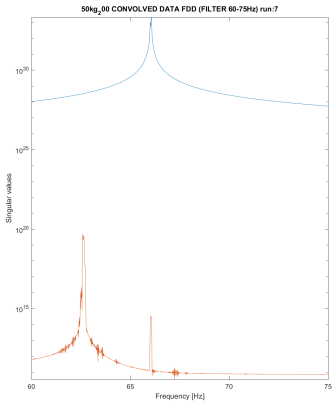


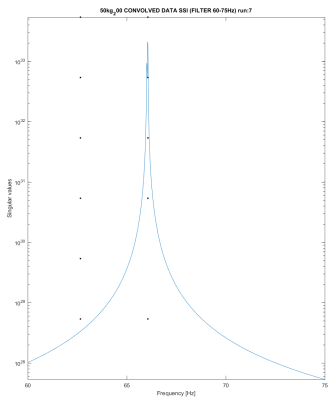
(b) 50kg FDD SSI output, run 6

Figure A1.50kg: Run 6



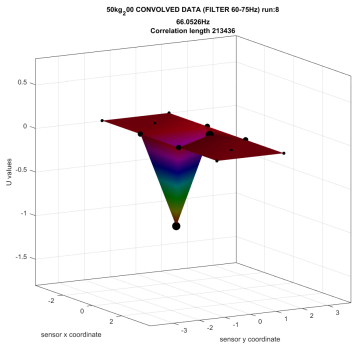
(a) 50kg mode shape, run 7



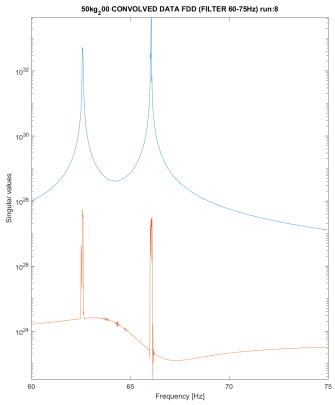


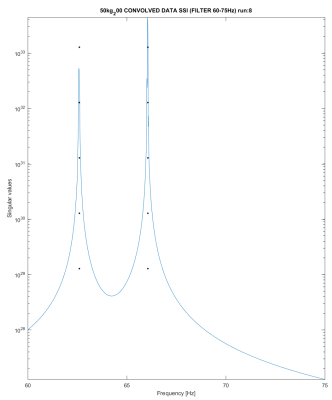
(b) 50kg FDD SSI output, run 7

Figure A1.50kg: Run 7



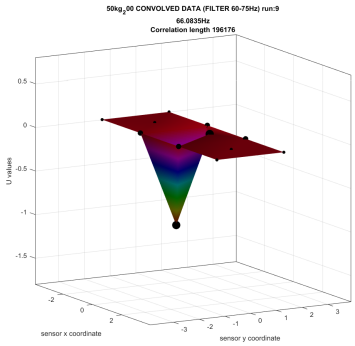
(a) 50kg mode shape, run 8



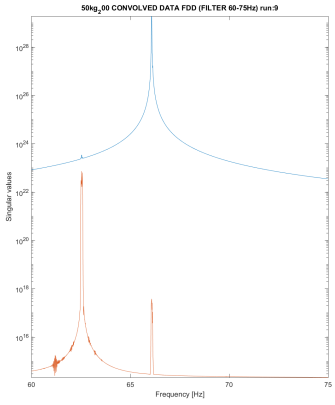


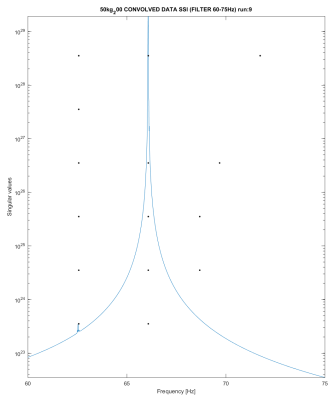
(b) 50kg FDD SSI output, run 8

Figure A1.50kg: Run 8



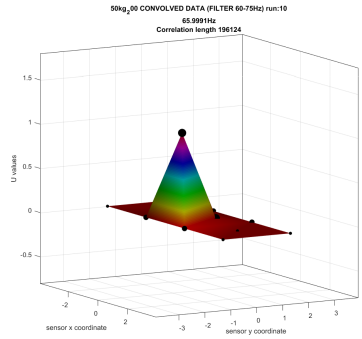
(a) 50kg mode shape, run 9



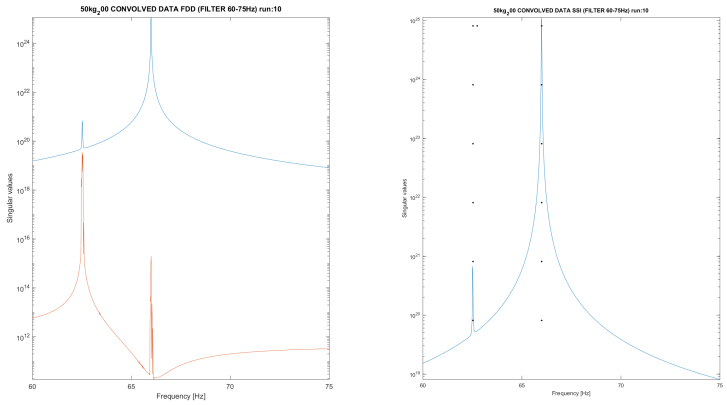


(b) 50kg FDD SSI output, run 9

Figure A1.50kg: Run 9

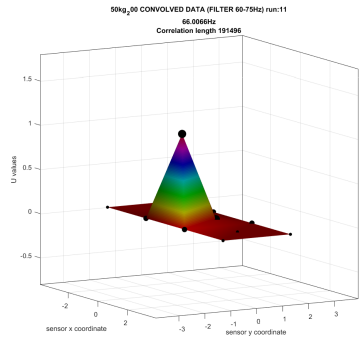


(a) 50kg mode shape, run 10

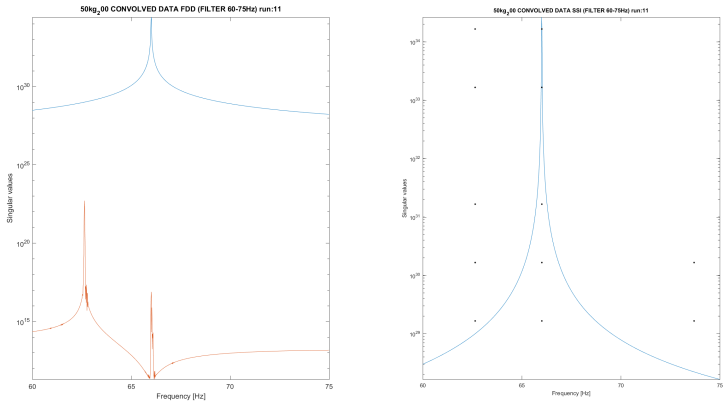


(b) 50kg FDD SSI output, run 10

Figure A1.50kg: Run 10

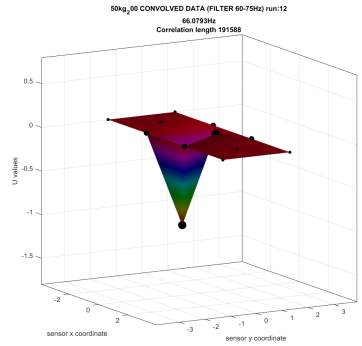


(a) 50kg mode shape, run 11

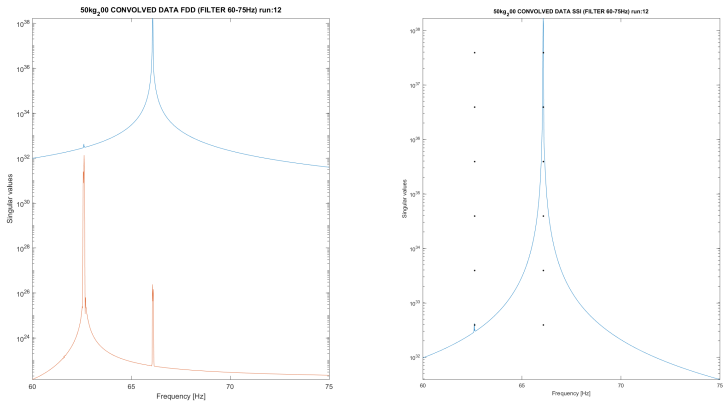


(b) 50kg FDD SSI output, run 11

Figure A1.50kg: Run 11

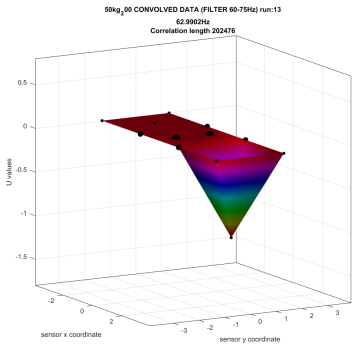


(a) 50kg mode shape, run 12

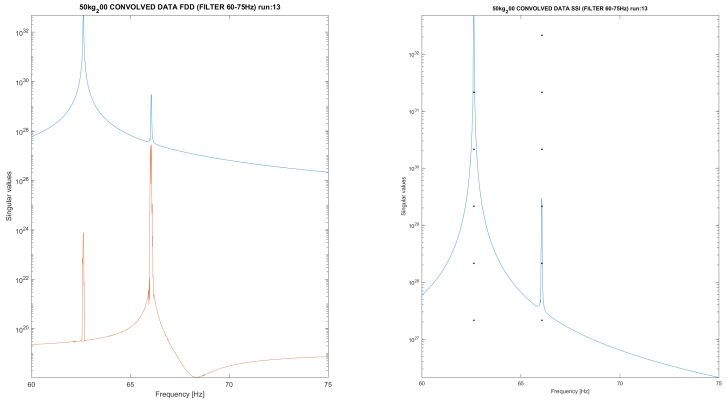


(b) 50kg FDD SSI output, run 12

Figure A1.50kg: Run 12

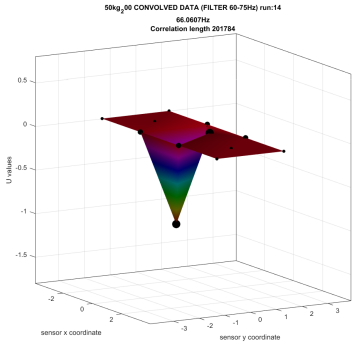


(a) 50kg mode shape, run 13

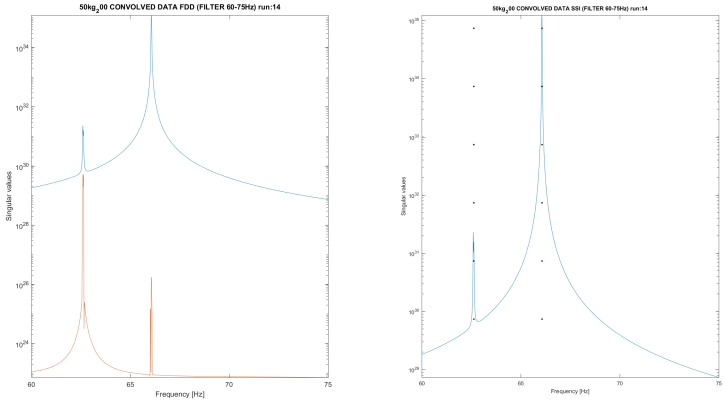


(b) 50kg FDD SSI output, run 13

Figure A1.50kg: Run 13

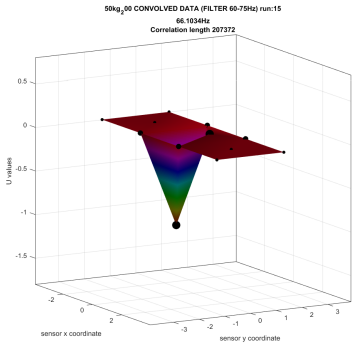


(a) 50kg mode shape, run 14

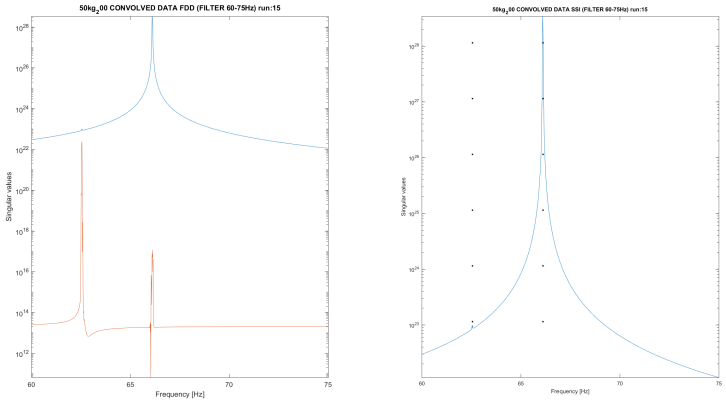


(b) 50kg FDD SSI output, run 14

Figure A1.50kg: Run 14

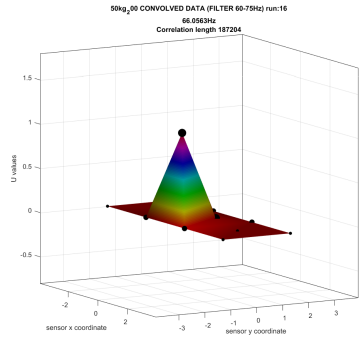


(a) 50kg mode shape, run 15

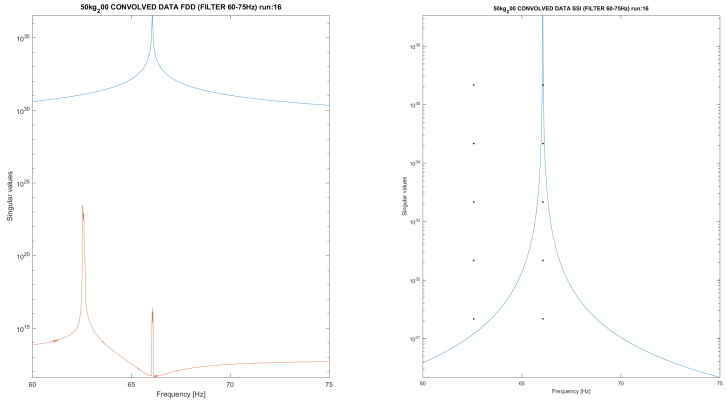


(b) 50kg FDD SSI output, run 15

Figure A1.50kg: Run 15

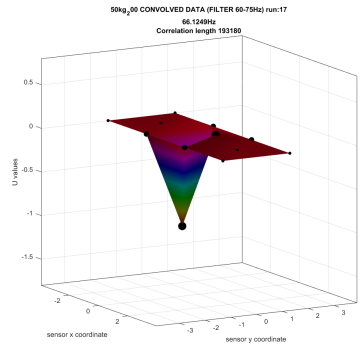


(a) 50kg mode shape, run 16

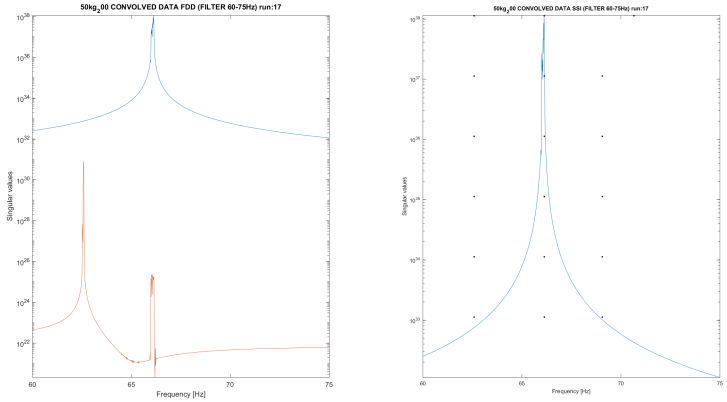


(b) 50kg FDD SSI output, run 16

Figure A1.50kg: Run 16

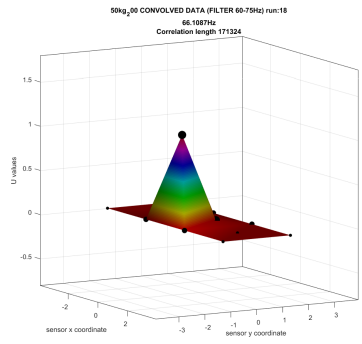


(a) 50kg mode shape, run 17

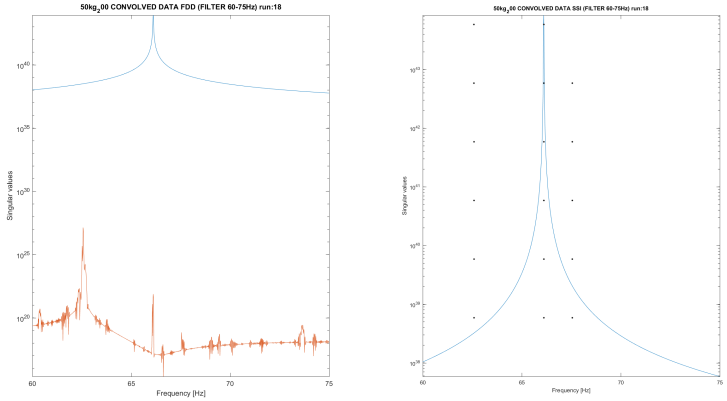


(b) 50kg FDD SSI output, run 17

Figure A1.50kg: Run 17

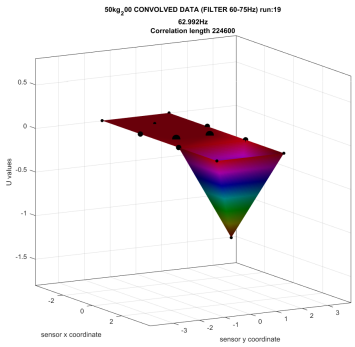


(a) 50kg mode shape, run 18

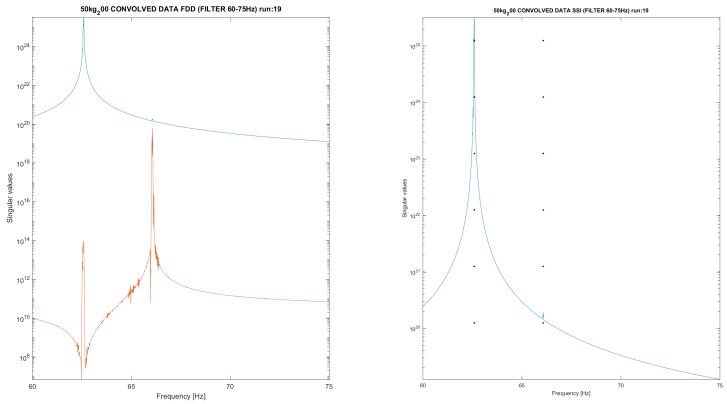


(b) 50kg FDD SSI output, run 18

Figure A1.50kg: Run 18

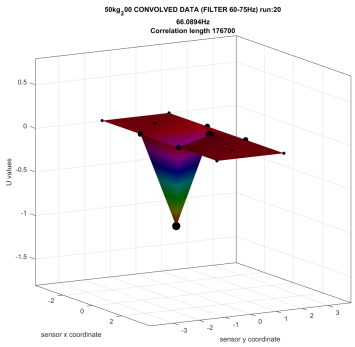


(a) 50kg mode shape, run 19

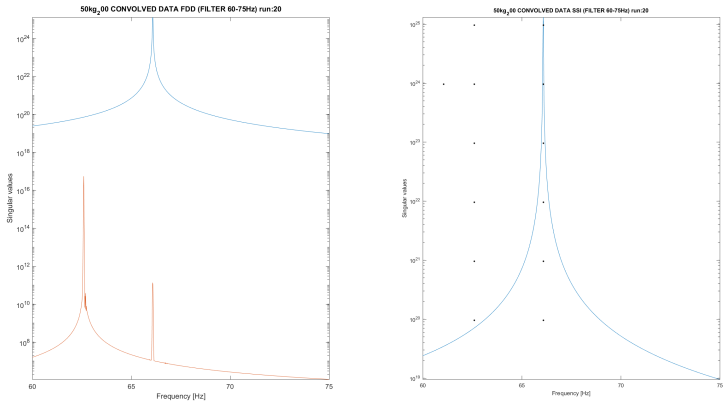


(b) 50kg FDD SSI output, run 19

Figure A1.50kg: Run 19

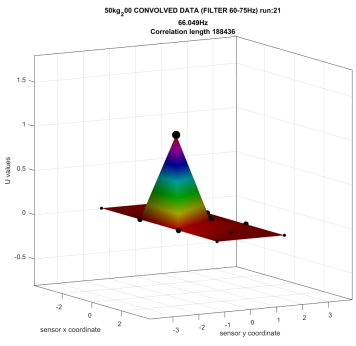


(a) 50kg mode shape, run 20

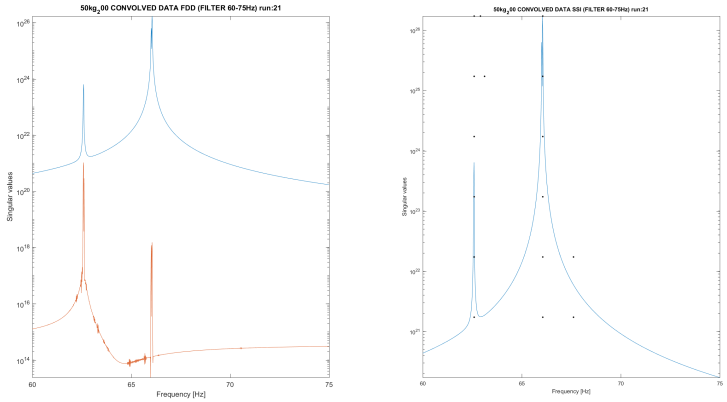


(b) 50kg FDD SSI output, run 20

Figure A1.50kg: Run 20

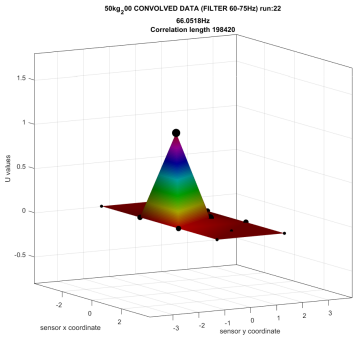


(a) 50kg mode shape, run 21

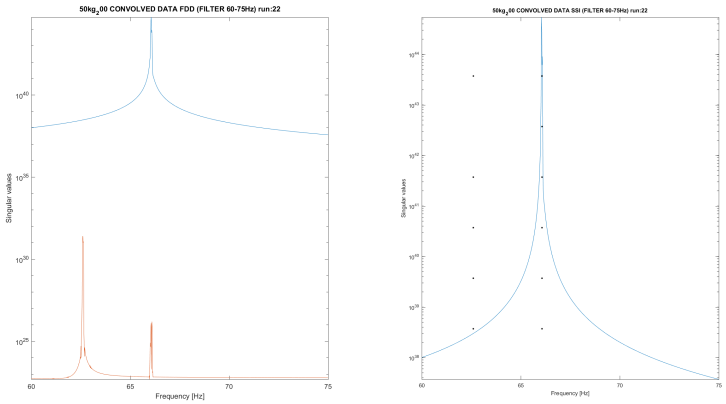


(b) 50kg FDD SSI output, run 21

Figure A1.50kg: Run 21

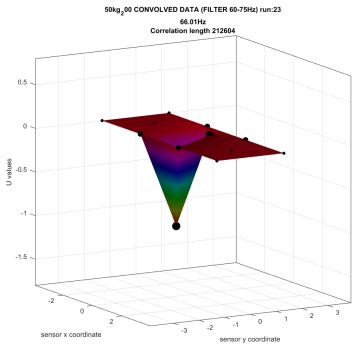


(a) 50kg mode shape, run 22

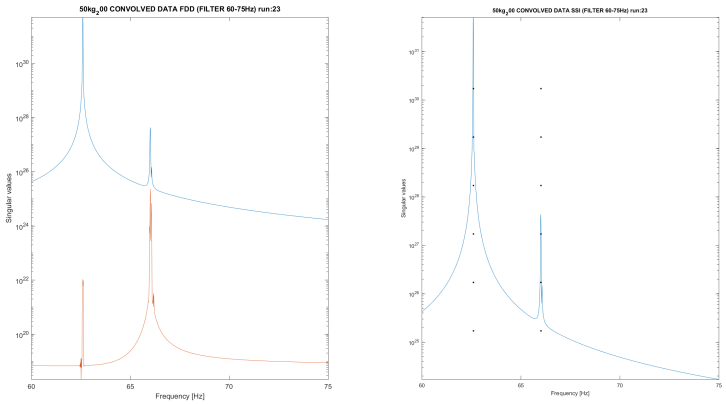


(b) 50kg FDD SSI output, run 22

Figure A1.50kg: Run 22

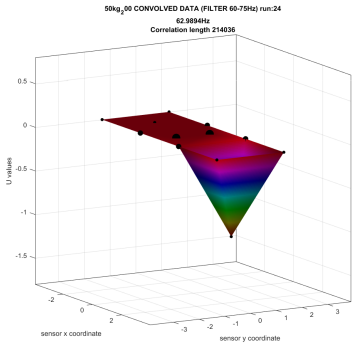


(a) 50kg mode shape, run 23

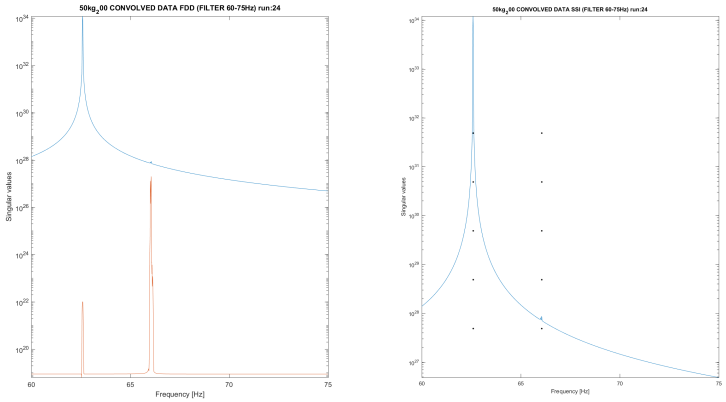


(b) 50kg FDD SSI output, run 23

Figure A1.50kg: Run 23

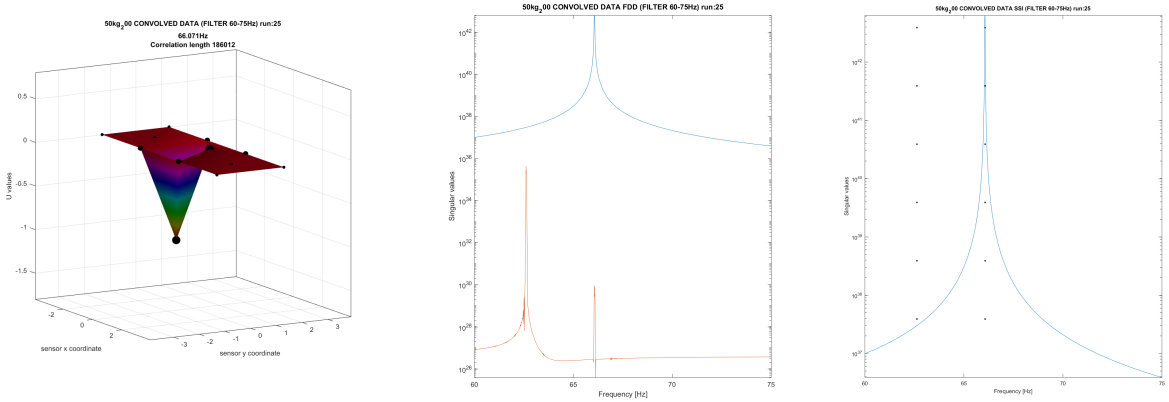


(a) 50kg mode shape, run 24



(b) 50kg FDD SSI output, run 24

Figure A1.50kg: Run 24

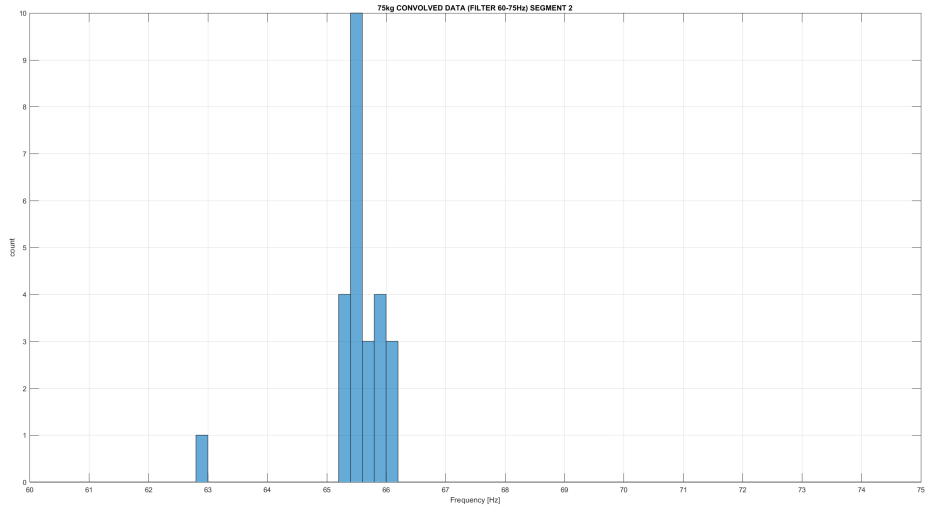


(a) 50kg mode shape, run 25

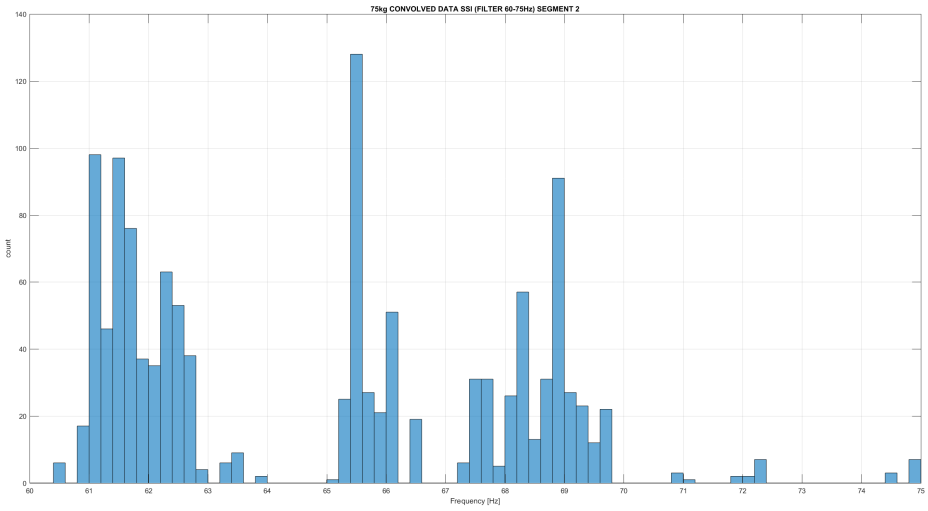
(b) 50kg FDD SSI output, run 25

Figure A1.50kg: Run 25

75kg data segment 2

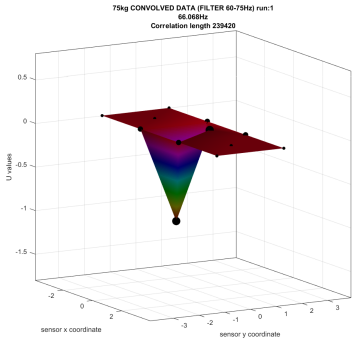


(a) 75kg FDD histogram

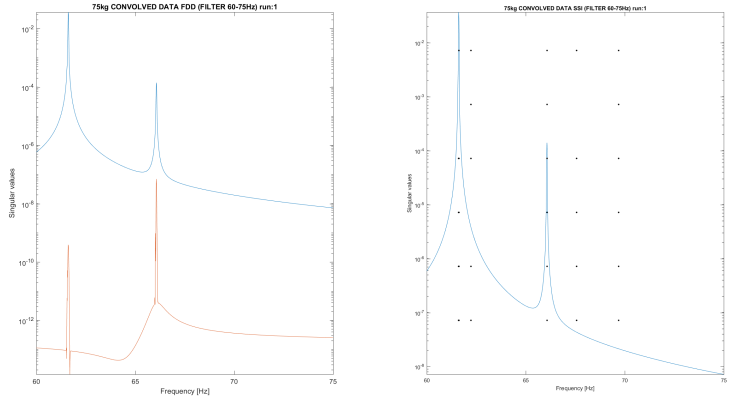


(b) 75kg SSI histogram

Figure A1.75kg: Histograms of identified modes, 75kg data

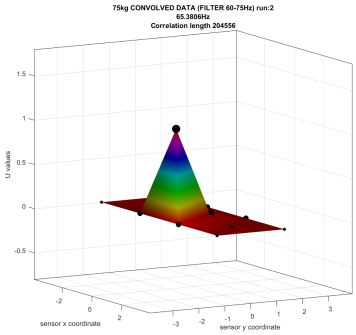


(a) 75kg mode shape, run 1

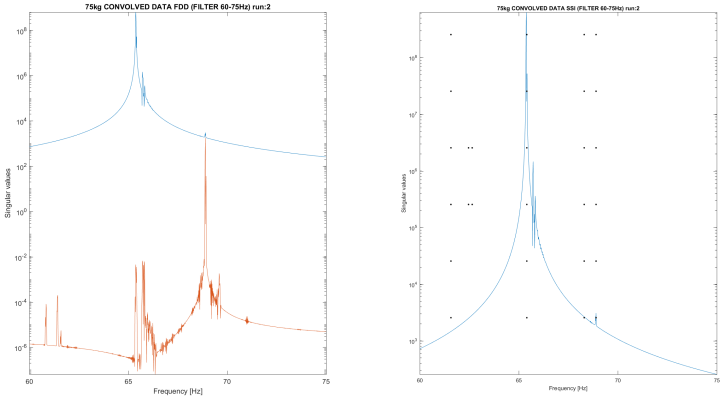


(b) 75kg FDD SSI output, run 1

Figure A1.75kg: Run 1

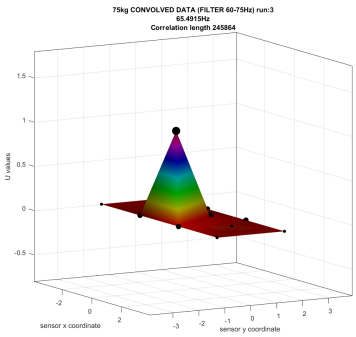


(a) 75kg mode shape, run 2

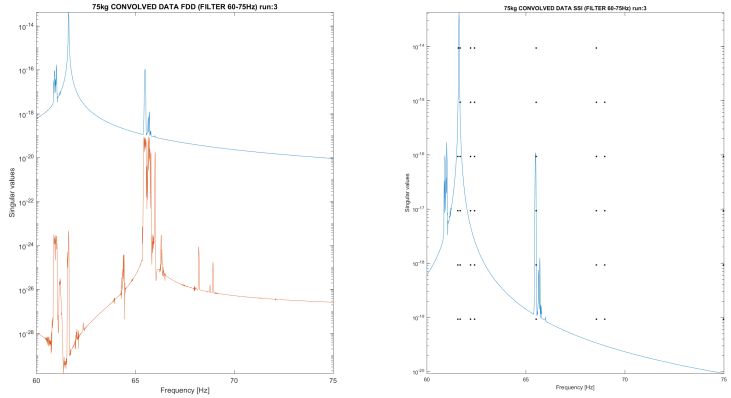


(b) 75kg FDD SSI output, run 2

Figure A1.75kg: Run 2

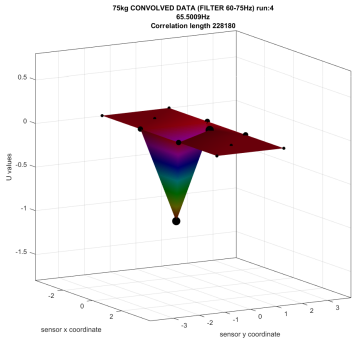


(a) 75kg mode shape, run 3

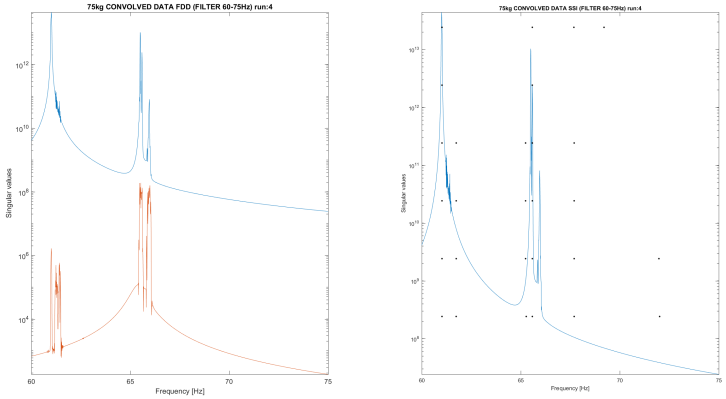


(b) 75kg FDD SSI output, run 3

Figure A1.75kg: Run 3

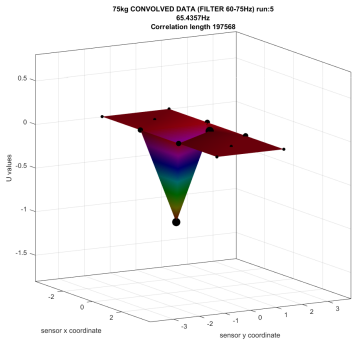


(a) 75kg mode shape, run 4

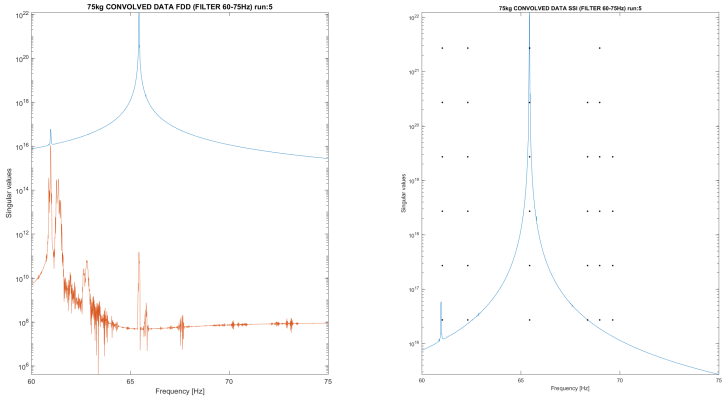


(b) 75kg FDD SSI output, run 4

Figure A1.75kg: Run 4

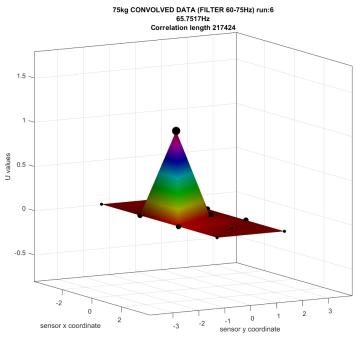


(a) 75kg mode shape, run 5

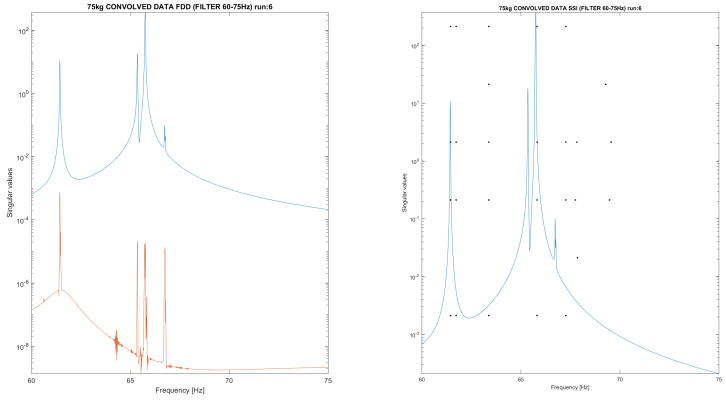


(b) 75kg FDD SSI output, run 5

Figure A1.75kg: Run 5

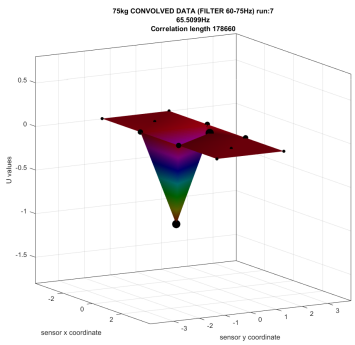


(a) 75kg mode shape, run 6

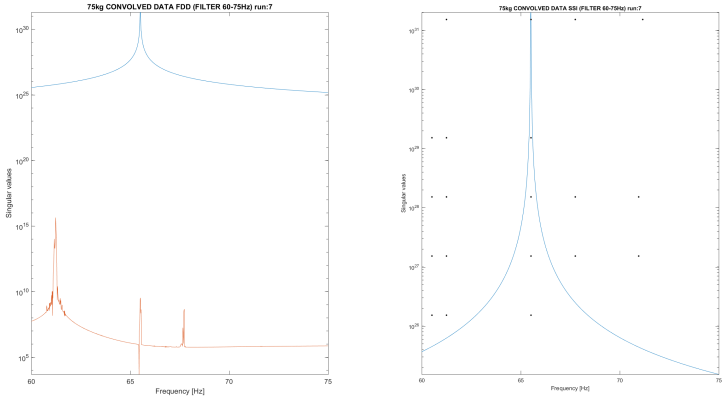


(b) 75kg FDD SSI output, run 6

Figure A1.75kg: Run 6

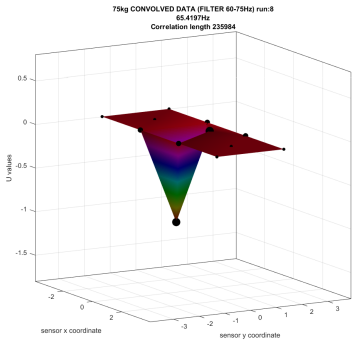


(a) 75kg mode shape, run 7

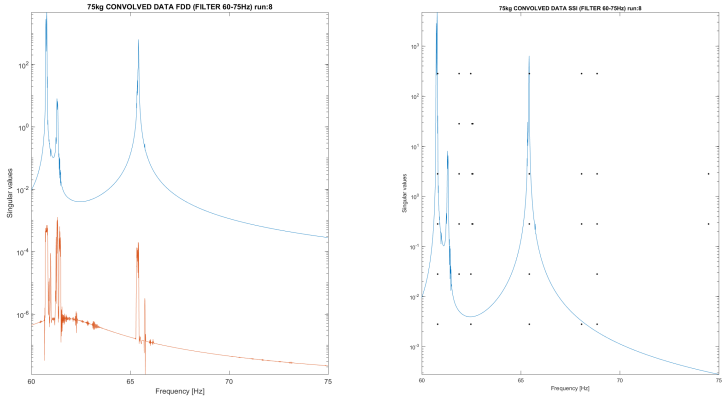


(b) 75kg FDD SSI output, run 7

Figure A1.75kg: Run 7

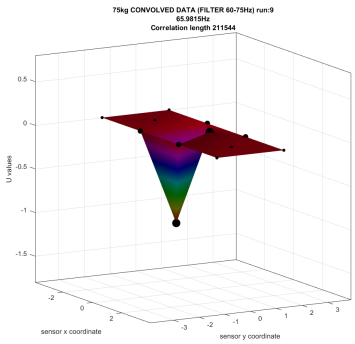


(a) 75kg mode shape, run 8

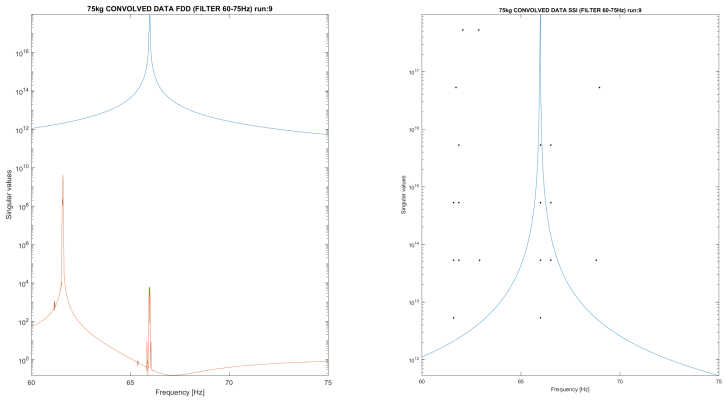


(b) 75kg FDD SSI output, run 8

Figure A1.75kg: Run 8

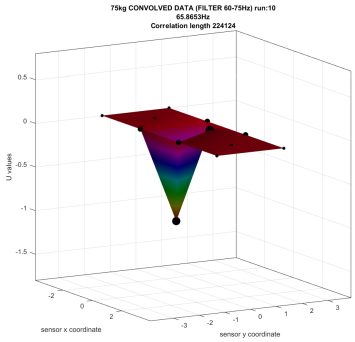


(a) 75kg mode shape, run 9

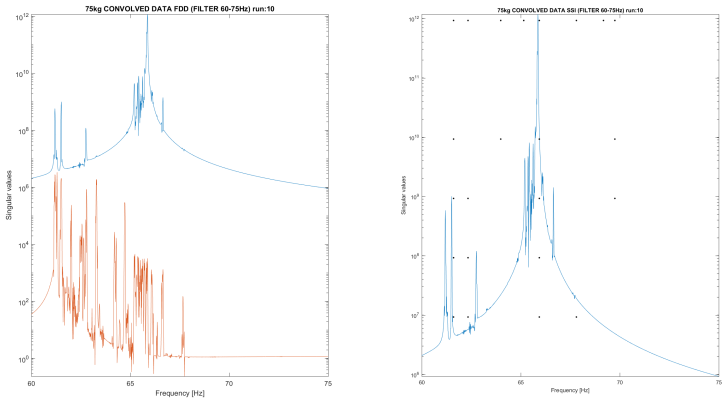


(b) 75kg FDD SSI output, run 9

Figure A1.75kg: Run 9

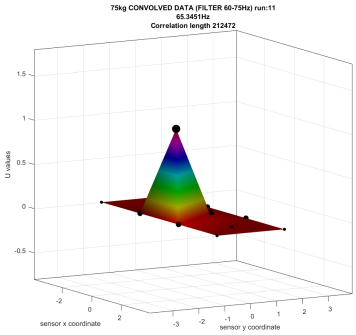


(a) 75kg mode shape, run 10

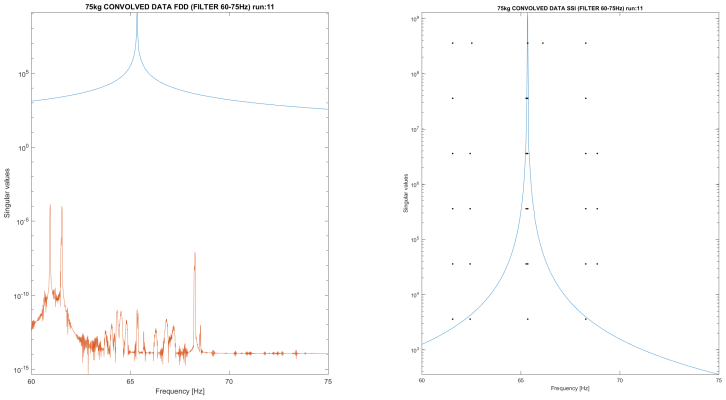


(b) 75kg FDD SSI output, run 10

Figure A1.75kg: Run 10

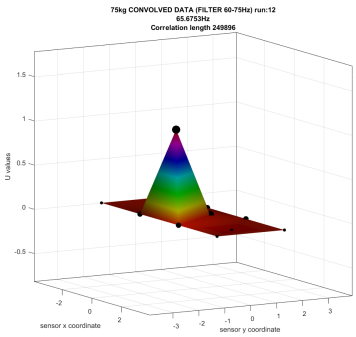


(a) 75kg mode shape, run 11

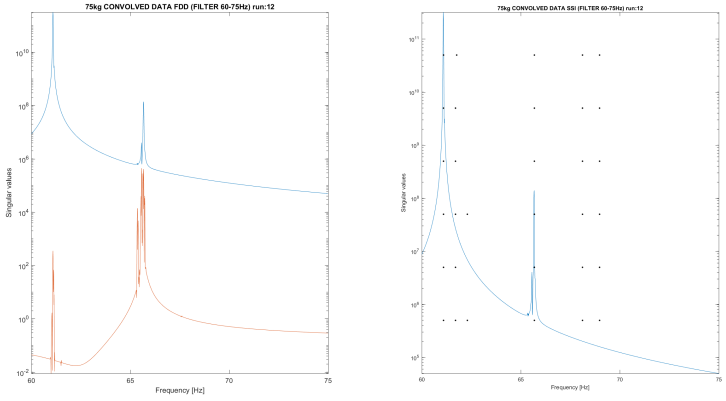


(b) 75kg FDD SSI output, run 11

Figure A1.75kg: Run 11

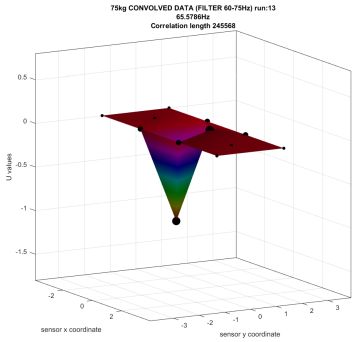


(a) 75kg mode shape, run 12

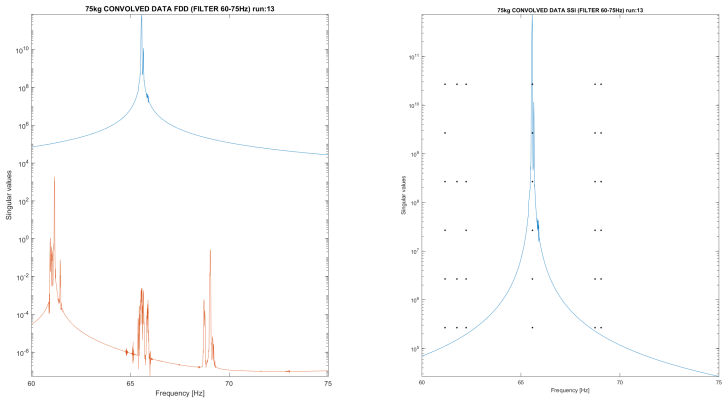


(b) 75kg FDD SSI output, run 12

Figure A1.75kg: Run 12

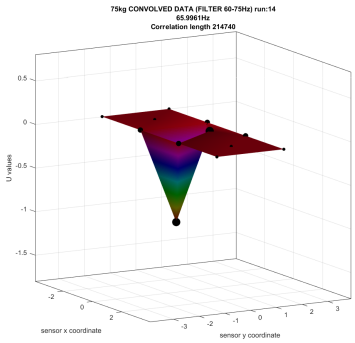


(a) 75kg mode shape, run 13

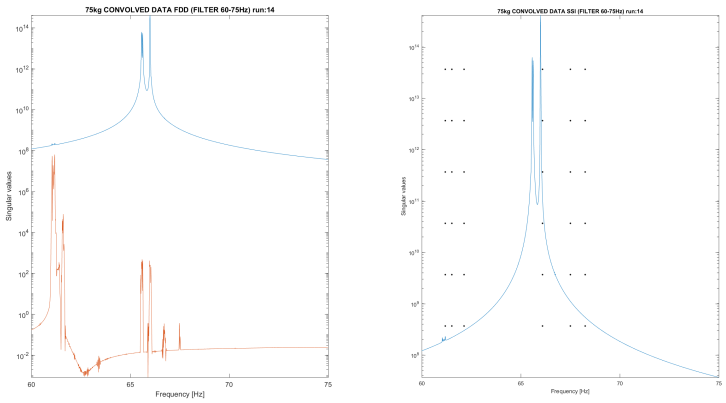


(b) 75kg FDD SSI output, run 13

Figure A1.75kg: Run 13

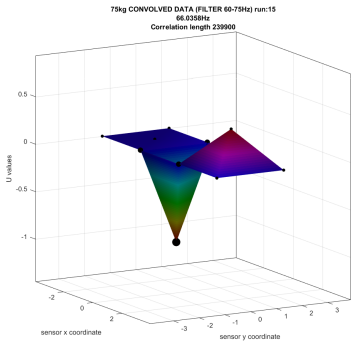


(a) 75kg mode shape, run 14

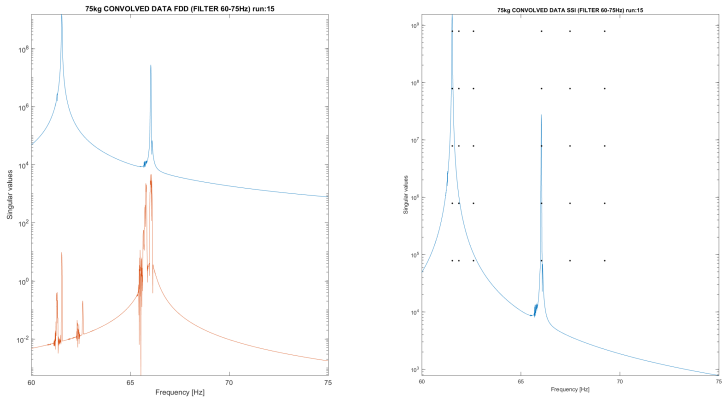


(b) 75kg FDD SSI output, run 14

Figure A1.75kg: Run 14

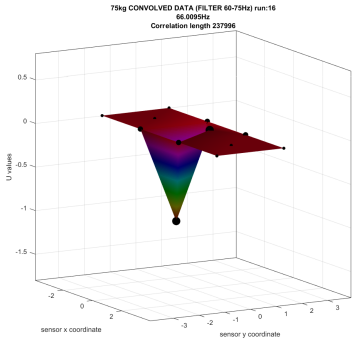


(a) 75kg mode shape, run 15

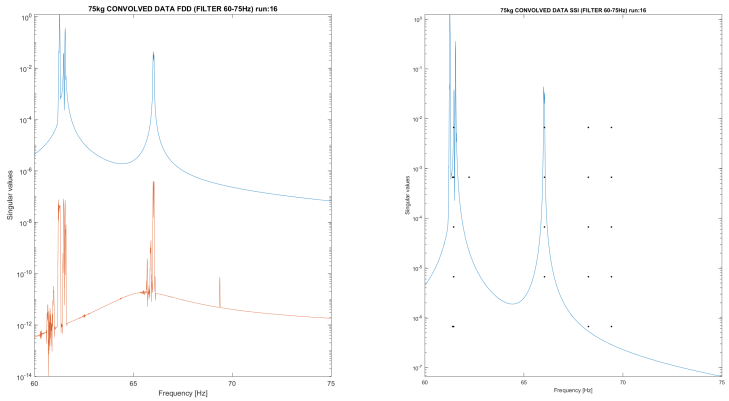


(b) 75kg FDD SSI output, run 15

Figure A1.75kg: Run 15

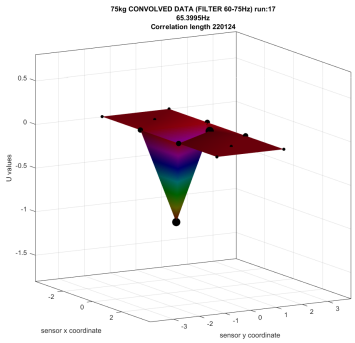


(a) 75kg mode shape, run 16

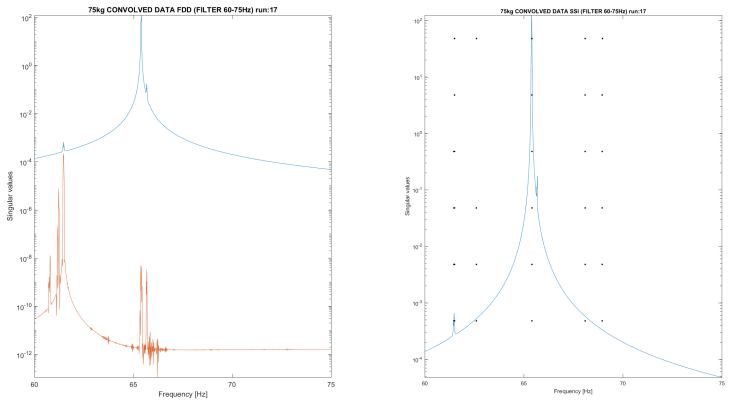


(b) 75kg FDD SSI output, run 16

Figure A1.75kg: Run 16

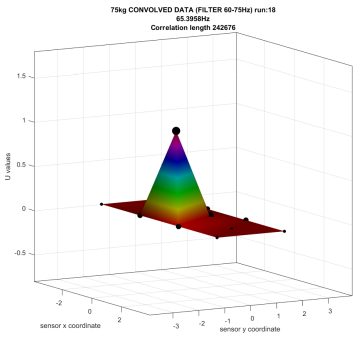


(a) 75kg mode shape, run 17

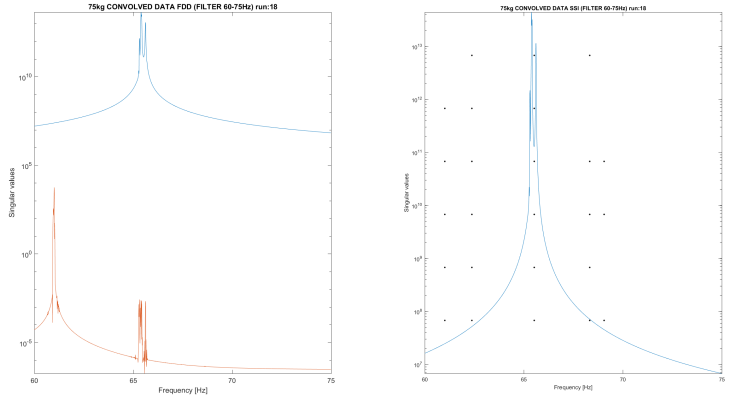


(b) 75kg FDD SSI output, run 17

Figure A1.75kg: Run 17

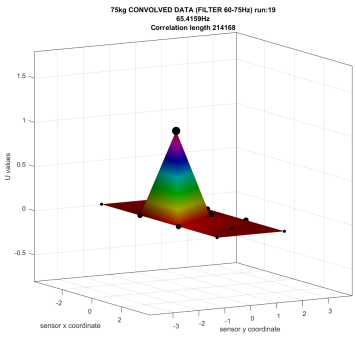


(a) 75kg mode shape, run 18

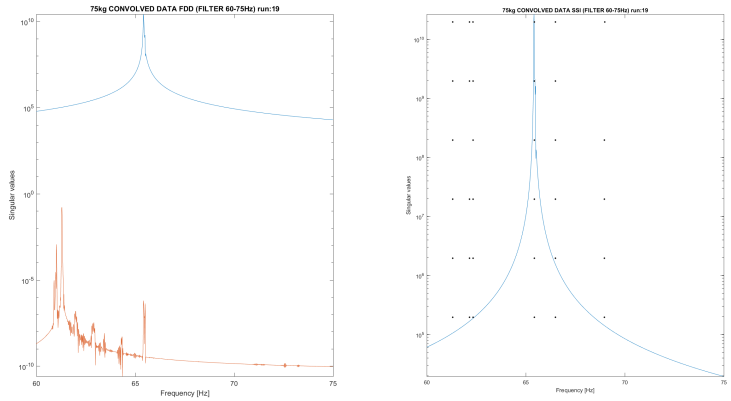


(b) 75kg FDD SSI output, run 18

Figure A1.75kg: Run 18

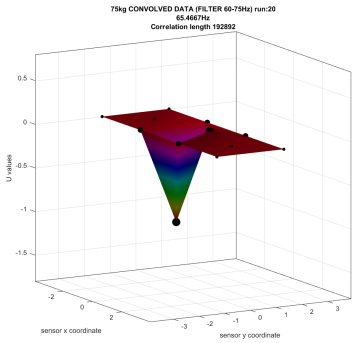


(a) 75kg mode shape, run 19

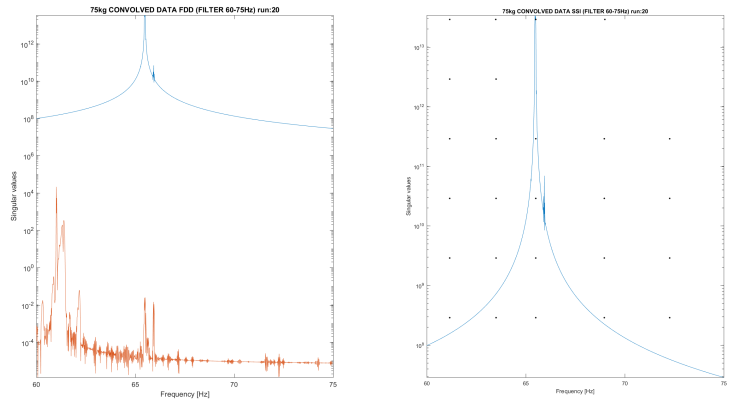


(b) 75kg FDD SSI output, run 19

Figure A1.75kg: Run 19

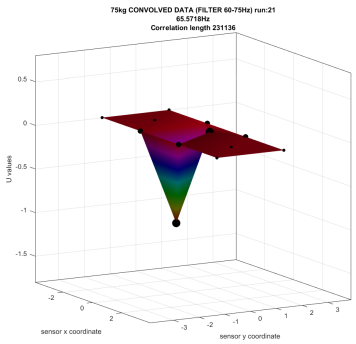


(a) 75kg mode shape, run 20

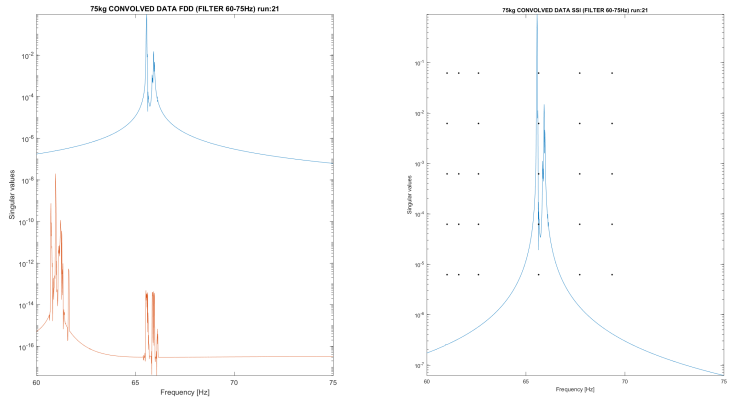


(b) 75kg FDD SSI output, run 20

Figure A1.75kg: Run 20

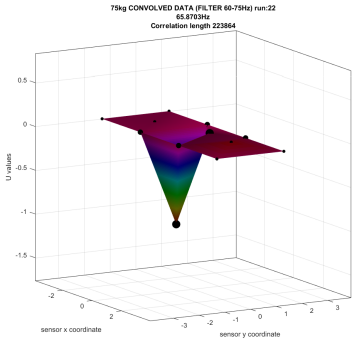


(a) 75kg mode shape, run 21

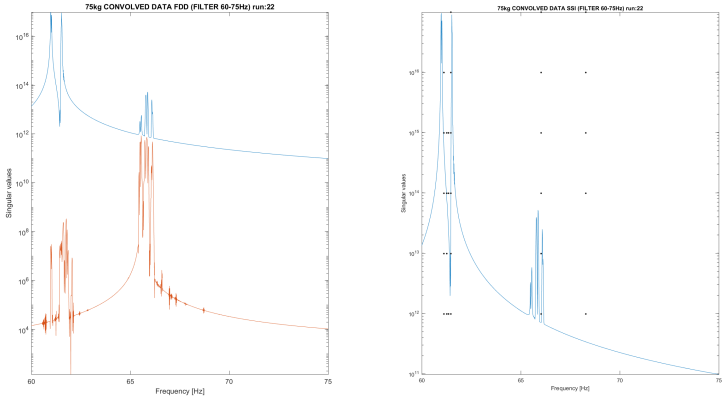


(b) 75kg FDD SSI output, run 21

Figure A1.75kg: Run 21

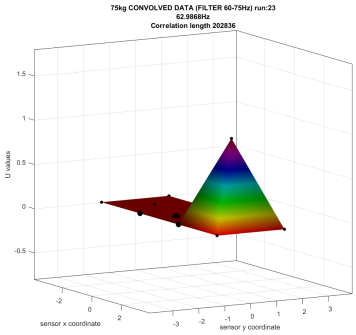


(a) 75kg mode shape, run 22

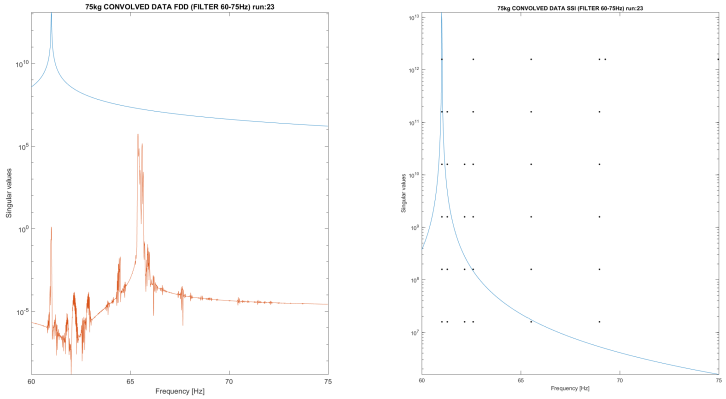


(b) 75kg FDD SSI output, run 22

Figure A1.75kg: Run 22

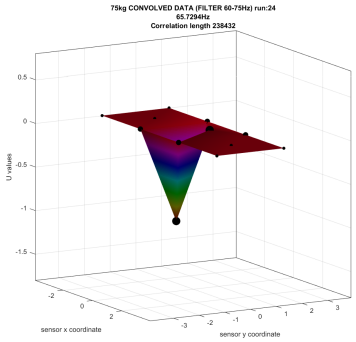


(a) 75kg mode shape, run 23

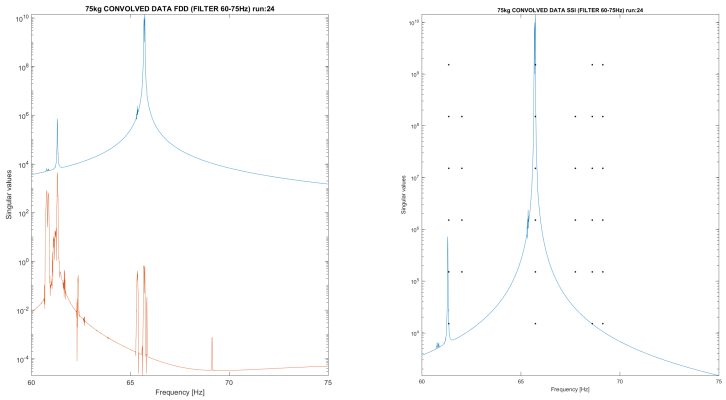


(b) 75kg FDD SSI output, run 23

Figure A1.75kg: Run 23

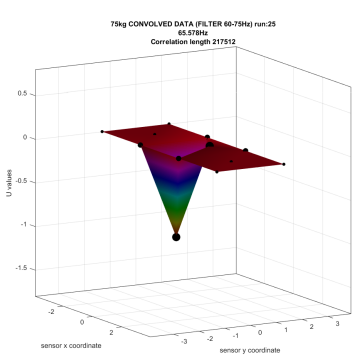


(a) 75kg mode shape, run 24

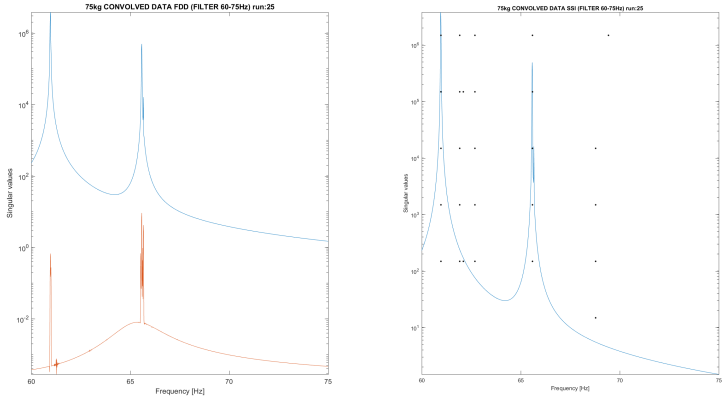


(b) 75kg FDD SSI output, run 24

Figure A1.75kg: Run 24



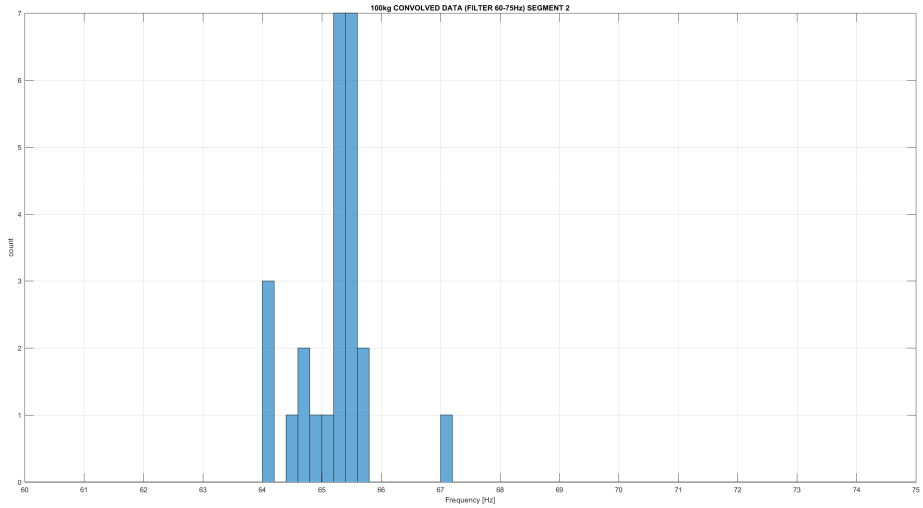
(a) 75kg mode shape, run 25



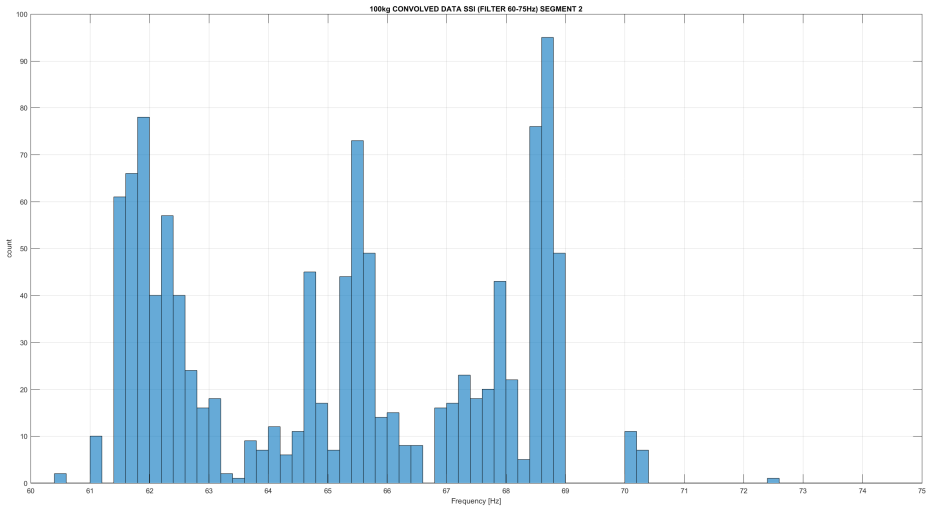
(b) 75kg FDD SSI output, run 25

Figure A1.75kg: Run 25

100kg data segment 2

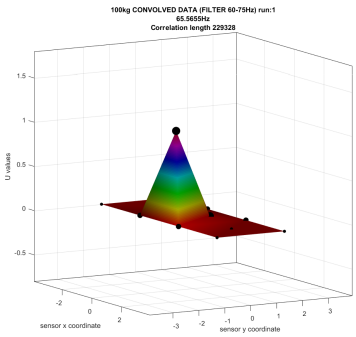


(a) 100kg FDD histogram

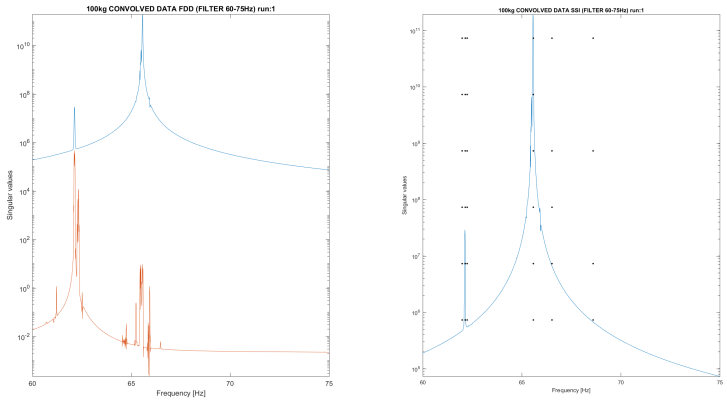


(b) 100kg SSI histogram

Figure A1.100kg: Histograms of identified modes, 100kg data

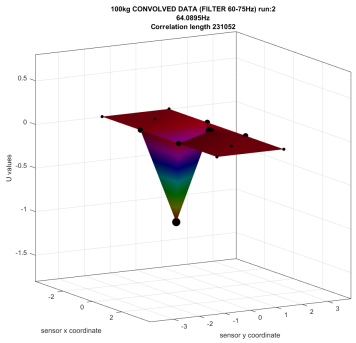


(a) 100kg mode shape, run 1

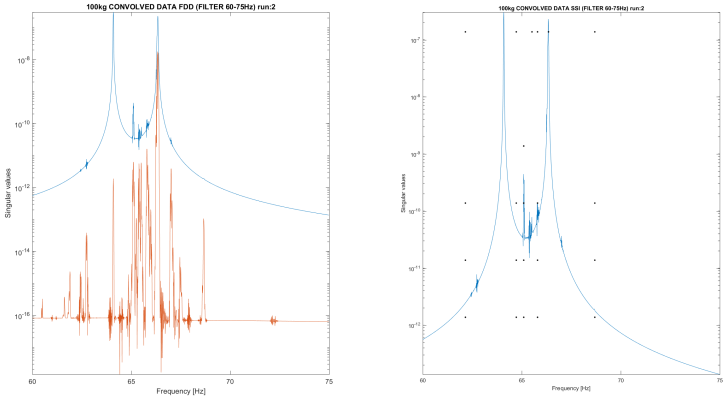


(b) 100kg FDD SSI output, run 1

Figure A1.100kg: Run 1

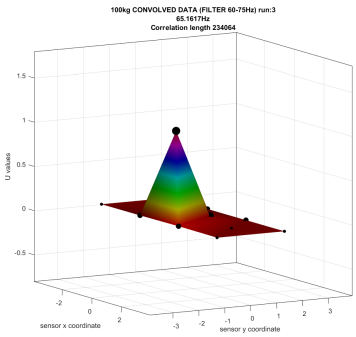


(a) 100kg mode shape, run 2

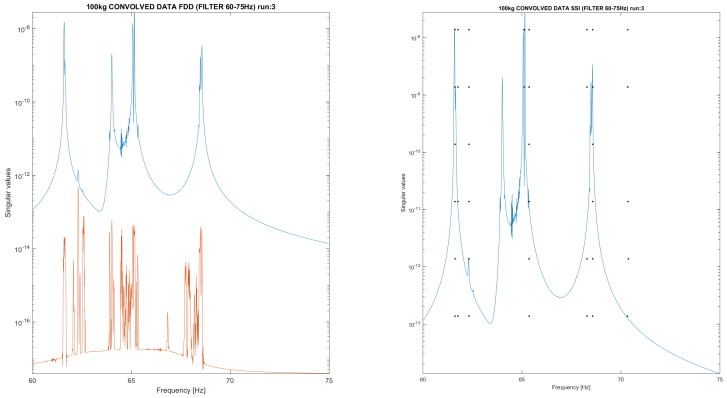


(b) 100kg FDD SSI output, run 2

Figure A1.100kg: Run 2

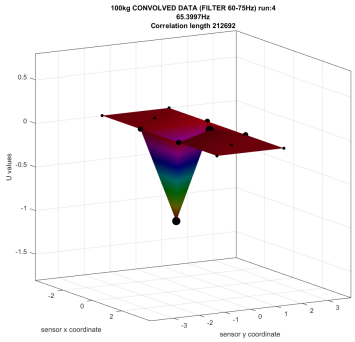


(a) 100kg mode shape, run 3

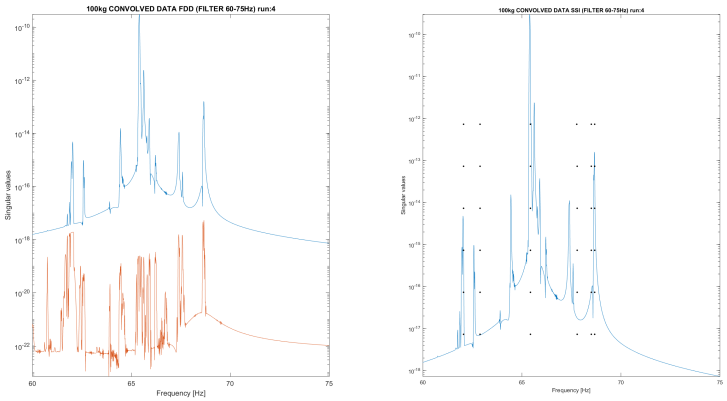


(b) 100kg FDD SSI output, run 3

Figure A1.100kg: Run 3

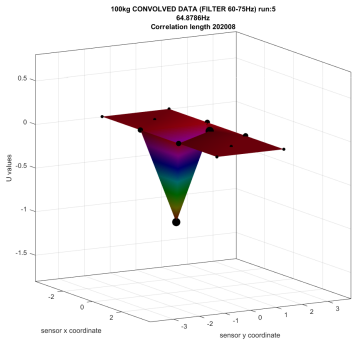


(a) 100kg mode shape, run 4

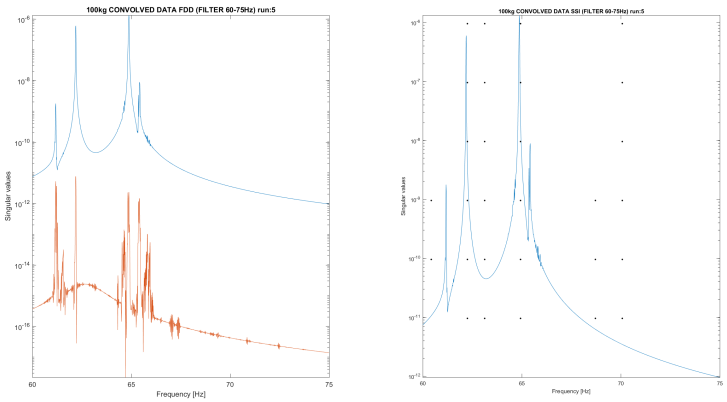


(b) 100kg FDD SSI output, run 4

Figure A1.100kg: Run 4

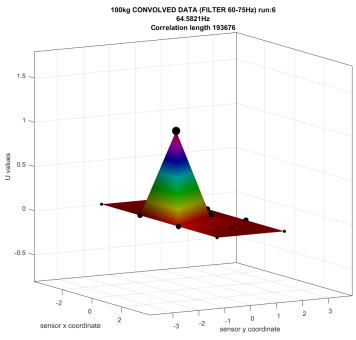


(a) 100kg mode shape, run 5

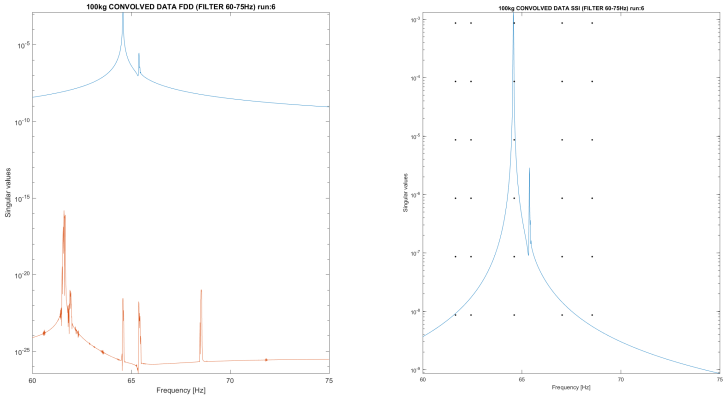


(b) 100kg FDD SSI output, run 5

Figure A1.100kg: Run 5

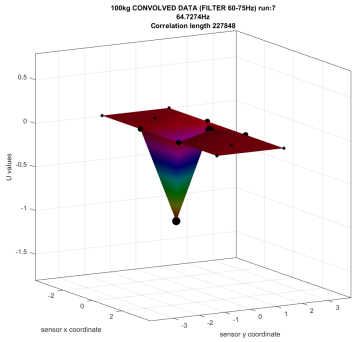


(a) 100kg mode shape, run 6

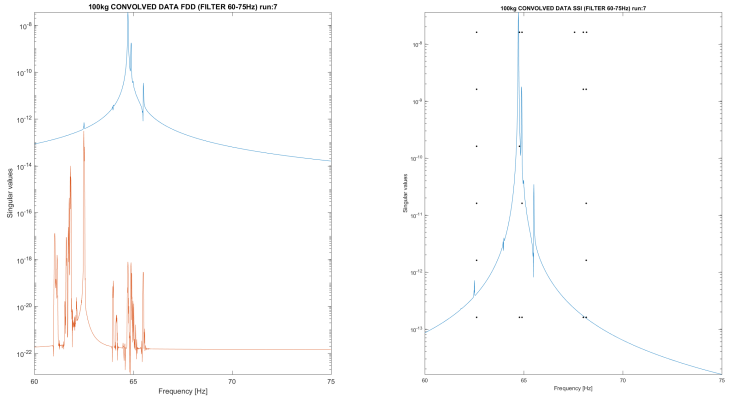


(b) 100kg FDD SSI output, run 6

Figure A1.100kg: Run 6

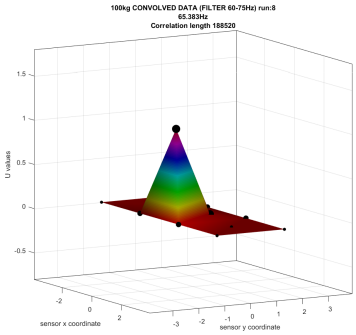


(a) 100kg mode shape, run 7

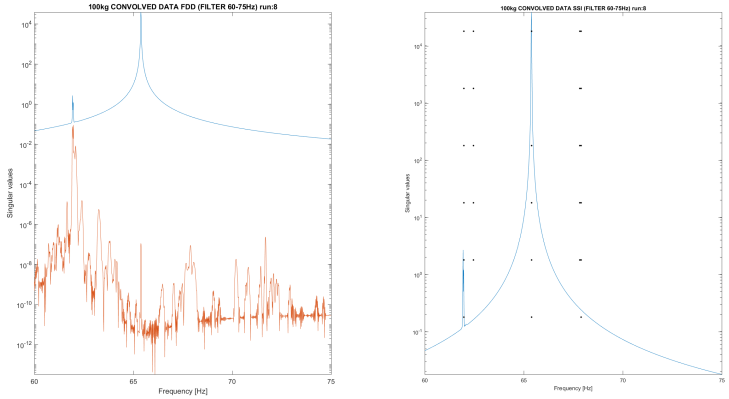


(b) 100kg FDD SSI output, run 7

Figure A1.100kg: Run 7

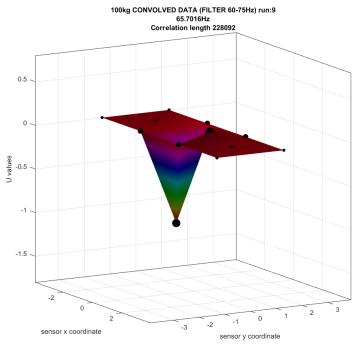


(a) 100kg mode shape, run 8

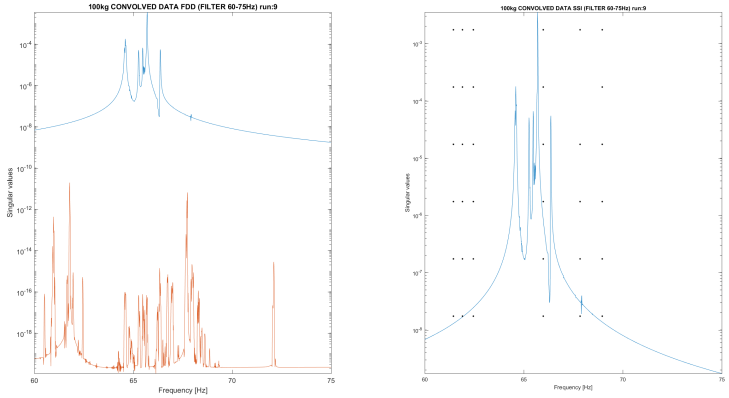


(b) 100kg FDD SSI output, run 8

Figure A1.100kg: Run 8

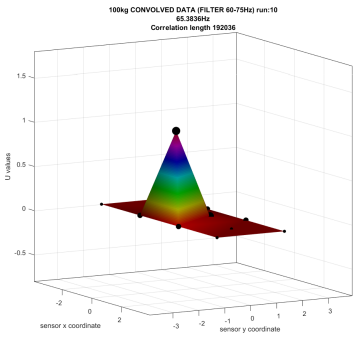


(a) 100kg mode shape, run 9

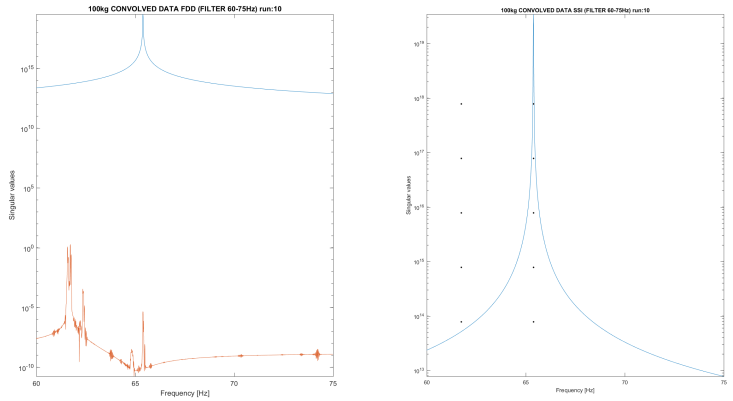


(b) 100kg FDD SSI output, run 9

Figure A1.100kg: Run 9

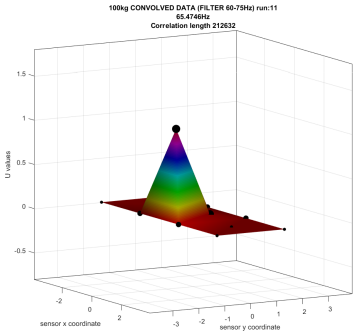


(a) 100kg mode shape, run 10

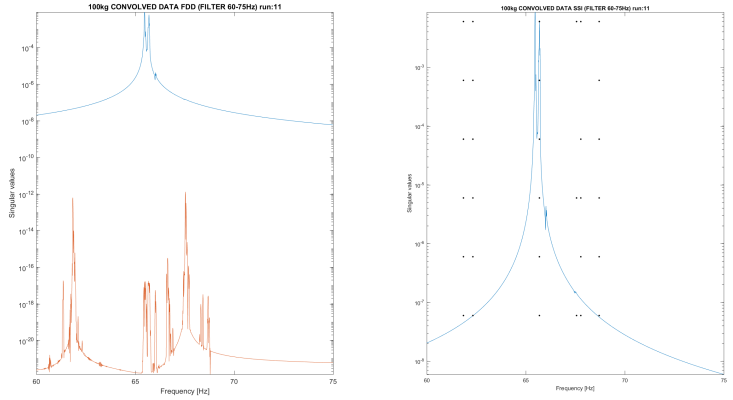


(b) 100kg FDD SSI output, run 10

Figure A1.100kg: Run 10

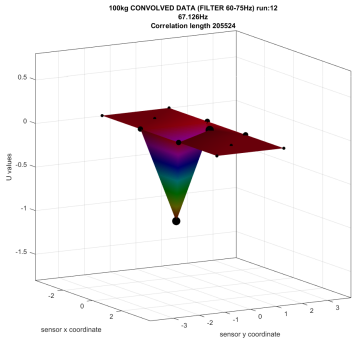


(a) 100kg mode shape, run 11

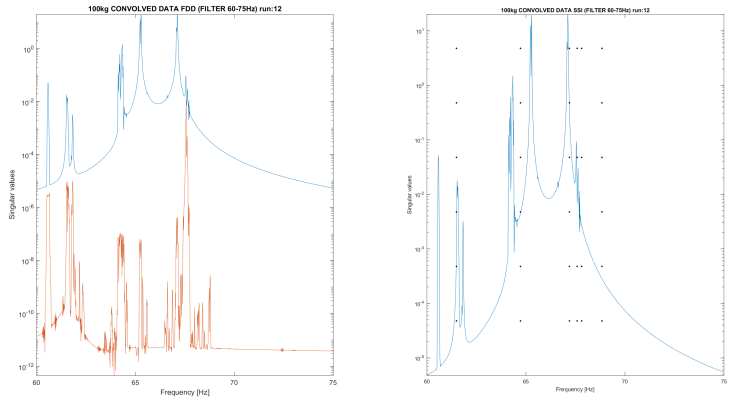


(b) 100kg FDD SSI output, run 11

Figure A1.100kg: Run 11

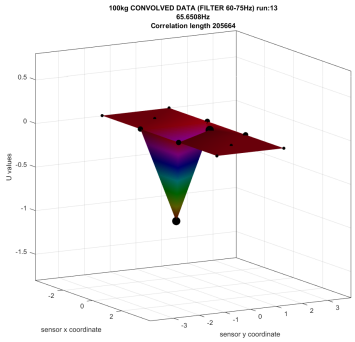


(a) 100kg mode shape, run 12

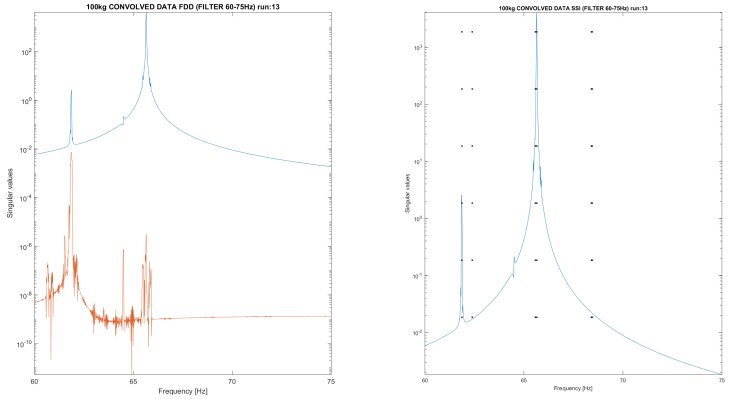


(b) 100kg FDD SSI output, run 12

Figure A1.100kg: Run 12

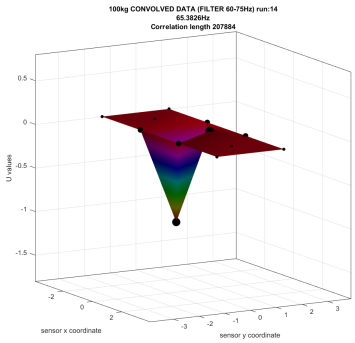


(a) 100kg mode shape, run 13

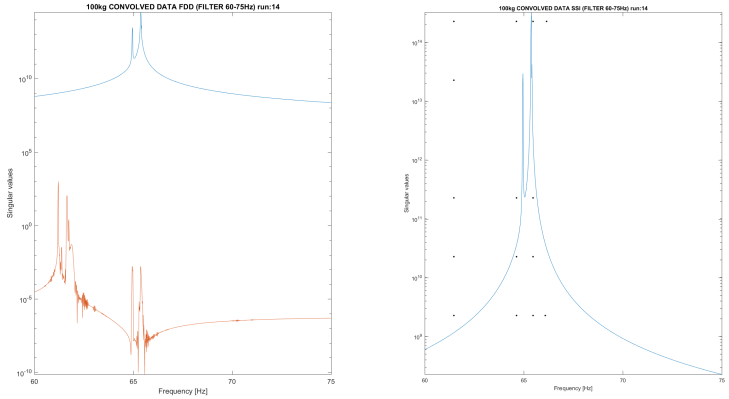


(b) 100kg FDD SSI output, run 13

Figure A1.100kg: Run 13

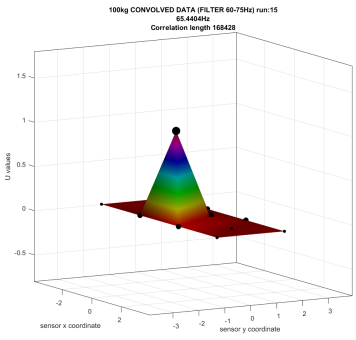


(a) 100kg mode shape, run 14

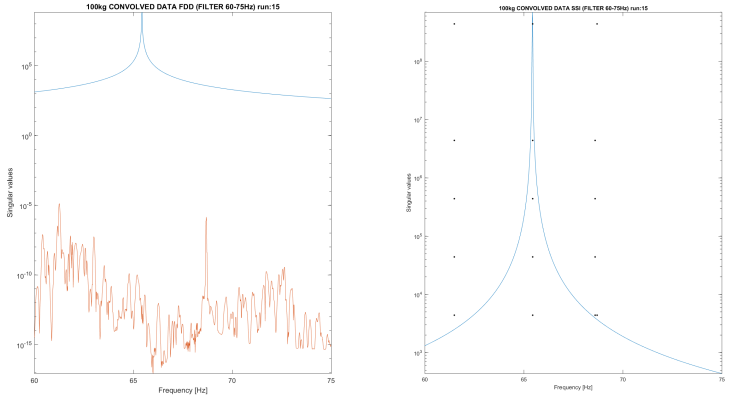


(b) 100kg FDD SSI output, run 14

Figure A1.100kg: Run 14

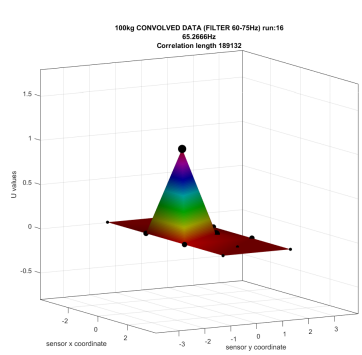


(a) 100kg mode shape, run 15

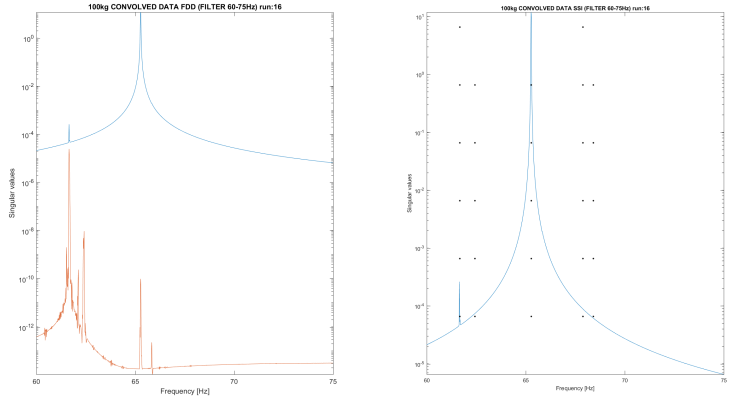


(b) 100kg FDD SSI output, run 15

Figure A1.100kg: Run 15

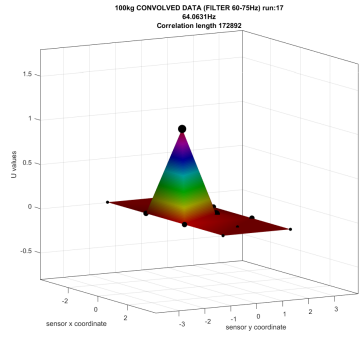


(a) 100kg mode shape, run 16

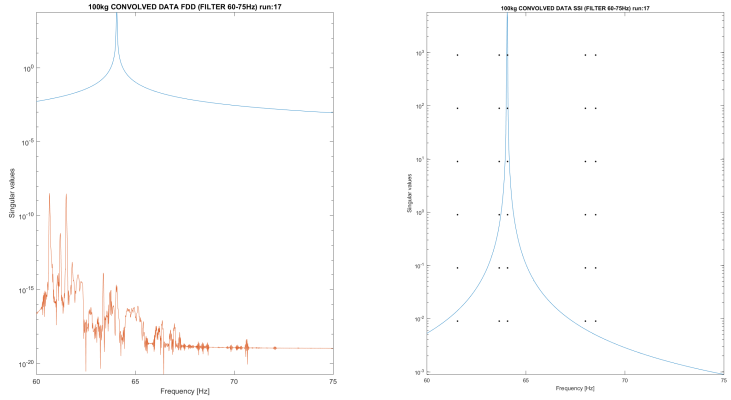


(b) 100kg FDD SSI output, run 16

Figure A1.100kg: Run 16

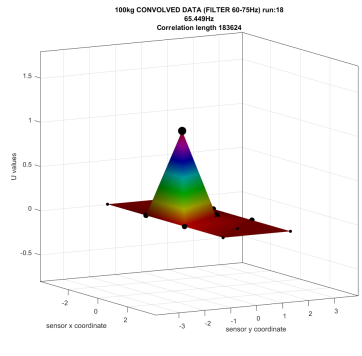


(a) 100kg mode shape, run 17

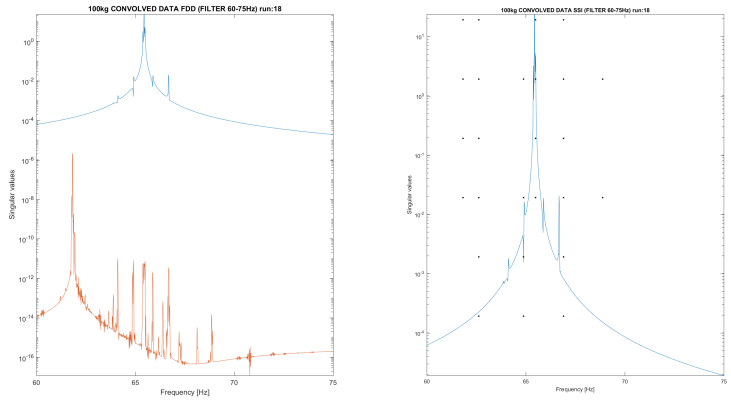


(b) 100kg FDD SSI output, run 17

Figure A1.100kg: Run 17

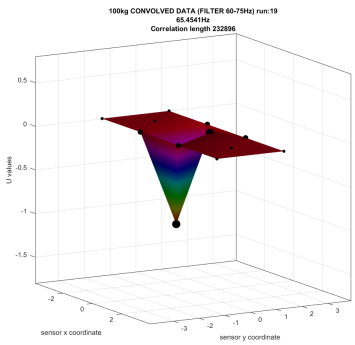


(a) 100kg mode shape, run 18

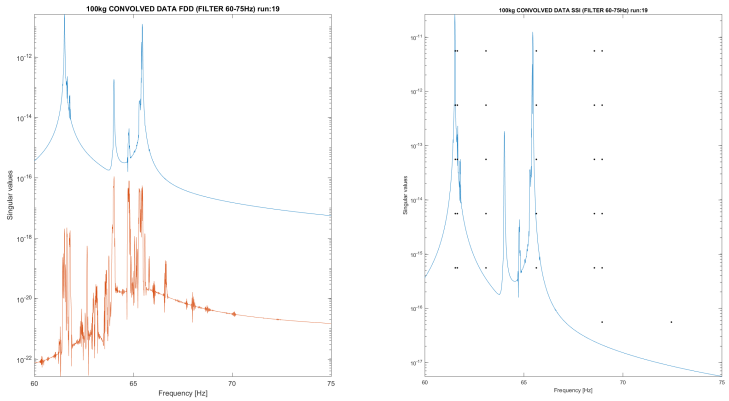


(b) 100kg FDD SSI output, run 18

Figure A1.100kg: Run 18

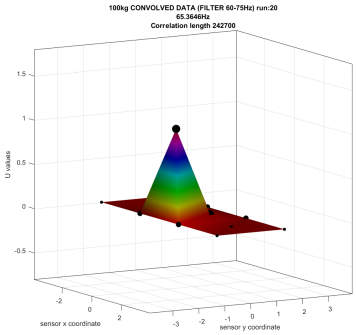


(a) 100kg mode shape, run 19

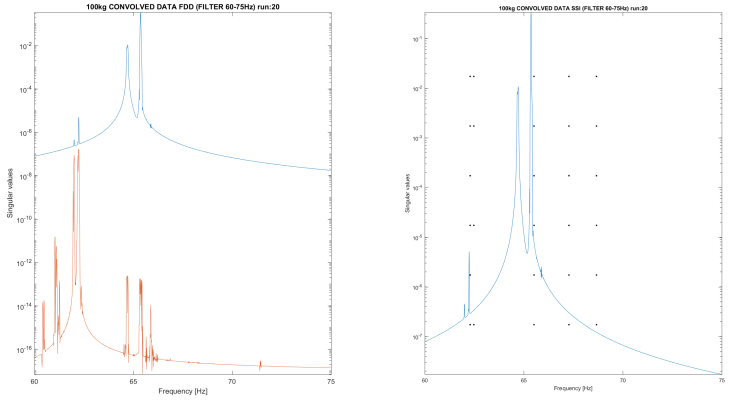


(b) 100kg FDD SSI output, run 19

Figure A1.100kg: Run 19

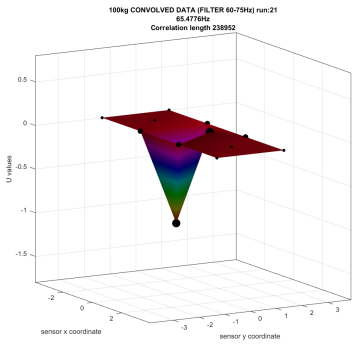


(a) 100kg mode shape, run 20

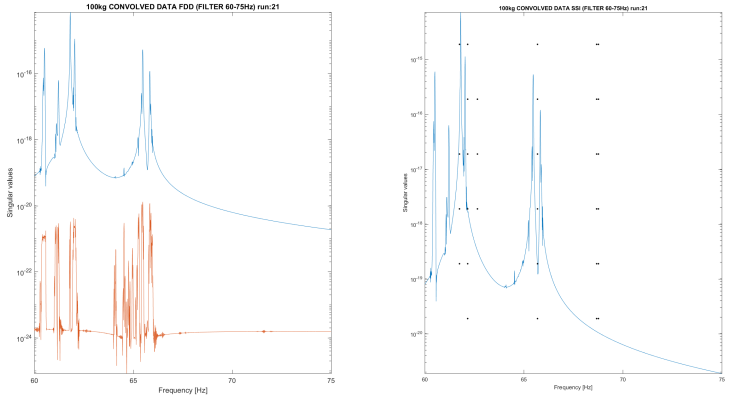


(b) 100kg FDD SSI output, run 20

Figure A1.100kg: Run 20

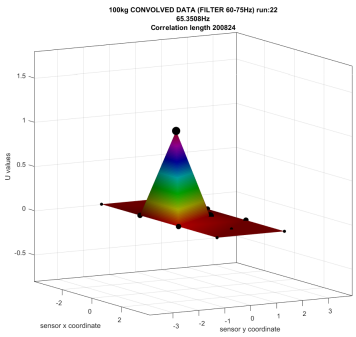


(a) 100kg mode shape, run 21

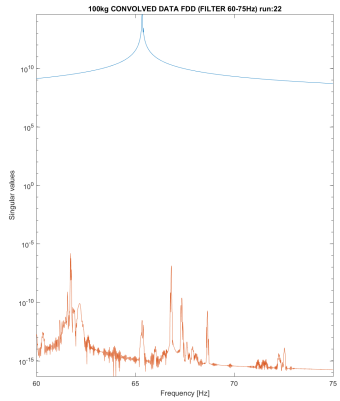


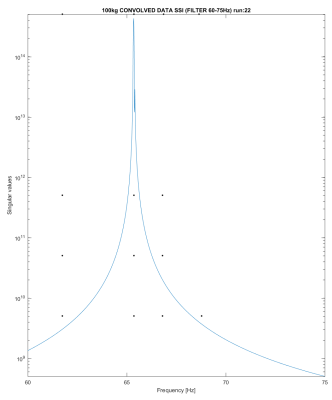
(b) 100kg FDD SSI output, run 21

Figure A1.100kg: Run 21



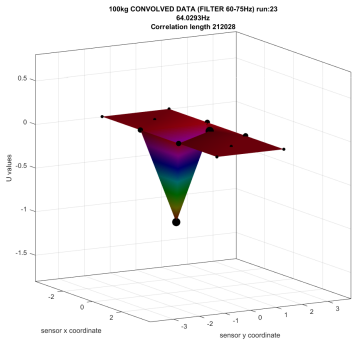
(a) 100kg mode shape, run 22



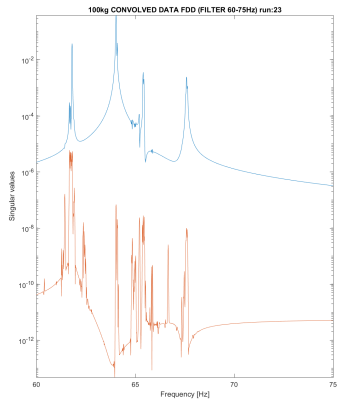


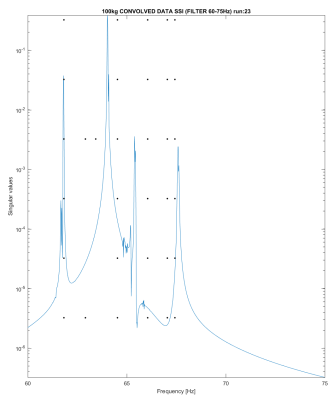
(b) 100kg FDD SSI output, run 22

Figure A1.100kg: Run 22



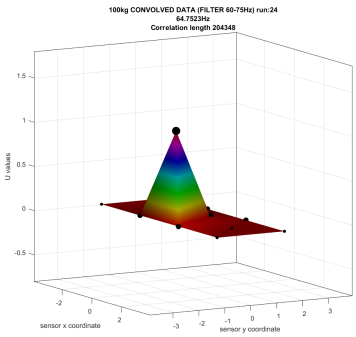
(a) 100kg mode shape, run 23



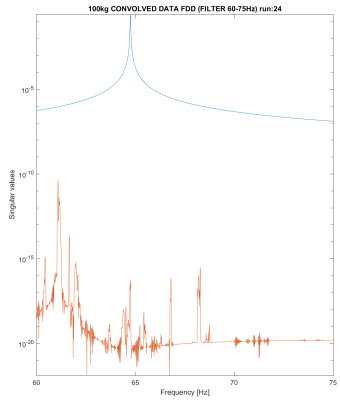


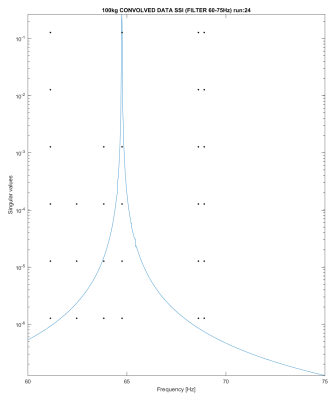
(b) 100kg FDD SSI output, run 23

Figure A1.100kg: Run 23



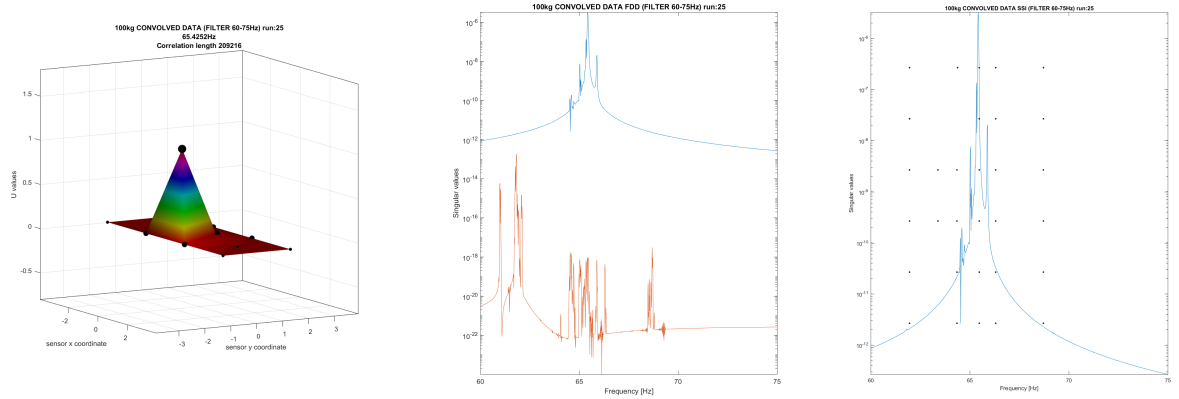
(a) 100kg mode shape, run 24





(b) 100kg FDD SSI output, run 24

Figure A1.100kg: Run 24

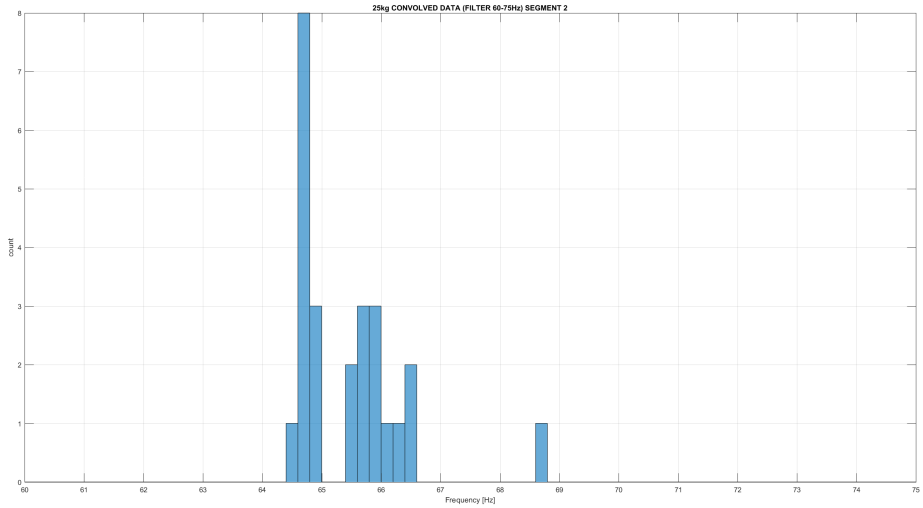


(a) 100kg mode shape, run 25

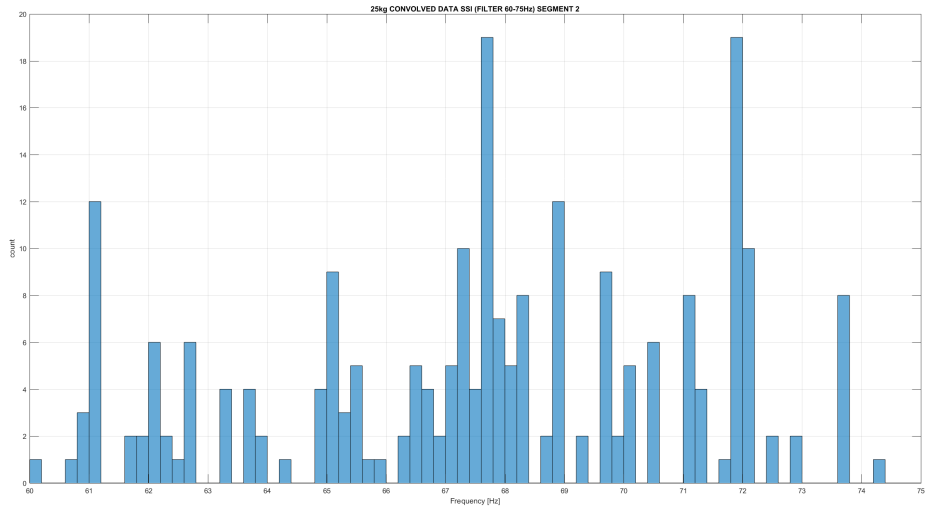
(b) 100kg FDD SSI output, run 25

Figure A1.100kg: Run 25

Data (28.03.2017) 25kg-50kg segment 2 (Unreduced order PF)

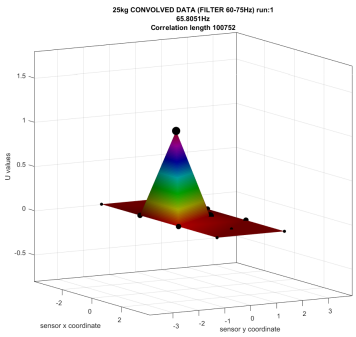


(a) 25kg FDD histogram

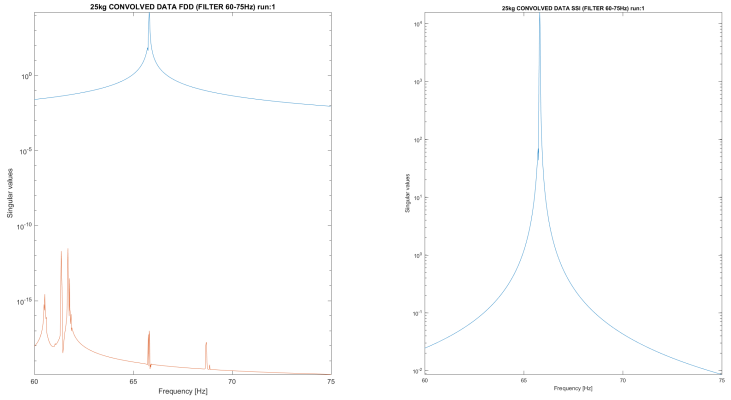


(b) 25kg SSI histogram

Figure A1.25kg: Histograms of identified modes, 25kg data

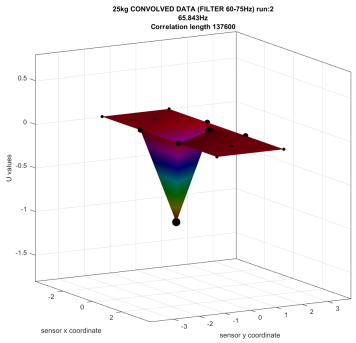


(a) 25kg mode shape, run 1

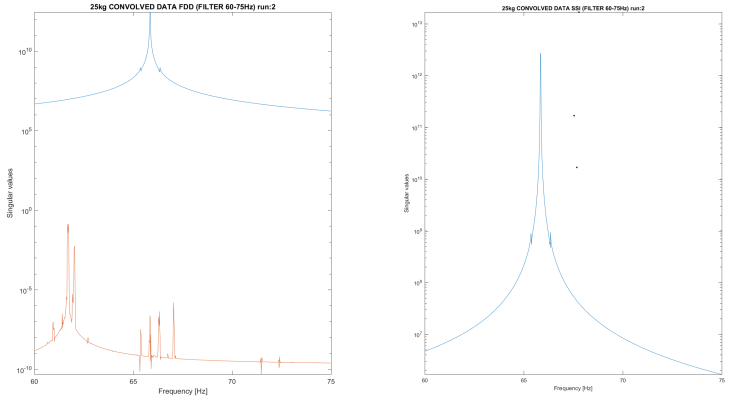


(b) 25kg FDD SSI output, run 1

Figure A1.25kg: Run 1

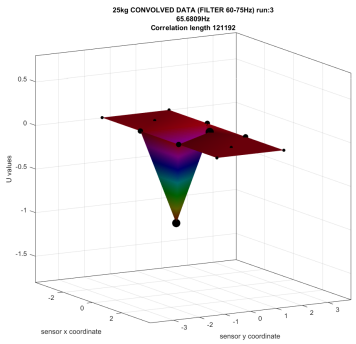


(a) 25kg mode shape, run 2

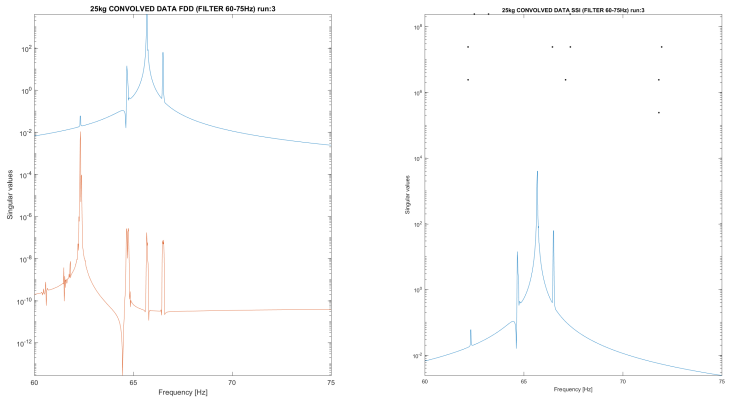


(b) 25kg FDD SSI output, run 2

Figure A1.25kg: Run 2

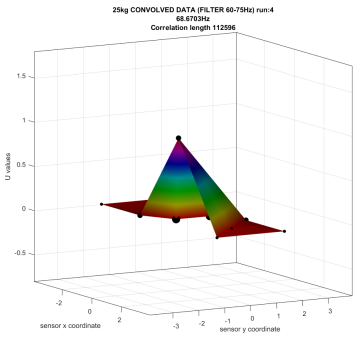


(a) 25kg mode shape, run 3

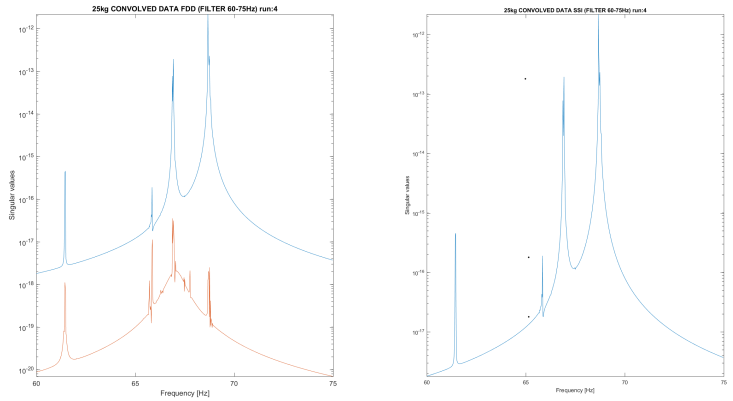


(b) 25kg FDD SSI output, run 3

Figure A1.25kg: Run 3

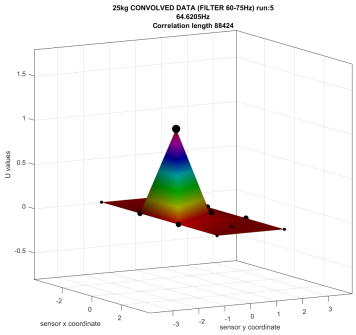


(a) 25kg mode shape, run 4

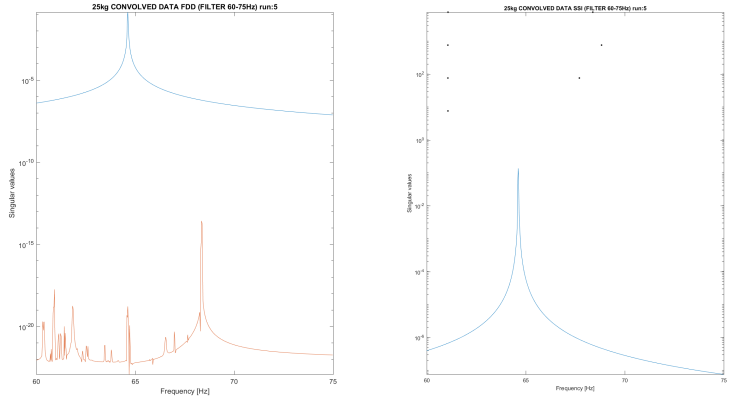


(b) 25kg FDD SSI output, run 4

Figure A1.25kg: Run 4

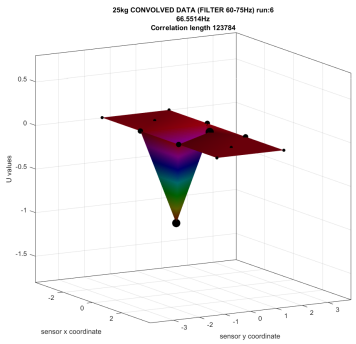


(a) 25kg mode shape, run 5

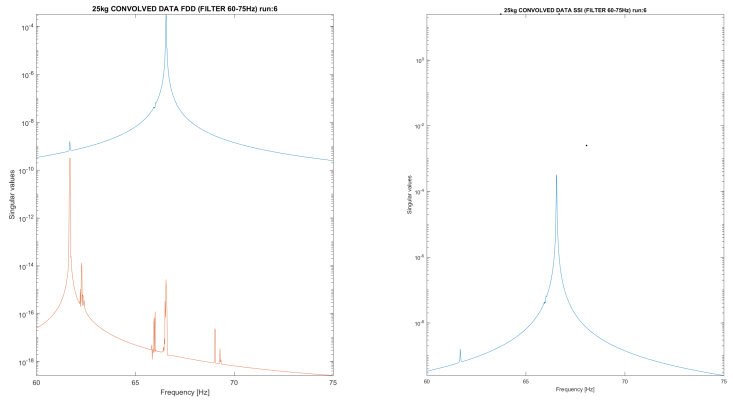


(b) 25kg FDD SSI output, run 5

Figure A1.25kg: Run 5

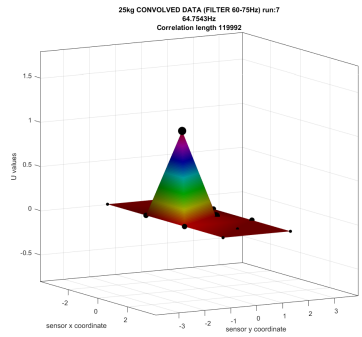


(a) 25kg mode shape, run 6

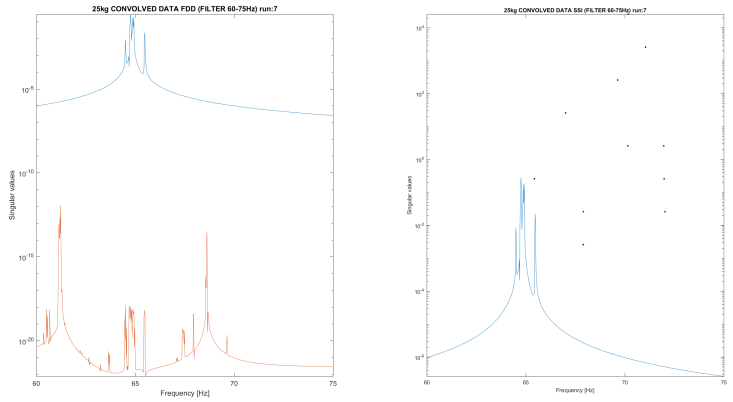


(b) 25kg FDD SSI output, run 6

Figure A1.25kg: Run 6

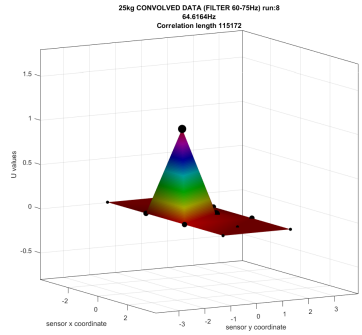


(a) 25kg mode shape, run 7

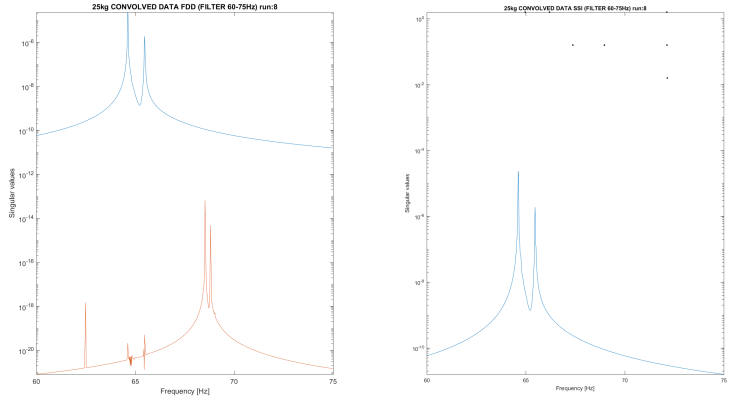


(b) 25kg FDD SSI output, run 7

Figure A1.25kg: Run 7

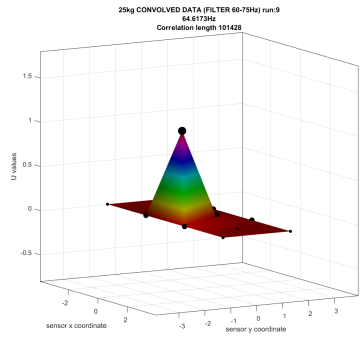


(a) 25kg mode shape, run 8

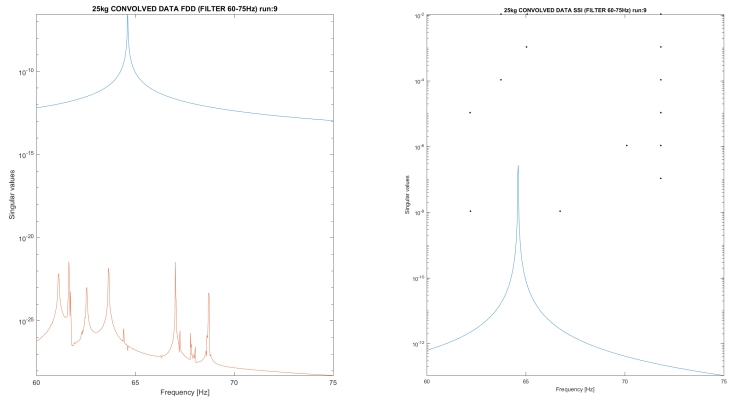


(b) 25kg FDD SSI output, run 8

Figure A1.25kg: Run 8

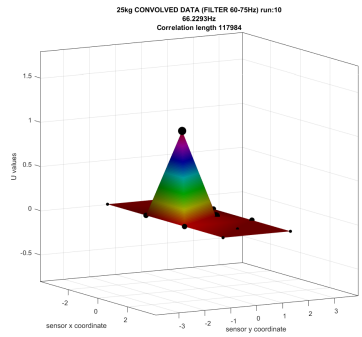


(a) 25kg mode shape, run 9

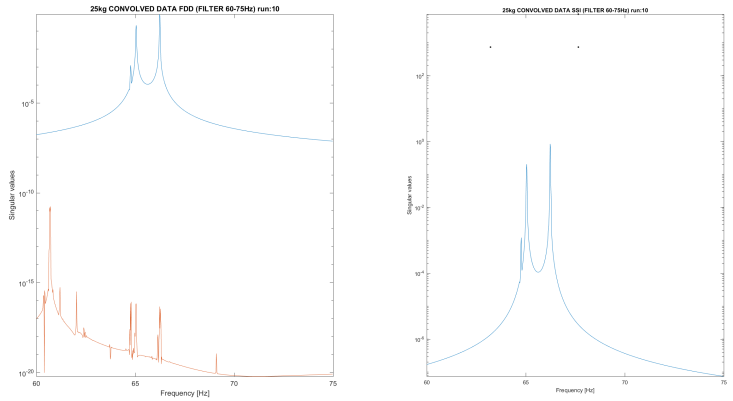


(b) 25kg FDD SSI output, run 9

Figure A1.25kg: Run 9

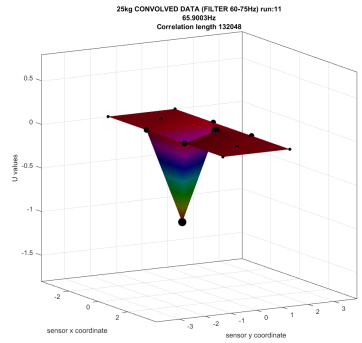


(a) 25kg mode shape, run 10

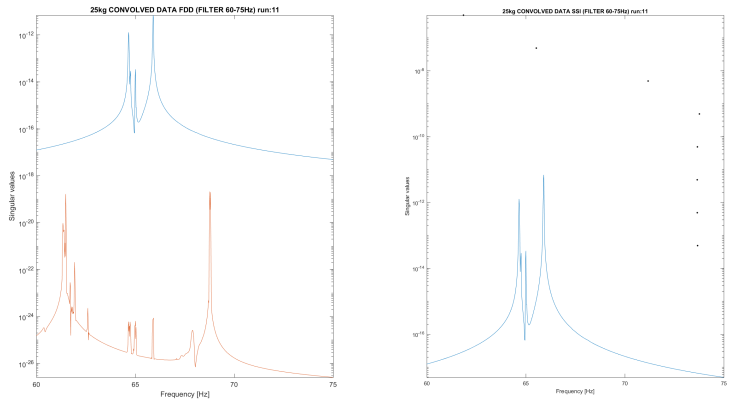


(b) 25kg FDD SSI output, run 10

Figure A1.25kg: Run 10

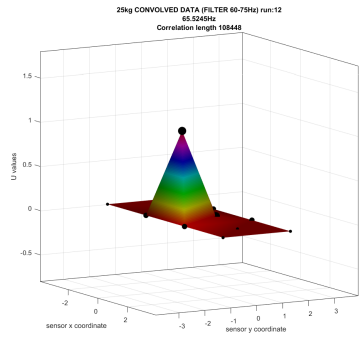


(a) 25kg mode shape, run 11

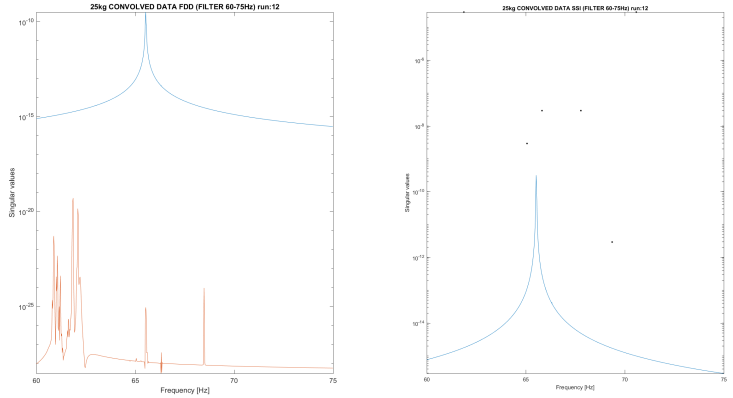


(b) 25kg FDD SSI output, run 11

Figure A1.25kg: Run 11

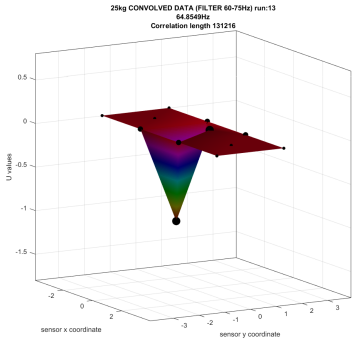


(a) 25kg mode shape, run 12

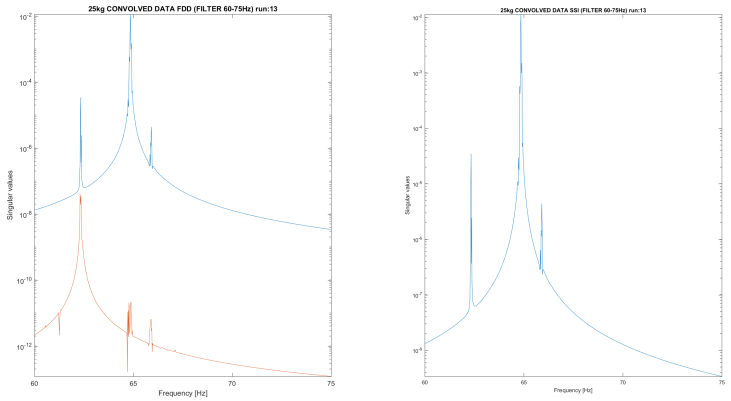


(b) 25kg FDD SSI output, run 12

Figure A1.25kg: Run 12

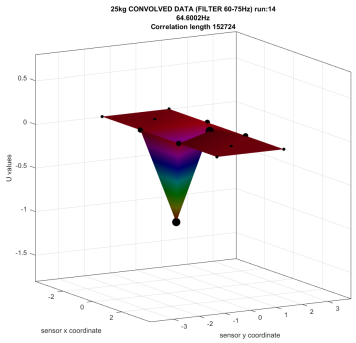


(a) 25kg mode shape, run 13

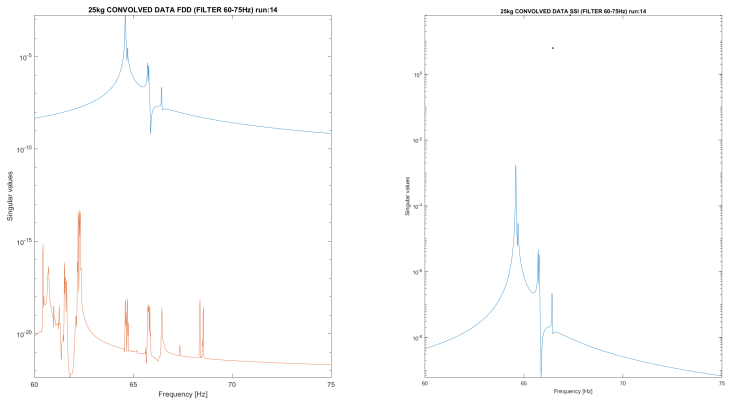


(b) 25kg FDD SSI output, run 13

Figure A1.25kg: Run 13

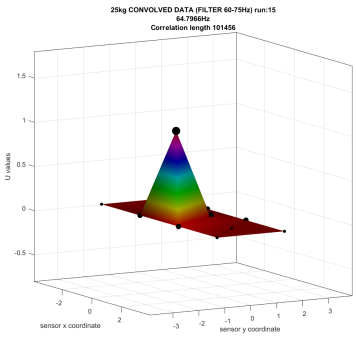


(a) 25kg mode shape, run 14

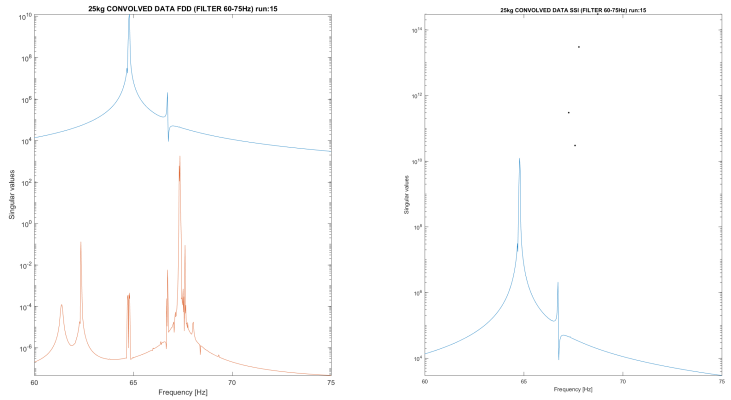


(b) 25kg FDD SSI output, run 14

Figure A1.25kg: Run 14

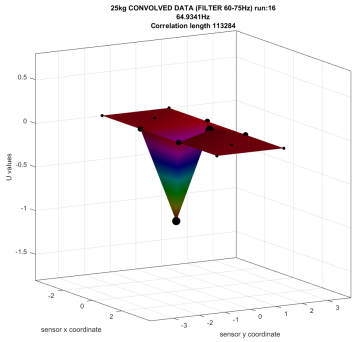


(a) 25kg mode shape, run 15

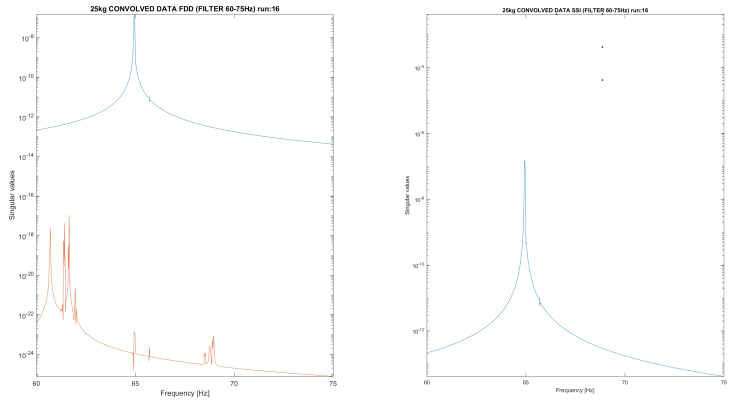


(b) 25kg FDD SSI output, run 15

Figure A1.25kg: Run 15

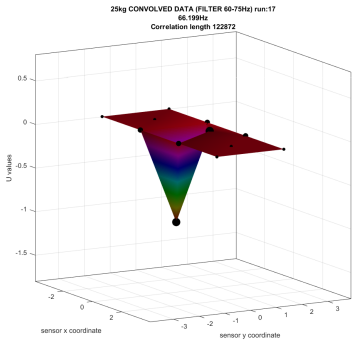


(a) 25kg mode shape, run 16

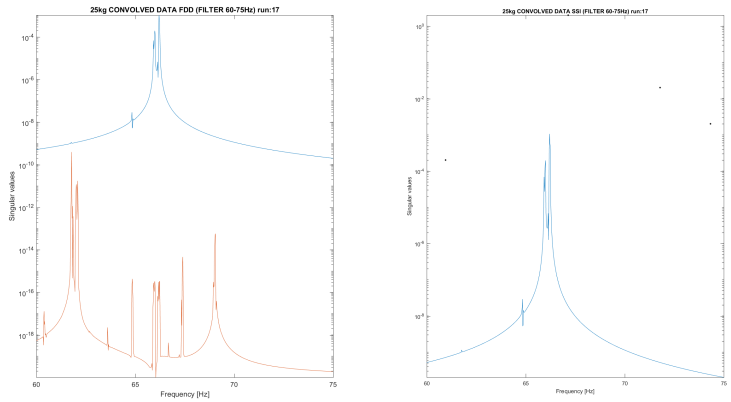


(b) 25kg FDD SSI output, run 16

Figure A1.25kg: Run 16

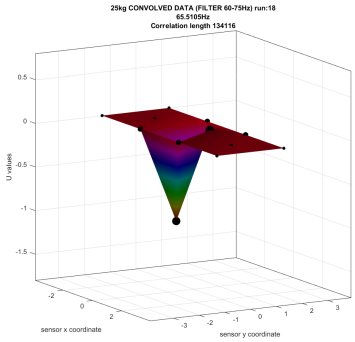


(a) 25kg mode shape, run 17

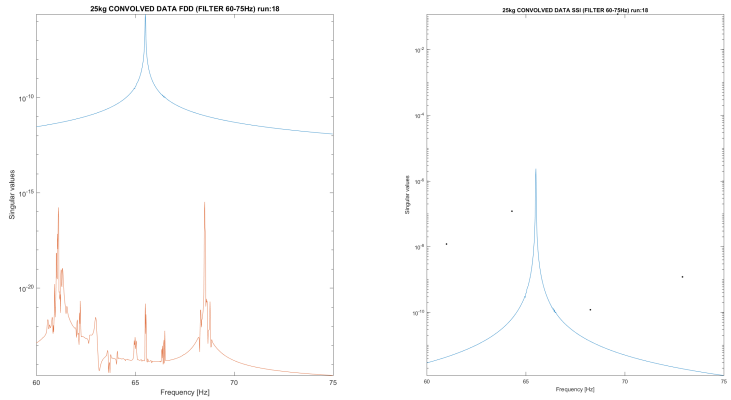


(b) 25kg FDD SSI output, run 17

Figure A1.25kg: Run 17

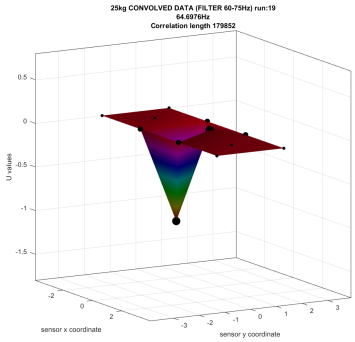


(a) 25kg mode shape, run 18

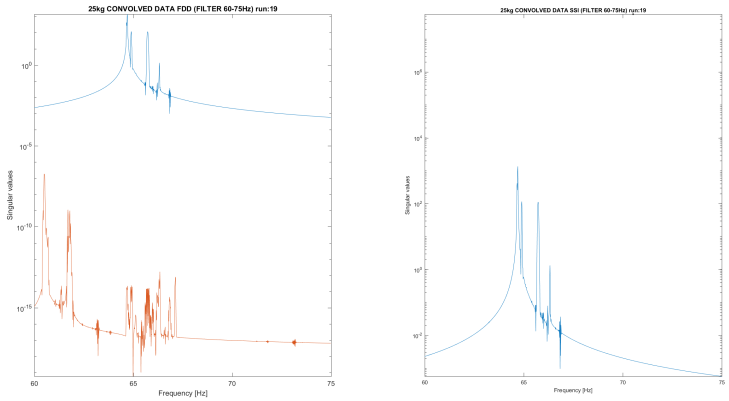


(b) 25kg FDD SSI output, run 18

Figure A1.25kg: Run 18

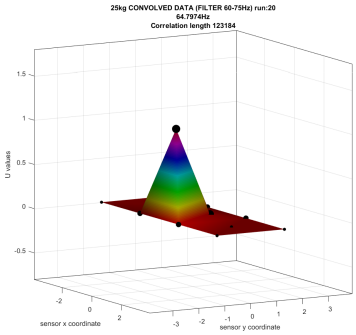


(a) 25kg mode shape, run 19

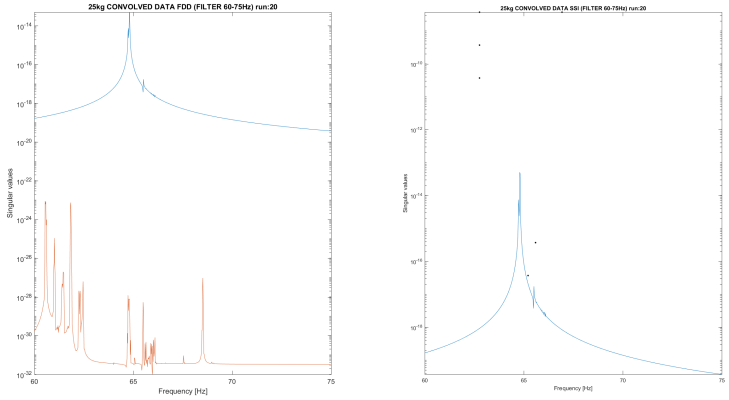


(b) 25kg FDD SSI output, run 19

Figure A1.25kg: Run 19

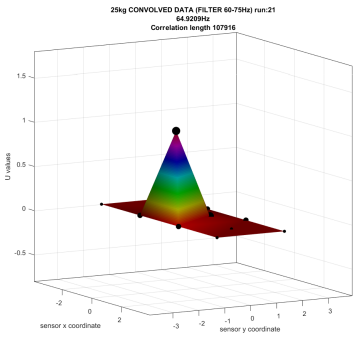


(a) 25kg mode shape, run 20

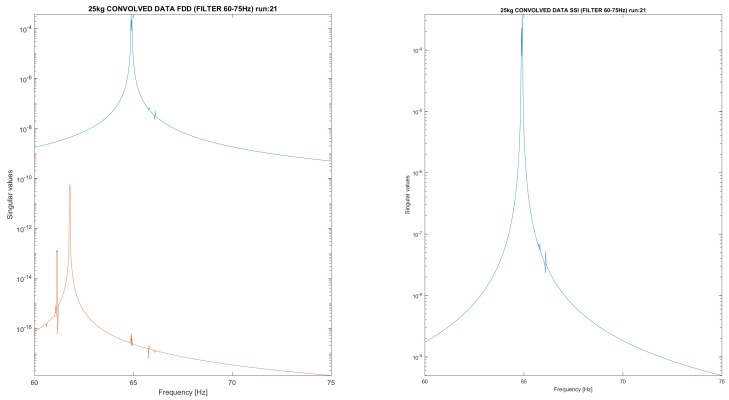


(b) 25kg FDD SSI output, run 20

Figure A1.25kg: Run 20

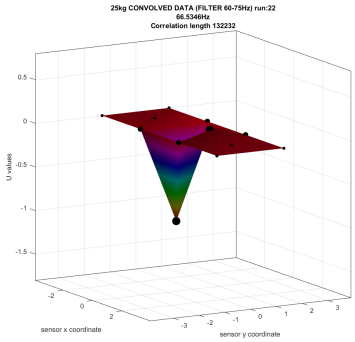


(a) 25kg mode shape, run 21

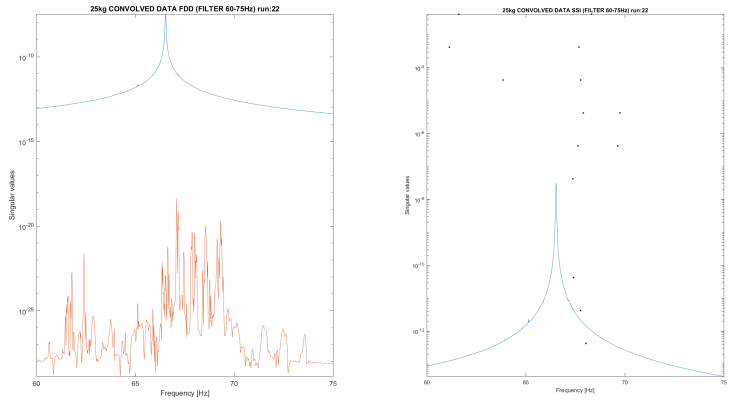


(b) 25kg FDD SSI output, run 21

Figure A1.25kg: Run 21

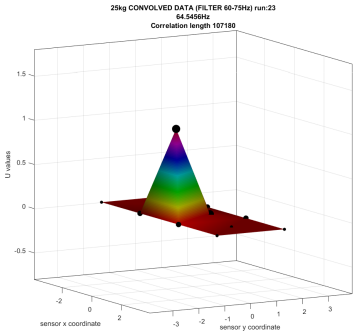


(a) 25kg mode shape, run 22

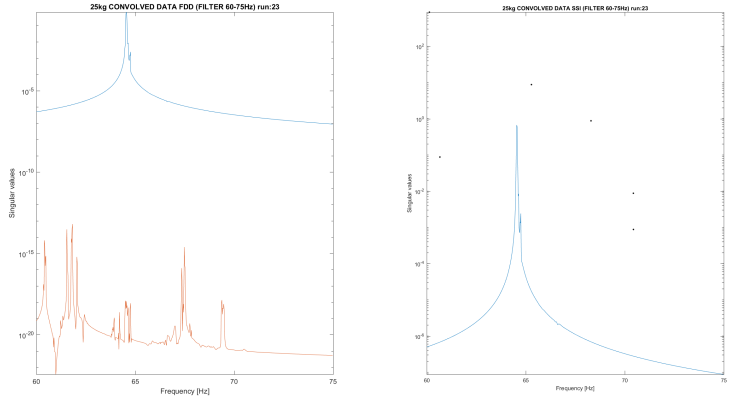


(b) 25kg FDD SSI output, run 22

Figure A1.25kg: Run 22

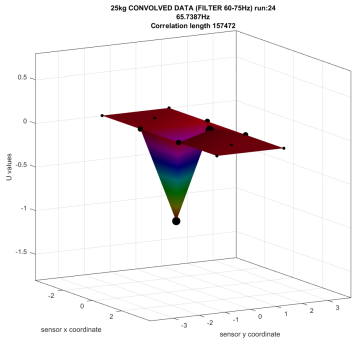


(a) 25kg mode shape, run 23

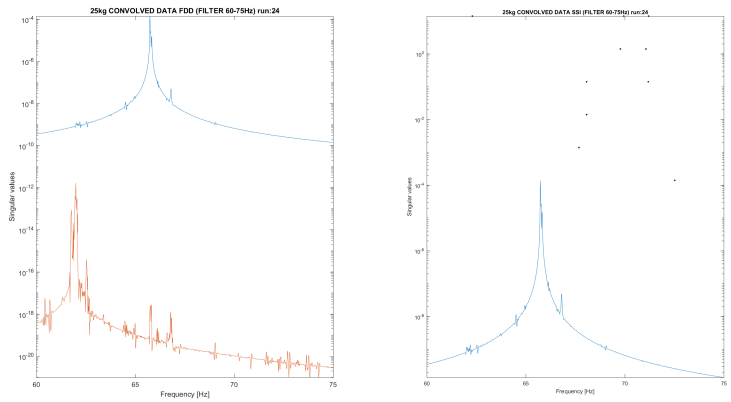


(b) 25kg FDD SSI output, run 23

Figure A1.25kg: Run 23

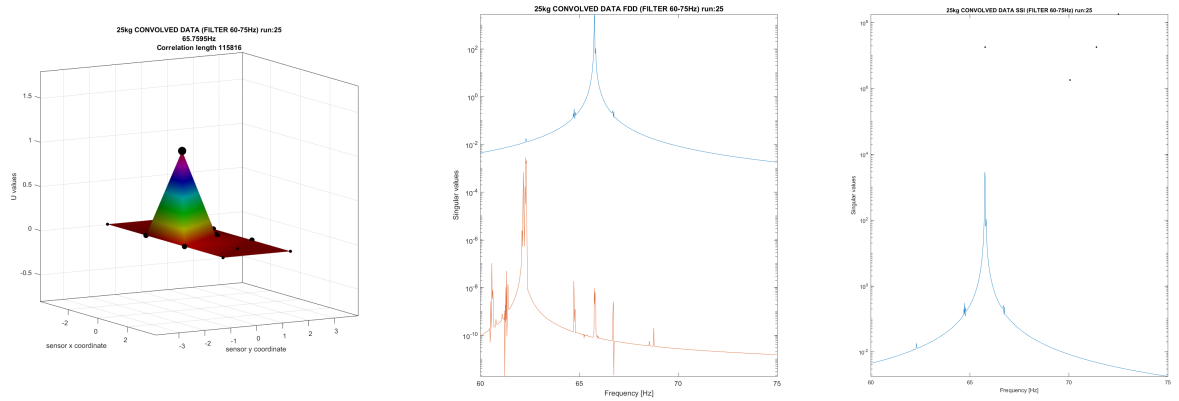


(a) 25kg mode shape, run 24



(b) 25kg FDD SSI output, run 24

Figure A1.25kg: Run 24

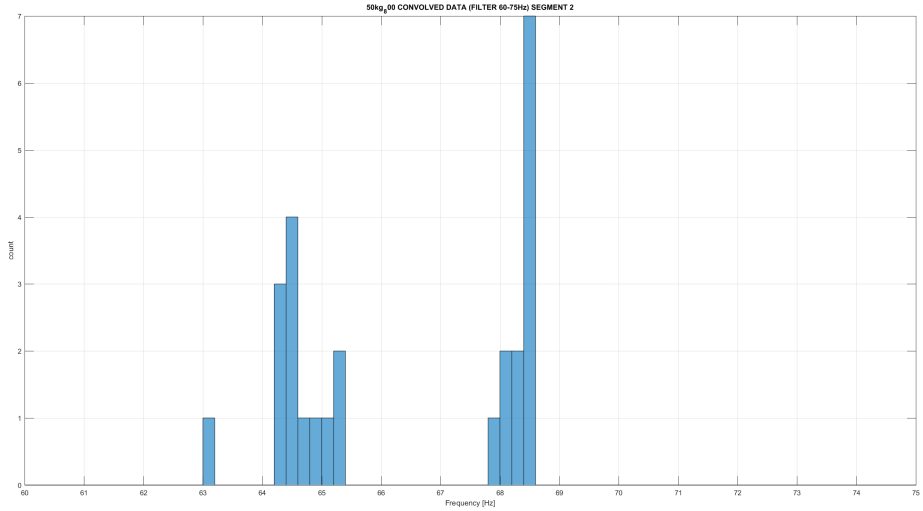


(a) 25kg mode shape, run 25

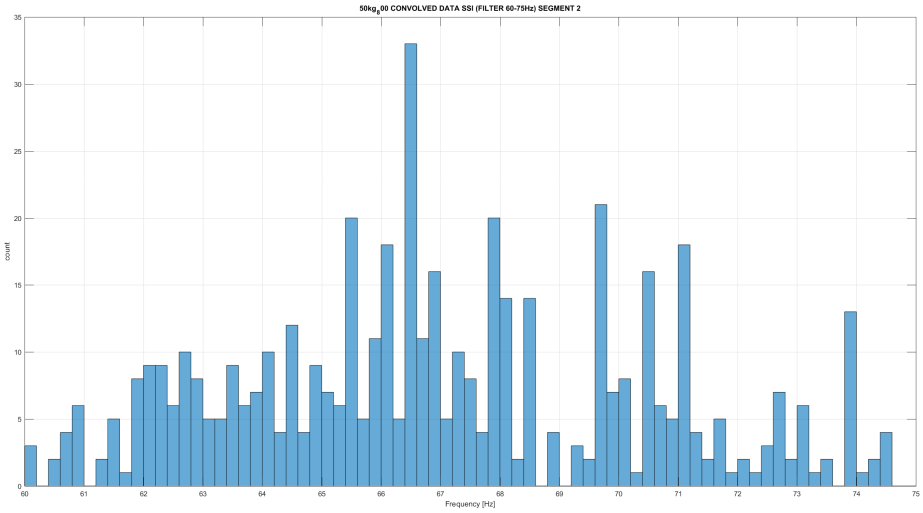
(b) 25kg FDD SSI output, run 25

Figure A1.25kg: Run 25

50kg data segment 2 (28.03.2017)

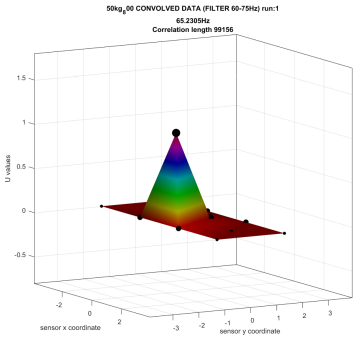


(a) 50kg FDD histogram

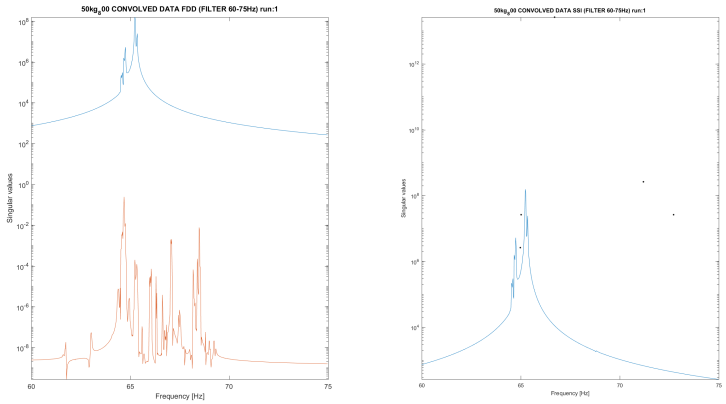


(b) 50kg SSI histogram

Figure A1.50kg: Histograms of identified modes, 50kg data

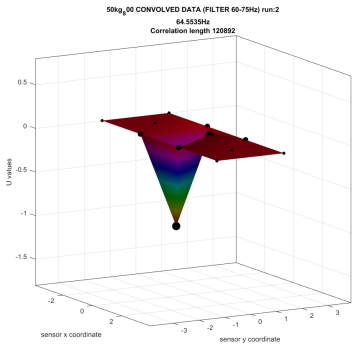


(a) 50kg mode shape, run 1

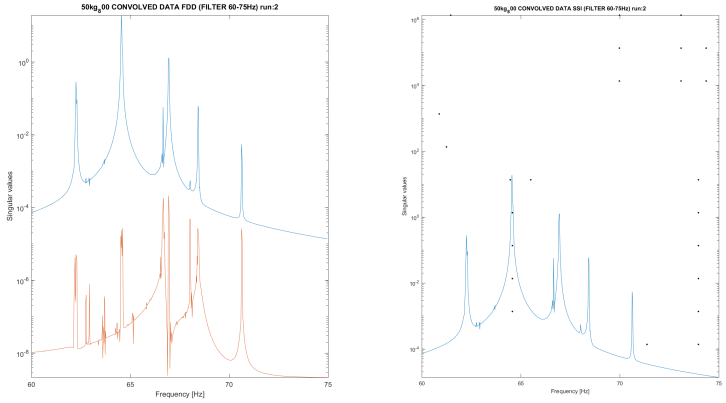


(b) 50kg FDD SSI output, run 1

Figure A1.50kg (28.03.2017): Run 1

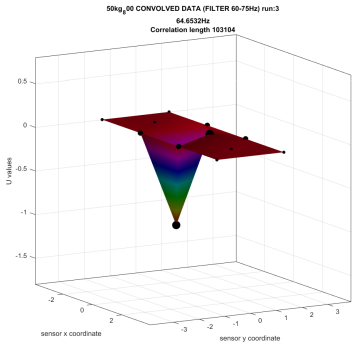


(a) 50kg mode shape, run 2

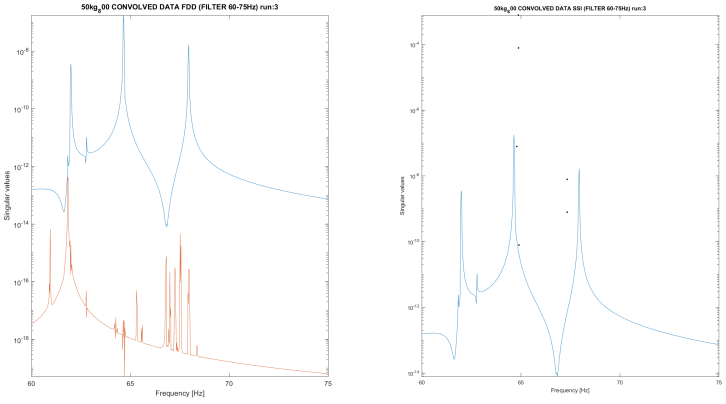


(b) 50kg FDD SSI output, run 2

Figure A1.50kg (28.03.2017): Run 2

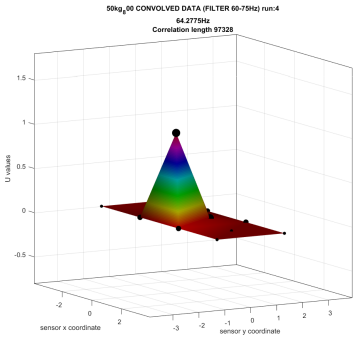


(a) 50kg mode shape, run 3

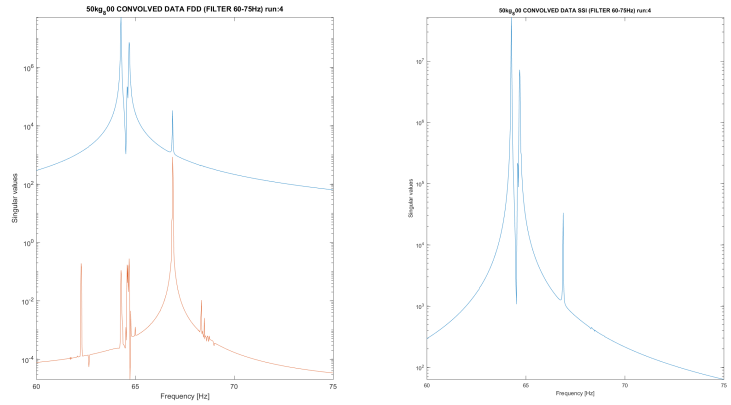


(b) 50kg FDD SSI output, run 3

Figure A1.50kg (28.03.2017): Run 3

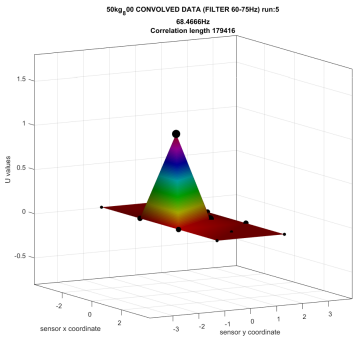


(a) 50kg mode shape, run 4

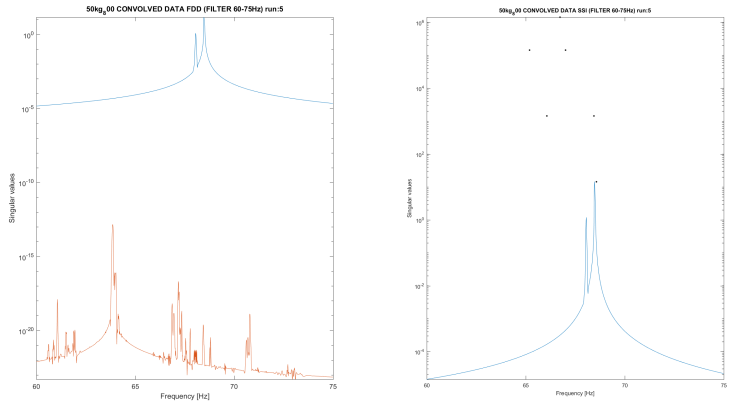


(b) 50kg FDD SSI output, run 4

Figure A1.50kg (28.03.2017): Run 4

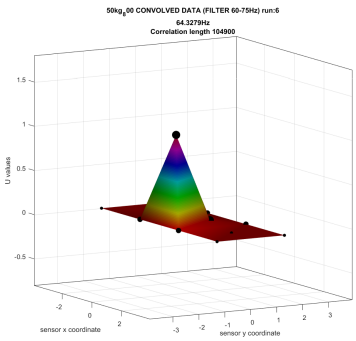


(a) 50kg mode shape, run 5

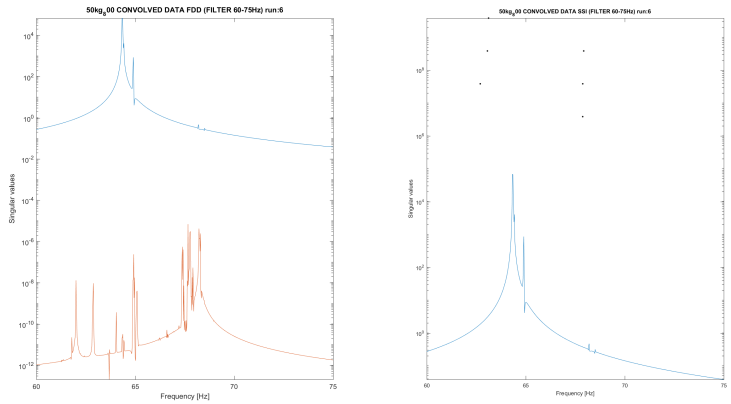


(b) 50kg FDD SSI output, run 5

Figure A1.50kg (28.03.2017): Run 5

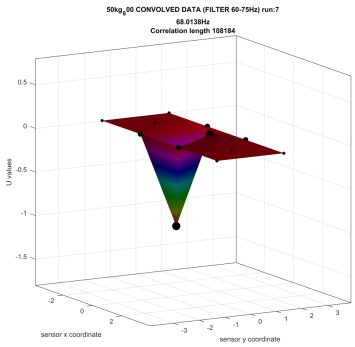


(a) 50kg mode shape, run 6

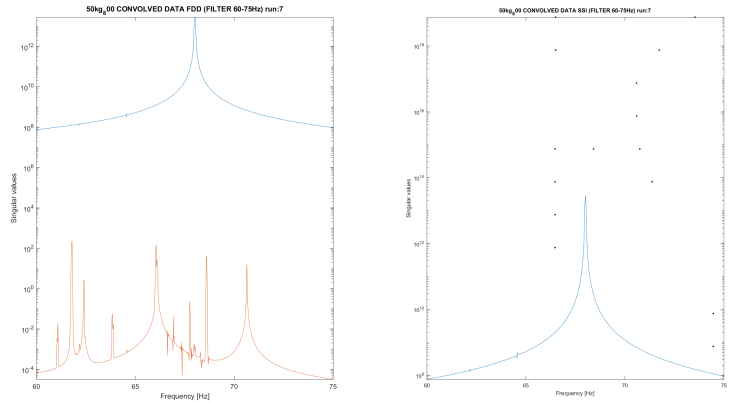


(b) 50kg FDD SSI output, run 6

Figure A1.50kg (28.03.2017): Run 6

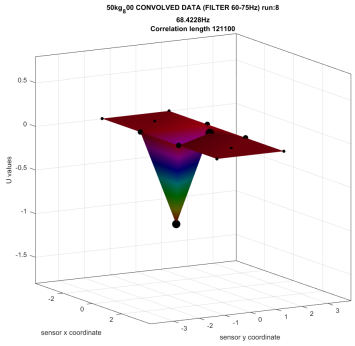


(a) 50kg mode shape, run 7

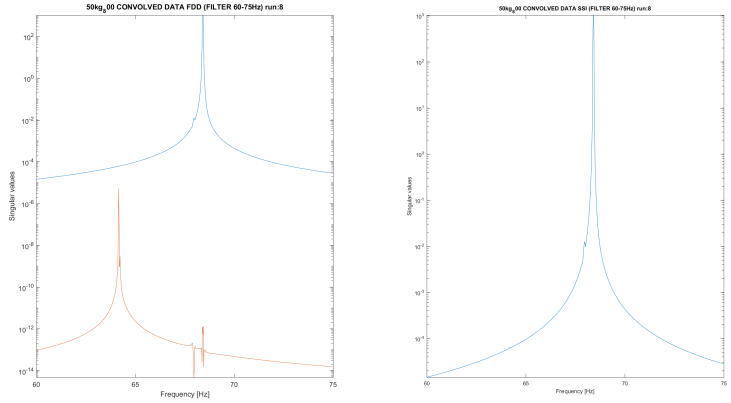


(b) 50kg FDD SSI output, run 7

Figure A1.50kg (28.03.2017): Run 7

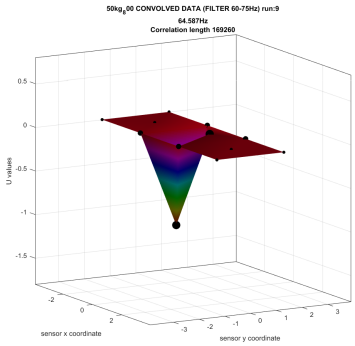


(a) 50kg mode shape, run 8

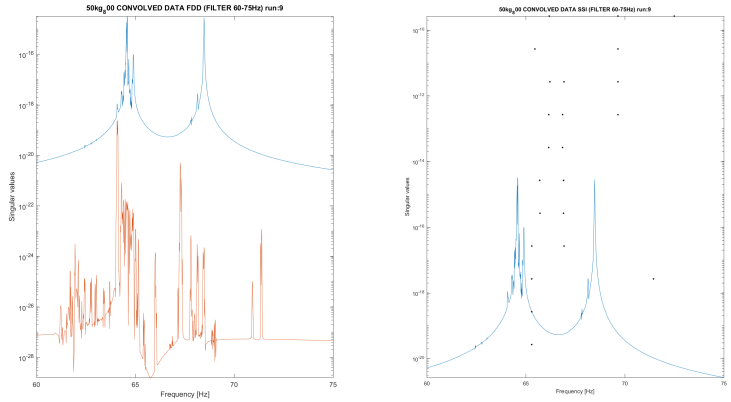


(b) 50kg FDD SSI output, run 8

Figure A1.50kg (28.03.2017): Run 8

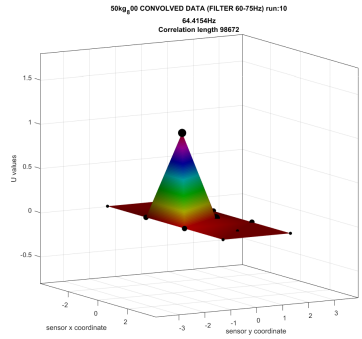


(a) 50kg mode shape, run 9

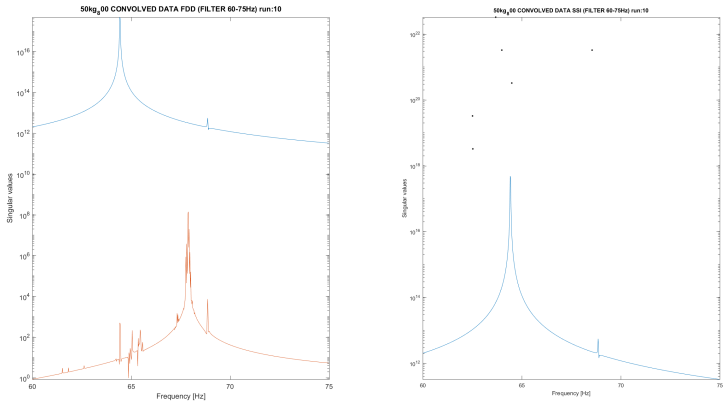


(b) 50kg FDD SSI output, run 9

Figure A1.50kg (28.03.2017): Run 9

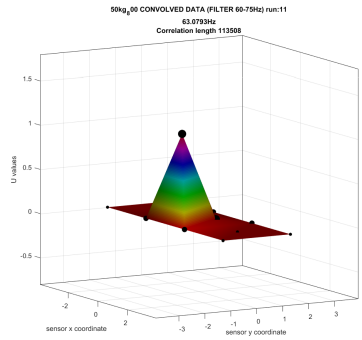


(a) 50kg mode shape, run 10

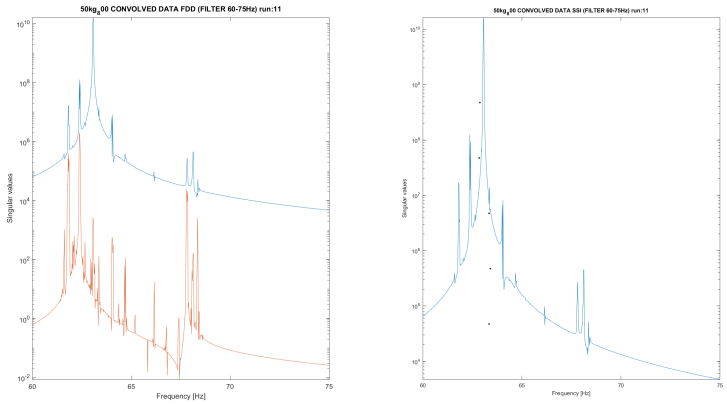


(b) 50kg FDD SSI output, run 10

Figure A1.50kg (28.03.2017): Run 10

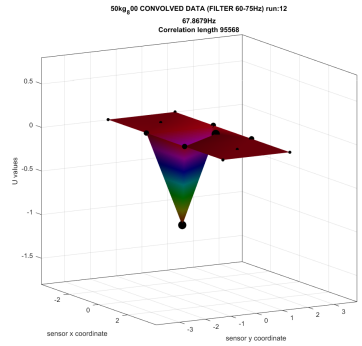


(a) 50kg mode shape, run 11

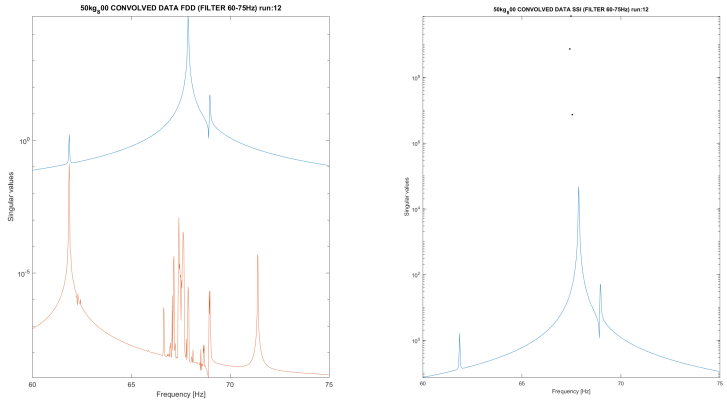


(b) 50kg FDD SSI output, run 11

Figure A1.50kg (28.03.2017): Run 11

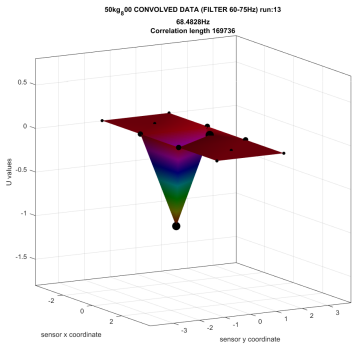


(a) 50kg mode shape, run 12

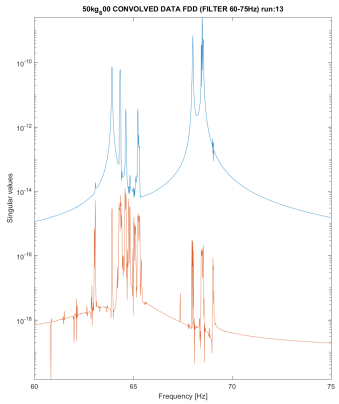


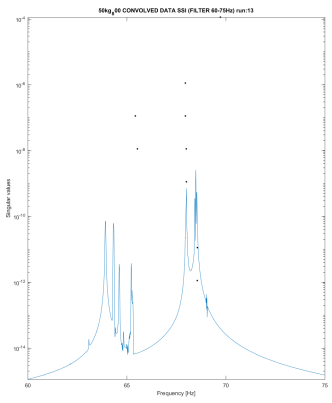
(b) 50kg FDD SSI output, run 12

Figure A1.50kg (28.03.2017): Run 12



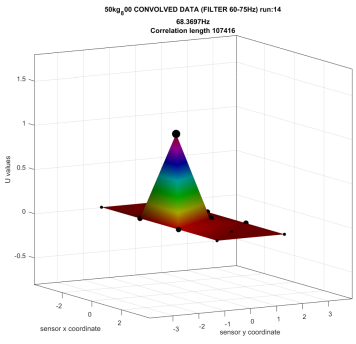
(a) 50kg mode shape, run 13



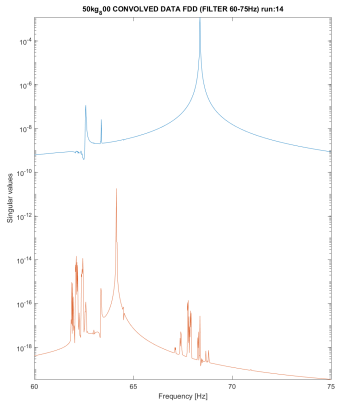


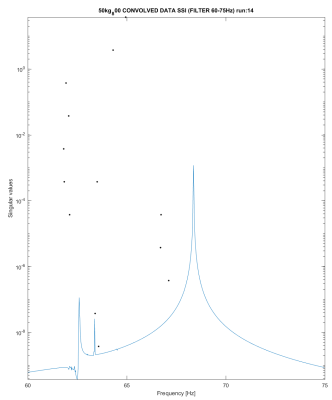
(b) 50kg FDD SSI output, run 13

Figure A1.50kg (28.03.2017): Run 13



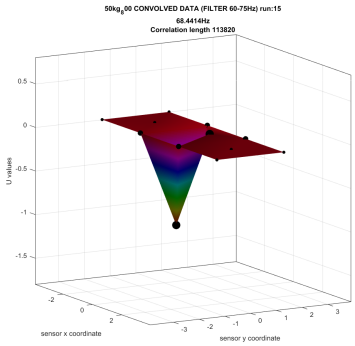
(a) 50kg mode shape, run 14



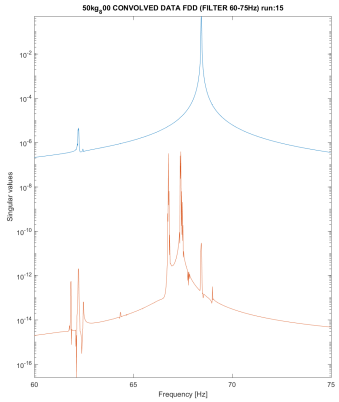


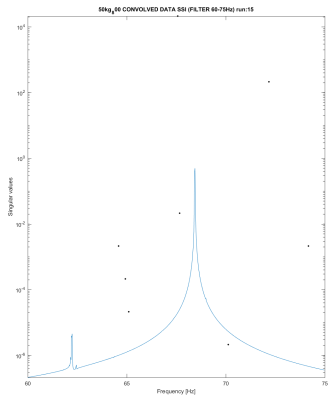
(b) 50kg FDD SSI output, run 14

Figure A1.50kg (28.03.2017): Run 14



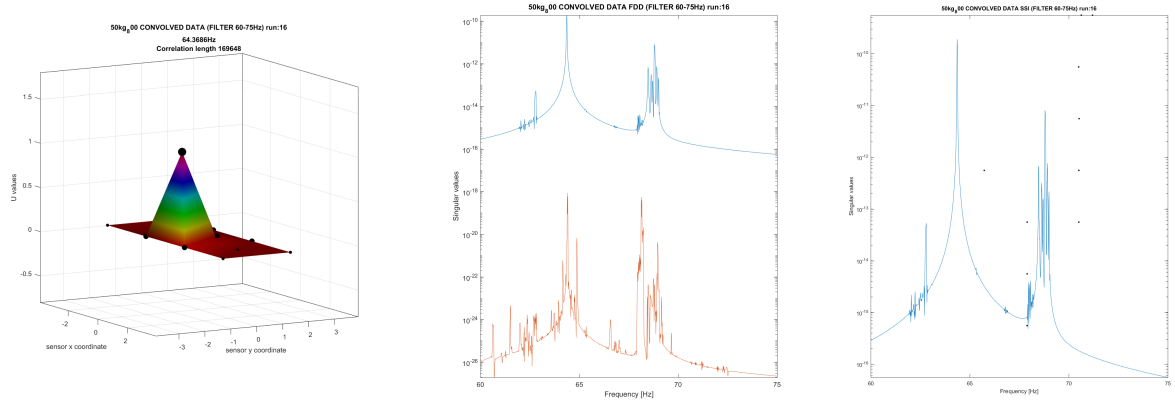
(a) 50kg mode shape, run 15





(b) 50kg FDD SSI output, run 15

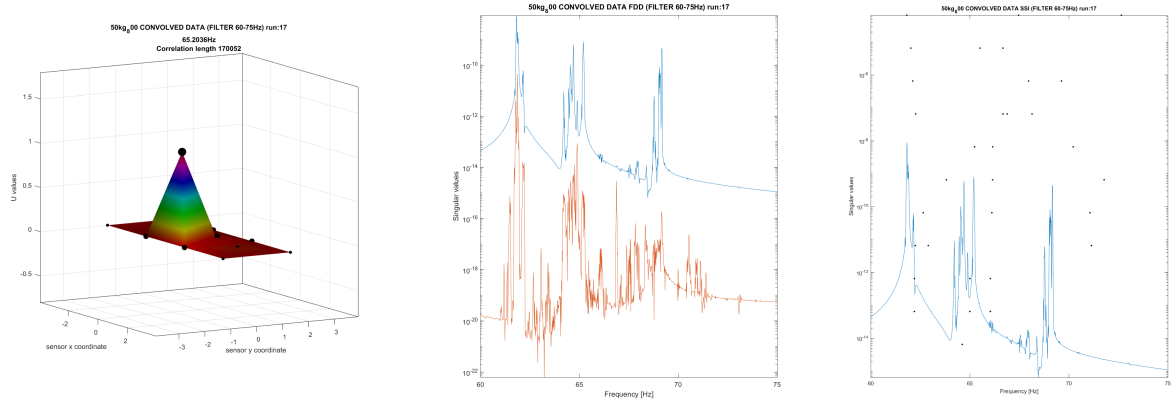
Figure A1.50kg (28.03.2017): Run 15



(a) 50kg mode shape, run 16

(b) 50kg FDD SSI output, run 16

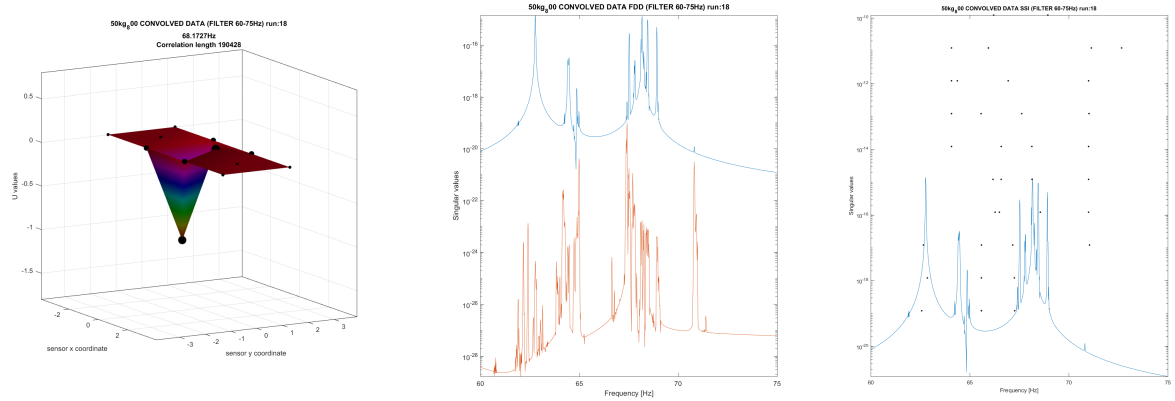
Figure A1.50kg (28.03.2017): Run 16



(a) 50kg mode shape, run 17

(b) 50kg FDD SSI output, run 17

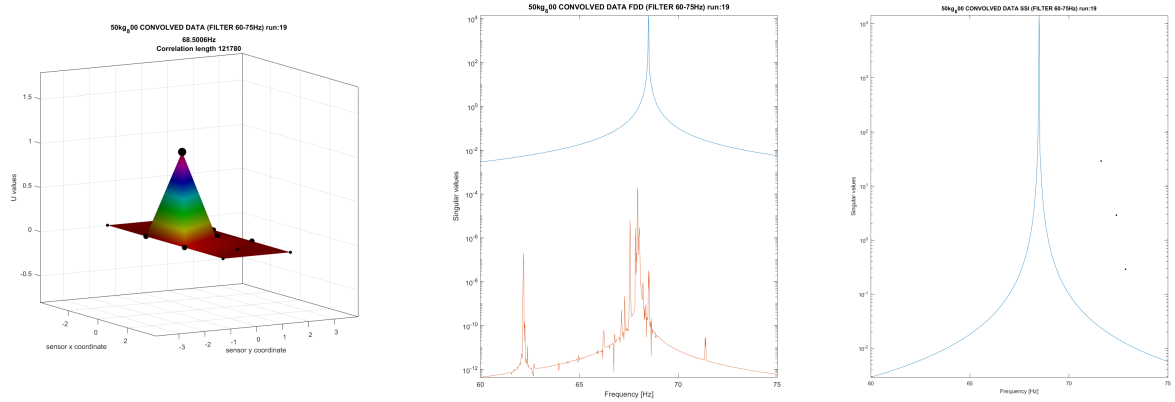
Figure A1.50kg (28.03.2017): Run 17



(a) 50kg mode shape, run 18

(b) 50kg FDD SSI output, run 18

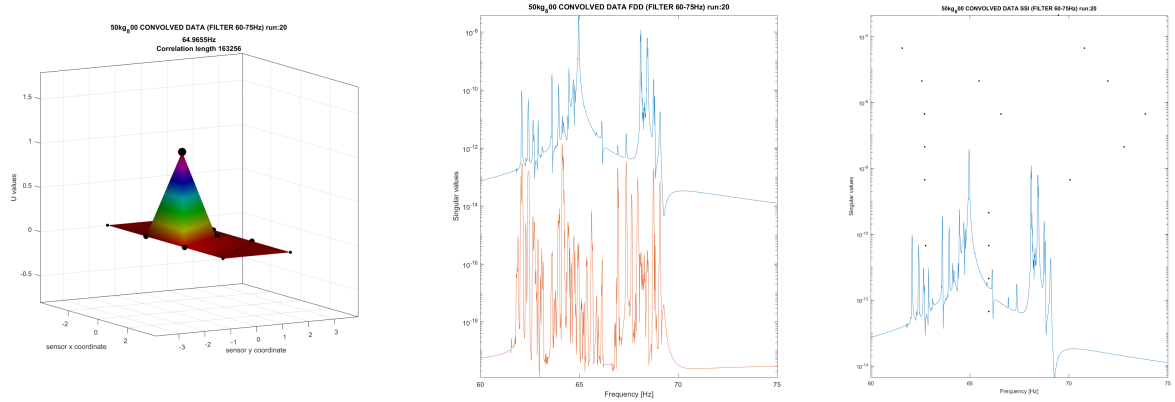
Figure A1.50kg (28.03.2017): Run 18



(a) 50kg mode shape, run 19

(b) 50kg FDD SSI output, run 19

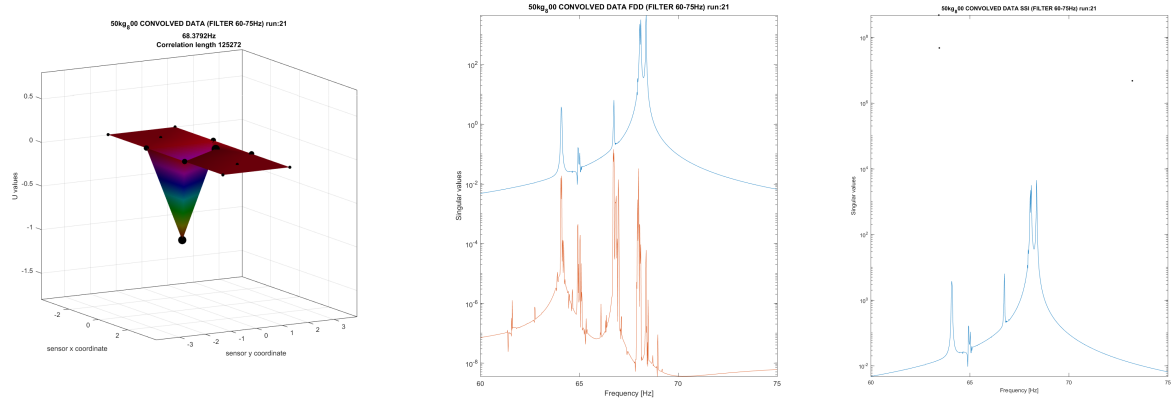
Figure A1.50kg (28.03.2017): Run 19



(a) 50kg mode shape, run 20

(b) 50kg FDD SSI output, run 20

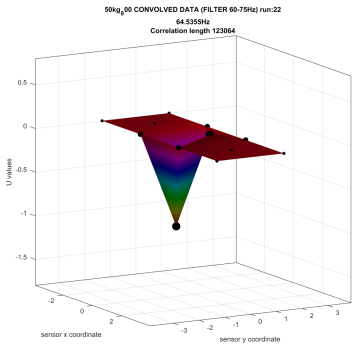
Figure A1.50kg (28.03.2017): Run 20



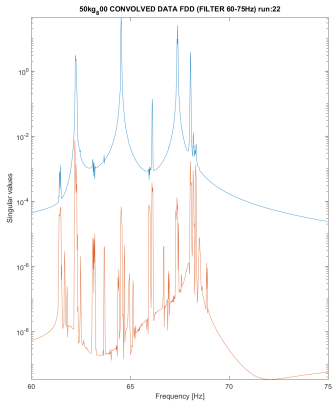
(a) 50kg mode shape, run 21

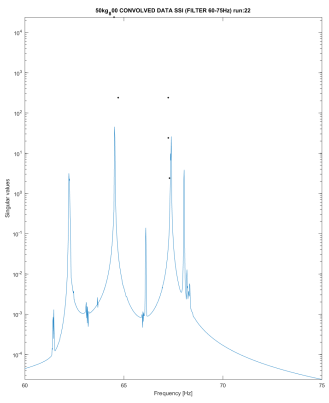
(b) 50kg FDD SSI output, run 21

Figure A1.50kg (28.03.2017): Run 21



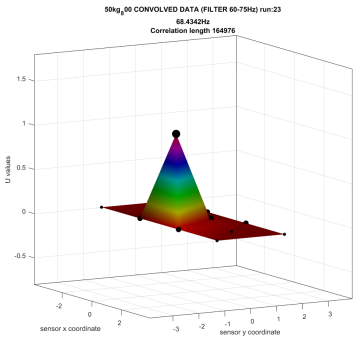
(a) 50kg mode shape, run 22



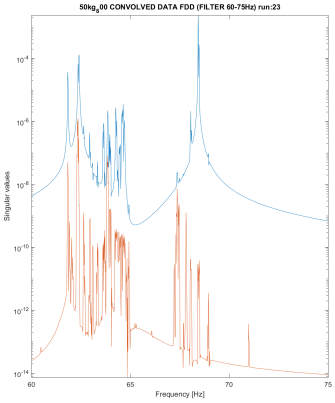


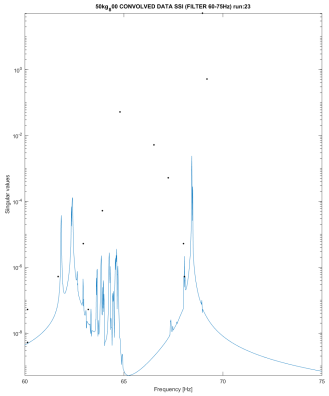
(b) 50kg FDD SSI output, run 22

Figure A1.50kg (28.03.2017): Run 22



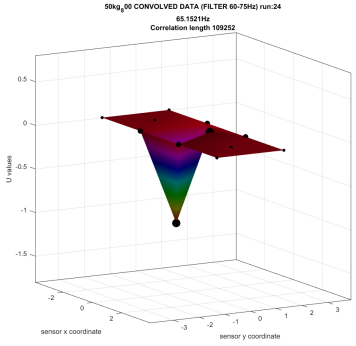
(a) 50kg mode shape, run 23



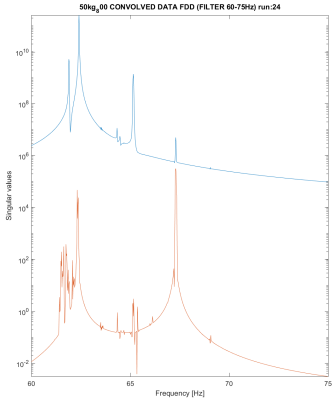


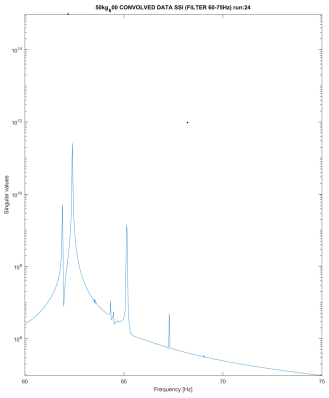
(b) 50kg FDD SSI output, run 23

Figure A1.50kg (28.03.2017): Run 23



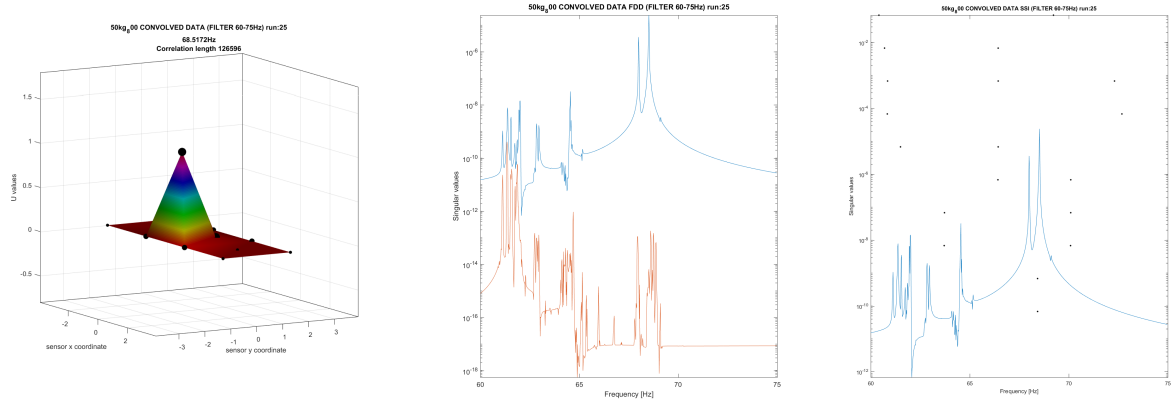
(a) 50kg mode shape, run 24





(b) 50kg FDD SSI output, run 24

Figure A1.50kg (28.03.2017): Run 24



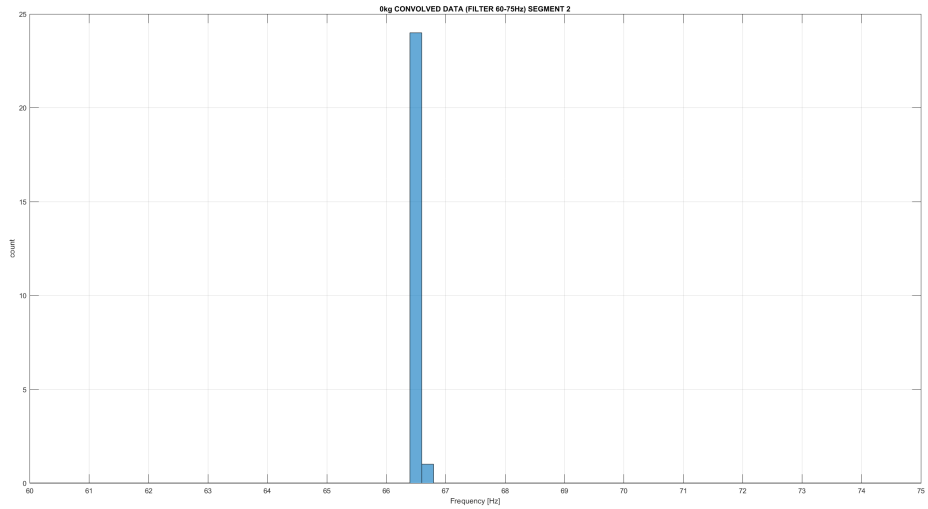
(a) 50kg mode shape, run 25

(b) 50kg FDD SSI output, run 25

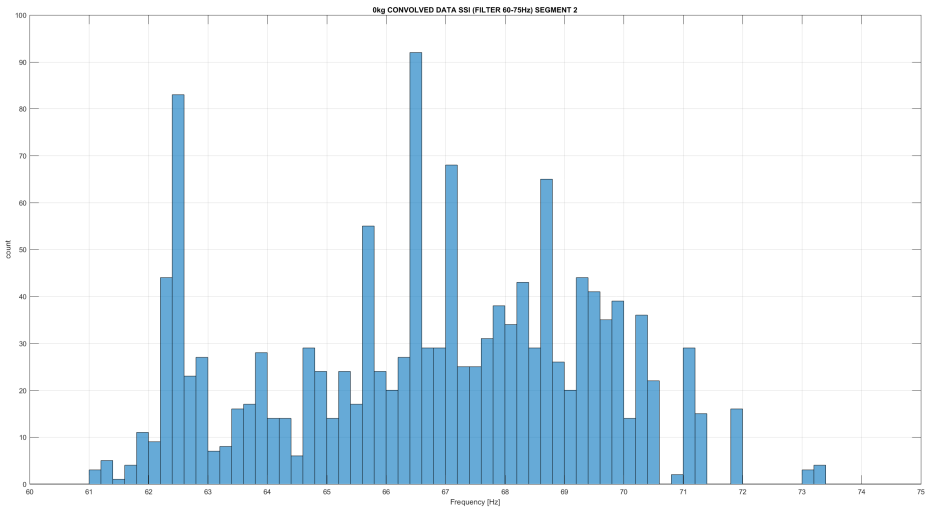
Figure A1.50kg (28.03.2017): Run 25

Appendix A2

Data 0kg-50kg-75kg-100kg segment 2 (Reduced order PF)

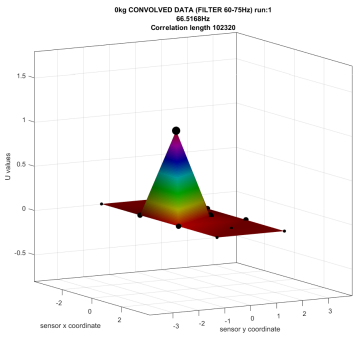


(a) 0kg FDD histogram

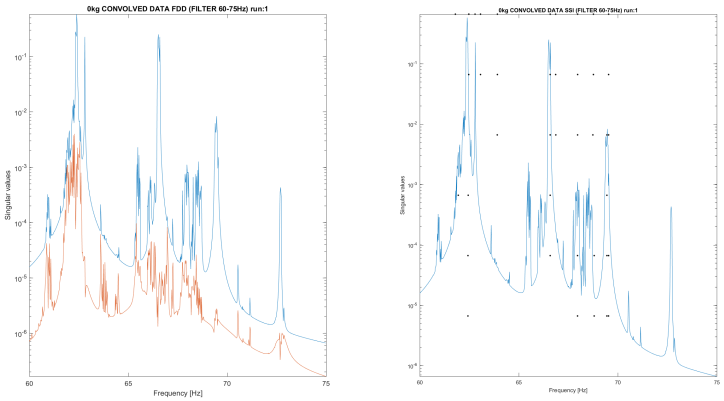


(b) 0kg SSI histogram

Figure A2.0kg: Histograms of identified modes, 0kg data

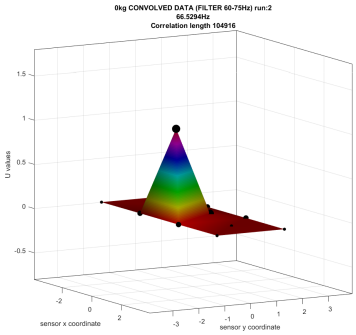


(a) 0kg mode shape, run 1

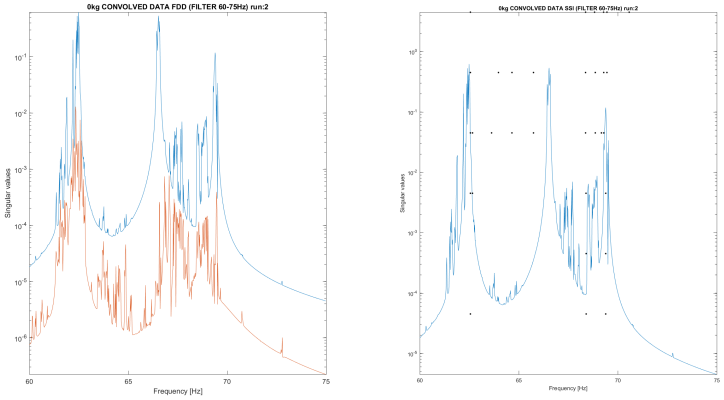


(b) 0kg FDD SSI output, run 1

Figure A2.0kg: Run 1

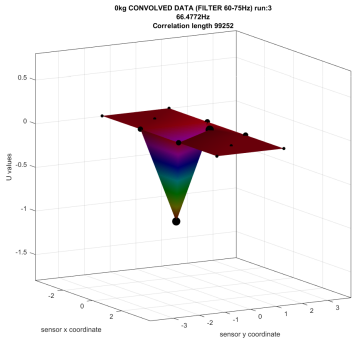


(a) 0kg mode shape, run 2

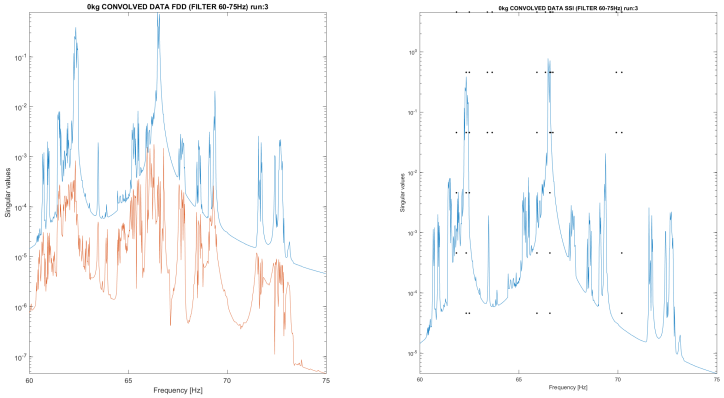


(b) 0kg FDD SSI output, run 2

Figure A2.0kg: Run 2

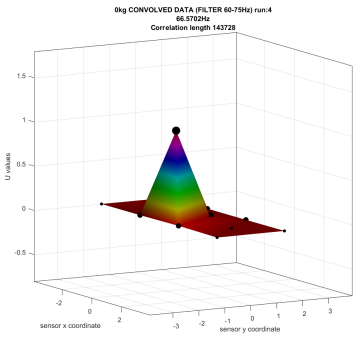


(a) 0kg mode shape, run 3

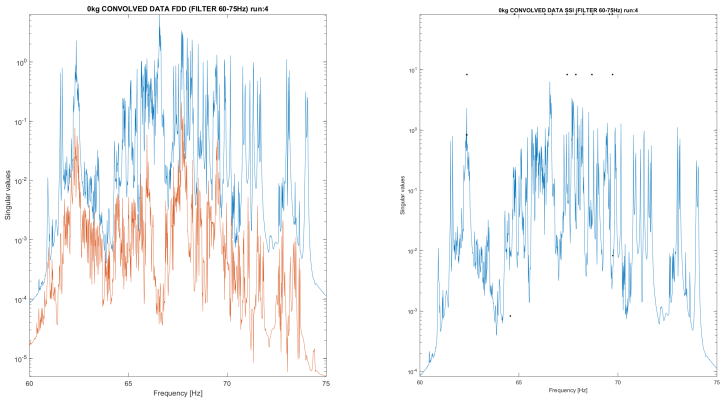


(b) 0kg FDD SSI output, run 3

Figure A2.0kg: Run 3

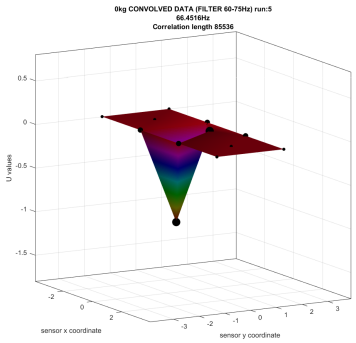


(a) 0kg mode shape, run 4

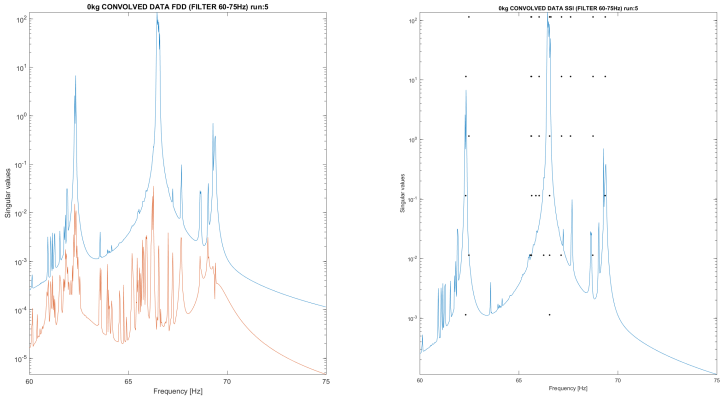


(b) 0kg FDD SSI output, run 4

Figure A2.0kg: Run 4

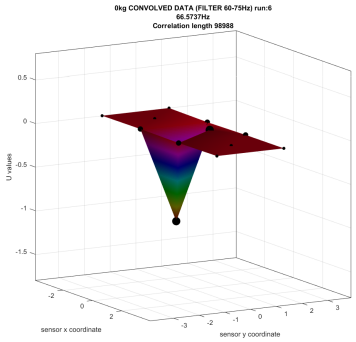


(a) 0kg mode shape, run 5

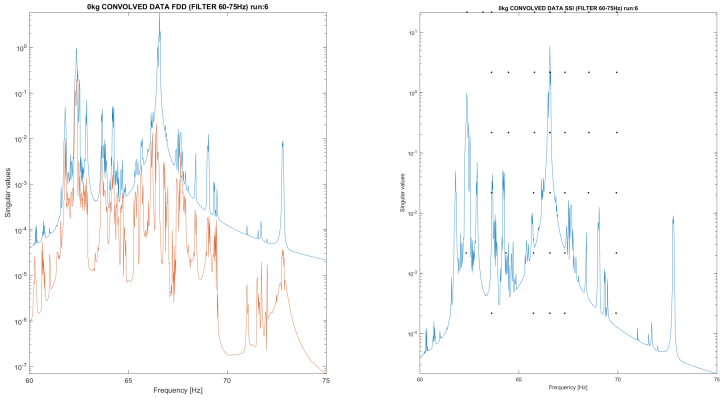


(b) 0kg FDD SSI output, run 5

Figure A2.0kg: Run 5

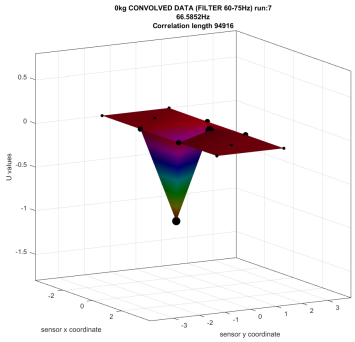


(a) 0kg mode shape, run 6

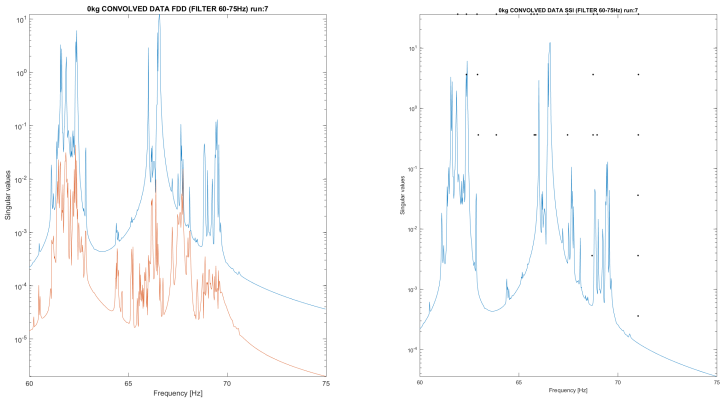


(b) 0kg FDD SSI output, run 6

Figure A2.0kg: Run 6

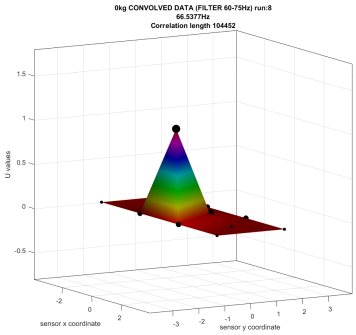


(a) 0kg mode shape, run 7

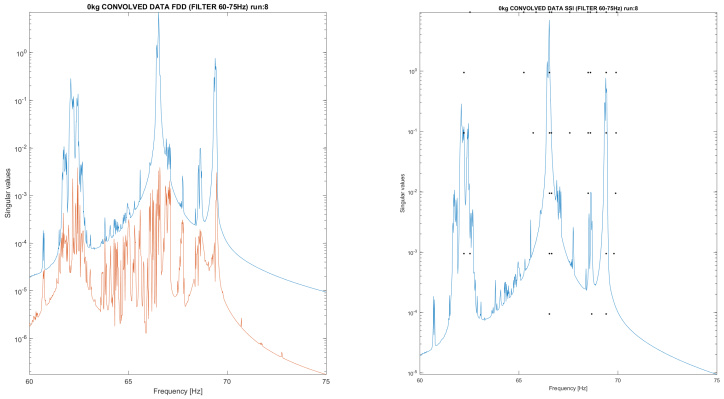


(b) 0kg FDD SSI output, run 7

Figure A2.0kg: Run 7

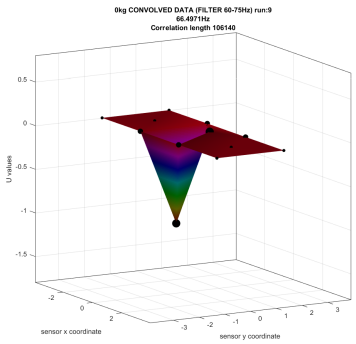


(a) 0kg mode shape, run 8

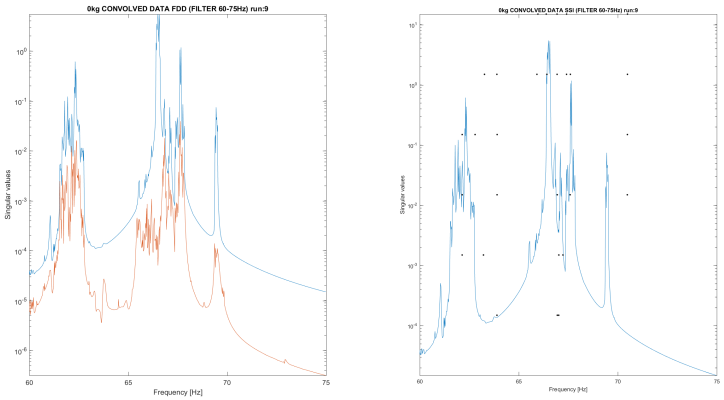


(b) 0kg FDD SSI output, run 8

Figure A2.0kg: Run 8

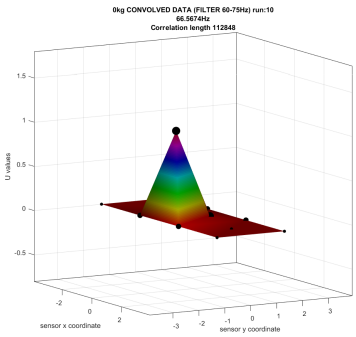


(a) 0kg mode shape, run 9

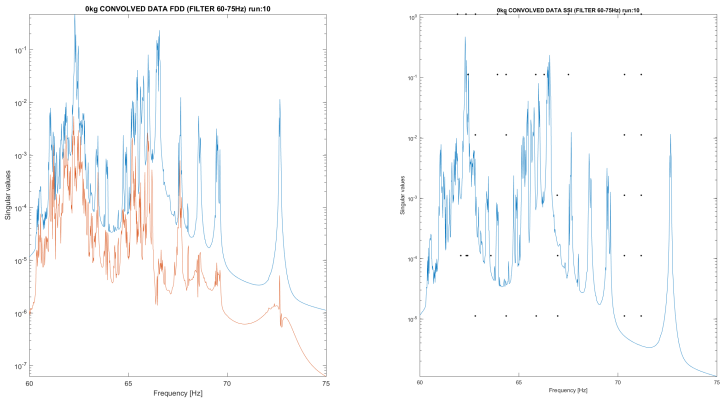


(b) 0kg FDD SSI output, run 9

Figure A2.0kg: Run 9

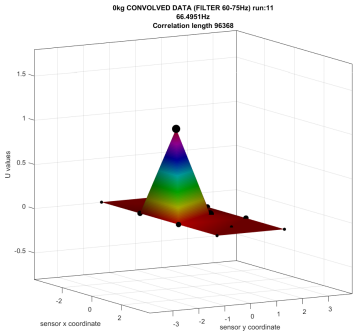


(a) 0kg mode shape, run 10

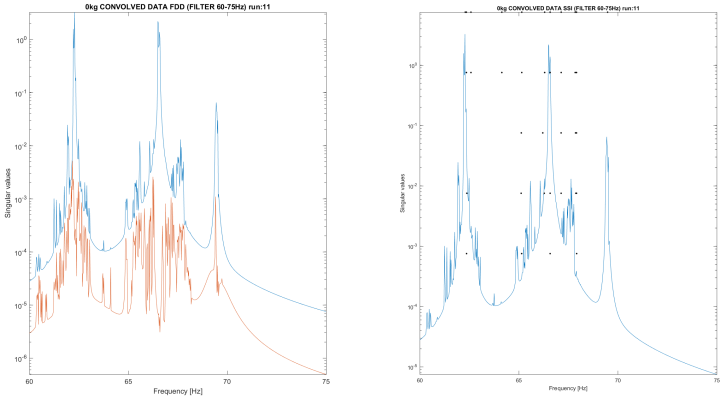


(b) 0kg FDD SSI output, run 10

Figure A2.0kg: Run 10

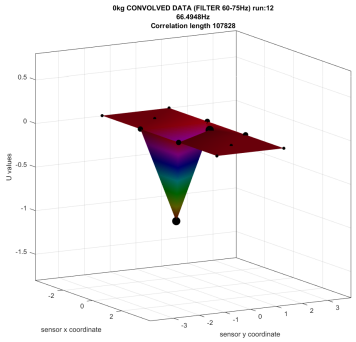


(a) 0kg mode shape, run 11

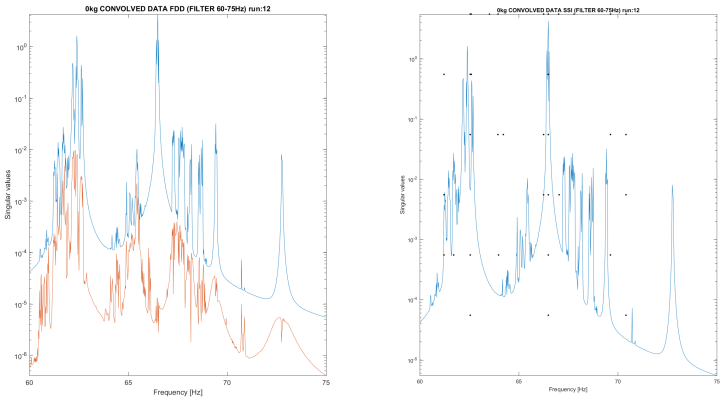


(b) 0kg FDD SSI output, run 11

Figure A2.0kg: Run 11

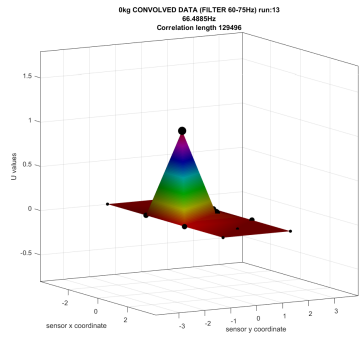


(a) 0kg mode shape, run 12

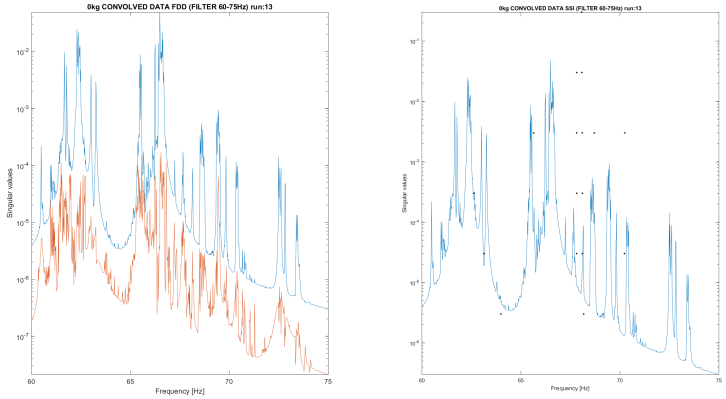


(b) 0kg FDD SSI output, run 12

Figure A2.0kg: Run 12

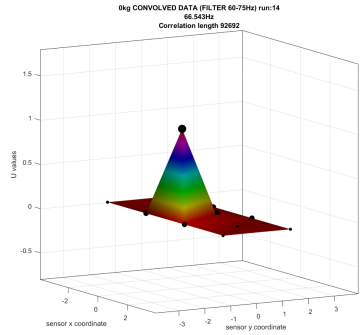


(a) 0kg mode shape, run 13

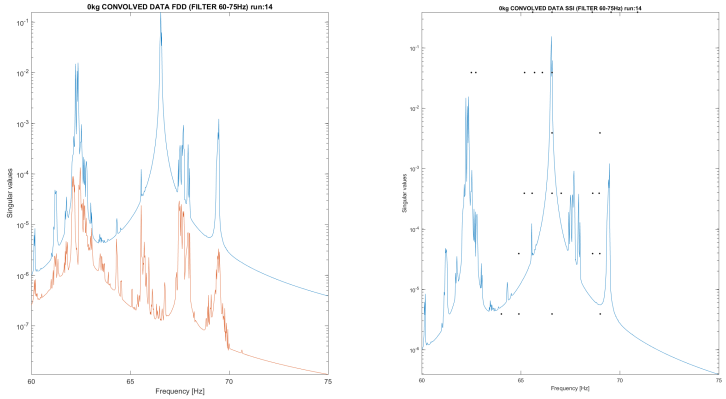


(b) 0kg FDD SSI output, run 13

Figure A2.0kg: Run 13

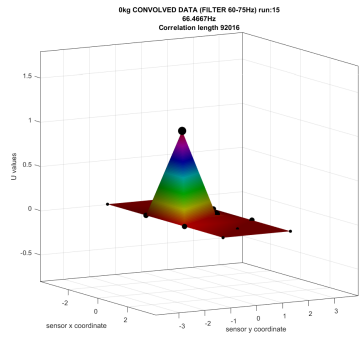


(a) 0kg mode shape, run 14

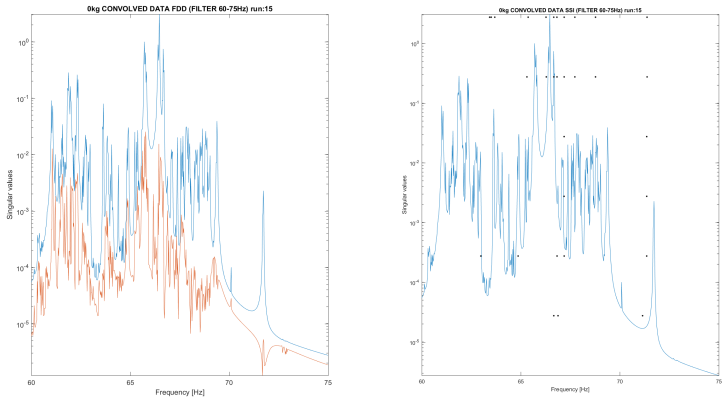


(b) 0kg FDD SSI output, run 14

Figure A2.0kg: Run 14

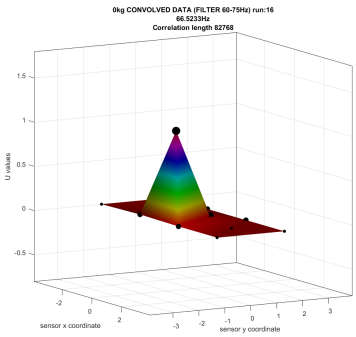


(a) 0kg mode shape, run 15

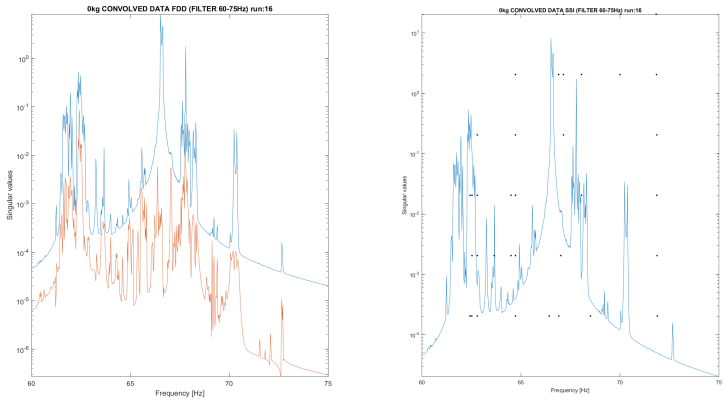


(b) 0kg FDD SSI output, run 15

Figure A2.0kg: Run 15

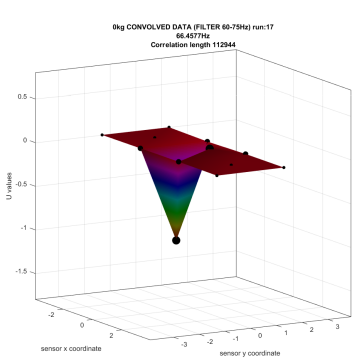


(a) 0kg mode shape, run 16

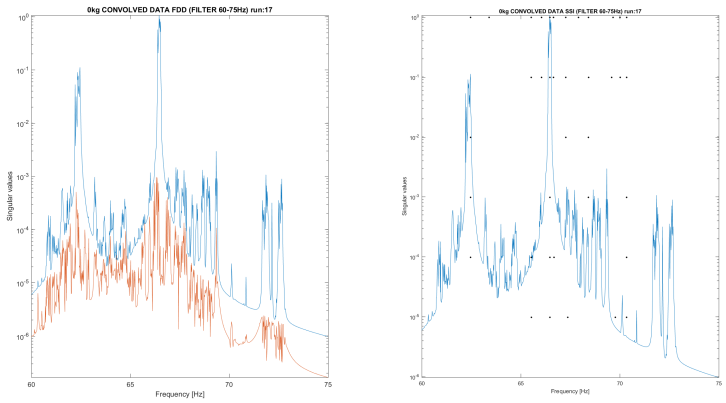


(b) 0kg FDD SSI output, run 16

Figure A2.0kg: Run 16

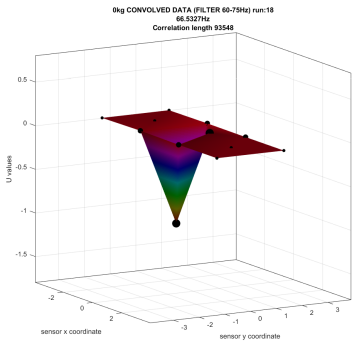


(a) 0kg mode shape, run 17

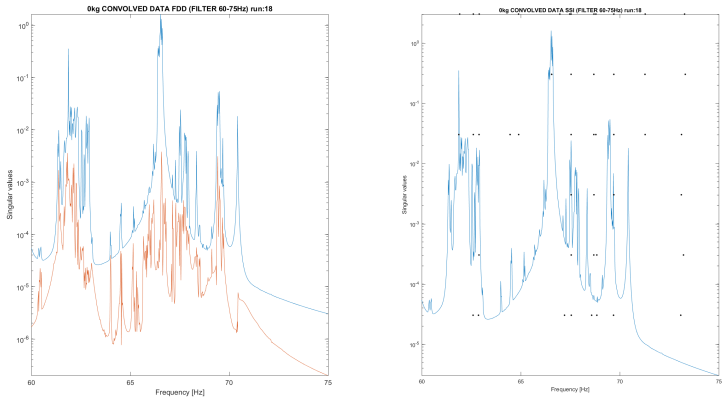


(b) 0kg FDD SSI output, run 17

Figure A2.0kg: Run 17

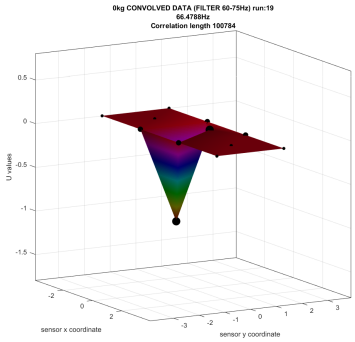


(a) 0kg mode shape, run 18

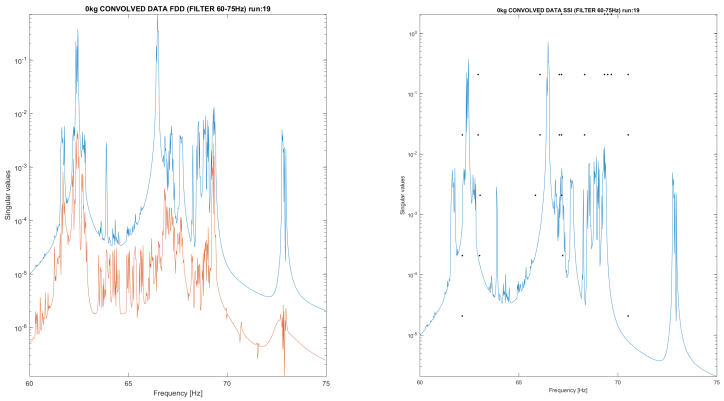


(b) 0kg FDD SSI output, run 18

Figure A2.0kg: Run 18

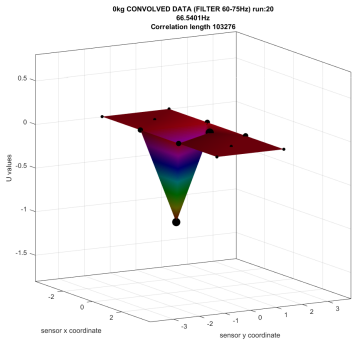


(a) 0kg mode shape, run 19

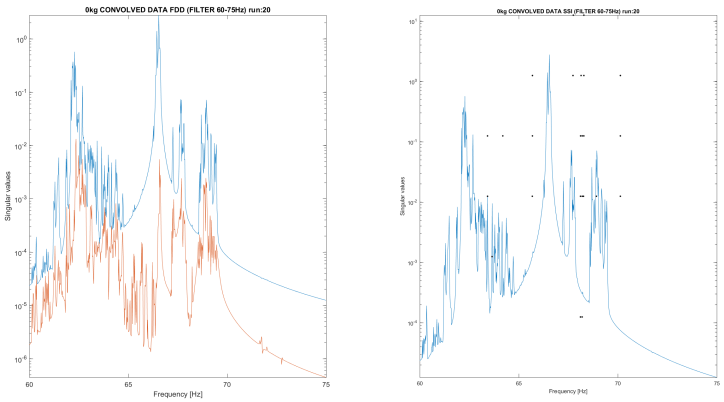


(b) 0kg FDD SSI output, run 19

Figure A2.0kg: Run 19

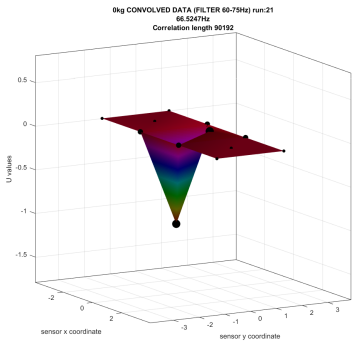


(a) 0kg mode shape, run 20

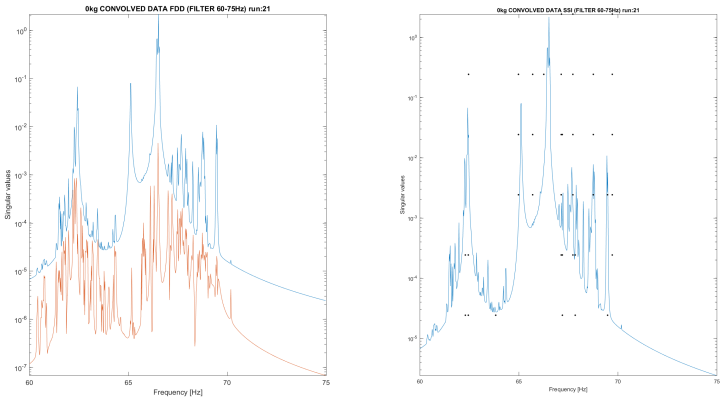


(b) 0kg FDD SSI output, run 21

Figure A2.0kg: Run 20

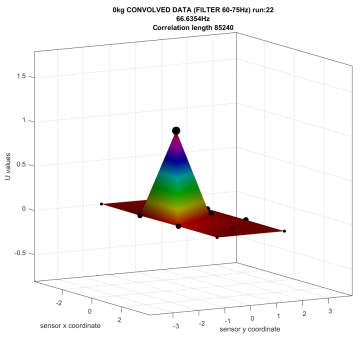


(a) 0kg mode shape, run 21

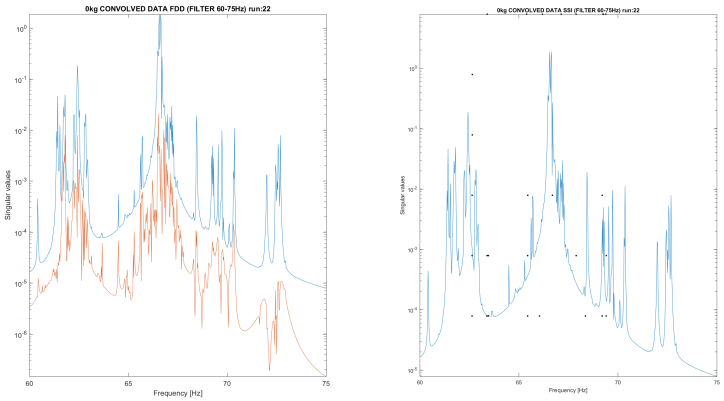


(b) 0kg FDD SSI output, run 21

Figure A2.0kg: Run 21

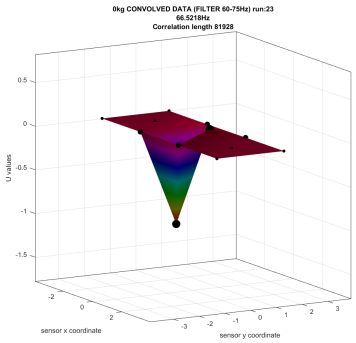


(a) 0kg mode shape, run 22

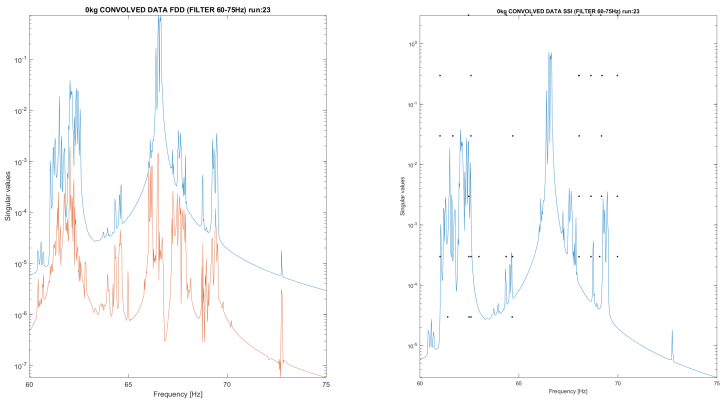


(b) 0kg FDD SSI output, run 22

Figure A2.0kg: Run 22

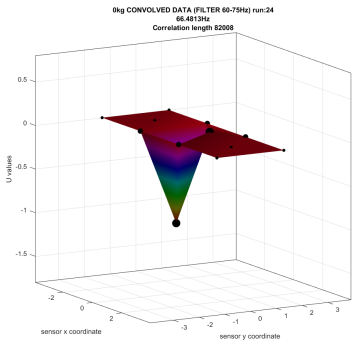


(a) 0kg mode shape, run 23

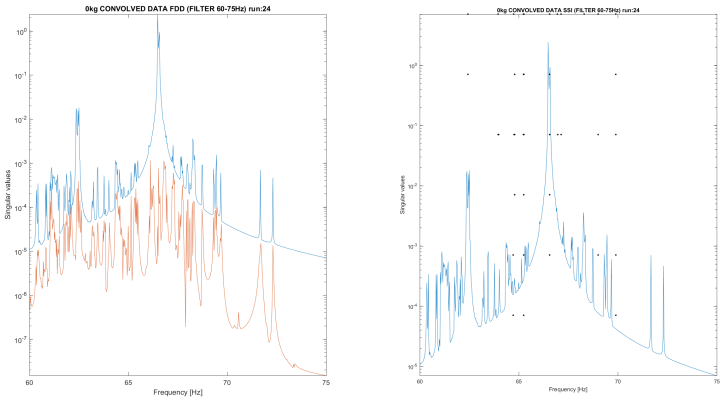


(b) 0kg FDD SSI output, run 23

Figure A2.0kg: Run 23

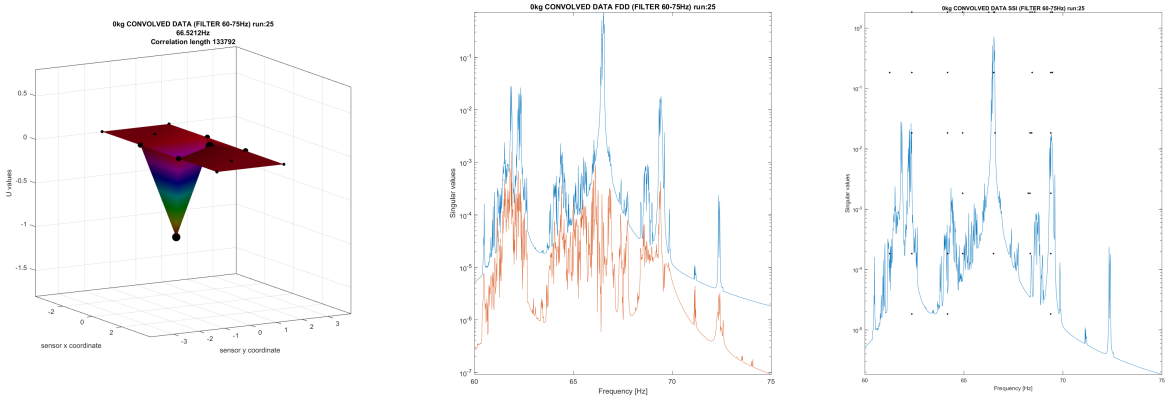


(a) 0kg mode shape, run 24



(b) 0kg FDD SSI output, run 24

Figure A2.0kg: Run 24

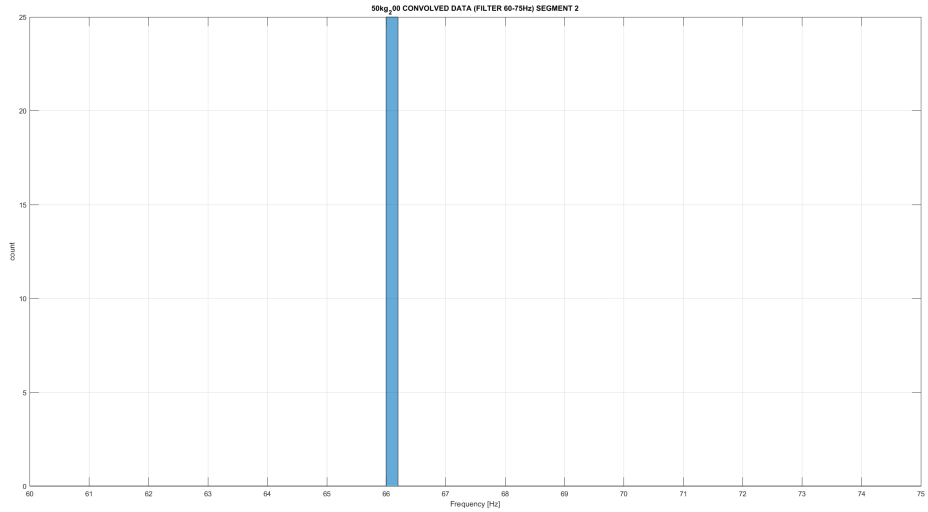


(a) 0kg mode shape, run 25

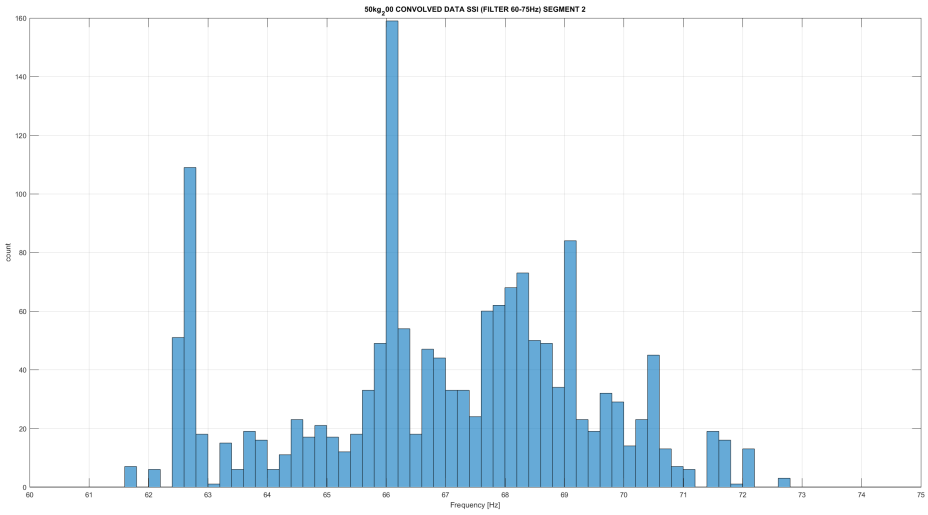
(b) 0kg FDD SSI output, run 25

Figure A2.0kg: Run 25

50kg data segment 2

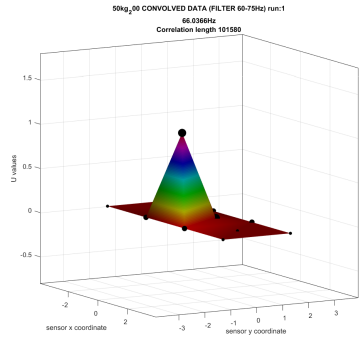


(a) 50kg FDD histogram

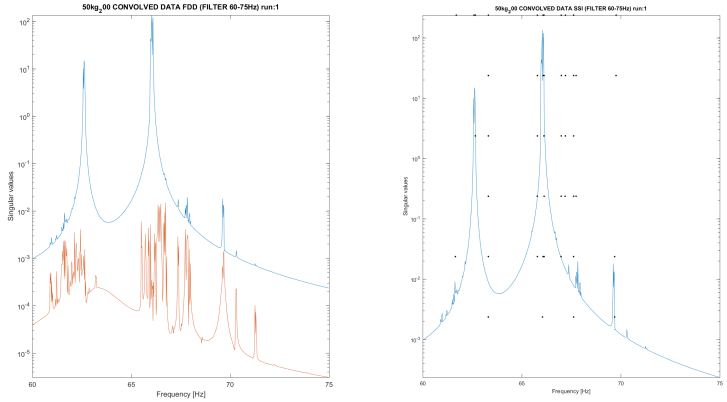


(b) 50kg SSI histogram

Figure A2.50kg: Histograms of identified modes, 50kg data

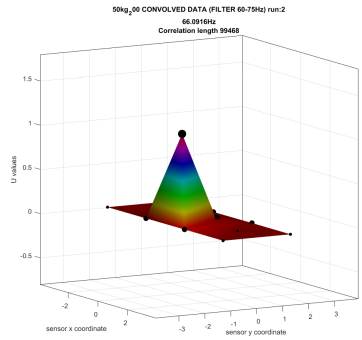


(a) 50kg mode shape, run 1

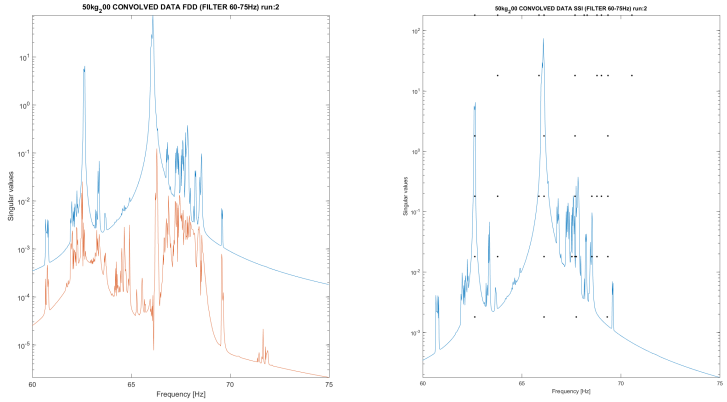


(b) 50kg FDD SSI output, run 1

Figure A2.50kg: Run 1

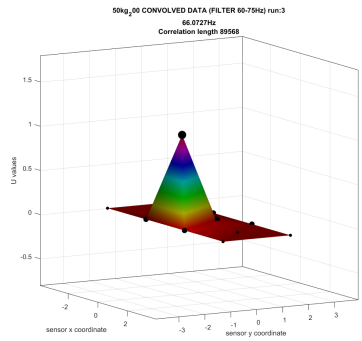


(a) 50kg mode shape, run 2

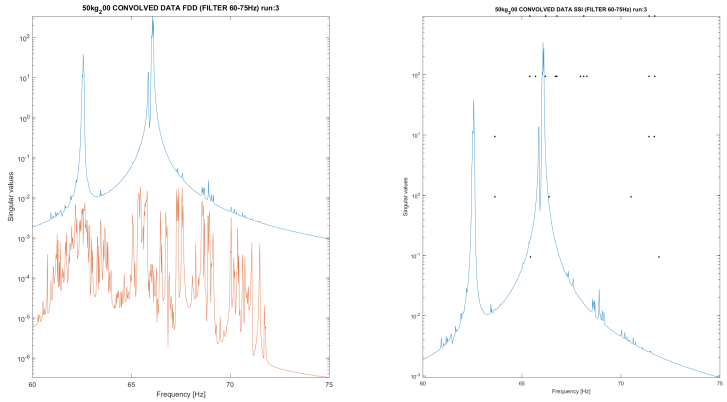


(b) 50kg FDD SSI output, run 2

Figure A2.50kg: Run 2

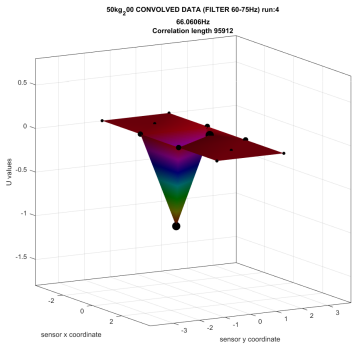


(a) 50kg mode shape, run 3

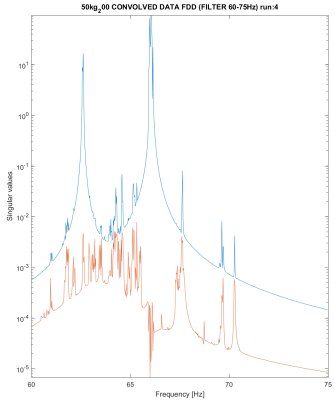


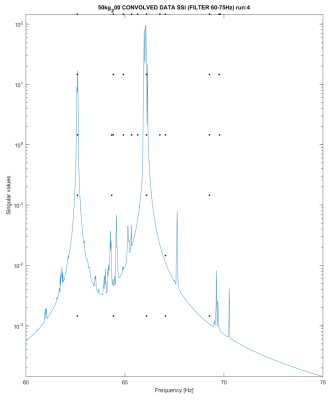
(b) 50kg FDD SSI output, run 3

Figure A2.50kg: Run 3



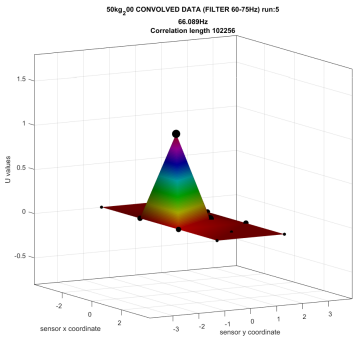
(a) 50kg mode shape, run 4



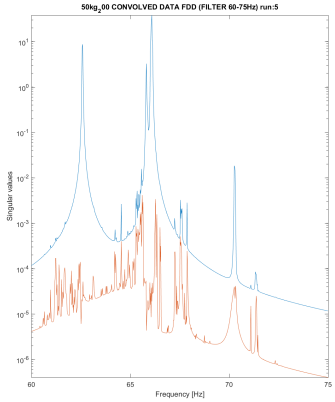


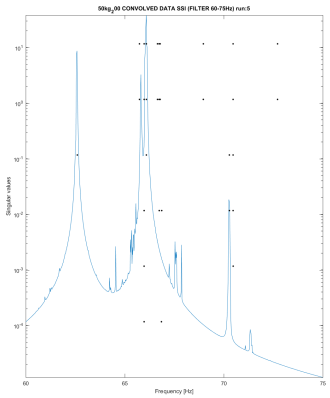
(b) 50kg FDD SSI output, run 4

Figure A2.50kg: Run 4



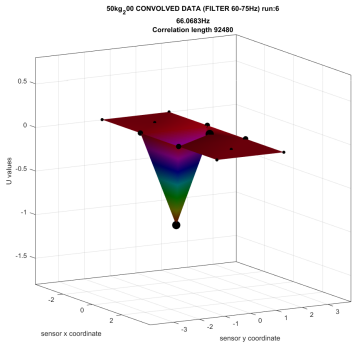
(a) 50kg mode shape, run 5



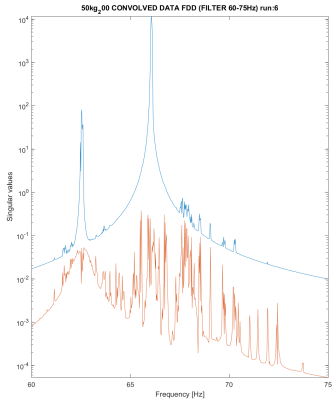


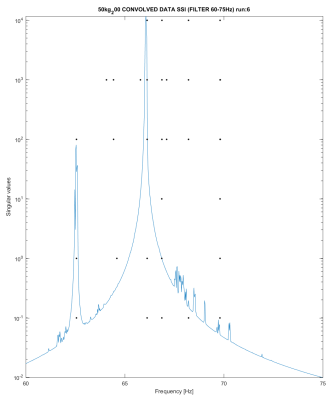
(b) 50kg FDD SSI output, run 5

Figure A2.50kg: Run 5



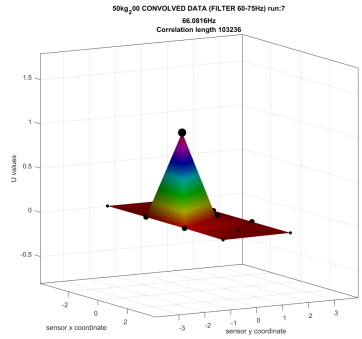
(a) 50kg mode shape, run 6



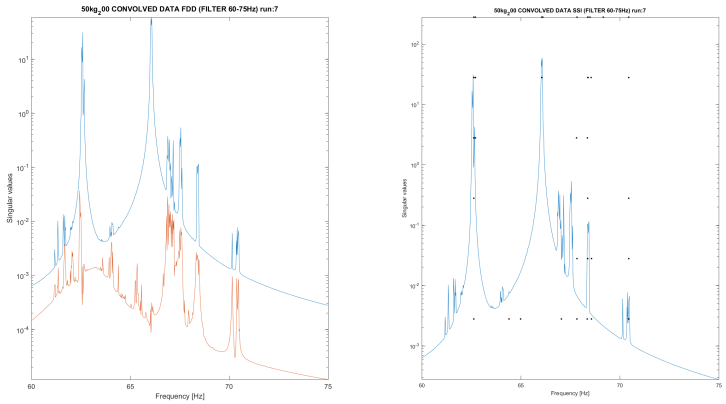


(b) 50kg FDD SSI output, run 6

Figure A2.50kg: Run 6

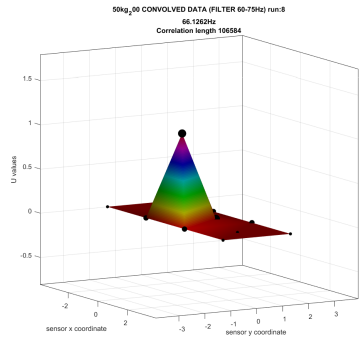


(a) 50kg mode shape, run 7

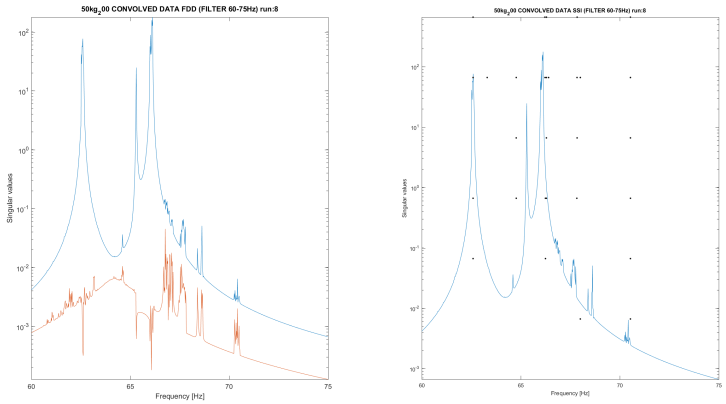


(b) 50kg FDD SSI output, run 7

Figure A2.50kg: Run 7

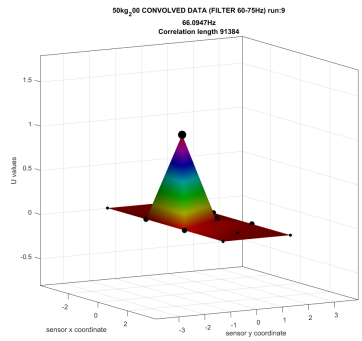


(a) 50kg mode shape, run 8

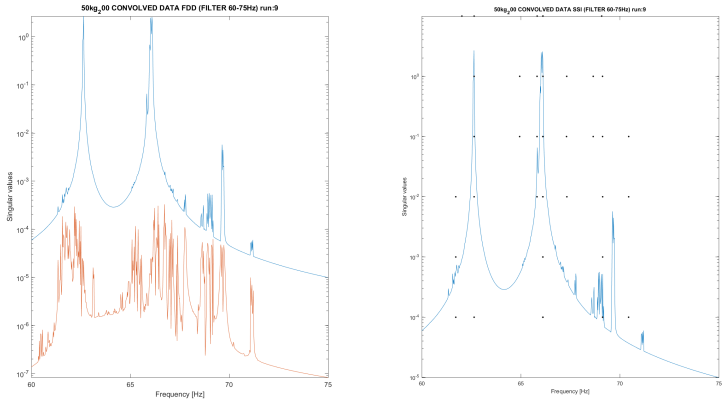


(b) 50kg FDD SSI output, run 8

Figure A2.50kg: Run 8

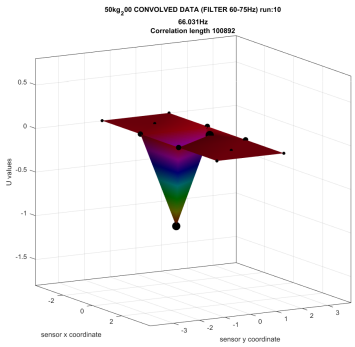


(a) 50kg mode shape, run 9

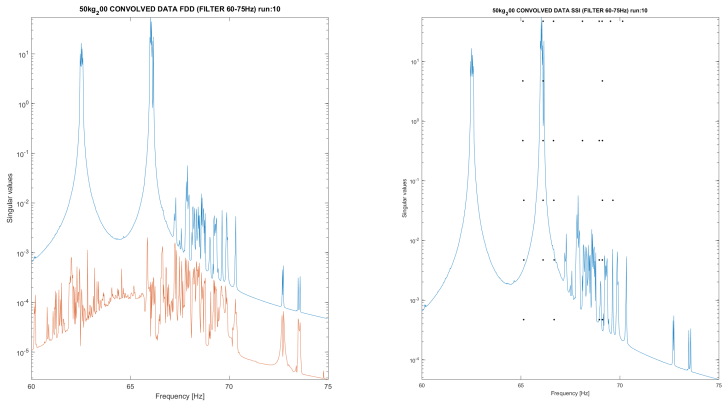


(b) 50kg FDD SSI output, run 9

Figure A2.50kg: Run 9

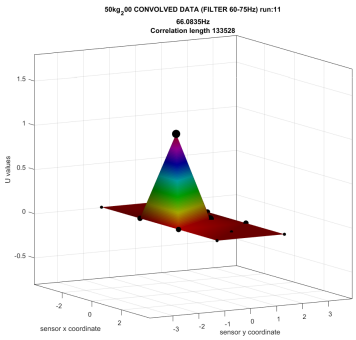


(a) 50kg mode shape, run 10

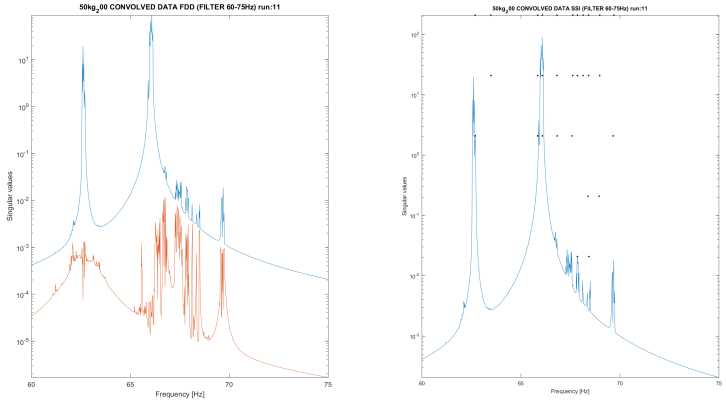


(b) 50kg FDD SSI output, run 10

Figure A2.50kg: Run 10

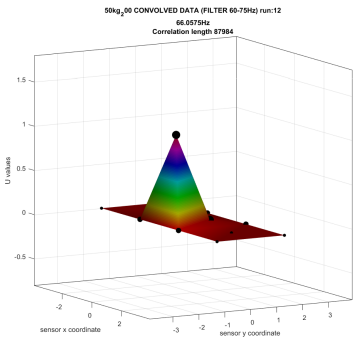


(a) 50kg mode shape, run 11

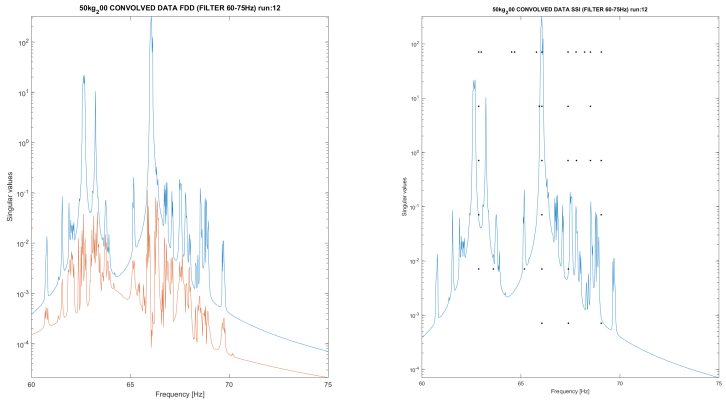


(b) 50kg FDD SSI output, run 11

Figure A2.50kg: Run 11

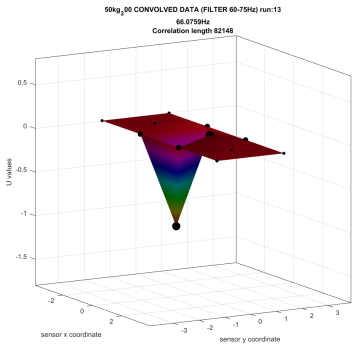


(a) 50kg mode shape, run 12

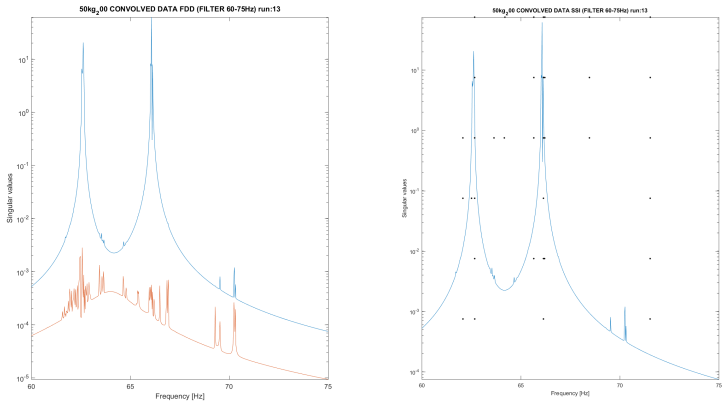


(b) 50kg FDD SSI output, run 12

Figure A2.50kg: Run 12

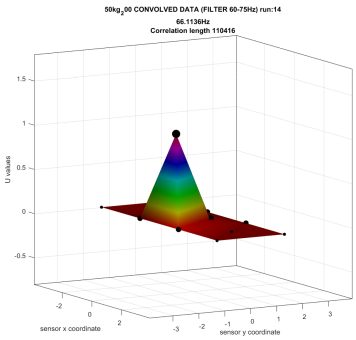


(a) 50kg mode shape, run 13

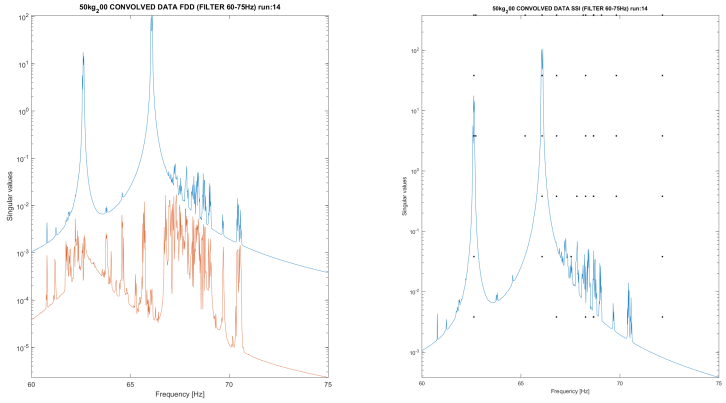


(b) 50kg FDD SSI output, run 13

Figure A2.50kg: Run 13

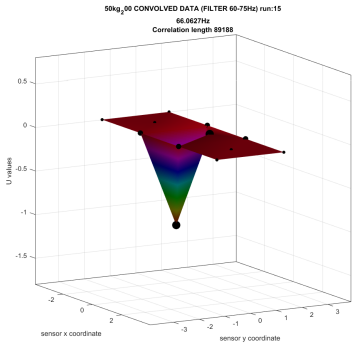


(a) 50kg mode shape, run 14

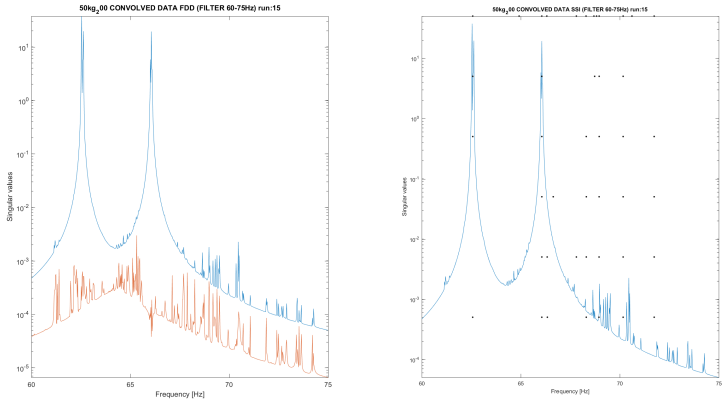


(b) 50kg FDD SSI output, run 14

Figure A2.50kg: Run 14

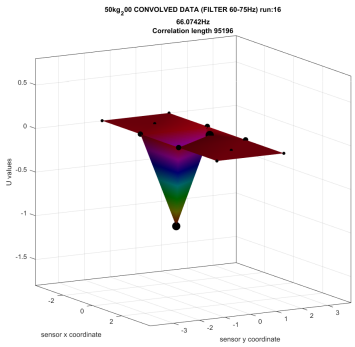


(a) 50kg mode shape, run 15

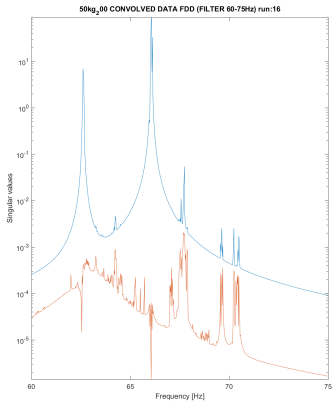


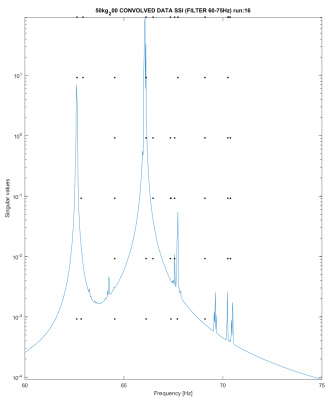
(b) 50kg FDD SSI output, run 15

Figure A2.50kg: Run 15



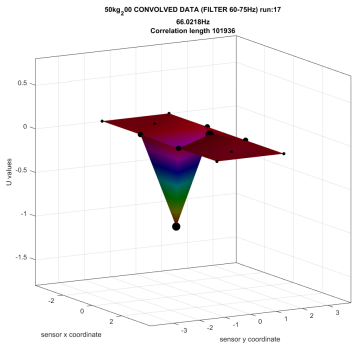
(a) 50kg mode shape, run 16



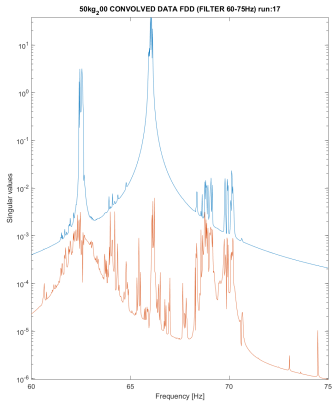


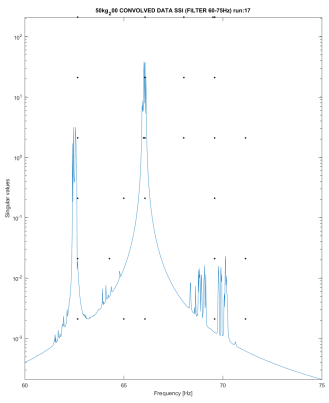
(b) 50kg FDD SSI output, run 16

Figure A2.50kg: Run 16



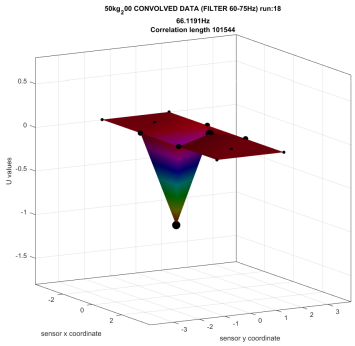
(a) 50kg mode shape, run 17



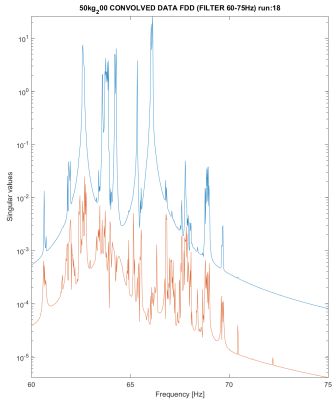


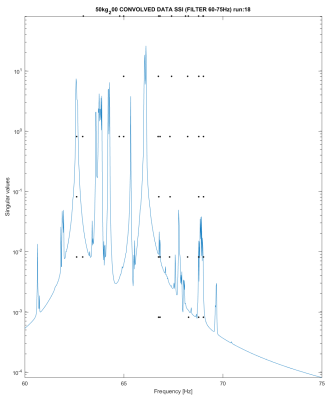
(b) 50kg FDD SSI output, run 17

Figure A2.50kg: Run 17



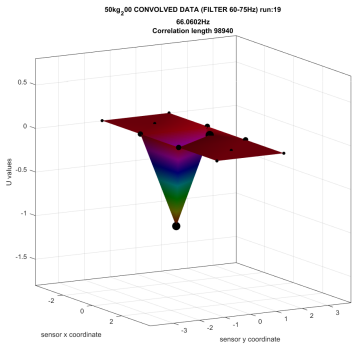
(a) 50kg mode shape, run 18



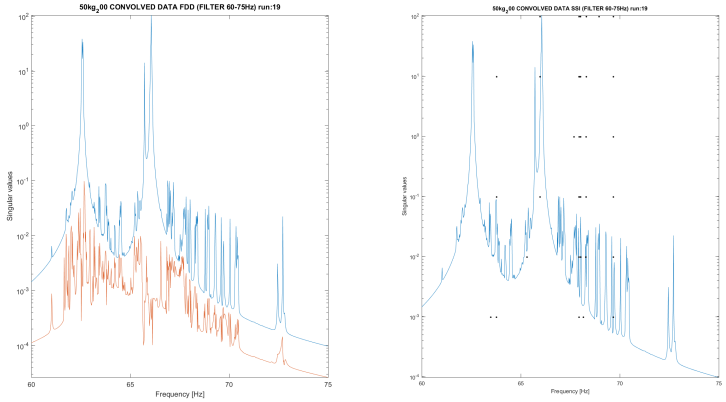


(b) 50kg FDD SSI output, run 18

Figure A2.50kg: Run 18

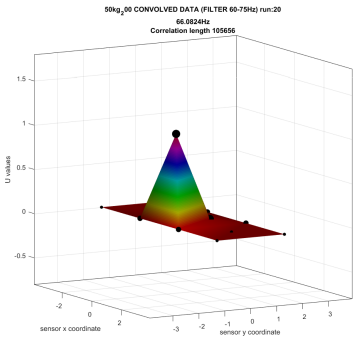


(a) 50kg mode shape, run 19

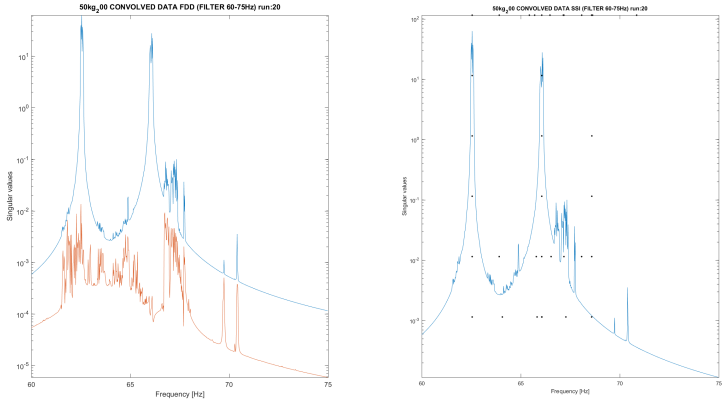


(b) 50kg FDD SSI output, run 19

Figure A2.50kg: Run 19

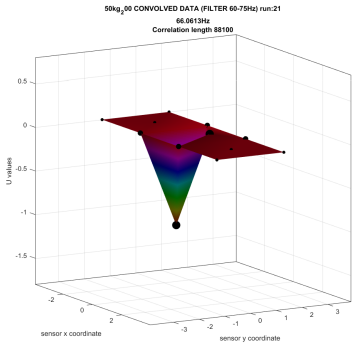


(a) 50kg mode shape, run 20

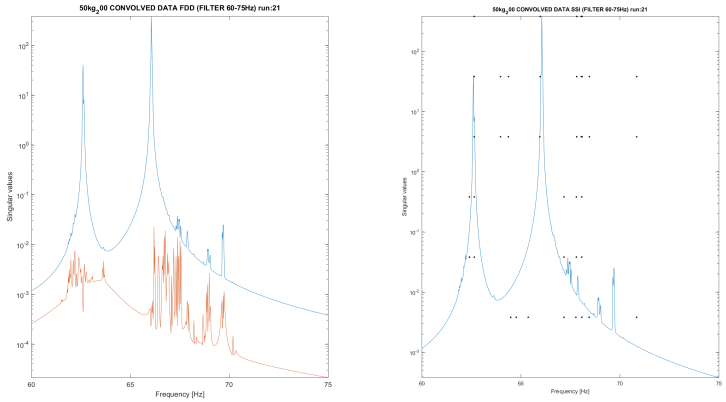


(b) 50kg FDD SSI output, run 20

Figure A2.50kg: Run 20

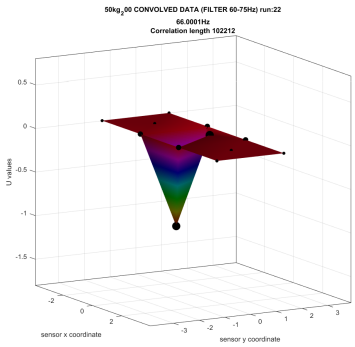


(a) 50kg mode shape, run 21

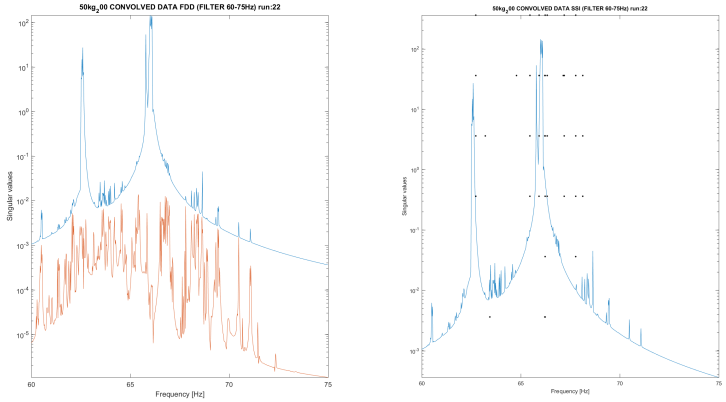


(b) 50kg FDD SSI output, run 21

Figure A2.50kg: Run 21

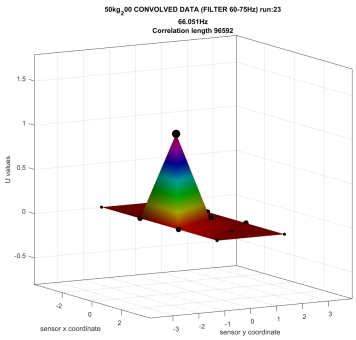


(a) 50kg mode shape, run 22

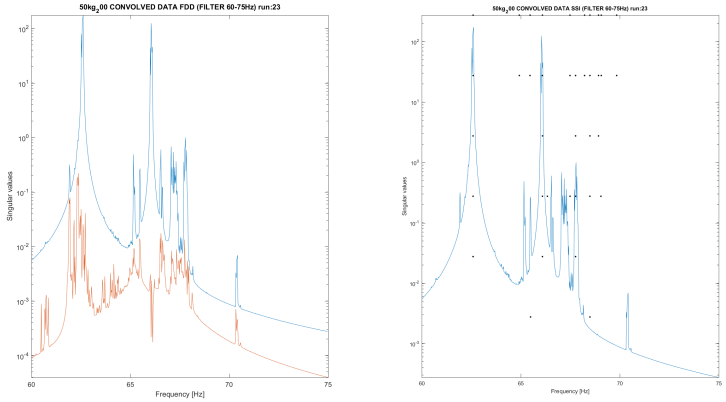


(b) 50kg FDD SSI output, run 22

Figure A2.50kg: Run 22

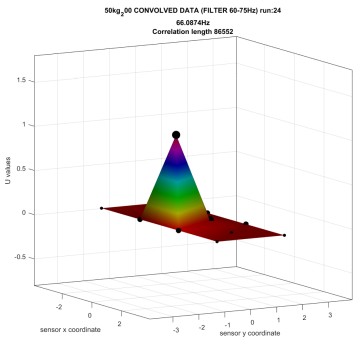


(a) 50kg mode shape, run 23

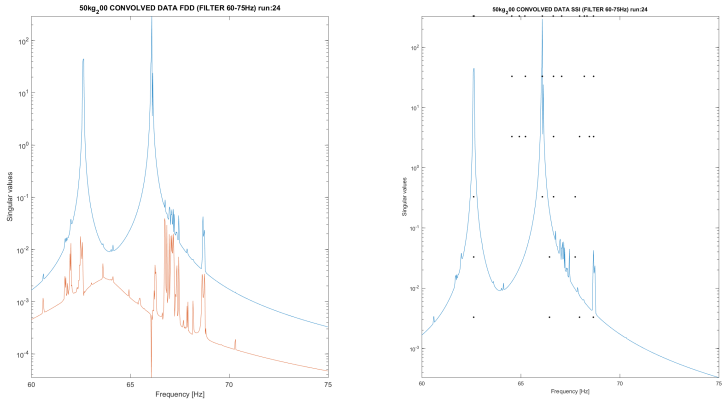


(b) 50kg FDD SSI output, run 23

Figure A2.50kg: Run 23

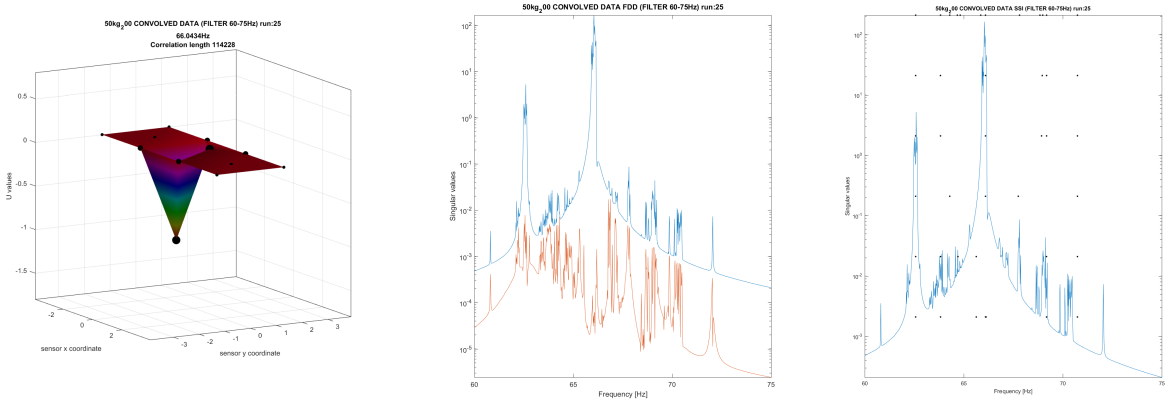


(a) 50kg mode shape, run 24



(b) 50kg FDD SSI output, run 24

Figure A2.50kg: Run 24

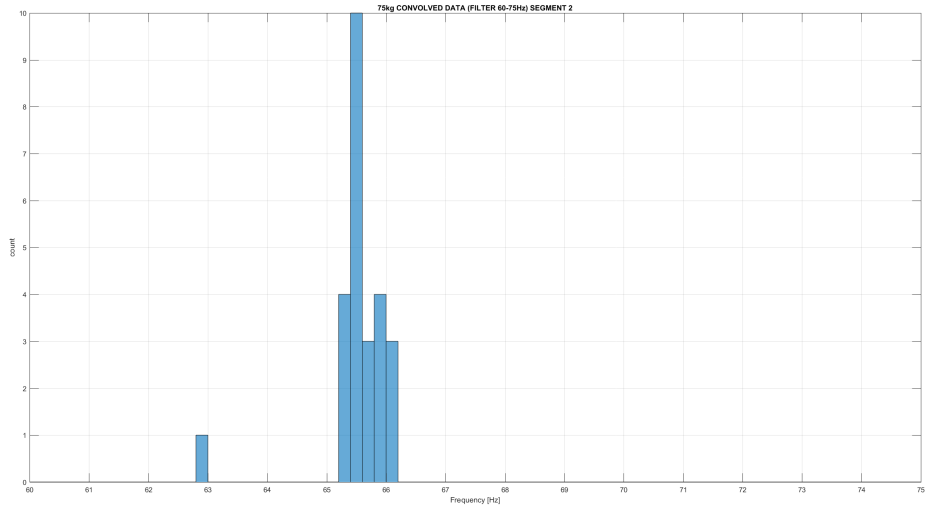


(a) 50kg mode shape, run 25

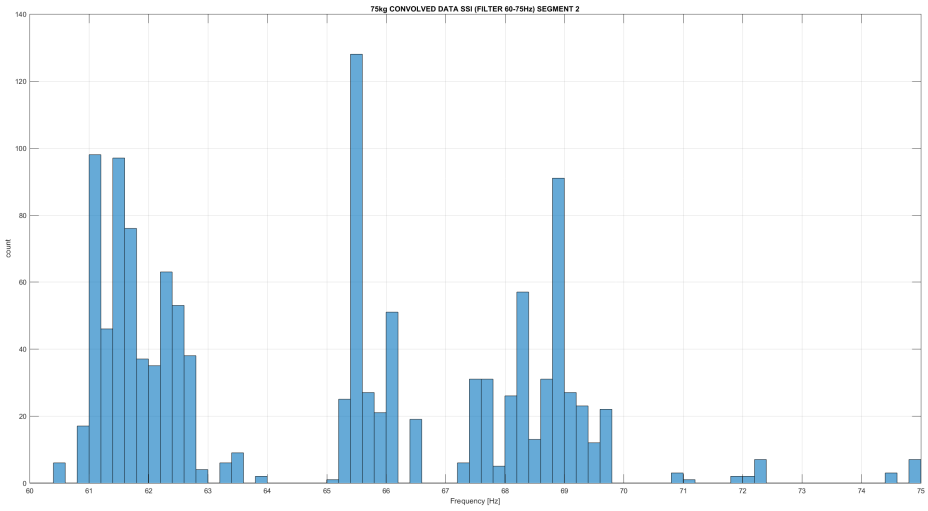
(b) 50kg FDD SSI output, run 25

Figure A2.50kg: Run 25

75kg data segment 2

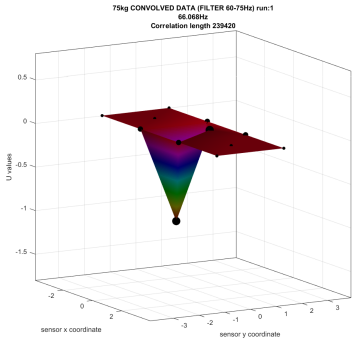


(a) 75kg FDD histogram

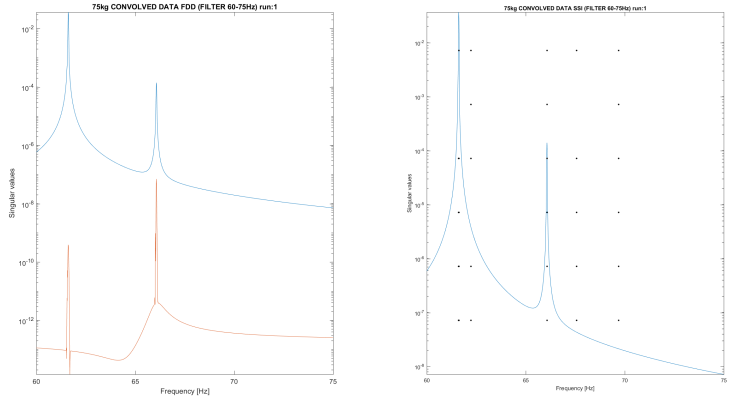


(b) 75kg SSI histogram

Figure A2.75kg: Histograms of identified modes, 75kg data

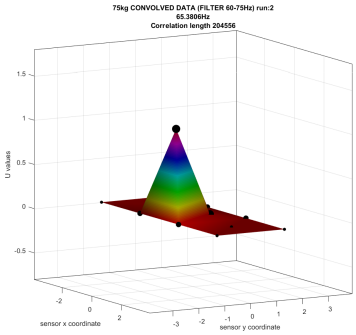


(a) 75kg mode shape, run 1

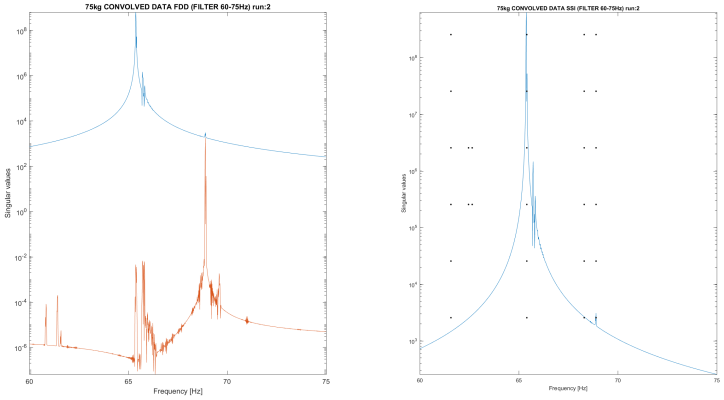


(b) 75kg FDD SSI output, run 1

Figure A2.75kg: Run 1

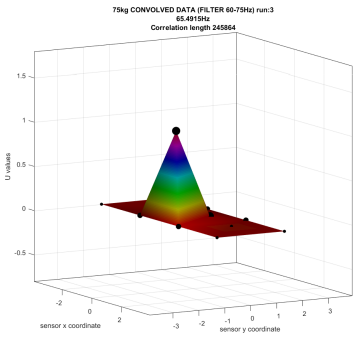


(a) 75kg mode shape, run 2

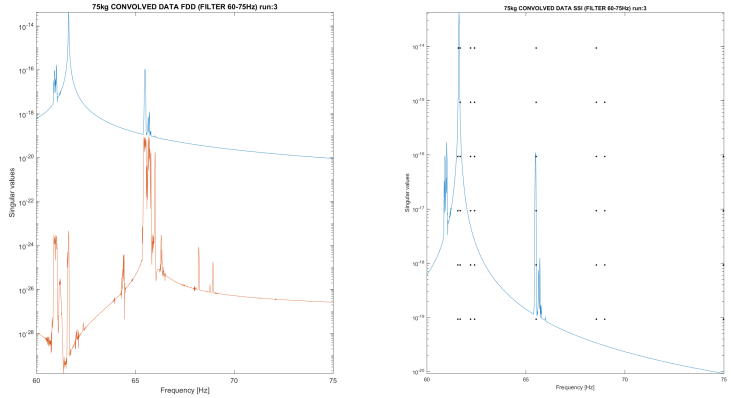


(b) 75kg FDD SSI output, run 2

Figure A2.75kg: Run 2

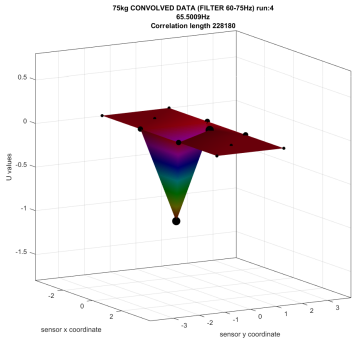


(a) 75kg mode shape, run 3

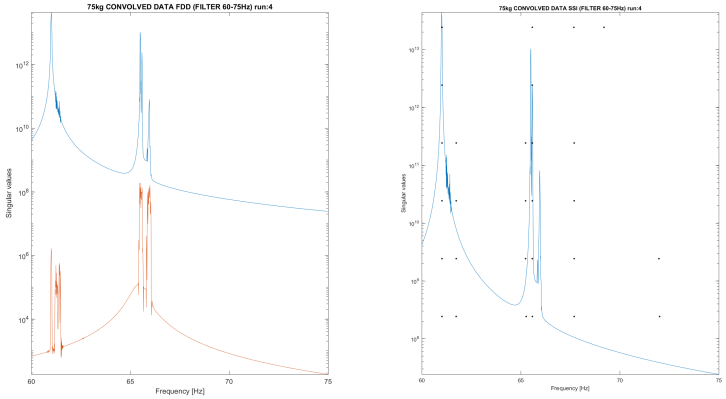


(b) 75kg FDD SSI output, run 3

Figure A2.75kg: Run 3

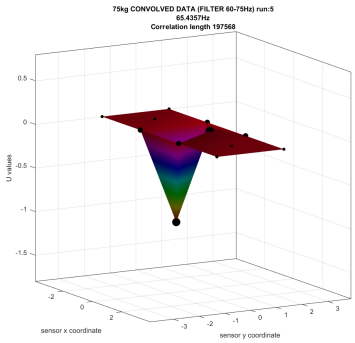


(a) 75kg mode shape, run 4

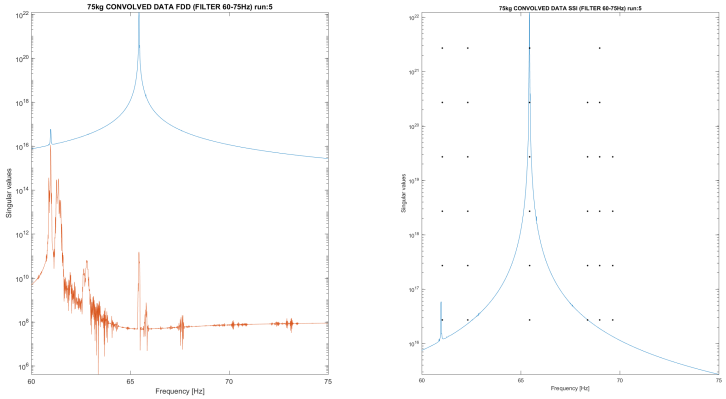


(b) 75kg FDD SSI output, run 4

Figure A2.75kg: Run 4

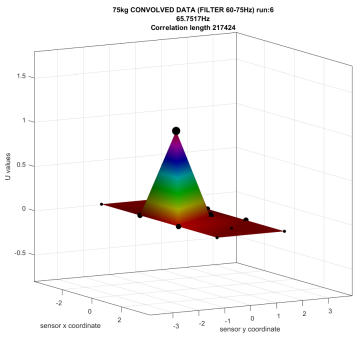


(a) 75kg mode shape, run 5

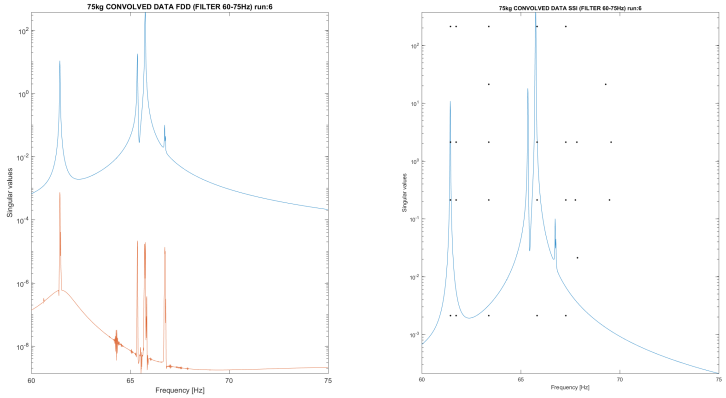


(b) 75kg FDD SSI output, run 5

Figure A2.75kg: Run 5

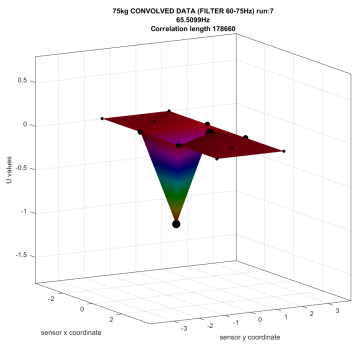


(a) 75kg mode shape, run 6

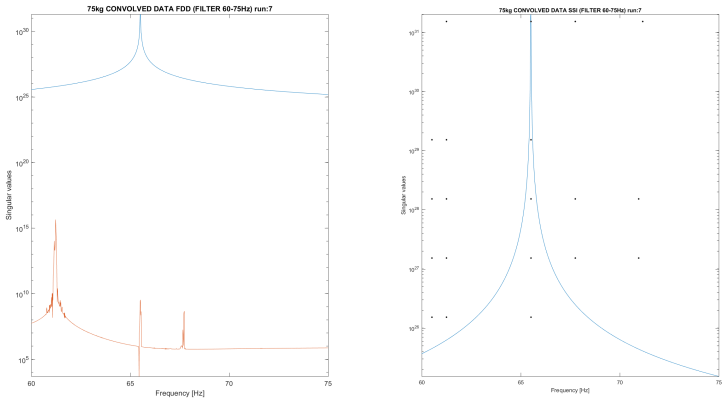


(b) 75kg FDD SSI output, run 6

Figure A2.75kg: Run 6

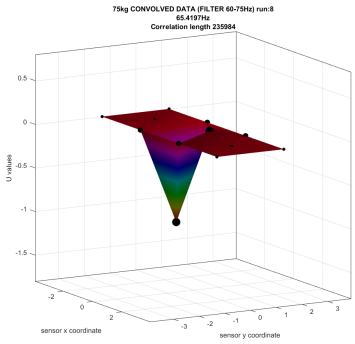


(a) 75kg mode shape, run 7

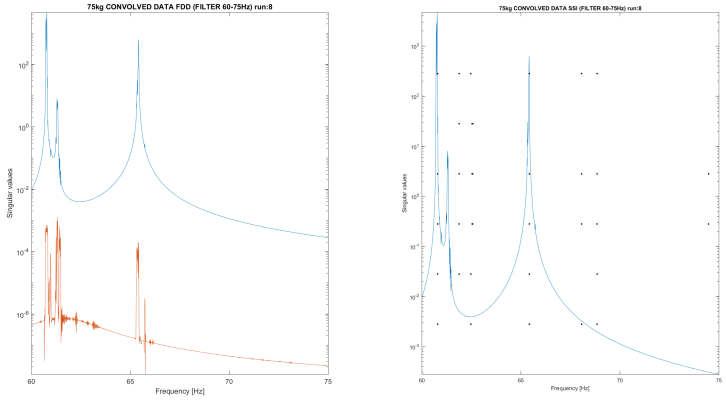


(b) 75kg FDD SSI output, run 7

Figure A2.75kg: Run 7

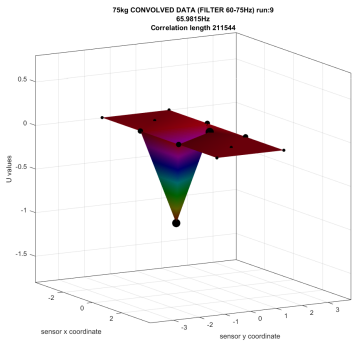


(a) 75kg mode shape, run 8

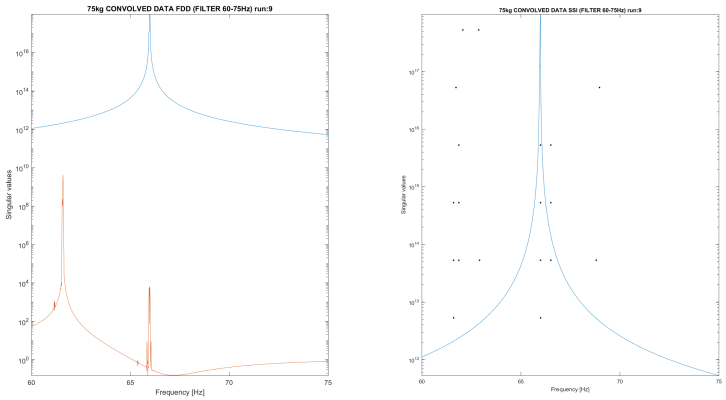


(b) 75kg FDD SSI output, run 8

Figure A2.75kg: Run 8

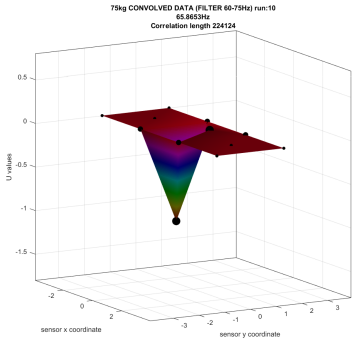


(a) 75kg mode shape, run 9

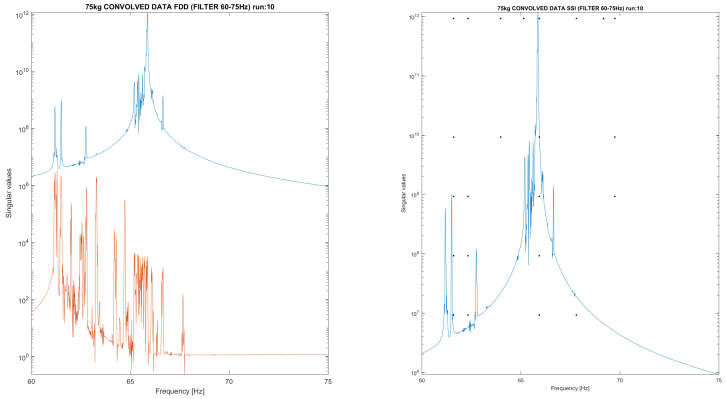


(b) 75kg FDD SSI output, run 9

Figure A2.75kg: Run 9

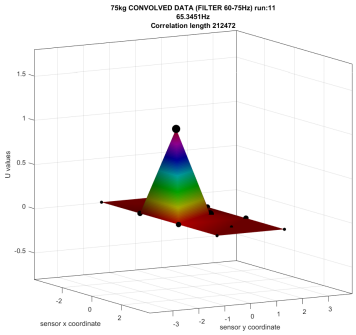


(a) 75kg mode shape, run 10

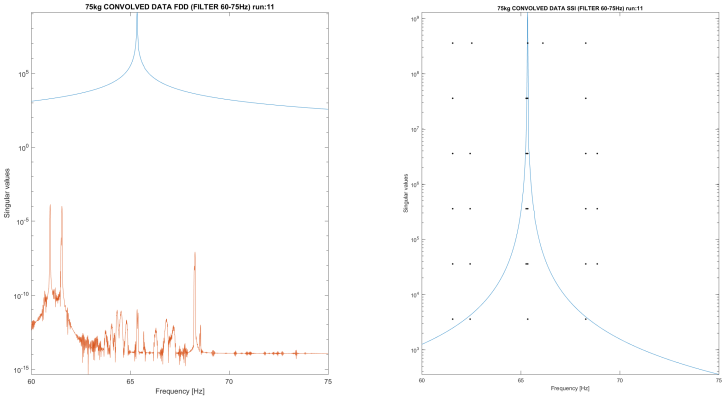


(b) 75kg FDD SSI output, run 10

Figure A2.75kg: Run 10

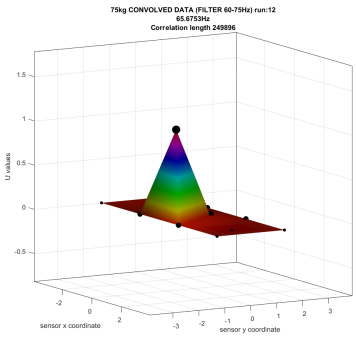


(a) 75kg mode shape, run 11

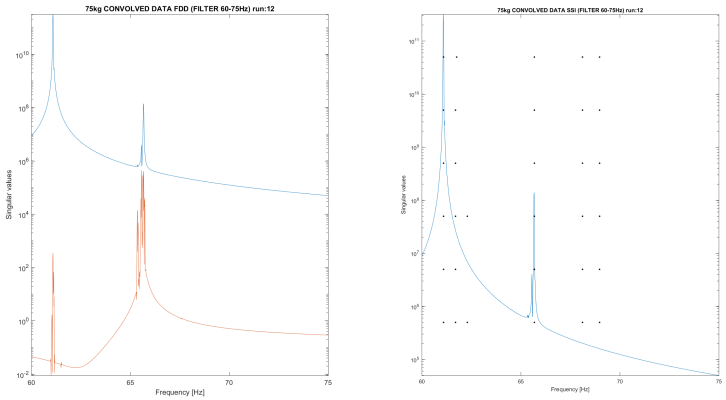


(b) 75kg FDD SSI output, run 11

Figure A2.75kg: Run 11

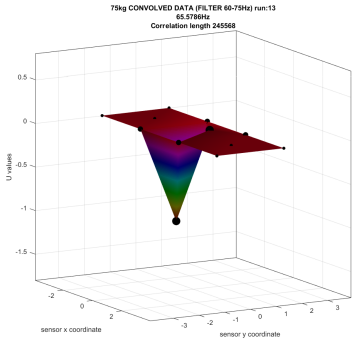


(a) 75kg mode shape, run 12

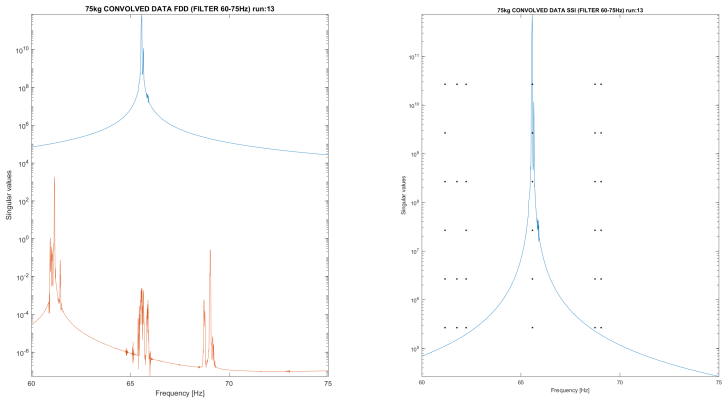


(b) 75kg FDD SSI output, run 12

Figure A2.75kg: Run 12

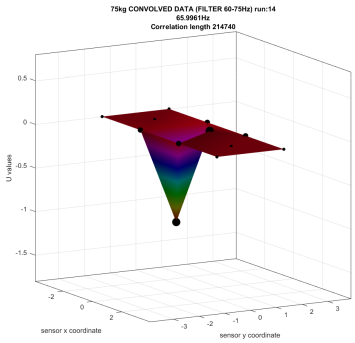


(a) 75kg mode shape, run 13

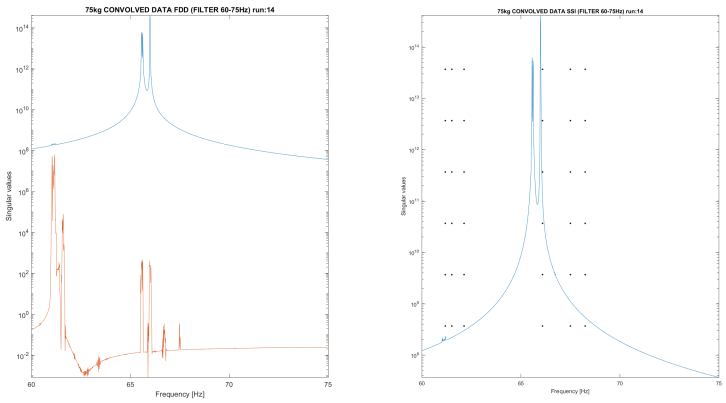


(b) 75kg FDD SSI output, run 13

Figure A2.75kg: Run 13

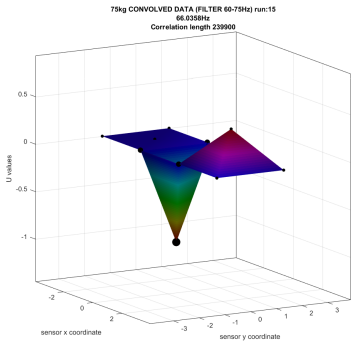


(a) 75kg mode shape, run 14

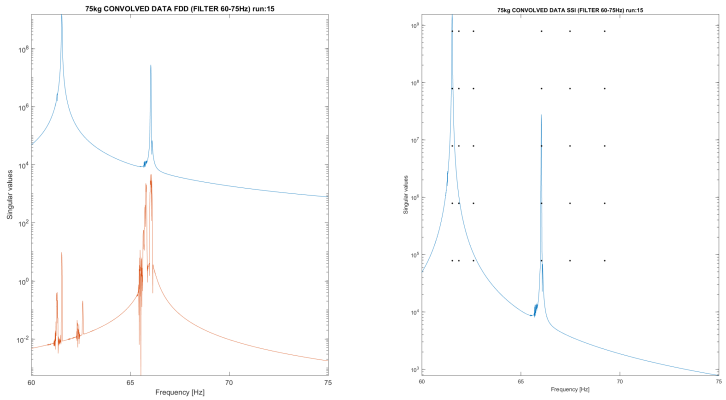


(b) 75kg FDD SSI output, run 14

Figure A2.75kg: Run 14

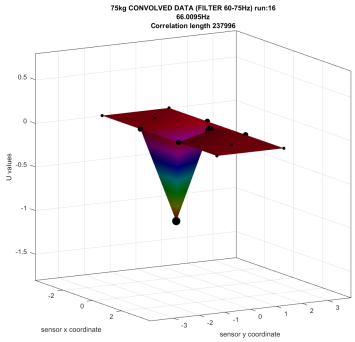


(a) 75kg mode shape, run 15

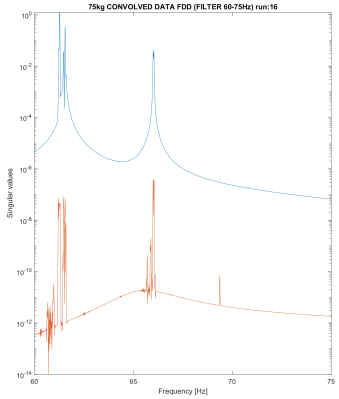


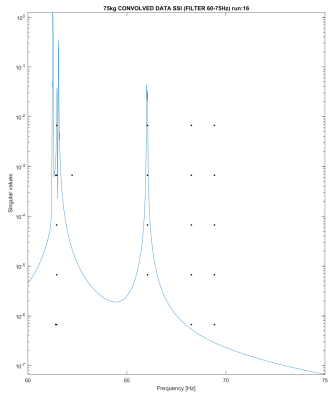
(b) 75kg FDD SSI output, run 15

Figure A2.75kg: Run 15



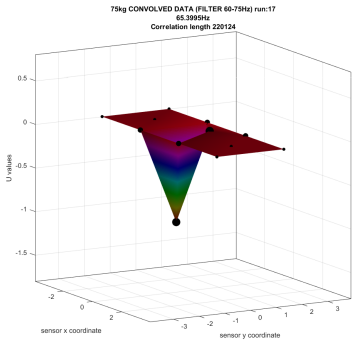
(a) 75kg mode shape, run 16



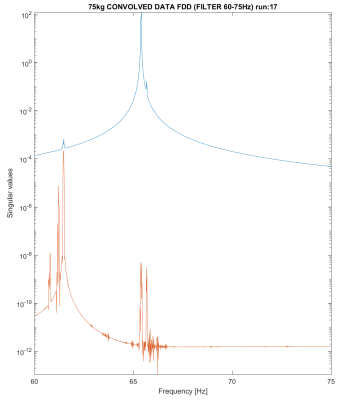


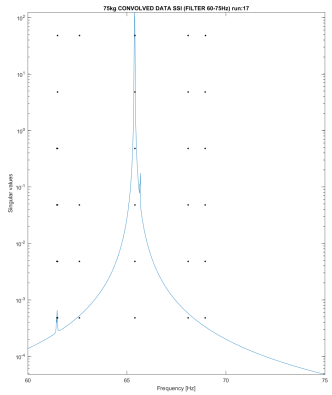
(b) 75kg FDD SSI output, run 16

Figure A2.75kg: Run 16



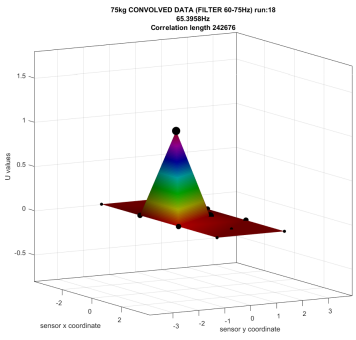
(a) 75kg mode shape, run 17



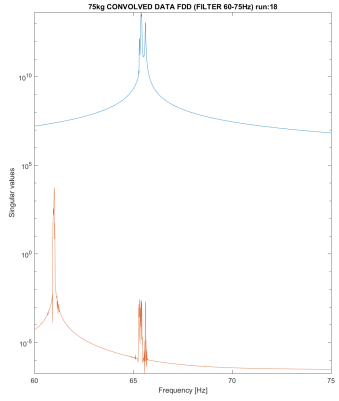


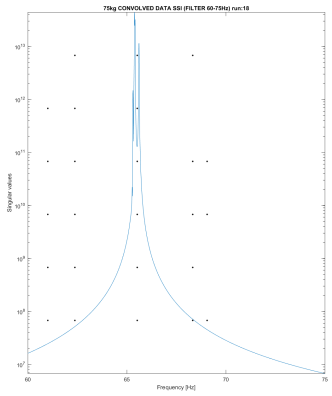
(b) 75kg FDD SSI output, run 17

Figure A2.75kg: Run 17



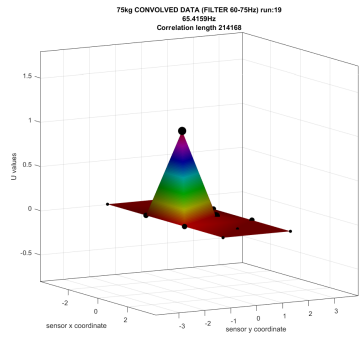
(a) 75kg mode shape, run 18



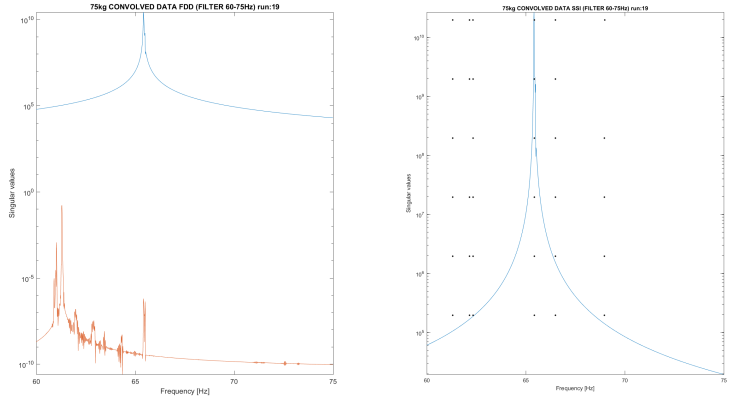


(b) 75kg FDD SSI output, run 18

Figure A2.75kg: Run 18

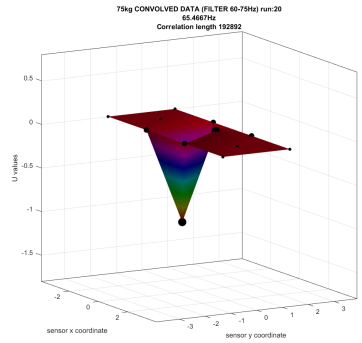


(a) 75kg mode shape, run 19

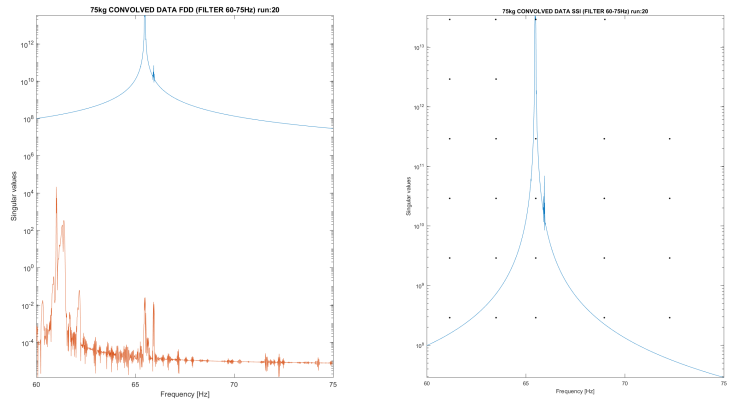


(b) 75kg FDD SSI output, run 19

Figure A2.75kg: Run 19

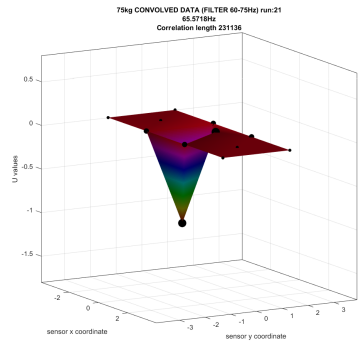


(a) 75kg mode shape, run 20

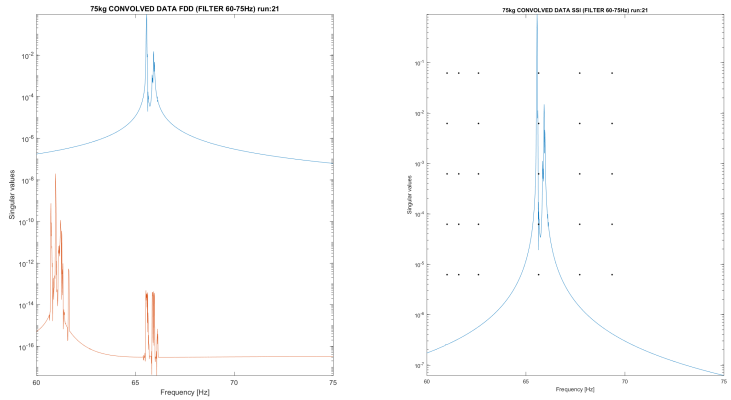


(b) 75kg FDD SSI output, run 20

Figure A2.75kg: Run 20

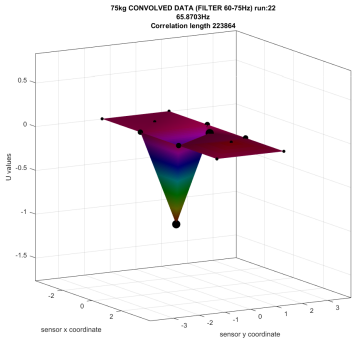


(a) 75kg mode shape, run 21

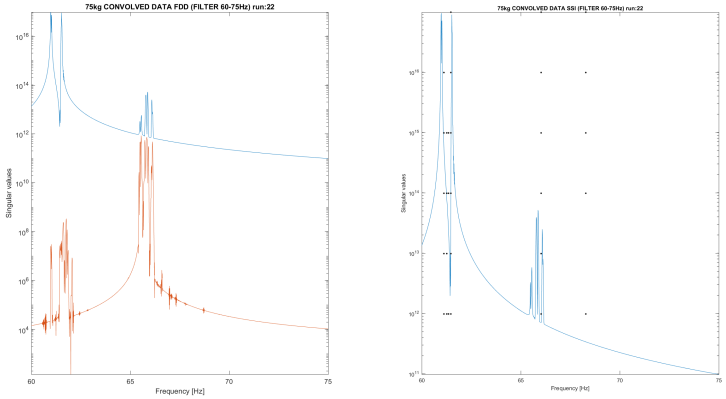


(b) 75kg FDD SSI output, run 21

Figure A2.75kg: Run 21

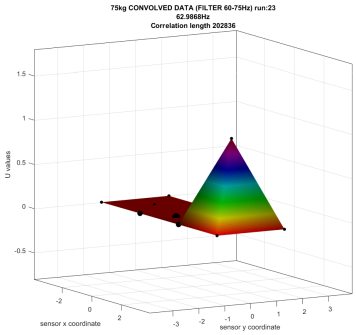


(a) 75kg mode shape, run 22

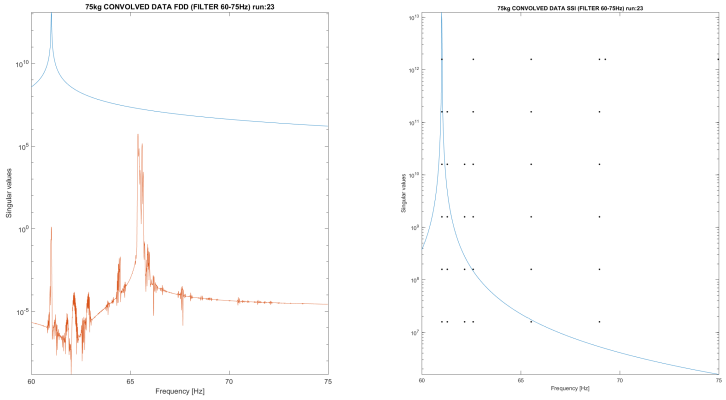


(b) 75kg FDD SSI output, run 22

Figure A2.75kg: Run 22

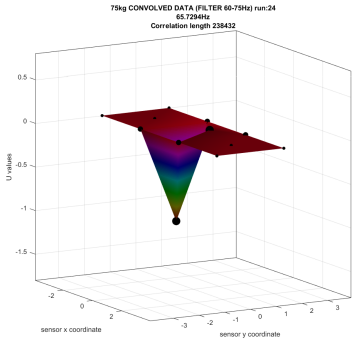


(a) 75kg mode shape, run 23

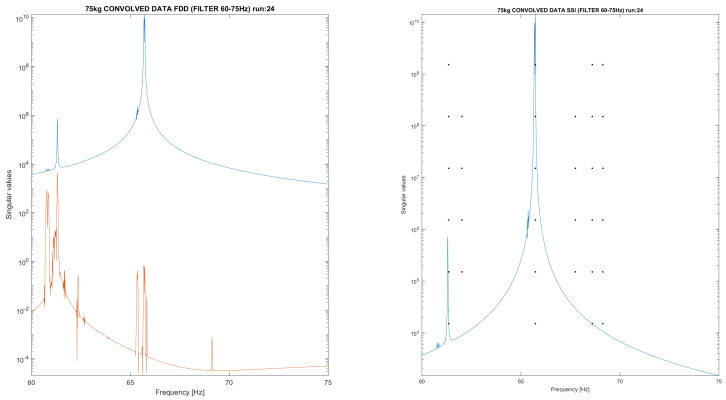


(b) 75kg FDD SSI output, run 23

Figure A2.75kg: Run 23

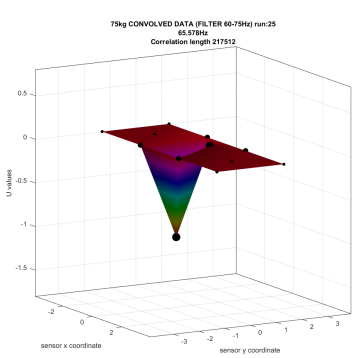


(a) 75kg mode shape, run 24

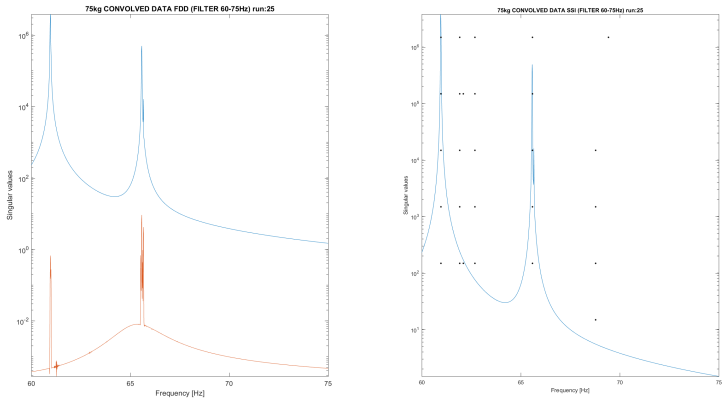


(b) 75kg FDD SSI output, run 24

Figure A2.75kg: Run 24



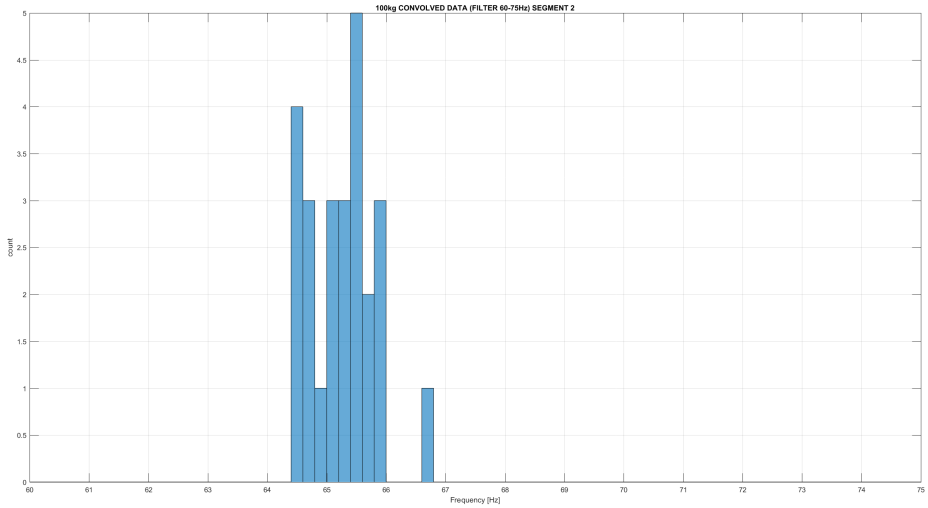
(a) 75kg mode shape, run 25



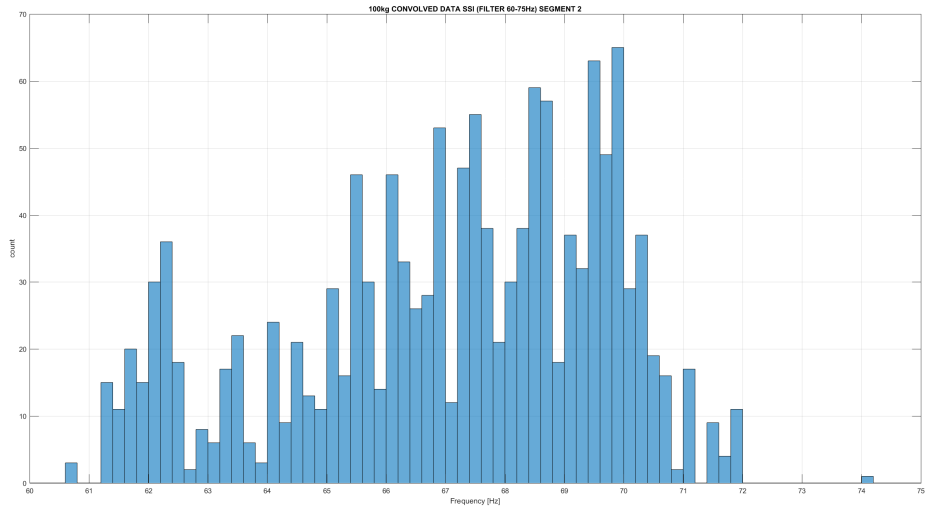
(b) 75kg FDD SSI output, run 25

Figure A2.75kg: Run 25

100kg data segment 2

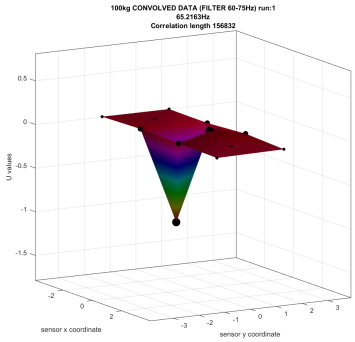


(a) 100kg FDD histogram

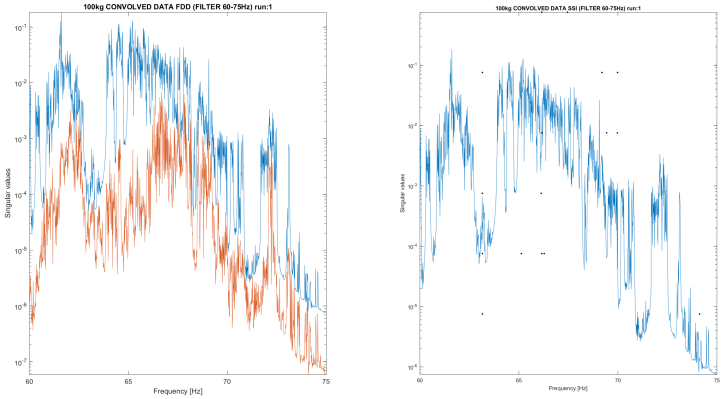


(b) 100kg SSI histogram

Figure A2.100kg: Histograms of identified modes, 100kg data

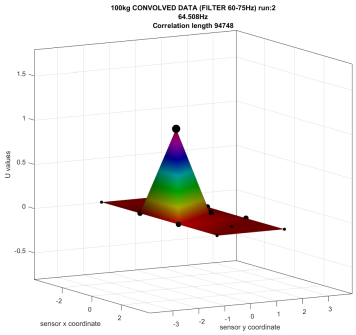


(a) 100kg mode shape, run 1

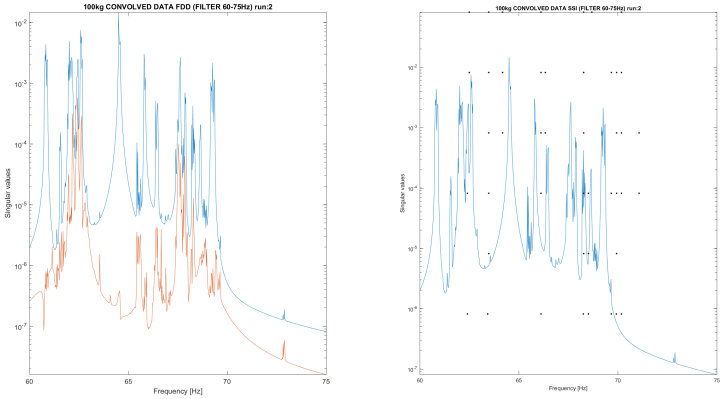


(b) 100kg FDD SSI output, run 1

Figure A2.100kg: Run 1

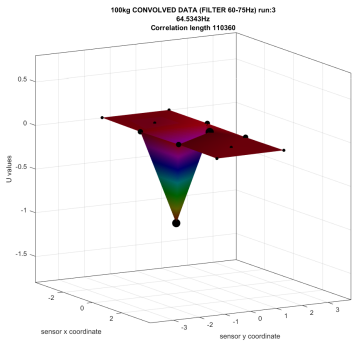


(a) 100kg mode shape, run 2

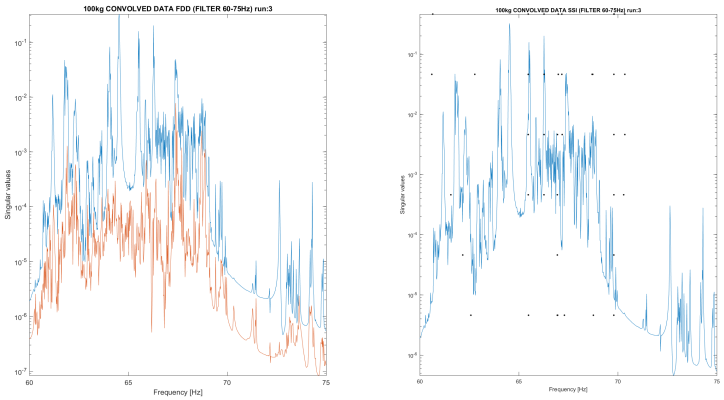


(b) 100kg FDD SSI output, run 2

Figure A2.100kg: Run 2

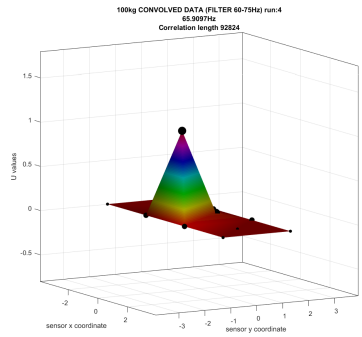


(a) 100kg mode shape, run 3

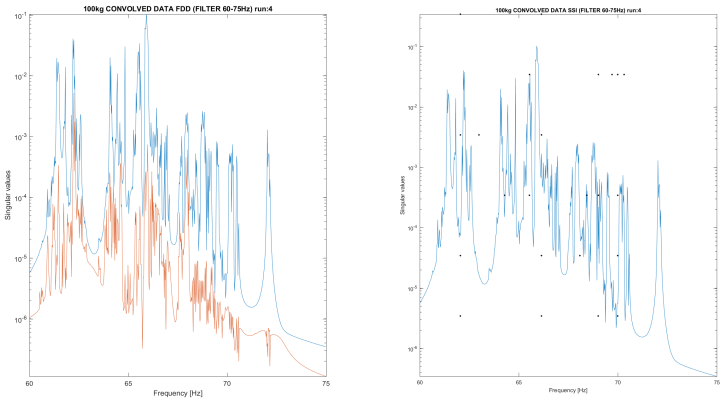


(b) 100kg FDD SSI output, run 3

Figure A2.100kg: Run 3

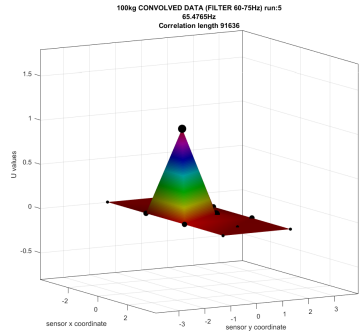


(a) 100kg mode shape, run 4

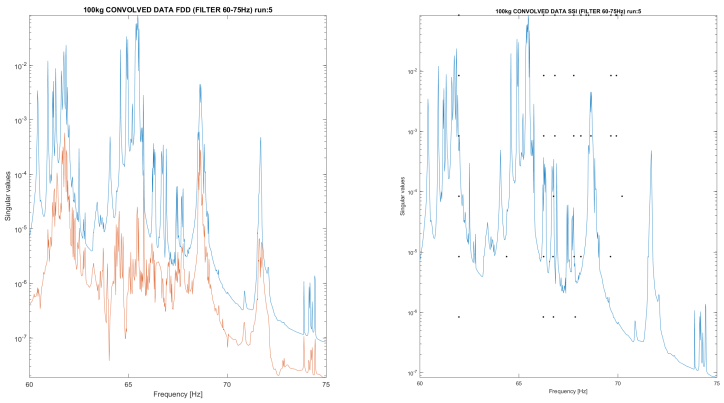


(b) 100kg FDD SSI output, run 4

Figure A2.100kg: Run 4

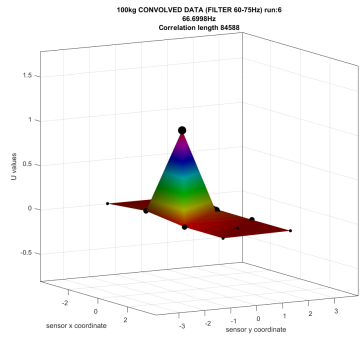


(a) 100kg mode shape, run 5

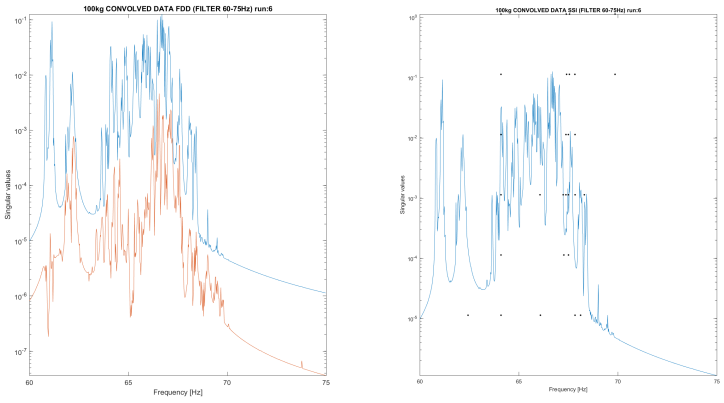


(b) 100kg FDD SSI output, run 5

Figure A2.100kg: Run 5

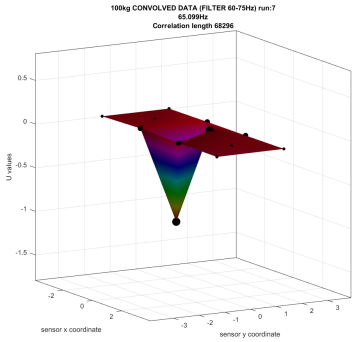


(a) 100kg mode shape, run 6

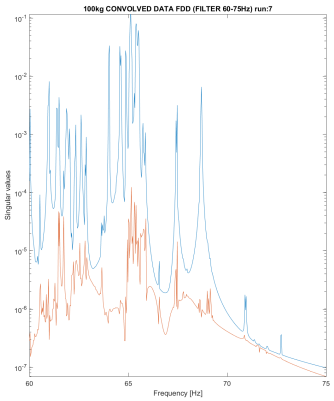


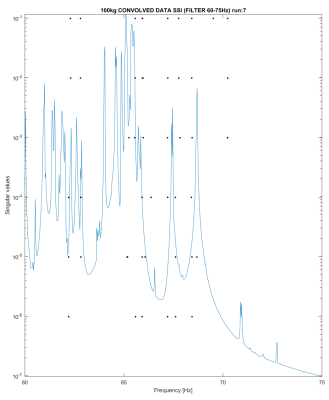
(b) 100kg FDD SSI output, run 6

Figure A2.100kg: Run 6



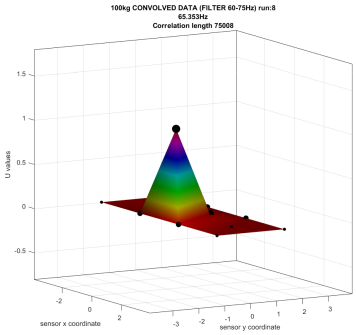
(a) 100kg mode shape, run 7



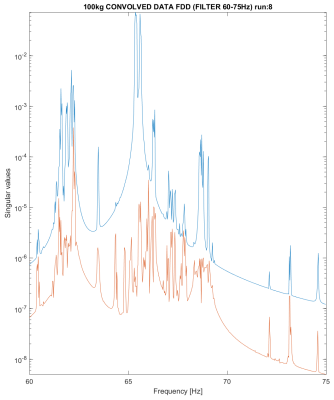


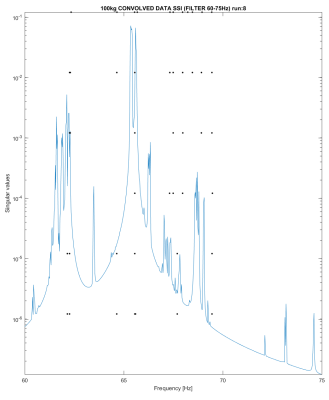
(b) 100kg FDD SSI output, run 7

Figure A2.100kg: Run 7



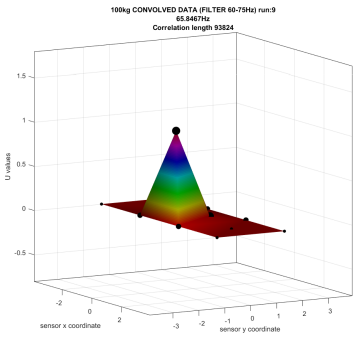
(a) 100kg mode shape, run 8



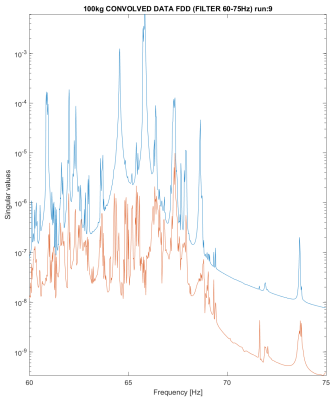


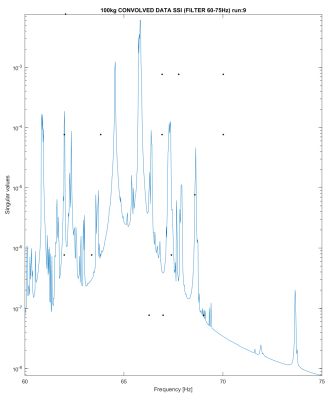
(b) 100kg FDD SSI output, run 8

Figure A2.100kg: Run 8



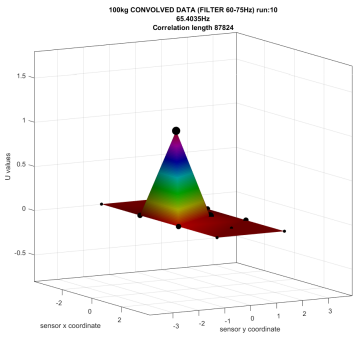
(a) 100kg mode shape, run 9



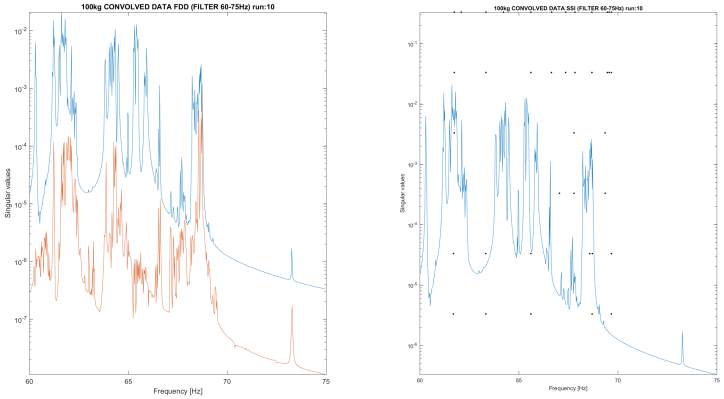


(b) 100kg FDD SSI output, run 9

Figure A2.100kg: Run 9

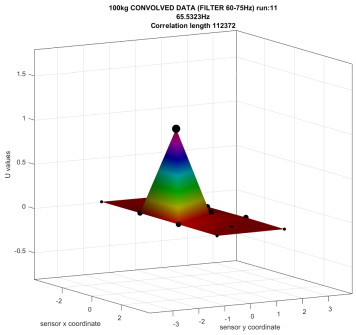


(a) 100kg mode shape, run 10

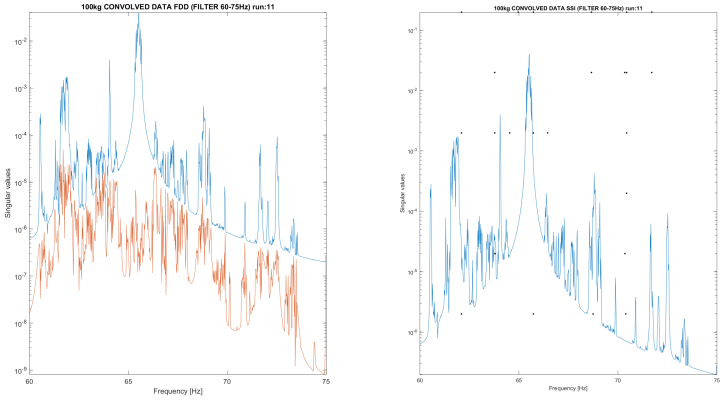


(b) 100kg FDD SSI output, run 10

Figure A2.100kg: Run 10

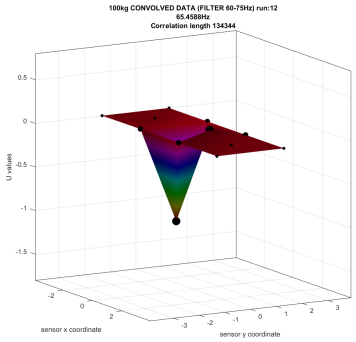


(a) 100kg mode shape, run 11

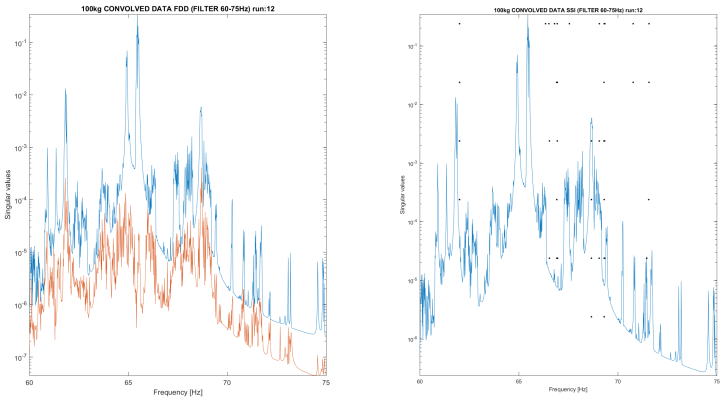


(b) 100kg FDD SSI output, run 11

Figure A2.100kg: Run 11

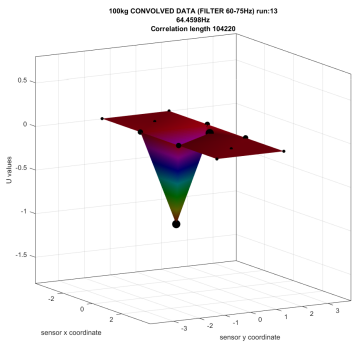


(a) 100kg mode shape, run 12

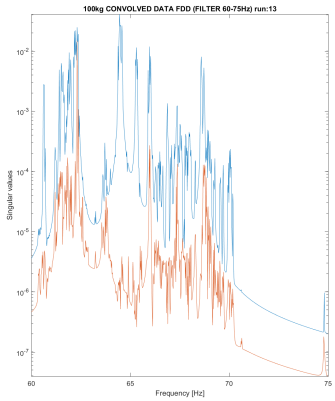


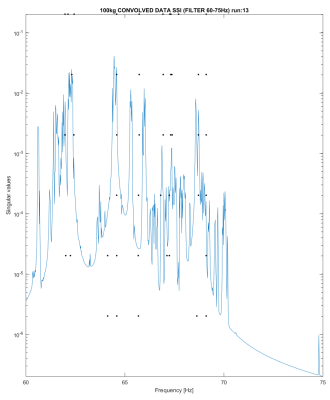
(b) 100kg FDD SSI output, run 12

Figure A2.100kg: Run 12



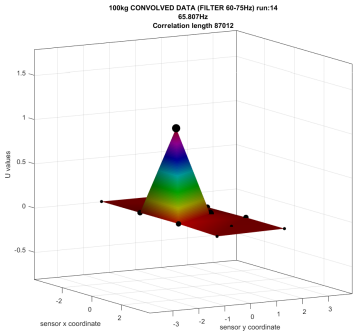
(a) 100kg mode shape, run 13



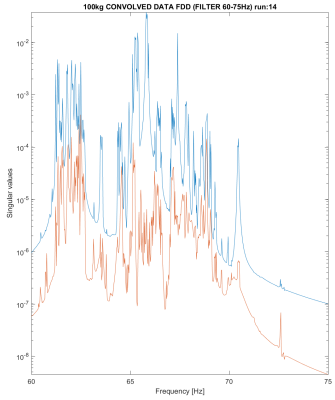


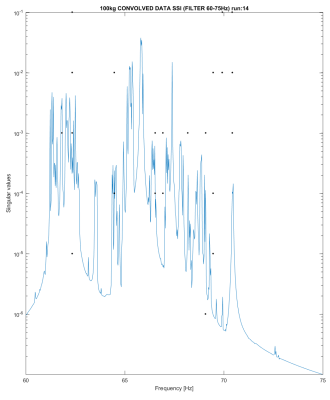
(b) 100kg FDD SSI output, run 13

Figure A2.100kg: Run 13



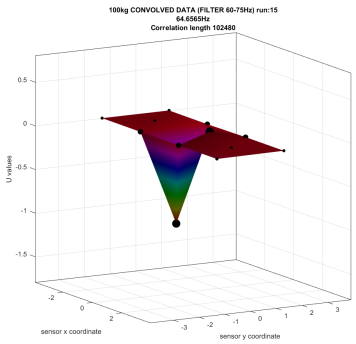
(a) 100kg mode shape, run 14



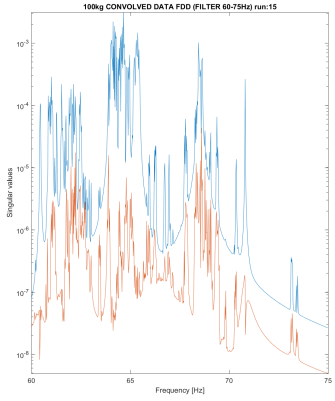


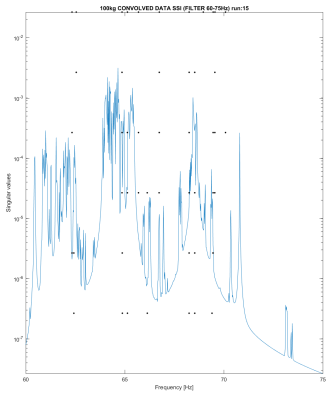
(b) 100kg FDD SSI output, run 14

Figure A2.100kg: Run 14



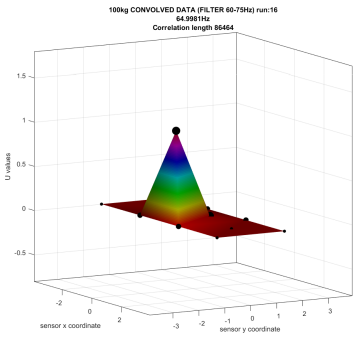
(a) 100kg mode shape, run 15



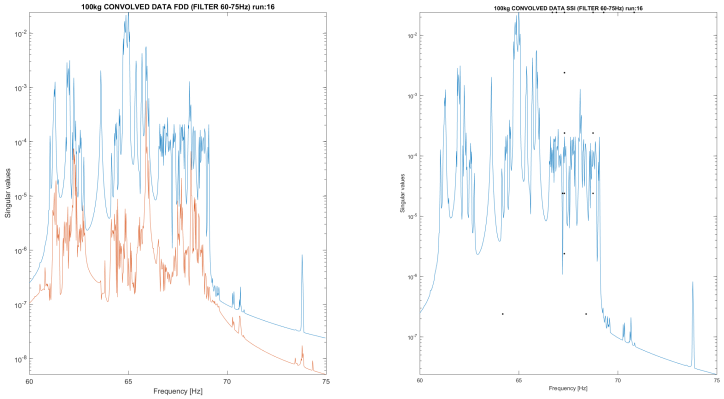


(b) 100kg FDD SSI output, run 15

Figure A2.100kg: Run 15

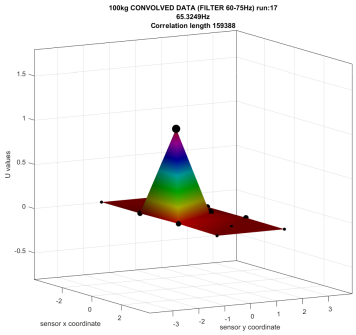


(a) 100kg mode shape, run 16

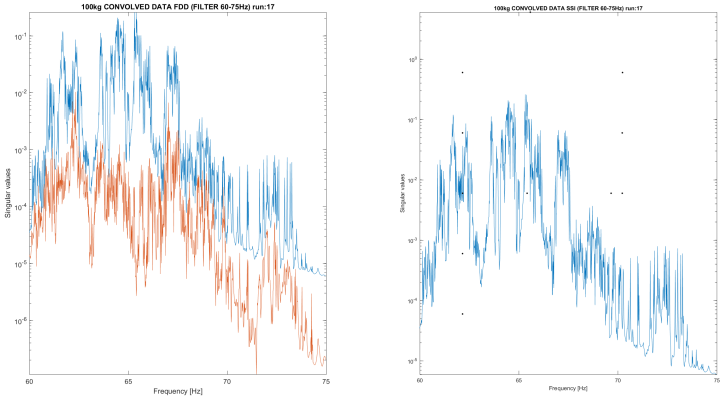


(b) 100kg FDD SSI output, run 16

Figure A2.100kg: Run 16

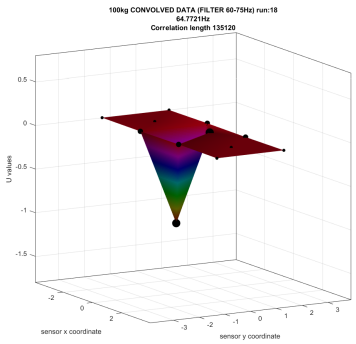


(a) 100kg mode shape, run 17

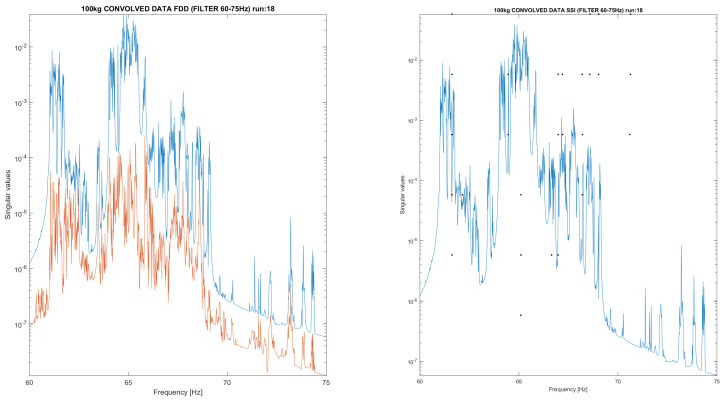


(b) 100kg FDD SSI output, run 17

Figure A2.100kg: Run 17

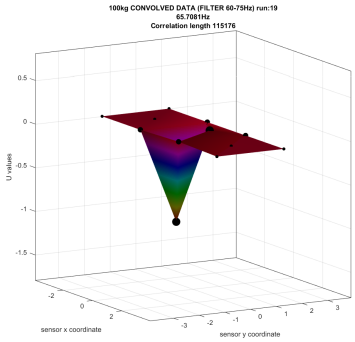


(a) 100kg mode shape, run 18

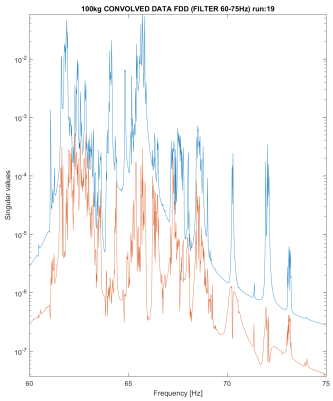


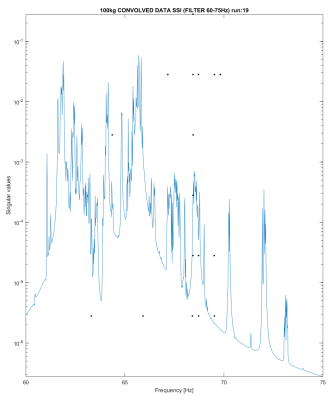
(b) 100kg FDD SSI output, run 18

Figure A2.100kg: Run 18



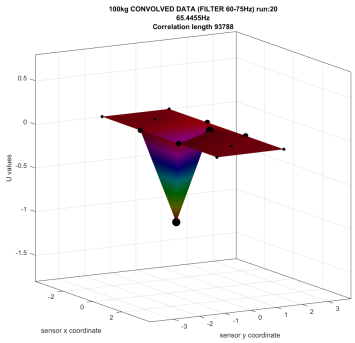
(a) 100kg mode shape, run 19



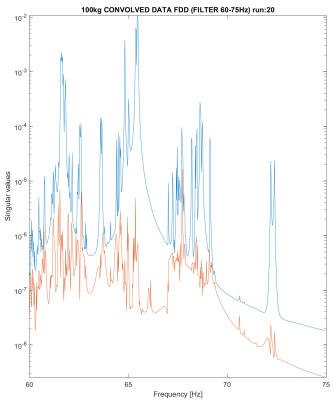


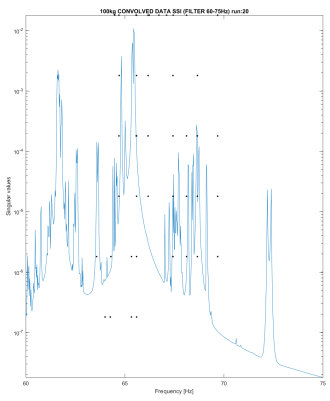
(b) 100kg FDD SSI output, run 19

Figure A2.100kg: Run 19



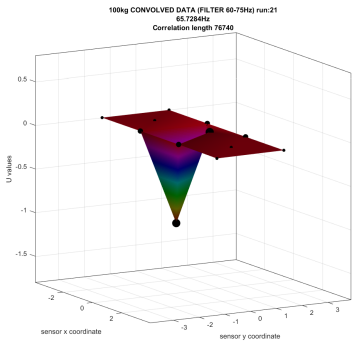
(a) 100kg mode shape, run 20



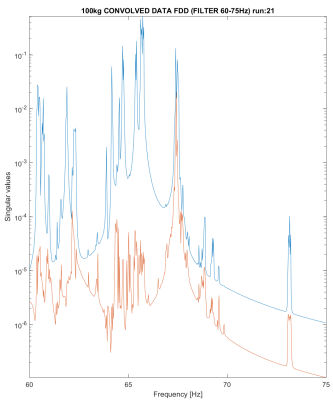


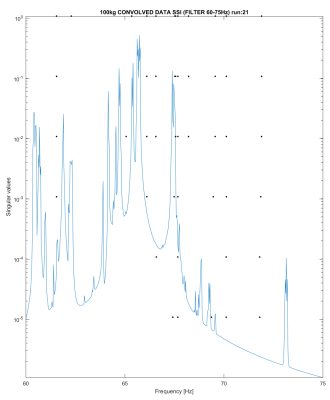
(b) 100kg FDD SSI output, run 20

Figure A2.100kg: Run 20



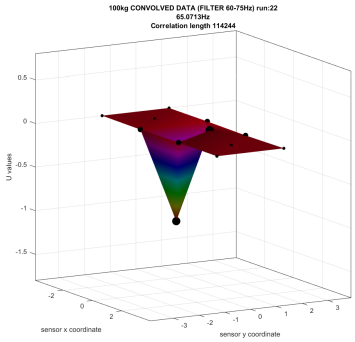
(a) 100kg mode shape, run 21



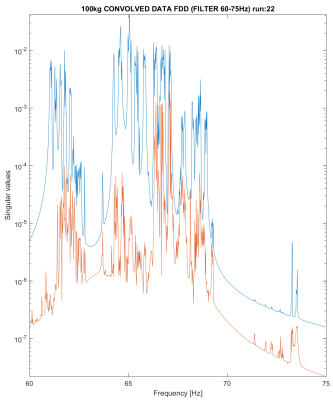


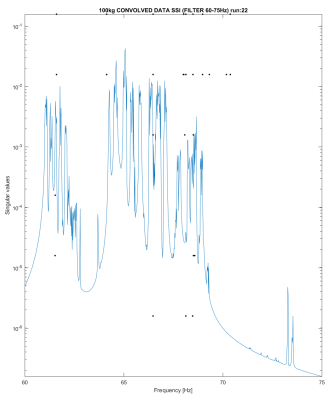
(b) 100kg FDD SSI output, run 21

Figure A2.100kg: Run 21



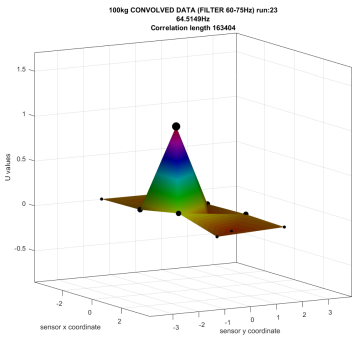
(a) 100kg mode shape, run 22



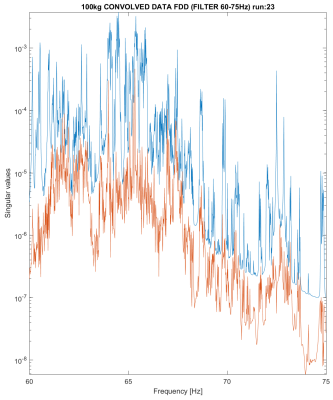


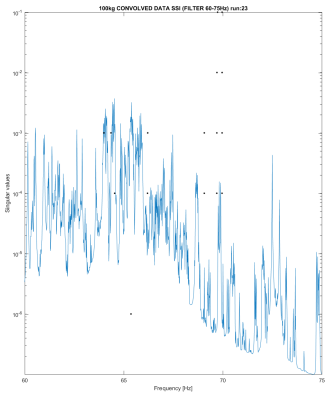
(b) 100kg FDD SSI output, run 22

Figure A2.100kg: Run 22



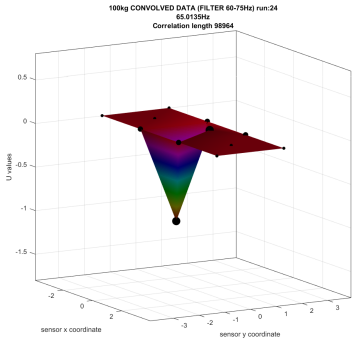
(a) 100kg mode shape, run 23



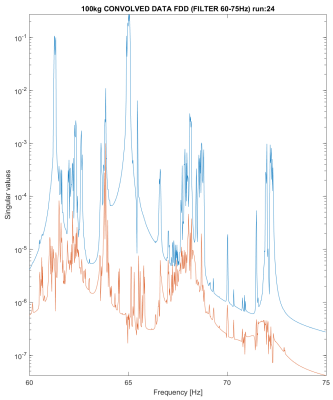


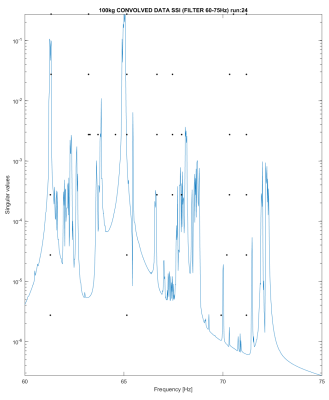
(b) 100kg FDD SSI output, run 23

Figure A2.100kg: Run 23



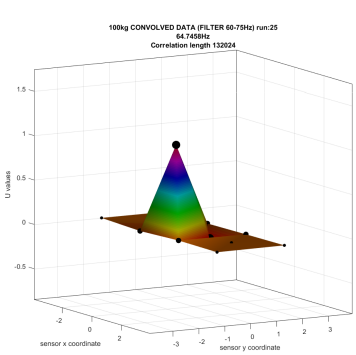
(a) 100kg mode shape, run 24



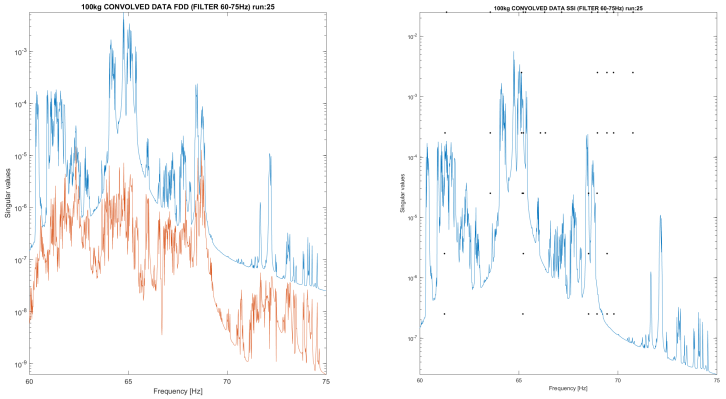


(b) 100kg FDD SSI output, run 24

Figure A2.100kg: Run 24



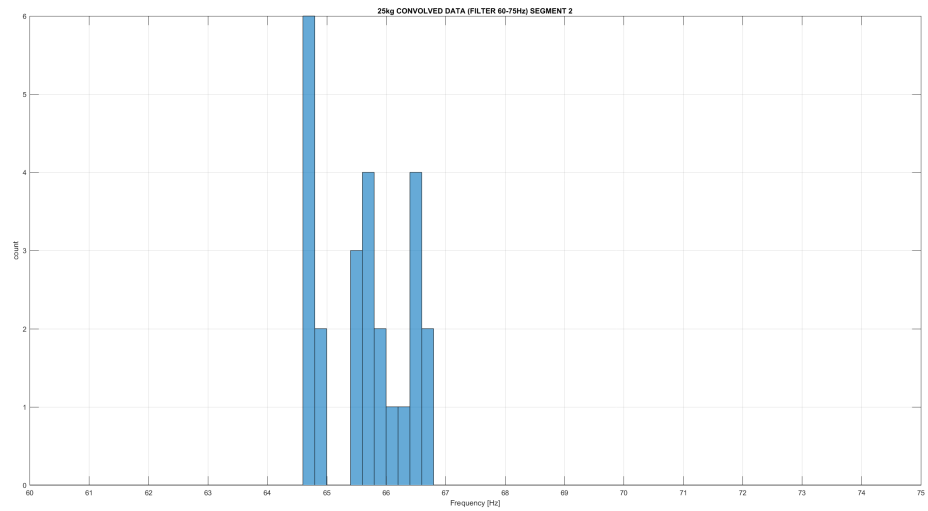
(a) 100kg mode shape, run 25



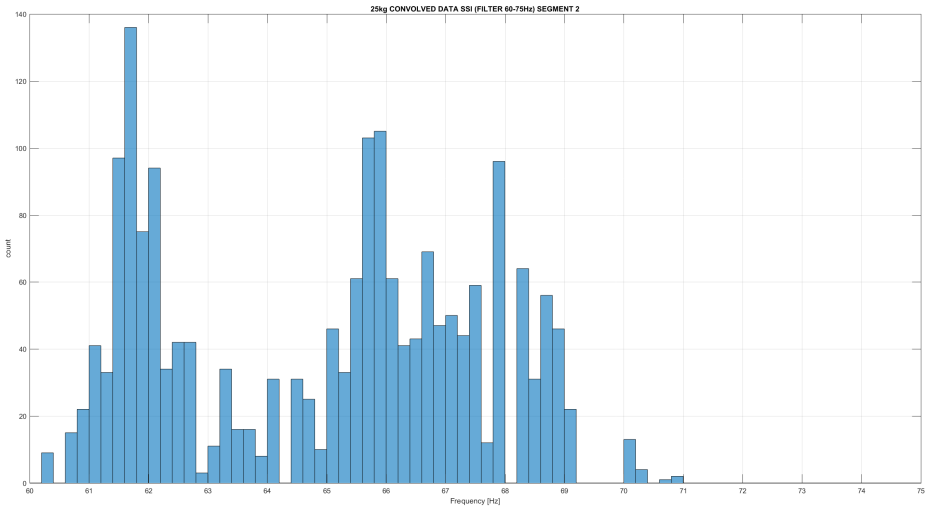
(b) 100kg FDD SSI output, run 25

Figure A2.100kg: Run 25

Data (28.03.2017) 25kg-50kg segment 2 (Reduced order PF)

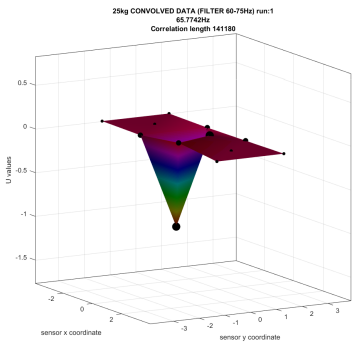


(a) 25kg FDD histogram

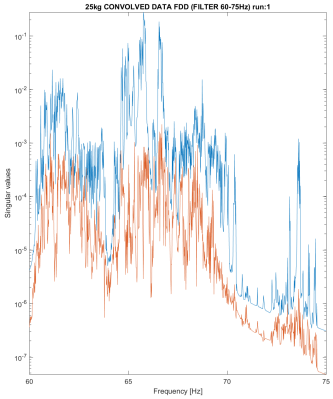


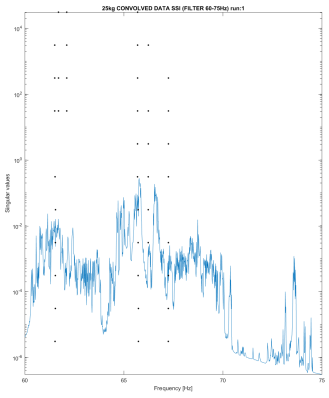
(b) 25kg SSI histogram

Figure A2.25kg: Histograms of identified modes, 25kg data



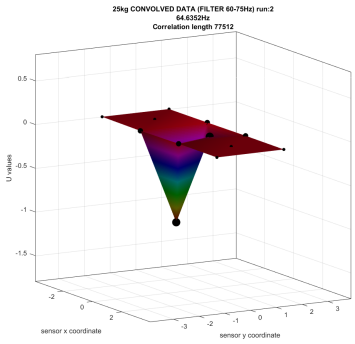
(a) 25kg mode shape, run 1



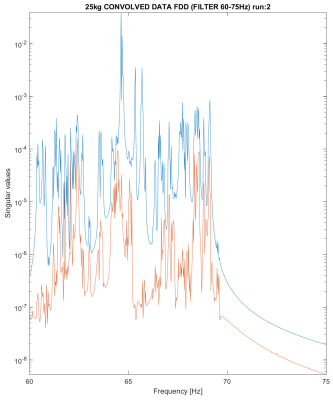


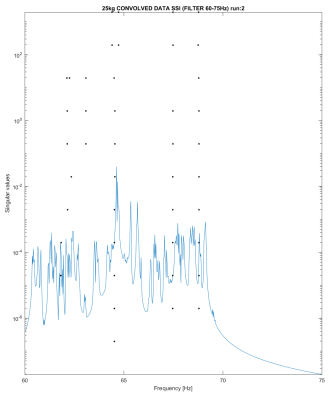
(b) 25kg FDD SSI output, run 1

Figure A2.25kg: Run 1



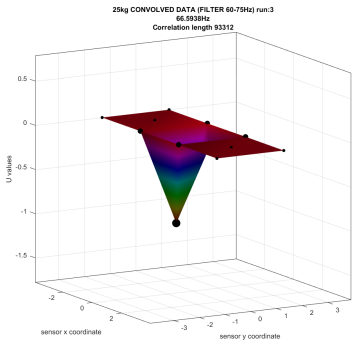
(a) 25kg mode shape, run 2



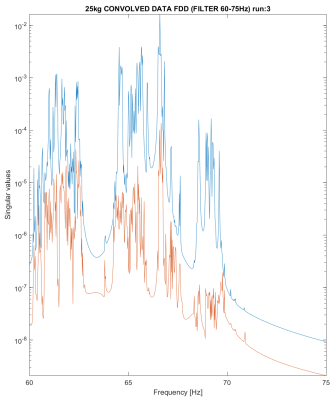


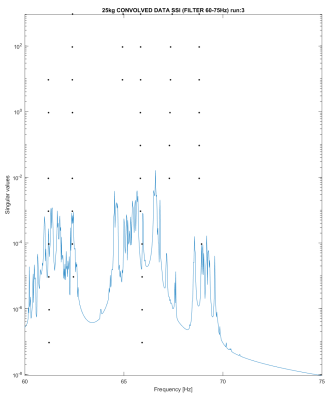
(b) 25kg FDD SSI output, run 2

Figure A2.25kg: Run 2



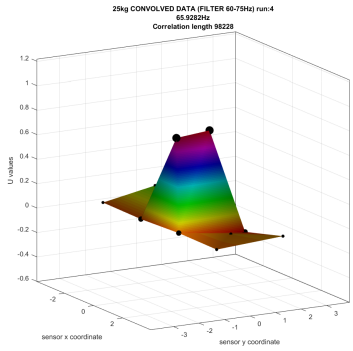
(a) 25kg mode shape, run 3



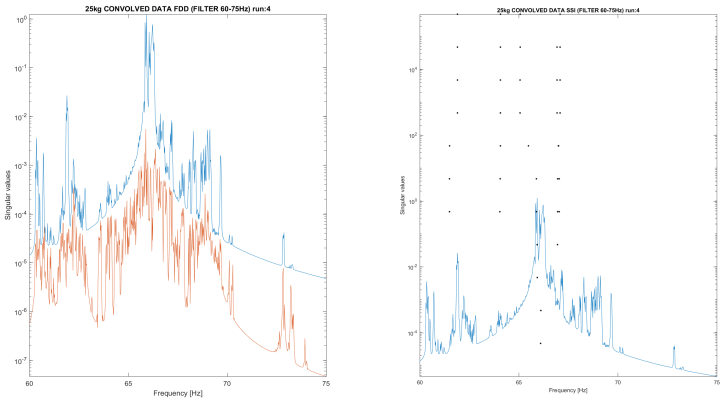


(b) 25kg FDD SSI output, run 3

Figure A2.25kg: Run 3

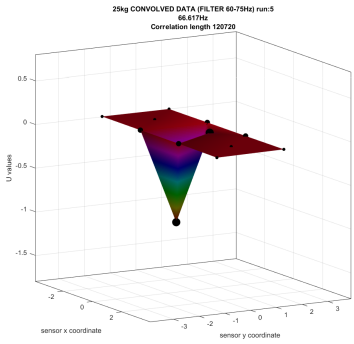


(a) 25kg mode shape, run 4

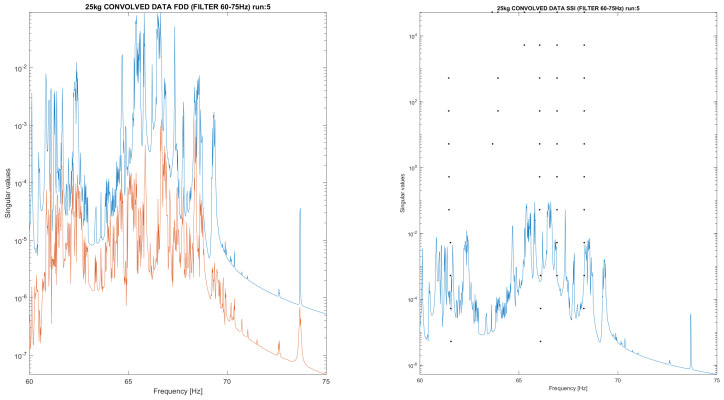


(b) 25kg FDD SSI output, run 4

Figure A2.25kg: Run 4

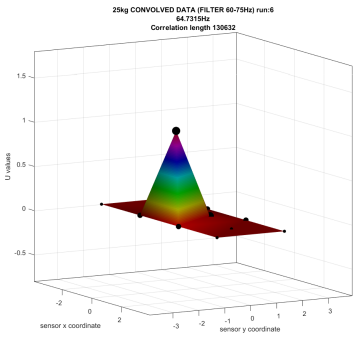


(a) 25kg mode shape, run 5

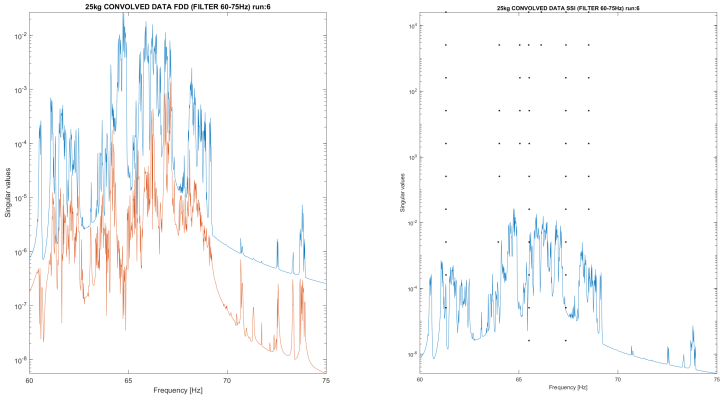


(b) 25kg FDD SSI output, run 5

Figure A2.25kg: Run 5

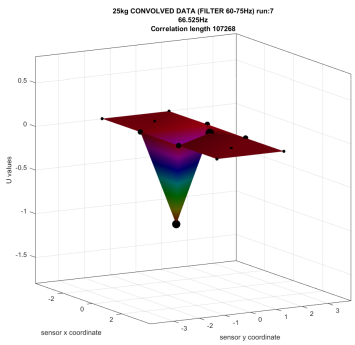


(a) 25kg mode shape, run 6

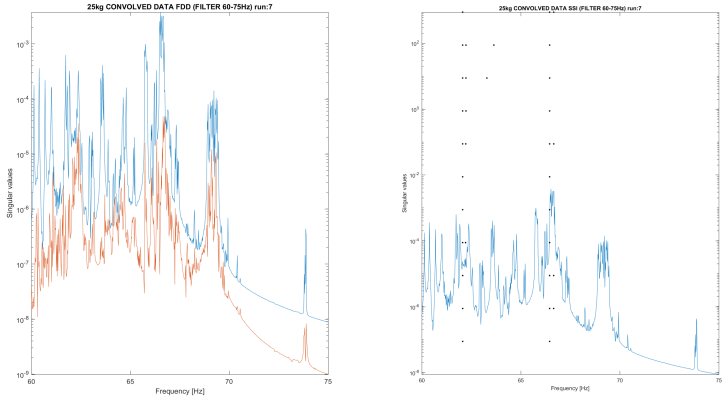


(b) 25kg FDD SSI output, run 6

Figure A2.25kg: Run 6

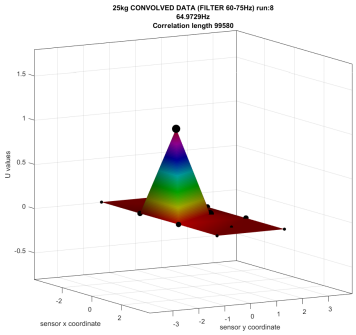


(a) 25kg mode shape, run 7

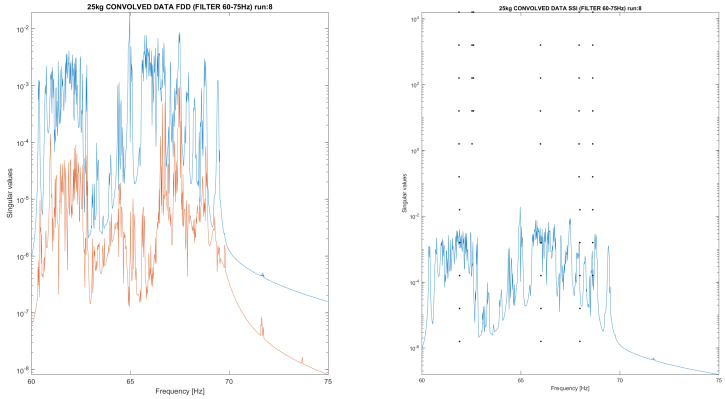


(b) 25kg FDD SSI output, run 7

Figure A2.25kg: Run 7

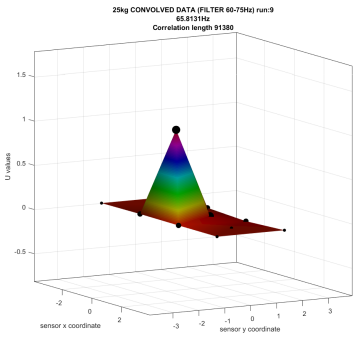


(a) 25kg mode shape, run 8

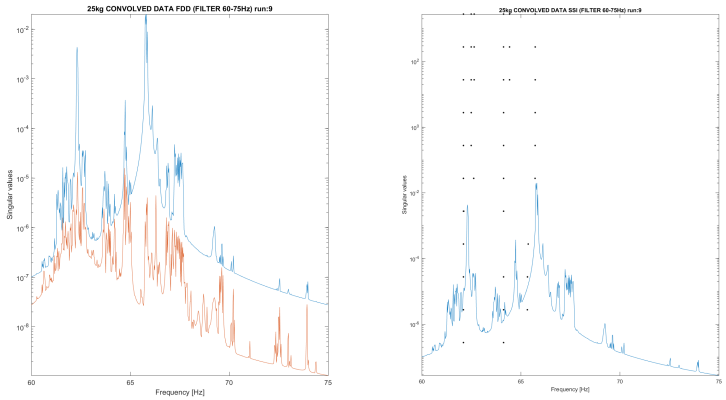


(b) 25kg FDD SSI output, run 8

Figure A2.25kg: Run 8

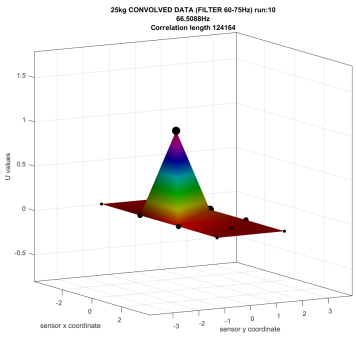


(a) 25kg mode shape, run 9

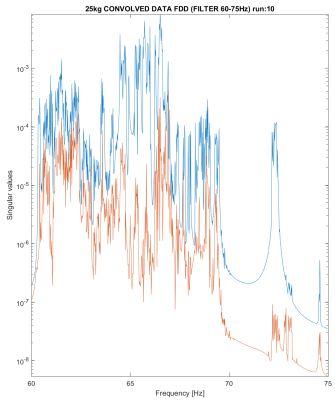


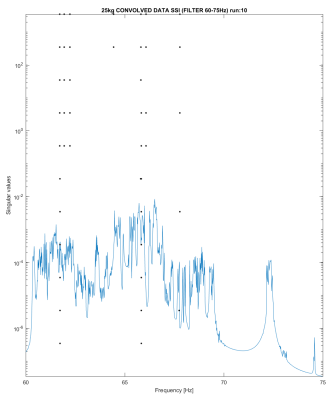
(b) 25kg FDD SSI output, run 9

Figure A2.25kg: Run 9



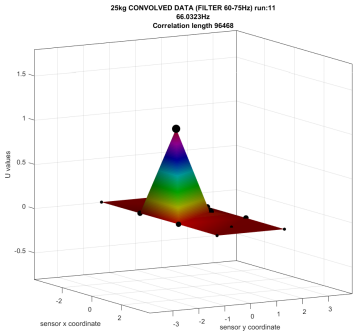
(a) 25kg mode shape, run 10



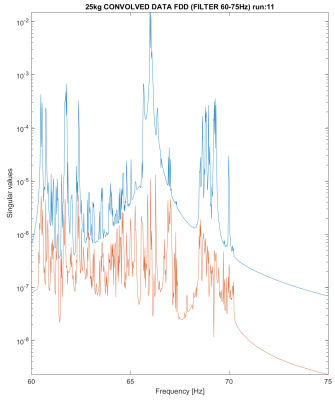


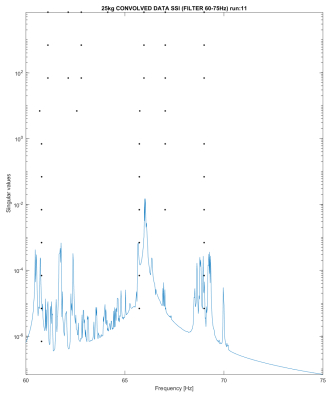
(b) 25kg FDD SSI output, run 10

Figure A2.25kg: Run 10



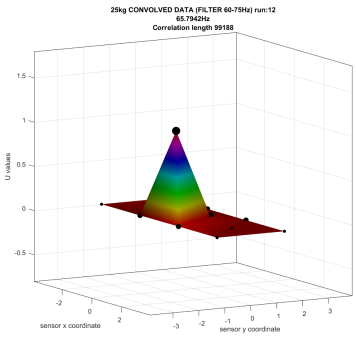
(a) 25kg mode shape, run 11



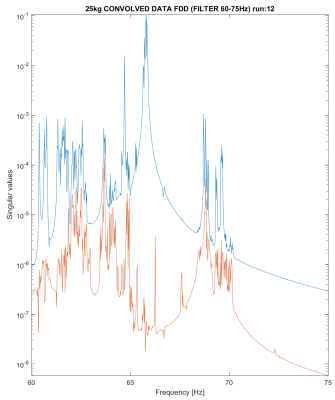


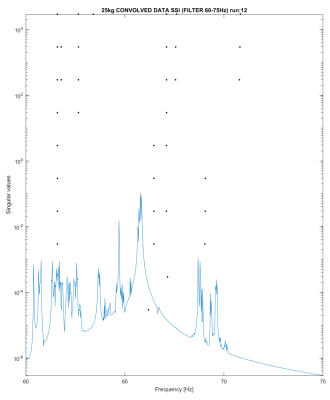
(b) 25kg FDD SSI output, run 11

Figure A2.25kg: Run 11



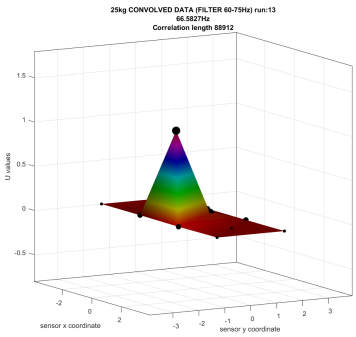
(a) 25kg mode shape, run 12



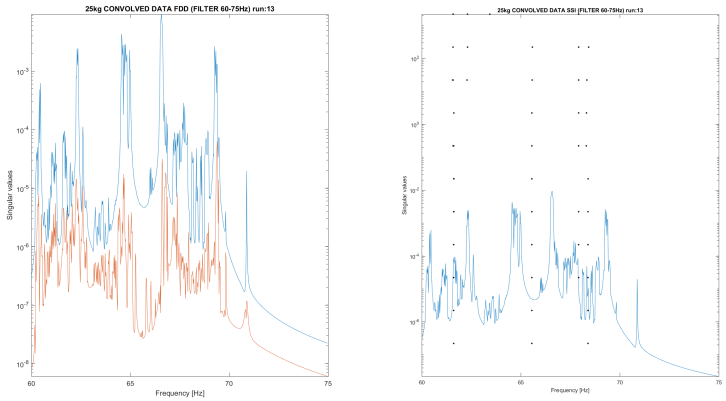


(b) 25kg FDD SSI output, run 12

Figure A2.25kg: Run 12

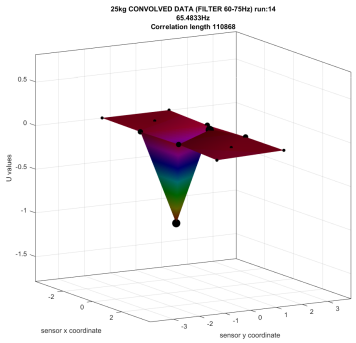


(a) 25kg mode shape, run 13

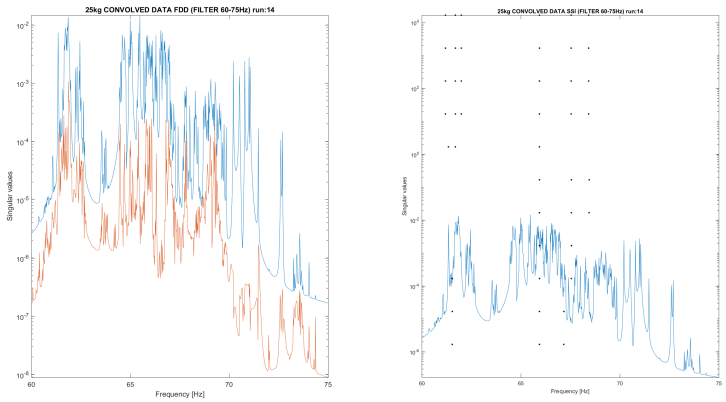


(b) 25kg FDD SSI output, run 13

Figure A2.25kg: Run 13

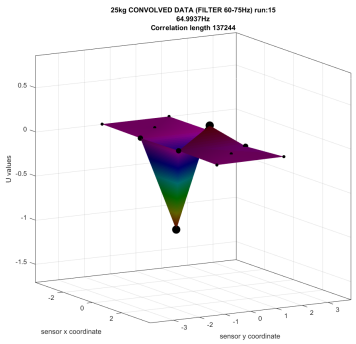


(a) 25kg mode shape, run 14

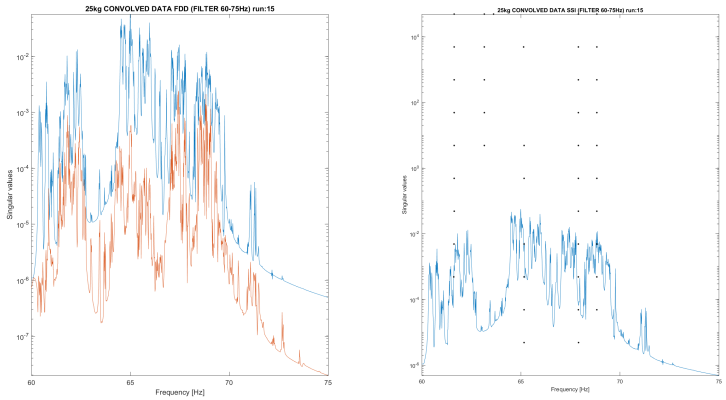


(b) 25kg FDD SSI output, run 14

Figure A2.25kg: Run 14

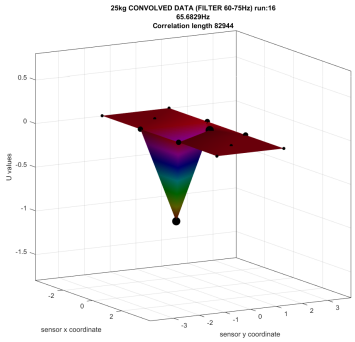


(a) 25kg mode shape, run 15

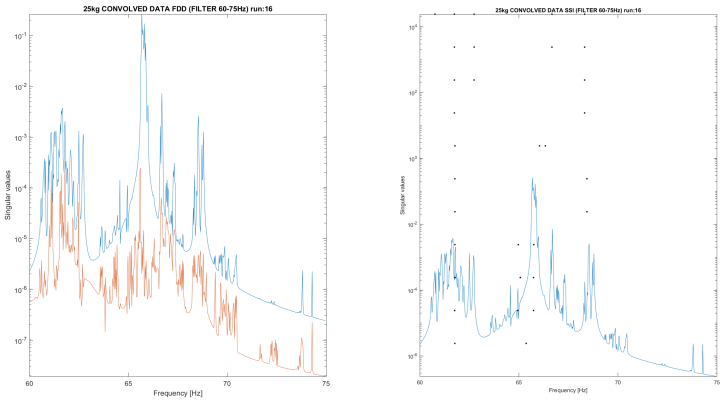


(b) 25kg FDD SSI output, run 15

Figure A2.25kg: Run 15

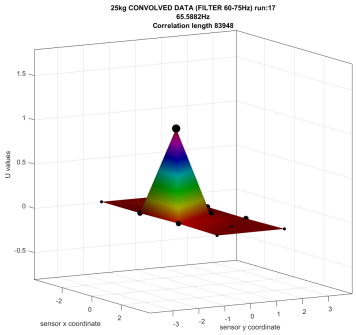


(a) 25kg mode shape, run 16

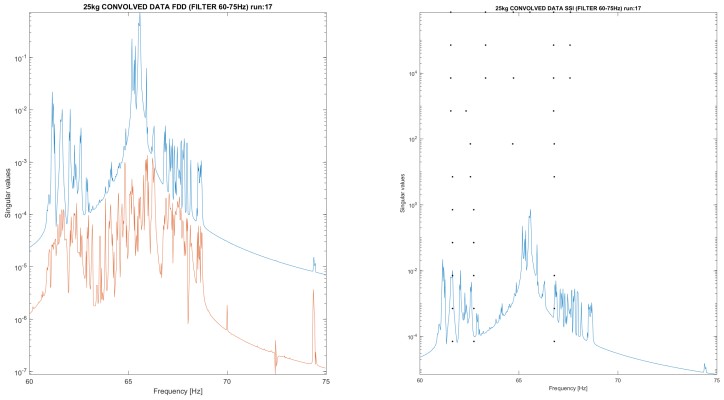


(b) 25kg FDD SSI output, run 16

Figure A2.25kg: Run 16

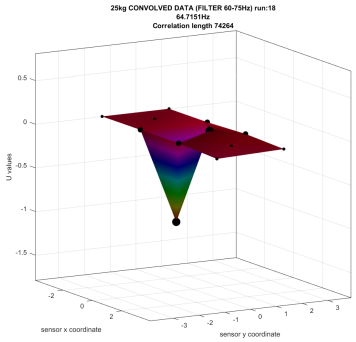


(a) 25kg mode shape, run 17

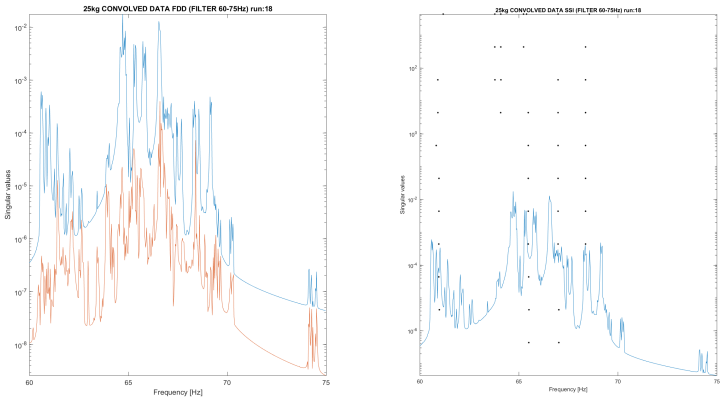


(b) 25kg FDD SSI output, run 17

Figure A2.25kg: Run 17

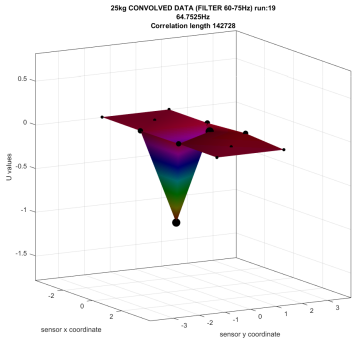


(a) 25kg mode shape, run 18

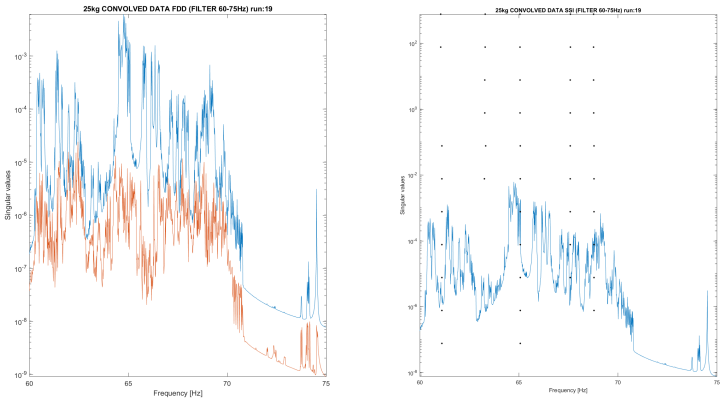


(b) 25kg FDD SSI output, run 18

Figure A2.25kg: Run 18

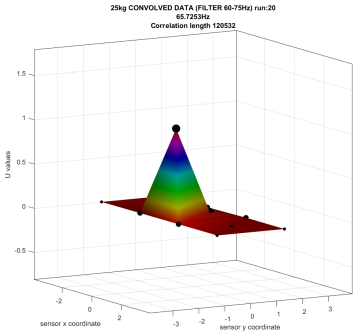


(a) 25kg mode shape, run 19

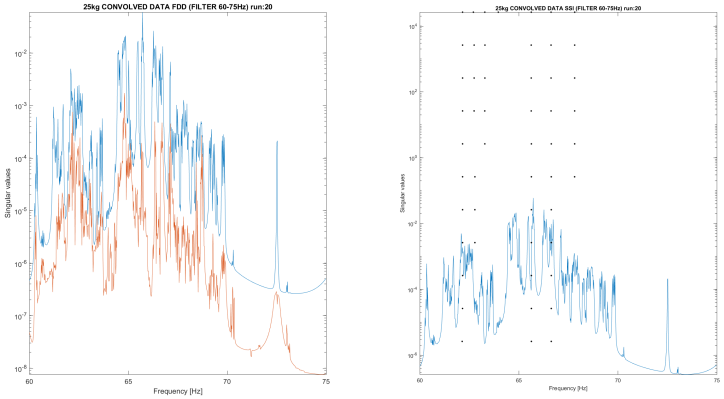


(b) 25kg FDD SSI output, run 19

Figure A2.25kg: Run 19

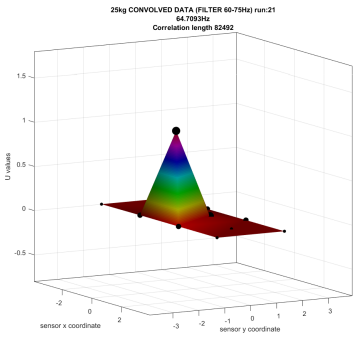


(a) 25kg mode shape, run 20

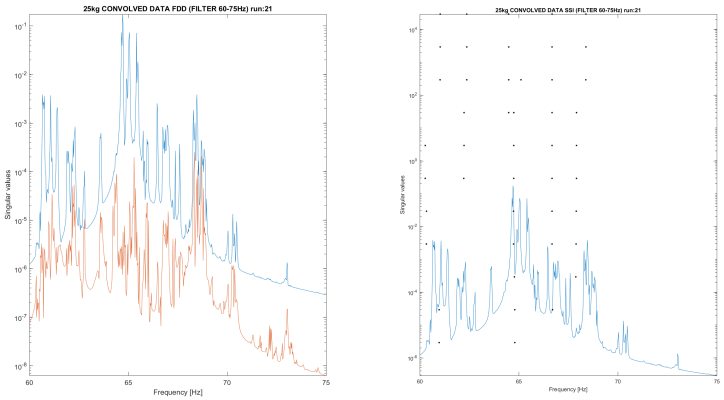


(b) 25kg FDD SSI output, run 20

Figure A2.25kg: Run 20

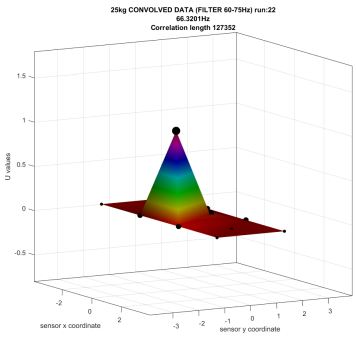


(a) 25kg mode shape, run 21

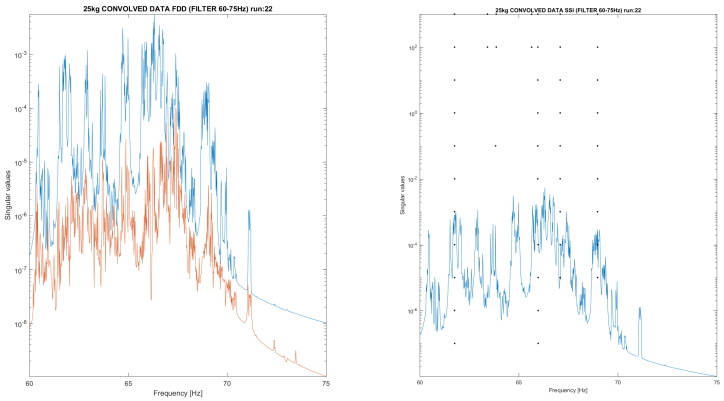


(b) 25kg FDD SSI output, run 21

Figure A2.25kg: Run 21

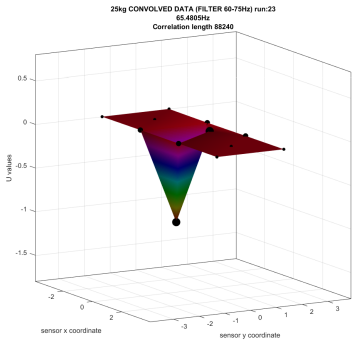


(a) 25kg mode shape, run 22

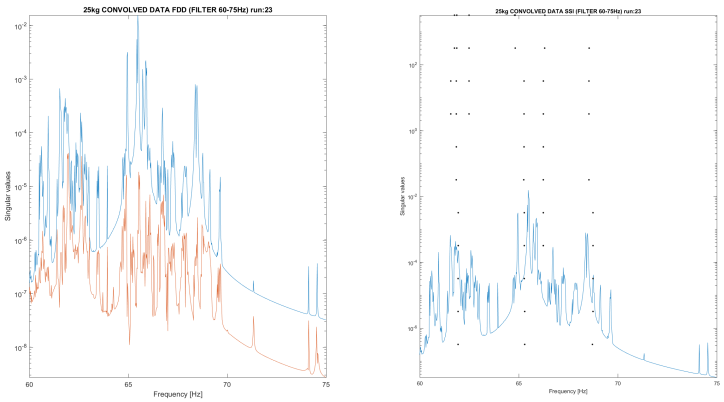


(b) 25kg FDD SSI output, run 22

Figure A2.25kg: Run 22

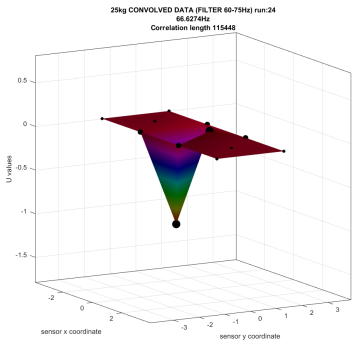


(a) 25kg mode shape, run 23

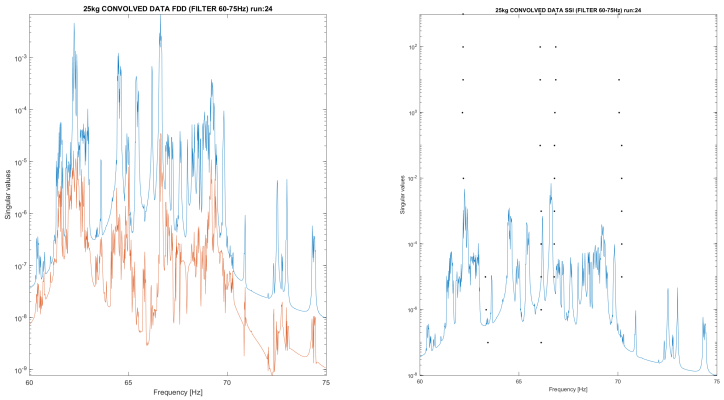


(b) 25kg FDD SSI output, run 23

Figure A2.25kg: Run 23

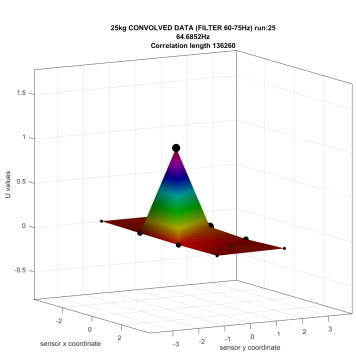


(a) 25kg mode shape, run 24

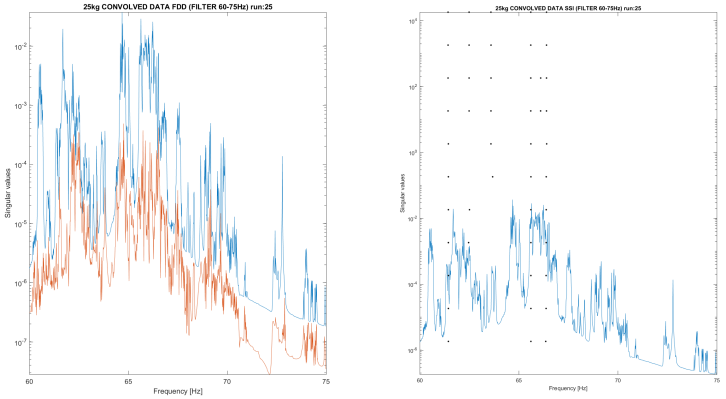


(b) 25kg FDD SSI output, run 24

Figure A2.25kg: Run 24



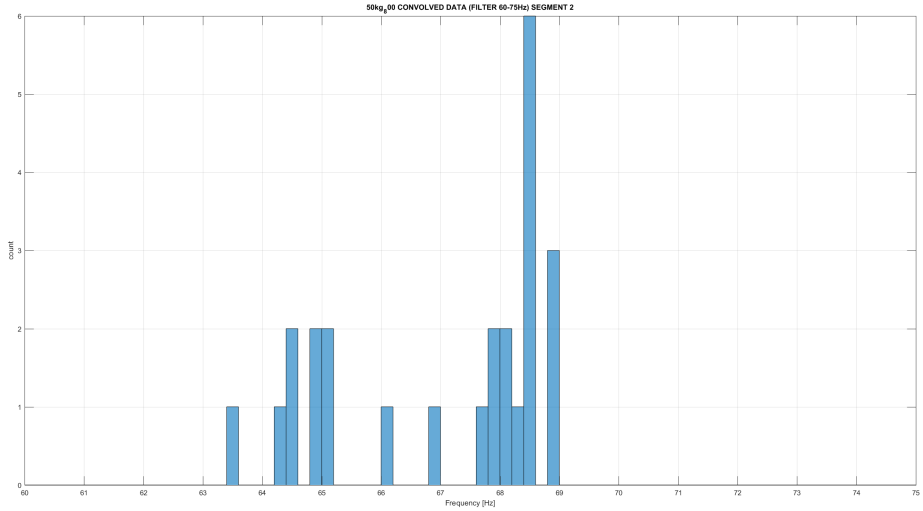
(a) 25kg mode shape, run 25



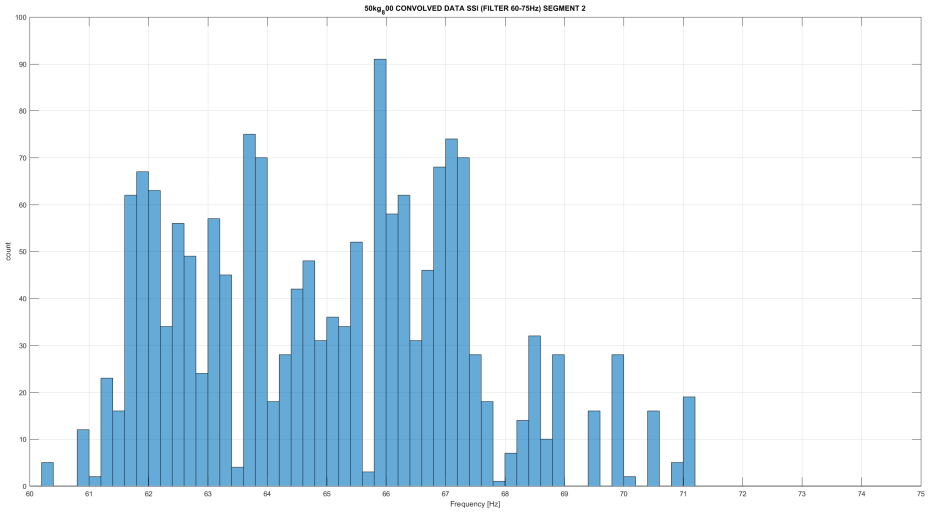
(b) 25kg FDD SSI output, run 25

Figure A2.25kg: Run 25

50kg data segment 2 (28.03.2017)

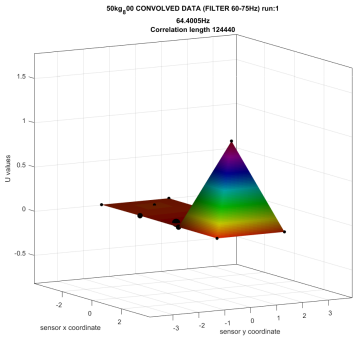


(a) 50kg FDD histogram

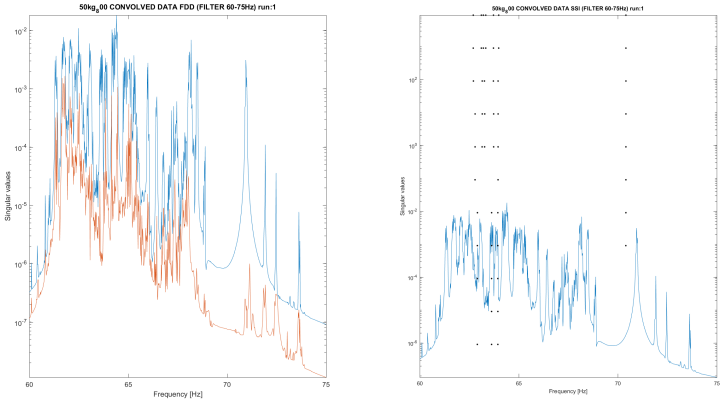


(b) 50kg SSI histogram

Figure A2.50kg: Histograms of identified modes, 50kg data

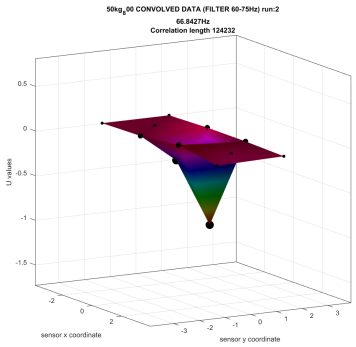


(a) 50kg mode shape, run 1

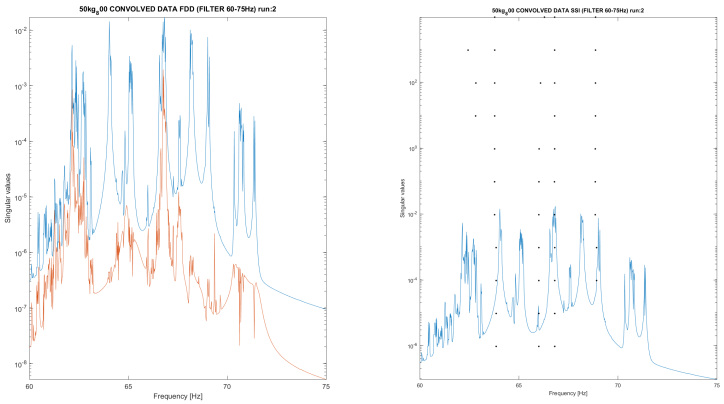


(b) 50kg FDD SSI output, run 1

Figure A2.50kg (28.03.2017): Run 1

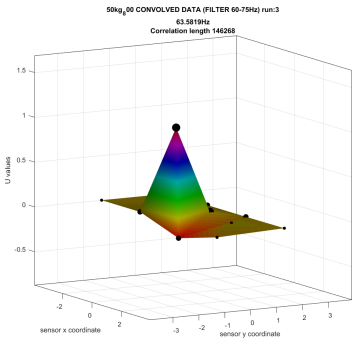


(a) 50kg mode shape, run 2

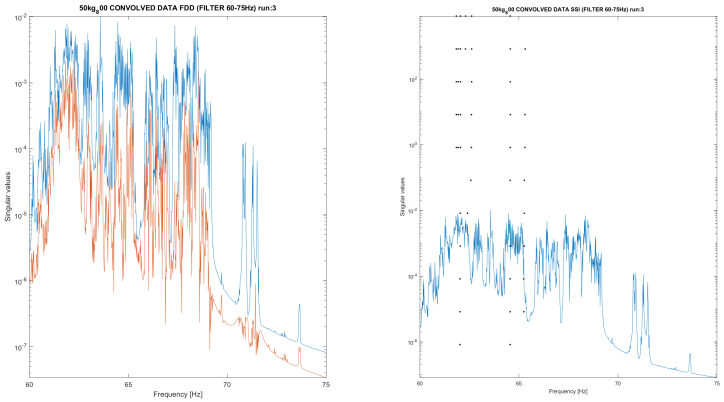


(b) 50kg FDD SSI output, run 2

Figure A2.50kg (28.03.2017): Run 2

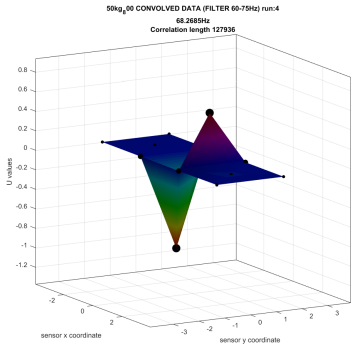


(a) 50kg mode shape, run 3

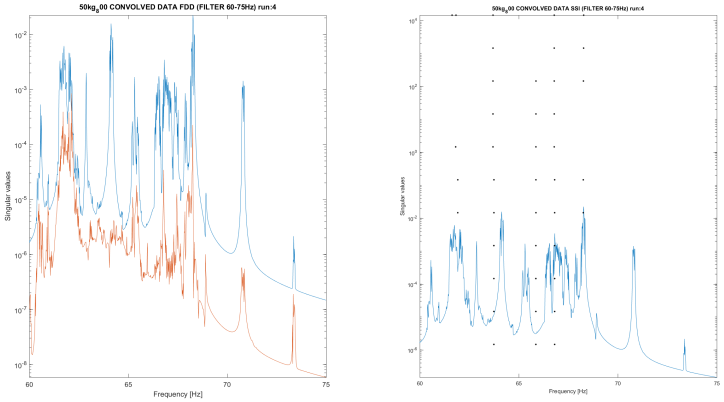


(b) 50kg FDD SSI output, run 3

Figure A2.50kg (28.03.2017): Run 3

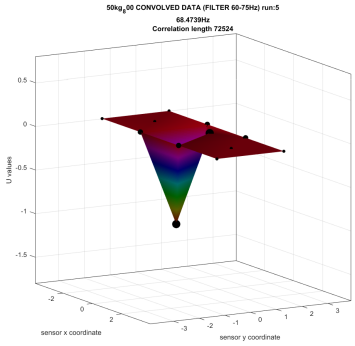


(a) 50kg mode shape, run 4

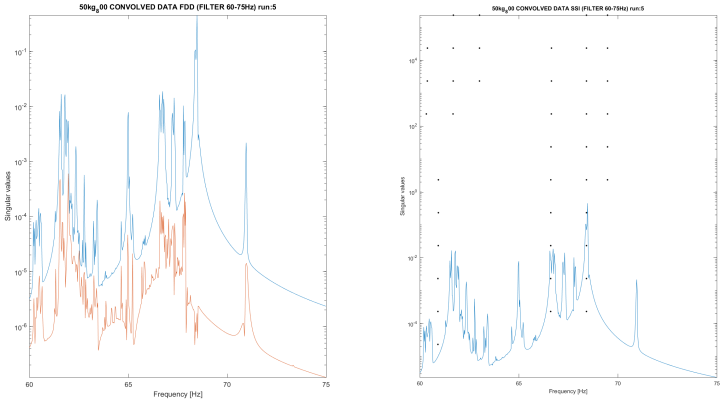


(b) 50kg FDD SSI output, run 4

Figure A2.50kg (28.03.2017): Run 4

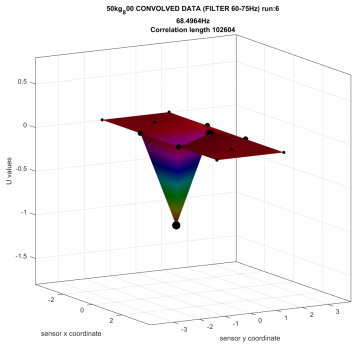


(a) 50kg mode shape, run 5

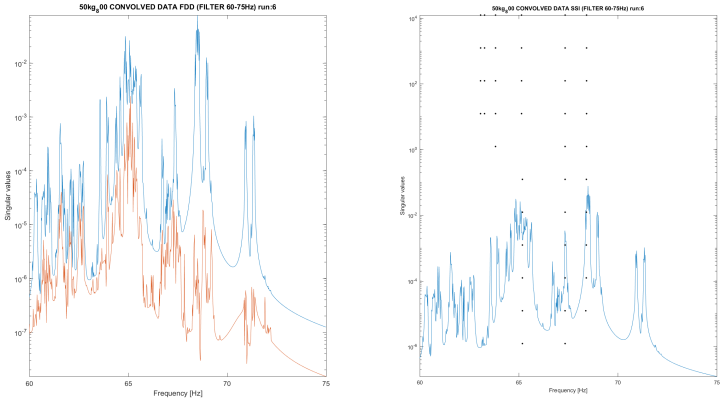


(b) 50kg FDD SSI output, run 5

Figure A2.50kg (28.03.2017): Run 5

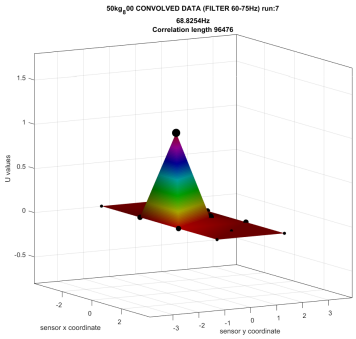


(a) 50kg mode shape, run 6

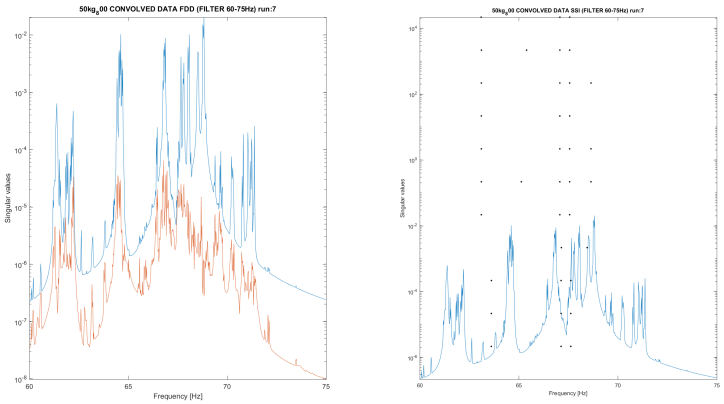


(b) 50kg FDD SSI output, run 6

Figure A2.50kg (28.03.2017): Run 6

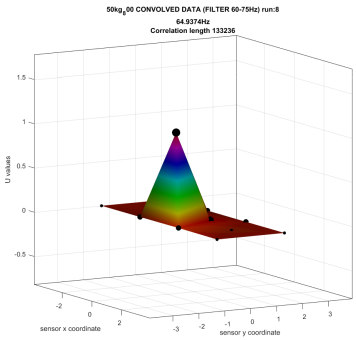


(a) 50kg mode shape, run 7

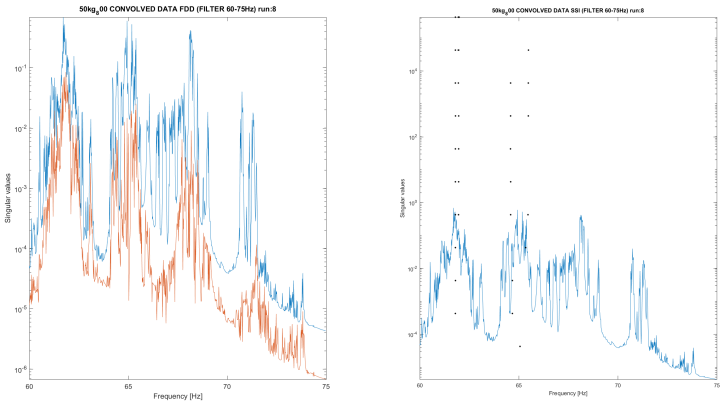


(b) 50kg FDD SSI output, run 7

Figure A2.50kg (28.03.2017): Run 7

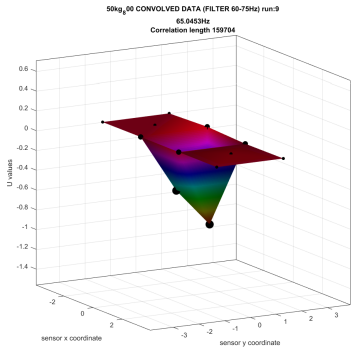


(a) 50kg mode shape, run 8

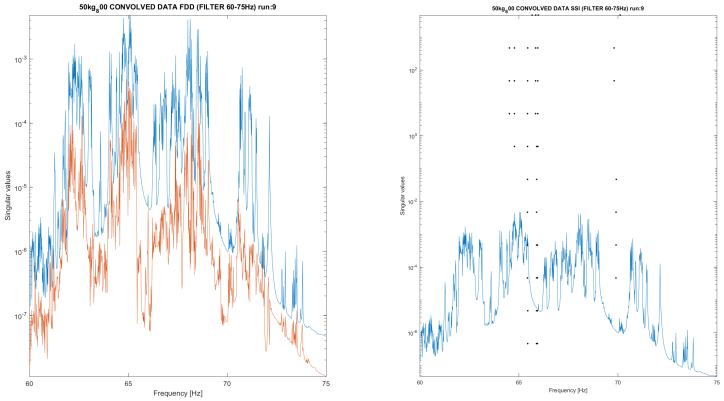


(b) 50kg FDD SSI output, run 8

Figure A2.50kg (28.03.2017): Run 8

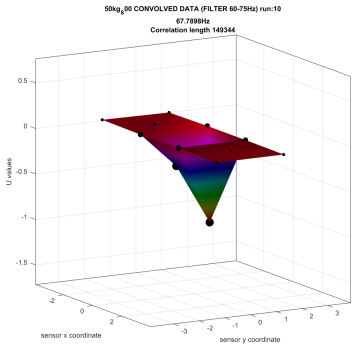


(a) 50kg mode shape, run 9

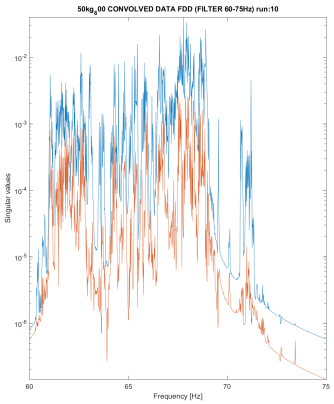


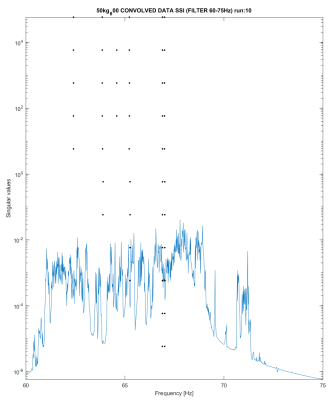
(b) 50kg FDD SSI output, run 9

Figure A2.50kg (28.03.2017): Run 9



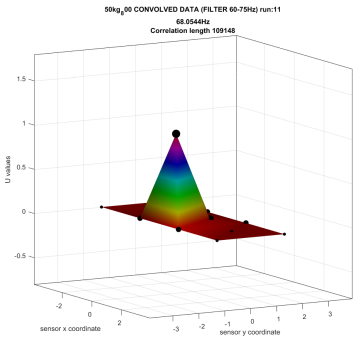
(a) 50kg mode shape, run 10



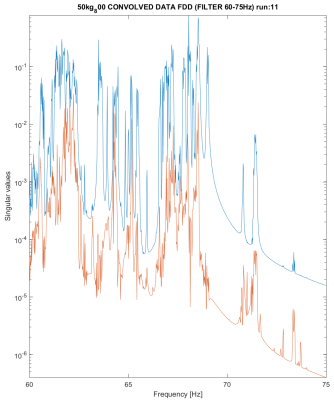


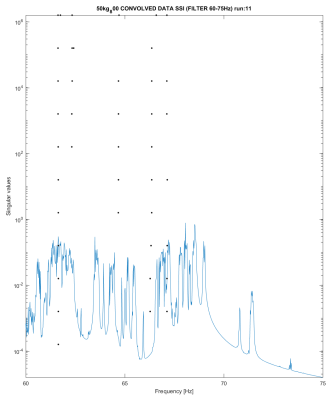
(b) 50kg FDD SSI output, run 10

Figure A2.50kg (28.03.2017): Run 10



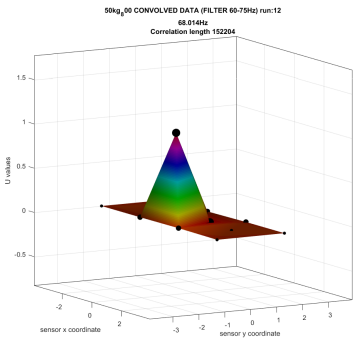
(a) 50kg mode shape, run 11



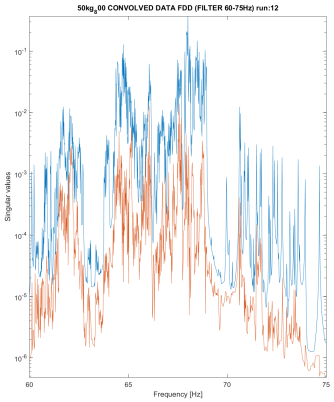


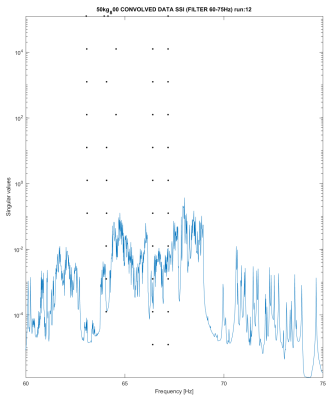
(b) 50kg FDD SSI output, run 11

Figure A2.50kg (28.03.2017): Run 11



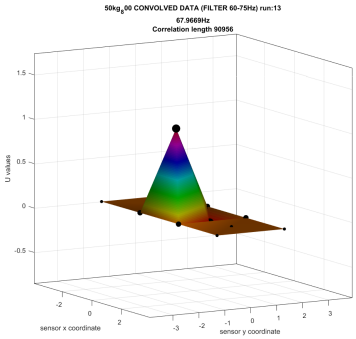
(a) 50kg mode shape, run 12



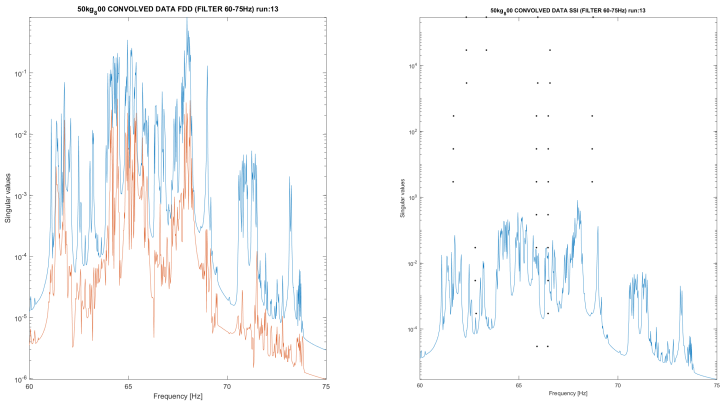


(b) 50kg FDD SSI output, run 12

Figure A2.50kg (28.03.2017): Run 12

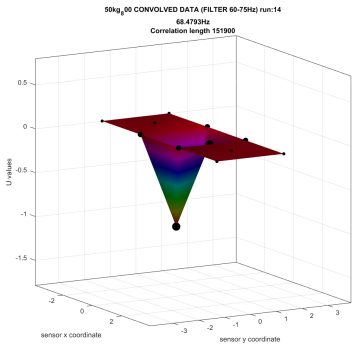


(a) 50kg mode shape, run 13

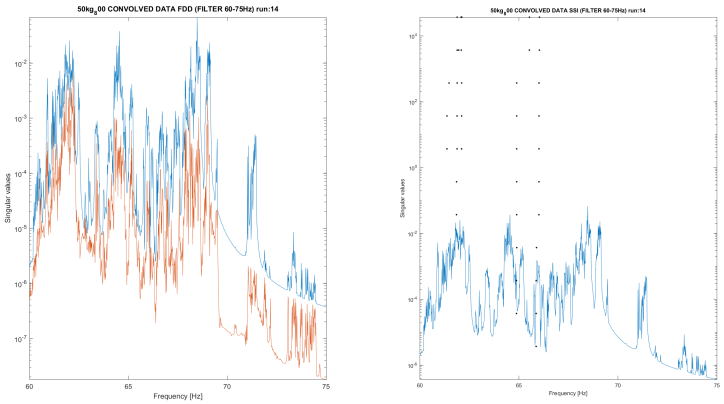


(b) 50kg FDD SSI output, run 13

Figure A2.50kg (28.03.2017): Run 13

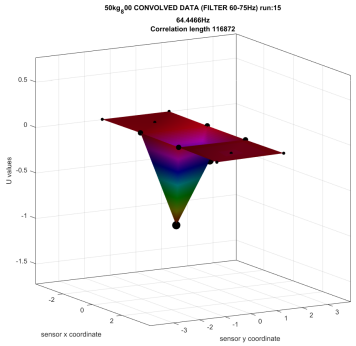


(a) 50kg mode shape, run 14

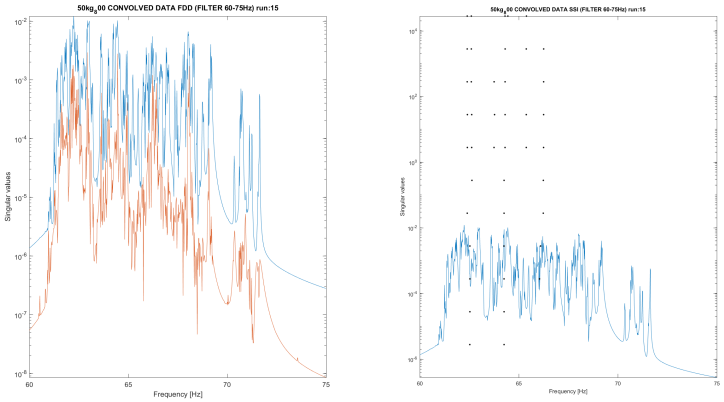


(b) 50kg FDD SSI output, run 14

Figure A2.50kg (28.03.2017): Run 14

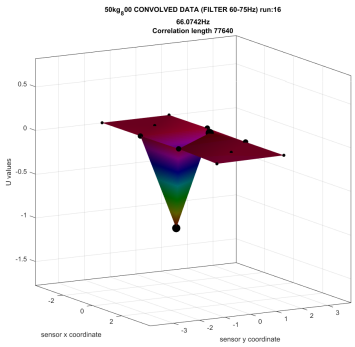


(a) 50kg mode shape, run 15

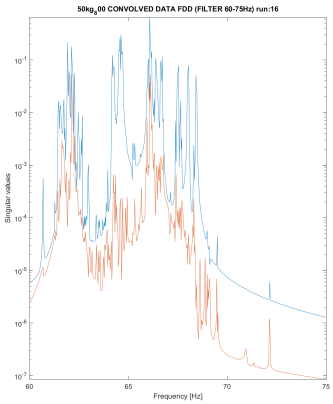


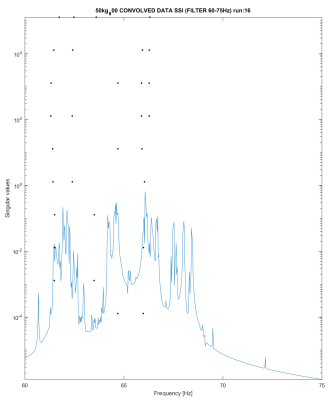
(b) 50kg FDD SSI output, run 15

Figure A2.50kg (28.03.2017): Run 15



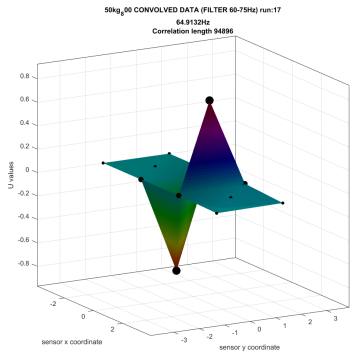
(a) 50kg mode shape, run 16



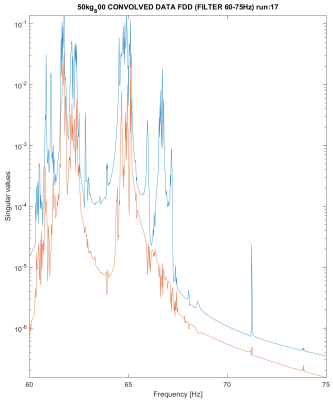


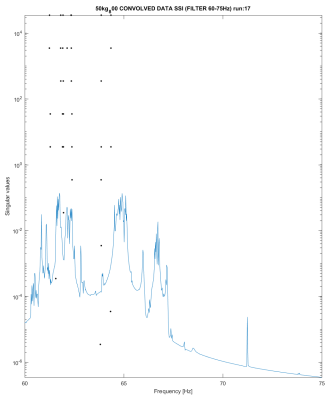
(b) 50kg FDD SSI output, run 16

Figure A2.50kg (28.03.2017): Run 16



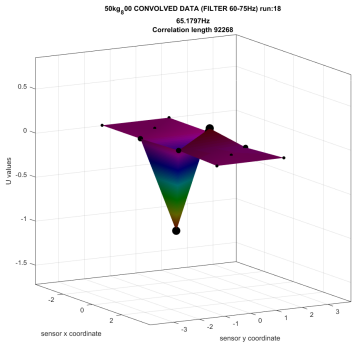
(a) 50kg mode shape, run 17



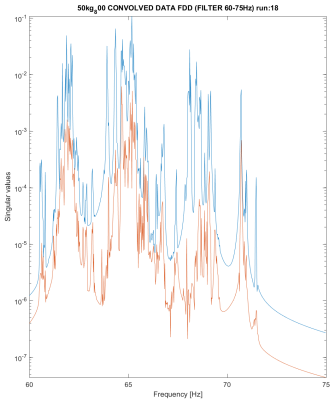


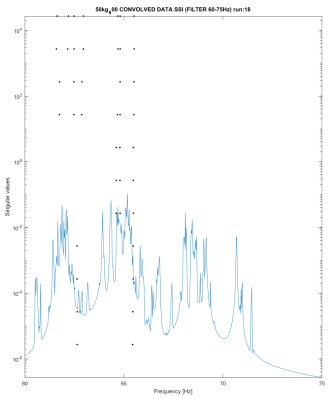
(b) 50kg FDD SSI output, run 17

Figure A2.50kg (28.03.2017): Run 17



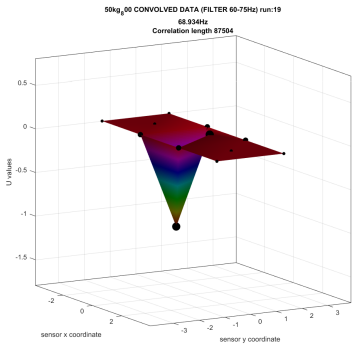
(a) 50kg mode shape, run 18



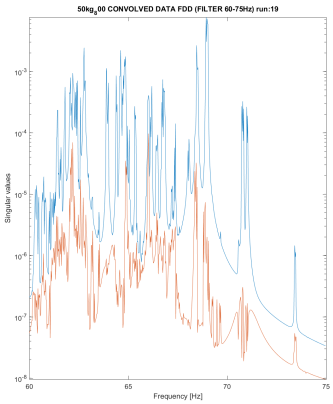


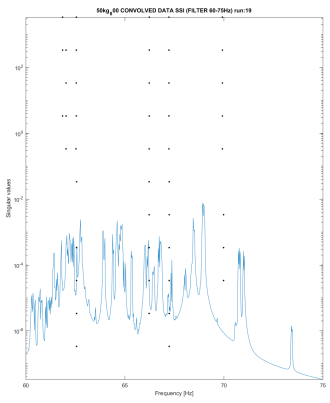
(b) 50kg FDD SSI output, run 18

Figure A2.50kg (28.03.2017): Run 18



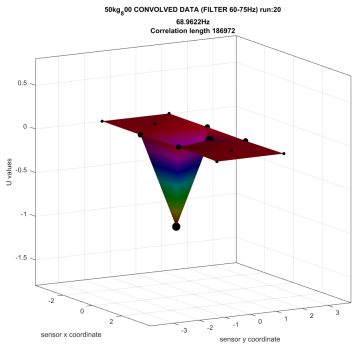
(a) 50kg mode shape, run 19



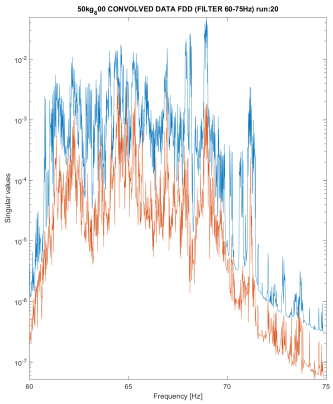


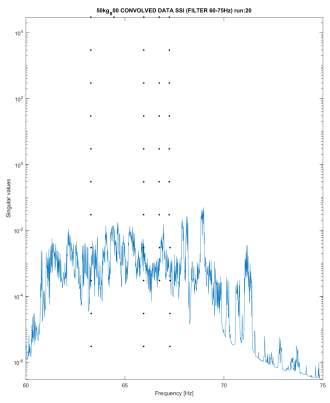
(b) 50kg FDD SSI output, run 19

Figure A2.50kg (28.03.2017): Run 19



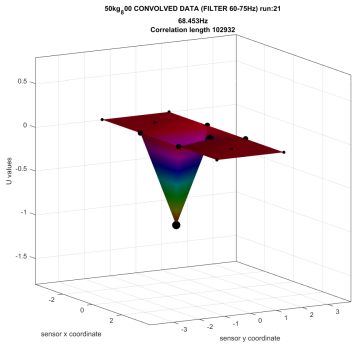
(a) 50kg mode shape, run 20



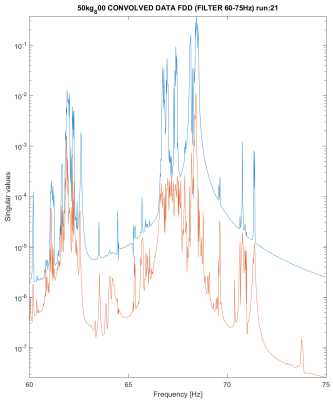


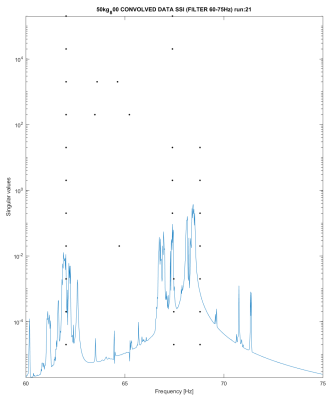
(b) 50kg FDD SSI output, run 20

Figure A2.50kg (28.03.2017): Run 20



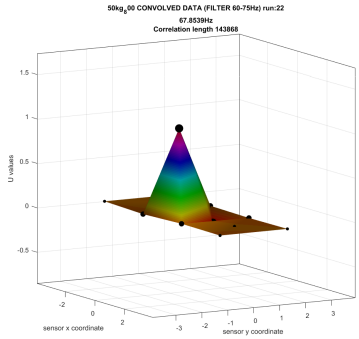
(a) 50kg mode shape, run 21

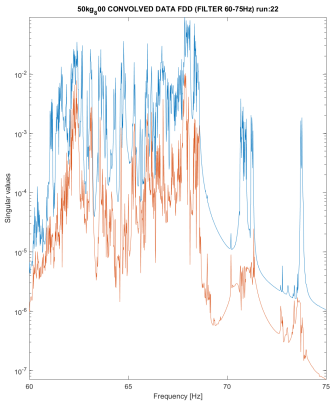


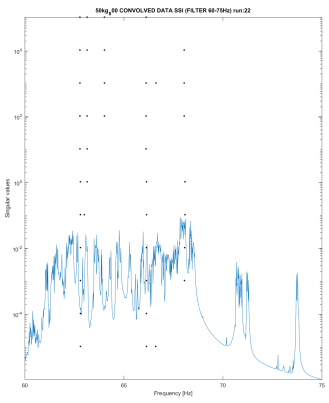


(b) 50kg FDD SSI output, run 21

Figure A2.50kg (28.03.2017): Run 21



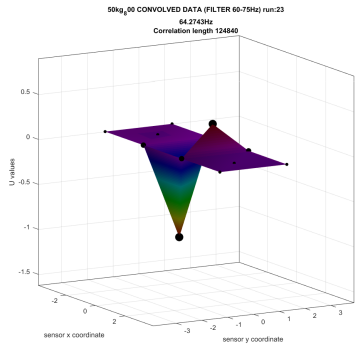


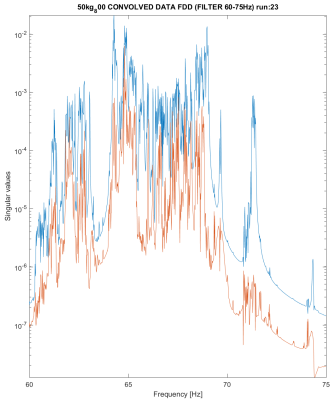


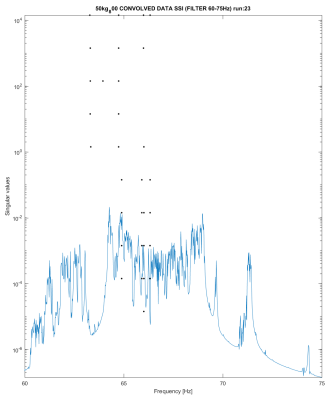
(a) 50kg mode shape, run 22

(b) 50kg FDD SSI output, run 22

Figure A2.50kg (28.03.2017): Run 22



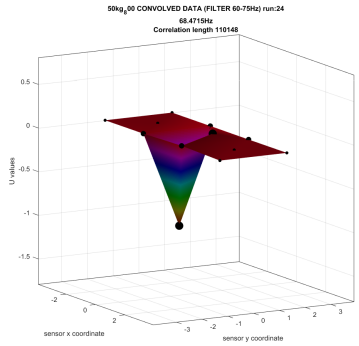


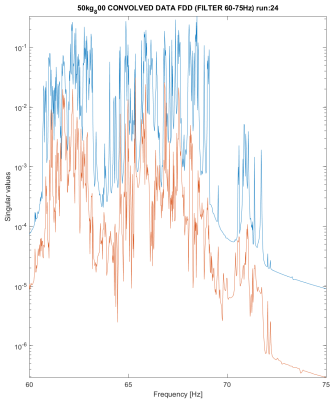


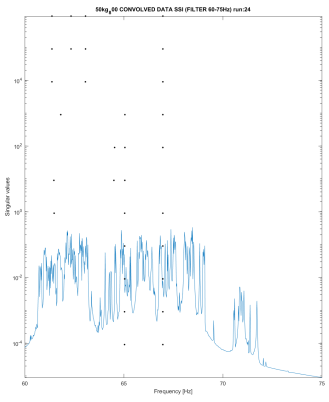
(a) 50kg mode shape, run 23

(b) 50kg FDD SSI output, run 23

Figure A2.50kg (28.03.2017): Run 23



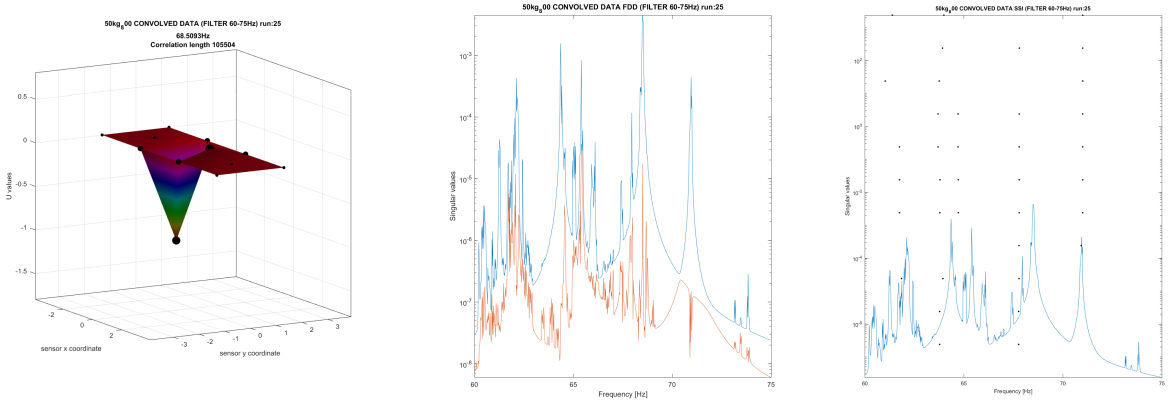




(a) 50kg mode shape, run 24

(b) 50kg FDD SSI output, run 24

Figure A2.50kg (28.03.2017): Run 24



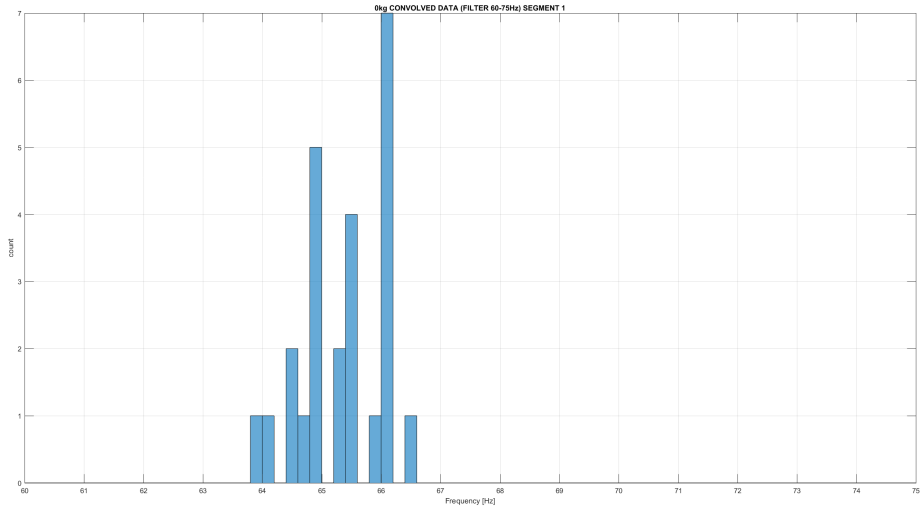
(a) 50kg mode shape, run 25

(b) 50kg FDD SSI output, run 25

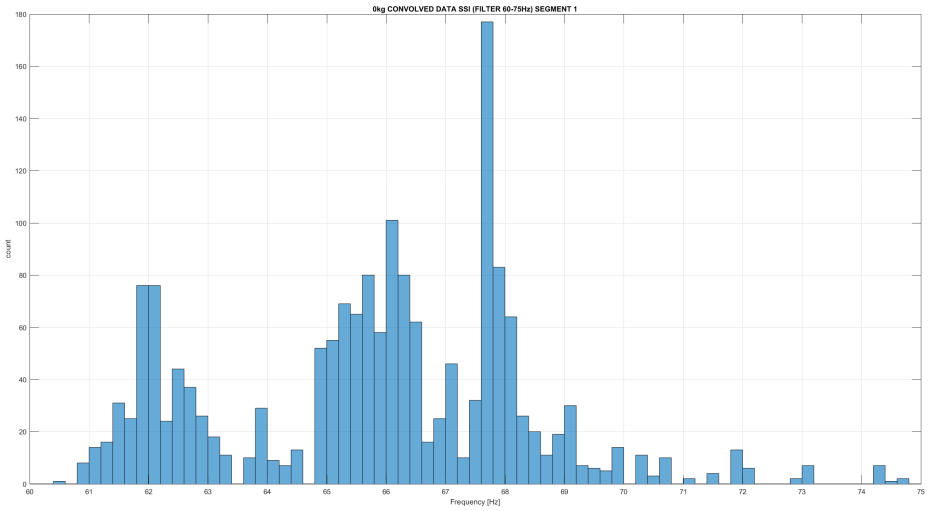
Figure A2.50kg (28.03.2017): Run 25

Appendix A3

Data 0kg-50kg-75kg-100kg segment 1 (Unreduced order PF)

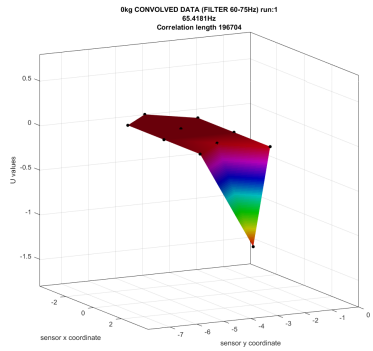


(a) 0kg FDD histogram

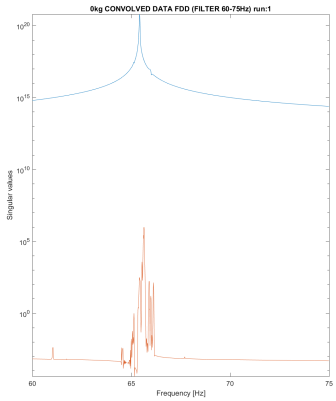


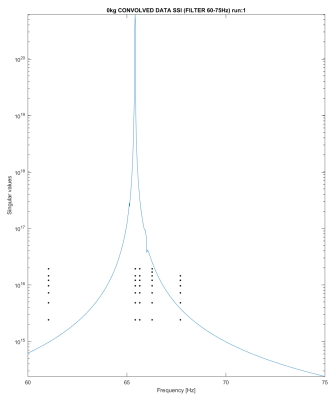
(b) 0kg SSI histogram

Figure A3.0kg: Histograms of identified modes, 0kg data (segment 1)



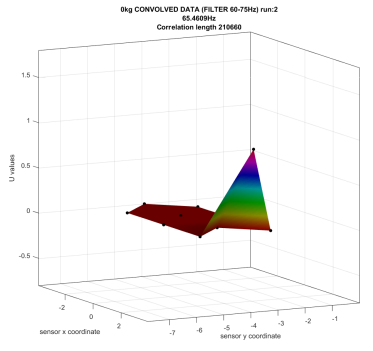
(a) 0kg mode shape, run 1



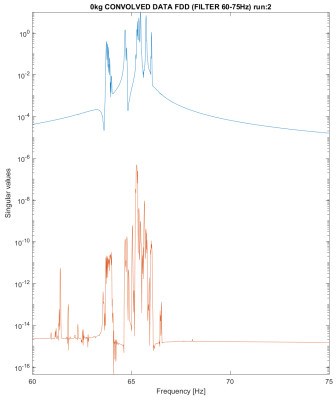


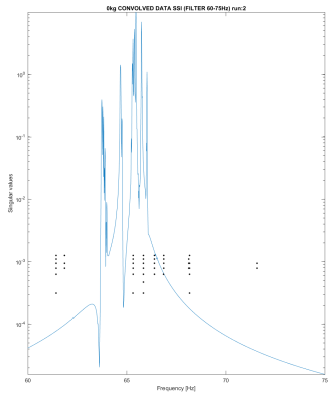
(b) 0kg FDD SSI output, run 1

Figure A3.0kg: Run 1 (segment 1)



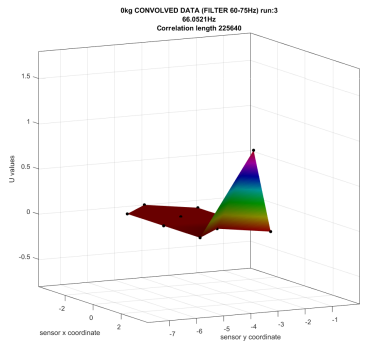
(a) 0kg mode shape, run 2



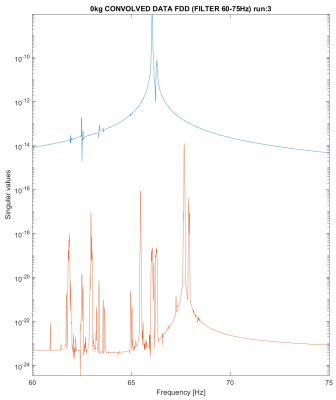


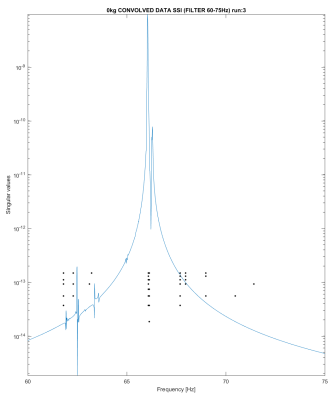
(b) 0kg FDD SSI output, run 2

Figure A3.0kg: Run 2 (segment 1)



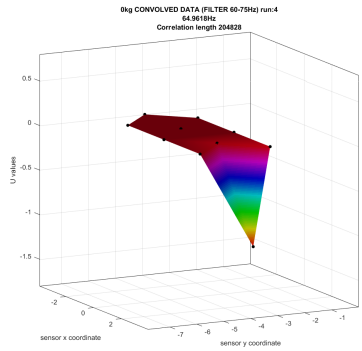
(a) 0kg mode shape, run 3



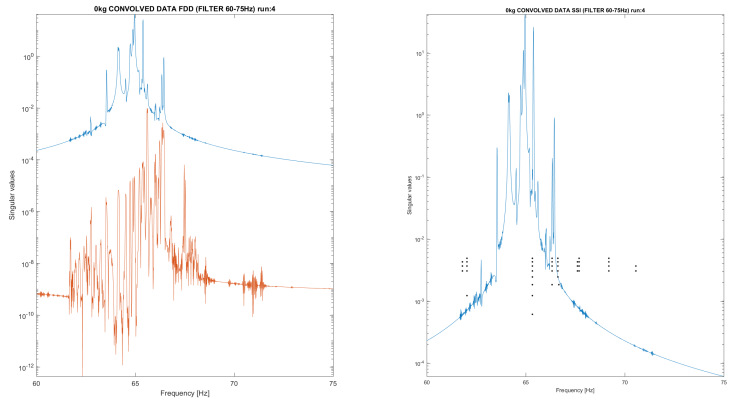


(b) 0kg FDD SSI output, run 3

Figure A3.0kg: Run 3 (segment 1)

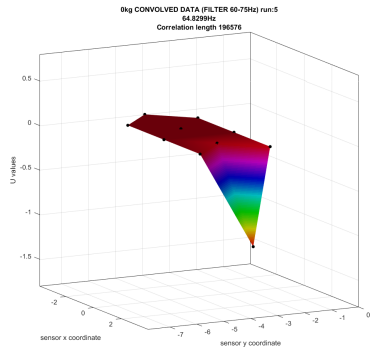


(a) 0kg mode shape, run 4

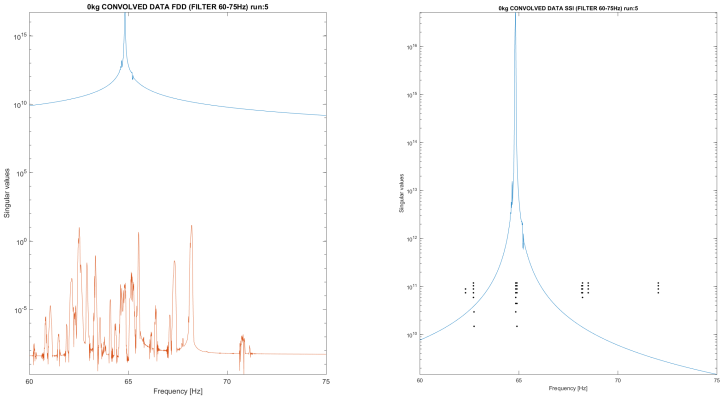


(b) 0kg FDD SSI output, run 4

Figure A3.0kg: Run 4 (segment 1)

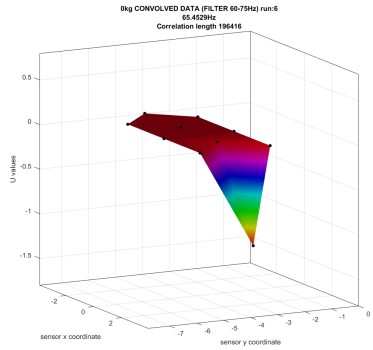


(a) 0kg mode shape, run 5

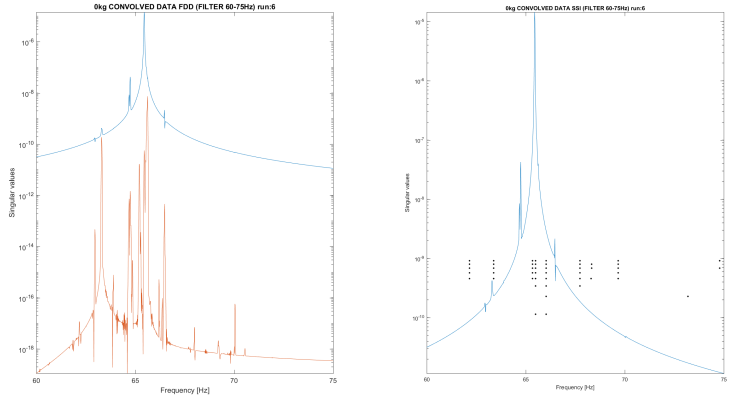


(b) 0kg FDD SSI output, run 5

Figure A3.0kg: Run 5 (segment 1)

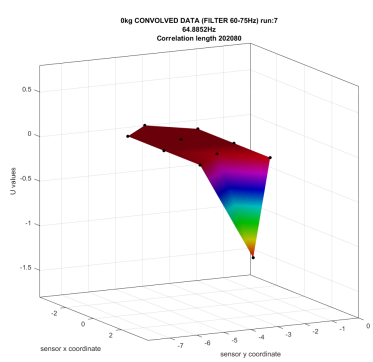


(a) 0kg mode shape, run 6

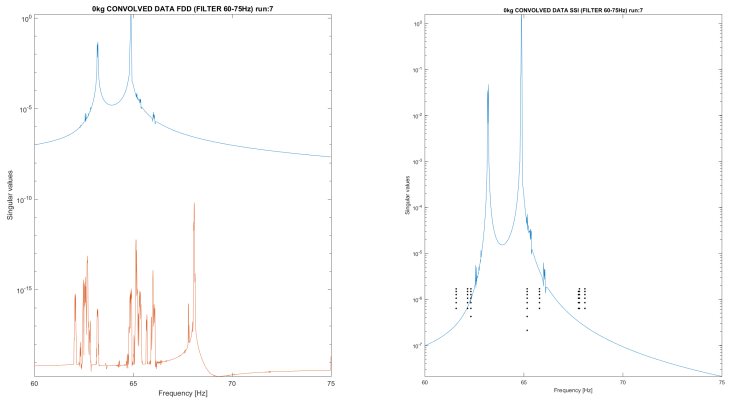


(b) 0kg FDD SSI output, run 6

Figure A3.0kg: Run 6 (segment 1)

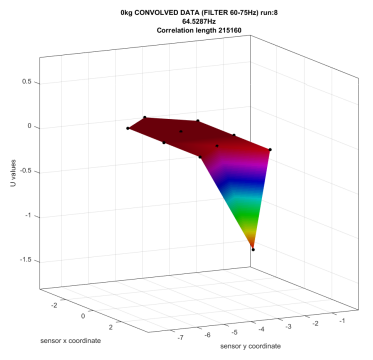


(a) 0kg mode shape, run 7

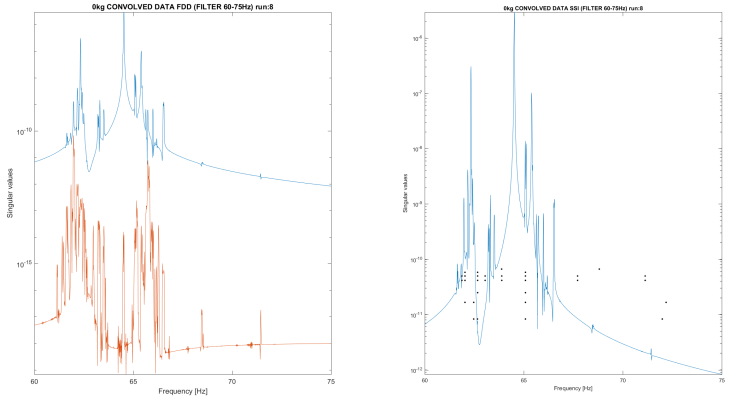


(b) 0kg FDD SSI output, run 7

Figure A3.0kg: Run 7 (segment 1)

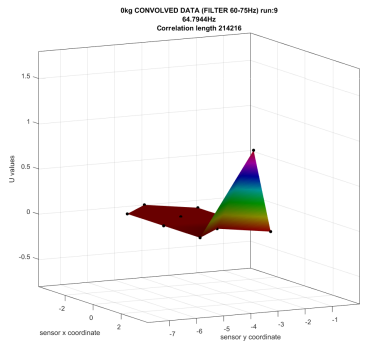


(a) 0kg mode shape, run 8

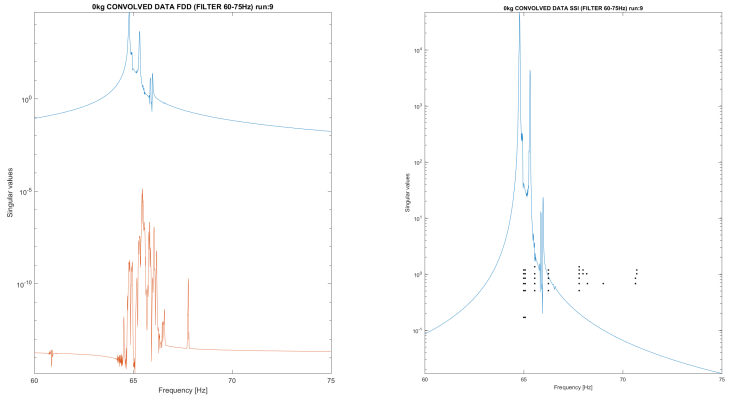


(b) 0kg FDD SSI output, run 8

Figure A3.0kg: Run 8 (segment 1)

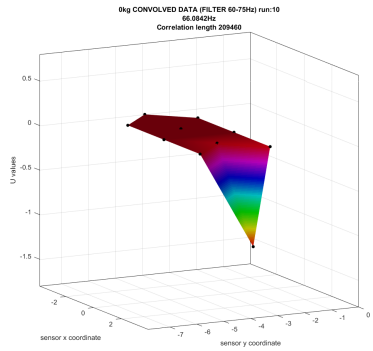


(a) 0kg mode shape, run 9

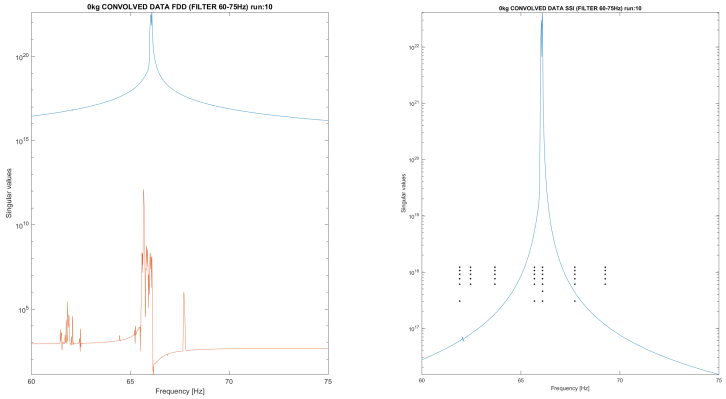


(b) 0kg FDD SSI output, run 9

Figure A3.0kg: Run 9 (segment 1)

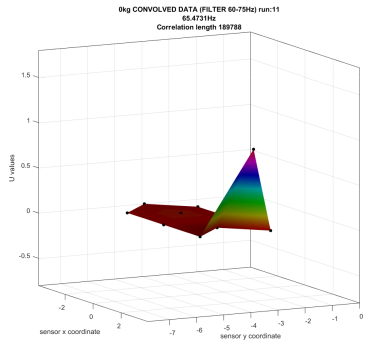


(a) 0kg mode shape, run 10

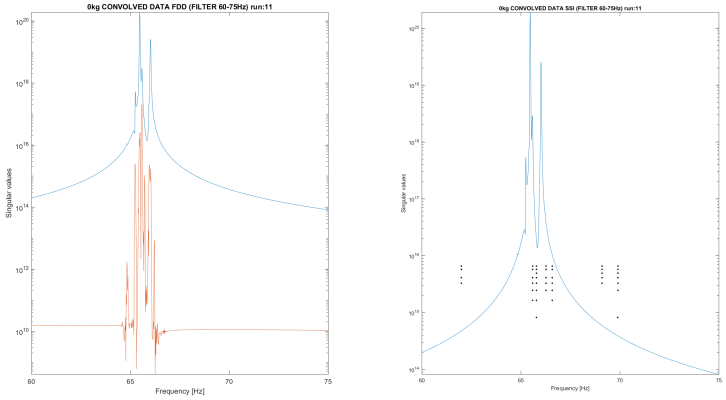


(b) 0kg FDD SSI output, run 10

Figure A3.0kg: Run 10 (segment 1)

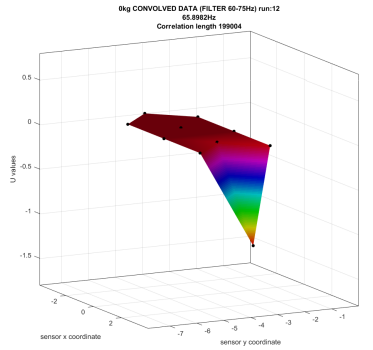


(a) 0kg mode shape, run 11

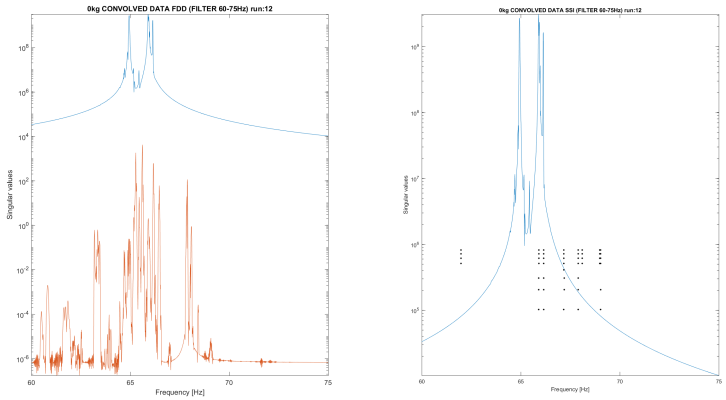


(b) 0kg FDD SSI output, run 11

Figure A3.0kg: Run 11 (segment 1)

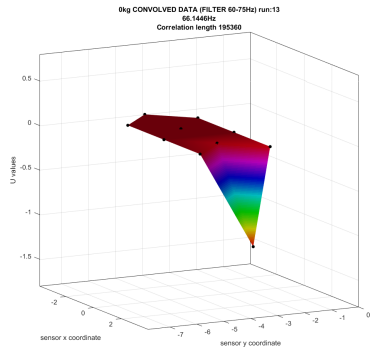


(a) 0kg mode shape, run 12

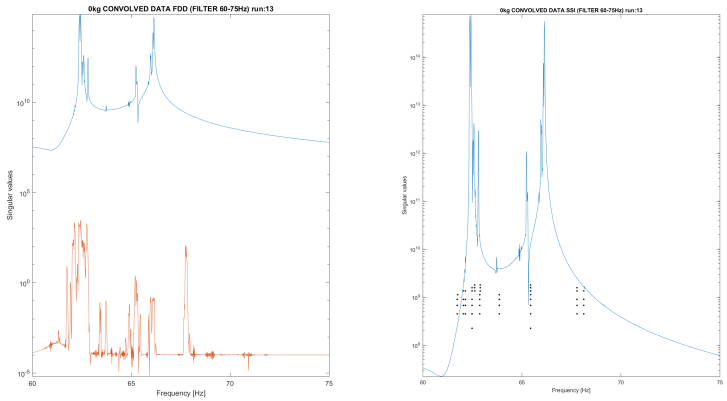


(b) 0kg FDD SSI output, run 12

Figure A3.0kg: Run 12 (segment 1)

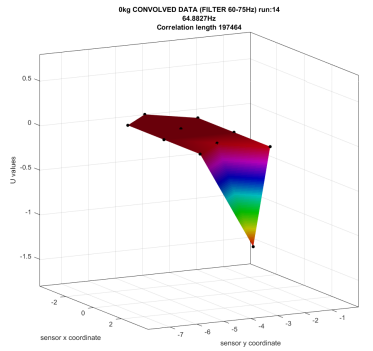


(a) 0kg mode shape, run 13

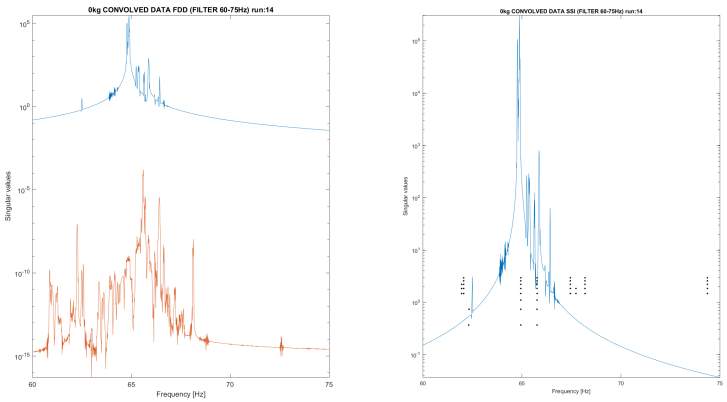


(b) 0kg FDD SSI output, run 13

Figure A3.0kg: Run 13 (segment 1)

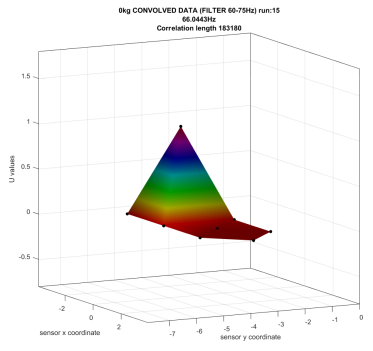


(a) 0kg mode shape, run 14

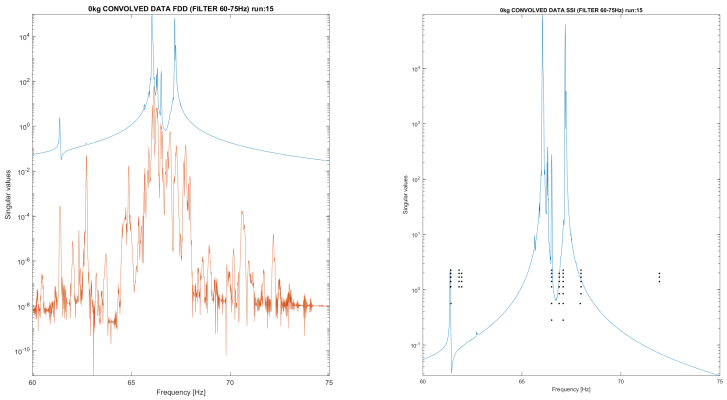


(b) 0kg FDD SSI output, run 14

Figure A3.0kg: Run 14 (segment 1)

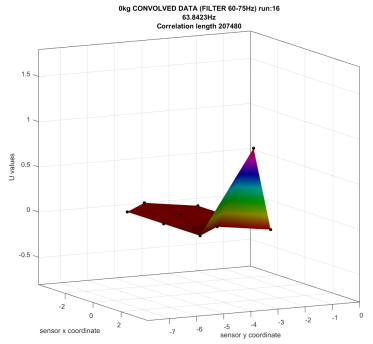


(a) 0kg mode shape, run 15

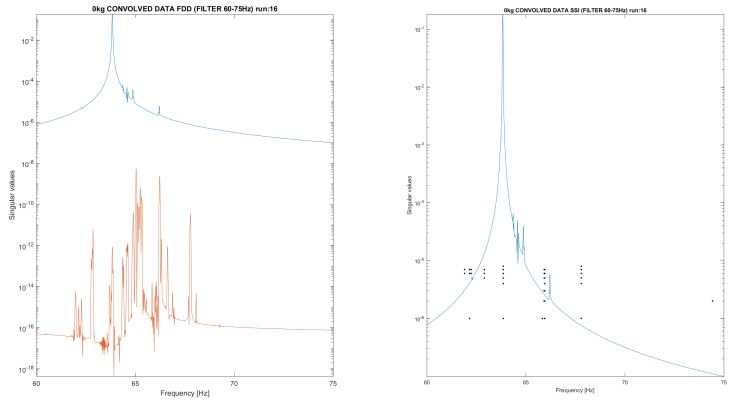


(b) 0kg FDD SSI output, run 15

Figure A3.0kg: Run 15 (segment 1)

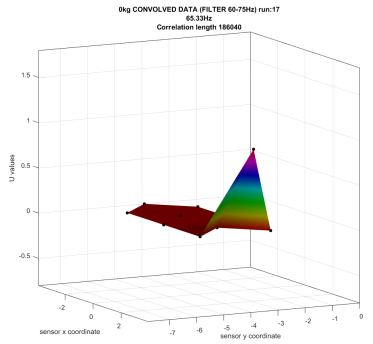


(a) 0kg mode shape, run 16

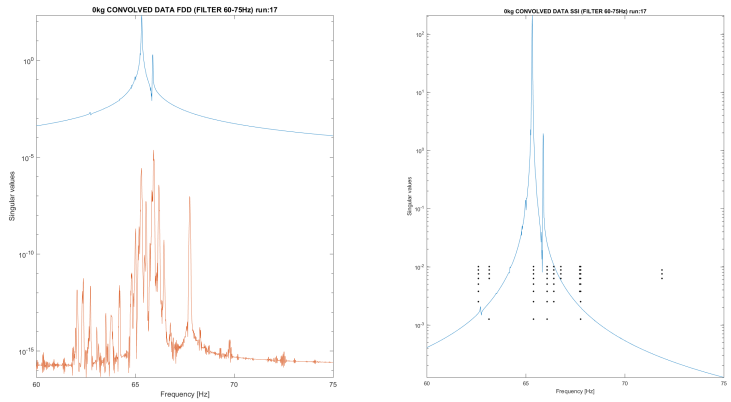


(b) 0kg FDD SSI output, run 16

Figure A3.0kg: Run 16 (segment 1)

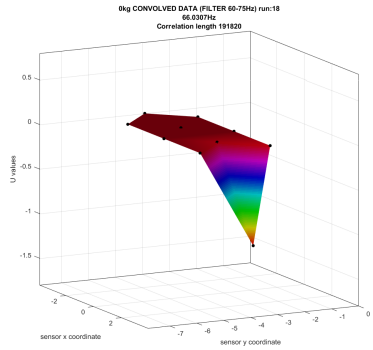


(a) 0kg mode shape, run 17

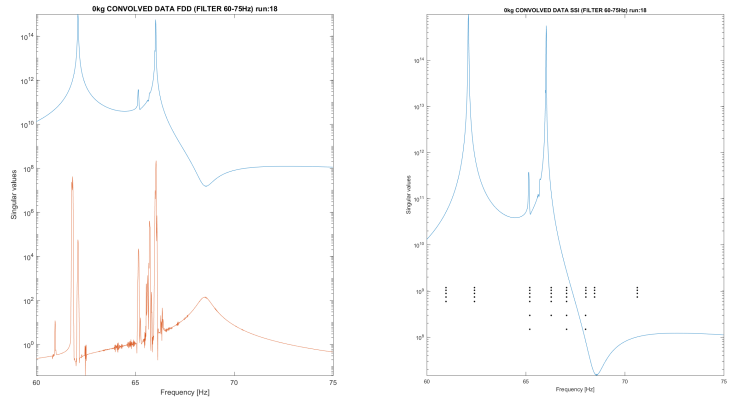


(b) 0kg FDD SSI output, run 17

Figure A3.0kg: Run 17 (segment 1)

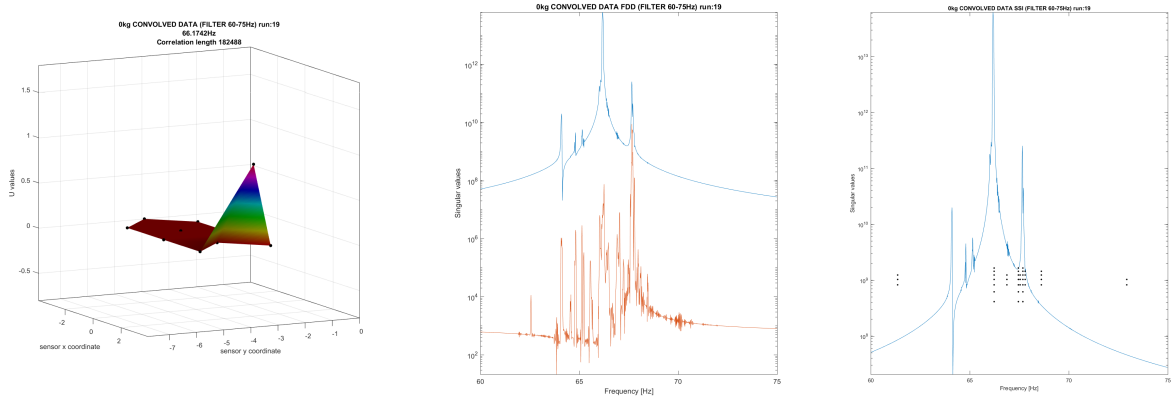


(a) 0kg mode shape, run 18



(b) 0kg FDD SSI output, run 18

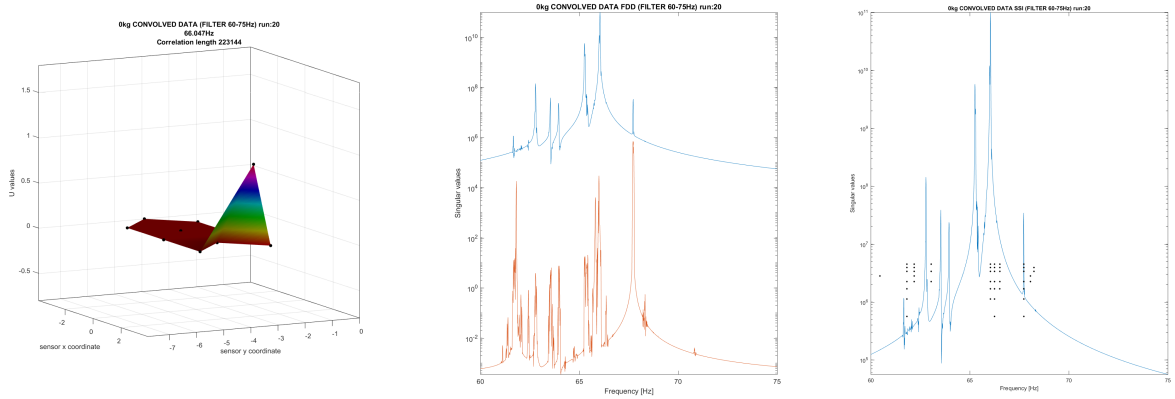
Figure A3.0kg: Run 18 (segment 1)



(a) 0kg mode shape, run 19

(b) 0kg FDD SSI output, run 19

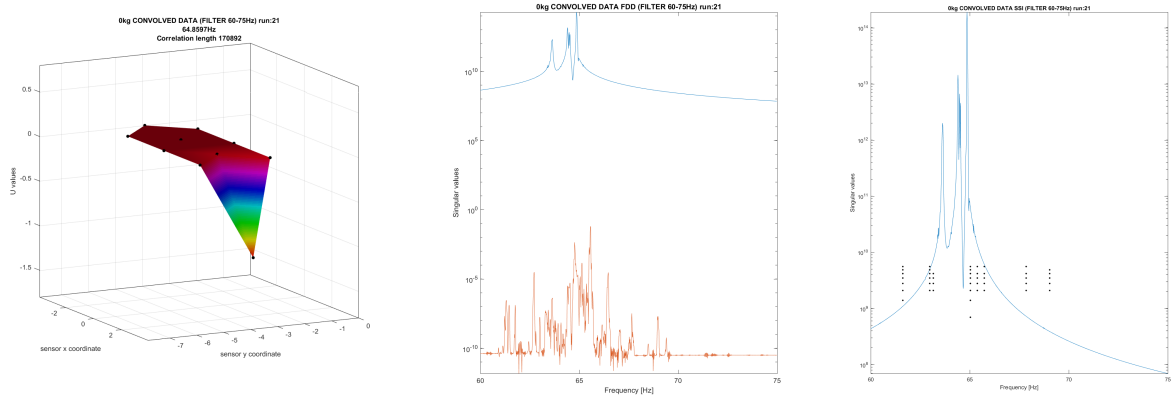
Figure A3.0kg: Run 19 (segment 1)



(a) 0kg mode shape, run 20

(b) 0kg FDD SSI output, run 20

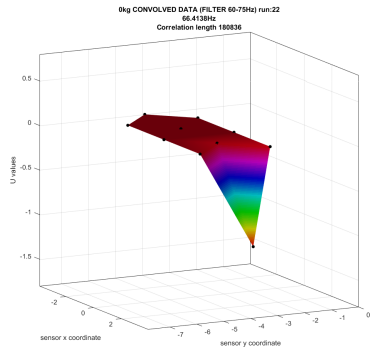
Figure A3.0kg: Run 20 (segment 1)



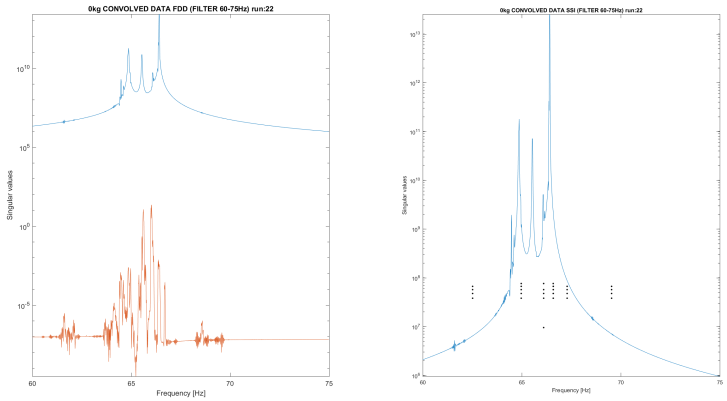
(a) 0kg mode shape, run 21

(b) 0kg FDD SSI output, run 21

Figure A3.0kg: Run 21 (segment 1)

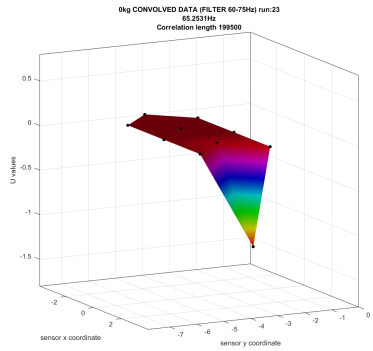


(a) 0kg mode shape, run 22

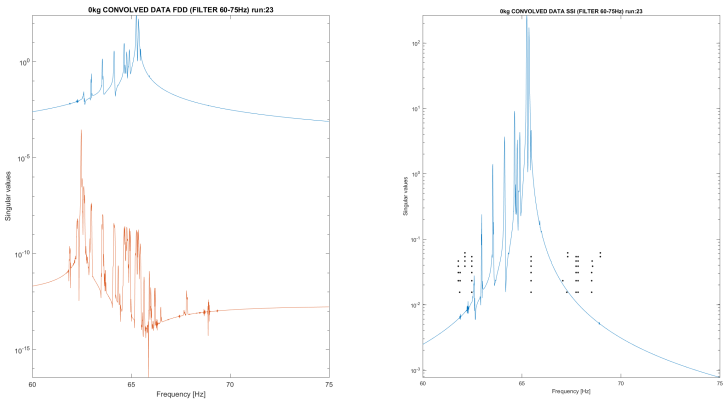


(b) 0kg FDD SSI output, run 22

Figure A3.0kg: Run 22 (segment 1)

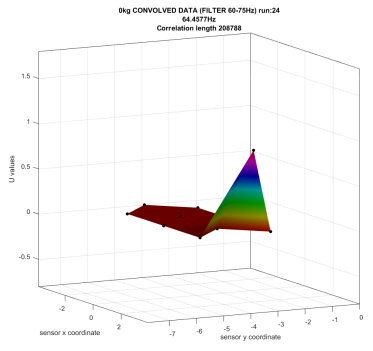


(a) 0kg mode shape, run 23

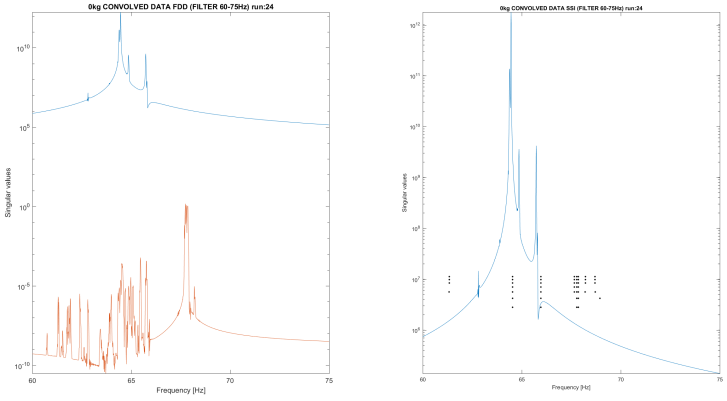


(b) 0kg FDD SSI output, run 23

Figure A3.0kg: Run 23 (segment 1)

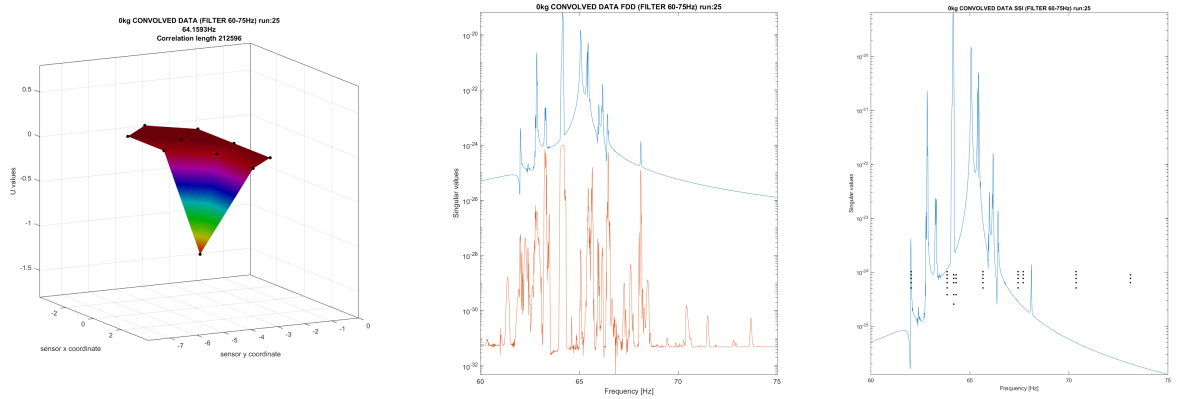


(a) 0kg mode shape, run 24



(b) 0kg FDD SSI output, run 24

Figure A3.0kg: Run 24 (segment 1)

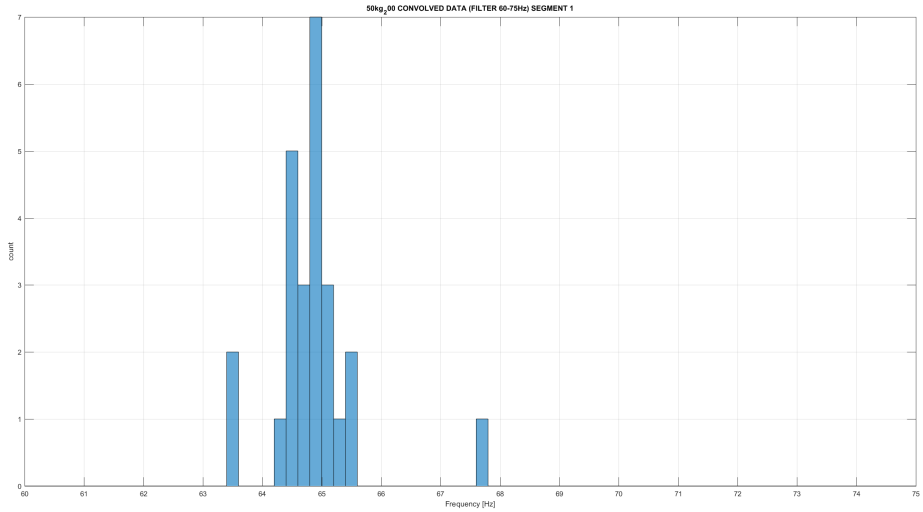


(a) 0kg mode shape, run 25

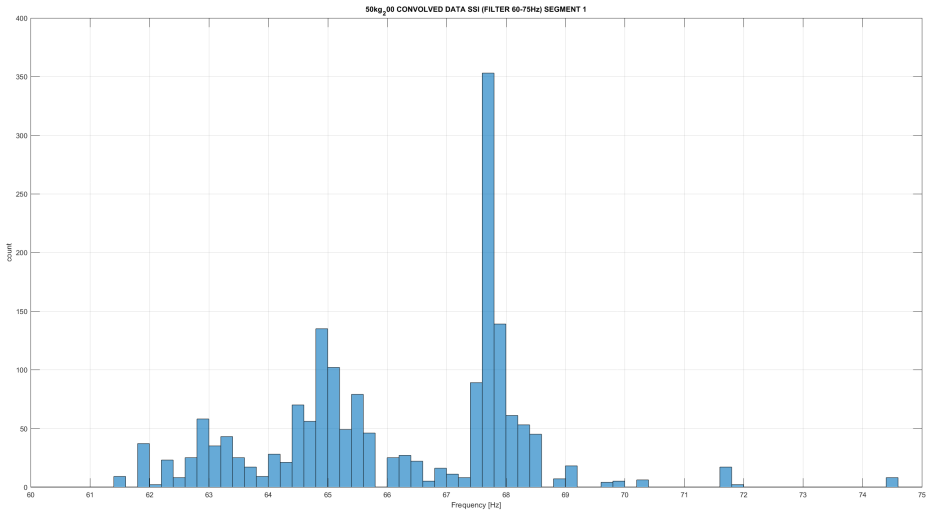
(b) 0kg FDD SSI output, run 25

Figure A3.0kg: Run 25 (segment 1)

50kg data segment 1

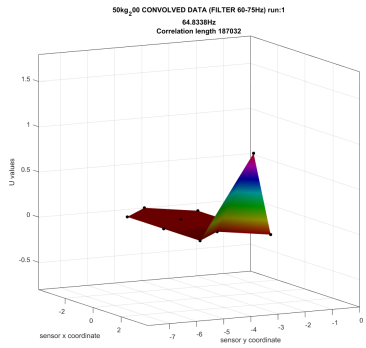


(a) 50kg FDD histogram

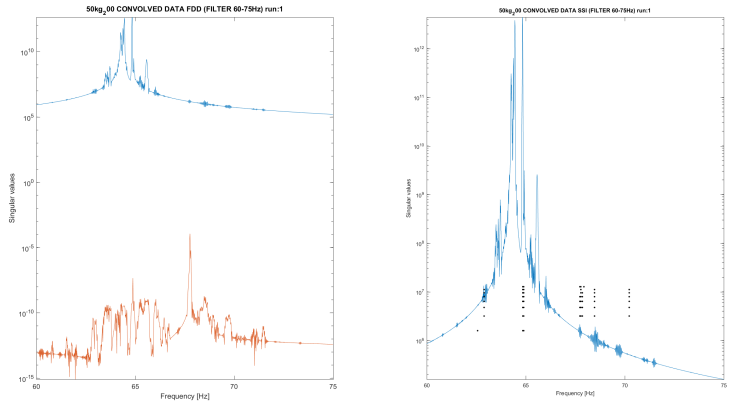


(b) 50kg SSI histogram

Figure A3.50kg: Histograms of identified modes, 50kg data (segment 1)

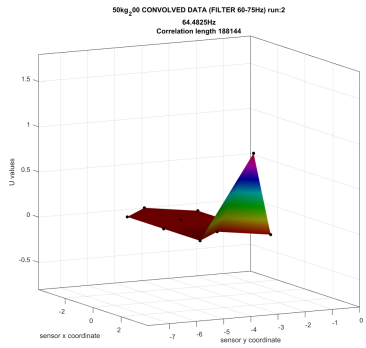


(a) 50kg mode shape, run 1

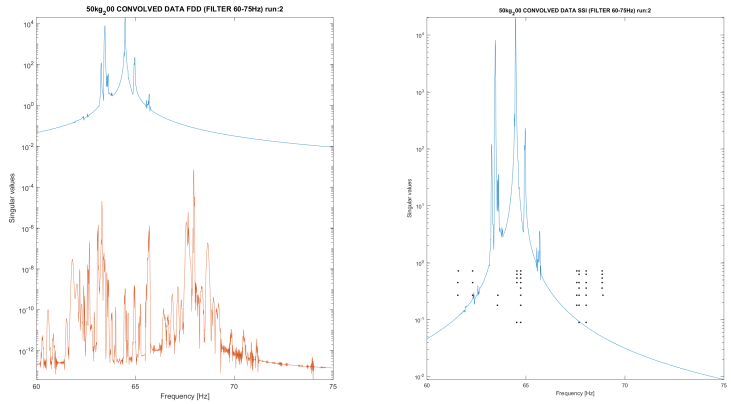


(b) 50kg FDD SSI output, run 1

Figure A3.50kg: Run 1 (segment 1)

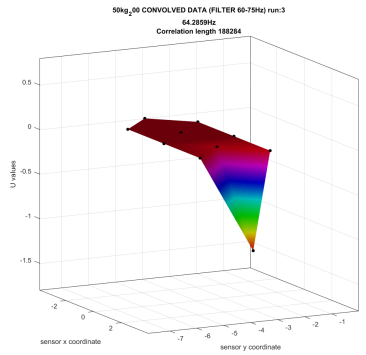


(a) 50kg mode shape, run 2

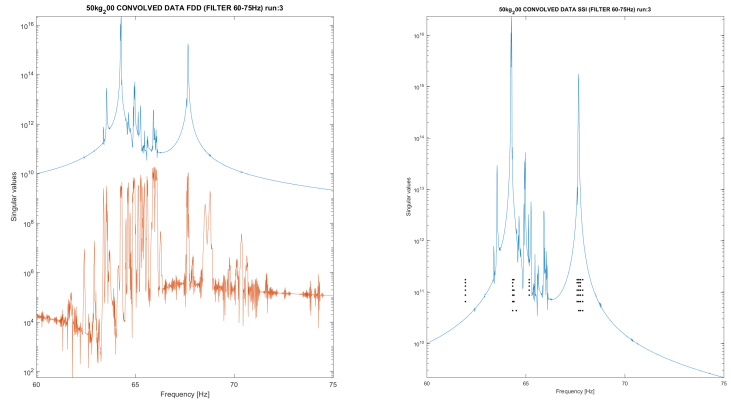


(b) 50kg FDD SSI output, run 2

Figure A3.50kg: Run 2 (segment 1)

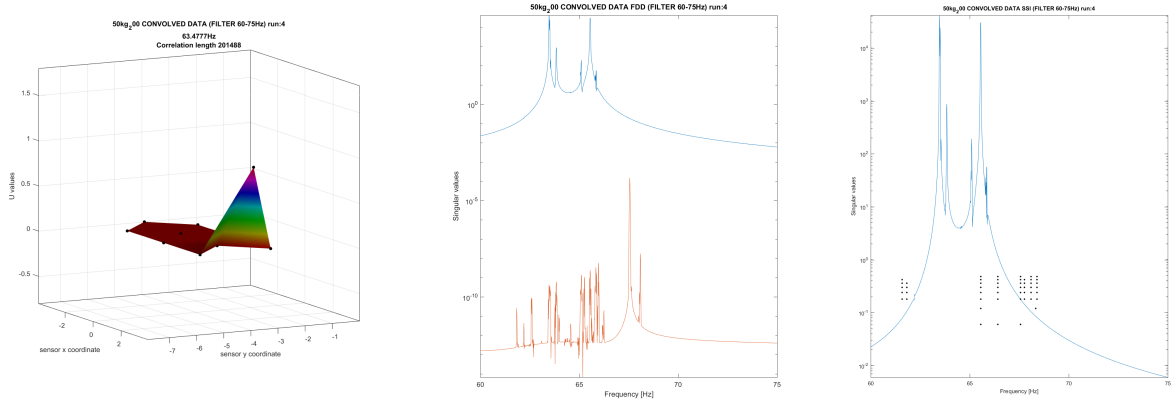


(a) 50kg mode shape, run 3



(b) 50kg FDD SSI output, run 3

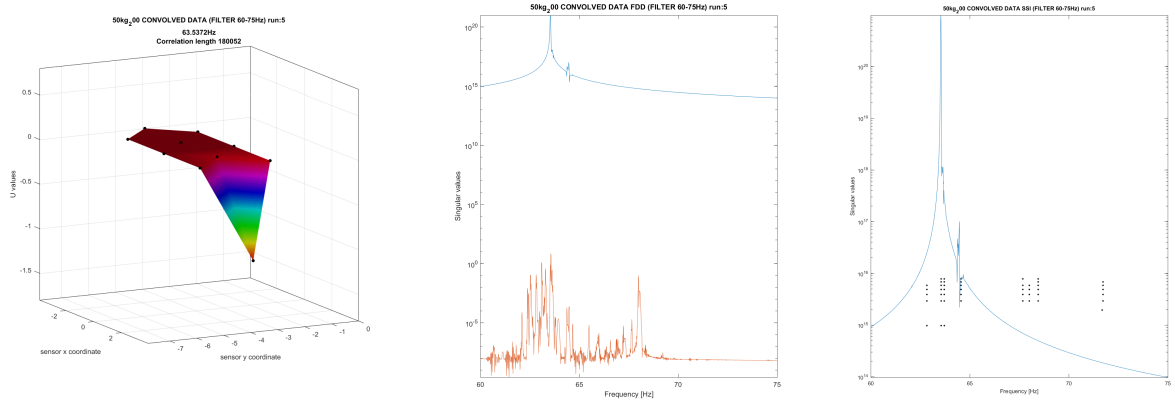
Figure A3.50kg: Run 3 (segment 1)



(a) 50kg mode shape, run 4

(b) 50kg FDD SSI output, run 4

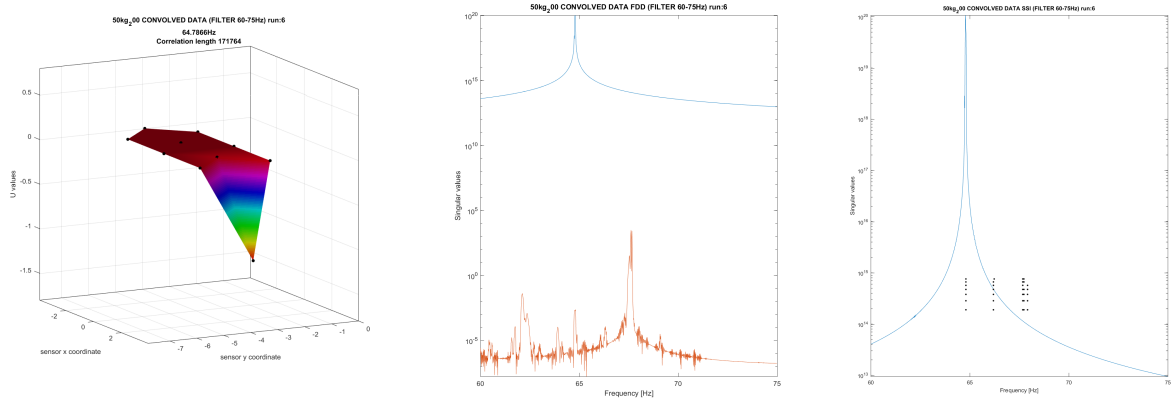
Figure A3.50kg: Run 4 (segment 1)



(a) 50kg mode shape, run 5

(b) 50kg FDD SSI output, run 5

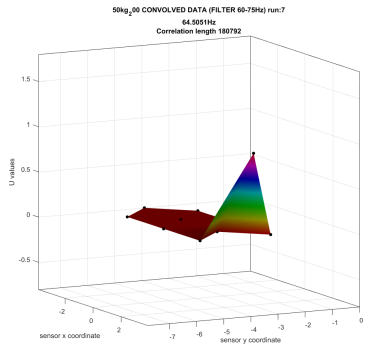
Figure A3.50kg: Run 5 (segment 1)



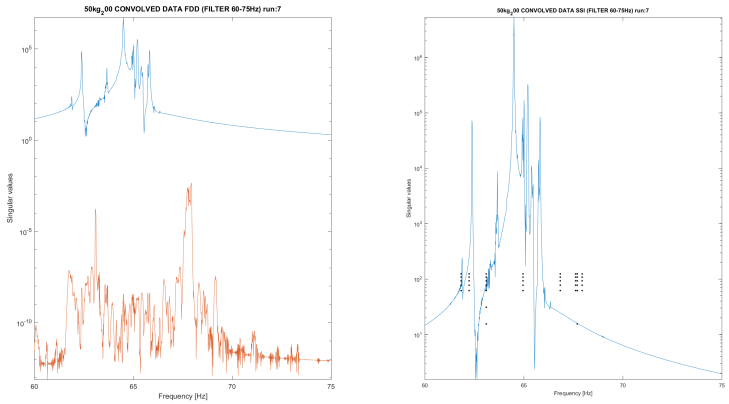
(a) 50kg mode shape, run 6

(b) 50kg FDD SSI output, run 6

Figure A3.50kg: Run 6 (segment 1)

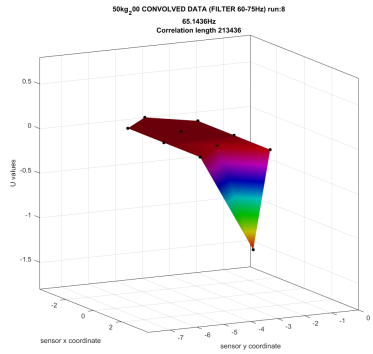


(a) 50kg mode shape, run 7

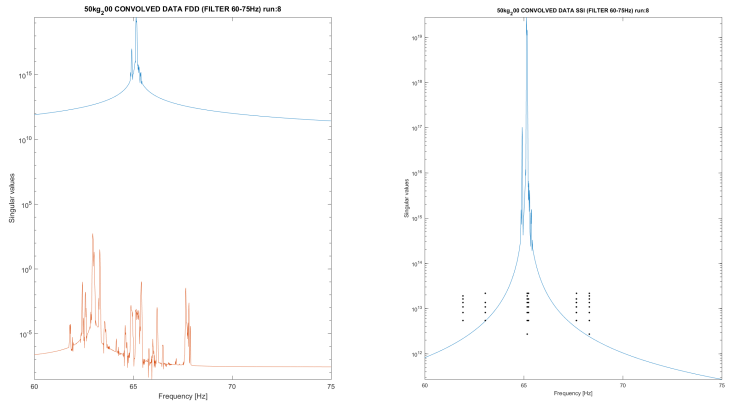


(b) 50kg FDD SSI output, run 7

Figure A3.50kg: Run 7 (segment 1)

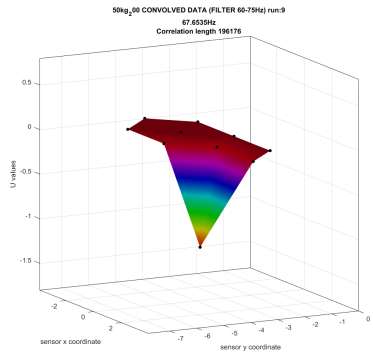


(a) 50kg mode shape, run 8

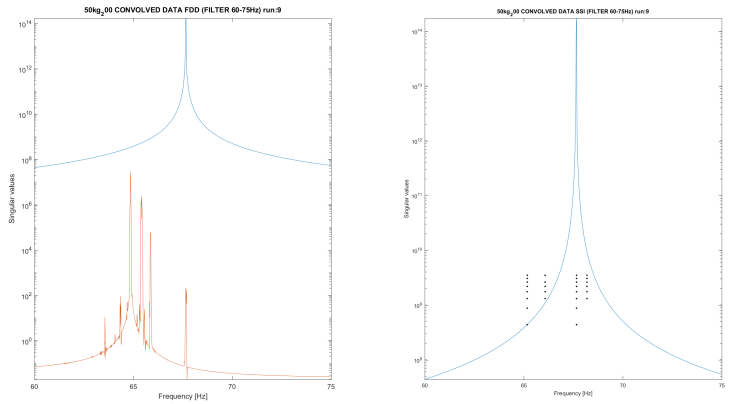


(b) 50kg FDD SSI output, run 8

Figure A3.50kg: Run 8 (segment 1)

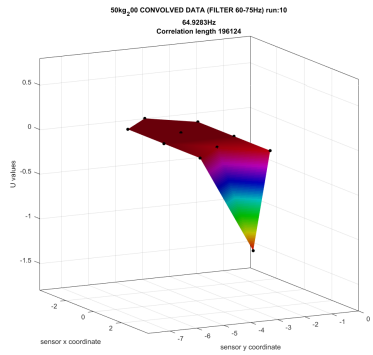


(a) 50kg mode shape, run 9

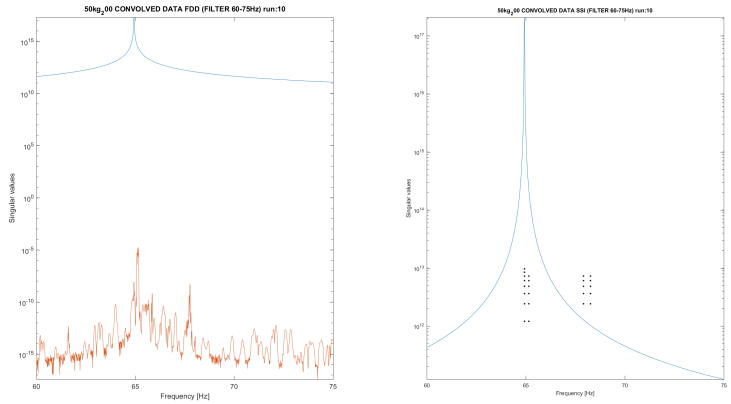


(b) 50kg FDD SSI output, run 9

Figure A3.50kg: Run 9 (segment 1)

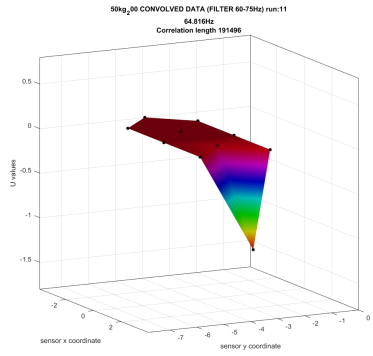


(a) 50kg mode shape, run 10

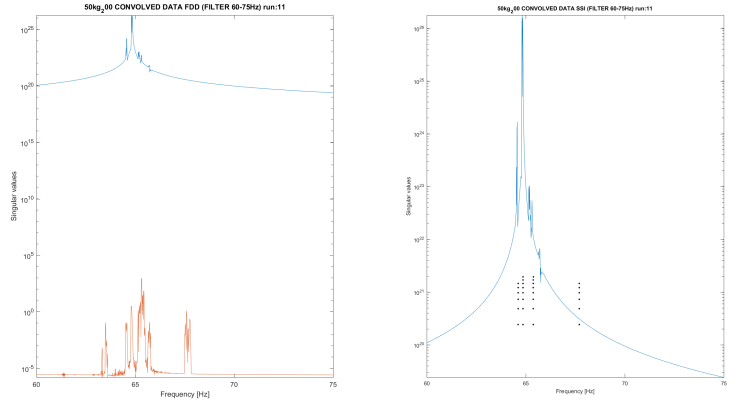


(b) 50kg FDD SSI output, run 10

Figure A3.50kg: Run 10 (segment 1)

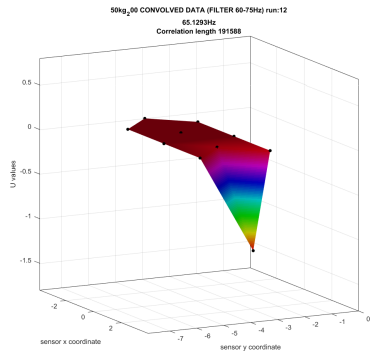


(a) 50kg mode shape, run 11

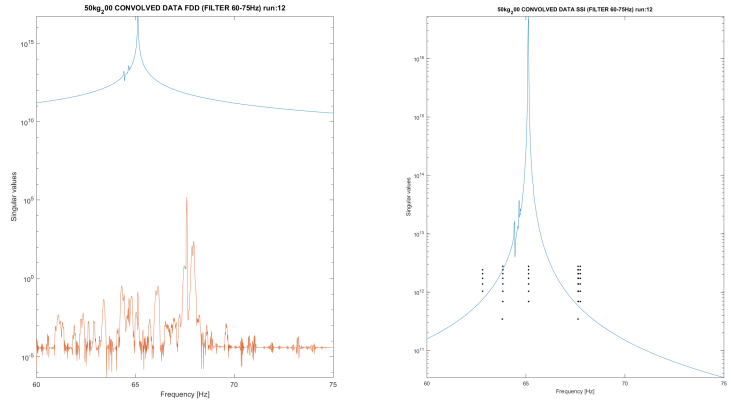


(b) 50kg FDD SSI output, run 11

Figure A3.50kg: Run 11 (segment 1)

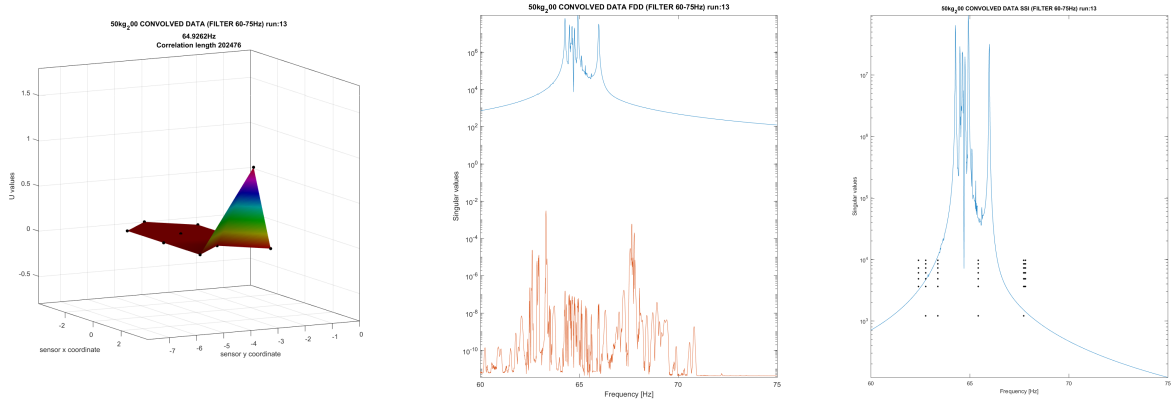


(a) 50kg mode shape, run 12



(b) 50kg FDD SSI output, run 12

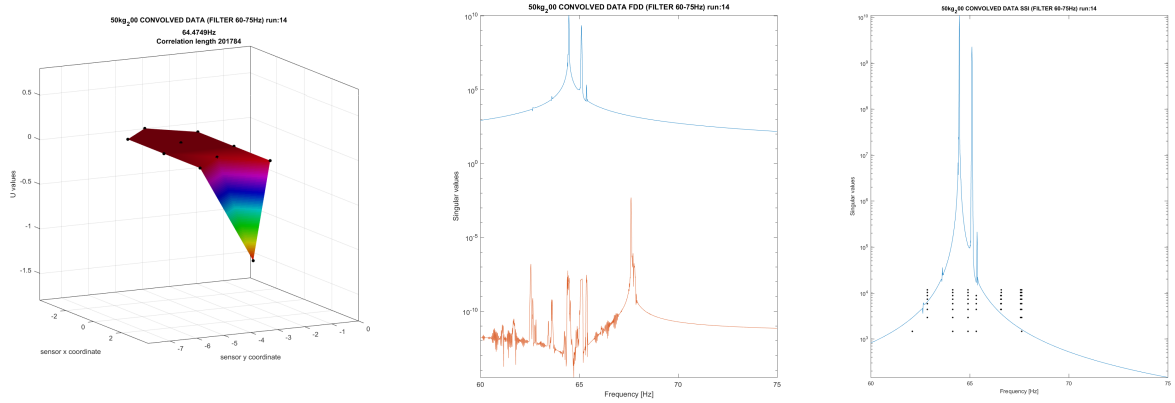
Figure A3.50kg: Run 12 (segment 1)



(a) 50kg mode shape, run 13

(b) 50kg FDD SSI output, run 13

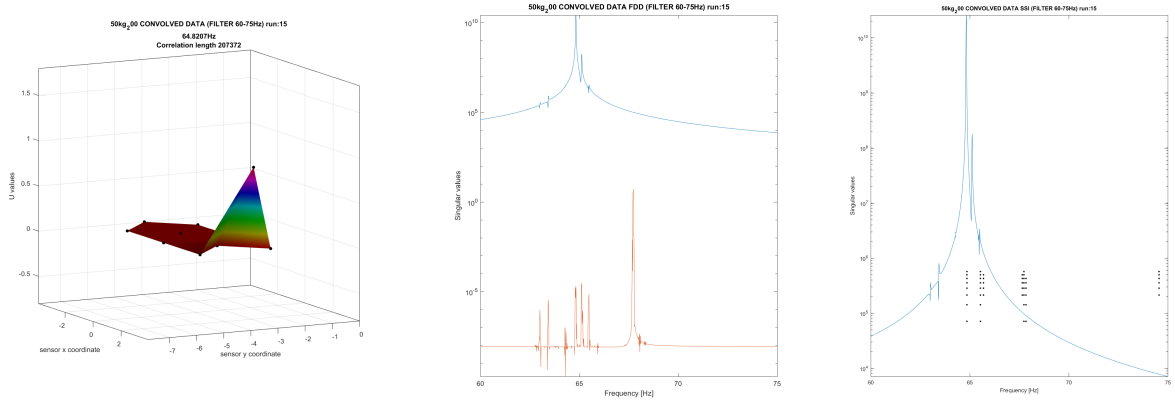
Figure A3.50kg: Run 13 (segment 1)



(a) 50kg mode shape, run 14

(b) 50kg FDD SSI output, run 14

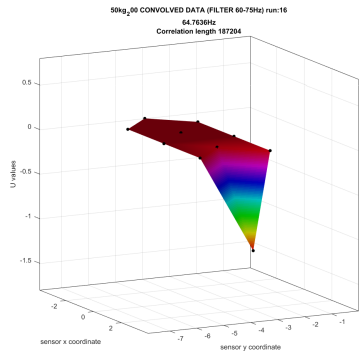
Figure A3.50kg: Run 14 (segment 1)



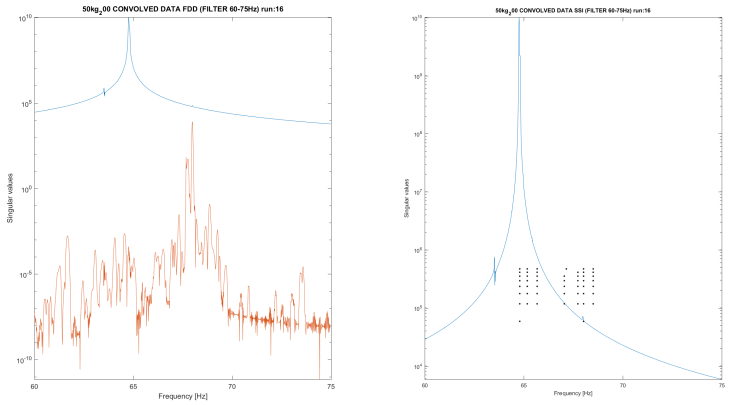
(a) 50kg mode shape, run 15

(b) 50kg FDD SSI output, run 15

Figure A3.50kg: Run 15 (segment 1)

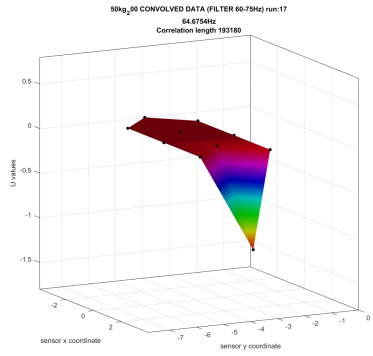


(a) 50kg mode shape, run 16

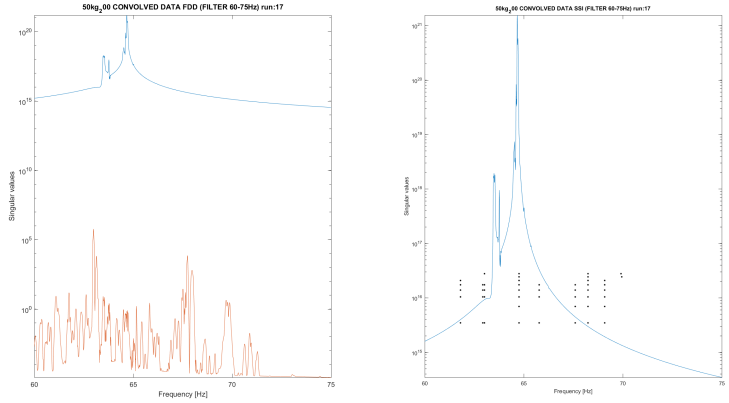


(b) 50kg FDD SSI output, run 16

Figure A3.50kg: Run 16 (segment 1)

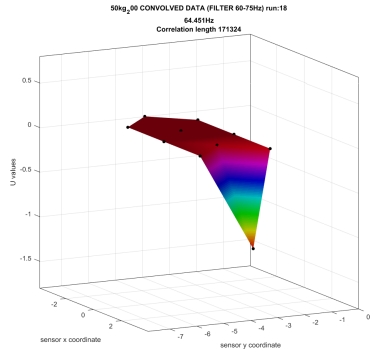


(a) 50kg mode shape, run 17

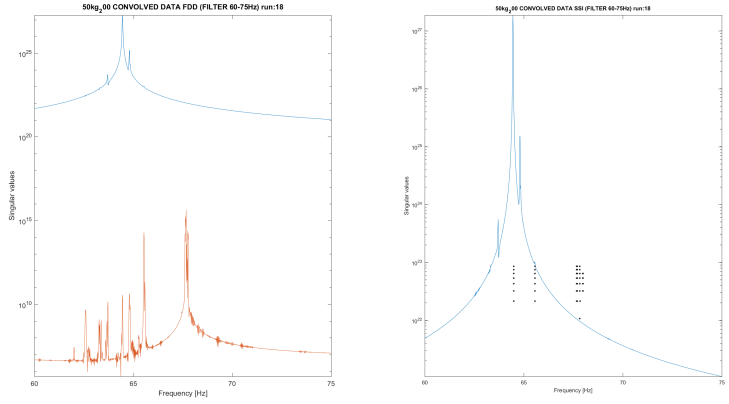


(b) 50kg FDD SSI output, run 17

Figure A3.50kg: Run 17 (segment 1)

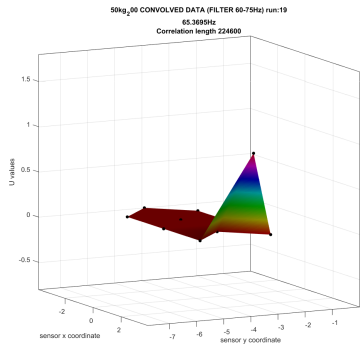


(a) 50kg mode shape, run 18

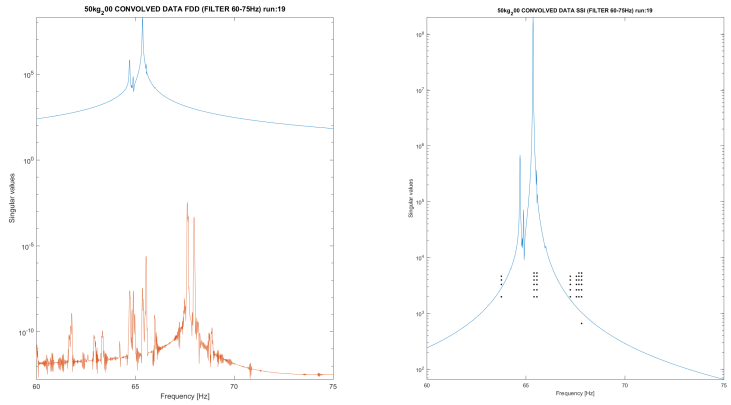


(b) 50kg FDD SSI output, run 18

Figure A3.50kg: Run 18 (segment 1)

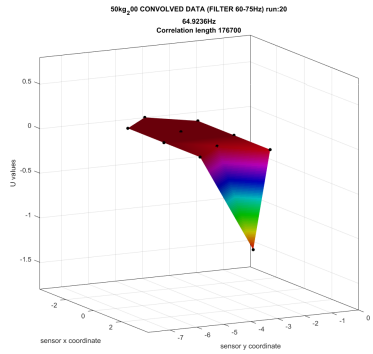


(a) 50kg mode shape, run 19

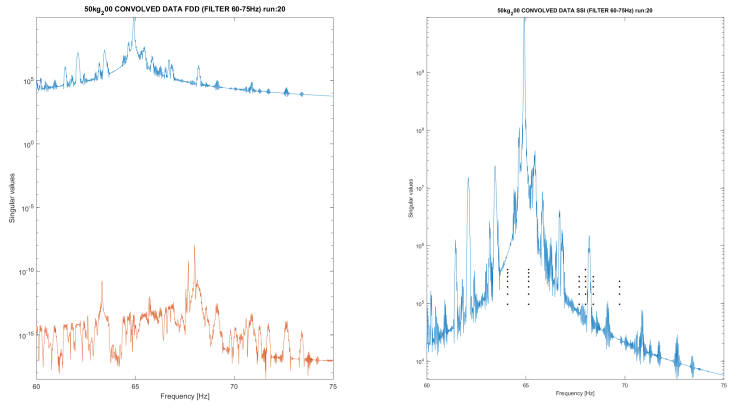


(b) 50kg FDD SSI output, run 19

Figure A3.50kg: Run 19 (segment 1)

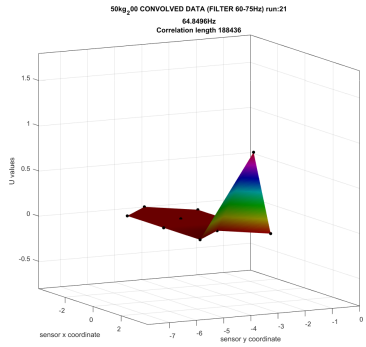


(a) 50kg mode shape, run 20

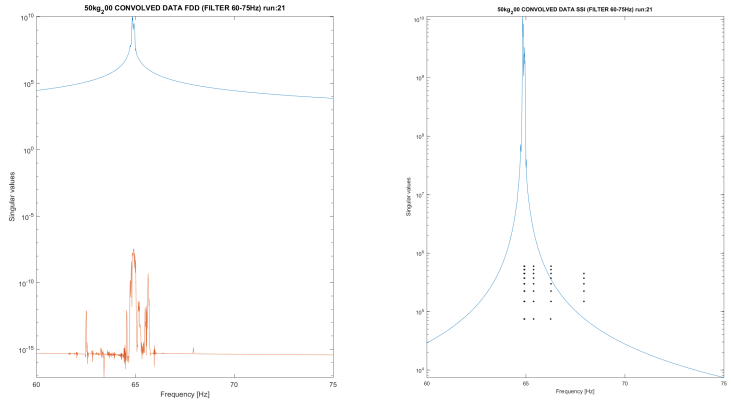


(b) 50kg FDD SSI output, run 20

Figure A3.50kg: Run 20 (segment 1)

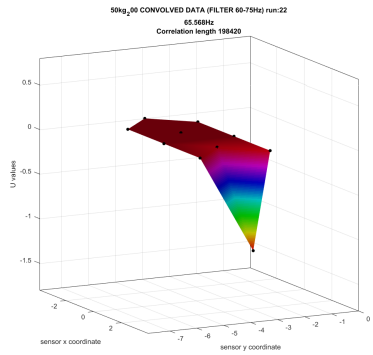


(a) 50kg mode shape, run 21

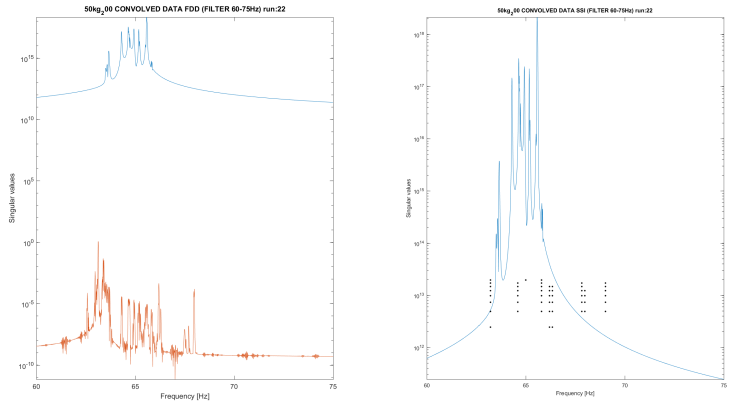


(b) 50kg FDD SSI output, run 21

Figure A3.50kg: Run 21 (segment 1)

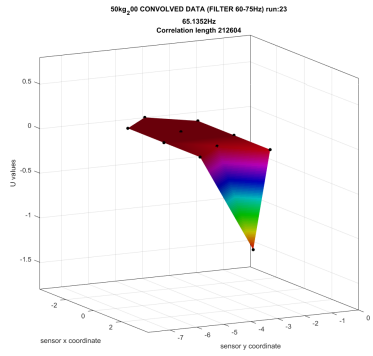


(a) 50kg mode shape, run 22

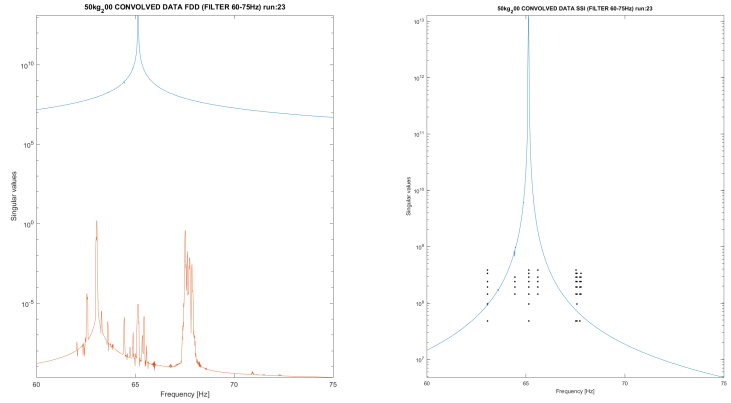


(b) 50kg FDD SSI output, run 22

Figure A3.50kg: Run 22 (segment 1)

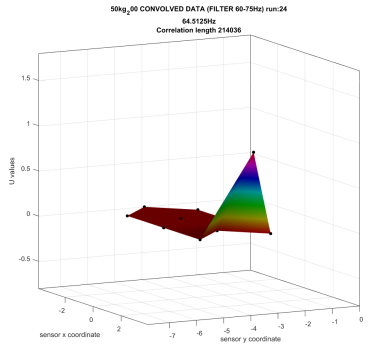


(a) 50kg mode shape, run 23

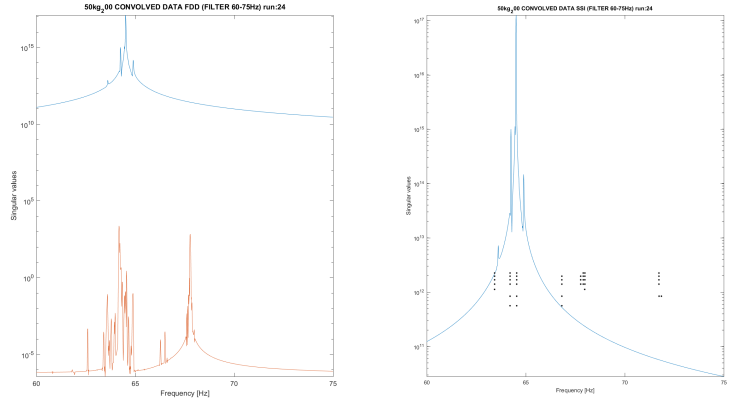


(b) 50kg FDD SSI output, run 23

Figure A3.50kg: Run 23 (segment 1)

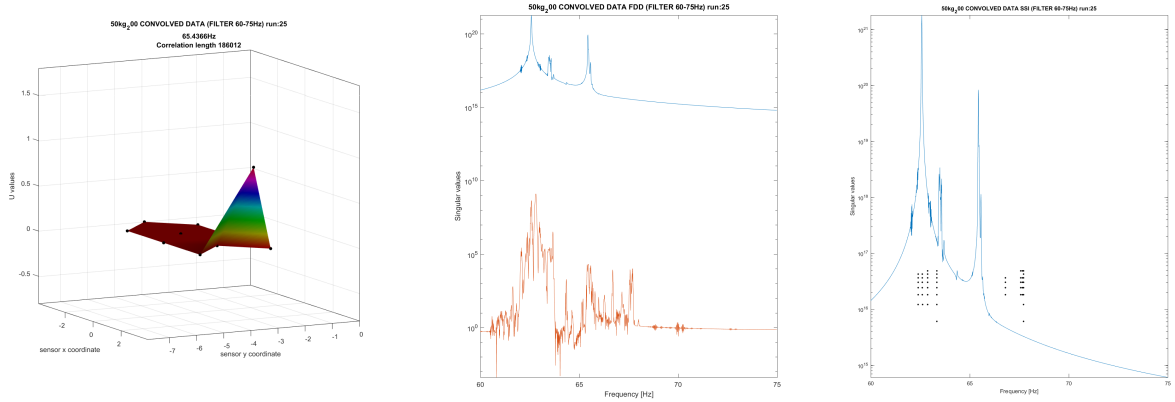


(a) 50kg mode shape, run 24



(b) 50kg FDD SSI output, run 24

Figure A3.50kg: Run 24 (segment 1)

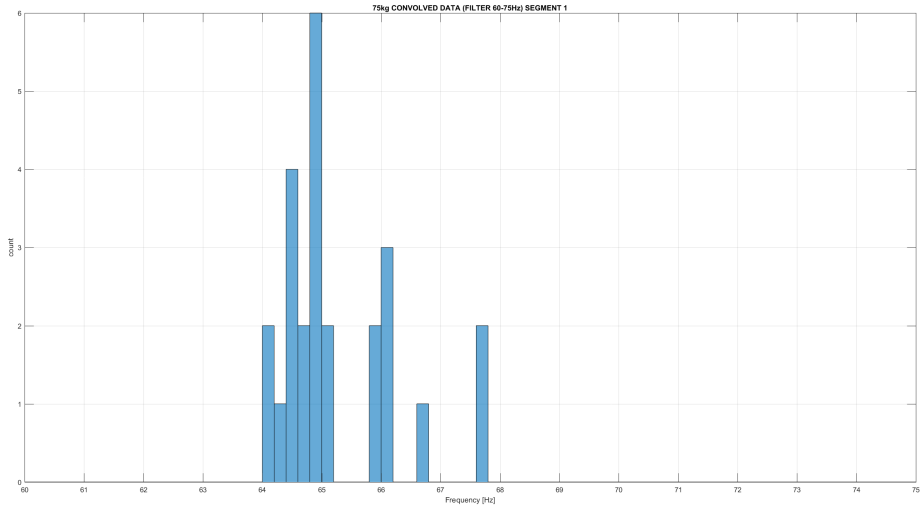


(a) 50kg mode shape, run 25

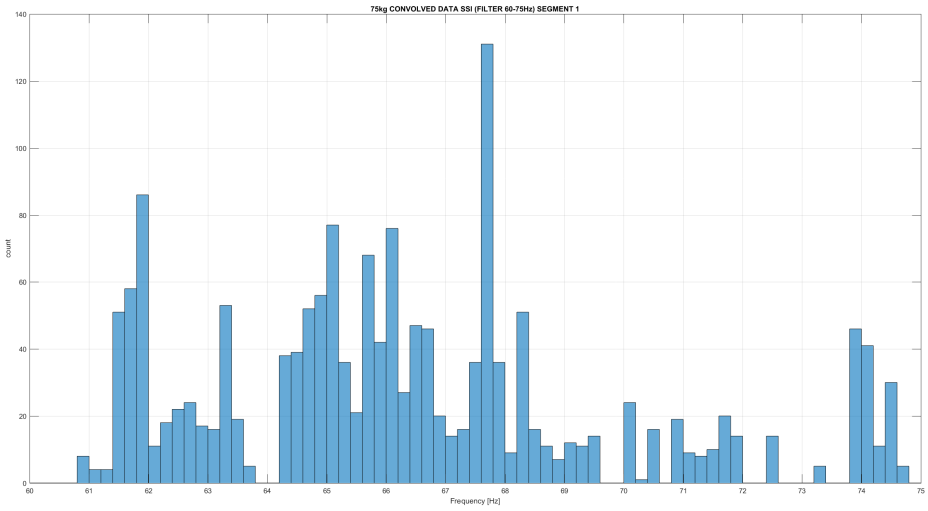
(b) 50kg FDD SSI output, run 25

Figure A3.50kg: Run 25 (segment 1)

75kg data segment 1

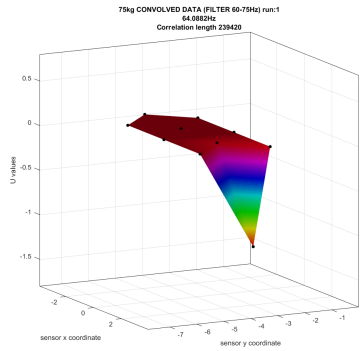


(a) 75kg FDD histogram

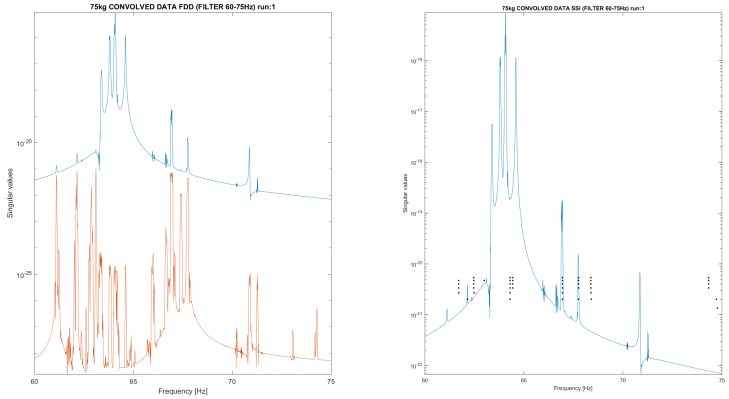


(b) 75kg SSI histogram

Figure A3.75kg: Histograms of identified modes, 75kg data (segment 1)

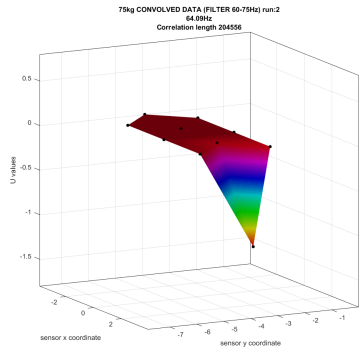


(a) 75kg mode shape, run 1

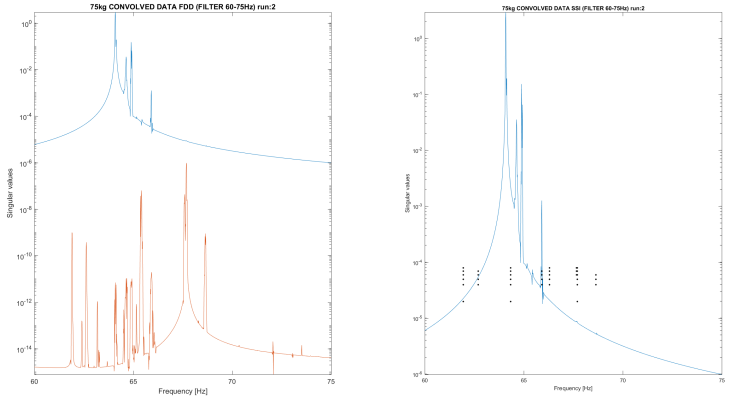


(b) 75kg FDD SSI output, run 1

Figure A3.75kg: Run 1 (segment 1)

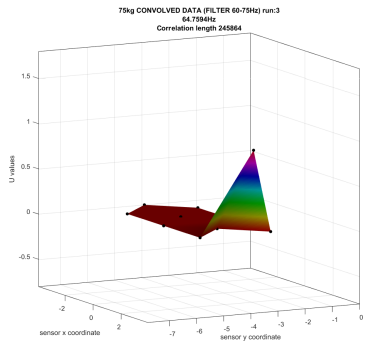


(a) 75kg mode shape, run 2

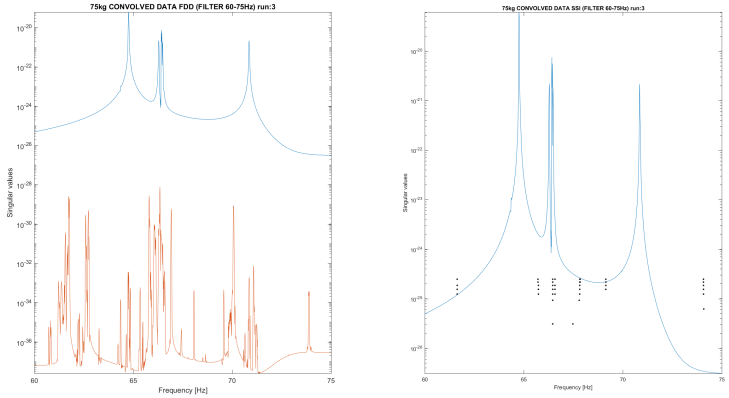


(b) 75kg FDD SSI output, run 2

Figure A3.75kg: Run 2 (segment 1)

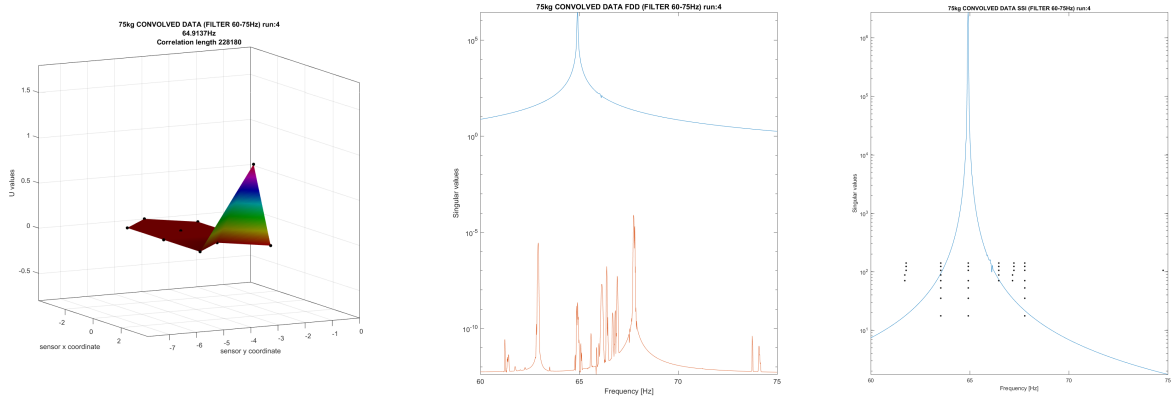


(a) 75kg mode shape, run 3



(b) 75kg FDD SSI output, run 3

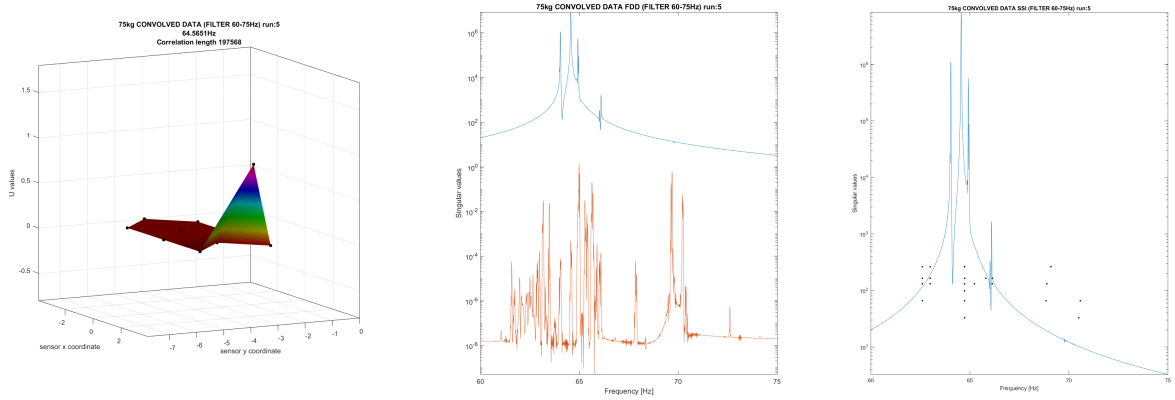
Figure A3.75kg: Run 3 (segment 1)



(a) 75kg mode shape, run 4

(b) 75kg FDD SSI output, run 4

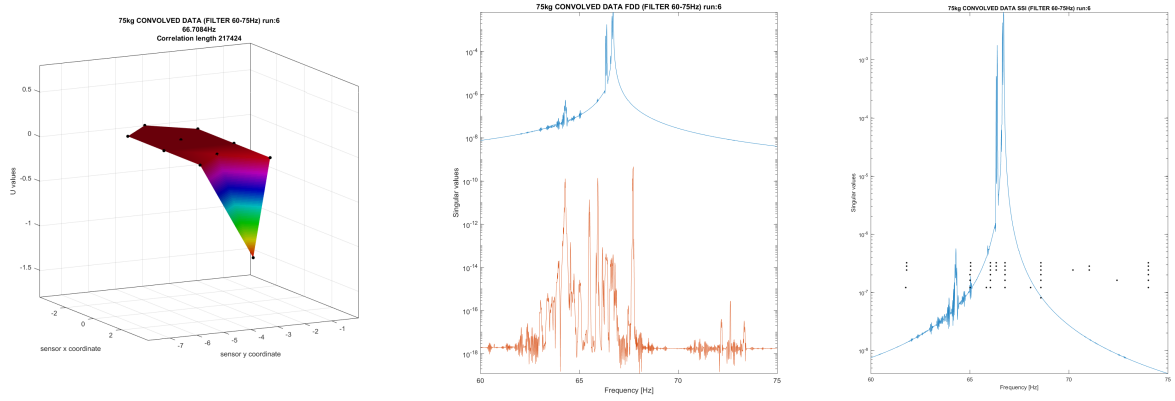
Figure A3.75kg: Run 4 (segment 1)



(a) 75kg mode shape, run 5

(b) 75kg FDD SSI output, run 5

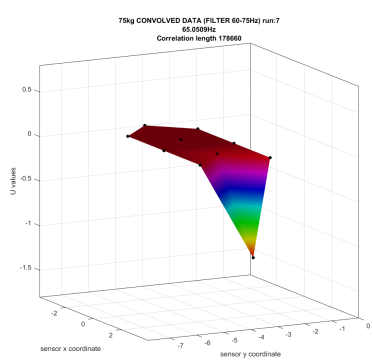
Figure A3.75kg: Run 5 (segment 1)



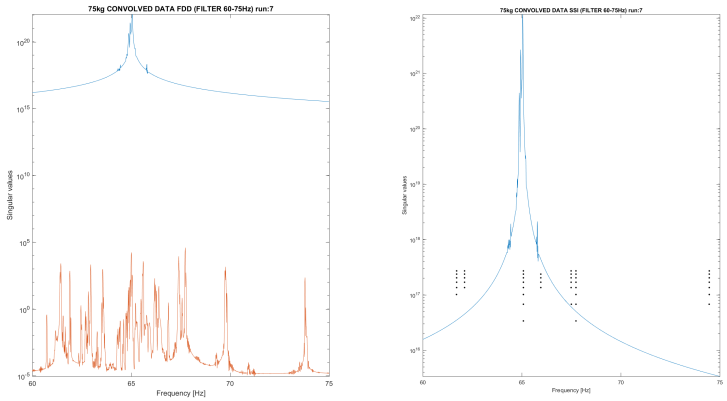
(a) 75kg mode shape, run 6

(b) 75kg FDD SSI output, run 6

Figure A3.75kg: Run 6 (segment 1)

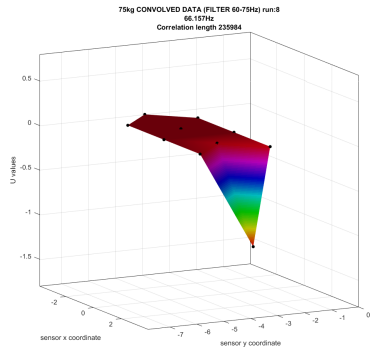


(a) 75kg mode shape, run 7

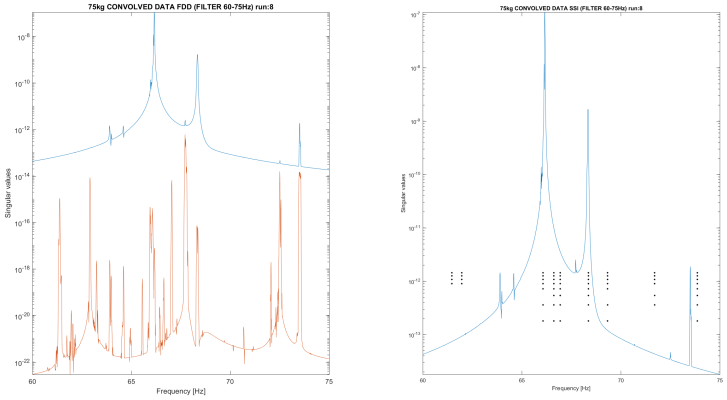


(b) 75kg FDD SSI output, run 7

Figure A3.75kg: Run 7 (segment 1)

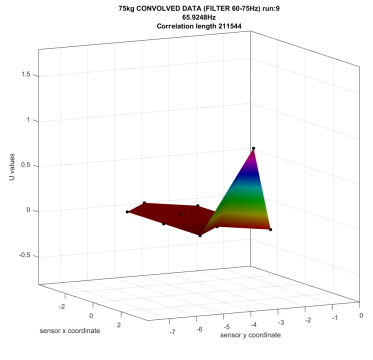


(a) 75kg mode shape, run 8

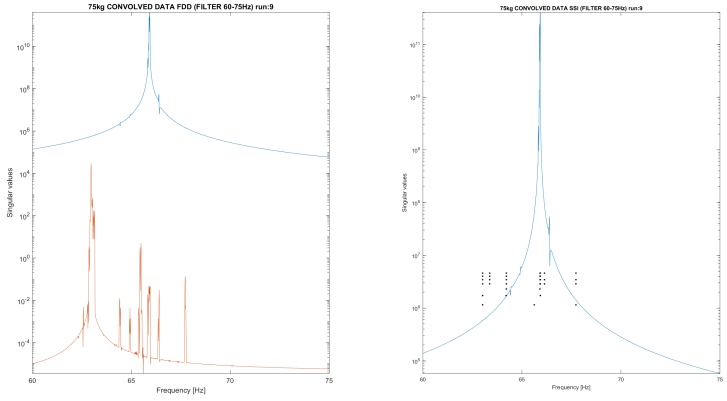


(b) 75kg FDD SSI output, run 8

Figure A3.75kg: Run 8 (segment 1)

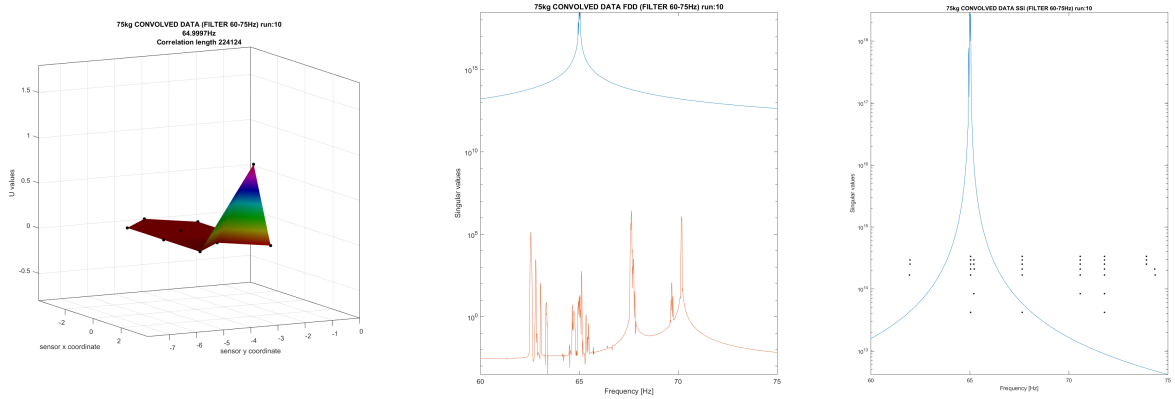


(a) 75kg mode shape, run 9



(b) 75kg FDD SSI output, run 9

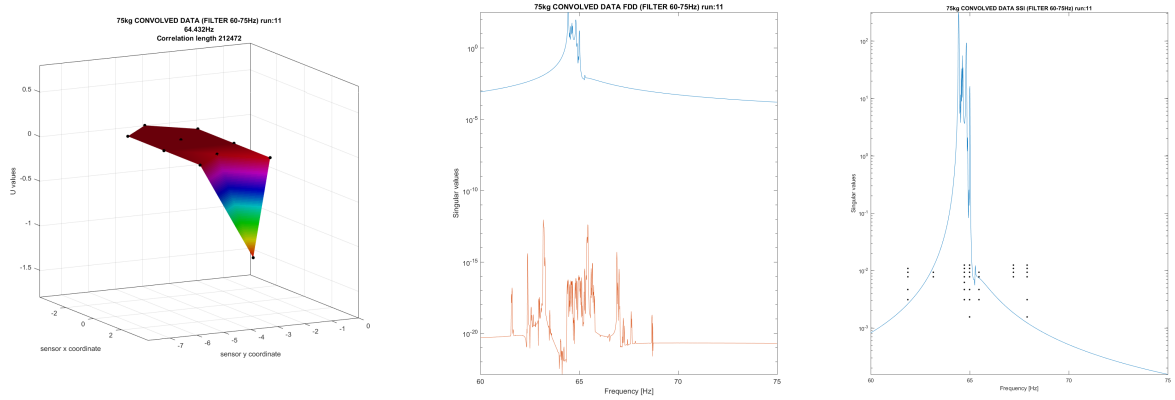
Figure A3.75kg: Run 9 (segment 1)



(a) 75kg mode shape, run 10

(b) 75kg FDD SSI output, run 10

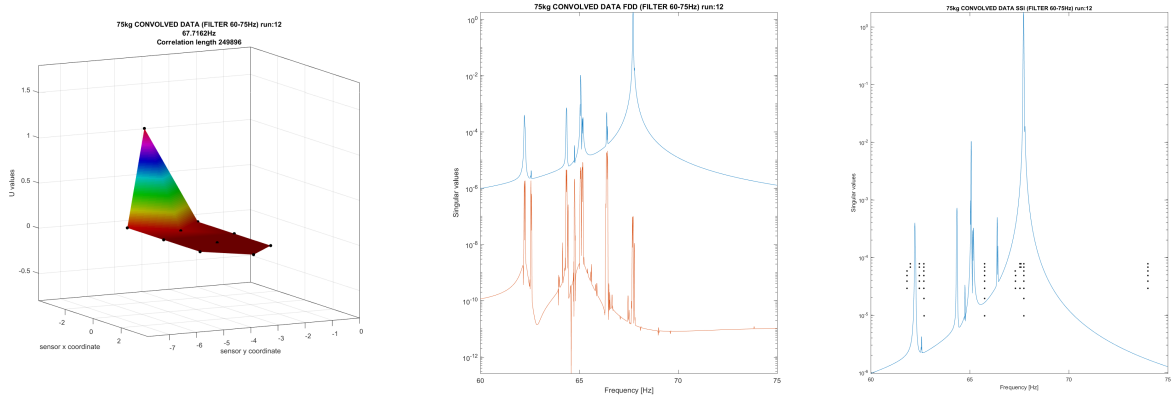
Figure A3.75kg: Run 10 (segment 1)



(a) 75kg mode shape, run 11

(b) 75kg FDD SSI output, run 11

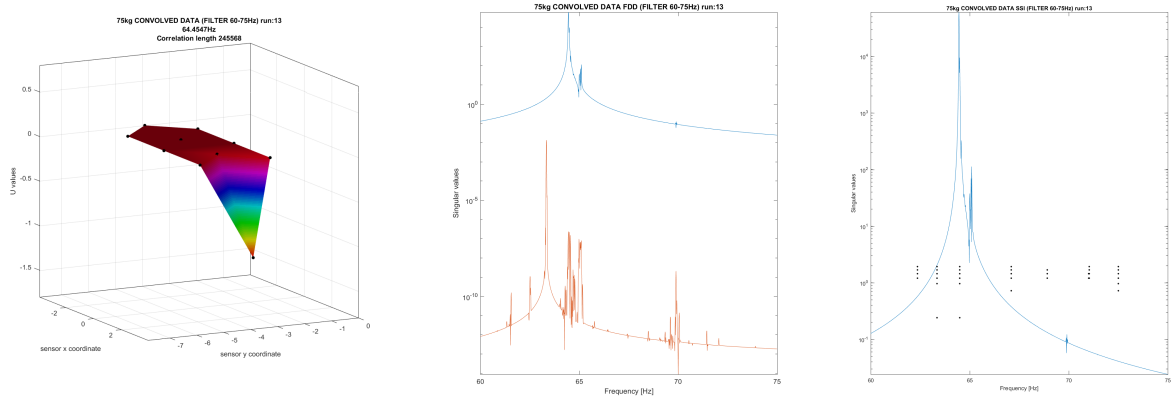
Figure A3.75kg: Run 11 (segment 1)



(a) 75kg mode shape, run 12

(b) 75kg FDD SSI output, run 12

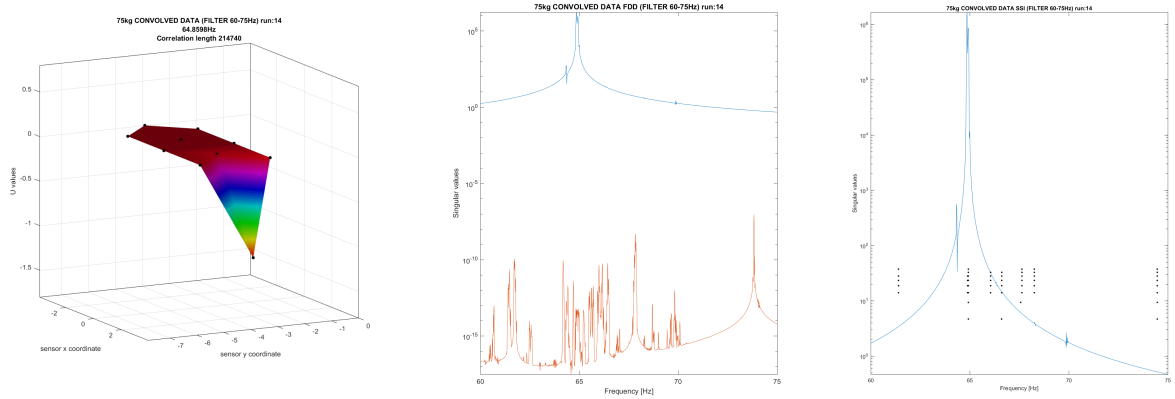
Figure A3.75kg: Run 12 (segment 1)



(a) 75kg mode shape, run 13

(b) 75kg FDD SSI output, run 13

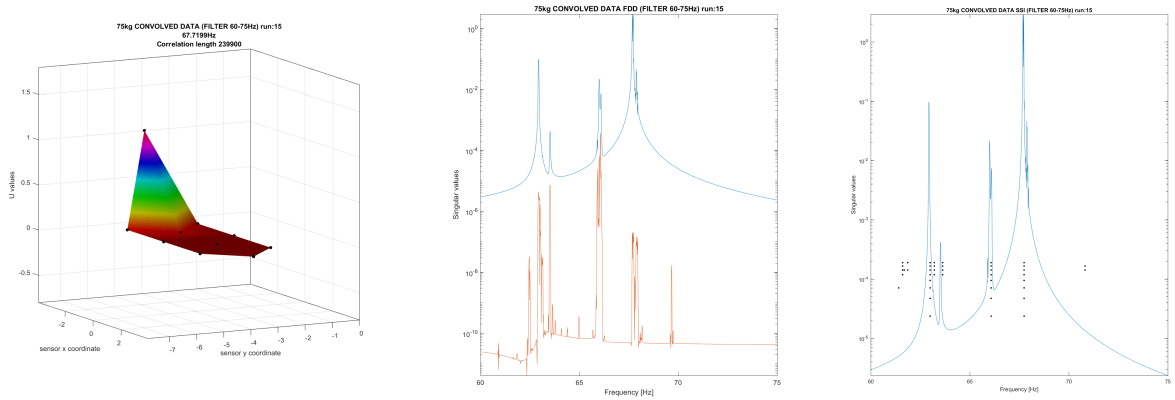
Figure A3.75kg: Run 13 (segment 1)



(a) 75kg mode shape, run 14

(b) 75kg FDD SSI output, run 14

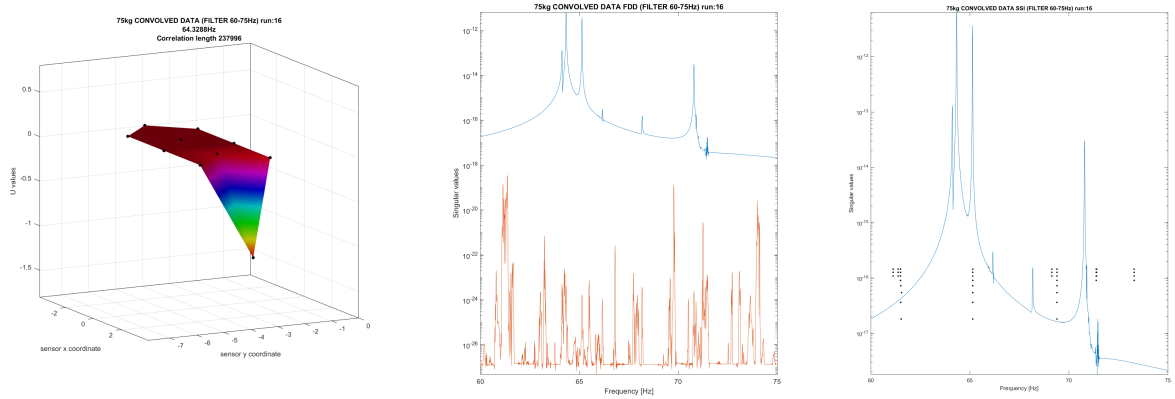
Figure A3.75kg: Run 14 (segment 1)



(a) 75kg mode shape, run 15

(b) 75kg FDD SSI output, run 15

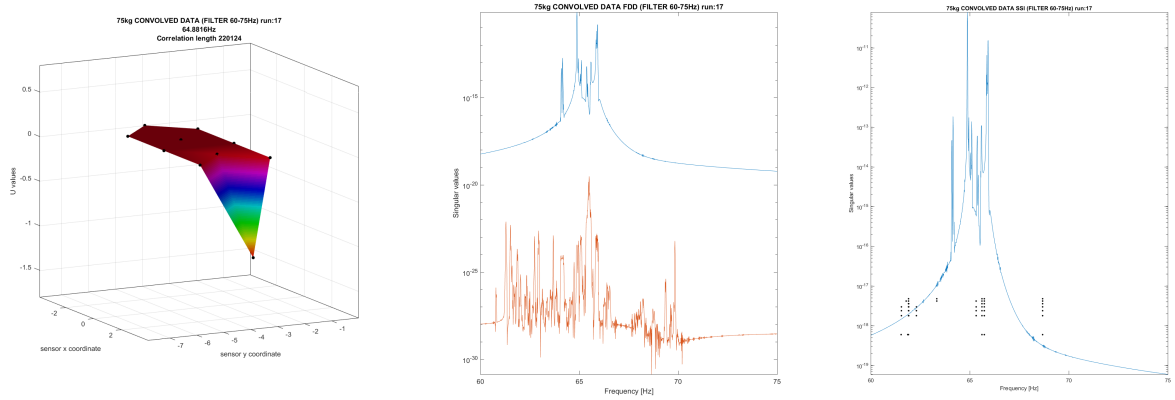
Figure A3.75kg: Run 15 (segment 1)



(a) 75kg mode shape, run 16

(b) 75kg FDD SSI output, run 16

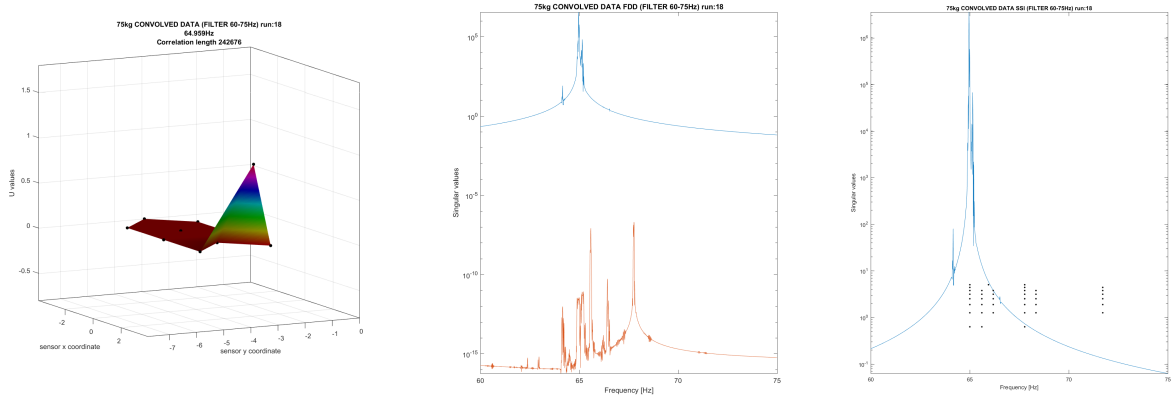
Figure A3.75kg: Run 16 (segment 1)



(a) 75kg mode shape, run 17

(b) 75kg FDD SSI output, run 17

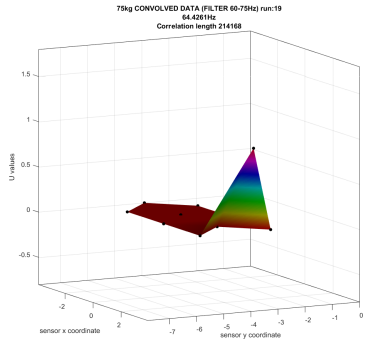
Figure A3.75kg: Run 17 (segment 1)

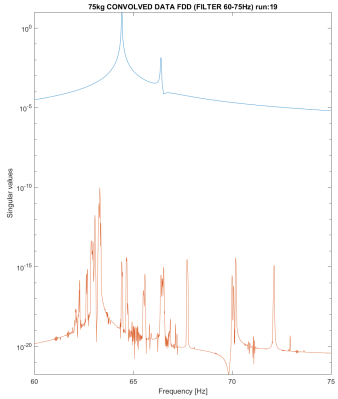


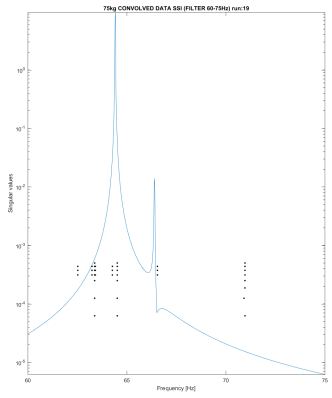
(a) 75kg mode shape, run 18

(b) 75kg FDD SSI output, run 18

Figure A3.75kg: Run 18 (segment 1)



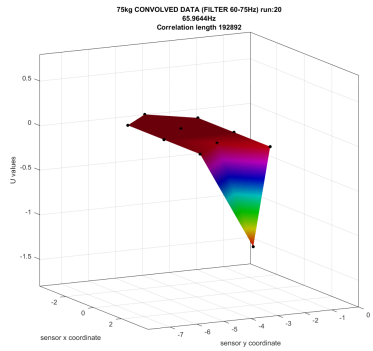


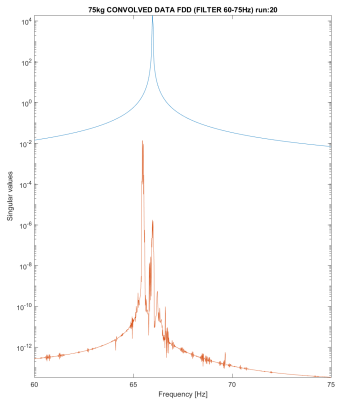


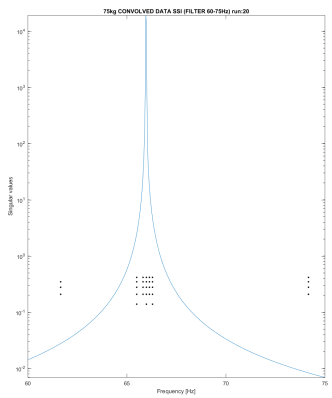
(a) 75kg mode shape, run 19

(b) 75kg FDD SSI output, run 19

Figure A3.75kg: Run 19 (segment 1)



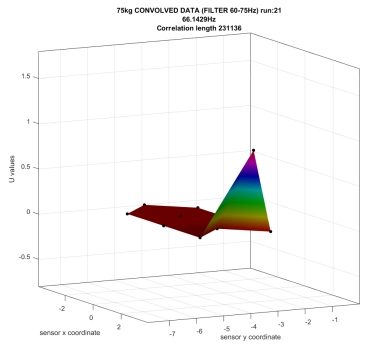


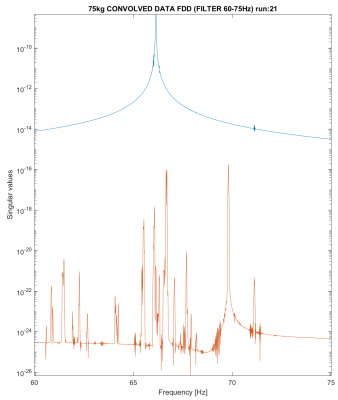


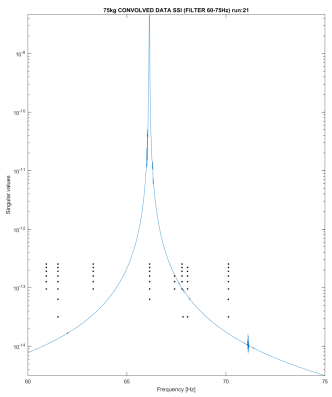
(a) 75kg mode shape, run 20

(b) 75kg FDD SSI output, run 20

Figure A3.75kg: Run 20 (segment 1)



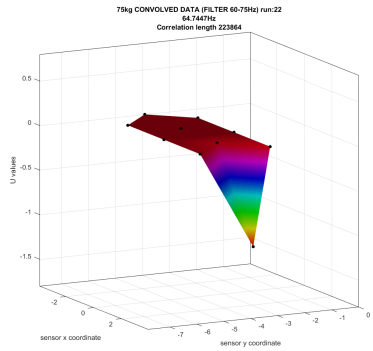




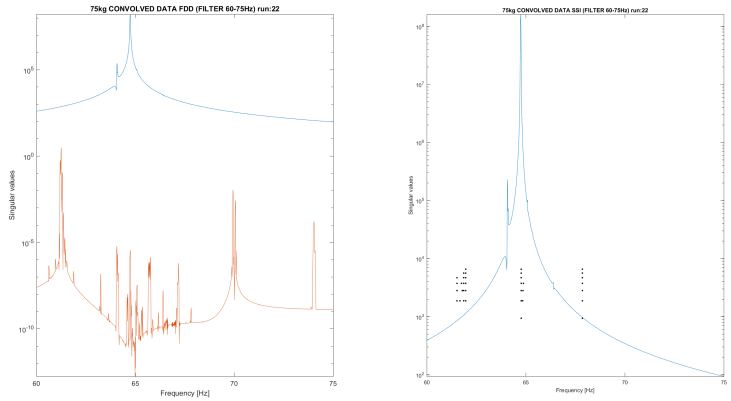
(a) 75kg mode shape, run 21

(b) 75kg FDD SSI output, run 21

Figure A3.75kg: Run 21 (segment 1)

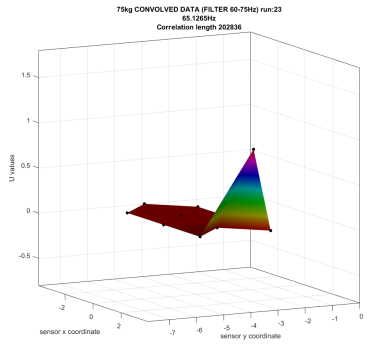


(a) 75kg mode shape, run 22

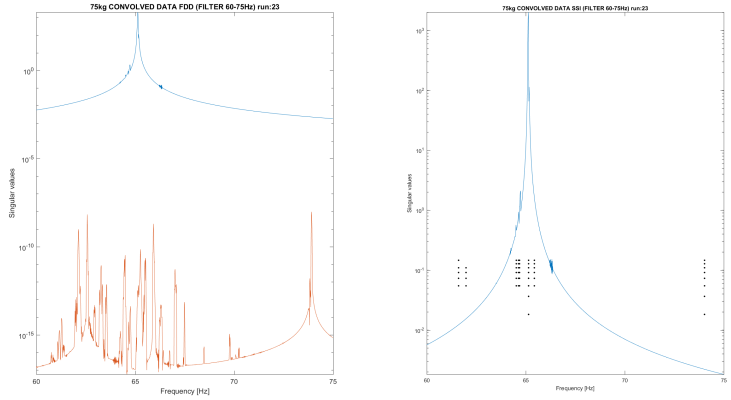


(b) 75kg FDD SSI output, run 22

Figure A3.75kg: Run 22 (segment 1)

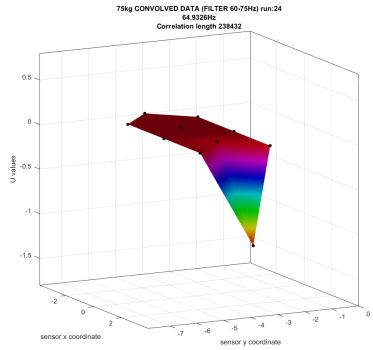


(a) 75kg mode shape, run 23

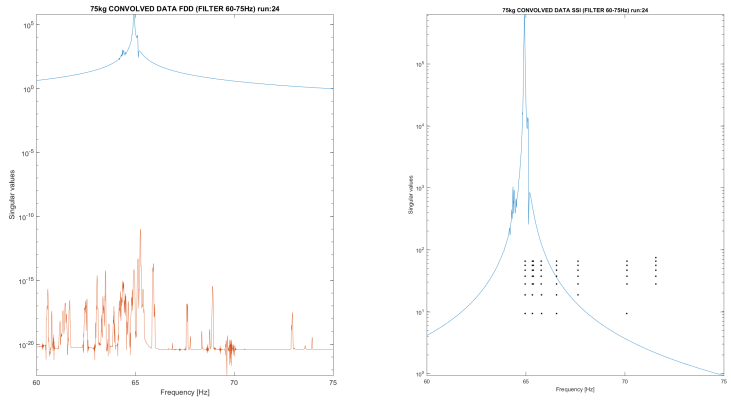


(b) 75kg FDD SSI output, run 23

Figure A3.75kg: Run 23 (segment 1)

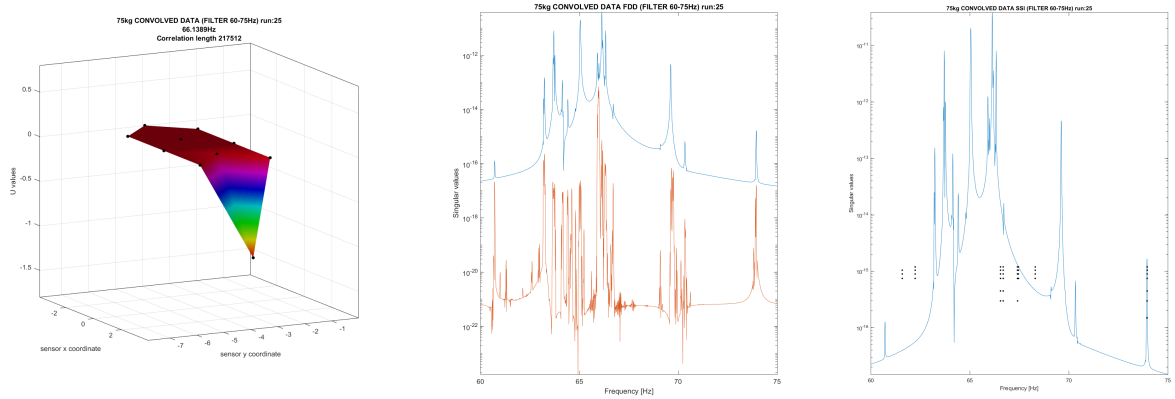


(a) 75kg mode shape, run 24



(b) 75kg FDD SSI output, run 24

Figure A3.75kg: Run 24 (segment 1)

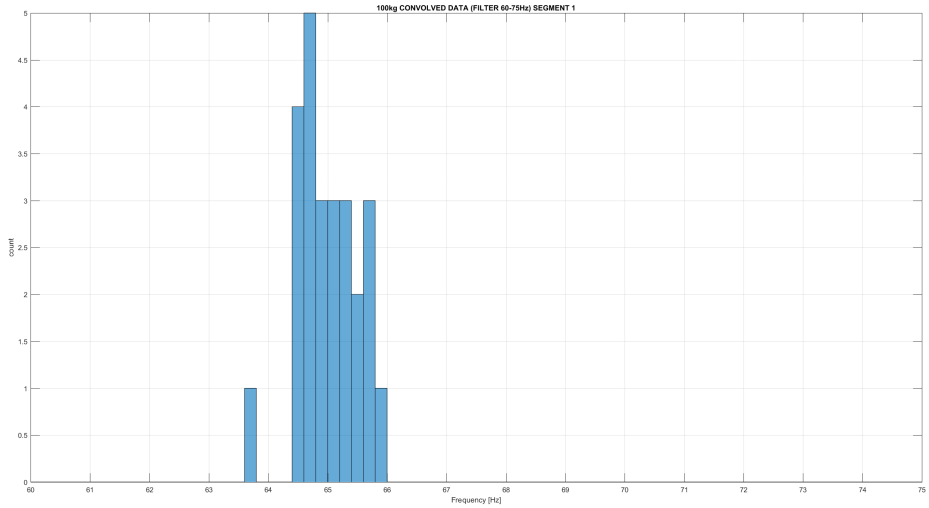


(a) 75kg mode shape, run 25

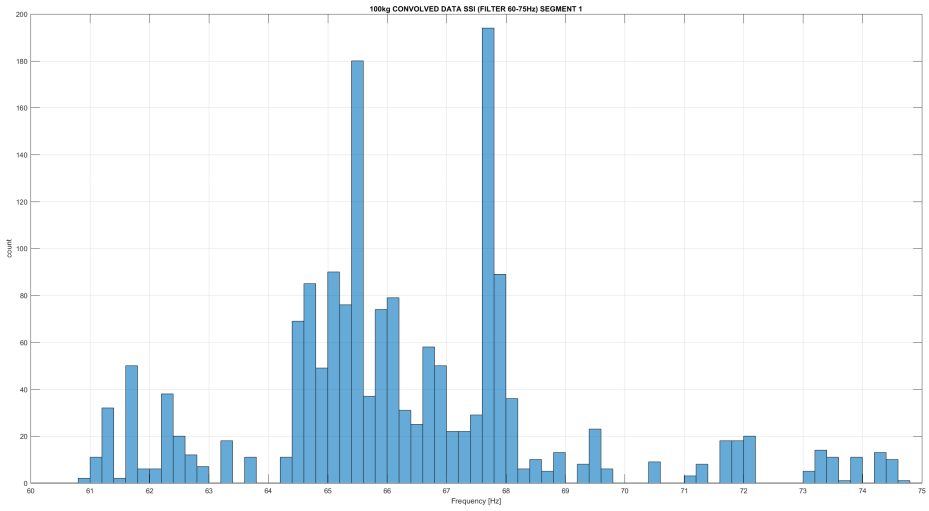
(b) 75kg FDD SSI output, run 25

Figure A3.75kg: Run 25 (segment 1)

100kg data segment 1

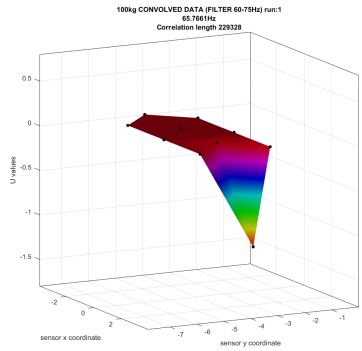


(a) 100kg FDD histogram

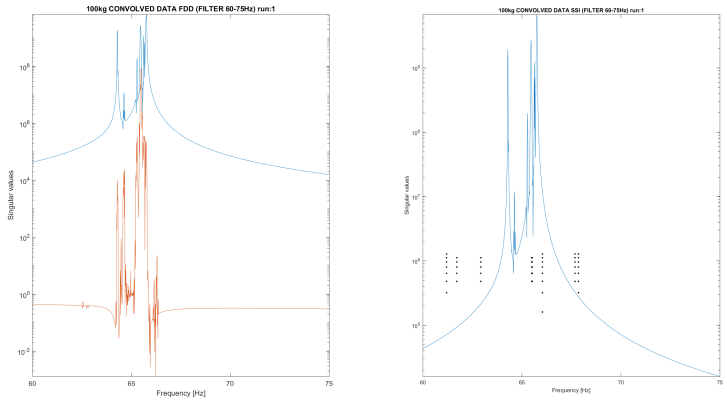


(b) 100kg SSI histogram

Figure A3.100kg: Histograms of identified modes, 100kg data (segment 1)

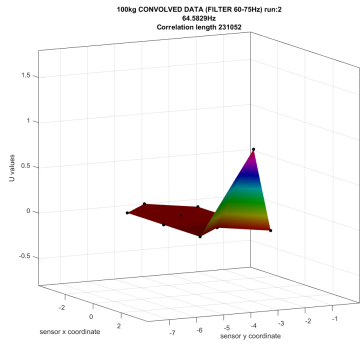


(a) 100kg mode shape, run 1

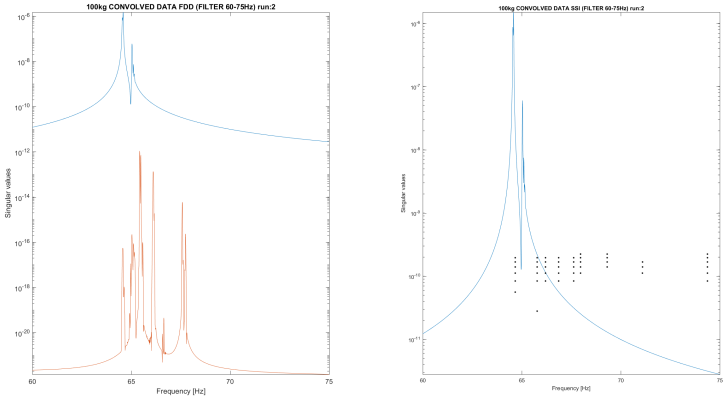


(b) 100kg FDD SSI output, run 1

Figure A3.100kg: Run 1 (segment 1)

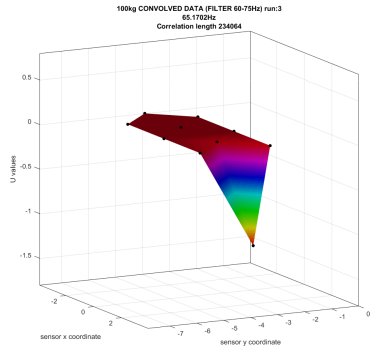


(a) 100kg mode shape, run 2

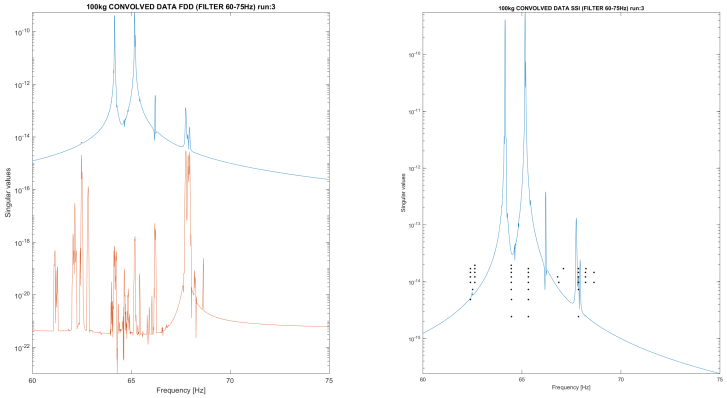


(b) 100kg FDD SSI output, run 2

Figure A3.100kg: Run 2 (segment 1)

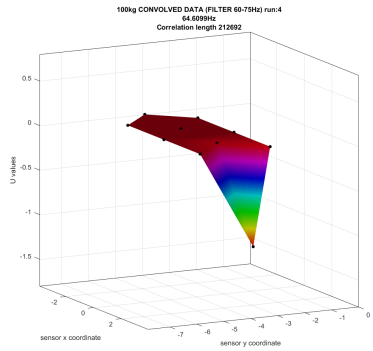


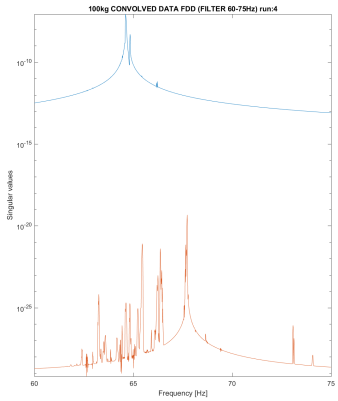
(a) 100kg mode shape, run 3

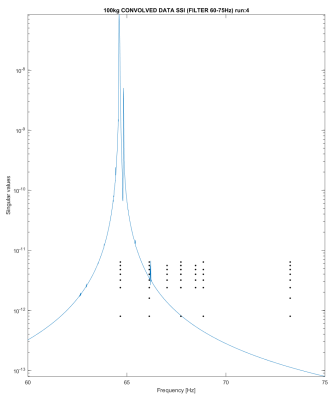


(b) 100kg FDD SSI output, run 3

Figure A3.100kg: Run 3 (segment 1)



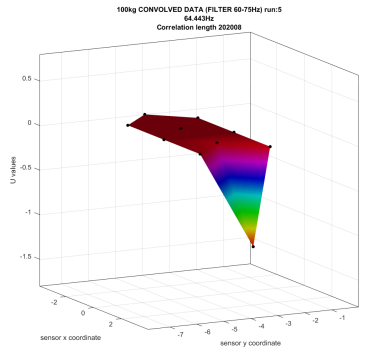


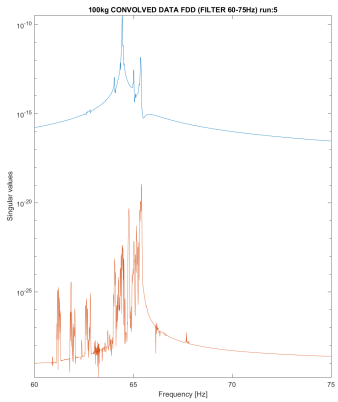


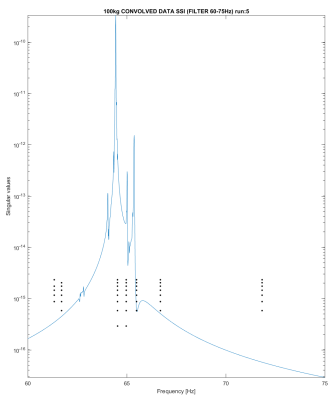
(a) 100kg mode shape, run 4

(b) 100kg FDD SSI output, run 4

Figure A3.100kg: Run 4 (segment 1)



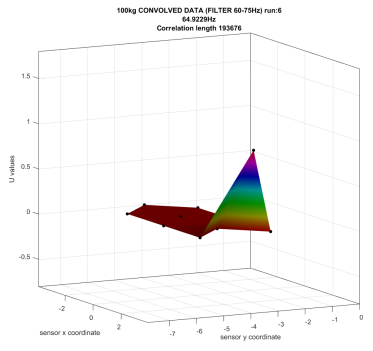


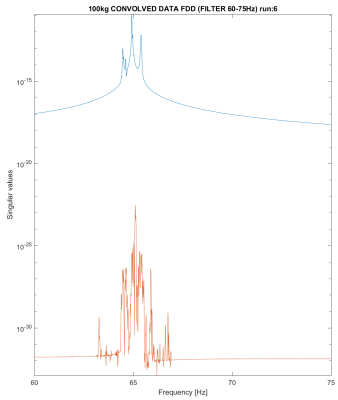


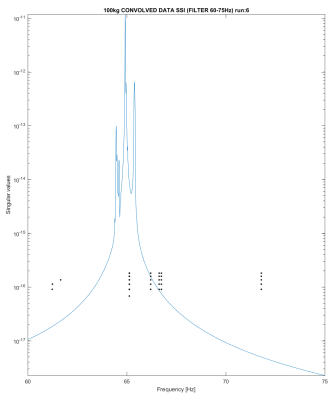
(a) 100kg mode shape, run 5

(b) 100kg FDD SSI output, run 5

Figure A3.100kg: Run 5 (segment 1)



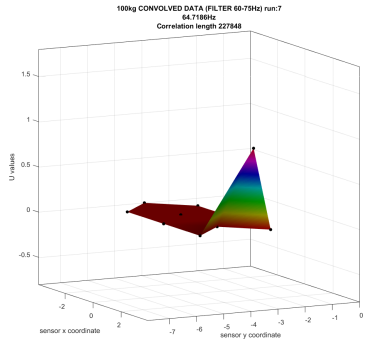




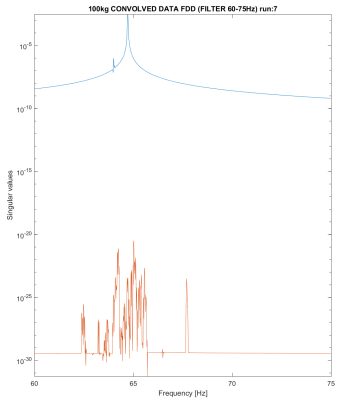
(a) 100kg mode shape, run 6

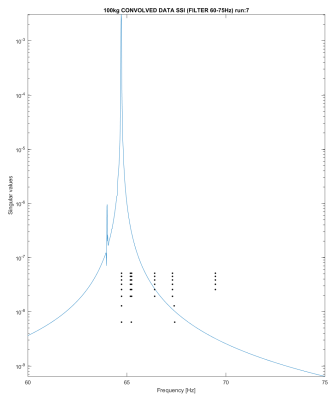
(b) 100kg FDD SSI output, run 6

Figure A3.100kg: Run 6 (segment 1)



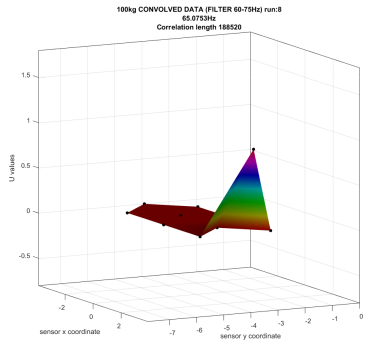
(a) 100kg mode shape, run 7



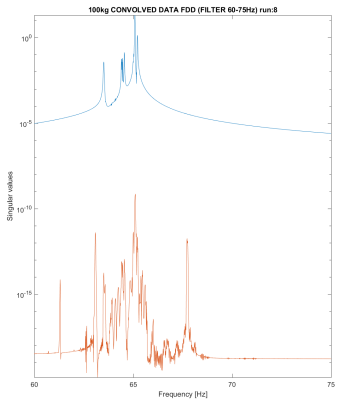


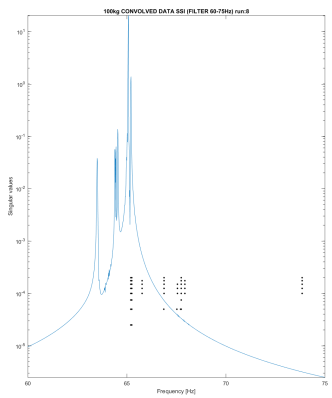
(b) 100kg FDD SSI output, run 7

Figure A3.100kg: Run 7 (segment 1)



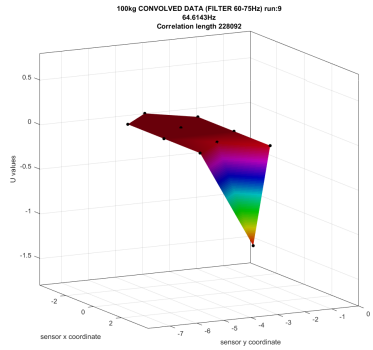
(a) 100kg mode shape, run 8



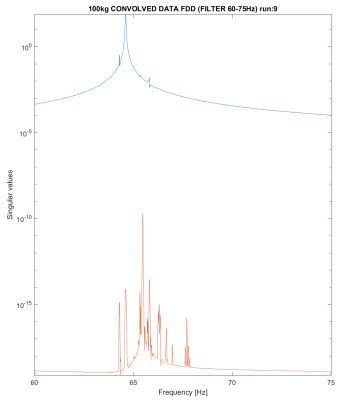


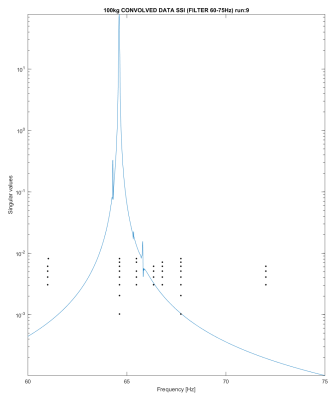
(b) 100kg FDD SSI output, run 8

Figure A3.100kg: Run 8 (segment 1)



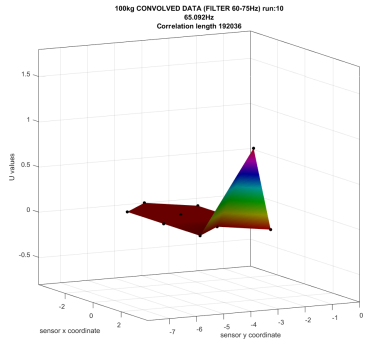
(a) 100kg mode shape, run 9

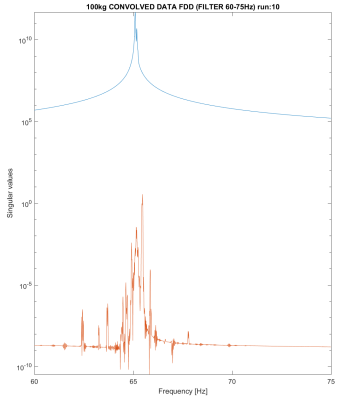


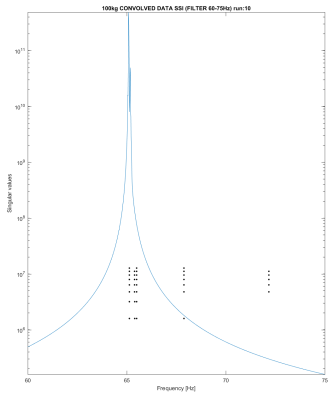


(b) 100kg FDD SSI output, run 9

Figure A3.100kg: Run 9 (segment 1)



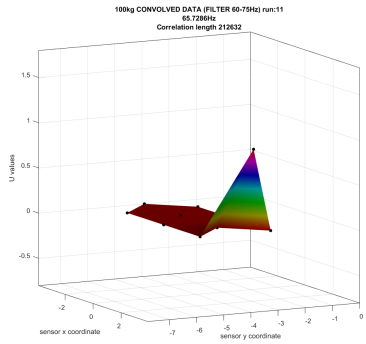


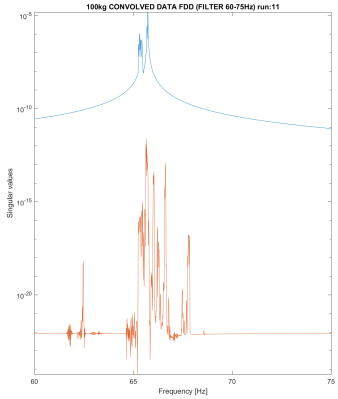


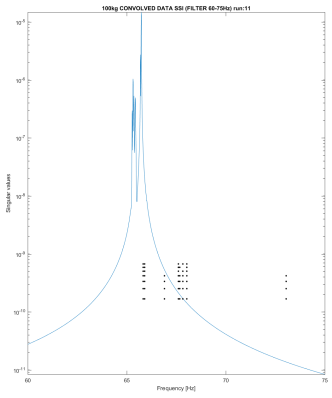
(a) 100kg mode shape, run 10

(b) 100kg FDD SSI output, run 10

Figure A3.100kg: Run 10 (segment 1)



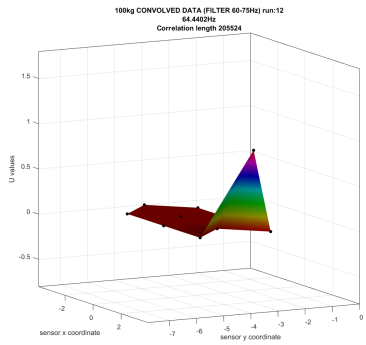


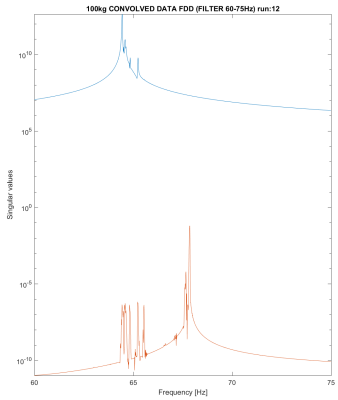


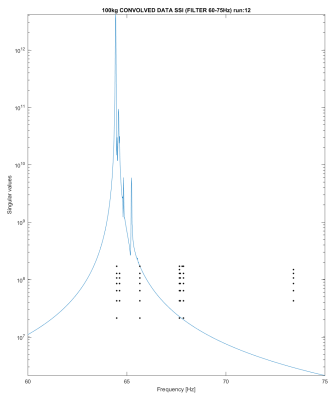
(a) 100kg mode shape, run 11

(b) 100kg FDD SSI output, run 11

Figure A3.100kg: Run 11 (segment 1)



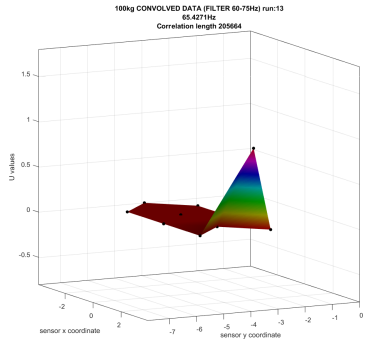




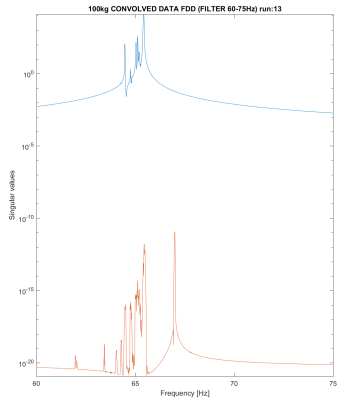
(a) 100kg mode shape, run 12

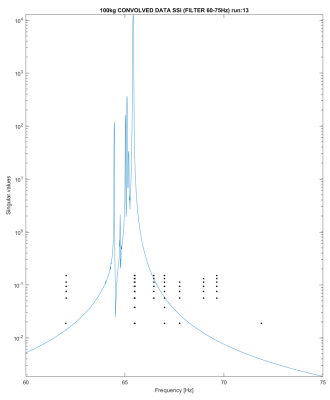
(b) 100kg FDD SSI output, run 12

Figure A3.100kg: Run 12 (segment 1)



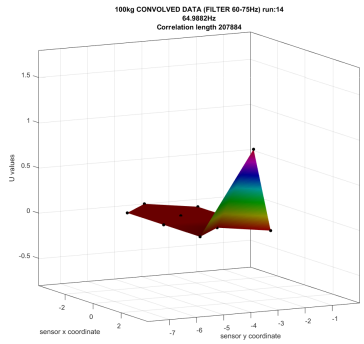
(a) 100kg mode shape, run 13



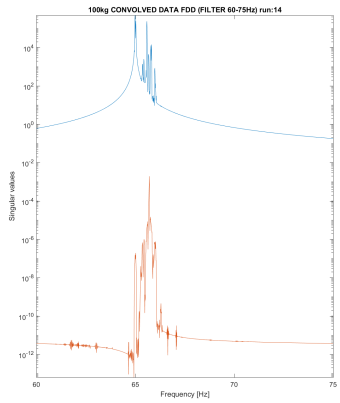


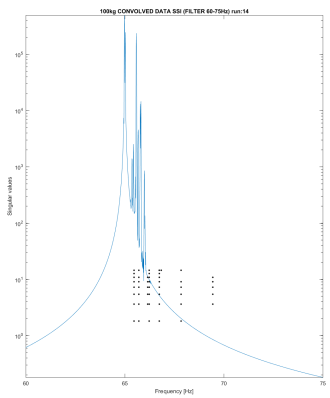
(b) 100kg FDD SSI output, run 13

Figure A3.100kg: Run 13 (segment 1)



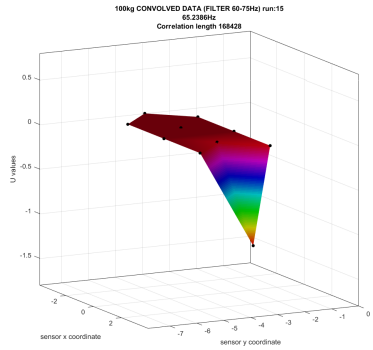
(a) 100kg mode shape, run 14



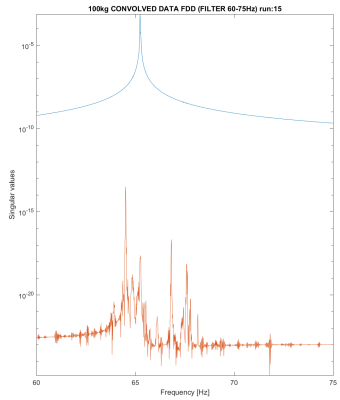


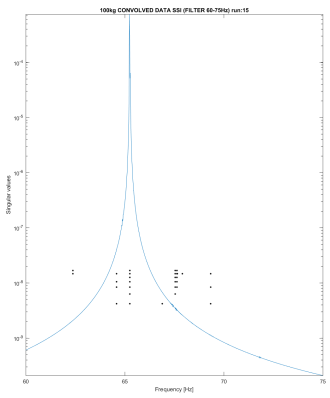
(b) 100kg FDD SSI output, run 14

Figure A3.100kg: Run 14 (segment 1)



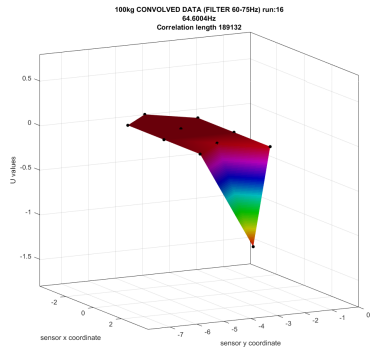
(a) 100kg mode shape, run 15



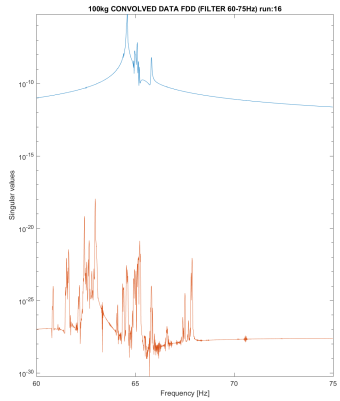


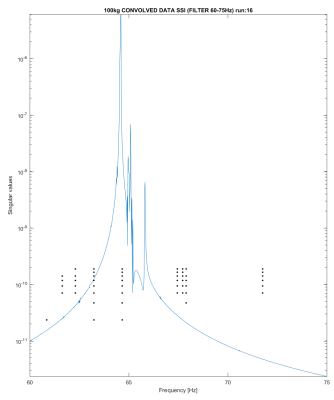
(b) 100kg FDD SSI output, run 15

Figure A3.100kg: Run 15 (segment 1)



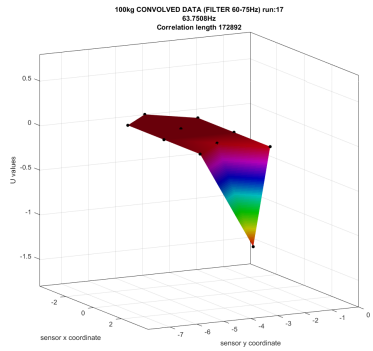
(a) 100kg mode shape, run 16



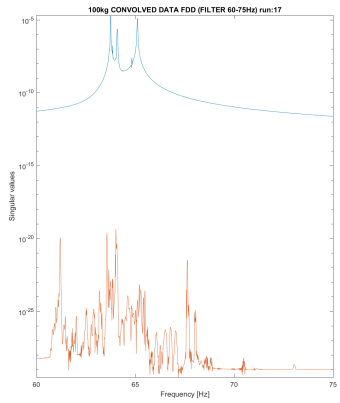


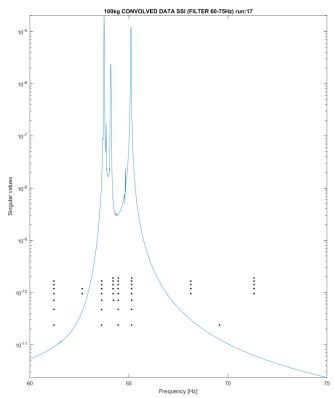
(b) 100kg FDD SSI output, run 16

Figure A3.100kg: Run 16 (segment 1)



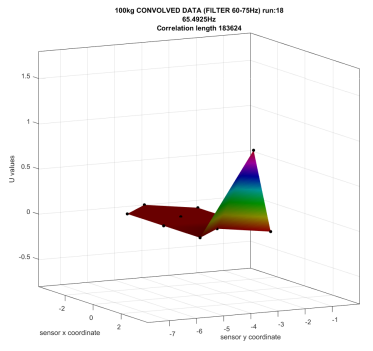
(a) 100kg mode shape, run 17



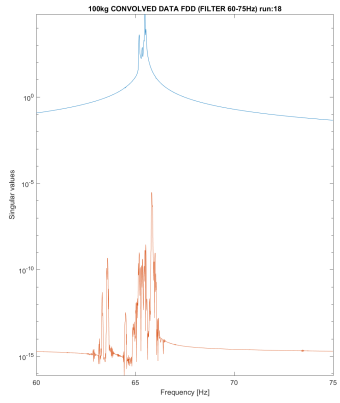


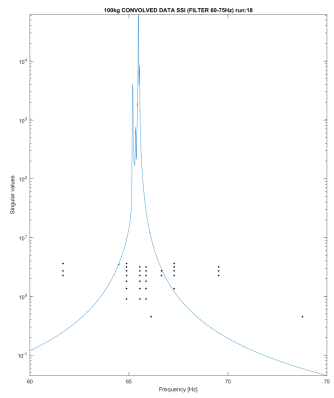
(b) 100kg FDD SSI output, run 17

Figure A3.100kg: Run 17 (segment 1)



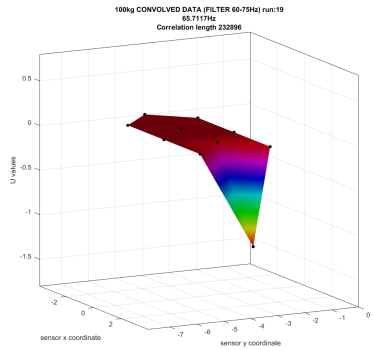
(a) 100kg mode shape, run 18



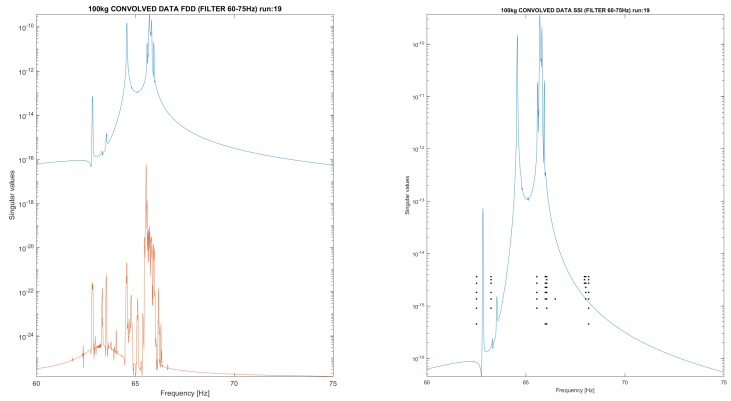


(b) 100kg FDD SSI output, run 18

Figure A3.100kg: Run 18 (segment 1)

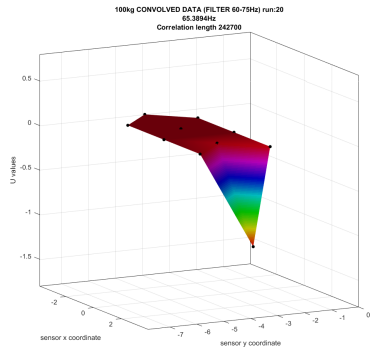


(a) 100kg mode shape, run 19

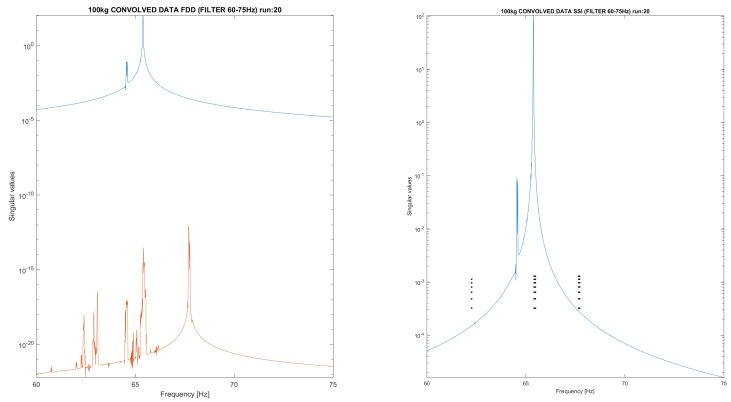


(b) 100kg FDD SSI output, run 19

Figure A3.100kg: Run 19 (segment 1)

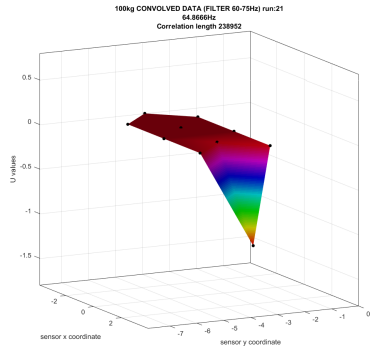


(a) 100kg mode shape, run 20

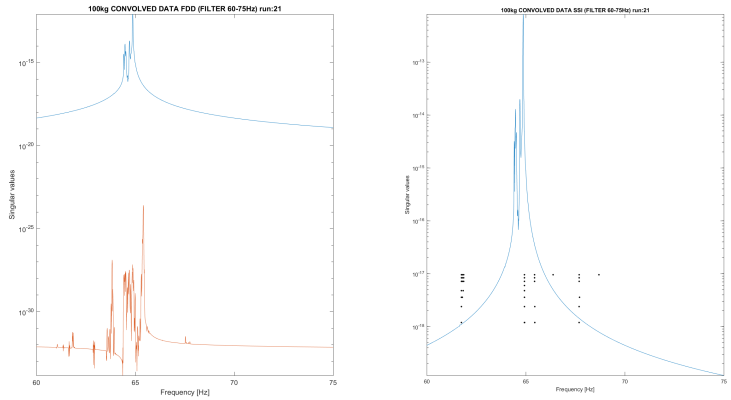


(b) 100kg FDD SSI output, run 20

Figure A3.100kg: Run 20 (segment 1)

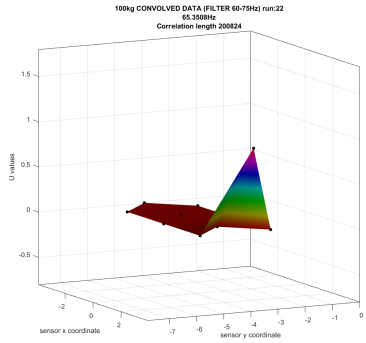


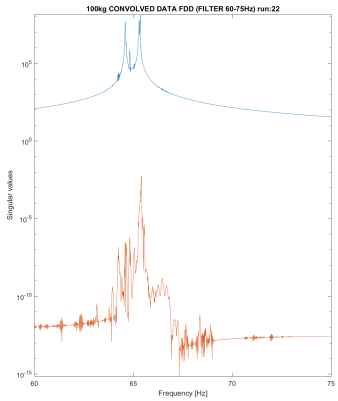
(a) 100kg mode shape, run 21

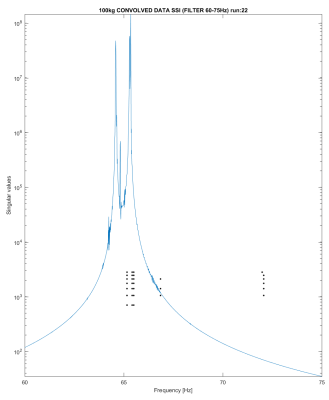


(b) 100kg FDD SSI output, run 21

Figure A3.100kg: Run 21 (segment 1)



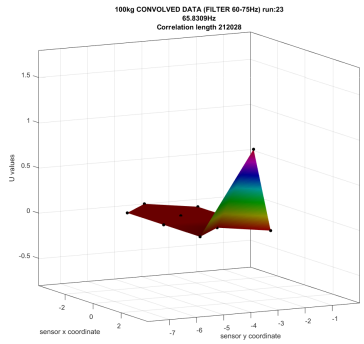


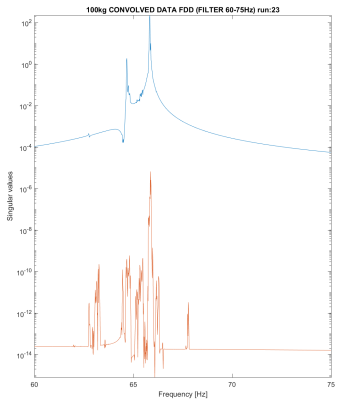


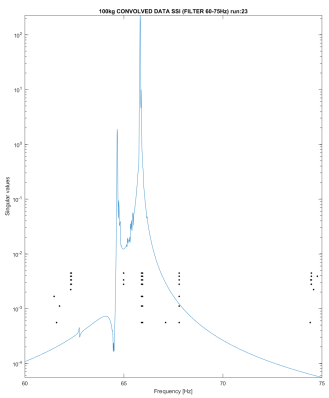
(a) 100kg mode shape, run 22

(b) 100kg FDD SSI output, run 22

Figure A3.100kg: Run 22 (segment 1)



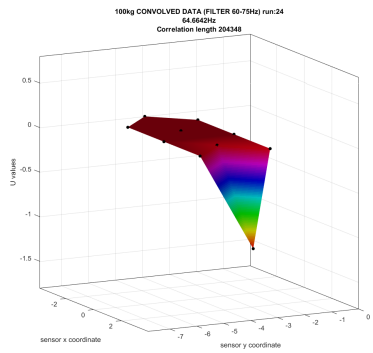


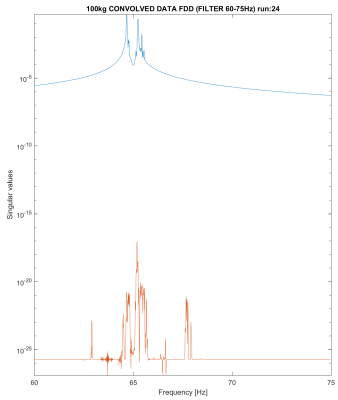


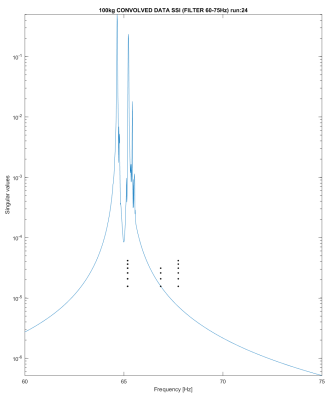
(a) 100kg mode shape, run 23

(b) 100kg FDD SSI output, run 23

Figure A3.100kg: Run 23 (segment 1)



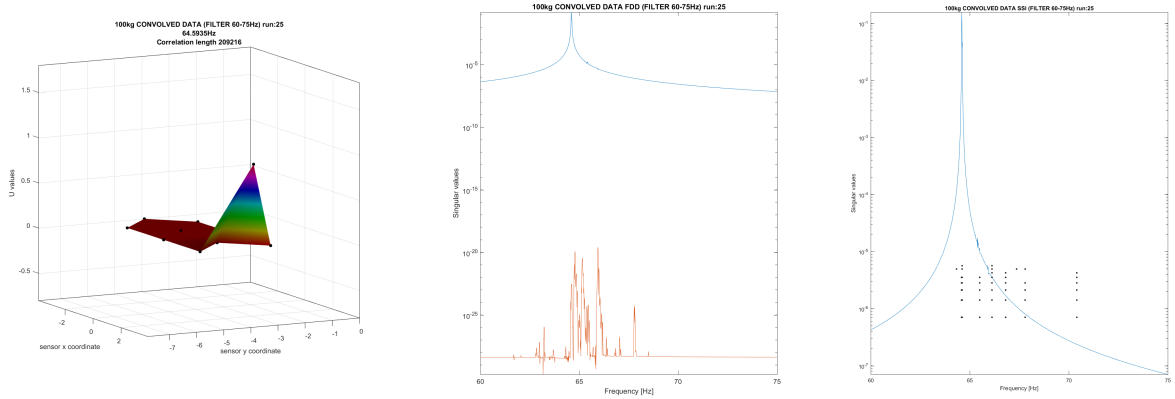




(a) 100kg mode shape, run 24

(b) 100kg FDD SSI output, run 24

Figure A3.100kg: Run 24 (segment 1)

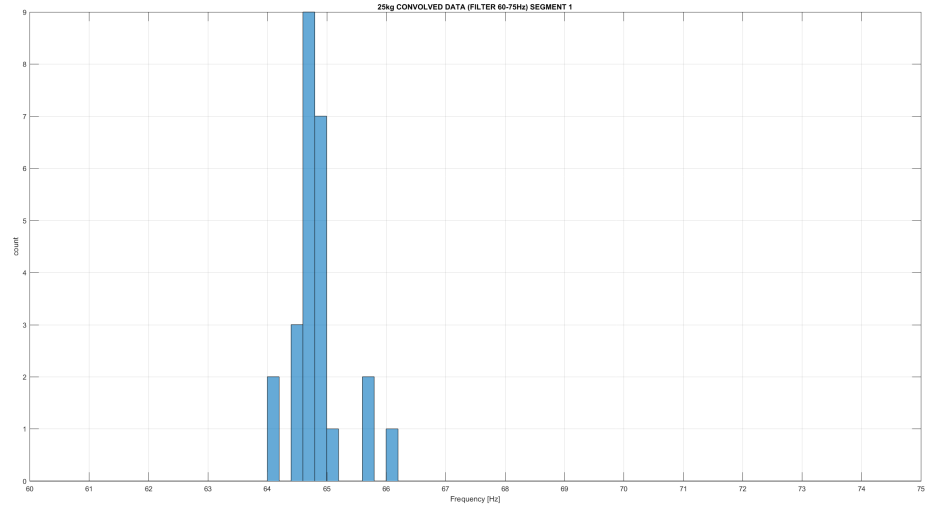


(a) 100kg mode shape, run 25

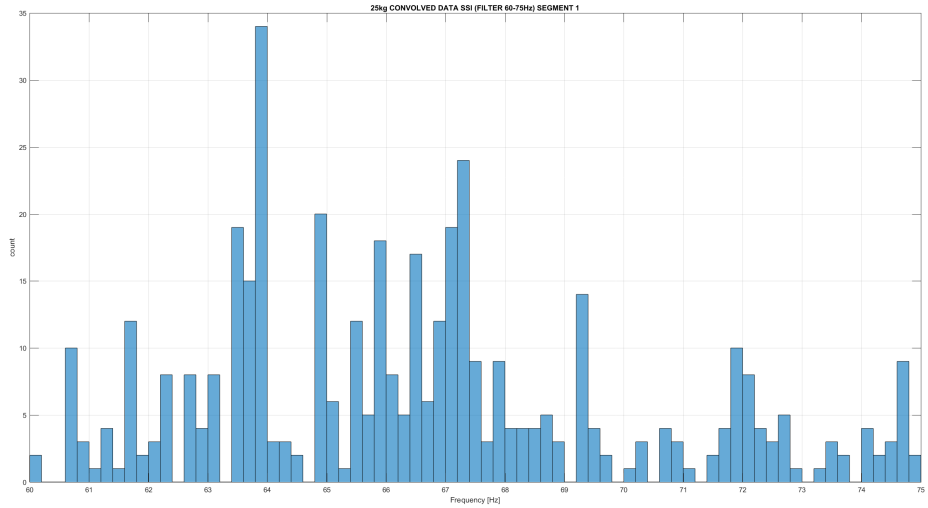
(b) 100kg FDD SSI output, run 25

Figure A3.100kg: Run 25 (segment 1)

Data (28.03.2017) 25kg-50kg segment 1 (Unreduced order PF)

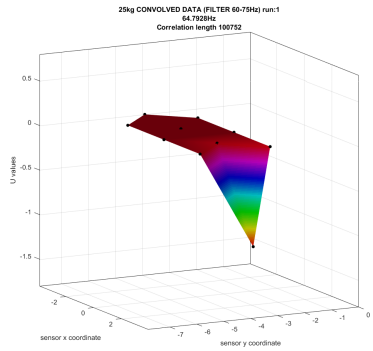


(a) 25kg FDD histogram

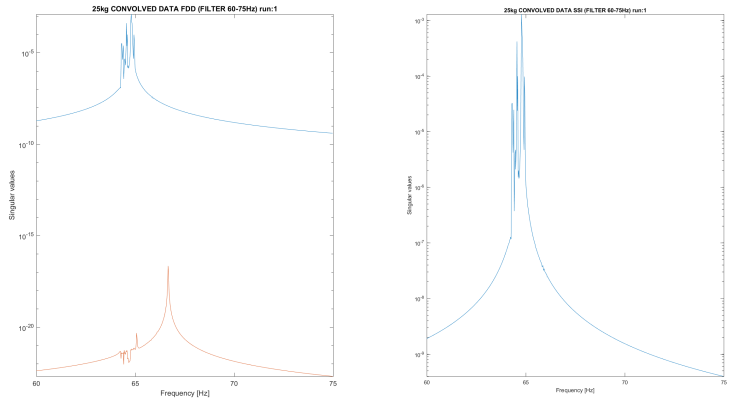


(b) 25kg SSI histogram

Figure A3.25kg: Histograms of identified modes, 25kg data (segment 1)

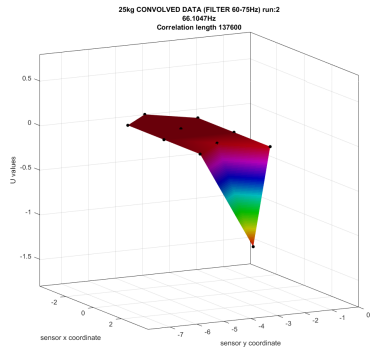


(a) 25kg mode shape, run 1

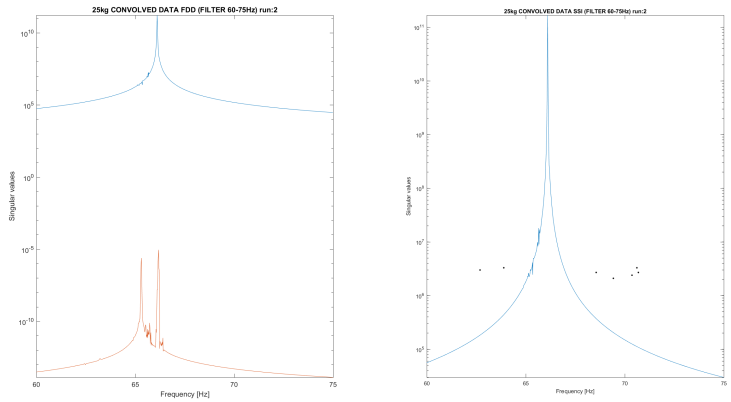


(b) 25kg FDD SSI output, run 1

Figure A3.25kg: Run 1 (segment 1)

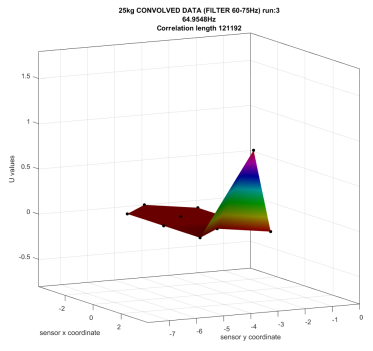


(a) 25kg mode shape, run 2

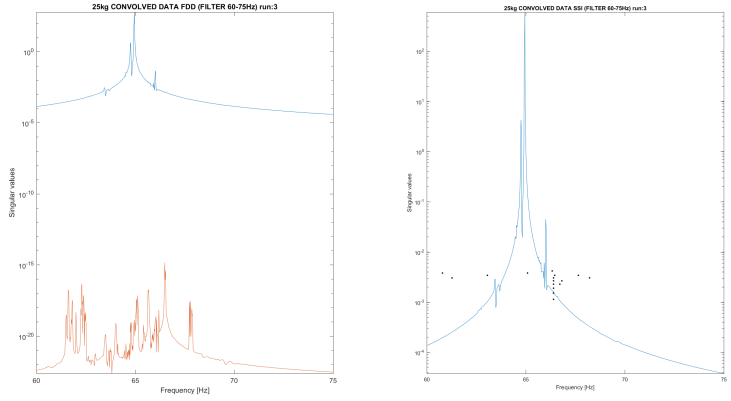


(b) 25kg FDD SSI output, run 2

Figure A3.25kg: Run 2 (segment 1)

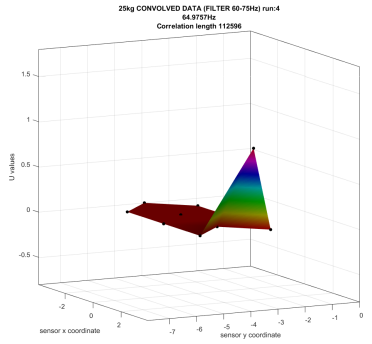


(a) 25kg mode shape, run 3

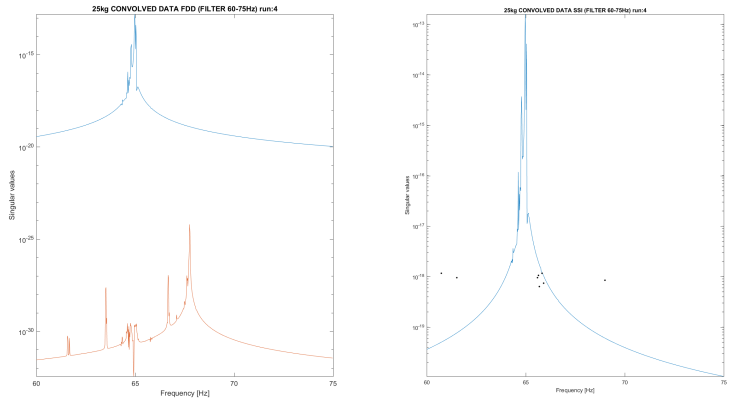


(b) 25kg FDD SSI output, run 3

Figure A3.25kg: Run 3 (segment 1)

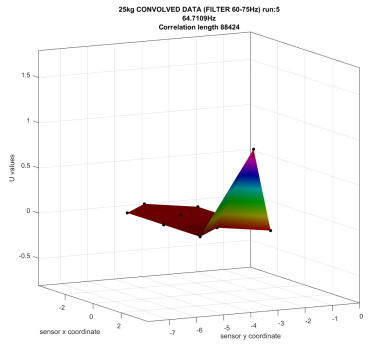


(a) 25kg mode shape, run 4

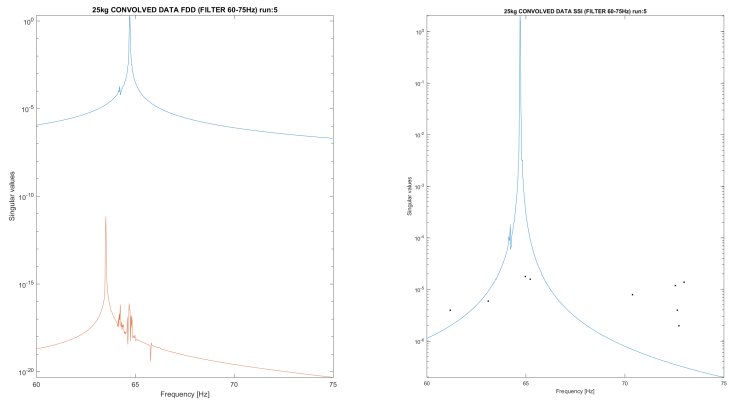


(b) 25kg FDD SSI output, run 4

Figure A3.25kg: Run 4 (segment 1)

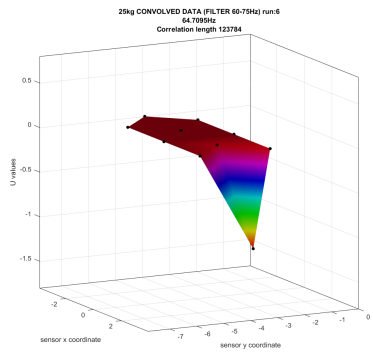


(a) 25kg mode shape, run 5

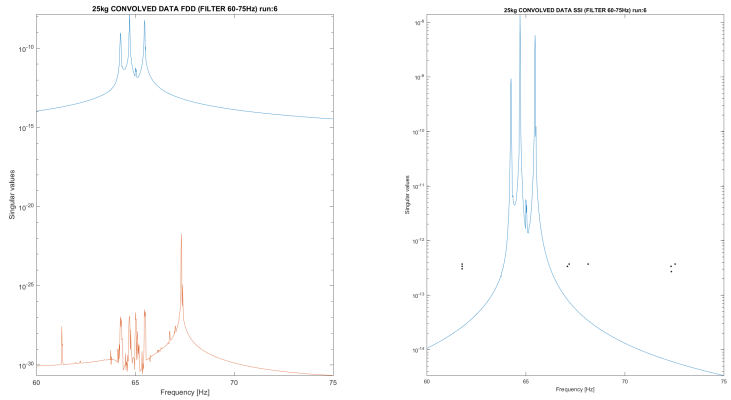


(b) 25kg FDD SSI output, run 5

Figure A3.25kg: Run 5 (segment 1)

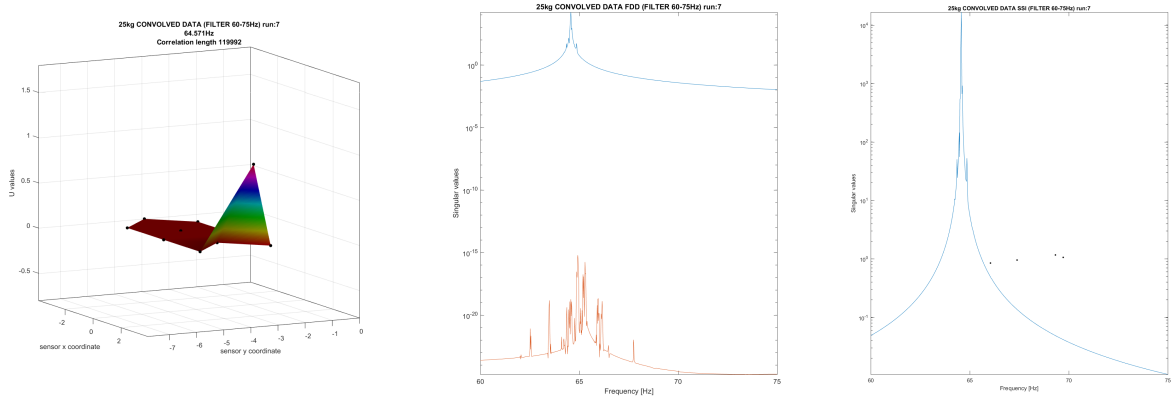


(a) 25kg mode shape, run 6



(b) 25kg FDD SSI output, run 6

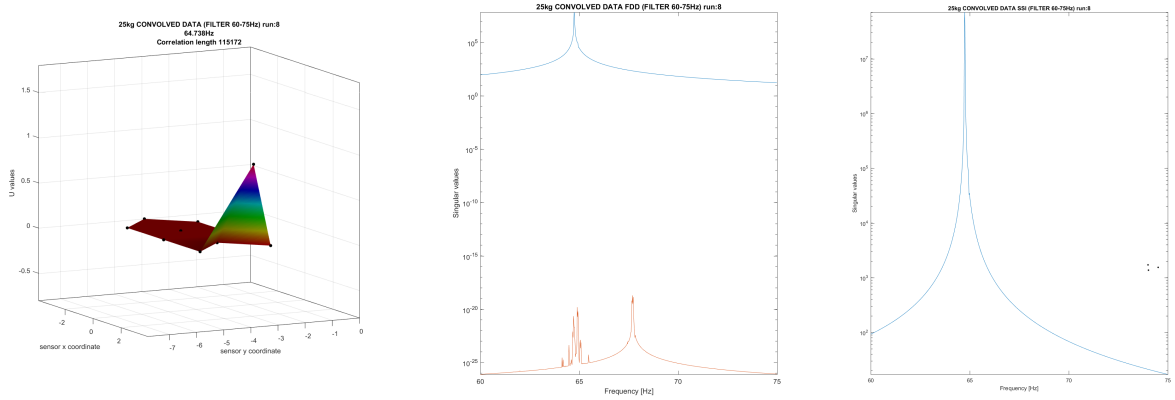
Figure A3.25kg: Run 6 (segment 1)



(a) 25kg mode shape, run 7

(b) 25kg FDD SSI output, run 7

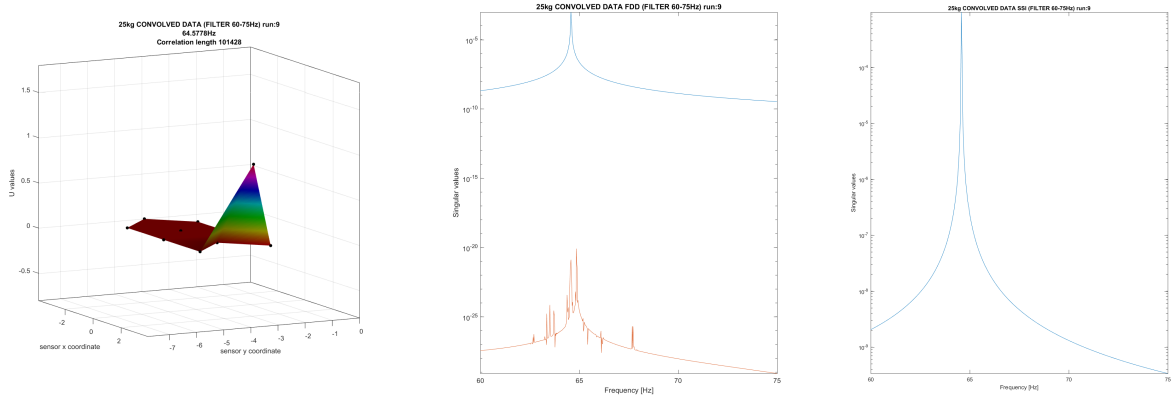
Figure A3.25kg: Run 7 (segment 1)



(a) 25kg mode shape, run 8

(b) 25kg FDD SSI output, run 8

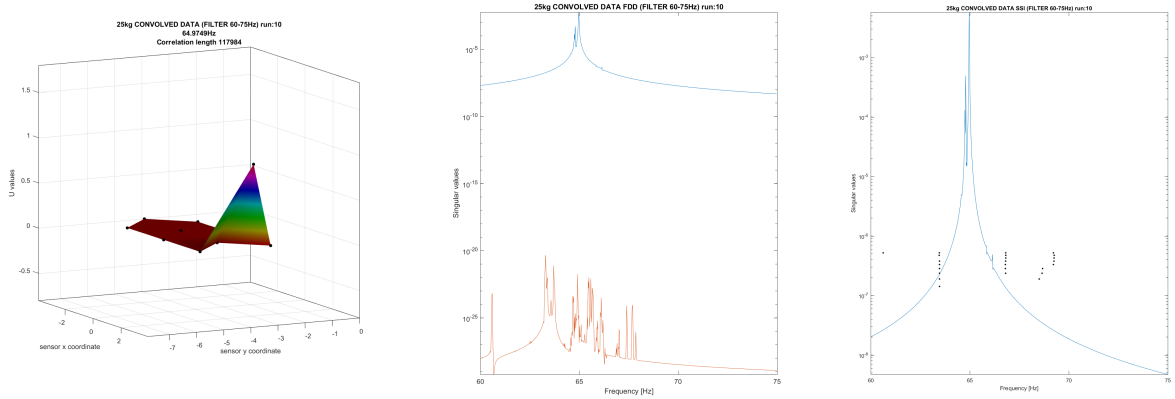
Figure A3.25kg: Run 8 (segment 1)



(a) 25kg mode shape, run 9

(b) 25kg FDD SSI output, run 9

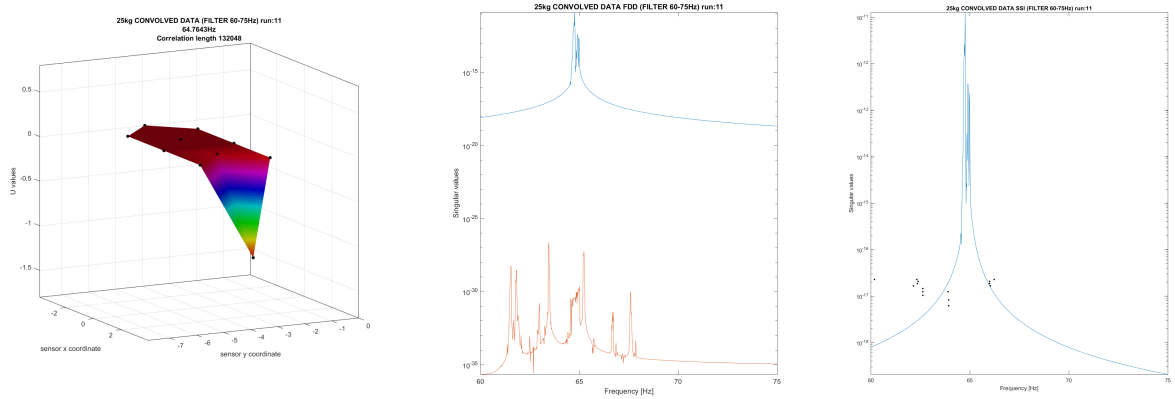
Figure A3.25kg: Run 9 (segment 1)



(a) 25kg mode shape, run 10

(b) 25kg FDD SSI output, run 10

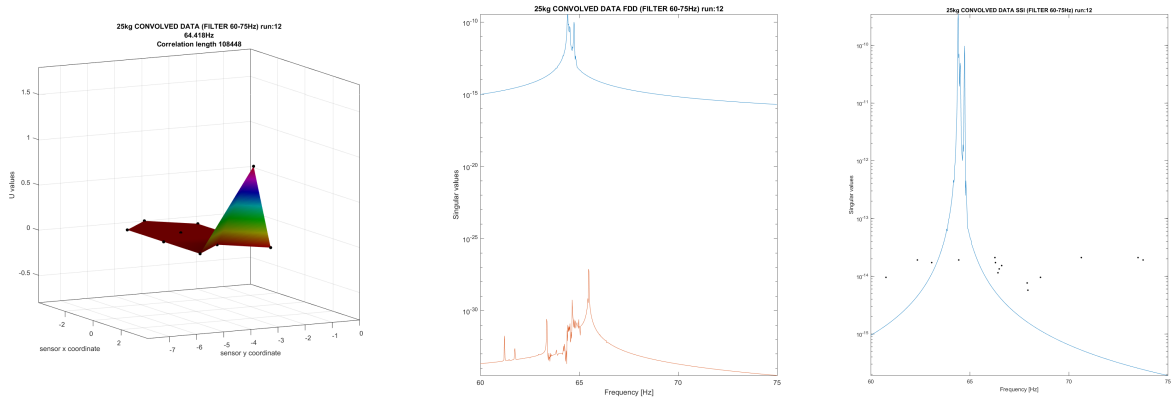
Figure A3.25kg: Run 10 (segment 1)



(a) 25kg mode shape, run 11

(b) 25kg FDD SSI output, run 11

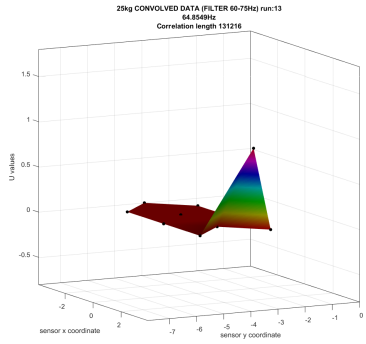
Figure A3.25kg: Run 11 (segment 1)



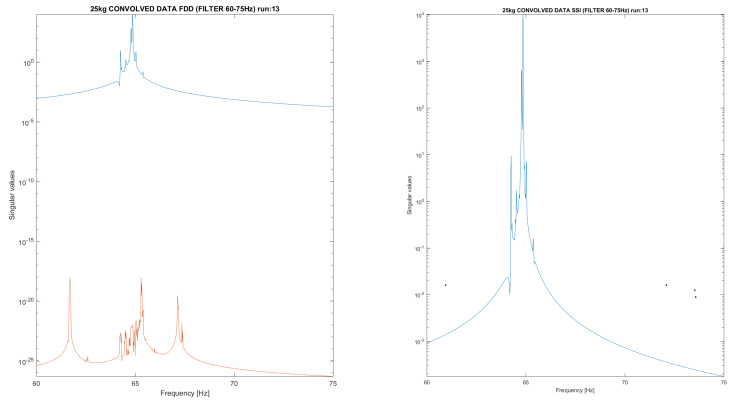
(a) 25kg mode shape, run 12

(b) 25kg FDD SSI output, run 12

Figure A3.25kg: Run 12 (segment 1)

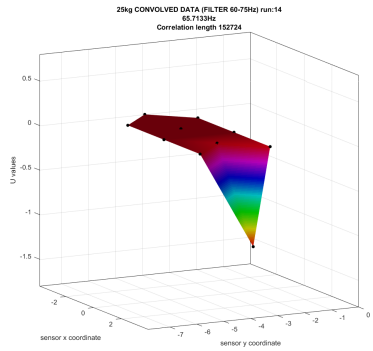


(a) 25kg mode shape, run 13

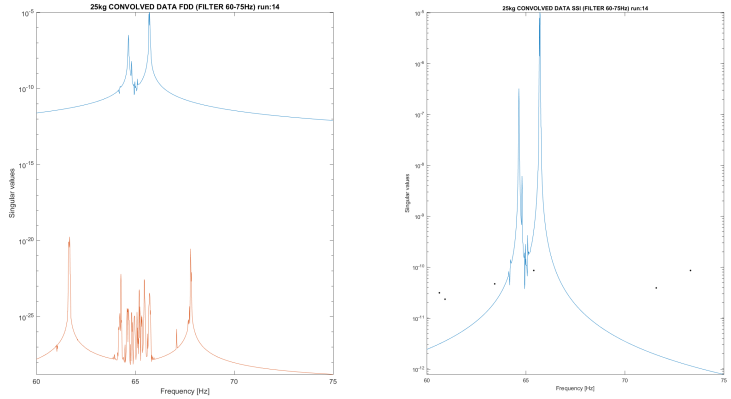


(b) 25kg FDD SSI output, run 13

Figure A3.25kg: Run 13 (segment 1)

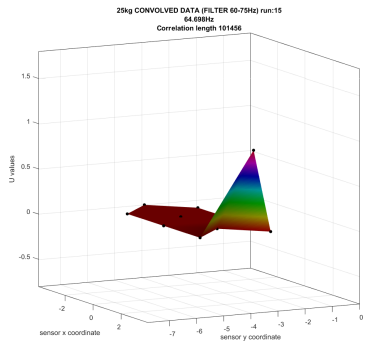


(a) 25kg mode shape, run 14

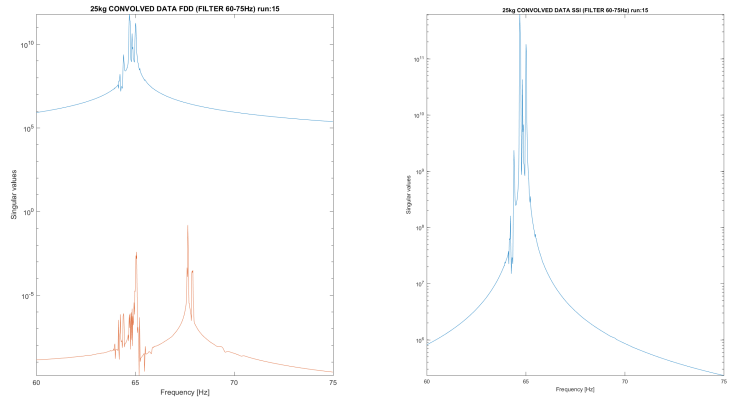


(b) 25kg FDD SSI output, run 14

Figure A3.25kg: Run 14 (segment 1)

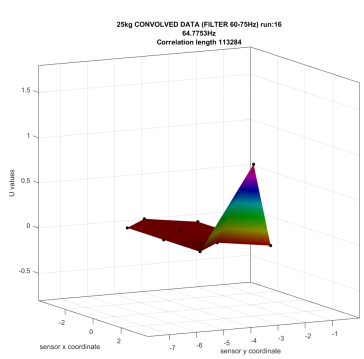


(a) 25kg mode shape, run 15

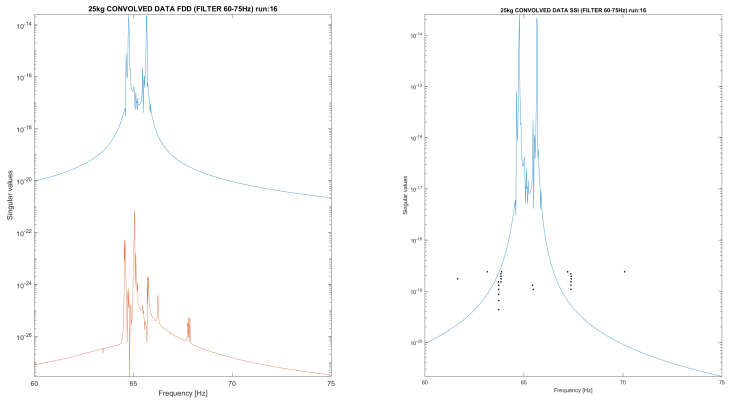


(b) 25kg FDD SSI output, run 15

Figure A3.25kg: Run 15 (segment 1)

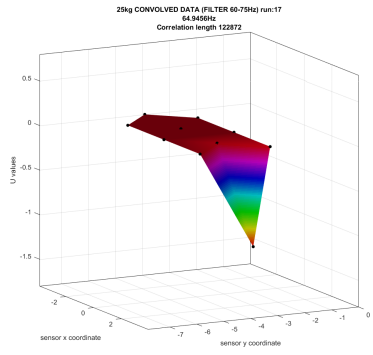


(a) 25kg mode shape, run 16

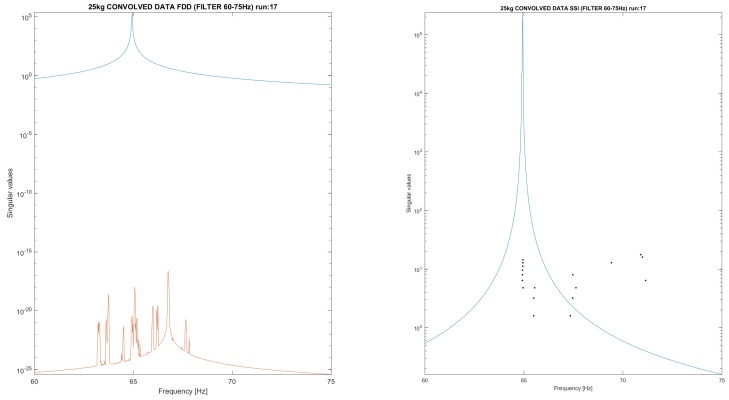


(b) 25kg FDD SSI output, run 16

Figure A3.25kg: Run 16 (segment 1)

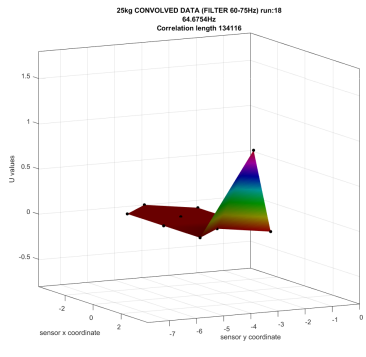


(a) 25kg mode shape, run 17

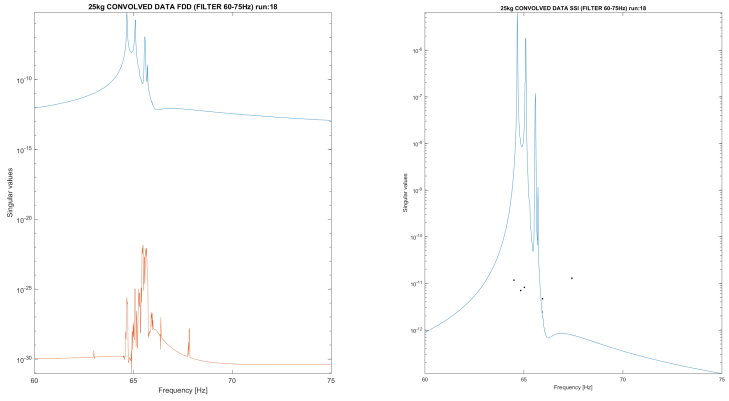


(b) 25kg FDD SSI output, run 17

Figure A3.25kg: Run 17 (segment 1)

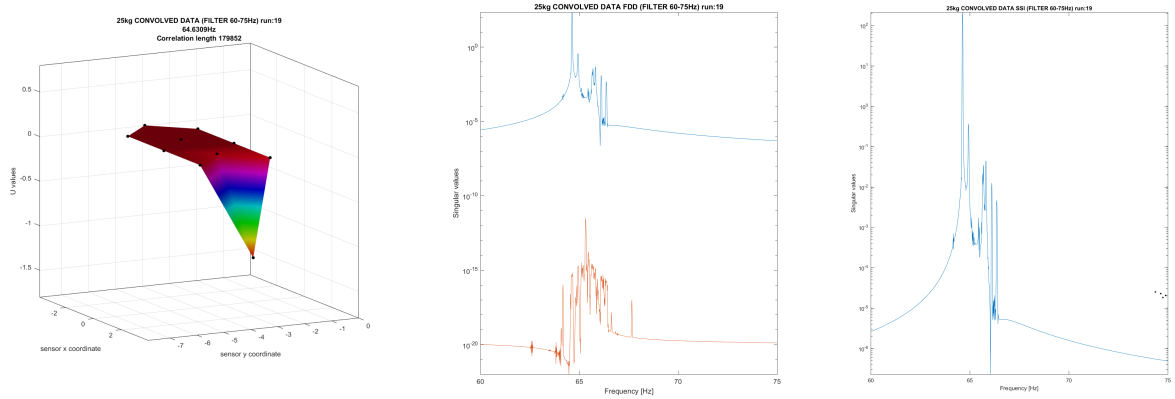


(a) 25kg mode shape, run 18



(b) 25kg FDD SSI output, run 18

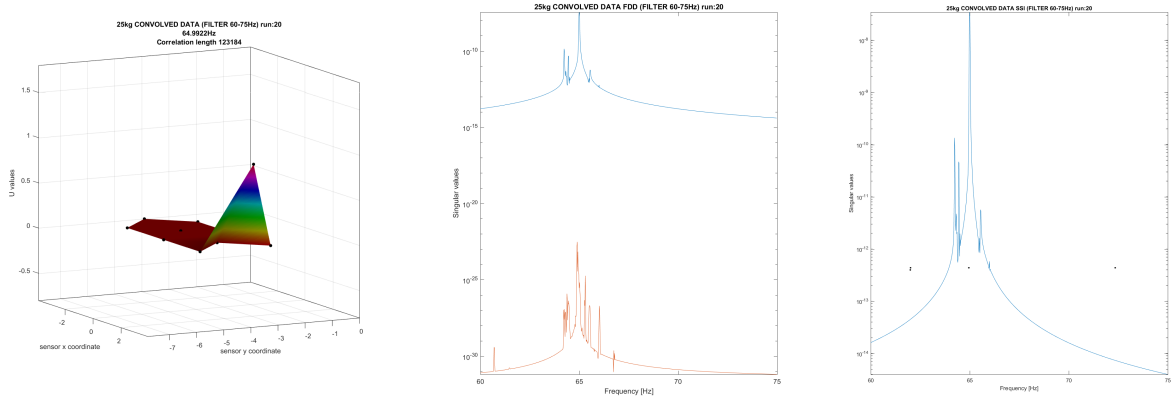
Figure A3.25kg: Run 18 (segment 1)



(a) 25kg mode shape, run 19

(b) 25kg FDD SSI output, run 19

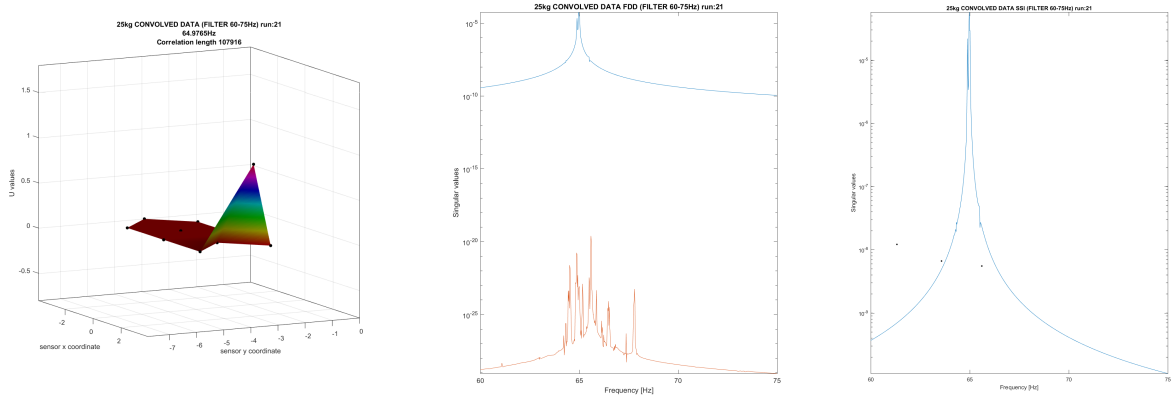
Figure A3.25kg: Run 19 (segment 1)



(a) 25kg mode shape, run 20

(b) 25kg FDD SSI output, run 20

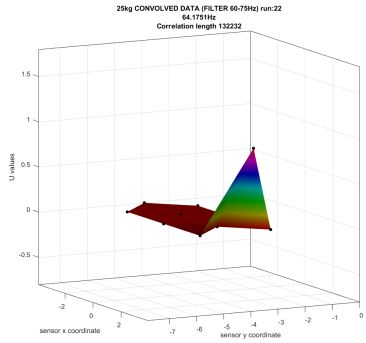
Figure A3.25kg: Run 20 (segment 1)



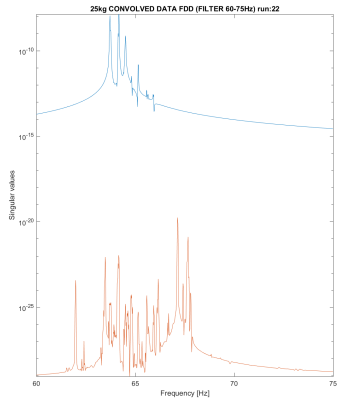
(a) 25kg mode shape, run 21

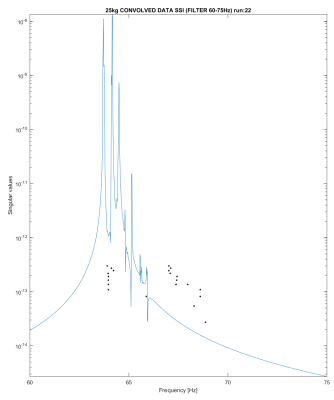
(b) 25kg FDD SSI output, run 21

Figure A3.25kg: Run 21 (segment 1)



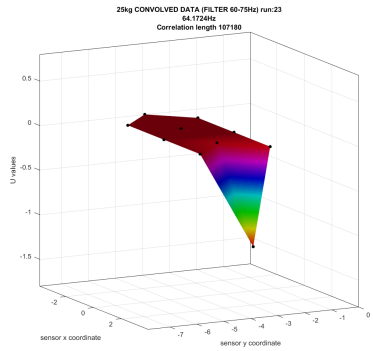
(a) 25kg mode shape, run 22



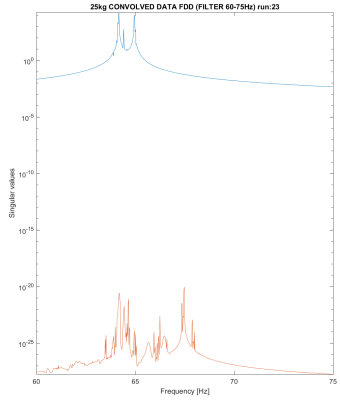


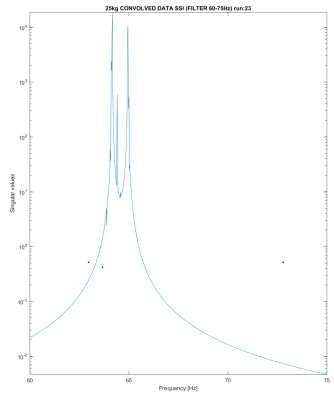
(b) 25kg FDD SSI output, run 22

Figure A3.25kg: Run 22 (segment 1)



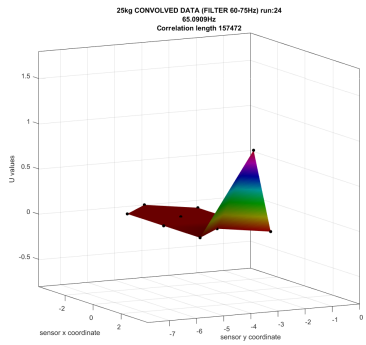
(a) 25kg mode shape, run 23



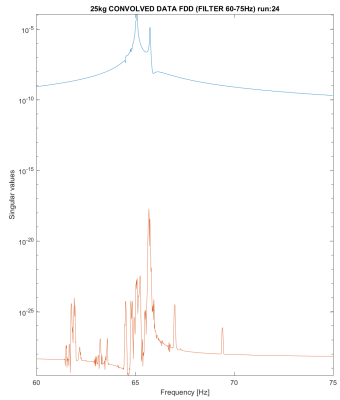


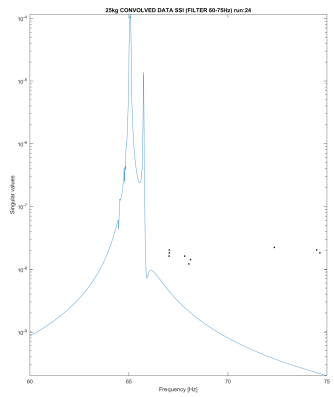
(b) 25kg FDD SSI output, run 23

Figure A3.25kg: Run 23 (segment 1)



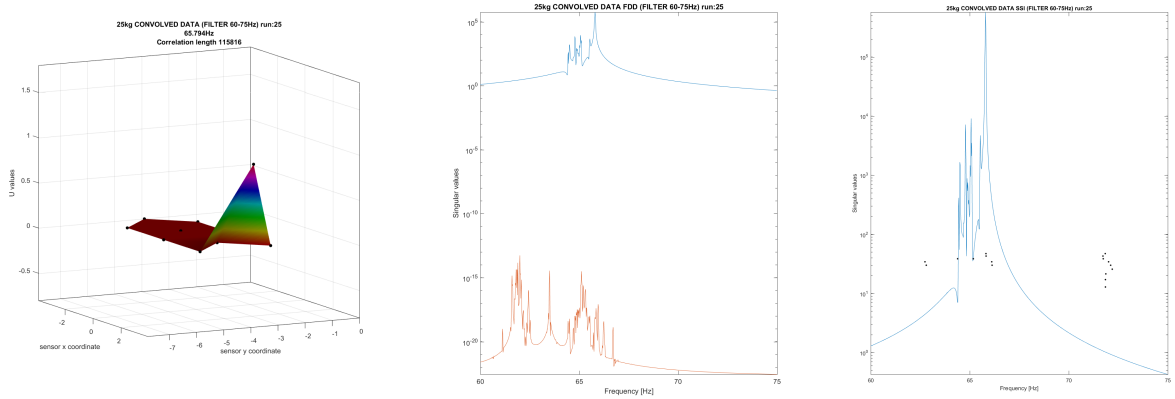
(a) 25kg mode shape, run 24





(b) 25kg FDD SSI output, run 24

Figure A3.25kg: Run 24 (segment 1)

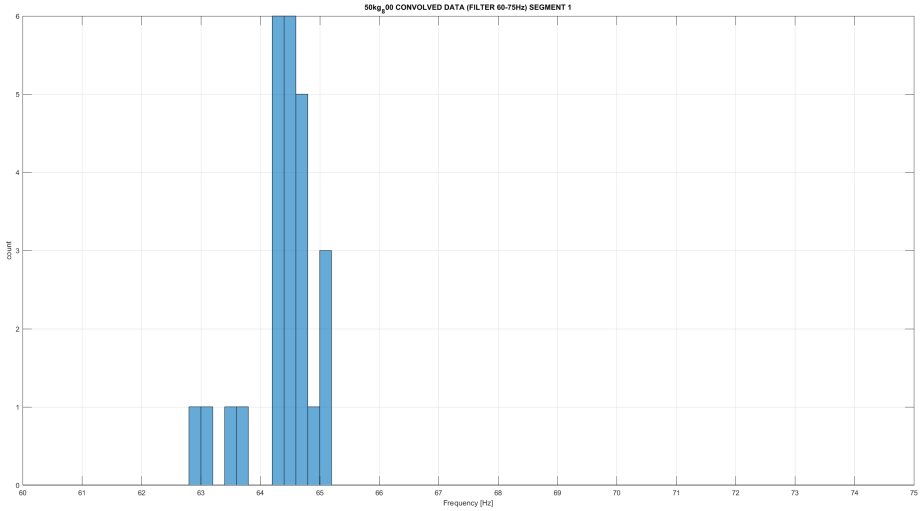


(a) 25kg mode shape, run 25

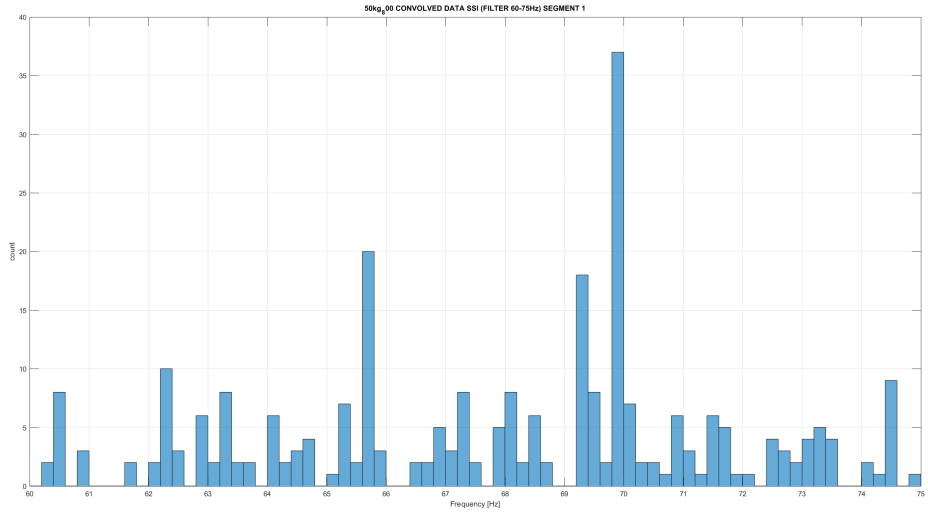
(b) 25kg FDD SSI output, run 25

Figure A3.25kg: Run 25 (segment 1)

50kg data segment 1 (28.03.2017)

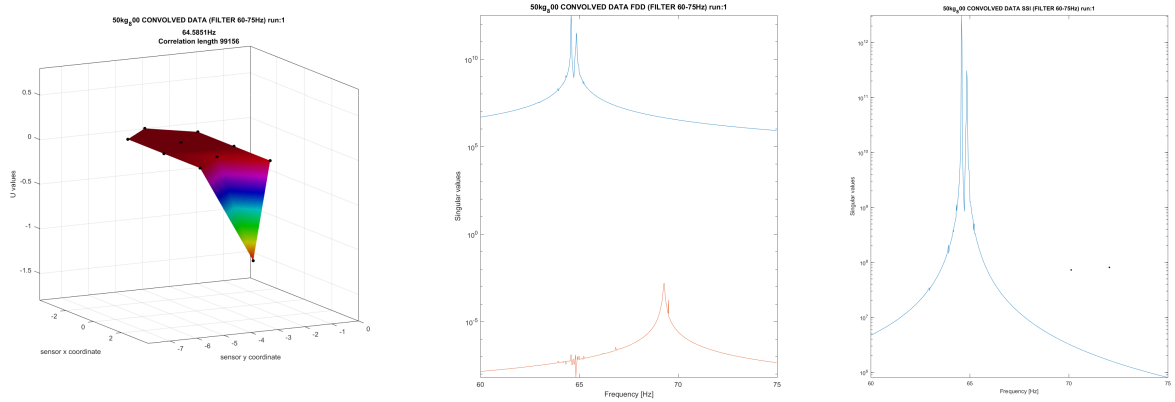


(a) 50kg FDD histogram



(b) 50kg SSI histogram

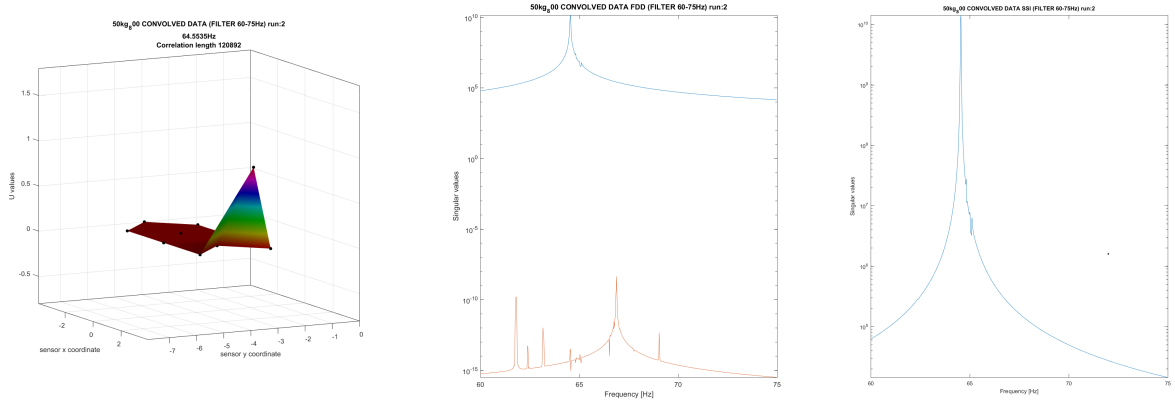
Figure A3.50kg: Histograms of identified modes, 50kg data (segment 1)



(a) 50kg mode shape, run 1

(b) 50kg FDD SSI output, run 1

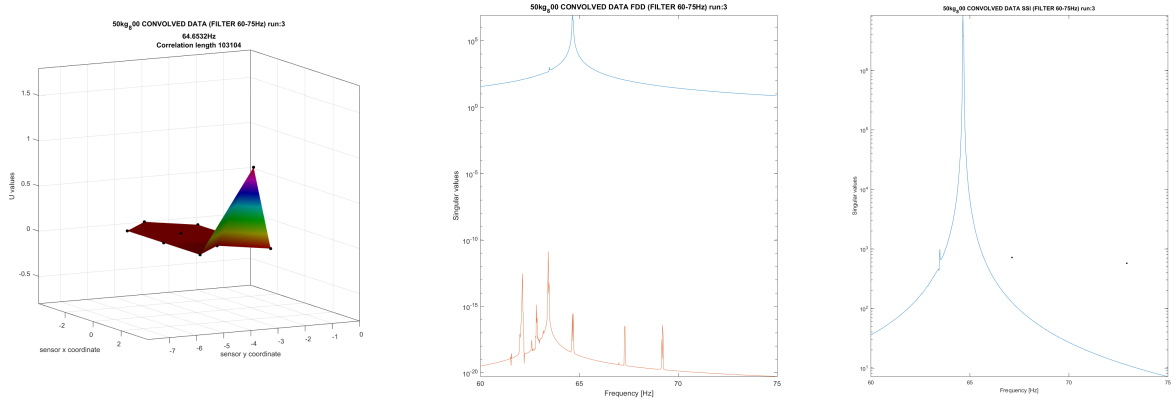
Figure A3.50kg (28.03.2017): Run 1 (segment 1)



(a) 50kg mode shape, run 2

(b) 50kg FDD SSI output, run 2

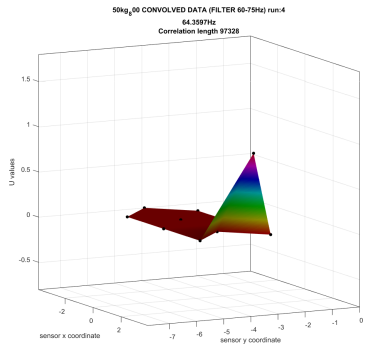
Figure A3.50kg (28.03.2017): Run 2 (segment 1)



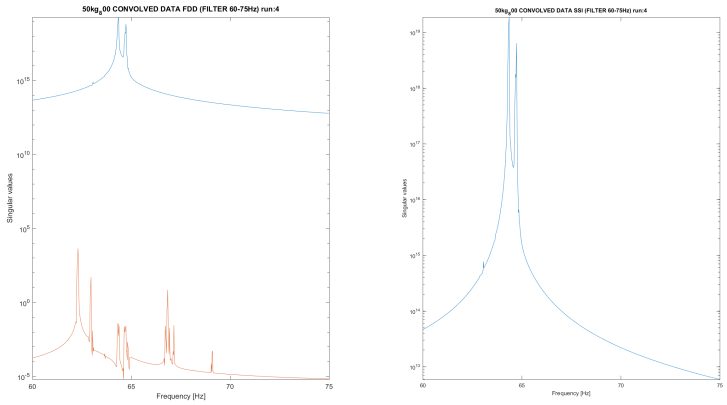
(a) 50kg mode shape, run 3

(b) 50kg FDD SSI output, run 3

Figure A3.50kg (28.03.2017): Run 3 (segment 1)

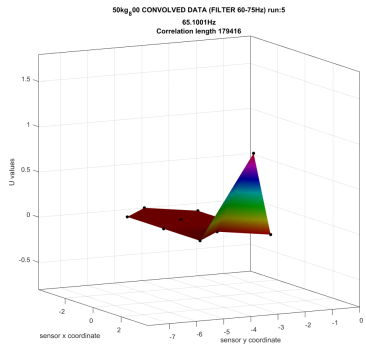


(a) 50kg mode shape, run 4

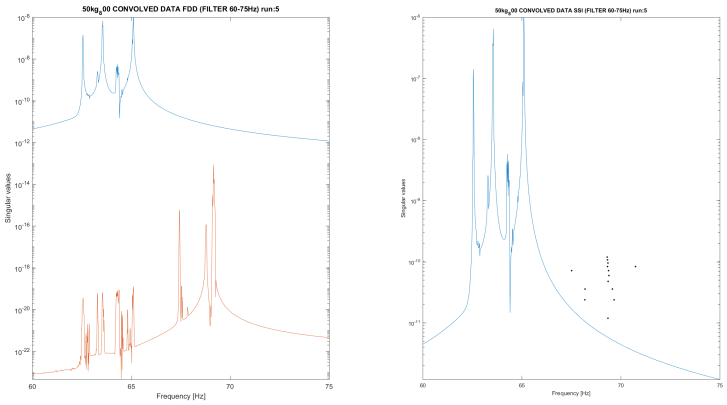


(b) 50kg FDD SSI output, run 4

Figure A3.50kg (28.03.2017): Run 4 (segment 1)

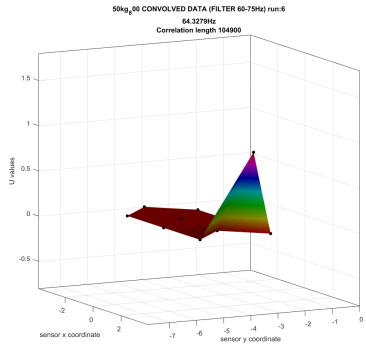


(a) 50kg mode shape, run 5

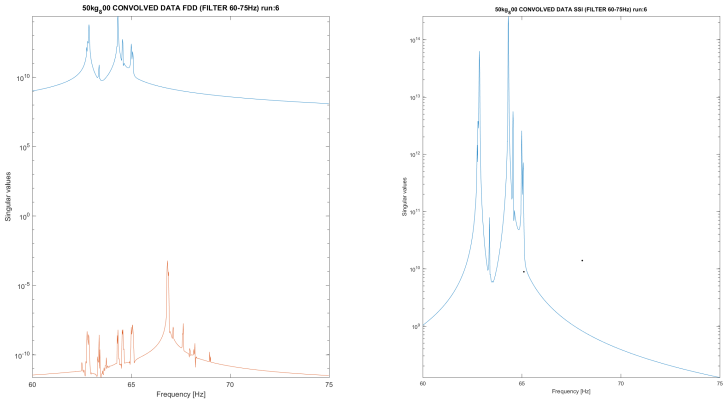


(b) 50kg FDD SSI output, run 5

Figure A3.50kg (28.03.2017): Run 5 (segment 1)

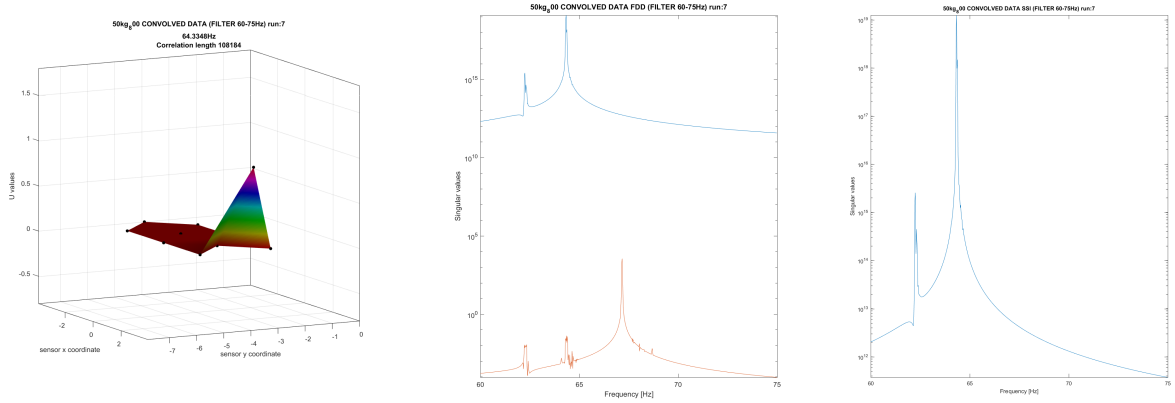


(a) 50kg mode shape, run 6



(b) 50kg FDD SSI output, run 6

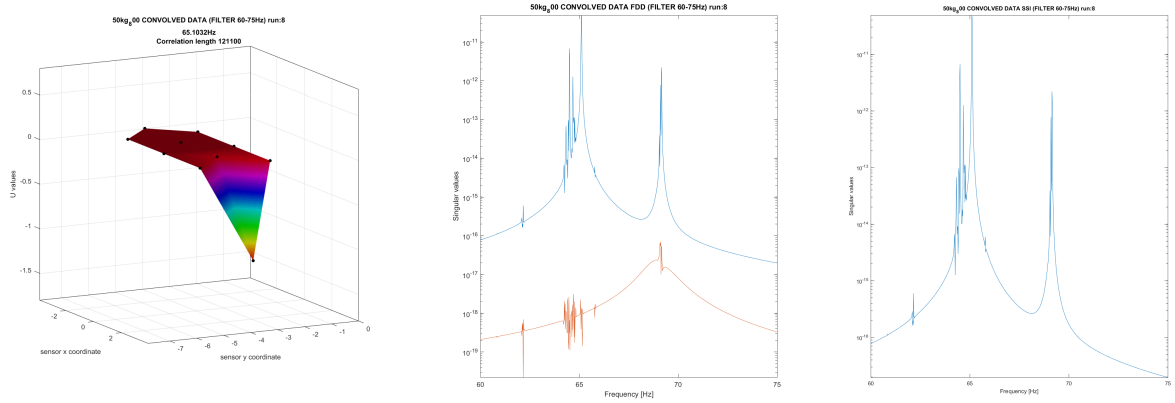
Figure A3.50kg (28.03.2017): Run 6 (segment 1)



(a) 50kg mode shape, run 7

(b) 50kg FDD SSI output, run 7

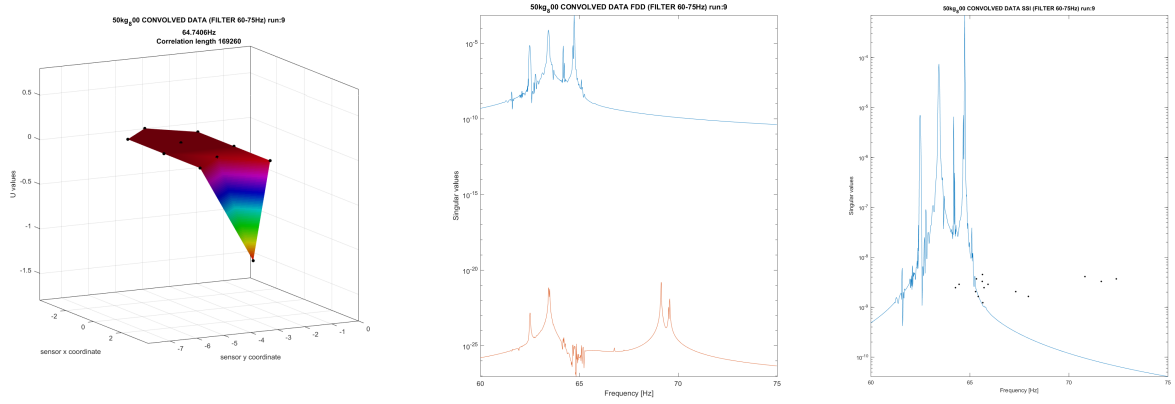
Figure A3.50kg (28.03.2017): Run 7 (segment 1)



(a) 50kg mode shape, run 8

(b) 50kg FDD SSI output, run 8

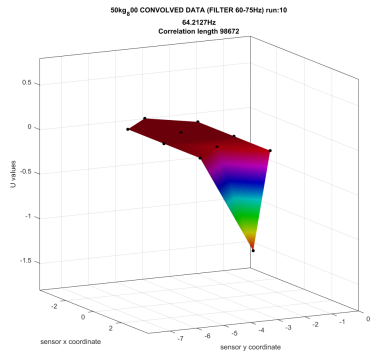
Figure A3.50kg (28.03.2017): Run 8 (segment 1)



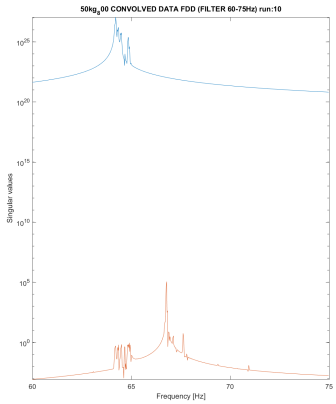
(a) 50kg mode shape, run 9

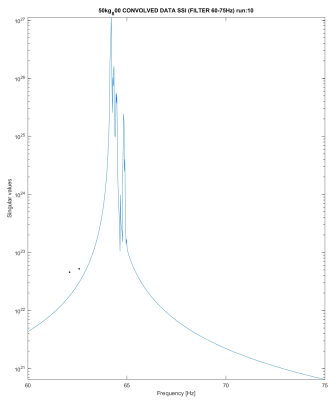
(b) 50kg FDD SSI output, run 9

Figure A3.50kg (28.03.2017): Run 9 (segment 1)



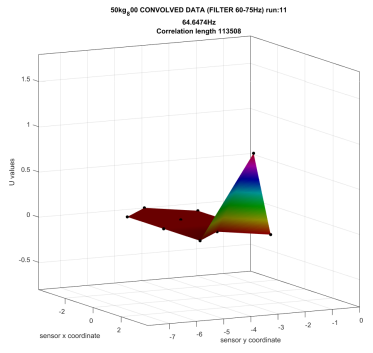
(a) 50kg mode shape, run 10



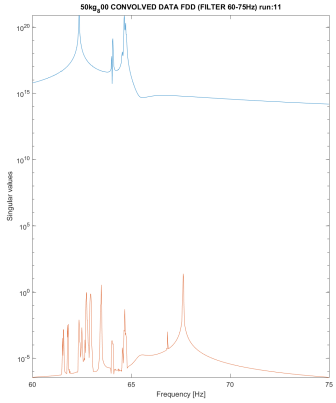


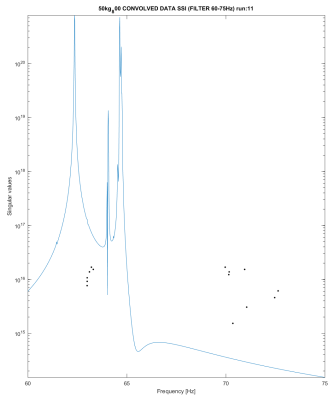
(b) 50kg FDD SSI output, run 10

Figure A3.50kg (28.03.2017): Run 10 (segment 1)



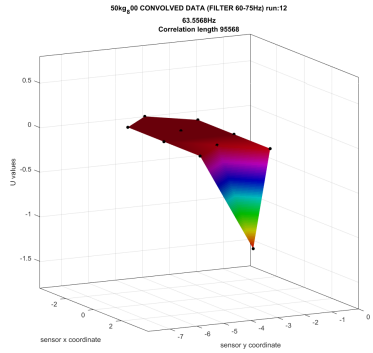
(a) 50kg mode shape, run 11



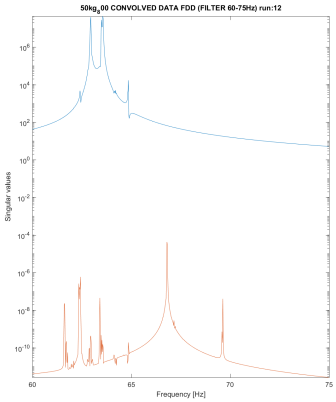


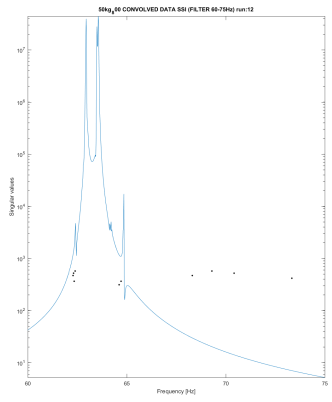
(b) 50kg FDD SSI output, run 11

Figure A3.50kg (28.03.2017): Run 11 (segment 1)



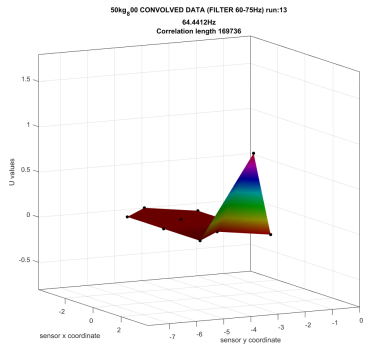
(a) 50kg mode shape, run 12



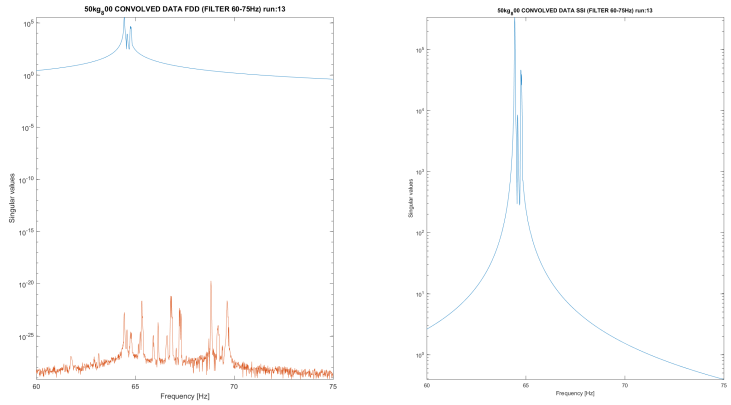


(b) 50kg FDD SSI output, run 12

Figure A3.50kg (28.03.2017): Run 12 (segment 1)

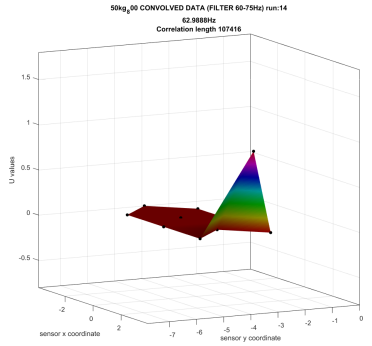


(a) 50kg mode shape, run 13

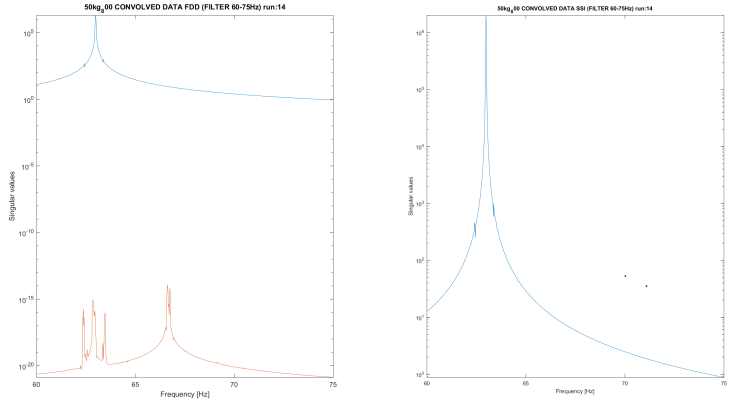


(b) 50kg FDD SSI output, run 13

Figure A3.50kg (28.03.2017): Run 13 (segment 1)

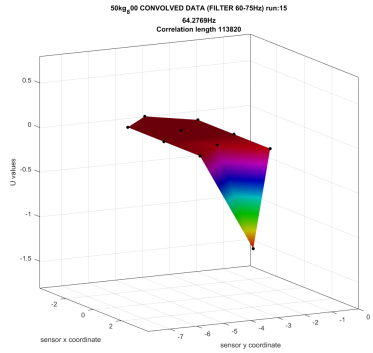


(a) 50kg mode shape, run 14

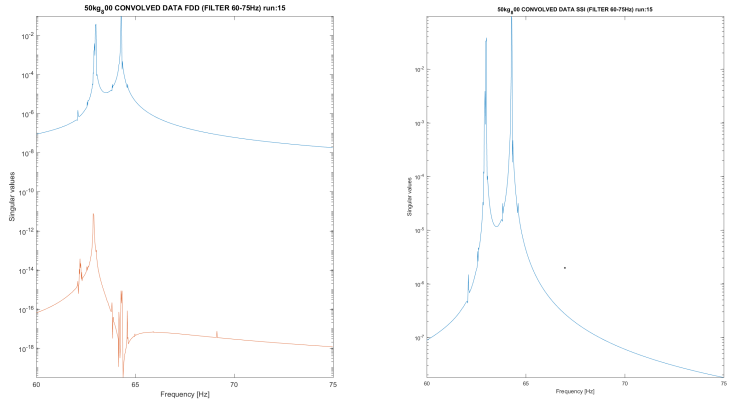


(b) 50kg FDD SSI output, run 14

Figure A3.50kg (28.03.2017): Run 14 (segment 1)

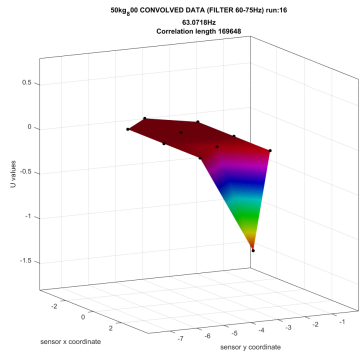


(a) 50kg mode shape, run 15

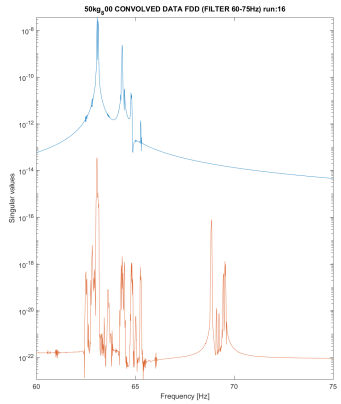


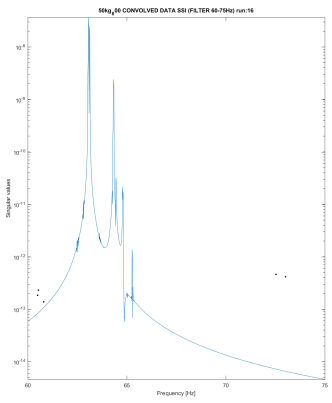
(b) 50kg FDD SSI output, run 15

Figure A3.50kg (28.03.2017): Run 15 (segment 1)



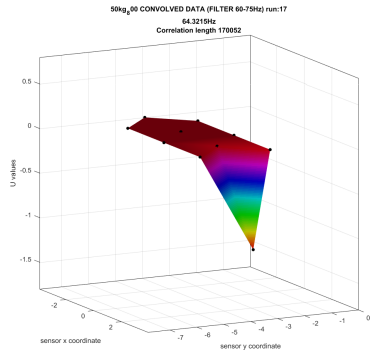
(a) 50kg mode shape, run 16



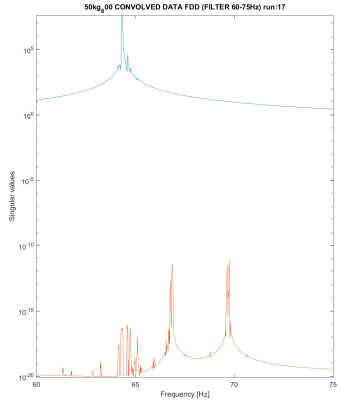


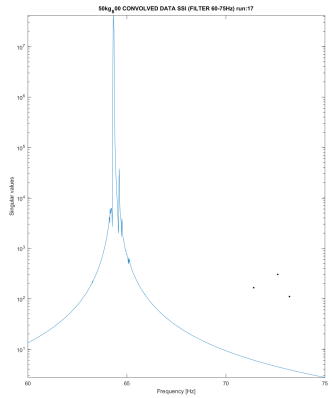
(b) 50kg FDD SSI output, run 16

Figure A3.50kg (28.03.2017): Run 16 (segment 1)



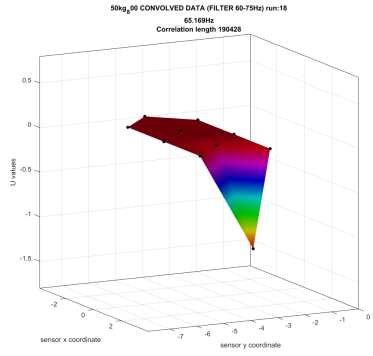
(a) 50kg mode shape, run 17



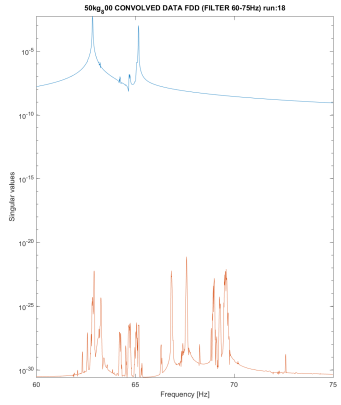


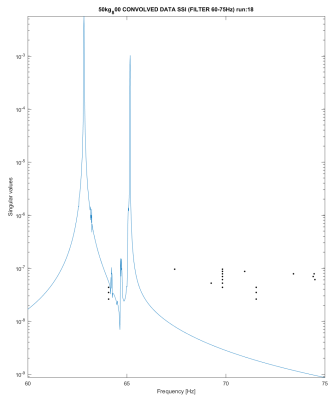
(b) 50kg FDD SSI output, run 17

Figure A3.50kg (28.03.2017): Run 17 (segment 1)



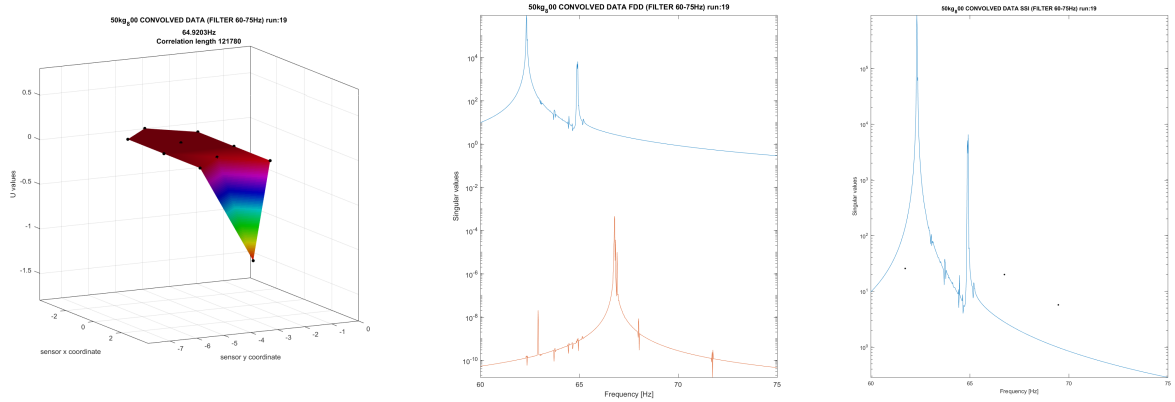
(a) 50kg mode shape, run 18





(b) 50kg FDD SSI output, run 18

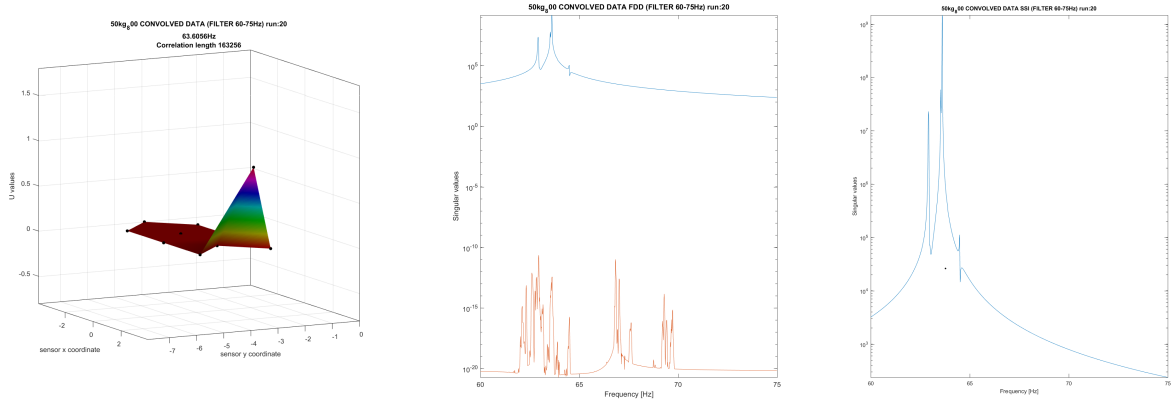
Figure A3.50kg (28.03.2017): Run 18 (segment 1)



(a) 50kg mode shape, run 19

(b) 50kg FDD SSI output, run 19

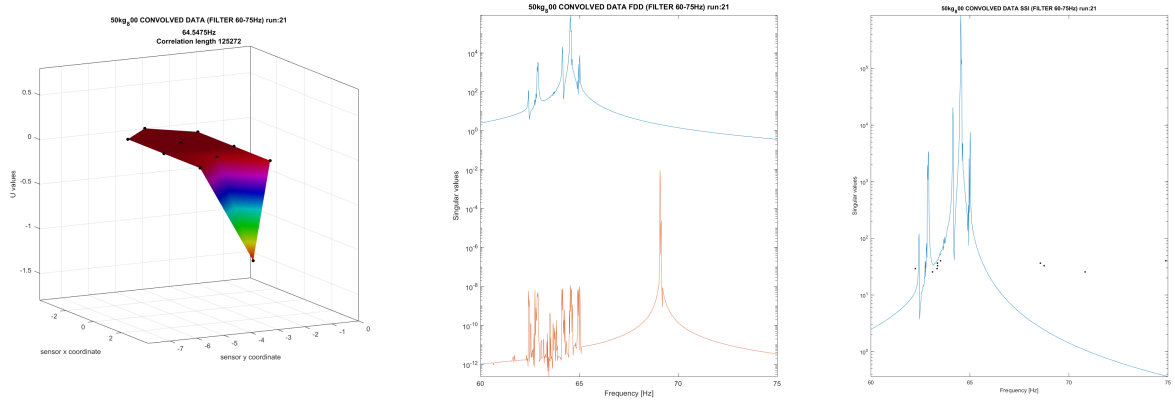
Figure A3.50kg (28.03.2017): Run 19 (segment 1)



(a) 50kg mode shape, run 20

(b) 50kg FDD SSI output, run 20

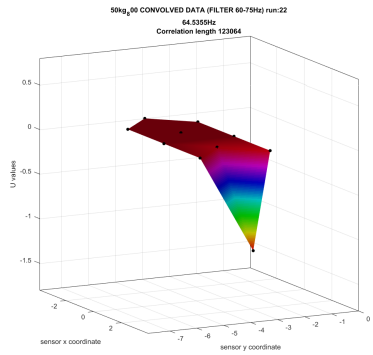
Figure A3.50kg (28.03.2017): Run 20 (segment 1)



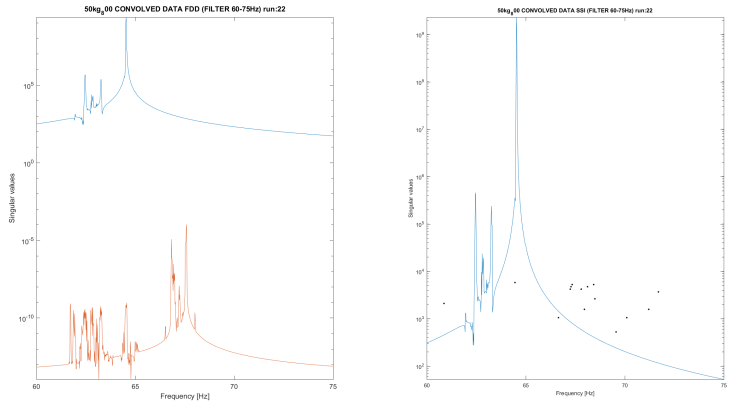
(a) 50kg mode shape, run 21

(b) 50kg FDD SSI output, run 21

Figure A3.50kg (28.03.2017): Run 21 (segment 1)

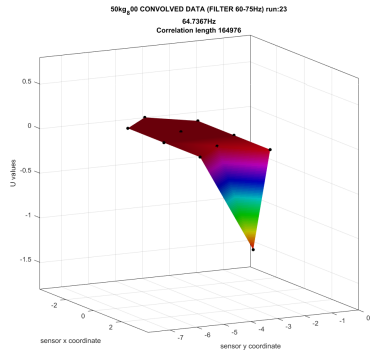


(a) 50kg mode shape, run 22

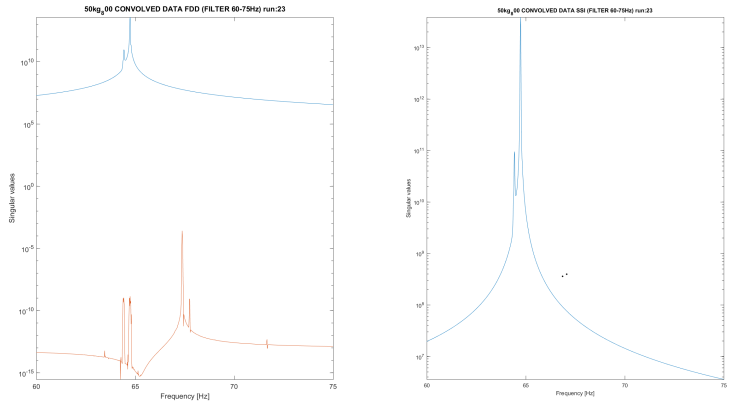


(b) 50kg FDD SSI output, run 22

Figure A3.50kg (28.03.2017): Run 22 (segment 1)

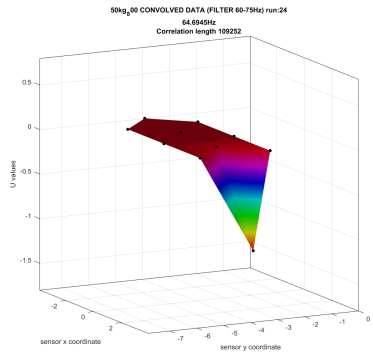


(a) 50kg mode shape, run 23

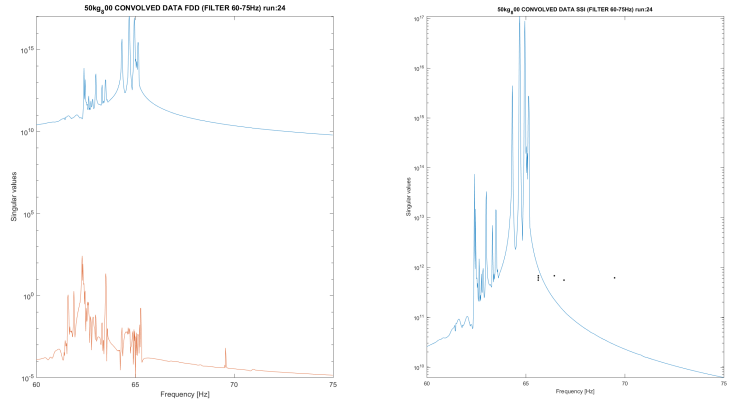


(b) 50kg FDD SSI output, run 23

Figure A3.50kg (28.03.2017): Run 23 (segment 1)

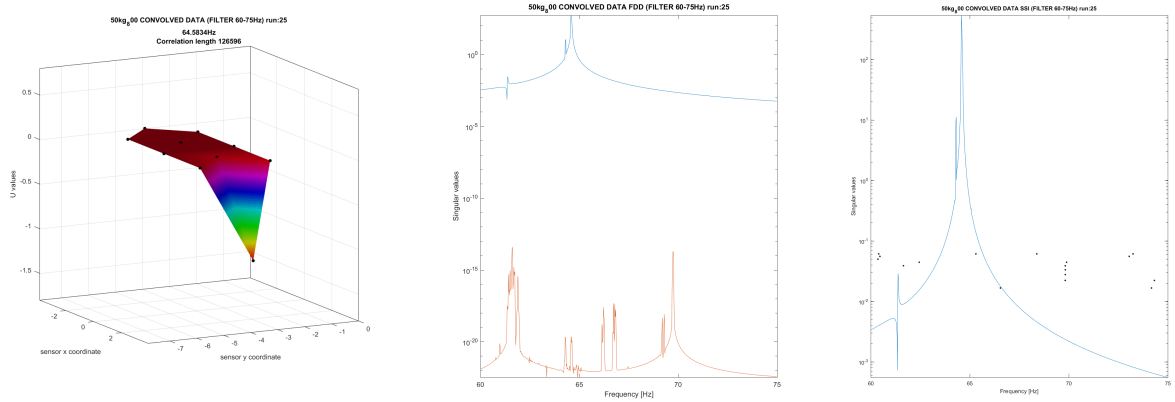


(a) 50kg mode shape, run 24



(b) 50kg FDD SSI output, run 24

Figure A3.50kg (28.03.2017): Run 24 (segment 1)

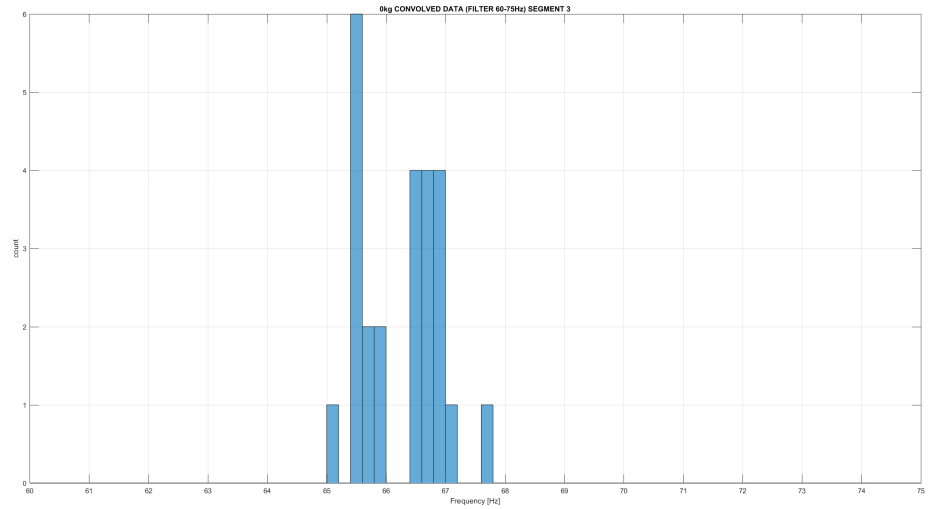


(a) 50kg mode shape, run 25

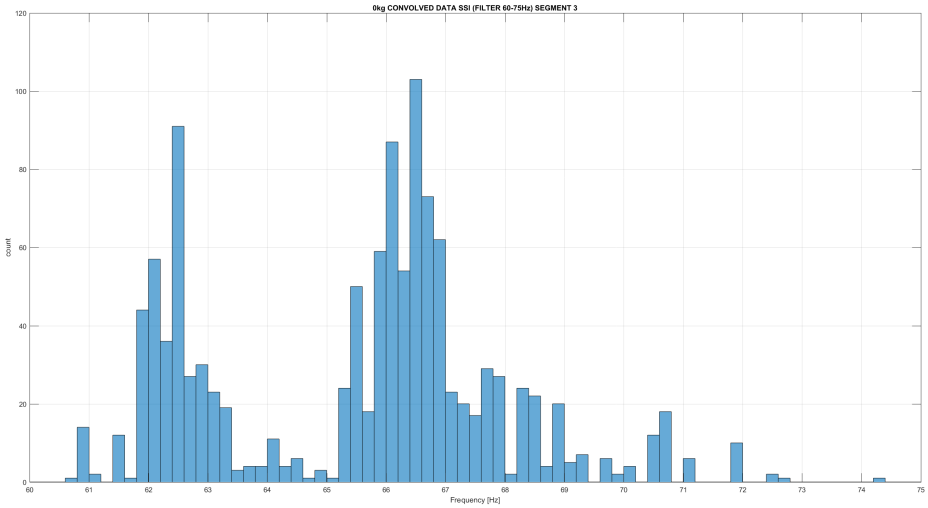
(b) 50kg FDD SSI output, run 25

Figure A3.50kg (28.03.2017): Run 25 (segment 1)

Data 0kg-50kg-75kg-100kg segment 3 (Unreduced order PF)

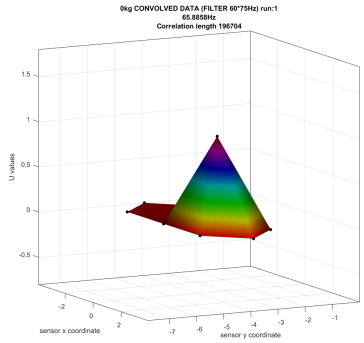


(a) 0kg FDD histogram

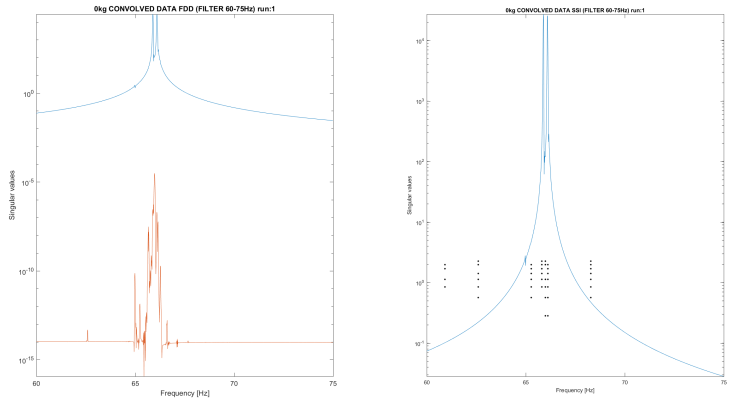


(b) 0kg SSI histogram

Figure A3.0kg: Histograms of identified modes, 0kg data (segment 3)

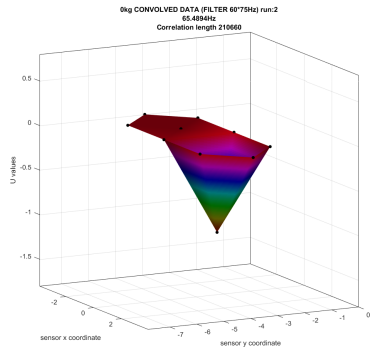


(a) 0kg mode shape, run 1

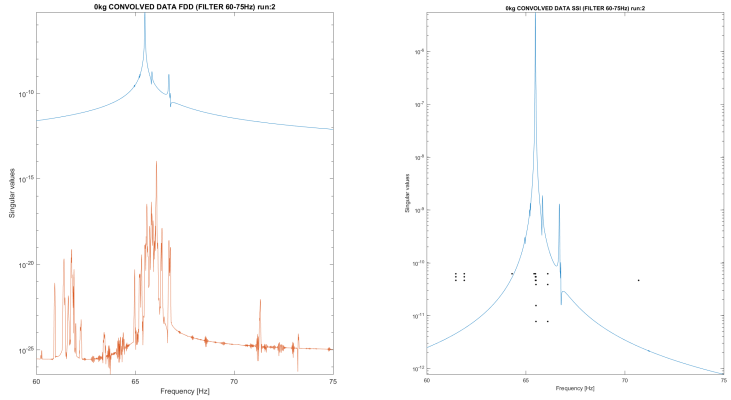


(b) 0kg FDD SSI output, run 1

Figure A3.0kg: Run 1 (segment 3)

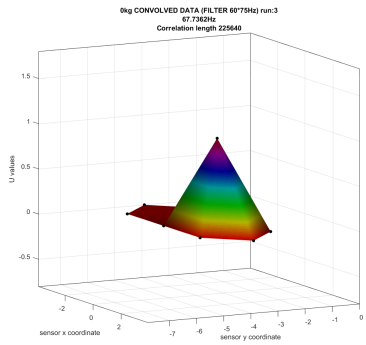


(a) 0kg mode shape, run 2

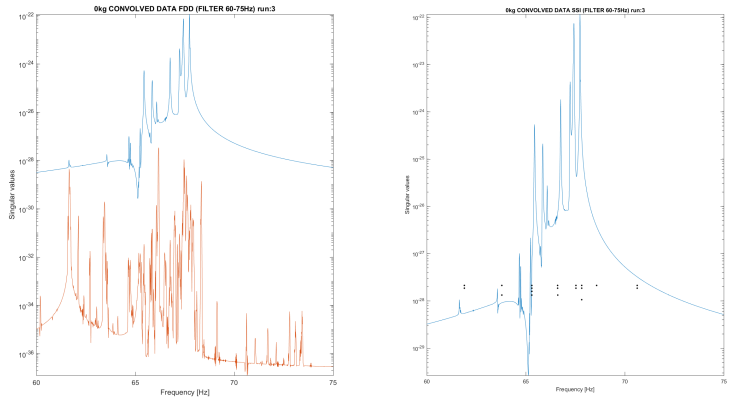


(b) 0kg FDD SSI output, run 2

Figure A3.0kg: Run 2 (segment 3)

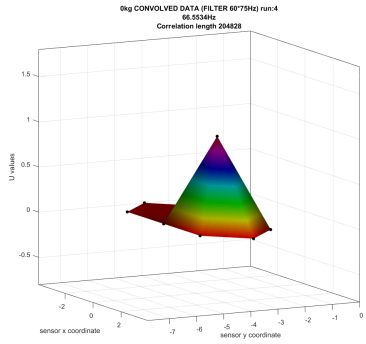


(a) 0kg mode shape, run 3

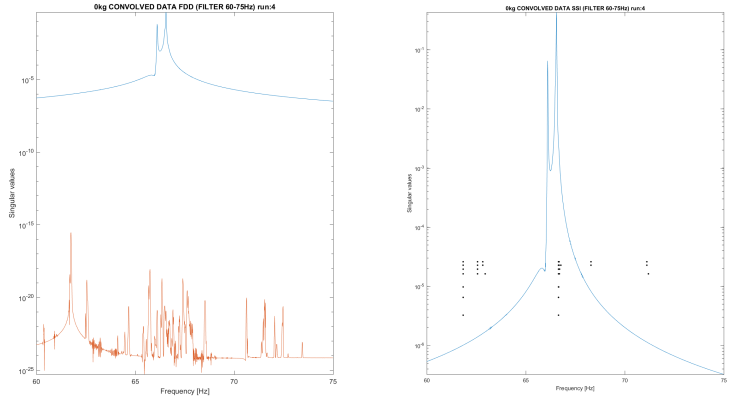


(b) 0kg FDD SSI output, run 3

Figure A3.0kg: Run 3 (segment 3)

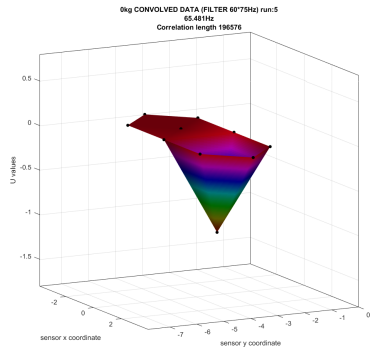


(a) 0kg mode shape, run 4

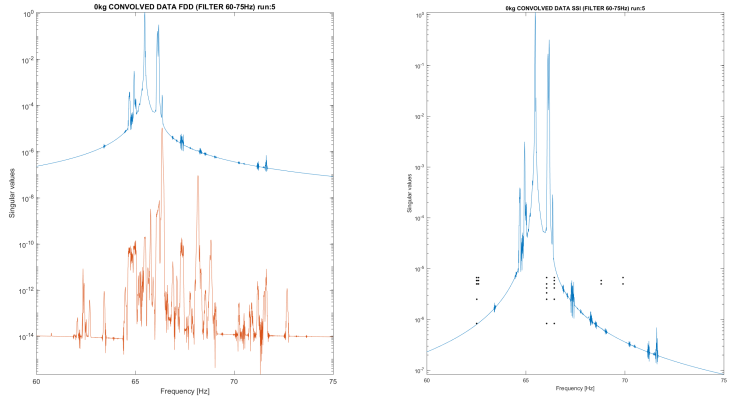


(b) 0kg FDD SSI output, run 4

Figure A3.0kg: Run 4 (segment 3)

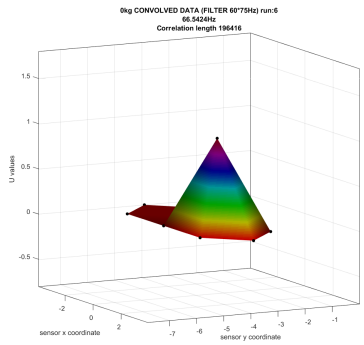


(a) 0kg mode shape, run 5

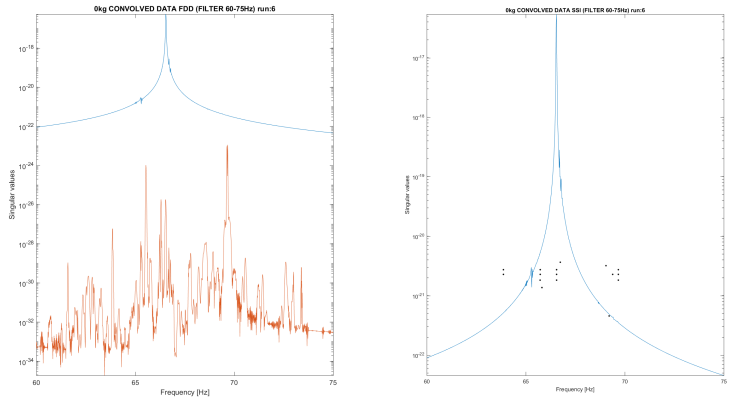


(b) 0kg FDD SSI output, run 5

Figure A3.0kg: Run 5 (segment 3)

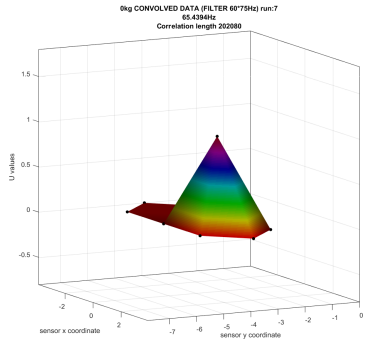


(a) 0kg mode shape, run 6

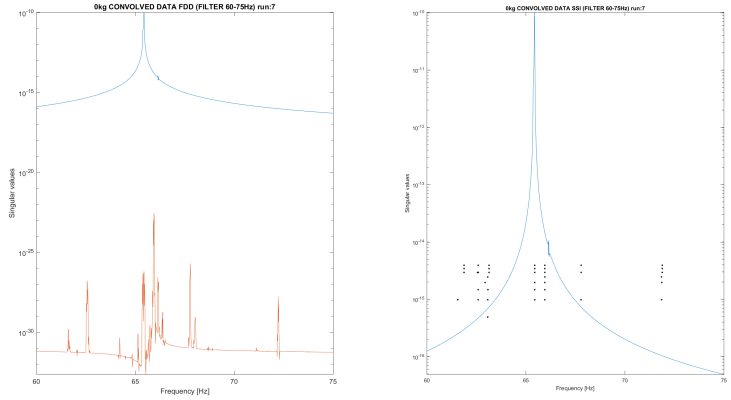


(b) 0kg FDD SSI output, run 6

Figure A3.0kg: Run 6 (segment 3)

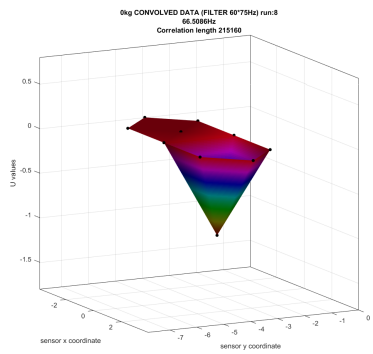


(a) 0kg mode shape, run 7

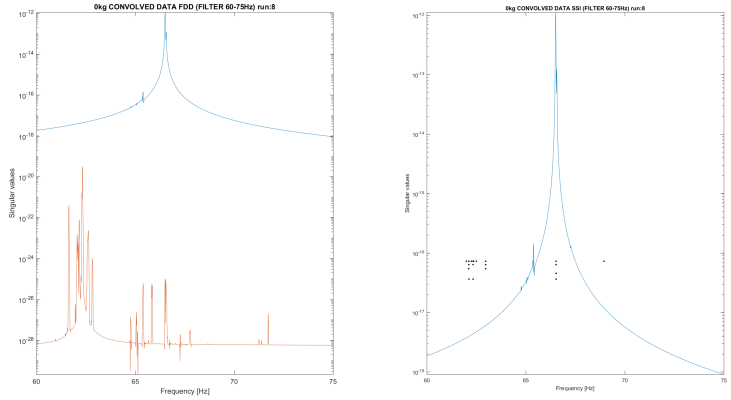


(b) 0kg FDD SSI output, run 7

Figure A3.0kg: Run 7 (segment 3)

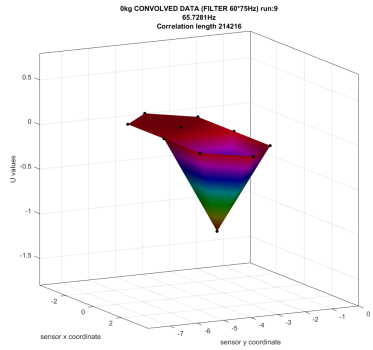


(a) 0kg mode shape, run 8

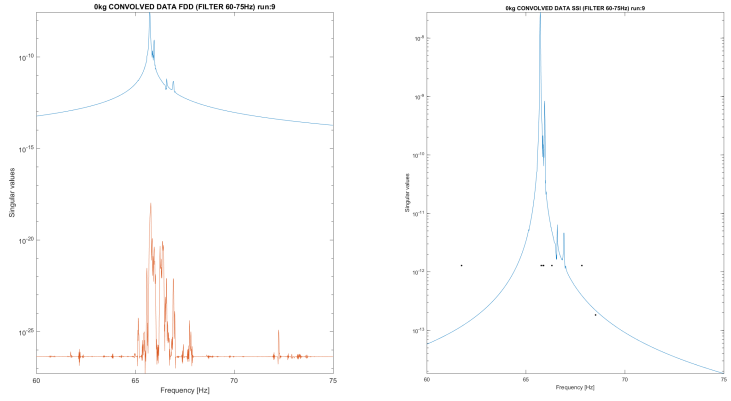


(b) 0kg FDD SSI output, run 8

Figure A3.0kg: Run 8 (segment 3)

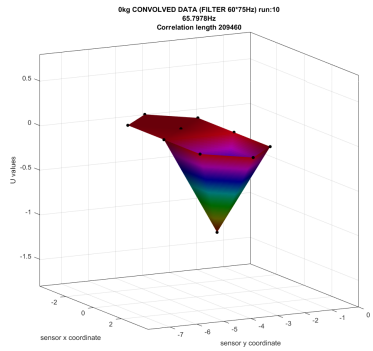


(a) 0kg mode shape, run 9

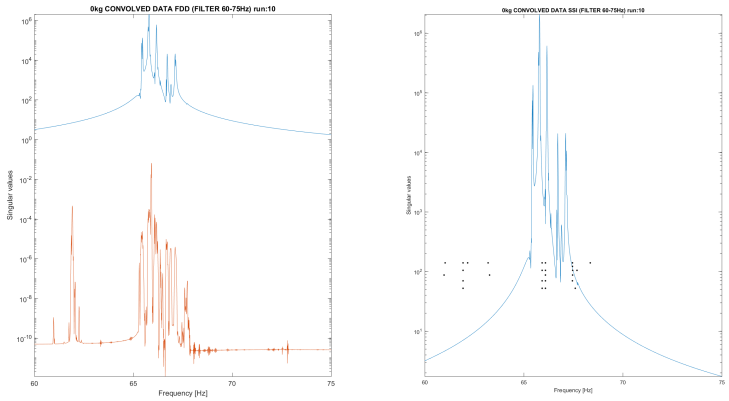


(b) 0kg FDD SSI output, run 9

Figure A3.0kg: Run 9 (segment 3)

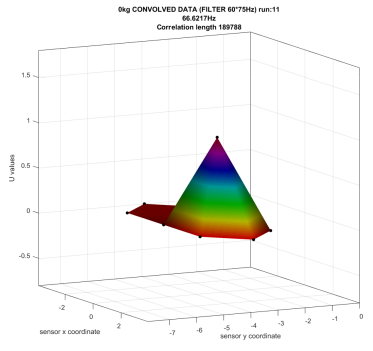


(a) 0kg mode shape, run 10

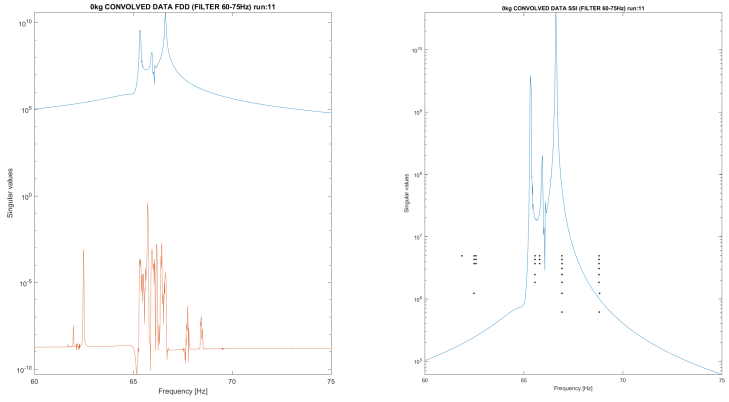


(b) 0kg FDD SSI output, run 10

Figure A3.0kg: Run 10 (segment 3)

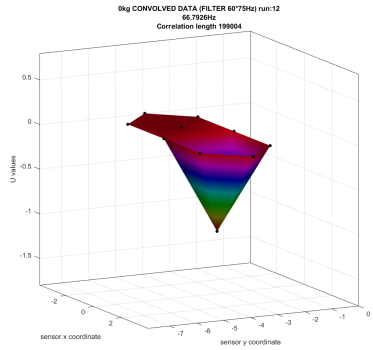


(a) 0kg mode shape, run 11

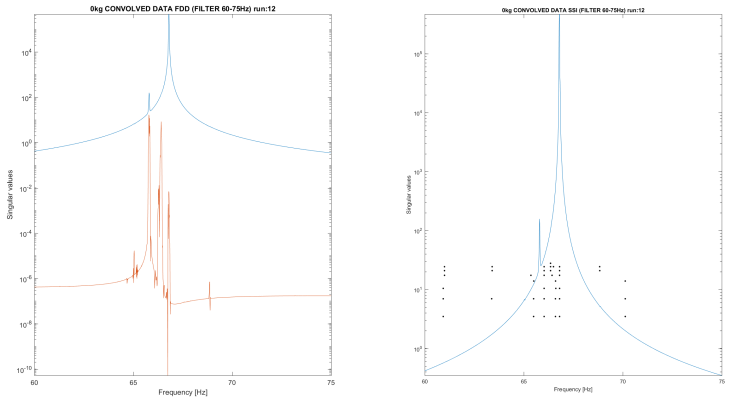


(b) 0kg FDD SSI output, run 11

Figure A3.0kg: Run 11 (segment 3)

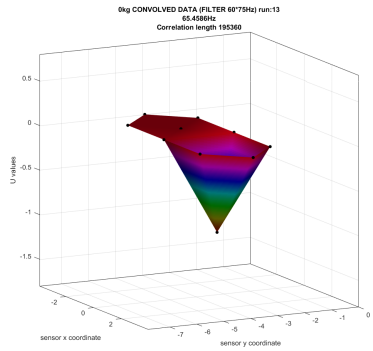


(a) 0kg mode shape, run 12

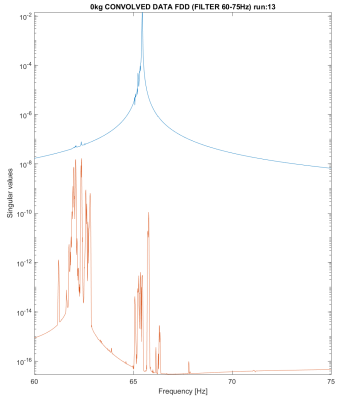


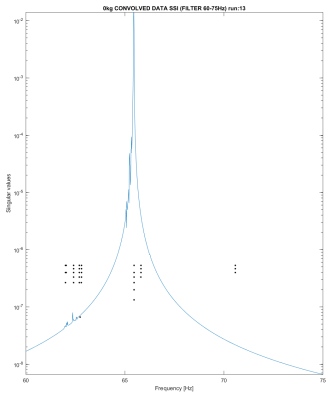
(b) 0kg FDD SSI output, run 12

Figure A3.0kg: Run 12 (segment 3)



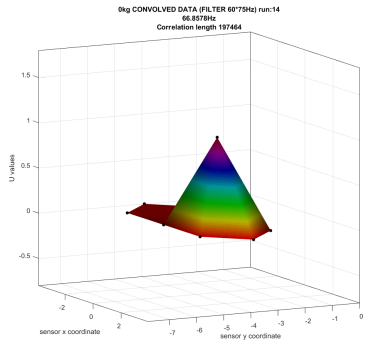
(a) 0kg mode shape, run 13



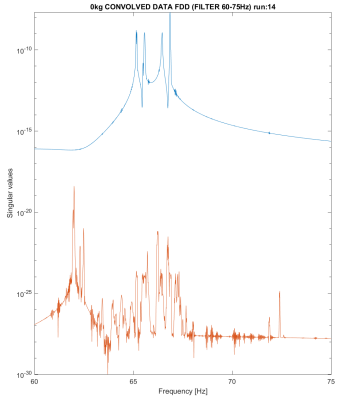


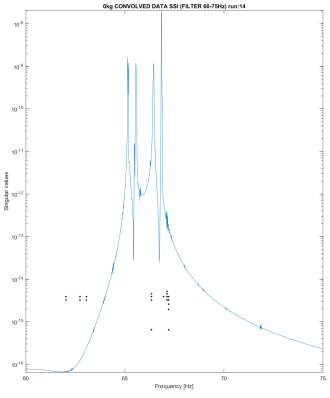
(b) 0kg FDD SSI output, run 13

Figure A3.0kg: Run 13 (segment 3)



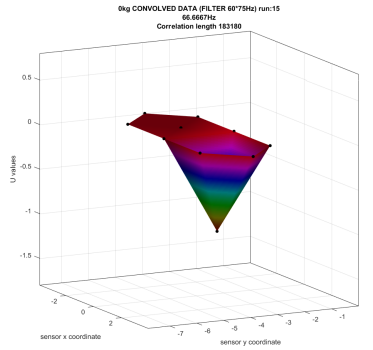
(a) 0kg mode shape, run 14



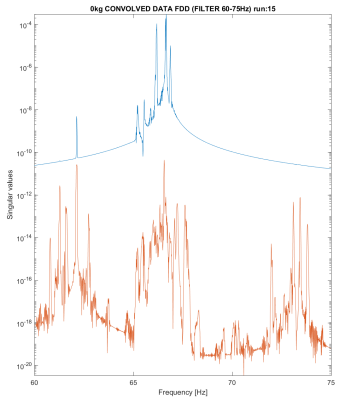


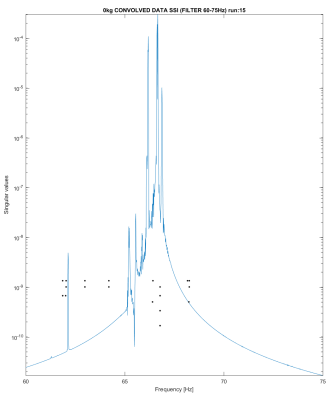
(b) 0kg FDD SSI output, run 14

Figure A3.0kg: Run 14 (segment 3)



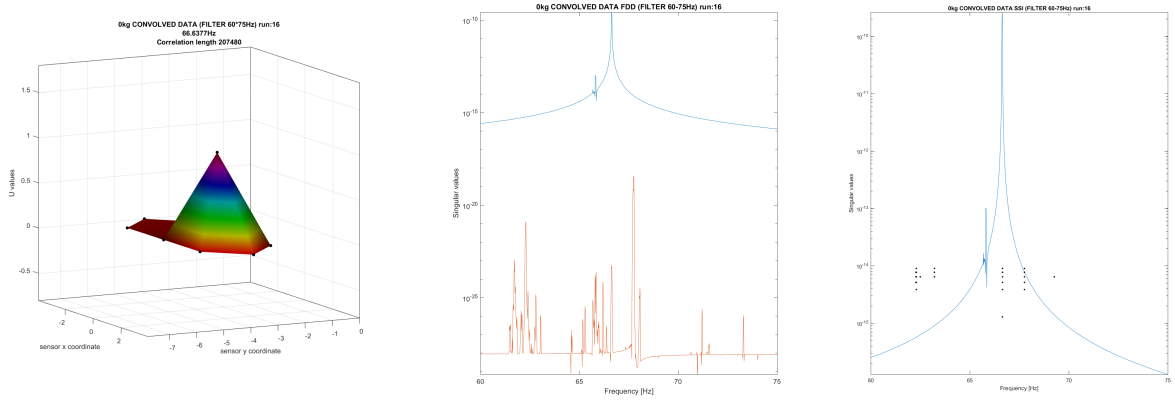
(a) 0kg mode shape, run 15





(b) 0kg FDD SSI output, run 15

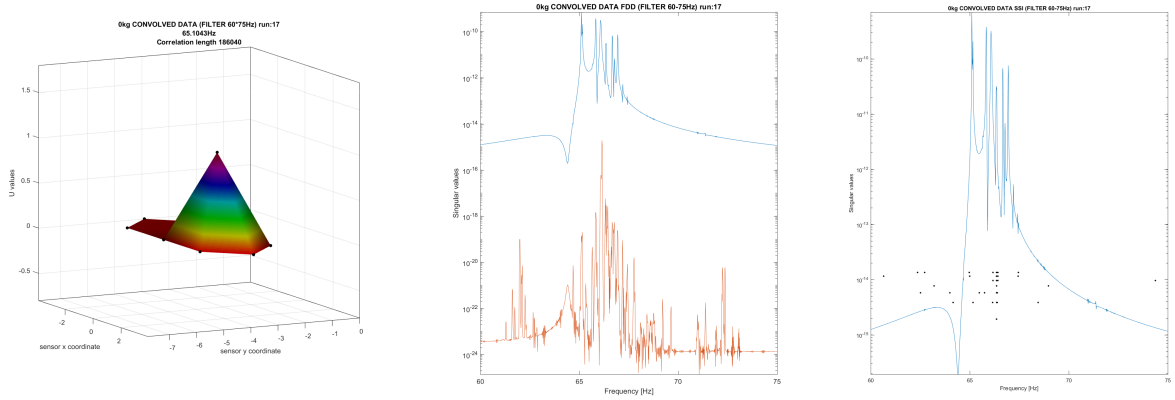
Figure A3.0kg: Run 15 (segment 3)



(a) 0kg mode shape, run 16

(b) 0kg FDD SSI output, run 16

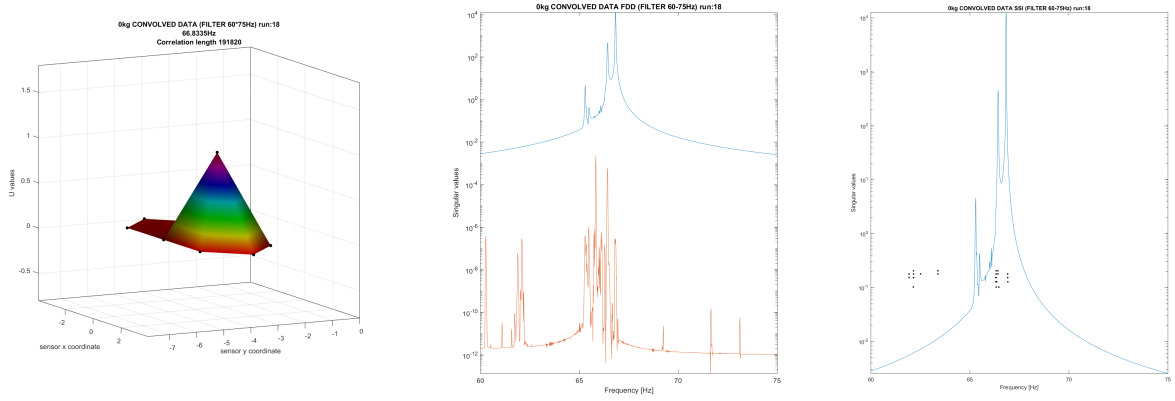
Figure A3.0kg: Run 16 (segment 3)



(a) 0kg mode shape, run 17

(b) 0kg FDD SSI output, run 17

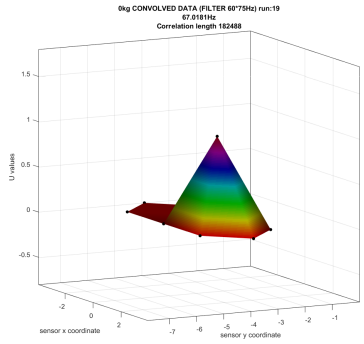
Figure A3.0kg: Run 17 (segment 3)



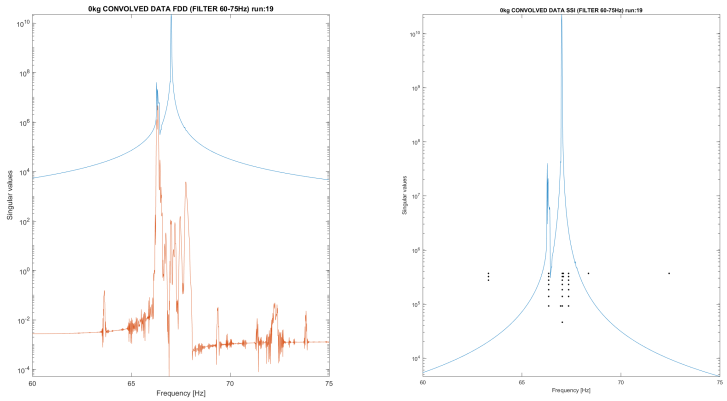
(a) 0kg mode shape, run 18

(b) 0kg FDD SSI output, run 18

Figure A3.0kg: Run 18 (segment 3)

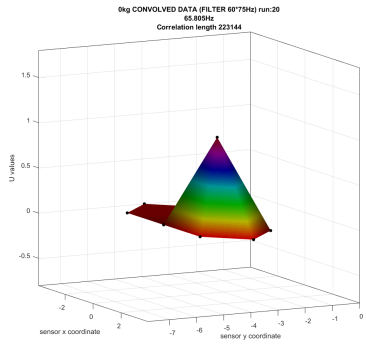


(a) 0kg mode shape, run 19

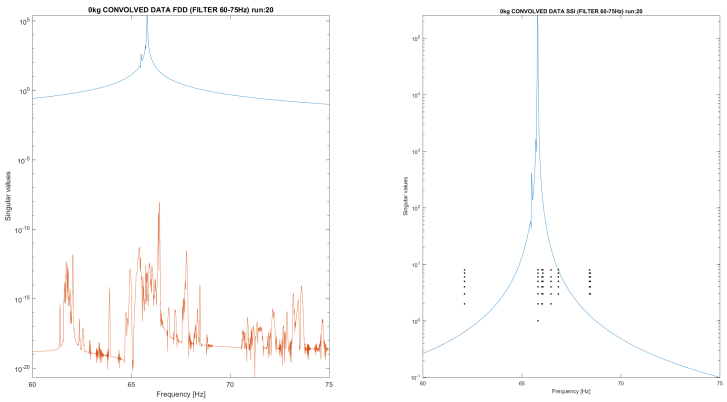


(b) 0kg FDD SSI output, run 19

Figure A3.0kg: Run 19 (segment 3)

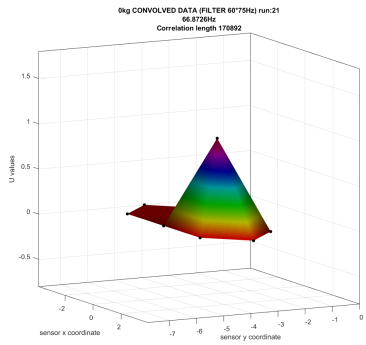


(a) 0kg mode shape, run 20

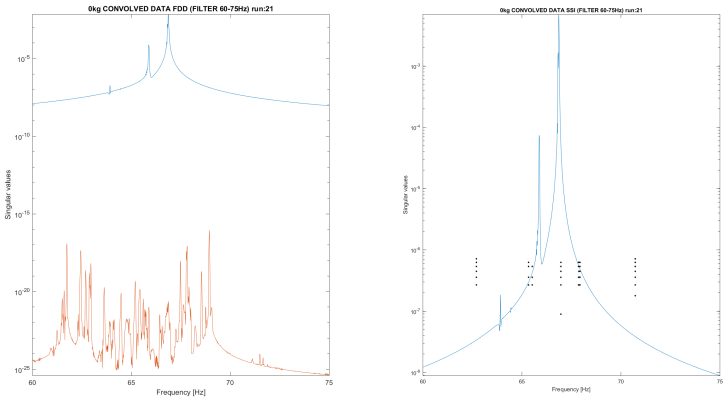


(b) 0kg FDD SSI output, run 20

Figure A3.0kg: Run 20 (segment 3)

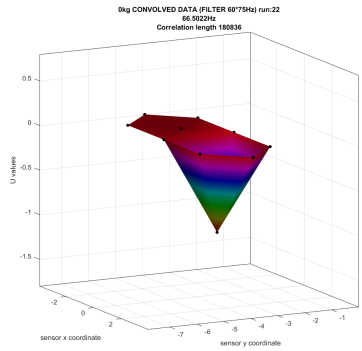


(a) 0kg mode shape, run 21

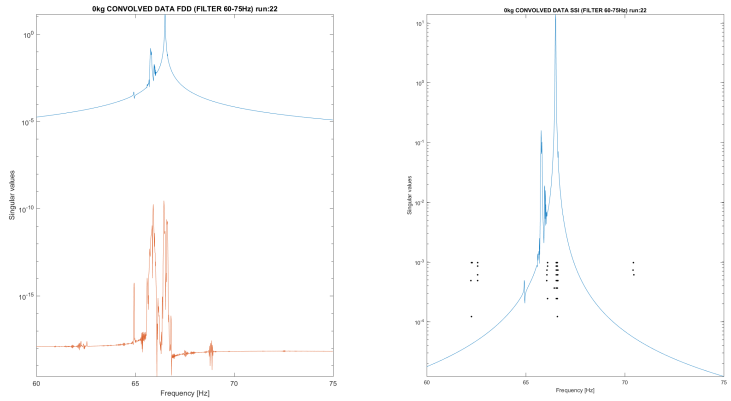


(b) 0kg FDD SSI output, run 21

Figure A3.0kg: Run 21 (segment 3)

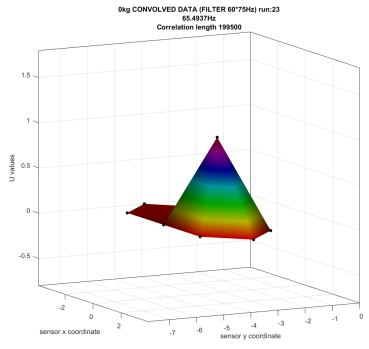


(a) 0kg mode shape, run 22

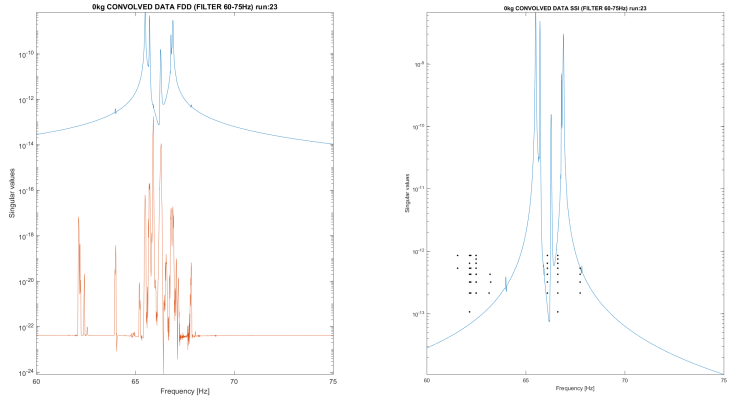


(b) 0kg FDD SSI output, run 22

Figure A3.0kg: Run 22 (segment 3)

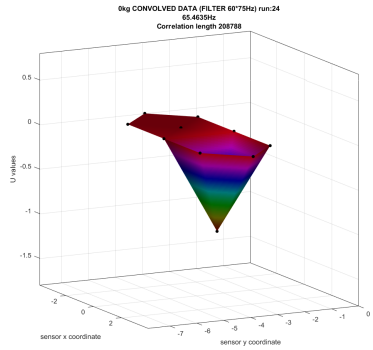


(a) 0kg mode shape, run 23

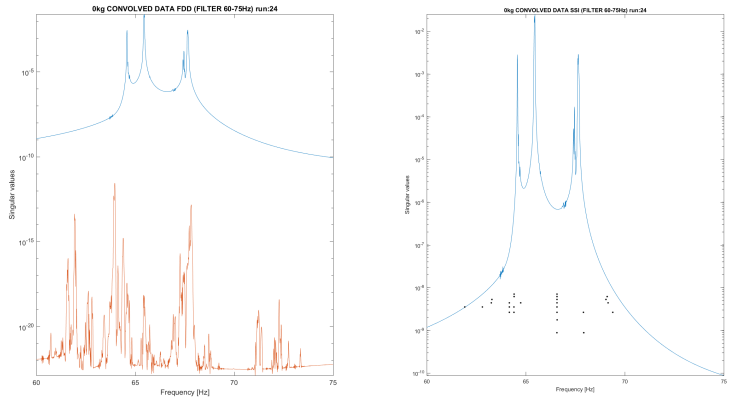


(b) 0kg FDD SSI output, run 23

Figure A3.0kg: Run 23 (segment 3)

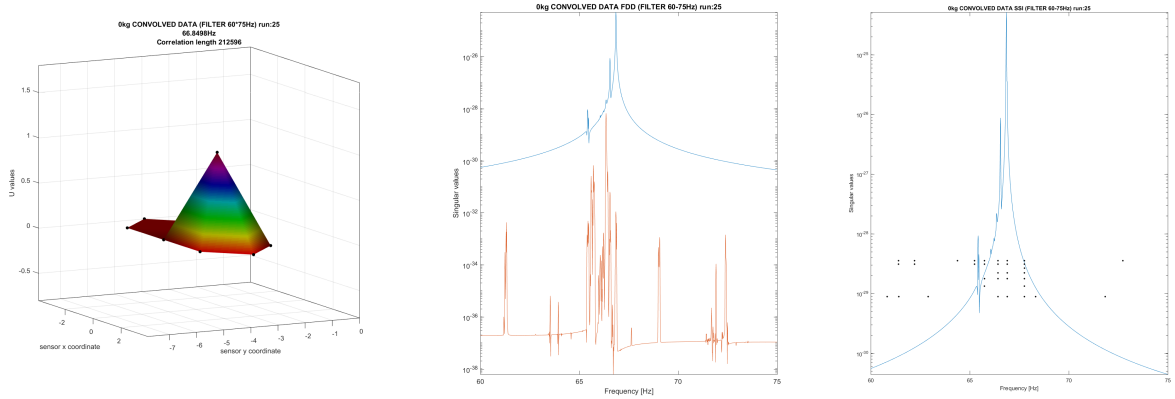


(a) 0kg mode shape, run 24



(b) 0kg FDD SSI output, run 24

Figure A3.0kg: Run 24 (segment 3)

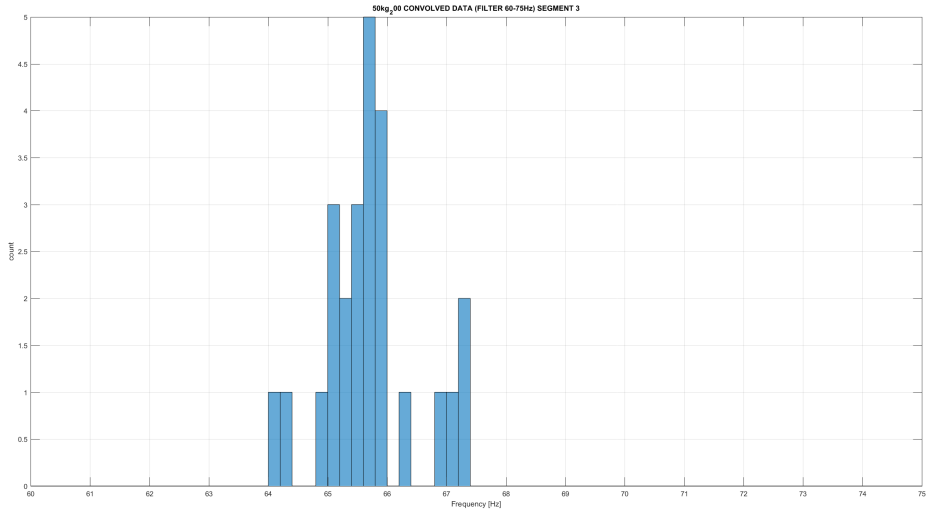


(a) 0kg mode shape, run 25

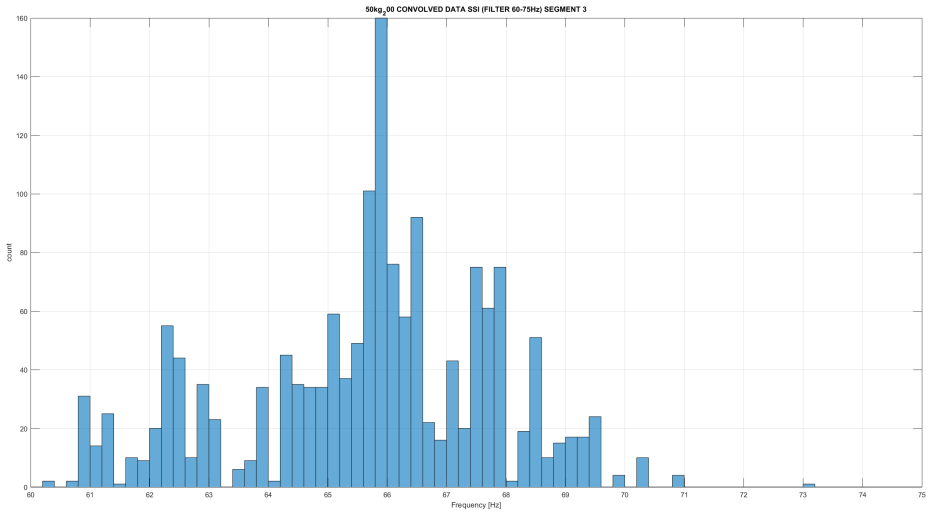
(b) 0kg FDD SSI output, run 25

Figure A3.0kg: Run 25 (segment 3)

50kg data segment 3

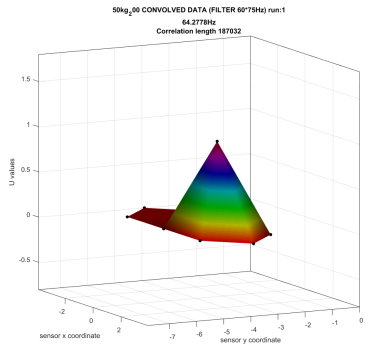


(a) 50kg FDD histogram

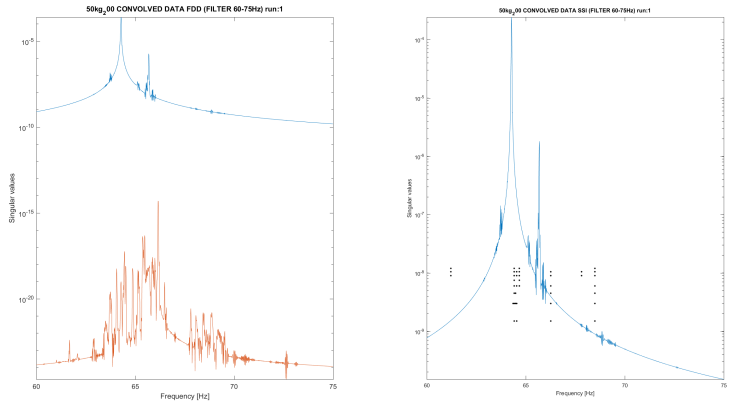


(b) 50kg SSI histogram

Figure A3.50kg: Histograms of identified modes, 50kg data (segment 3)

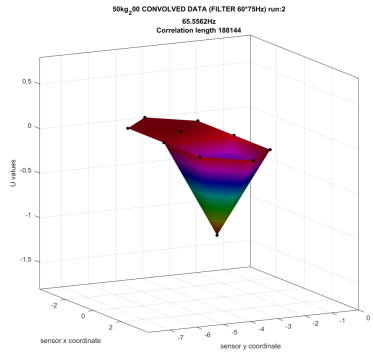


(a) 50kg mode shape, run 1

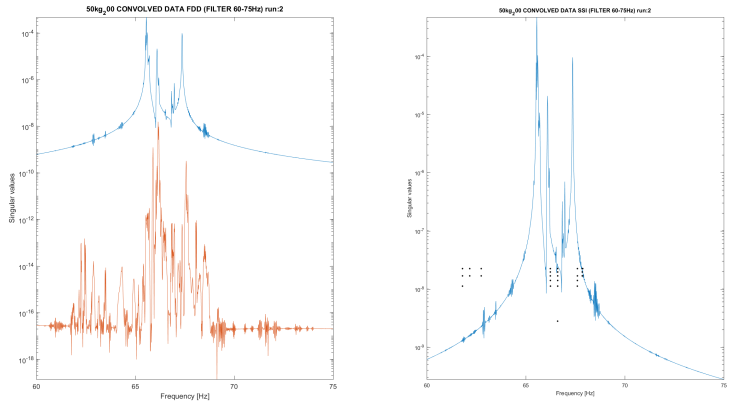


(b) 50kg FDD SSI output, run 1

Figure A3.50kg: Run 1 (segment 3)

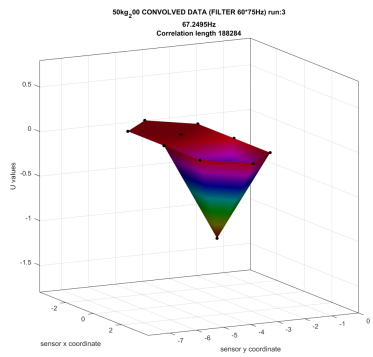


(a) 50kg mode shape, run 2

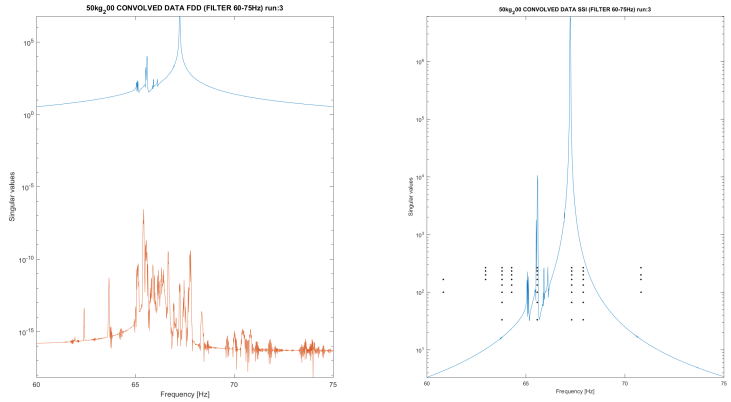


(b) 50kg FDD SSI output, run 2

Figure A3.50kg: Run 2 (segment 3)

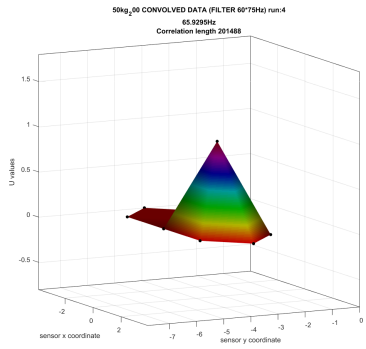


(a) 50kg mode shape, run 3

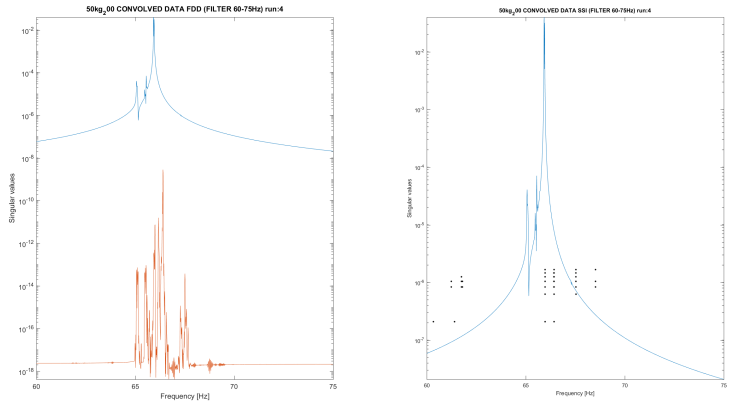


(b) 50kg FDD SSI output, run 3

Figure A3.50kg: Run 3 (segment 3)

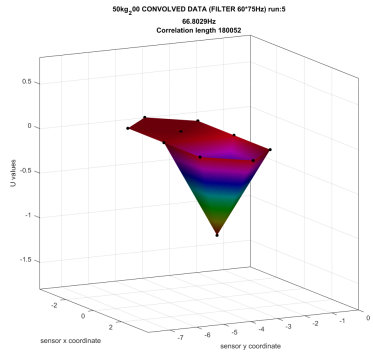


(a) 50kg mode shape, run 4

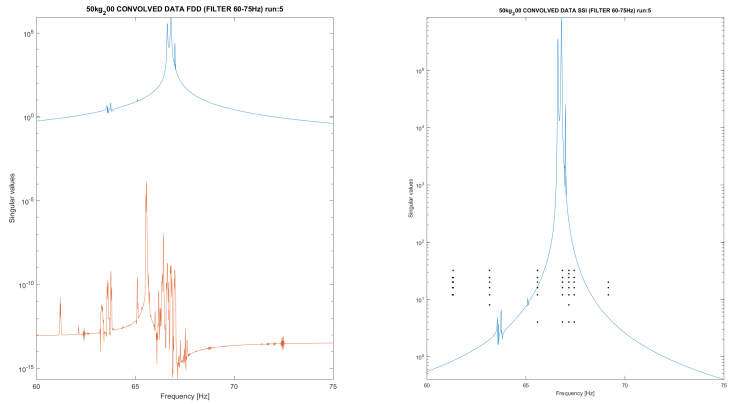


(b) 50kg FDD SSI output, run 4

Figure A3.50kg: Run 4 (segment 3)

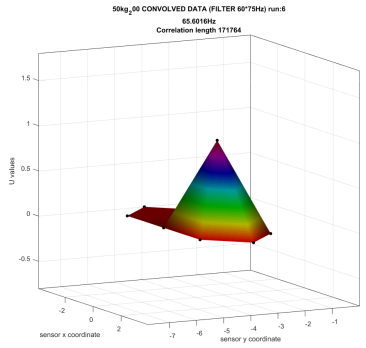


(a) 50kg mode shape, run 5

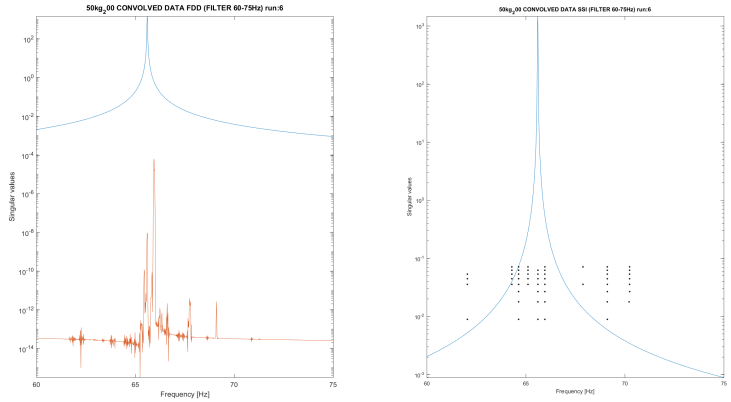


(b) 50kg FDD SSI output, run 5

Figure A3.50kg: Run 5 (segment 3)

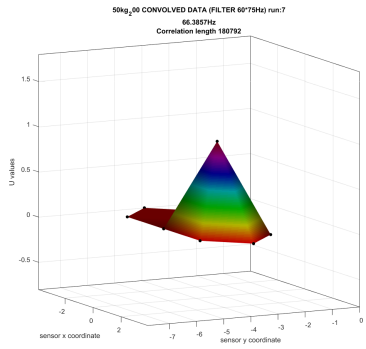


(a) 50kg mode shape, run 6

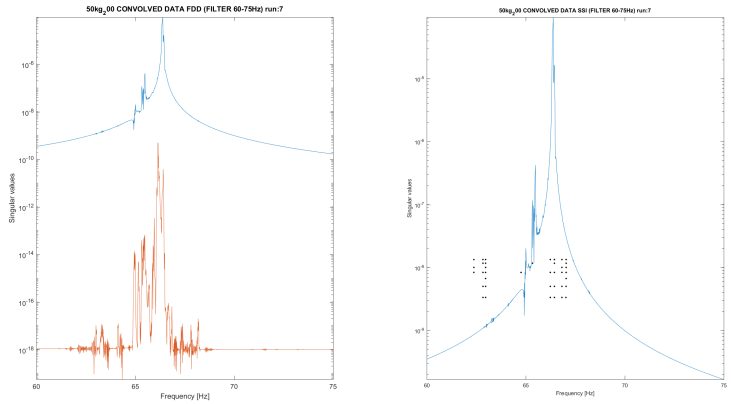


(b) 50kg FDD SSI output, run 6

Figure A3.50kg: Run 6 (segment 3)

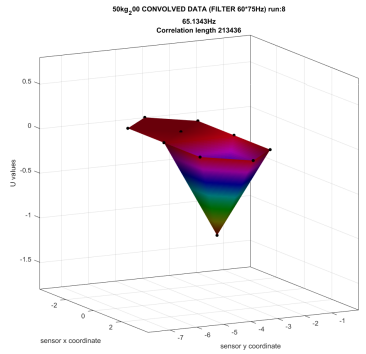


(a) 50kg mode shape, run 7

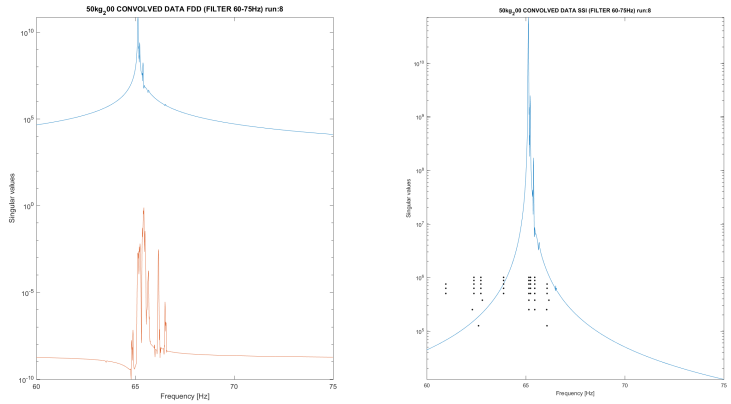


(b) 50kg FDD SSI output, run 7

Figure A3.50kg: Run 7 (segment 3)

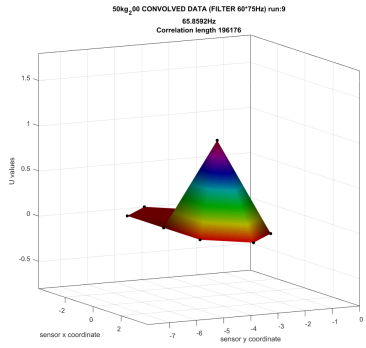


(a) 50kg mode shape, run 8

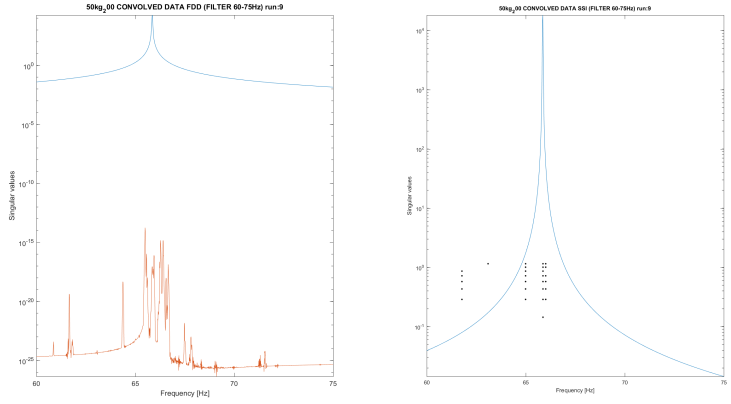


(b) 50kg FDD SSI output, run 8

Figure A3.50kg: Run 8 (segment 3)

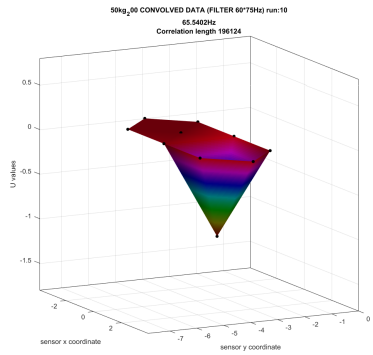


(a) 50kg mode shape, run 9

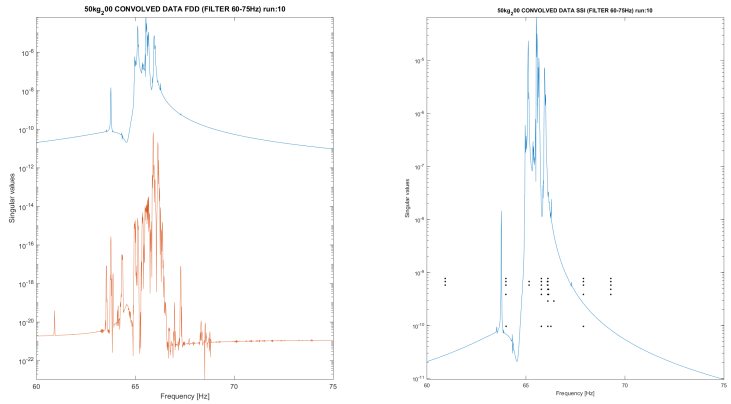


(b) 50kg FDD SSI output, run 9

Figure A3.50kg: Run 9 (segment 3)

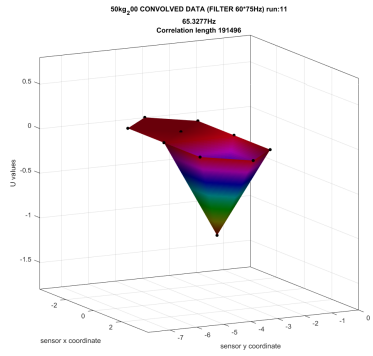


(a) 50kg mode shape, run 10

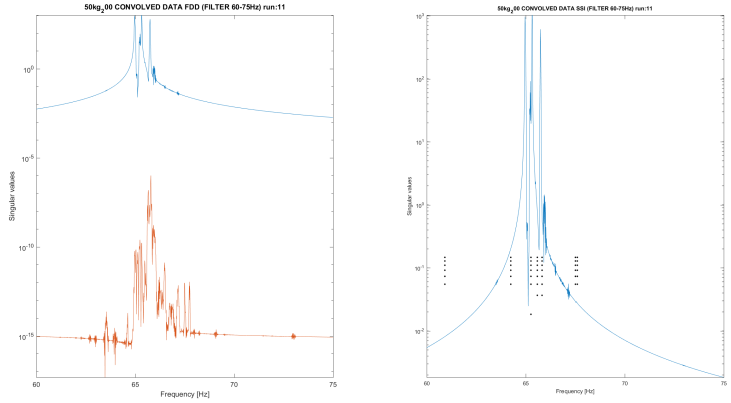


(b) 50kg FDD SSI output, run 10

Figure A3.50kg: Run 10 (segment 3)

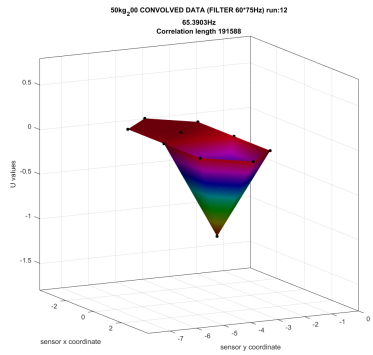


(a) 50kg mode shape, run 11

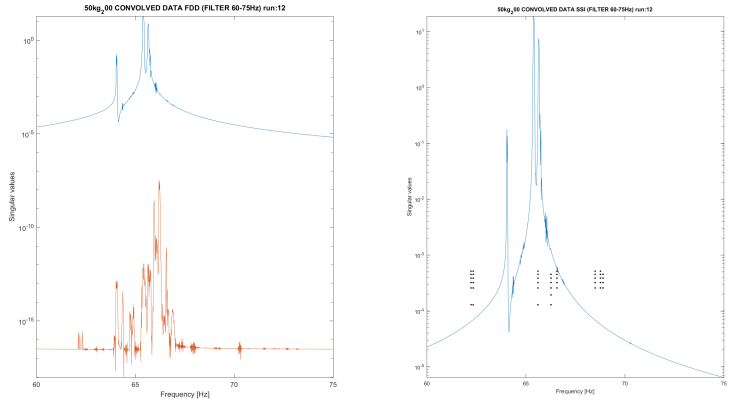


(b) 50kg FDD SSI output, run 11

Figure A3.50kg: Run 11 (segment 3)

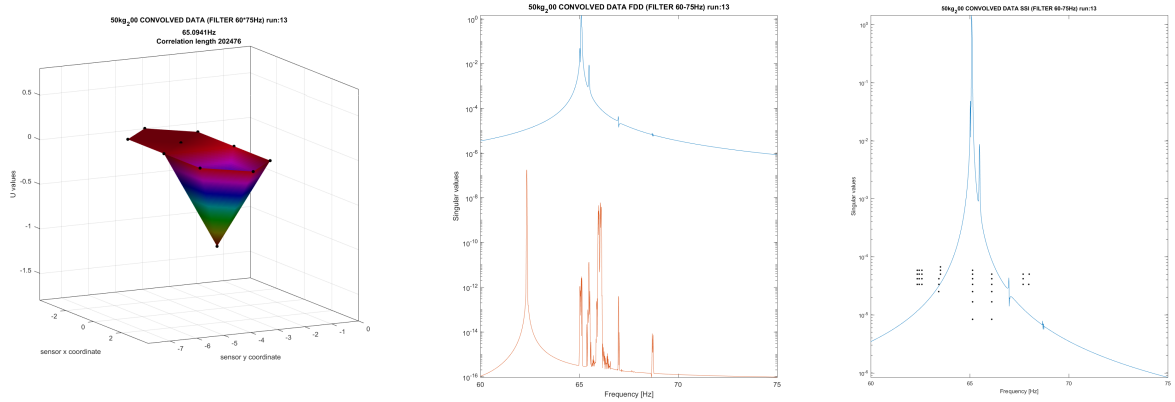


(a) 50kg mode shape, run 12



(b) 50kg FDD SSI output, run 12

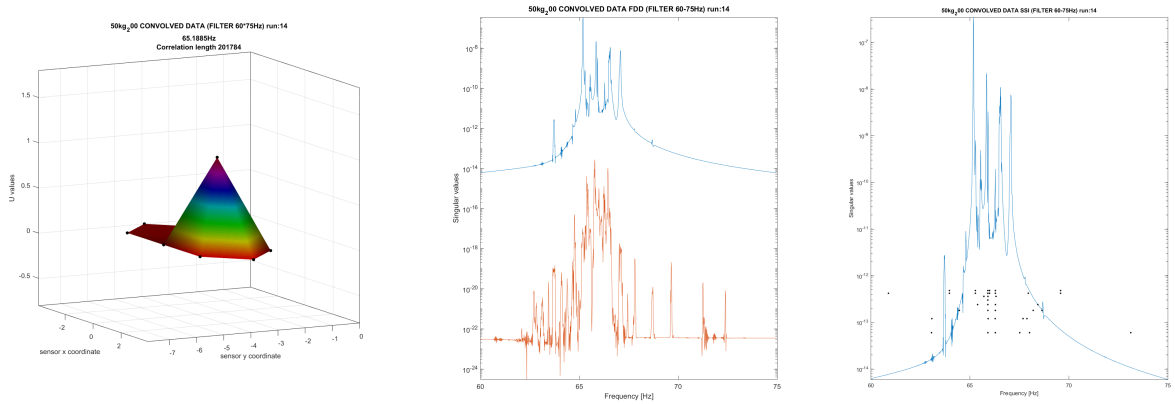
Figure A3.50kg: Run 12 (segment 3)



(a) 50kg mode shape, run 13

(b) 50kg FDD SSI output, run 13

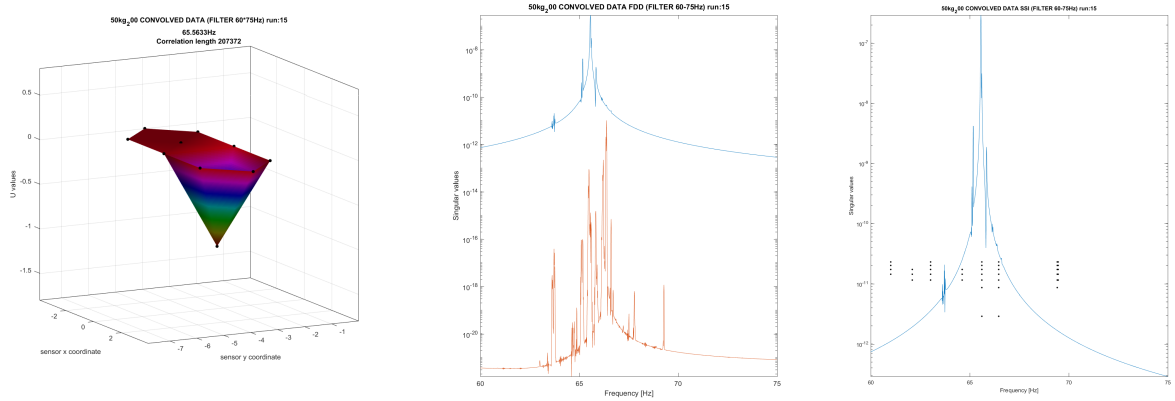
Figure A3.50kg: Run 13 (segment 3)



(a) 50kg mode shape, run 14

(b) 50kg FDD SSI output, run 14

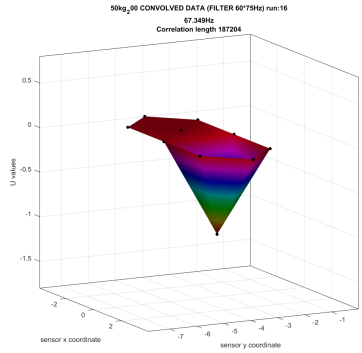
Figure A3.50kg: Run 14 (segment 3)



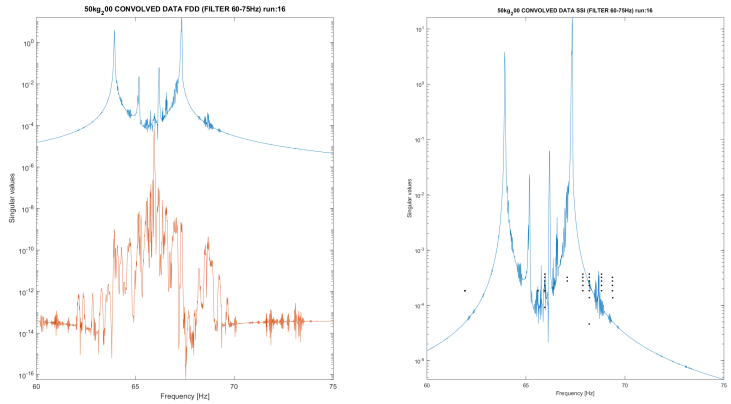
(a) 50kg mode shape, run 15

(b) 50kg FDD SSI output, run 15

Figure A3.50kg: Run 15 (segment 3)

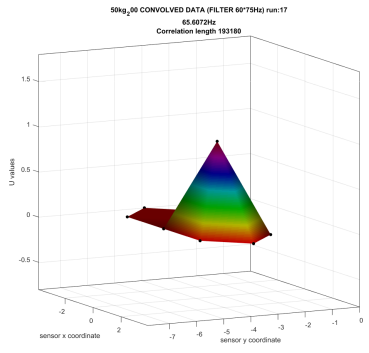


(a) 50kg mode shape, run 16

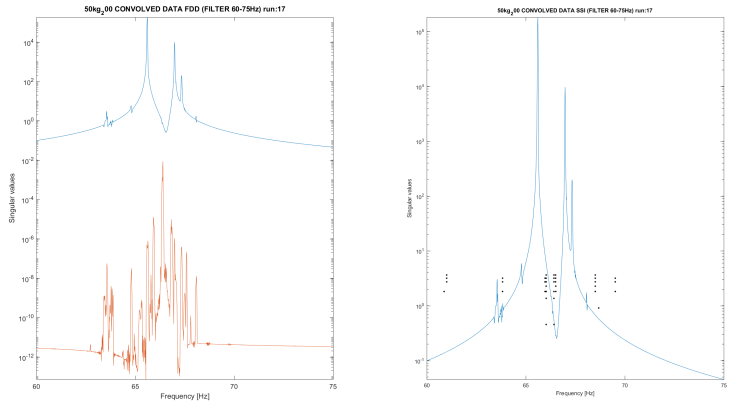


(b) 50kg FDD SSI output, run 16

Figure A3.50kg: Run 16 (segment 3)

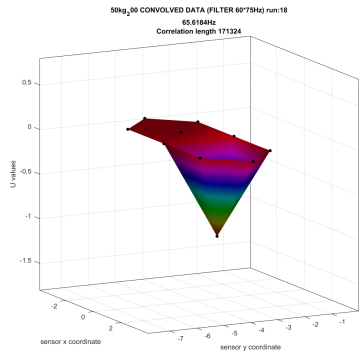


(a) 50kg mode shape, run 17

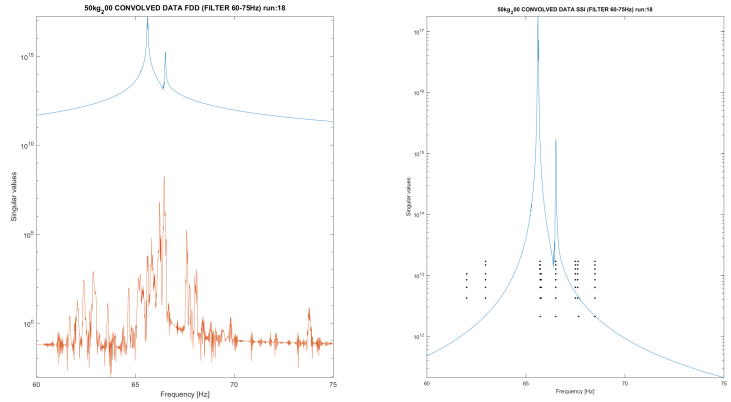


(b) 50kg FDD SSI output, run 17

Figure A3.50kg: Run 17 (segment 3)

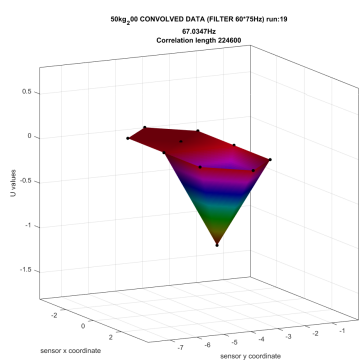


(a) 50kg mode shape, run 18

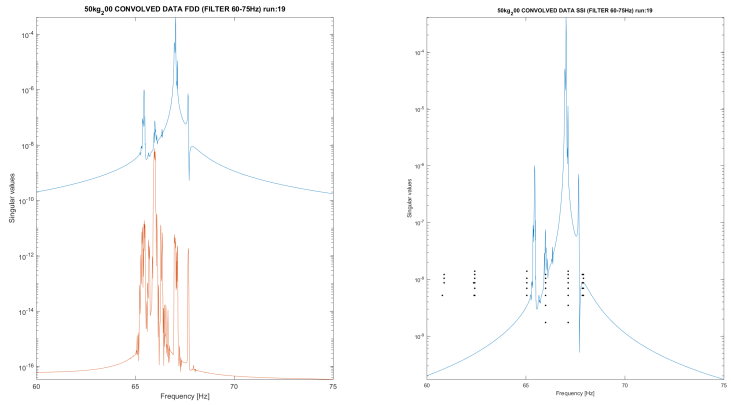


(b) 50kg FDD SSI output, run 18

Figure A3.50kg: Run 18 (segment 3)

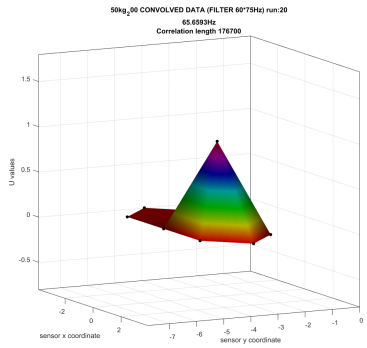


(a) 50kg mode shape, run 19

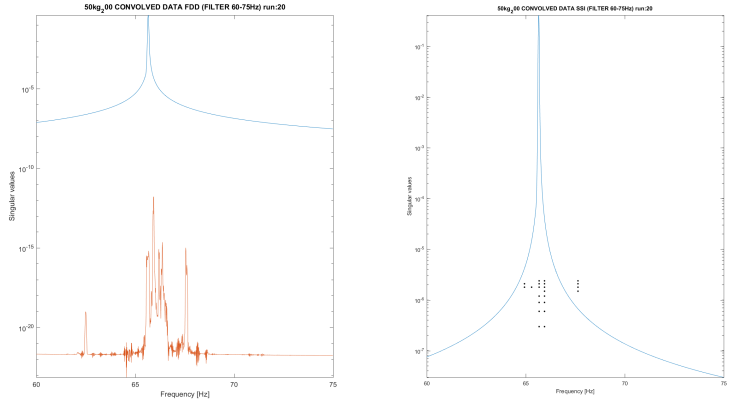


(b) 50kg FDD SSI output, run 19

Figure A3.50kg: Run 19 (segment 3)

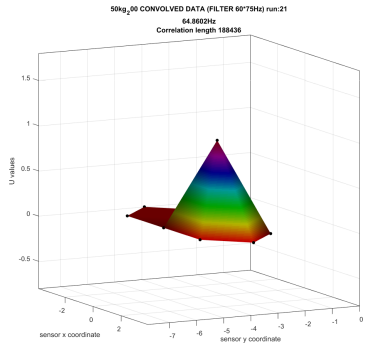


(a) 50kg mode shape, run 20

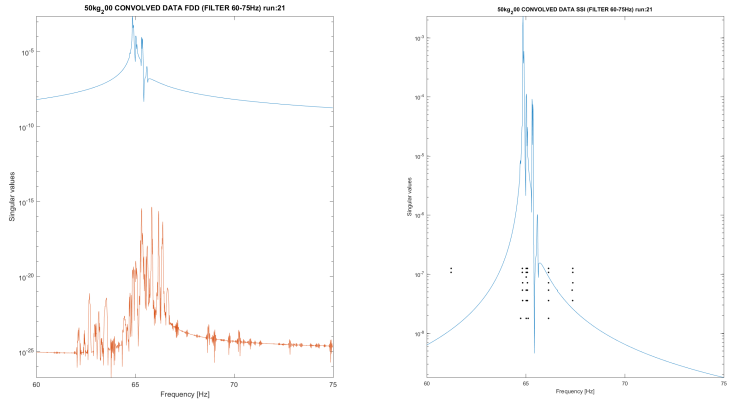


(b) 50kg FDD SSI output, run 20

Figure A3.50kg: Run 20 (segment 3)

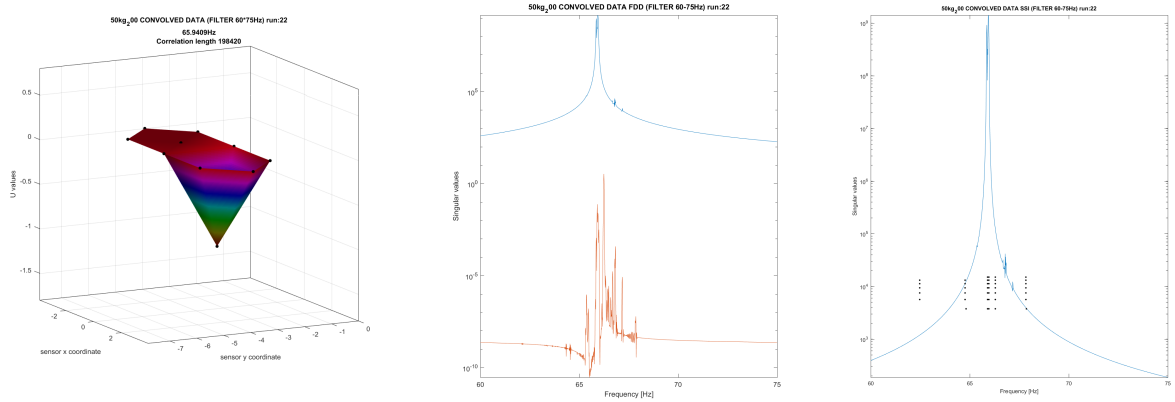


(a) 50kg mode shape, run 21



(b) 50kg FDD SSI output, run 21

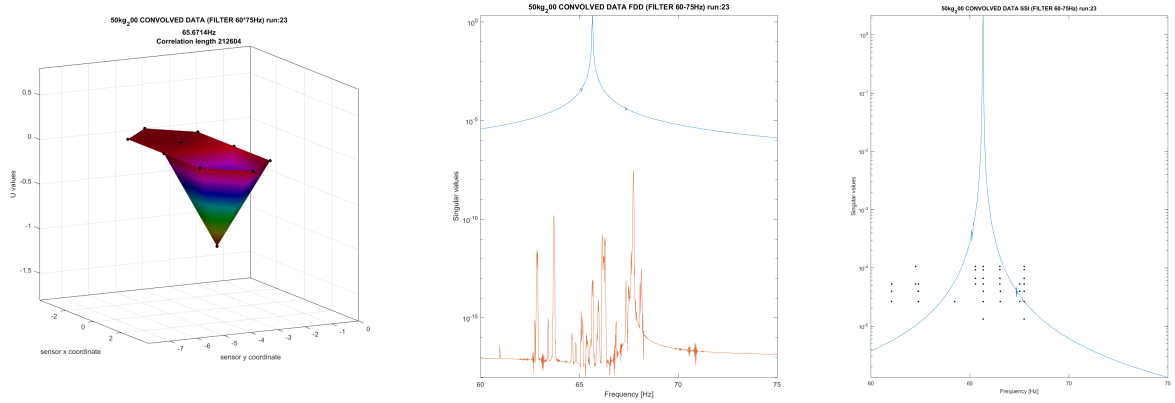
Figure A3.50kg: Run 21 (segment 3)



(a) 50kg mode shape, run 22

(b) 50kg FDD SSI output, run 22

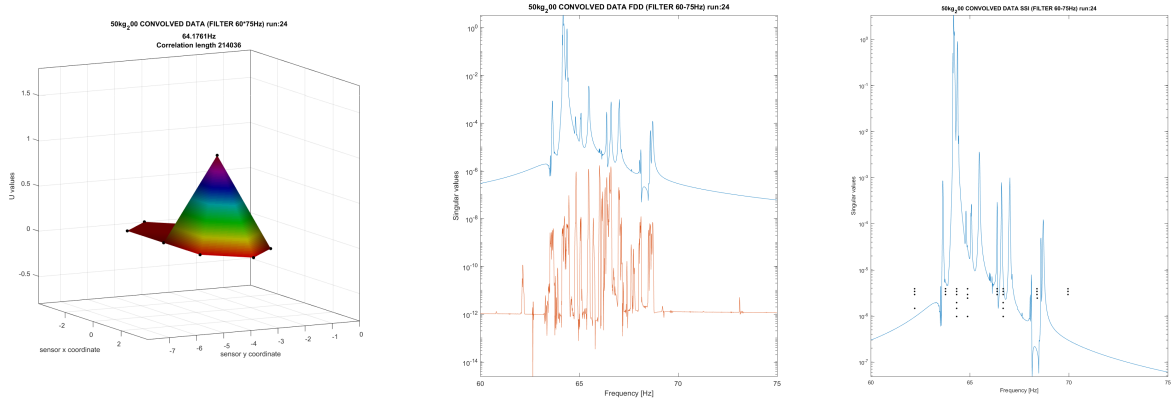
Figure A3.50kg: Run 22 (segment 3)



(a) 50kg mode shape, run 23

(b) 50kg FDD SSI output, run 23

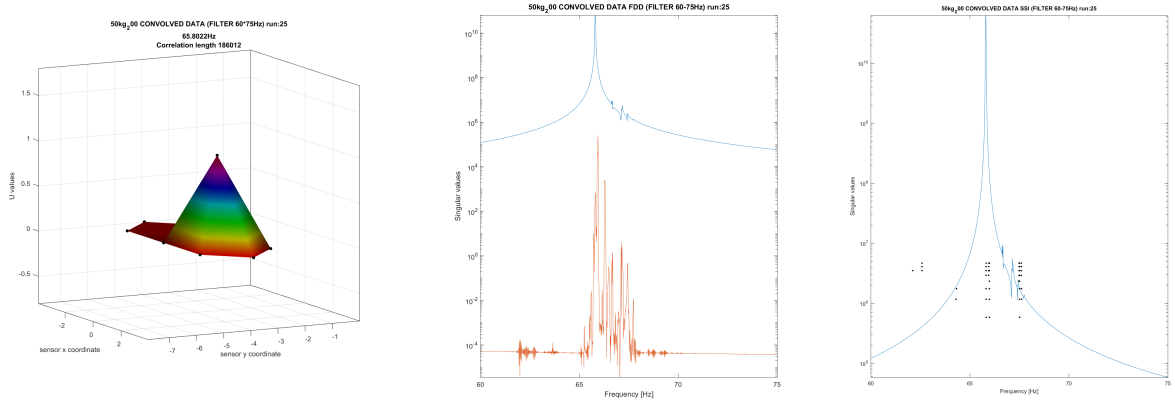
Figure A3.50kg: Run 23 (segment 3)



(a) 50kg mode shape, run 24

(b) 50kg FDD SSI output, run 24

Figure A3.50kg: Run 24 (segment 3)

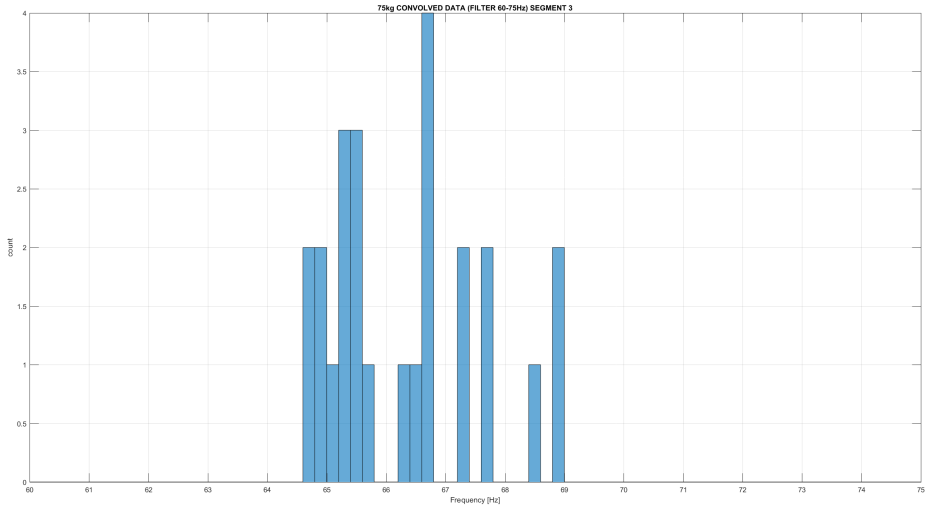


(a) 50kg mode shape, run 25

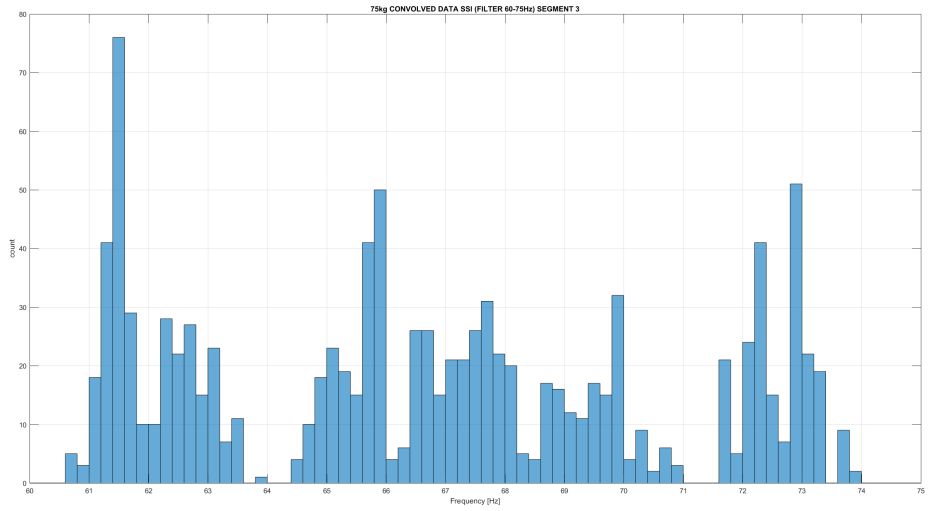
(b) 50kg FDD SSI output, run 25

Figure A3.50kg: Run 25 (segment 3)

75kg data segment 3

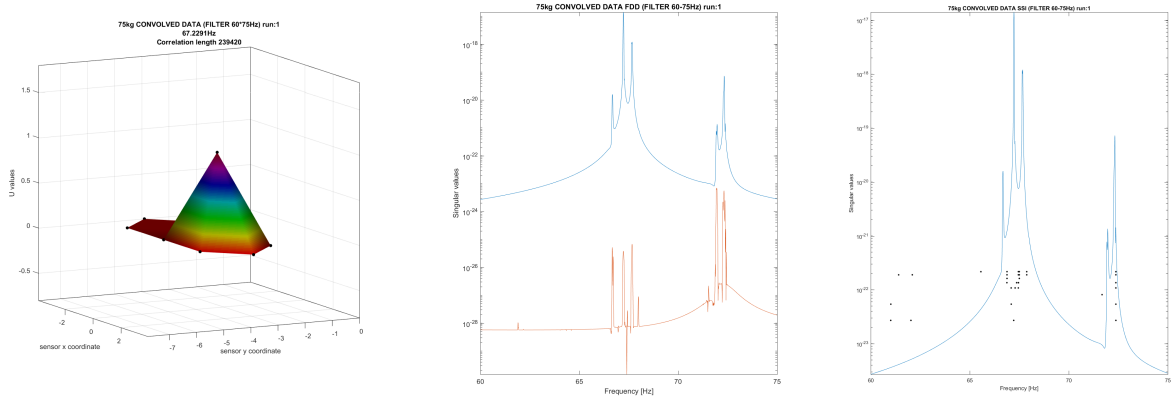


(a) 75kg FDD histogram



(b) 75kg SSI histogram

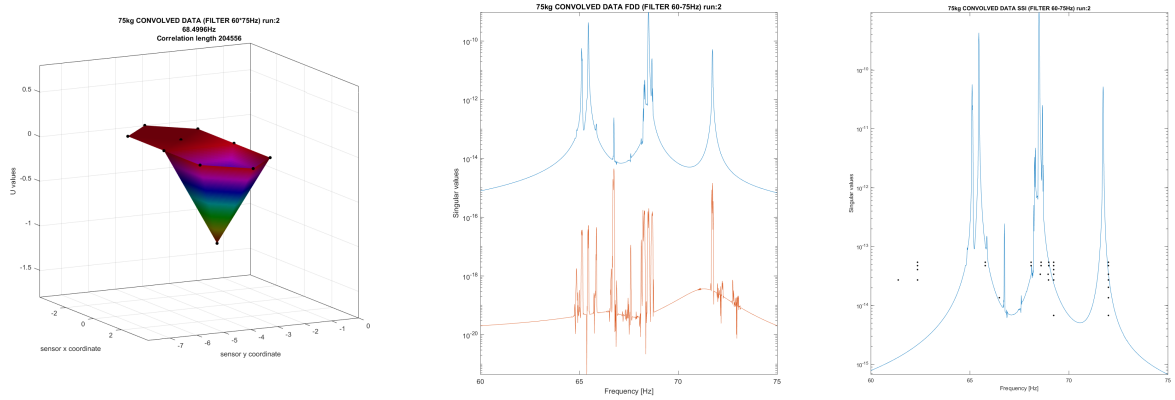
Figure A3.75kg: Histograms of identified modes, 75kg data (segment 3)



(a) 75kg mode shape, run 1

(b) 75kg FDD SSI output, run 1

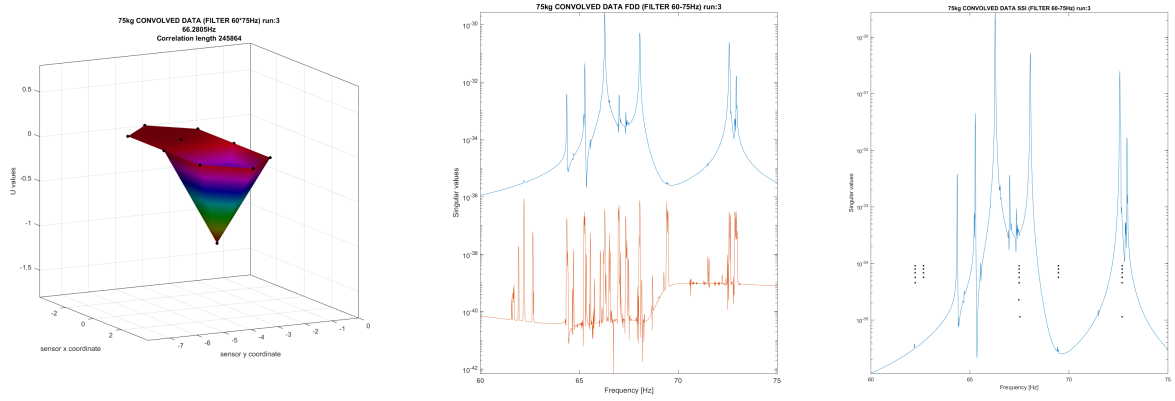
Figure A3.75kg: Run 1 (segment 3)



(a) 75kg mode shape, run 2

(b) 75kg FDD SSI output, run 2

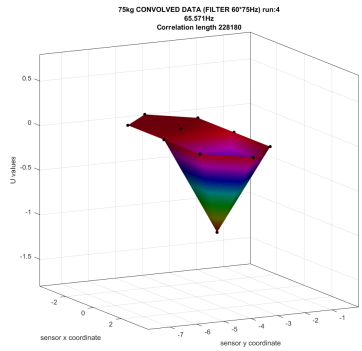
Figure A3.75kg: Run 2 (segment 3)



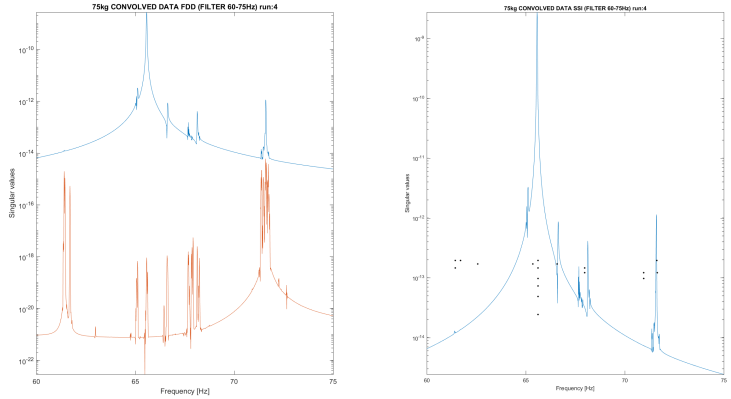
(a) 75kg mode shape, run 3

(b) 75kg FDD SSI output, run 3

Figure A3.75kg: Run 3 (segment 3)

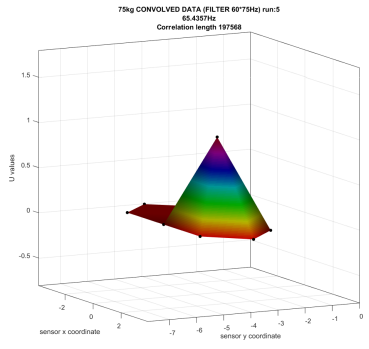


(a) 75kg mode shape, run 4

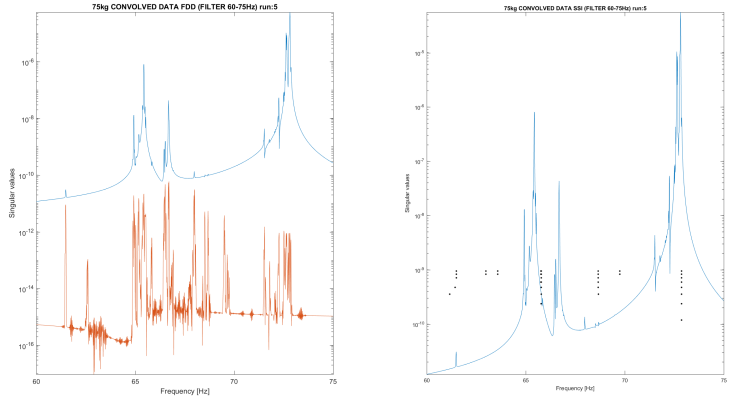


(b) 75kg FDD SSI output, run 4

Figure A3.75kg: Run 4 (segment 3)

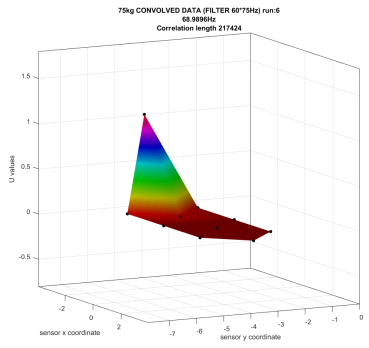


(a) 75kg mode shape, run 5

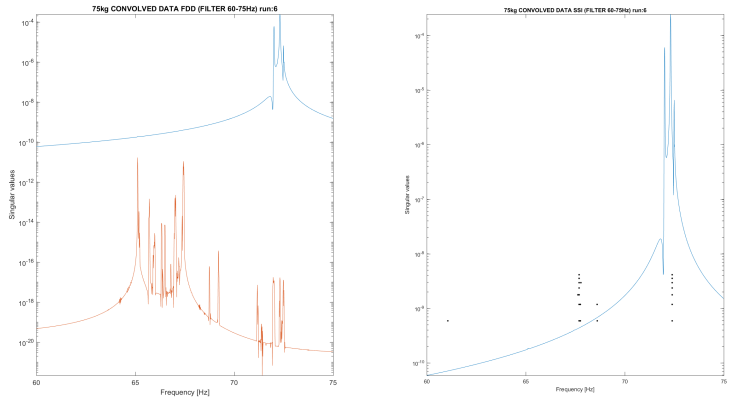


(b) 75kg FDD SSI output, run 5

Figure A3.75kg: Run 5 (segment 3)

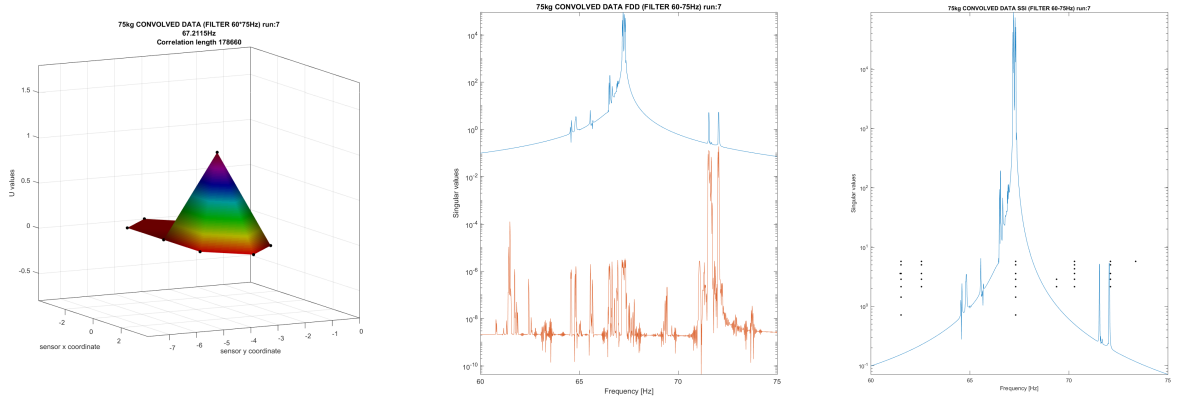


(a) 75kg mode shape, run 6



(b) 75kg FDD SSI output, run 6

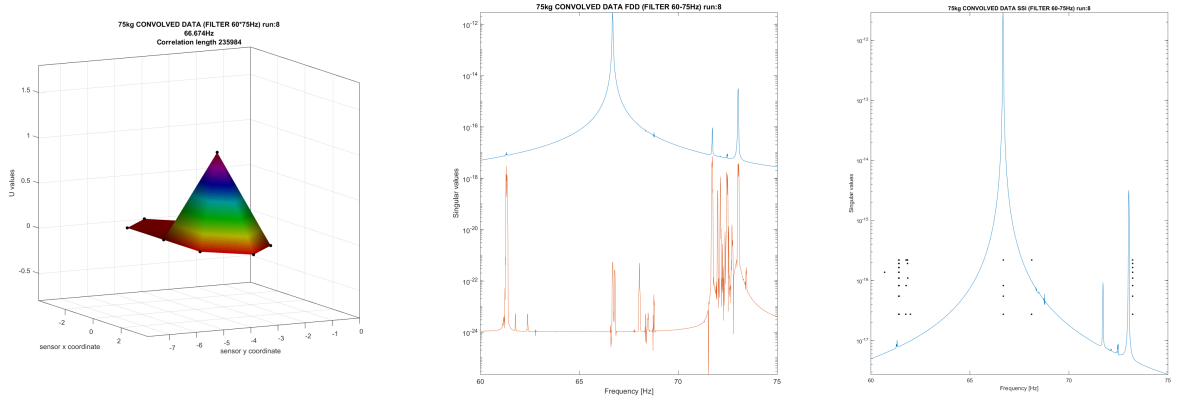
Figure A3.75kg: Run 6 (segment 3)



(a) 75kg mode shape, run 7

(b) 75kg FDD SSI output, run 7

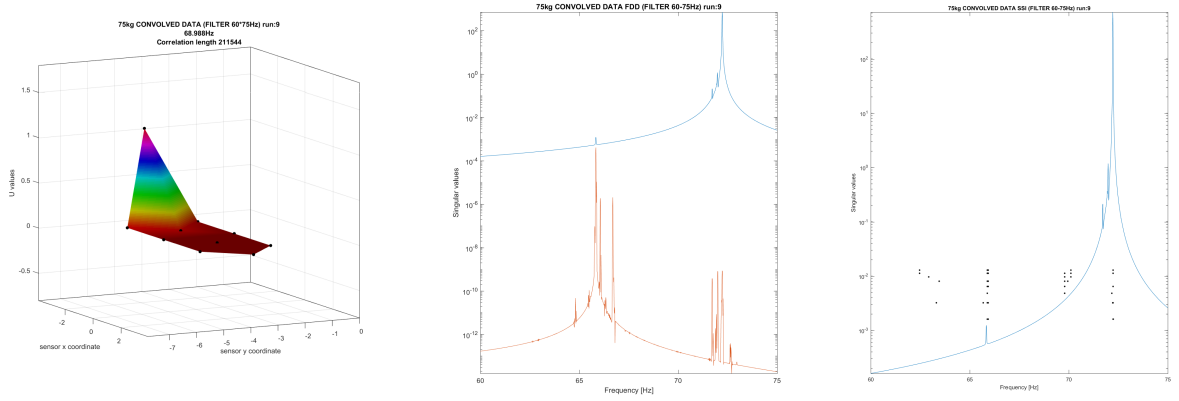
Figure A3.75kg: Run 7 (segment 3)



(a) 75kg mode shape, run 8

(b) 75kg FDD SSI output, run 8

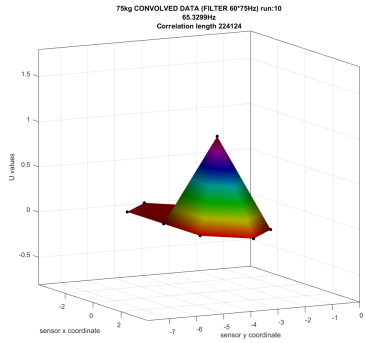
Figure A3.75kg: Run 8 (segment 3)

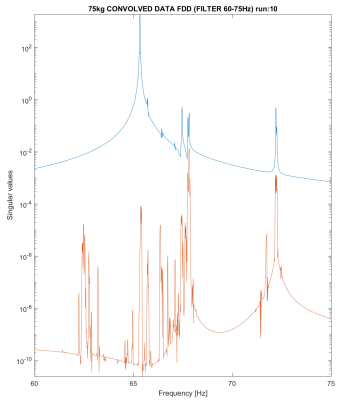


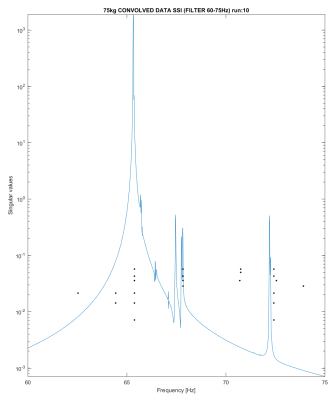
(a) 75kg mode shape, run 9

(b) 75kg FDD SSI output, run 9

Figure A3.75kg: Run 9 (segment 3)



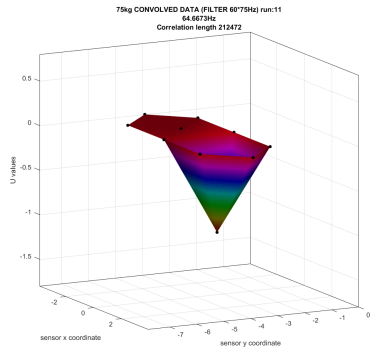


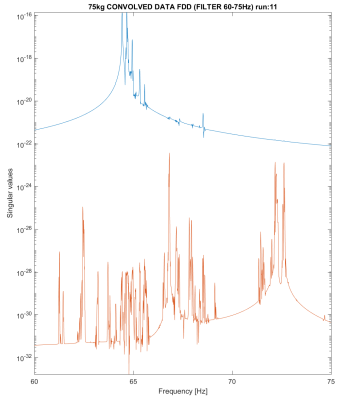


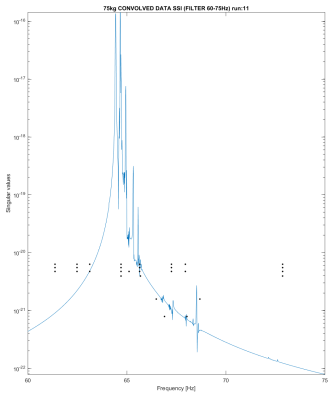
(a) 75kg mode shape, run 10

(b) 75kg FDD SSI output, run 10

Figure A3.75kg: Run 10 (segment 3)



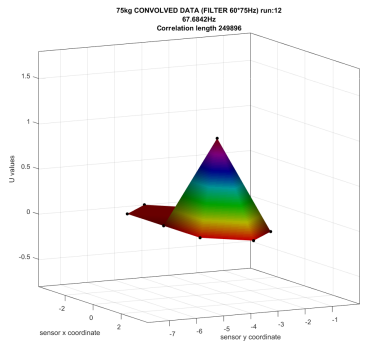


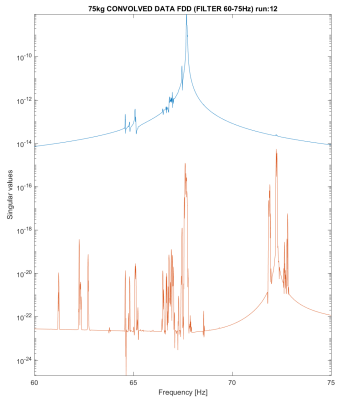


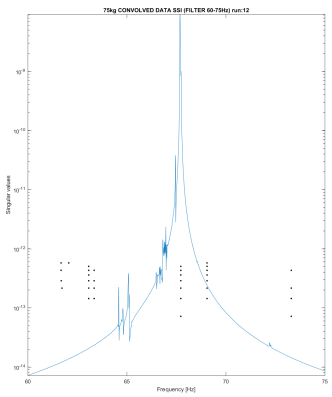
(a) 75kg mode shape, run 11

(b) 75kg FDD SSI output, run 11

Figure A3.75kg: Run 11 (segment 3)



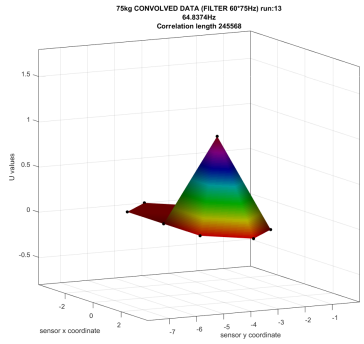




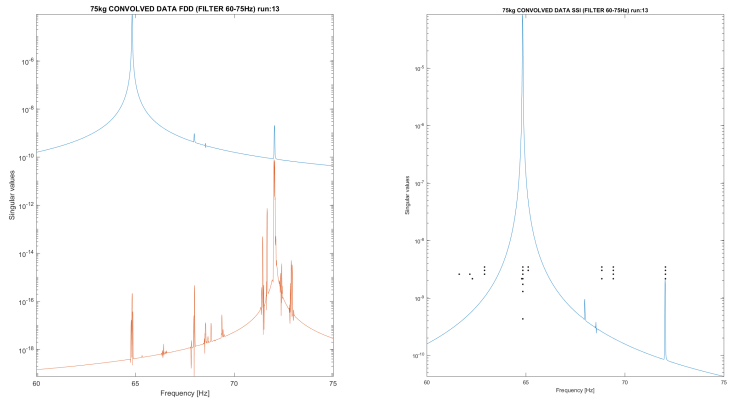
(a) 75kg mode shape, run 12

(b) 75kg FDD SSI output, run 12

Figure A3.75kg: Run 12 (segment 3)

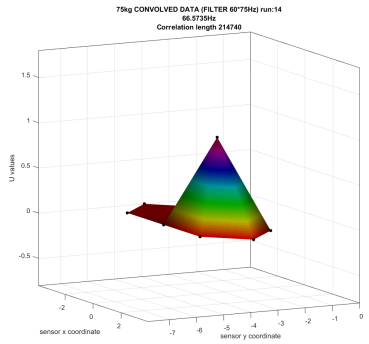


(a) 75kg mode shape, run 13

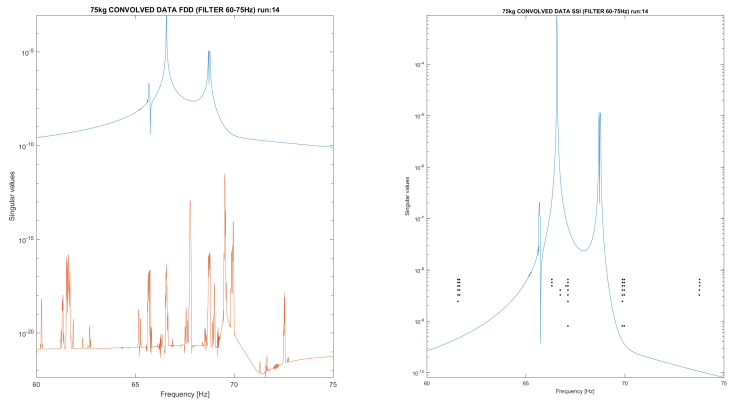


(b) 75kg FDD SSI output, run 13

Figure A3.75kg: Run 13 (segment 3)

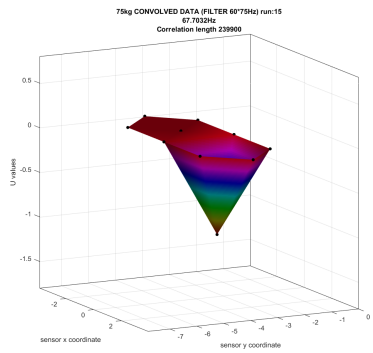


(a) 75kg mode shape, run 14

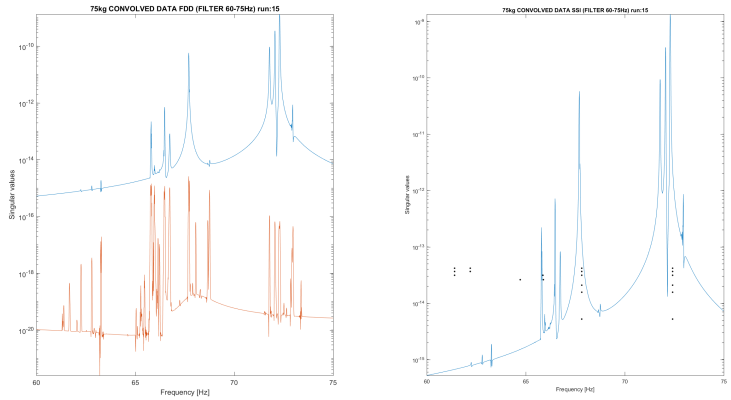


(b) 75kg FDD SSI output, run 14

Figure A3.75kg: Run 14 (segment 3)

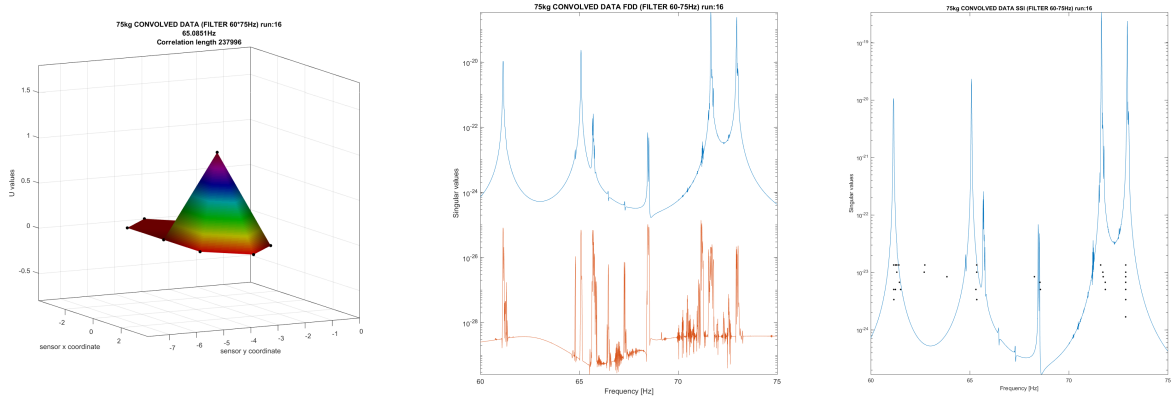


(a) 75kg mode shape, run 15



(b) 75kg FDD SSI output, run 15

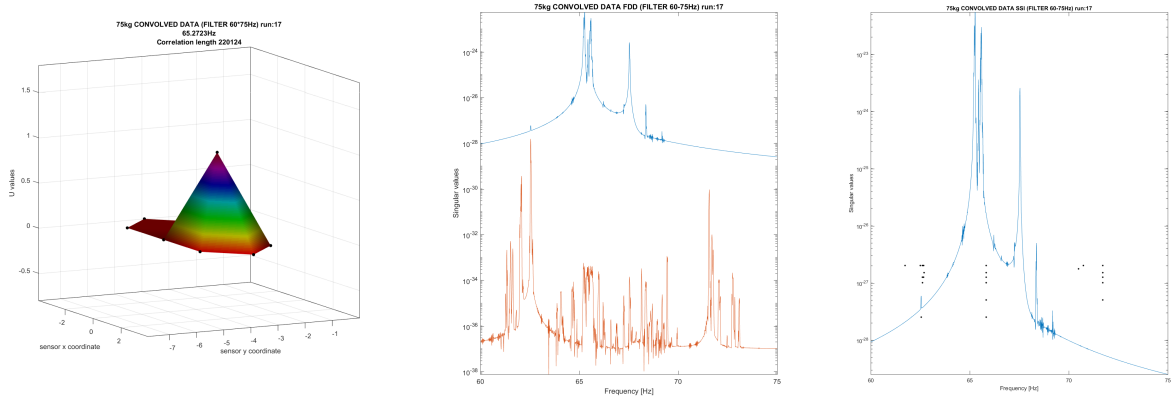
Figure A3.75kg: Run 15 (segment 3)



(a) 75kg mode shape, run 16

(b) 75kg FDD SSI output, run 16

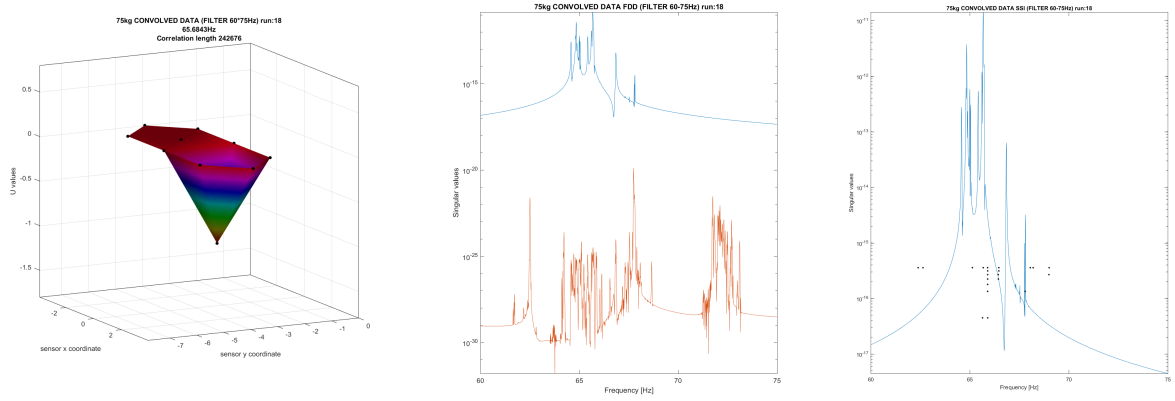
Figure A3.75kg: Run 16 (segment 3)



(a) 75kg mode shape, run 17

(b) 75kg FDD SSI output, run 17

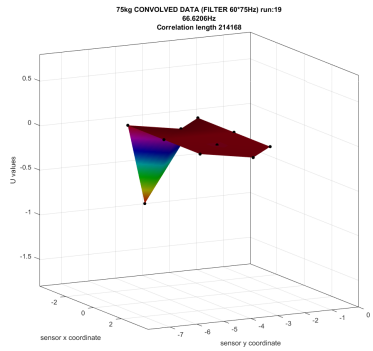
Figure A3.75kg: Run 17 (segment 3)



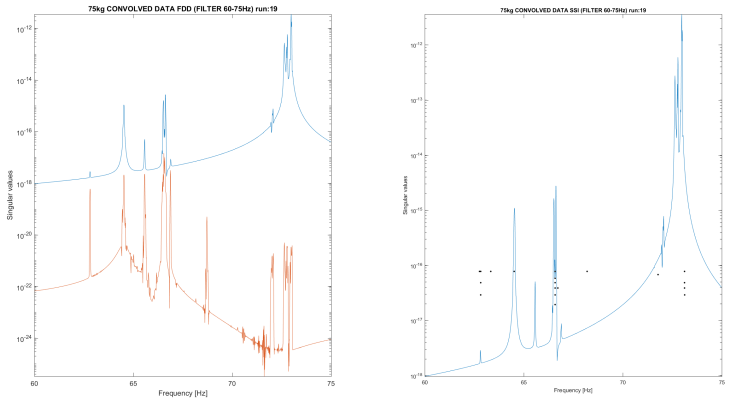
(a) 75kg mode shape, run 18

(b) 75kg FDD SSI output, run 18

Figure A3.75kg: Run 18 (segment 3)

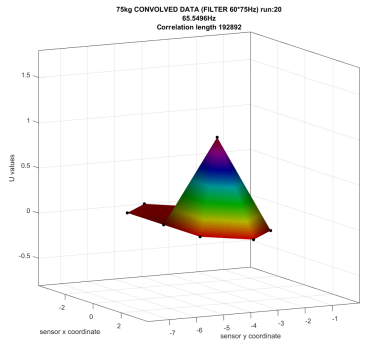


(a) 75kg mode shape, run 19

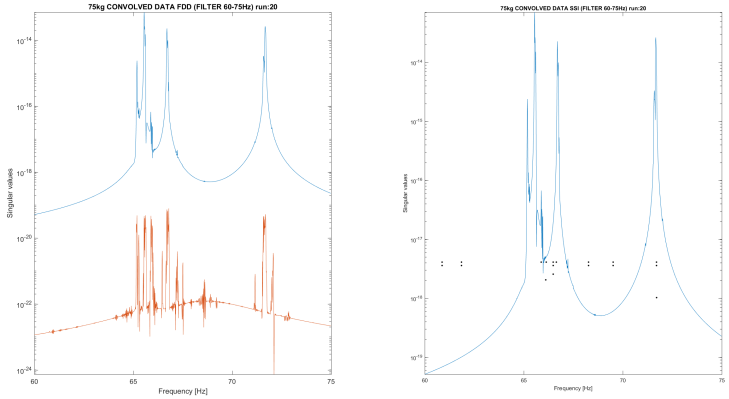


(b) 75kg FDD SSI output, run 19

Figure A3.75kg: Run 19 (segment 3)

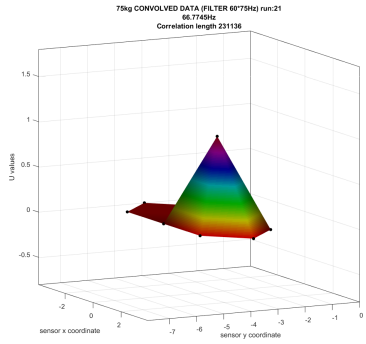


(a) 75kg mode shape, run 20

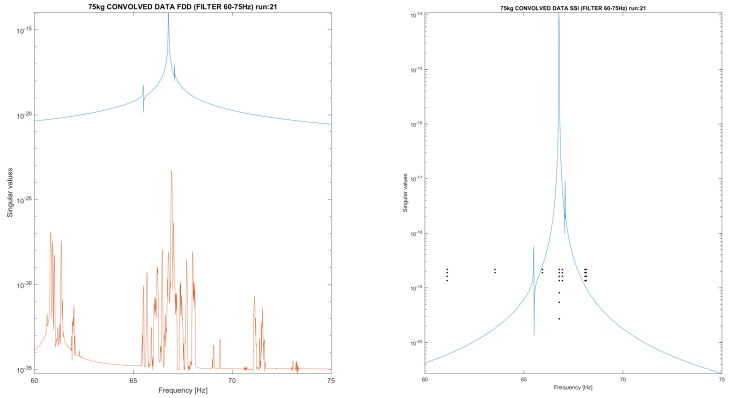


(b) 75kg FDD SSI output, run 20

Figure A3.75kg: Run 20 (segment 3)

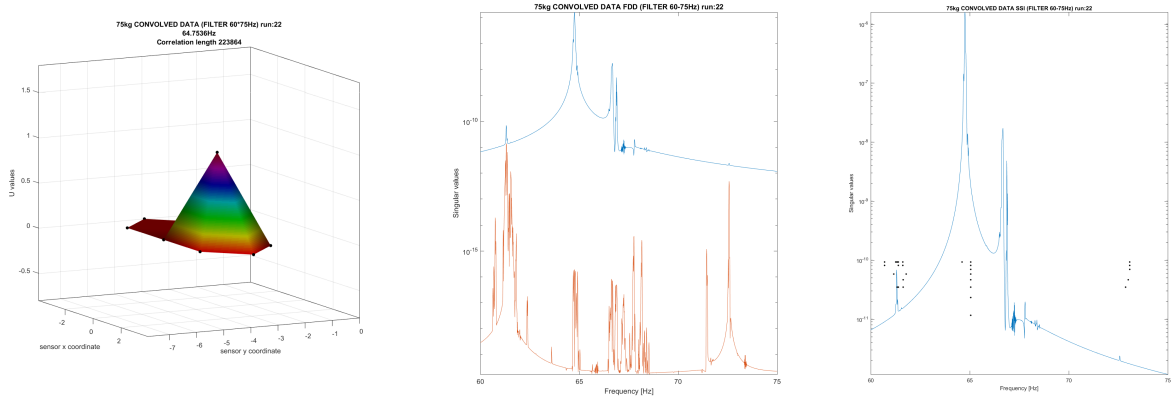


(a) 75kg mode shape, run 21



(b) 75kg FDD SSI output, run 21

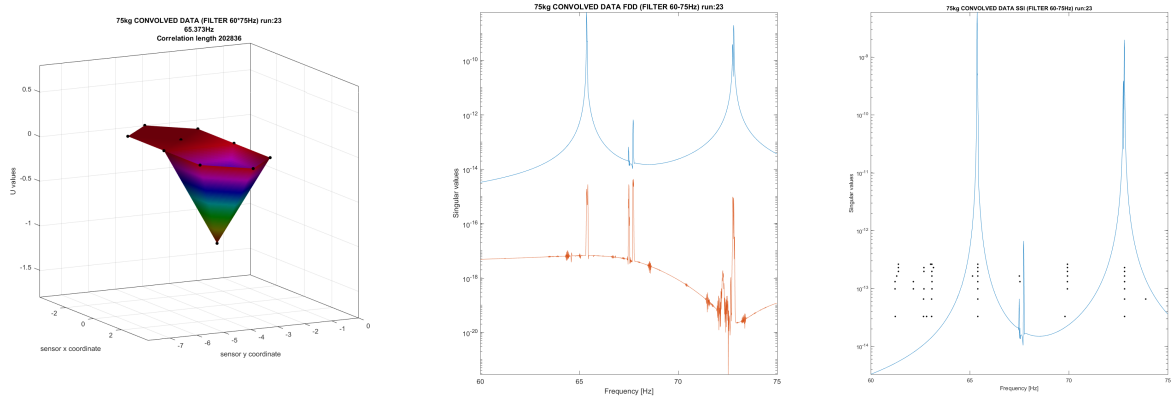
Figure A3.75kg: Run 21 (segment 3)



(a) 75kg mode shape, run 22

(b) 75kg FDD SSI output, run 22

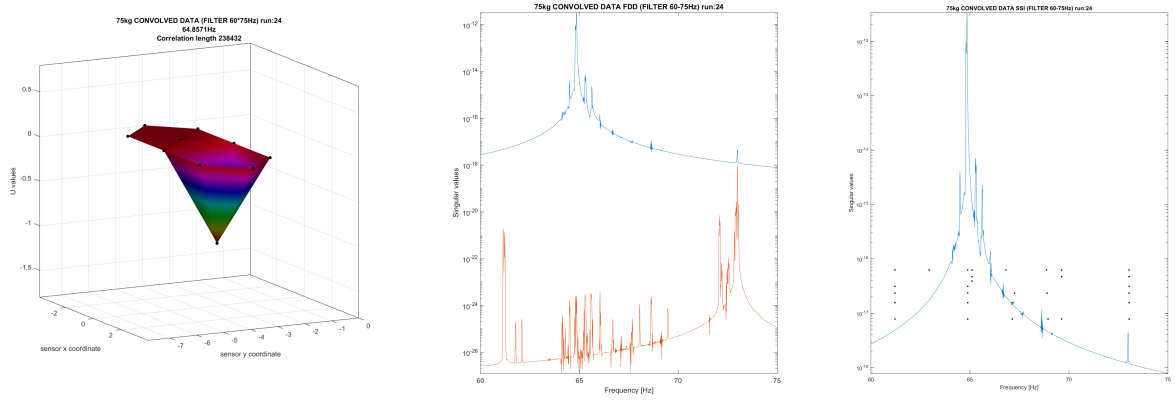
Figure A3.75kg: Run 22 (segment 3)



(a) 75kg mode shape, run 23

(b) 75kg FDD SSI output, run 23

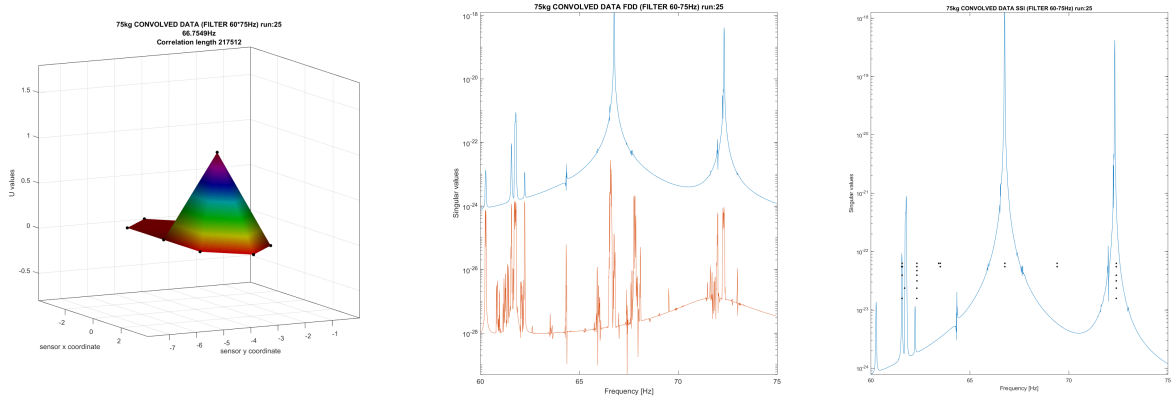
Figure A3.75kg: Run 23 (segment 3)



(a) 75kg mode shape, run 24

(b) 75kg FDD SSI output, run 24

Figure A3.75kg: Run 24 (segment 3)

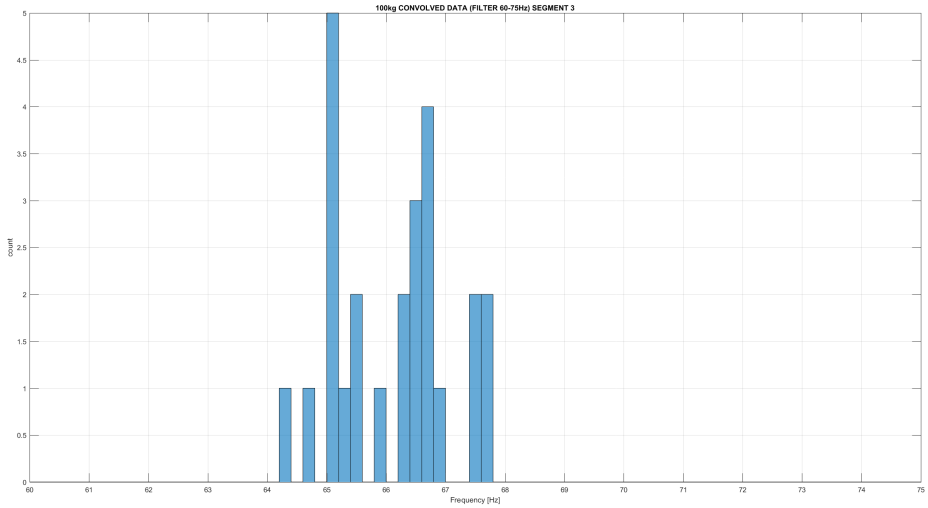


(a) 75kg mode shape, run 25

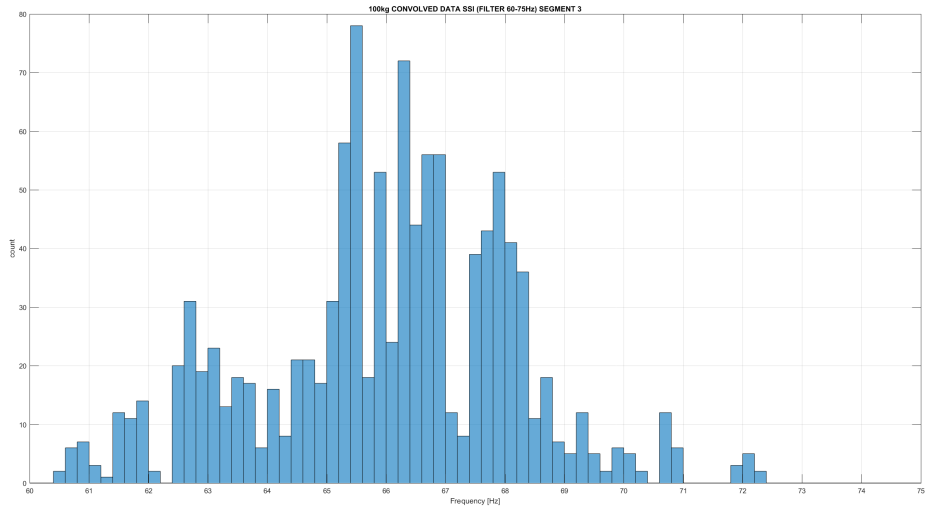
(b) 75kg FDD SSI output, run 25

Figure A3.75kg: Run 25 (segment 3)

100kg data segment 3

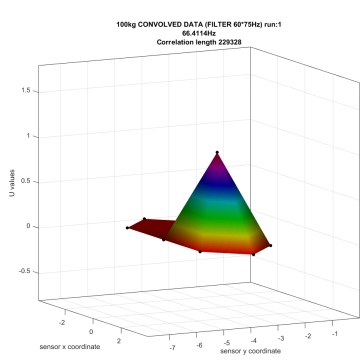


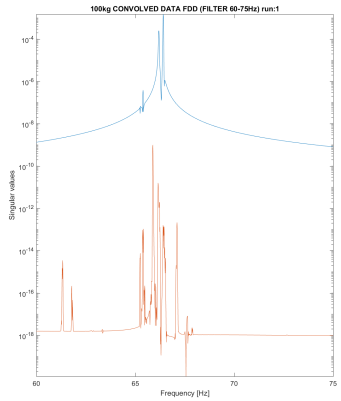
(a) 100kg FDD histogram

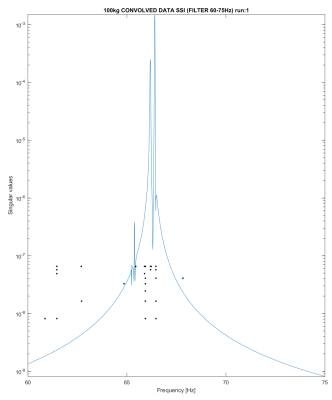


(b) 100kg SSI histogram

Figure A3.100kg: Histograms of identified modes, 100kg data (segment 3)



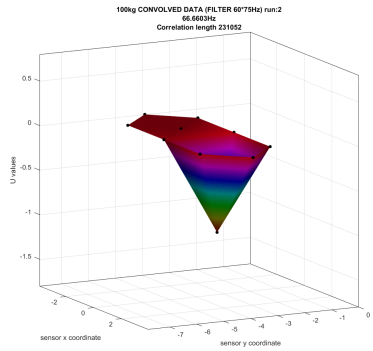


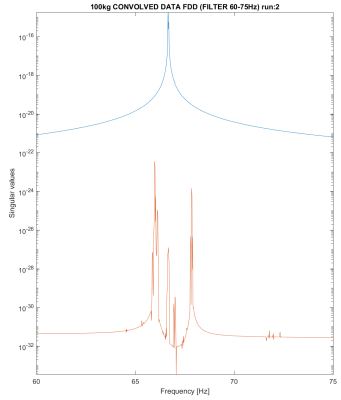


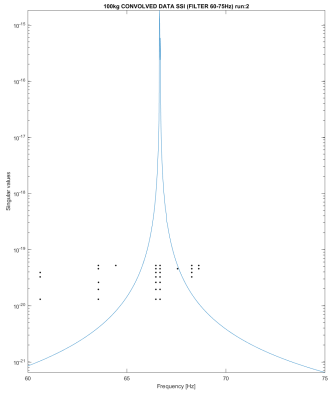
(a) 100kg mode shape, run 1

(b) 100kg FDD SSI output, run 1

Figure A3.100kg: Run 1 (segment 3)



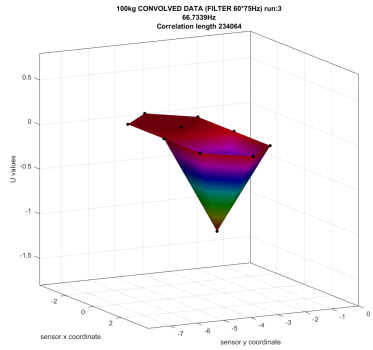


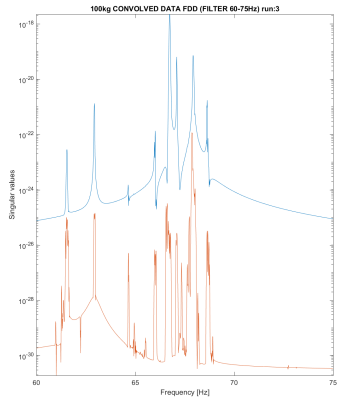


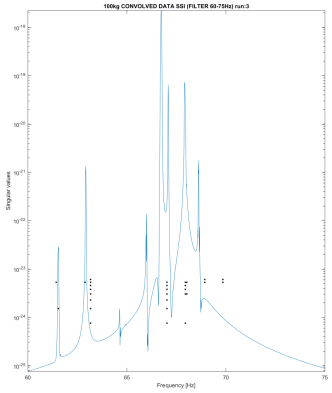
(a) 100kg mode shape, run 2

(b) 100kg FDD SSI output, run 2

Figure A3.100kg: Run 2 (segment 3)



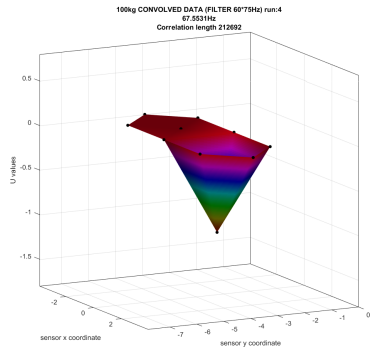




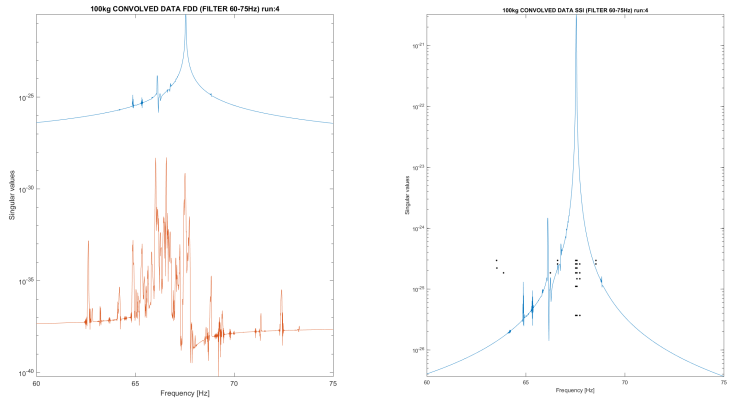
(a) 100kg mode shape, run 3

(b) 100kg FDD SSI output, run 3

Figure A3.100kg: Run 3 (segment 3)

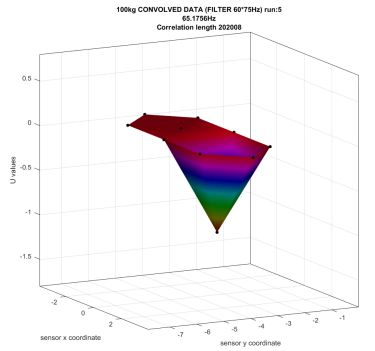


(a) 100kg mode shape, run 4

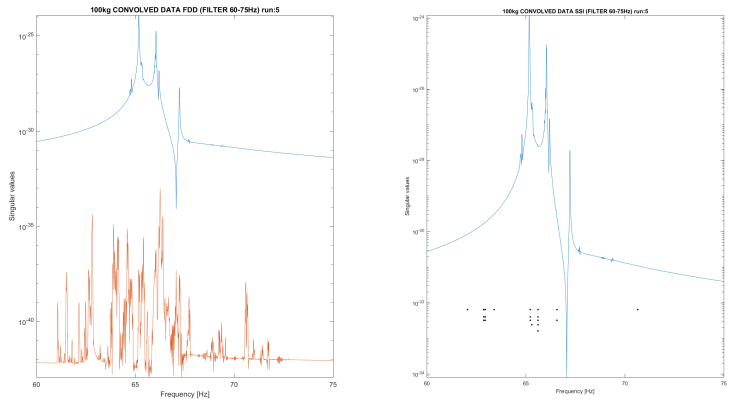


(b) 100kg FDD SSI output, run 4

Figure A3.100kg: Run 4 (segment 3)

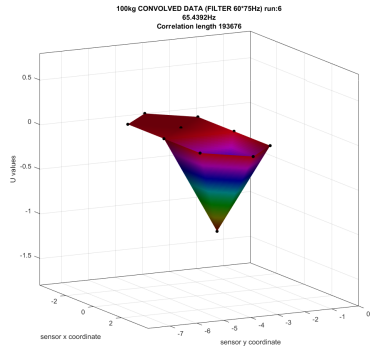


(a) 100kg mode shape, run 5

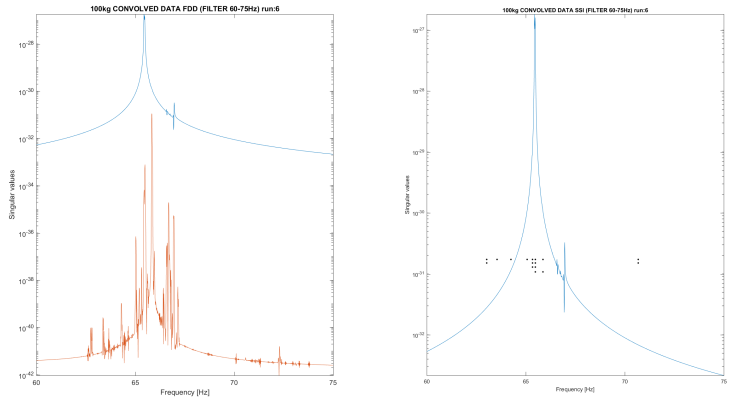


(b) 100kg FDD SSI output, run 5

Figure A3.100kg: Run 5 (segment 3)

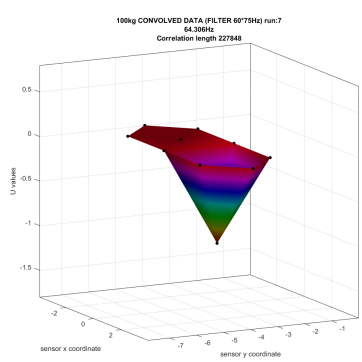


(a) 100kg mode shape, run 6

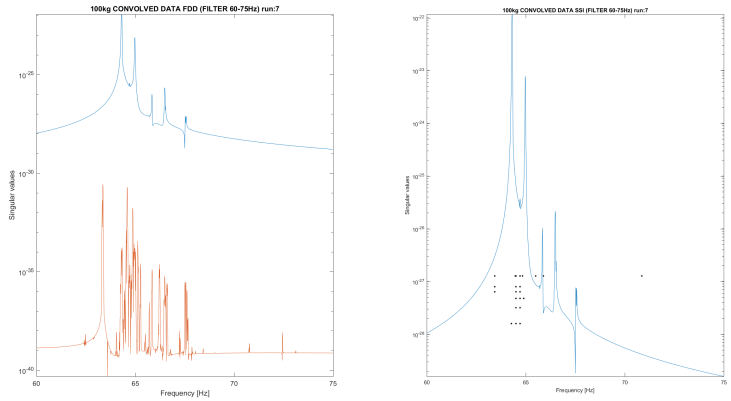


(b) 100kg FDD SSI output, run 6

Figure A3.100kg: Run 6 (segment 3)

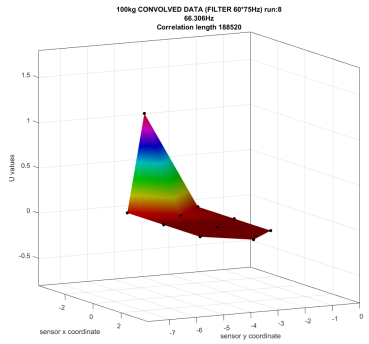


(a) 100kg mode shape, run 7

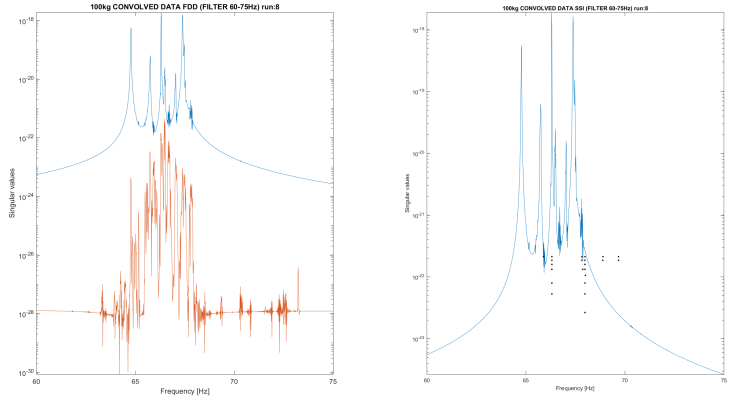


(b) 100kg FDD SSI output, run 7

Figure A3.100kg: Run 7 (segment 3)

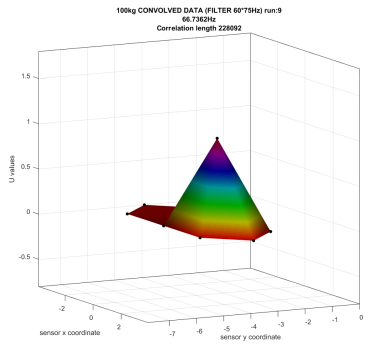


(a) 100kg mode shape, run 8

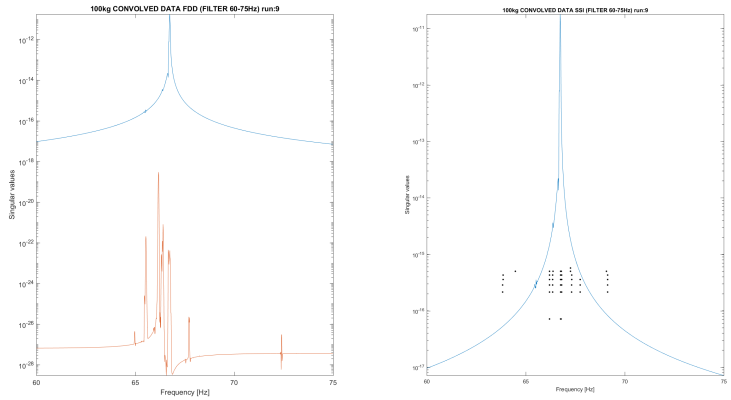


(b) 100kg FDD SSI output, run 8

Figure A3.100kg: Run 8 (segment 3)

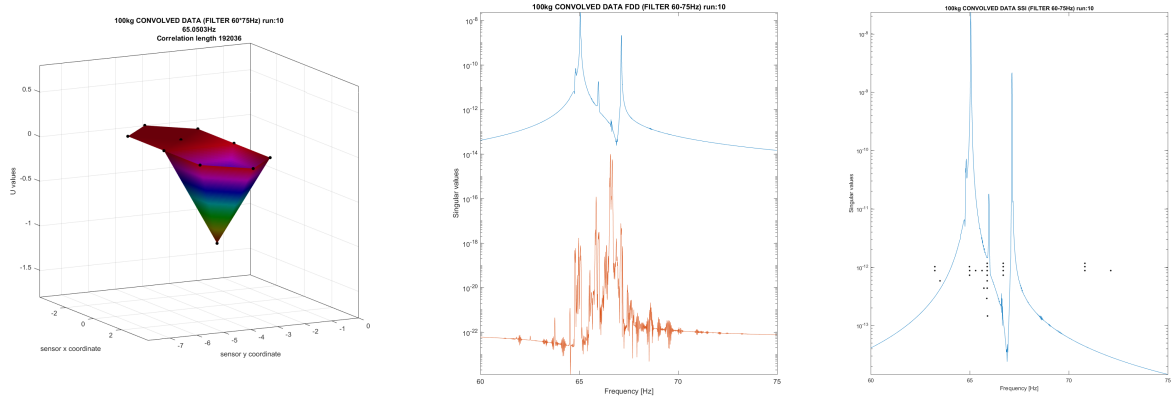


(a) 100kg mode shape, run 9



(b) 100kg FDD SSI output, run 9

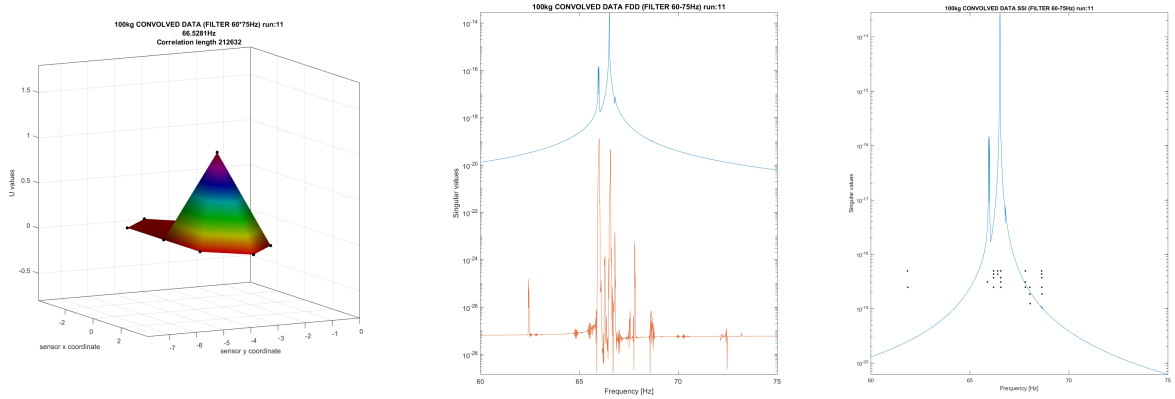
Figure A3.100kg: Run 9 (segment 3)



(a) 100kg mode shape, run 10

(b) 100kg FDD SSI output, run 10

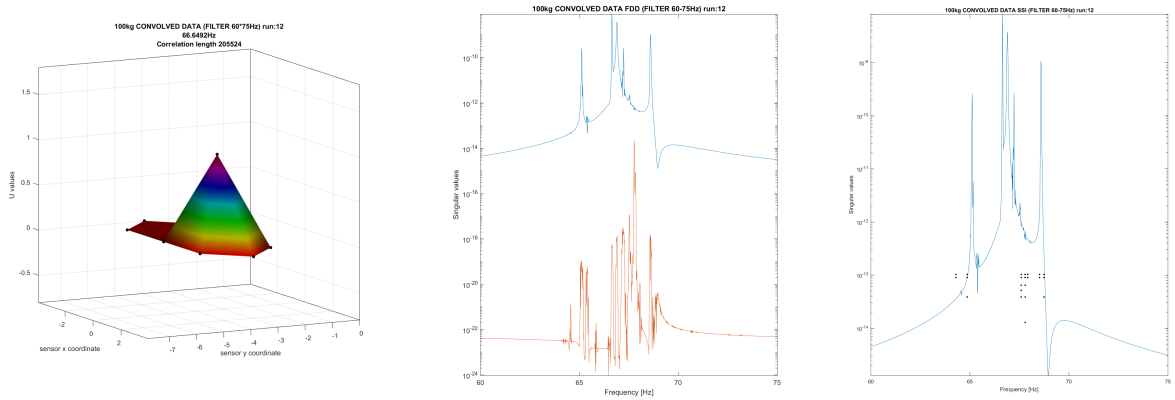
Figure A3.100kg: Run 10 (segment 3)



(a) 100kg mode shape, run 11

(b) 100kg FDD SSI output, run 11

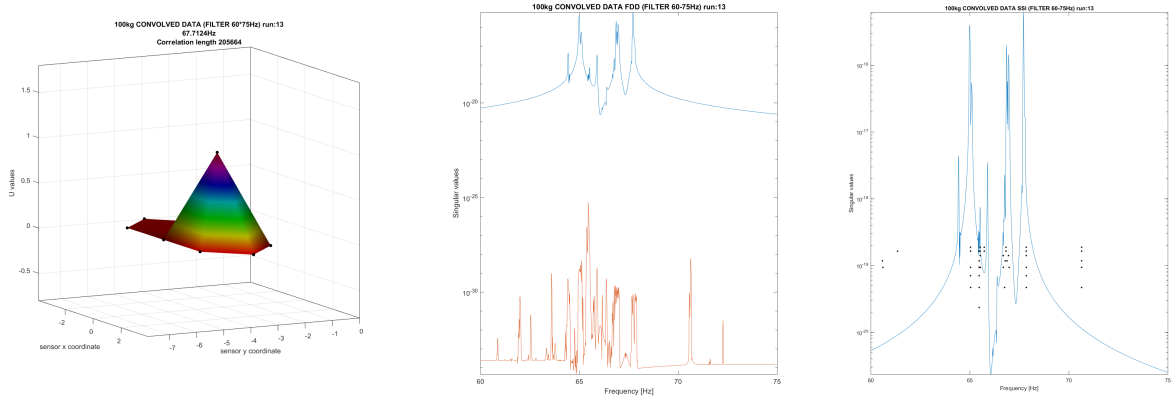
Figure A3.100kg: Run 11 (segment 3)



(a) 100kg mode shape, run 12

(b) 100kg FDD SSI output, run 12

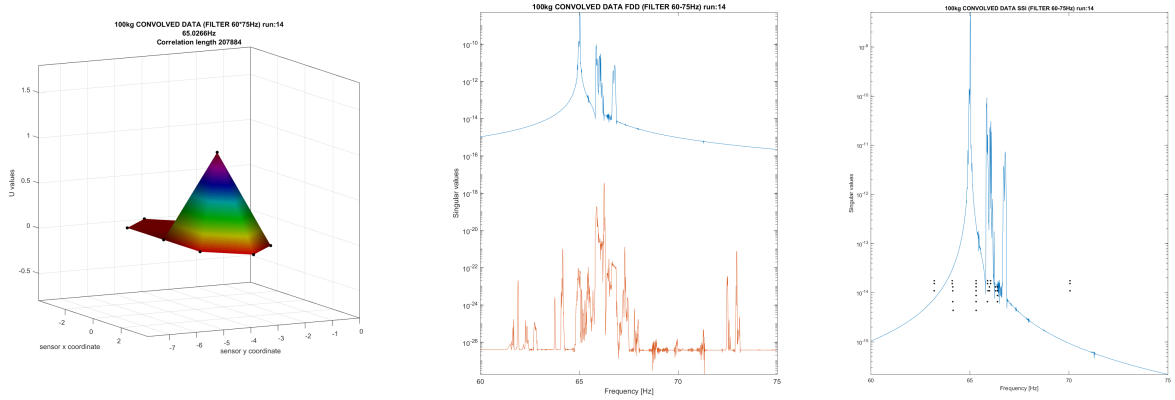
Figure A3.100kg: Run 12 (segment 3)



(a) 100kg mode shape, run 13

(b) 100kg FDD SSI output, run 13

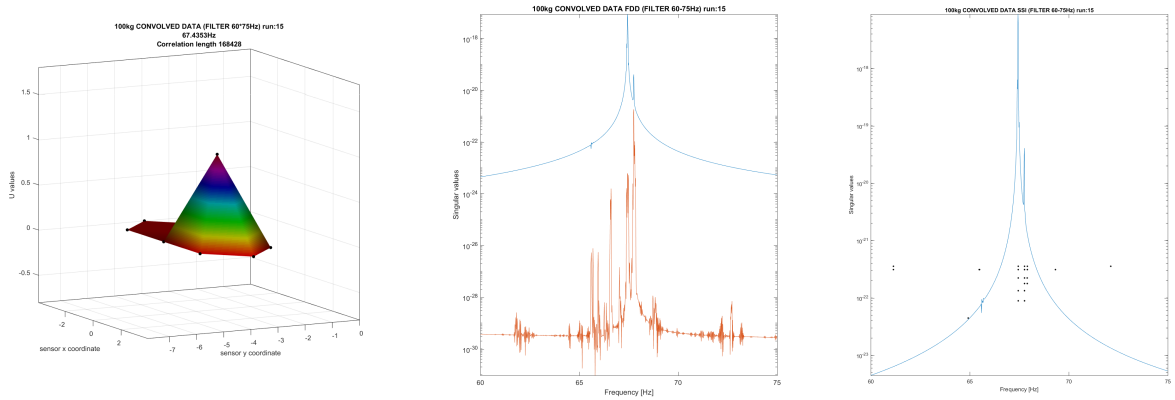
Figure A3.100kg: Run 13 (segment 3)



(a) 100kg mode shape, run 14

(b) 100kg FDD SSI output, run 14

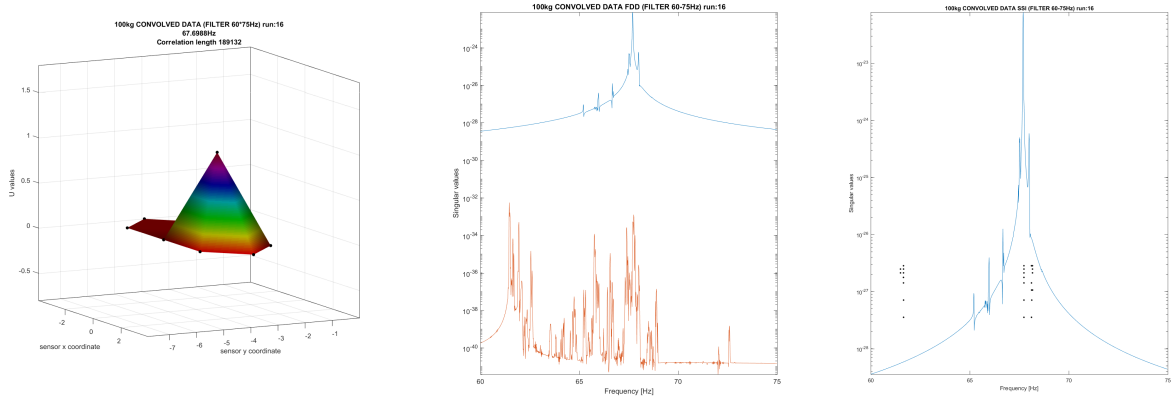
Figure A3.100kg: Run 14 (segment 3)



(a) 100kg mode shape, run 15

(b) 100kg FDD SSI output, run 15

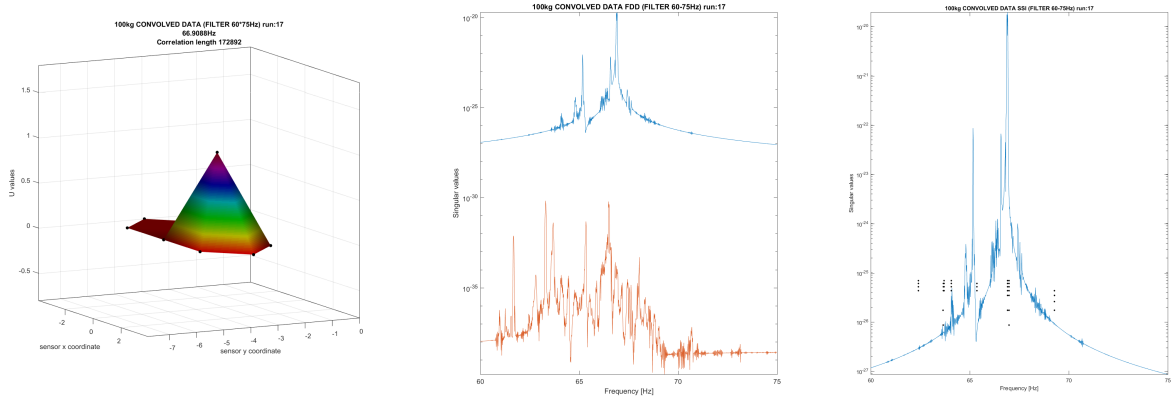
Figure A3.100kg: Run 15 (segment 3)



(a) 100kg mode shape, run 16

(b) 100kg FDD SSI output, run 16

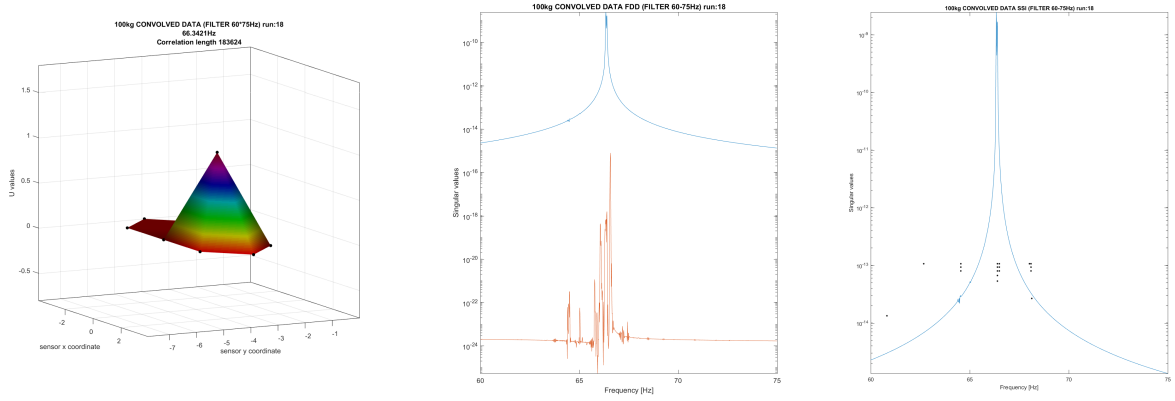
Figure A3.100kg: Run 16 (segment 3)



(a) 100kg mode shape, run 17

(b) 100kg FDD SSI output, run 17

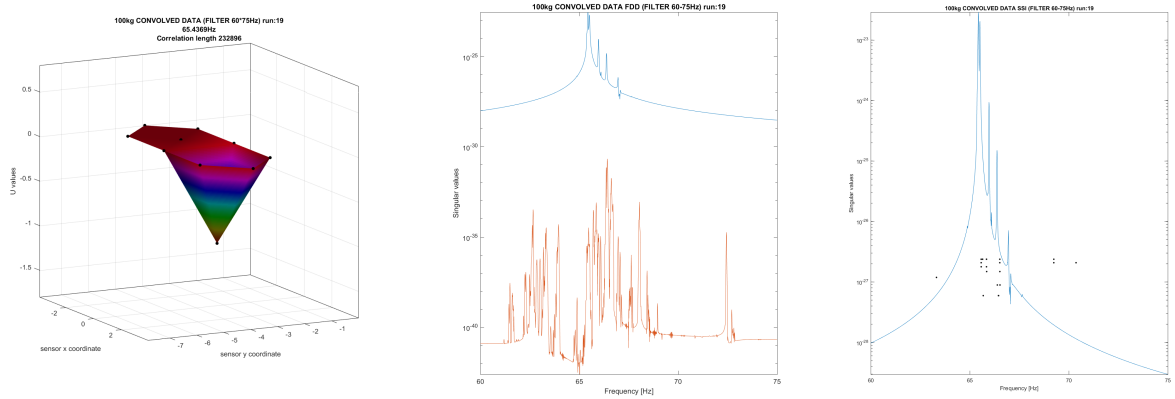
Figure A3.100kg: Run 17 (segment 3)



(a) 100kg mode shape, run 18

(b) 100kg FDD SSI output, run 18

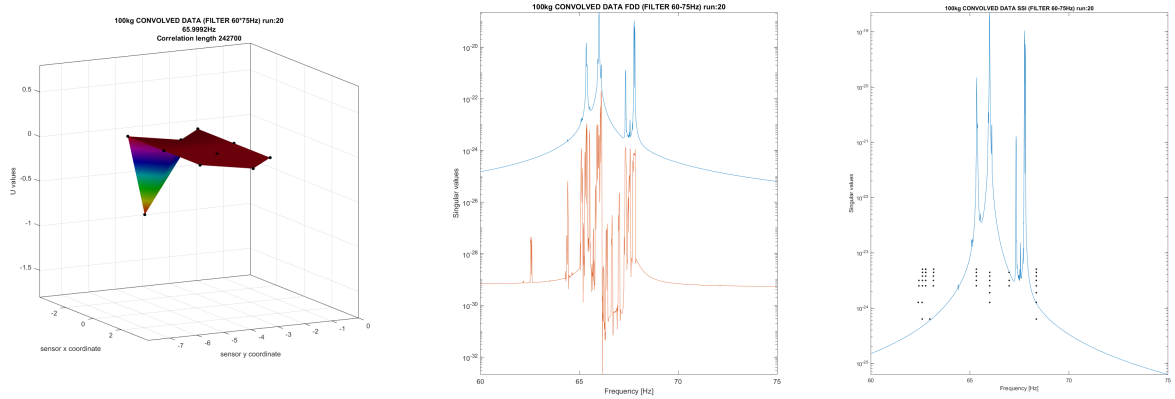
Figure A3.100kg: Run 18 (segment 3)



(a) 100kg mode shape, run 19

(b) 100kg FDD SSI output, run 19

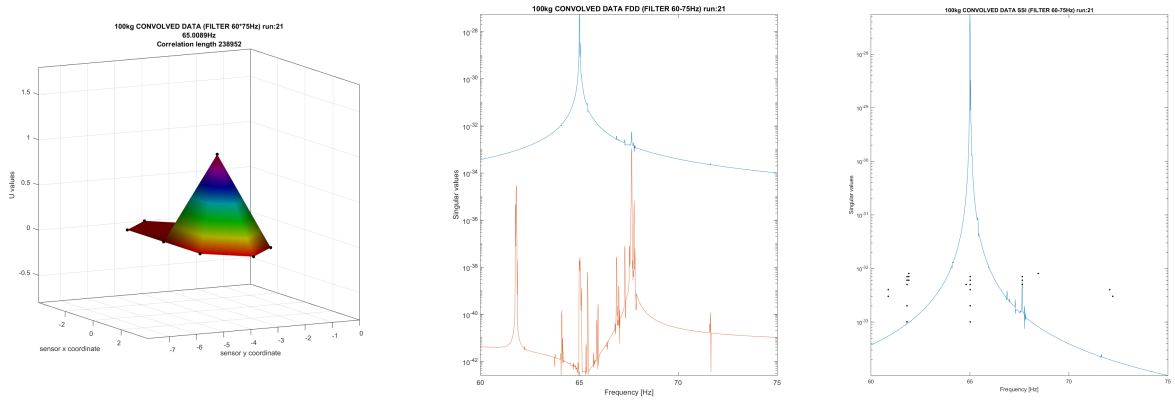
Figure A3.100kg: Run 19 (segment 3)



(a) 100kg mode shape, run 20

(b) 100kg FDD SSI output, run 20

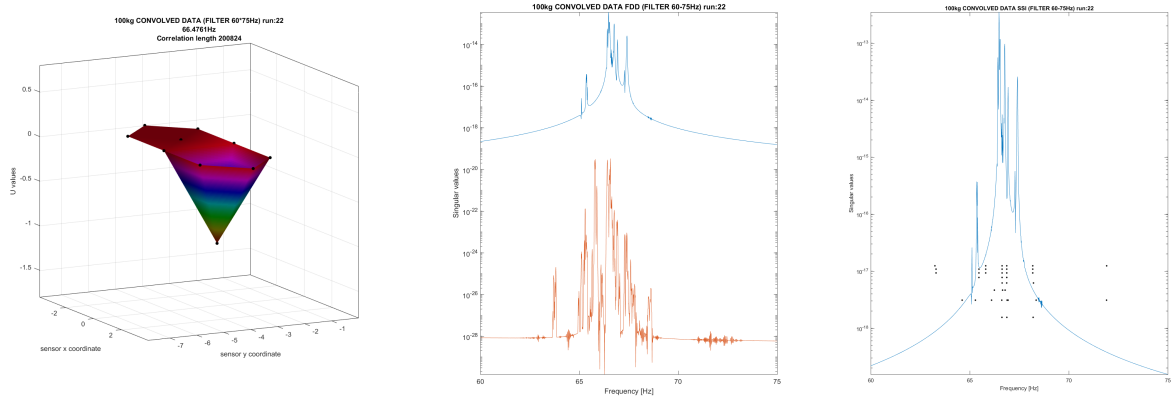
Figure A3.100kg: Run 20 (segment 3)



(a) 100kg mode shape, run 21

(b) 100kg FDD SSI output, run 21

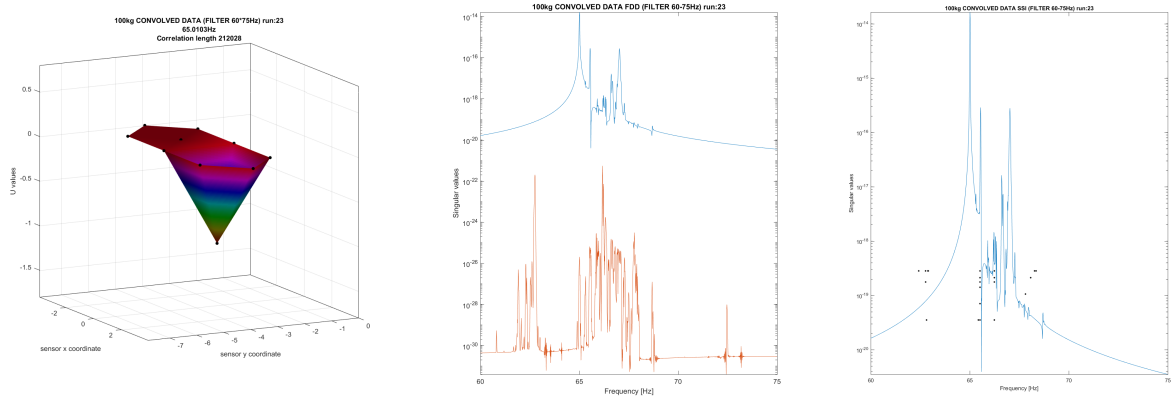
Figure A3.100kg: Run 21 (segment 3)



(a) 100kg mode shape, run 22

(b) 100kg FDD SSI output, run 22

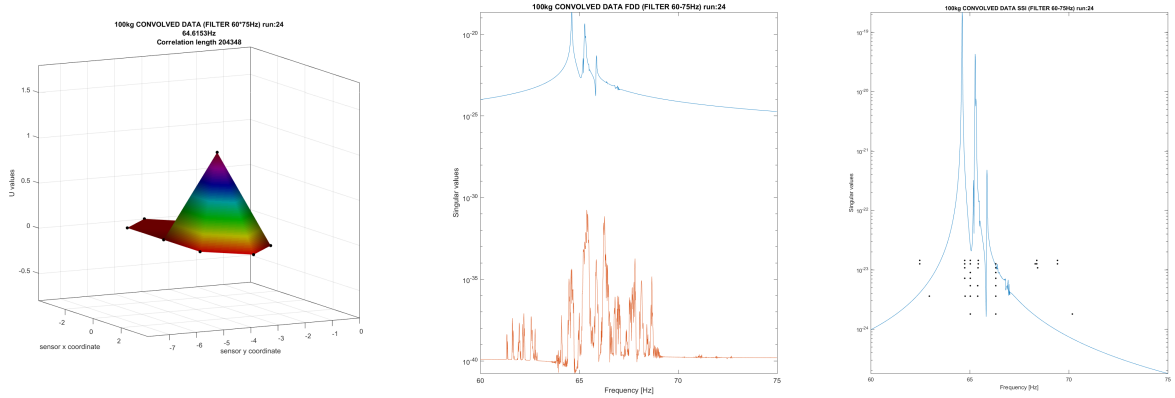
Figure A3.100kg: Run 22 (segment 3)



(a) 100kg mode shape, run 23

(b) 100kg FDD SSI output, run 23

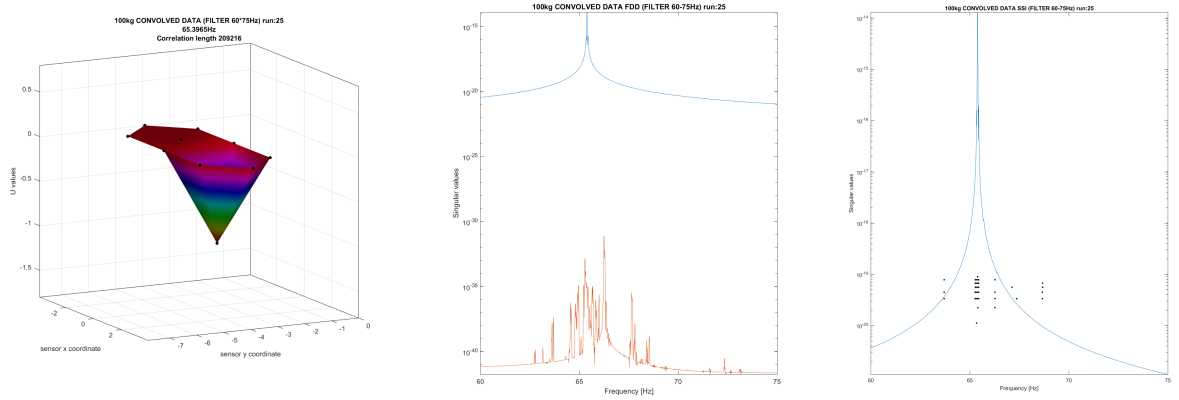
Figure A3.100kg: Run 23 (segment 3)



(a) 100kg mode shape, run 24

(b) 100kg FDD SSI output, run 24

Figure A3.100kg: Run 24 (segment 3)

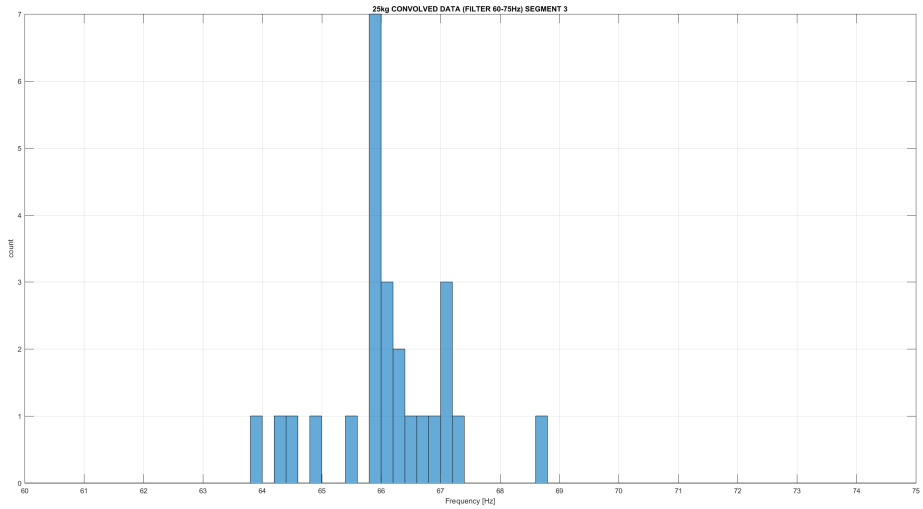


(a) 100kg mode shape, run 25

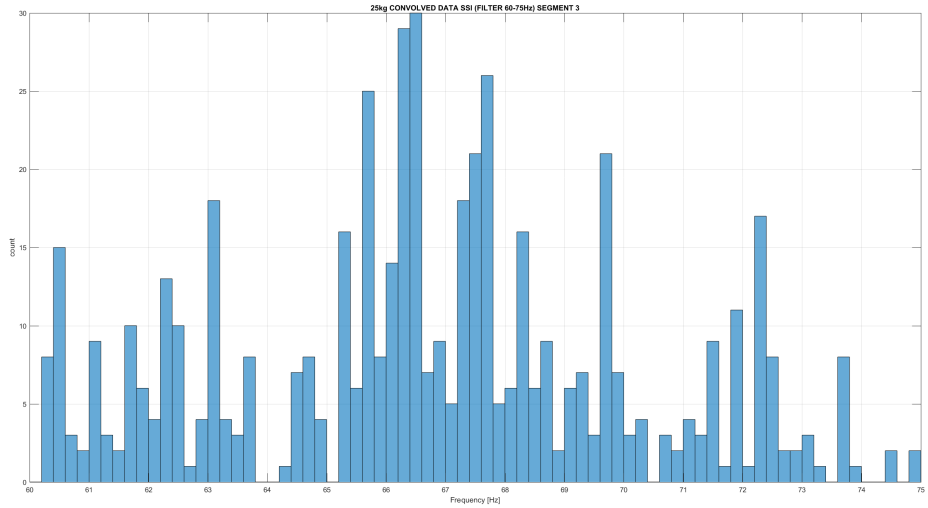
(b) 100kg FDD SSI output, run 25

Figure A3.100kg: Run 25 (segment 3)

Data (28.03.2017) 25kg-50kg segment 3 (Unreduced order PF)

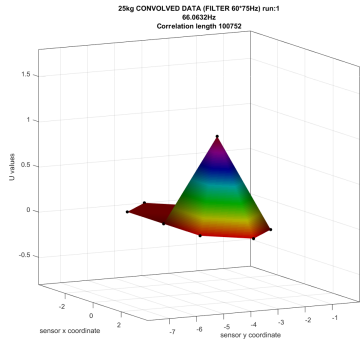


(a) 25kg FDD histogram

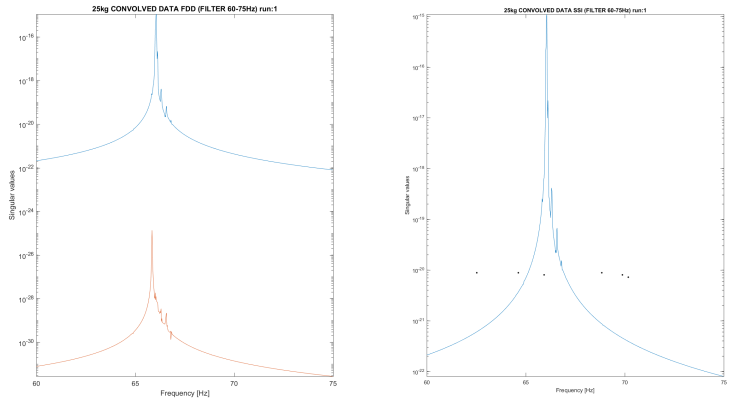


(b) 25kg SSI histogram

Figure A3.25kg: Histograms of identified modes, 25kg data (segment 3)

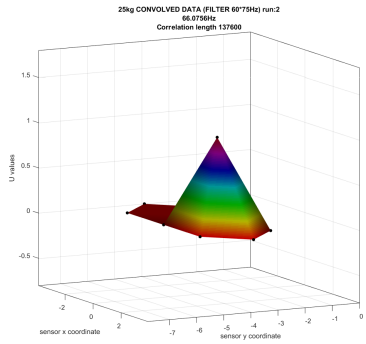


(a) 25kg mode shape, run 1

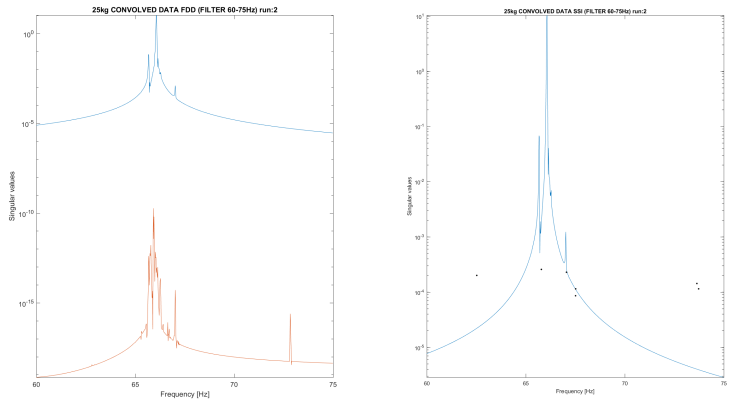


(b) 25kg FDD SSI output, run 1

Figure A3.25kg: Run 1 (segment 3)

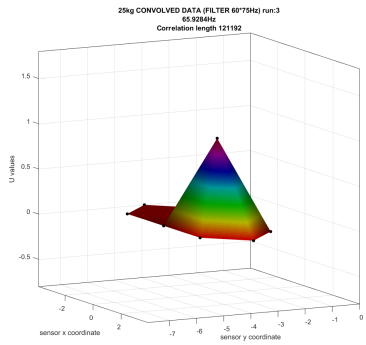


(a) 25kg mode shape, run 2

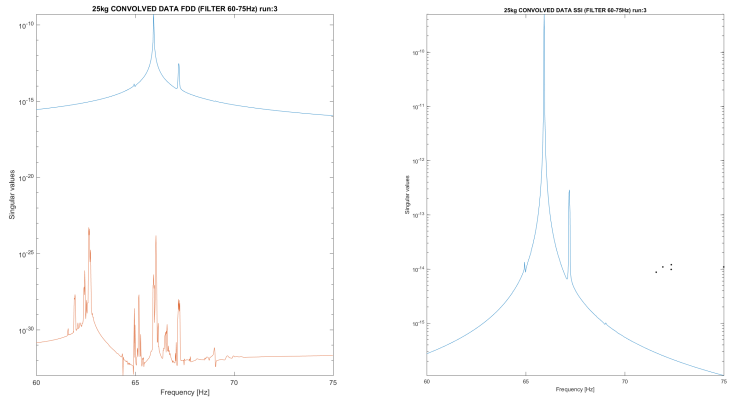


(b) 25kg FDD SSI output, run 2

Figure A3.25kg: Run 2 (segment 3)

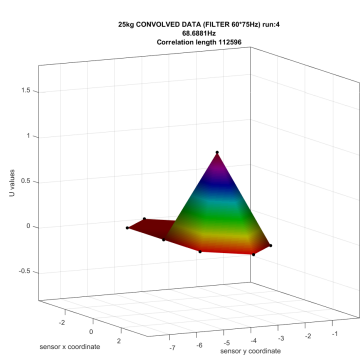


(a) 25kg mode shape, run 3

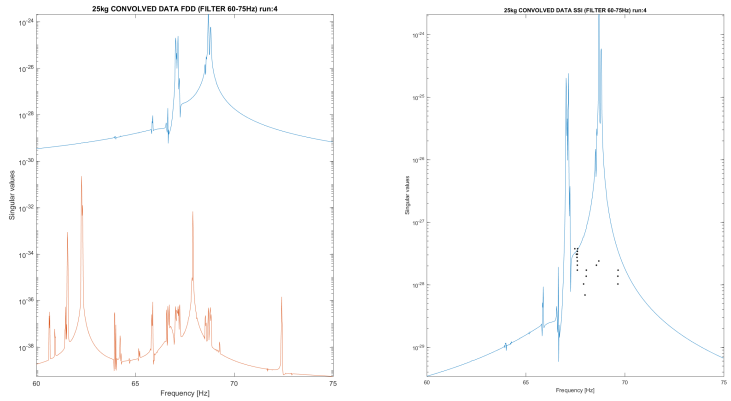


(b) 25kg FDD SSI output, run 3

Figure A3.25kg: Run 3 (segment 3)

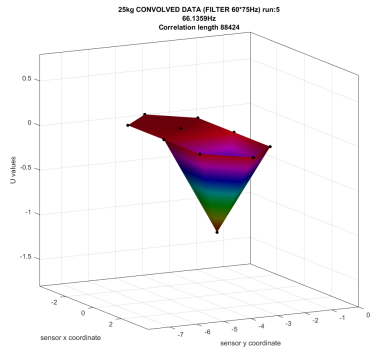


(a) 25kg mode shape, run 4

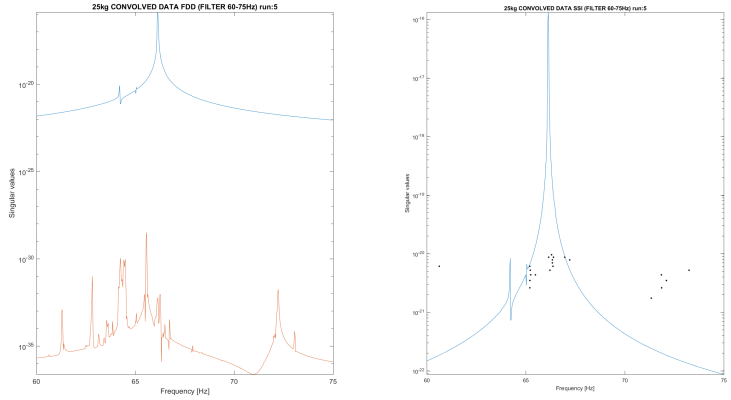


(b) 25kg FDD SSI output, run 4

Figure A3.25kg: Run 4 (segment 3)

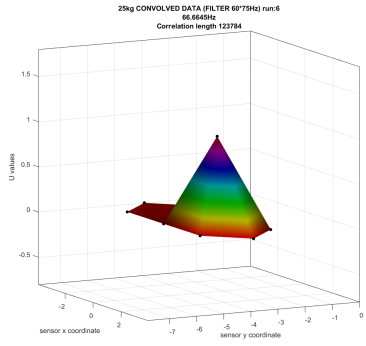


(a) 25kg mode shape, run 5

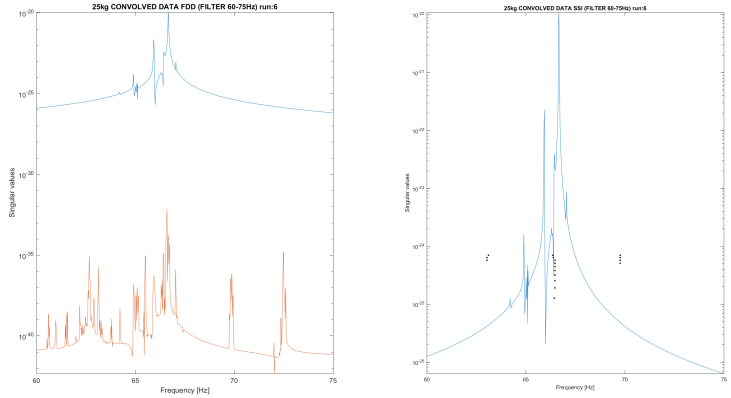


(b) 25kg FDD SSI output, run 5

Figure A3.25kg: Run 5 (segment 3)

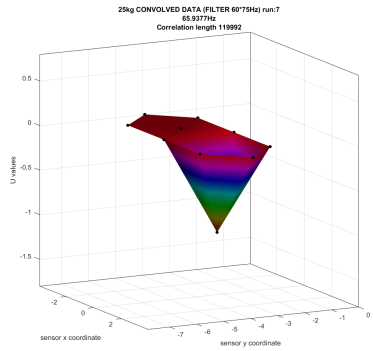


(a) 25kg mode shape, run 6

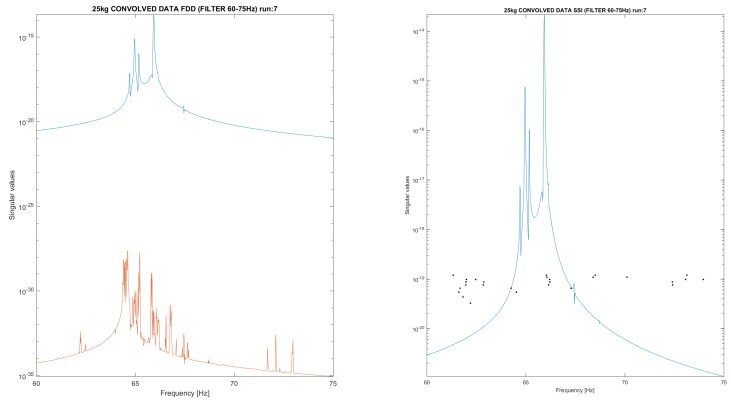


(b) 25kg FDD SSI output, run 6

Figure A3.25kg: Run 6 (segment 3)

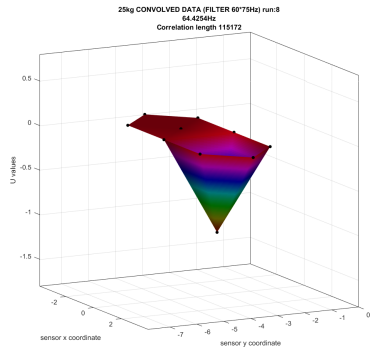


(a) 25kg mode shape, run 7

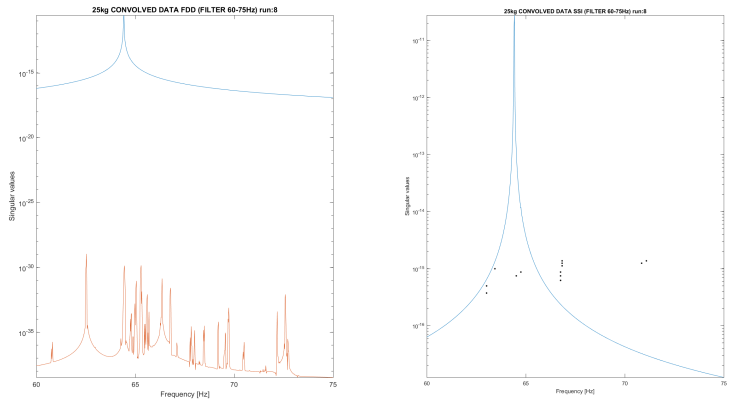


(b) 25kg FDD SSI output, run 7

Figure A3.25kg: Run 7 (segment 3)

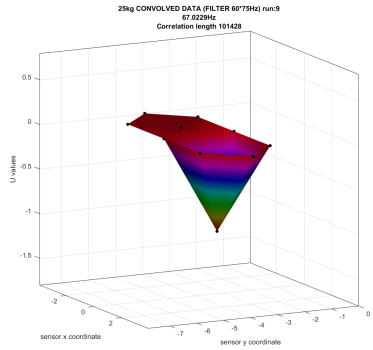


(a) 25kg mode shape, run 8

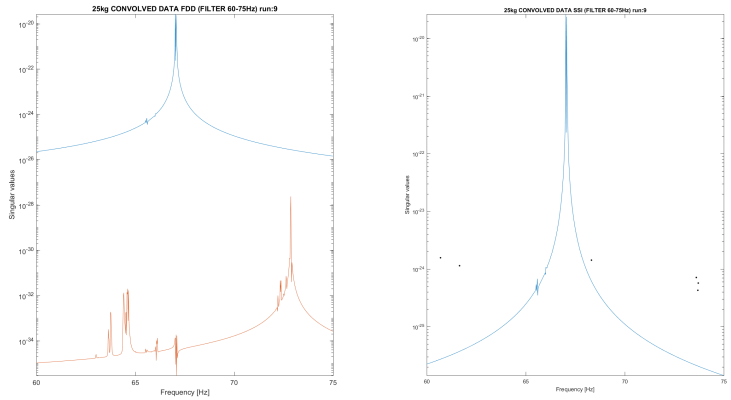


(b) 25kg FDD SSI output, run 8

Figure A3.25kg: Run 8 (segment 3)

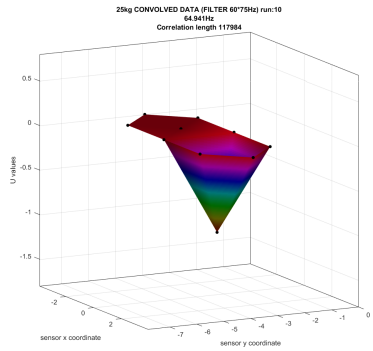


(a) 25kg mode shape, run 9

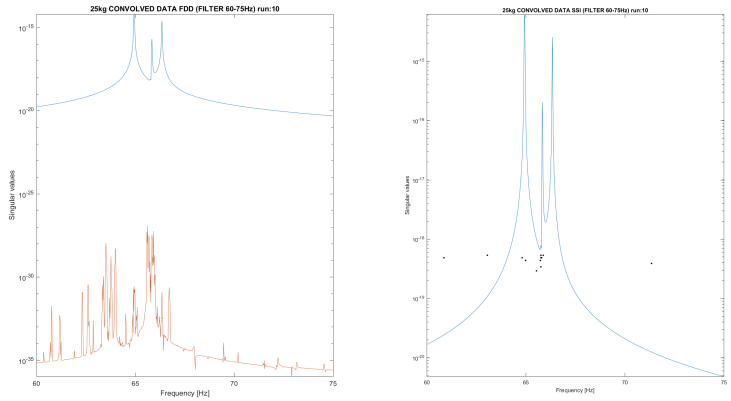


(b) 25kg FDD SSI output, run 9

Figure A3.25kg: Run 9 (segment 3)

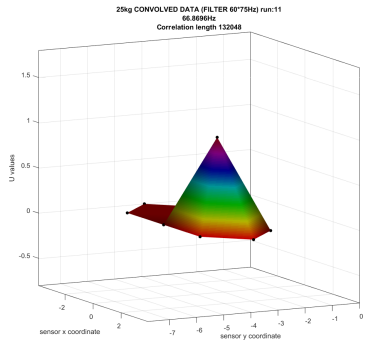


(a) 25kg mode shape, run 10

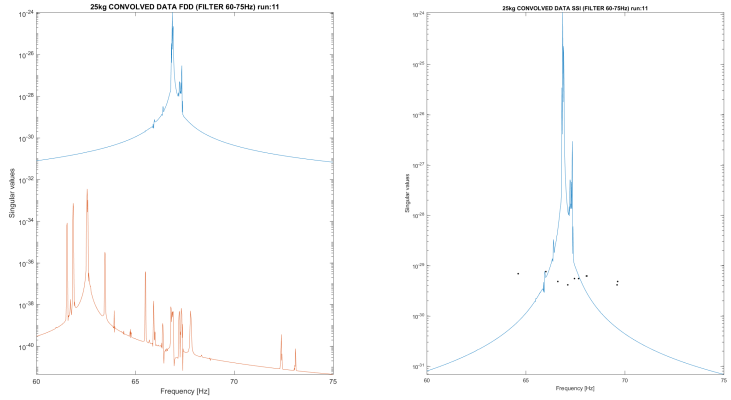


(b) 25kg FDD SSI output, run 10

Figure A3.25kg: Run 10 (segment 3)

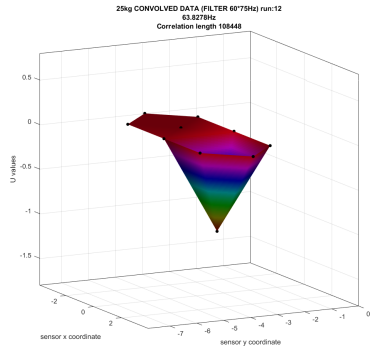


(a) 25kg mode shape, run 11

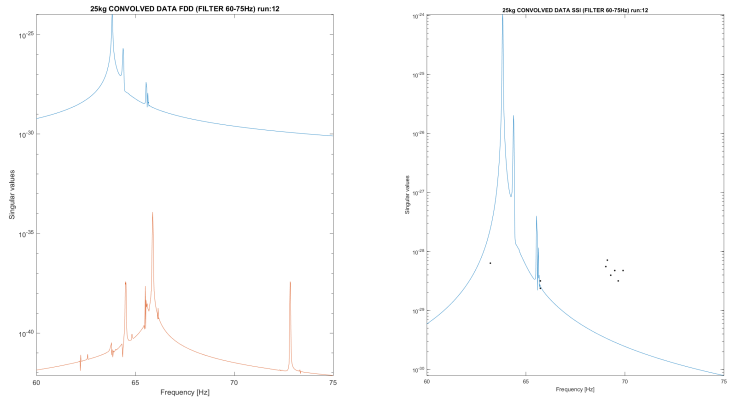


(b) 25kg FDD SSI output, run 11

Figure A3.25kg: Run 11 (segment 3)

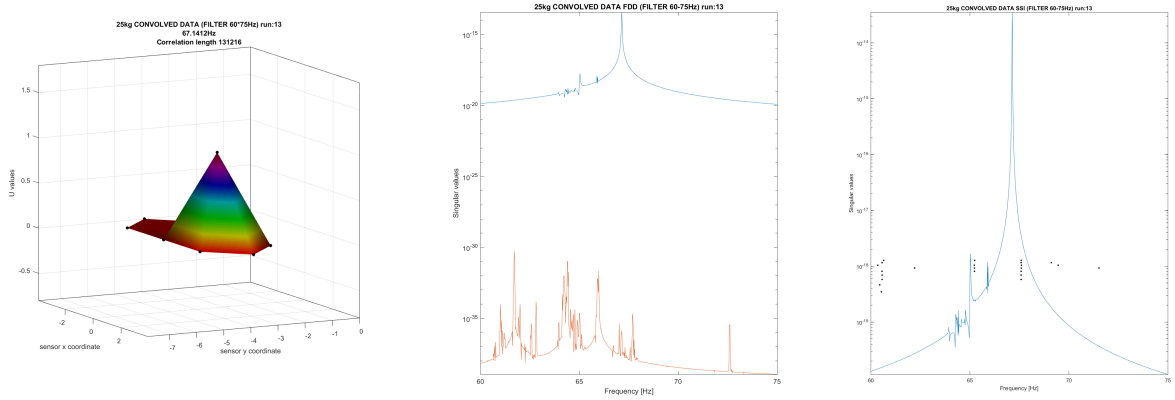


(a) 25kg mode shape, run 12



(b) 25kg FDD SSI output, run 12

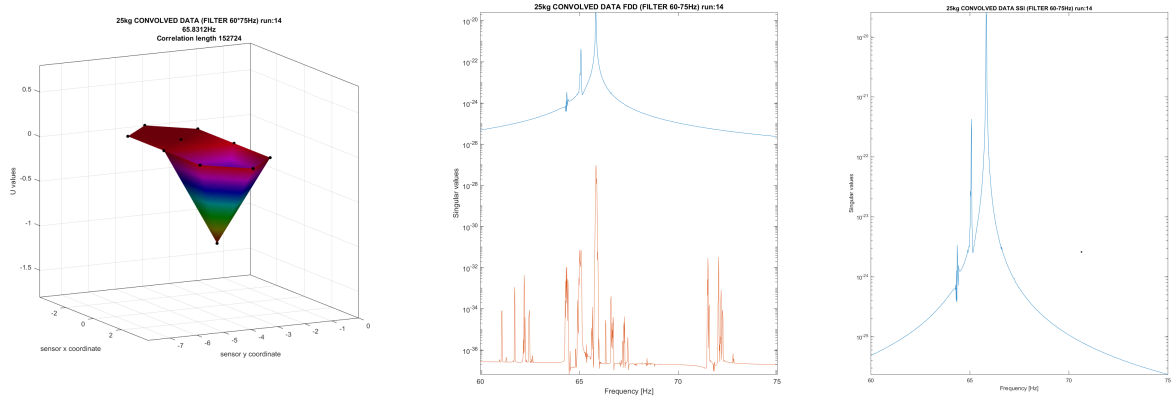
Figure A3.25kg: Run 12 (segment 3)



(a) 25kg mode shape, run 13

(b) 25kg FDD SSI output, run 13

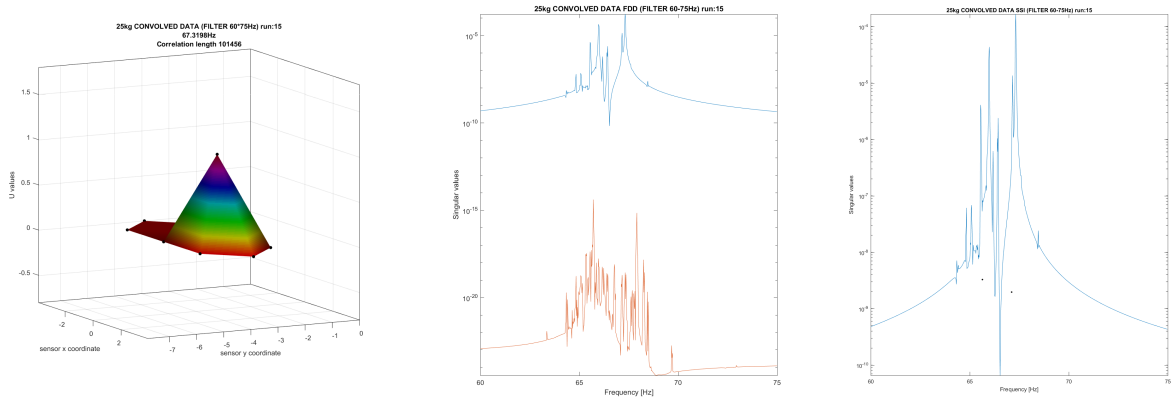
Figure A3.25kg: Run 13 (segment 3)



(a) 25kg mode shape, run 14

(b) 25kg FDD SSI output, run 14

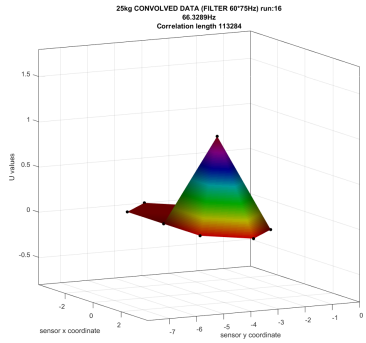
Figure A3.25kg: Run 14 (segment 3)

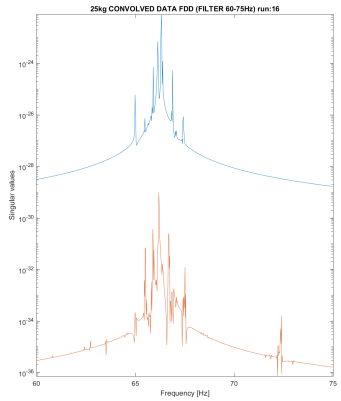


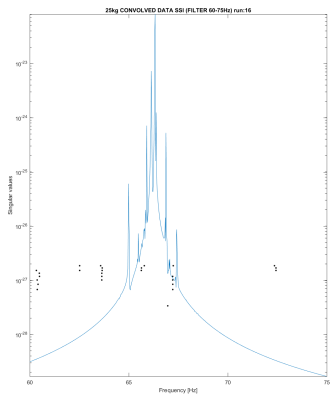
(a) 25kg mode shape, run 15

(b) 25kg FDD SSI output, run 15

Figure A3.25kg: Run 15 (segment 3)



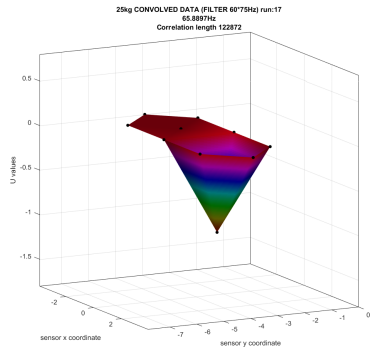


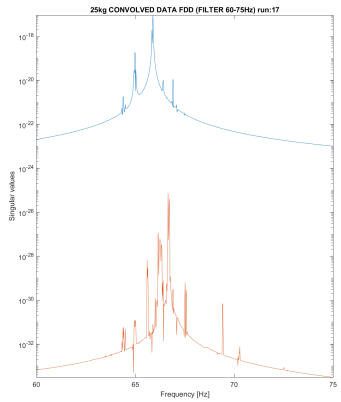


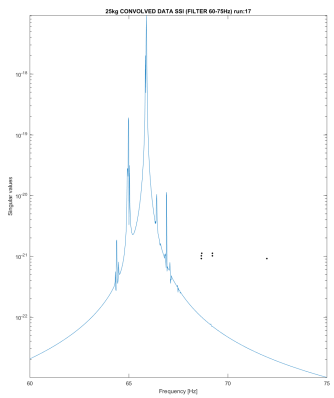
(a) 25kg mode shape, run 16

(b) 25kg FDD SSI output, run 16

Figure A3.25kg: Run 16 (segment 3)



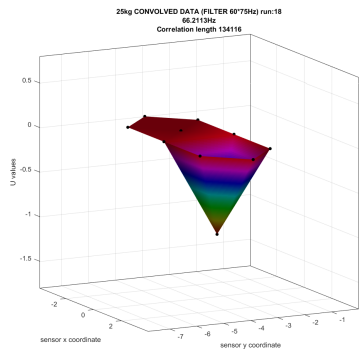


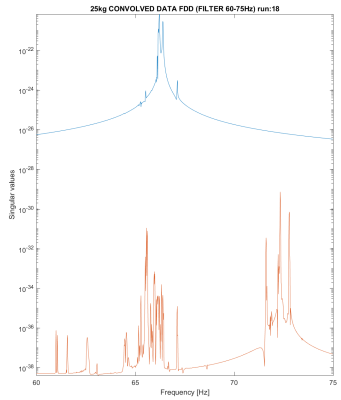


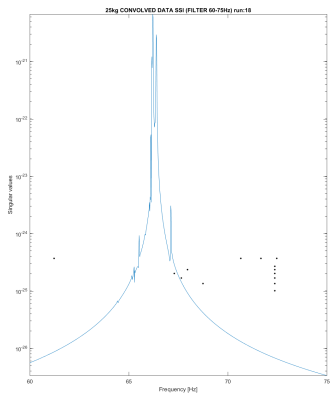
(a) 25kg mode shape, run 17

(b) 25kg FDD SSI output, run 17

Figure A3.25kg: Run 17 (segment 3)



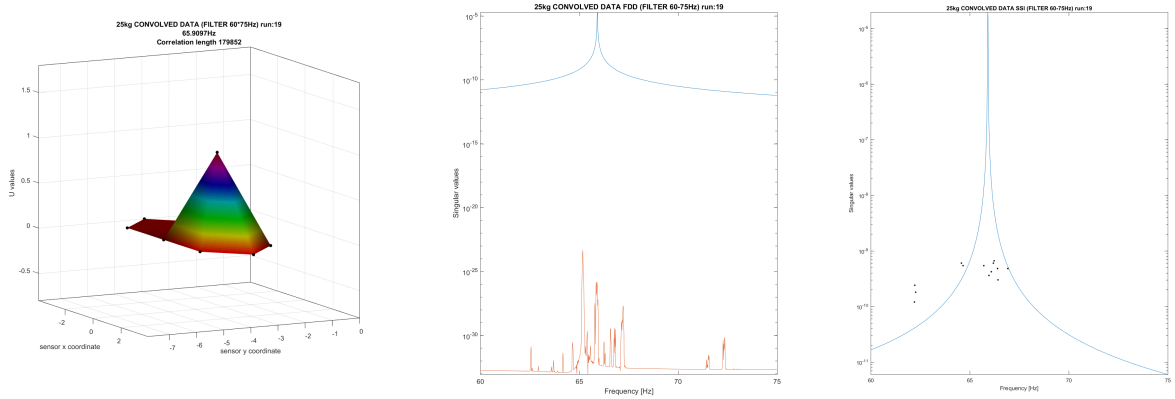




(a) 25kg mode shape, run 18

(b) 25kg FDD SSI output, run 18

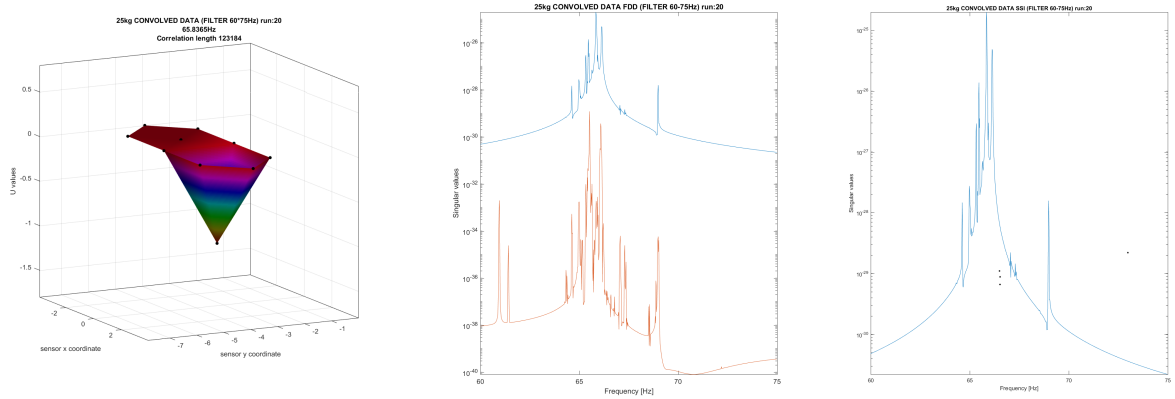
Figure A3.25kg: Run 18 (segment 3)



(a) 25kg mode shape, run 19

(b) 25kg FDD SSI output, run 19

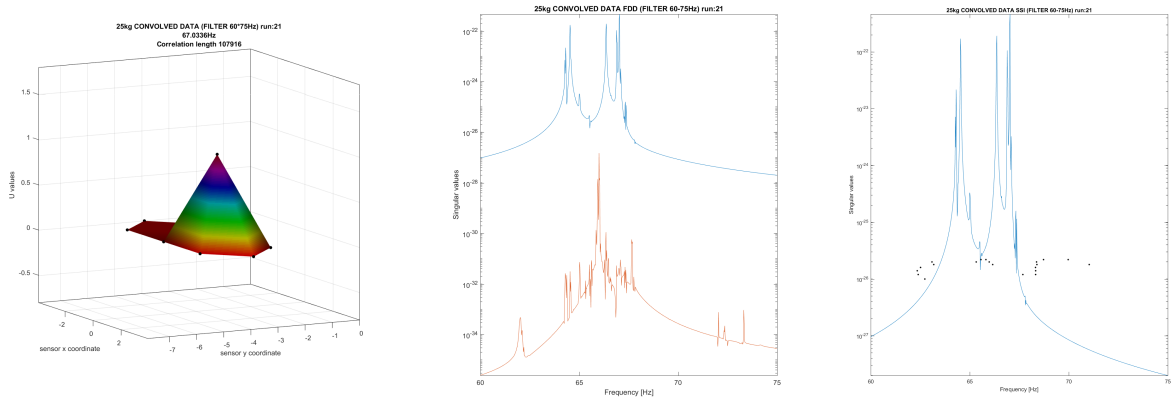
Figure A3.25kg: Run 19 (segment 3)



(a) 25kg mode shape, run 20

(b) 25kg FDD SSI output, run 20

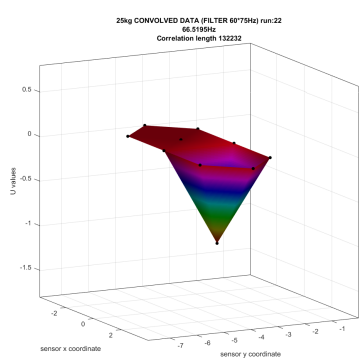
Figure A3.25kg: Run 20 (segment 3)



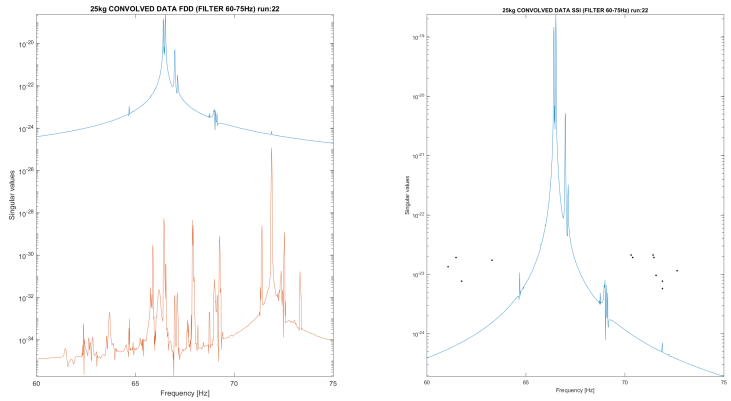
(a) 25kg mode shape, run 21

(b) 25kg FDD SSI output, run 21

Figure A3.25kg: Run 21 (segment 3)

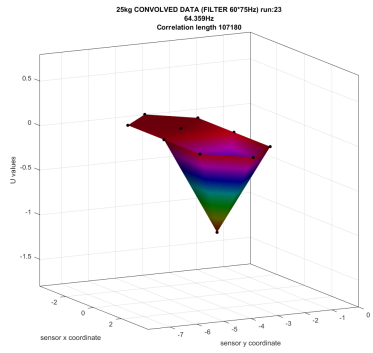


(a) 25kg mode shape, run 22

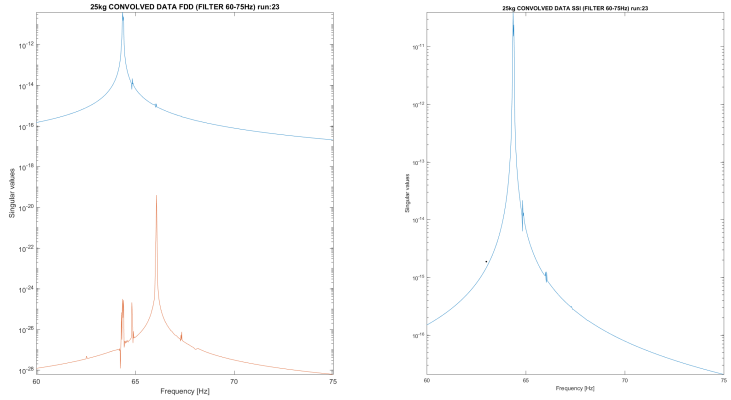


(b) 25kg FDD SSI output, run 22

Figure A3.25kg: Run 22 (segment 3)

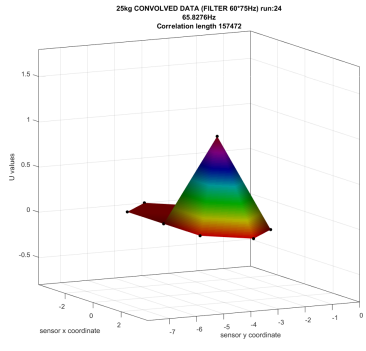


(a) 25kg mode shape, run 23

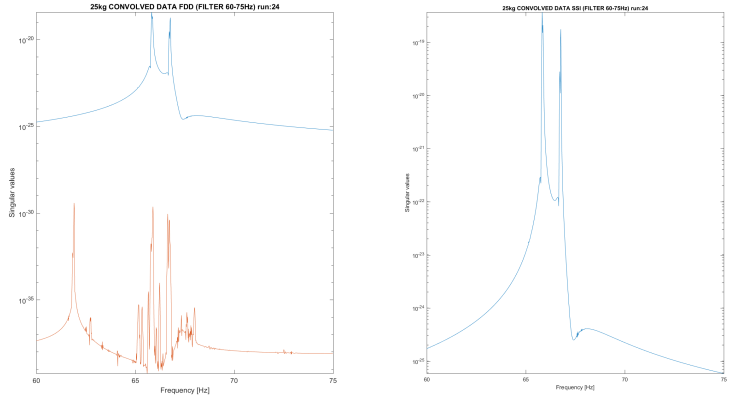


(b) 25kg FDD SSI output, run 23

Figure A3.25kg: Run 23 (segment 3)

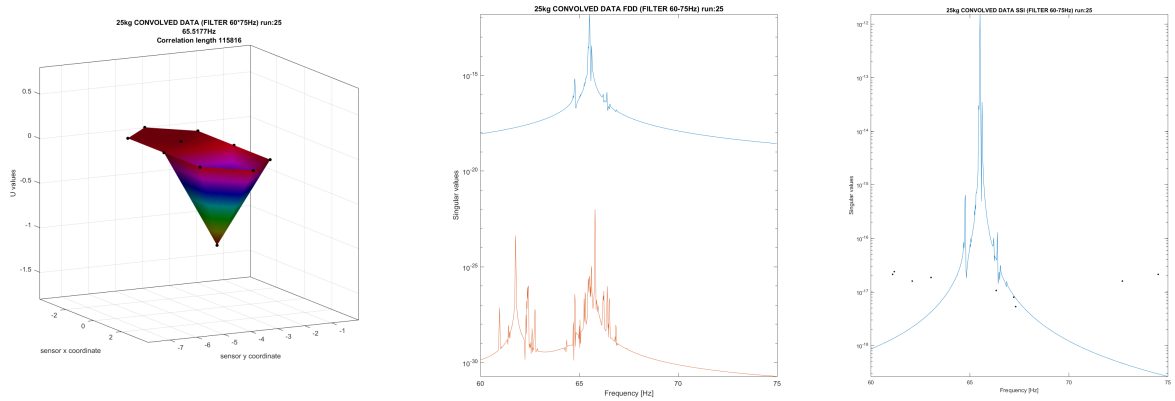


(a) 25kg mode shape, run 24



(b) 25kg FDD SSI output, run 24

Figure A3.25kg: Run 24 (segment 3)

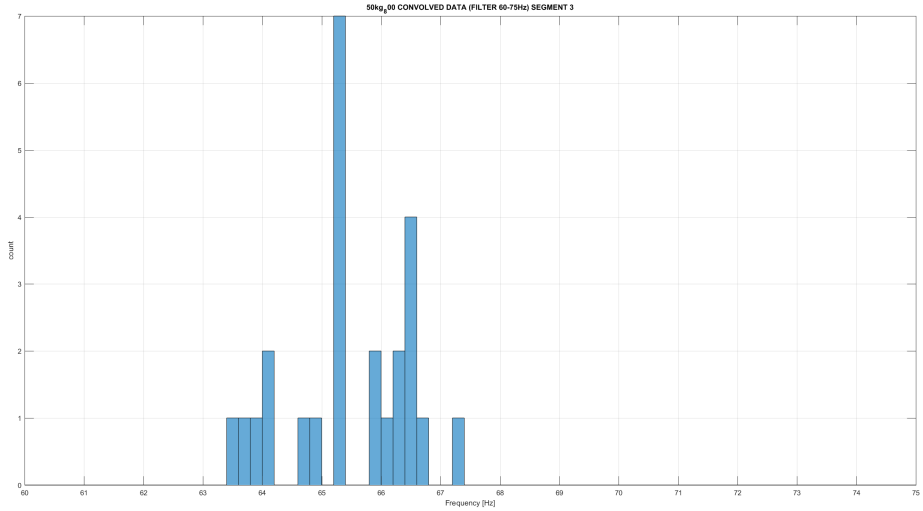


(a) 25kg mode shape, run 25

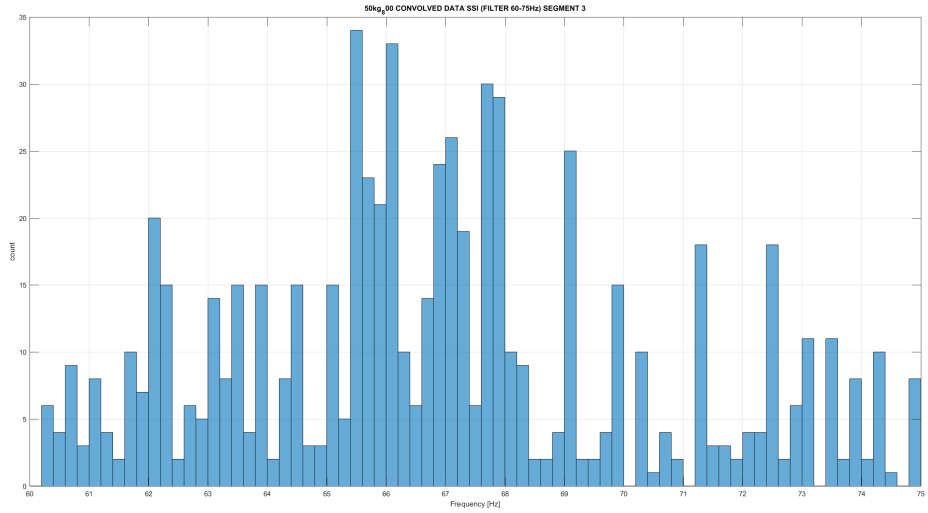
(b) 25kg FDD SSI output, run 25

Figure A3.25kg: Run 25 (segment 3)

50kg data segment 3 (28.03.2017)

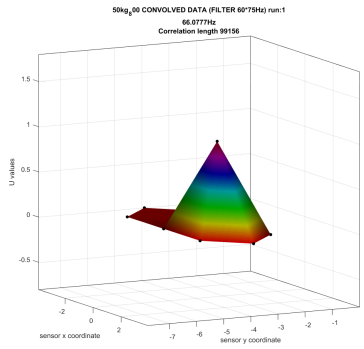


(a) 50kg FDD histogram

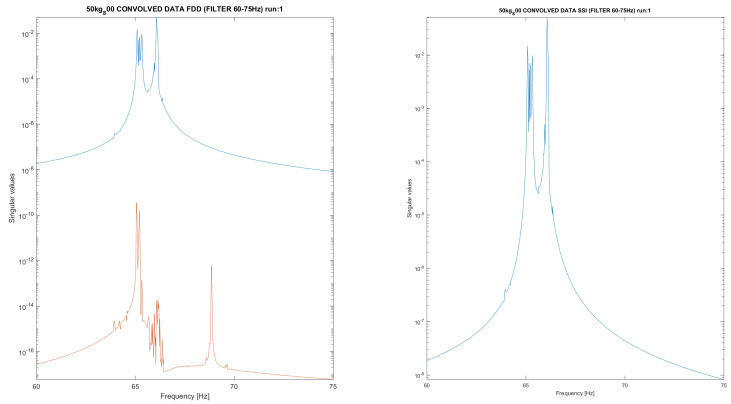


(b) 50kg SSI histogram

Figure A3.50kg: Histograms of identified modes, 50kg data (segment 3)

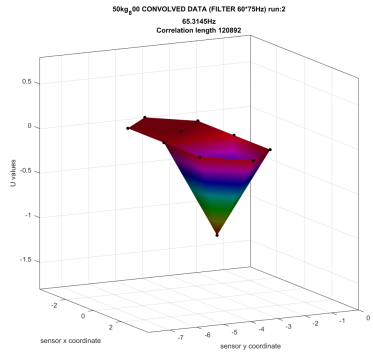


(a) 50kg mode shape, run 1

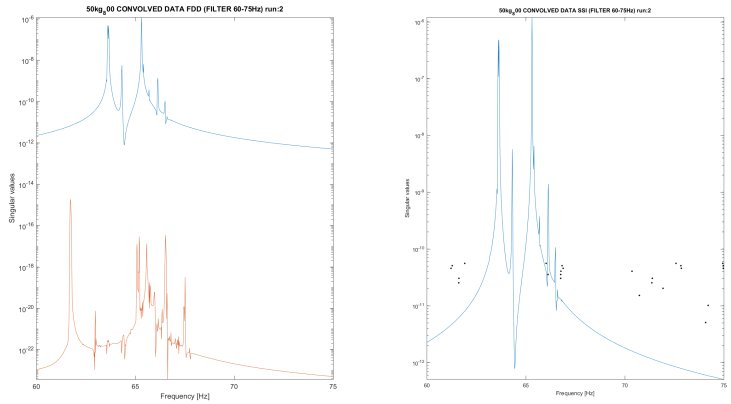


(b) 50kg FDD SSI output, run 1

Figure A3.50kg (28.03.2017): Run 1 (segment 3)

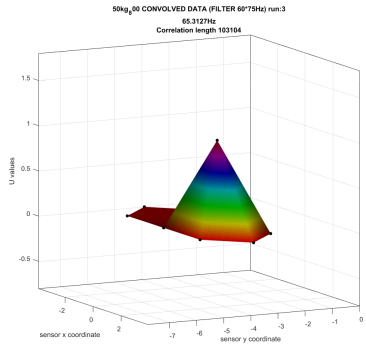


(a) 50kg mode shape, run 2

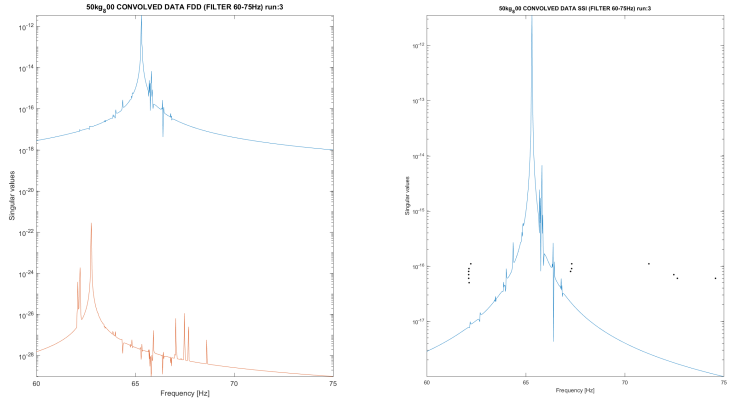


(b) 50kg FDD SSI output, run 2

Figure A3.50kg (28.03.2017): Run 2 (segment 3)

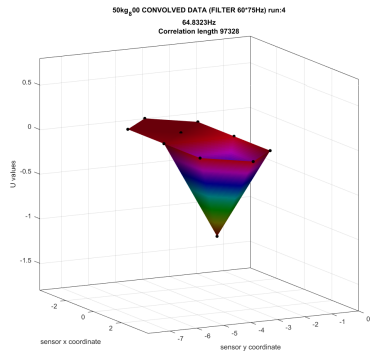


(a) 50kg mode shape, run 3

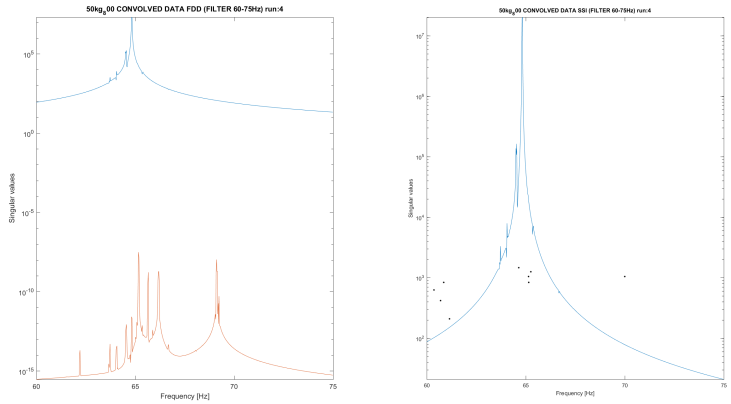


(b) 50kg FDD SSI output, run 3

Figure A3.50kg (28.03.2017): Run 3 (segment 3)

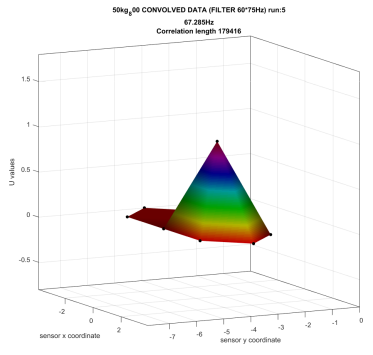


(a) 50kg mode shape, run 4

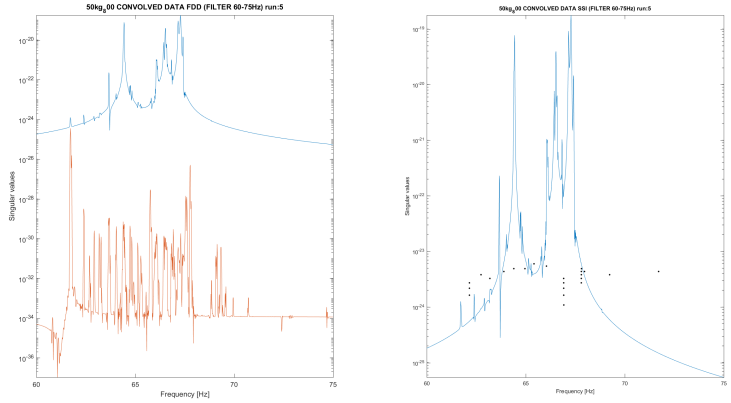


(b) 50kg FDD SSI output, run 4

Figure A3.50kg (28.03.2017): Run 4 (segment 3)

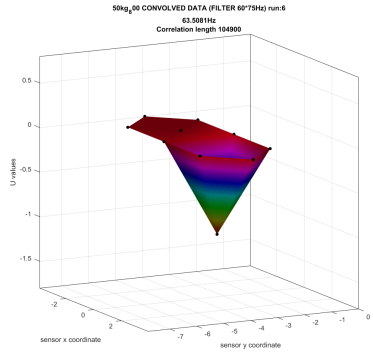


(a) 50kg mode shape, run 5

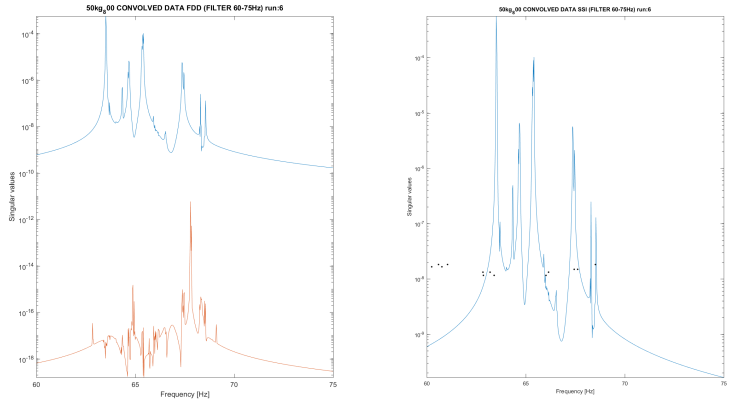


(b) 50kg FDD SSI output, run 5

Figure A3.50kg (28.03.2017): Run 5 (segment 3)

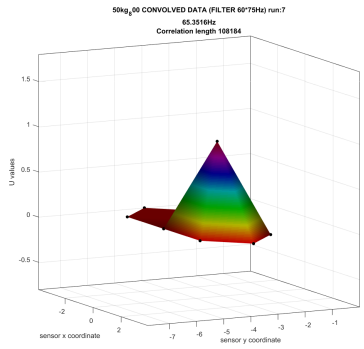


(a) 50kg mode shape, run 6

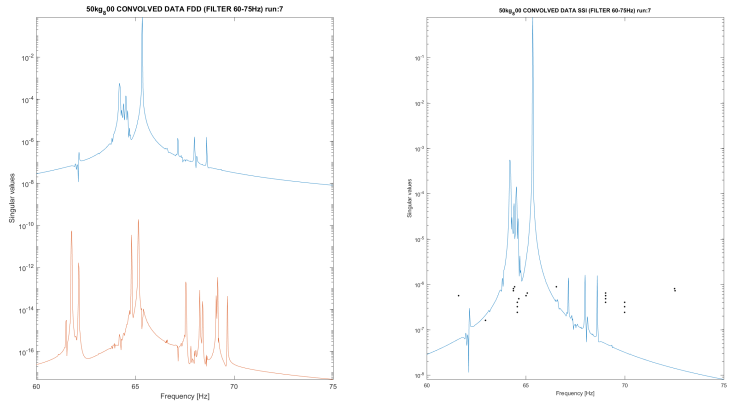


(b) 50kg FDD SSI output, run 6

Figure A3.50kg (28.03.2017): Run 6 (segment 3)

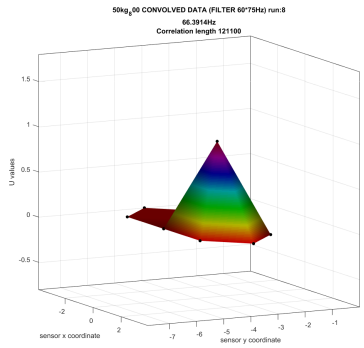


(a) 50kg mode shape, run 7

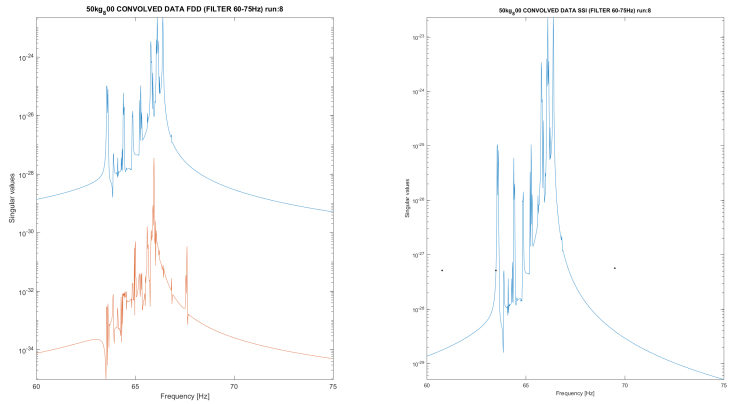


(b) 50kg FDD SSI output, run 7

Figure A3.50kg (28.03.2017): Run 7 (segment 3)

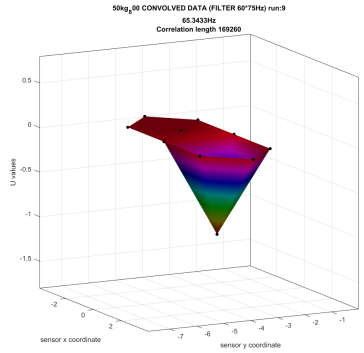


(a) 50kg mode shape, run 8

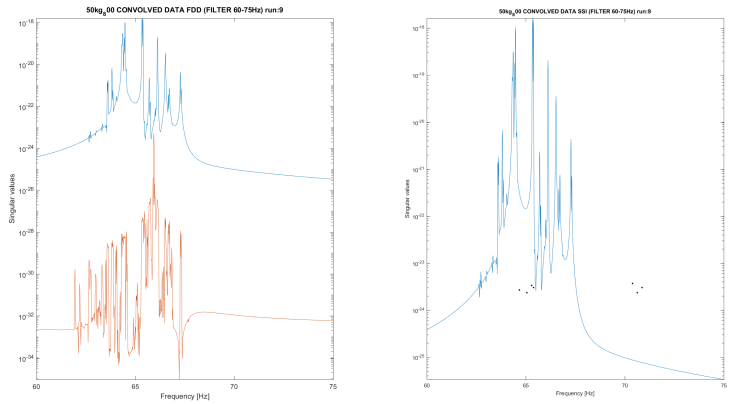


(b) 50kg FDD SSI output, run 8

Figure A3.50kg (28.03.2017): Run 8 (segment 3)

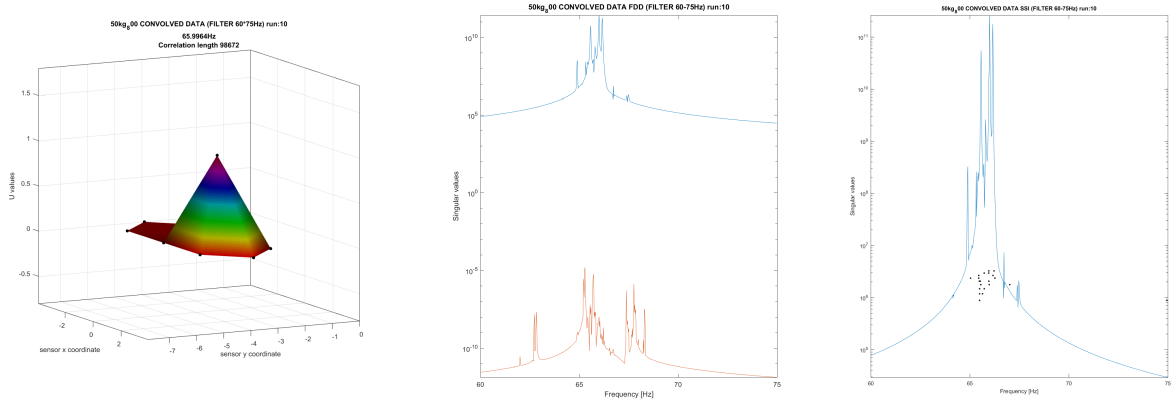


(a) 50kg mode shape, run 9



(b) 50kg FDD SSI output, run 9

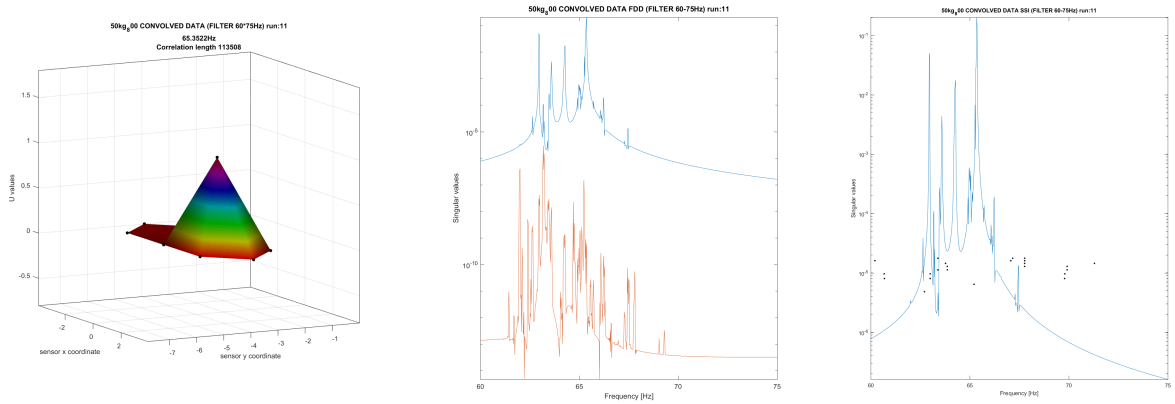
Figure A3.50kg (28.03.2017): Run 9 (segment 3)



(a) 50kg mode shape, run 10

(b) 50kg FDD SSI output, run 10

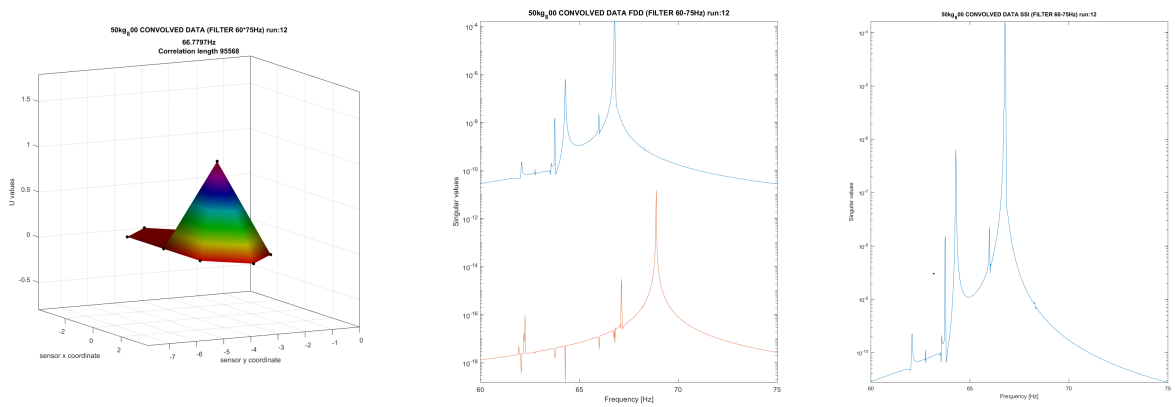
Figure A3.50kg (28.03.2017): Run 10 (segment 3)



(a) 50kg mode shape, run 11

(b) 50kg FDD SSI output, run 11

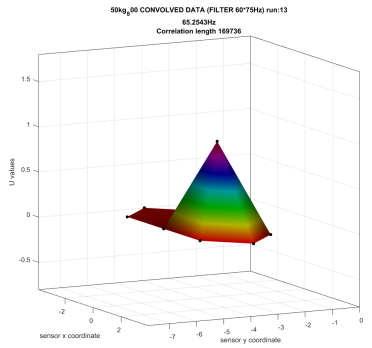
Figure A3.50kg (28.03.2017): Run 11 (segment 3)



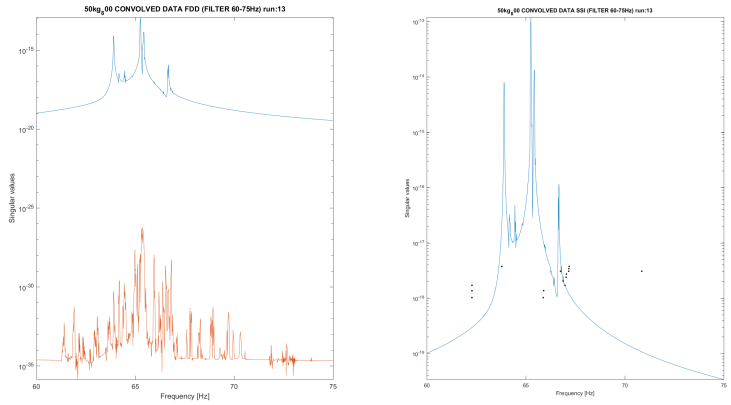
(a) 50kg mode shape, run 12

(b) 50kg FDD SSI output, run 12

Figure A3.50kg (28.03.2017): Run 12 (segment 3)

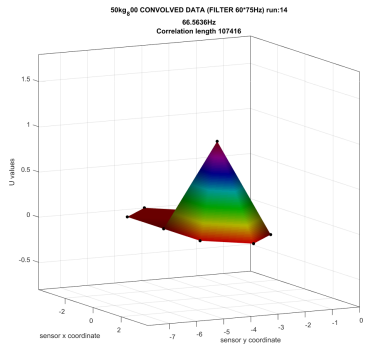


(a) 50kg mode shape, run 13

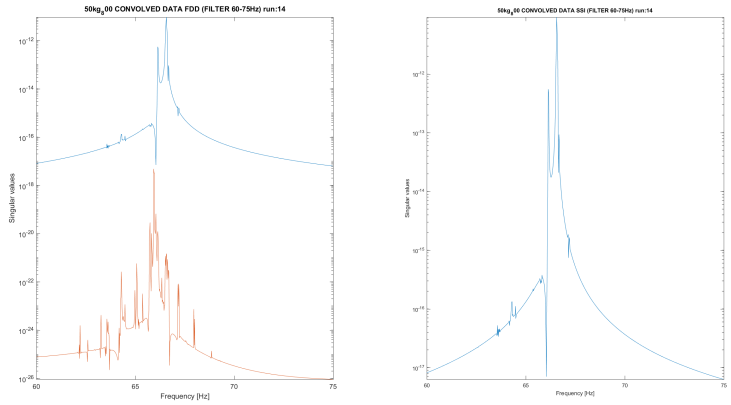


(b) 50kg FDD SSI output, run 13

Figure A3.50kg (28.03.2017): Run 13 (segment 3)

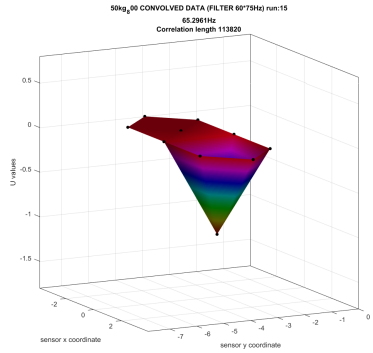


(a) 50kg mode shape, run 14

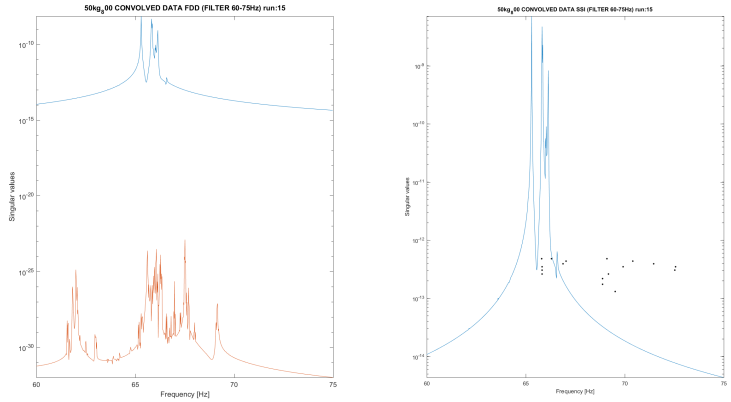


(b) 50kg FDD SSI output, run 14

Figure A3.50kg (28.03.2017): Run 14 (segment 3)

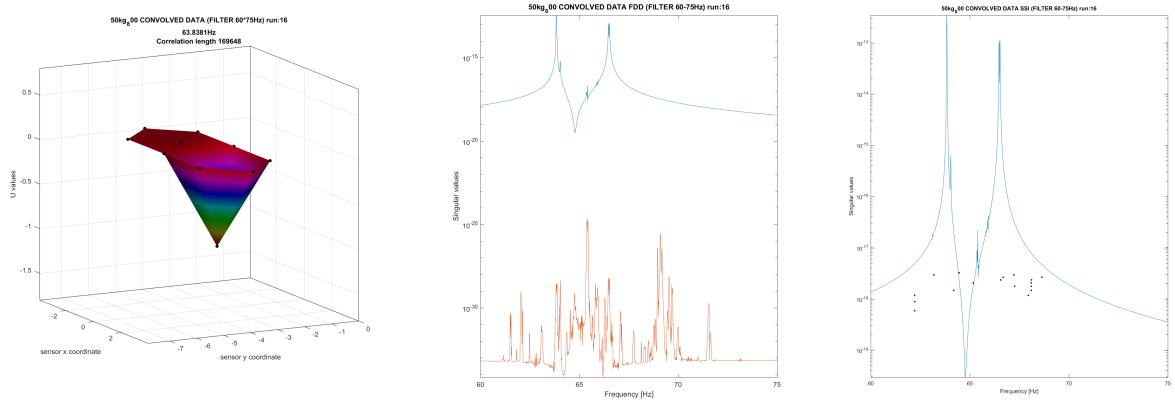


(a) 50kg mode shape, run 15



(b) 50kg FDD SSI output, run 15

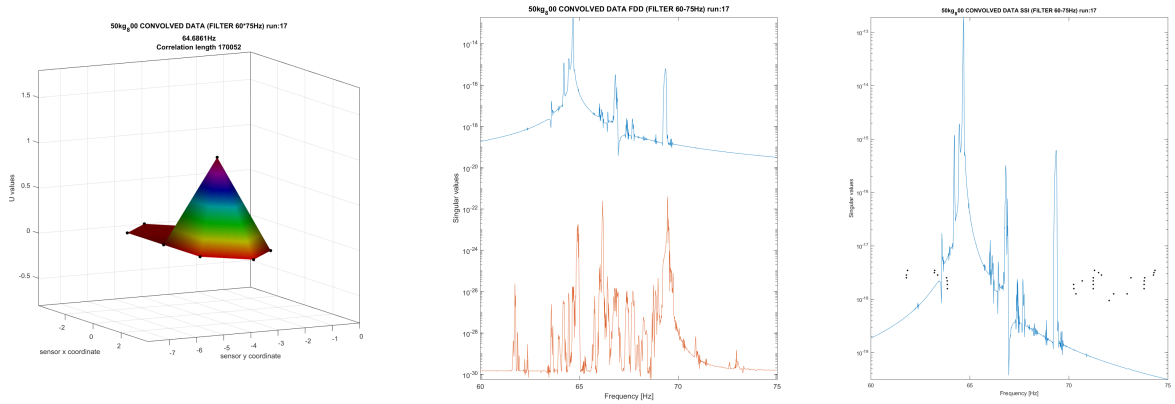
Figure A3.50kg (28.03.2017): Run 15 (segment 3)



(a) 50kg mode shape, run 16

(b) 50kg FDD SSI output, run 16

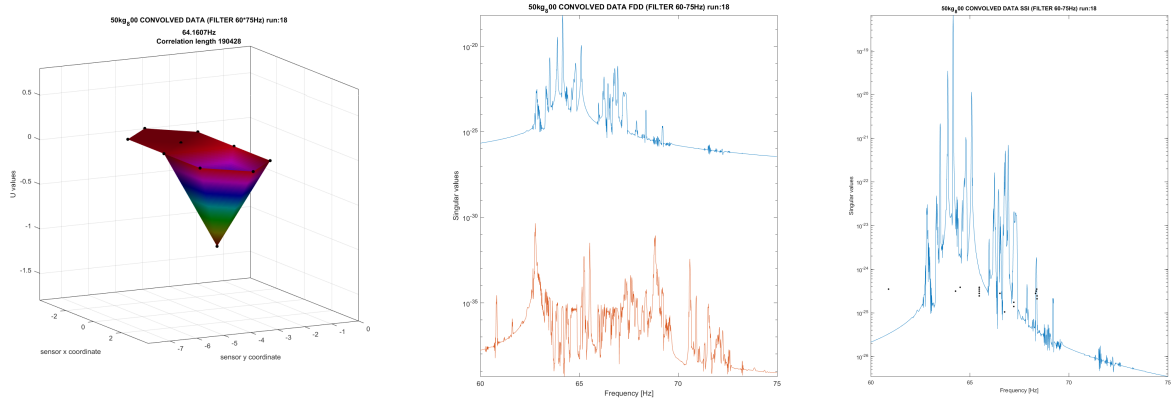
Figure A3.50kg (28.03.2017): Run 16 (segment 3)



(a) 50kg mode shape, run 17

(b) 50kg FDD SSI output, run 17

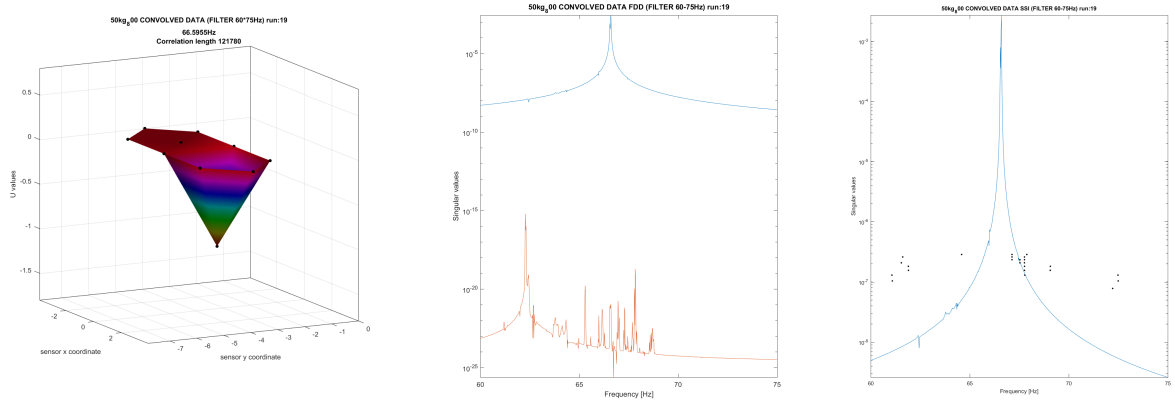
Figure A3.50kg (28.03.2017): Run 17 (segment 3)



(a) 50kg mode shape, run 18

(b) 50kg FDD SSI output, run 18

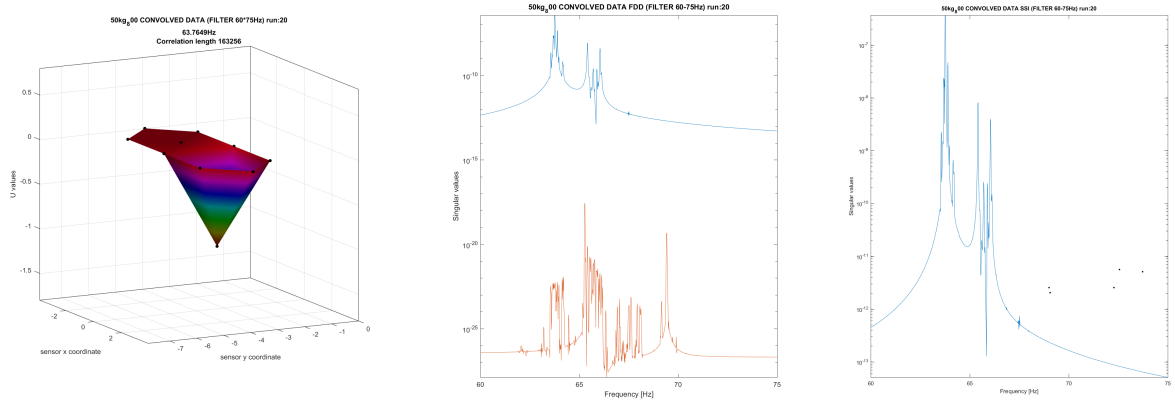
Figure A3.50kg (28.03.2017): Run 18 (segment 3)



(a) 50kg mode shape, run 19

(b) 50kg FDD SSI output, run 19

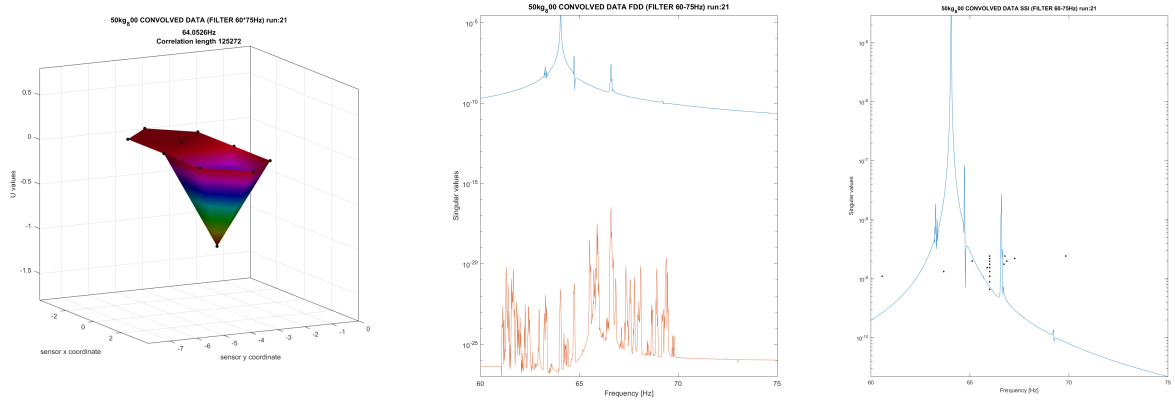
Figure A3.50kg (28.03.2017): Run 19 (segment 3)



(a) 50kg mode shape, run 20

(b) 50kg FDD SSI output, run 20

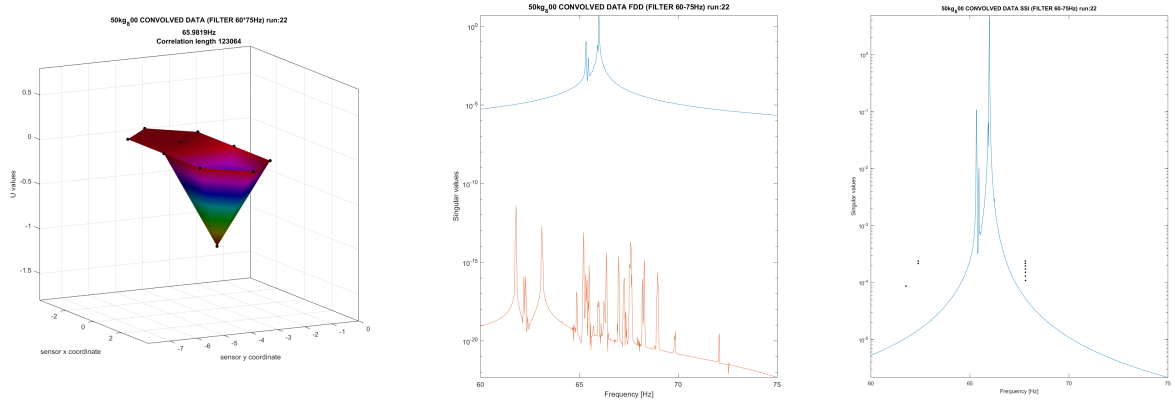
Figure A3.50kg (28.03.2017): Run 20 (segment 3)



(a) 50kg mode shape, run 21

(b) 50kg FDD SSI output, run 21

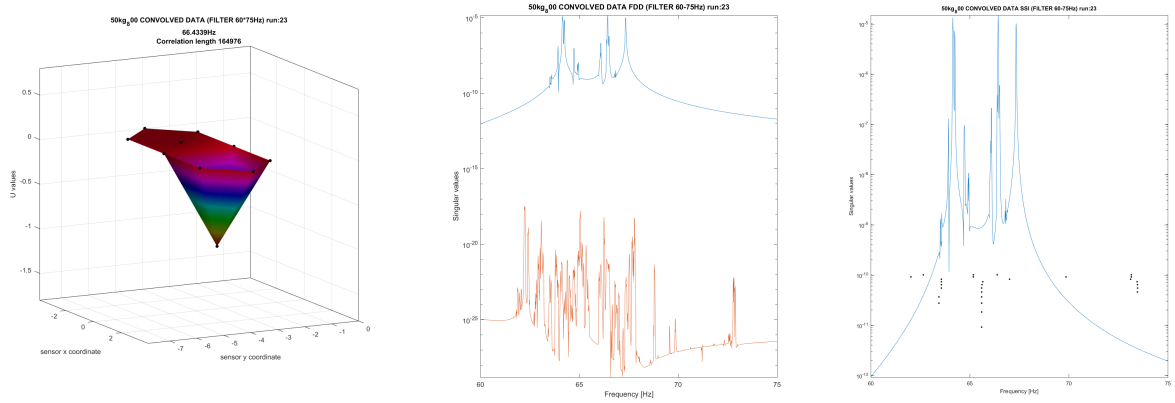
Figure A3.50kg (28.03.2017): Run 21 (segment 3)



(a) 50kg mode shape, run 22

(b) 50kg FDD SSI output, run 22

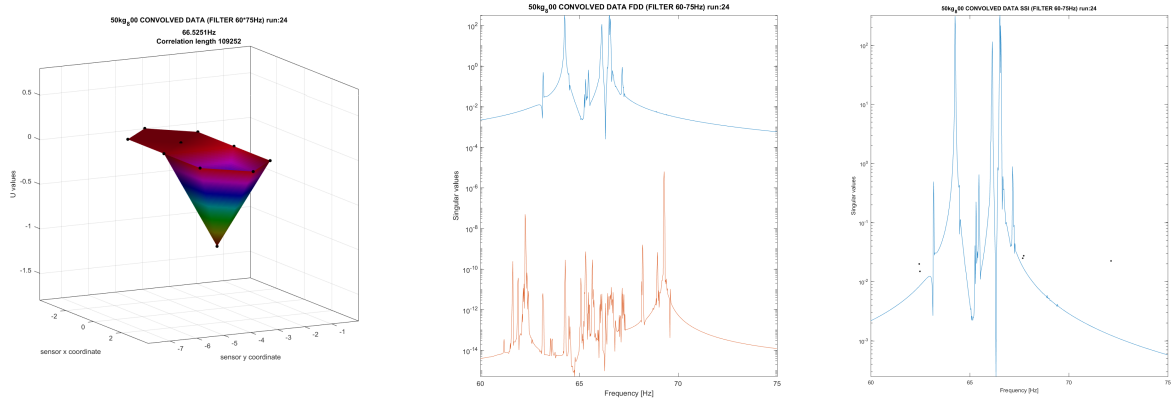
Figure A3.50kg (28.03.2017): Run 22 (segment 3)



(a) 50kg mode shape, run 23

(b) 50kg FDD SSI output, run 23

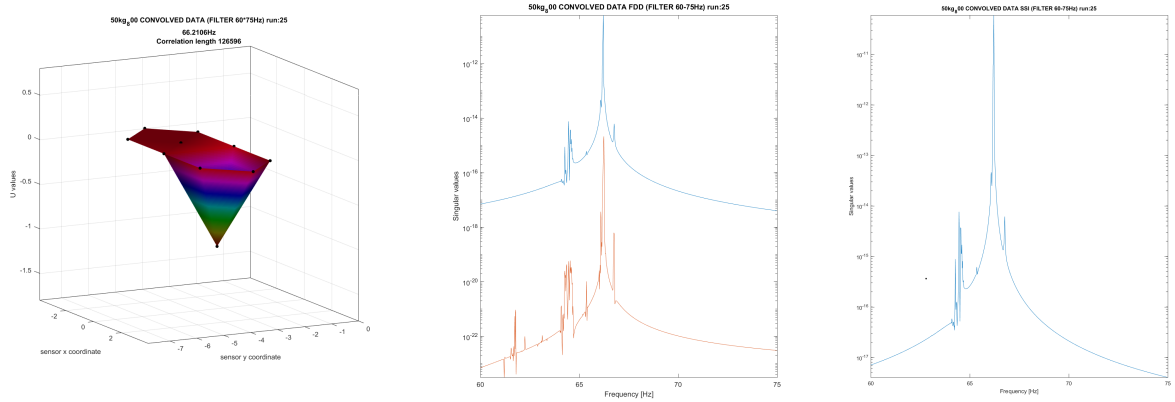
Figure A3.50kg (28.03.2017): Run 23 (segment 3)



(a) 50kg mode shape, run 24

(b) 50kg FDD SSI output, run 24

Figure A3.50kg (28.03.2017): Run 24 (segment 3)



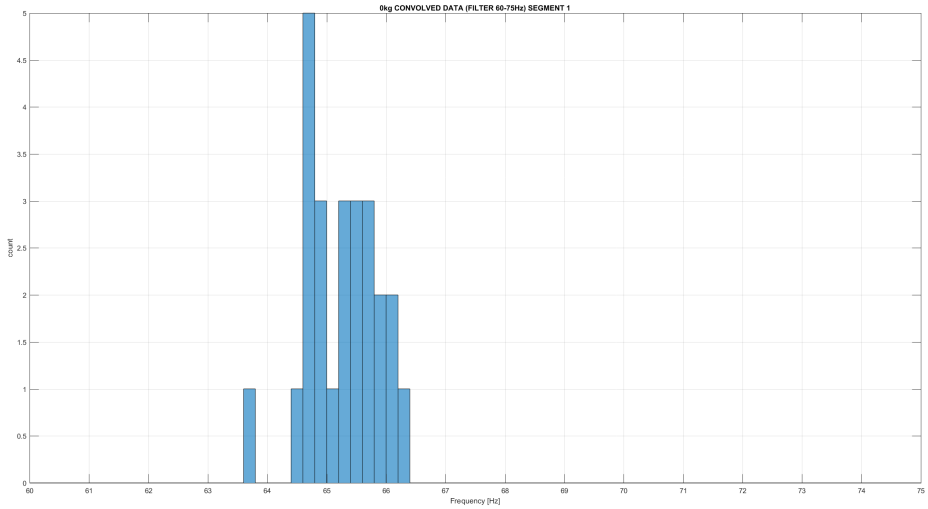
(a) 50kg mode shape, run 25

(b) 50kg FDD SSI output, run 25

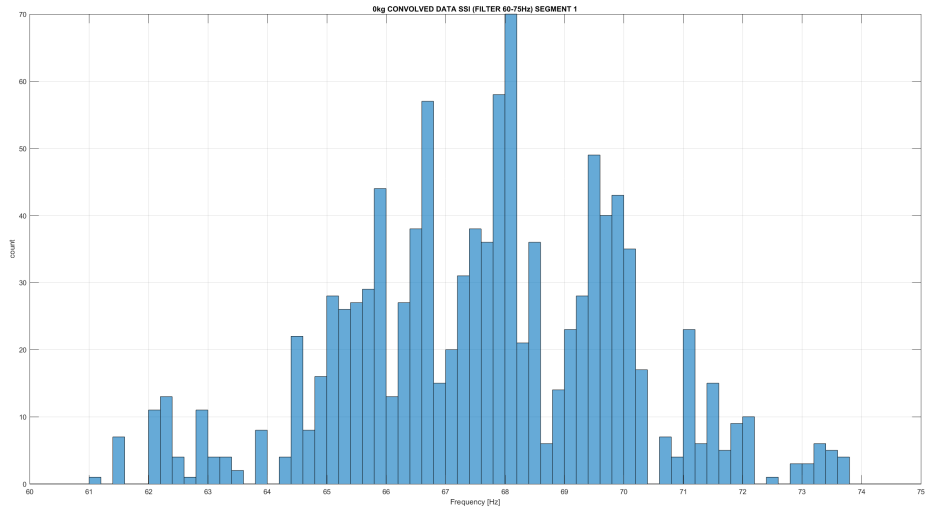
Figure A3.50kg (28.03.2017): Run 25 (segment 3)

Appendix A4

Data 0kg-50kg-75kg-100kg segment 1 (Reduced order PF)

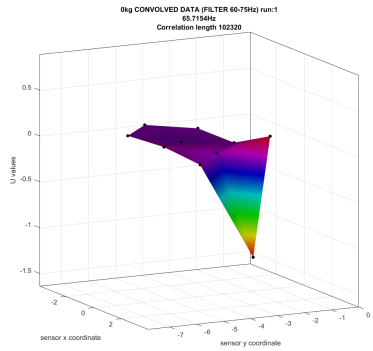


(a) 0kg FDD histogram

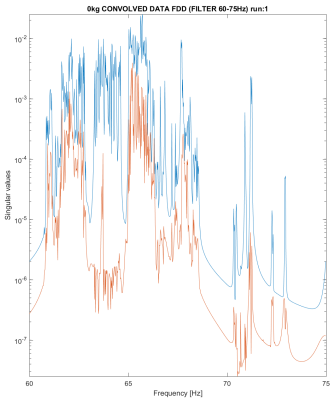


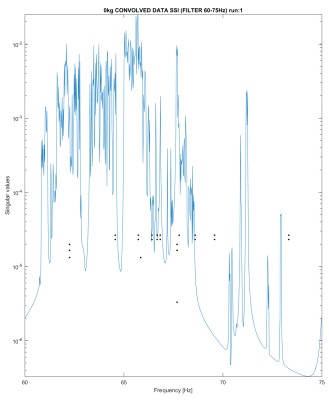
(b) 0kg SSI histogram

Figure A4.0kg: Histograms of identified modes, 0kg data (segment 1)



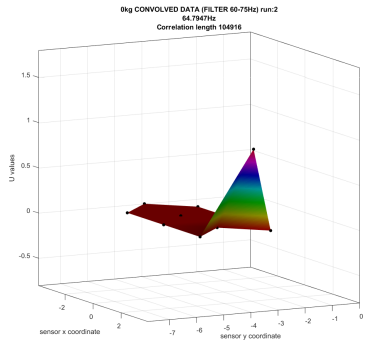
(a) 0kg mode shape, run 1



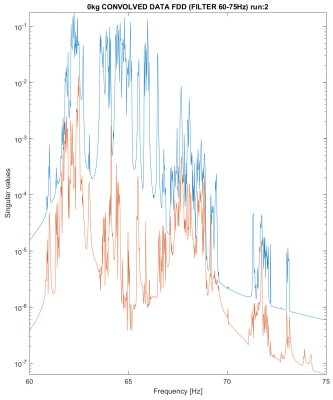


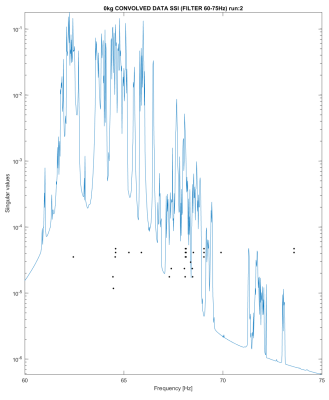
(b) 0kg FDD SSI output, run 1

Figure A4.0kg: Run 1 (segment 1)



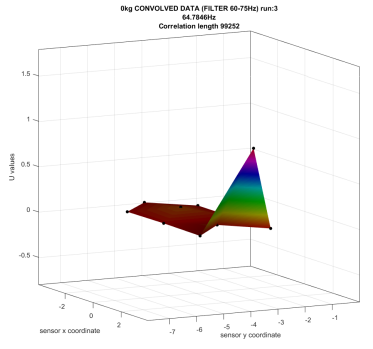
(a) 0kg mode shape, run 2



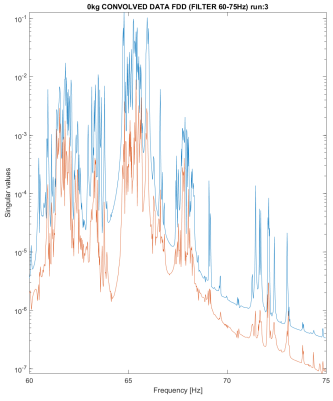


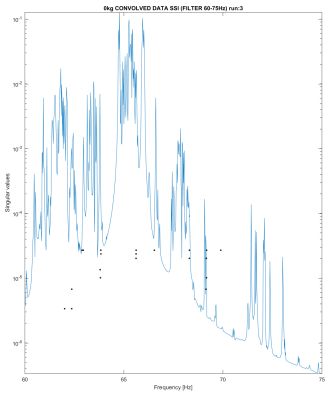
(b) 0kg FDD SSI output, run 2

Figure A4.0kg: Run 2 (segment 1)



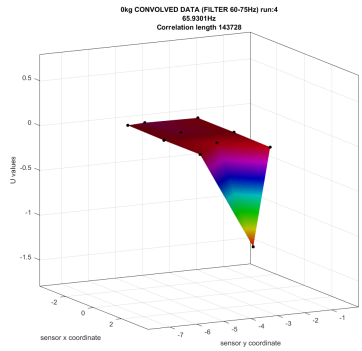
(a) 0kg mode shape, run 3



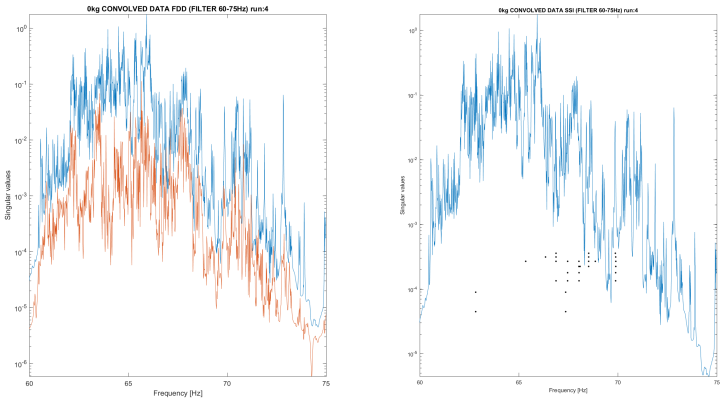


(b) 0kg FDD SSI output, run 3

Figure A4.0kg: Run 3 (segment 1)

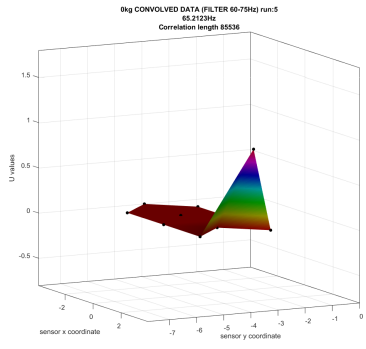


(a) 0kg mode shape, run 4

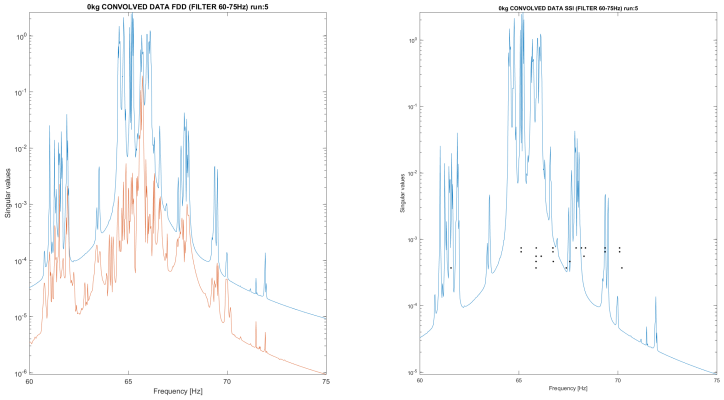


(b) 0kg FDD SSI output, run 4

Figure A4.0kg: Run 4 (segment 1)

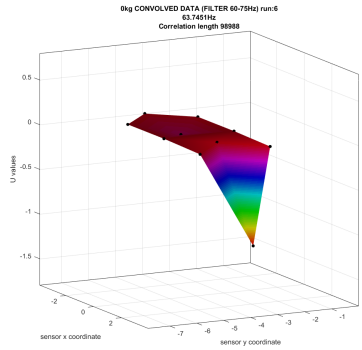


(a) 0kg mode shape, run 5

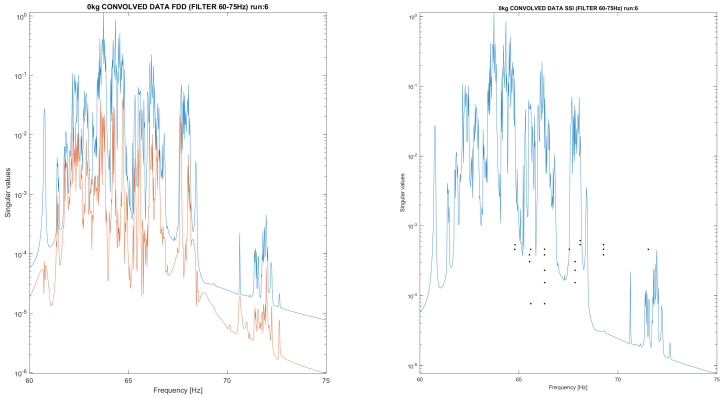


(b) 0kg FDD SSI output, run 5

Figure A4.0kg: Run 5 (segment 1)

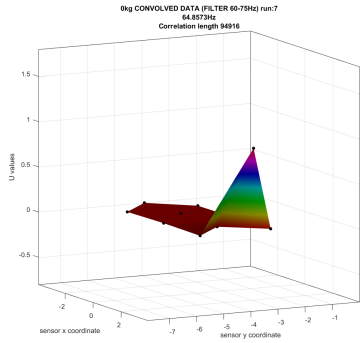


(a) 0kg mode shape, run 6

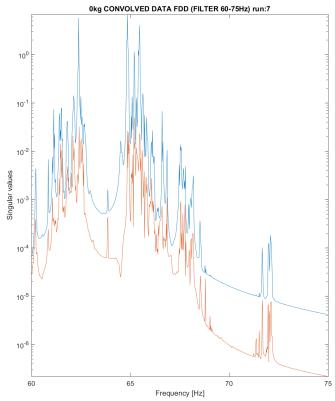


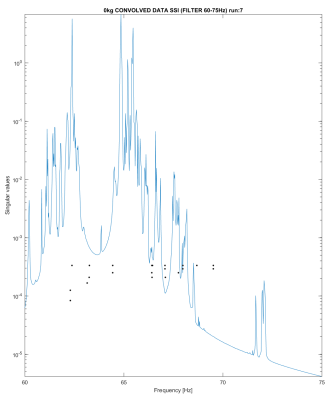
(b) 0kg FDD SSI output, run 6

Figure A4.0kg: Run 6 (segment 1)



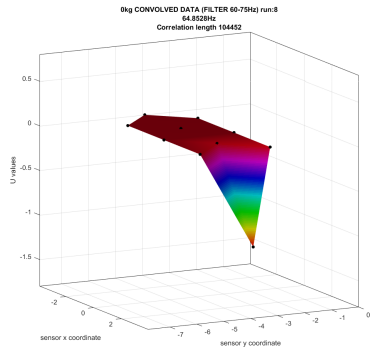
(a) 0kg mode shape, run 7



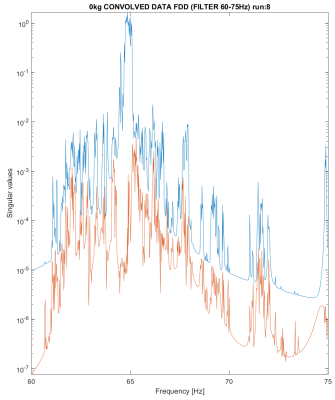


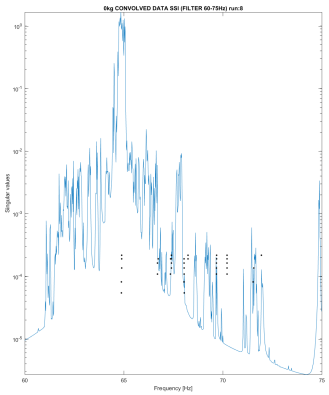
(b) 0kg FDD SSI output, run 7

Figure A4.0kg: Run 7 (segment 1)



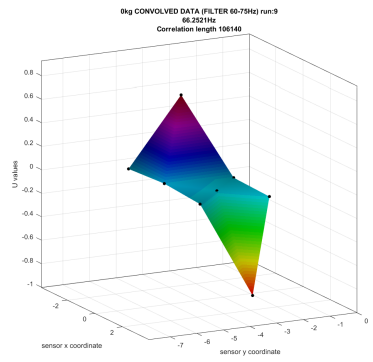
(a) 0kg mode shape, run 8



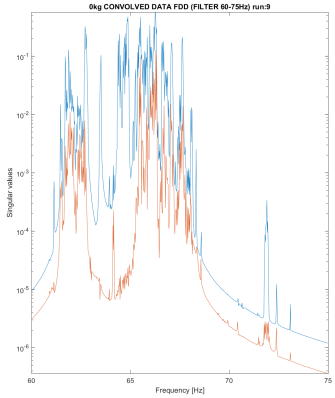


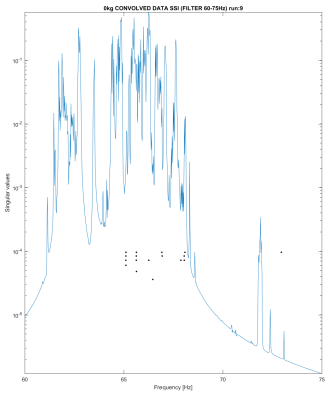
(b) 0kg FDD SSI output, run 8

Figure A4.0kg: Run 8 (segment 1)



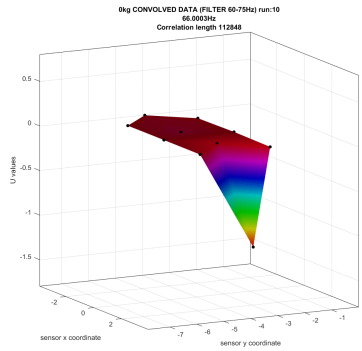
(a) 0kg mode shape, run 9



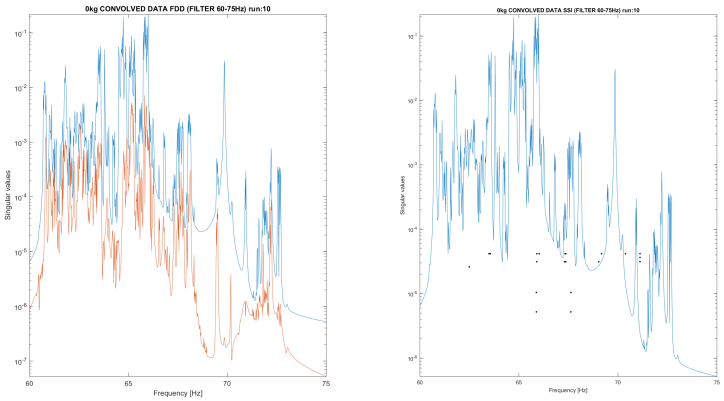


(b) 0kg FDD SSI output, run 9

Figure A4.0kg: Run 9 (segment 1)

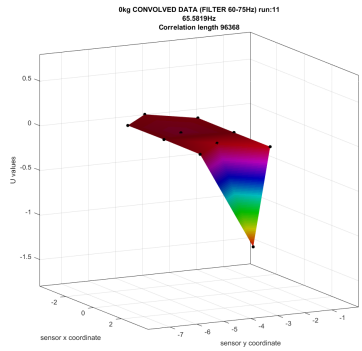


(a) 0kg mode shape, run 10

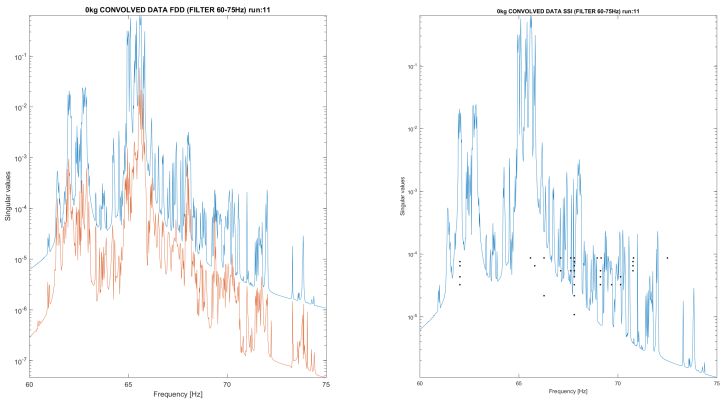


(b) 0kg FDD SSI output, run 10

Figure A4.0kg: Run 10 (segment 1)

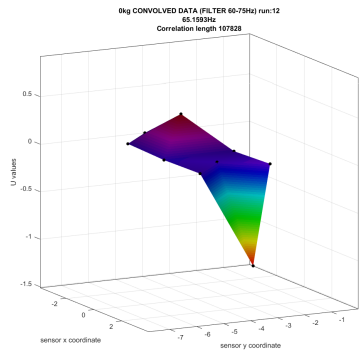


(a) 0kg mode shape, run 11

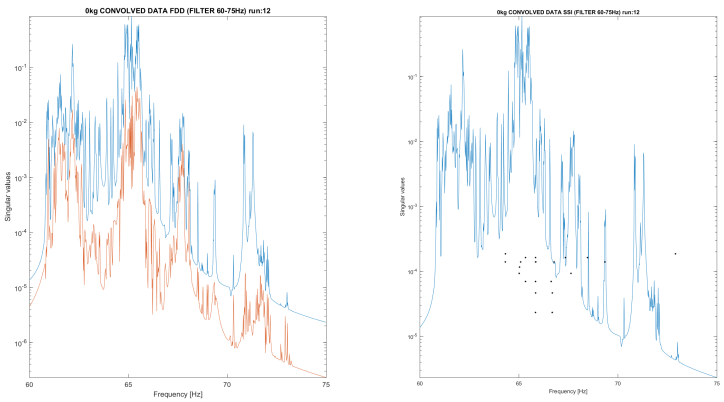


(b) 0kg FDD SSI output, run 11

Figure A4.0kg: Run 11 (segment 1)

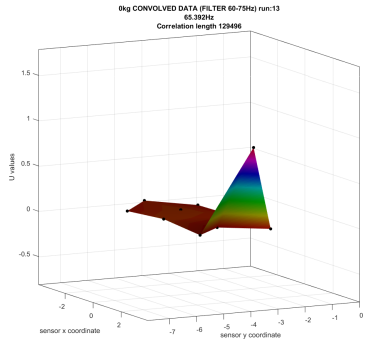


(a) 0kg mode shape, run 12

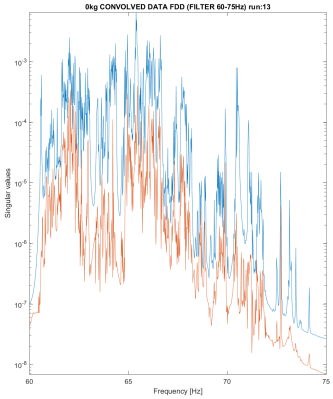


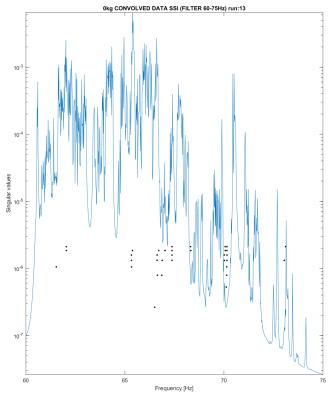
(b) 0kg FDD SSI output, run 12

Figure A4.0kg: Run 12 (segment 1)



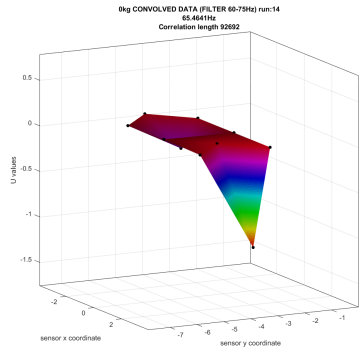
(a) 0kg mode shape, run 13



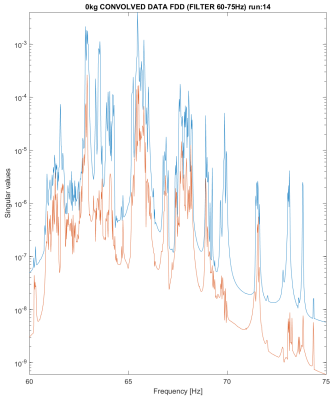


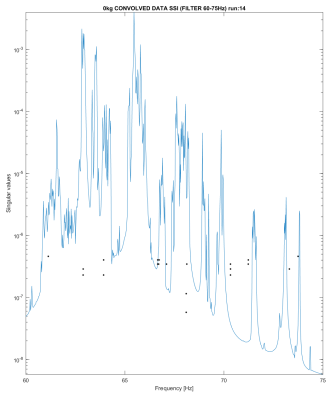
(b) 0kg FDD SSI output, run 13

Figure A4.0kg: Run 13 (segment 1)



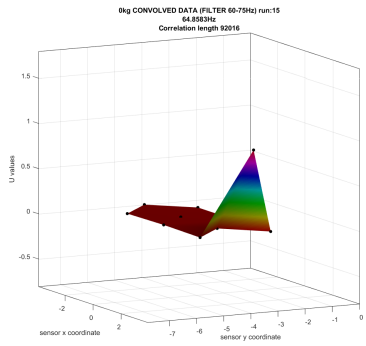
(a) 0kg mode shape, run 14



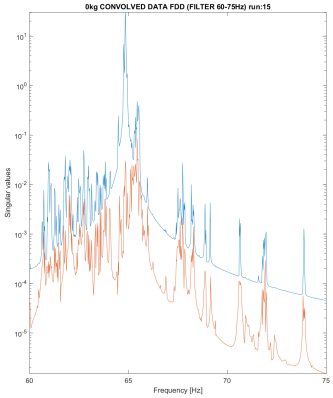


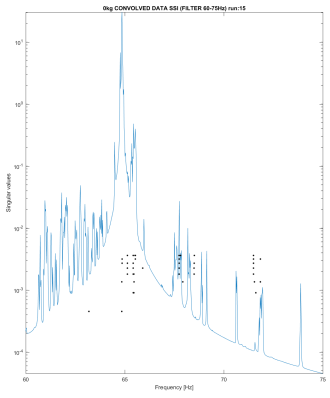
(b) 0kg FDD SSI output, run 14

Figure A4.0kg: Run 14 (segment 1)



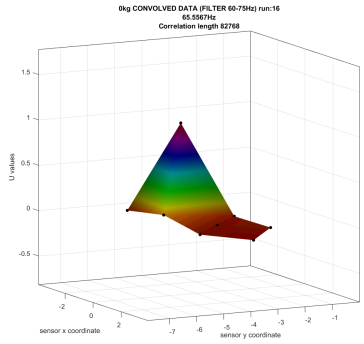
(a) 0kg mode shape, run 15



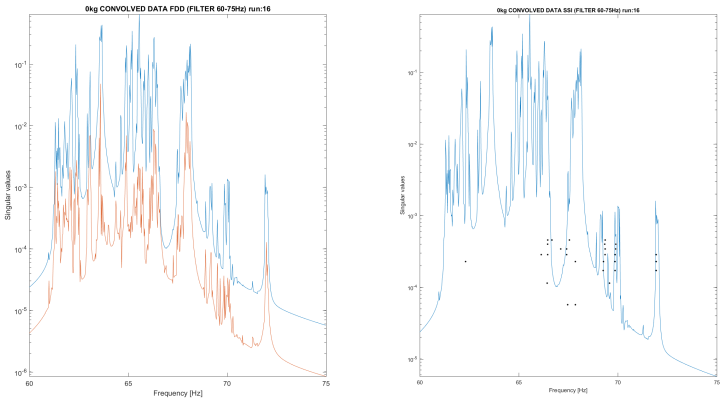


(b) 0kg FDD SSI output, run 15

Figure A4.0kg: Run 15 (segment 1)

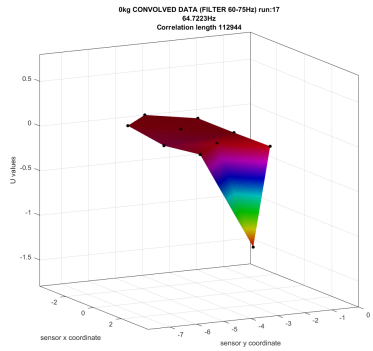


(a) 0kg mode shape, run 16

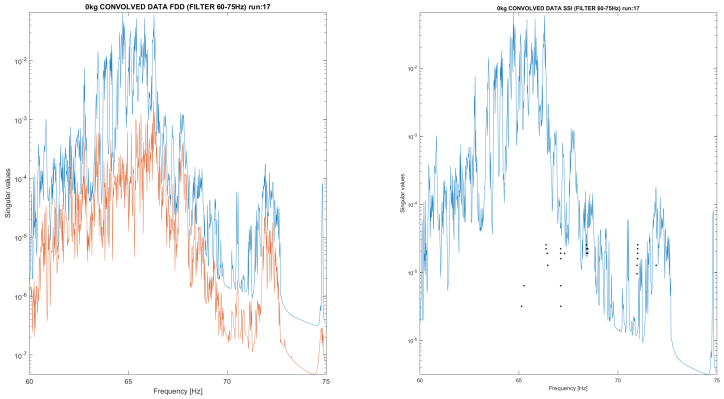


(b) 0kg FDD SSI output, run 16

Figure A4.0kg: Run 16 (segment 1)

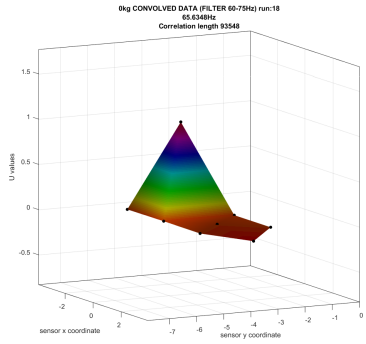


(a) 0kg mode shape, run 17

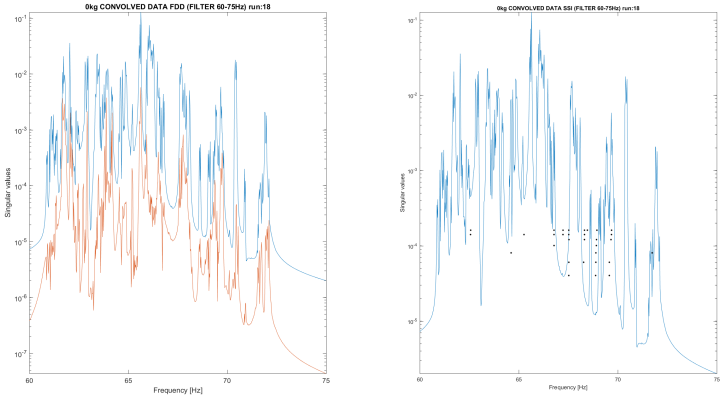


(b) 0kg FDD SSI output, run 17

Figure A4.0kg: Run 17 (segment 1)

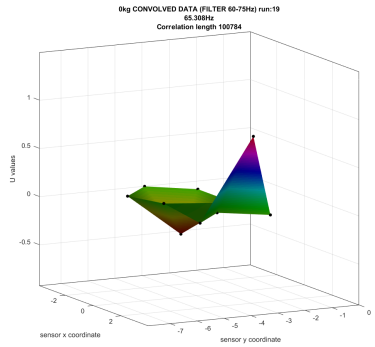


(a) 0kg mode shape, run 18

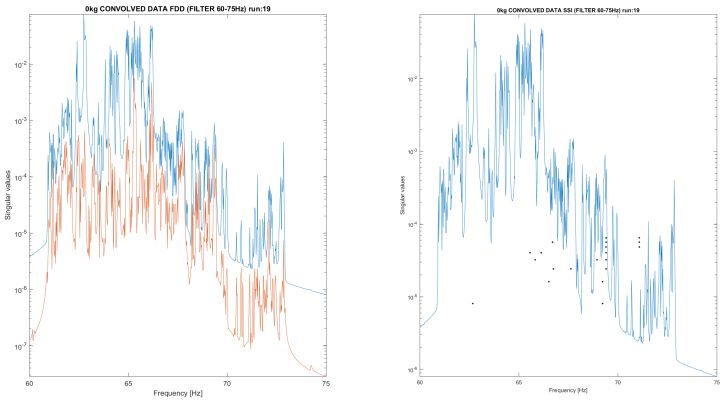


(b) 0kg FDD SSI output, run 18

Figure A4.0kg: Run 18 (segment 1)

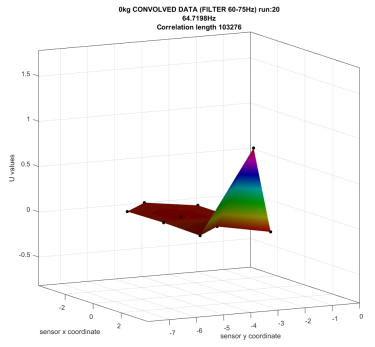


(a) 0kg mode shape, run 19

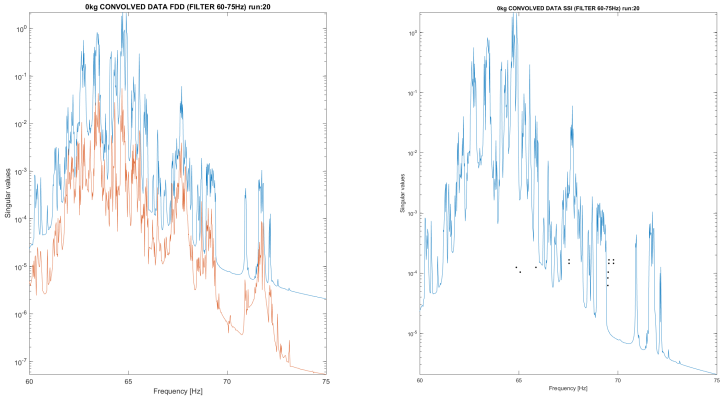


(b) 0kg FDD SSI output, run 19

Figure A4.0kg: Run 19 (segment 1)

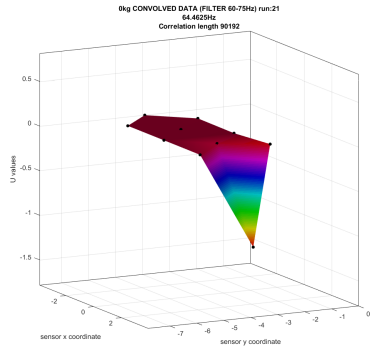


(a) 0kg mode shape, run 20

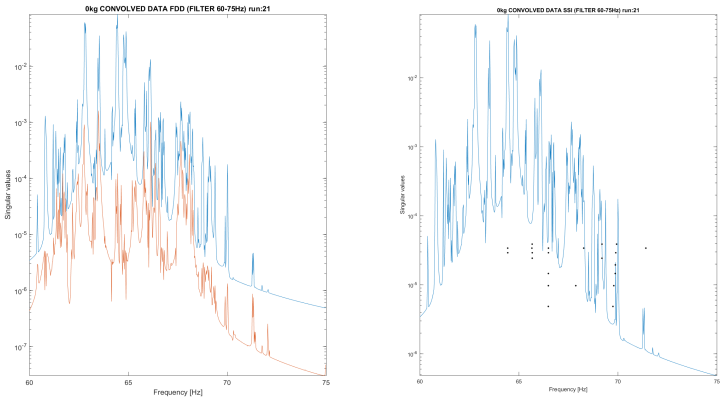


(b) 0kg FDD SSI output, run 21

Figure A4.0kg: Run 20 (segment 1)

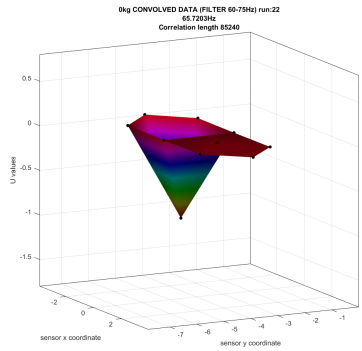


(a) 0kg mode shape, run 21

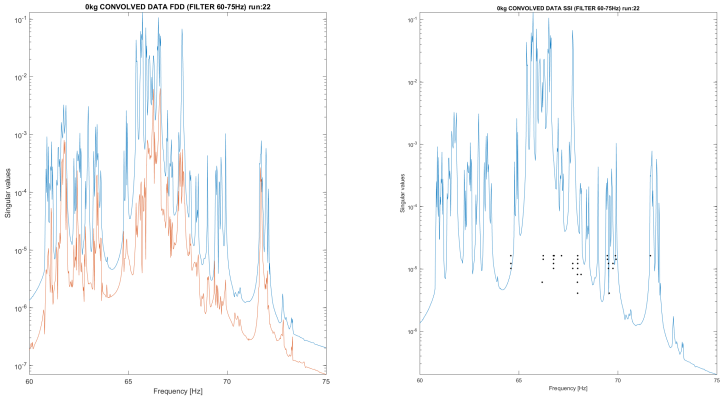


(b) 0kg FDD SSI output, run 21

Figure A4.0kg: Run 21 (segment 1)

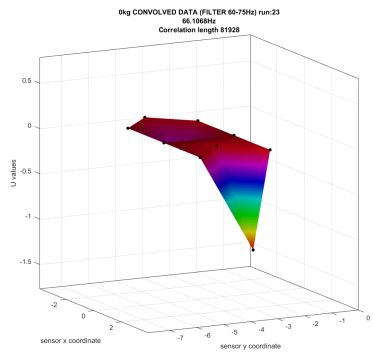


(a) 0kg mode shape, run 22

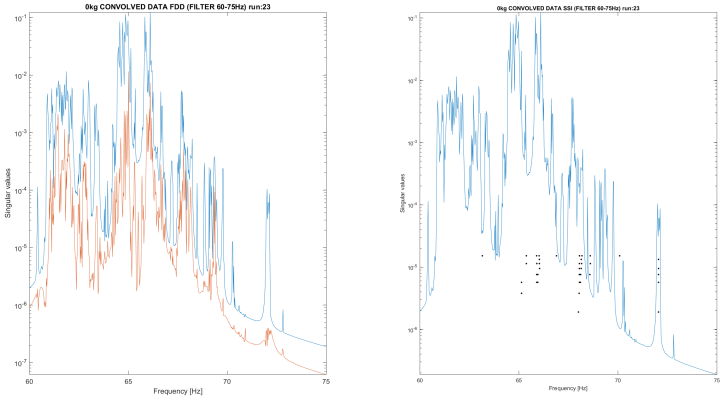


(b) 0kg FDD SSI output, run 22

Figure A4.0kg: Run 22 (segment 1)

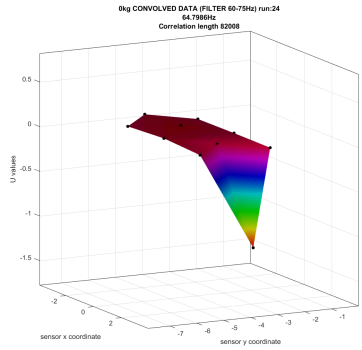


(a) 0kg mode shape, run 23

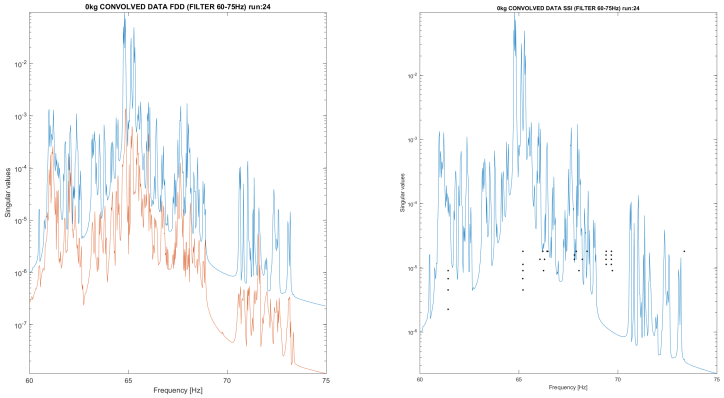


(b) 0kg FDD SSI output, run 23

Figure A4.0kg: Run 23 (segment 1)

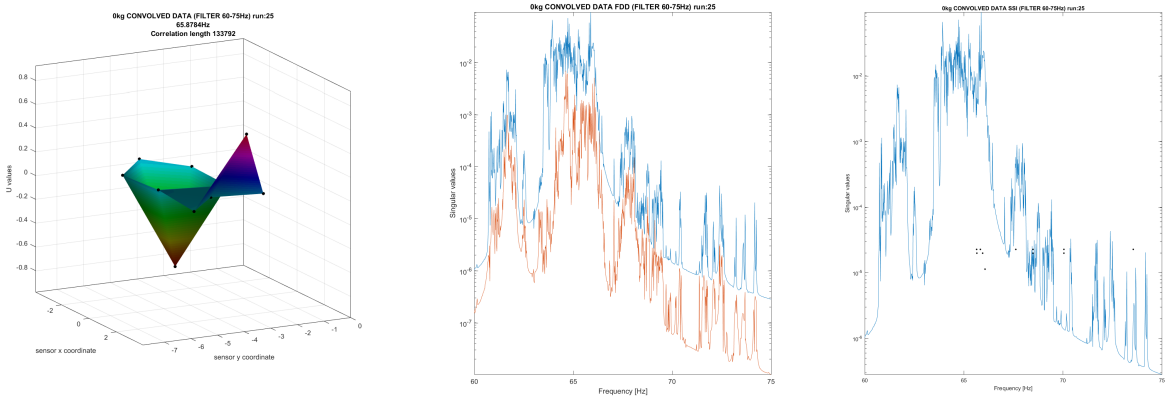


(a) 0kg mode shape, run 24



(b) 0kg FDD SSI output, run 24

Figure A4.0kg: Run 24 (segment 1)

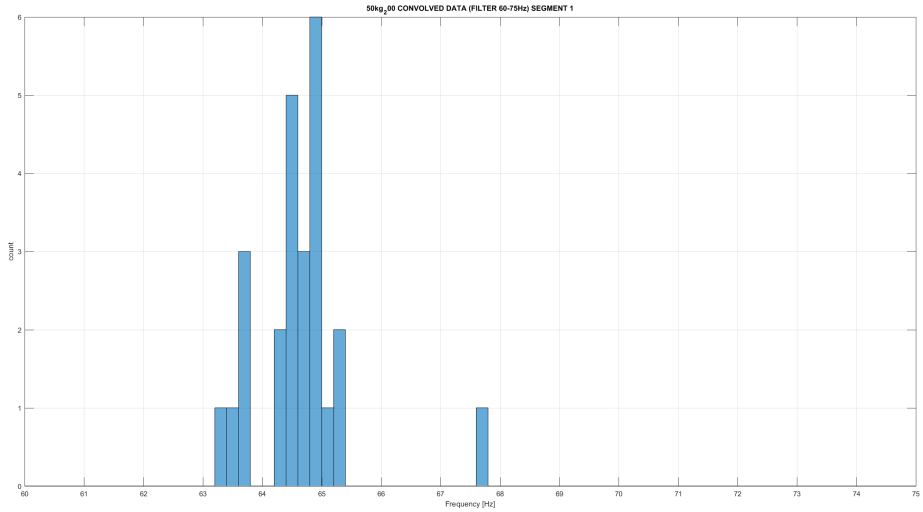


(a) 0kg mode shape, run 25

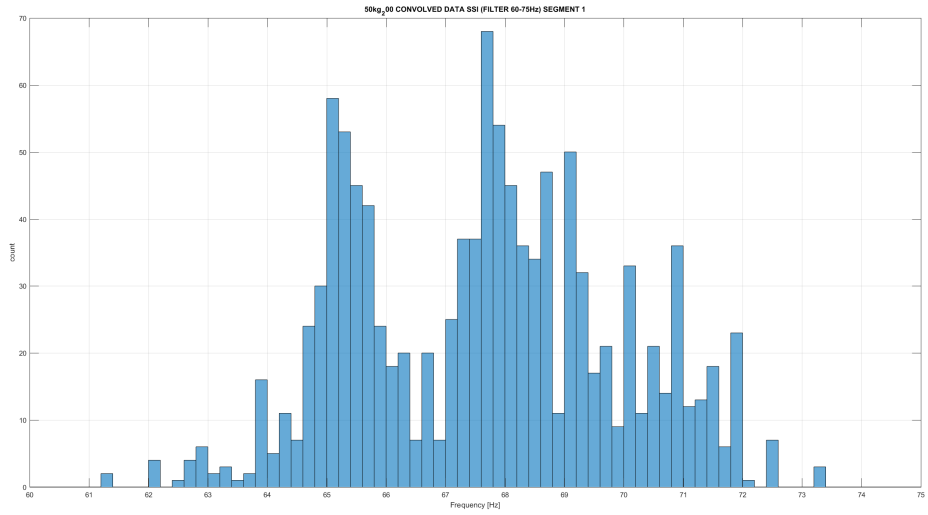
(b) 0kg FDD SSI output, run 25

Figure A4.0kg: Run 25 (segment 1)

50kg data segment 1

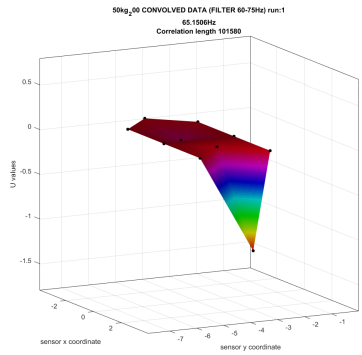


(a) 50kg FDD histogram

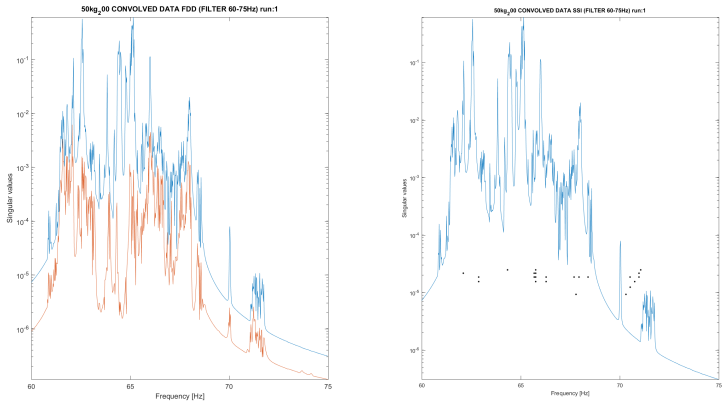


(b) 50kg SSI histogram

Figure A4.50kg: Histograms of identified modes, 50kg data (segment 1)

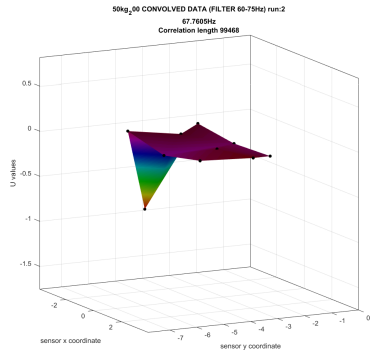


(a) 50kg mode shape, run 1

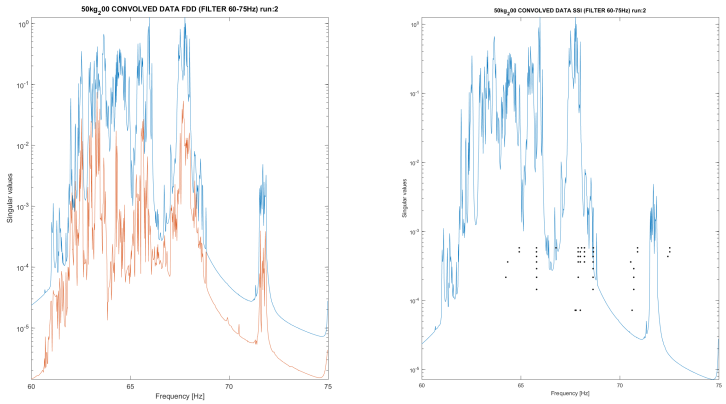


(b) 50kg FDD SSI output, run 1

Figure A4.50kg: Run 1 (segment 1)

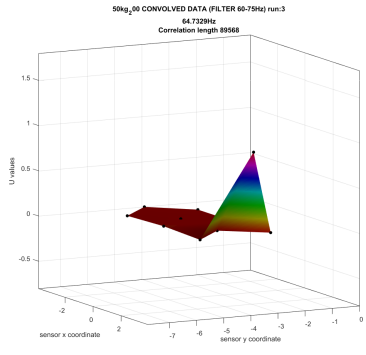


(a) 50kg mode shape, run 2

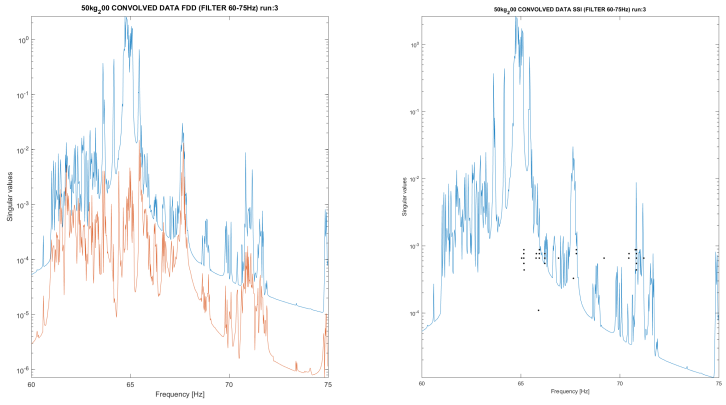


(b) 50kg FDD SSI output, run 2

Figure A4.50kg: Run 2 (segment 1)

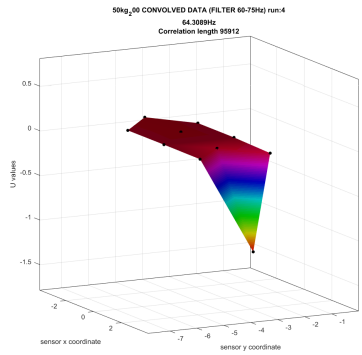


(a) 50kg mode shape, run 3

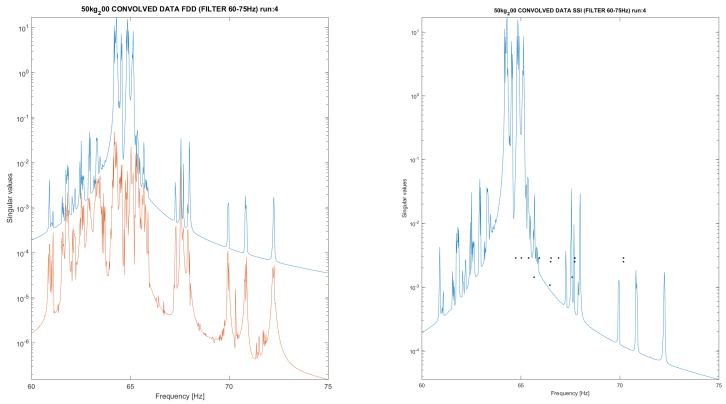


(b) 50kg FDD SSI output, run 3

Figure A4.50kg: Run 3 (segment 1)

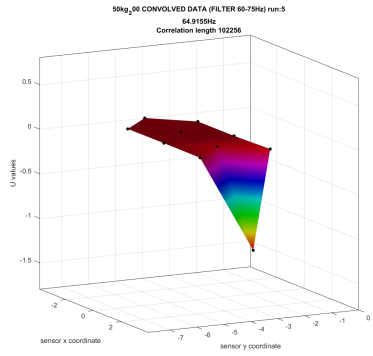


(a) 50kg mode shape, run 4

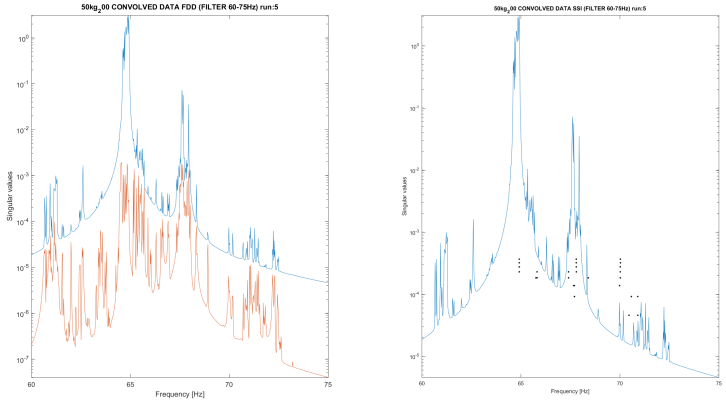


(b) 50kg FDD SSI output, run 4

Figure A4.50kg: Run 4 (segment 1)

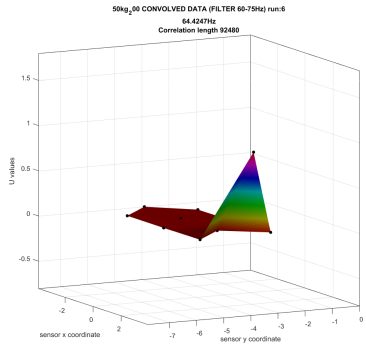


(a) 50kg mode shape, run 5

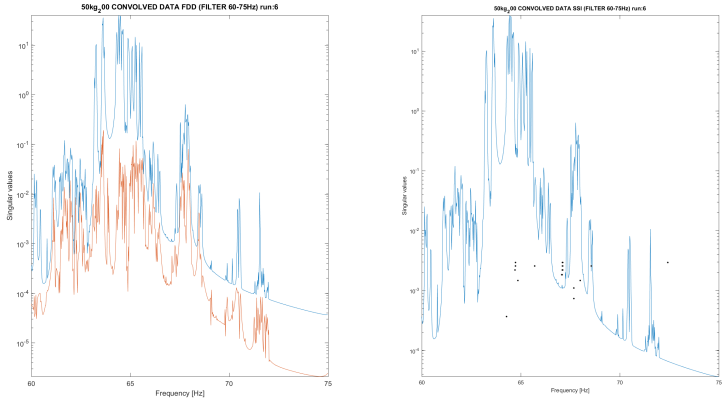


(b) 50kg FDD SSI output, run 5

Figure A4.50kg: Run 5 (segment 1)

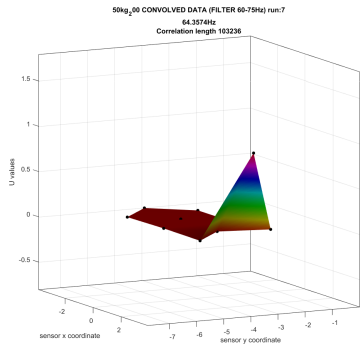


(a) 50kg mode shape, run 6

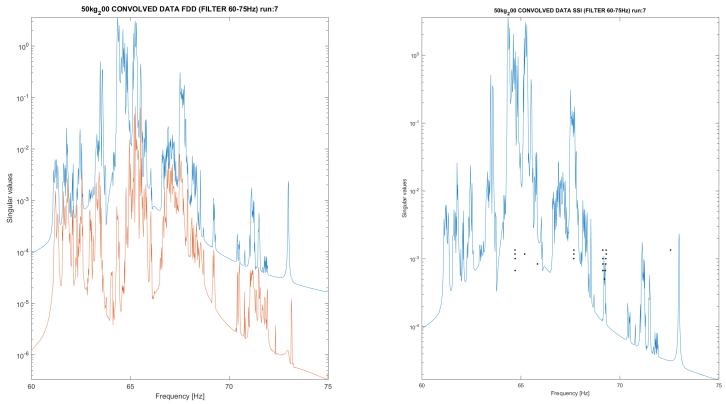


(b) 50kg FDD SSI output, run 6

Figure A4.50kg: Run 6 (segment 1)

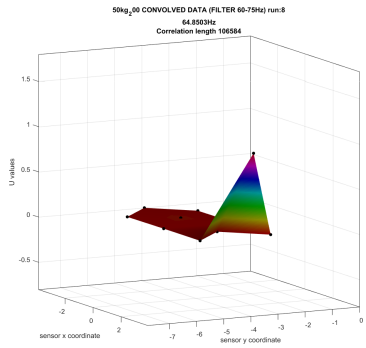


(a) 50kg mode shape, run 7

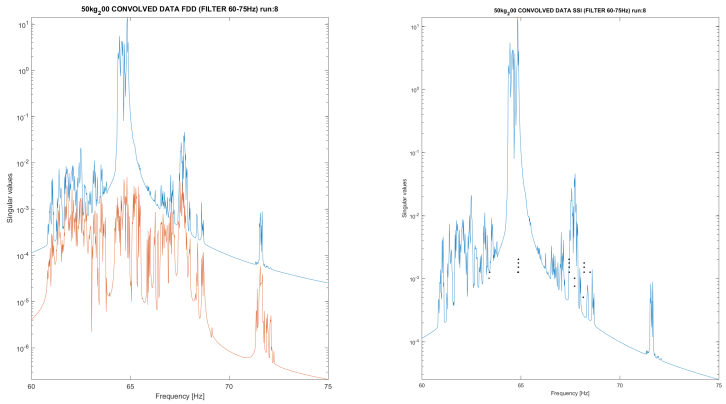


(b) 50kg FDD SSI output, run 7

Figure A4.50kg: Run 7 (segment 1)

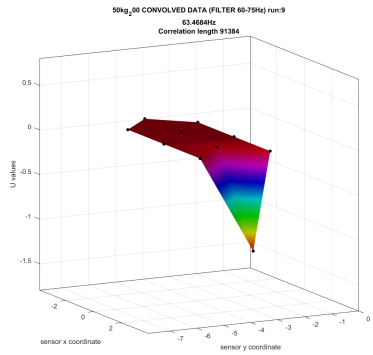


(a) 50kg mode shape, run 8

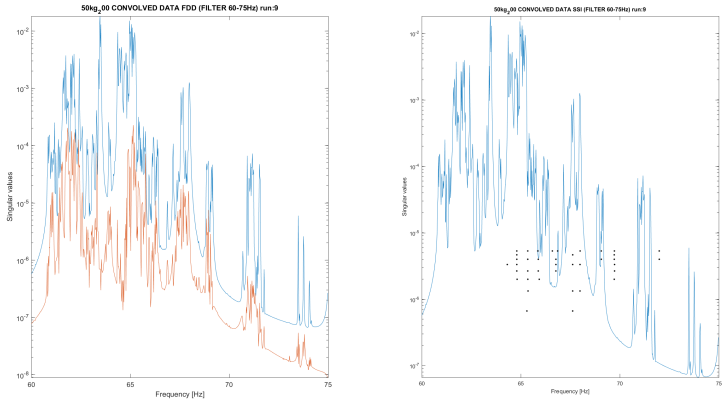


(b) 50kg FDD SSI output, run 8

Figure A4.50kg: Run 8 (segment 1)

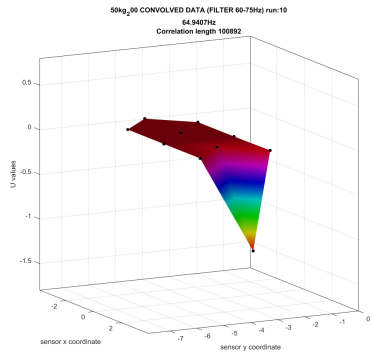


(a) 50kg mode shape, run 9

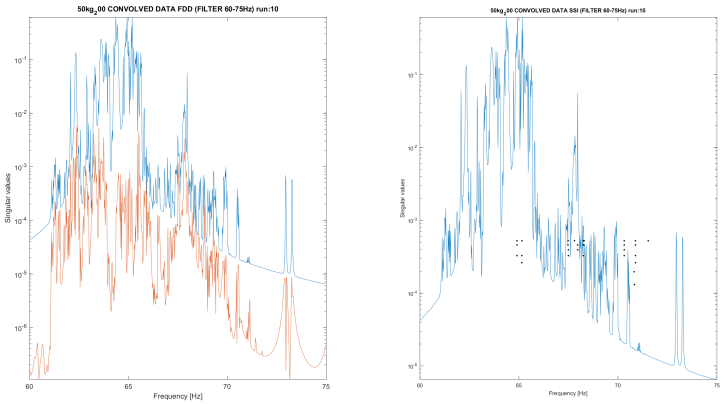


(b) 50kg FDD SSI output, run 9

Figure A4.50kg: Run 9 (segment 1)

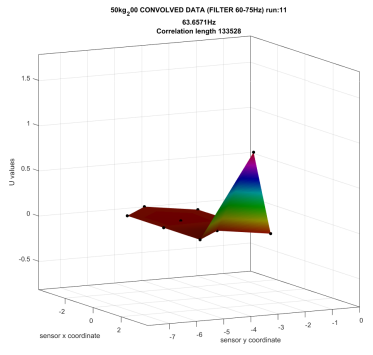


(a) 50kg mode shape, run 10

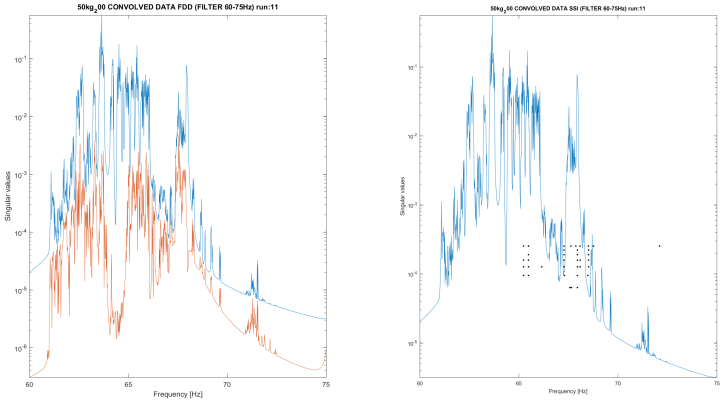


(b) 50kg FDD SSI output, run 10

Figure A4.50kg: Run 10 (segment 1)

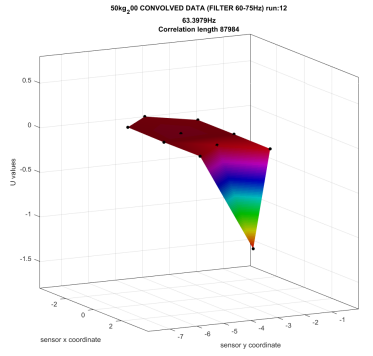


(a) 50kg mode shape, run 11

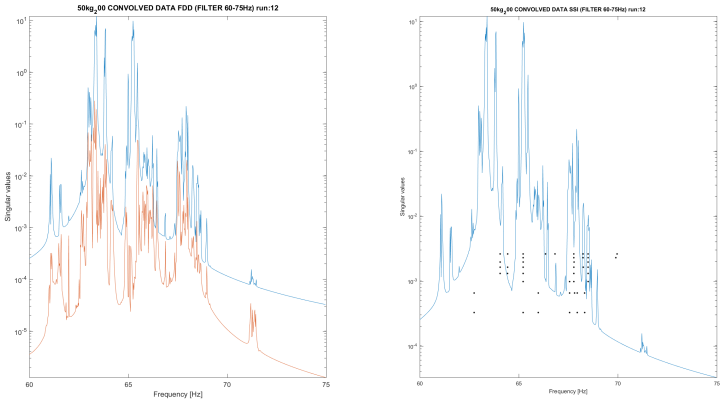


(b) 50kg FDD SSI output, run 11

Figure A4.50kg: Run 11 (segment 1)

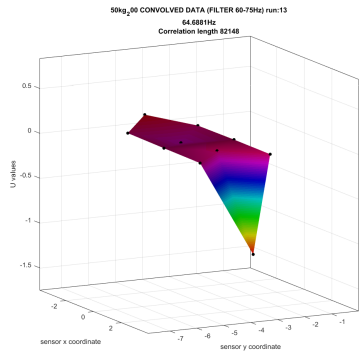


(a) 50kg mode shape, run 12

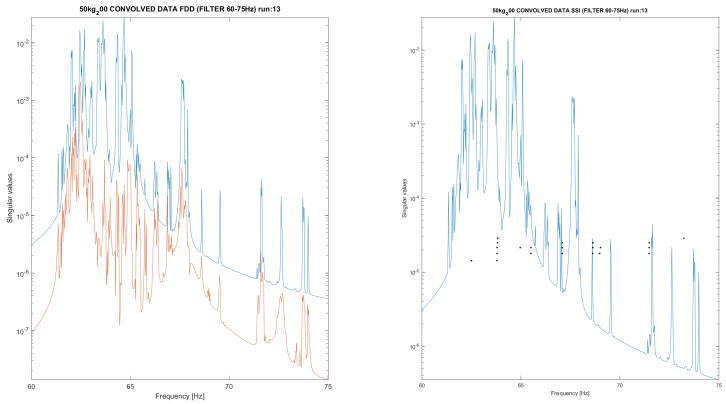


(b) 50kg FDD SSI output, run 12

Figure A4.50kg: Run 12 (segment 1)

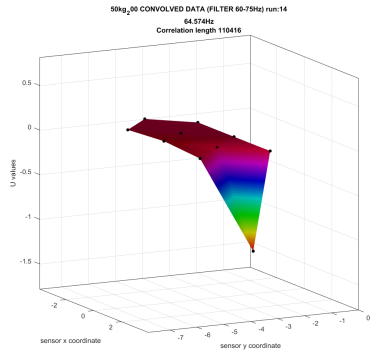


(a) 50kg mode shape, run 13

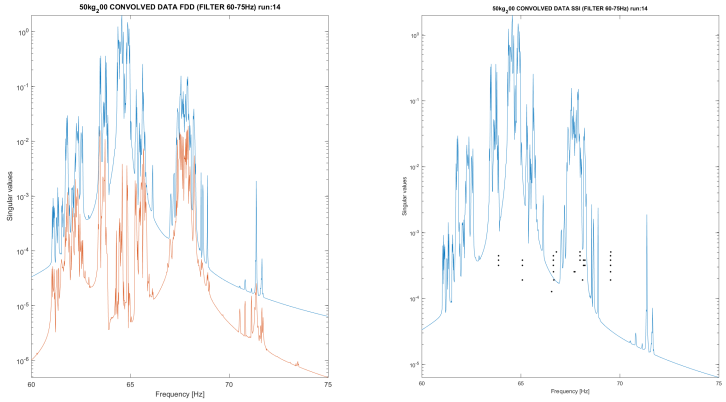


(b) 50kg FDD SSI output, run 13

Figure A4.50kg: Run 13 (segment 1)

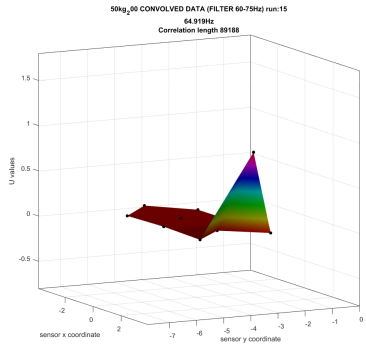


(a) 50kg mode shape, run 14

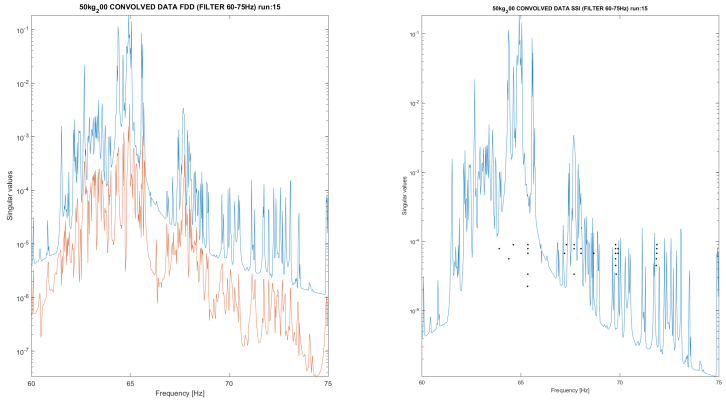


(b) 50kg FDD SSI output, run 14

Figure A4.50kg: Run 14 (segment 1)

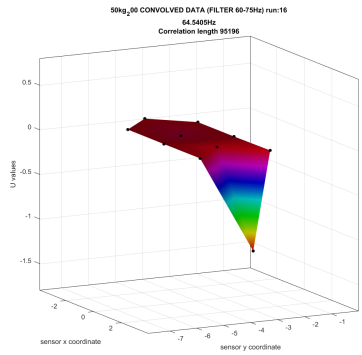


(a) 50kg mode shape, run 15

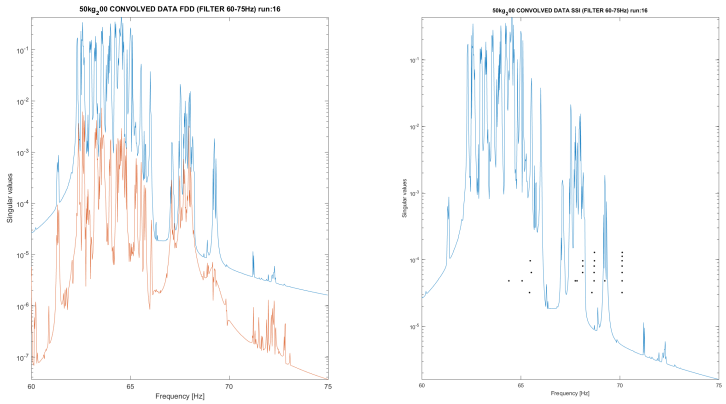


(b) 50kg FDD SSI output, run 15

Figure A4.50kg: Run 15 (segment 1)

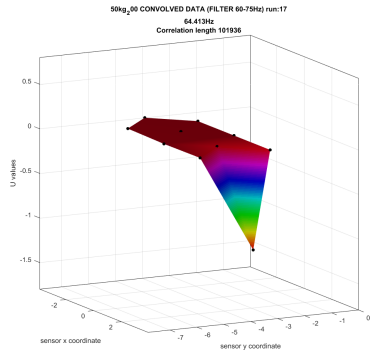


(a) 50kg mode shape, run 16

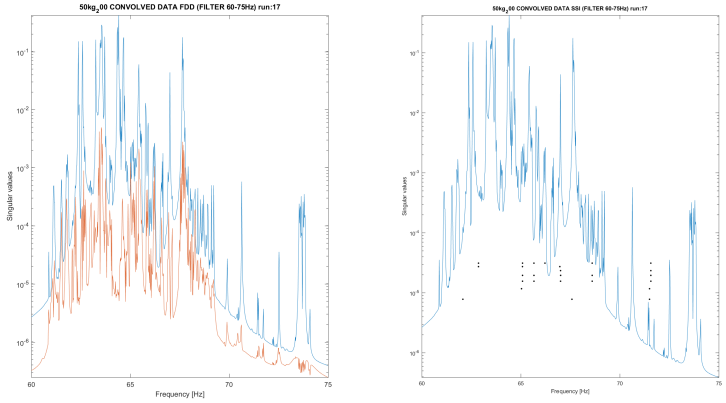


(b) 50kg FDD SSI output, run 16

Figure A4.50kg: Run 16 (segment 1)

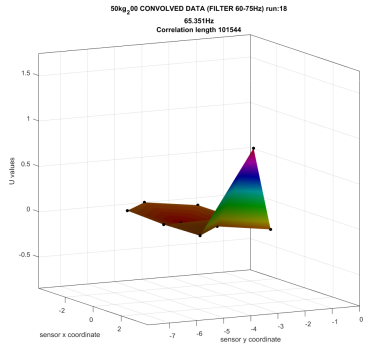


(a) 50kg mode shape, run 17

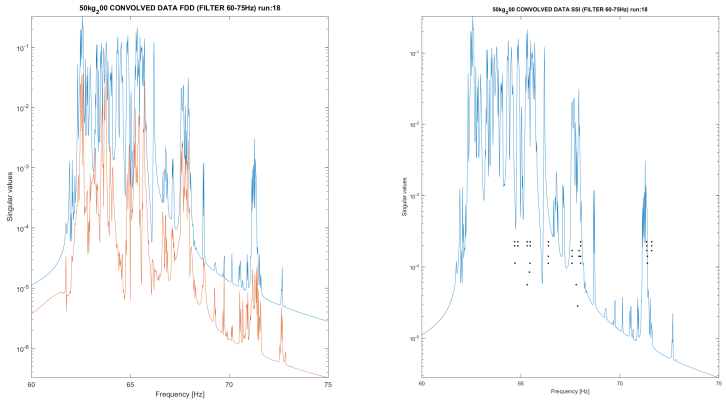


(b) 50kg FDD SSI output, run 17

Figure A4.50kg: Run 17 (segment 1)

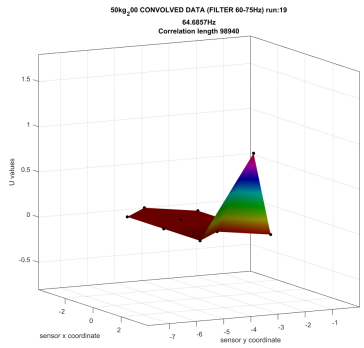


(a) 50kg mode shape, run 18

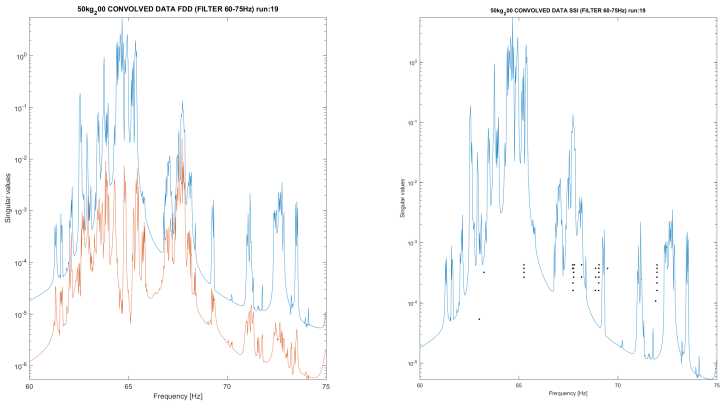


(b) 50kg FDD SSI output, run 18

Figure A4.50kg: Run 18 (segment 1)

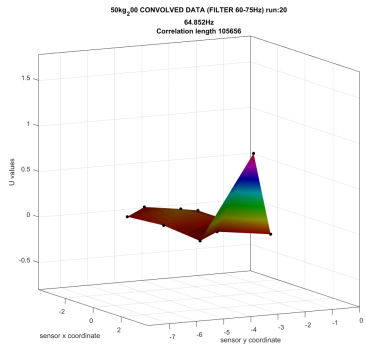


(a) 50kg mode shape, run 19

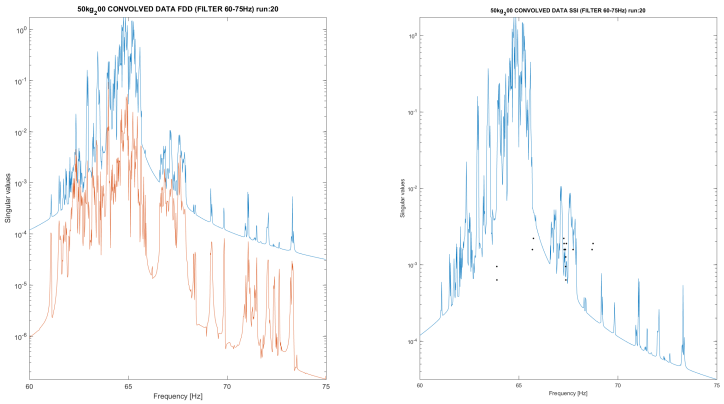


(b) 50kg FDD SSI output, run 19

Figure A4.50kg: Run 19 (segment 1)

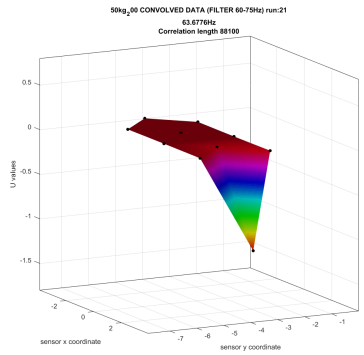


(a) 50kg mode shape, run 20

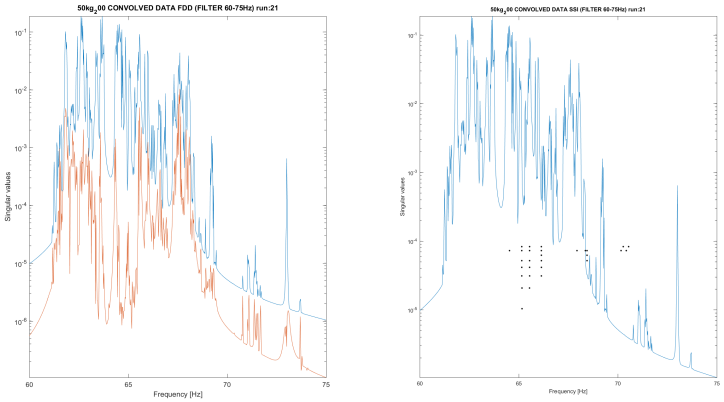


(b) 50kg FDD SSI output, run 20

Figure A4.50kg: Run 20 (segment 1)

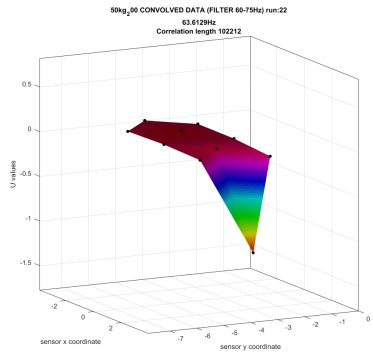


(a) 50kg mode shape, run 21

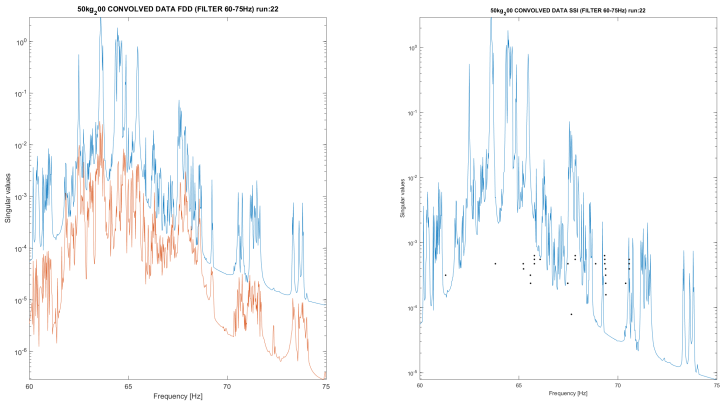


(b) 50kg FDD SSI output, run 21

Figure A4.50kg: Run 21 (segment 1)

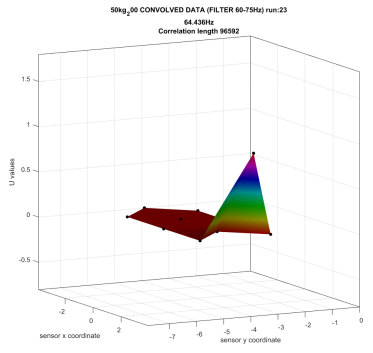


(a) 50kg mode shape, run 22

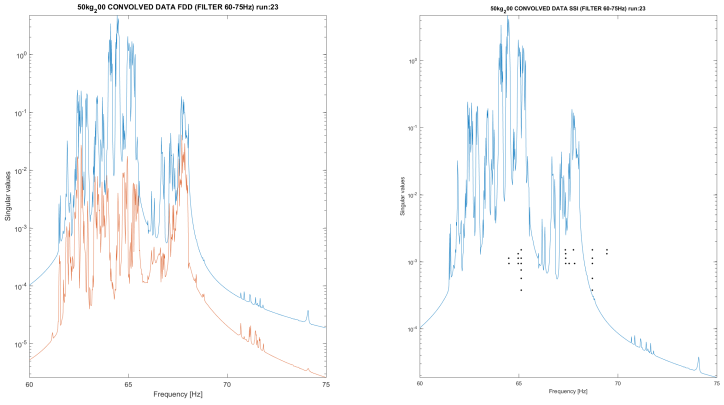


(b) 50kg FDD SSI output, run 22

Figure A4.50kg: Run 22 (segment 1)

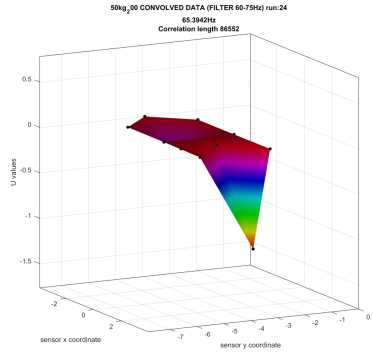


(a) 50kg mode shape, run 23

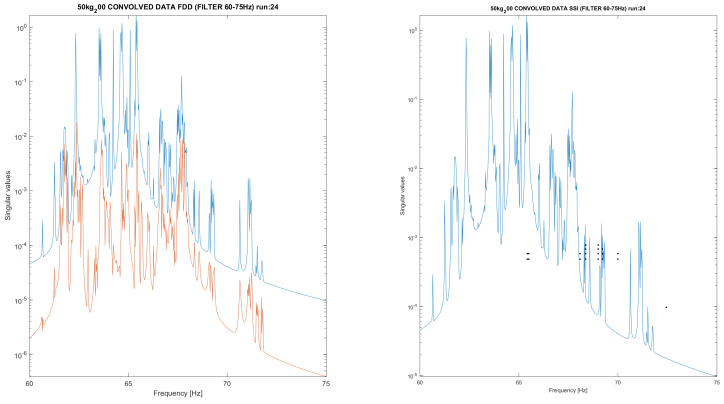


(b) 50kg FDD SSI output, run 23

Figure A4.50kg: Run 23 (segment 1)

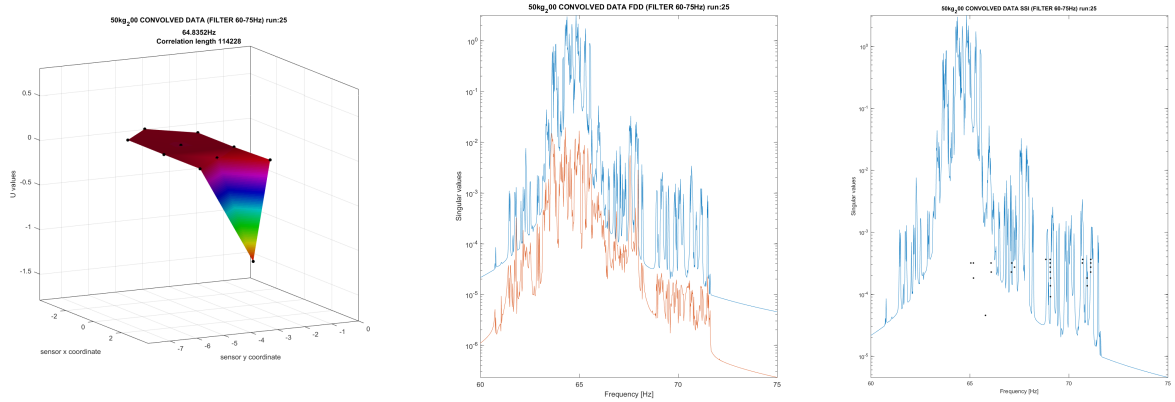


(a) 50kg mode shape, run 24



(b) 50kg FDD SSI output, run 24

Figure A4.50kg: Run 24 (segment 1)

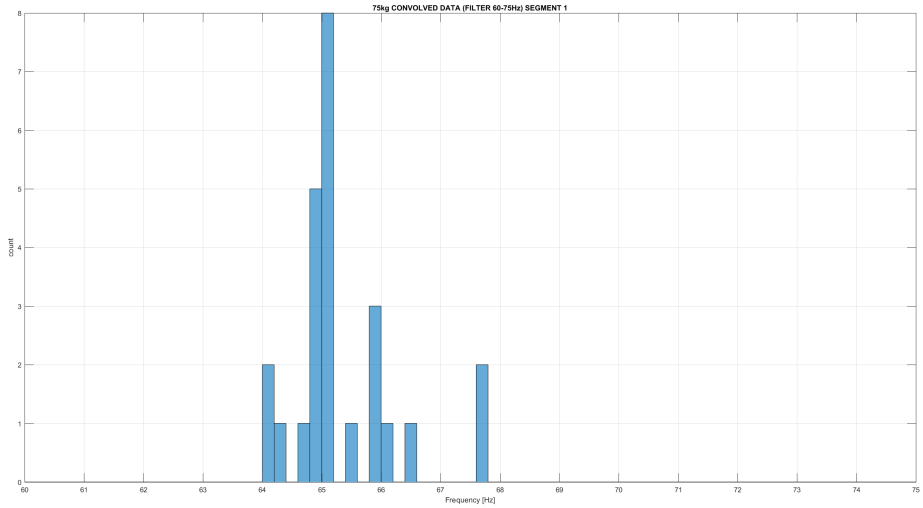


(a) 50kg mode shape, run 25

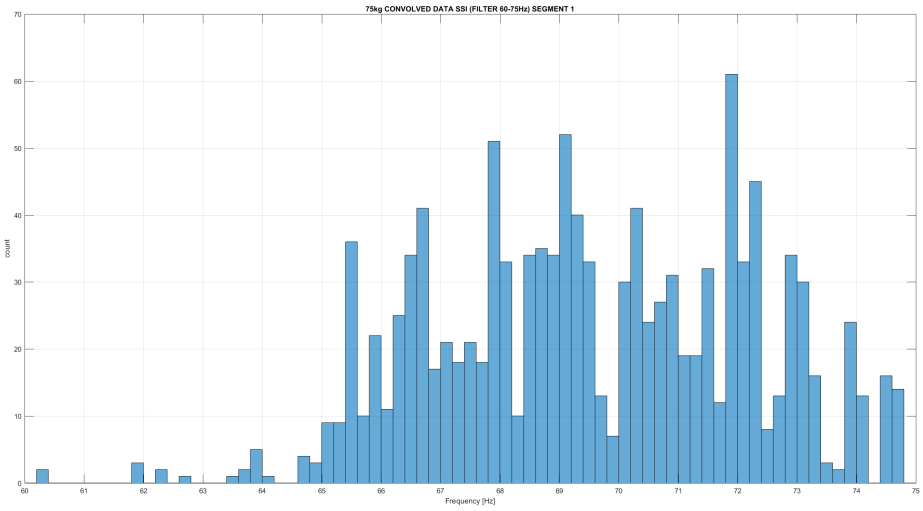
(b) 50kg FDD SSI output, run 25

Figure A4.50kg: Run 25 (segment 1)

75kg data segment 1

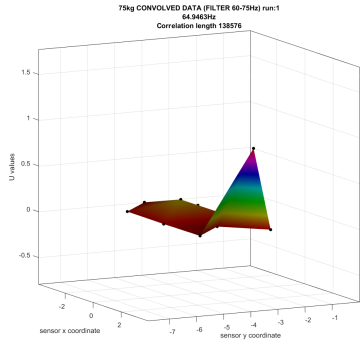


(a) 75kg FDD histogram

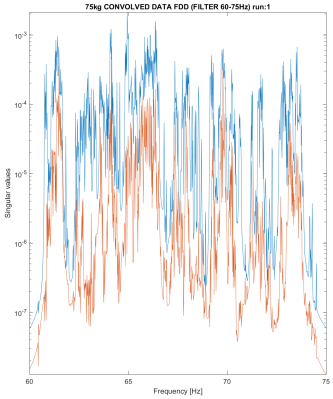


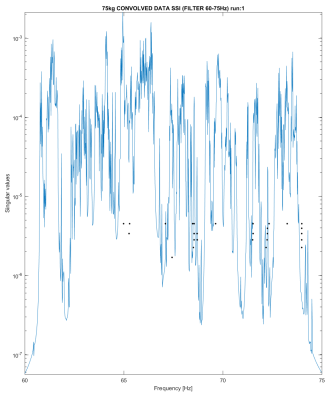
(b) 75kg SSI histogram

Figure A4.75kg: Histograms of identified modes, 75kg data (segment 1)



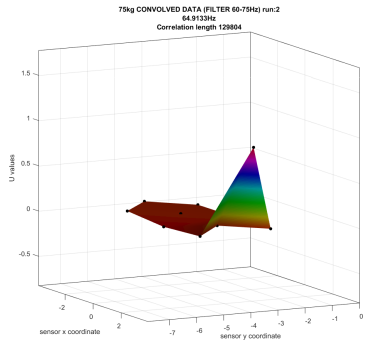
(a) 75kg mode shape, run 1



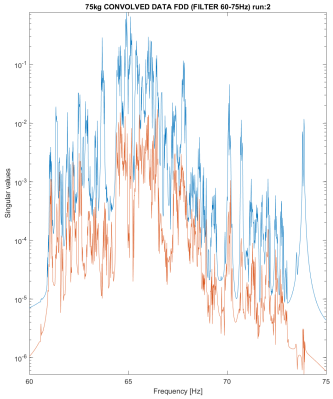


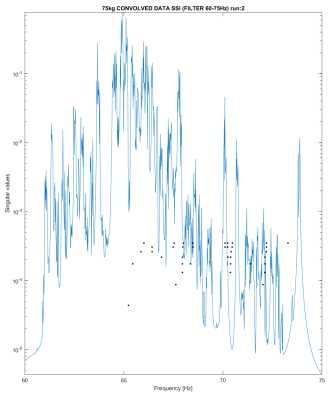
(b) 75kg FDD SSI output, run 1

Figure A4.75kg: Run 1 (segment 1)



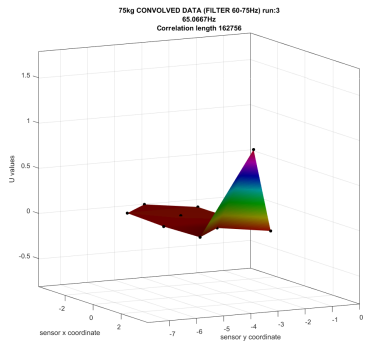
(a) 75kg mode shape, run 2



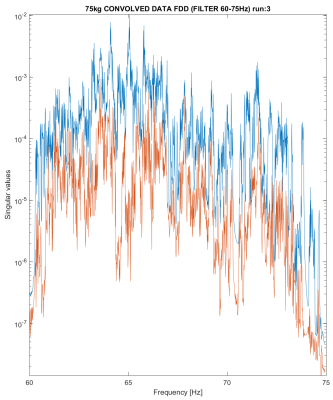


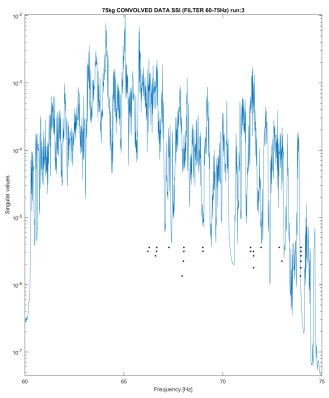
(b) 75kg FDD SSI output, run 2

Figure A4.75kg: Run 2 (segment 1)



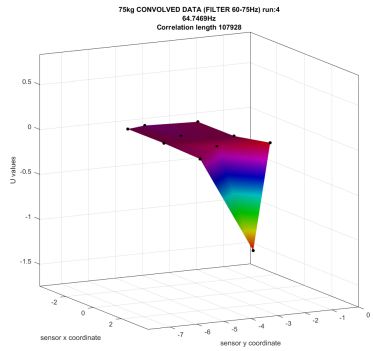
(a) 75kg mode shape, run 3



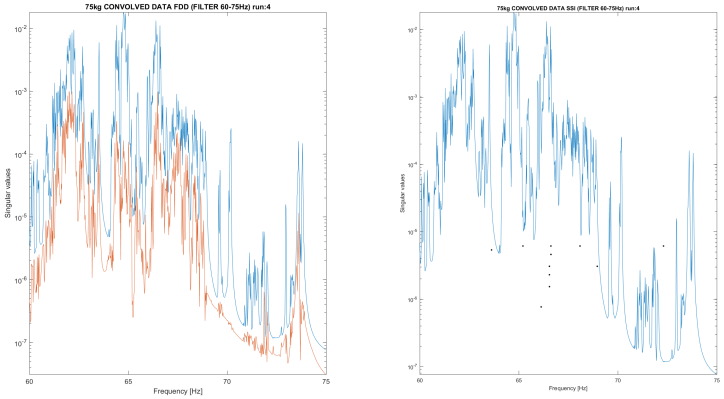


(b) 75kg FDD SSI output, run 3

Figure A4.75kg: Run 3 (segment 1)

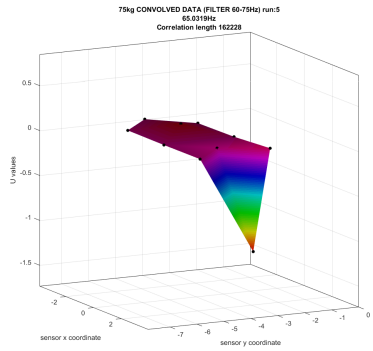


(a) 75kg mode shape, run 4

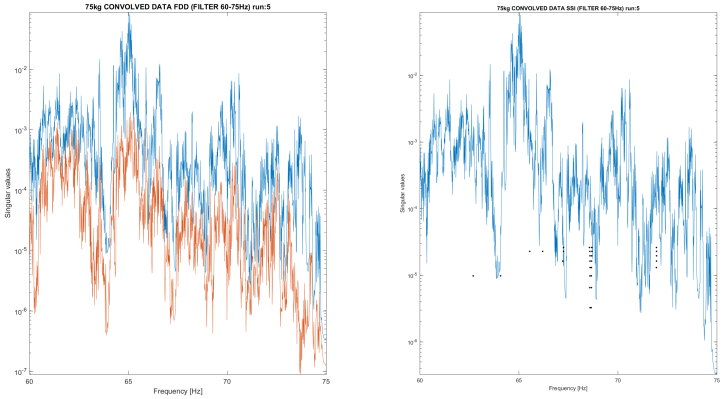


(b) 75kg FDD SSI output, run 4

Figure A4.75kg: Run 4 (segment 1)

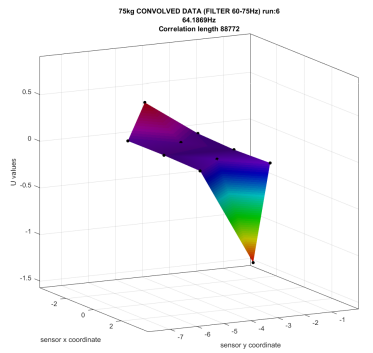


(a) 75kg mode shape, run 5

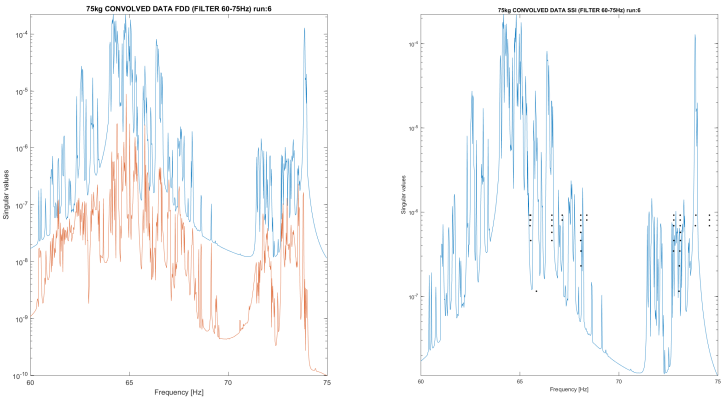


(b) 75kg FDD SSI output, run 5

Figure A4.75kg: Run 5 (segment 1)

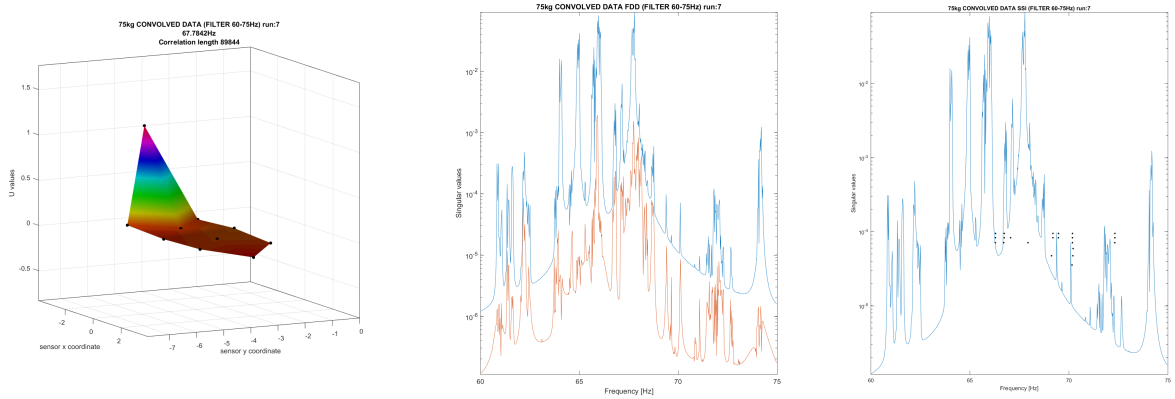


(a) 75kg mode shape, run 6



(b) 75kg FDD SSI output, run 6

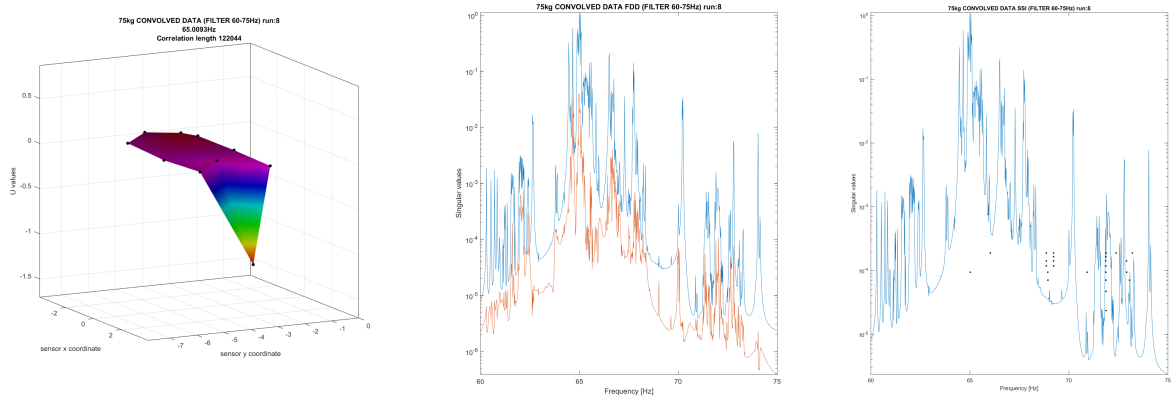
Figure A4.75kg: Run 6 (segment 1)



(a) 75kg mode shape, run 7

(b) 75kg FDD SSI output, run 7

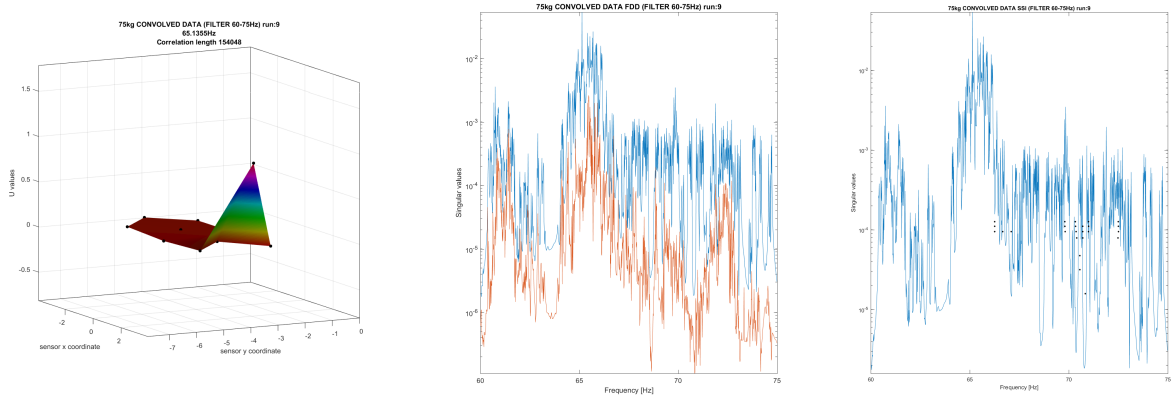
Figure A4.75kg: Run 7 (segment 1)



(a) 75kg mode shape, run 8

(b) 75kg FDD SSI output, run 8

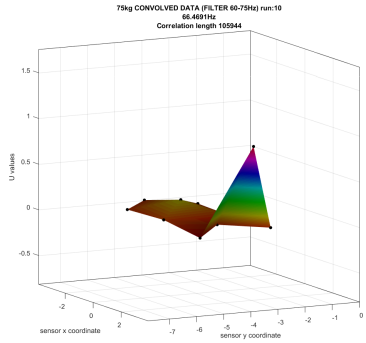
Figure A4.75kg: Run 8 (segment 1)

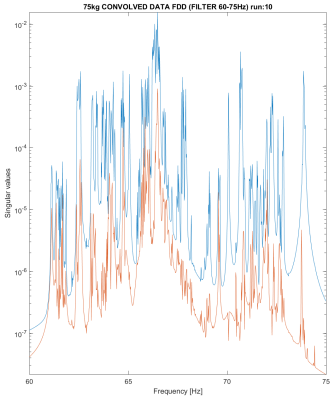


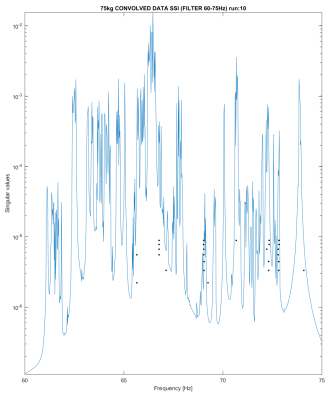
(a) 75kg mode shape, run 9

(b) 75kg FDD SSI output, run 9

Figure A4.75kg: Run 9 (segment 1)



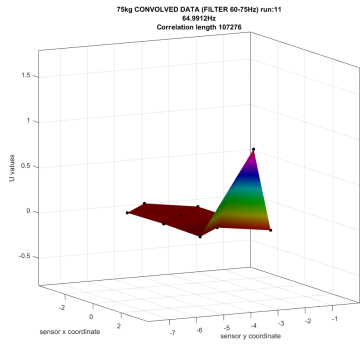


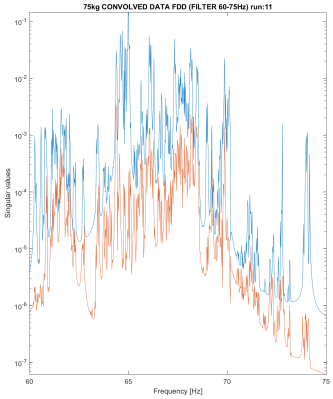


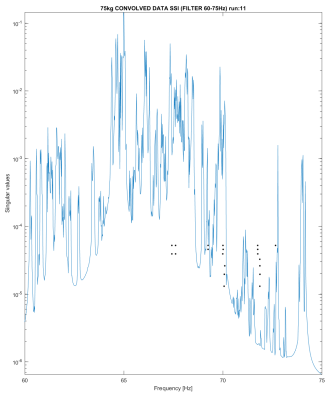
(a) 75kg mode shape, run 10

(b) 75kg FDD SSI output, run 10

Figure A4.75kg: Run 10 (segment 1)



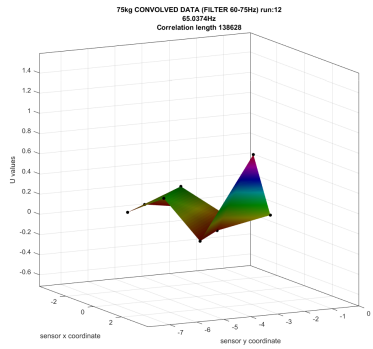


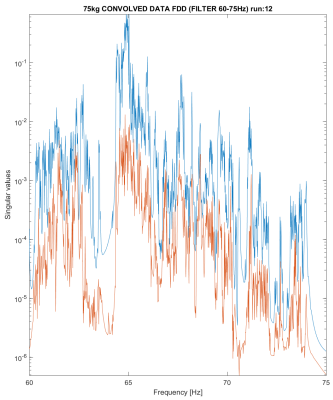


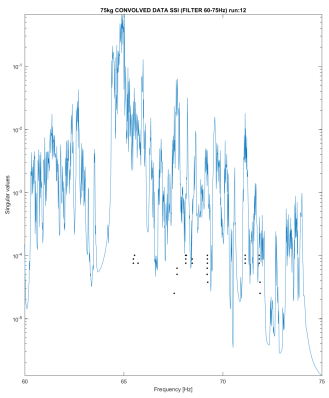
(a) 75kg mode shape, run 11

(b) 75kg FDD SSI output, run 11

Figure A4.75kg: Run 11 (segment 1)



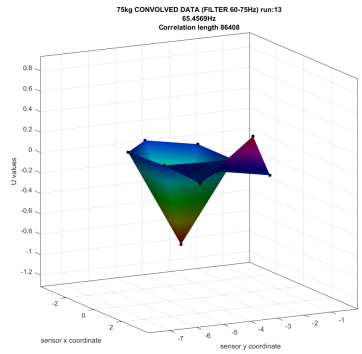




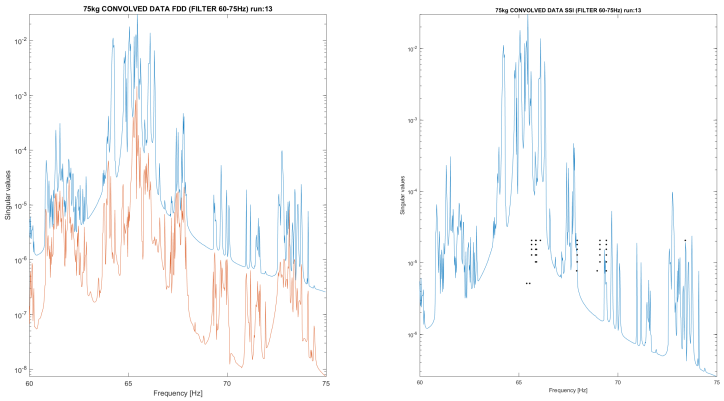
(a) 75kg mode shape, run 12

(b) 75kg FDD SSI output, run 12

Figure A4.75kg: Run 12 (segment 1)

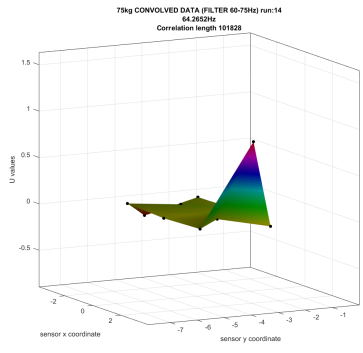


(a) 75kg mode shape, run 13

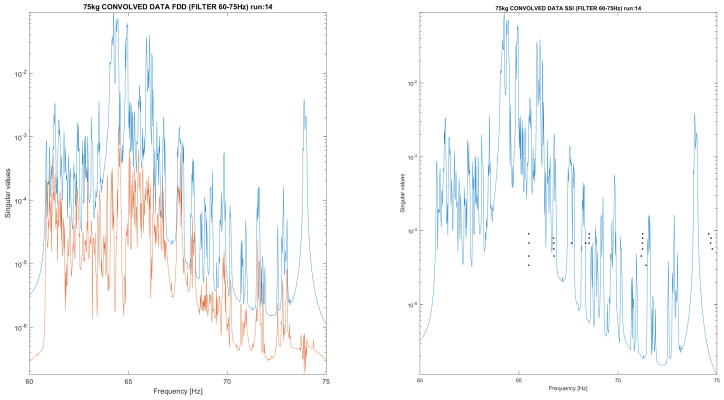


(b) 75kg FDD SSI output, run 13

Figure A4.75kg: Run 13 (segment 1)

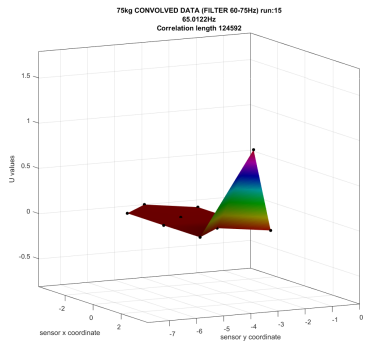


(a) 75kg mode shape, run 14

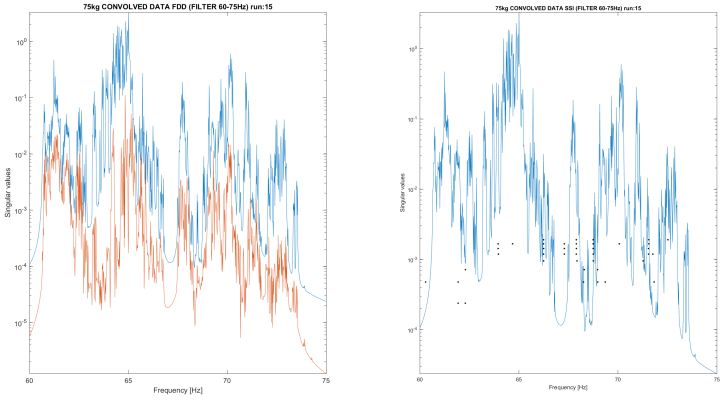


(b) 75kg FDD SSI output, run 14

Figure A4.75kg: Run 14 (segment 1)

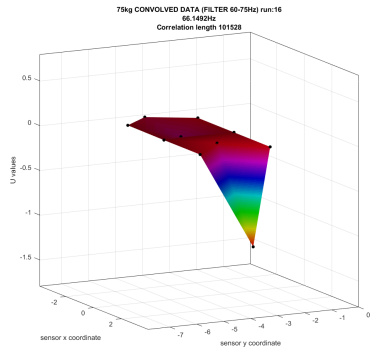


(a) 75kg mode shape, run 15

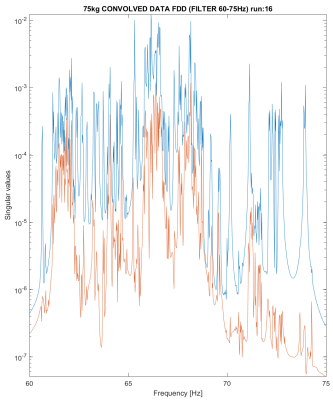


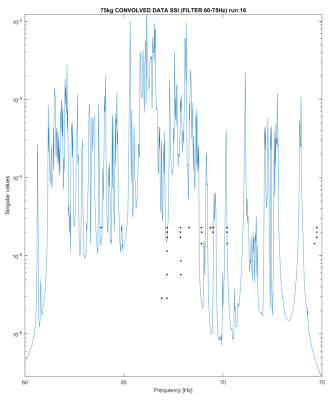
(b) 75kg FDD SSI output, run 15

Figure A4.75kg: Run 15 (segment 1)



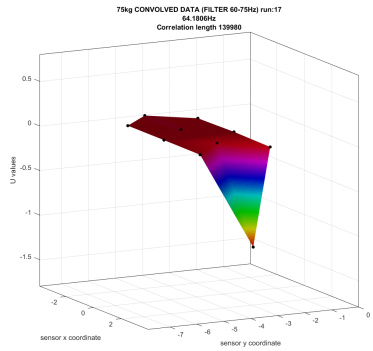
(a) 75kg mode shape, run 16



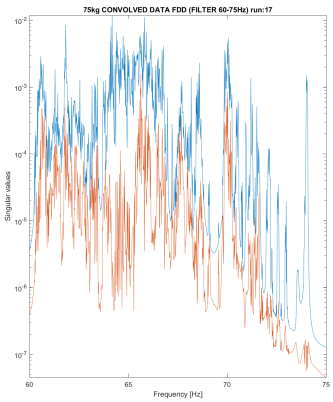


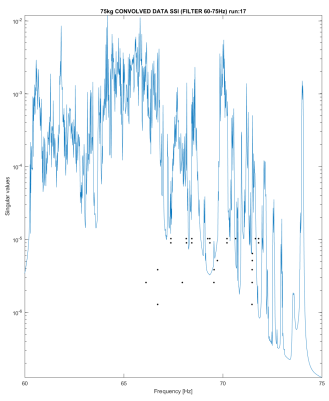
(b) 75kg FDD SSI output, run 16

Figure A4.75kg: Run 16 (segment 1)



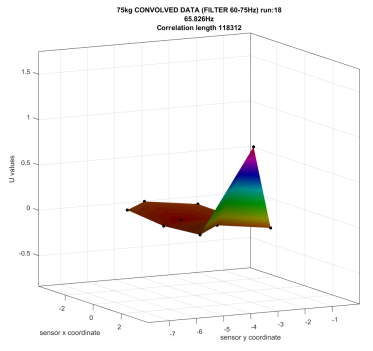
(a) 75kg mode shape, run 17



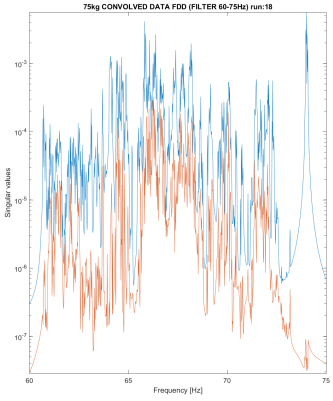


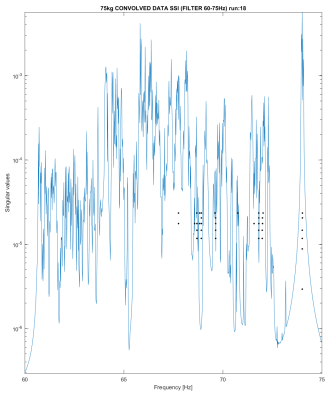
(b) 75kg FDD SSI output, run 17

Figure A4.75kg: Run 17 (segment 1)



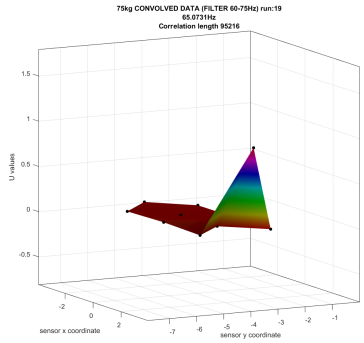
(a) 75kg mode shape, run 18

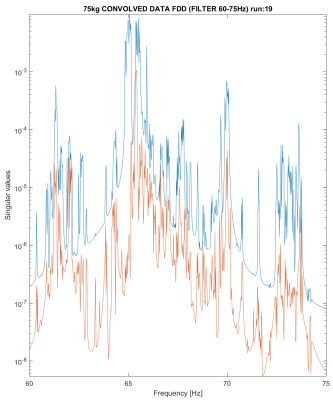


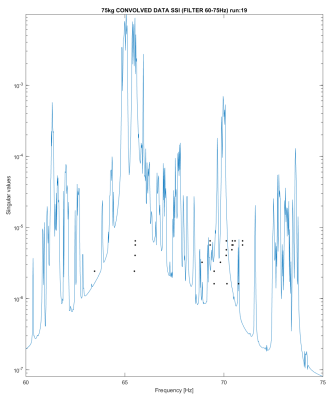


(b) 75kg FDD SSI output, run 18

Figure A4.75kg: Run 18 (segment 1)



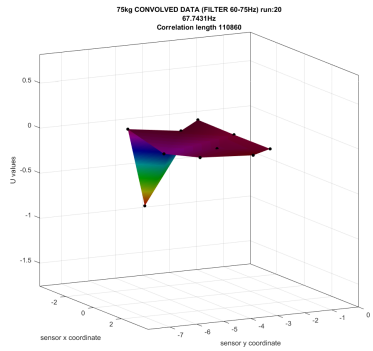


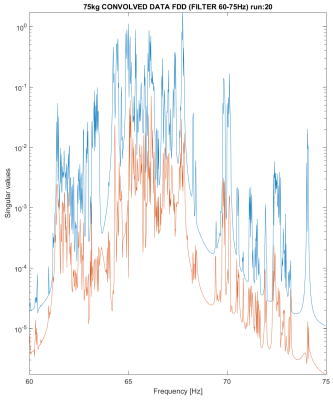


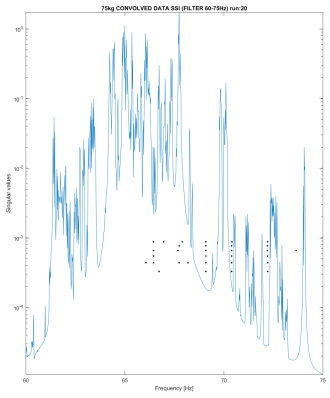
(a) 75kg mode shape, run 19

(b) 75kg FDD SSI output, run 19

Figure A4.75kg: Run 19 (segment 1)



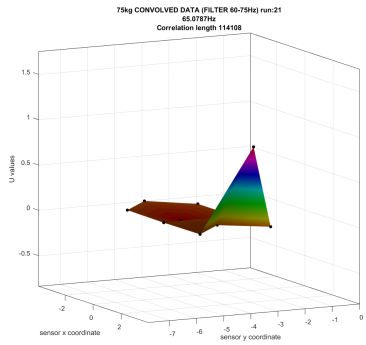


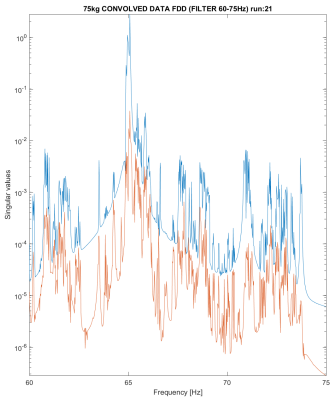


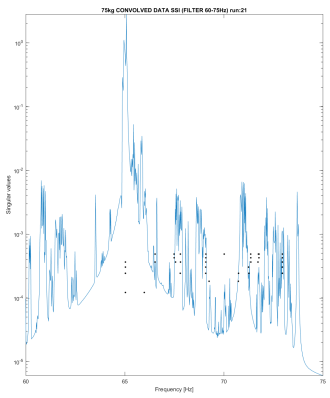
(a) 75kg mode shape, run 20

(b) 75kg FDD SSI output, run 20

Figure A4.75kg: Run 20 (segment 1)



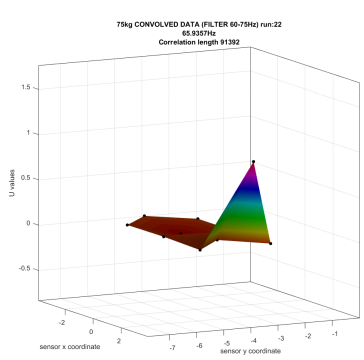




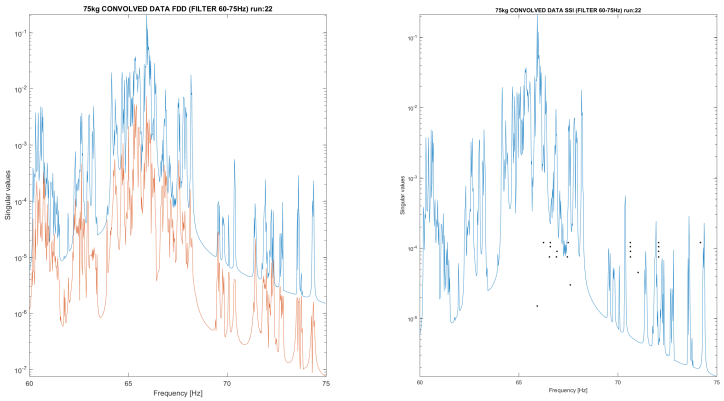
(a) 75kg mode shape, run 21

(b) 75kg FDD SSI output, run 21

Figure A4.75kg: Run 21 (segment 1)

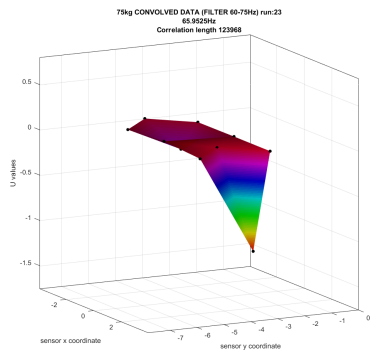


(a) 75kg mode shape, run 22

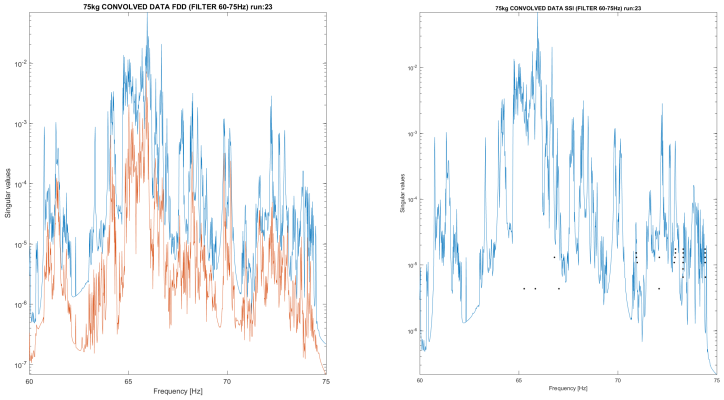


(b) 75kg FDD SSI output, run 22

Figure A4.75kg: Run 22 (segment 1)

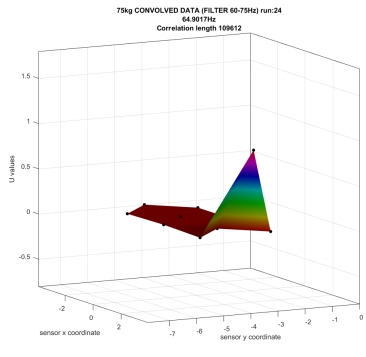


(a) 75kg mode shape, run 23

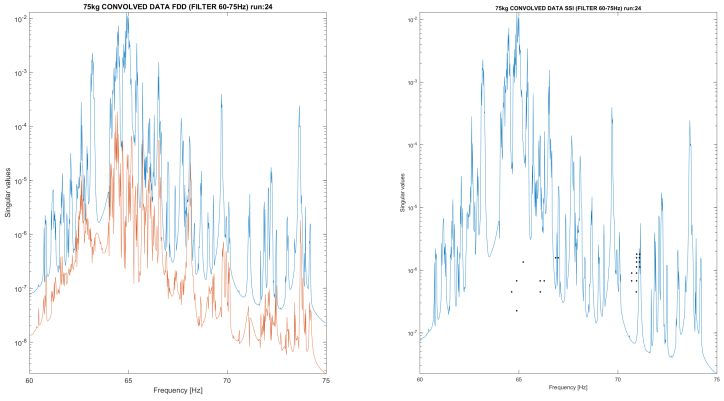


(b) 75kg FDD SSI output, run 23

Figure A4.75kg: Run 23 (segment 1)

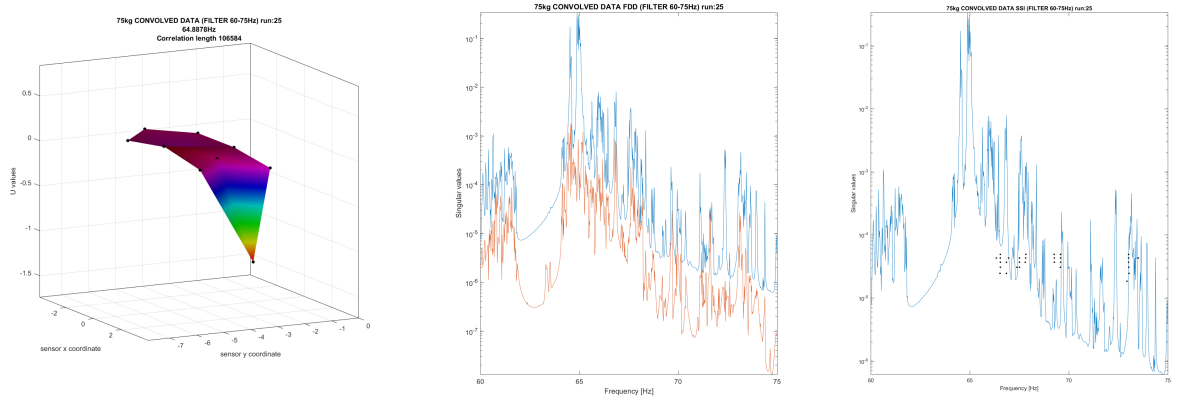


(a) 75kg mode shape, run 24



(b) 75kg FDD SSI output, run 24

Figure A4.75kg: Run 24 (segment 1)

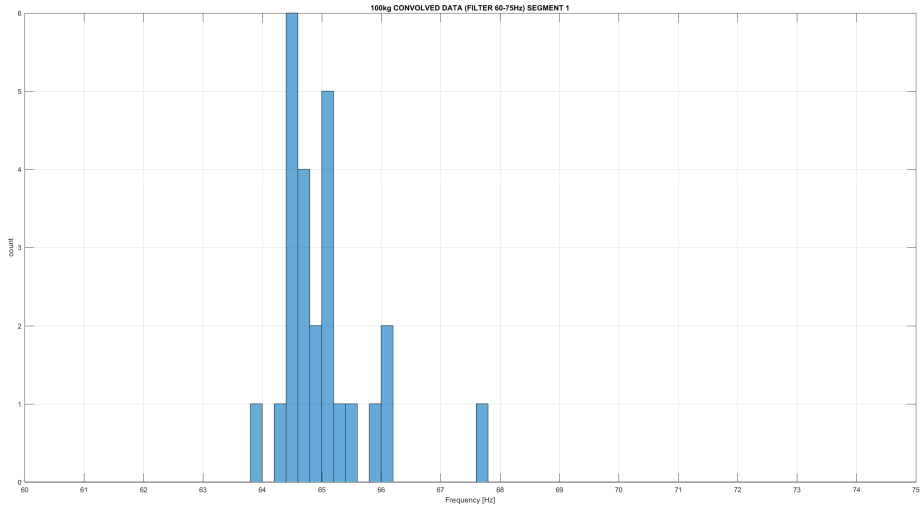


(a) 75kg mode shape, run 25

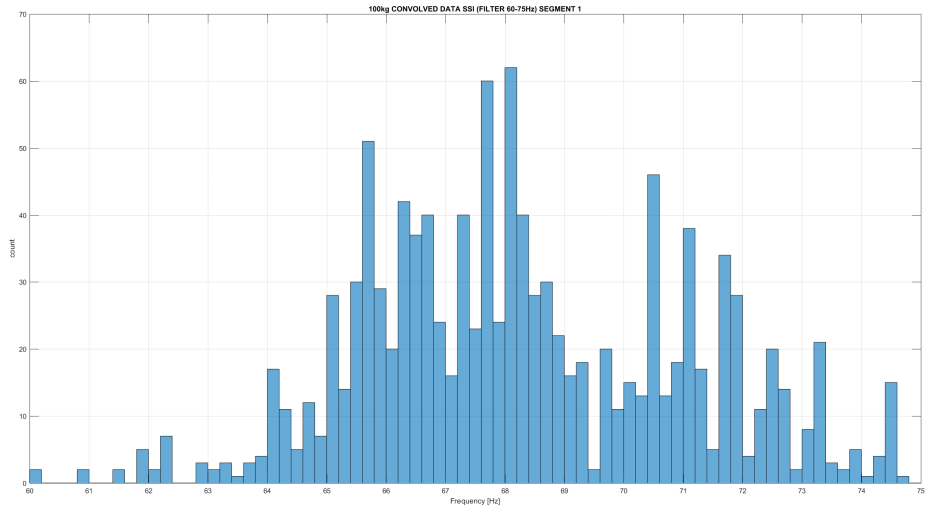
(b) 75kg FDD SSI output, run 25

Figure A4.75kg: Run 25 (segment 1)

100kg data segment 1

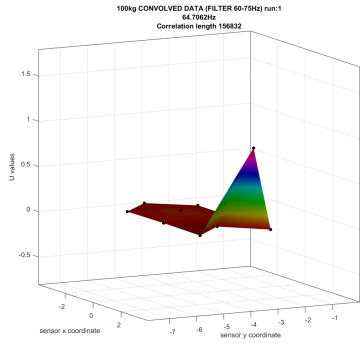


(a) 100kg FDD histogram

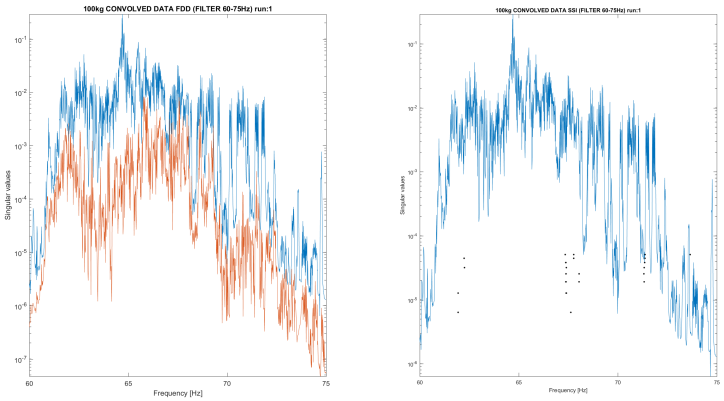


(b) 100kg SSI histogram

Figure A4.100kg: Histograms of identified modes, 100kg data (segment 1)

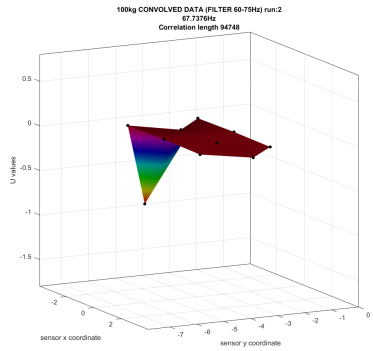


(a) 100kg mode shape, run 1

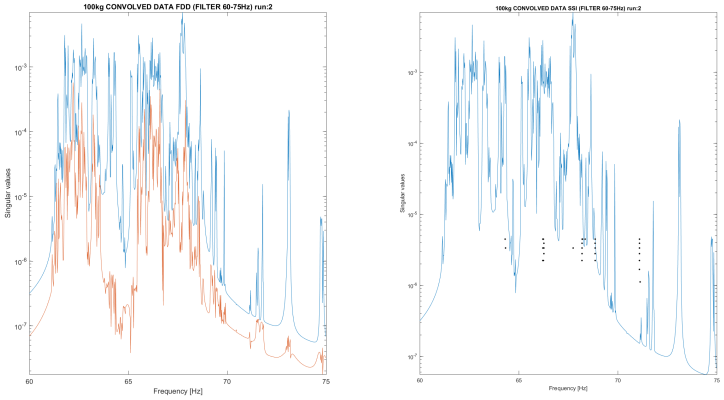


(b) 100kg FDD SSI output, run 1

Figure A4.100kg: Run 1 (segment 1)

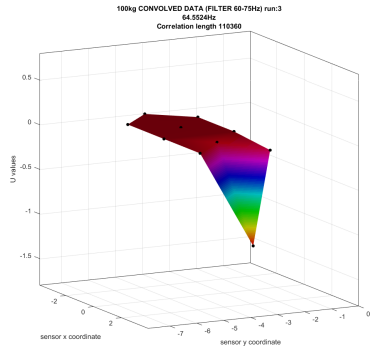


(a) 100kg mode shape, run 2

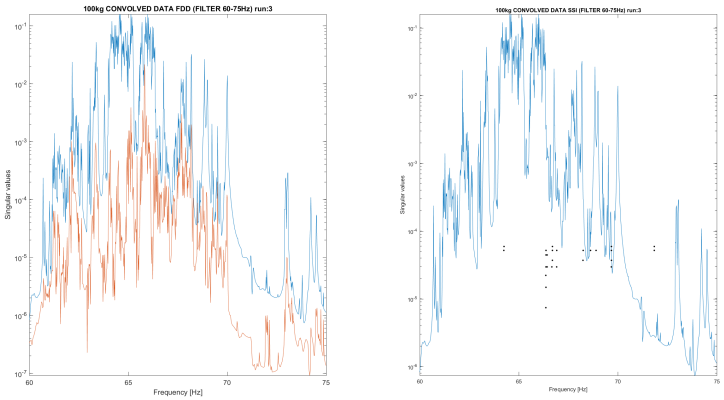


(b) 100kg FDD SSI output, run 2

Figure A4.100kg: Run 2 (segment 1)

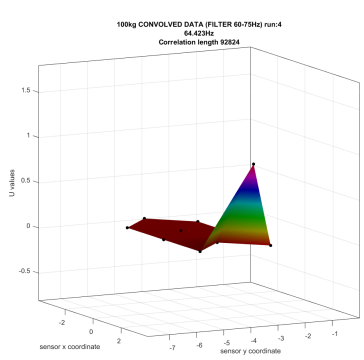


(a) 100kg mode shape, run 3

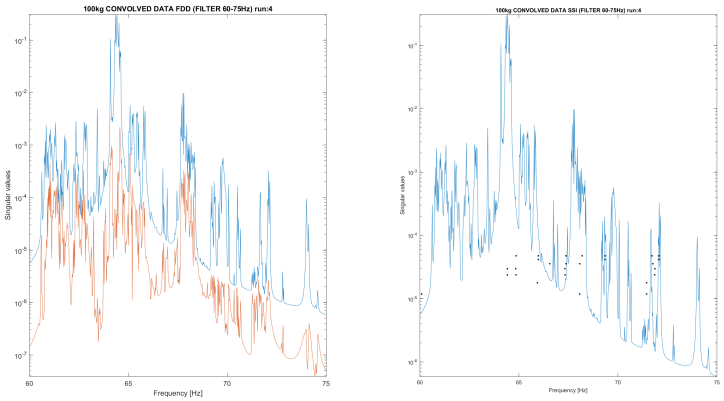


(b) 100kg FDD SSI output, run 3

Figure A4.100kg: Run 3 (segment 1)

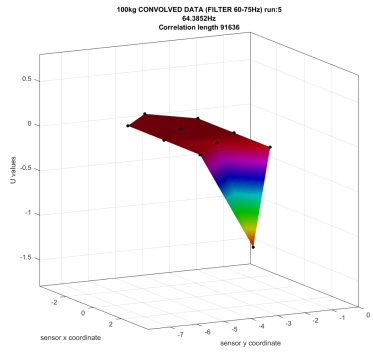


(a) 100kg mode shape, run 4

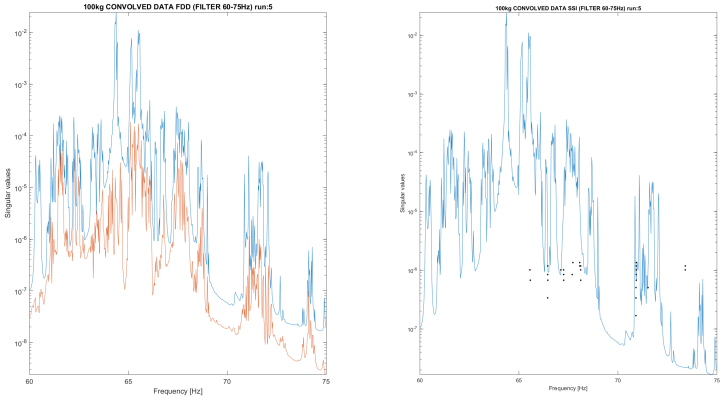


(b) 100kg FDD SSI output, run 4

Figure A4.100kg: Run 4 (segment 1)

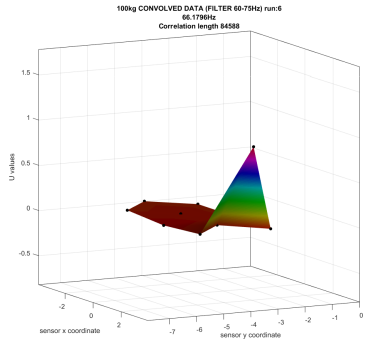


(a) 100kg mode shape, run 5

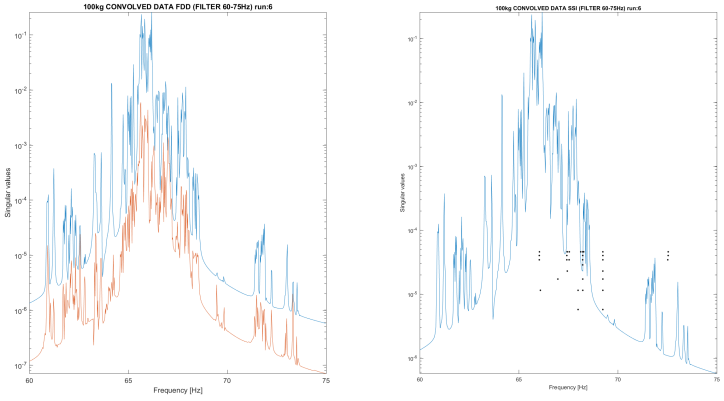


(b) 100kg FDD SSI output, run 5

Figure A4.100kg: Run 5 (segment 1)

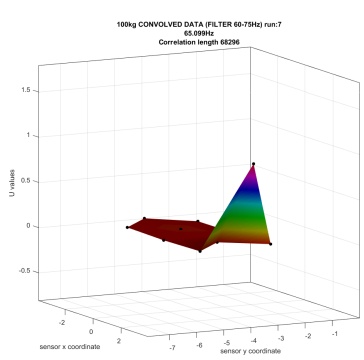


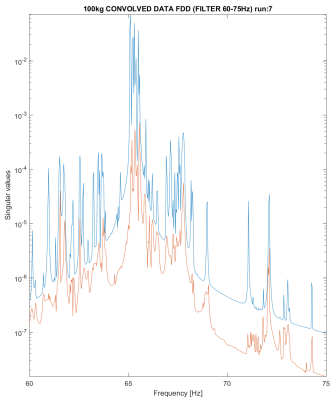
(a) 100kg mode shape, run 6

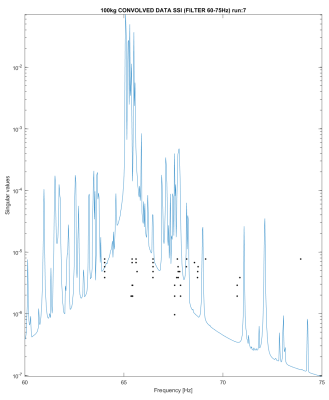


(b) 100kg FDD SSI output, run 6

Figure A4.100kg: Run 6 (segment 1)



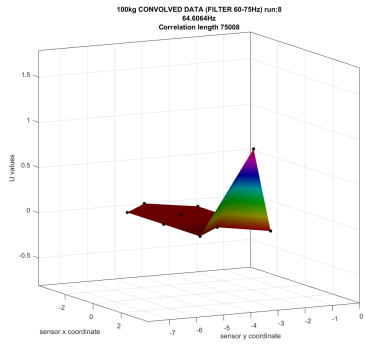


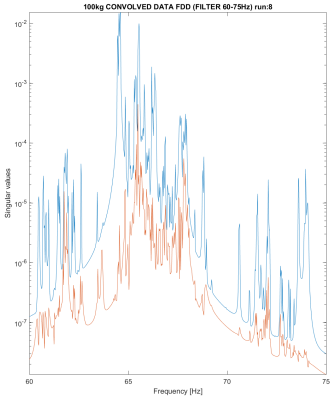


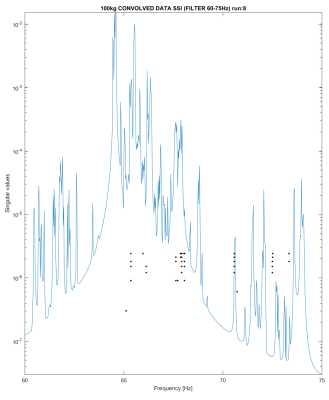
(a) 100kg mode shape, run 7

(b) 100kg FDD SSI output, run 7

Figure A4.100kg: Run 7 (segment 1)



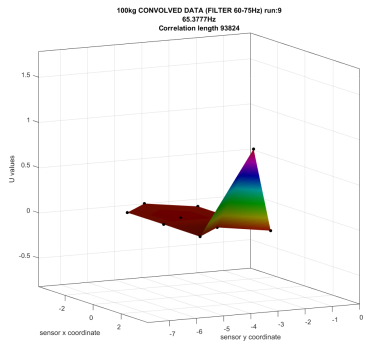


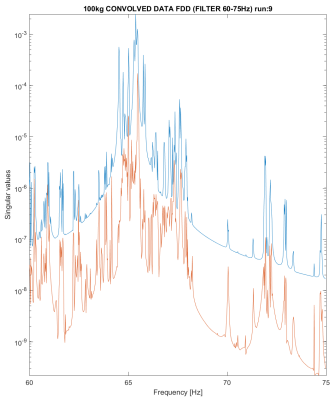


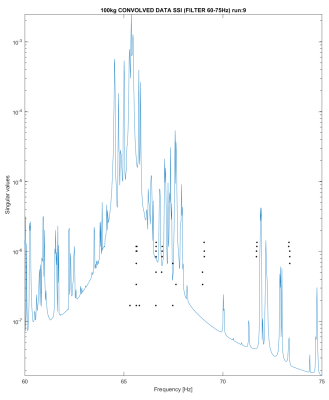
(a) 100kg mode shape, run 8

(b) 100kg FDD SSI output, run 8

Figure A4.100kg: Run 8 (segment 1)



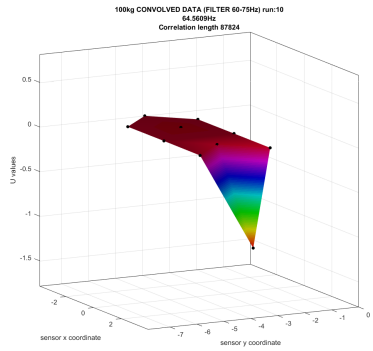




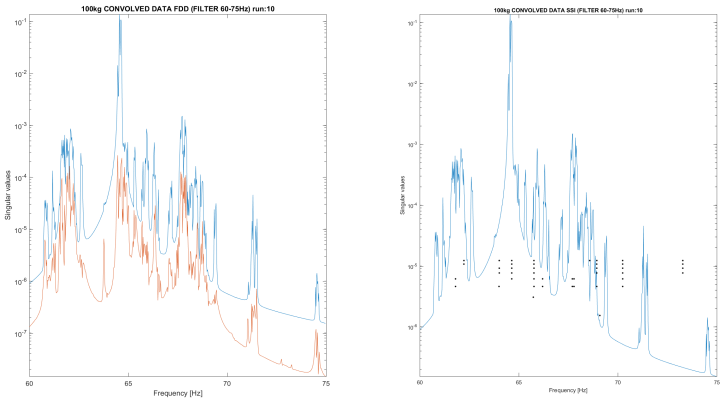
(a) 100kg mode shape, run 9

(b) 100kg FDD SSI output, run 9

Figure A4.100kg: Run 9 (segment 1)

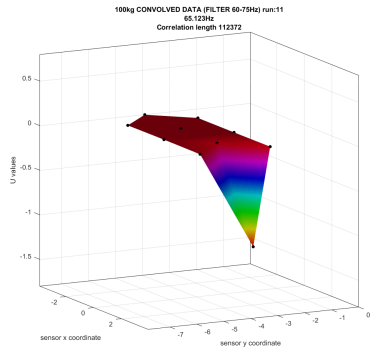


(a) 100kg mode shape, run 10

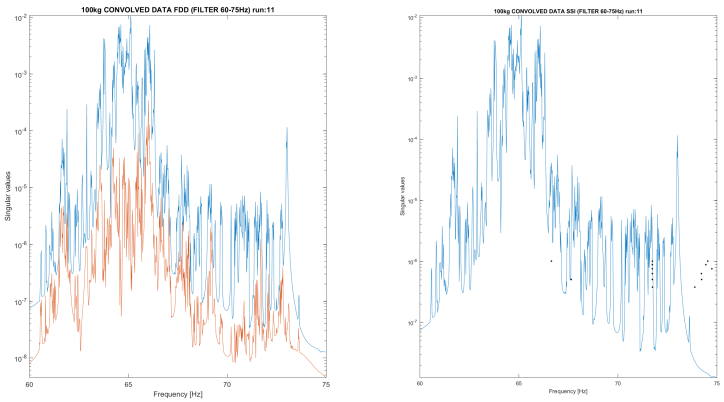


(b) 100kg FDD SSI output, run 10

Figure A4.100kg: Run 10 (segment 1)

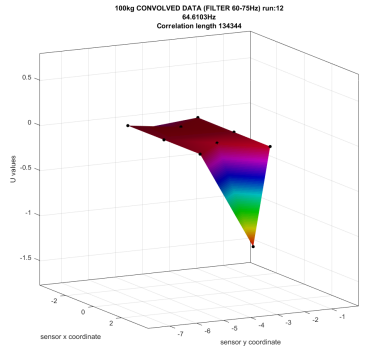


(a) 100kg mode shape, run 11

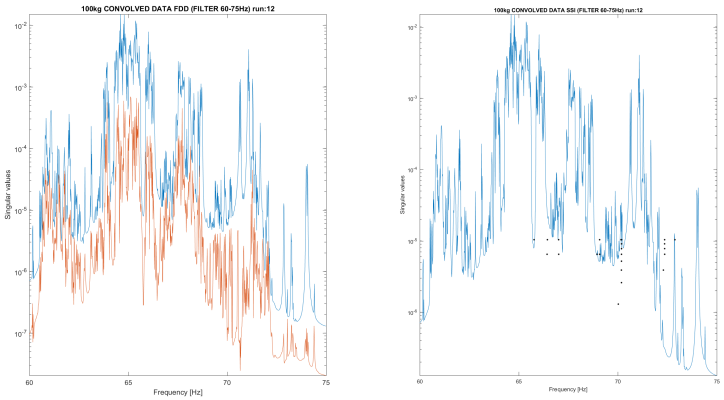


(b) 100kg FDD SSI output, run 11

Figure A4.100kg: Run 11 (segment 1)

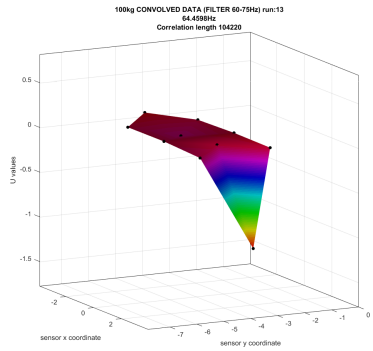


(a) 100kg mode shape, run 12

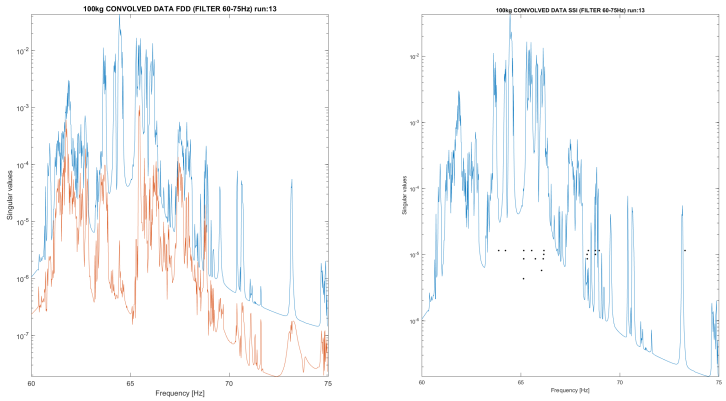


(b) 100kg FDD SSI output, run 12

Figure A4.100kg: Run 12 (segment 1)

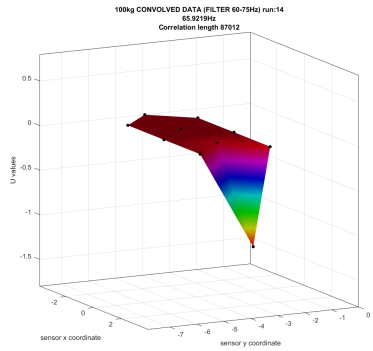


(a) 100kg mode shape, run 13

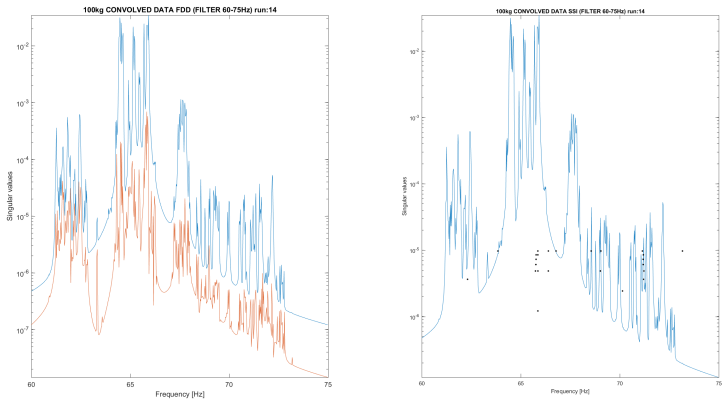


(b) 100kg FDD SSI output, run 13

Figure A4.100kg: Run 13 (segment 1)

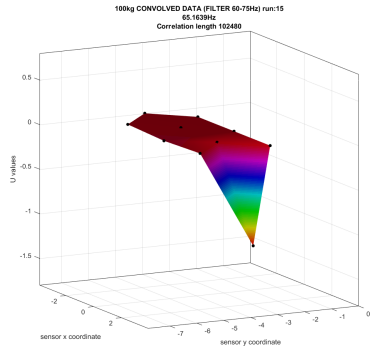


(a) 100kg mode shape, run 14

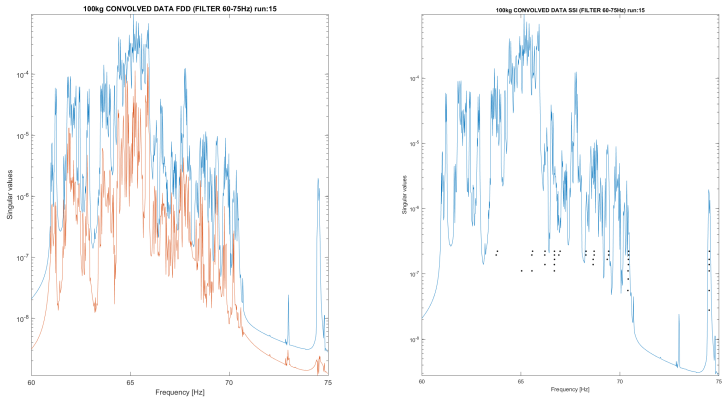


(b) 100kg FDD SSI output, run 14

Figure A4.100kg: Run 14 (segment 1)

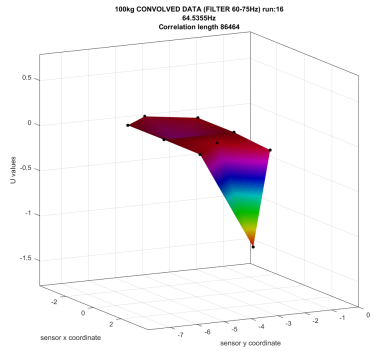


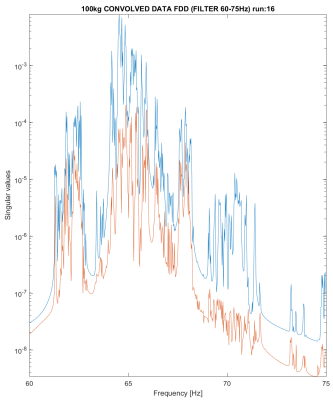
(a) 100kg mode shape, run 15

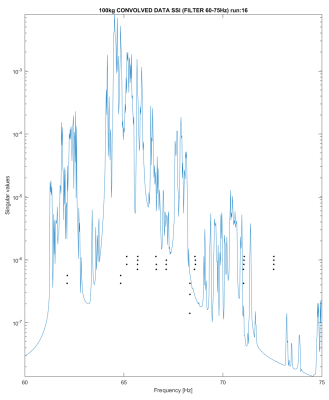


(b) 100kg FDD SSI output, run 15

Figure A4.100kg: Run 15 (segment 1)



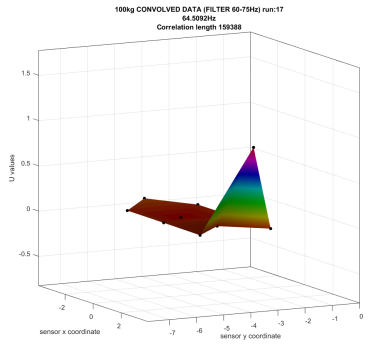


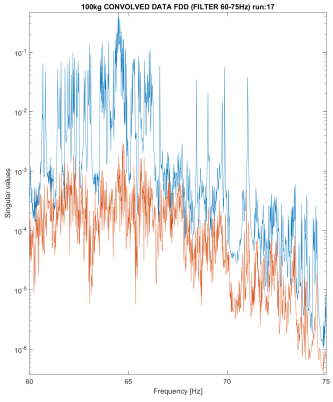


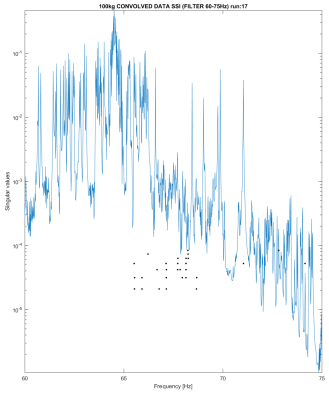
(a) 100kg mode shape, run 16

(b) 100kg FDD SSI output, run 16

Figure A4.100kg: Run 16 (segment 1)



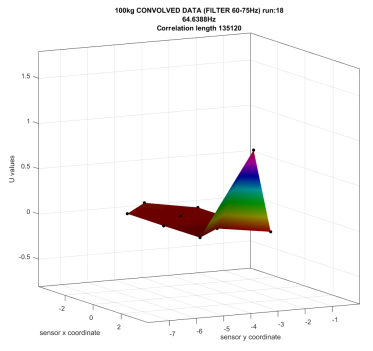


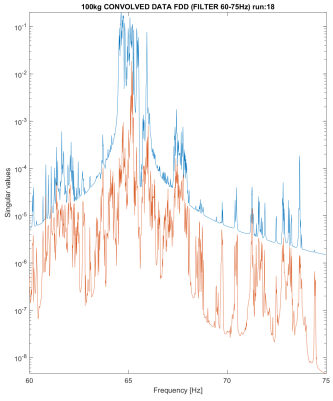


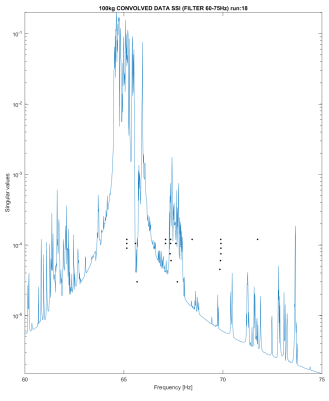
(a) 100kg mode shape, run 17

(b) 100kg FDD SSI output, run 17

Figure A4.100kg: Run 17 (segment 1)



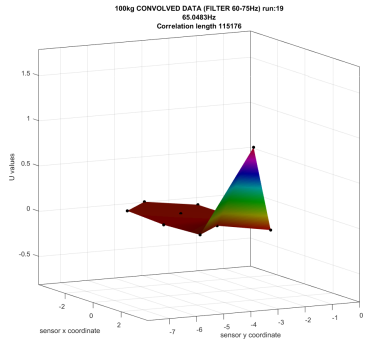


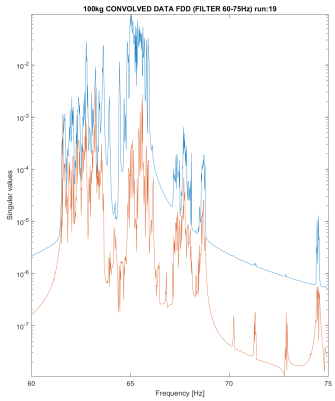


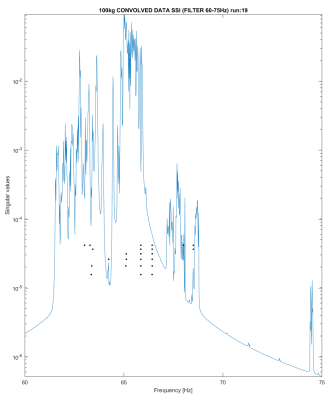
(a) 100kg mode shape, run 18

(b) 100kg FDD SSI output, run 18

Figure A4.100kg: Run 18 (segment 1)



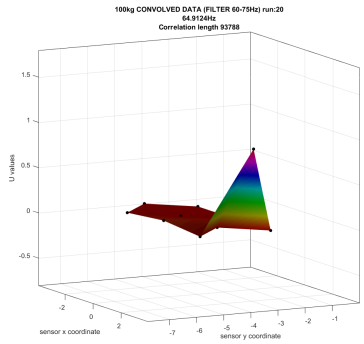


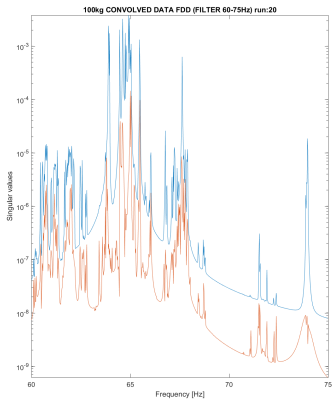


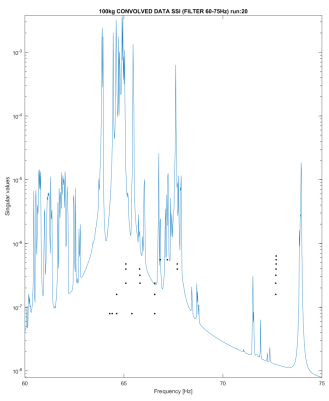
(a) 100kg mode shape, run 19

(b) 100kg FDD SSI output, run 19

Figure A4.100kg: Run 19 (segment 1)



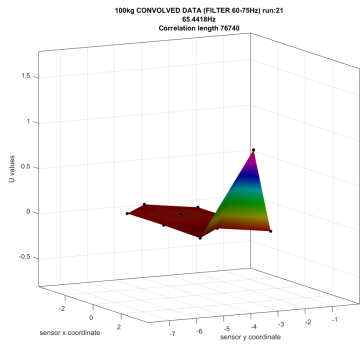


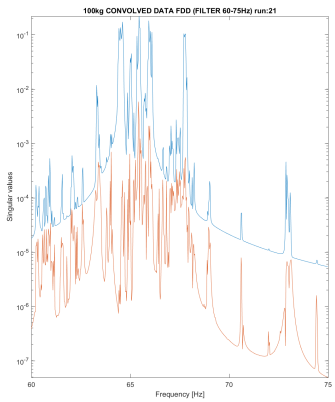


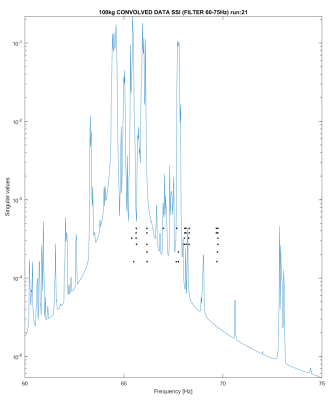
(a) 100kg mode shape, run 20

(b) 100kg FDD SSI output, run 20

Figure A4.100kg: Run 20 (segment 1)



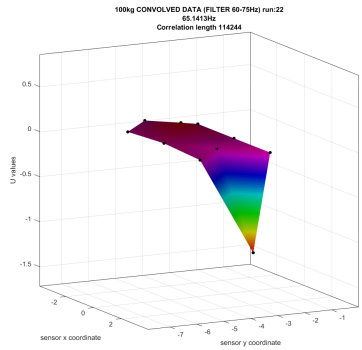




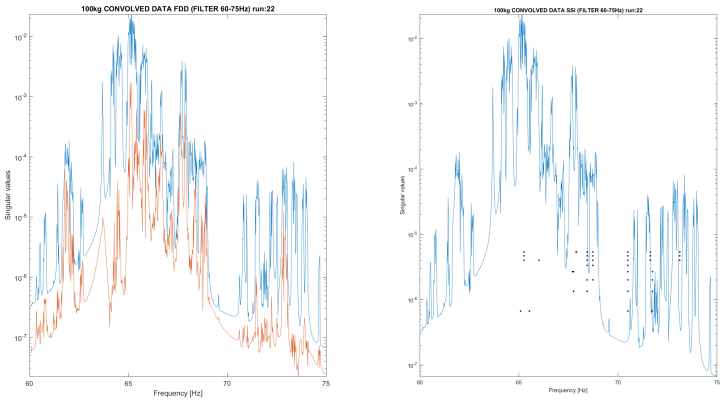
(a) 100kg mode shape, run 21

(b) 100kg FDD SSI output, run 21

Figure A4.100kg: Run 21 (segment 1)

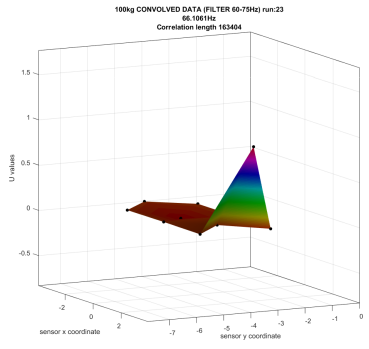


(a) 100kg mode shape, run 22

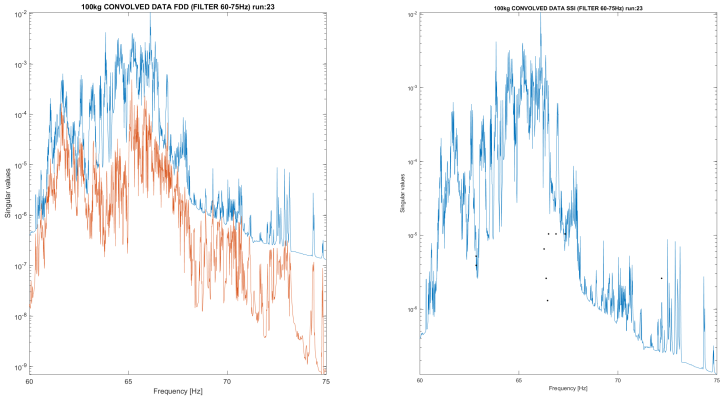


(b) 100kg FDD SSI output, run 22

Figure A4.100kg: Run 22 (segment 1)

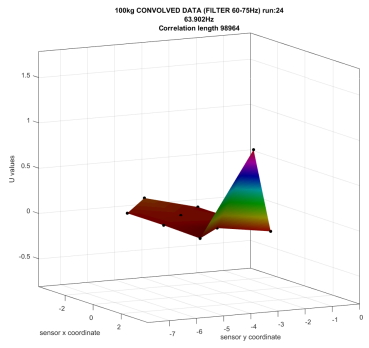


(a) 100kg mode shape, run 23

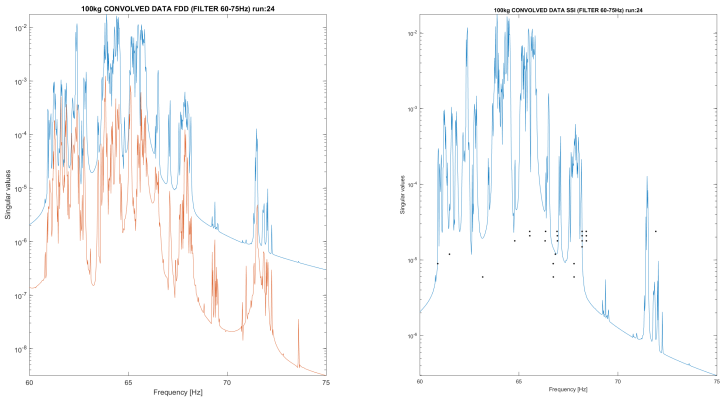


(b) 100kg FDD SSI output, run 23

Figure A4.100kg: Run 23 (segment 1)

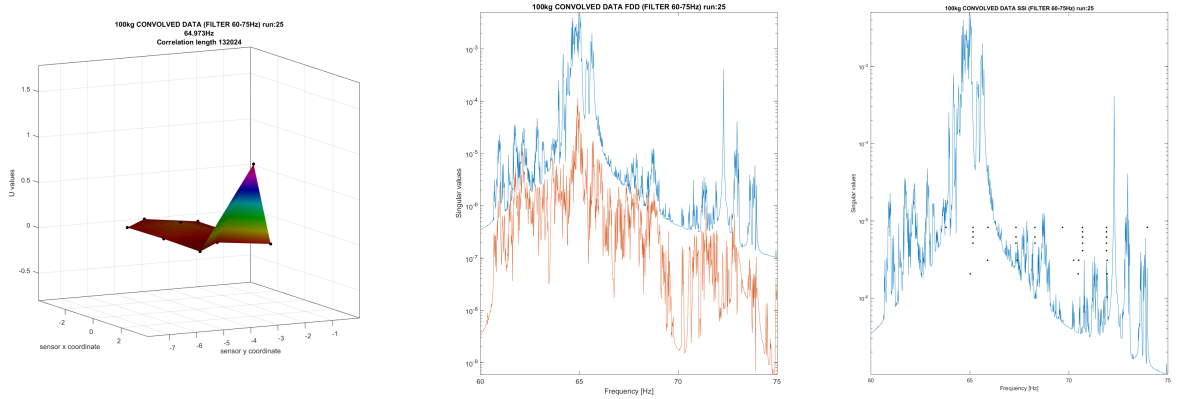


(a) 100kg mode shape, run 24



(b) 100kg FDD SSI output, run 24

Figure A4.100kg: Run 24 (segment 1)

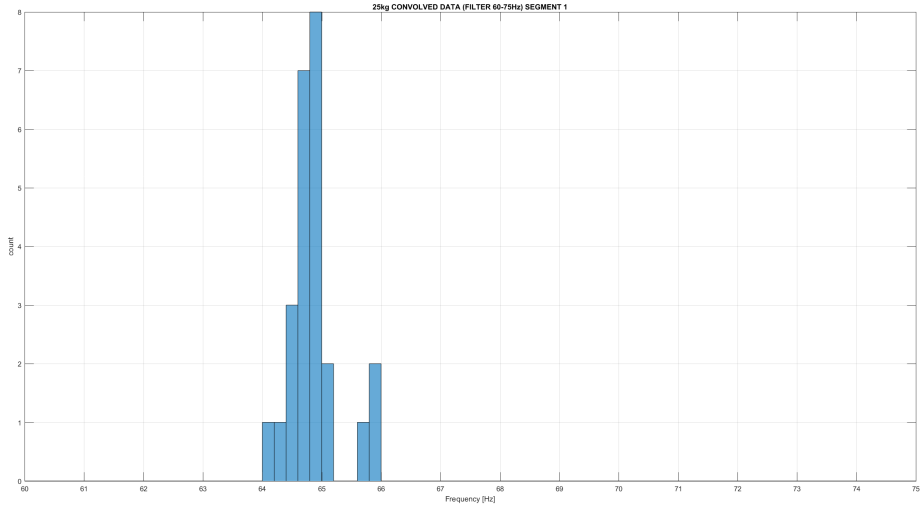


(a) 100kg mode shape, run 25

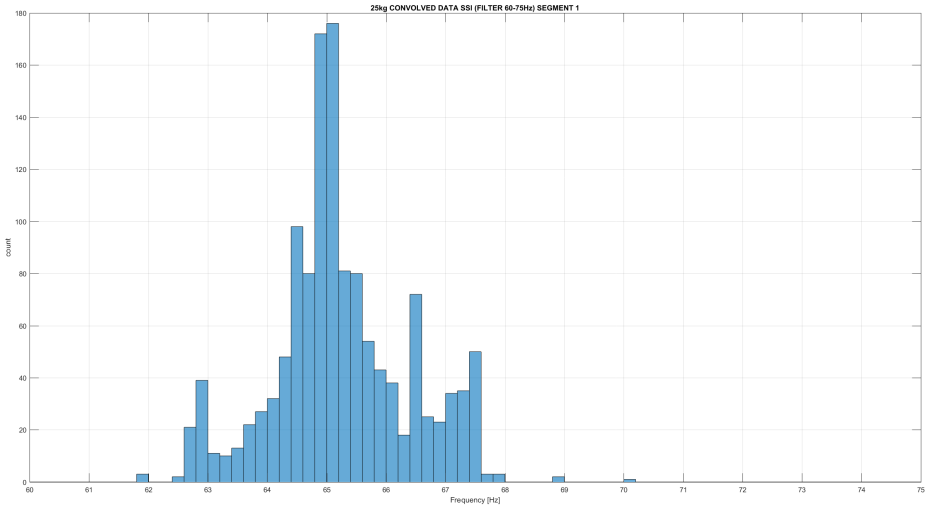
(b) 100kg FDD SSI output, run 25

Figure A4.100kg: Run 25 (segment 1)

Data (28.03.2017) 25kg-50kg segment 1 (Reduced order PF)

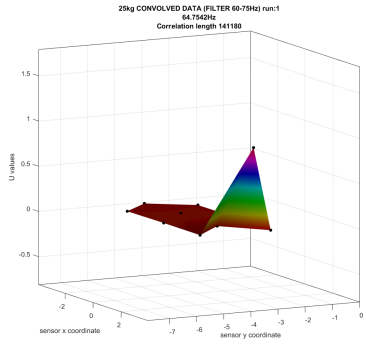


(a) 25kg FDD histogram

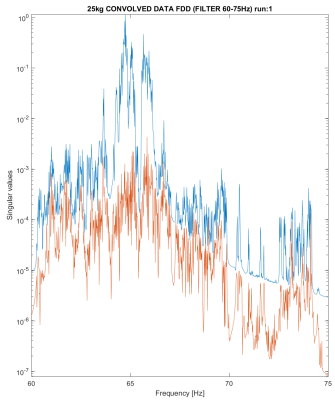


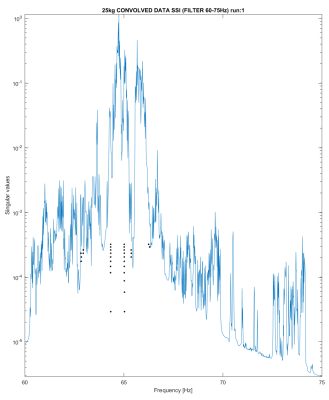
(b) 25kg SSI histogram

Figure A4.25kg: Histograms of identified modes, 25kg data (segment 1)



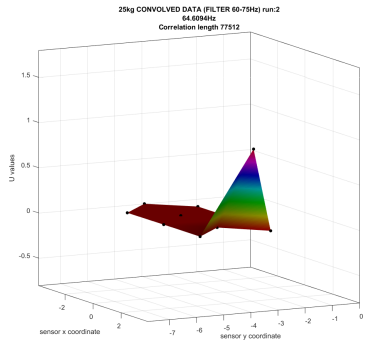
(a) 25kg mode shape, run 1



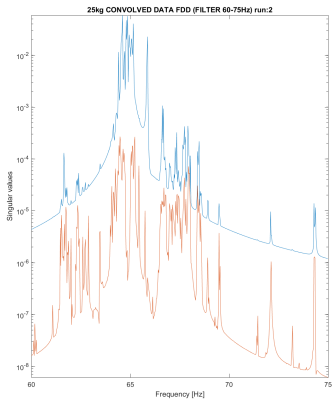


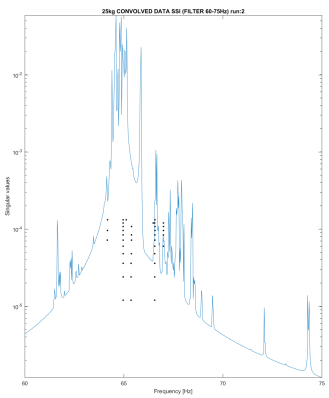
(b) 25kg FDD SSI output, run 1

Figure A4.25kg: Run 1 (segment 1)



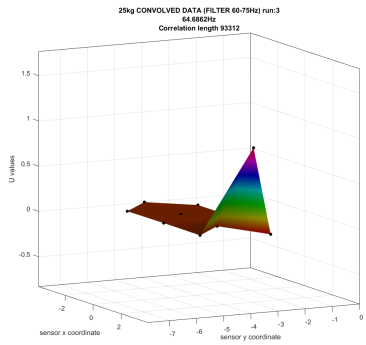
(a) 25kg mode shape, run 2



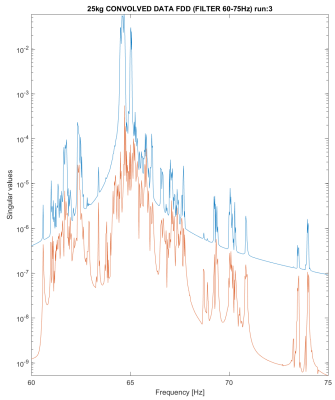


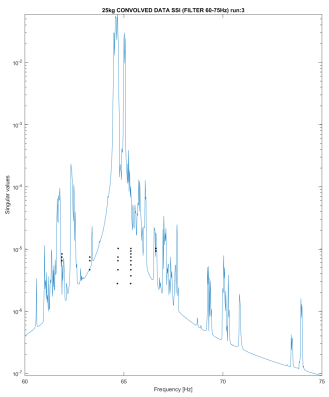
(b) 25kg FDD SSI output, run 2

Figure A4.25kg: Run 2 (segment 1)



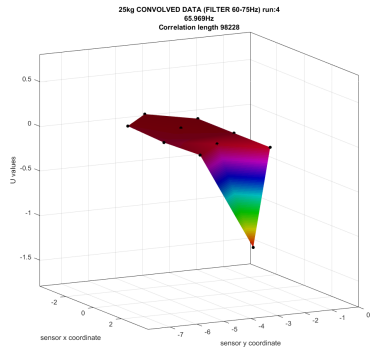
(a) 25kg mode shape, run 3



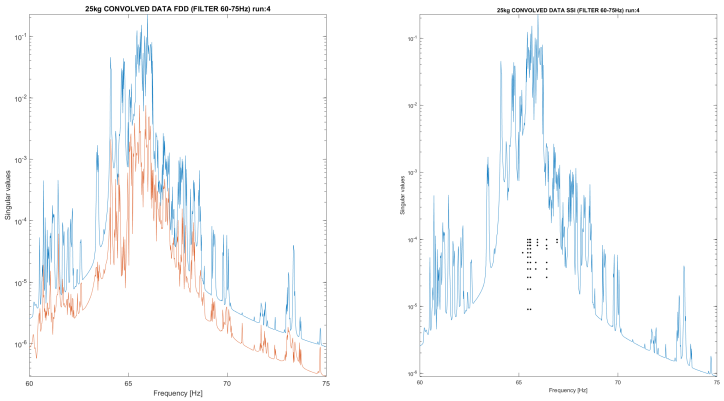


(b) 25kg FDD SSI output, run 3

Figure A4.25kg: Run 3 (segment 1)

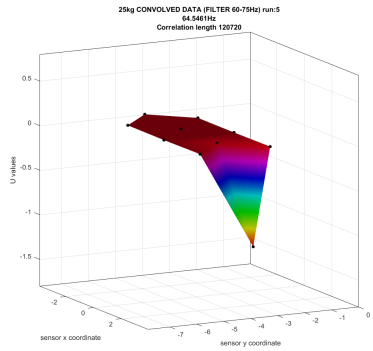


(a) 25kg mode shape, run 4

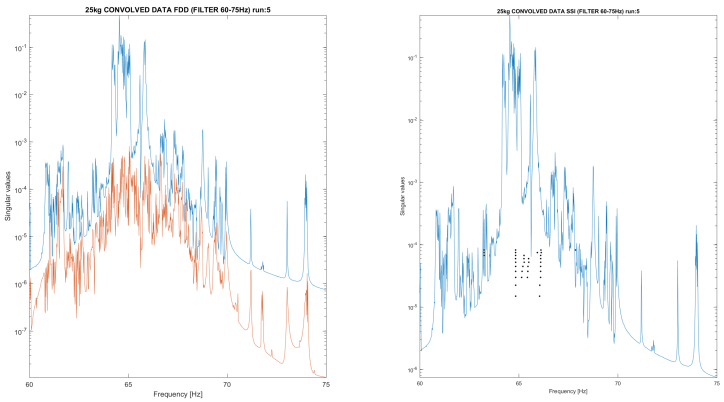


(b) 25kg FDD SSI output, run 4

Figure A4.25kg: Run 4 (segment 1)

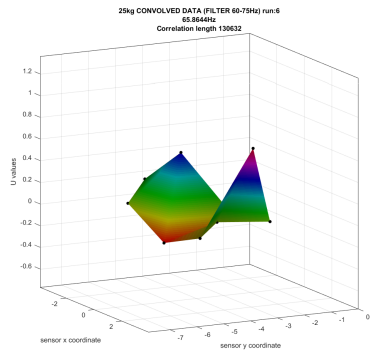


(a) 25kg mode shape, run 5

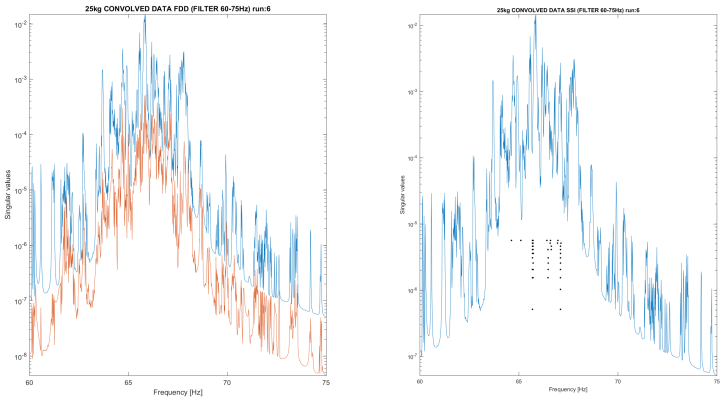


(b) 25kg FDD SSI output, run 5

Figure A4.25kg: Run 5 (segment 1)

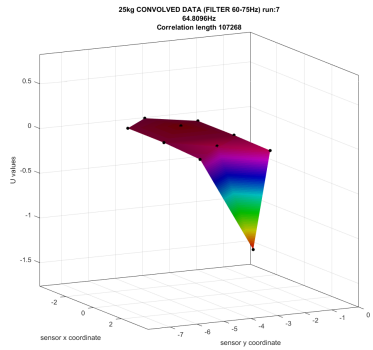


(a) 25kg mode shape, run 6

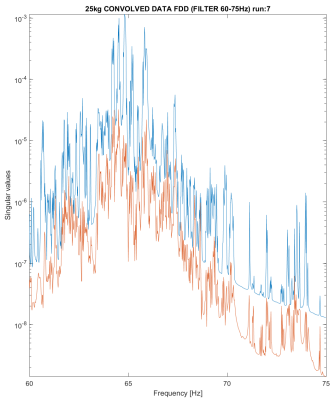


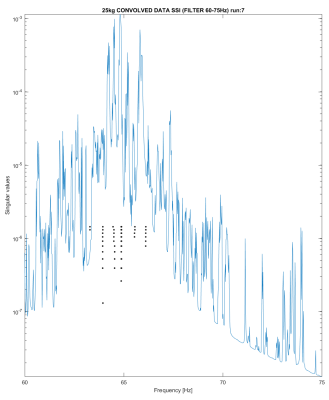
(b) 25kg FDD SSI output, run 6

Figure A4.25kg: Run 6 (segment 1)



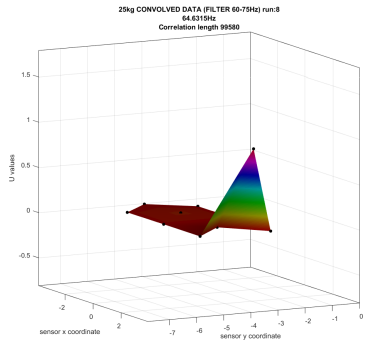
(a) 25kg mode shape, run 7



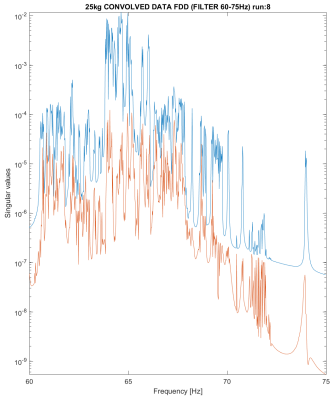


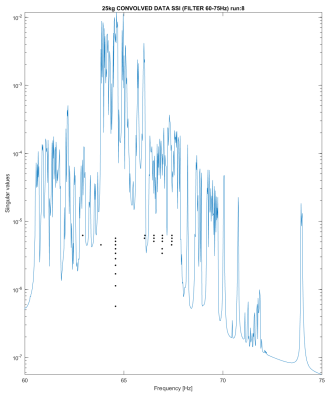
(b) 25kg FDD SSI output, run 7

Figure A4.25kg: Run 7 (segment 1)



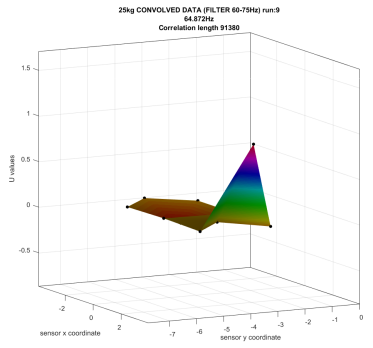
(a) 25kg mode shape, run 8



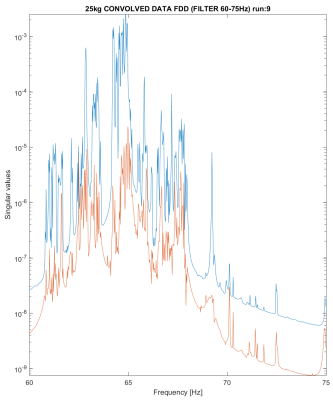


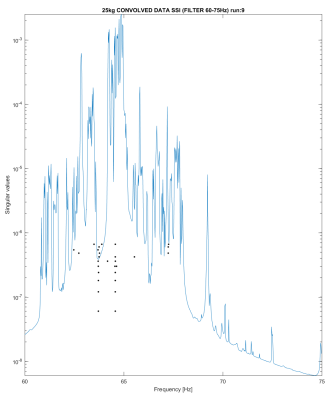
(b) 25kg FDD SSI output, run 8

Figure A4.25kg: Run 8 (segment 1)



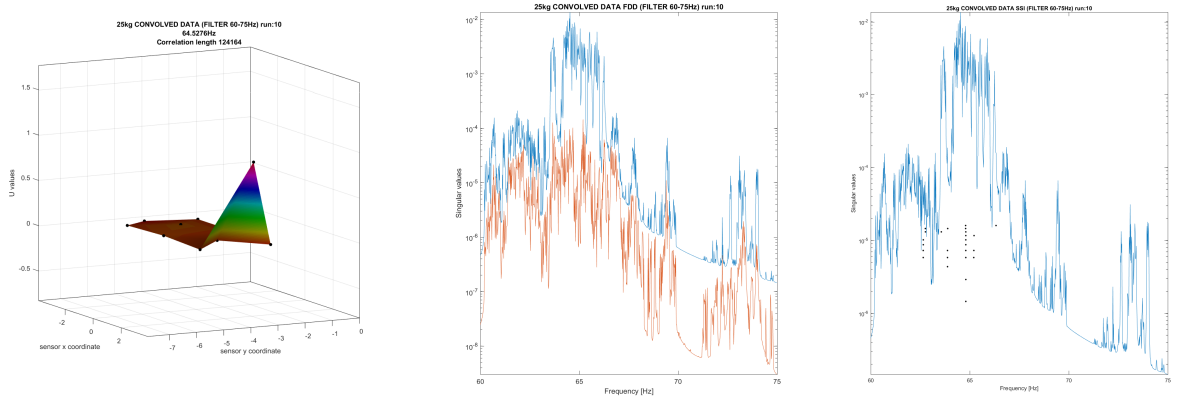
(a) 25kg mode shape, run 9





(b) 25kg FDD SSI output, run 9

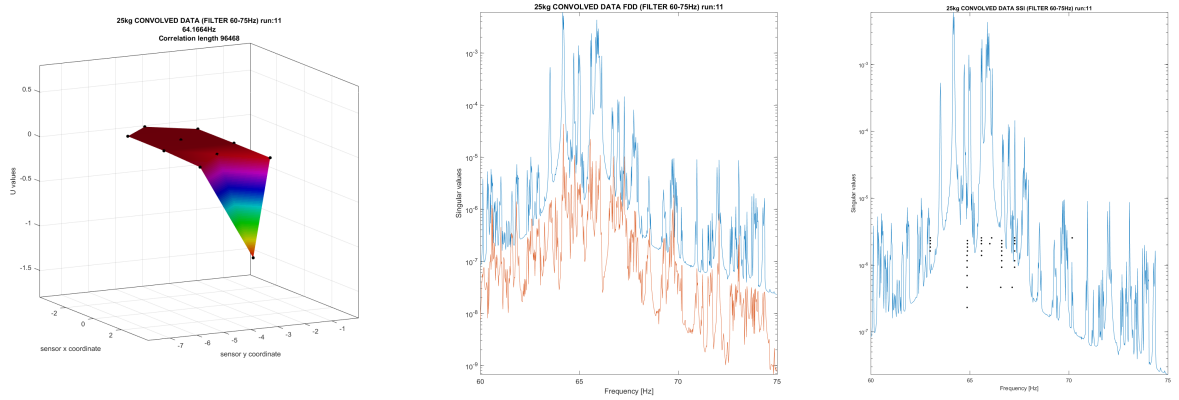
Figure A4.25kg: Run 9 (segment 1)



(a) 25kg mode shape, run 10

(b) 25kg FDD SSI output, run 10

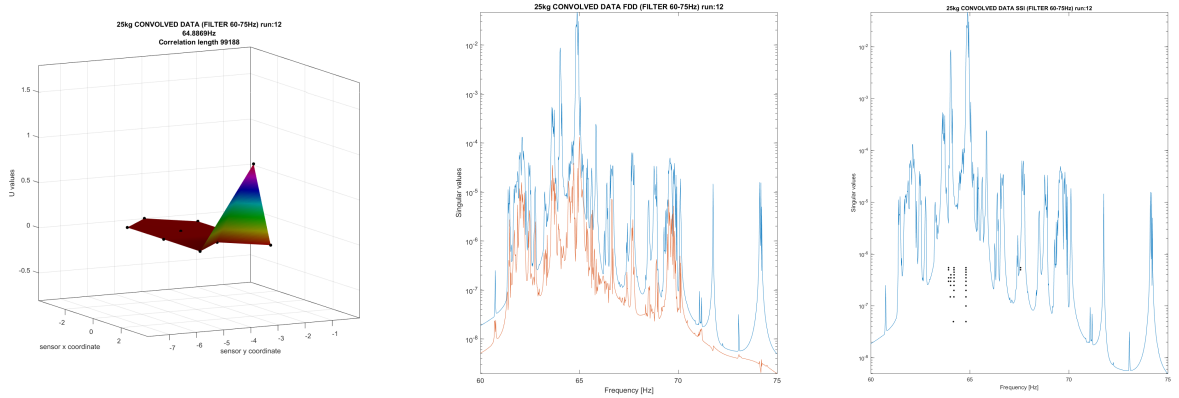
Figure A4.25kg: Run 10 (segment 1)



(a) 25kg mode shape, run 11

(b) 25kg FDD SSI output, run 11

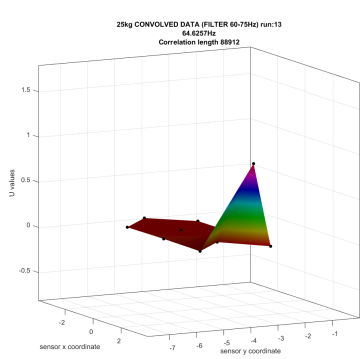
Figure A4.25kg: Run 11 (segment 1)

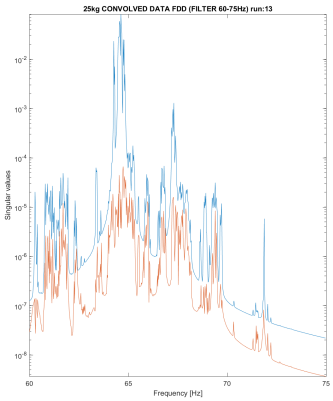


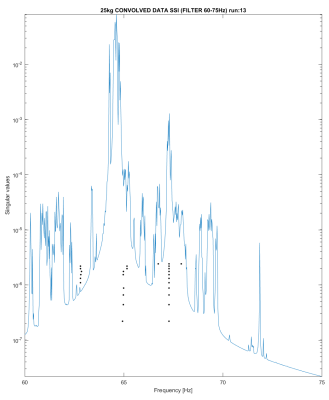
(a) 25kg mode shape, run 12

(b) 25kg FDD SSI output, run 12

Figure A4.25kg: Run 12 (segment 1)



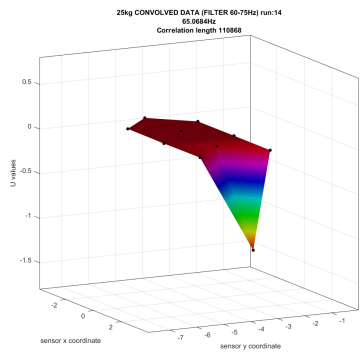


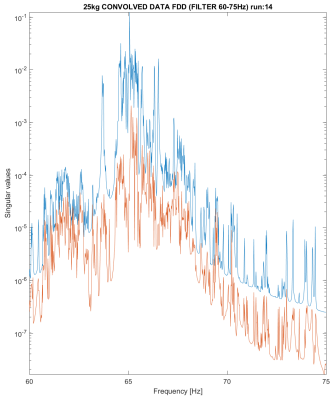


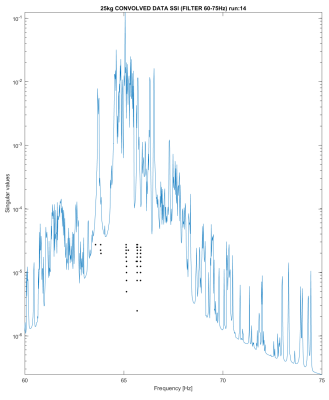
(a) 25kg mode shape, run 13

(b) 25kg FDD SSI output, run 13

Figure A4.25kg: Run 13 (segment 1)



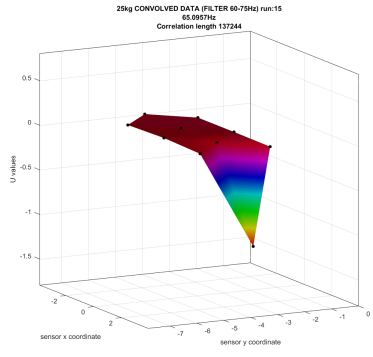


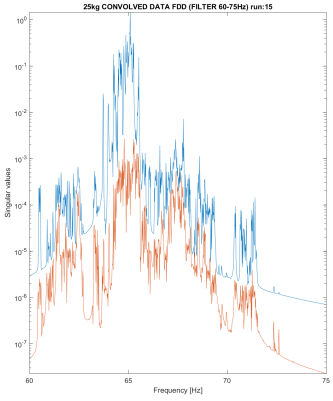


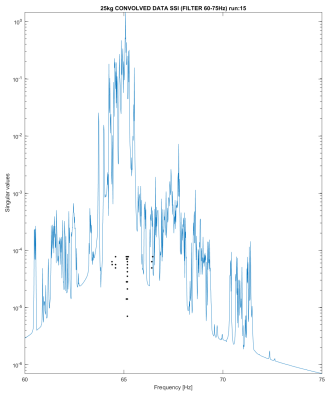
(a) 25kg mode shape, run 14

(b) 25kg FDD SSI output, run 14

Figure A4.25kg: Run 14 (segment 1)



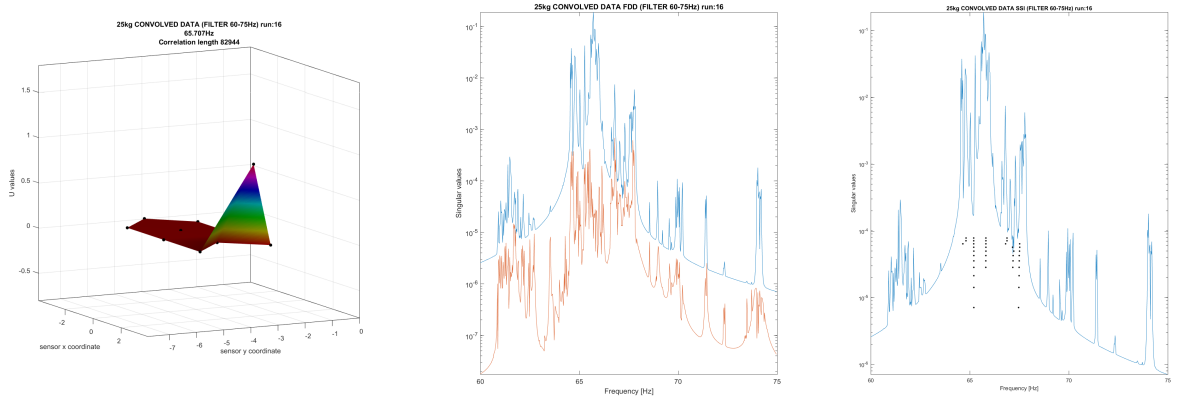




(a) 25kg mode shape, run 15

(b) 25kg FDD SSI output, run 15

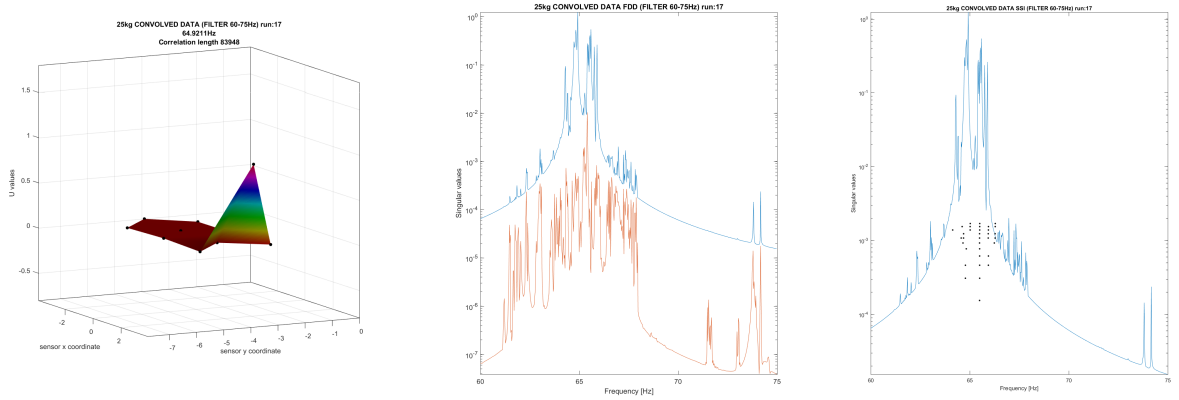
Figure A4.25kg: Run 15 (segment 1)



(a) 25kg mode shape, run 16

(b) 25kg FDD SSI output, run 16

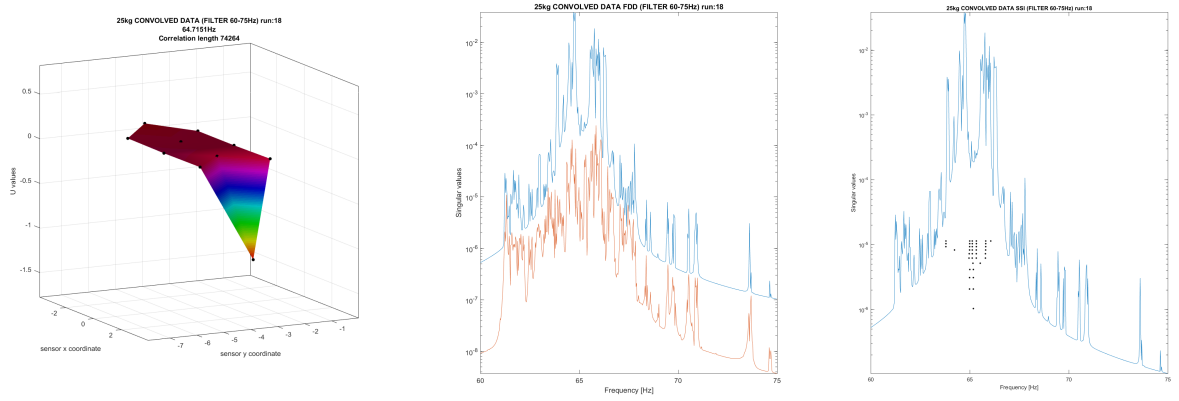
Figure A4.25kg: Run 16 (segment 1)



(a) 25kg mode shape, run 17

(b) 25kg FDD SSI output, run 17

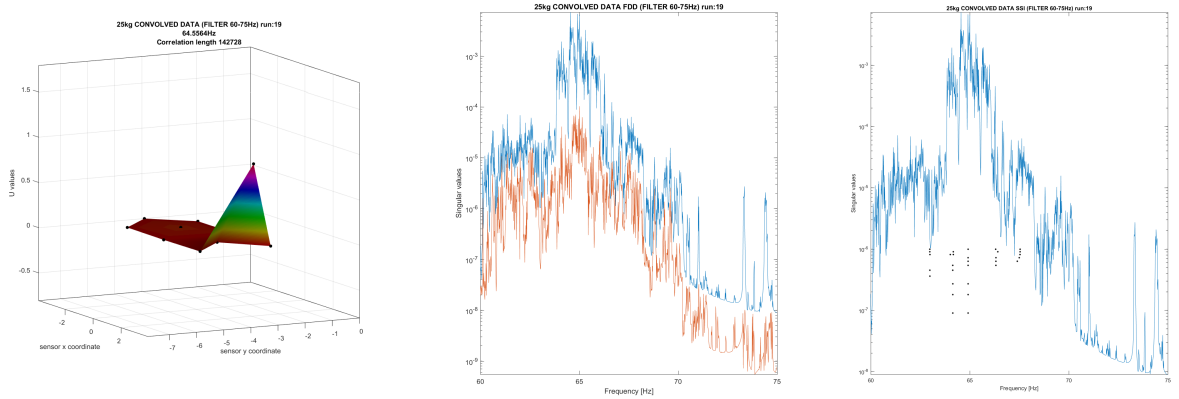
Figure A4.25kg: Run 17 (segment 1)



(a) 25kg mode shape, run 18

(b) 25kg FDD SSI output, run 18

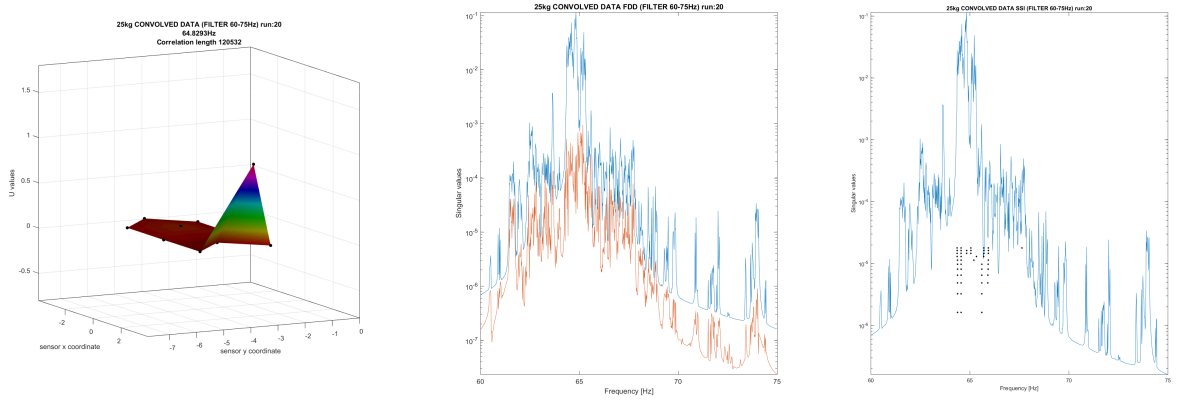
Figure A4.25kg: Run 18 (segment 1)



(a) 25kg mode shape, run 19

(b) 25kg FDD SSI output, run 19

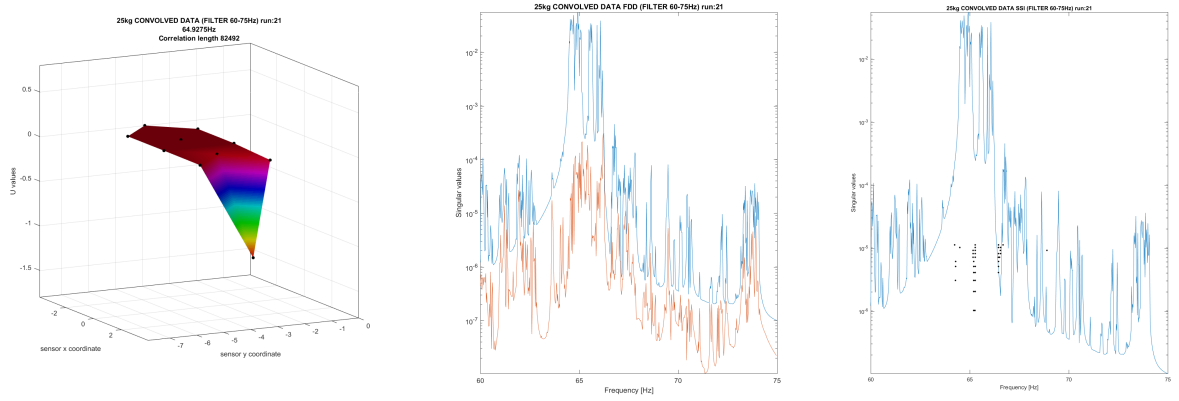
Figure A4.25kg: Run 19 (segment 1)



(a) 25kg mode shape, run 20

(b) 25kg FDD SSI output, run 20

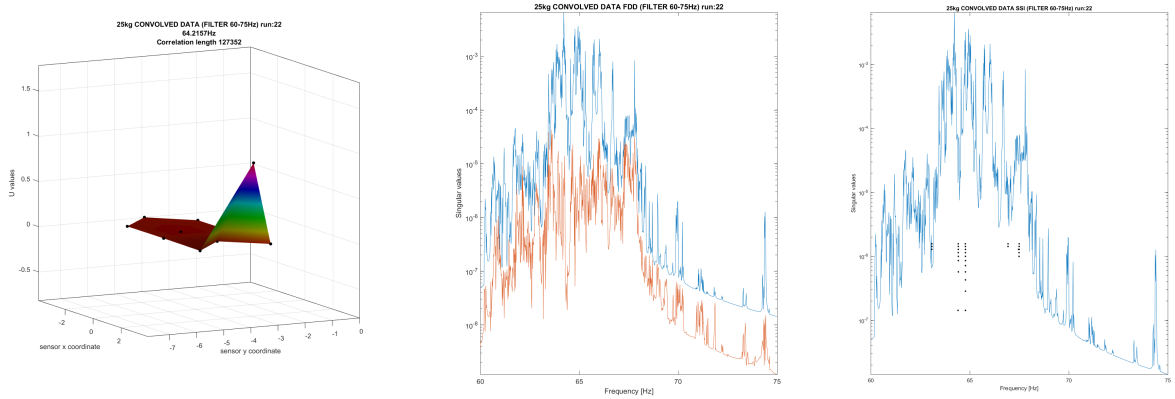
Figure A4.25kg: Run 20 (segment 1)



(a) 25kg mode shape, run 21

(b) 25kg FDD SSI output, run 21

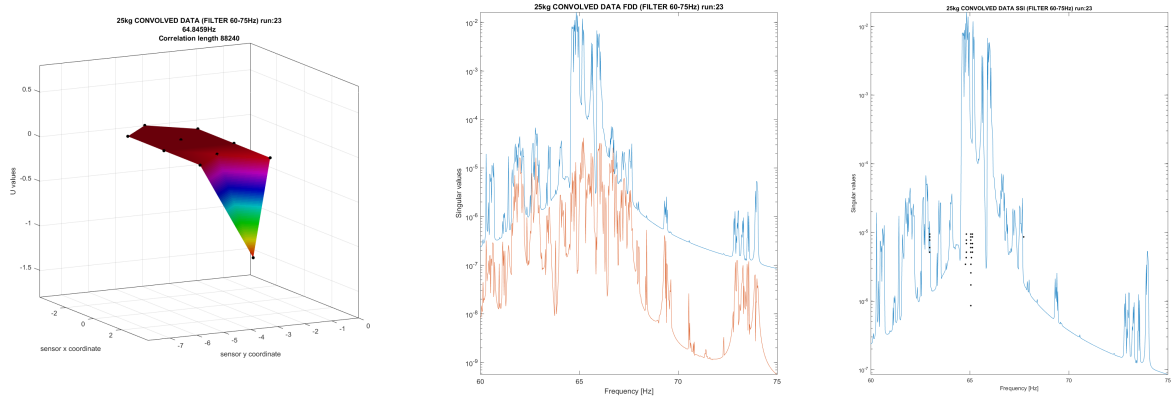
Figure A4.25kg: Run 21 (segment 1)



(a) 25kg mode shape, run 22

(b) 25kg FDD SSI output, run 22

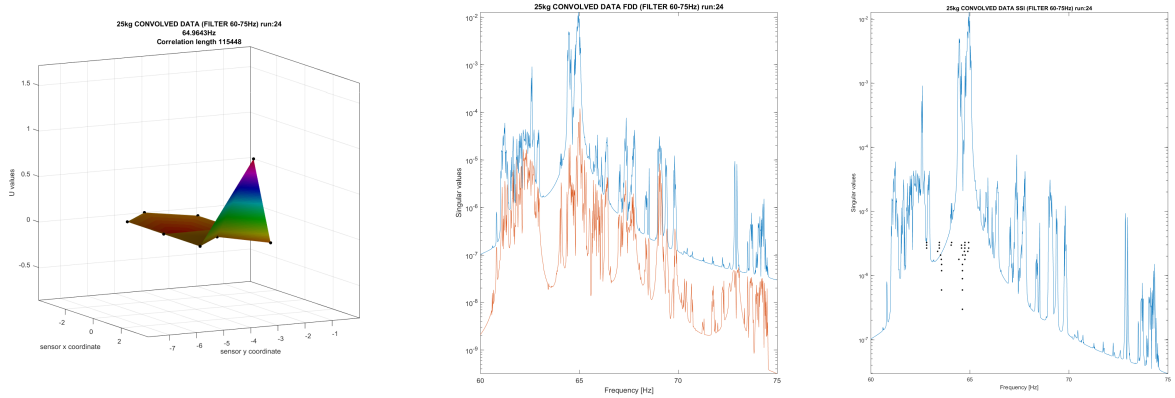
Figure A4.25kg: Run 22 (segment 1)



(a) 25kg mode shape, run 23

(b) 25kg FDD SSI output, run 23

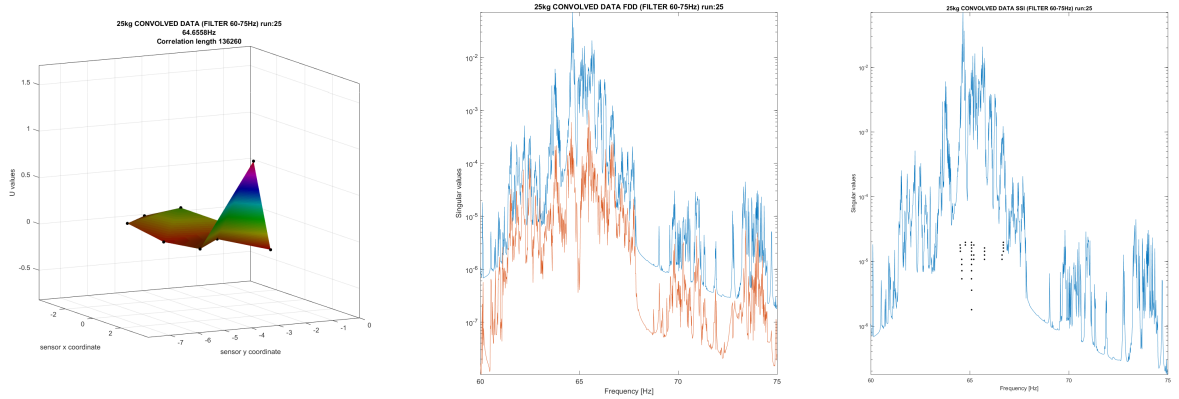
Figure A4.25kg: Run 23 (segment 1)



(a) 25kg mode shape, run 24

(b) 25kg FDD SSI output, run 24

Figure A4.25kg: Run 24 (segment 1)

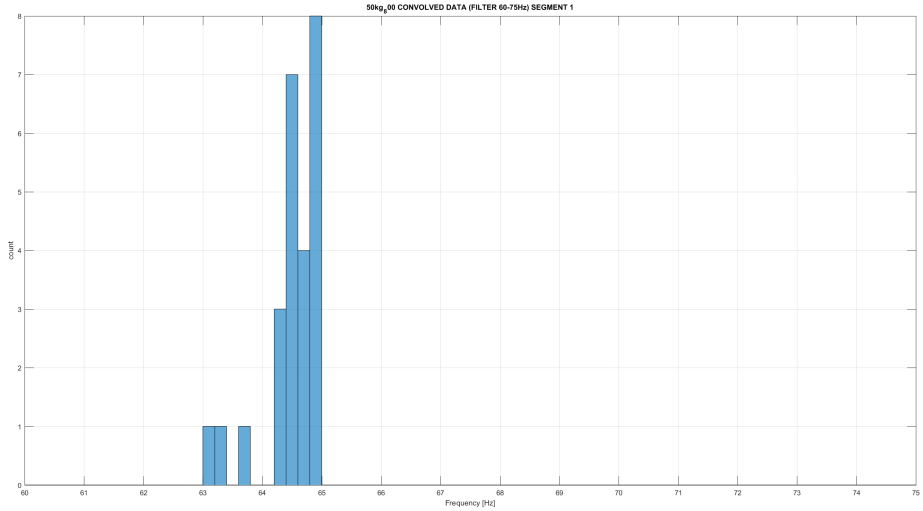


(a) 25kg mode shape, run 25

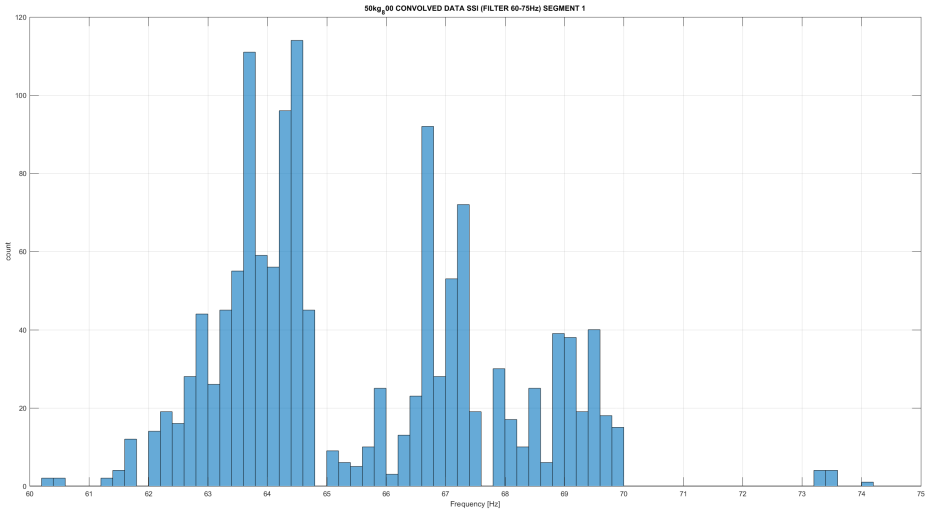
(b) 25kg FDD SSI output, run 25

Figure A4.25kg: Run 25 (segment 1)

50kg data segment 1 (28.03.2017)

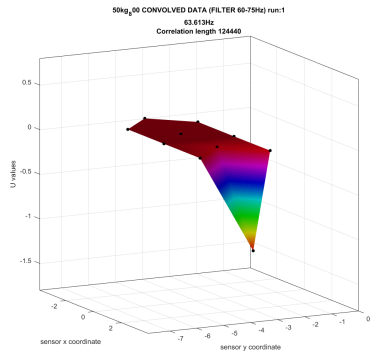


(a) 50kg FDD histogram

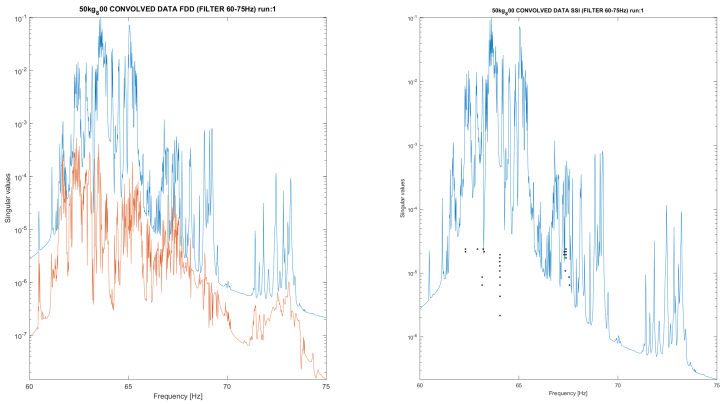


(b) 50kg SSI histogram

Figure A4.50kg: Histograms of identified modes, 50kg data (segment 1)

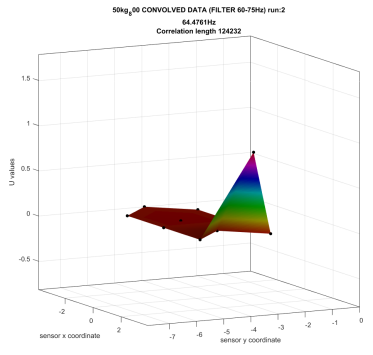


(a) 50kg mode shape, run 1

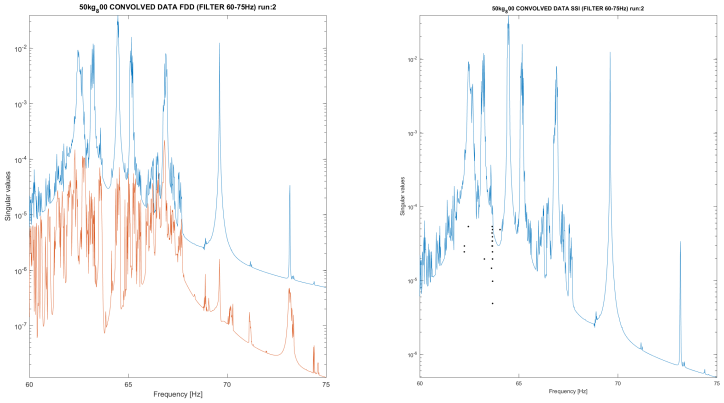


(b) 50kg FDD SSI output, run 1

Figure A4.50kg (28.03.2017): Run 1 (segment 1)

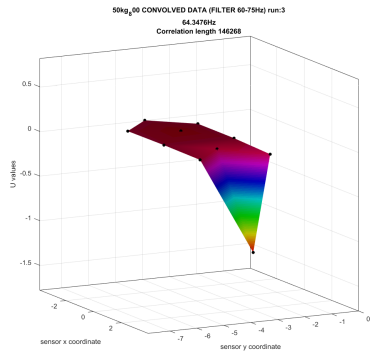


(a) 50kg mode shape, run 2

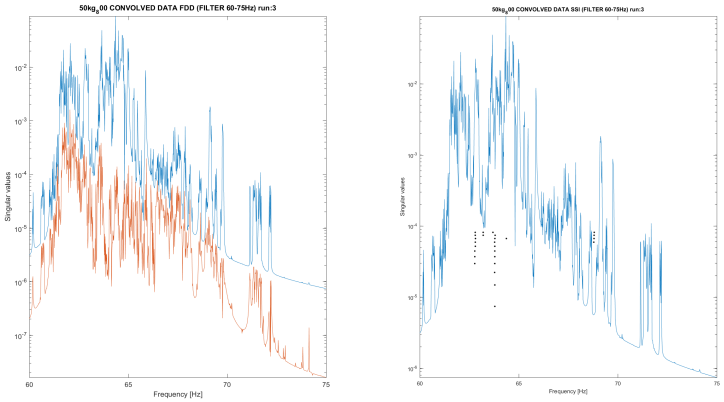


(b) 50kg FDD SSI output, run 2

Figure A4.50kg (28.03.2017): Run 2 (segment 1)

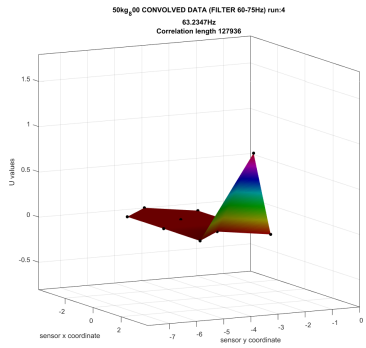


(a) 50kg mode shape, run 3

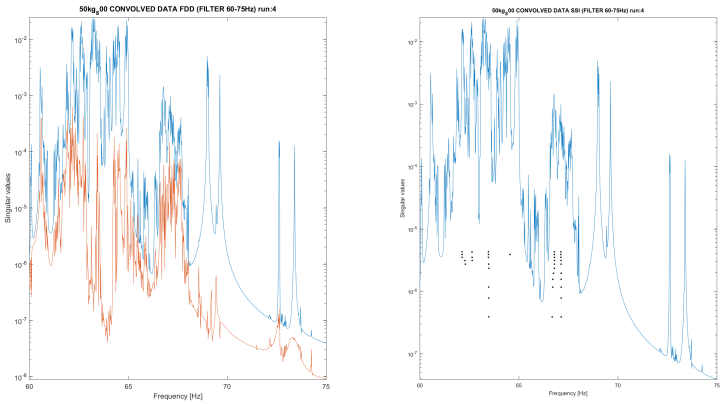


(b) 50kg FDD SSI output, run 3

Figure A4.50kg (28.03.2017): Run 3 (segment 1)

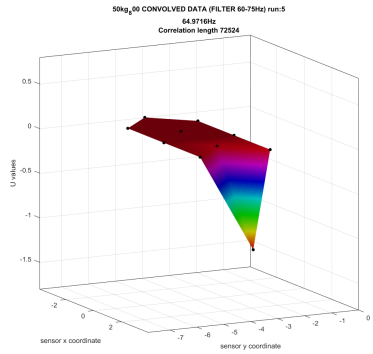


(a) 50kg mode shape, run 4

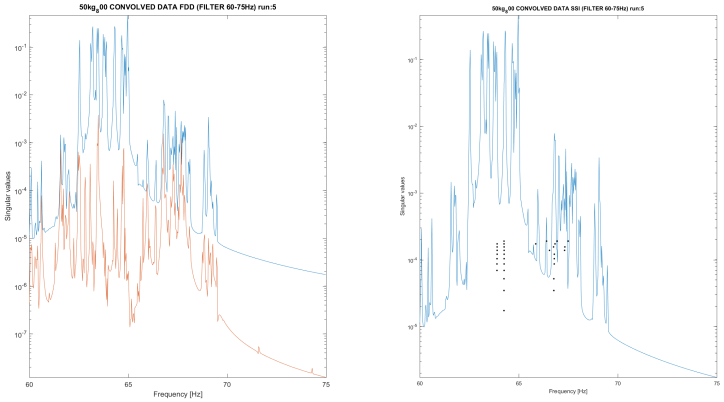


(b) 50kg FDD SSI output, run 4

Figure A4.50kg (28.03.2017): Run 4 (segment 1)

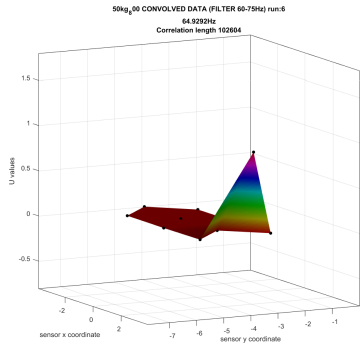


(a) 50kg mode shape, run 5

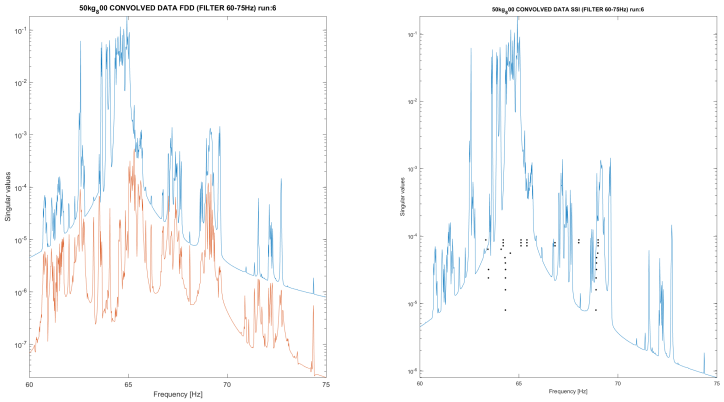


(b) 50kg FDD SSI output, run 5

Figure A4.50kg (28.03.2017): Run 5 (segment 1)

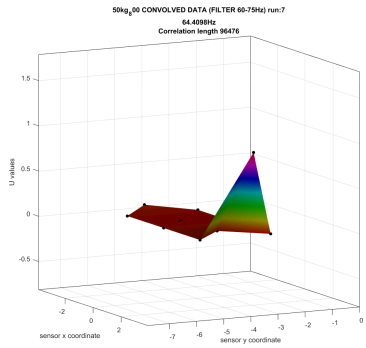


(a) 50kg mode shape, run 6

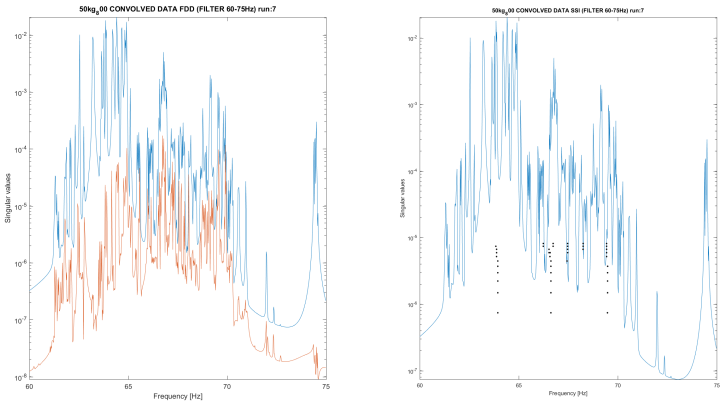


(b) 50kg FDD SSI output, run 6

Figure A4.50kg (28.03.2017): Run 6 (segment 1)

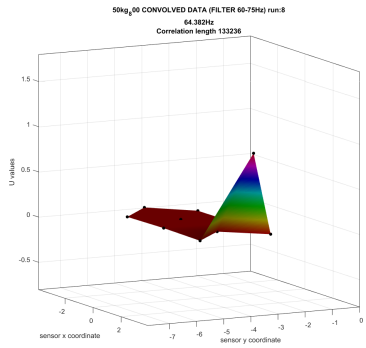


(a) 50kg mode shape, run 7

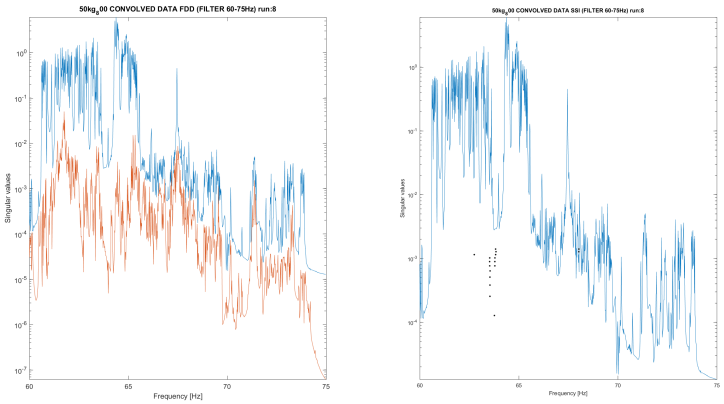


(b) 50kg FDD SSI output, run 7

Figure A4.50kg (28.03.2017): Run 7 (segment 1)

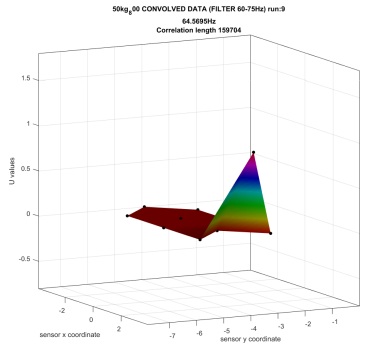


(a) 50kg mode shape, run 8

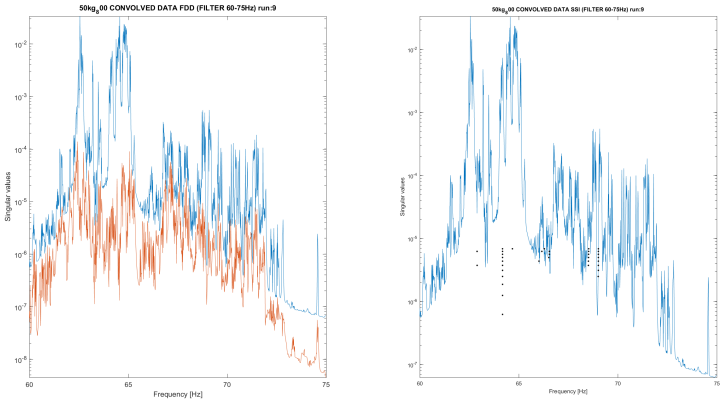


(b) 50kg FDD SSI output, run 8

Figure A4.50kg (28.03.2017): Run 8 (segment 1)

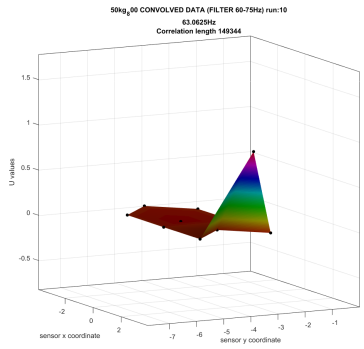


(a) 50kg mode shape, run 9

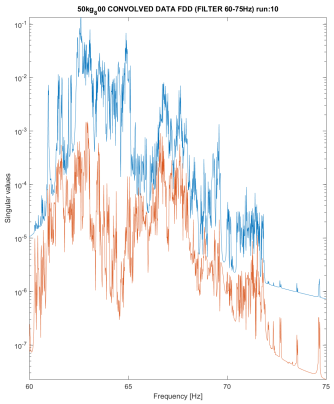


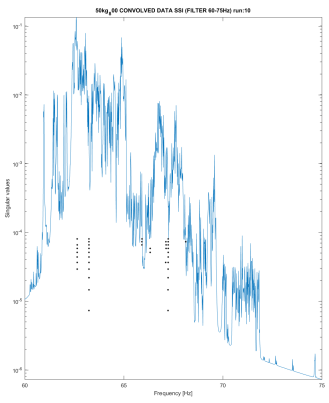
(b) 50kg FDD SSI output, run 9

Figure A4.50kg (28.03.2017): Run 9 (segment 1)



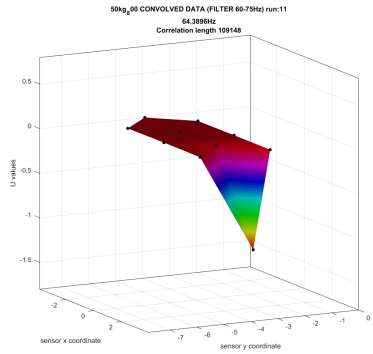
(a) 50kg mode shape, run 10



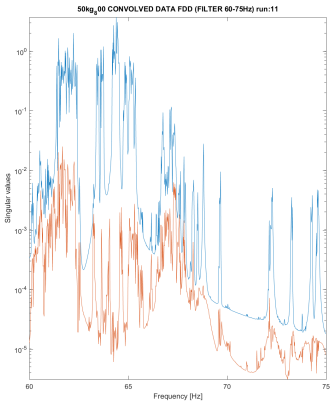


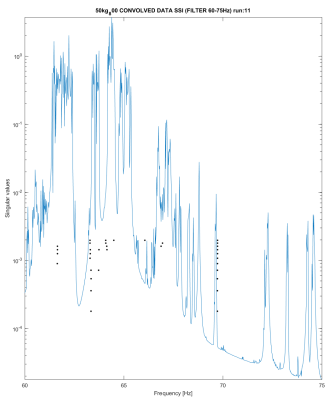
(b) 50kg FDD SSI output, run 10

Figure A4.50kg (28.03.2017): Run 10 (segment 1)



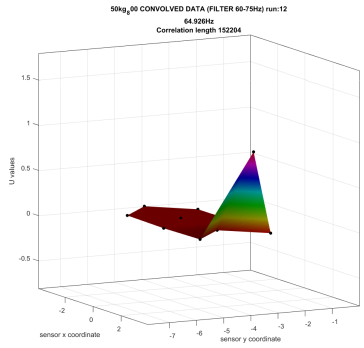
(a) 50kg mode shape, run 11



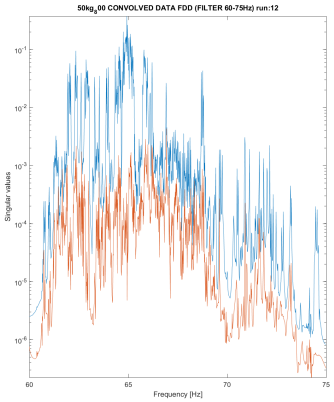


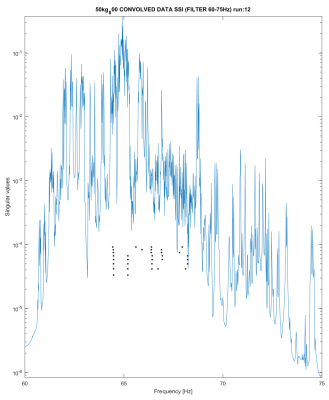
(b) 50kg FDD SSI output, run 11

Figure A4.50kg (28.03.2017): Run 11 (segment 1)



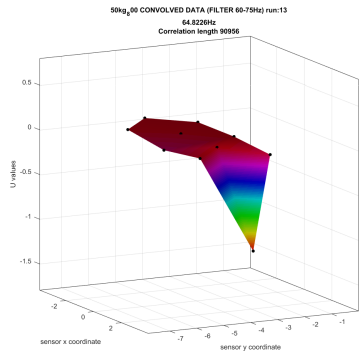
(a) 50kg mode shape, run 12



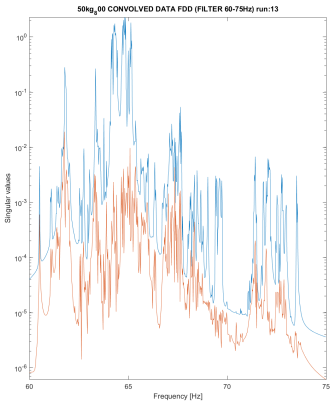


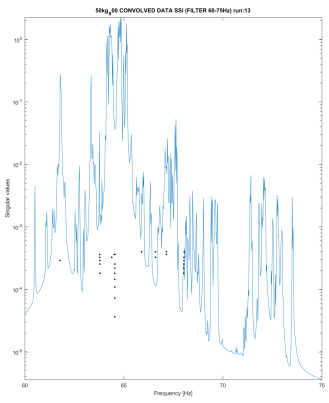
(b) 50kg FDD SSI output, run 12

Figure A4.50kg (28.03.2017): Run 12 (segment 1)



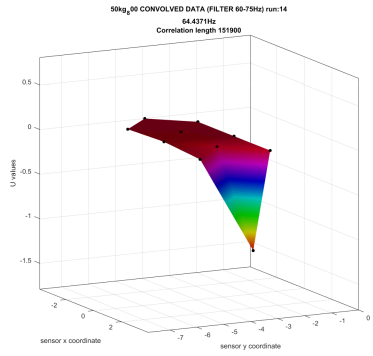
(a) 50kg mode shape, run 13



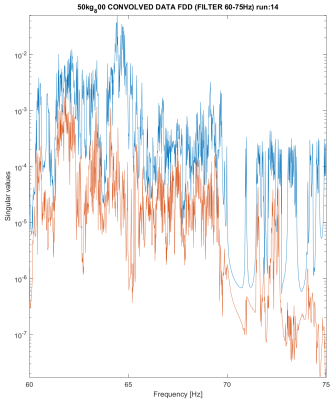


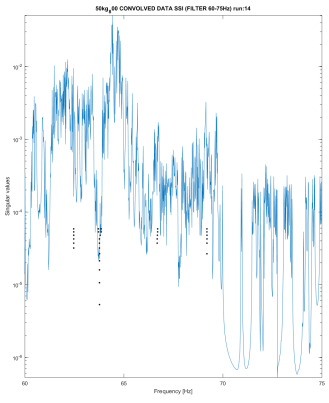
(b) 50kg FDD SSI output, run 13

Figure A4.50kg (28.03.2017): Run 13 (segment 1)



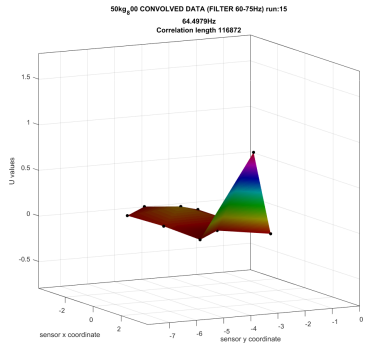
(a) 50kg mode shape, run 14



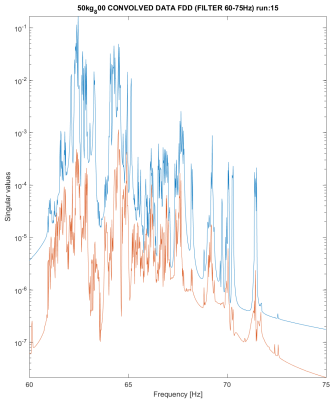


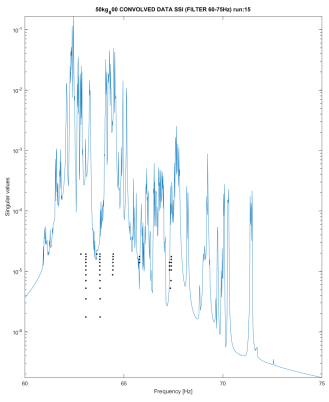
(b) 50kg FDD SSI output, run 14

Figure A4.50kg (28.03.2017): Run 14 (segment 1)



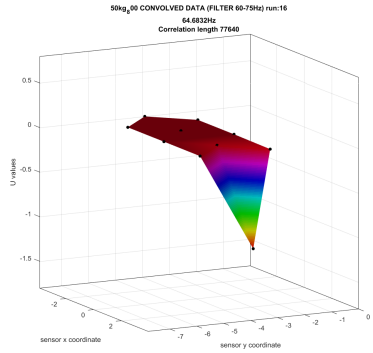
(a) 50kg mode shape, run 15



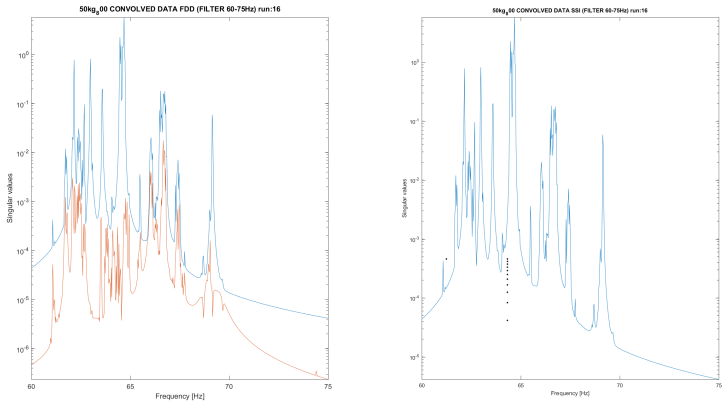


(b) 50kg FDD SSI output, run 15

Figure A4.50kg (28.03.2017): Run 15 (segment 1)

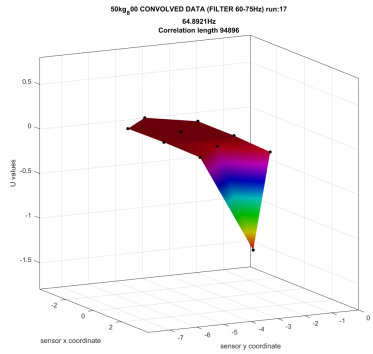


(a) 50kg mode shape, run 16

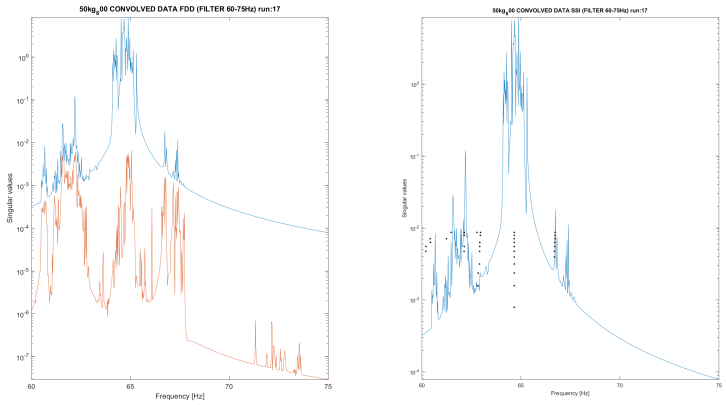


(b) 50kg FDD SSI output, run 16

Figure A4.50kg (28.03.2017): Run 16 (segment 1)

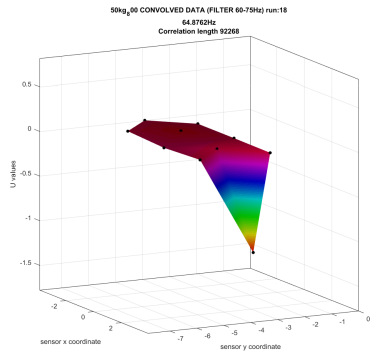


(a) 50kg mode shape, run 17

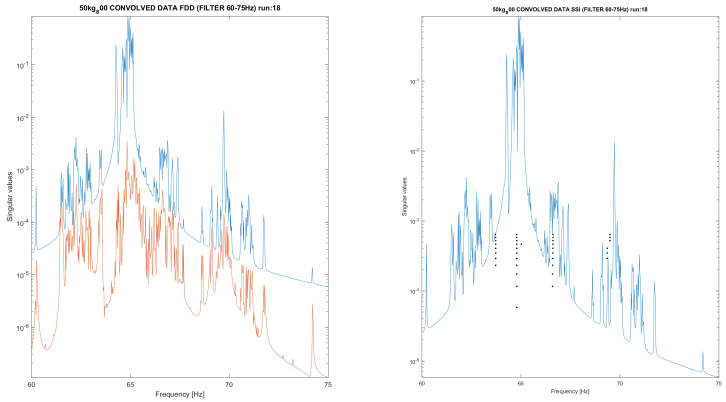


(b) 50kg FDD SSI output, run 17

Figure A4.50kg (28.03.2017): Run 17 (segment 1)

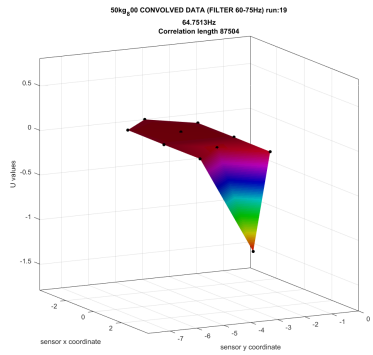


(a) 50kg mode shape, run 18

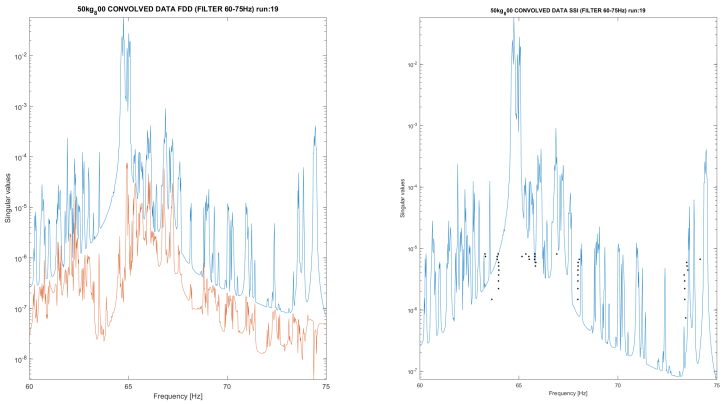


(b) 50kg FDD SSI output, run 18

Figure A4.50kg (28.03.2017): Run 18 (segment 1)

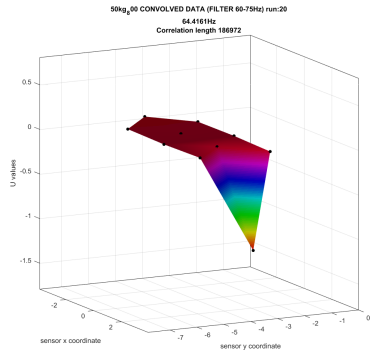


(a) 50kg mode shape, run 19

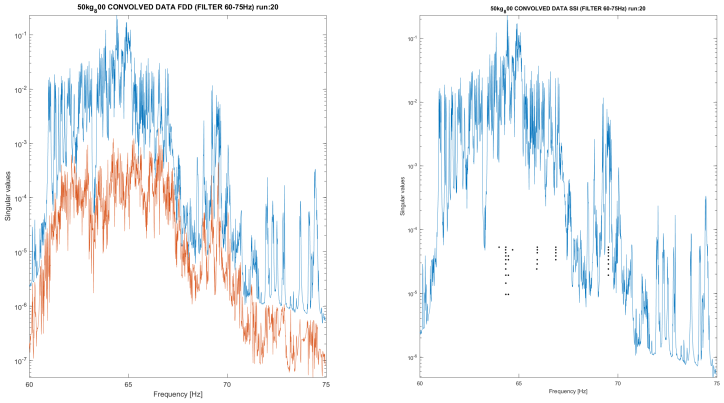


(b) 50kg FDD SSI output, run 19

Figure A4.50kg (28.03.2017): Run 19 (segment 1)

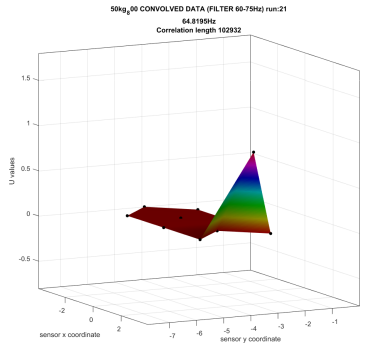


(a) 50kg mode shape, run 20

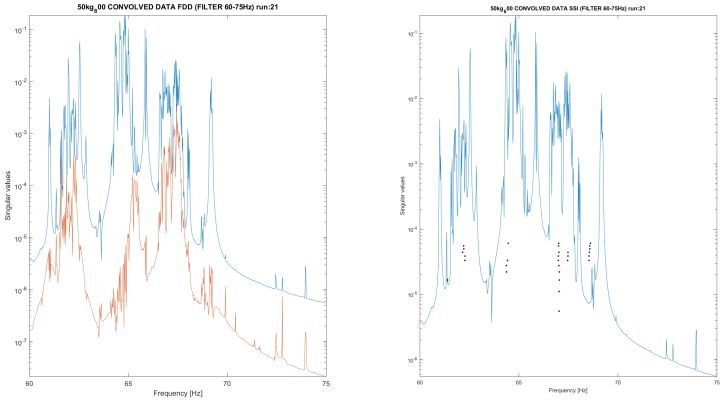


(b) 50kg FDD SSI output, run 20

Figure A4.50kg (28.03.2017): Run 20 (segment 1)

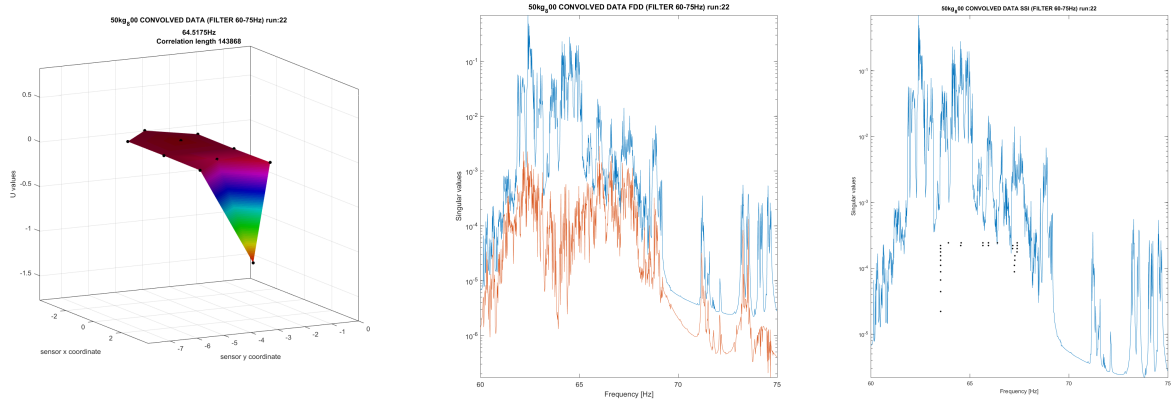


(a) 50kg mode shape, run 21



(b) 50kg FDD SSI output, run 21

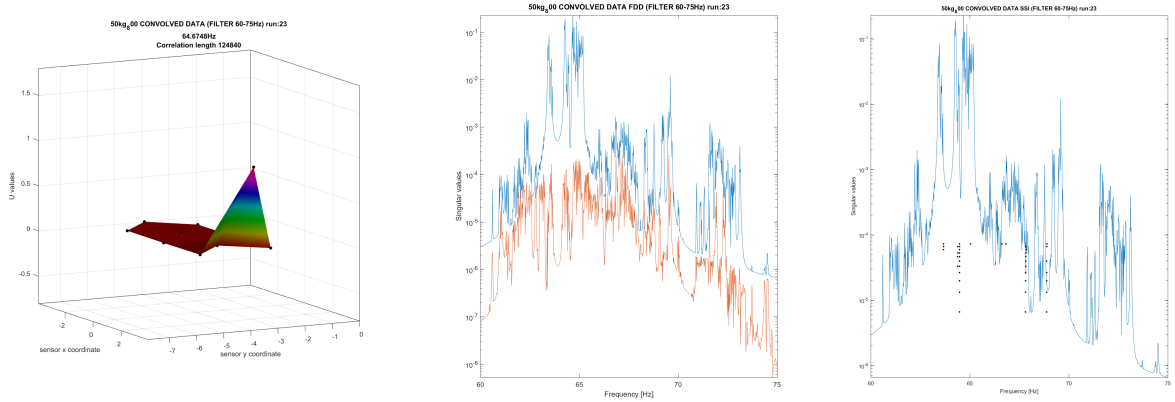
Figure A4.50kg (28.03.2017): Run 21 (segment 1)



(a) 50kg mode shape, run 22

(b) 50kg FDD SSI output, run 22

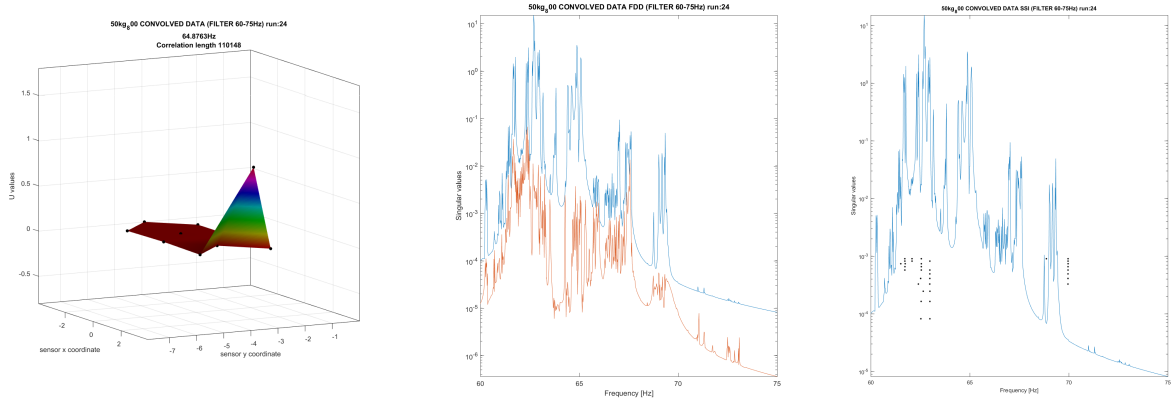
Figure A4.50kg (28.03.2017): Run 22 (segment 1)



(a) 50kg mode shape, run 23

(b) 50kg FDD SSI output, run 23

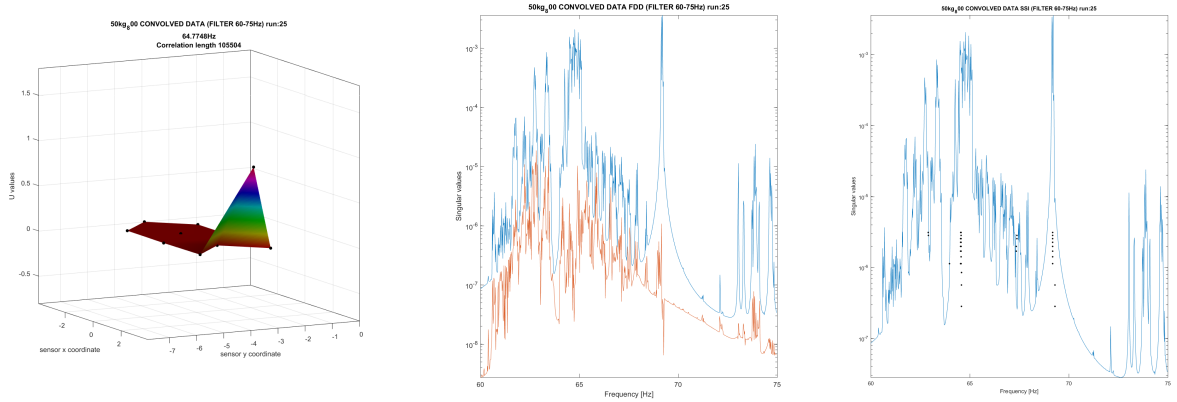
Figure A4.50kg (28.03.2017): Run 23 (segment 1)



(a) 50kg mode shape, run 24

(b) 50kg FDD SSI output, run 24

Figure A4.50kg (28.03.2017): Run 24 (segment 1)

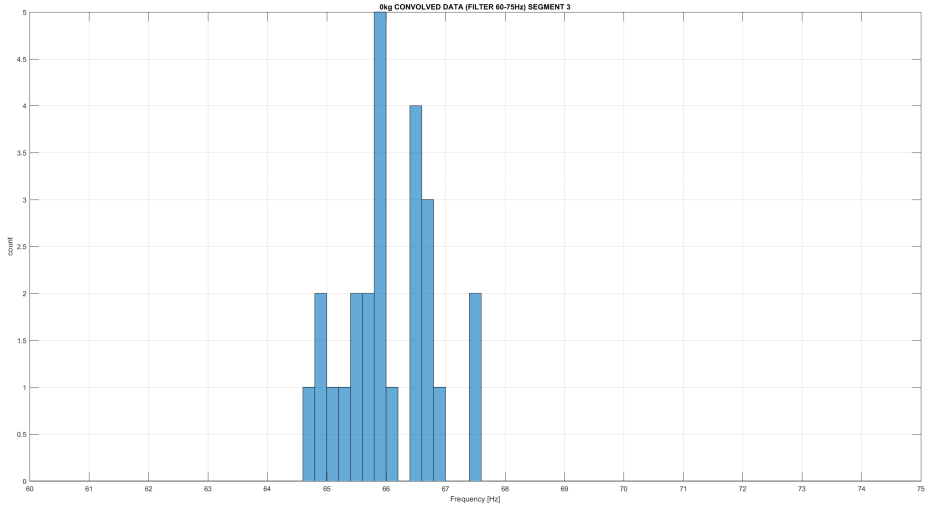


(a) 50kg mode shape, run 25

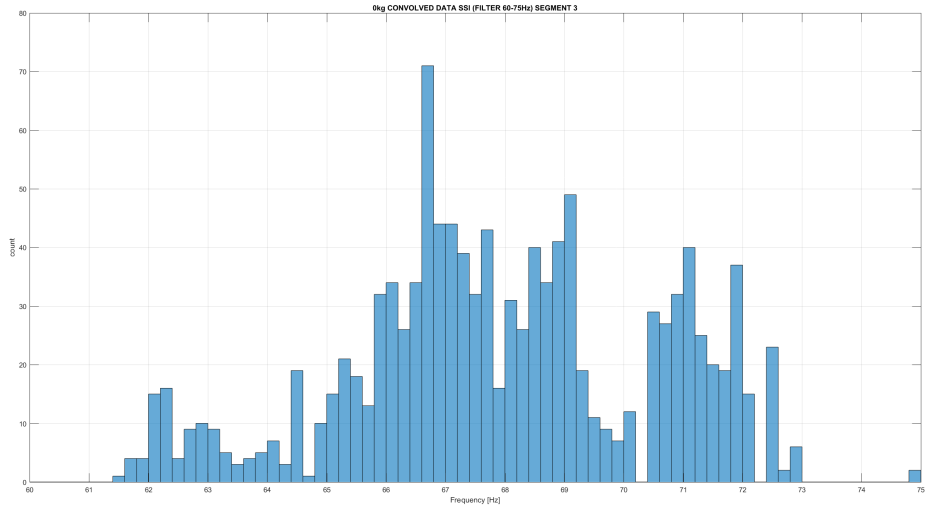
(b) 50kg FDD SSI output, run 25

Figure A4.50kg (28.03.2017): Run 25 (segment 1)

Data 0kg-50kg-75kg-100kg segment 3 (Reduced order PF)

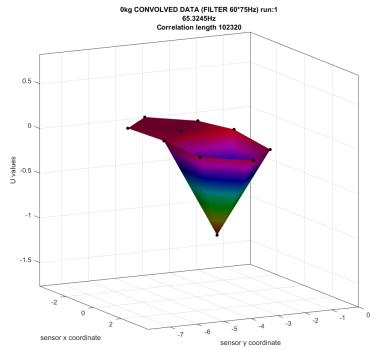


(a) 0kg FDD histogram

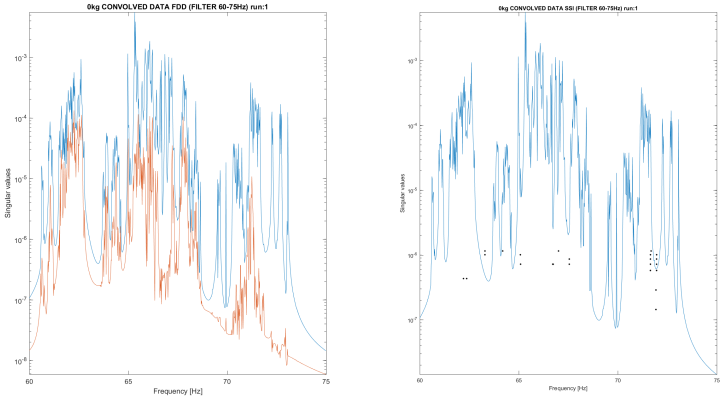


(b) 0kg SSI histogram

Figure A4.0kg: Histograms of identified modes, 0kg data (segment 3)

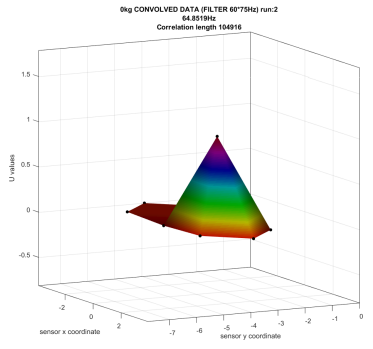


(a) 0kg mode shape, run 1

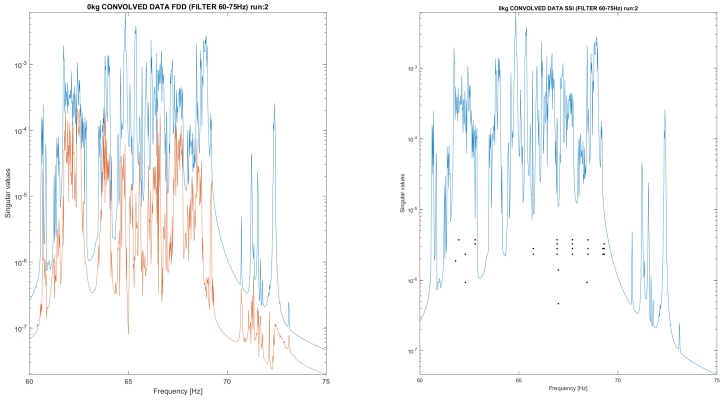


(b) 0kg FDD SSI output, run 1

Figure A4.0kg: Run 1 (segment 3)

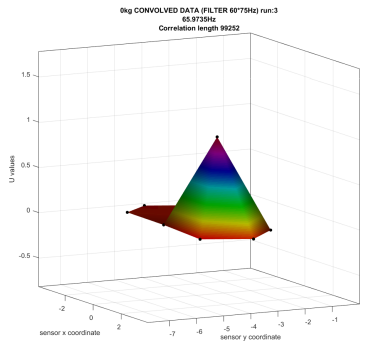


(a) 0kg mode shape, run 2

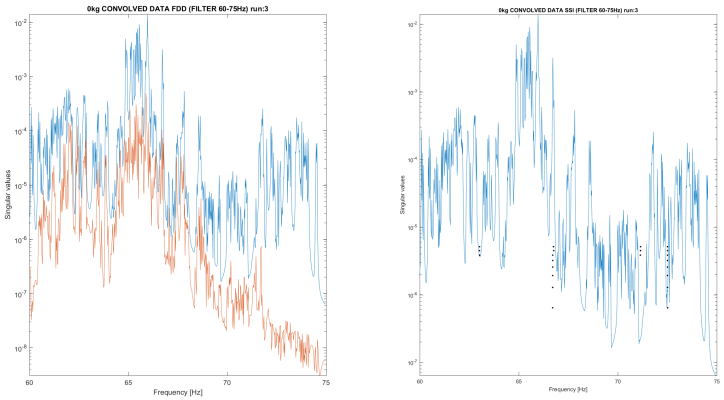


(b) 0kg FDD SSI output, run 2

Figure A4.0kg: Run 2 (segment 3)

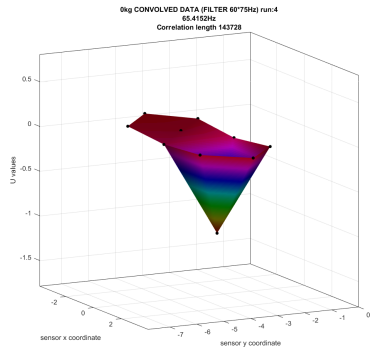


(a) 0kg mode shape, run 3

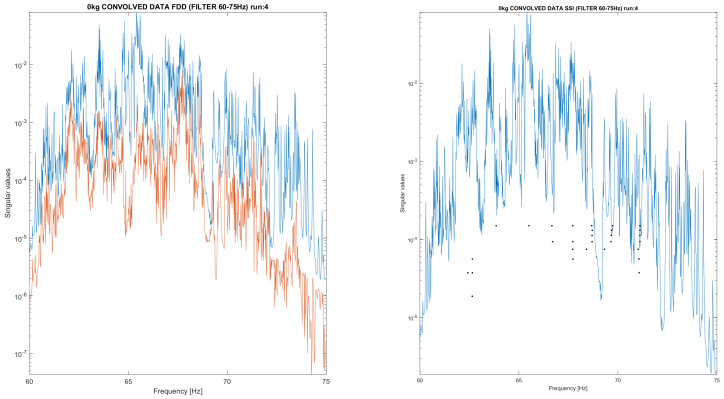


(b) 0kg FDD SSI output, run 3

Figure A4.0kg: Run 3 (segment 3)

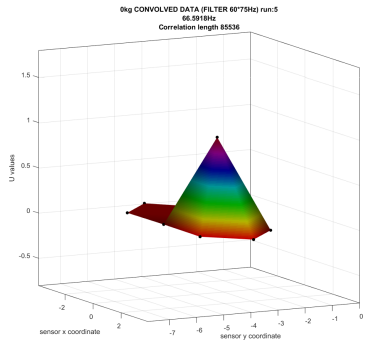


(a) 0kg mode shape, run 4

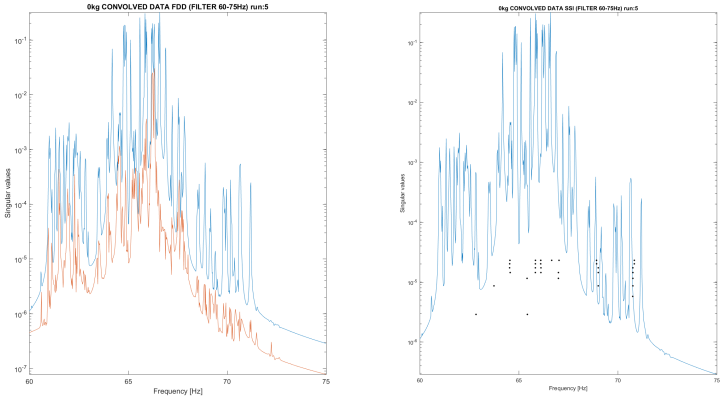


(b) 0kg FDD SSI output, run 4

Figure A4.0kg: Run 4 (segment 3)

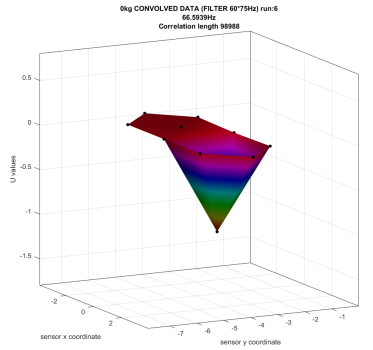


(a) 0kg mode shape, run 5

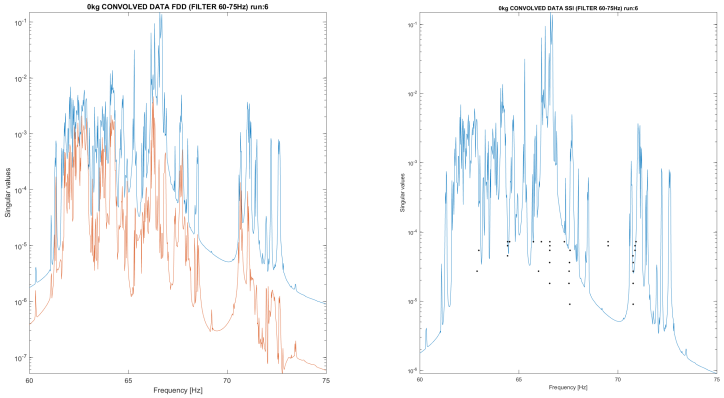


(b) 0kg FDD SSI output, run 5

Figure A4.0kg: Run 5 (segment 3)

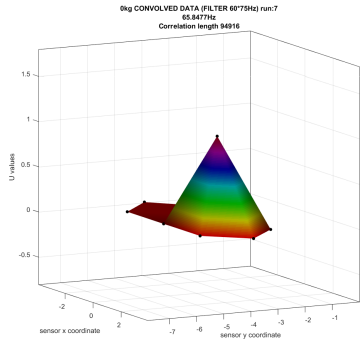


(a) 0kg mode shape, run 6

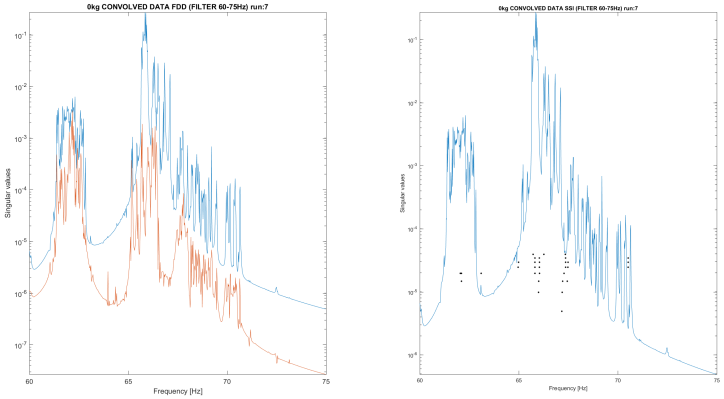


(b) 0kg FDD SSI output, run 6

Figure A4.0kg: Run 6 (segment 3)

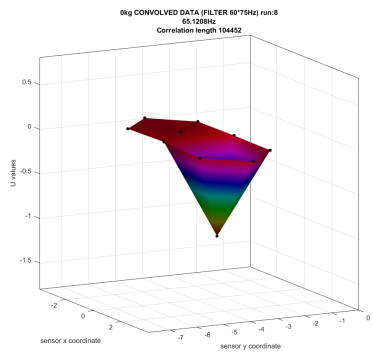


(a) 0kg mode shape, run 7

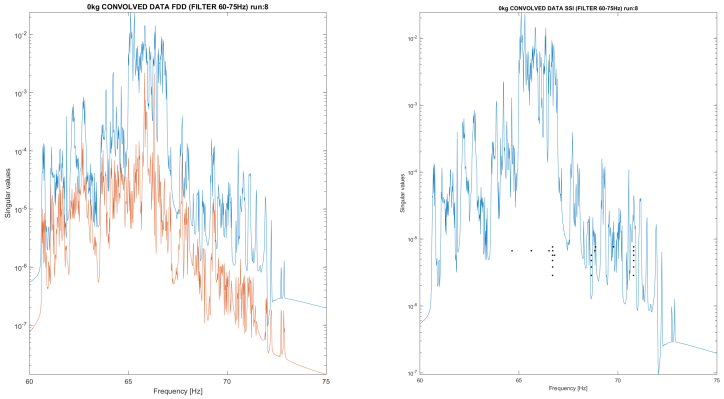


(b) 0kg FDD SSI output, run 7

Figure A4.0kg: Run 7 (segment 3)

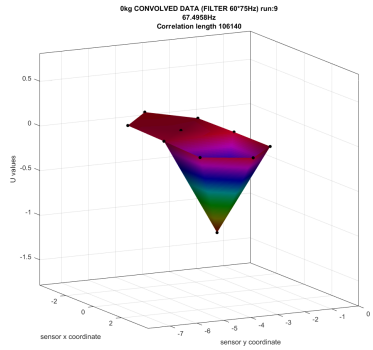


(a) 0kg mode shape, run 8

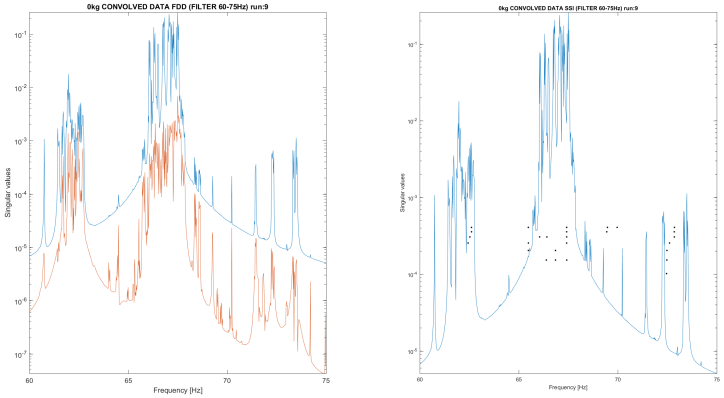


(b) 0kg FDD SSI output, run 8

Figure A4.0kg: Run 8 (segment 3)

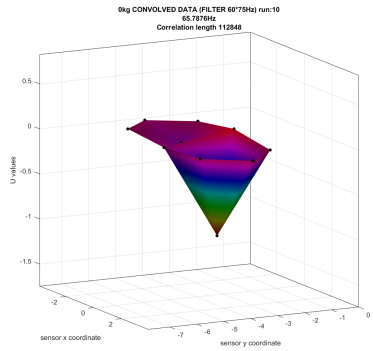


(a) 0kg mode shape, run 9

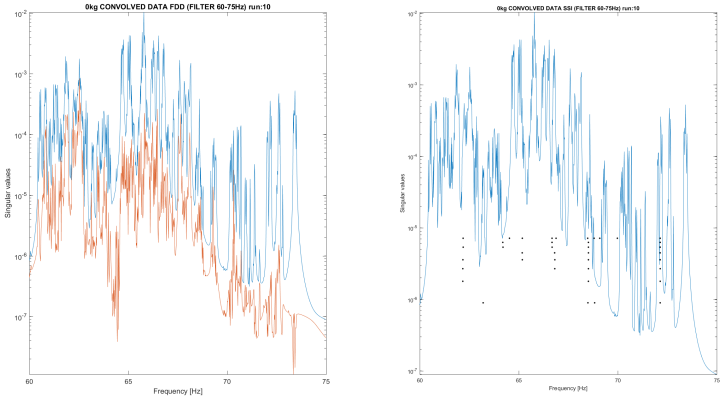


(b) 0kg FDD SSI output, run 9

Figure A4.0kg: Run 9 (segment 3)

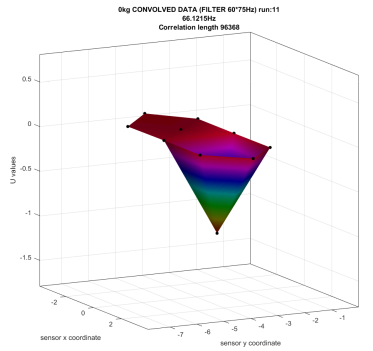


(a) 0kg mode shape, run 10

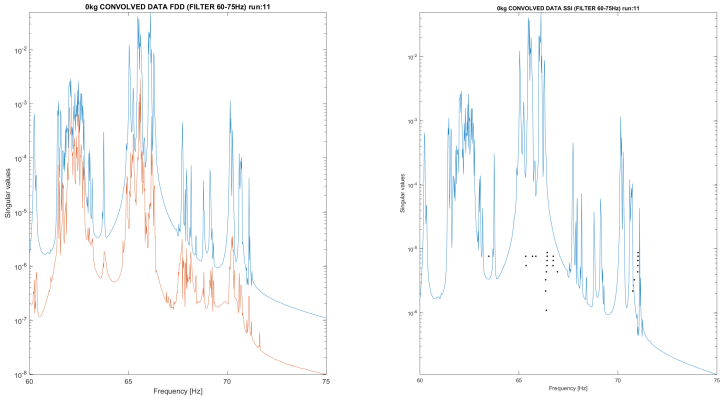


(b) 0kg FDD SSI output, run 10

Figure A4.0kg: Run 10 (segment 3)

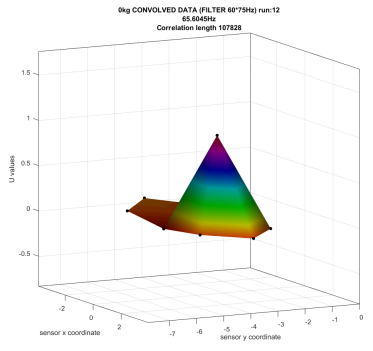


(a) 0kg mode shape, run 11

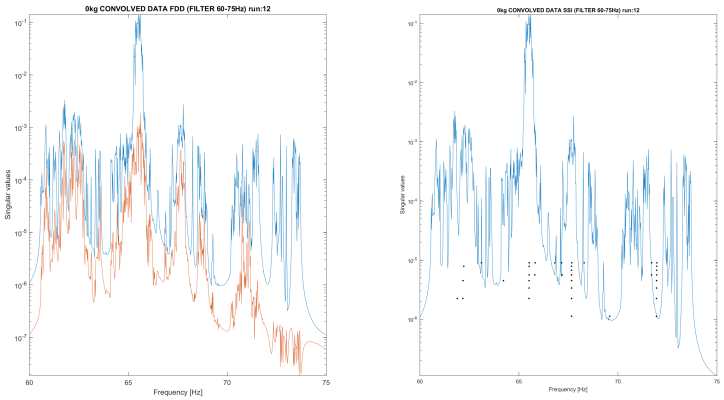


(b) 0kg FDD SSI output, run 11

Figure A4.0kg: Run 11 (segment 3)

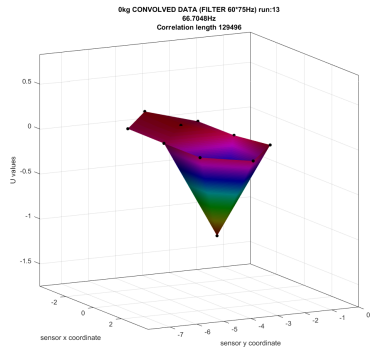


(a) 0kg mode shape, run 12

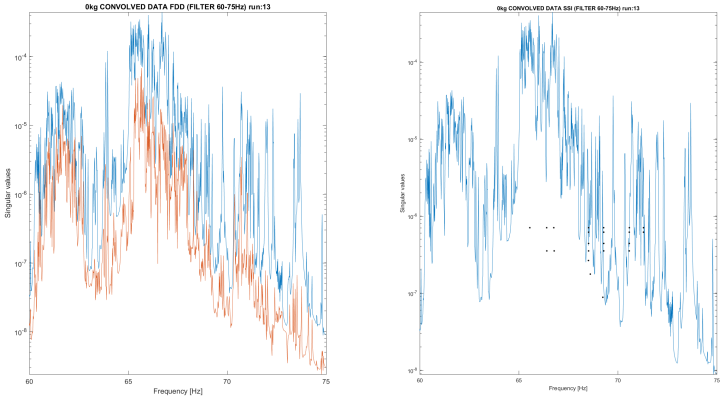


(b) 0kg FDD SSI output, run 12

Figure A4.0kg: Run 12 (segment 3)

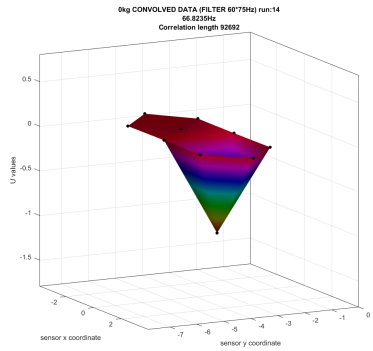


(a) 0kg mode shape, run 13

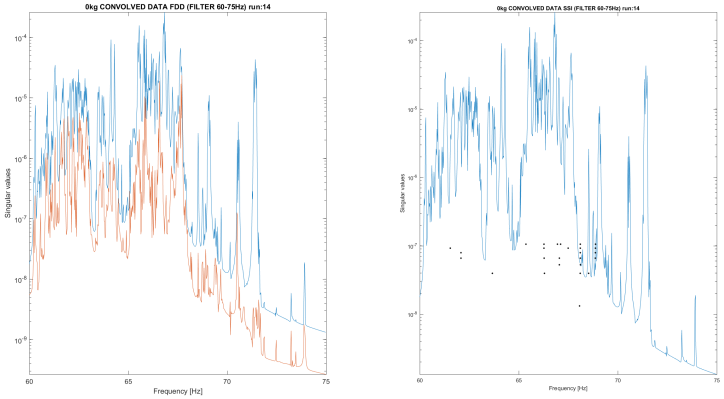


(b) 0kg FDD SSI output, run 13

Figure A4.0kg: Run 13 (segment 3)

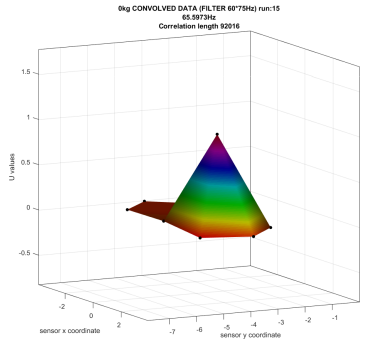


(a) 0kg mode shape, run 14

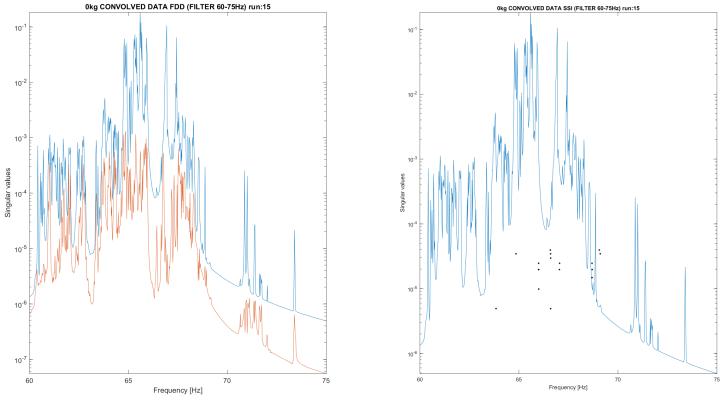


(b) 0kg FDD SSI output, run 14

Figure A4.0kg: Run 14 (segment 3)

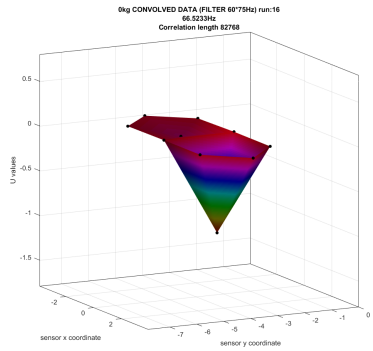


(a) 0kg mode shape, run 15

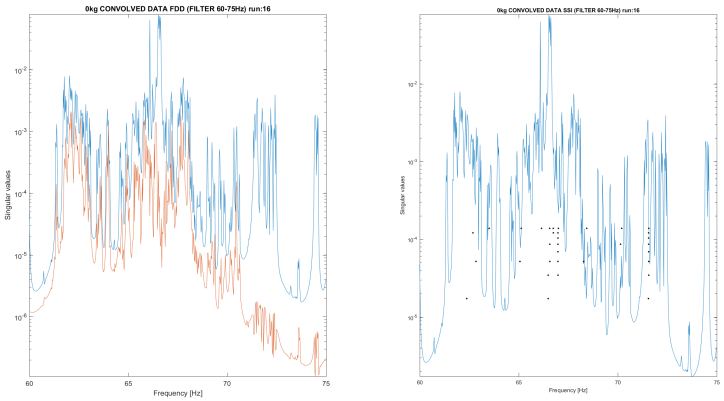


(b) 0kg FDD SSI output, run 15

Figure A4.0kg: Run 15 (segment 3)

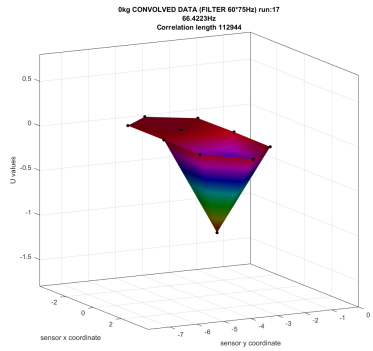


(a) 0kg mode shape, run 16

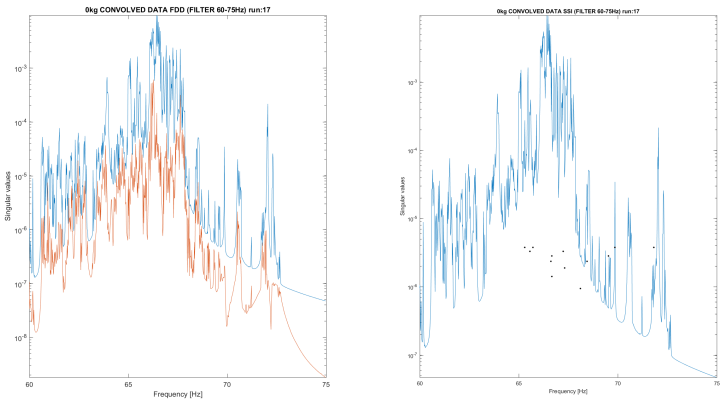


(b) 0kg FDD SSI output, run 16

Figure A4.0kg: Run 16 (segment 3)

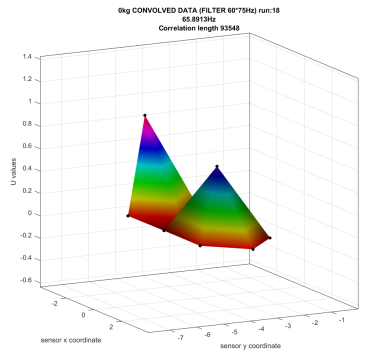


(a) 0kg mode shape, run 17

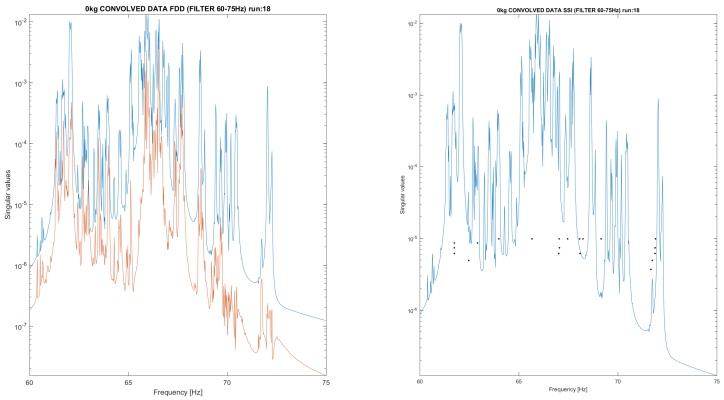


(b) 0kg FDD SSI output, run 17

Figure A4.0kg: Run 17 (segment 3)

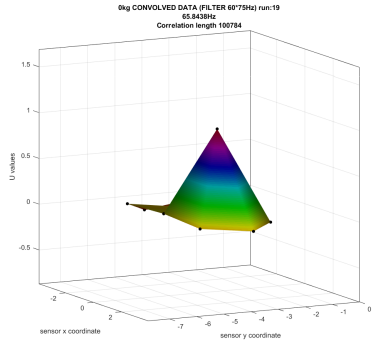


(a) 0kg mode shape, run 18

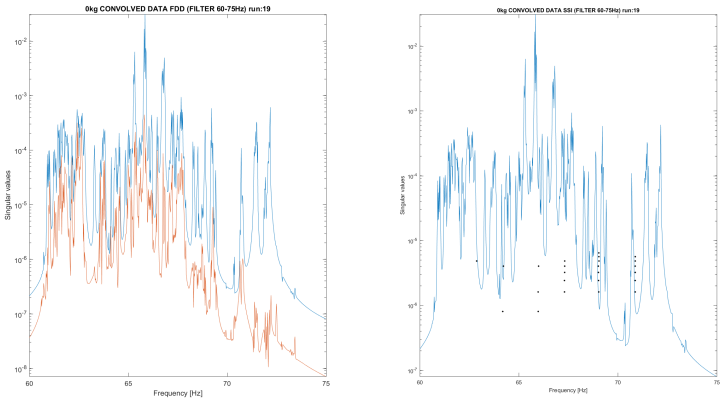


(b) 0kg FDD SSI output, run 18

Figure A4.0kg: Run 18 (segment 3)

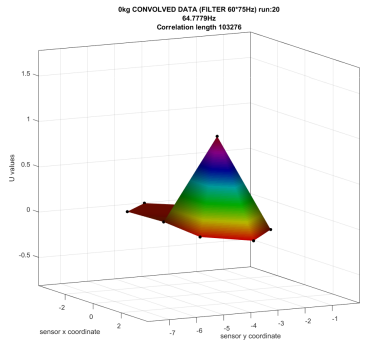


(a) 0kg mode shape, run 19

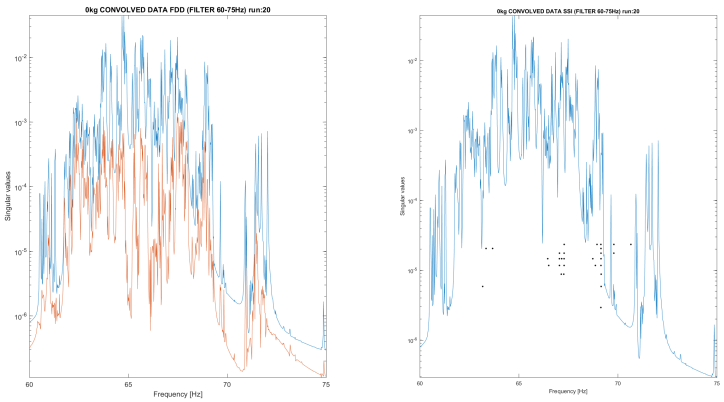


(b) 0kg FDD SSI output, run 19

Figure A4.0kg: Run 19 (segment 3)

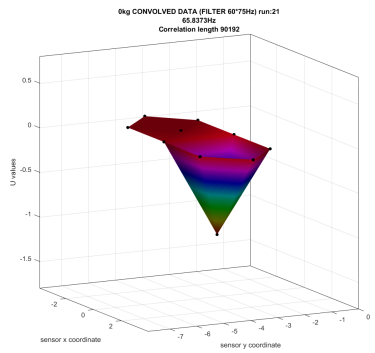


(a) 0kg mode shape, run 20

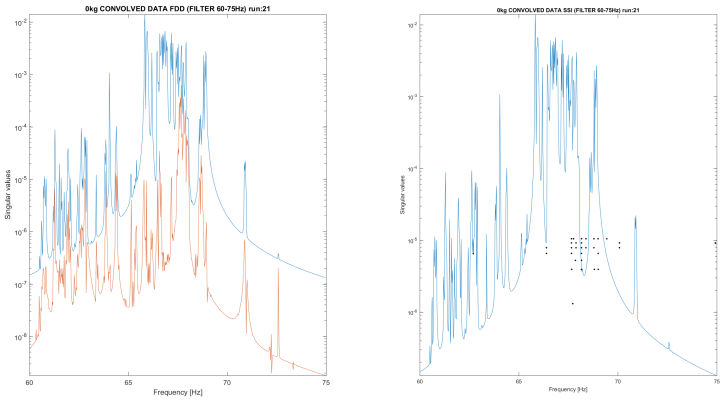


(b) 0kg FDD SSI output, run 21

Figure A4.0kg: Run 20 (segment 3)

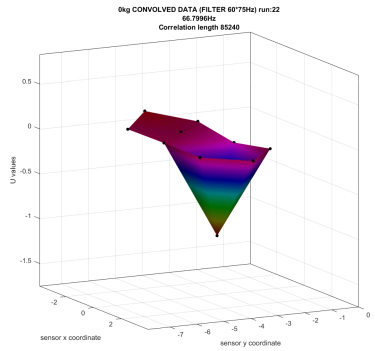


(a) 0kg mode shape, run 21

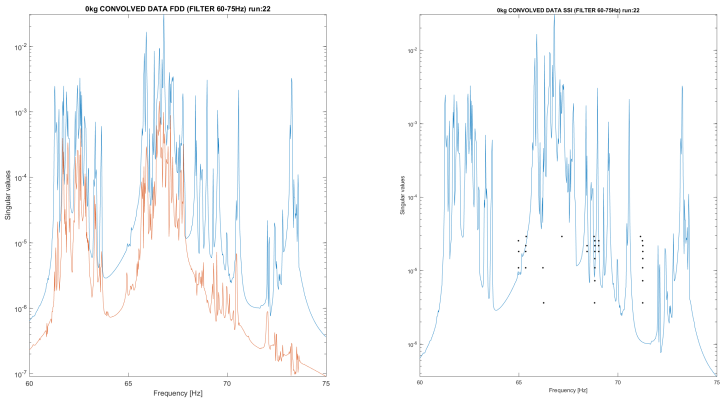


(b) 0kg FDD SSI output, run 21

Figure A4.0kg: Run 21 (segment 3)

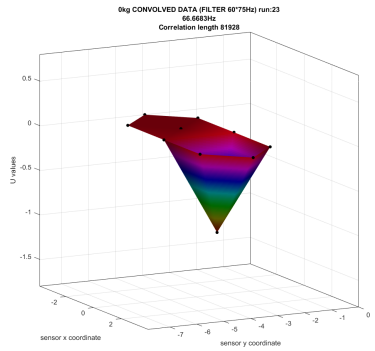


(a) 0kg mode shape, run 22

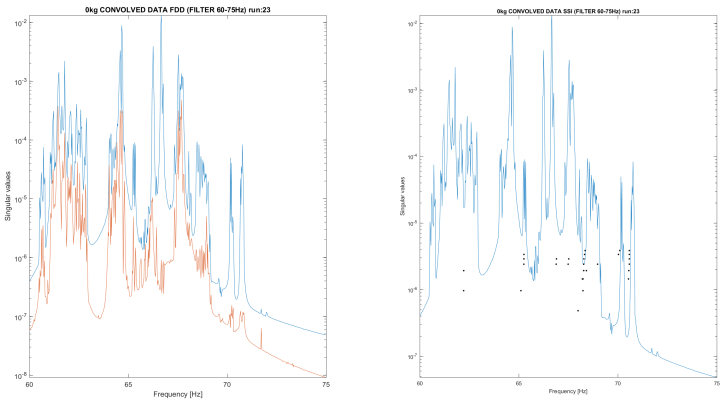


(b) 0kg FDD SSI output, run 22

Figure A4.0kg: Run 22 (segment 3)

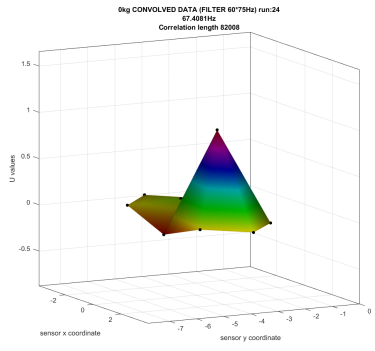


(a) 0kg mode shape, run 23

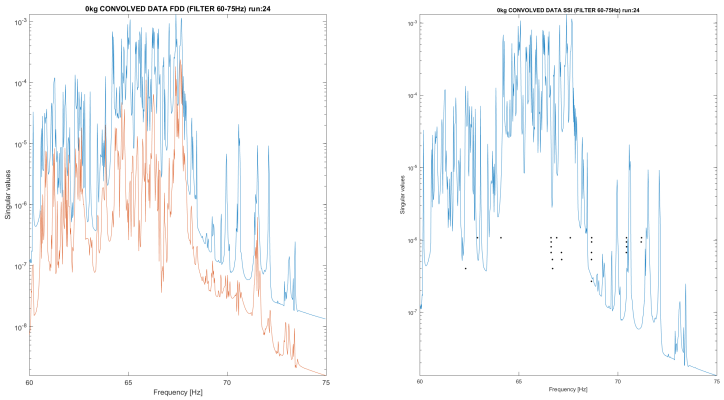


(b) 0kg FDD SSI output, run 23

Figure A4.0kg: Run 23 (segment 3)

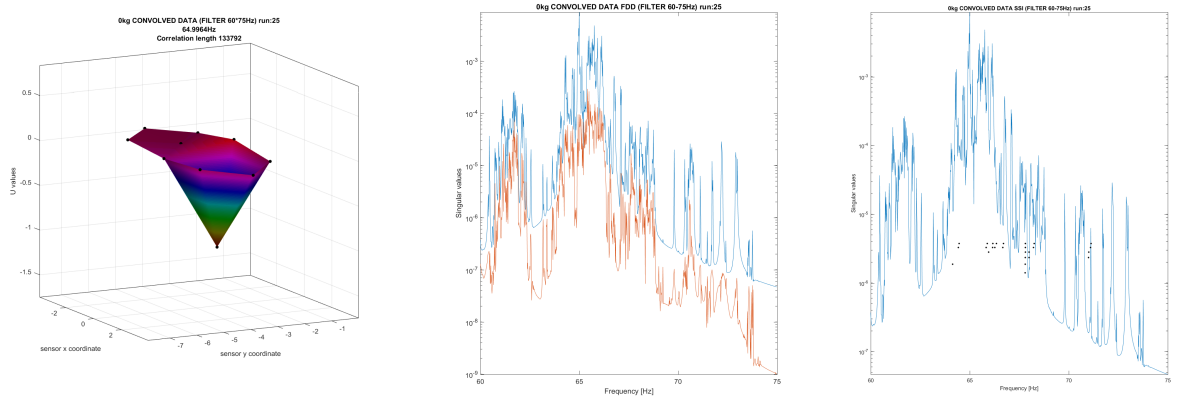


(a) 0kg mode shape, run 24



(b) 0kg FDD SSI output, run 24

Figure A4.0kg: Run 24 (segment 3)

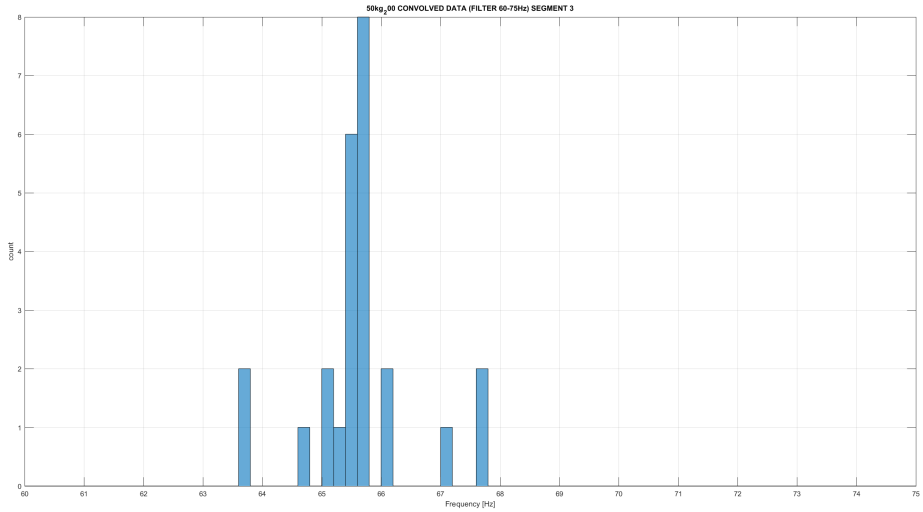


(a) 0kg mode shape, run 25

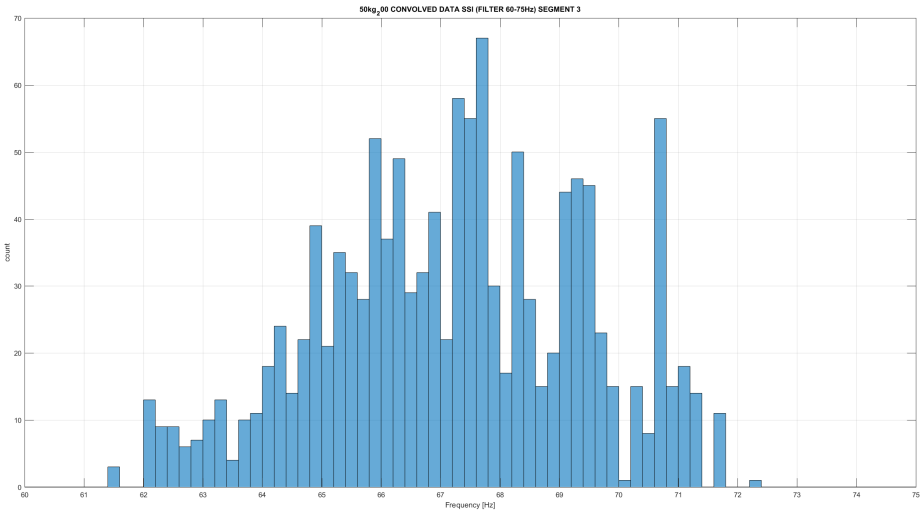
(b) 0kg FDD SSI output, run 25

Figure A4.0kg: Run 25 (segment 3)

50kg data segment 3

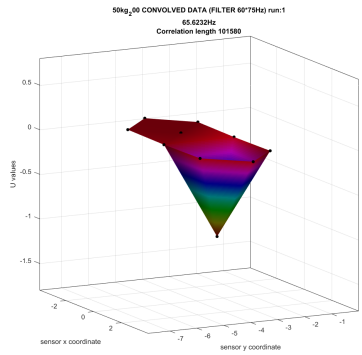


(a) 50kg FDD histogram

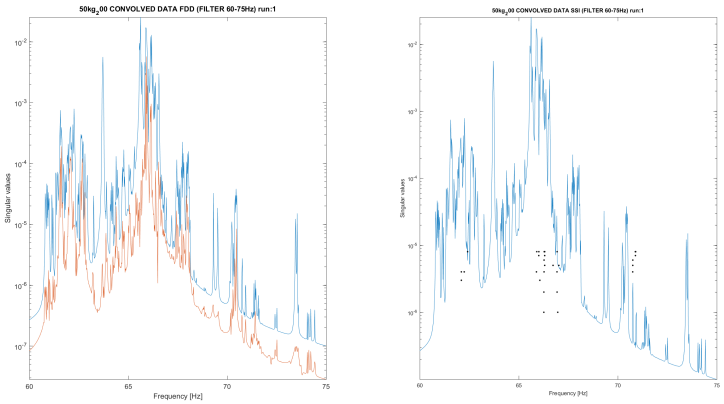


(b) 50kg SSI histogram

Figure A4.50kg: Histograms of identified modes, 50kg data (segment 3)

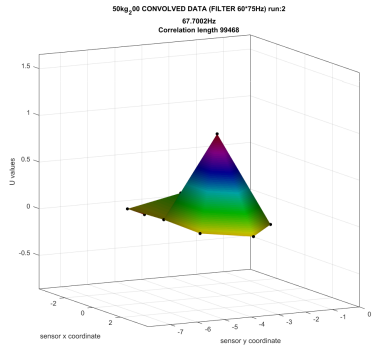


(a) 50kg mode shape, run 1

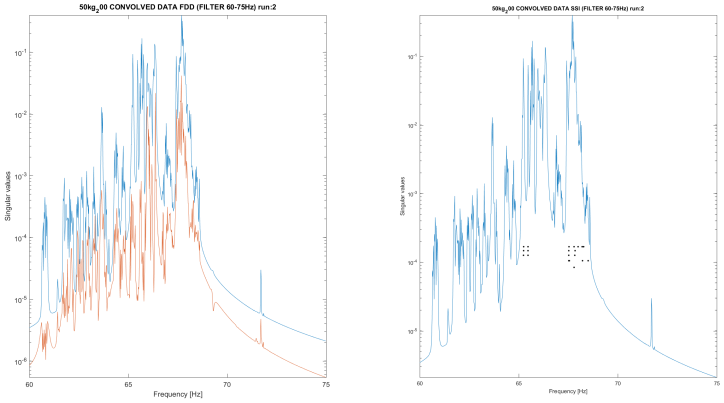


(b) 50kg FDD SSI output, run 1

Figure A4.50kg: Run 1 (segment 3)

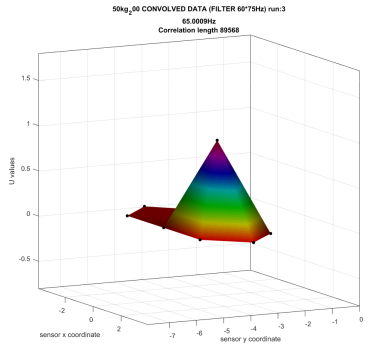


(a) 50kg mode shape, run 2

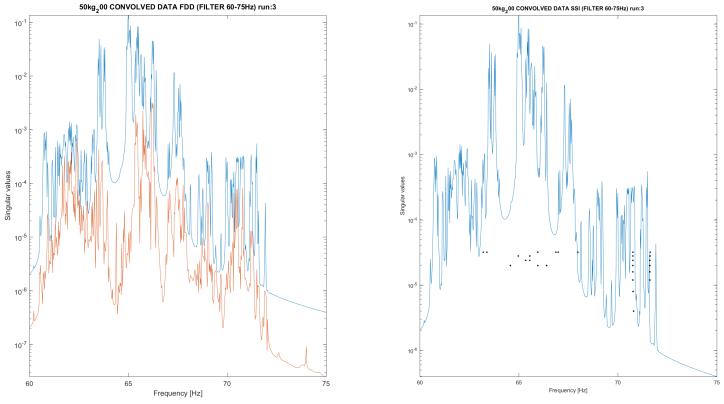


(b) 50kg FDD SSI output, run 2

Figure A4.50kg: Run 2 (segment 3)

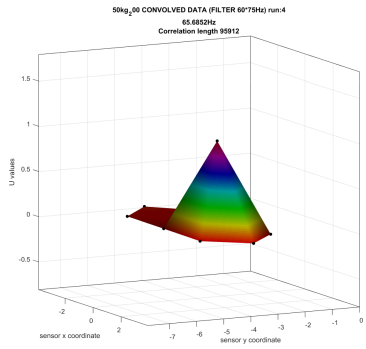


(a) 50kg mode shape, run 3

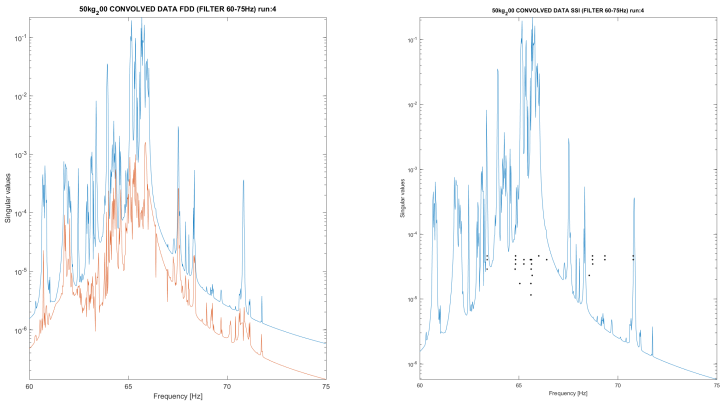


(b) 50kg FDD SSI output, run 3

Figure A4.50kg: Run 3 (segment 3)

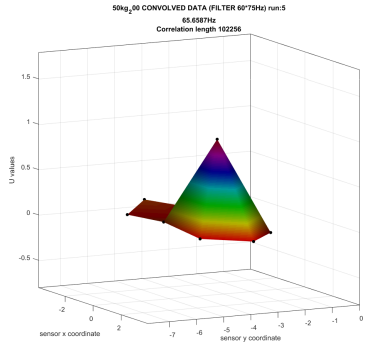


(a) 50kg mode shape, run 4

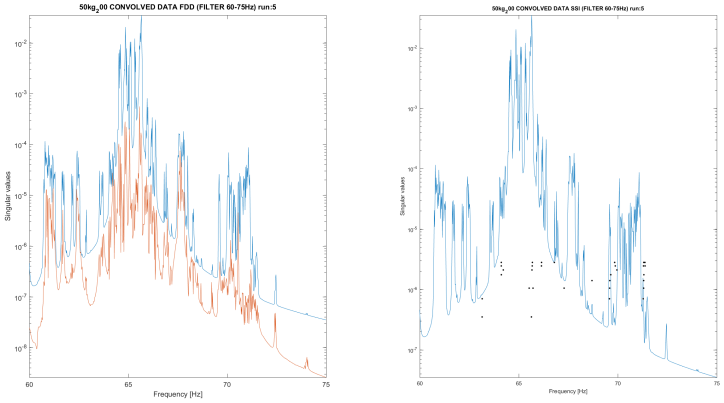


(b) 50kg FDD SSI output, run 4

Figure A4.50kg: Run 4 (segment 3)

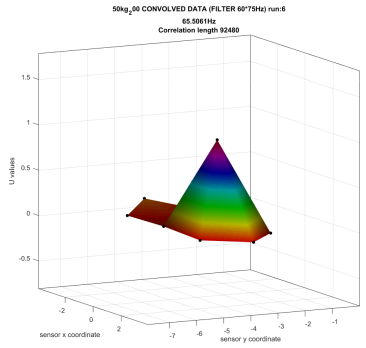


(a) 50kg mode shape, run 5

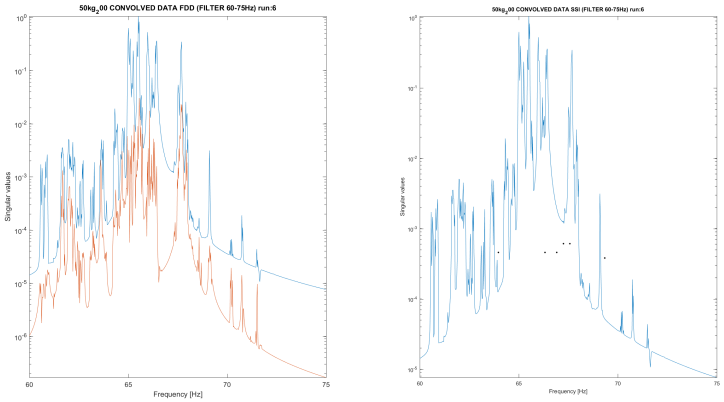


(b) 50kg FDD SSI output, run 5

Figure A4.50kg: Run 5 (segment 3)

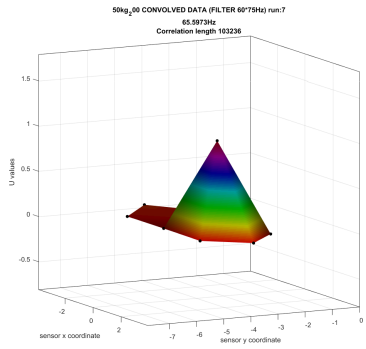


(a) 50kg mode shape, run 6

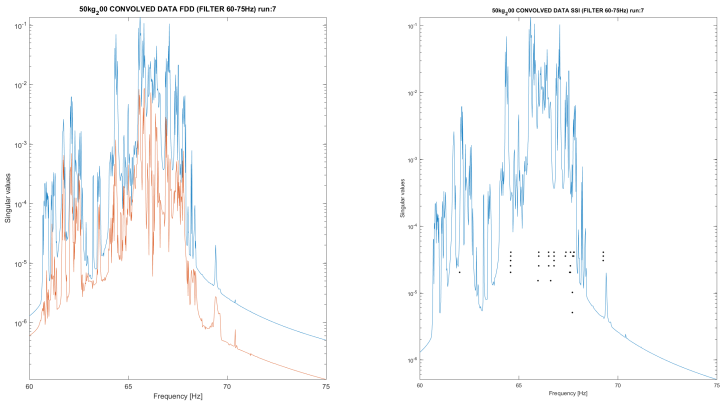


(b) 50kg FDD SSI output, run 6

Figure A4.50kg: Run 6 (segment 3)

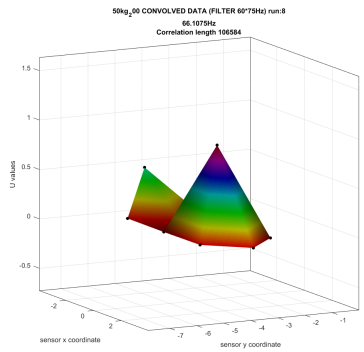


(a) 50kg mode shape, run 7

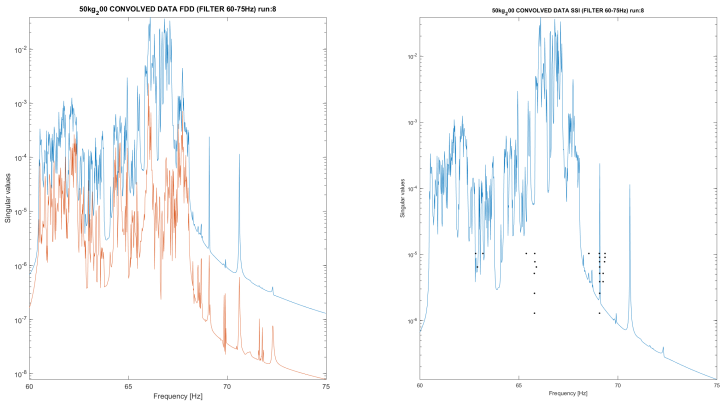


(b) 50kg FDD SSI output, run 7

Figure A4.50kg: Run 7 (segment 3)

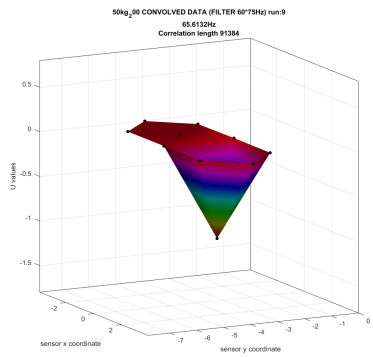


(a) 50kg mode shape, run 8

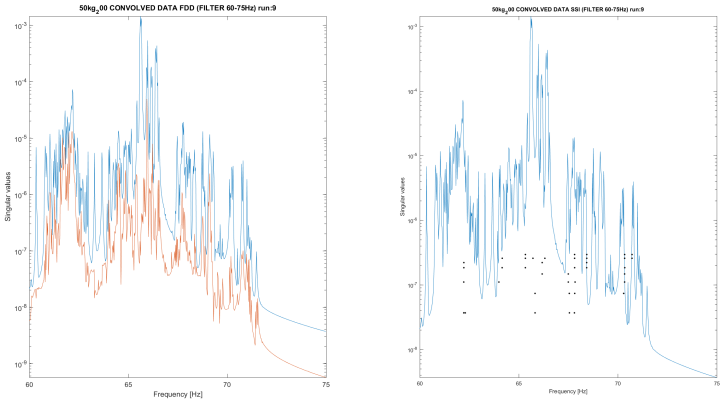


(b) 50kg FDD SSI output, run 8

Figure A4.50kg: Run 8 (segment 3)

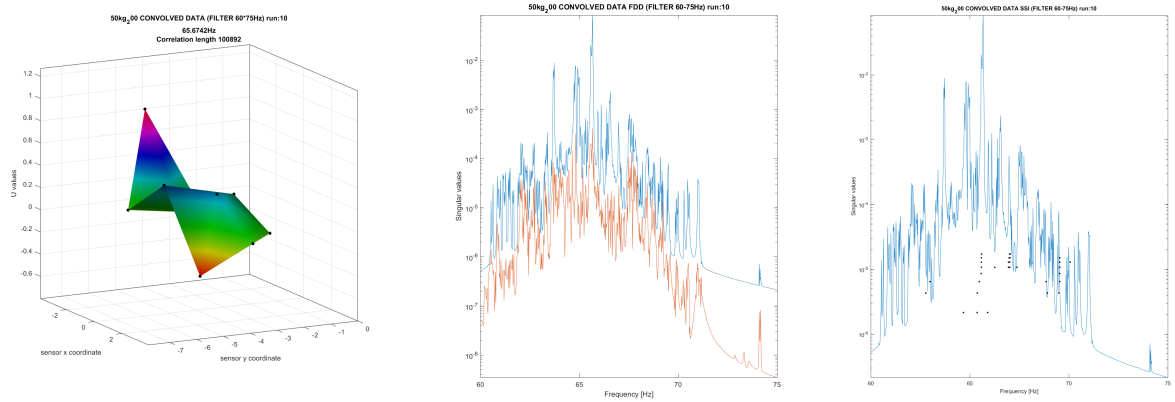


(a) 50kg mode shape, run 9



(b) 50kg FDD SSI output, run 9

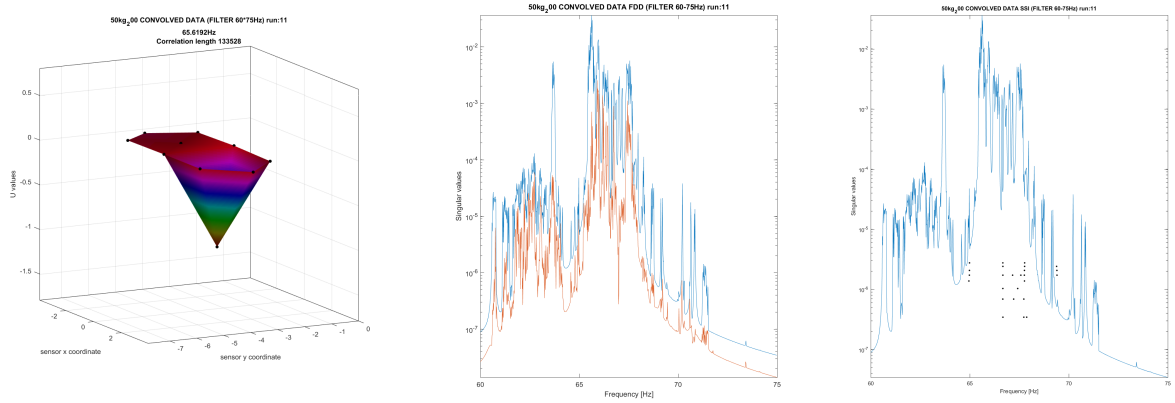
Figure A4.50kg: Run 9 (segment 3)



(a) 50kg mode shape, run 10

(b) 50kg FDD SSI output, run 10

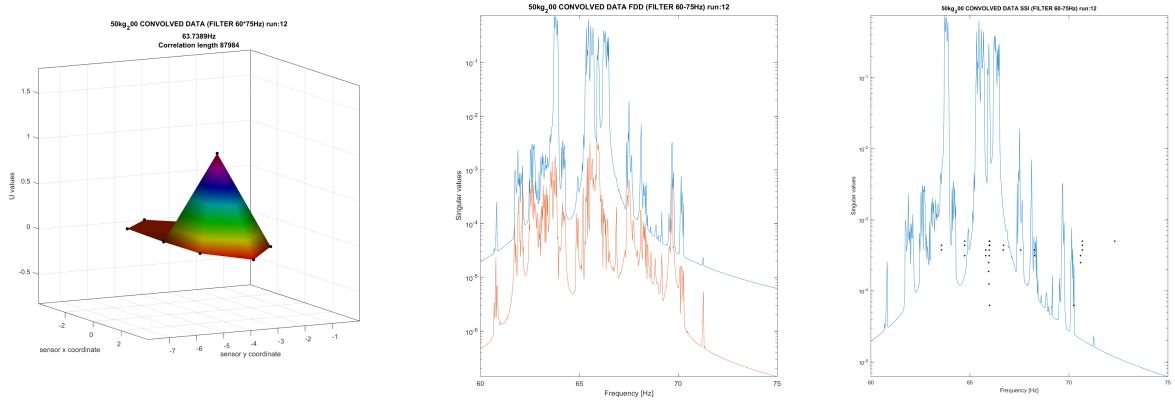
Figure A4.50kg: Run 10 (segment 3)



(a) 50kg mode shape, run 11

(b) 50kg FDD SSI output, run 11

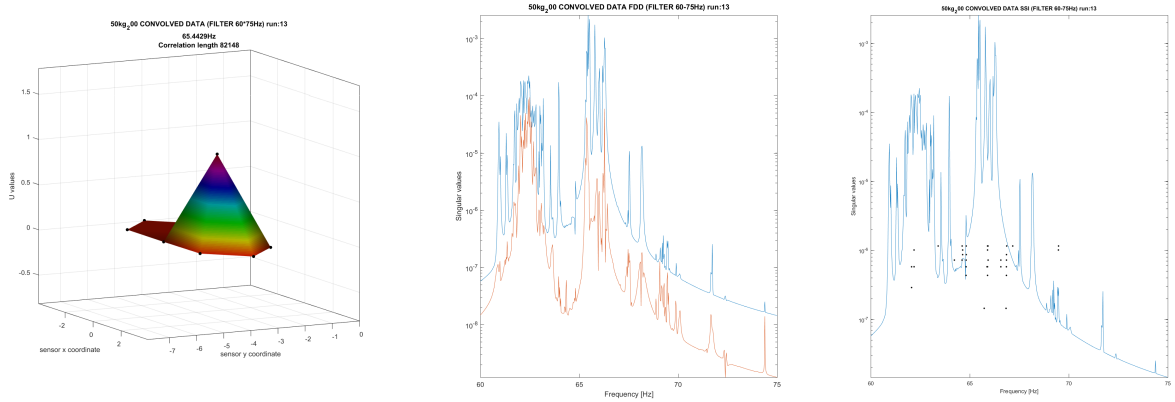
Figure A4.50kg: Run 11 (segment 3)



(a) 50kg mode shape, run 12

(b) 50kg FDD SSI output, run 12

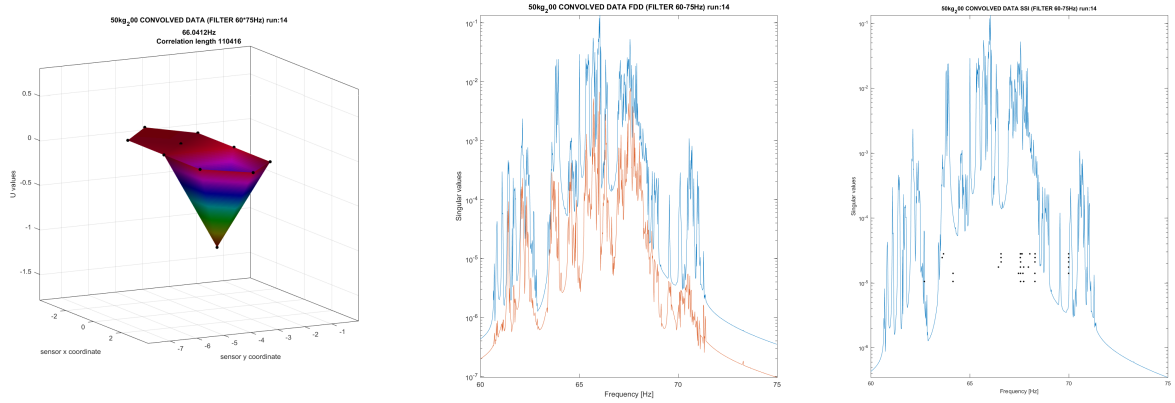
Figure A4.50kg: Run 12 (segment 3)



(a) 50kg mode shape, run 13

(b) 50kg FDD SSI output, run 13

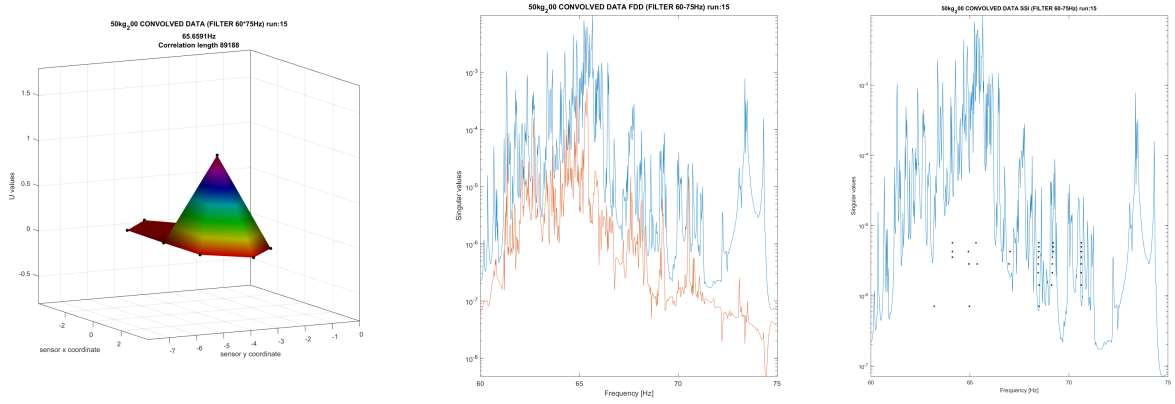
Figure A4.50kg: Run 13 (segment 3)



(a) 50kg mode shape, run 14

(b) 50kg FDD SSI output, run 14

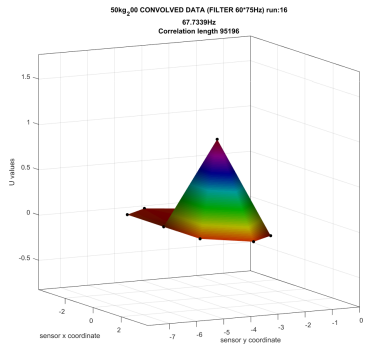
Figure A4.50kg: Run 14 (segment 3)



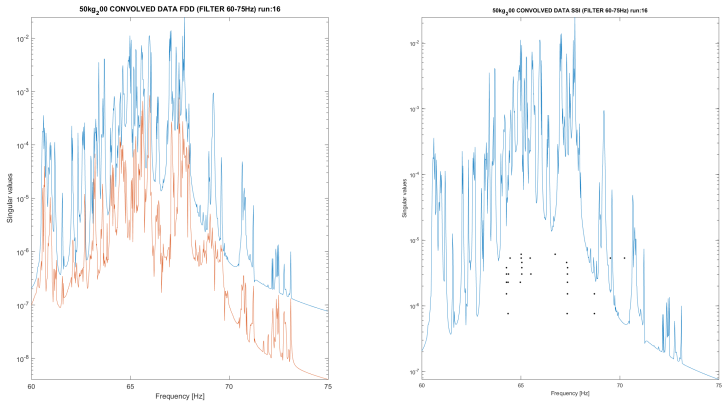
(a) 50kg mode shape, run 15

(b) 50kg FDD SSI output, run 15

Figure A4.50kg: Run 15 (segment 3)

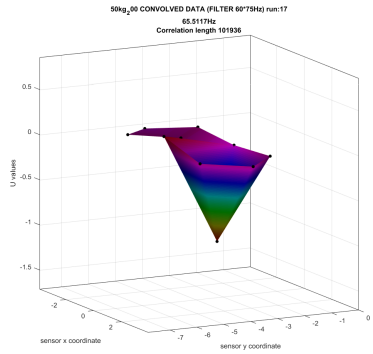


(a) 50kg mode shape, run 16

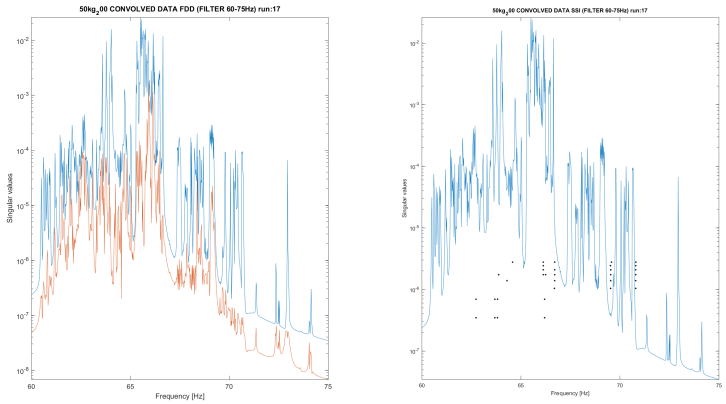


(b) 50kg FDD SSI output, run 16

Figure A4.50kg: Run 16 (segment 3)

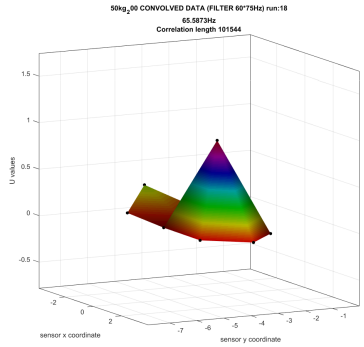


(a) 50kg mode shape, run 17

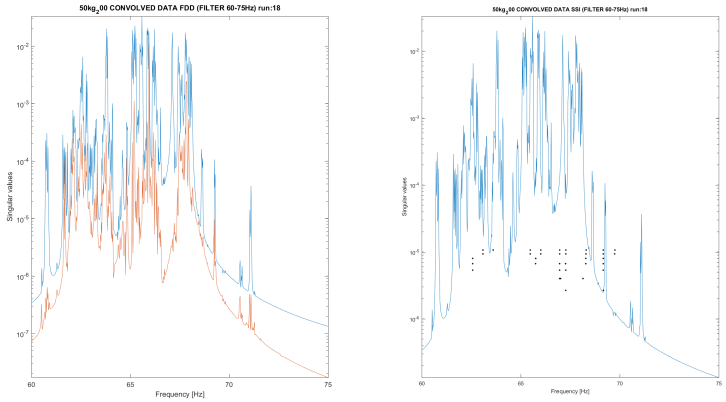


(b) 50kg FDD SSI output, run 17

Figure A4.50kg: Run 17 (segment 3)

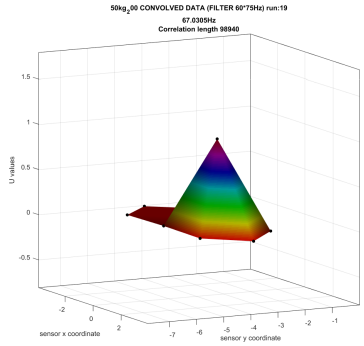


(a) 50kg mode shape, run 18

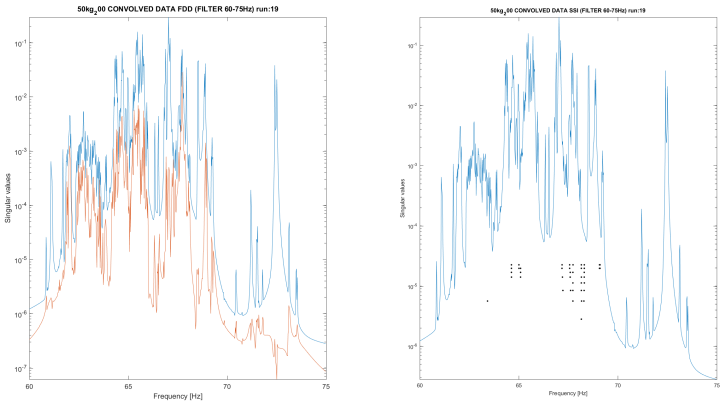


(b) 50kg FDD SSI output, run 18

Figure A4.50kg: Run 18 (segment 3)

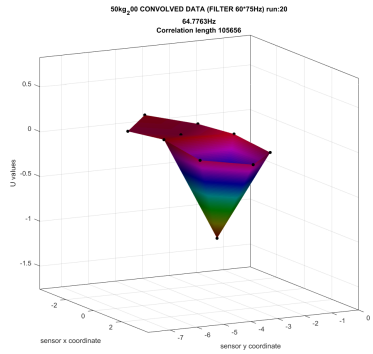


(a) 50kg mode shape, run 19

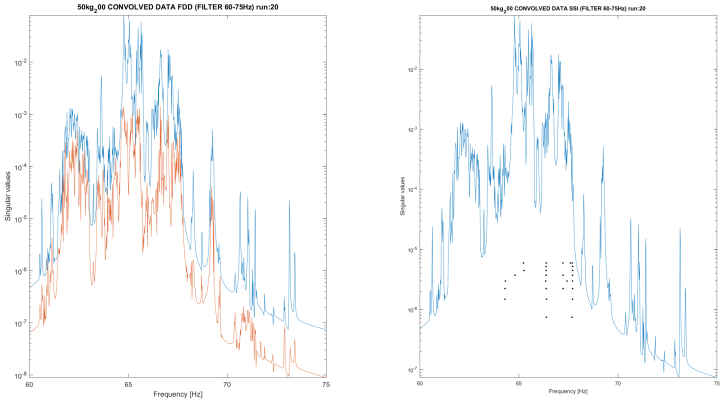


(b) 50kg FDD SSI output, run 19

Figure A4.50kg: Run 19 (segment 3)

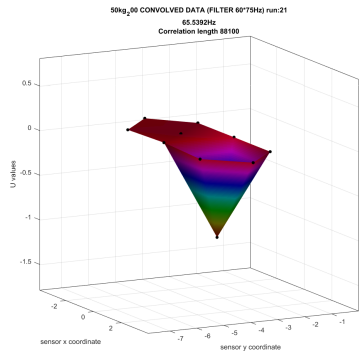


(a) 50kg mode shape, run 20

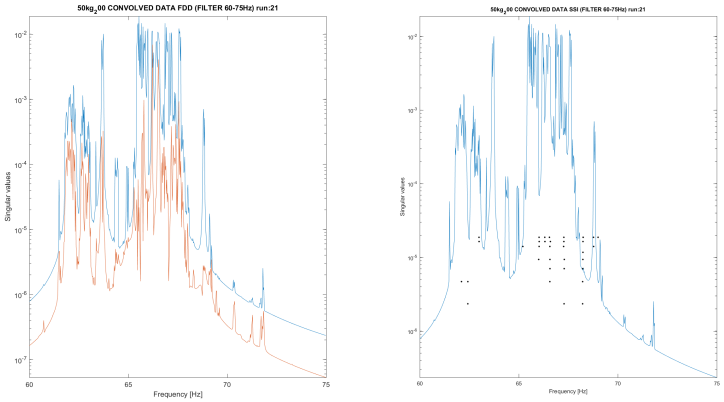


(b) 50kg FDD SSI output, run 20

Figure A4.50kg: Run 20 (segment 3)

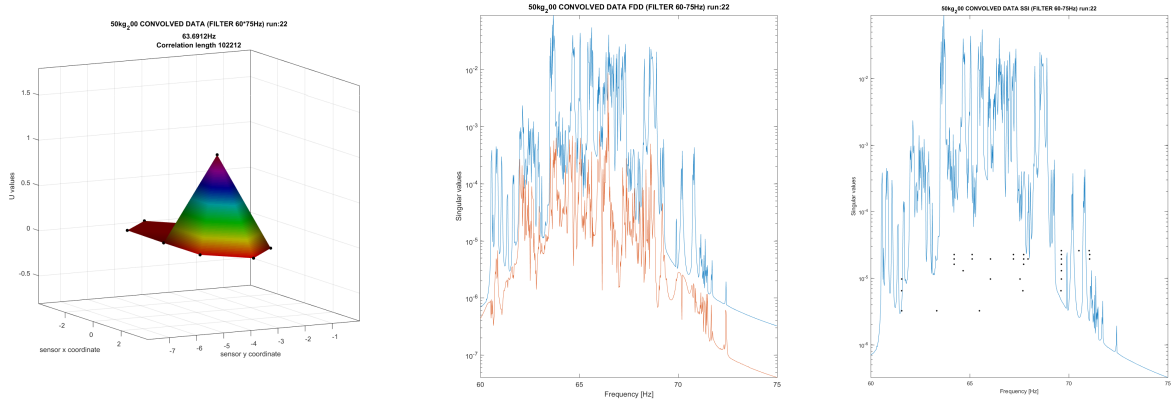


(a) 50kg mode shape, run 21



(b) 50kg FDD SSI output, run 21

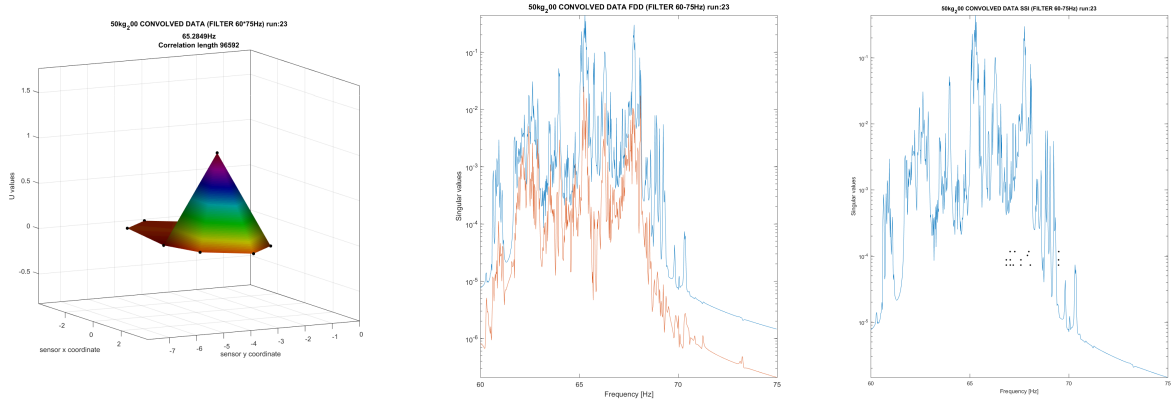
Figure A4.50kg: Run 21 (segment 3)



(a) 50kg mode shape, run 22

(b) 50kg FDD SSI output, run 22

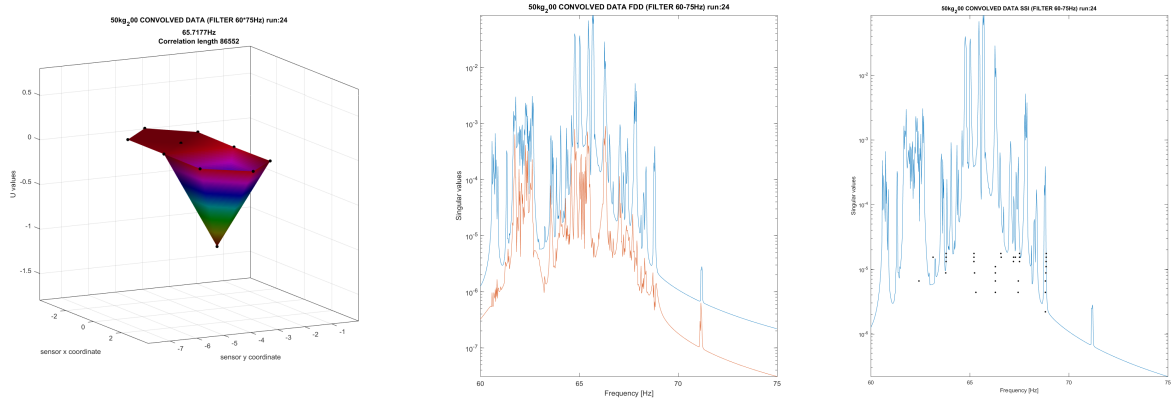
Figure A4.50kg: Run 22 (segment 3)



(a) 50kg mode shape, run 23

(b) 50kg FDD SSI output, run 23

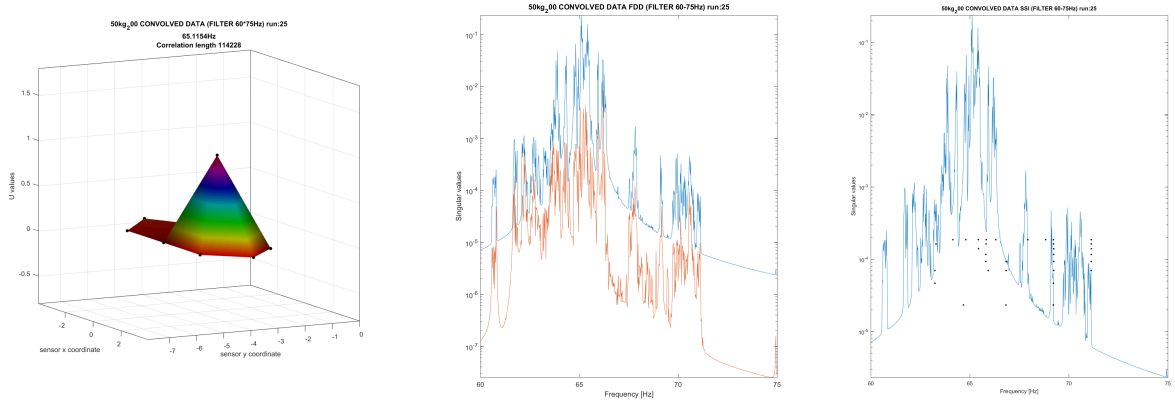
Figure A4.50kg: Run 23 (segment 3)



(a) 50kg mode shape, run 24

(b) 50kg FDD SSI output, run 24

Figure A4.50kg: Run 24 (segment 3)

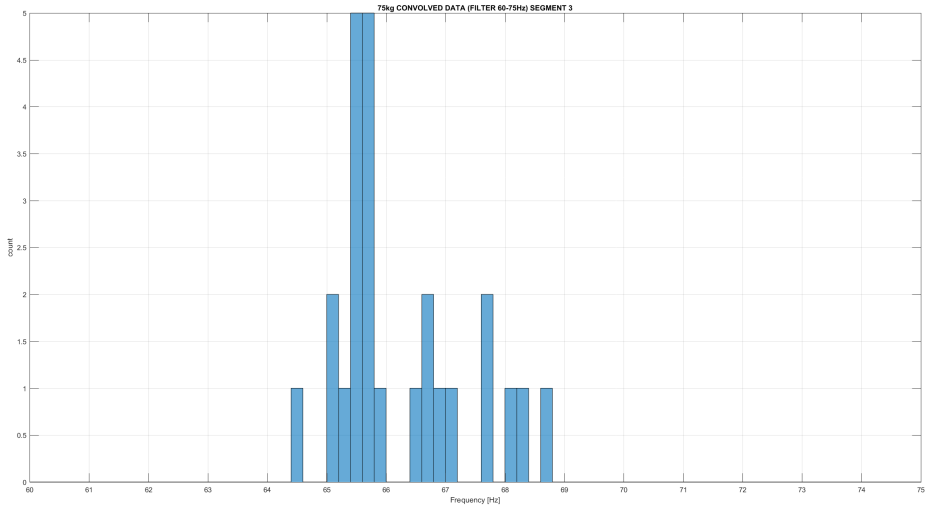


(a) 50kg mode shape, run 25

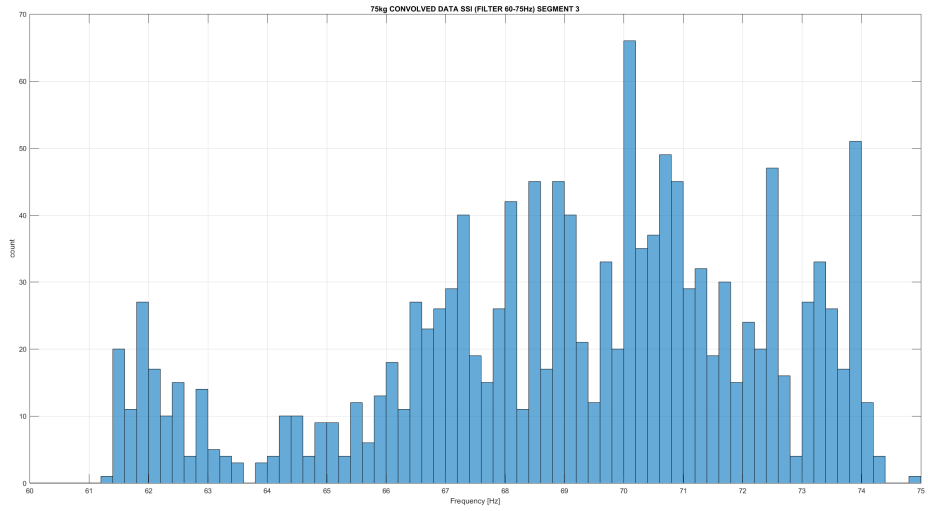
(b) 50kg FDD SSI output, run 25

Figure A4.50kg: Run 25 (segment 3)

75kg data segment 3

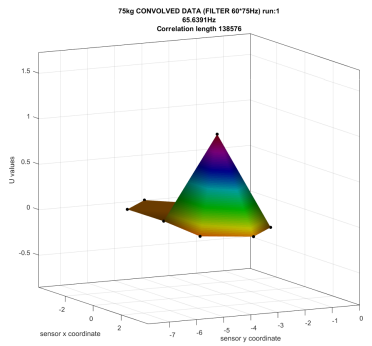


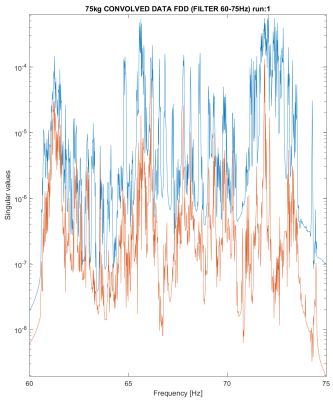
(a) 75kg FDD histogram

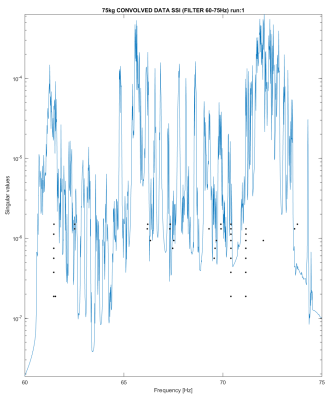


(b) 75kg SSI histogram

Figure A4.75kg: Histograms of identified modes, 75kg data (segment 3)



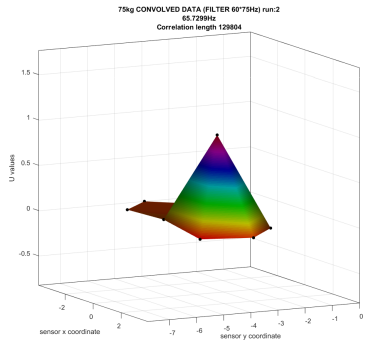


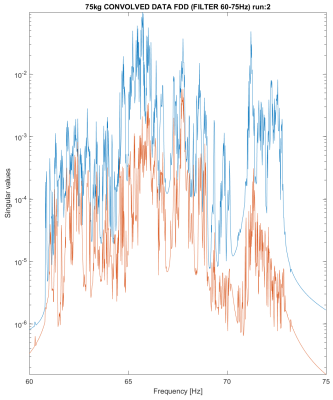


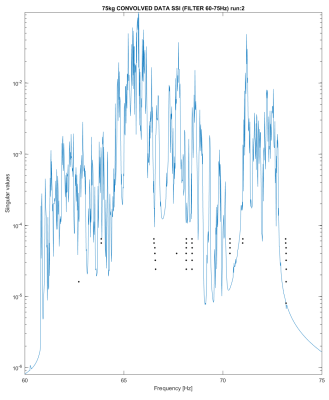
(a) 75kg mode shape, run 1

(b) 75kg FDD SSI output, run 1

Figure A4.75kg: Run 1 (segment 3)



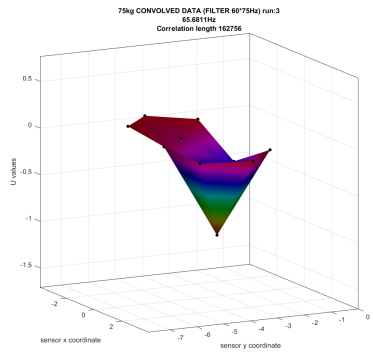


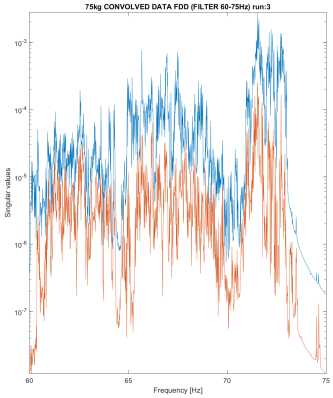


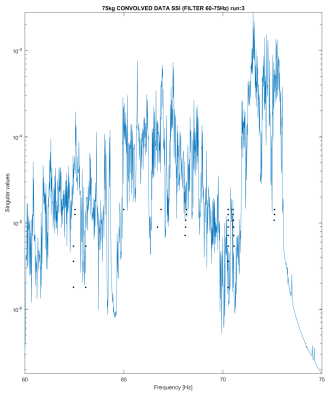
(a) 75kg mode shape, run 2

(b) 75kg FDD SSI output, run 2

Figure A4.75kg: Run 2 (segment 3)



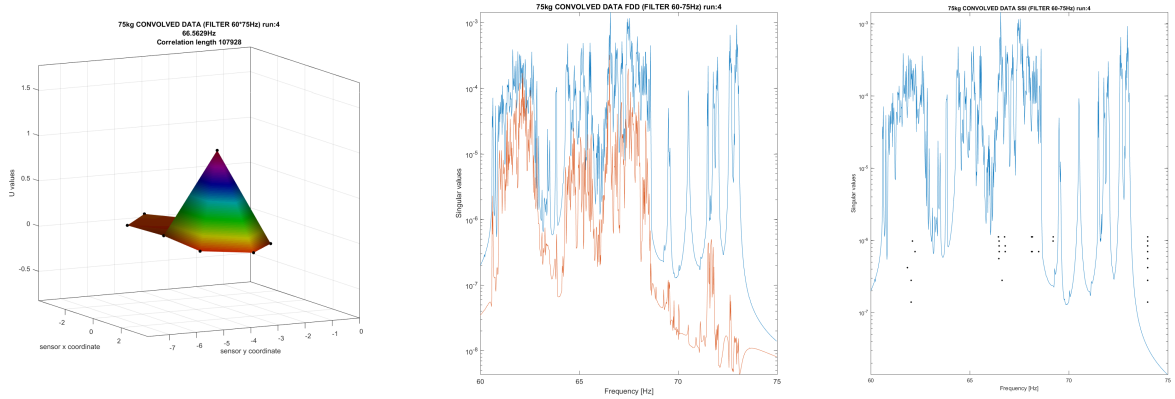




(a) 75kg mode shape, run 3

(b) 75kg FDD SSI output, run 3

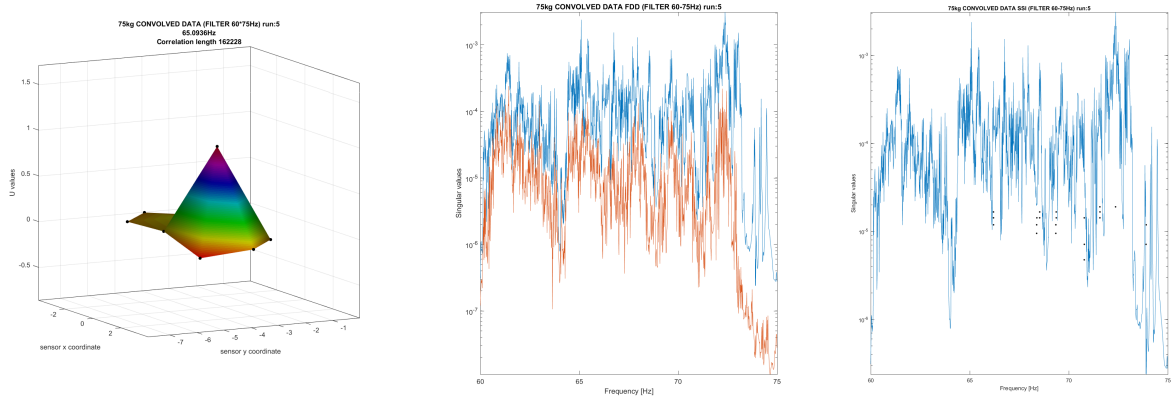
Figure A4.75kg: Run 3 (segment 3)



(a) 75kg mode shape, run 4

(b) 75kg FDD SSI output, run 4

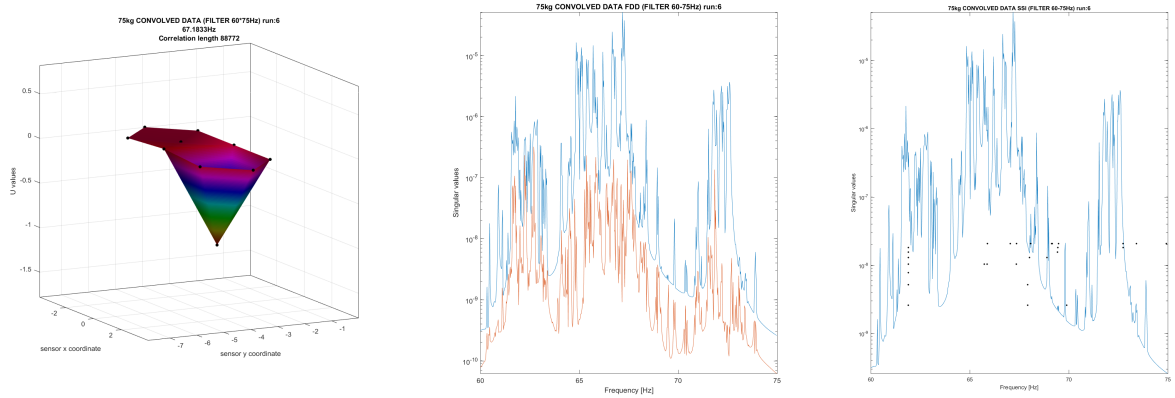
Figure A4.75kg: Run 4 (segment 3)



(a) 75kg mode shape, run 5

(b) 75kg FDD SSI output, run 5

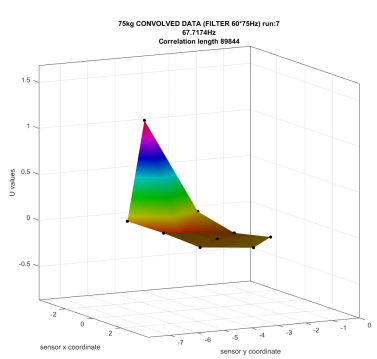
Figure A4.75kg: Run 5 (segment 3)



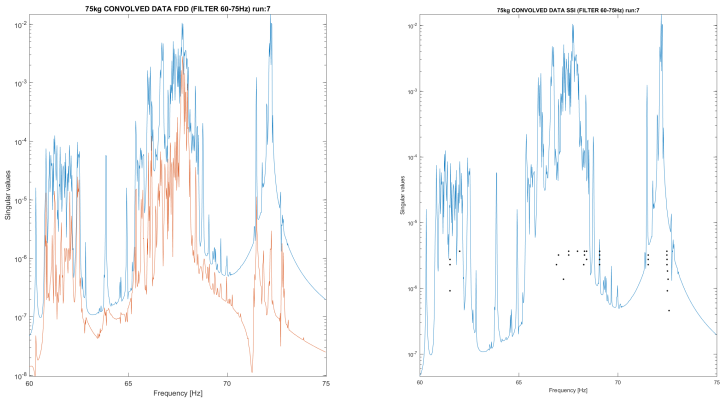
(a) 75kg mode shape, run 6

(b) 75kg FDD SSI output, run 6

Figure A4.75kg: Run 6 (segment 3)

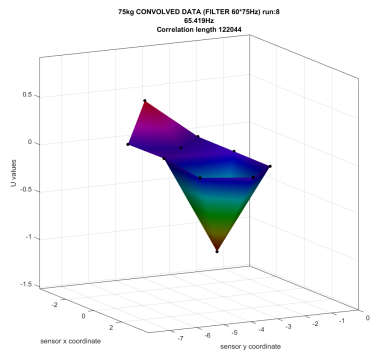


(a) 75kg mode shape, run 7

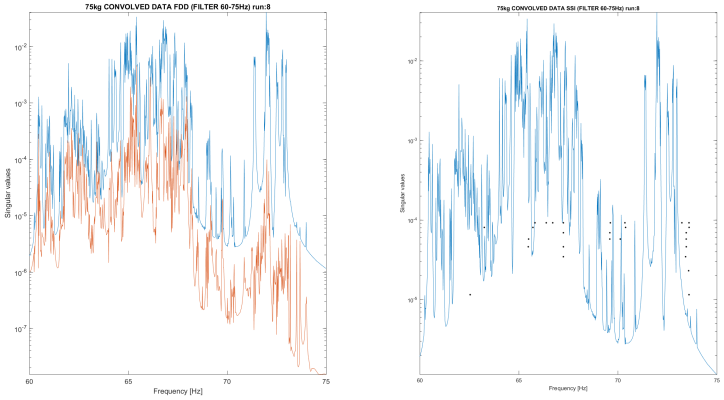


(b) 75kg FDD SSI output, run 7

Figure A4.75kg: Run 7 (segment 3)

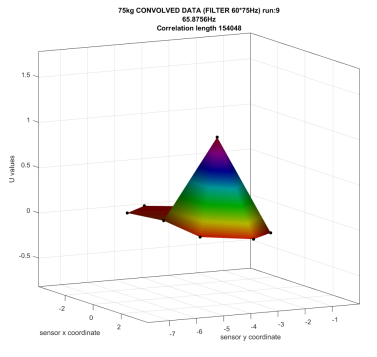


(a) 75kg mode shape, run 8

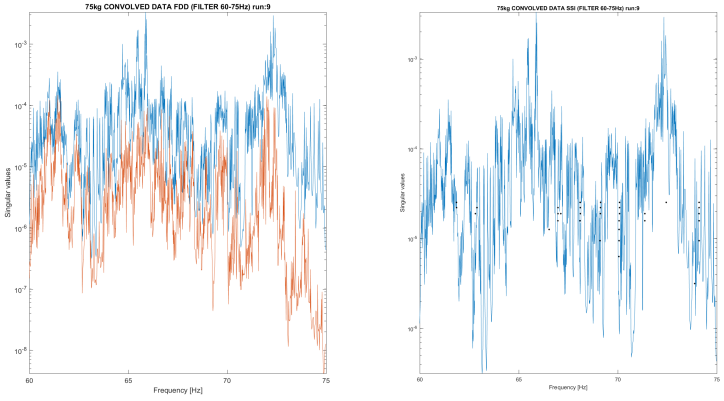


(b) 75kg FDD SSI output, run 8

Figure A4.75kg: Run 8 (segment 3)

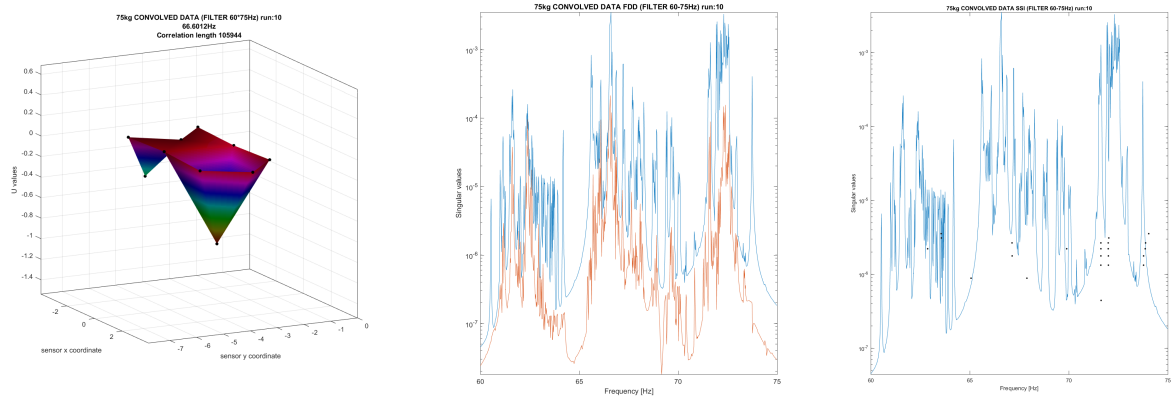


(a) 75kg mode shape, run 9



(b) 75kg FDD SSI output, run 9

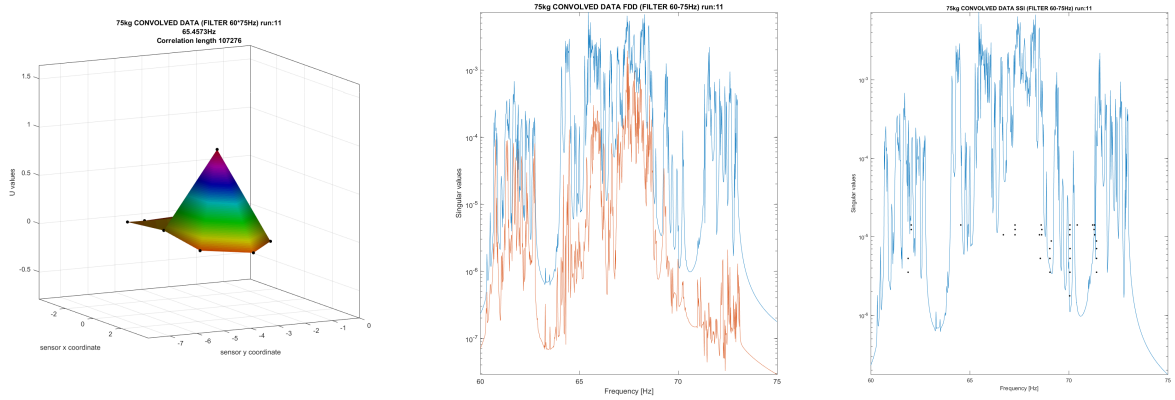
Figure A4.75kg: Run 9 (segment 3)



(a) 75kg mode shape, run 10

(b) 75kg FDD SSI output, run 10

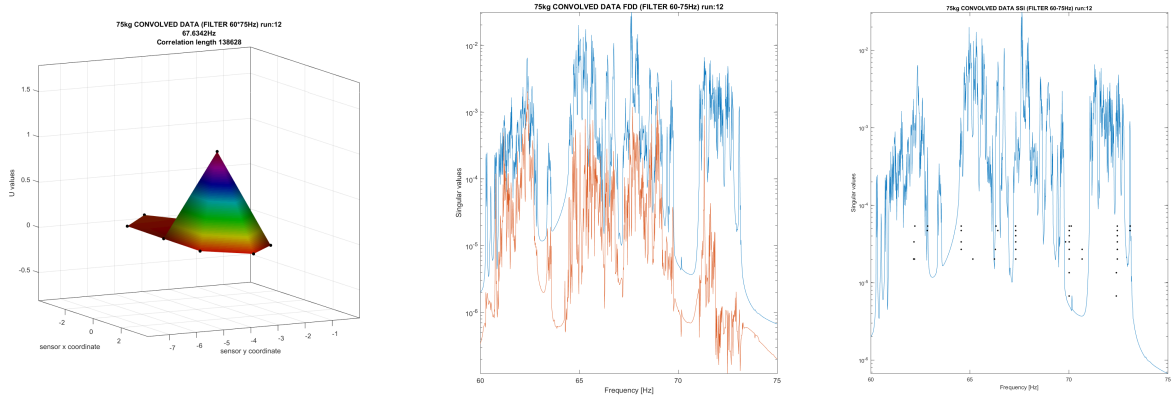
Figure A4.75kg: Run 10 (segment 3)



(a) 75kg mode shape, run 11

(b) 75kg FDD SSI output, run 11

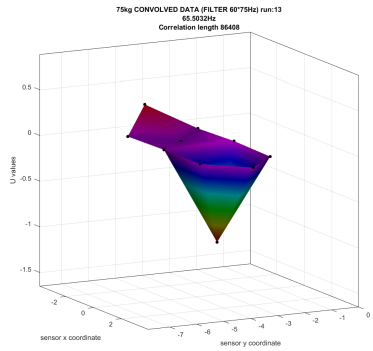
Figure A4.75kg: Run 11 (segment 3)



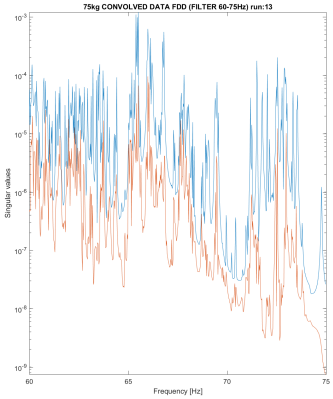
(a) 75kg mode shape, run 12

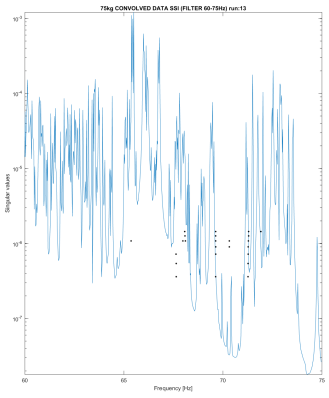
(b) 75kg FDD SSI output, run 12

Figure A4.75kg: Run 12 (segment 3)



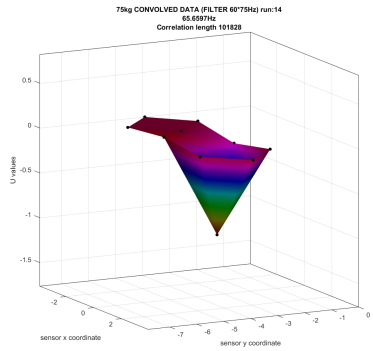
(a) 75kg mode shape, run 13



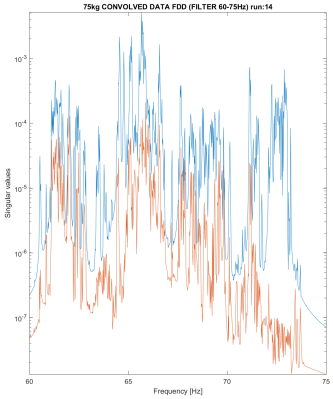


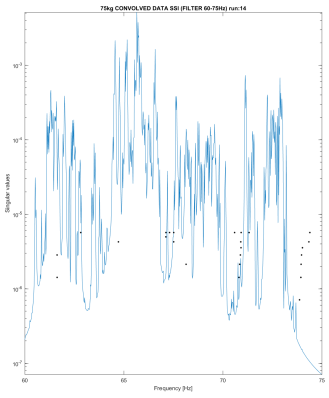
(b) 75kg FDD SSI output, run 13

Figure A4.75kg: Run 13 (segment 3)



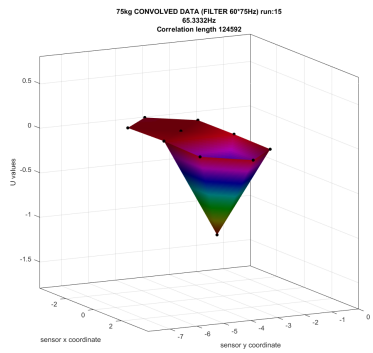
(a) 75kg mode shape, run 14



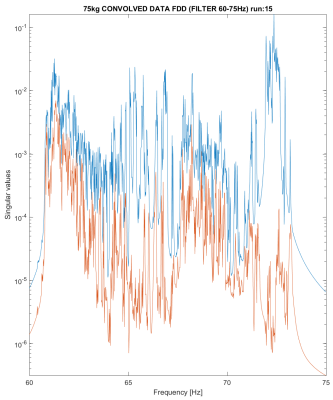


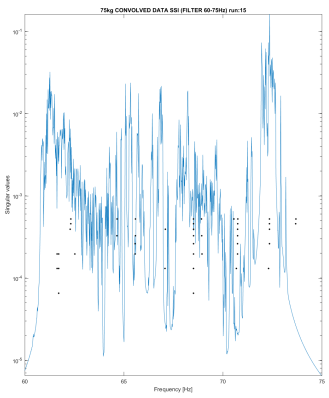
(b) 75kg FDD SSI output, run 14

Figure A4.75kg: Run 14 (segment 3)



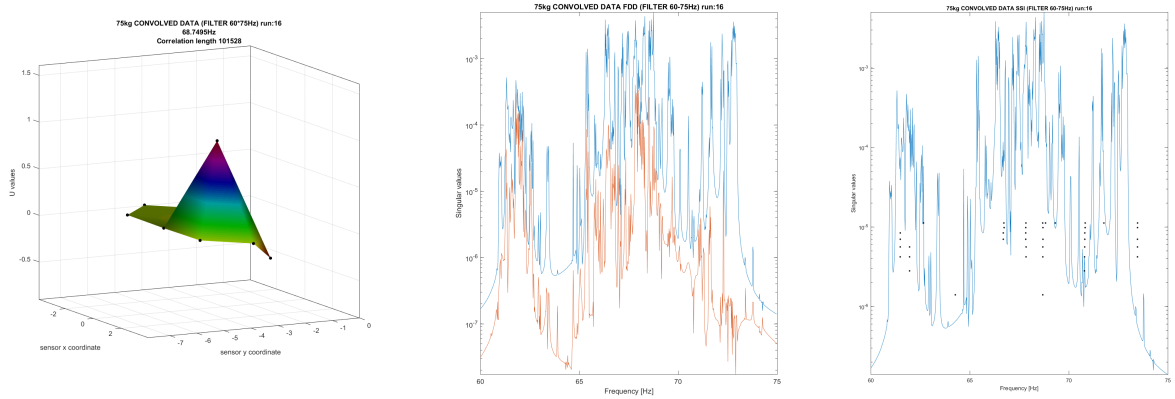
(a) 75kg mode shape, run 15





(b) 75kg FDD SSI output, run 15

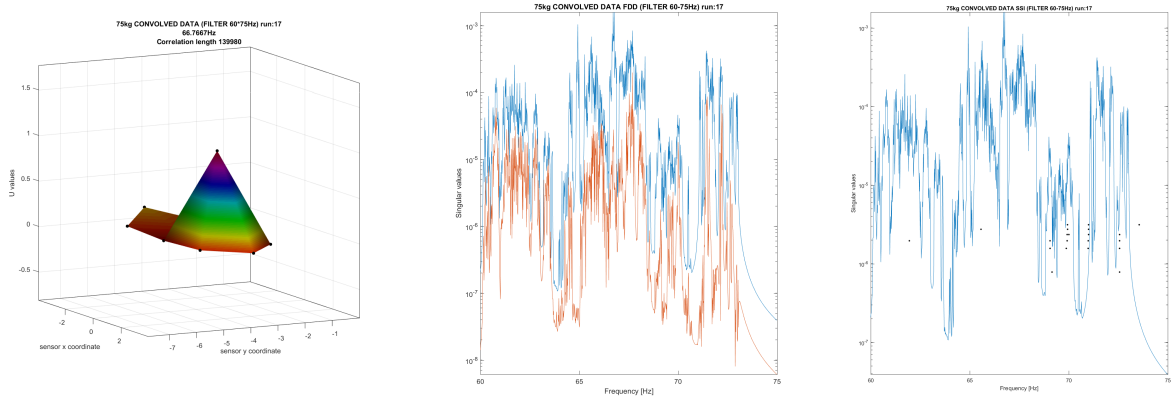
Figure A4.75kg: Run 15 (segment 3)



(a) 75kg mode shape, run 16

(b) 75kg FDD SSI output, run 16

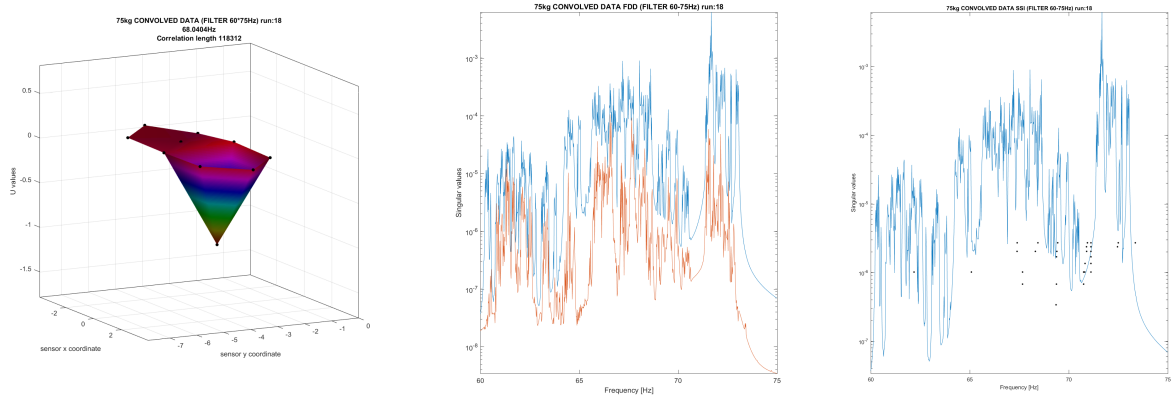
Figure A4.75kg: Run 16 (segment 3)



(a) 75kg mode shape, run 17

(b) 75kg FDD SSI output, run 17

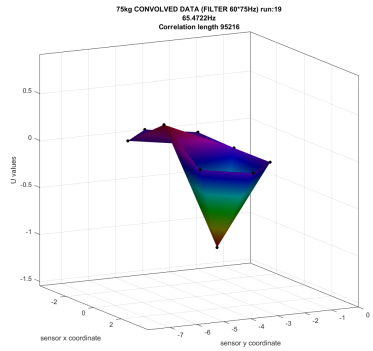
Figure A4.75kg: Run 17 (segment 3)



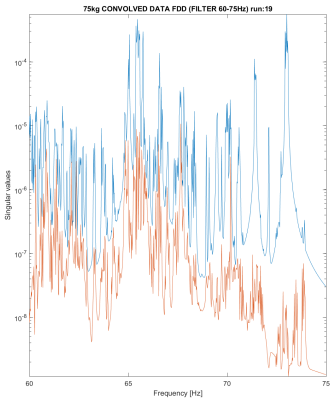
(a) 75kg mode shape, run 18

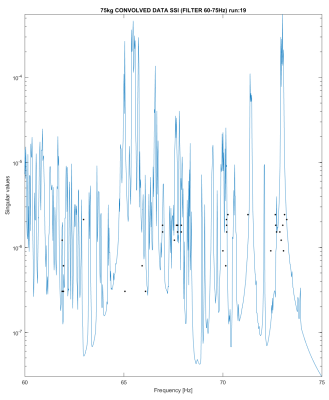
(b) 75kg FDD SSI output, run 18

Figure A4.75kg: Run 18 (segment 3)



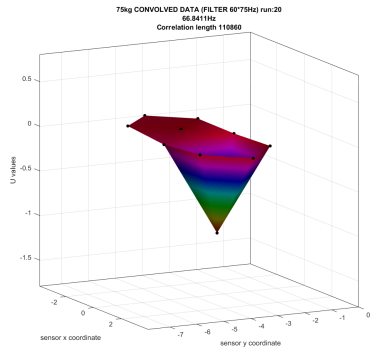
(a) 75kg mode shape, run 19



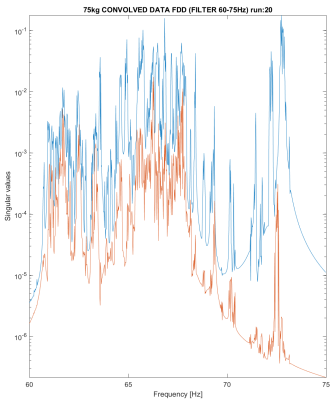


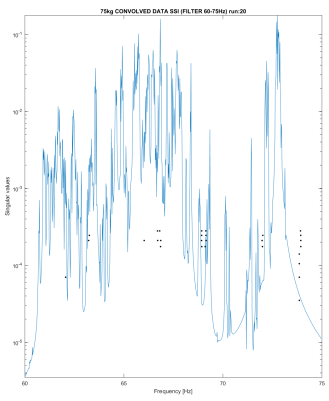
(b) 75kg FDD SSI output, run 19

Figure A4.75kg: Run 19 (segment 3)



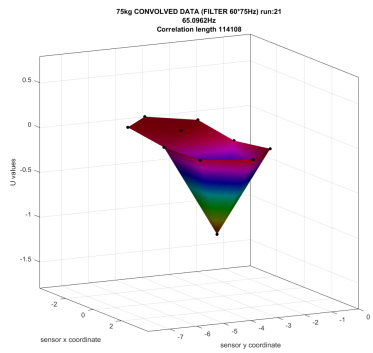
(a) 75kg mode shape, run 20



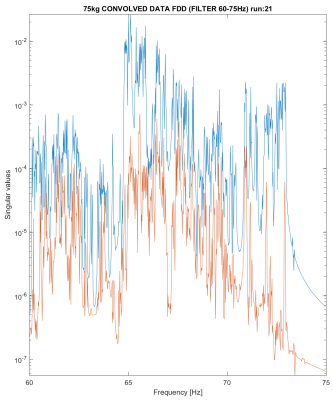


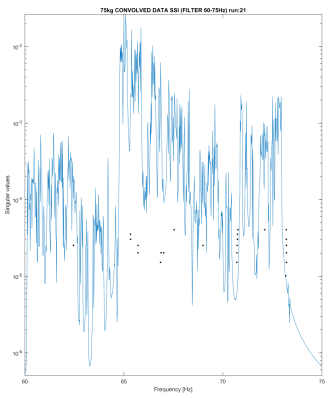
(b) 75kg FDD SSI output, run 20

Figure A4.75kg: Run 20 (segment 3)



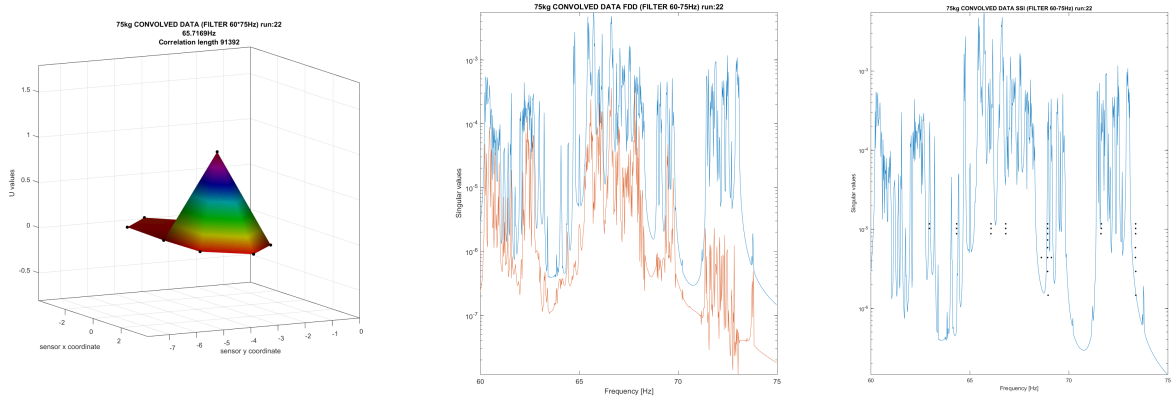
(a) 75kg mode shape, run 21





(b) 75kg FDD SSI output, run 21

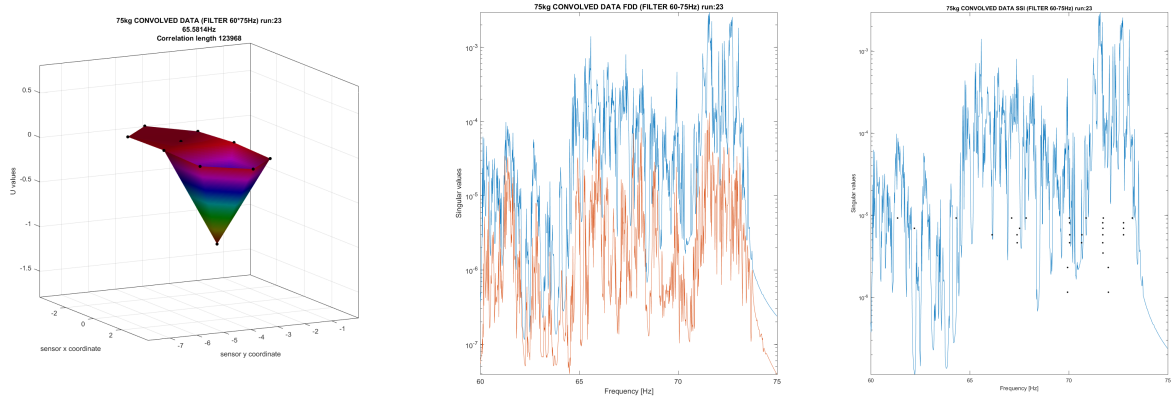
Figure A4.75kg: Run 21 (segment 3)



(a) 75kg mode shape, run 22

(b) 75kg FDD SSI output, run 22

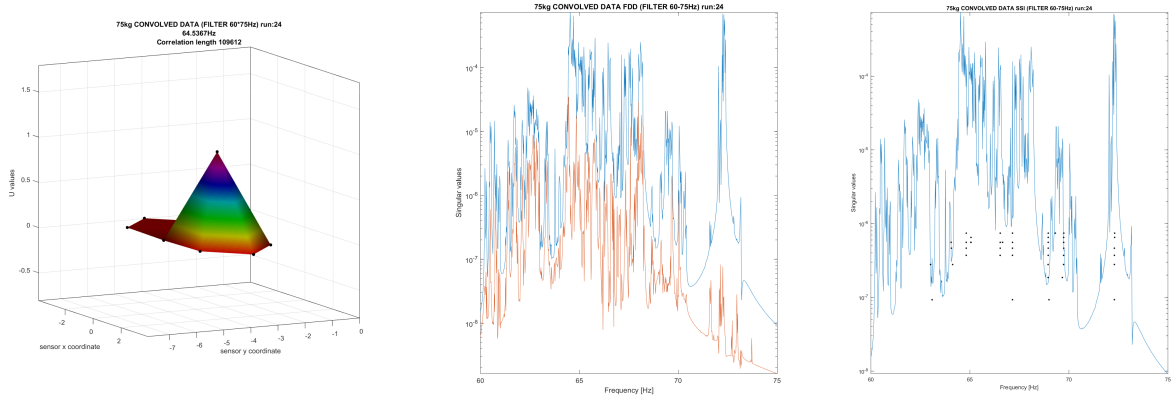
Figure A4.75kg: Run 22 (segment 3)



(a) 75kg mode shape, run 23

(b) 75kg FDD SSI output, run 23

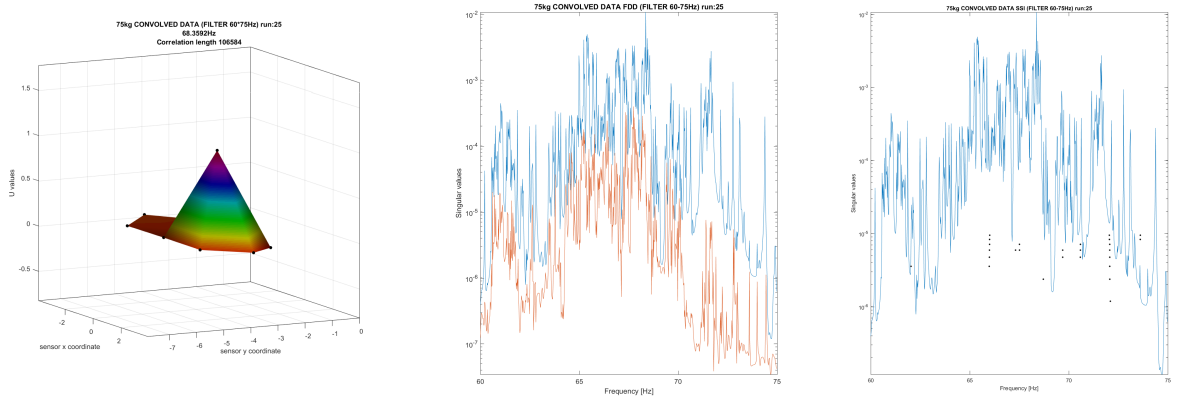
Figure A4.75kg: Run 23 (segment 3)



(a) 75kg mode shape, run 24

(b) 75kg FDD SSI output, run 24

Figure A4.75kg: Run 24 (segment 3)

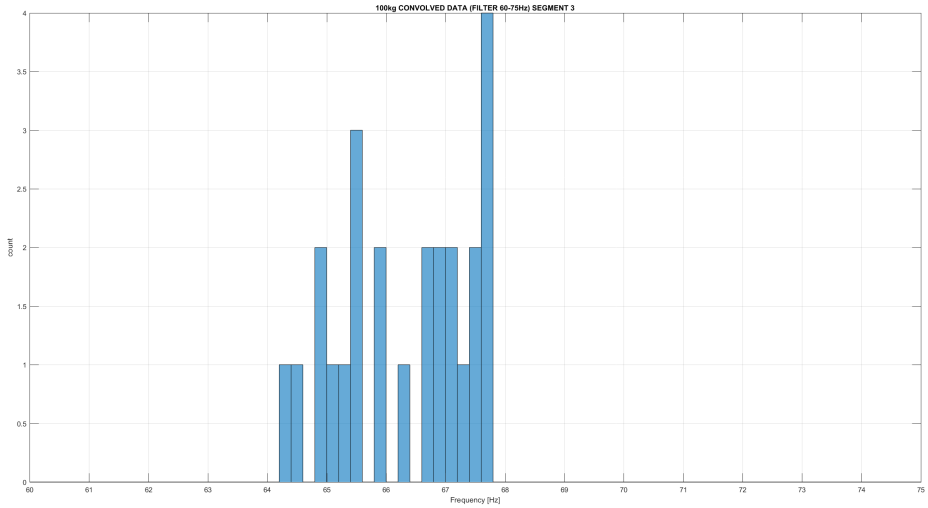


(a) 75kg mode shape, run 25

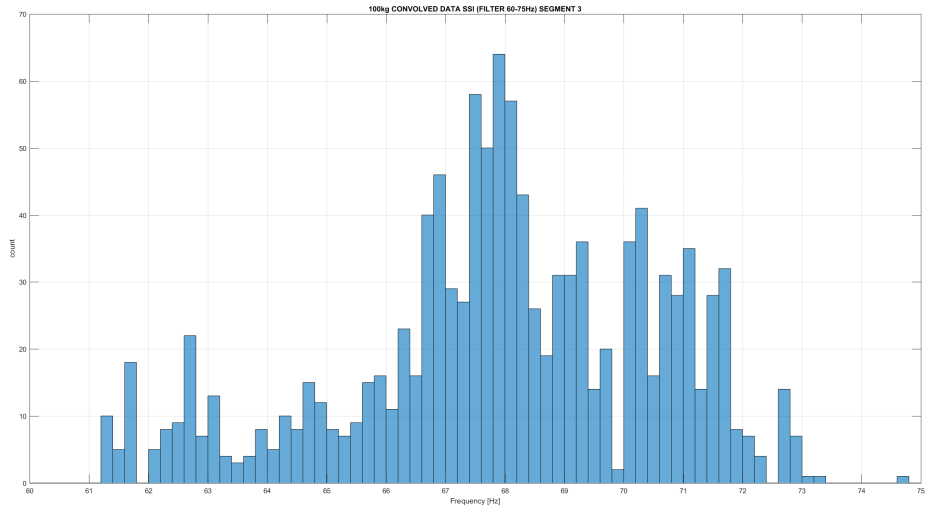
(b) 75kg FDD SSI output, run 25

Figure A4.75kg: Run 25 (segment 3)

100kg data segment 3

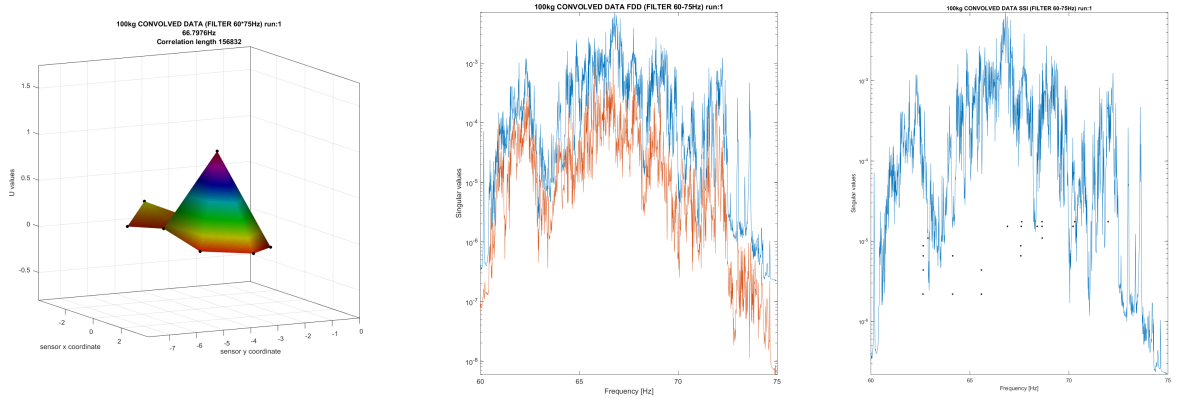


(a) 100kg FDD histogram



(b) 100kg SSI histogram

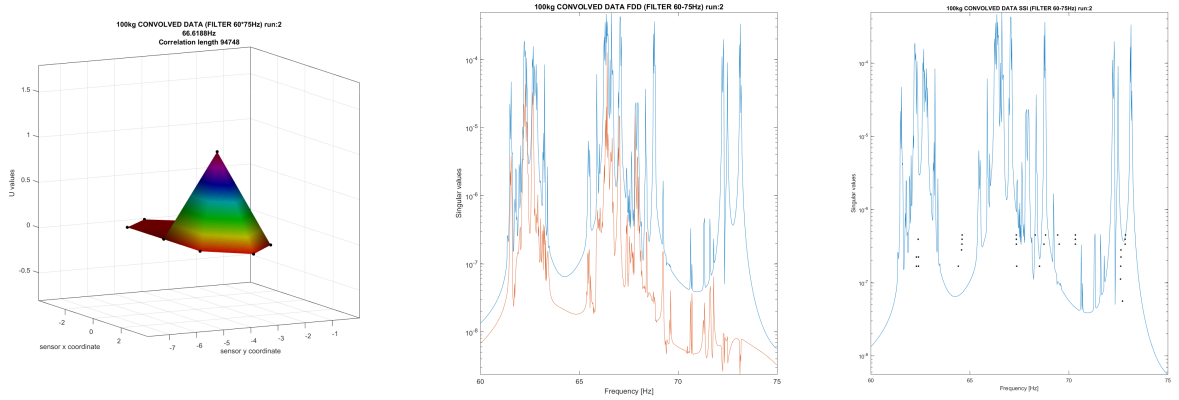
Figure A4.100kg: Histograms of identified modes, 100kg data (segment 3)



(a) 100kg mode shape, run 1

(b) 100kg FDD SSI output, run 1

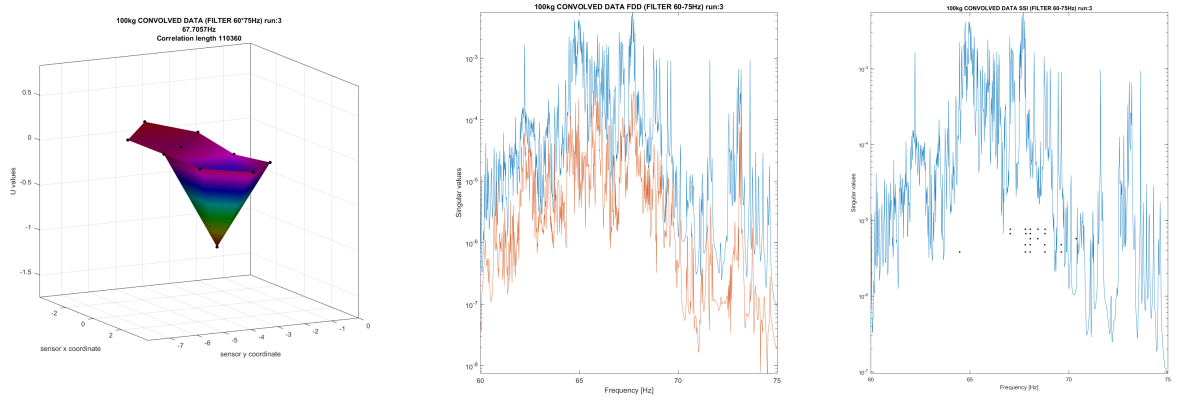
Figure A4.100kg: Run 1 (segment 3)



(a) 100kg mode shape, run 2

(b) 100kg FDD SSI output, run 2

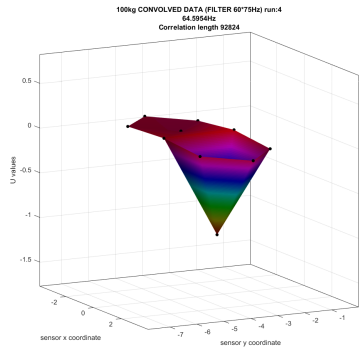
Figure A4.100kg: Run 2 (segment 3)



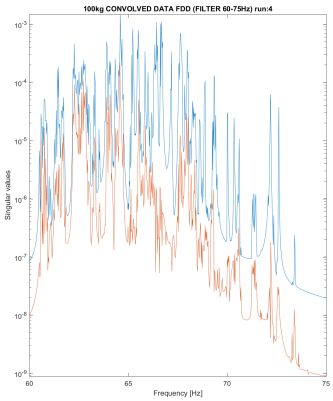
(a) 100kg mode shape, run 3

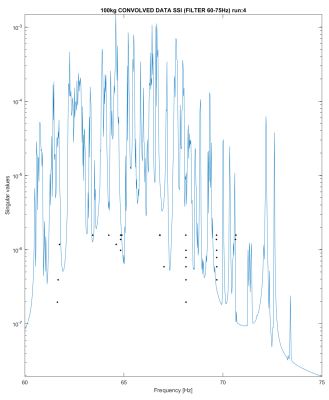
(b) 100kg FDD SSI output, run 3

Figure A4.100kg: Run 3 (segment 3)



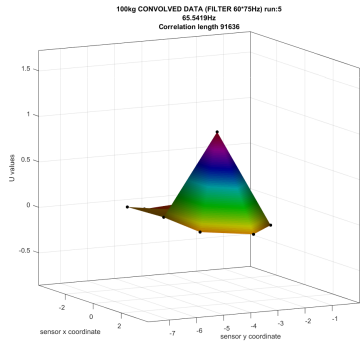
(a) 100kg mode shape, run 4



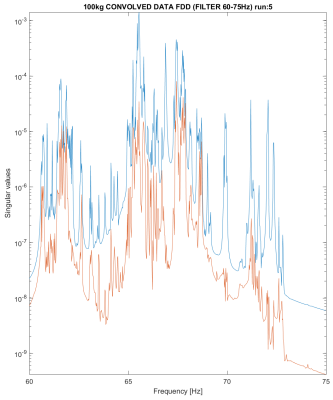


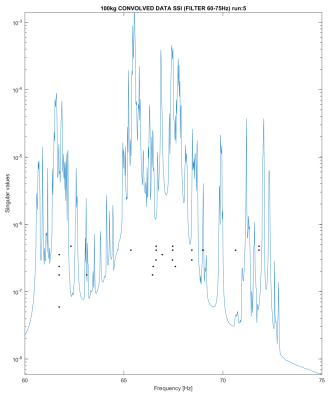
(b) 100kg FDD SSI output, run 4

Figure A4.100kg: Run 4 (segment 3)



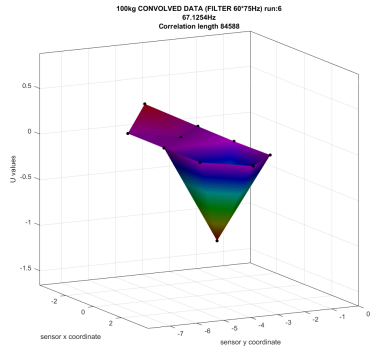
(a) 100kg mode shape, run 5



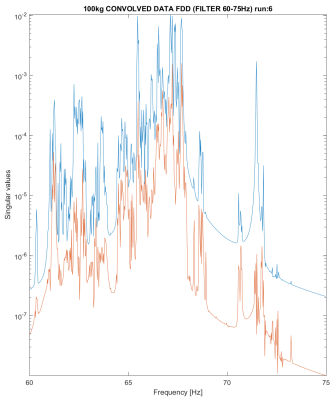


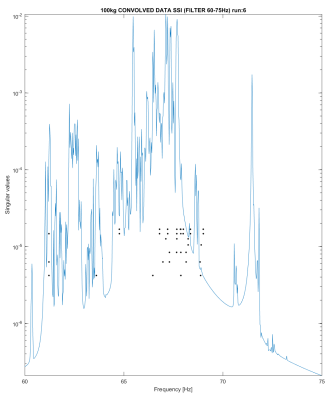
(b) 100kg FDD SSI output, run 5

Figure A4.100kg: Run 5 (segment 3)



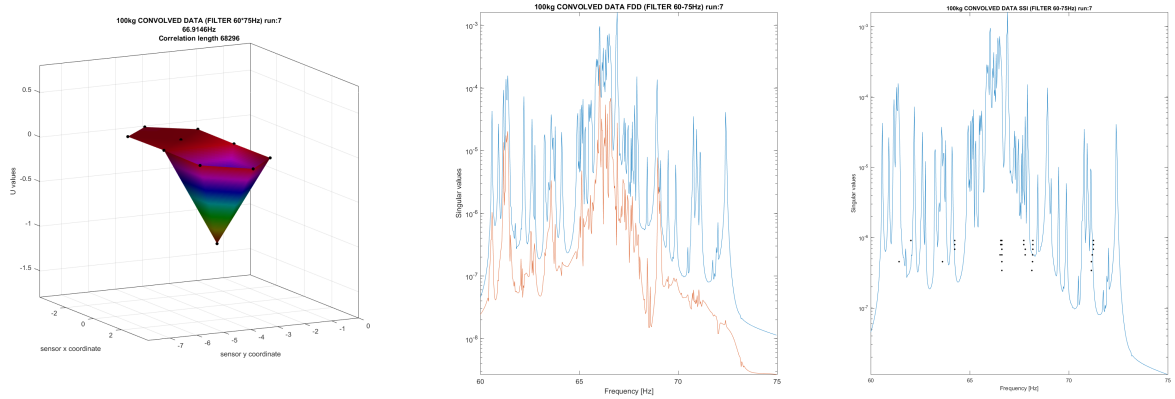
(a) 100kg mode shape, run 6





(b) 100kg FDD SSI output, run 6

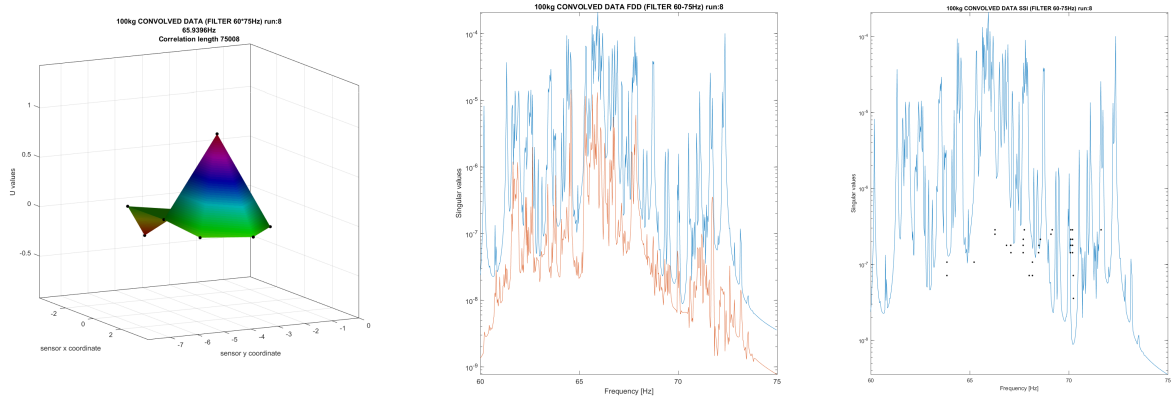
Figure A4.100kg: Run 6 (segment 3)



(a) 100kg mode shape, run 7

(b) 100kg FDD SSI output, run 7

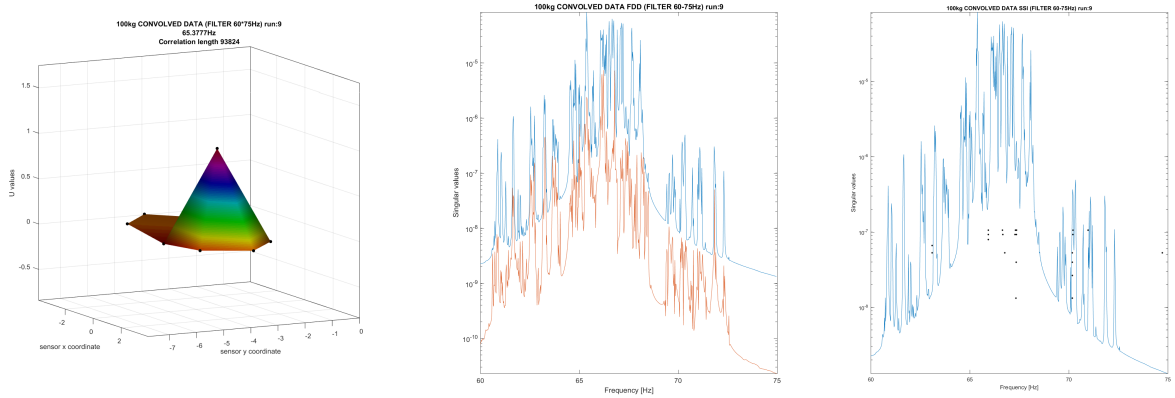
Figure A4.100kg: Run 7 (segment 3)



(a) 100kg mode shape, run 8

(b) 100kg FDD SSI output, run 8

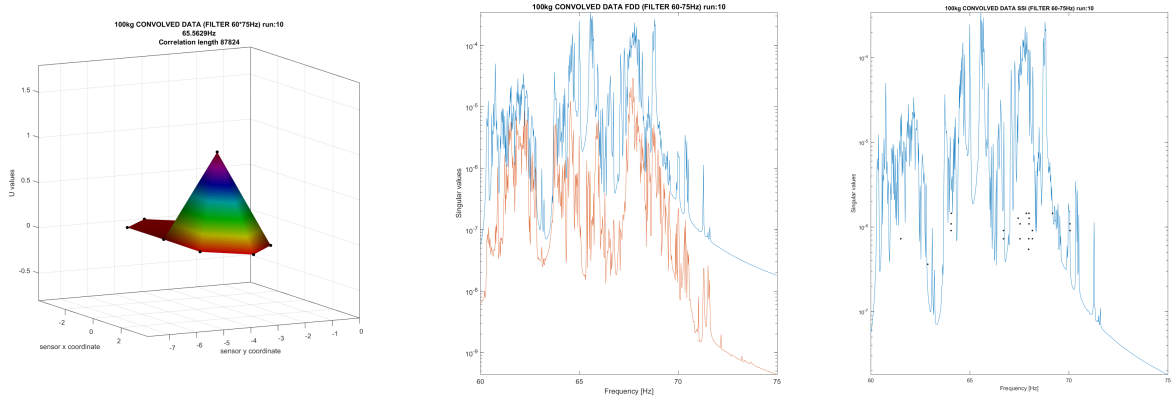
Figure A4.100kg: Run 8 (segment 3)



(a) 100kg mode shape, run 9

(b) 100kg FDD SSI output, run 9

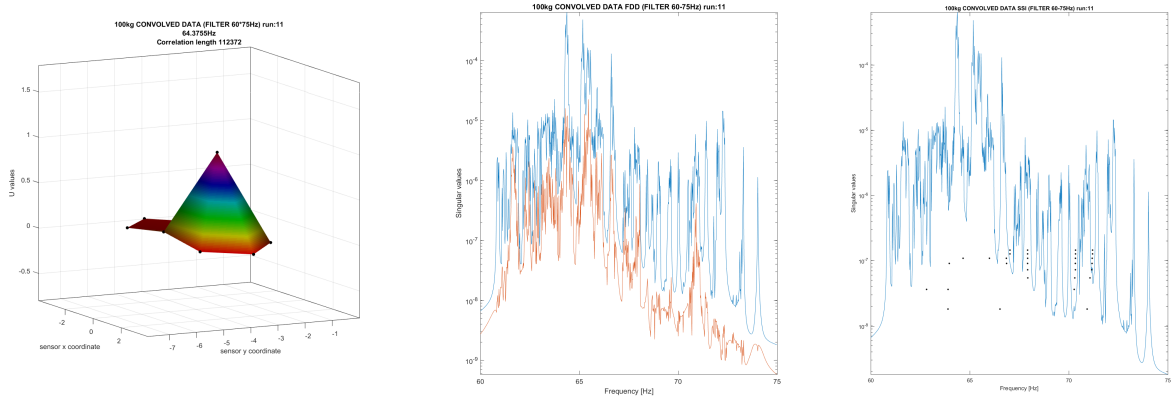
Figure A4.100kg: Run 9 (segment 3)



(a) 100kg mode shape, run 10

(b) 100kg FDD SSI output, run 10

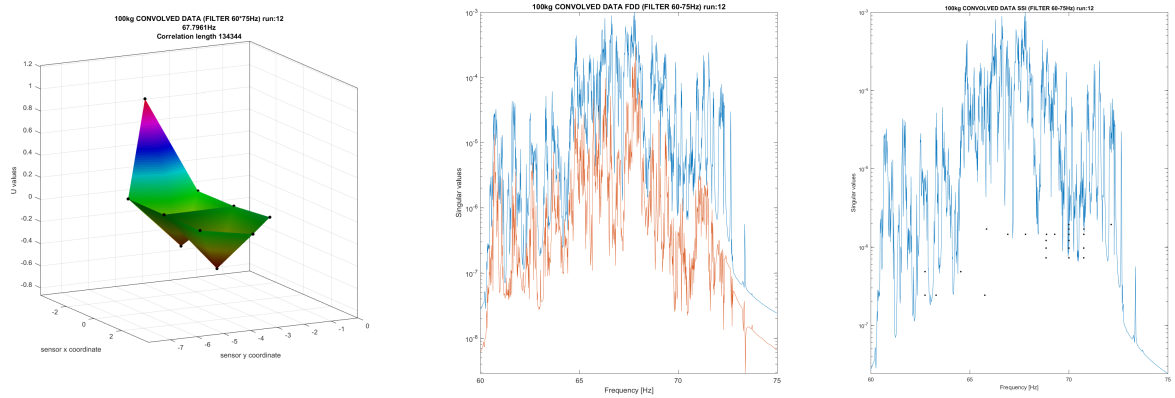
Figure A4.100kg: Run 10 (segment 3)



(a) 100kg mode shape, run 11

(b) 100kg FDD SSI output, run 11

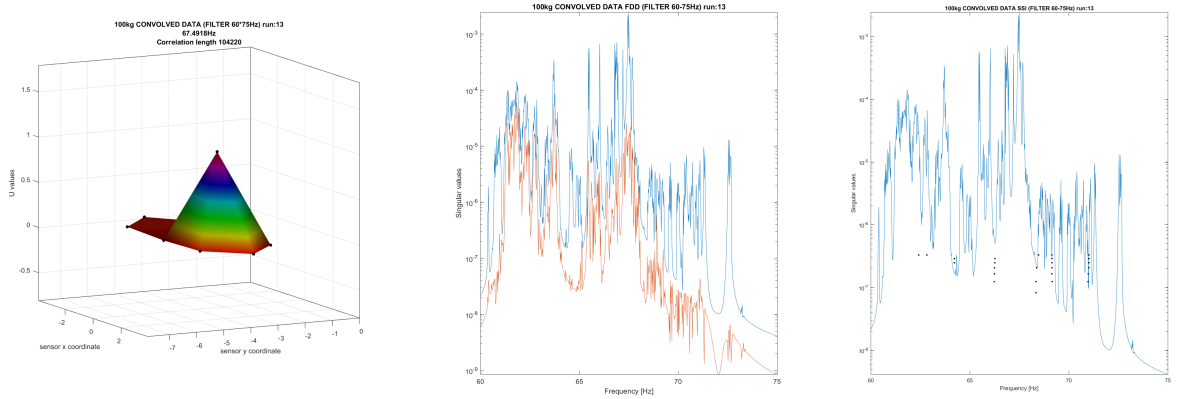
Figure A4.100kg: Run 11 (segment 3)



(a) 100kg mode shape, run 12

(b) 100kg FDD SSI output, run 12

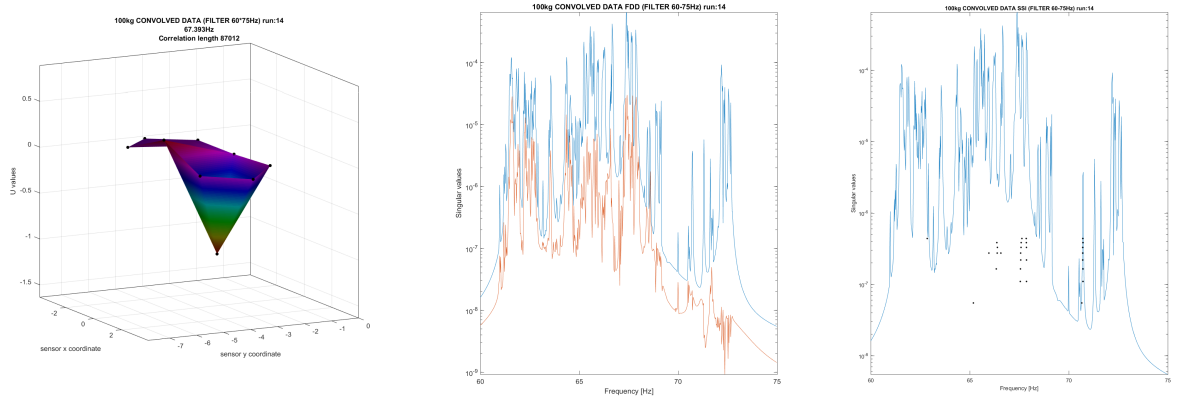
Figure A4.100kg: Run 12 (segment 3)



(a) 100kg mode shape, run 13

(b) 100kg FDD SSI output, run 13

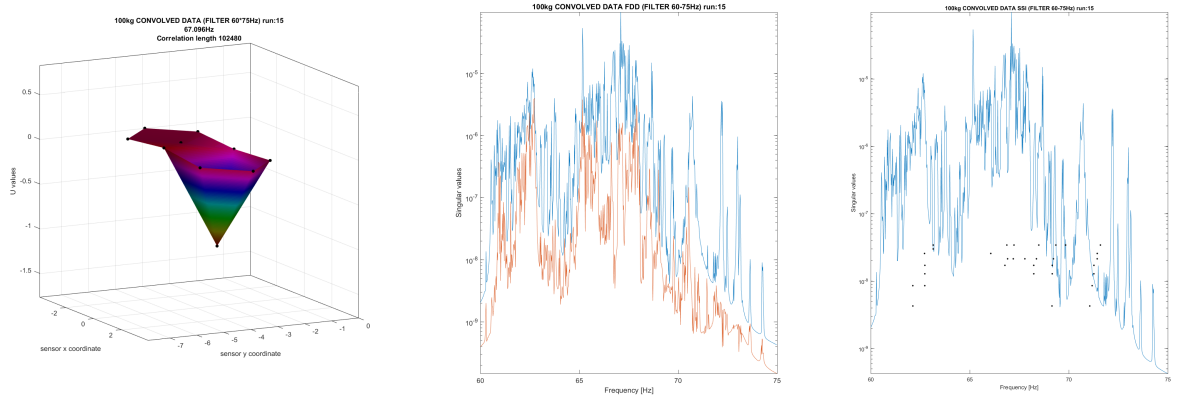
Figure A4.100kg: Run 13 (segment 3)



(a) 100kg mode shape, run 14

(b) 100kg FDD SSI output, run 14

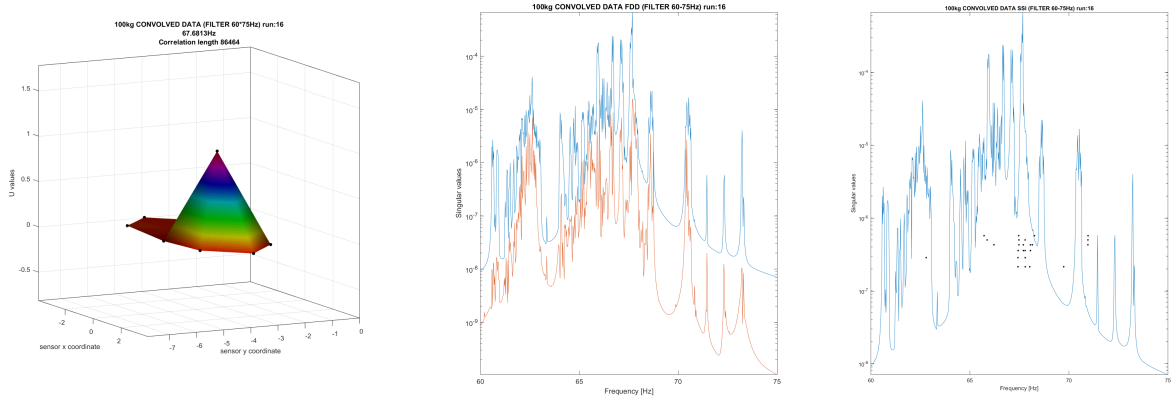
Figure A4.100kg: Run 14 (segment 3)



(a) 100kg mode shape, run 15

(b) 100kg FDD SSI output, run 15

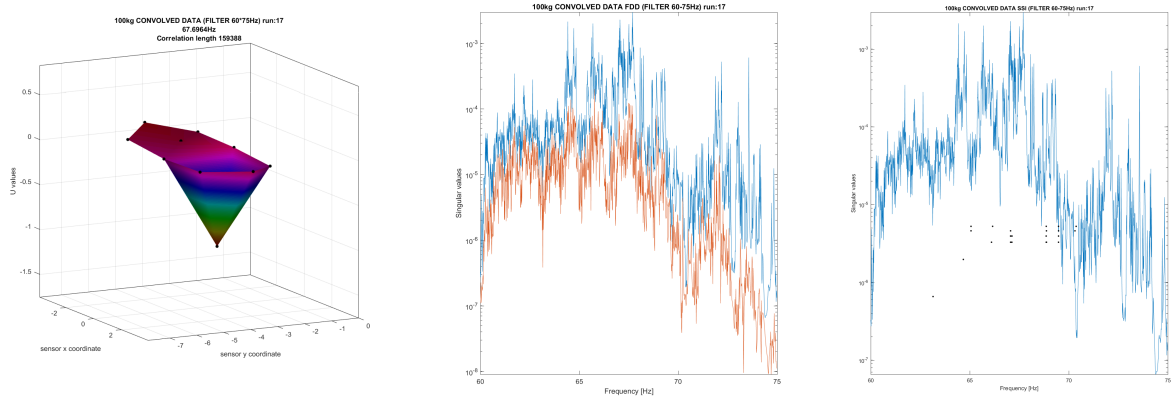
Figure A4.100kg: Run 15 (segment 3)



(a) 100kg mode shape, run 16

(b) 100kg FDD SSI output, run 16

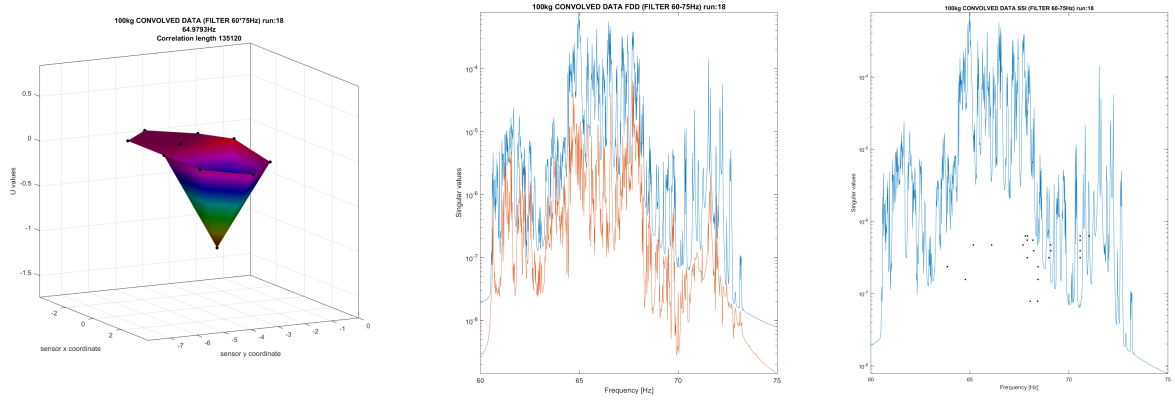
Figure A4.100kg: Run 16 (segment 3)



(a) 100kg mode shape, run 17

(b) 100kg FDD SSI output, run 17

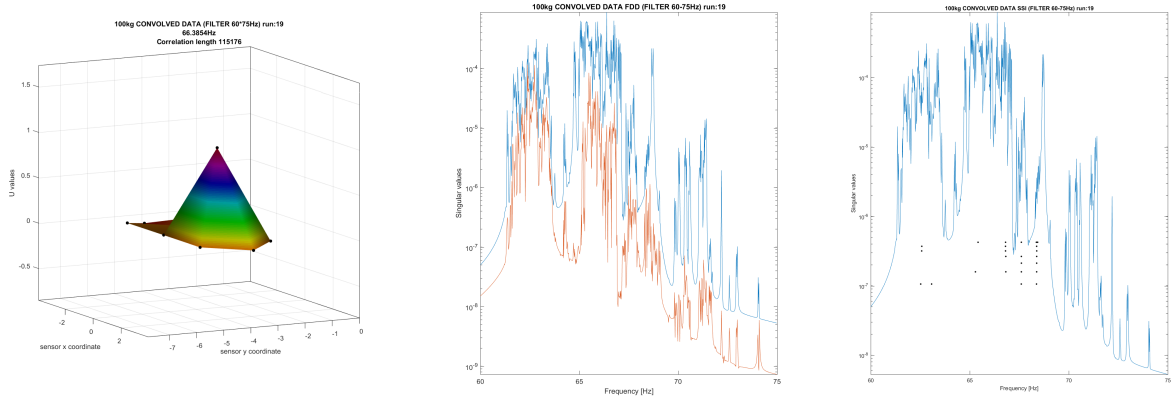
Figure A4.100kg: Run 17 (segment 3)



(a) 100kg mode shape, run 18

(b) 100kg FDD SSI output, run 18

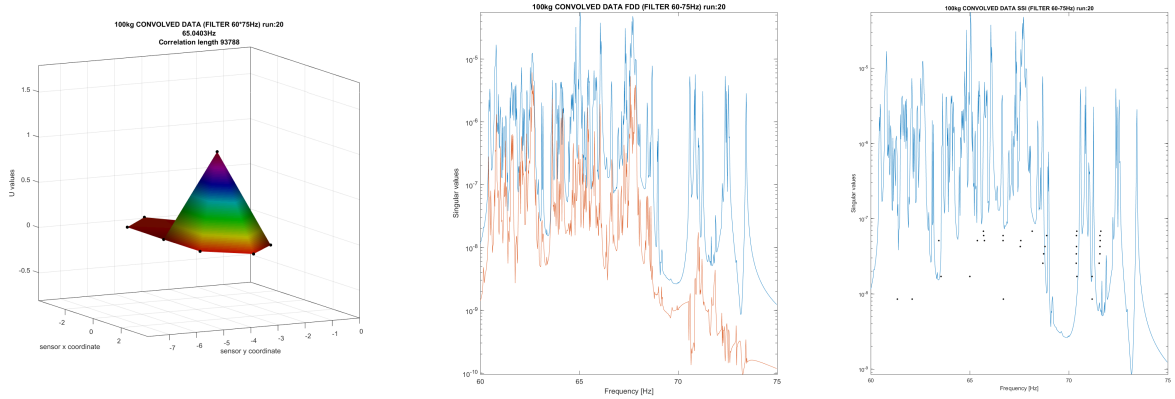
Figure A4.100kg: Run 18 (segment 3)



(a) 100kg mode shape, run 19

(b) 100kg FDD SSI output, run 19

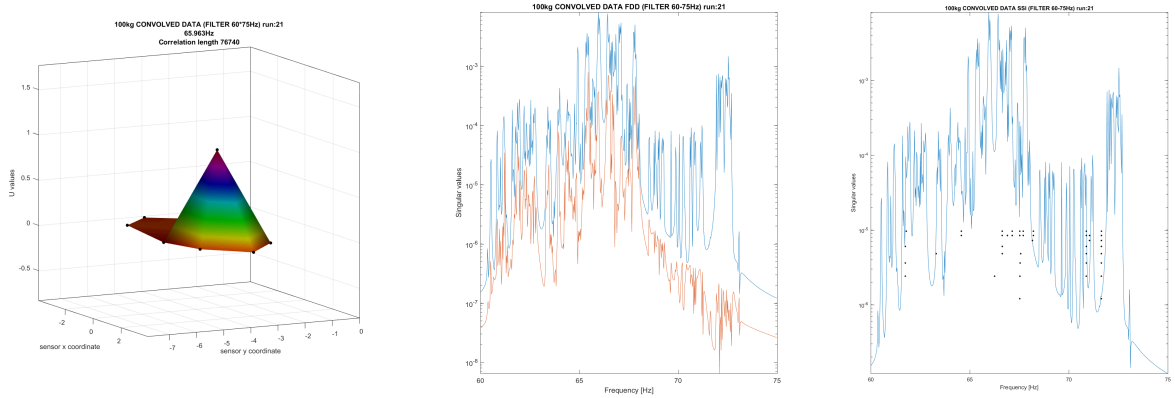
Figure A4.100kg: Run 19 (segment 3)



(a) 100kg mode shape, run 20

(b) 100kg FDD SSI output, run 20

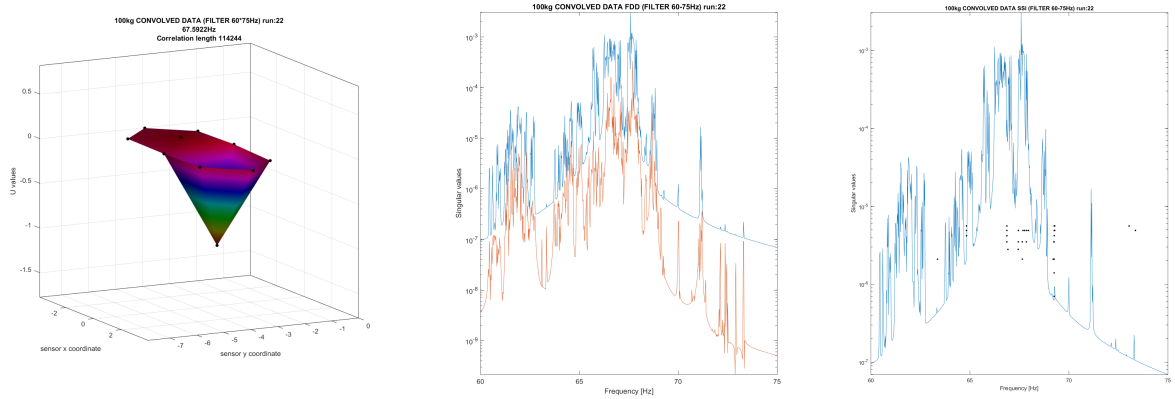
Figure A4.100kg: Run 20 (segment 3)



(a) 100kg mode shape, run 21

(b) 100kg FDD SSI output, run 21

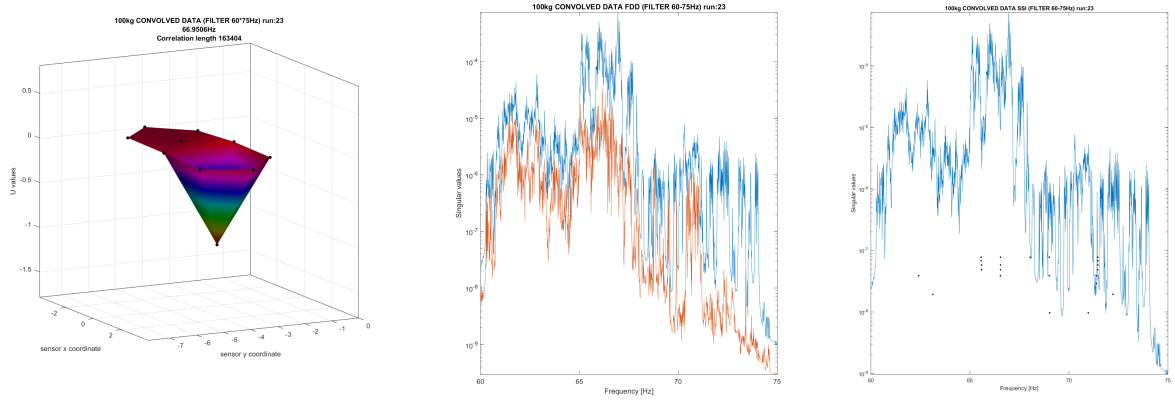
Figure A4.100kg: Run 21 (segment 3)



(a) 100kg mode shape, run 22

(b) 100kg FDD SSI output, run 22

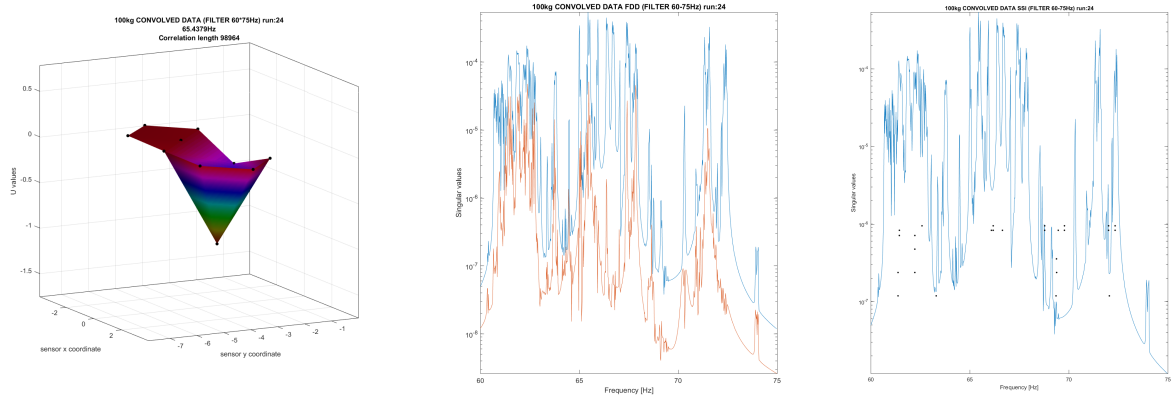
Figure A4.100kg: Run 22 (segment 3)



(a) 100kg mode shape, run 23

(b) 100kg FDD SSI output, run 23

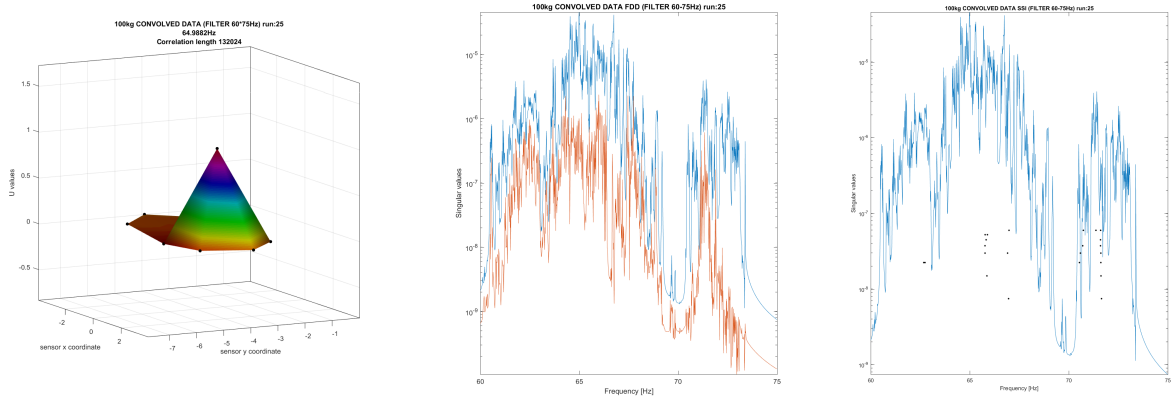
Figure A4.100kg: Run 23 (segment 3)



(a) 100kg mode shape, run 24

(b) 100kg FDD SSI output, run 24

Figure A4.100kg: Run 24 (segment 3)

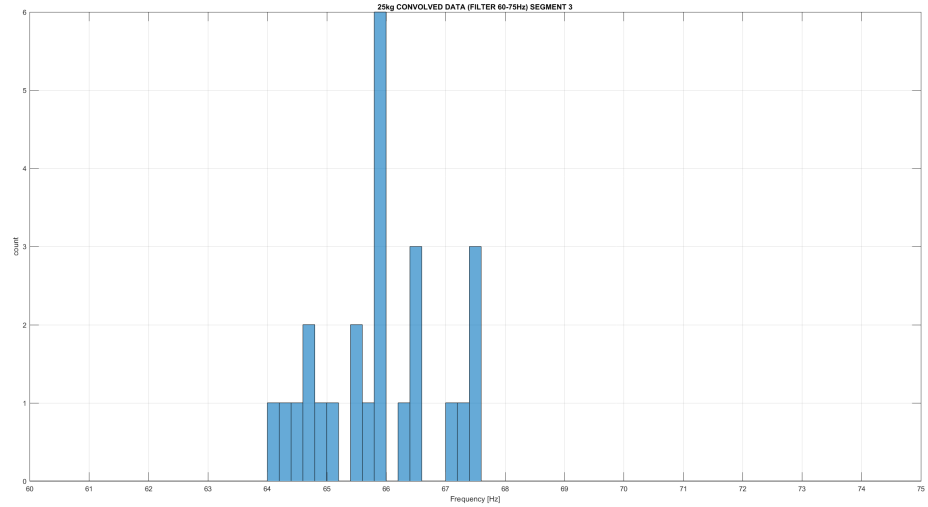


(a) 100kg mode shape, run 25

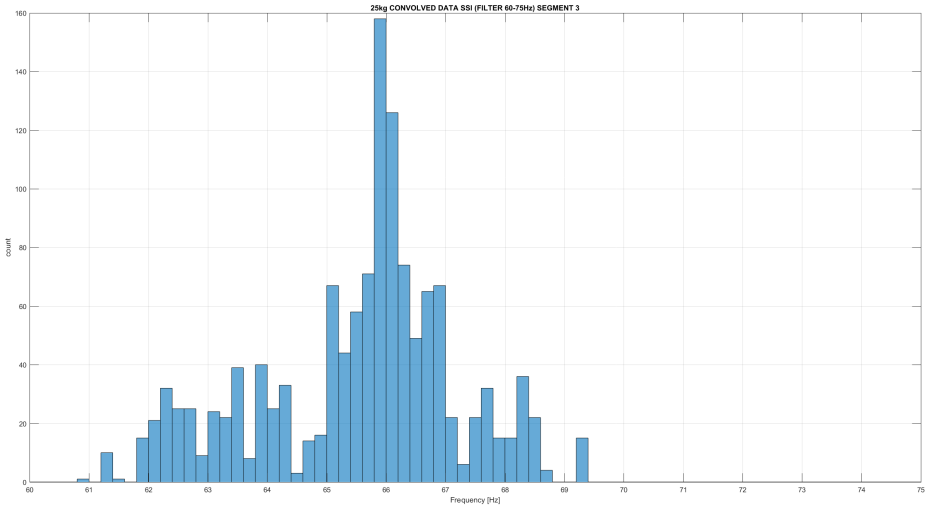
(b) 100kg FDD SSI output, run 25

Figure A4.100kg: Run 25 (segment 3)

Data (28.03.2017) 25kg-50kg segment 3 (Reduced order PF)

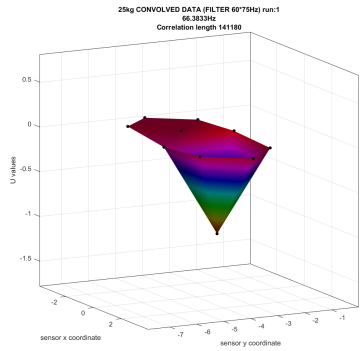


(a) 25kg FDD histogram

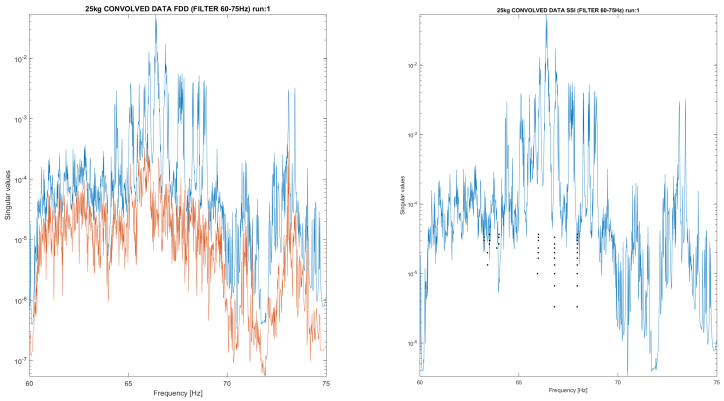


(b) 25kg SSI histogram

Figure A4.25kg: Histograms of identified modes, 25kg data (segment 3)

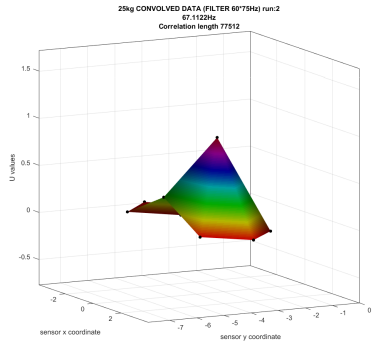


(a) 25kg mode shape, run 1

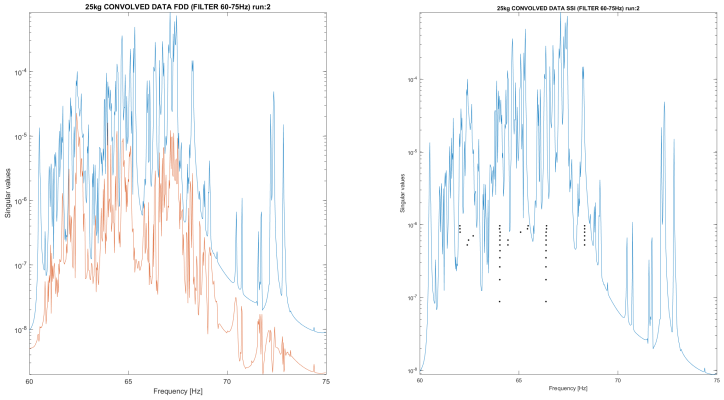


(b) 25kg FDD SSI output, run 1

Figure A4.25kg: Run 1 (segment 3)

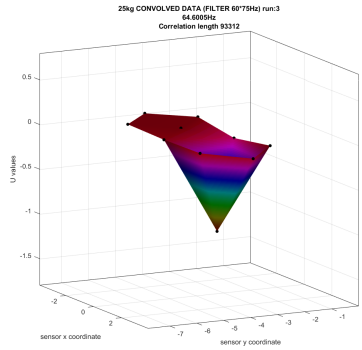


(a) 25kg mode shape, run 2

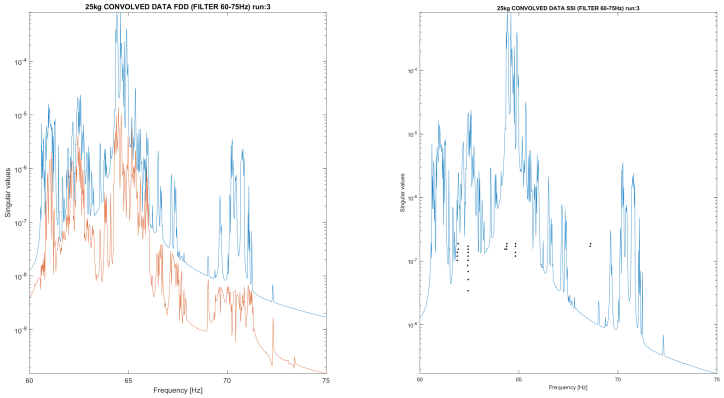


(b) 25kg FDD SSI output, run 2

Figure A4.25kg: Run 2 (segment 3)

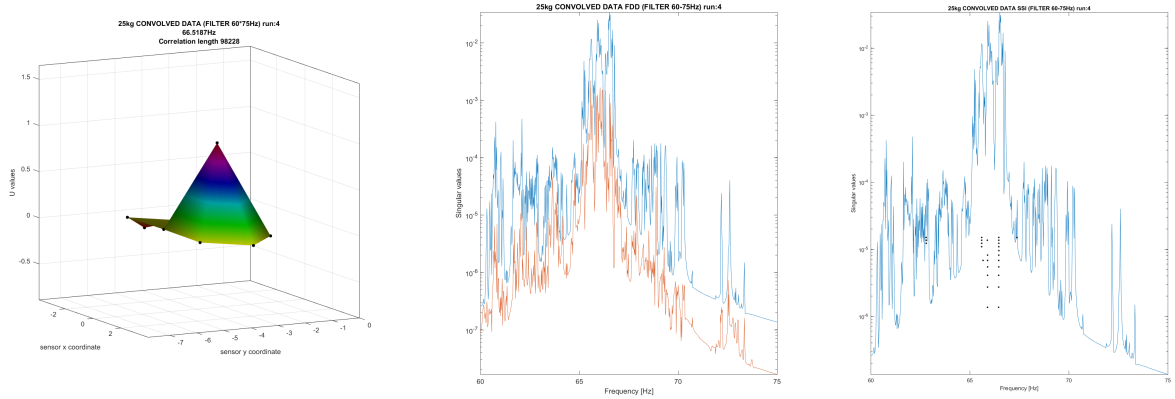


(a) 25kg mode shape, run 3



(b) 25kg FDD SSI output, run 3

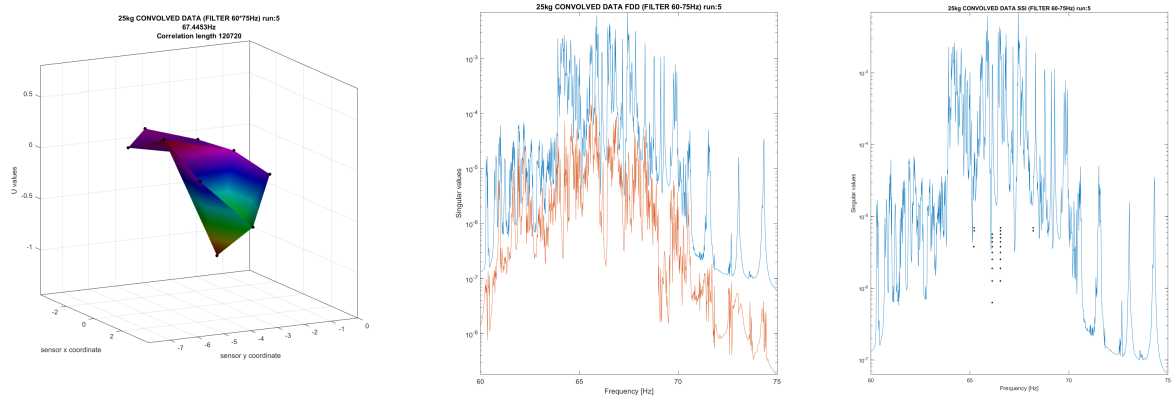
Figure A4.25kg: Run 3 (segment 3)



(a) 25kg mode shape, run 4

(b) 25kg FDD SSI output, run 4

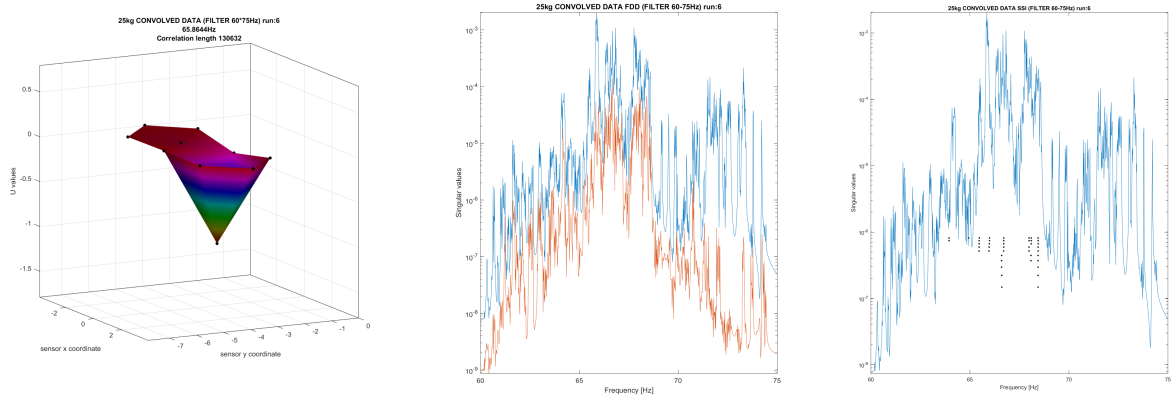
Figure A4.25kg: Run 4 (segment 3)



(a) 25kg mode shape, run 5

(b) 25kg FDD SSI output, run 5

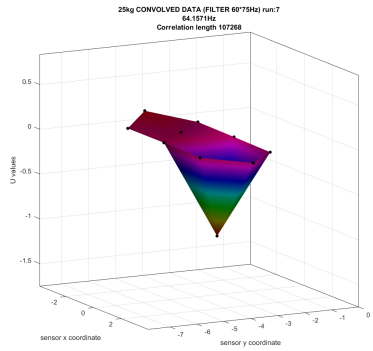
Figure A4.25kg: Run 5 (segment 3)



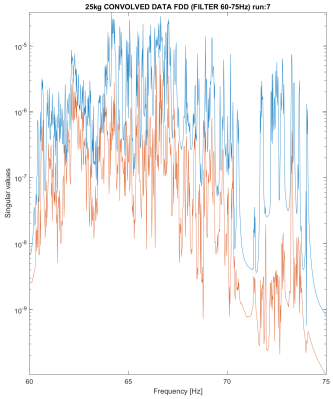
(a) 25kg mode shape, run 6

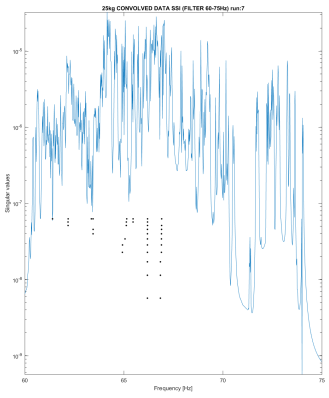
(b) 25kg FDD SSI output, run 6

Figure A4.25kg: Run 6 (segment 3)



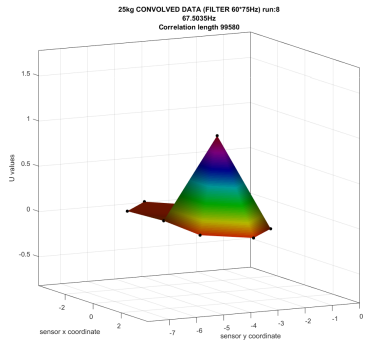
(a) 25kg mode shape, run 7



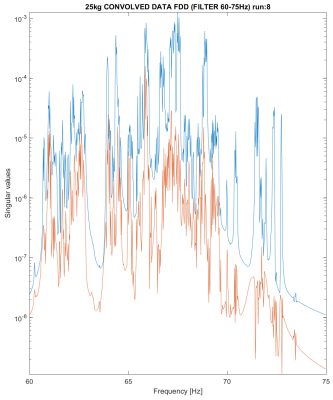


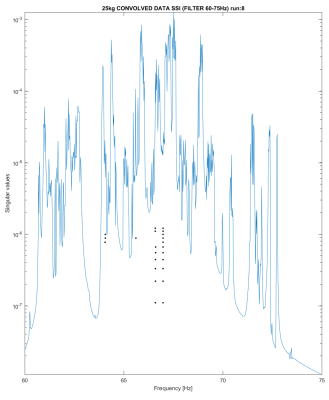
(b) 25kg FDD SSI output, run 7

Figure A4.25kg: Run 7 (segment 3)



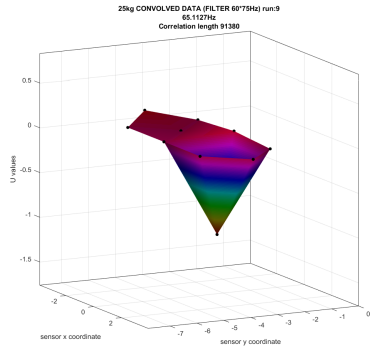
(a) 25kg mode shape, run 8



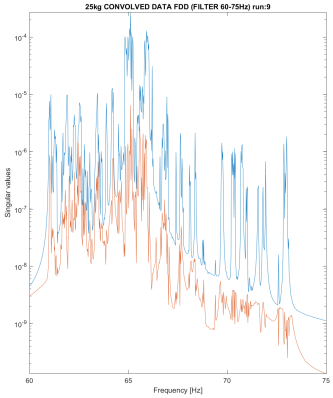


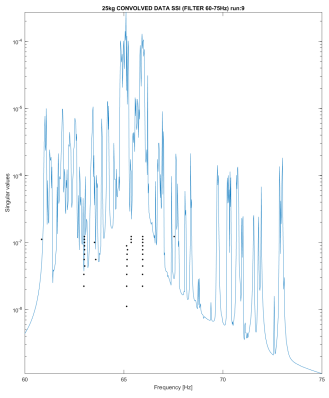
(b) 25kg FDD SSI output, run 8

Figure A4.25kg: Run 8 (segment 3)



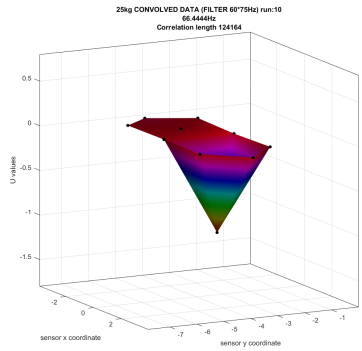
(a) 25kg mode shape, run 9



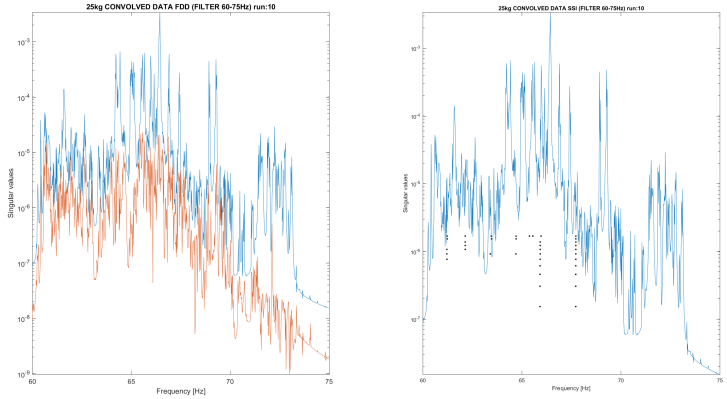


(b) 25kg FDD SSI output, run 9

Figure A4.25kg: Run 9 (segment 3)

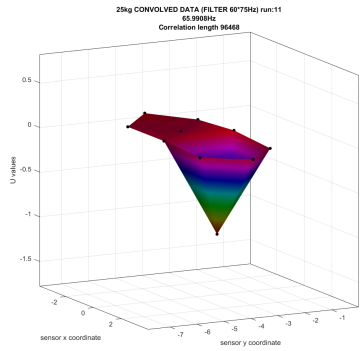


(a) 25kg mode shape, run 10

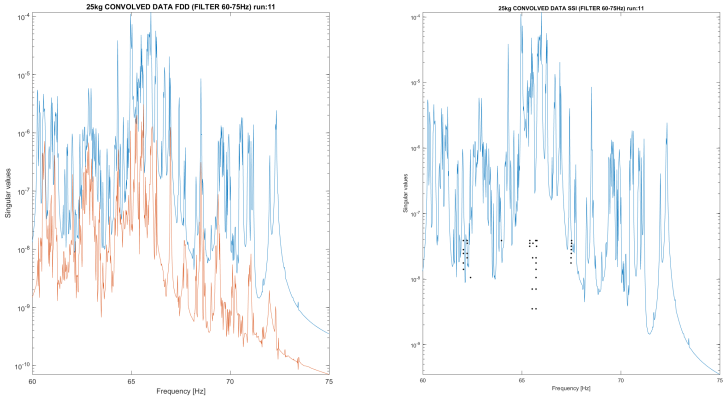


(b) 25kg FDD SSI output, run 10

Figure A4.25kg: Run 10 (segment 3)

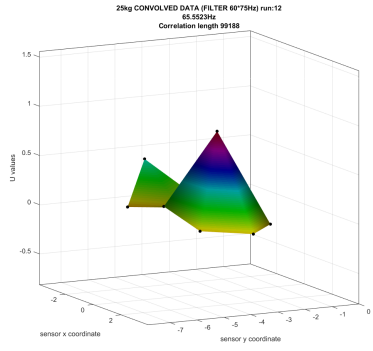


(a) 25kg mode shape, run 11

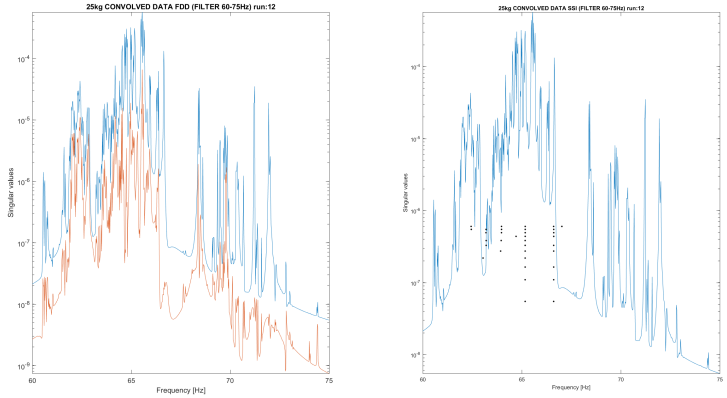


(b) 25kg FDD SSI output, run 11

Figure A4.25kg: Run 11 (segment 3)

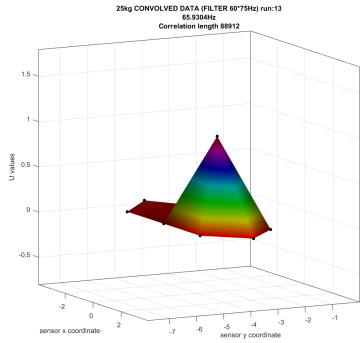


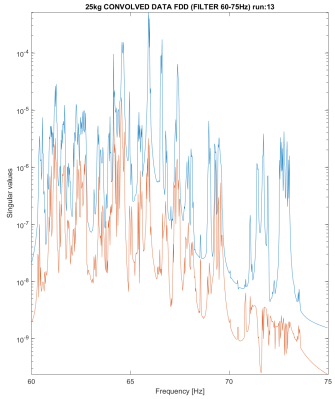
(a) 25kg mode shape, run 12

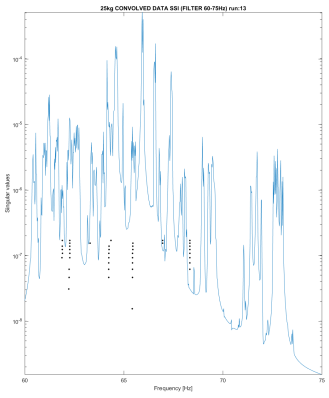


(b) 25kg FDD SSI output, run 12

Figure A4.25kg: Run 12 (segment 3)



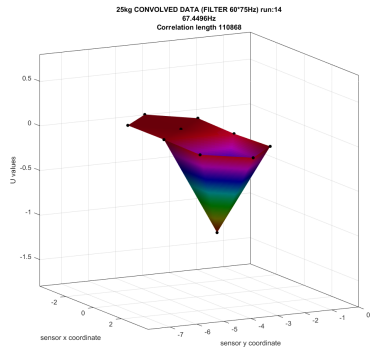


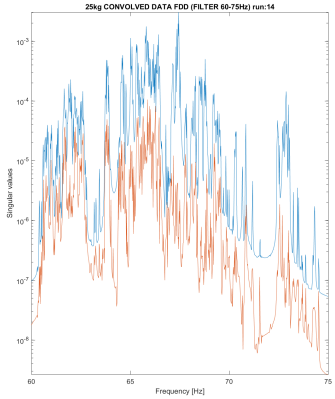


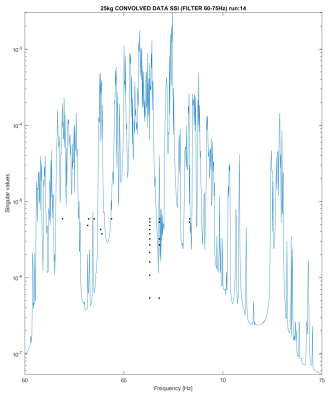
(a) 25kg mode shape, run 13

(b) 25kg FDD SSI output, run 13

Figure A4.25kg: Run 13 (segment 3)



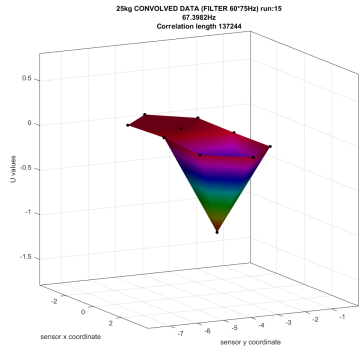


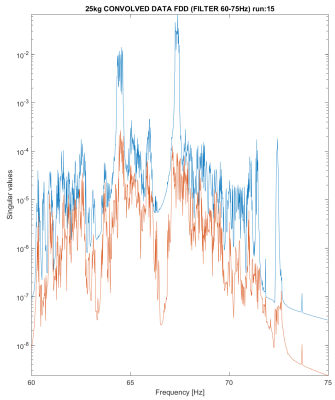


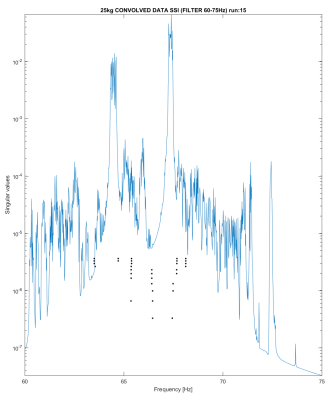
(a) 25kg mode shape, run 14

(b) 25kg FDD SSI output, run 14

Figure A4.25kg: Run 14 (segment 3)



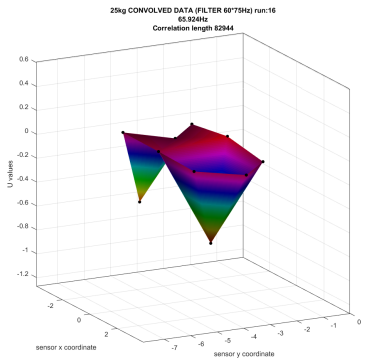




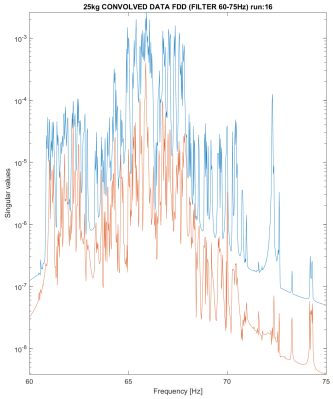
(a) 25kg mode shape, run 15

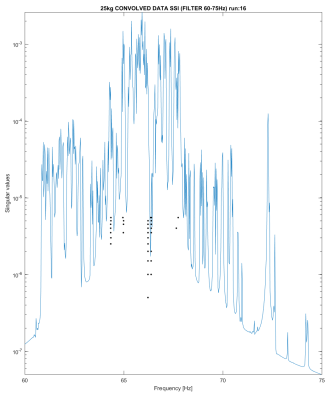
(b) 25kg FDD SSI output, run 15

Figure A4.25kg: Run 15 (segment 3)



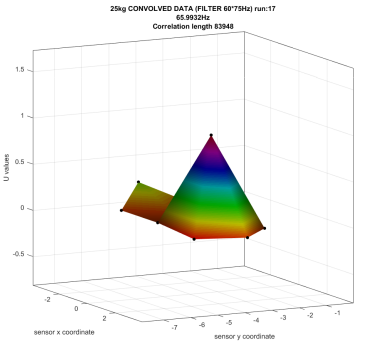
(a) 25kg mode shape, run 16



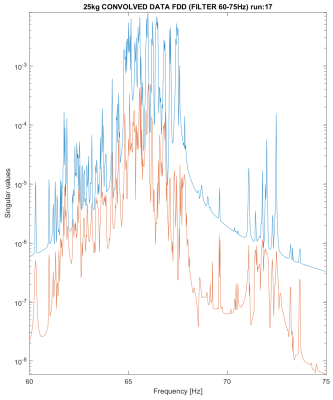


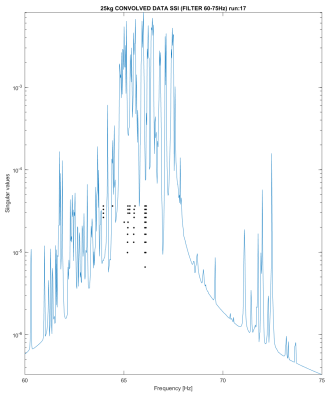
(b) 25kg FDD SSI output, run 16

Figure A4.25kg: Run 16 (segment 3)



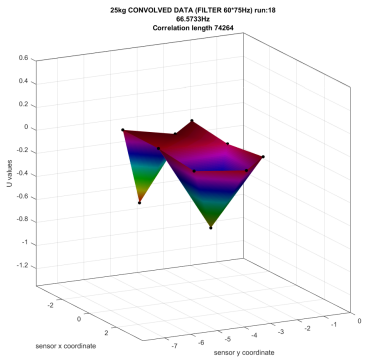
(a) 25kg mode shape, run 17



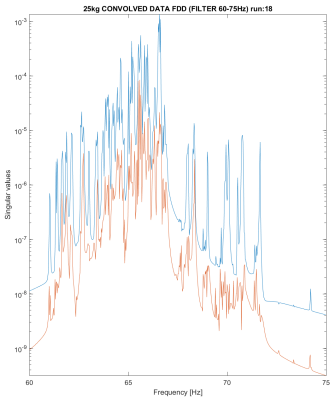


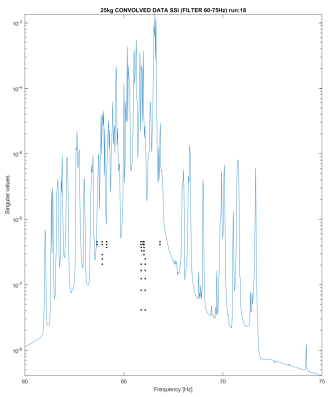
(b) 25kg FDD SSI output, run 17

Figure A4.25kg: Run 17 (segment 3)



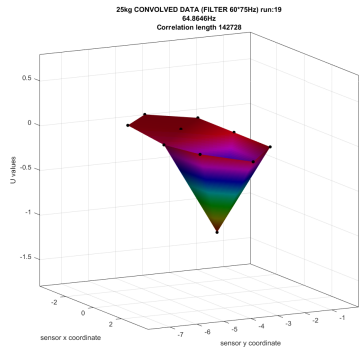
(a) 25kg mode shape, run 18



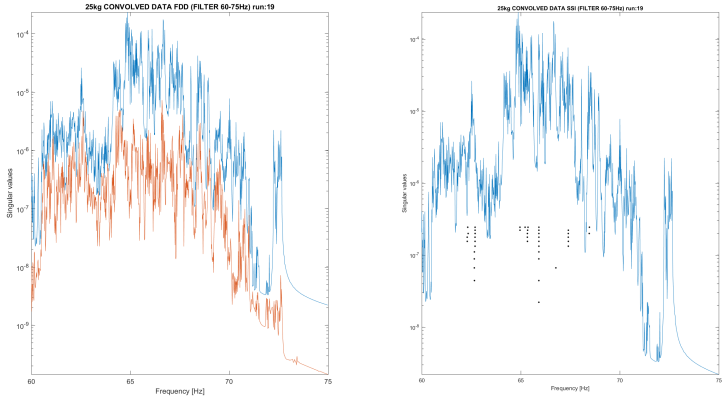


(b) 25kg FDD SSI output, run 18

Figure A4.25kg: Run 18 (segment 3)

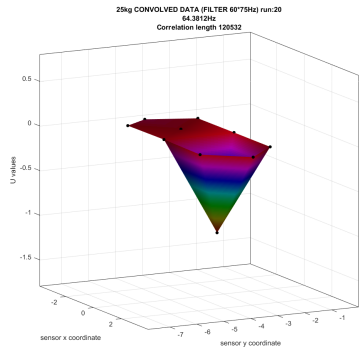


(a) 25kg mode shape, run 19

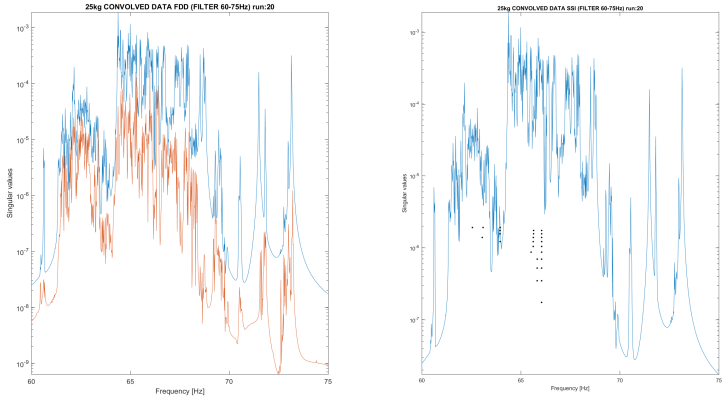


(b) 25kg FDD SSI output, run 19

Figure A4.25kg: Run 19 (segment 3)

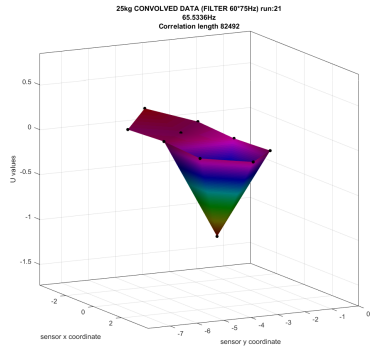


(a) 25kg mode shape, run 20

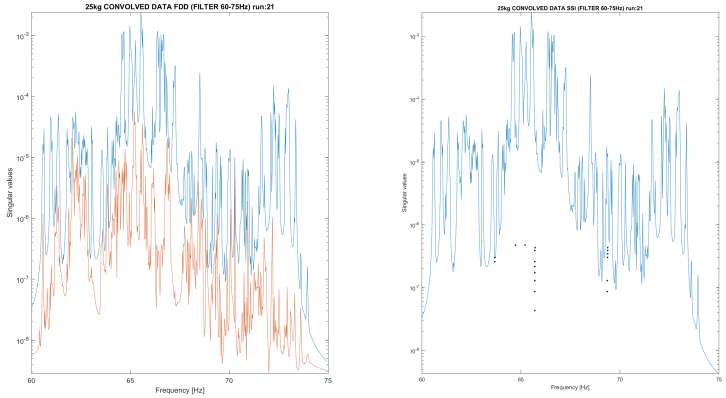


(b) 25kg FDD SSI output, run 20

Figure A4.25kg: Run 20 (segment 3)

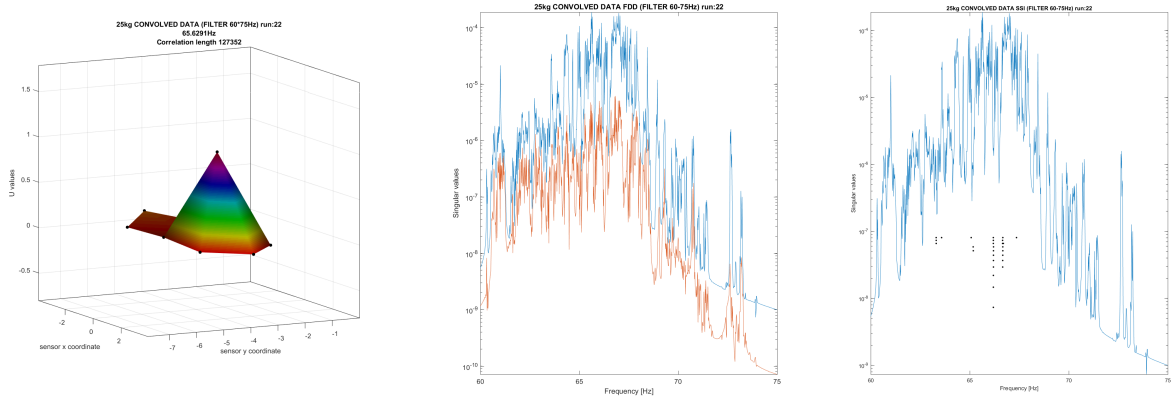


(a) 25kg mode shape, run 21



(b) 25kg FDD SSI output, run 21

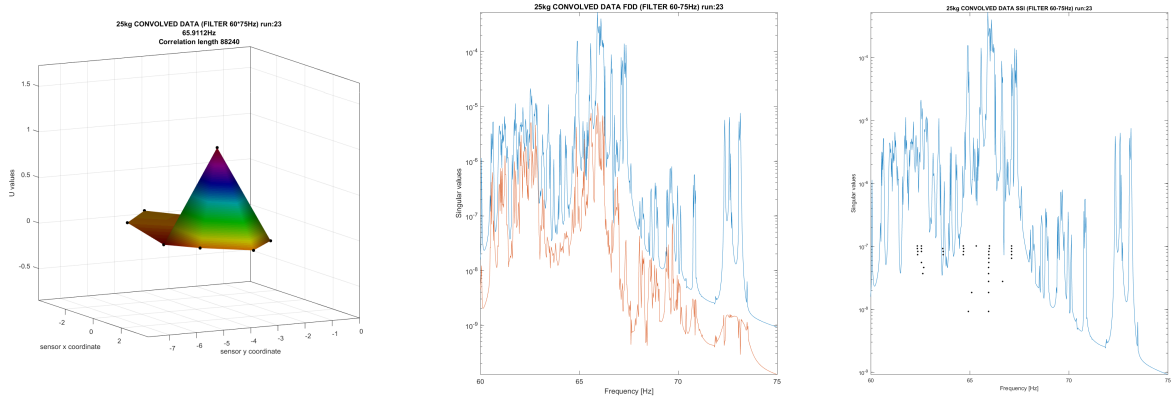
Figure A4.25kg: Run 21 (segment 3)



(a) 25kg mode shape, run 22

(b) 25kg FDD SSI output, run 22

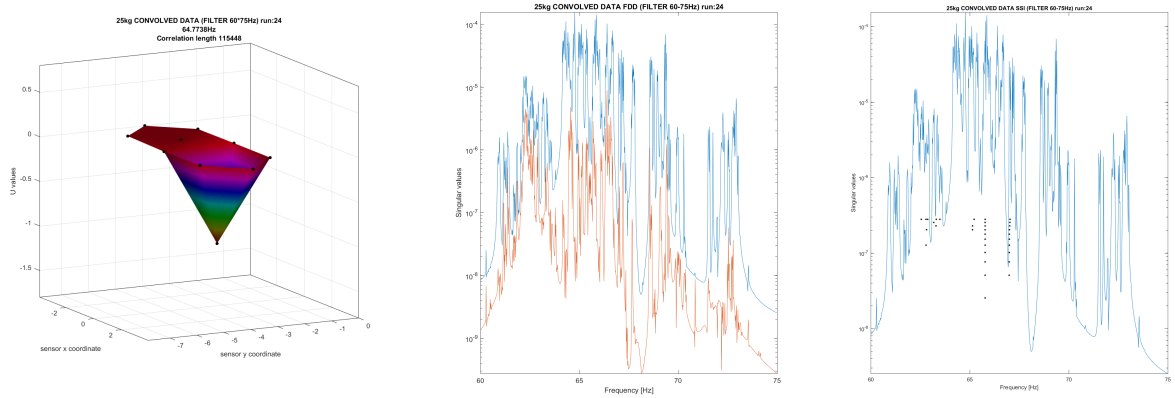
Figure A4.25kg: Run 22 (segment 3)



(a) 25kg mode shape, run 23

(b) 25kg FDD SSI output, run 23

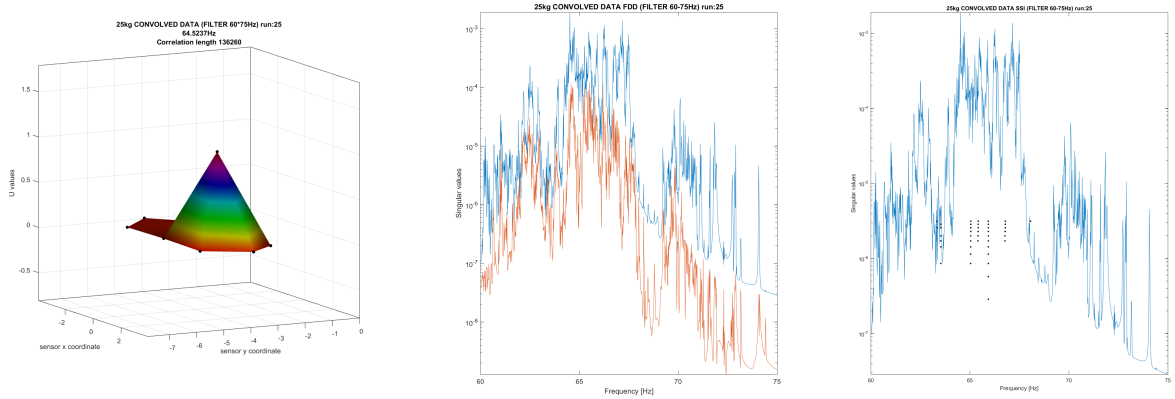
Figure A4.25kg: Run 23 (segment 3)



(a) 25kg mode shape, run 24

(b) 25kg FDD SSI output, run 24

Figure A4.25kg: Run 24 (segment 3)

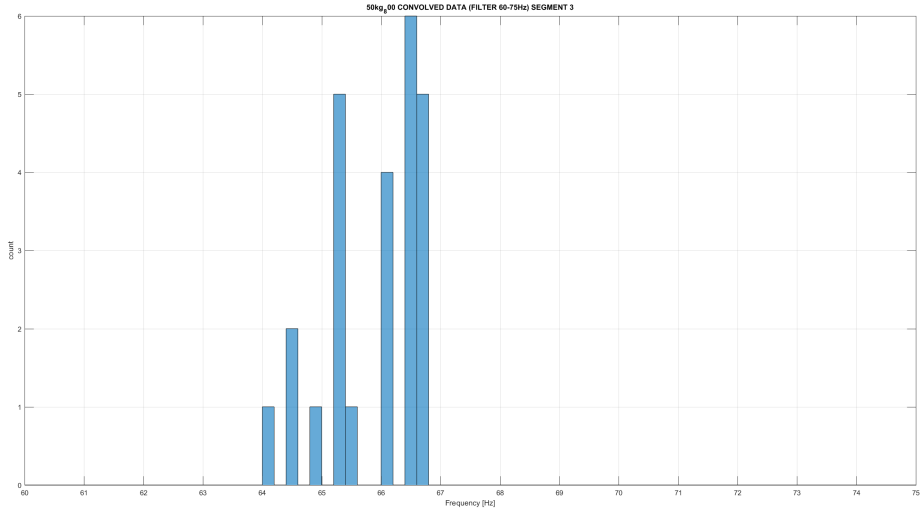


(a) 25kg mode shape, run 25

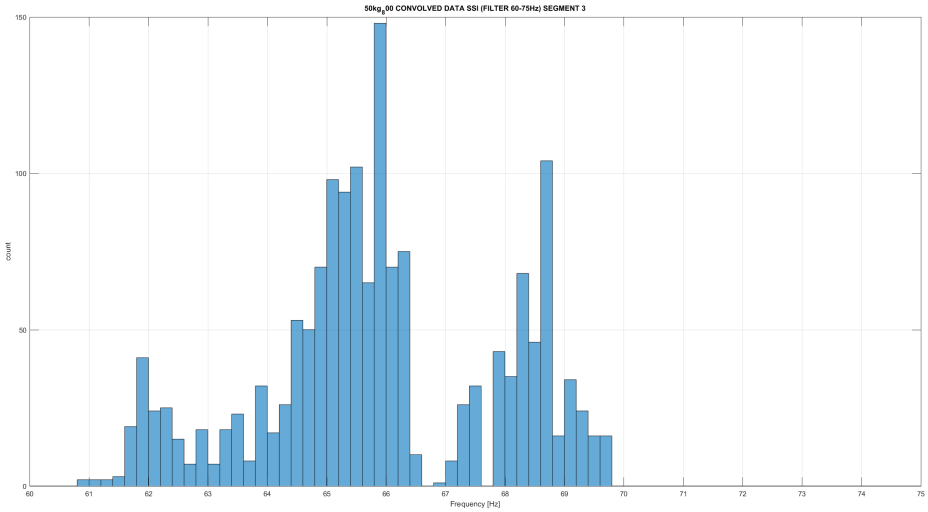
(b) 25kg FDD SSI output, run 25

Figure A4.25kg: Run 25 (segment 3)

50kg data segment 3 (28.03.2017)

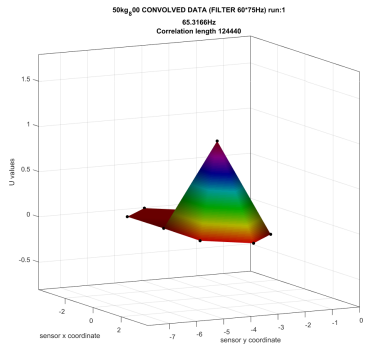


(a) 50kg FDD histogram

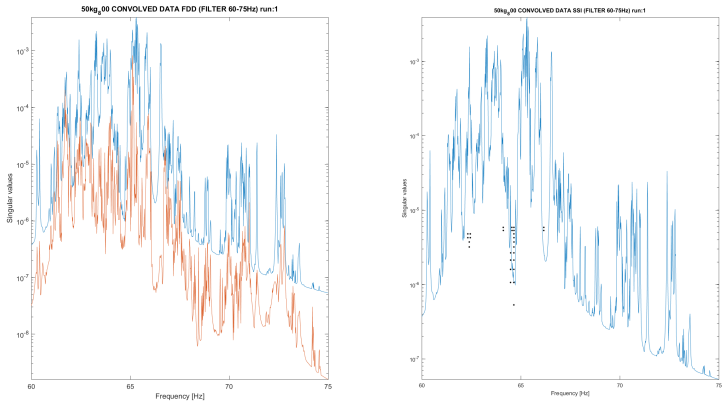


(b) 50kg SSI histogram

Figure A4.50kg: Histograms of identified modes, 50kg data (segment 3)

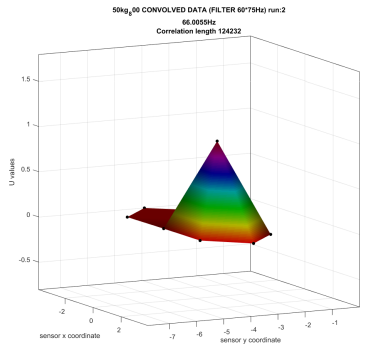


(a) 50kg mode shape, run 1

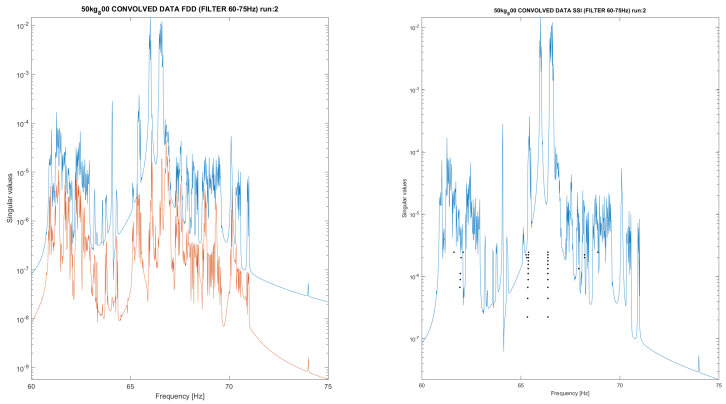


(b) 50kg FDD SSI output, run 1

Figure A4.50kg (28.03.2017): Run 1 (segment 3)

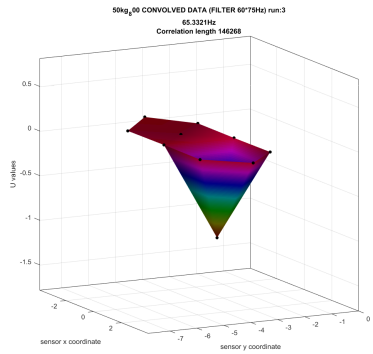


(a) 50kg mode shape, run 2

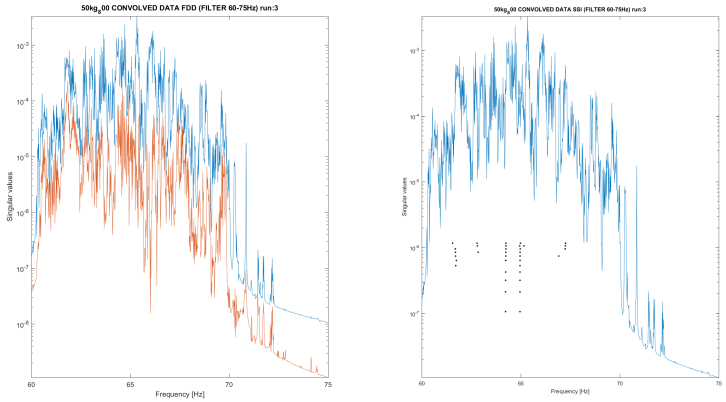


(b) 50kg FDD SSI output, run 2

Figure A4.50kg (28.03.2017): Run 2 (segment 3)

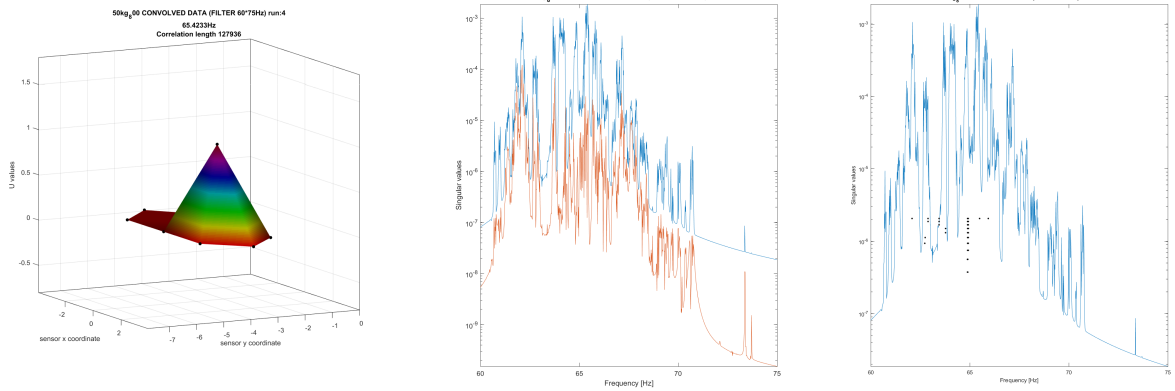


(a) 50kg mode shape, run 3



(b) 50kg FDD SSI output, run 3

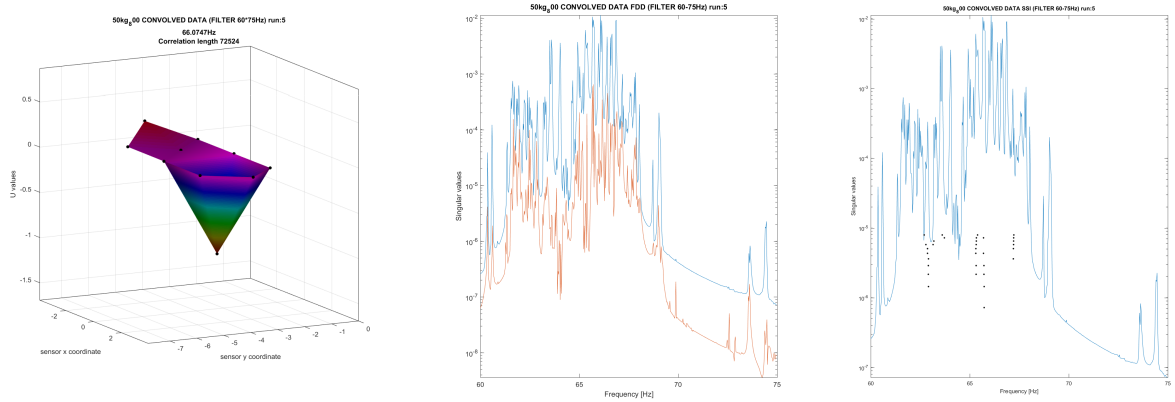
Figure A4.50kg (28.03.2017): Run 3 (segment 3)



(a) 50kg mode shape, run 4

(b) 50kg FDD SSI output, run 4

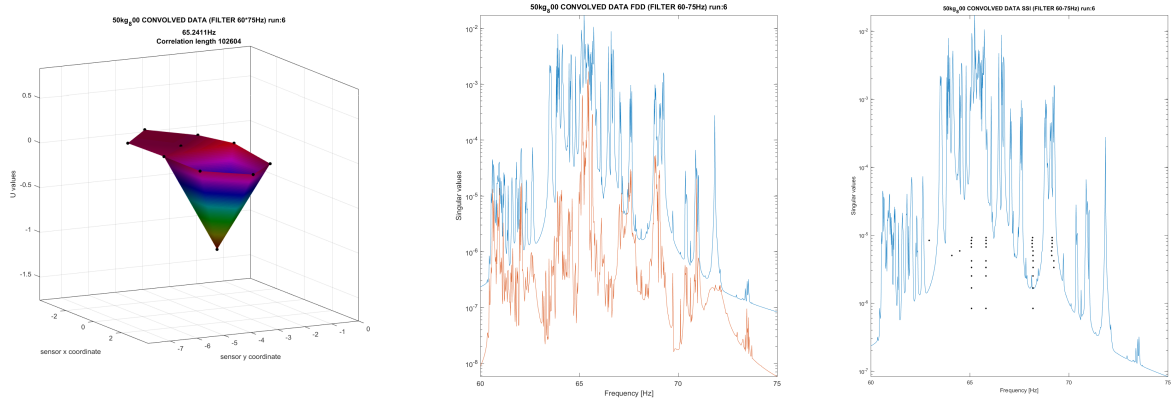
Figure A4.50kg (28.03.2017): Run 4 (segment 3)



(a) 50kg mode shape, run 5

(b) 50kg FDD SSI output, run 5

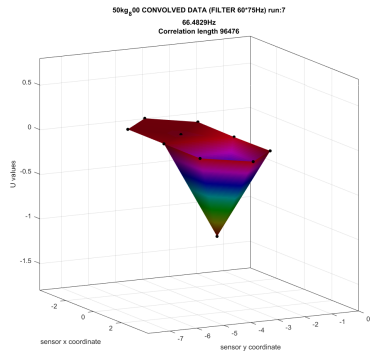
Figure A4.50kg (28.03.2017): Run 5 (segment 3)



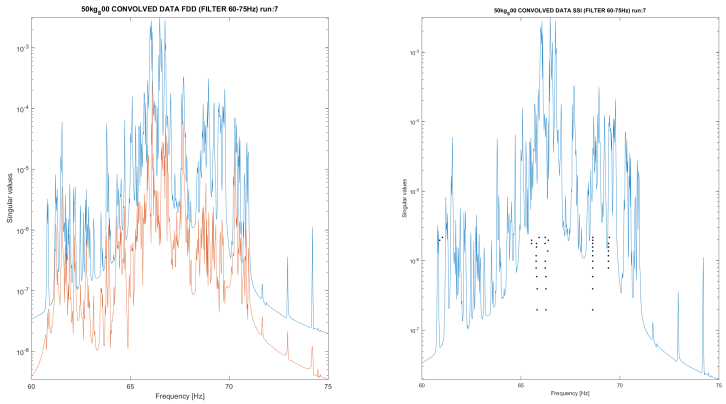
(a) 50kg mode shape, run 6

(b) 50kg FDD SSI output, run 6

Figure A4.50kg (28.03.2017): Run 6 (segment 3)

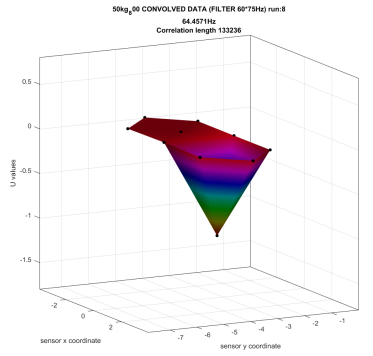


(a) 50kg mode shape, run 7

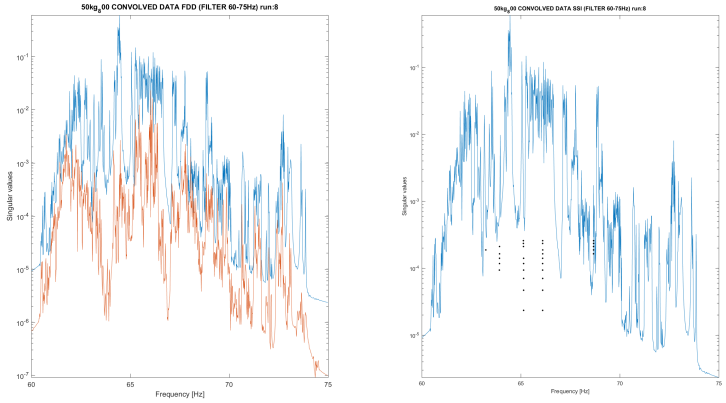


(b) 50kg FDD SSI output, run 7

Figure A4.50kg (28.03.2017): Run 7 (segment 3)

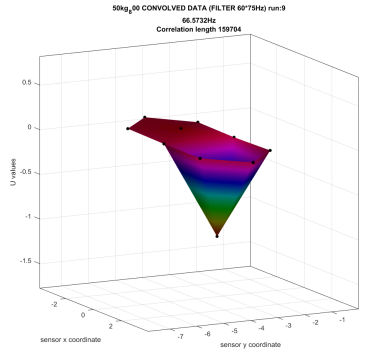


(a) 50kg mode shape, run 8

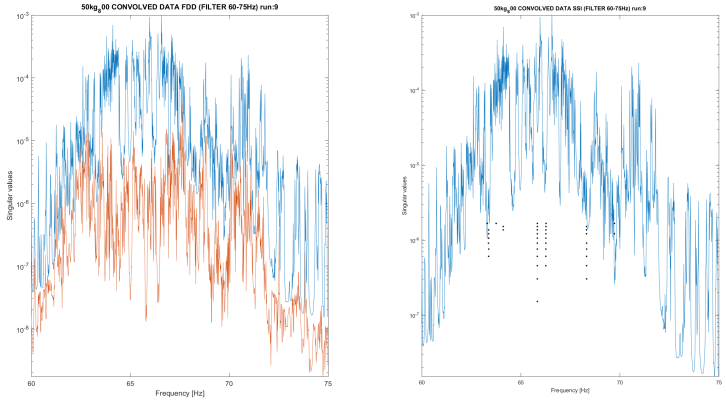


(b) 50kg FDD SSI output, run 8

Figure A4.50kg (28.03.2017): Run 8 (segment 3)

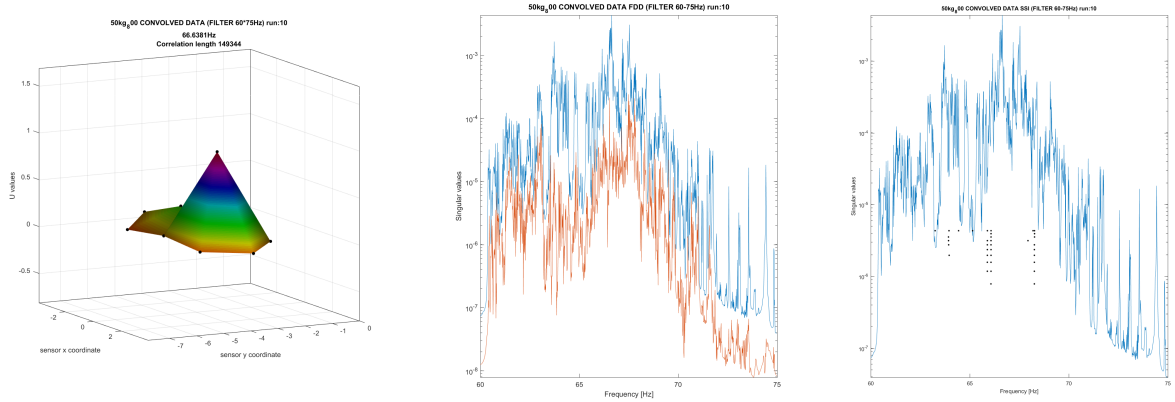


(a) 50kg mode shape, run 9



(b) 50kg FDD SSI output, run 9

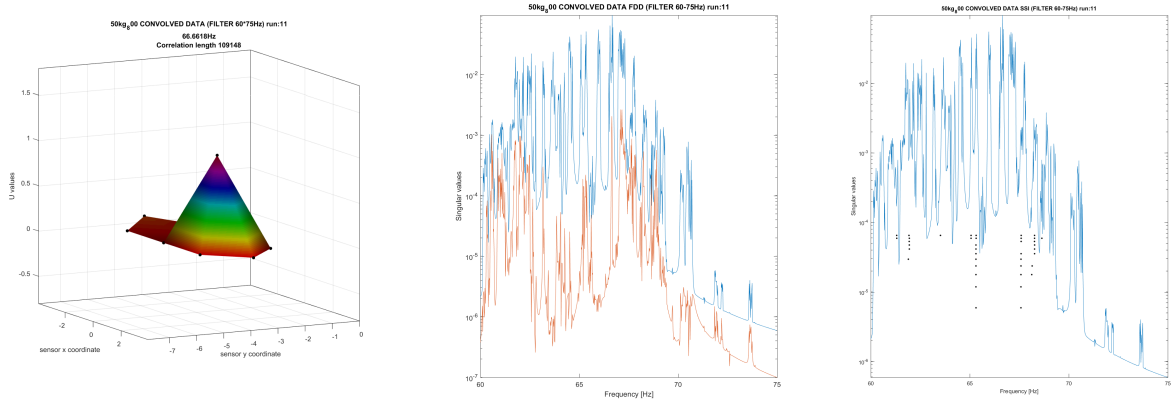
Figure A4.50kg (28.03.2017): Run 9 (segment 3)



(a) 50kg mode shape, run 10

(b) 50kg FDD SSI output, run 10

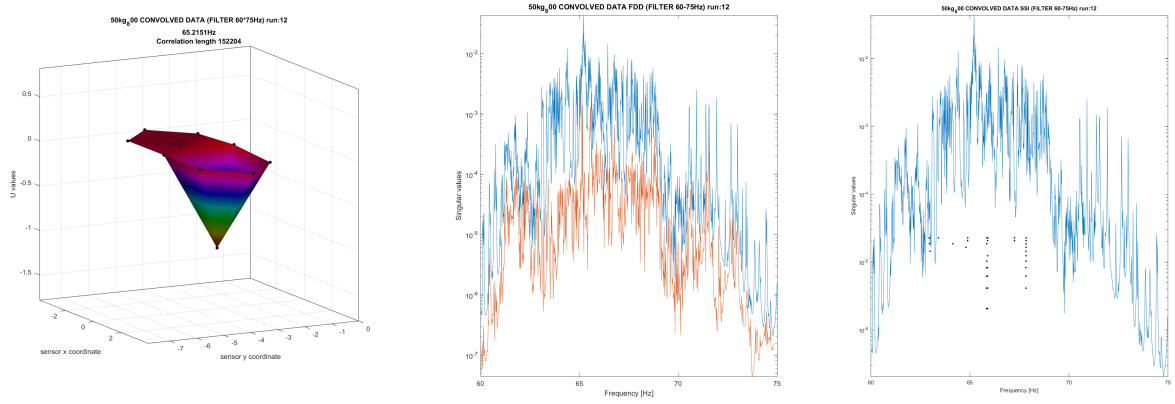
Figure A4.50kg (28.03.2017): Run 10 (segment 3)



(a) 50kg mode shape, run 11

(b) 50kg FDD SSI output, run 11

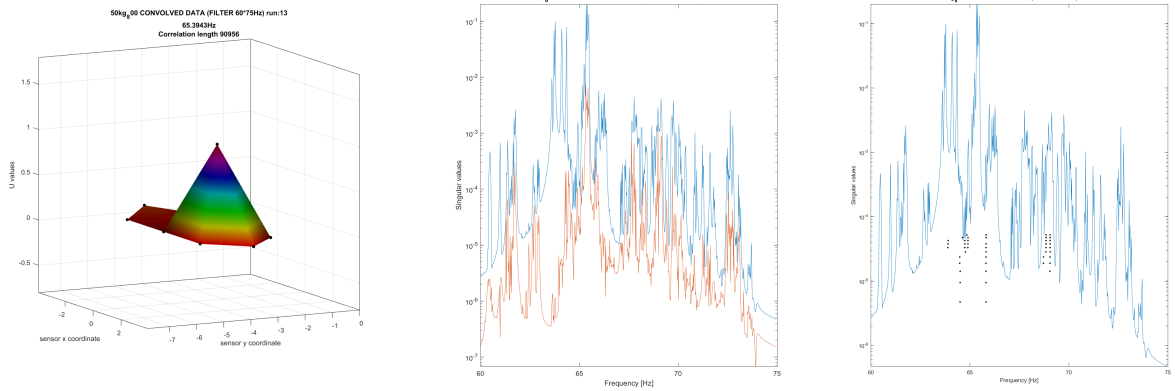
Figure A4.50kg (28.03.2017): Run 11 (segment 3)



(a) 50kg mode shape, run 12

(b) 50kg FDD SSI output, run 12

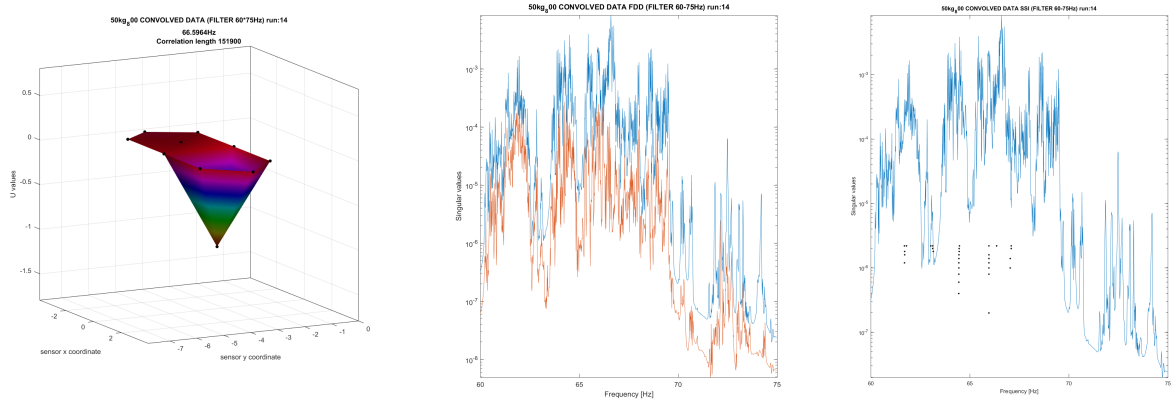
Figure A4.50kg (28.03.2017): Run 12 (segment 3)



(a) 50kg mode shape, run 13

(b) 50kg FDD SSI output, run 13

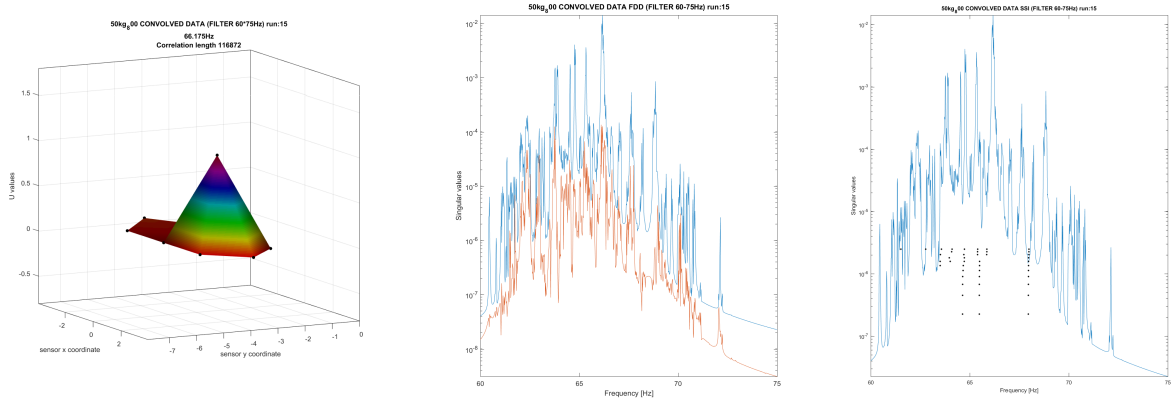
Figure A4.50kg (28.03.2017): Run 13 (segment 3)



(a) 50kg mode shape, run 14

(b) 50kg FDD SSI output, run 14

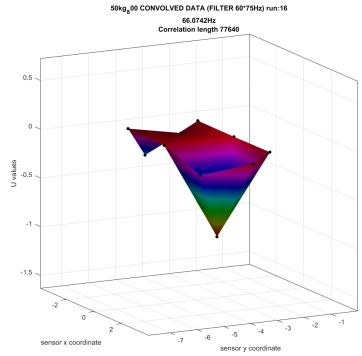
Figure A4.50kg (28.03.2017): Run 14 (segment 3)



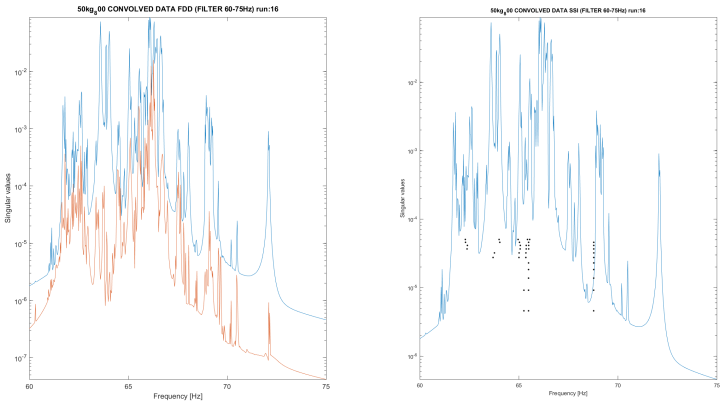
(a) 50kg mode shape, run 15

(b) 50kg FDD SSI output, run 15

Figure A4.50kg (28.03.2017): Run 15 (segment 3)

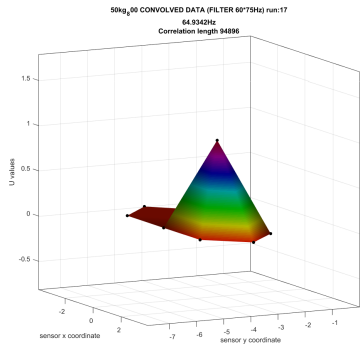


(a) 50kg mode shape, run 16

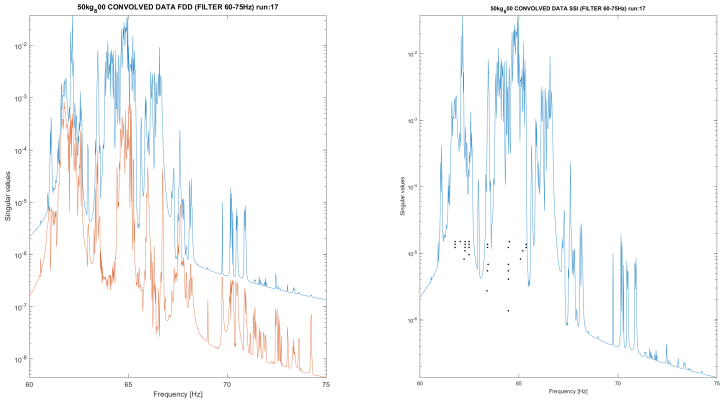


(b) 50kg FDD SSI output, run 16

Figure A4.50kg (28.03.2017): Run 16 (segment 3)

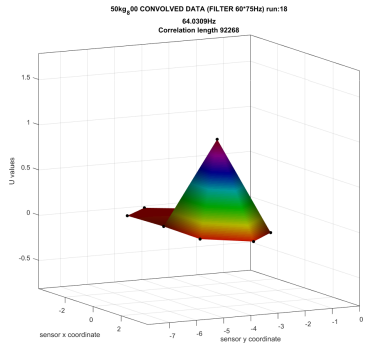


(a) 50kg mode shape, run 17

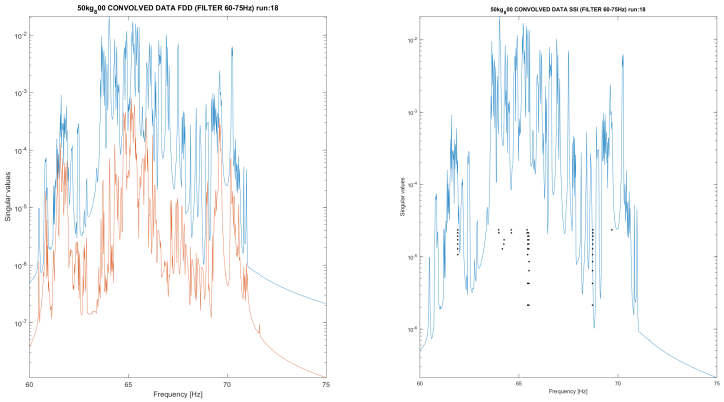


(b) 50kg FDD SSI output, run 17

Figure A4.50kg (28.03.2017): Run 17 (segment 3)

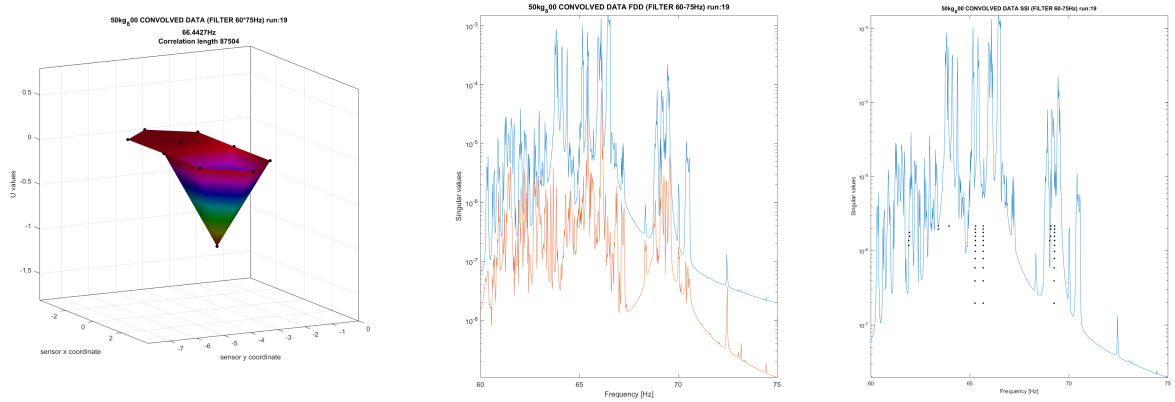


(a) 50kg mode shape, run 18



(b) 50kg FDD SSI output, run 18

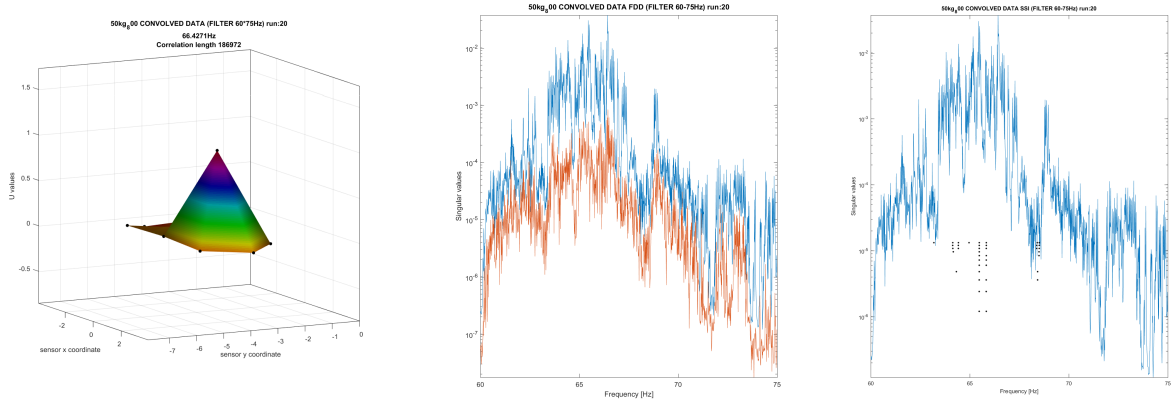
Figure A4.50kg (28.03.2017): Run 18 (segment 3)



(a) 50kg mode shape, run 19

(b) 50kg FDD SSI output, run 19

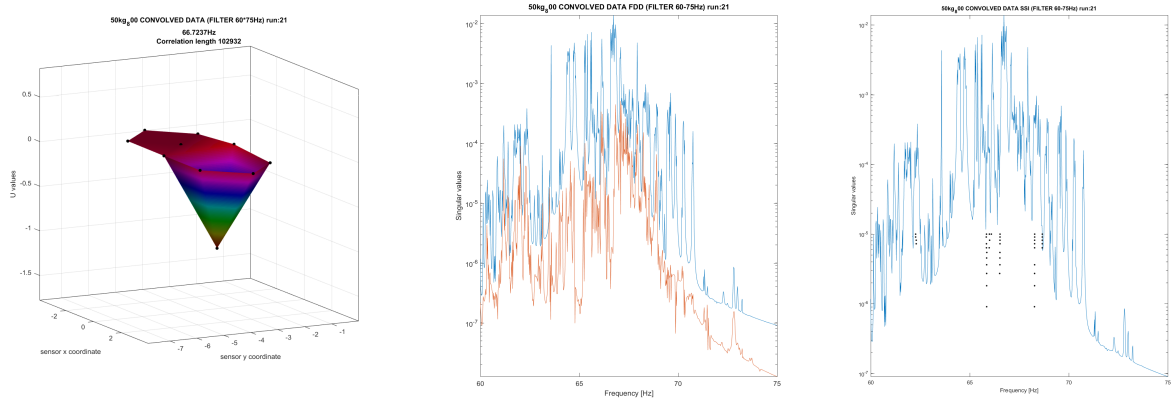
Figure A4.50kg (28.03.2017): Run 19 (segment 3)



(a) 50kg mode shape, run 20

(b) 50kg FDD SSI output, run 20

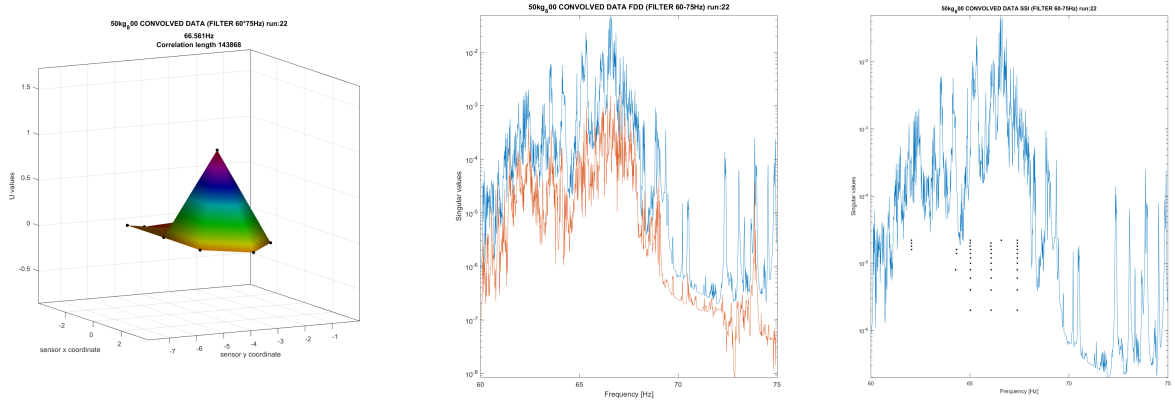
Figure A4.50kg (28.03.2017): Run 20 (segment 3)



(a) 50kg mode shape, run 21

(b) 50kg FDD SSI output, run 21

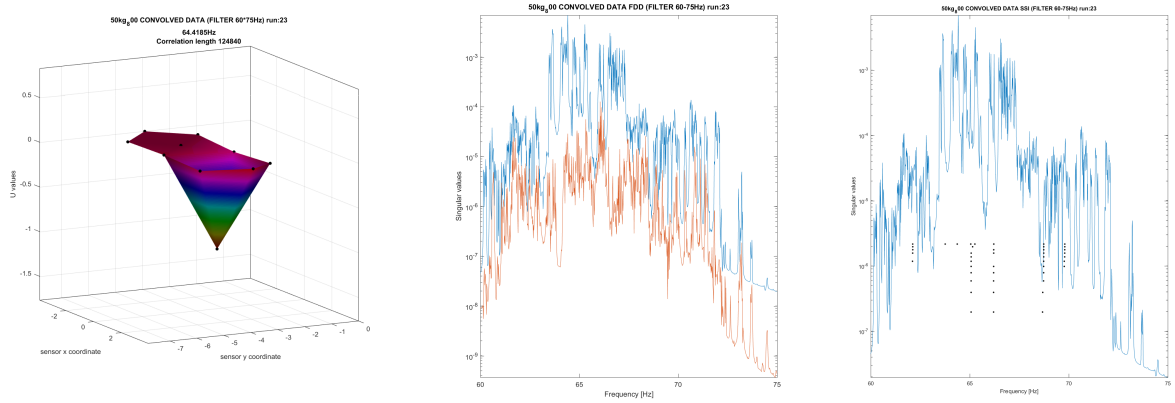
Figure A4.50kg (28.03.2017): Run 21 (segment 3)



(a) 50kg mode shape, run 22

(b) 50kg FDD SSI output, run 22

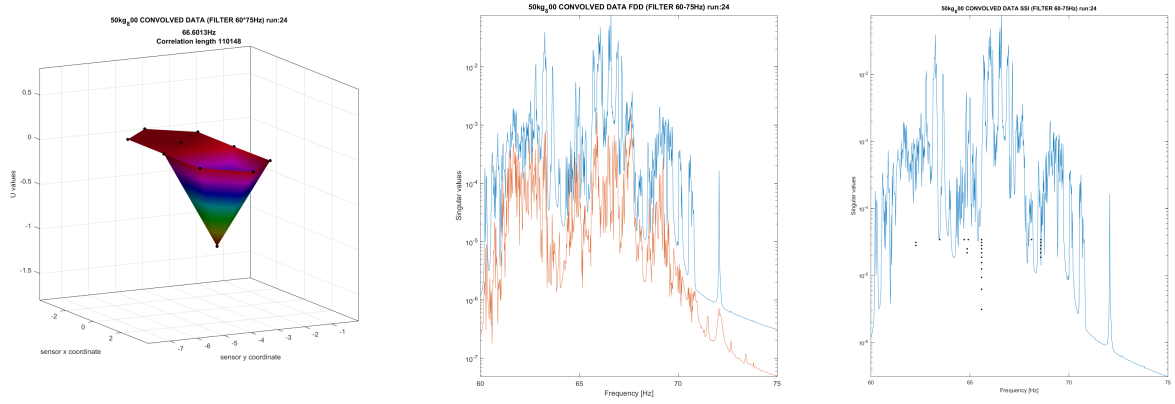
Figure A4.50kg (28.03.2017): Run 22 (segment 3)



(a) 50kg mode shape, run 23

(b) 50kg FDD SSI output, run 23

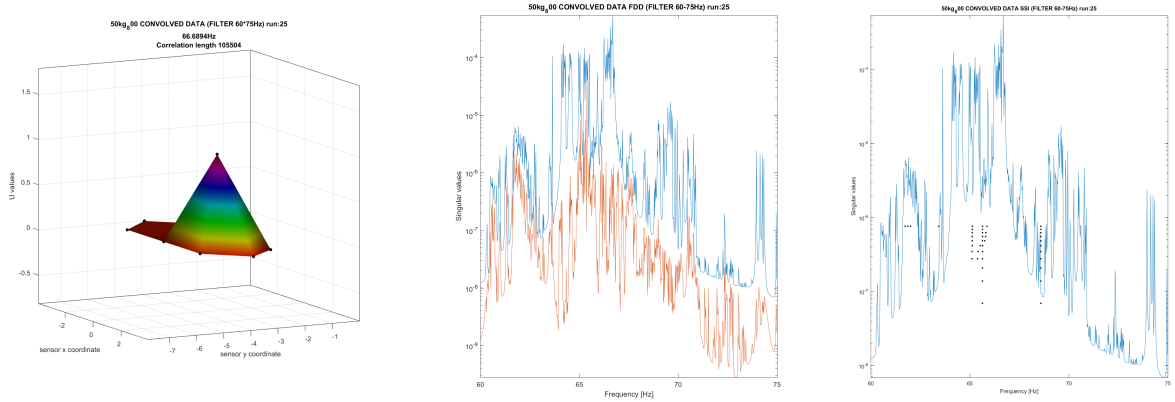
Figure A4.50kg (28.03.2017): Run 23 (segment 3)



(a) 50kg mode shape, run 24

(b) 50kg FDD SSI output, run 24

Figure A4.50kg (28.03.2017): Run 24 (segment 3)



(a) 50kg mode shape, run 25

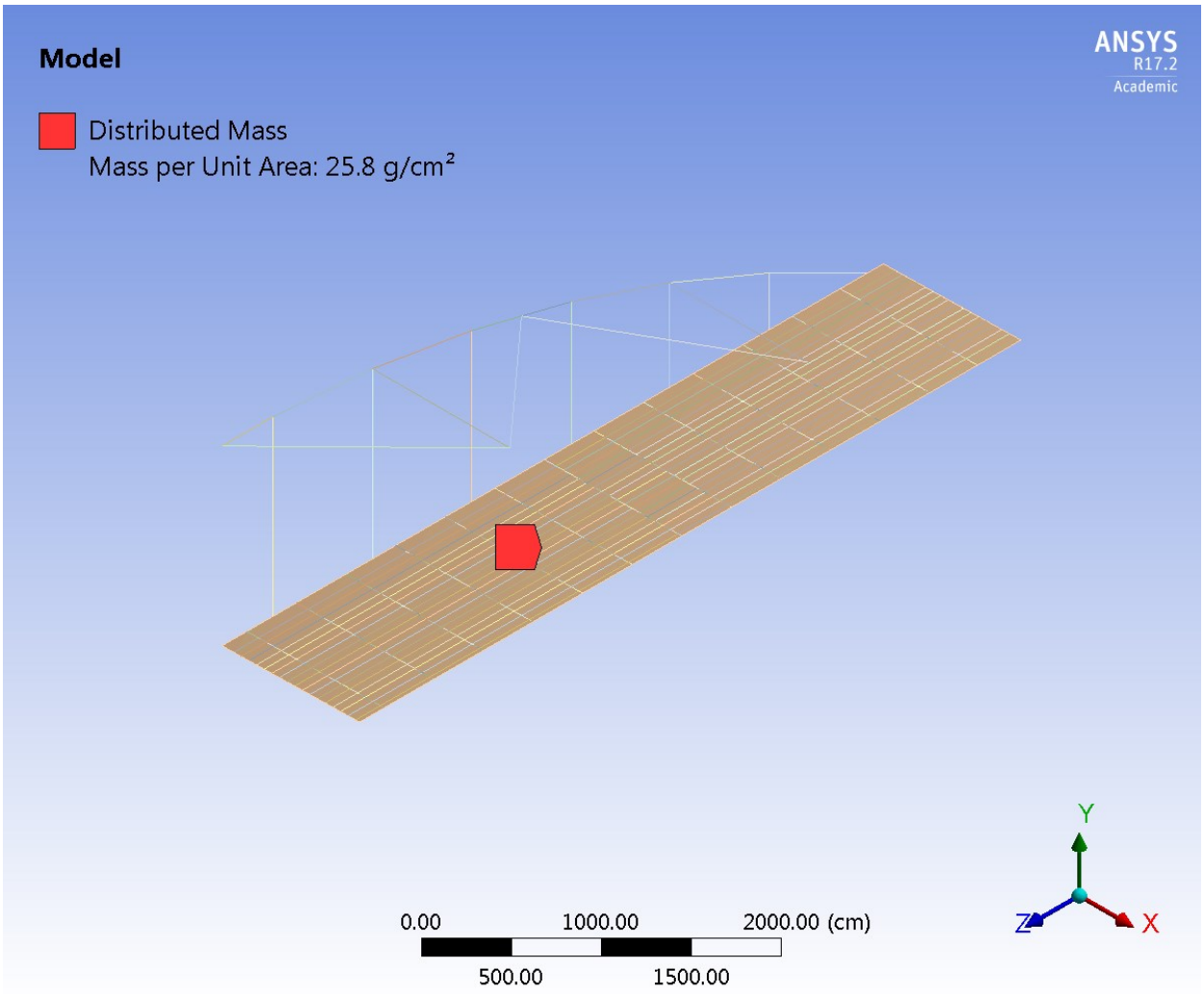
(b) 50kg FDD SSI output, run 25

Figure A4.50kg (28.03.2017): Run 25 (segment 3)

Appendix F1

Global model

First Saved	Sunday, July 08, 2018
Last Saved	Monday, July 09, 2018
Product Version	17.2 Release
Save Project Before Solution	No
Save Project After Solution	No



Contents

- **Units**
- **Model (B3)**
  - Geometry
    - Line_structures
      - Parts
    - deck
    - Distributed Mass
  - Coordinate Systems
  - Connections
    - Contacts
      - Contact Regions
  - Mesh
  - Named Selections
  - **Modal (B4)**
    - Pre-Stress (None)
    - Analysis Settings
    - Loads
    - Solution (B5)
      - Solution Information
- **Material Data**
  - Structural Steel

Units

TABLE 1

Unit System	Metric (cm, g, dyne, s, V, A) Degrees rad/s Celsius
Angle	Degrees
Rotational Velocity	rad/s
Temperature	Celsius

Model (B3)

Geometry

TABLE 2
Model (B3) > Geometry

Object Name	*Geometry*
State	Fully Defined
Definition	
Source	C:\Users\Korisnik\Desktop\The final\ansys17\Global model\Global_model_files\dp0\Geom\DM\Geom.agdb
Type	DesignModeler
Length Unit	Meters
Element Control	Program Controlled
Display Style	Body Color

Bounding Box	
Length X	1080.2 cm
Length Y	1358.4 cm
Length Z	5200. cm
Properties	
Volume	2.2302e+007 cm³
Mass	3.2002e+008 g
Scale Factor Value	1.
Statistics	
Bodies	564
Active Bodies	564
Nodes	96222
Elements	82555
Mesh Metric	None
Basic Geometry Options	
Parameters	Independent
Parameter Key	
Attributes	Yes
Attribute Key	
Named Selections	Yes
Named Selection Key	
Material Properties	Yes
Advanced Geometry Options	
Use Associativity	Yes
Coordinate Systems	Yes
Coordinate System Key	
Reader Mode Saves Updated File	Yes
Use Instances	Yes
Smart CAD Update	Yes
Compare Parts On Update	No
Attach File Via Temp File	Yes
Temporary Directory	C:\Users\Korisnik\AppData\Local\Temp
Analysis Type	3-D
Decompose Disjoint Geometry	Yes
Enclosure and Symmetry Processing	Yes

TABLE 57
Model (B3) > Geometry > Masses

Object Name	*Distributed Mass*
State	Fully Defined
Scope	
Scoping Method	Geometry Selection

Geometry	1 Face
Definition	
Mass Type	Mass per Unit Area
Mass per Unit Area	25.8 g/cm²
Suppressed	No

Coordinate Systems

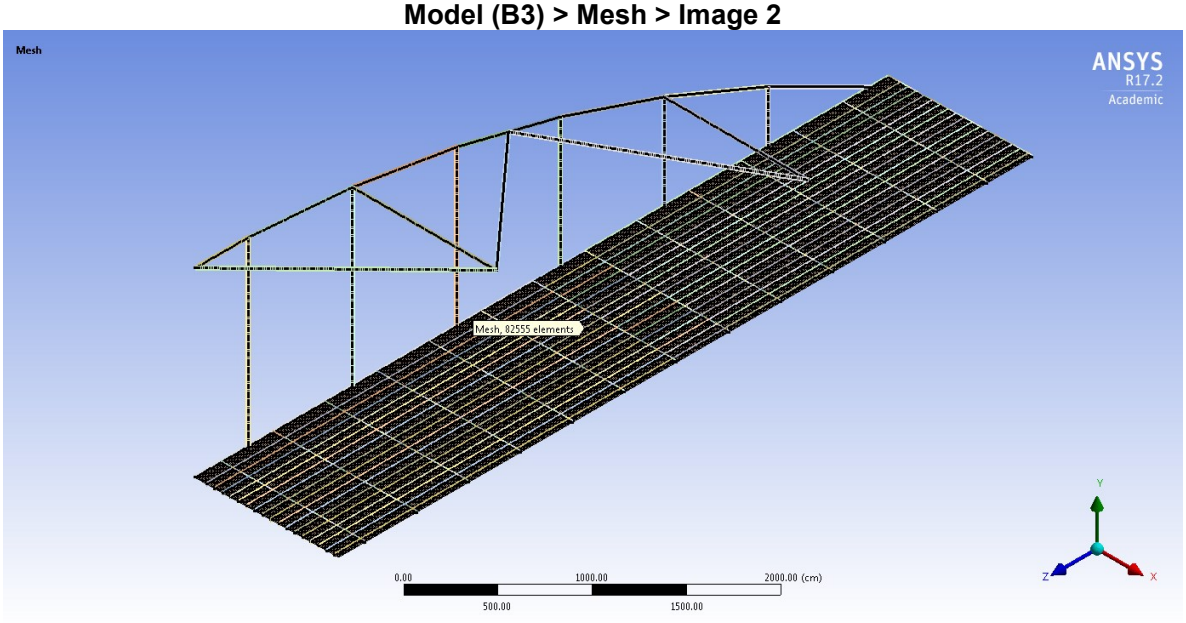
Mesh

TABLE 111
Model (B3) > Mesh

Object Name	*Mesh*
State	Solved
Display	
Display Style	Body Color
Defaults	
Physics Preference	Mechanical
Relevance	0
Shape Checking	Standard Mechanical
Element Midside Nodes	Program Controlled
Sizing	
Size Function	Curvature
Use Uniform Size Function For Sheets	No
Relevance Center	Coarse
Initial Size Seed	Active Assembly
Smoothing	Medium
Span Angle Center	Coarse
Curvature Normal Angle	Default (30.0 °)
Min Size	1.0 cm
Max Face Size	9.0 cm
Growth Rate	Default
Automatic Mesh Based Defeaturing	On
Defeature Size	Default (0.750 cm)
Minimum Edge Length	1.10 cm
Inflation	
Use Automatic Inflation	None
Inflation Option	Smooth Transition
Transition Ratio	0.272
Maximum Layers	2
Growth Rate	1.2
Inflation Algorithm	Pre
View Advanced Options	No
Advanced	
Number of CPUs for Parallel Part Meshing	Program Controlled
Straight Sided Elements	No
Number of Retries	0
Rigid Body Behavior	Dimensionally Reduced

Mesh Morphing	Disabled
Triangle Surface Mesher	Program Controlled
Topology Checking	No
Use Sheet Thickness for Pinch	No
Pinch Tolerance	Default (0.90 cm)
Generate Pinch on Refresh	No
Sheet Loop Removal	No
Statistics	
Nodes	96222
Elements	82555
Mesh Metric	None

FIGURE 1
Model (B3) > Mesh > Image 2



Named Selections

TABLE 112
Model (B3) > Named Selections > Named Selections

Object Name	*Beam_frame*
State	Fully Defined
Scope	
Scoping Method	Geometry Selection
Geometry	490 Bodies
Definition	
Send to Solver	Yes
Visible	Yes
Program Controlled Inflation	Exclude
Statistics	
Type	Imported
Total Selection	490 Bodies
Suppressed	0

Used by Mesh Worksheet	No

Modal (B4)

TABLE 113
Model (B3) > Analysis

Object Name	*Modal (B4)*
State	Solved
Definition	
Physics Type	Structural
Analysis Type	Modal
Solver Target	Mechanical APDL
Options	
Environment Temperature	22. °C
Generate Input Only	No

TABLE 114
Model (B3) > Modal (B4) > Initial Condition

Object Name	*Pre-Stress (None)*
State	Fully Defined
Definition	
Pre-Stress Environment	None

TABLE 115
Model (B3) > Modal (B4) > Analysis Settings

Object Name	*Analysis Settings*
State	Fully Defined
Options	
Max Modes to Find	500
Limit Search to Range	No
Solver Controls	
Damped	No
Solver Type	Program Controlled
Rotordynamics Controls	
Coriolis Effect	Off
Campbell Diagram	Off
Output Controls	
Stress	No
Strain	No
Nodal Forces	No
Calculate Reactions	No
General Miscellaneous	No
Analysis Data Management	
Solver Files Directory	C:\Users\Korisnik\Desktop\The final\ansys17\Global model\Global_model_files\dp0\SYS-1\MECH\
Future Analysis	None
Scratch Solver Files Directory	

Save MAPDL db	No
Delete Unneeded Files	Yes
Solver Units	Active System
Solver Unit System	cgs

FIGURE 2
Model (B3) > Modal (B4) > Image

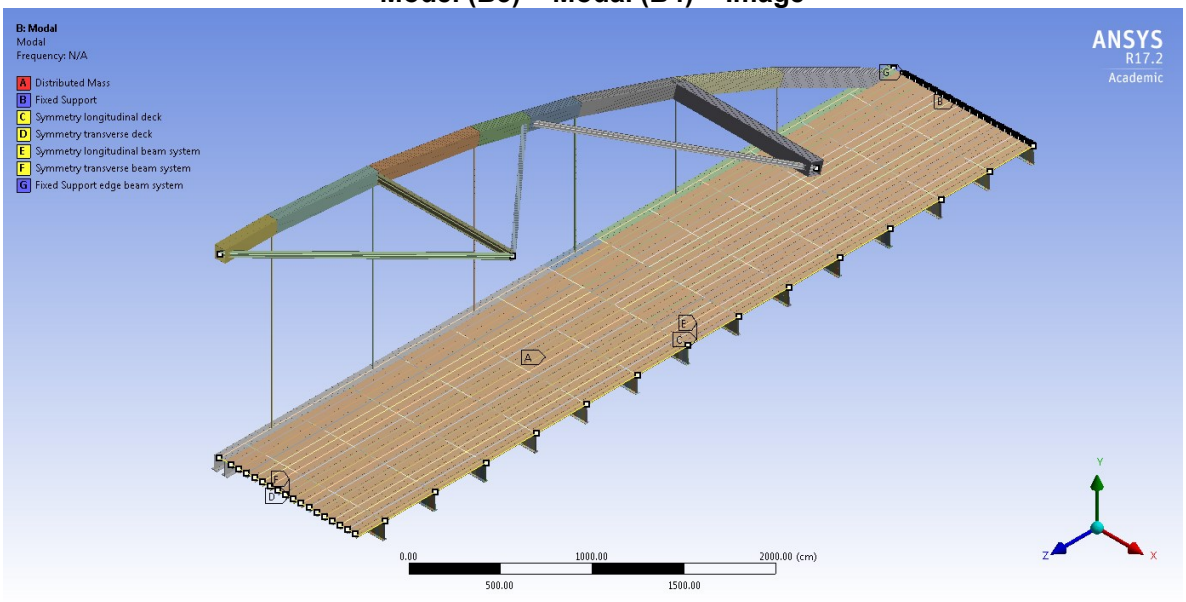


FIGURE 3
Model (B3) > Modal (B4) > Image 2

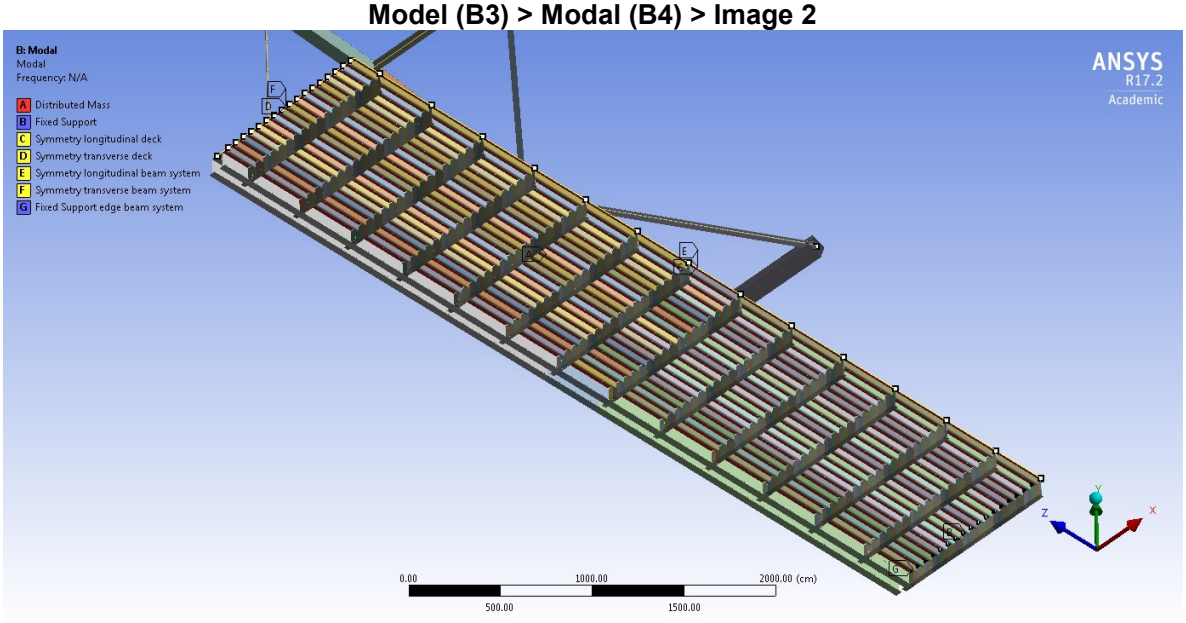


TABLE 116
Model (B3) > Modal (B4) > Loads

Object Name	*Fixed Support*	*Symmetry longitudinal deck*	*Symmetry transverse deck*	*Symmetry longitudinal beam system*	*Symmetry transverse beam system*	*Fixed Support edge beam system*
State	Fully Defined					

Scope						
Scoping Method	Geometry Selection					
Geometry	1 Edge			15 Vertices	19 Vertices	70 Vertices
Coordinate System		Global Coordinate System				
X Coordinate		1080.2 cm	540.1 cm	1080.2 cm	540.1 cm	
Y Coordinate		124.8 cm	114.4 cm	124.8 cm	114.4 cm	
Z Coordinate		2600. cm	5200. cm	2600. cm	5200. cm	
Location		Defined				
Definition						
Type	Fixed Support	Remote Displacement				Fixed Support
Suppressed	No					
X Component		0. cm	Free	0. cm	Free	
Y Component		Free				
Z Component		Free	0. cm	Free	0. cm	
Rotation X		Free				
Rotation Y		Free				
Rotation Z		0. °				
Behavior		Deformable				
Rotation X			0. °			
Rotation Y			Free			
Rotation Z			Free			
Rotation X				Free		
Rotation Y				Free		
Rotation Z				0. °		
Rotation X					0. °	
Rotation Y					Free	
Rotation Z					Free	
Advanced						
Pinball Region		All				

Solution (B5)

TABLE 117
Model (B3) > Modal (B4) > Solution

Object Name	*Solution (B5)*
State	Solved
Adaptive Mesh Refinement	
Max Refinement Loops	1.
Refinement Depth	2.
Information	
Status	Done
MAPDL Elapsed Time	4 h 36 m

MAPDL Memory Used	3.4648 GB
MAPDL Result File Size	6.9992 GB
Post Processing	
Beam Section Results	No

The following bar chart indicates the frequency at each calculated mode.

FIGURE 4
Model (B3) > Modal (B4) > Solution (B5)

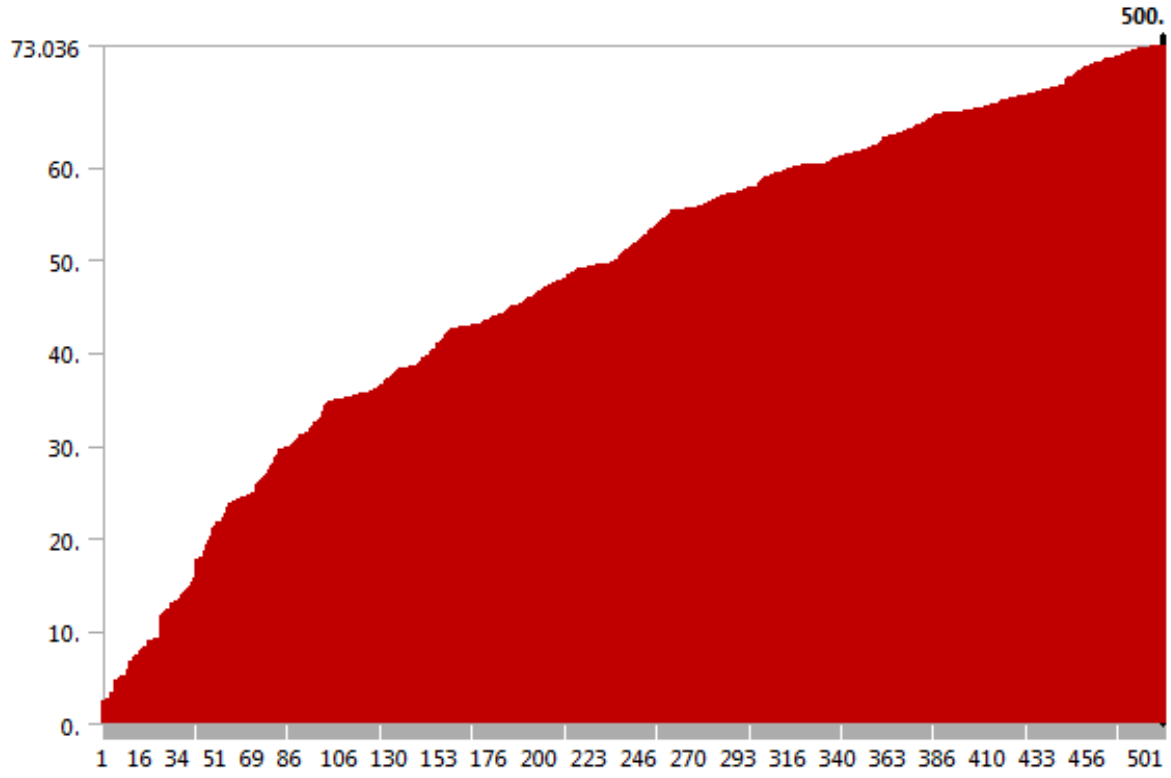


TABLE 118
Model (B3) > Modal (B4) > Solution (B5)

Mode	Frequency [Hz]
1.	2.0506
2.	2.4292
3.	2.4323
4.	2.6782
5.	2.6823
6.	3.3047
7.	3.3124
8.	4.7557
9.	4.7685
10.	4.9187
11.	5.055
12.	5.1089
13.	5.2381

14.	5.9291
15.	6.6922
16.	6.6995
17.	7.0657
18.	7.3753
19.	7.3938
20.	7.7394
21.	8.1356
22.	8.366
23.	8.8553
24.	8.8632
25.	8.9167
26.	9.1017
27.	9.1218
28.	9.2727
29.	11.599
30.	11.858
31.	12.18
32.	12.336
33.	12.392
34.	13.065
35.	13.094
36.	13.13
37.	13.139
38.	13.491
39.	13.849
40.	14.037
41.	14.446
42.	14.477
43.	14.837
44.	15.244
45.	15.771
46.	17.589
47.	17.787
48.	17.852
49.	17.888
50.	18.497
51.	19.241
52.	19.612
53.	20.162
54.	20.994
55.	21.317
56.	21.64
57.	21.689
58.	21.792
59.	22.076
60.	22.655
61.	23.298

62.	23.716
63.	23.841
64.	23.869
65.	23.983
66.	24.141
67.	24.36
68.	24.4
69.	24.439
70.	24.654
71.	24.673
72.	24.784
73.	24.882
74.	25.703
75.	25.94
76.	26.265
77.	26.417
78.	26.719
79.	26.859
80.	27.304
81.	27.731
82.	28.055
83.	28.644
84.	28.85
85.	29.508
86.	29.57
87.	29.645
88.	29.686
89.	29.725
90.	29.828
91.	30.047
92.	30.337
93.	30.57
94.	30.791
95.	31.062
96.	31.136
97.	31.209
98.	31.353
99.	31.426
100.	31.745
101.	31.995
102.	32.379
103.	32.465
104.	32.699
105.	32.89
106.	33.712
107.	34.315
108.	34.562
109.	34.768

110.	34.825
111.	34.856
112.	34.91
113.	34.98
114.	35.013
115.	35.031
116.	35.094
117.	35.118
118.	35.211
119.	35.245
120.	35.293
121.	35.328
122.	35.418
123.	35.574
124.	35.63
125.	35.641
126.	35.648
127.	35.73
128.	35.792
129.	35.949
130.	36.043
131.	36.178
132.	36.382
133.	36.522
134.	36.559
135.	36.971
136.	37.117
137.	37.175
138.	37.486
139.	37.661
140.	37.909
141.	38.081
142.	38.354
143.	38.361
144.	38.371
145.	38.384
146.	38.41
147.	38.441
148.	38.443
149.	38.452
150.	38.463
151.	38.755
152.	39.012
153.	39.433
154.	39.631
155.	39.704
156.	40.17
157.	40.298

158.	40.4
159.	40.893
160.	41.076
161.	41.21
162.	41.503
163.	41.793
164.	42.096
165.	42.367
166.	42.475
167.	42.503
168.	42.598
169.	42.611
170.	42.726
171.	42.771
172.	42.798
173.	42.8
174.	42.822
175.	42.886
176.	42.931
177.	42.994
178.	43.073
179.	43.087
180.	43.124
181.	43.294
182.	43.412
183.	43.446
184.	43.556
185.	43.598
186.	43.809
187.	43.916
188.	43.991
189.	44.054
190.	44.099
191.	44.227
192.	44.32
193.	44.594
194.	44.712
195.	44.924
196.	44.991
197.	45.049
198.	45.166
199.	45.209
200.	45.483
201.	45.719
202.	45.856
203.	45.909
204.	45.971
205.	46.185

206.	46.419
207.	46.556
208.	46.623
209.	46.735
210.	46.994
211.	47.045
212.	47.276
213.	47.37
214.	47.433
215.	47.596
216.	47.672
217.	47.738
218.	47.786
219.	47.866
220.	47.931
221.	48.282
222.	48.343
223.	48.68
224.	48.715
225.	48.789
226.	48.976
227.	48.996
228.	49.056
229.	49.144
230.	49.175
231.	49.238
232.	49.314
233.	49.339
234.	49.344
235.	49.446
236.	49.46
237.	49.503
238.	49.52
239.	49.551
240.	49.567
241.	49.724
242.	49.78
243.	49.868
244.	49.916
245.	50.309
246.	50.564
247.	50.828
248.	51.035
249.	51.11
250.	51.215
251.	51.5
252.	51.664
253.	51.756

254.	52.077
255.	52.152
256.	52.326
257.	52.668
258.	52.72
259.	53.022
260.	53.345
261.	53.362
262.	53.459
263.	53.684
264.	53.949
265.	54.121
266.	54.37
267.	54.372
268.	54.649
269.	54.811
270.	55.321
271.	55.381
272.	55.387
273.	55.398
274.	55.406
275.	55.433
276.	55.446
277.	55.463
278.	55.471
279.	55.481
280.	55.484
281.	55.486
282.	55.58
283.	55.75
284.	55.789
285.	55.909
286.	55.924
287.	56.124
288.	56.258
289.	56.364
290.	56.441
291.	56.63
292.	56.718
293.	56.878
294.	56.901
295.	56.981
296.	57.073
297.	57.105
298.	57.156
299.	57.169
300.	57.211
301.	57.305

302.	57.398
303.	57.426
304.	57.527
305.	57.626
306.	57.714
307.	57.846
308.	57.87
309.	57.884
310.	57.902
311.	58.208
312.	58.443
313.	58.741
314.	58.82
315.	58.832
316.	58.942
317.	59.042
318.	59.074
319.	59.291
320.	59.293
321.	59.351
322.	59.417
323.	59.528
324.	59.593
325.	59.795
326.	59.917
327.	60.001
328.	60.057
329.	60.114
330.	60.137
331.	60.186
332.	60.196
333.	60.208
334.	60.218
335.	60.226
336.	60.24
337.	60.247
338.	60.276
339.	60.329
340.	60.333
341.	60.335
342.	60.348
343.	60.384
344.	60.491
345.	60.664
346.	60.868
347.	60.914
348.	60.972
349.	61.115

350.	61.201
351.	61.22
352.	61.281
353.	61.361
354.	61.404
355.	61.446
356.	61.544
357.	61.625
358.	61.635
359.	61.693
360.	61.765
361.	61.818
362.	61.937
363.	61.959
364.	62.097
365.	62.212
366.	62.281
367.	62.35
368.	62.448
369.	62.623
370.	63.069
371.	63.116
372.	63.347
373.	63.418
374.	63.452
375.	63.508
376.	63.563
377.	63.637
378.	63.739
379.	63.762
380.	63.96
381.	64.045
382.	64.076
383.	64.155
384.	64.27
385.	64.417
386.	64.511
387.	64.617
388.	64.763
389.	64.823
390.	65.022
391.	65.221
392.	65.259
393.	65.5
394.	65.557
395.	65.571
396.	65.64
397.	65.68

398.	65.769
399.	65.785
400.	65.797
401.	65.812
402.	65.821
403.	65.845
404.	65.854
405.	65.872
406.	65.893
407.	65.974
408.	66.057
409.	66.064
410.	66.07
411.	66.073
412.	66.181
413.	66.231
414.	66.271
415.	66.282
416.	66.412
417.	66.453
418.	66.523
419.	66.585
420.	66.661
421.	66.697
422.	66.759
423.	66.808
424.	67.037
425.	67.11
426.	67.143
427.	67.305
428.	67.316
429.	67.392
430.	67.461
431.	67.519
432.	67.541
433.	67.609
434.	67.664
435.	67.693
436.	67.703
437.	67.753
438.	67.809
439.	67.897
440.	67.961
441.	67.994
442.	68.009
443.	68.162
444.	68.192
445.	68.289

446.	68.34
447.	68.355
448.	68.388
449.	68.458
450.	68.488
451.	68.555
452.	68.623
453.	68.792
454.	68.814
455.	68.888
456.	69.391
457.	69.626
458.	69.738
459.	69.957
460.	70.078
461.	70.244
462.	70.326
463.	70.542
464.	70.708
465.	70.774
466.	70.849
467.	70.921
468.	71.08
469.	71.15
470.	71.224
471.	71.259
472.	71.32
473.	71.575
474.	71.619
475.	71.623
476.	71.643
477.	71.69
478.	71.774
479.	71.883
480.	71.956
481.	71.967
482.	72.169
483.	72.213
484.	72.283
485.	72.346
486.	72.459
487.	72.525
488.	72.636
489.	72.676
490.	72.725
491.	72.792
492.	72.8
493.	72.838

494.	72.895
495.	72.911
496.	72.964
497.	72.985
498.	73.022
499.	73.03
500.	73.036

TABLE 119
Model (B3) > Modal (B4) > Solution (B5) > Solution Information

Object Name	*Solution Information*
State	Solved
Solution Information	
Solution Output	Solver Output
Newton-Raphson Residuals	0
Identify Element Violations	0
Update Interval	2.5 s
Display Points	All
FE Connection Visibility	
Activate Visibility	Yes
Display	All FE Connectors
Draw Connections Attached To	All Nodes
Line Color	Connection Type
Visible on Results	No
Line Thickness	Single
Display Type	Lines

Material Data

Structural Steel

TABLE 120
Structural Steel > Constants

Density	7.85 g cm^-3
Coefficient of Thermal Expansion	1.2e-005 C^-1
Specific Heat	4.34e+006 erg g^-1 C^-1
Thermal Conductivity	0.605 W cm^-1 C^-1
Resistivity	1.7e-005 ohm cm

TABLE 121
Structural Steel > Compressive Ultimate Strength

Compressive Ultimate Strength dyne cm^-2
0

TABLE 122
Structural Steel > Compressive Yield Strength

Compressive Yield Strength dyne cm^-2
2.5e+009

TABLE 123
Structural Steel > Tensile Yield Strength

Tensile Yield Strength dyne cm^-2
2.5e+009

TABLE 124
Structural Steel > Tensile Ultimate Strength

Tensile Ultimate Strength dyne cm^-2
4.6e+009

TABLE 125
Structural Steel > Isotropic Secant Coefficient of Thermal Expansion

Zero-Thermal-Strain Reference Temperature C
22

TABLE 126
Structural Steel > Alternating Stress Mean Stress

Alternating Stress dyne cm^-2	Cycles	Mean Stress dyne cm^-2
3.999e+010	10	0
2.827e+010	20	0
1.896e+010	50	0
1.413e+010	100	0
1.069e+010	200	0
4.41e+009	2000	0
2.62e+009	10000	0
2.14e+009	20000	0
1.38e+009	1.e+005	0
1.14e+009	2.e+005	0
8.62e+008	1.e+006	0

TABLE 127
Structural Steel > Strain-Life Parameters

Strength Coefficient dyne cm^-2	Strength Exponent	Ductility Coefficient	Ductility Exponent	Cyclic Strength Coefficient dyne cm^-2	Cyclic Strain Hardening Exponent
9.2e+009	-0.106	0.213	-0.47	1.e+010	0.2

TABLE 128
Structural Steel > Isotropic Elasticity

Temperature C	Young's Modulus dyne cm^-2	Poisson's Ratio	Bulk Modulus dyne cm^-2	Shear Modulus dyne cm^-2
	2.e+012	0.3	1.6667e+012	7.6923e+011

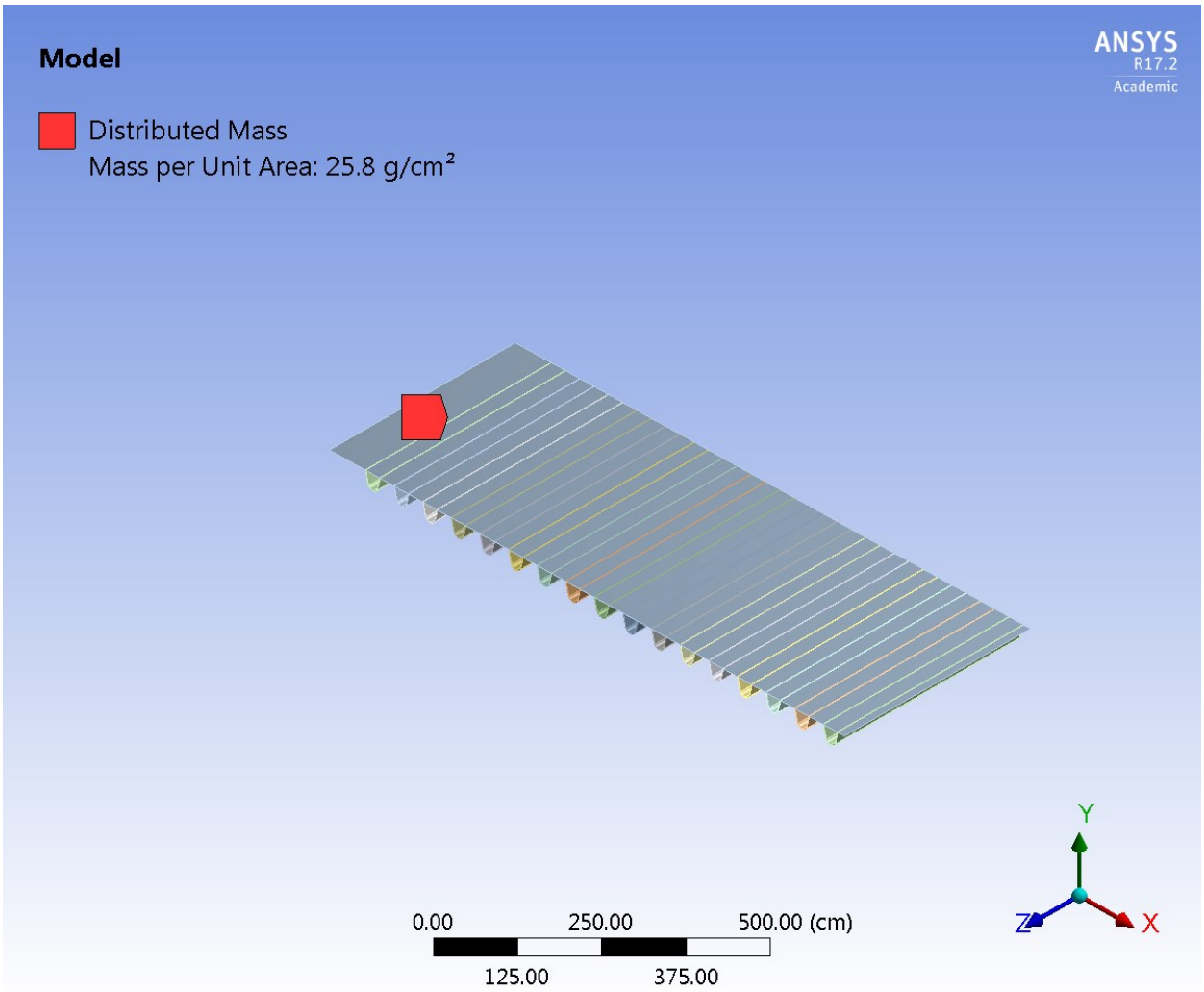
TABLE 129
Structural Steel > Isotropic Relative Permeability

Relative Permeability		
10000		
-1	-1	-1

Appendix F2

Local model 1

First Saved	Saturday, July 07, 2018
Last Saved	Saturday, July 07, 2018
Product Version	17.2 Release
Save Project Before Solution	No
Save Project After Solution	No



Contents

- **Units**
- **Model (B3)**
  - Geometry
    - Parts
    - 3D U stiffener
      - Parts
    - Added_mass
    - Distributed Mass
  - Coordinate Systems
  - Connections
    - Contacts
      - Contact Regions
      - Bonded - Longitudinal edge beam.2 To deck_mid
  - Mesh
  - Named Selections
  - **Modal (B4)**
    - Pre-Stress (None)
    - Analysis Settings
    - Loads
    - Solution (B5)
      - Solution Information
      - 0kg
        - Results
      - 50kg
        - Results
      - 75kg
        - Results
      - 100kg
        - Results
      - 1crack 35cm
        - Results
      - 2x cracks of 35cm
        - Results
      - 2 fully open U section cracks
        - Results
- **Material Data**
  - Structural Steel
  - 100kg

Units

TABLE 1

Unit System	Metric (cm, g, dyne, s, V, A) Degrees rad/s Celsius
Angle	Degrees
Rotational Velocity	rad/s
Temperature	Celsius

Model (B3)

Geometry

TABLE 2
Model (B3) > Geometry

Object Name	*Geometry*
State	Fully Defined
Definition	
Source	C:\Users\Korisnik\Desktop\The final\ansys17\local 3D model\3D_segment_files\dp0\Geom\DM\Geom.agdb
Type	DesignModeler
Length Unit	Meters
Element Control	Program Controlled
Display Style	Body Color
Bounding Box	
Length X	1080.2 cm
Length Y	50.42 cm
Length Z	390. cm
Properties	
Volume	9.9002e+005 cm³
Mass	1.8643e+007 g
Scale Factor Value	1.
Statistics	
Bodies	20
Active Bodies	19
Nodes	235106
Elements	50198
Mesh Metric	None
Basic Geometry Options	
Parameters	Independent
Parameter Key	
Attributes	Yes
Attribute Key	
Named Selections	Yes
Named Selection Key	
Material Properties	Yes
Advanced Geometry Options	
Use Associativity	Yes
Coordinate Systems	Yes
Coordinate System Key	
Reader Mode Saves Updated File	Yes
Use Instances	Yes
Smart CAD Update	Yes
Compare Parts On Update	No

Attach File Via Temp File	Yes
Temporary Directory	C:\Users\Korisnik\AppData\Local\Temp
Analysis Type	3-D
Decompose Disjoint Geometry	Yes
Enclosure and Symmetry Processing	Yes

TABLE 3
Model (B3) > Geometry > Parts

Object Name	*Longitudinal edge beam.2*	*deck_mid*
State	Meshed	
Graphics Properties		
Visible	Yes	
Transparency	1	
Definition		
Suppressed	No	
Coordinate System	Default Coordinate System	
Reference Temperature	By Environment	
Offset Mode	Refresh on Update	
Offset Type	User Defined	Middle
Offset X	61. cm	
Offset Y	104. cm	
Model Type	Beam	
Cross Section (For Solver)	Pre-Integrated	
Stiffness Behavior		Flexible
Thickness		1. cm
Thickness Mode		Refresh on Update
Behavior		None
Material		
Assignment	Structural Steel	
Nonlinear Effects	Yes	
Thermal Strain Effects	Yes	
Bounding Box		
Length X	3.1974e-012 cm	1080.2 cm
Length Y	0. cm	20.804 cm
Length Z	390. cm	
Properties		
Volume	2.7261e+005 cm³	4.2136e+005 cm³
Mass	2.14e+006 g	3.3076e+006 g
Length	390. cm	
Cross Section	end_long_1d	
Cross Section Area	699.01 cm²	
Cross Section IYY	1.0481e+006 cm²·cm²	
Cross Section IZZ	1.0948e+006 cm²·cm²	
Centroid X		540.1 cm
Centroid Y		114.4 cm
Centroid Z		2470. cm

Moment of Inertia Ip1		4.1924e+010 g·cm²
Moment of Inertia Ip2		3.6367e+011 g·cm²
Moment of Inertia Ip3		3.2174e+011 g·cm²
Surface Area(approx.)		4.2136e+005 cm²
Statistics		
Nodes	159	21206
Elements	79	20879
Mesh Metric	None	
CAD Attributes		
DMBodyGroup	2	3
DMSheetThickness		0.01

FIGURE 1
Model (B3) > Geometry > Longitudinal edge beam.2 > Image

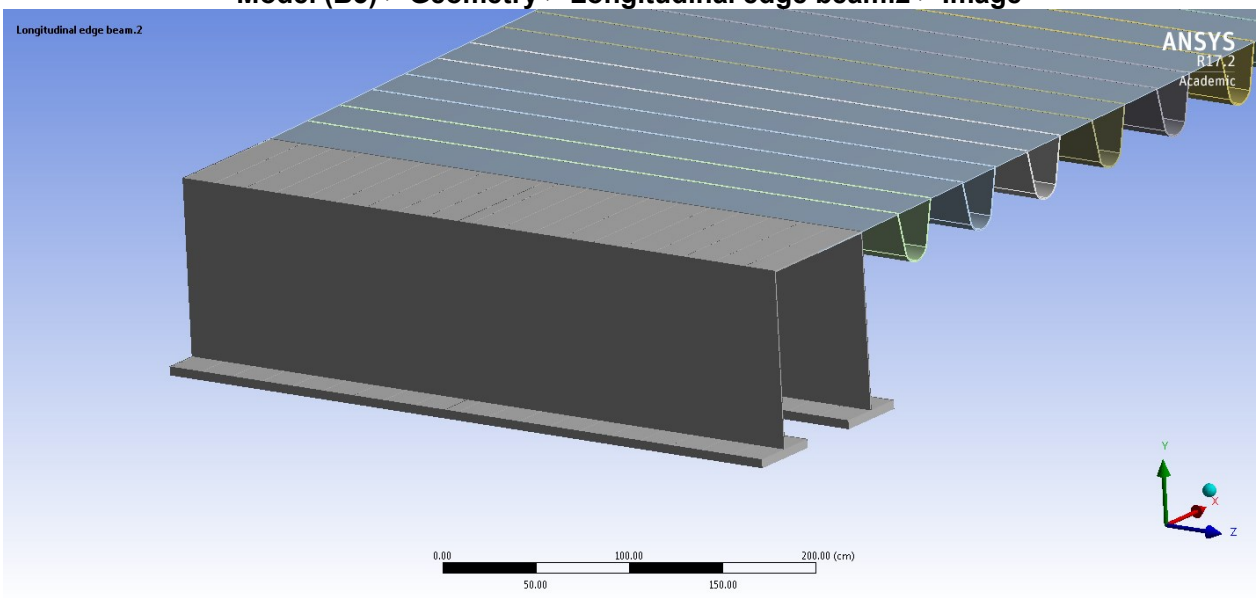


TABLE 4
Model (B3) > Geometry > Body Groups

Object Name	*3D U stiffener*
State	Meshed
Graphics Properties	
Visible	Yes
Definition	
Suppressed	No
Assignment	Structural Steel
Coordinate System	Default Coordinate System
Bounding Box	
Length X	990.61 cm
Length Y	50.107 cm
Length Z	387.6 cm
Properties	
Volume	2.9605e+005 cm³
Mass	2.324e+006 g

Centroid X	570.27 cm
Centroid Y	97.279 cm
Centroid Z	2470. cm
Moment of Inertia Ip1	2.9304e+010 g·cm²
Moment of Inertia Ip2	2.3022e+011 g·cm²
Moment of Inertia Ip3	2.0136e+011 g·cm²
Statistics	
Nodes	213741
Elements	29240
Mesh Metric	None
CAD Attributes	
DMBodyGroup	6

TABLE 5
Model (B3) > Geometry > 3D U stiffener > Parts

Object Name	*3D_U.1*	*3D_U.2*	*3D_U.3*	*3D_U.4*	*3D_U.5*	*3D_U.6*	*3D_U.7*	*3D_U.8*	*3D_U.9*	*3D_U.10*	*3D_U.11*
State	Meshed										
Graphics Properties											
Visible	Yes										
Transparency	1										
Definition											
Suppressed	No										
Stiffness Behavior	Flexible										
Coordinate System	Default Coordinate System										
Reference Temperature	By Environment										
Behavior	None										
Material											
Assignment	Structural Steel										
Nonlinear Effects	Yes										
Thermal Strain Effects	Yes										
Bounding Box											
Length X	30.601 cm										
Length Y	31.59 cm										
Length Z	387.6 cm										
Properties											
Volume	17414 cm³										
Mass	1.367e+005 g										
Centroid X	1050.3 cm	990.28 cm	930.28 cm	870.28 cm	810.28 cm	750.28 cm	690.28 cm	630.28 cm	570.27 cm	510.27 cm	450.27 cm

Centroid Y	106.51 cm	105.35 cm	104.2 cm	103.04 cm	101.92 cm	100.76 cm	99.604 cm	98.447 cm	97.29 cm	96.132 cm	94.975 cm
Centroid Z	2470. cm										
Moment of Inertia Ip1	1.7276e+009 g·cm²	1.7277e+009 g·cm²	1.7276e+009 g·cm²	1.7221e+009 g·cm²							
Moment of Inertia Ip2	1.7306e+009 g·cm²	1.7307e+009 g·cm²	1.7306e+009 g·cm²	1.7251e+009 g·cm²							
Moment of Inertia Ip3	2.8861e+007 g·cm²	2.8862e+007 g·cm²	2.8861e+007 g·cm²	2.8791e+007 g·cm²	2.8792e+007 g·cm²	2.8791e+007 g·cm²					
Statistics											
Nodes	12573										
Elements	1720										
Mesh Metric	None										

TABLE 6
Model (B3) > Geometry > 3D U stiffener > Parts

Object Name	*3D_U.12*	*3D_U.13*	*3D_U.14*	*3D_U.15*	*3D_U.16*	*3D_U.17*
State	Meshed					
Graphics Properties						
Visible	Yes					
Transparency	1					
Definition						
Suppressed	No					
Stiffness Behavior	Flexible					
Coordinate System	Default Coordinate System					
Reference Temperature	By Environment					
Behavior	None					
Material						
Assignment	Structural Steel					
Nonlinear Effects	Yes					
Thermal Strain Effects	Yes					
Bounding Box						
Length X	30.601 cm					
Length Y	31.59 cm					
Length Z	387.6 cm					
Properties						
Volume	17414 cm³					
Mass	1.367e+005 g					
Centroid X	390.27 cm	330.27 cm	270.27 cm	210.27 cm	150.27 cm	90.268 cm
Centroid Y	93.818 cm	92.66 cm	91.503 cm	90.345 cm	89.188 cm	87.994 cm
Centroid Z	2470. cm					
Moment of Inertia Ip1	1.7221e+009 g·cm²					1.7276e+009 g·cm²
Moment of Inertia Ip2	1.7251e+009 g·cm²					1.7306e+009 g·cm²
Moment of Inertia Ip3	2.8791e+007 g·cm²					2.8861e+007 g·cm²
Statistics						
Nodes	12573					
Elements	1720					
Mesh Metric	None					

TABLE 7
Model (B3) > Geometry > Parts

Object Name	*Added_mass*
State	Suppressed
Graphics Properties	
Visible	No
Definition	
Suppressed	Yes
Stiffness Behavior	Flexible
Coordinate System	Default Coordinate System
Reference Temperature	By Environment
Behavior	None
Material	
Assignment	100kg
Nonlinear Effects	Yes
Thermal Strain Effects	Yes
Bounding Box	
Length X	37.005 cm
Length Y	15.652 cm
Length Z	10. cm
Properties	
Volume	5083.3 cm³
Mass	99998 g
Centroid X	660.2 cm
Centroid Y	105.95 cm
Centroid Z	2470. cm
Moment of Inertia Ip1	2.6995e+006 g·cm²
Moment of Inertia Ip2	1.0508e+007 g·cm²
Moment of Inertia Ip3	1.1541e+007 g·cm²
Statistics	
Nodes	0
Elements	0
Mesh Metric	None

FIGURE 2
Model (B3) > Geometry > Added_mass > Image

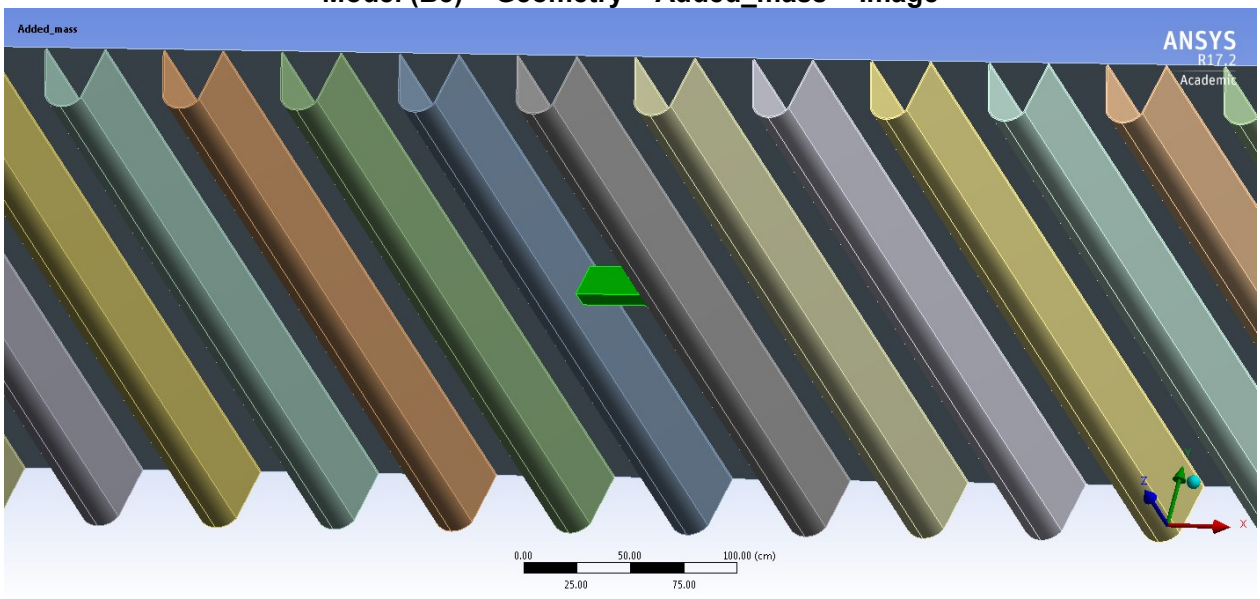


TABLE 8
Model (B3) > Geometry > Masses

Object Name	*Distributed Mass*
State	Fully Defined
Scope	
Scoping Method	Geometry Selection
Geometry	1 Face
Definition	
Mass Type	Mass per Unit Area
Mass per Unit Area	25.8 g/cm²
Suppressed	No

Coordinate Systems

TABLE 9
Model (B3) > Coordinate Systems > Coordinate System

Object Name	*Global Coordinate System*
State	Fully Defined
Definition	
Type	Cartesian
Coordinate System ID	0.
Origin	
Origin X	0. cm
Origin Y	0. cm
Origin Z	0. cm
Directional Vectors	
X Axis Data	[1. 0. 0.]
Y Axis Data	[0. 1. 0.]
Z Axis Data	[0. 0. 1.]

Connections

TABLE 10
Model (B3) > Connections

Object Name	*Connections*
State	Fully Defined
Auto Detection	
Generate Automatic Connection On Refresh	Yes
Transparency	
Enabled	Yes

TABLE 11
Model (B3) > Connections > Contacts

Object Name	*Contacts*	*Contacts 2*
State	Fully Defined	
Definition		
Connection Type	Contact	
Scope		
Scoping Method	Geometry Selection	
Geometry	All Bodies	
Auto Detection		
Tolerance Type	Slider	
Tolerance Slider	0.	
Tolerance Value	2.8739 cm	
Use Range	No	
Face/Face	Yes	No
Cylindrical Faces	Include	
Face/Edge	No	
Edge/Edge	No	
Priority	Include All	
Group By	Bodies	
Search Across	Bodies	
Statistics		
Connections	19	1
Active Connections	17	1

TABLE 12
Model (B3) > Connections > Contacts > Contact Regions

Object Name	*Contact Region*	*Contact Region 2*	*Contact Region 3*	*Contact Region 4*	*Contact Region 5*	*Contact Region 6*	*Contact Region 7*	*Contact Region 8*	*Contact Region 9*	*Contact Region 10*	*Contact Region 11*
State	Fully Defined										
Scope											
Scoping Method	Geometry Selection										
Contact	1 Face										
Target	2 Faces										

Contact Bodies	deck_mid										
Target Bodies	3D_U.1	3D_U.2	3D_U.3	3D_U.4	3D_U.5	3D_U.6	3D_U.7	3D_U.8	3D_U.9	3D_U.10	3D_U.11
Contact Shell Face	Program Controlled										
Shell Thickness Effect	No										
Definition											
Type	Bonded										
Scope Mode	Automatic										
Behavior	Program Controlled										
Trim Contact	Program Controlled										
Trim Tolerance	2.8739 cm										
Suppressed	No										
Advanced											
Formulation	Program Controlled										
Detection Method	Program Controlled										
Penetration Tolerance	Program Controlled										
Elastic Slip Tolerance	Program Controlled										
Normal Stiffness	Program Controlled										
Update Stiffness	Program Controlled										
Pinball Region	Program Controlled										
Geometric Modification											
Contact Geometry Correction	None										
Target Geometry Correction	None										

TABLE 13
Model (B3) > Connections > Contacts > Contact Regions

Object Name	*Contact Region 12*	*Contact Region 13*	*Contact Region 14*	*Contact Region 15*	*Contact Region 16*	*Contact Region 17*	*Contact Region 18*	*Contact Region 19*
State	Fully Defined						Suppressed	
Scope								

Scoping Method	Geometry Selection							
Contact	1 Face							
Target	2 Faces						No Selection	
Contact Bodies	deck_mid						3D_U.7	3D_U.8
Target Bodies	3D_U.12	3D_U.13	3D_U.14	3D_U.15	3D_U.16	3D_U.17	Added_mass	
Contact Shell Face	Program Controlled							
Shell Thickness Effect	No							
Definition								
Type	Bonded							
Scope Mode	Automatic							
Behavior	Program Controlled							
Trim Contact	Program Controlled							
Trim Tolerance	2.8739 cm							
Suppressed	No							
Advanced								
Formulation	Program Controlled							
Detection Method	Program Controlled							
Penetration Tolerance	Program Controlled							
Elastic Slip Tolerance	Program Controlled							
Normal Stiffness	Program Controlled							
Update Stiffness	Program Controlled							
Pinball Region	Program Controlled							
Geometric Modification								
Contact Geometry Correction	None							
Target Geometry Correction	None							

TABLE 14
Model (B3) > Connections > Contacts 2 > Contact Regions

Object Name	*Bonded - Longitudinal edge beam.2 To deck_mid*
State	Fully Defined
Scope	
Scoping Method	Geometry Selection
Contact	21 Edges
Target	1 Face
Contact Bodies	Longitudinal edge beam.2

Target Bodies	deck_mid
Target Shell Face	Program Controlled
Shell Thickness Effect	No
Definition	
Type	Bonded
Scope Mode	Manual
Trim Contact	Program Controlled
Suppressed	No
Advanced	
Formulation	Program Controlled
Penetration Tolerance	Program Controlled
Elastic Slip Tolerance	Program Controlled
Normal Stiffness	Program Controlled
Update Stiffness	Program Controlled
Pinball Region	Program Controlled
Geometric Modification	
Target Geometry Correction	None

Mesh

TABLE 15
Model (B3) > Mesh

Object Name	*Mesh*
State	Solved
Display	
Display Style	Body Color
Defaults	
Physics Preference	Mechanical
Relevance	0
Shape Checking	Standard Mechanical
Element Midside Nodes	Program Controlled
Sizing	
Size Function	Curvature
Use Uniform Size Function For Sheets	No
Relevance Center	Coarse
Initial Size Seed	Active Assembly
Smoothing	Medium
Transition	Fast
Span Angle Center	Coarse
Curvature Normal Angle	Default (30.0 °)
Min Size	Default (1.76420 cm)
Max Face Size	4.50 cm
Max Tet Size	4.50 cm
Growth Rate	Default
Automatic Mesh Based Defeaturing	On
Defeature Size	Default (1.32320 cm)
Minimum Edge Length	0.60 cm
Inflation	

Use Automatic Inflation	None
Inflation Option	Smooth Transition
Transition Ratio	0.272
Maximum Layers	5
Growth Rate	1.2
Inflation Algorithm	Pre
View Advanced Options	No
Advanced	
Number of CPUs for Parallel Part Meshing	Program Controlled
Straight Sided Elements	No
Number of Retries	0
Rigid Body Behavior	Dimensionally Reduced
Mesh Morphing	Disabled
Triangle Surface Mesher	Program Controlled
Topology Checking	No
Pinch Tolerance	Default (1.58780 cm)
Generate Pinch on Refresh	No
Sheet Loop Removal	No
Statistics	
Nodes	235106
Elements	50198
Mesh Metric	None

FIGURE 3
Model (B3) > Mesh > Image

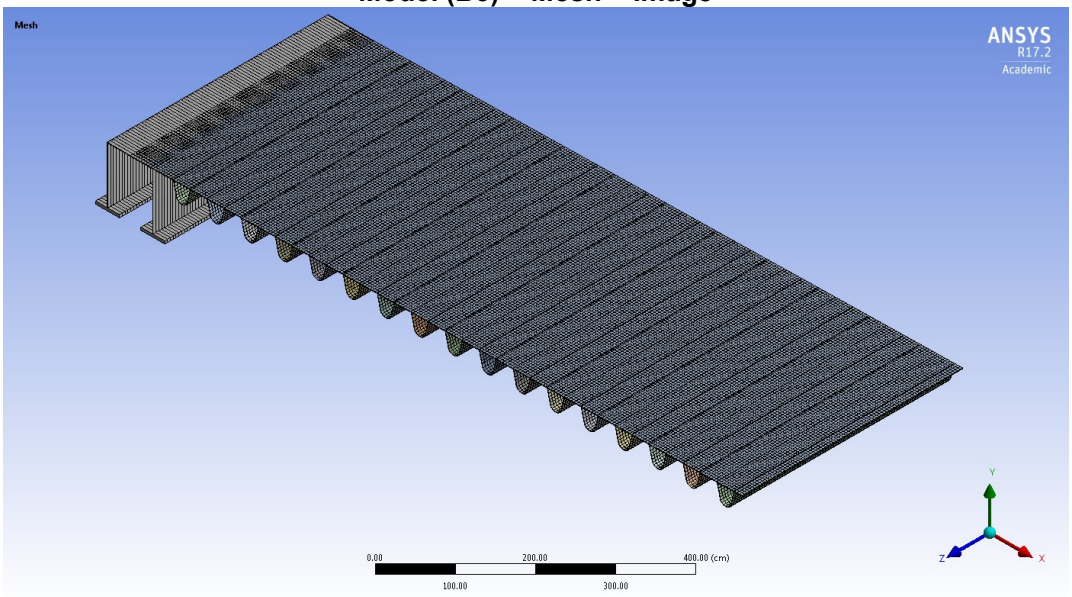
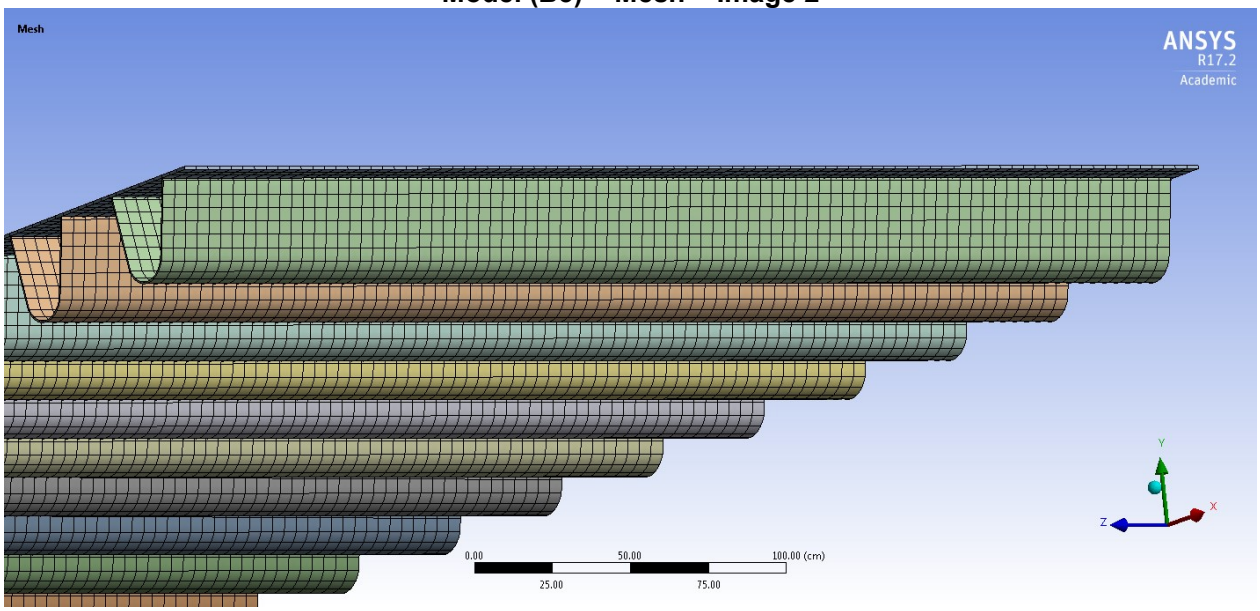


FIGURE 4
Model (B3) > Mesh > Image 2



Named Selections

TABLE 16
Model (B3) > Named Selections > Named Selections

Object Name	*U7_8_walls_face*	*U7_bottom_face*	*U8_bottom_face*
State	Fully Defined		
Scope			
Scoping Method	Geometry Selection		
Geometry	4 Faces	1 Face	
Definition			
Send to Solver	Yes		
Visible	Yes		
Program Controlled Inflation	Exclude		
Statistics			
Type	Imported		
Total Selection	4 Faces	1 Face	
Surface Area	49.259 cm²	20.066 cm²	20.415 cm²
Suppressed	0		
Used by Mesh Worksheet	No		

Modal (B4)

TABLE 17
Model (B3) > Analysis

Object Name	*Modal (B4)*
State	Solved
Definition	
Physics Type	Structural
Analysis Type	Modal

Solver Target	Mechanical APDL
Options	
Environment Temperature	22. °C
Generate Input Only	No

TABLE 18
Model (B3) > Modal (B4) > Initial Condition

Object Name	*Pre-Stress (None)*
State	Fully Defined
Definition	
Pre-Stress Environment	None

TABLE 19
Model (B3) > Modal (B4) > Analysis Settings

Object Name	*Analysis Settings*
State	Fully Defined
Options	
Max Modes to Find	20
Limit Search to Range	No
Solver Controls	
Damped	No
Solver Type	Program Controlled
Rotordynamics Controls	
Coriolis Effect	Off
Campbell Diagram	Off
Output Controls	
Stress	No
Strain	No
Nodal Forces	No
Calculate Reactions	No
General Miscellaneous	No
Analysis Data Management	
Solver Files Directory	C:\Users\Korisnik\Desktop\The final\ansys17\local 3D model\3D_segment_files\dp0\SYS-1\MECH\
Future Analysis	None
Scratch Solver Files Directory	
Save MAPDL db	No
Delete Unneeded Files	Yes
Solver Units	Active System
Solver Unit System	cgs

FIGURE 5
Model (B3) > Modal (B4) > Image

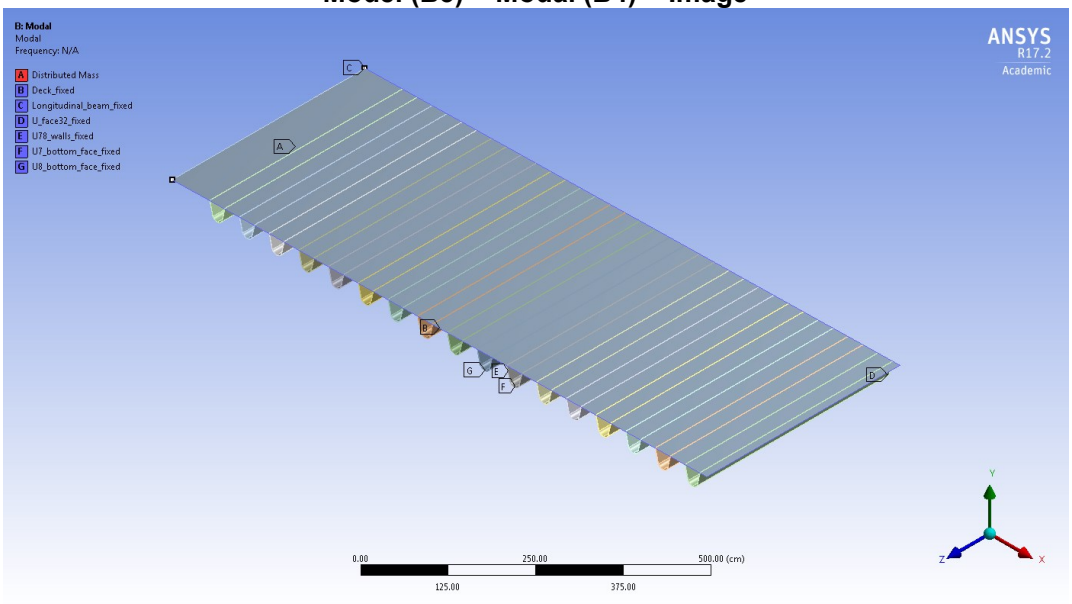


TABLE 20
Model (B3) > Modal (B4) > Loads

Object Name	*Deck_fixed*	*Longitudinal_beam_fixed*	*U_face32_fixed*	*U78_walls_fixed*	*U7_bottom_face_fixed*	*U8_bottom_face_fixed*
State	Fully Defined					
Scope						
Scoping Method	Geometry Selection			Named Selection		
Geometry	3 Edges	2 Vertices	32 Faces			
Named Selection				U7_8_walls_face	U7_bottom_face	U8_bottom_face
Definition						
Type	Fixed Support					
Suppressed	No					

FIGURE 6
Model (B3) > Modal (B4) > U7_bottom_face_fixed > Image 2

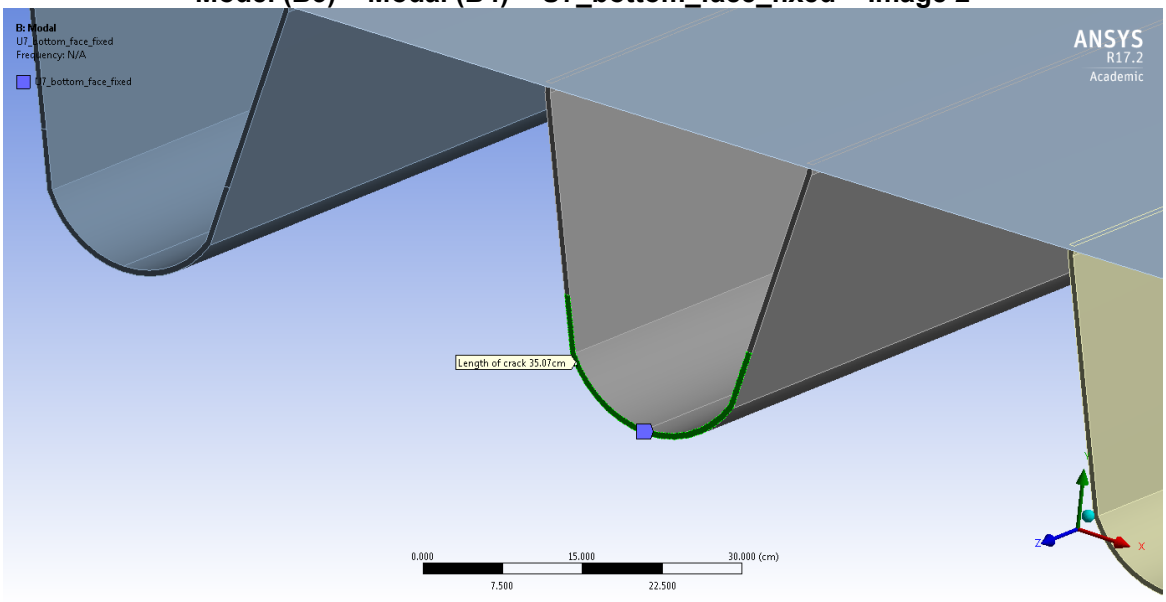


FIGURE 7
Model (B3) > Modal (B4) > U8_bottom_face_fixed > Image

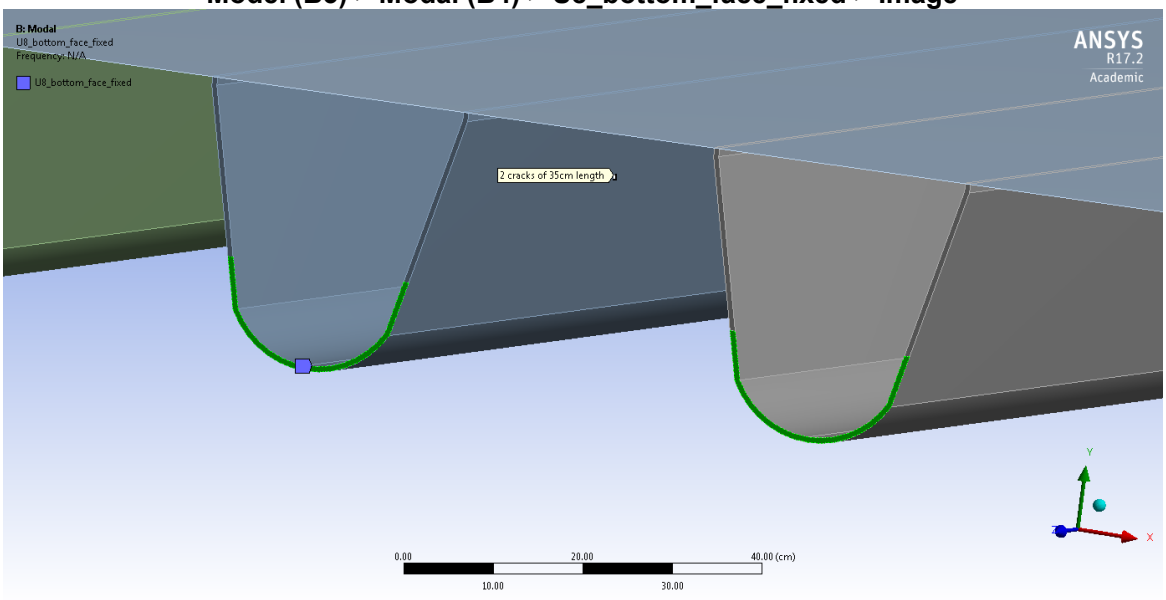
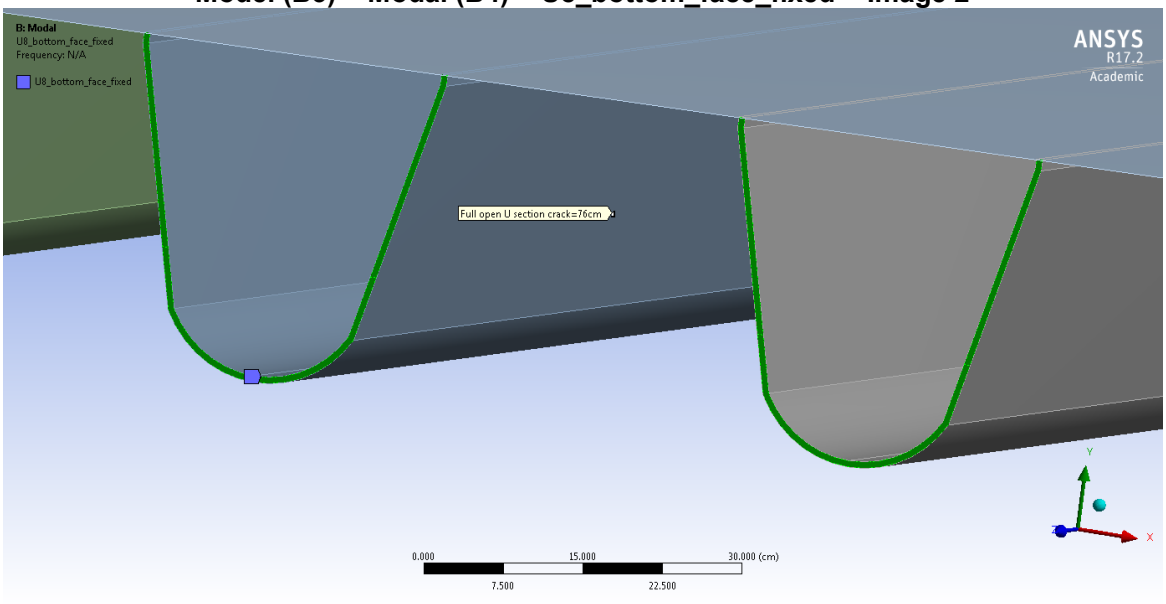


FIGURE 8
Model (B3) > Modal (B4) > U8_bottom_face_fixed > Image 2



Solution (B5)

TABLE 21
Model (B3) > Modal (B4) > Solution

Object Name	*Solution (B5)*
State	Solved
Adaptive Mesh Refinement	
Max Refinement Loops	1.
Refinement Depth	2.
Information	
Status	Done
MAPDL Elapsed Time	8 m 3 s
MAPDL Memory Used	5.2178 GB
MAPDL Result File Size	301.19 MB
Post Processing	
Beam Section Results	No

The following bar chart indicates the frequency at each calculated mode.

FIGURE 9
Model (B3) > Modal (B4) > Solution (B5)

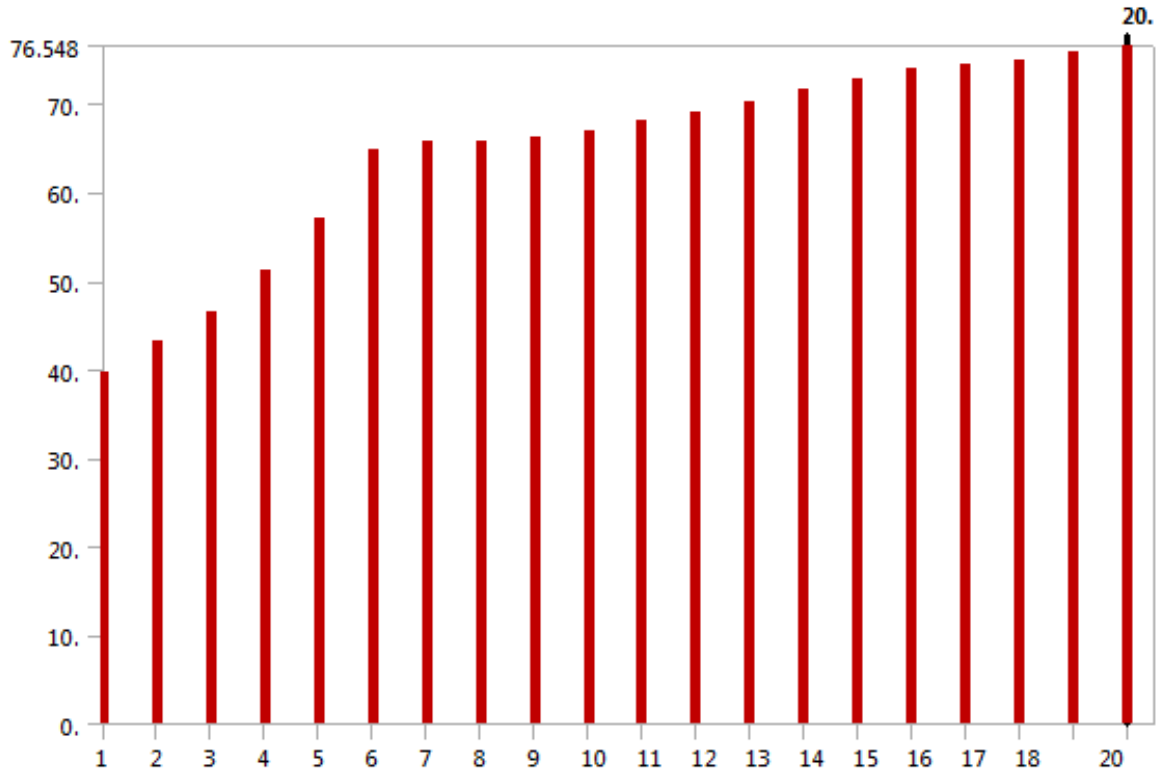


TABLE 22
Model (B3) > Modal (B4) > Solution (B5)

Mode	Frequency [Hz]
1.	39.626
2.	43.2
3.	46.543
4.	51.1
5.	57.156
6.	64.885
7.	65.635
8.	65.834
9.	66.292
10.	67.036
11.	68.014
12.	69.086
13.	70.317
14.	71.55
15.	72.751
16.	73.883
17.	74.361
18.	74.938
19.	75.771
20.	76.548

TABLE 23
Model (B3) > Modal (B4) > Solution (B5) > Solution Information

Object Name	*Solution Information*
State	Solved
Solution Information	
Solution Output	Solver Output
Newton-Raphson Residuals	0
Identify Element Violations	0
Update Interval	2.5 s
Display Points	All
FE Connection Visibility	
Activate Visibility	Yes
Display	All FE Connectors
Draw Connections Attached To	All Nodes
Line Color	Connection Type
Visible on Results	No
Line Thickness	Single
Display Type	Lines

0kg

TABLE 24
Model (B3) > Modal (B4) > Solution (B5) > 0kg > Results

Object Name	*0kg total deformation 1*	*0kg total deformation 2*	*0kg total deformation 3*	*0kg total deformation 4*	*0kg total deformation 5*	*0kg total deformation 6*	*0kg total deformation 7*	*0kg total deformation 8*	*0kg total deformation 9*	*0kg total deformation 10*	*0kg total deformation 11*
State	Solved	Suppressed									
Scope											
Scoping Method	Geometry Selection										
Geometry	All Bodies										
Definition											
Type	Total Deformation										
Mode	1.	2.	3.	4.	5.	6.	7.	8.	9.	10.	11.
Identifier											
Suppressed	No	Yes									
Results											
Minimum	0. cm										
Maximum	2.2466e-003 cm										
Minimum	Longitudinal										

Occurs On	edge beam.2	
Maximum Occurs On	deck_mid	
Information		
Frequency	39.626 Hz	

FIGURE 10
Model (B3) > Modal (B4) > Solution (B5) > 0kg > 0kg total deformation 1 > Image

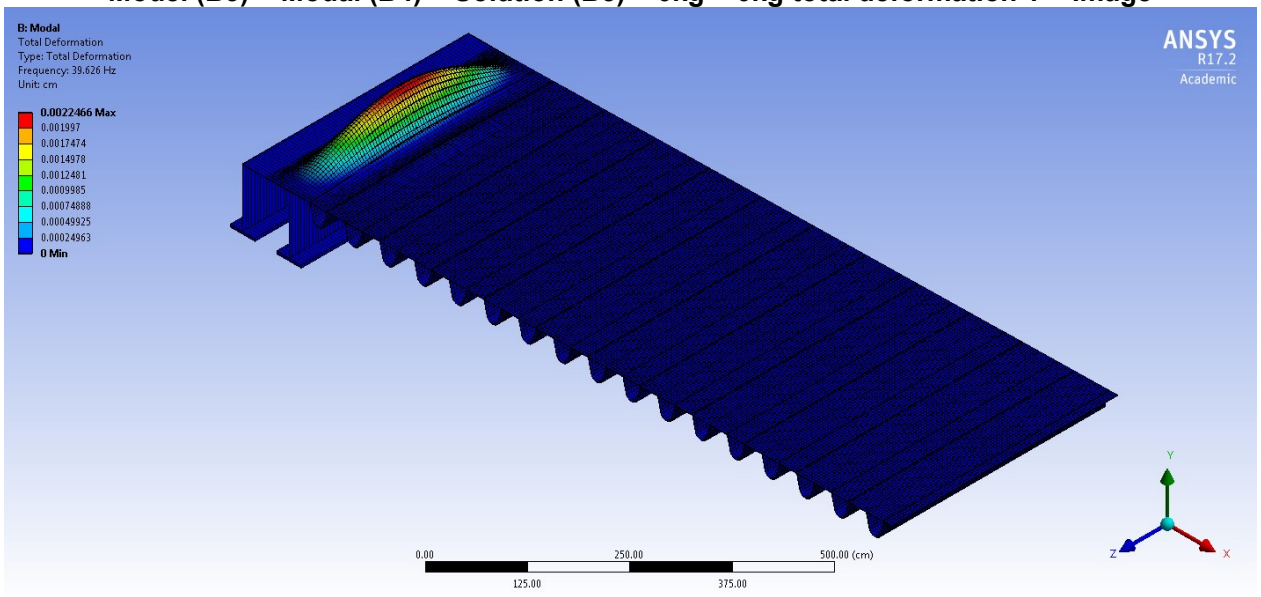


FIGURE 11
Model (B3) > Modal (B4) > Solution (B5) > 0kg > 0kg total deformation 2 > Image

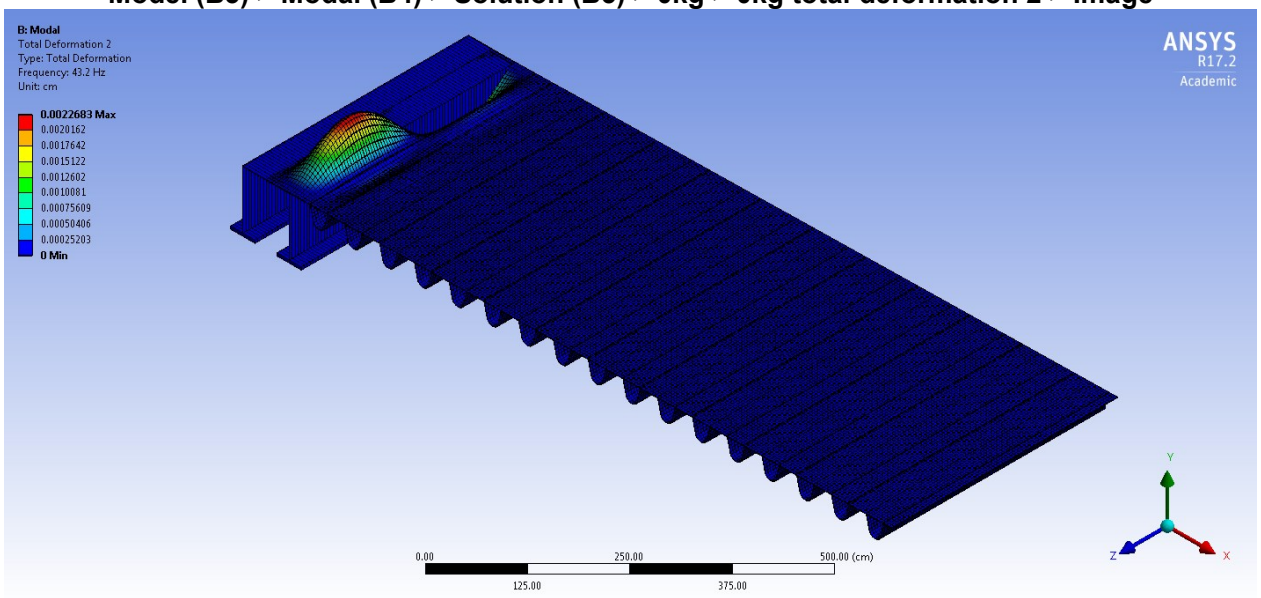


FIGURE 12
Model (B3) > Modal (B4) > Solution (B5) > 0kg > 0kg total deformation 3 > Image

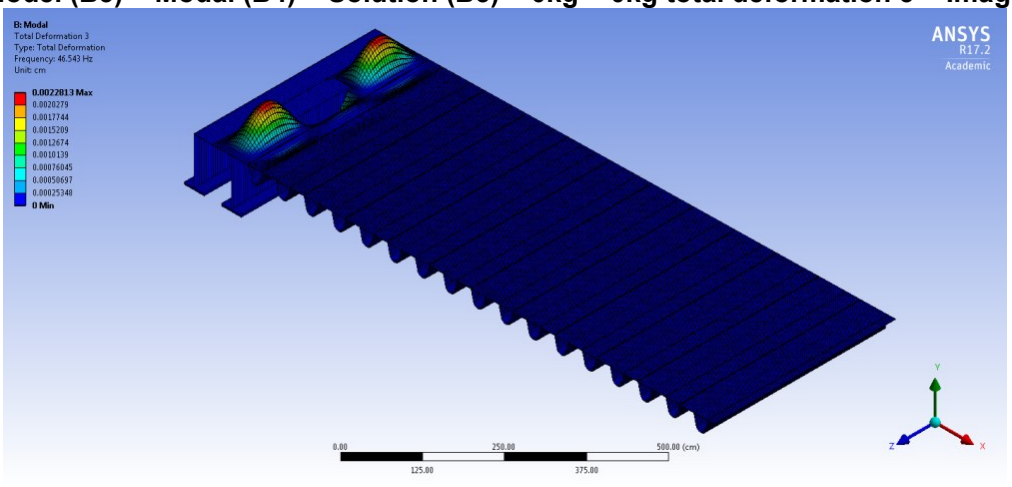


FIGURE 13
Model (B3) > Modal (B4) > Solution (B5) > 0kg > 0kg total deformation 4 > Image

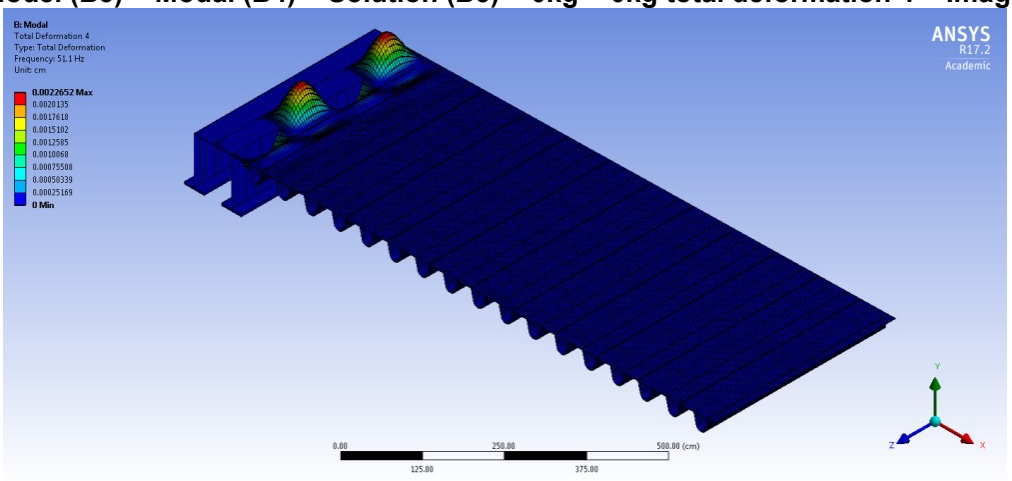


FIGURE 14
Model (B3) > Modal (B4) > Solution (B5) > 0kg > 0kg total deformation 5 > Image

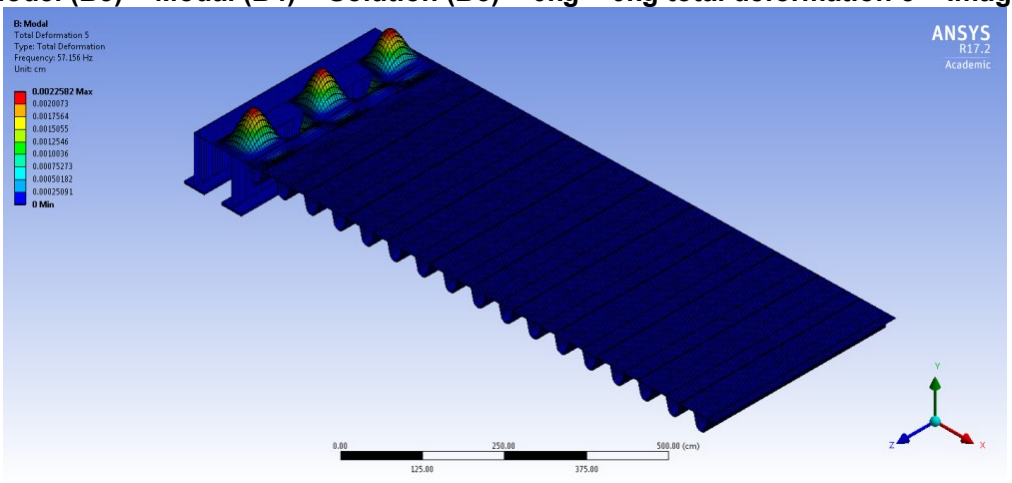


FIGURE 15
Model (B3) > Modal (B4) > Solution (B5) > 0kg > 0kg total deformation 6 > Image

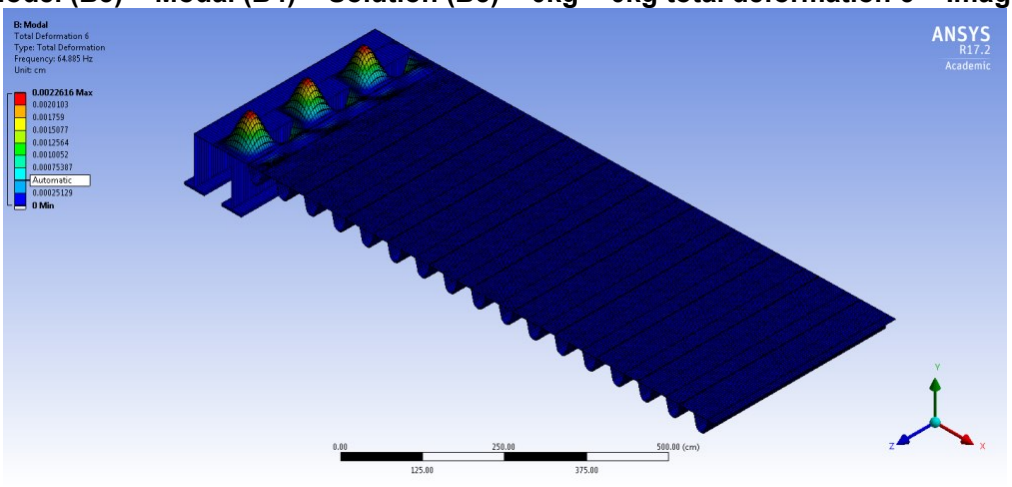


FIGURE 16
Model (B3) > Modal (B4) > Solution (B5) > 0kg > 0kg total deformation 7 > Image

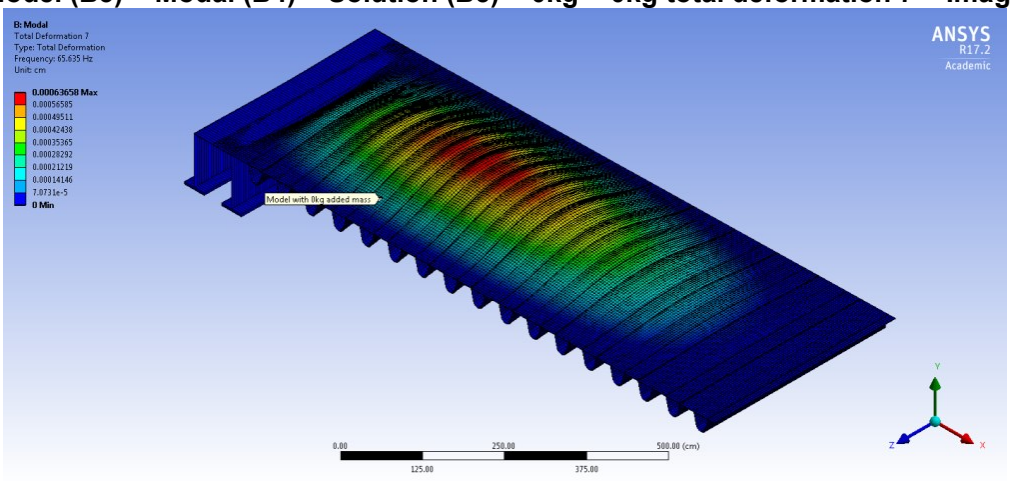


FIGURE 17
Model (B3) > Modal (B4) > Solution (B5) > 0kg > 0kg total deformation 8 > Image

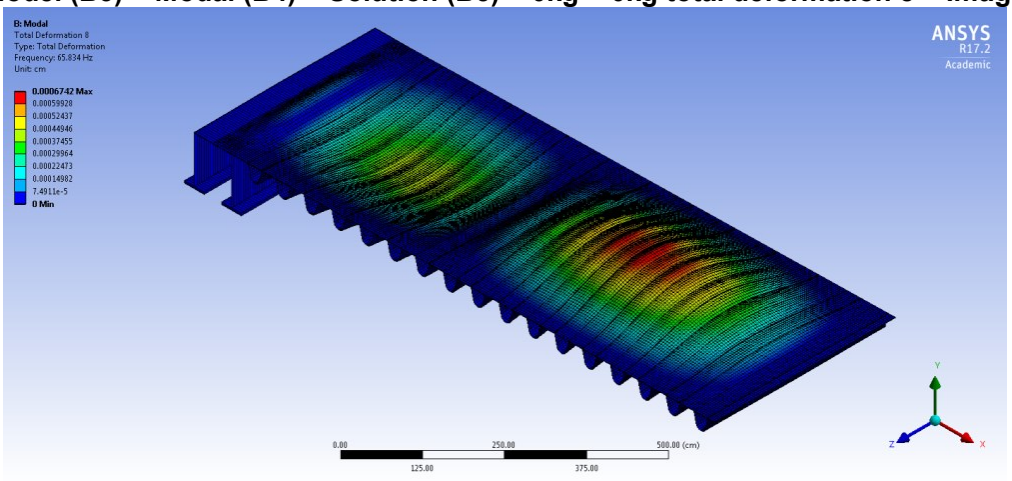


FIGURE 18
Model (B3) > Modal (B4) > Solution (B5) > 0kg > 0kg total deformation 9 > Image

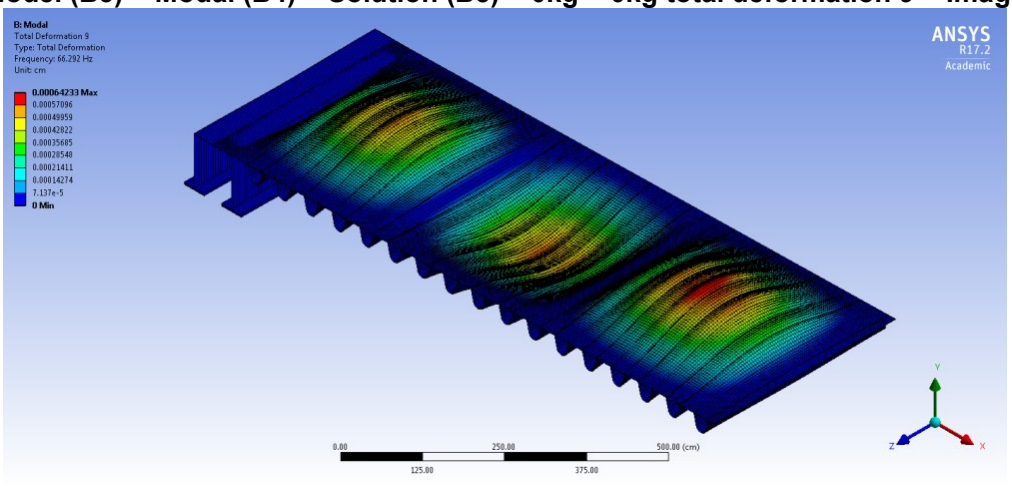


FIGURE 19
Model (B3) > Modal (B4) > Solution (B5) > 0kg > 0kg total deformation 10 > Image

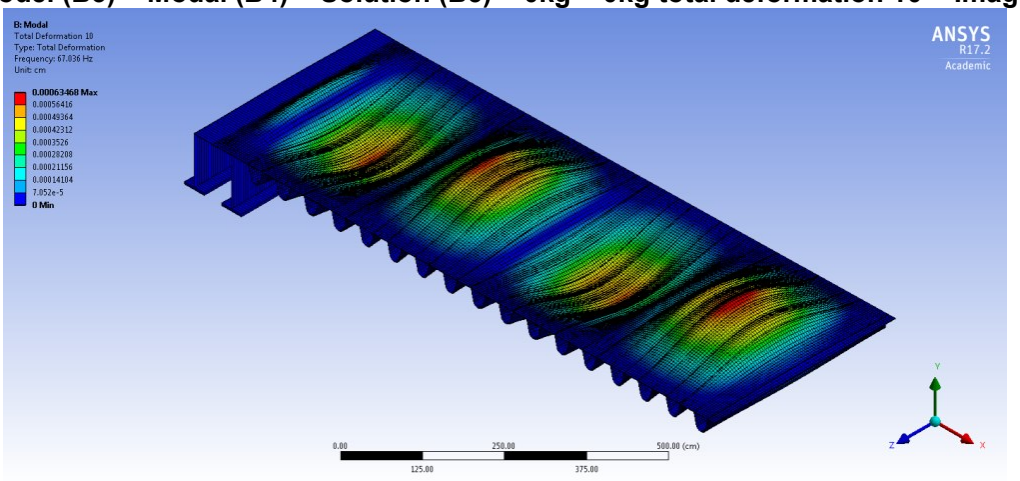


FIGURE 20
Model (B3) > Modal (B4) > Solution (B5) > 0kg > 0kg total deformation 11 > Image

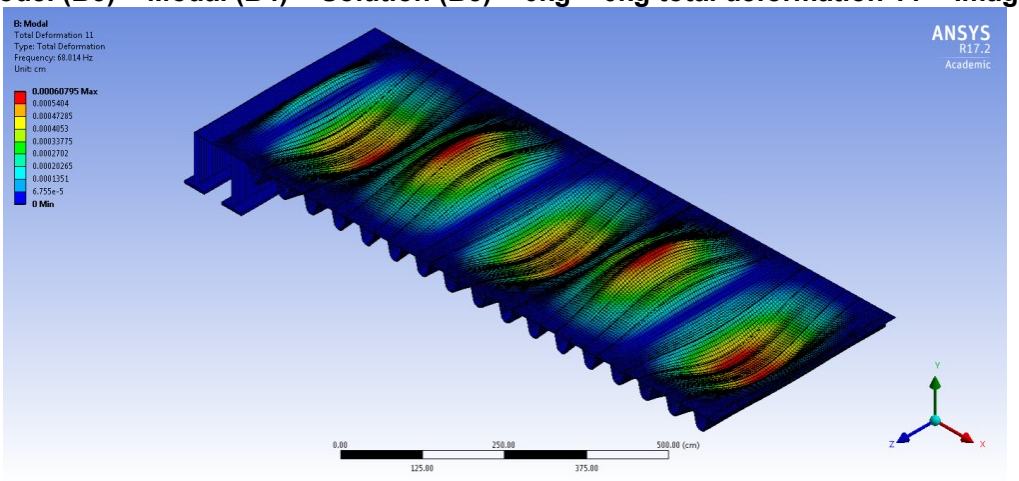


TABLE 26
Model (B3) > Modal (B4) > Solution (B5) > 0kg > Results

Object Name	*0kg total deformation 12*	*0kg total deformation 13*	*0kg total deformation 14*	*0kg total deformation 15*	*0kg total deformation 16*	*0kg total deformation 17*	*0kg total deformation 18*	*0kg total deformation 19*	*0kg total deformation 20*
State	Suppressed								
Scope									
Scoping Method	Geometry Selection								
Geometry	All Bodies								
Definition									
Type	Total Deformation								
Mode	12.	13.	14.	15.	16.	17.	18.	19.	20.
Identifier									
Suppressed	Yes								
Results									
Minimum									
Maximum									
Minimum Occurs On									
Maximum Occurs On									
Information									
Frequency									

FIGURE 21
Model (B3) > Modal (B4) > Solution (B5) > 0kg > 0kg total deformation 12 > Image

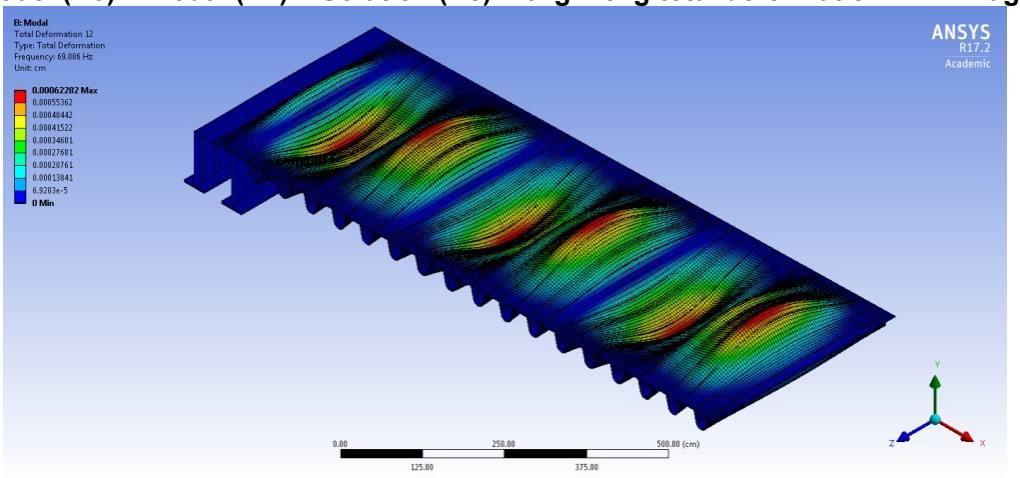


FIGURE 22
Model (B3) > Modal (B4) > Solution (B5) > 0kg > 0kg total deformation 13 > Image

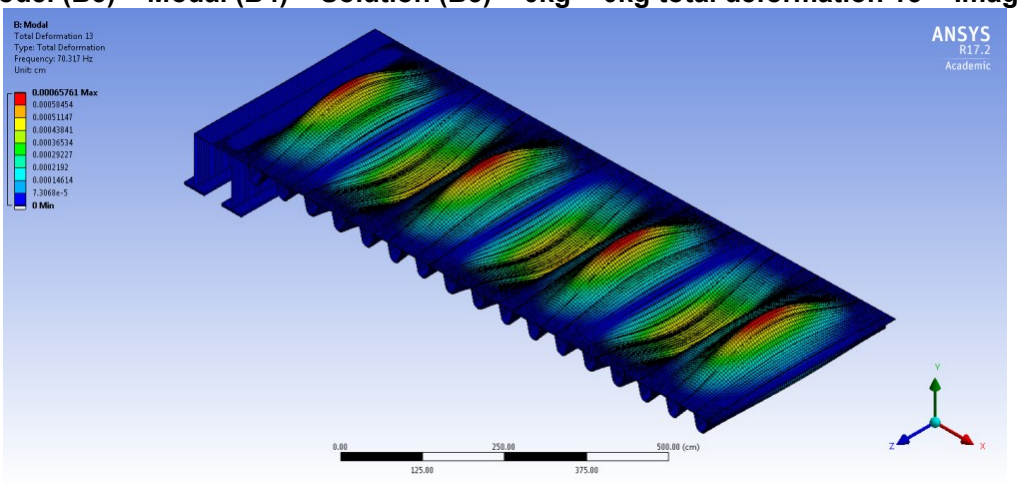


FIGURE 23
Model (B3) > Modal (B4) > Solution (B5) > 0kg > 0kg total deformation 14 > Image

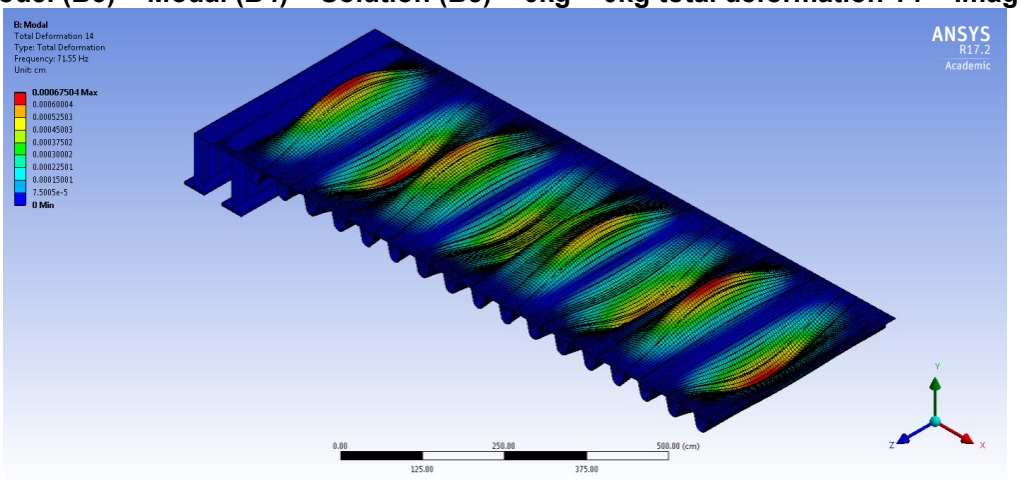


FIGURE 24
Model (B3) > Modal (B4) > Solution (B5) > 0kg > 0kg total deformation 15 > Image

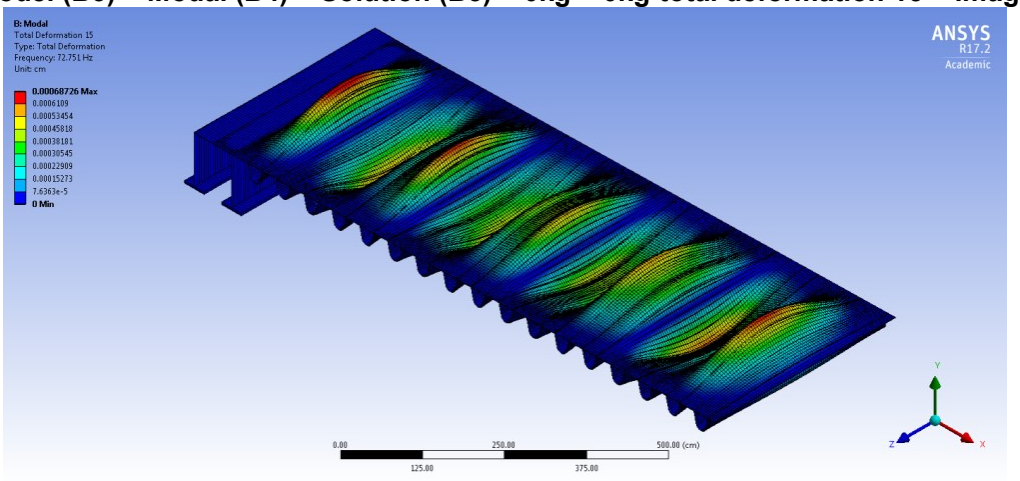


FIGURE 25
Model (B3) > Modal (B4) > Solution (B5) > 0kg > 0kg total deformation 16 > Image

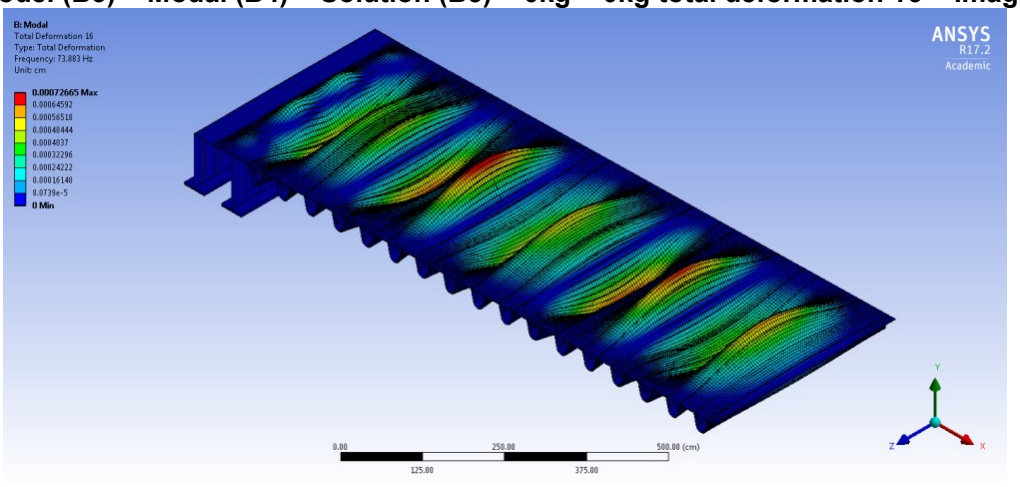


FIGURE 26
Model (B3) > Modal (B4) > Solution (B5) > 0kg > 0kg total deformation 17 > Image

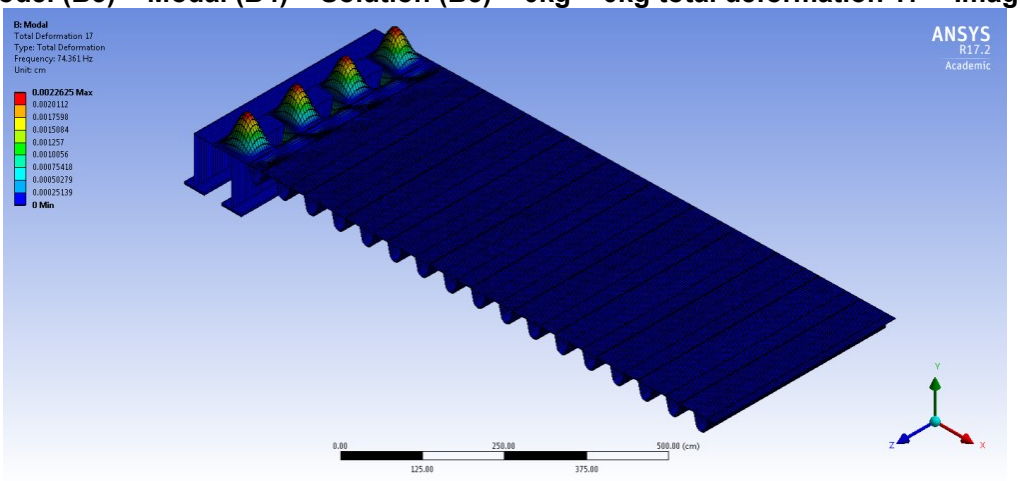


FIGURE 27
Model (B3) > Modal (B4) > Solution (B5) > 0kg > 0kg total deformation 18 > Image

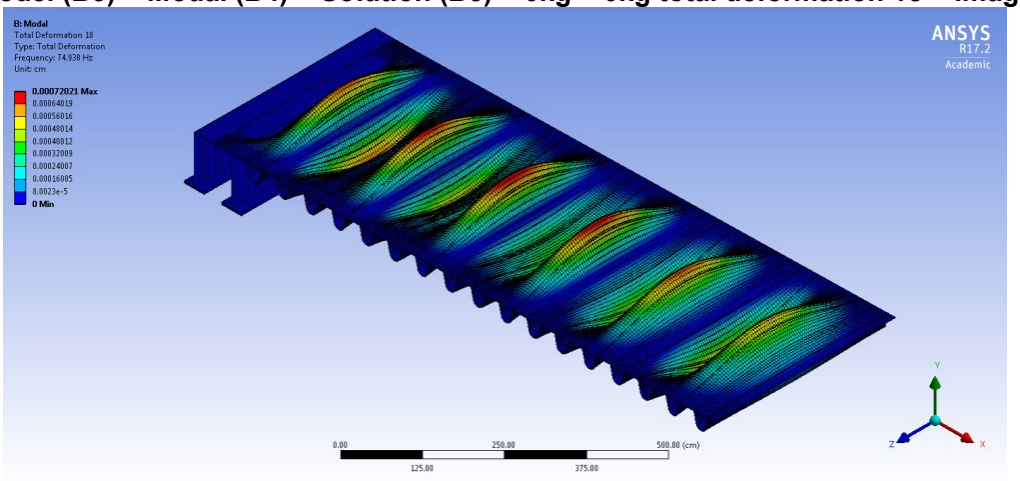


FIGURE 28
Model (B3) > Modal (B4) > Solution (B5) > 0kg > 0kg total deformation 19 > Image

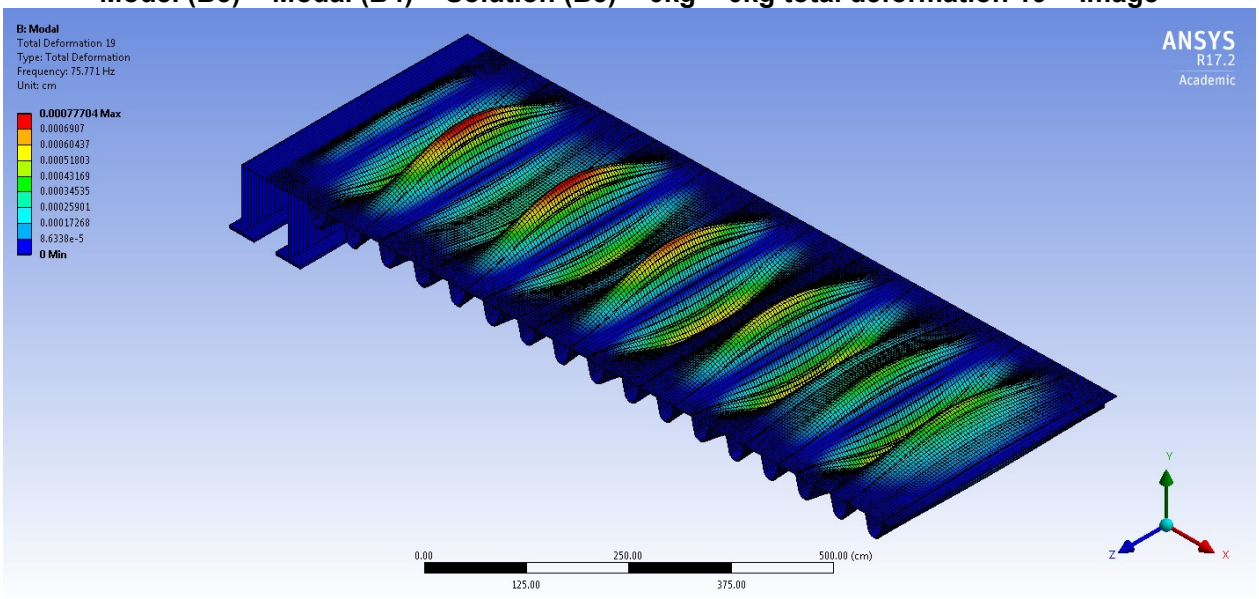
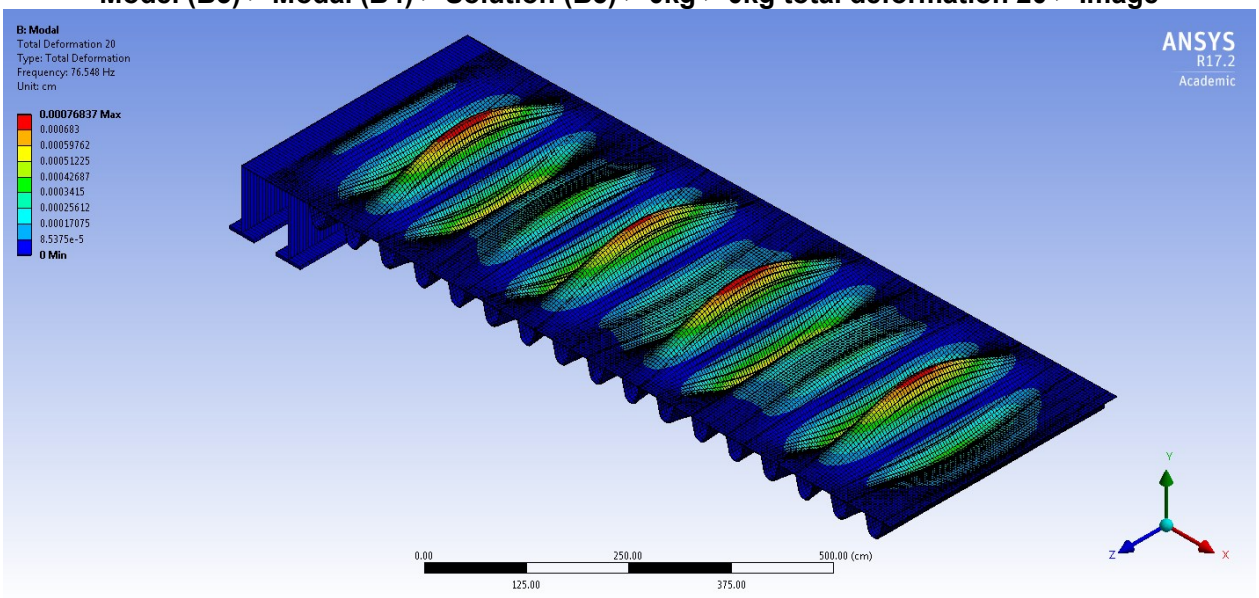


FIGURE 29
Model (B3) > Modal (B4) > Solution (B5) > 0kg > 0kg total deformation 20 > Image



50kg

TABLE 27
Model (B3) > Modal (B4) > Solution (B5) > 50kg > Results

Object Name	*50kg total deformation 1*	*50kg total deformation 2*	*50kg total deformation 3*	*50kg total deformation 4*	*50kg total deformation 5*	*50kg total deformation 6*	*50kg total deformation 7*	*50kg total deformation 8*	*50kg total deformation 9*	*50kg total deformation 10*	*50kg total deformation 11*
State	Suppressed										
Scope											

Scoping Method	Geometry Selection										
Geometry	All Bodies										
Definition											
Type	Total Deformation										
Mode	1.	2.	3.	4.	5.	6.	7.	8.	9.	10.	11.
Identifier											
Suppressed	Yes										
Results											
Minimum											
Maximum											
Minimum Occurs On											
Maximum Occurs On											
Information											
Frequency											

FIGURE 30
Model (B3) > Modal (B4) > Solution (B5) > 50kg > 50kg total deformation 1 > Image

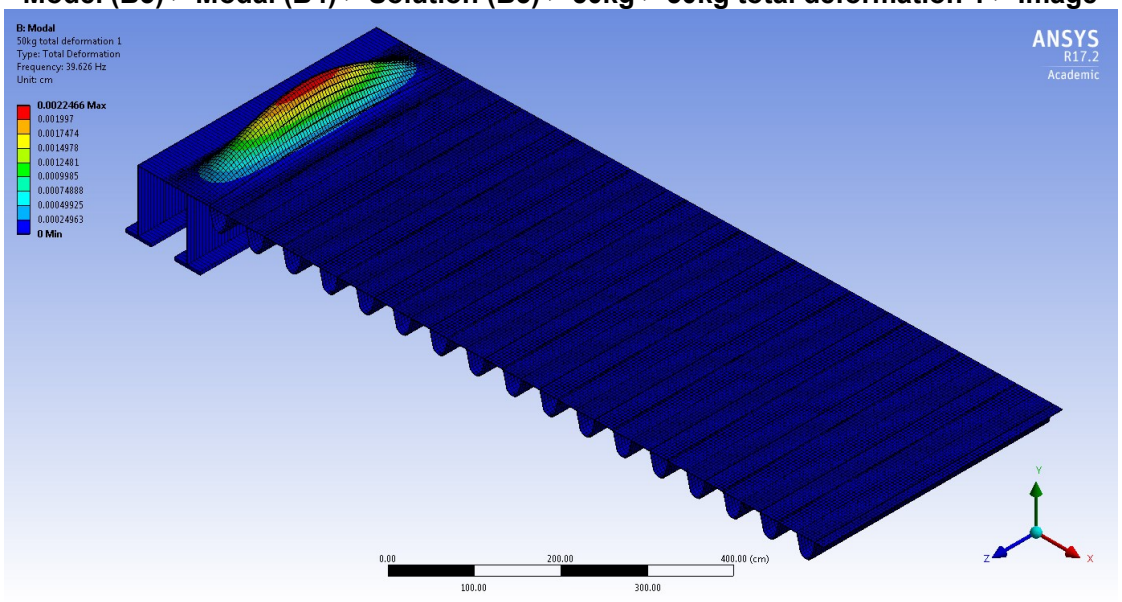


FIGURE 31
Model (B3) > Modal (B4) > Solution (B5) > 50kg > 50kg total deformation 2 > Image

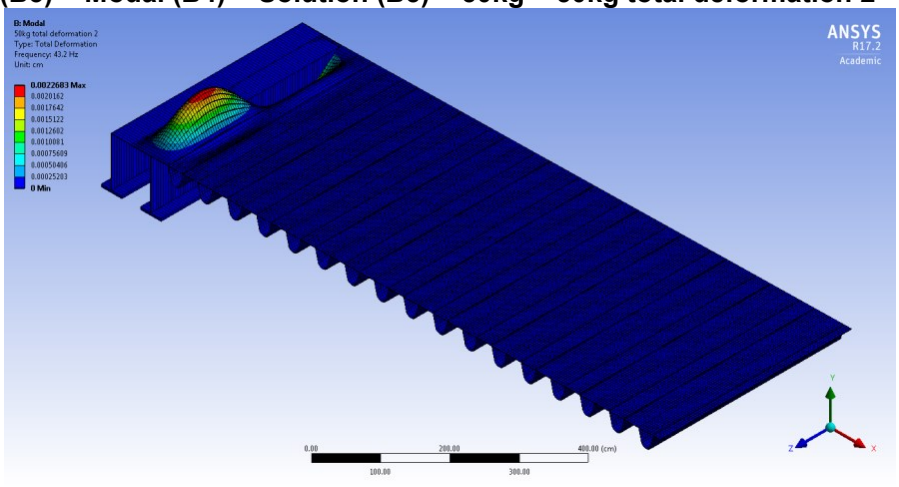


FIGURE 32
Model (B3) > Modal (B4) > Solution (B5) > 50kg > 50kg total deformation 3 > Image

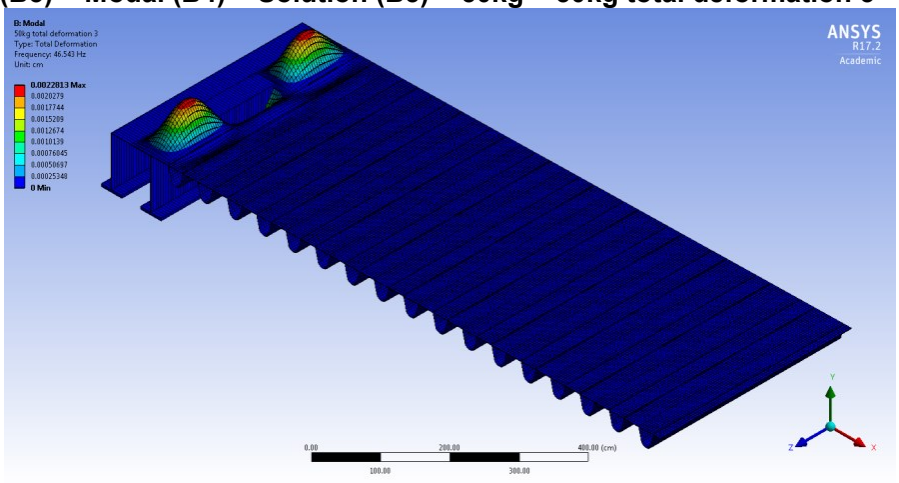


FIGURE 33
Model (B3) > Modal (B4) > Solution (B5) > 50kg > 50kg total deformation 4 > Image

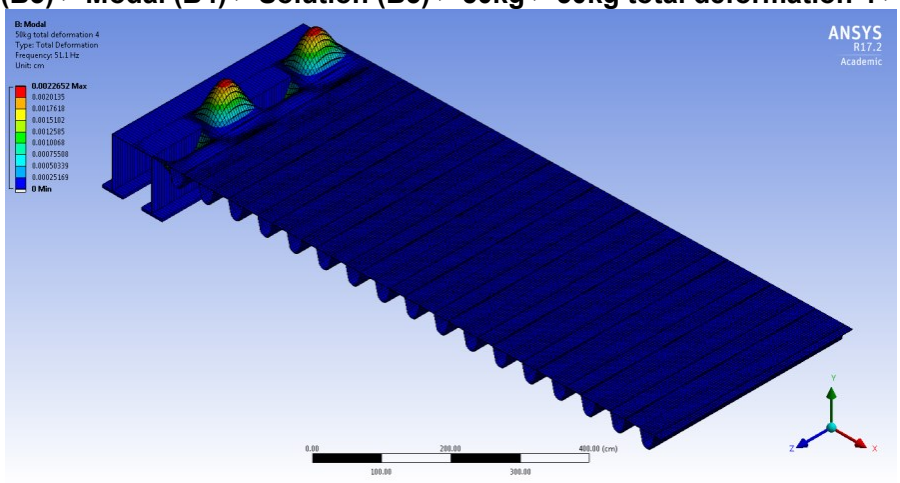


FIGURE 34
Model (B3) > Modal (B4) > Solution (B5) > 50kg > 50kg total deformation 5 > Image

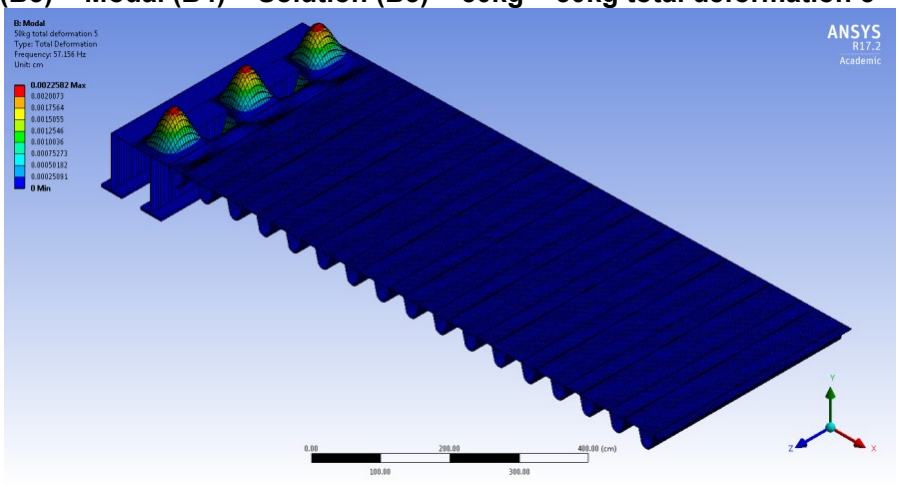


FIGURE 35
Model (B3) > Modal (B4) > Solution (B5) > 50kg > 50kg total deformation 6 > Image

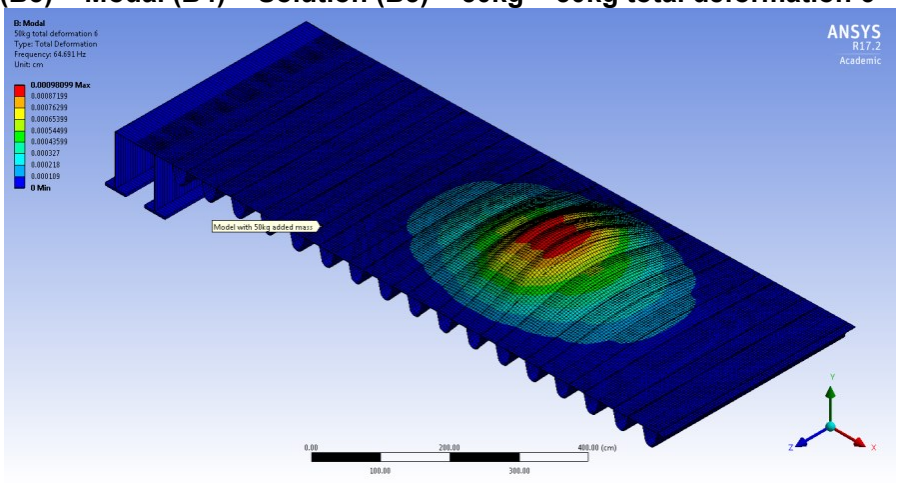


FIGURE 36
Model (B3) > Modal (B4) > Solution (B5) > 50kg > 50kg total deformation 7 > Image

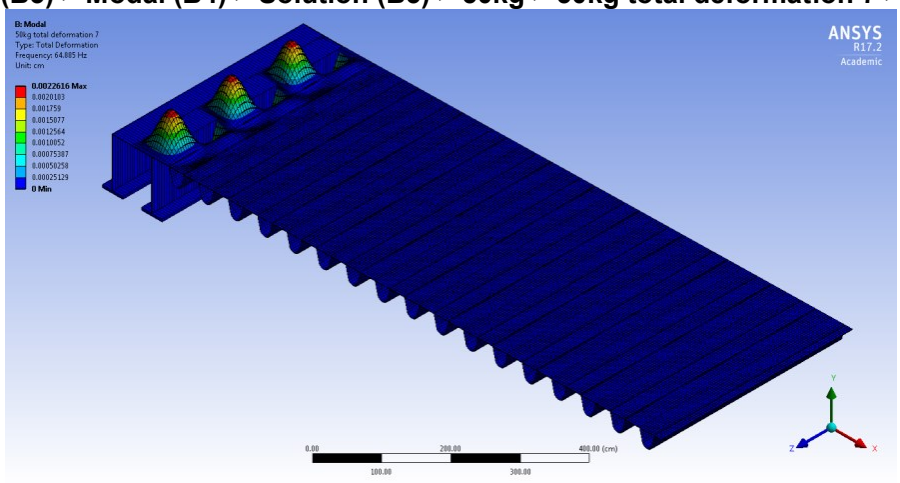


FIGURE 37
Model (B3) > Modal (B4) > Solution (B5) > 50kg > 50kg total deformation 8 > Image

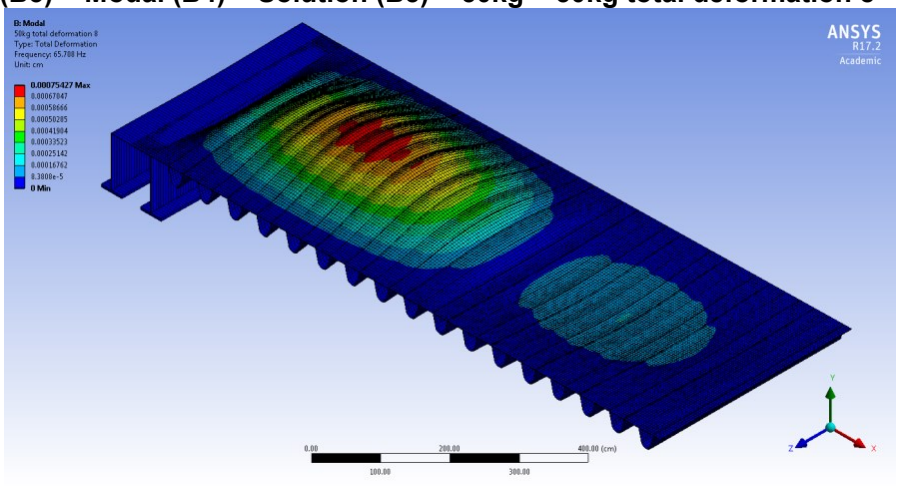


FIGURE 38
Model (B3) > Modal (B4) > Solution (B5) > 50kg > 50kg total deformation 9 > Image

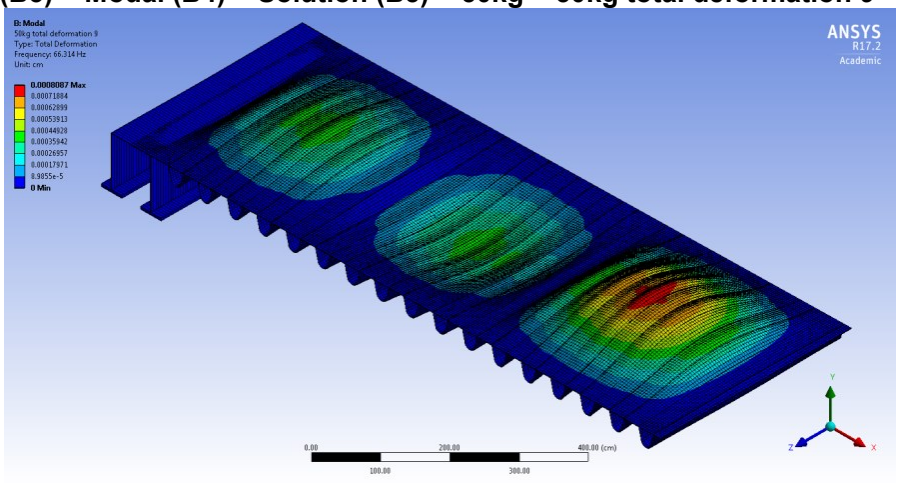


FIGURE 39
Model (B3) > Modal (B4) > Solution (B5) > 50kg > 50kg total deformation 10 > Image

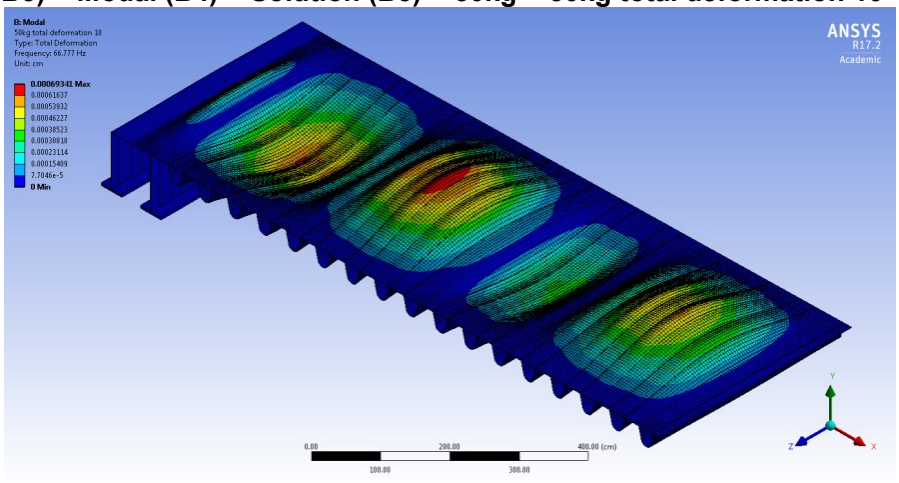


FIGURE 40
Model (B3) > Modal (B4) > Solution (B5) > 50kg > 50kg total deformation 11 > Image

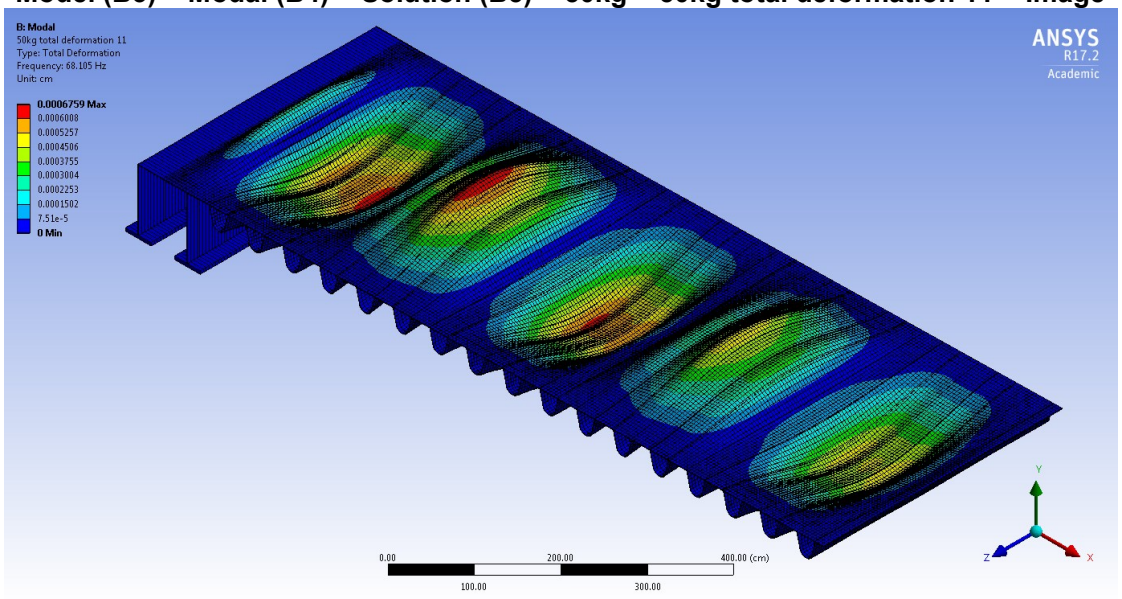
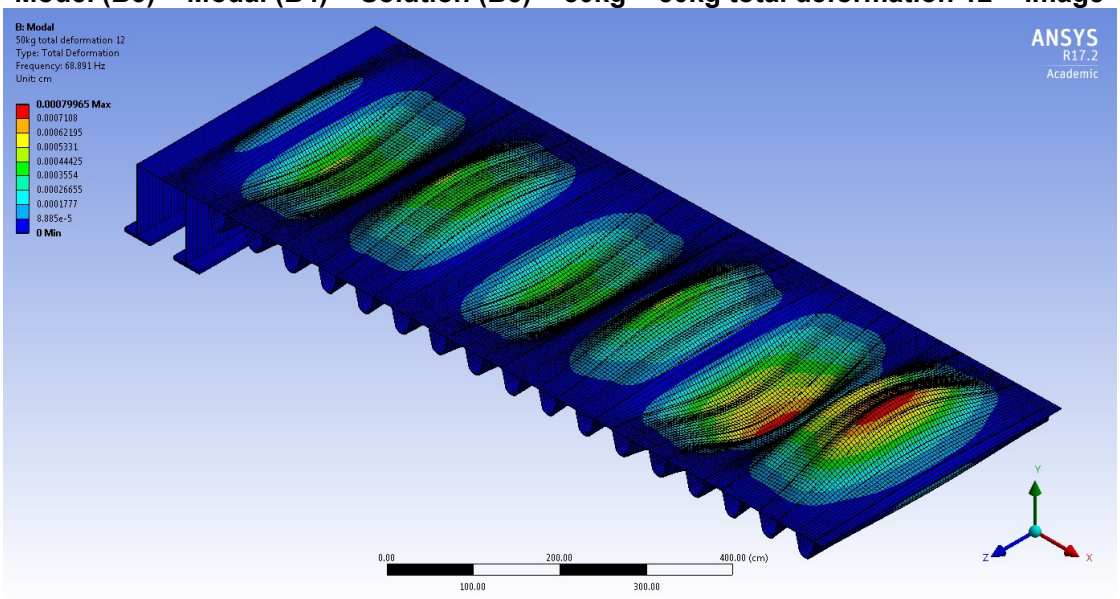


TABLE 28
Model (B3) > Modal (B4) > Solution (B5) > 50kg > Results

Object Name	*50kg total deformation 12*
State	Suppressed
Scope	
Scoping Method	Geometry Selection
Geometry	All Bodies
Definition	
Type	Total Deformation
Mode	12.
Identifier	
Suppressed	Yes
Results	
Minimum	
Maximum	
Minimum Occurs On	
Maximum Occurs On	
Information	
Frequency	

FIGURE 41
Model (B3) > Modal (B4) > Solution (B5) > 50kg > 50kg total deformation 12 > Image



75kg

TABLE 29
Model (B3) > Modal (B4) > Solution (B5) > 75kg > Results

Object Name	*75kg total deformation 1*	*75kg total deformation 2*	*75kg total deformation 3*	*75kg total deformation 4*	*75kg total deformation 5*	*75kg total deformation 6*	*75kg total deformation 7*	*75kg total deformation 8*	*75kg total deformation 9*	*75kg total deformation 10*	*75kg total deformation 11*
State	Suppressed										
Scope											
Scoping Method	Geometry Selection										
Geometry	All Bodies										
Definition											
Type	Total Deformation										
Mode	1.	2.	3.	4.	5.	6.	7.	8.	9.	10.	11.
Identifier											
Suppressed	Yes										
Results											
Minimum											
Maximum											
Minimum											

Occurs On	
Maximum Occurs On	
Information	
Frequency	

FIGURE 42
Model (B3) > Modal (B4) > Solution (B5) > 75kg > 75kg total deformation 1 > Image

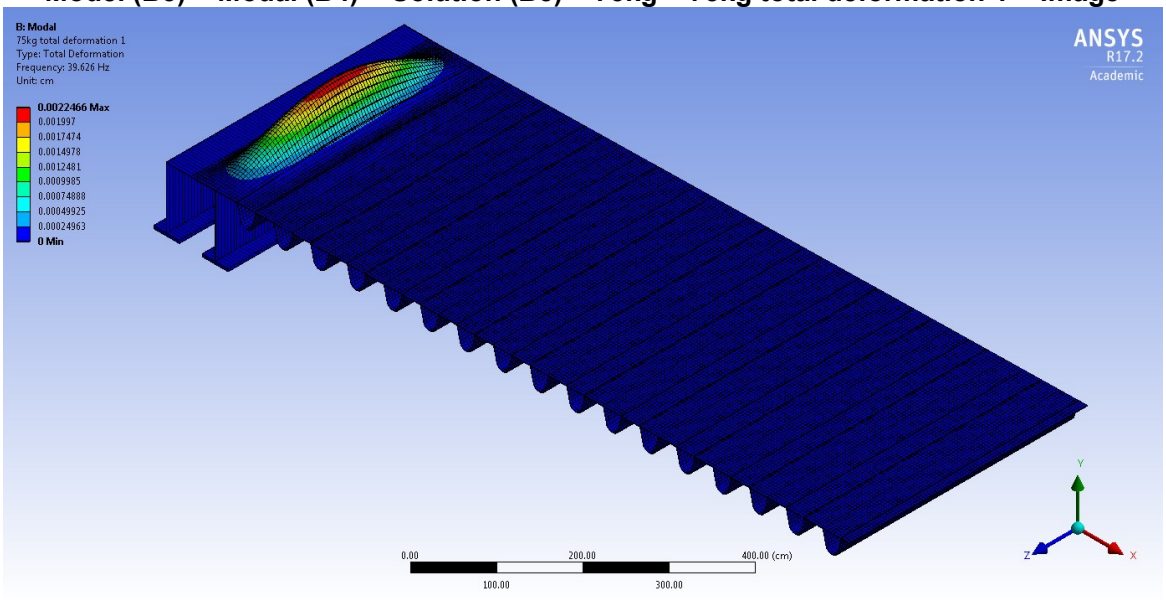


FIGURE 43
Model (B3) > Modal (B4) > Solution (B5) > 75kg > 75kg total deformation 2 > Image

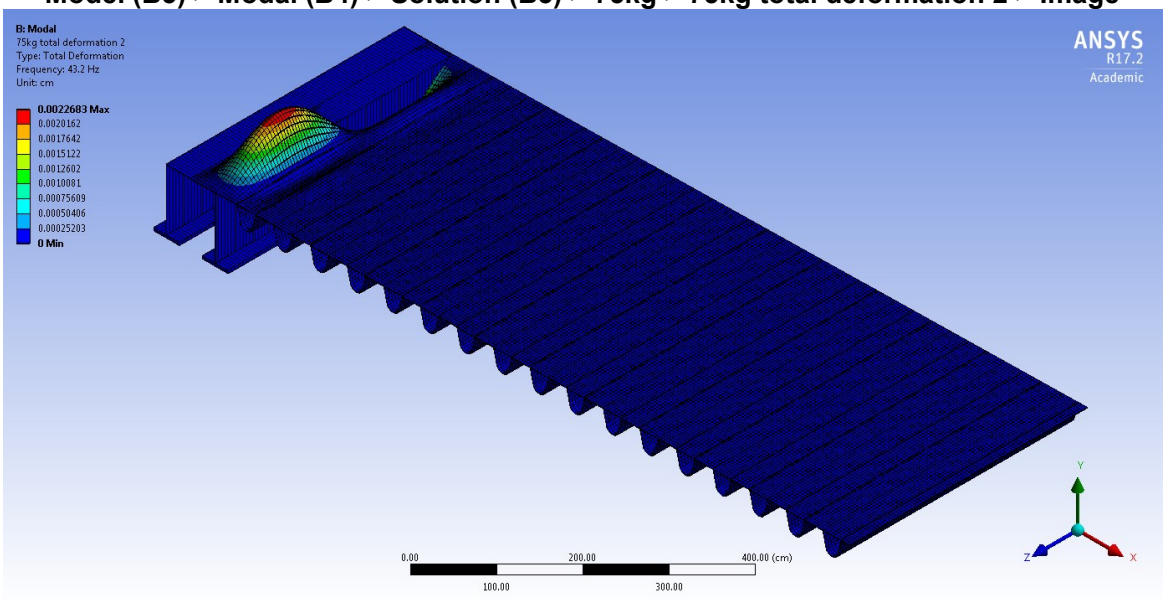


FIGURE 44
Model (B3) > Modal (B4) > Solution (B5) > 75kg > 75kg total deformation 3 > Image

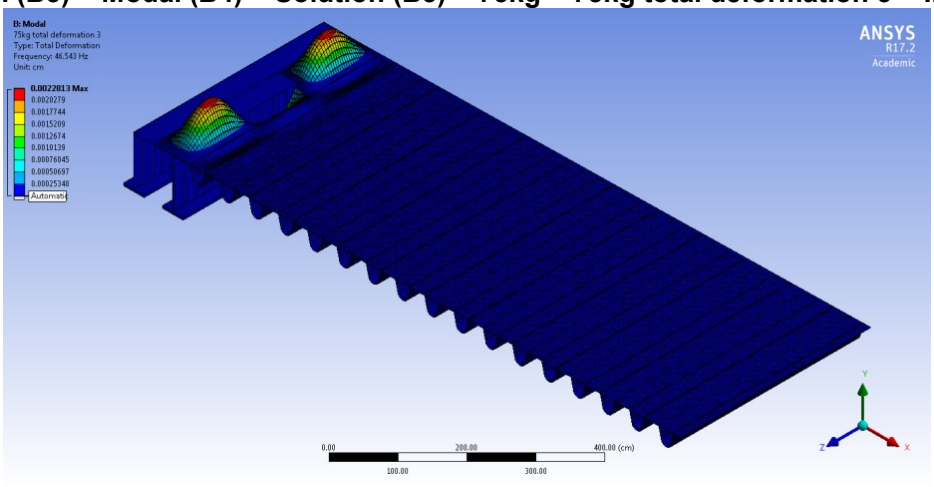


FIGURE 45
Model (B3) > Modal (B4) > Solution (B5) > 75kg > 75kg total deformation 4 > Image

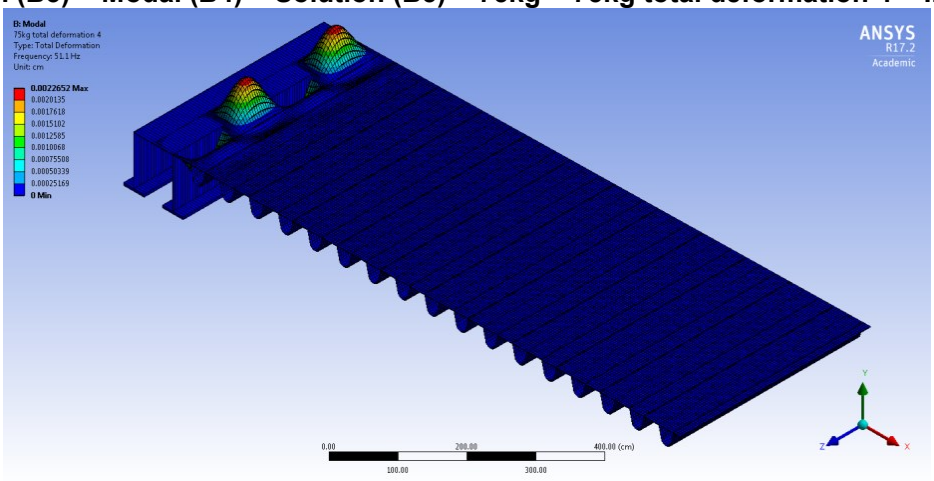


FIGURE 46
Model (B3) > Modal (B4) > Solution (B5) > 75kg > 75kg total deformation 5 > Image

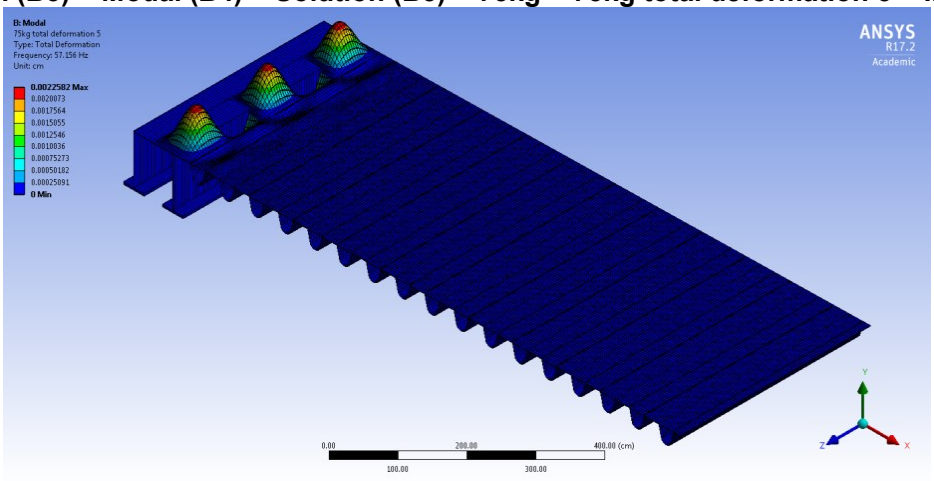


FIGURE 47
Model (B3) > Modal (B4) > Solution (B5) > 75kg > 75kg total deformation 6 > Image

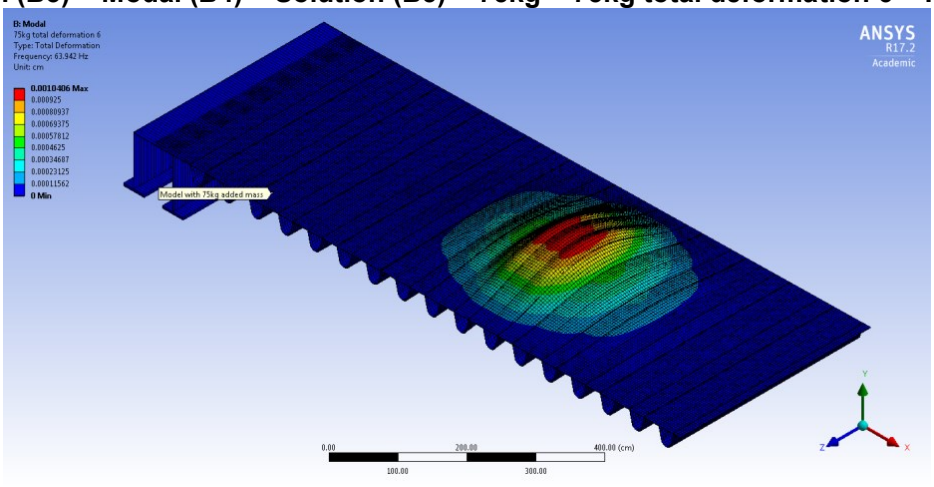


FIGURE 48
Model (B3) > Modal (B4) > Solution (B5) > 75kg > 75kg total deformation 7 > Image

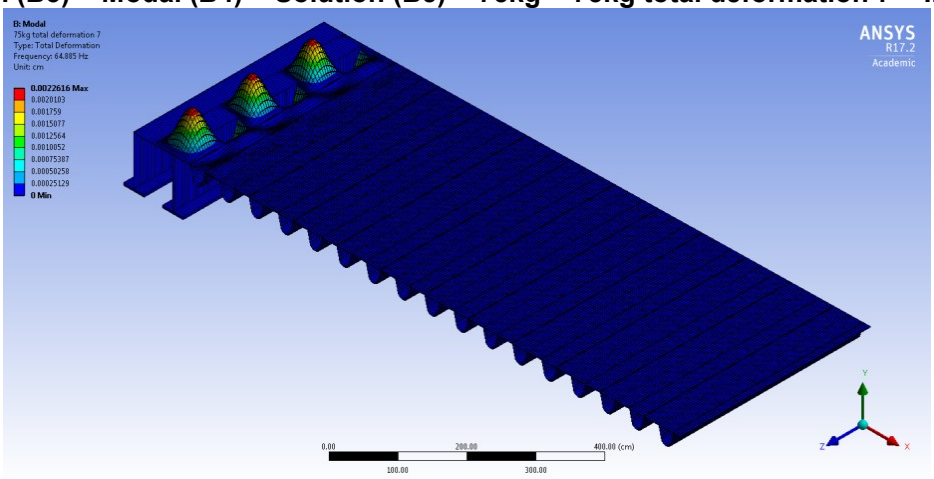


FIGURE 49
Model (B3) > Modal (B4) > Solution (B5) > 75kg > 75kg total deformation 8 > Image

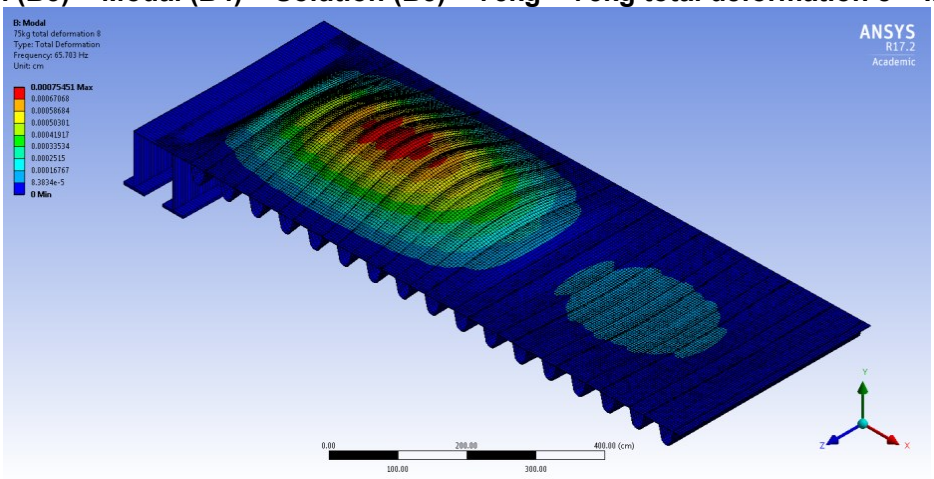


FIGURE 50
Model (B3) > Modal (B4) > Solution (B5) > 75kg > 75kg total deformation 9 > Image

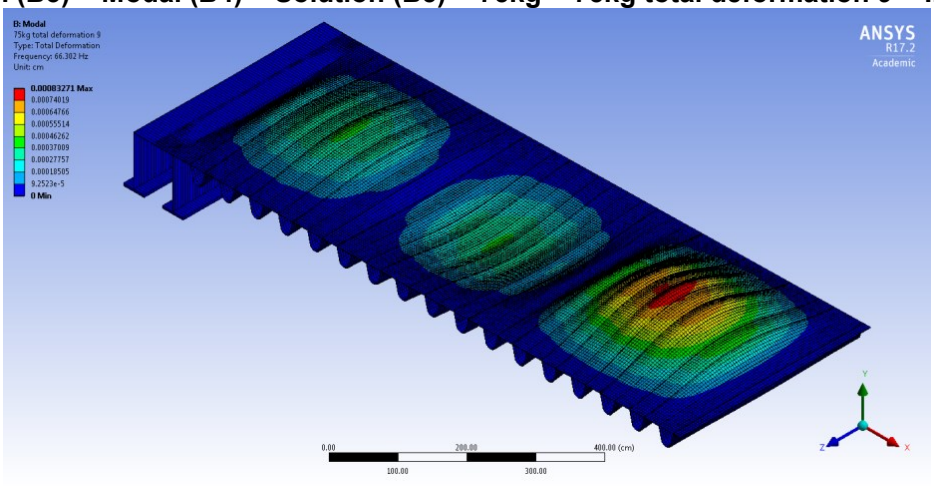


FIGURE 51
Model (B3) > Modal (B4) > Solution (B5) > 75kg > 75kg total deformation 10 > Image

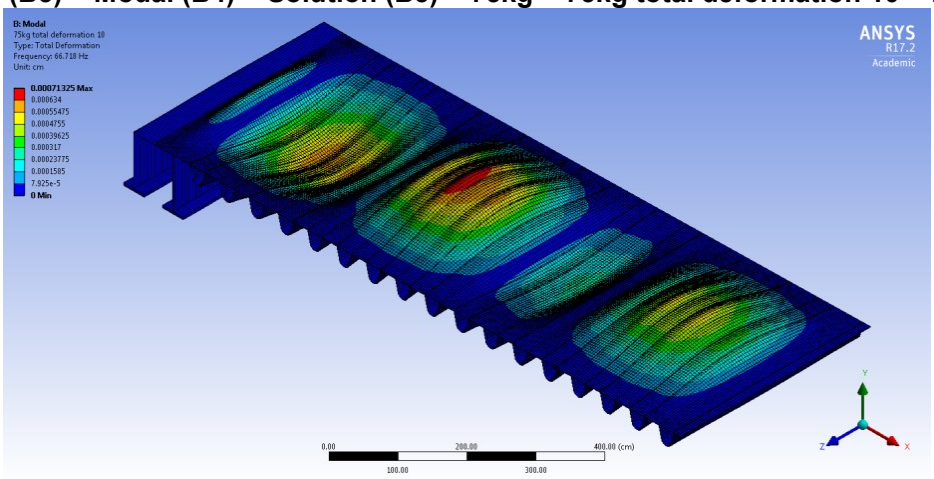


FIGURE 52
Model (B3) > Modal (B4) > Solution (B5) > 75kg > 75kg total deformation 11 > Image

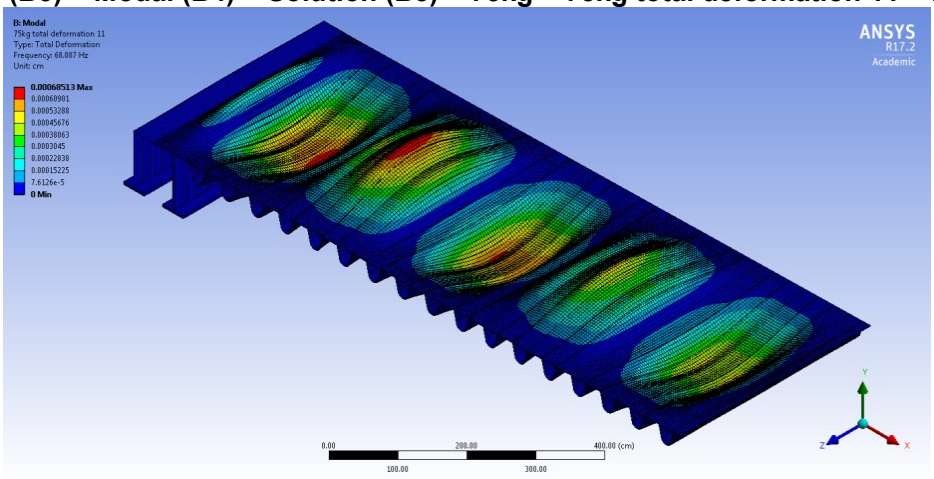
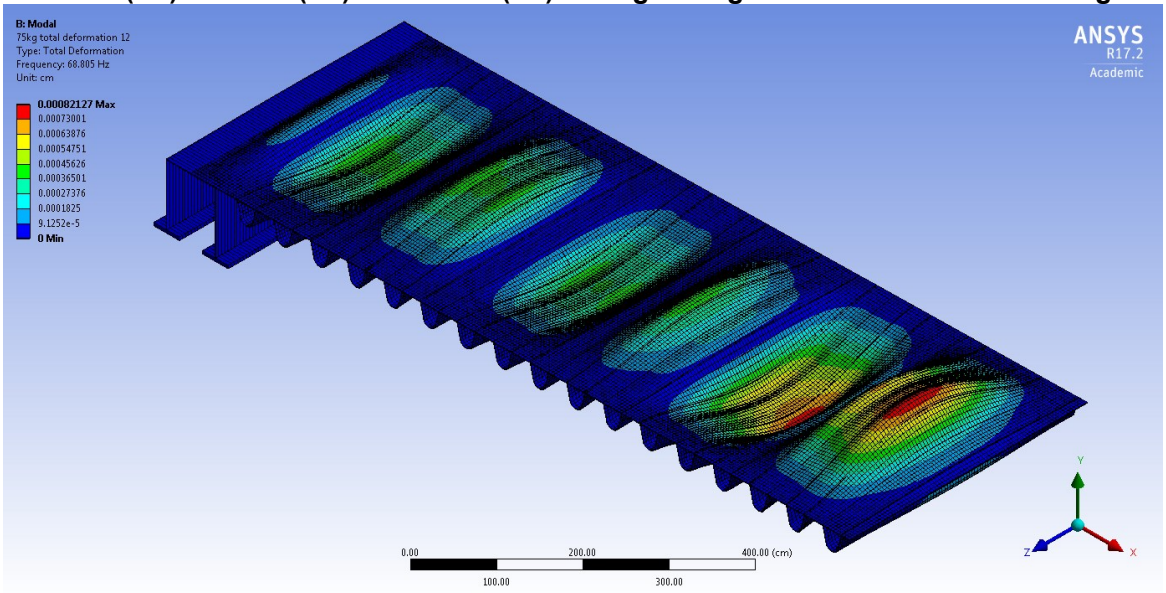


TABLE 30
Model (B3) > Modal (B4) > Solution (B5) > 75kg > Results

Object Name	*75kg total deformation 12*
State	Suppressed
Scope	
Scoping Method	Geometry Selection
Geometry	All Bodies
Definition	
Type	Total Deformation
Mode	12.
Identifier	
Suppressed	Yes
Results	
Minimum	
Maximum	
Minimum Occurs On	
Maximum Occurs On	
Information	
Frequency	

FIGURE 53
Model (B3) > Modal (B4) > Solution (B5) > 75kg > 75kg total deformation 12 > Image



100kg

TABLE 31
Model (B3) > Modal (B4) > Solution (B5) > 100kg > Results

Object Name	*100kg total deformation 1*	*100kg total deformation 2*	*100kg total deformation 3*	*100kg total deformation 4*	*100kg total deformation 5*	*100kg total deformation 6*	*100kg total deformation 7*	*100kg total deformation 8*	*100kg total deformation 9*	*100kg total deformation 10*	*100kg total deformation 11*
State	Suppressed										

Scope											
Scoping Method	Geometry Selection										
Geometry	All Bodies										
Definition											
Type	Total Deformation										
Mode	1.	2.	3.	4.	5.	6.	7.	8.	9.	10.	11.
Identifier											
Suppressed	Yes										
Results											
Minimum											
Maximum											
Minimum Occurs On											
Maximum Occurs On											
Information											
Frequency											

FIGURE 54
Model (B3) > Modal (B4) > Solution (B5) > 100kg > 100kg total deformation 1 > Image

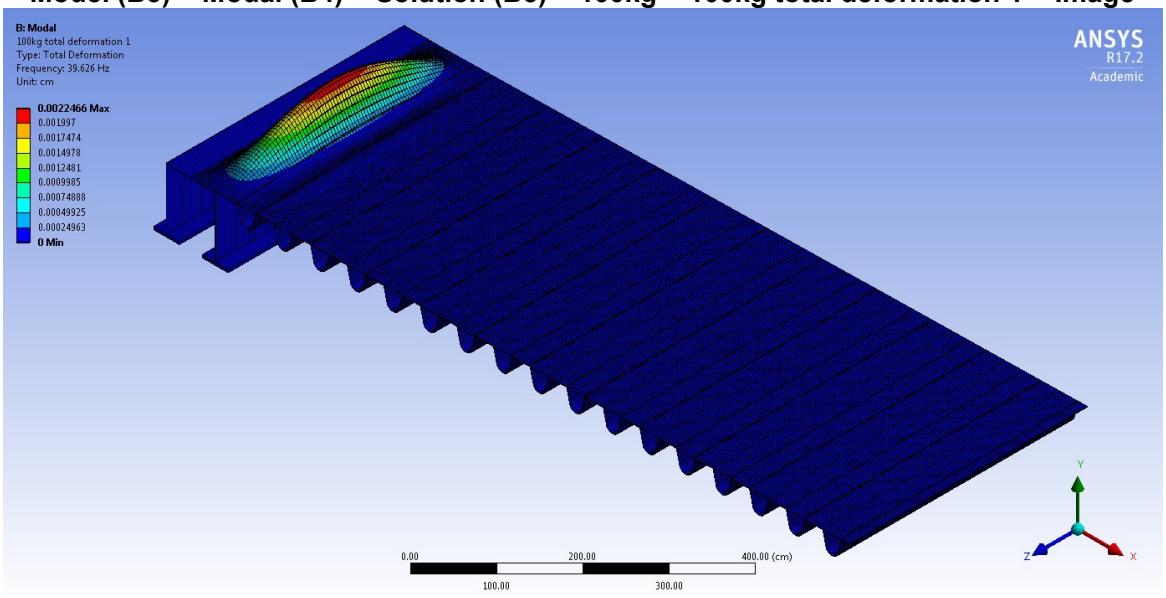


FIGURE 55
Model (B3) > Modal (B4) > Solution (B5) > 100kg > 100kg total deformation 2 > Image

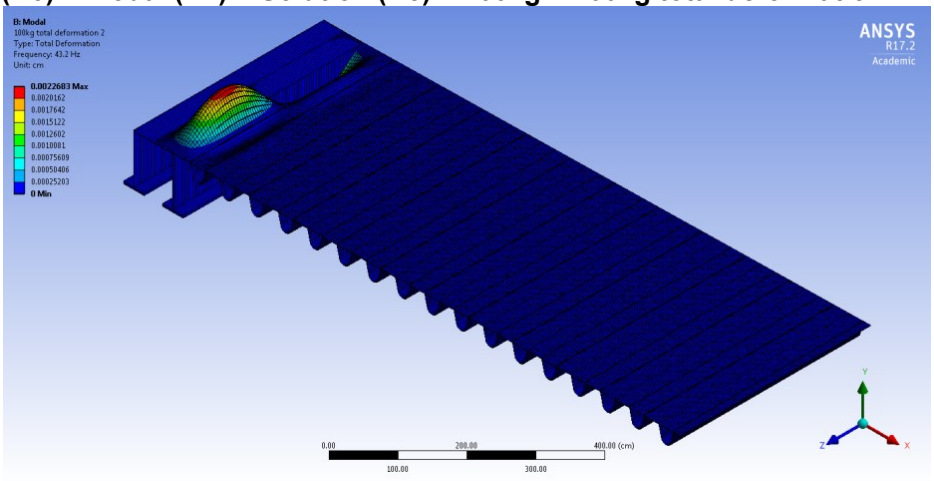


FIGURE 56
Model (B3) > Modal (B4) > Solution (B5) > 100kg > 100kg total deformation 3 > Image

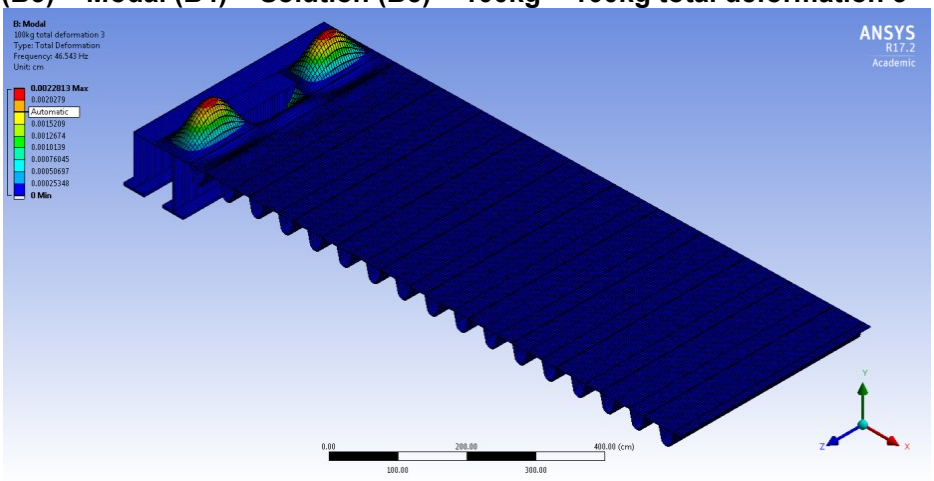


FIGURE 57
Model (B3) > Modal (B4) > Solution (B5) > 100kg > 100kg total deformation 4 > Image

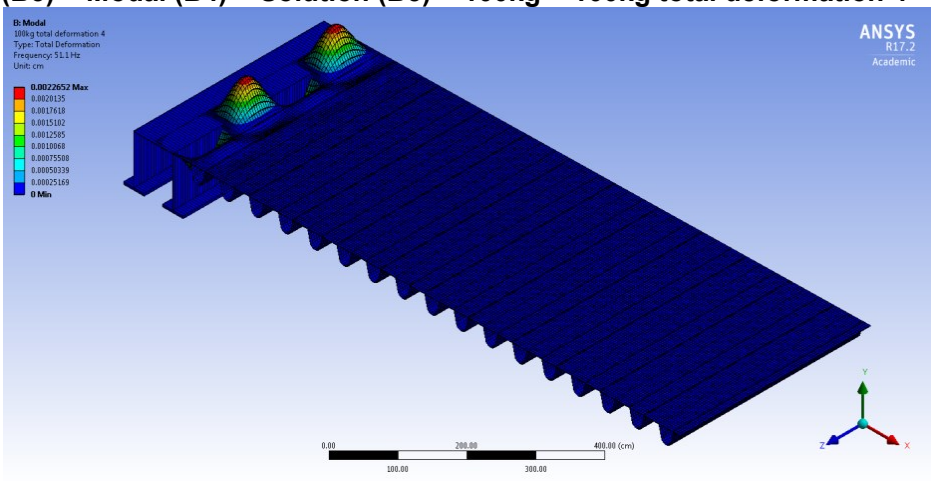


FIGURE 58
Model (B3) > Modal (B4) > Solution (B5) > 100kg > 100kg total deformation 5 > Image

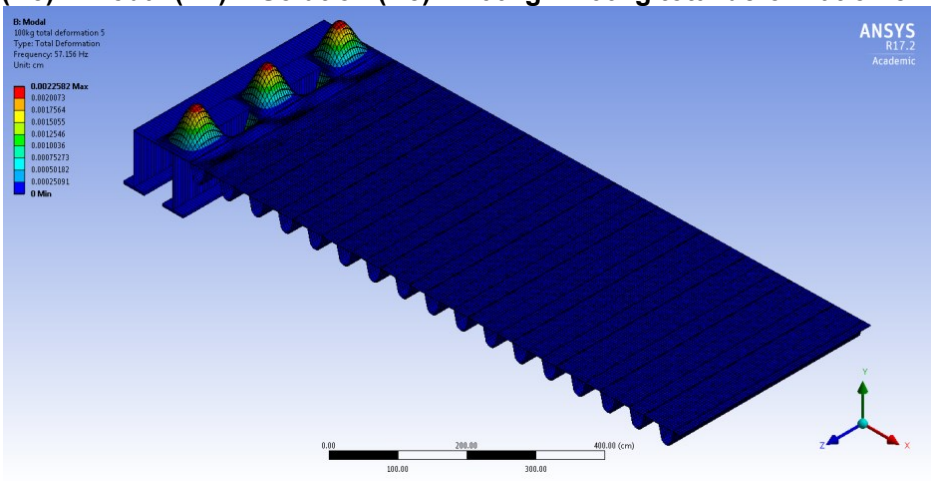


FIGURE 59
Model (B3) > Modal (B4) > Solution (B5) > 100kg > 100kg total deformation 6 > Image

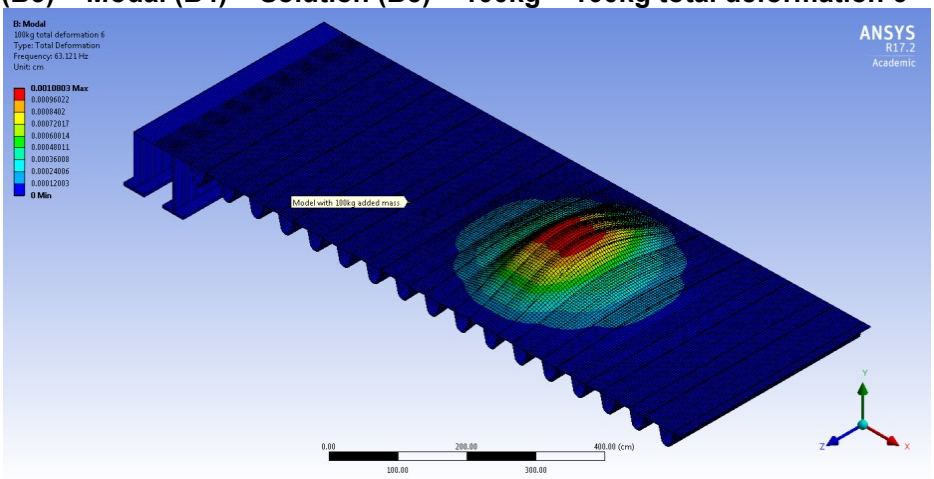


FIGURE 60
Model (B3) > Modal (B4) > Solution (B5) > 100kg > 100kg total deformation 7 > Image

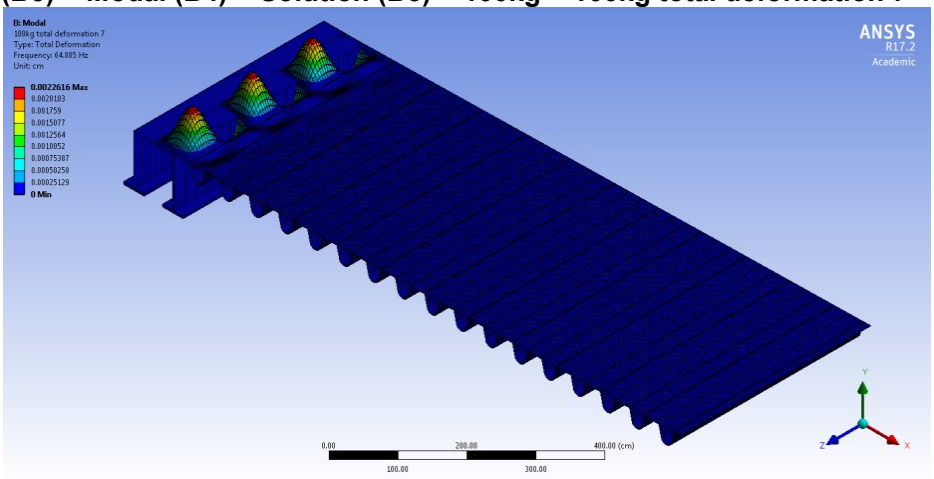


FIGURE 61
Model (B3) > Modal (B4) > Solution (B5) > 100kg > 100kg total deformation 8 > Image

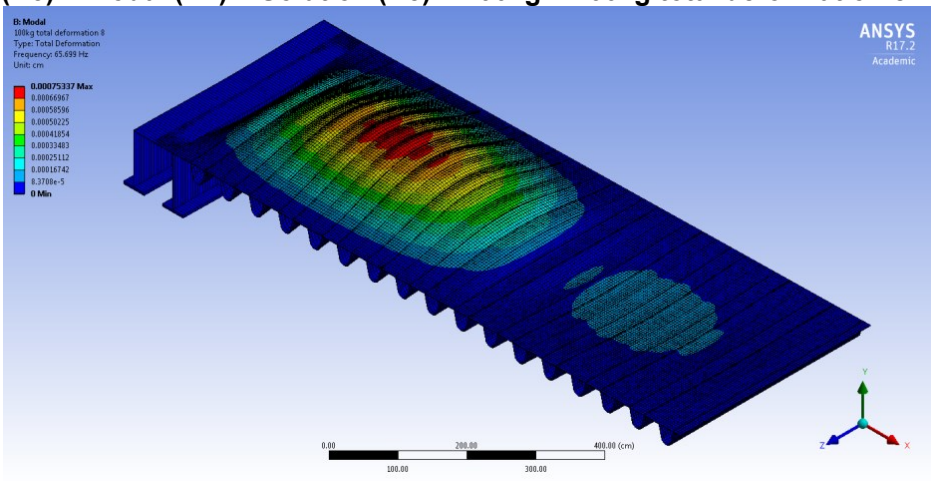


FIGURE 62
Model (B3) > Modal (B4) > Solution (B5) > 100kg > 100kg total deformation 9 > Image

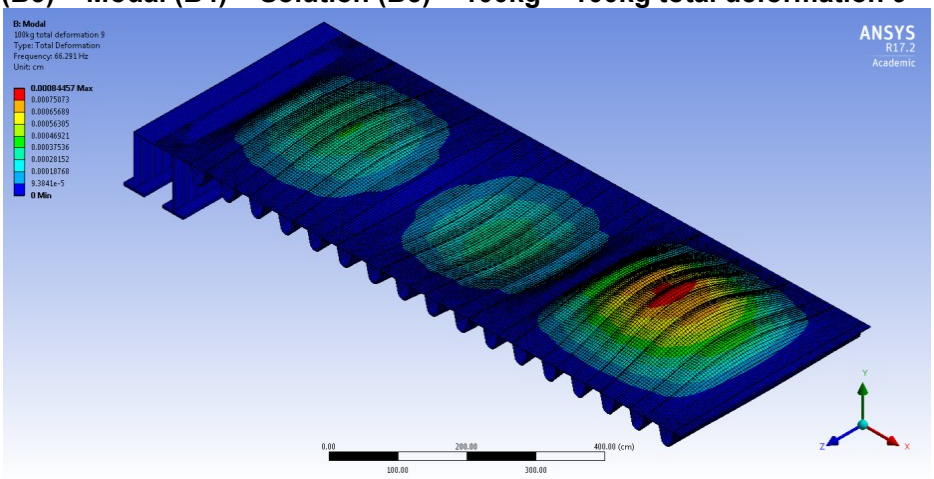


FIGURE 63
Model (B3) > Modal (B4) > Solution (B5) > 100kg > 100kg total deformation 10 > Image

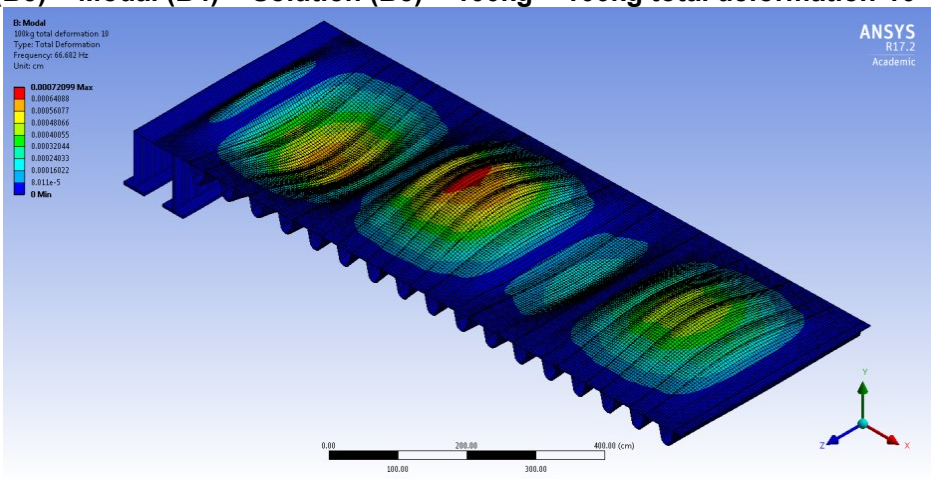


FIGURE 64
Model (B3) > Modal (B4) > Solution (B5) > 100kg > 100kg total deformation 11 > Image

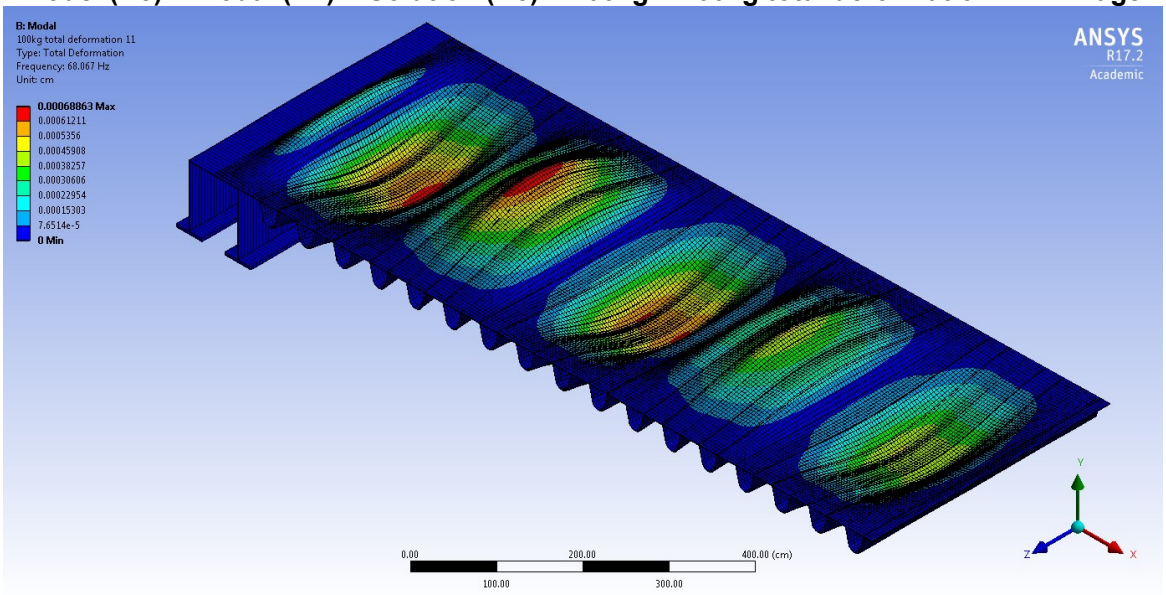
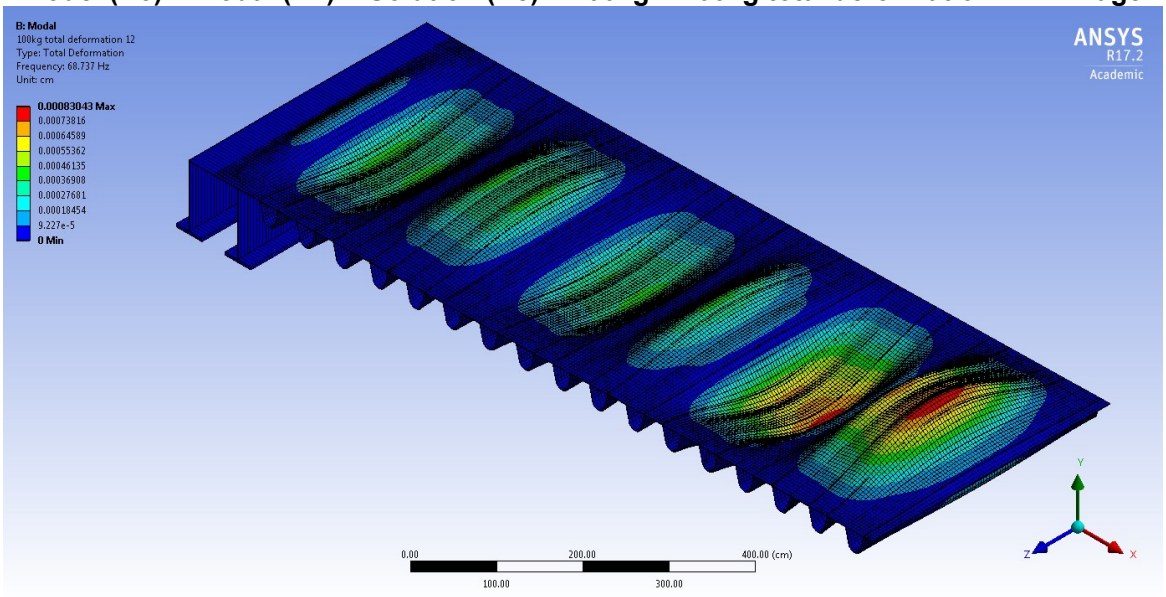


TABLE 32
Model (B3) > Modal (B4) > Solution (B5) > 100kg > Results

Object Name	*100kg total deformation 12*
State	Suppressed
Scope	
Scoping Method	Geometry Selection
Geometry	All Bodies
Definition	
Type	Total Deformation
Mode	12.
Identifier	
Suppressed	Yes
Results	
Minimum	
Maximum	
Minimum Occurs On	
Maximum Occurs On	
Information	
Frequency	

FIGURE 65
Model (B3) > Modal (B4) > Solution (B5) > 100kg > 100kg total deformation 12 > Image



1crack 35cm

TABLE 33
Model (B3) > Modal (B4) > Solution (B5) > 1crack 35cm > Results

Object Name	*1crack 35cm total deformation 1*	*1crack 35cm total deformation 2*	*1crack 35cm total deformation 3*	*1crack 35cm total deformation 4*	*1crack 35cm total deformation 5*	*1crack 35cm total deformation 6*	*1crack 35cm total deformation 7*	*1crack 35cm total deformation 8*	*1crack 35cm total deformation 9*	*1crack 35cm total deformation 10*	*1crack 35cm total deformation 11*
State	Suppressed										
Scope											
Scoping Method	Geometry Selection										
Geometry	All Bodies										
Definition											
Type	Total Deformation										
Mode	1.	2.	3.	4.	5.	6.	7.	8.	9.	10.	11.
Identifier											
Suppressed	Yes										

FIGURE 66
Model (B3) > Modal (B4) > Solution (B5) > 1crack 35cm > 1crack 35cm total deformation 1 > Image

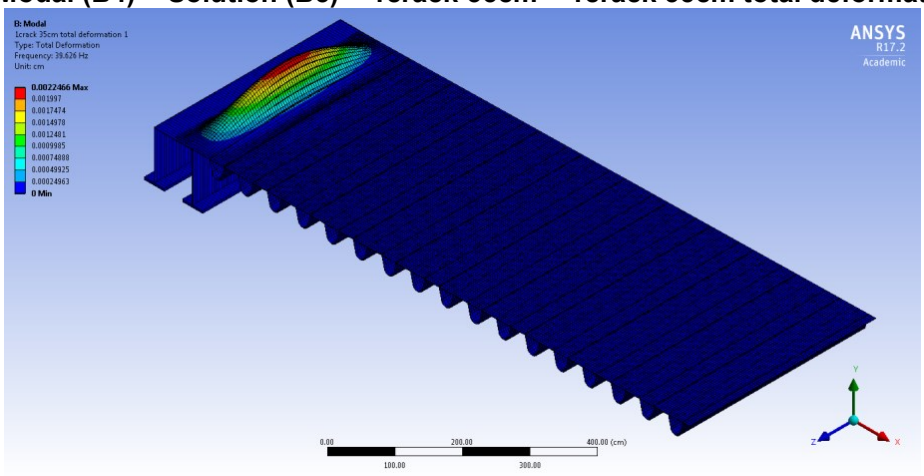


FIGURE 67
Model (B3) > Modal (B4) > Solution (B5) > 1crack 35cm > 1crack 35cm total deformation 2 > Image

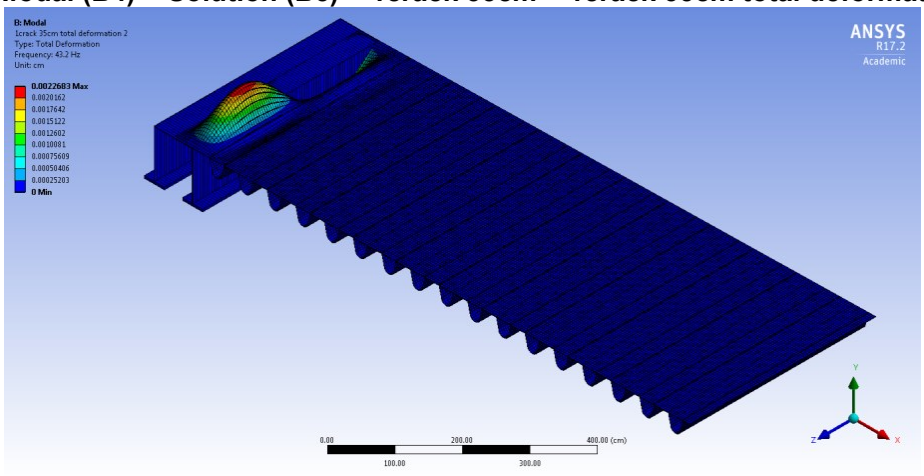


FIGURE 68
Model (B3) > Modal (B4) > Solution (B5) > 1crack 35cm > 1crack 35cm total deformation 3 > Image

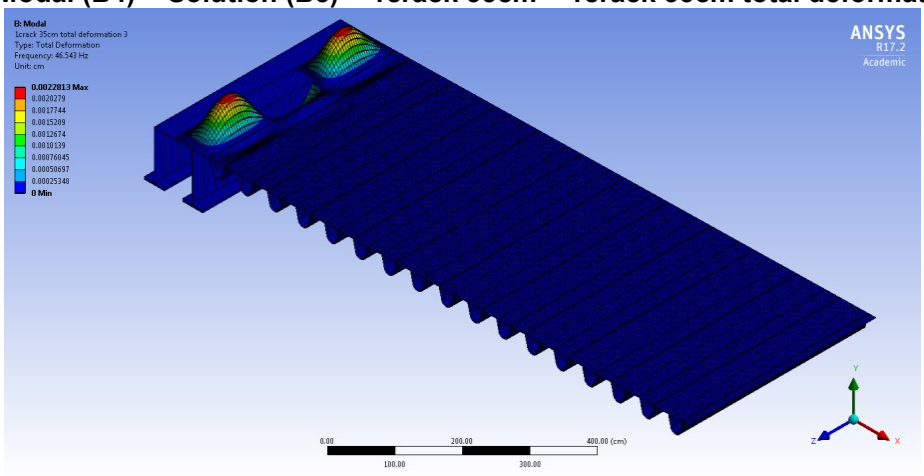


FIGURE 69
Model (B3) > Modal (B4) > Solution (B5) > 1crack 35cm > 1crack 35cm total deformation 4 > Image

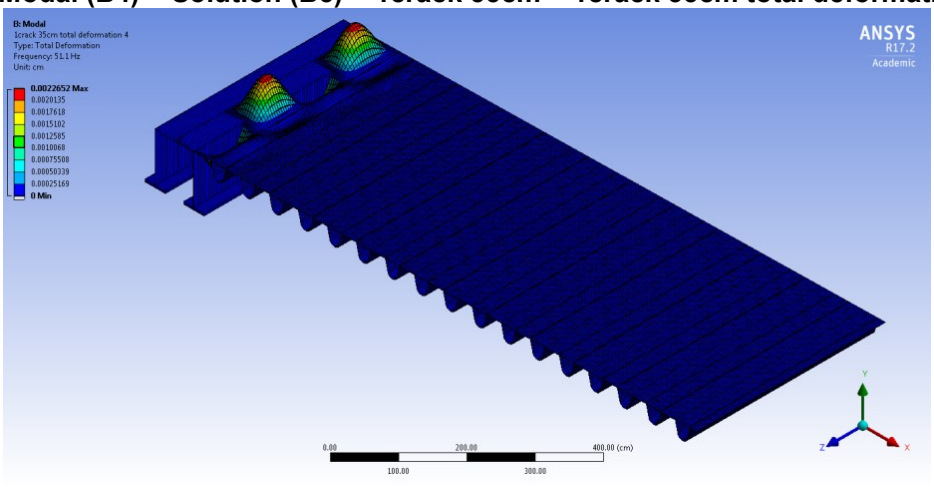


FIGURE 70
Model (B3) > Modal (B4) > Solution (B5) > 1crack 35cm > 1crack 35cm total deformation 5 > Image

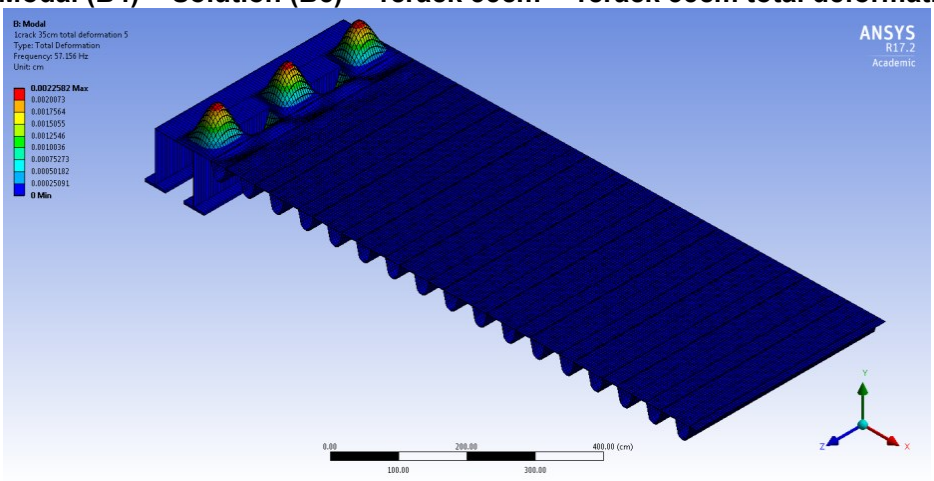


FIGURE 71
Model (B3) > Modal (B4) > Solution (B5) > 1crack 35cm > 1crack 35cm total deformation 6 > Image

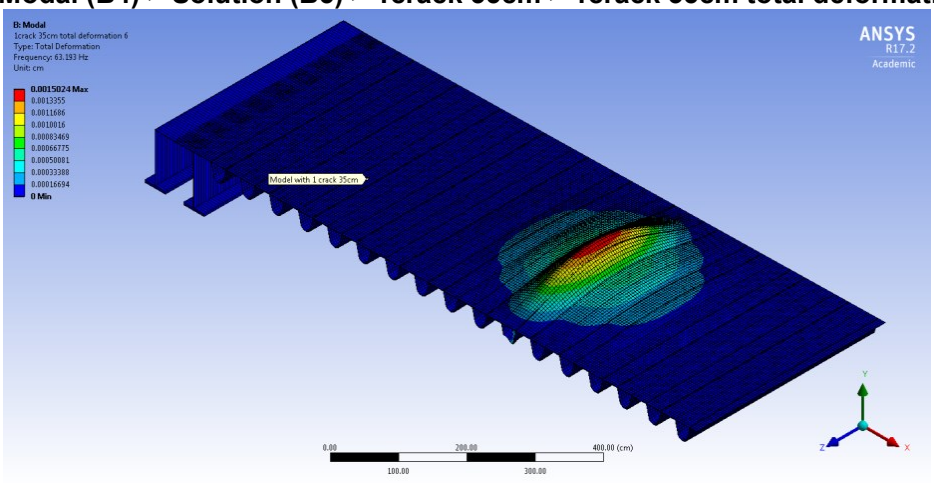


FIGURE 72
Model (B3) > Modal (B4) > Solution (B5) > 1crack 35cm > 1crack 35cm total deformation 7 > Image

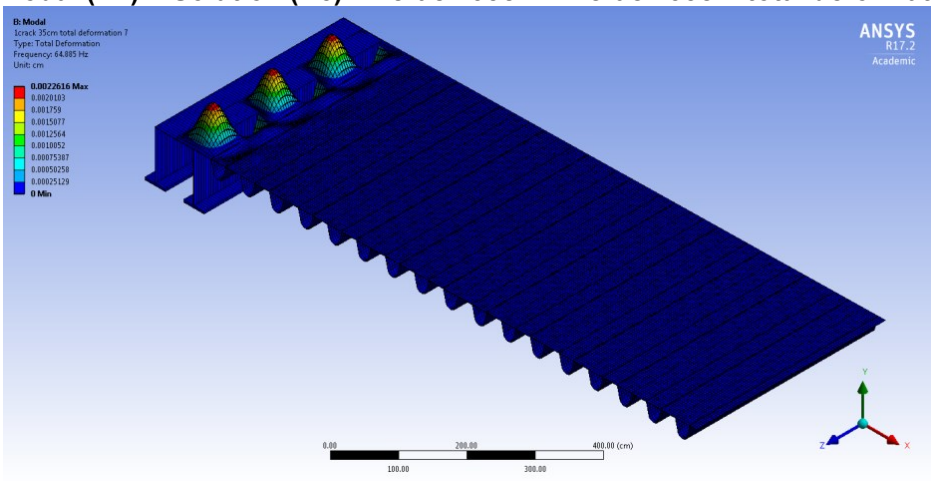


FIGURE 73
Model (B3) > Modal (B4) > Solution (B5) > 1crack 35cm > 1crack 35cm total deformation 8 > Image

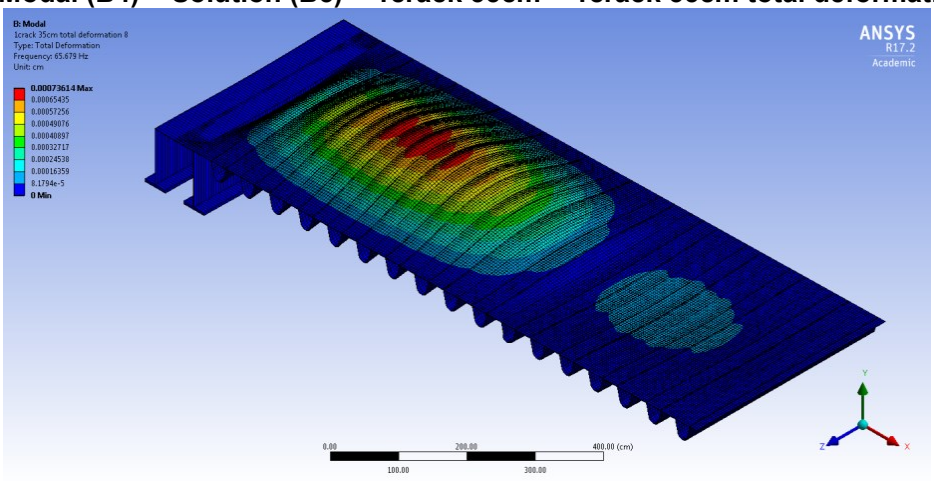


FIGURE 74
Model (B3) > Modal (B4) > Solution (B5) > 1crack 35cm > 1crack 35cm total deformation 9 > Image

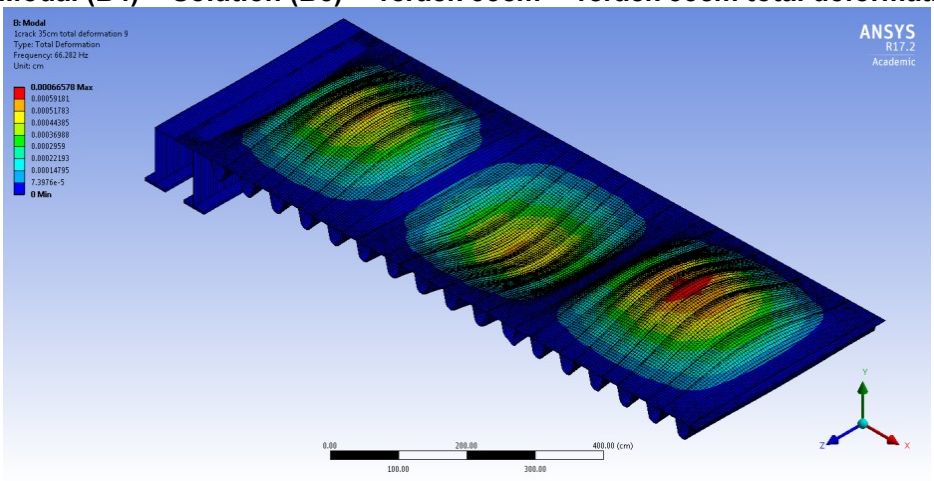


FIGURE 75
Model (B3) > Modal (B4) > Solution (B5) > 1crack 35cm > 1crack 35cm total deformation 10 > Image

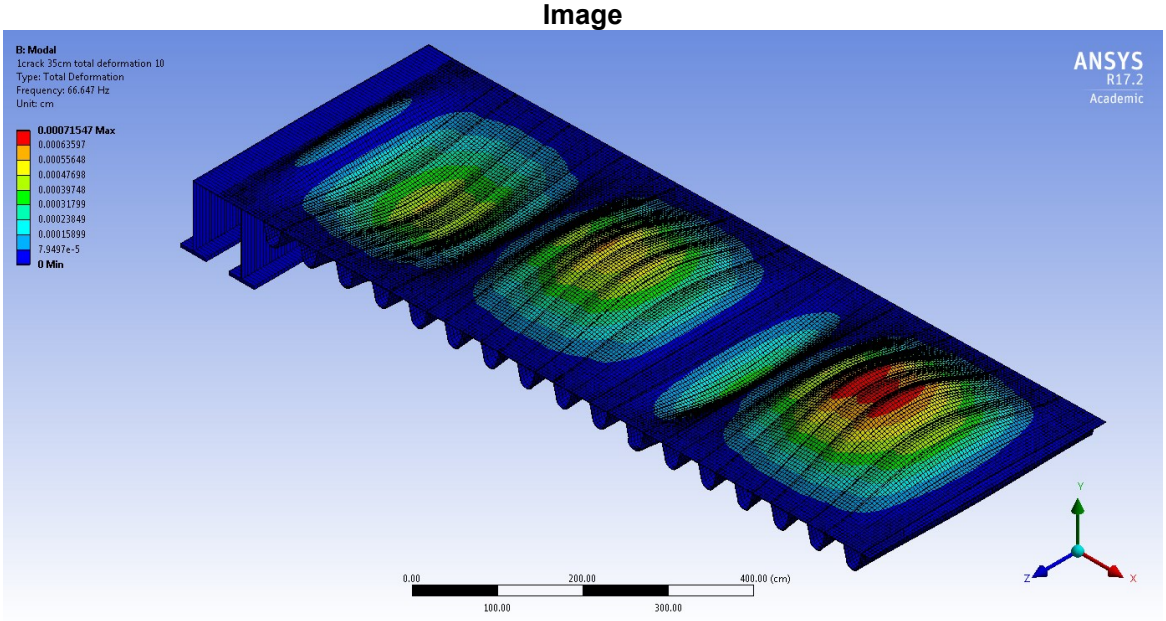


FIGURE 76
Model (B3) > Modal (B4) > Solution (B5) > 1crack 35cm > 1crack 35cm total deformation 11 > Image

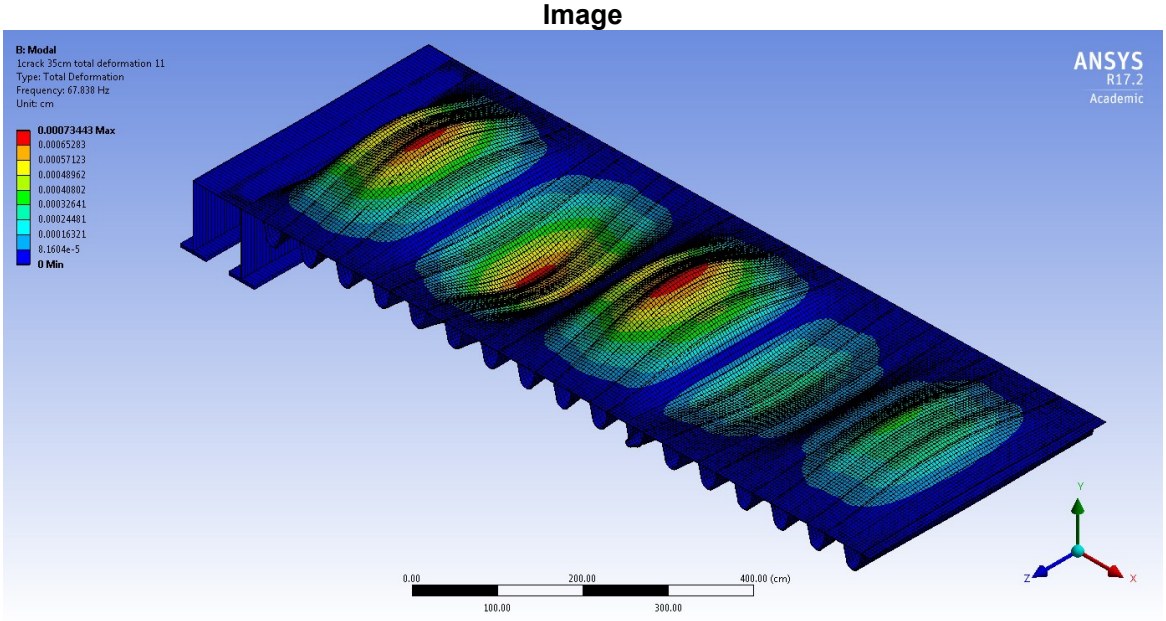
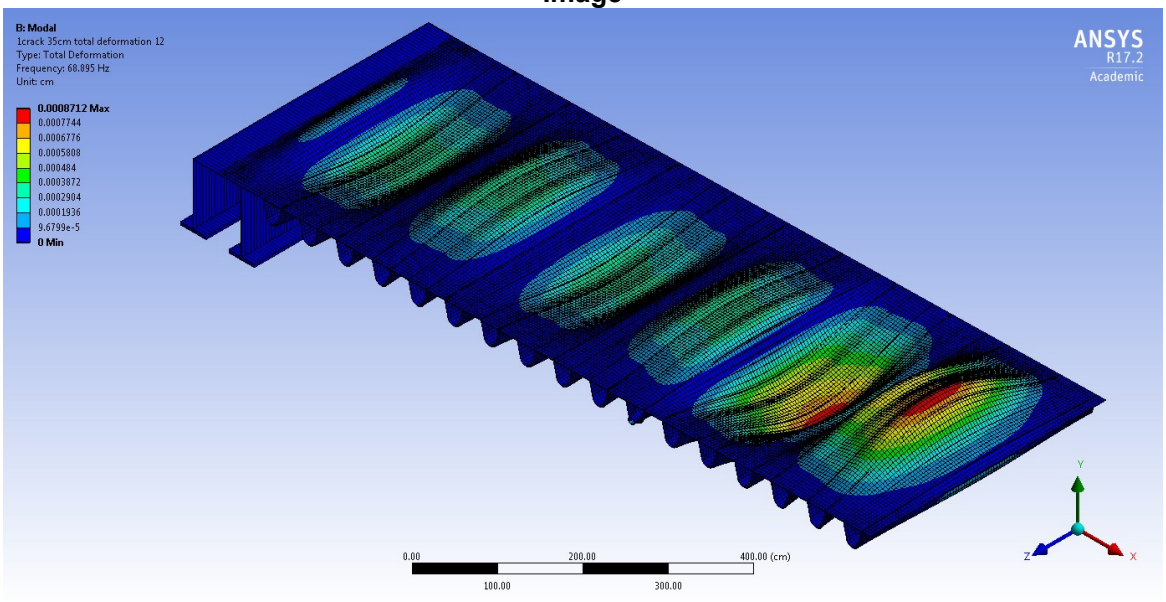


TABLE 34
Model (B3) > Modal (B4) > Solution (B5) > 1crack 35cm > Results

Object Name	*1crack 35cm total deformation 12*
State	Suppressed
Scope	
Scoping Method	Geometry Selection
Geometry	All Bodies
Definition	
Type	Total Deformation

Mode	12.
Identifier	
Suppressed	Yes
Results	
Minimum	
Maximum	
Minimum Occurs On	
Maximum Occurs On	
Information	
Frequency	

FIGURE 77
Model (B3) > Modal (B4) > Solution (B5) > 1crack 35cm > 1crack 35cm total deformation 12 > Image



2x cracks of 35cm

TABLE 35
Model (B3) > Modal (B4) > Solution (B5) > 2x cracks of 35cm > Results

Object Name	*2x cracks of 35cm total deformation 1*	*2x cracks of 35cm total deformation 2*	*2x cracks of 35cm total deformation 3*	*2x cracks of 35cm total deformation 4*	*2x cracks of 35cm total deformation 5*	*2x cracks of 35cm total deformation 6*	*2x cracks of 35cm total deformation 7*	*2x cracks of 35cm total deformation 8*	*2x cracks of 35cm total deformation 9*	*2x cracks of 35cm total deformation 10*	*2x cracks of 35cm total deformation 11*
State	Suppressed										
Scope											
Scoping Method	Geometry Selection										
Geometry	All Bodies										

Definition											
Type	Total Deformation										
Mode	1.	2.	3.	4.	5.	6.	7.	8.	9.	10.	11.
Identifier											
Suppressed	Yes										
Results											
Minimum											
Maximum											
Minimum Occurs On											
Maximum Occurs On											
Information											
Frequency											

FIGURE 78
Model (B3) > Modal (B4) > Solution (B5) > 2x cracks of 35cm > 2x cracks of 35cm total deformation 1 > Image

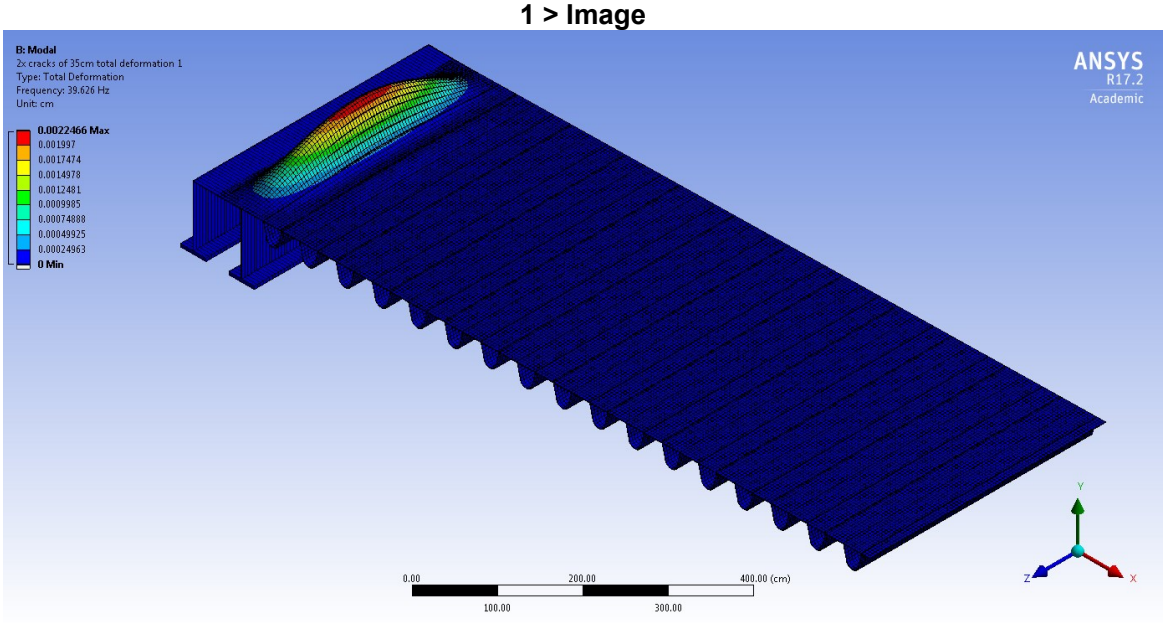


FIGURE 79
Model (B3) > Modal (B4) > Solution (B5) > 2x cracks of 35cm > 2x cracks of 35cm total deformation 2 > Image

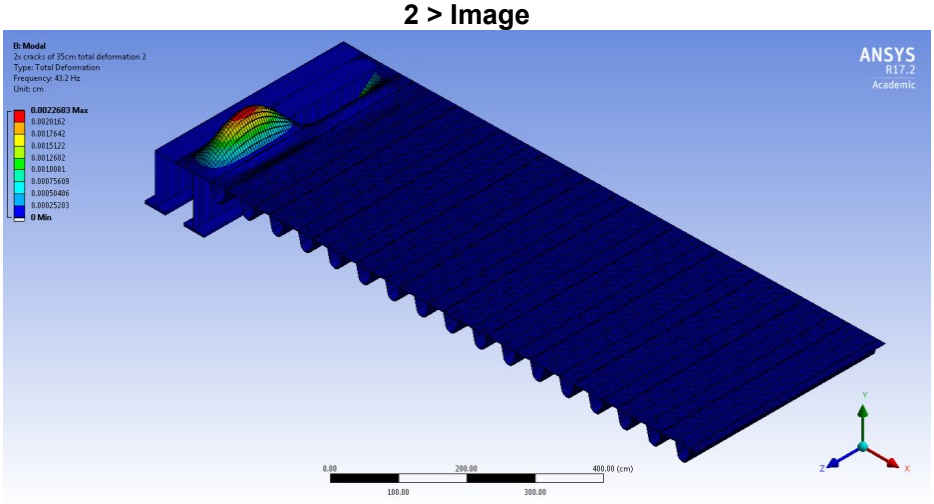


FIGURE 80
Model (B3) > Modal (B4) > Solution (B5) > 2x cracks of 35cm > 2x cracks of 35cm total deformation 3 > Image

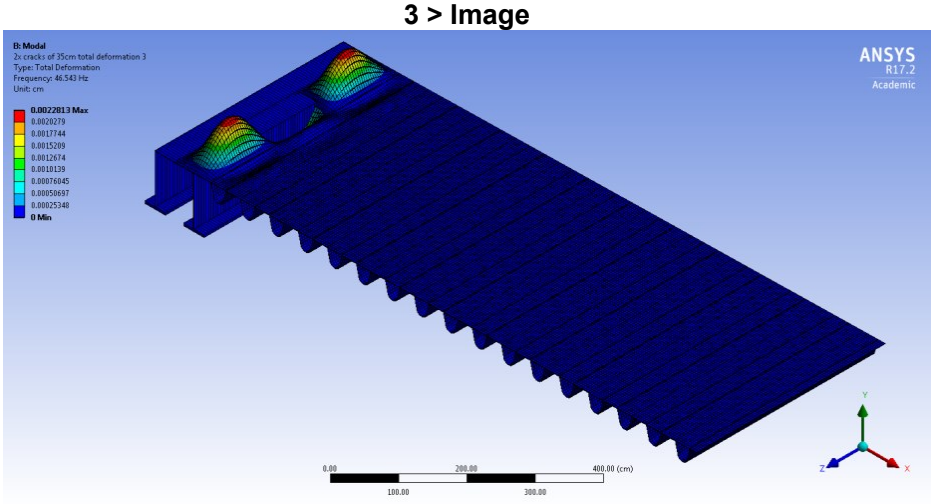


FIGURE 81
Model (B3) > Modal (B4) > Solution (B5) > 2x cracks of 35cm > 2x cracks of 35cm total deformation 4 > Image

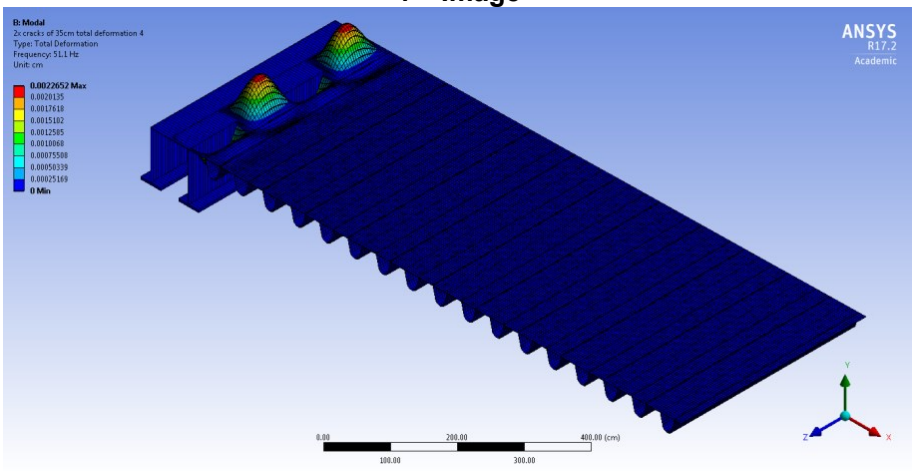


FIGURE 82
Model (B3) > Modal (B4) > Solution (B5) > 2x cracks of 35cm > 2x cracks of 35cm total deformation 5 > Image

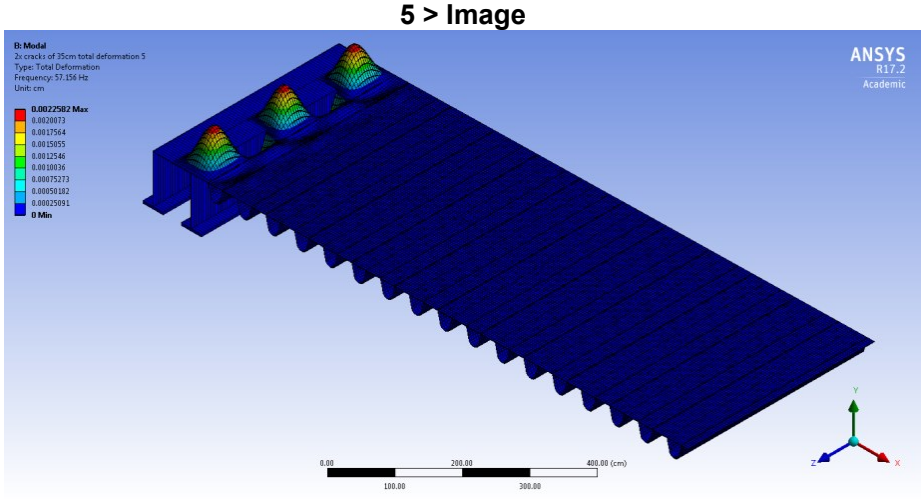


FIGURE 83
Model (B3) > Modal (B4) > Solution (B5) > 2x cracks of 35cm > 2x cracks of 35cm total deformation 6 > Image

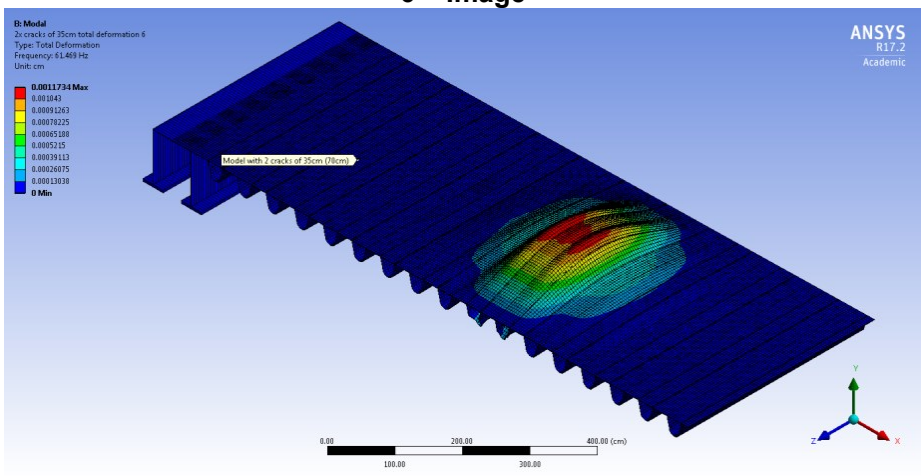


FIGURE 84
Model (B3) > Modal (B4) > Solution (B5) > 2x cracks of 35cm > 2x cracks of 35cm total deformation 7 > Image

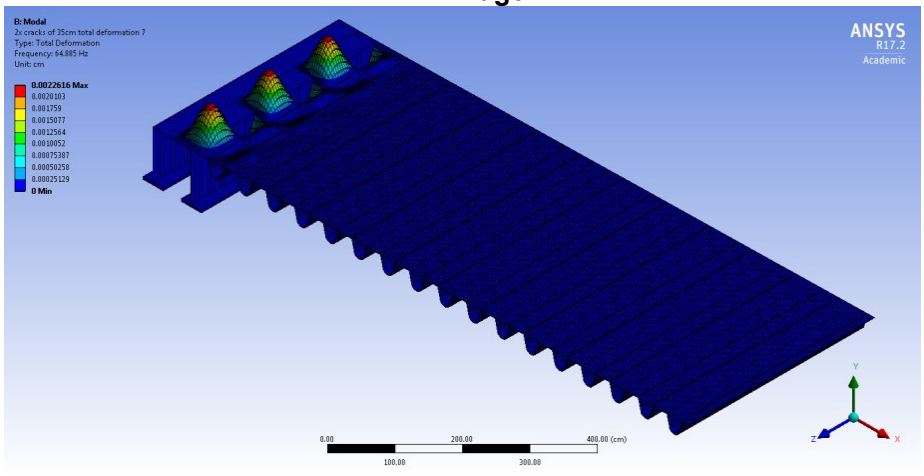


FIGURE 85
Model (B3) > Modal (B4) > Solution (B5) > 2x cracks of 35cm > 2x cracks of 35cm total deformation 8 > Image

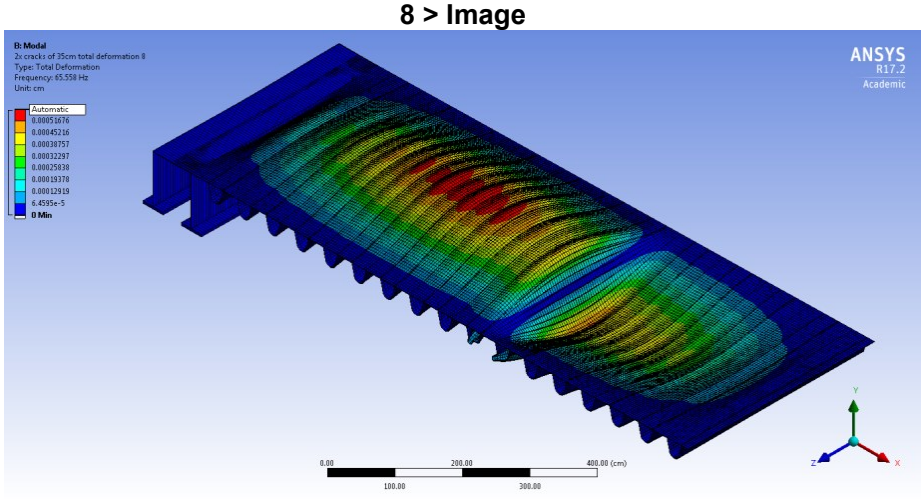


FIGURE 86
Model (B3) > Modal (B4) > Solution (B5) > 2x cracks of 35cm > 2x cracks of 35cm total deformation 9 > Image

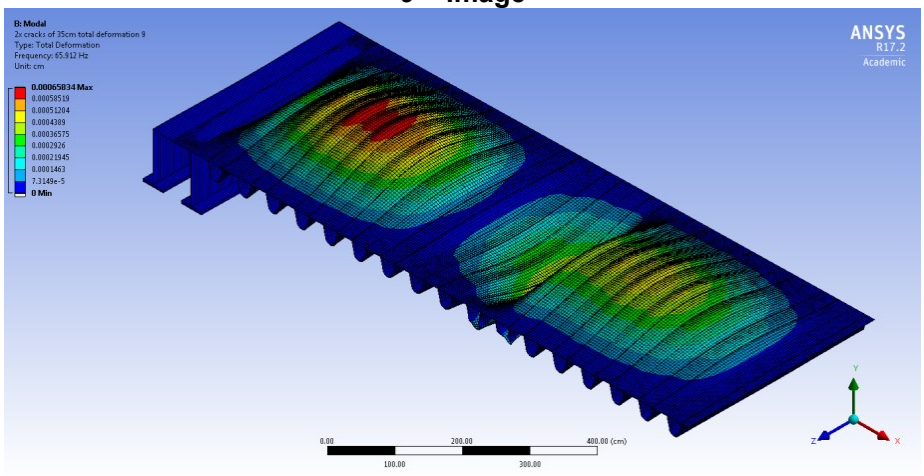


FIGURE 87
Model (B3) > Modal (B4) > Solution (B5) > 2x cracks of 35cm > 2x cracks of 35cm total deformation 10 > Image

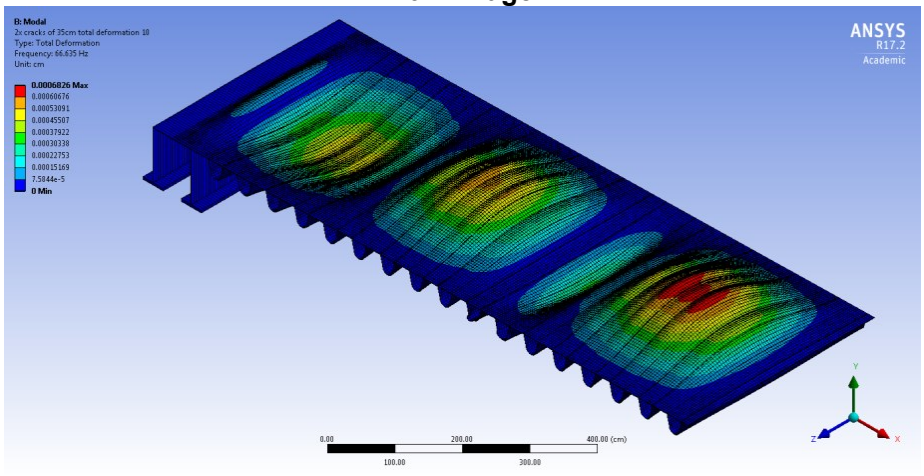


FIGURE 88
Model (B3) > Modal (B4) > Solution (B5) > 2x cracks of 35cm > 2x cracks of 35cm total deformation 11 > Image

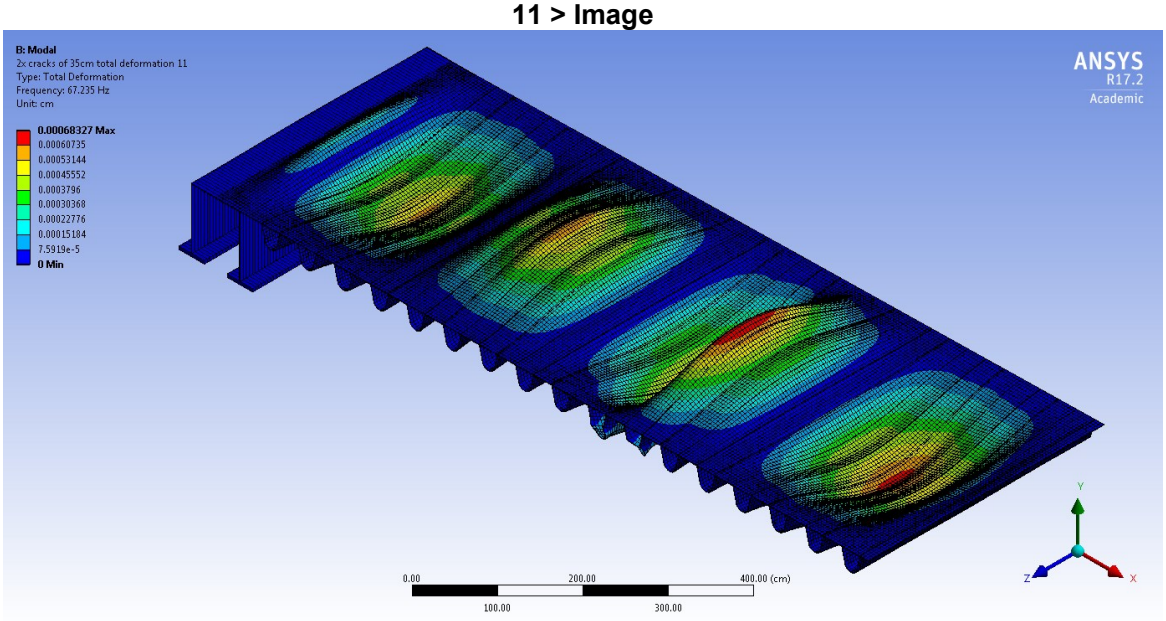
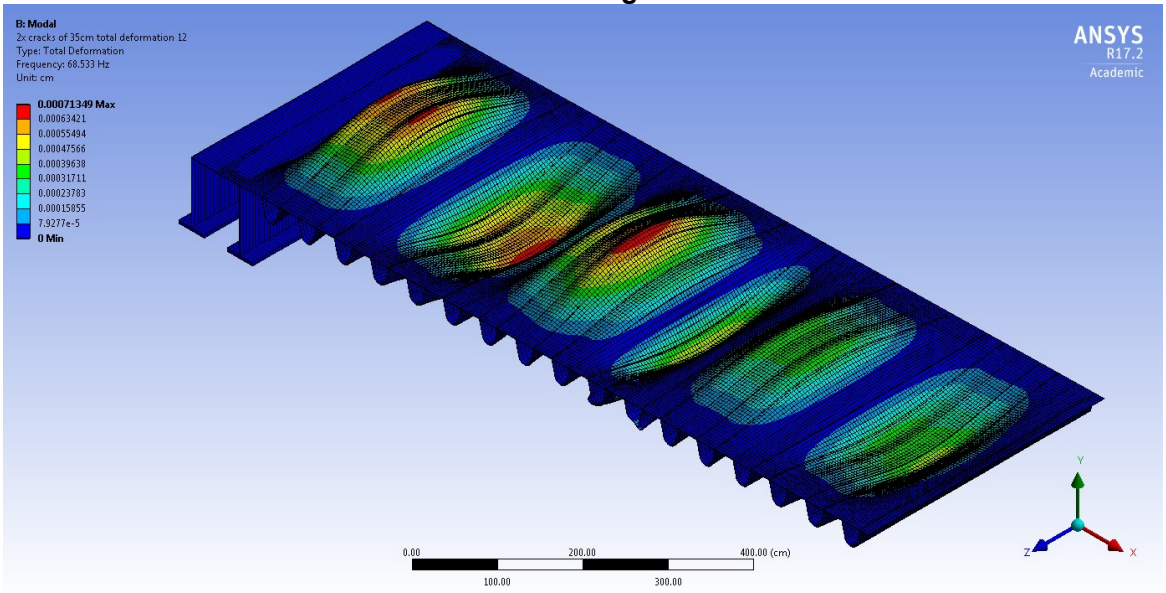


TABLE 36
Model (B3) > Modal (B4) > Solution (B5) > 2x cracks of 35cm > Results

Object Name	*2x cracks of 35cm total deformation 12*
State	Suppressed
Scope	
Scoping Method	Geometry Selection
Geometry	All Bodies
Definition	
Type	Total Deformation
Mode	12.
Identifier	
Suppressed	Yes
Results	
Minimum	
Maximum	
Minimum Occurs On	
Maximum Occurs On	
Information	
Frequency	

FIGURE 89
Model (B3) > Modal (B4) > Solution (B5) > 2x cracks of 35cm > 2x cracks of 35cm total deformation 12 > Image



2 fully open U section cracks

TABLE 37
Model (B3) > Modal (B4) > Solution (B5) > 2 fully open U section cracks > Results

Object Name	*2 fully open U section cracks 1*	*2 fully open U section cracks 2*	*2 fully open U section cracks 3*	*2 fully open U section cracks 4*	*2 fully open U section cracks 5*	*2 fully open U section cracks 6*	*2 fully open U section cracks 7*	*2 fully open U section cracks 8*	*2 fully open U section cracks 9*	*2 fully open U section cracks 10*	*2 fully open U section cracks 11*
State	Suppressed										
Scope											
Scoping Method	Geometry Selection										
Geometry	All Bodies										
Definition											
Type	Total Deformation										
Mode	1.	2.	3.	4.	5.	6.	7.	8.	9.	10.	11.
Identifier											
Suppressed	Yes										
Results											
Minimum											
Maximum											
Minimum Occurs On											
Maximum Occurs On											
Information											
Frequency											

FIGURE 90
Model (B3) > Modal (B4) > Solution (B5) > 2 fully open U section cracks > 2 fully open U section cracks 1 > Image

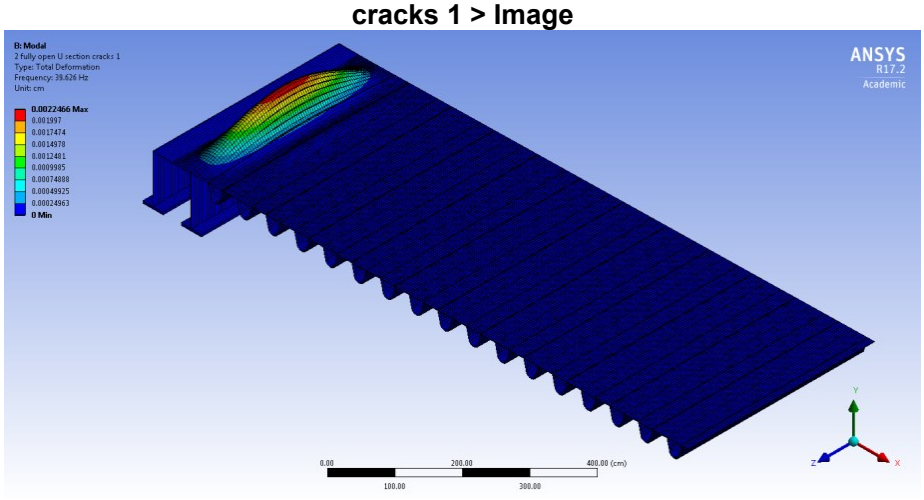


FIGURE 91
Model (B3) > Modal (B4) > Solution (B5) > 2 fully open U section cracks > 2 fully open U section cracks 2 > Image

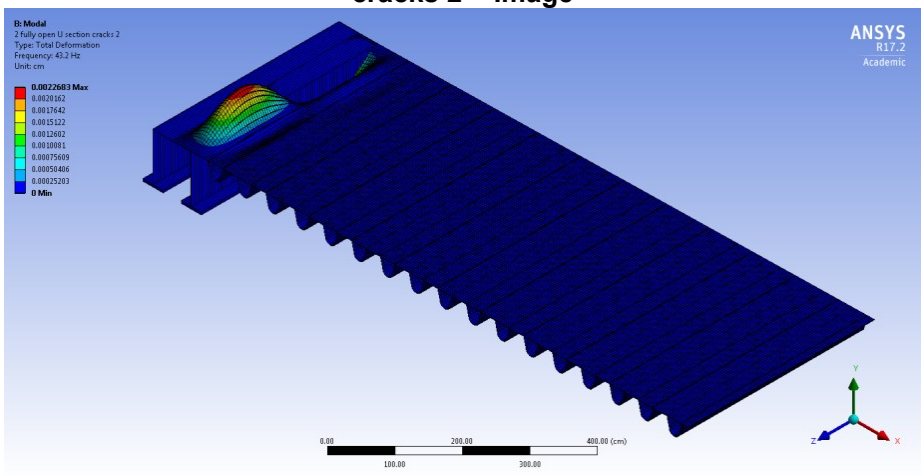


FIGURE 92
Model (B3) > Modal (B4) > Solution (B5) > 2 fully open U section cracks > 2 fully open U section cracks 3 > Image

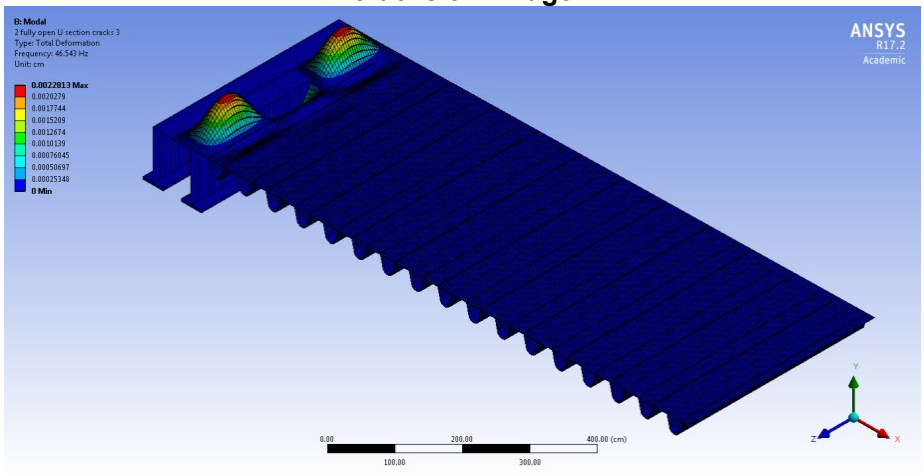


FIGURE 93
Model (B3) > Modal (B4) > Solution (B5) > 2 fully open U section cracks > 2 fully open U section cracks 4 > Image

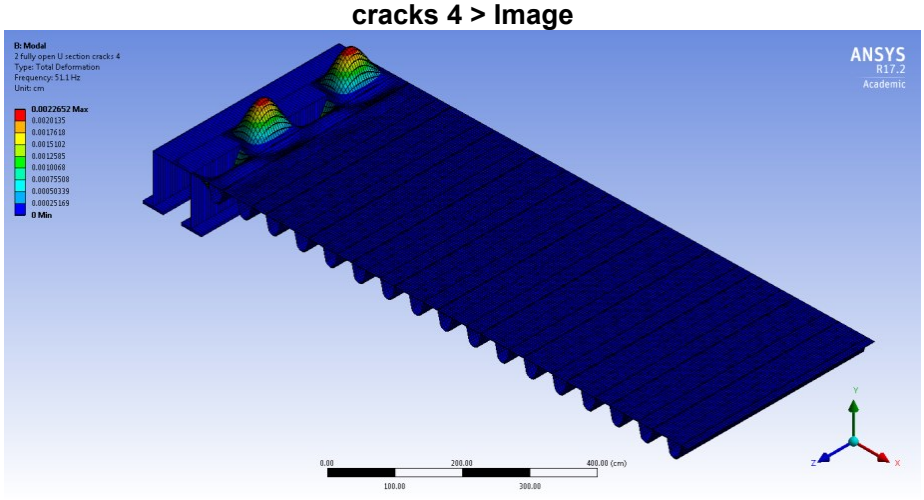


FIGURE 94
Model (B3) > Modal (B4) > Solution (B5) > 2 fully open U section cracks > 2 fully open U section cracks 5 > Image

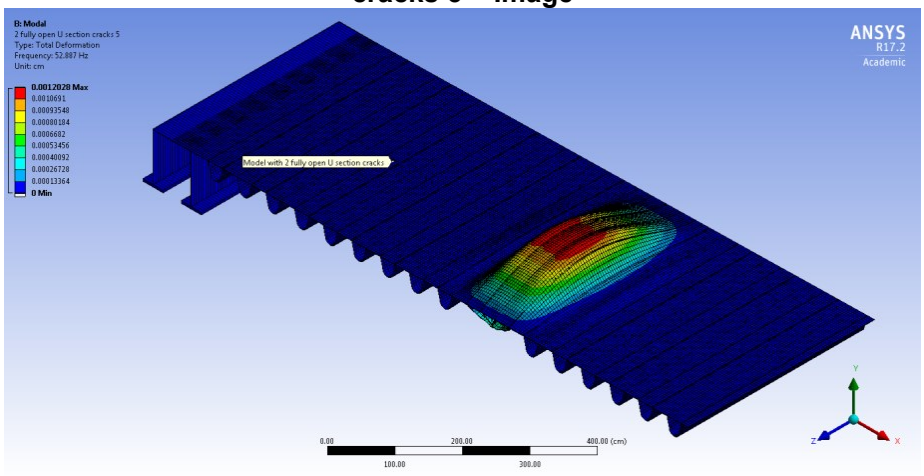


FIGURE 95
Model (B3) > Modal (B4) > Solution (B5) > 2 fully open U section cracks > 2 fully open U section cracks 6 > Image

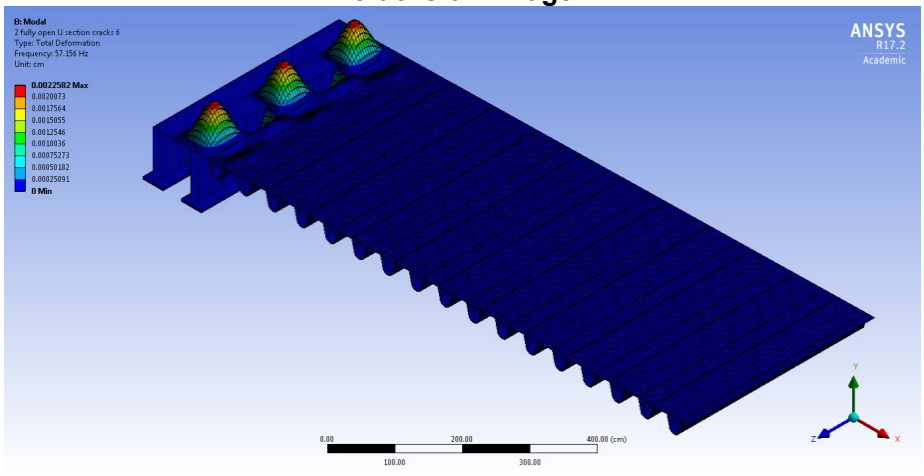


FIGURE 96
Model (B3) > Modal (B4) > Solution (B5) > 2 fully open U section cracks > 2 fully open U section cracks 7 > Image

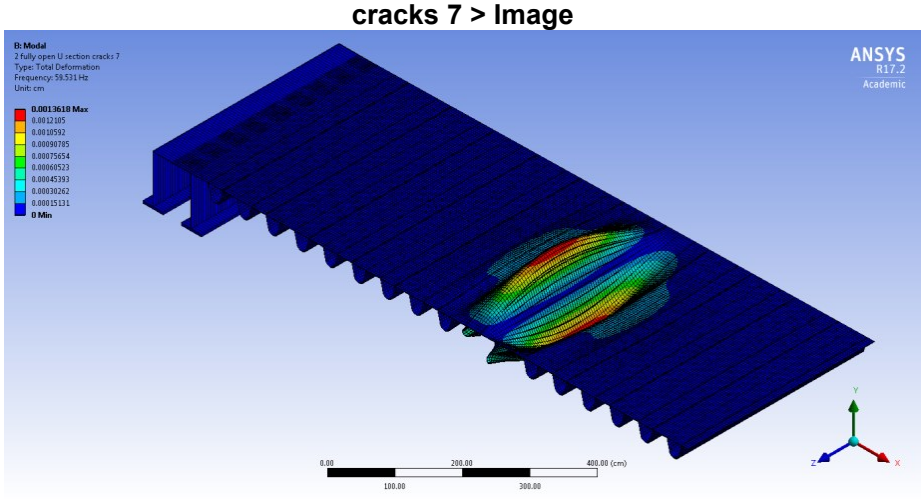


FIGURE 97
Model (B3) > Modal (B4) > Solution (B5) > 2 fully open U section cracks > 2 fully open U section cracks 8 > Image

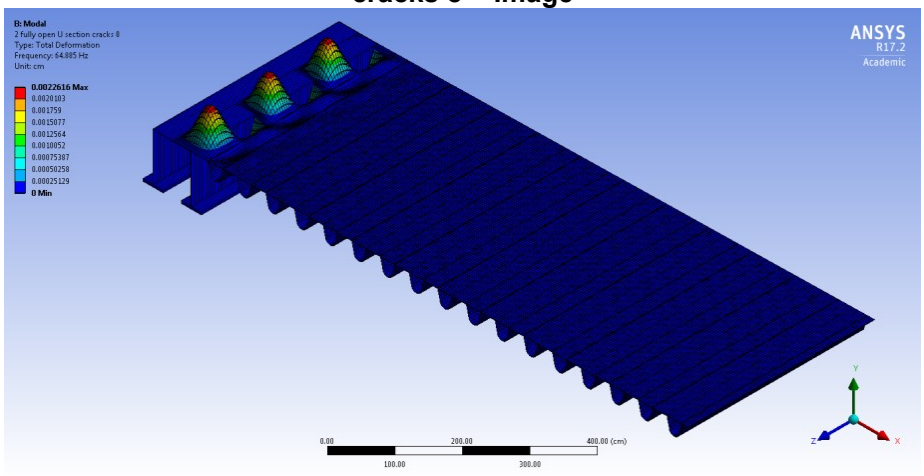


FIGURE 98
Model (B3) > Modal (B4) > Solution (B5) > 2 fully open U section cracks > 2 fully open U section cracks 9 > Image

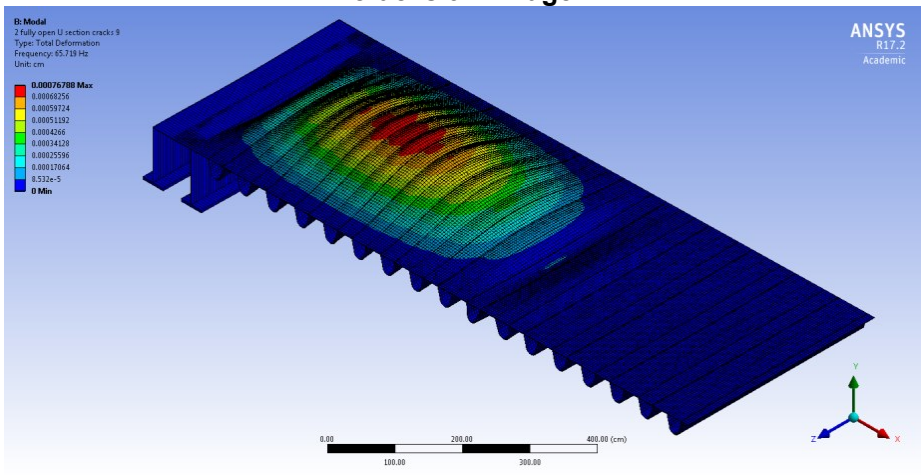


FIGURE 99
Model (B3) > Modal (B4) > Solution (B5) > 2 fully open U section cracks > 2 fully open U section cracks 10 > Image

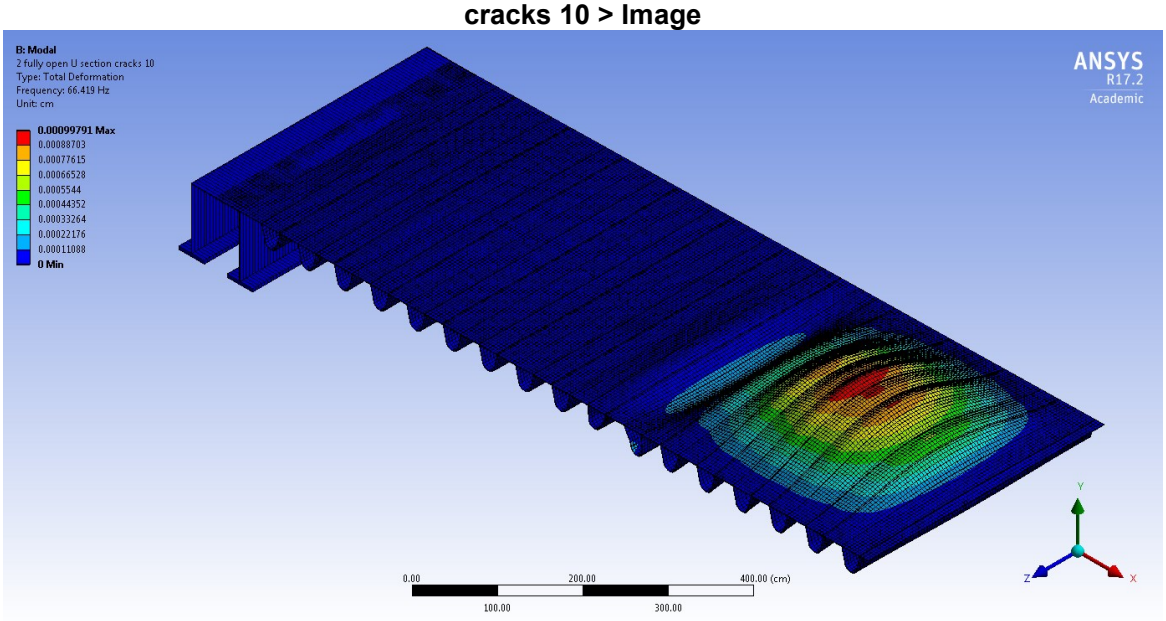


FIGURE 100
Model (B3) > Modal (B4) > Solution (B5) > 2 fully open U section cracks > 2 fully open U section cracks 11 > Image

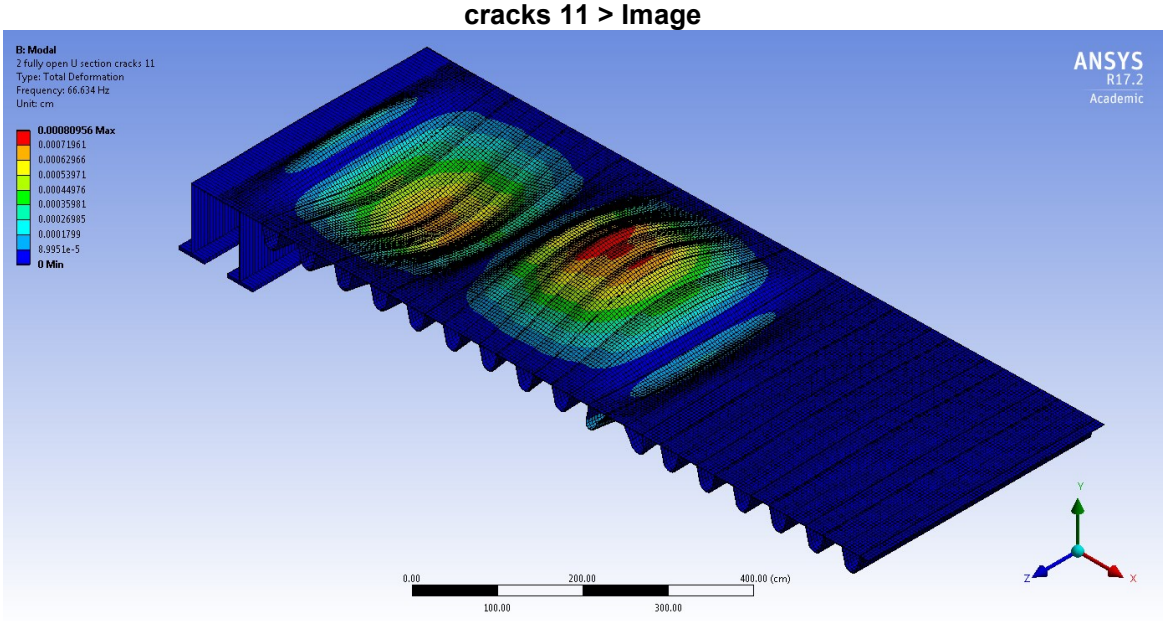
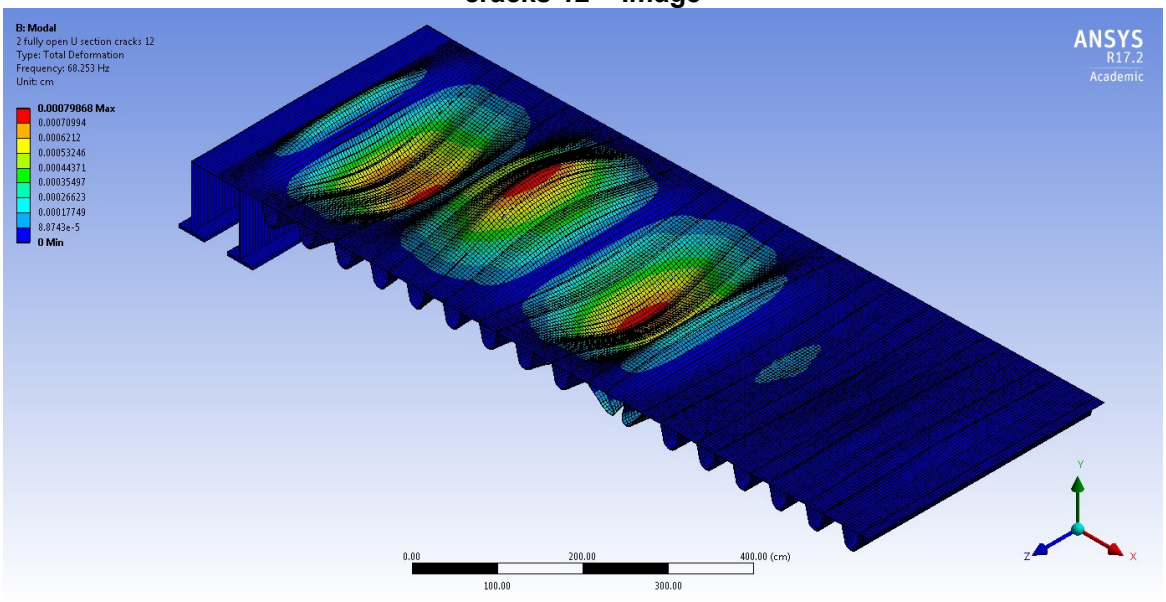


TABLE 38
Model (B3) > Modal (B4) > Solution (B5) > 2 fully open U section cracks > Results

Object Name	*2 fully open U section cracks 12*
State	Suppressed
Scope	
Scoping Method	Geometry Selection
Geometry	All Bodies
Definition	
Type	Total Deformation

Mode	12.
Identifier	
Suppressed	Yes
Results	
Minimum	
Maximum	
Minimum Occurs On	
Maximum Occurs On	
Information	
Frequency	

FIGURE 101
Model (B3) > Modal (B4) > Solution (B5) > 2 fully open U section cracks > 2 fully open U section cracks 12 > Image



Material Data

Structural Steel

TABLE 39
Structural Steel > Constants

Density	7.85 g cm^-3
Coefficient of Thermal Expansion	1.2e-005 C^-1
Specific Heat	4.34e+006 erg g^-1 C^-1
Thermal Conductivity	0.605 W cm^-1 C^-1
Resistivity	1.7e-005 ohm cm

TABLE 40
Structural Steel > Compressive Ultimate Strength

Compressive Ultimate Strength dyne cm^-2
0

TABLE 41
Structural Steel > Compressive Yield Strength

Compressive Yield Strength dyne cm^-2
2.5e+009

TABLE 42
Structural Steel > Tensile Yield Strength

Tensile Yield Strength dyne cm^-2
2.5e+009

TABLE 43
Structural Steel > Tensile Ultimate Strength

Tensile Ultimate Strength dyne cm^-2
4.6e+009

TABLE 44
Structural Steel > Isotropic Secant Coefficient of Thermal Expansion

Zero-Thermal-Strain Reference Temperature C
22

TABLE 45
Structural Steel > Alternating Stress Mean Stress

Alternating Stress dyne cm^-2	Cycles	Mean Stress dyne cm^-2
3.999e+010	10	0
2.827e+010	20	0
1.896e+010	50	0
1.413e+010	100	0
1.069e+010	200	0
4.41e+009	2000	0
2.62e+009	10000	0
2.14e+009	20000	0
1.38e+009	1.e+005	0
1.14e+009	2.e+005	0
8.62e+008	1.e+006	0

TABLE 46
Structural Steel > Strain-Life Parameters

Strength Coefficient dyne cm^-2	Strength Exponent	Ductility Coefficient	Ductility Exponent	Cyclic Strength Coefficient dyne cm^-2	Cyclic Strain Hardening Exponent
9.2e+009	-0.106	0.213	-0.47	1.e+010	0.2

TABLE 47
Structural Steel > Isotropic Elasticity

Temperature C	Young's Modulus dyne cm^-2	Poisson's Ratio	Bulk Modulus dyne cm^-2	Shear Modulus dyne cm^-2
	2.e+012	0.3	1.6667e+012	7.6923e+011

TABLE 48
Structural Steel > Isotropic Relative Permeability

Relative Permeability
10000

TABLE 49
Structural Steel > Color

Red	Green	Blue
-1	-1	-1

100kg

TABLE 50
100kg > Constants

Density	19.672 g cm^-3

TABLE 51
100kg > Isotropic Elasticity

Temperature C	Young's Modulus dyne cm^-2	Poisson's Ratio	Bulk Modulus dyne cm^-2	Shear Modulus dyne cm^-2
	2.e+012	0.3	1.6667e+012	7.6923e+011

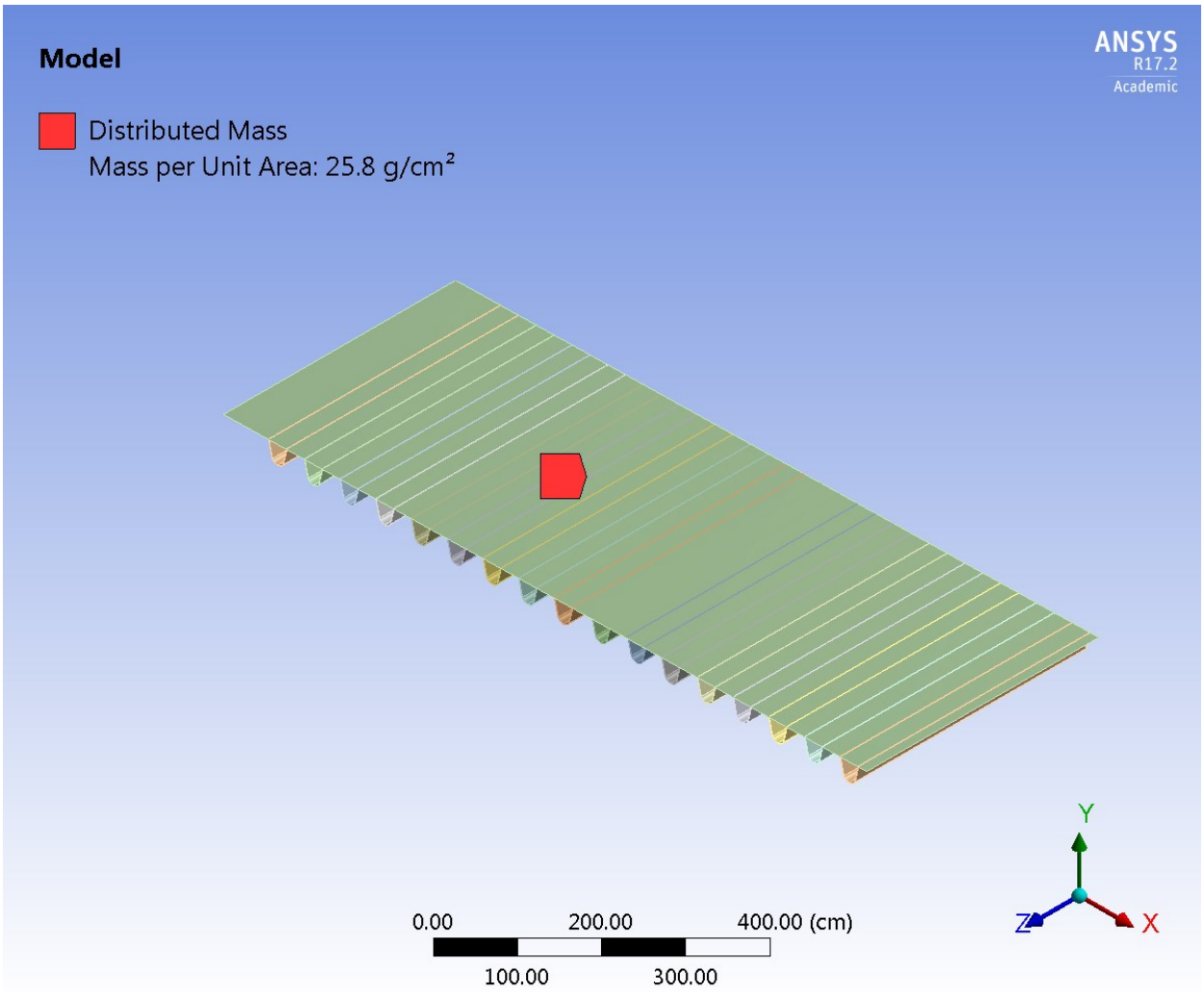
TABLE 52
100kg > Color

Red	Green	Blue
-1	-1	-1

Appendix F3

Local model 2

First Saved	Sunday, July 08, 2018
Last Saved	Sunday, July 08, 2018
Product Version	17.2 Release
Save Project Before Solution	No
Save Project After Solution	No



Contents

- **Units**
- **Model (B3)**
  - Geometry
    - Body Groups
      - Parts
      - Parts
      - Parts
      - Parts
    - Parts
    - Distributed Mass
  - Coordinate Systems
  - Connections
    - Line elements edge to deck face
      - Contact Regions
      - Contact Regions
      - Contact Regions
      - Contact Regions
      - Contact Regions
      - Contact Regions
  - Mesh
    - Mesh Controls
  - Named Selections
  - **Modal (B4)**
    - Pre-Stress (None)
    - Analysis Settings
    - Loads
    - Solution (B5)
      - Solution Information
      - 0kg
        - Results
      - 50kg
        - Results
      - 75kg
        - Results
      - 100kg
        - Results
      - 1crack35cm
        - Results
      - 2xcrack35cm
        - Results
      - Full 2xU crack
        - Results
- **Material Data**
  - Structural Steel no mass
  - Structural Steel
  - 100kg

Units

TABLE 1

Unit System	Metric (cm, g, dyne, s, V, A) Degrees rad/s Celsius
Angle	Degrees
Rotational Velocity	rad/s
Temperature	Celsius

Model (B3)

Geometry

TABLE 2
Model (B3) > Geometry

Object Name	*Geometry*
State	Fully Defined
Definition	
Source	C:\Users\Korisnik\Desktop\The final\ansys17\Local 3D model no mass\analysis\local_deck_model_staticBC_files\dp0\Geom\DM\Geom.agdb
Type	DesignModeler
Length Unit	Meters
Element Control	Program Controlled
Display Style	Body Color
Bounding Box	
Length X	1080.3 cm
Length Y	1463.2 cm
Length Z	5200. cm
Properties	
Volume	2.2811e+007 cm³
Mass	1.864e+007 g
Scale Factor Value	1.
Statistics	
Bodies	540
Active Bodies	533
Nodes	238483
Elements	81976
Mesh Metric	None
Basic Geometry Options	
Solid Bodies	Yes
Surface Bodies	Yes
Line Bodies	Yes
Parameters	Independent
Parameter Key	
Attributes	Yes
Attribute Key	
Named Selections	Yes
Named Selection Key	

Material Properties	Yes
Advanced Geometry Options	
Use Associativity	Yes
Coordinate Systems	Yes
Coordinate System Key	
Reader Mode Saves Updated File	Yes
Use Instances	Yes
Smart CAD Update	Yes
Compare Parts On Update	No
Attach File Via Temp File	Yes
Temporary Directory	C:\Users\Korisnik\AppData\Local\Temp
Analysis Type	3-D
Mixed Import Resolution	None
Decompose Disjoint Geometry	Yes
Enclosure and Symmetry Processing	Yes

TABLE 3
Model (B3) > Geometry > Body Groups

Object Name	*Transverse_3D*	*Line_structures*	*deck*	*3D U stiffener*
State	Hidden		Meshed	
Graphics Properties				
Visible	No		Yes	
Definition				
Suppressed	No			
Assignment	Structural Steel no mass	Multiple Materials		Structural Steel
Coordinate System	Default Coordinate System			
Bounding Box				
Length X	1080.3 cm	1080.2 cm		990.61 cm
Length Y	125.56 cm	1358.4 cm	20.804 cm	50.107 cm
Length Z	660. cm	5200. cm		387.6 cm
Properties				
Volume	6.9043e+005 cm³	1.5914e+007 cm³	5.6181e+006 cm³	2.9578e+005 cm³
Mass	0. g	2.14e+006 g	3.3076e+006 g	2.3218e+006 g
Centroid X	0. cm		0. cm	570.19 cm

Centroid Y	0. cm		0. cm	97.277 cm
Centroid Z	0. cm		0. cm	2469.8 cm
Moment of Inertia Ip1	0. g·cm²		0. g·cm²	2.9225e+010 g·cm²
Moment of Inertia Ip2	0. g·cm²		0. g·cm²	2.3013e+011 g·cm²
Moment of Inertia Ip3	0. g·cm²		0. g·cm²	2.0134e+011 g·cm²
Surface Area(approx.)			5.6181e+006 cm²	
Statistics				
Nodes	153521	12274	14761	57754
Elements	53590	6226	14506	7568
Mesh Metric	None			
CAD Attributes				
DMBodyGroup	1	2	3	6
DMSheetThickness			0.01	

FIGURE 1
Model (B3) > Geometry > Image

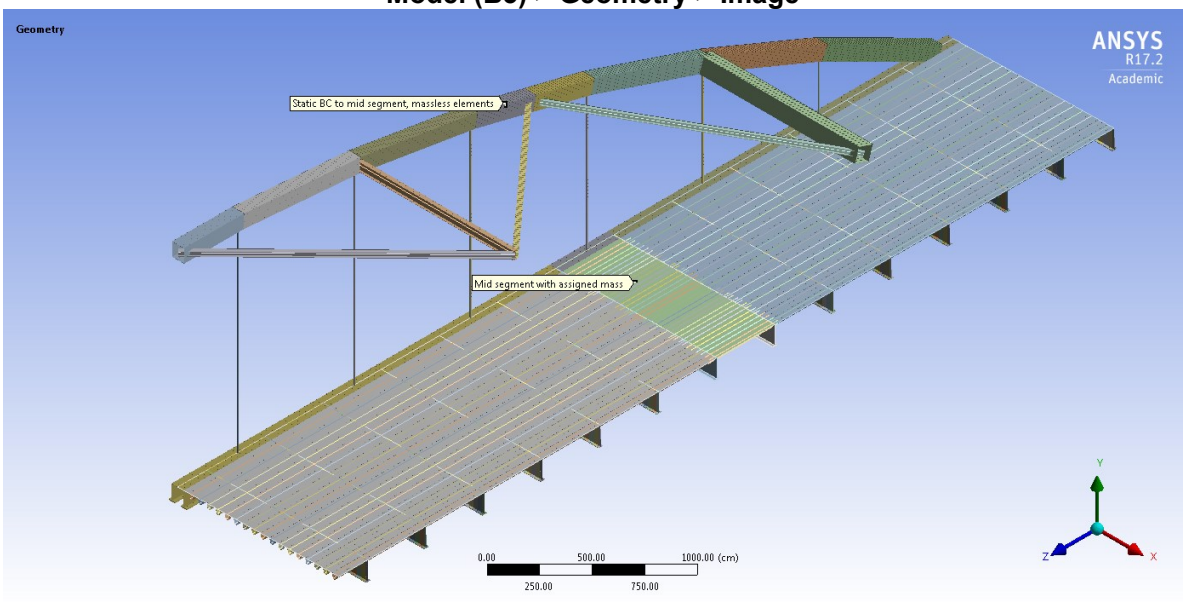


TABLE 57
Model (B3) > Geometry > Masses

Object Name	*Distributed Mass*
State	Fully Defined
Scope	
Scoping Method	Geometry Selection
Geometry	1 Face
Definition	
Mass Type	Mass per Unit Area
Mass per Unit Area	25.8 g/cm²
Suppressed	No

Coordinate Systems

TABLE 58
Model (B3) > Coordinate Systems > Coordinate System

Object Name	*Global Coordinate System*
State	Fully Defined
Definition	
Type	Cartesian
Coordinate System ID	0.
Origin	
Origin X	0. cm
Origin Y	0. cm
Origin Z	0. cm
Directional Vectors	
X Axis Data	[1. 0. 0.]
Y Axis Data	[0. 1. 0.]
Z Axis Data	[0. 0. 1.]

Mesh

TABLE 115
Model (B3) > Mesh

Object Name	*Mesh*
State	Solved
Display	
Display Style	Body Color
Defaults	
Physics Preference	Mechanical
Relevance	0
Shape Checking	Standard Mechanical
Element Midside Nodes	Program Controlled
Sizing	
Size Function	Curvature
Use Uniform Size Function For Sheets	No
Relevance Center	Coarse
Initial Size Seed	Active Assembly
Smoothing	Medium
Transition	Fast
Span Angle Center	Coarse
Curvature Normal Angle	Default (30.0 °)
Min Size	Default (2.29620 cm)
Max Face Size	25.0 cm
Max Tet Size	25.0 cm
Growth Rate	Default
Automatic Mesh Based Defeaturing	On
Defeature Size	Default (1.72220 cm)
Minimum Edge Length	0.60 cm
Inflation	

Use Automatic Inflation	None
Inflation Option	Smooth Transition
Transition Ratio	0.272
Maximum Layers	5
Growth Rate	1.2
Inflation Algorithm	Pre
View Advanced Options	No
Advanced	
Number of CPUs for Parallel Part Meshing	Program Controlled
Straight Sided Elements	No
Number of Retries	0
Rigid Body Behavior	Dimensionally Reduced
Mesh Morphing	Disabled
Triangle Surface Mesher	Program Controlled
Topology Checking	No
Pinch Tolerance	Default (2.06660 cm)
Generate Pinch on Refresh	No
Sheet Loop Removal	No
Statistics	
Nodes	238483
Elements	81976
Mesh Metric	None

TABLE 116
Model (B3) > Mesh > Mesh Controls

Object Name	*Body Sizing*	*Body Sizing 2*
State	Fully Defined	
Scope		
Scoping Method	Geometry Selection	
Geometry	2 Bodies	18 Bodies
Definition		
Suppressed	No	
Type	Element Size	
Element Size	8. cm	9. cm
Advanced		
Defeature Size	Default (1.7222 cm)	
Size Function	Uniform	
Behavior	Soft	
Growth Rate	Default (1.850)	

FIGURE 2
Model (B3) > Mesh > Image

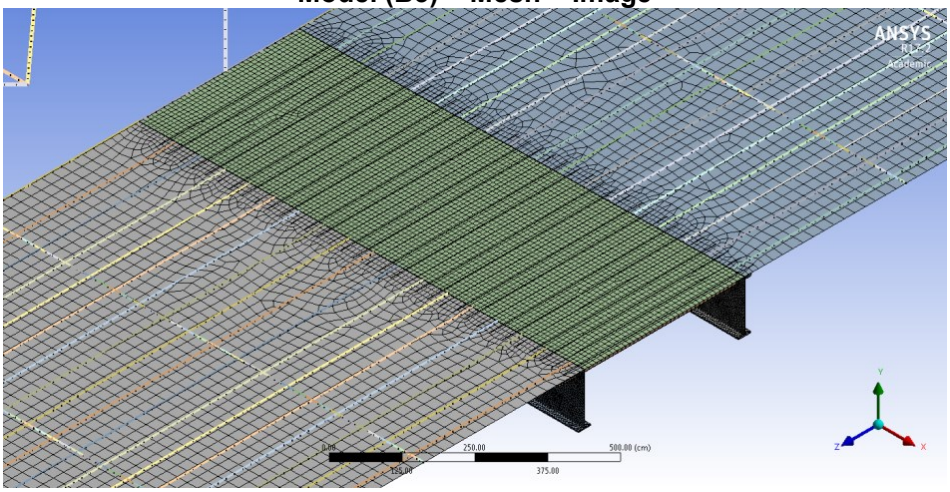


FIGURE 3
Model (B3) > Mesh > Image 2

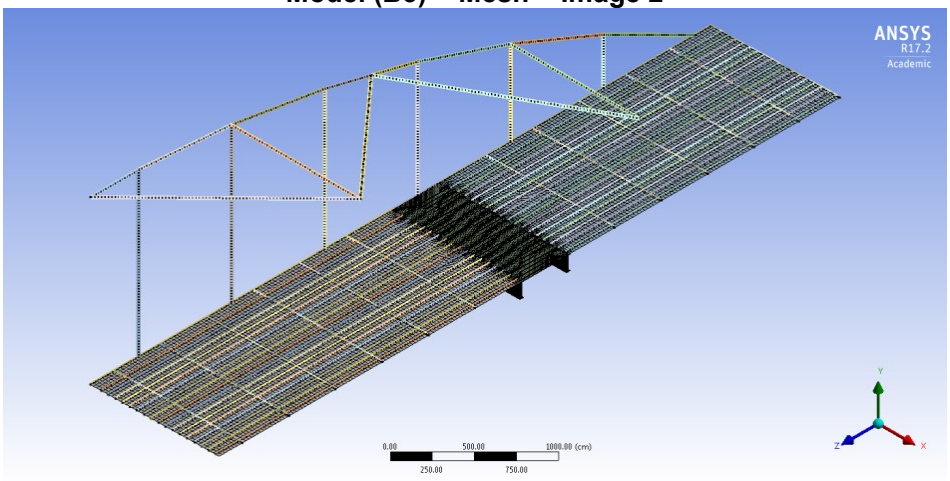


FIGURE 4
Model (B3) > Mesh > Image 4

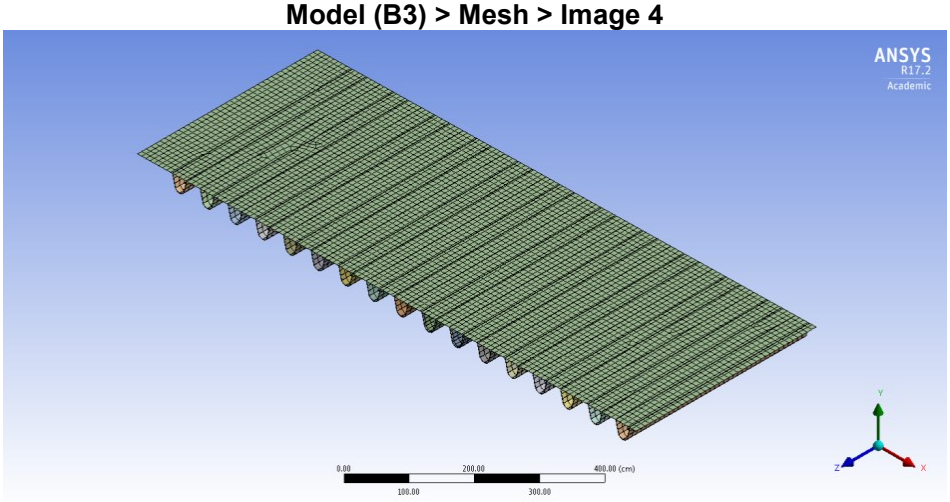
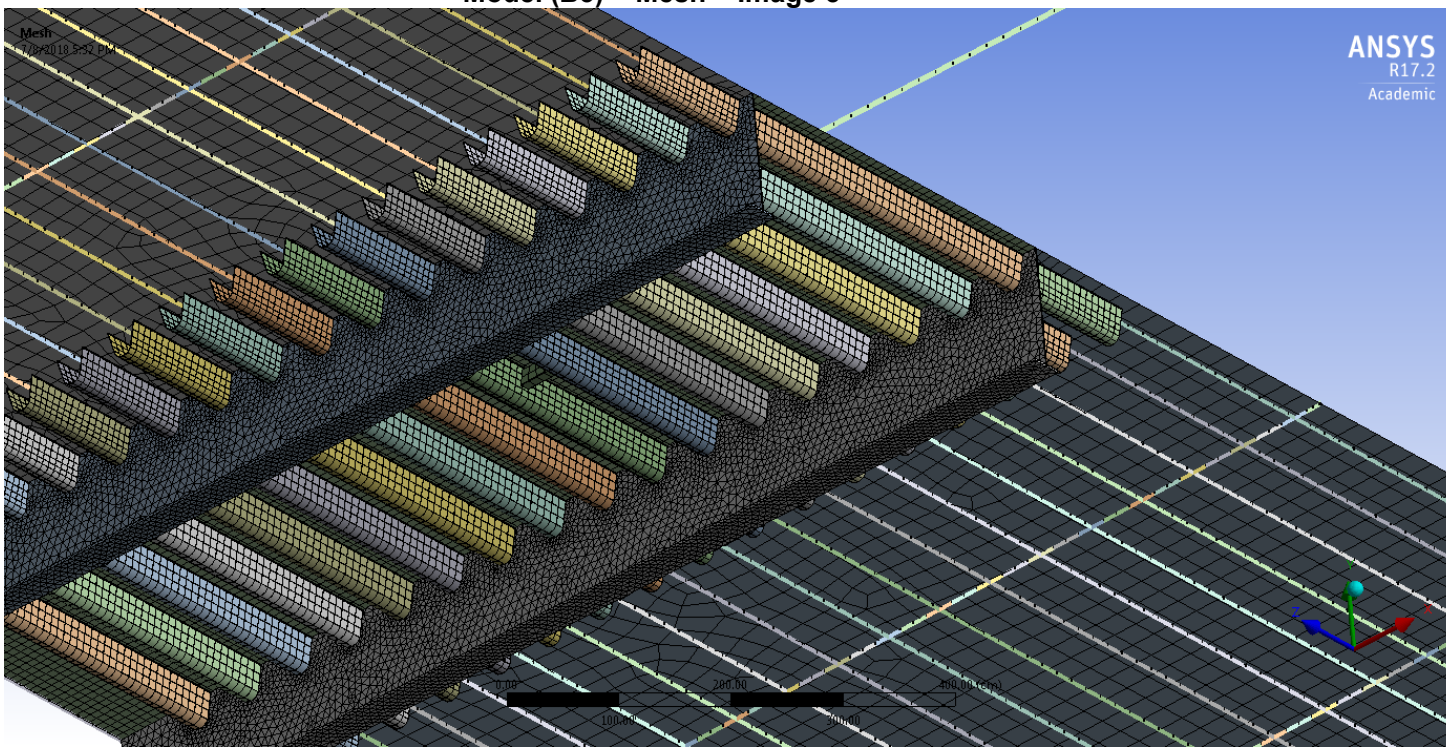


FIGURE 5
Model (B3) > Mesh > Image 5



Named Selections

TABLE 117
Model (B3) > Named Selections > Named Selections

Object Name	*Beam_frame*	*U7_8_walls_face*	*U7_bottom_face*	*U8_bottom_face*
State	Fully Defined			
Scope				
Scoping Method	Geometry Selection			
Geometry	420 Bodies	6 Faces	3 Faces	
Definition				
Send to Solver	Yes			
Visible	Yes			
Program Controlled Inflation	Exclude			
Statistics				
Type	Imported			
Total Selection	420 Bodies	10 Faces	4 Faces	
Suppressed	0	4	1	
Used by Mesh Worksheet	No			
Surface Area		139. cm²	65.009 cm²	65.357 cm²

Modal (B4)

TABLE 118
Model (B3) > Analysis

Object Name	*Modal (B4)*

State	Solved
Definition	
Physics Type	Structural
Analysis Type	Modal
Solver Target	Mechanical APDL
Options	
Environment Temperature	22. °C
Generate Input Only	No

TABLE 119
Model (B3) > Modal (B4) > Initial Condition

Object Name	*Pre-Stress (None)*
State	Fully Defined
Definition	
Pre-Stress Environment	None

TABLE 120
Model (B3) > Modal (B4) > Analysis Settings

Object Name	*Analysis Settings*
State	Fully Defined
Options	
Max Modes to Find	30
Limit Search to Range	No
Solver Controls	
Damped	No
Solver Type	Program Controlled
Rotordynamics Controls	
Coriolis Effect	Off
Campbell Diagram	Off
Output Controls	
Stress	No
Strain	No
Nodal Forces	No
Calculate Reactions	No
General Miscellaneous	No
Analysis Data Management	
Solver Files Directory	C:\Users\Korisnik\Desktop\The final\ansys17\Local 3D model no mass\analysis\local_deck_model_staticBC_files\dp0\SYS-1\MECH\
Future Analysis	None
Scratch Solver Files Directory	
Save MAPDL db	No
Delete Unneeded Files	Yes
Solver Units	Active System
Solver Unit System	cgs

FIGURE 6
Model (B3) > Modal (B4) > Image

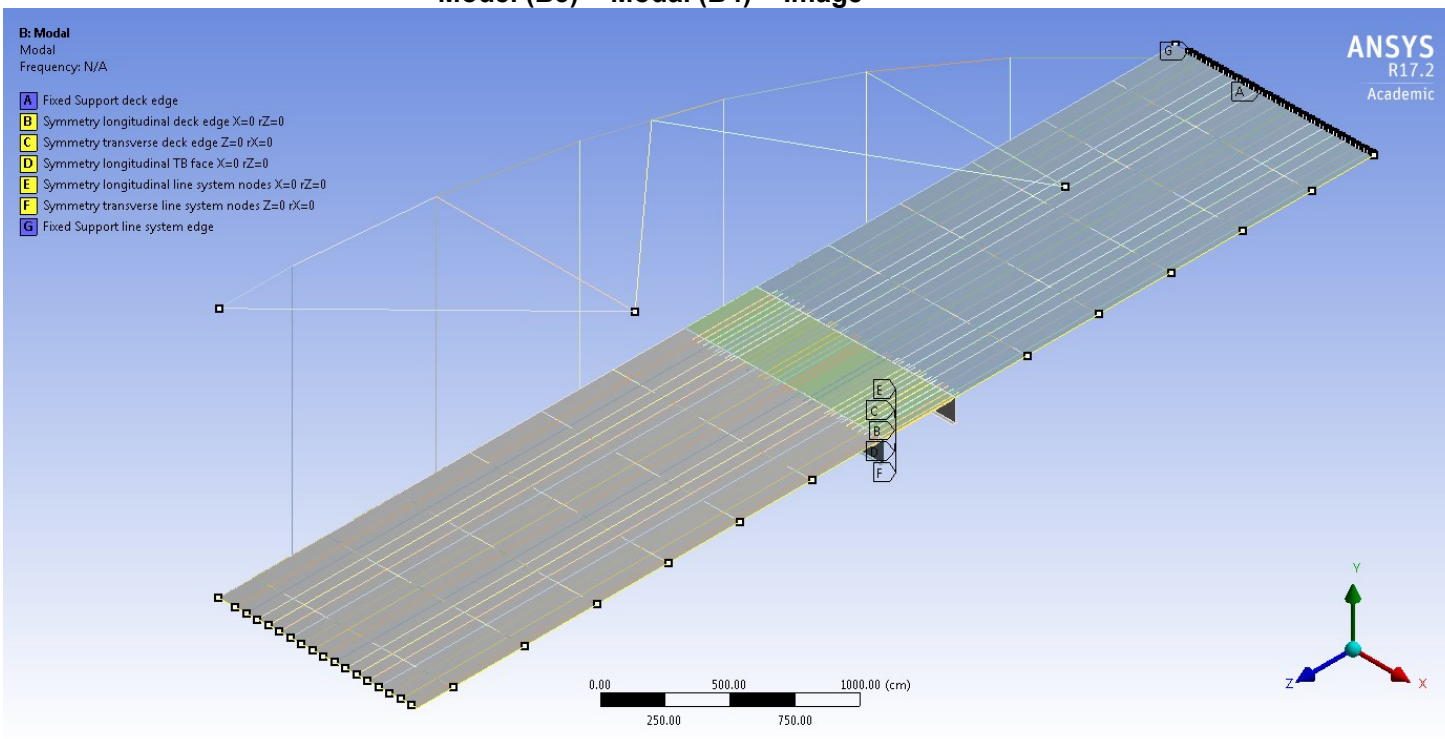


TABLE 121
Model (B3) > Modal (B4) > Loads

Object Name	*Fixed Support deck edge*	*Symmetry longitudinal deck edge X=0 rZ=0*	*Symmetry transverse deck edge Z=0 rX=0*	*Symmetry longitudinal TB face X=0 rZ=0*	*Symmetry longitudinal line system nodes X=0 rZ=0*	*Symmetry transverse line system nodes Z=0 rX=0*	*Fixed Support line system edge*
State	Fully Defined						
Scope							
Scoping Method	Geometry Selection						
Geometry	1 Edge	3 Edges	1 Edge	2 Faces	13 Vertices	19 Vertices	70 Vertices
Coordinate System		Global Coordinate System					
X Coordinate		1080.2 cm					
Y Coordinate		124.8 cm					
Z Coordinate		2600. cm					
Location		Defined					
Definition							
Type	Fixed Support	Remote Displacement					Fixed Support
Suppressed	No						

X Component		0. cm	Free	0. cm	Free	
Y Component		Free				
Z Component		Free	0. cm	Free	0. cm	
Rotation X		Free				
Rotation Y		Free				
Rotation Z		0. °				
Behavior		Deformable				
Rotation X			0. °			
Rotation Y			Free			
Rotation Z			Free			
Rotation X				Free		
Rotation Y				Free		
Rotation Z				0. °		
Rotation X					0. °	
Rotation Y					Free	
Rotation Z					Free	
Advanced						
Pinball Region		All				

FIGURE 7
Model (B3) > Modal (B4) > Fixed Support deck edge > Image

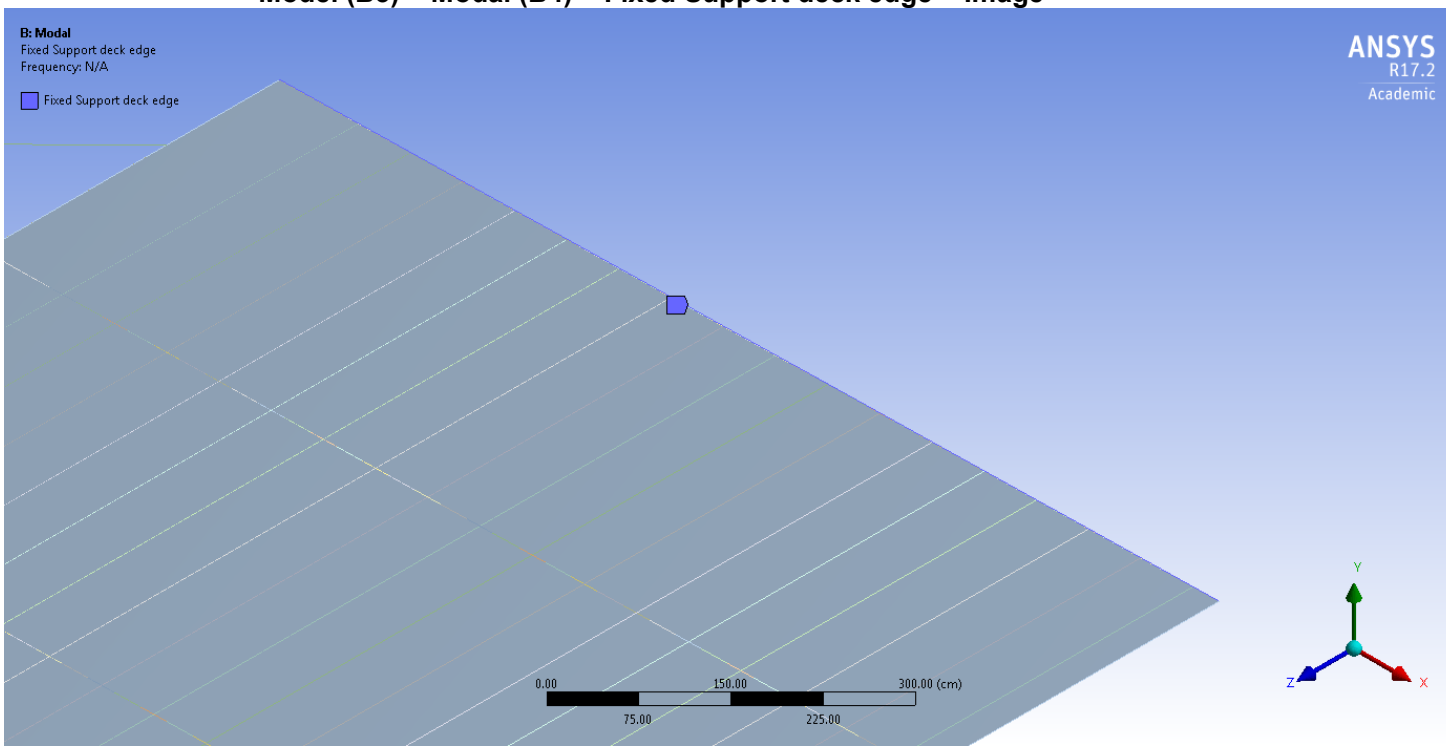


FIGURE 8
Model (B3) > Modal (B4) > Symmetry longitudinal deck edge X=0 rZ=0 > Image

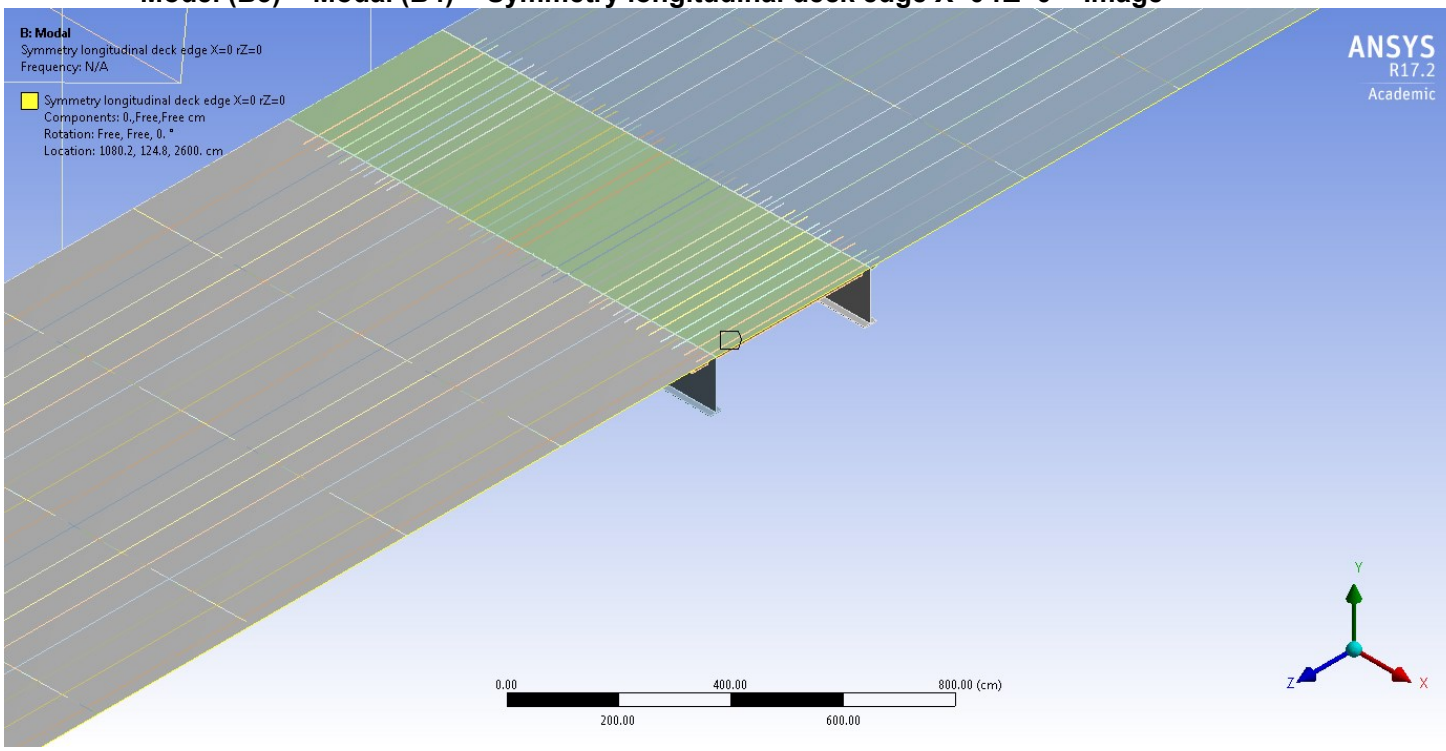


FIGURE 9
Model (B3) > Modal (B4) > Symmetry transverse deck edge Z=0 rX=0 > Image

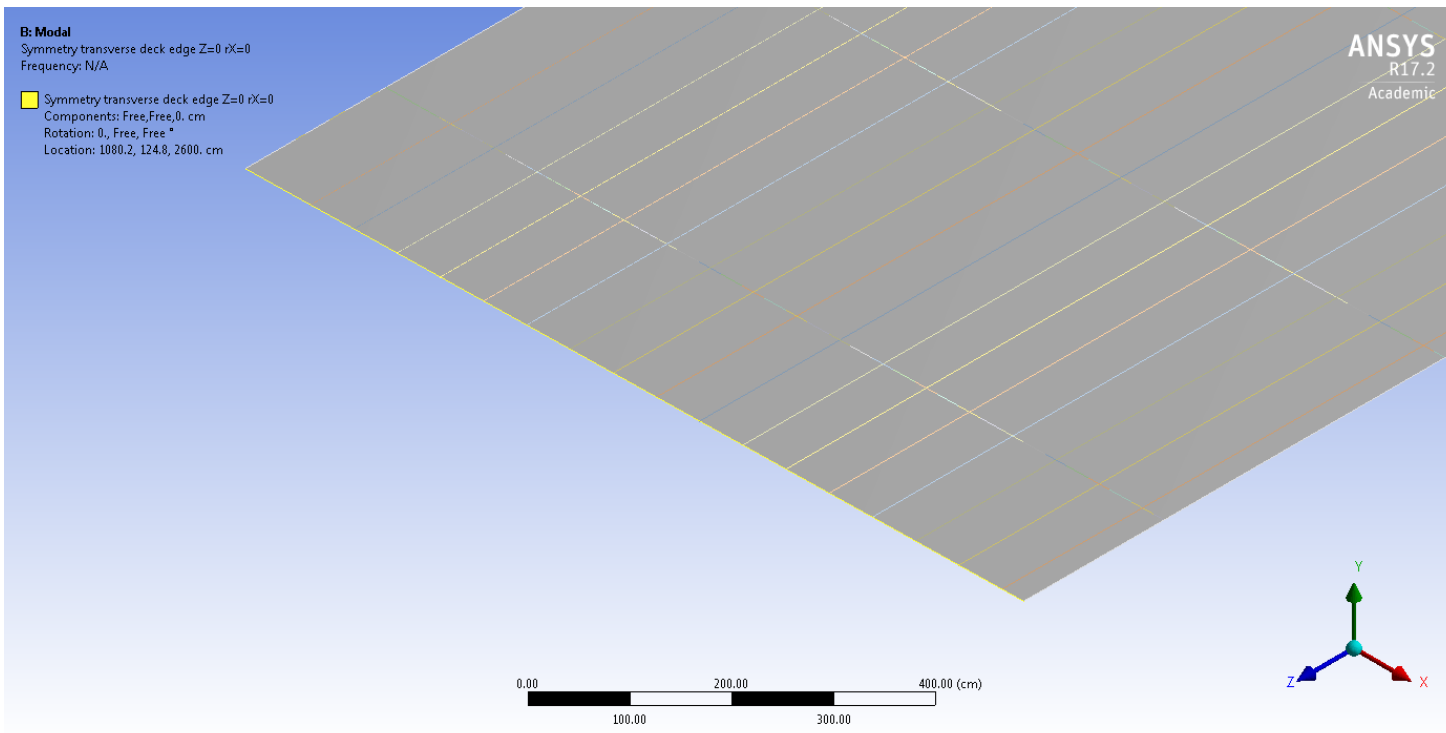


FIGURE 10
Model (B3) > Modal (B4) > Symmetry longitudinal TB face X=0 rZ=0 > Image

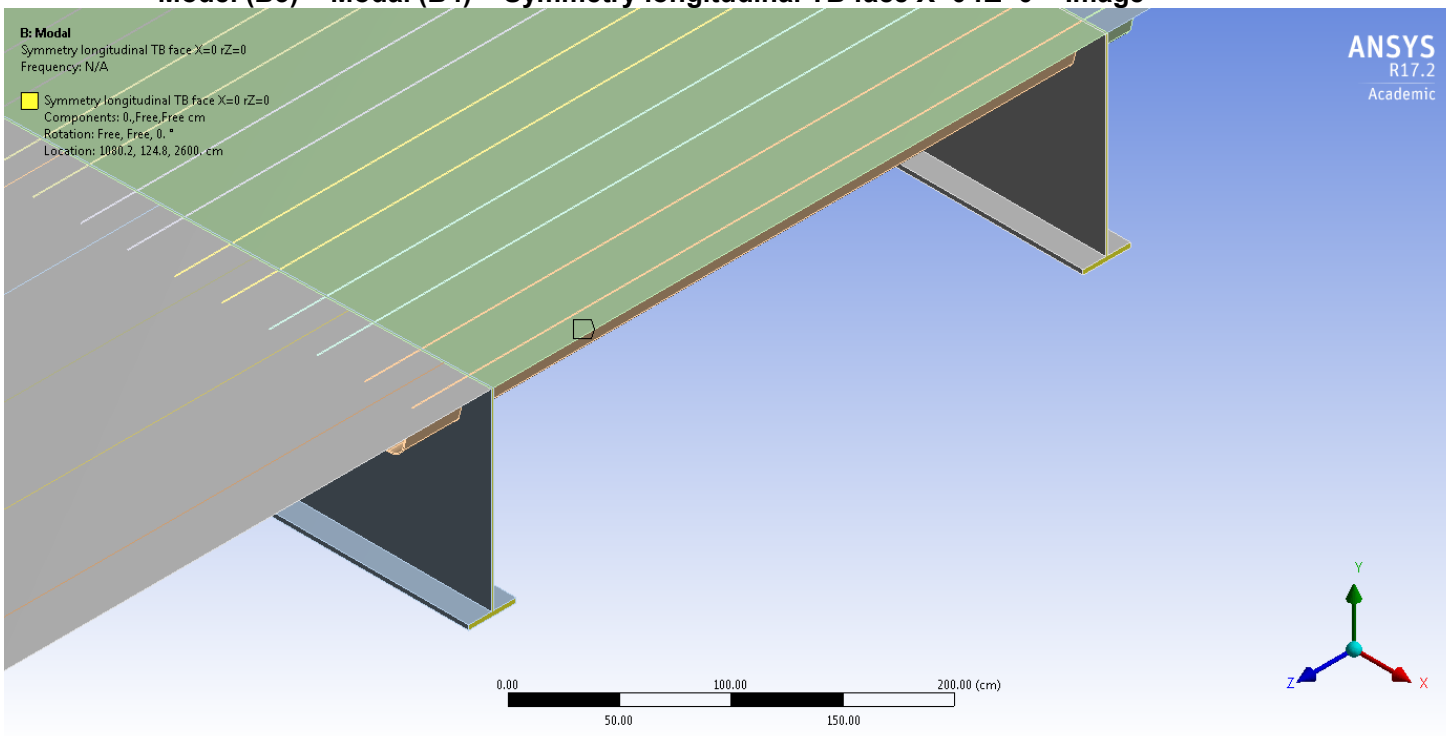


FIGURE 11
Model (B3) > Modal (B4) > Symmetry longitudinal line system nodes X=0 rZ=0 > Image

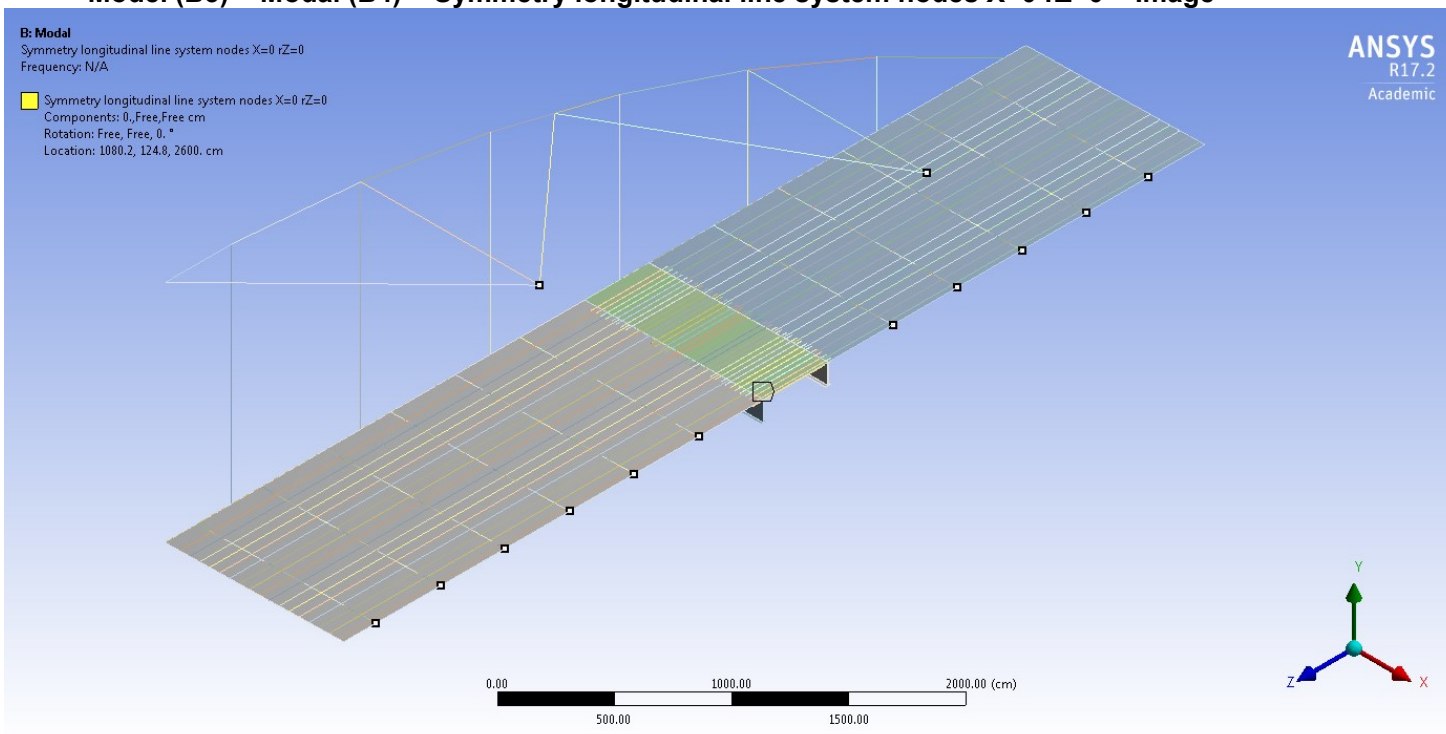


FIGURE 12
Model (B3) > Modal (B4) > Symmetry transverse line system nodes Z=0 rX=0 > Image

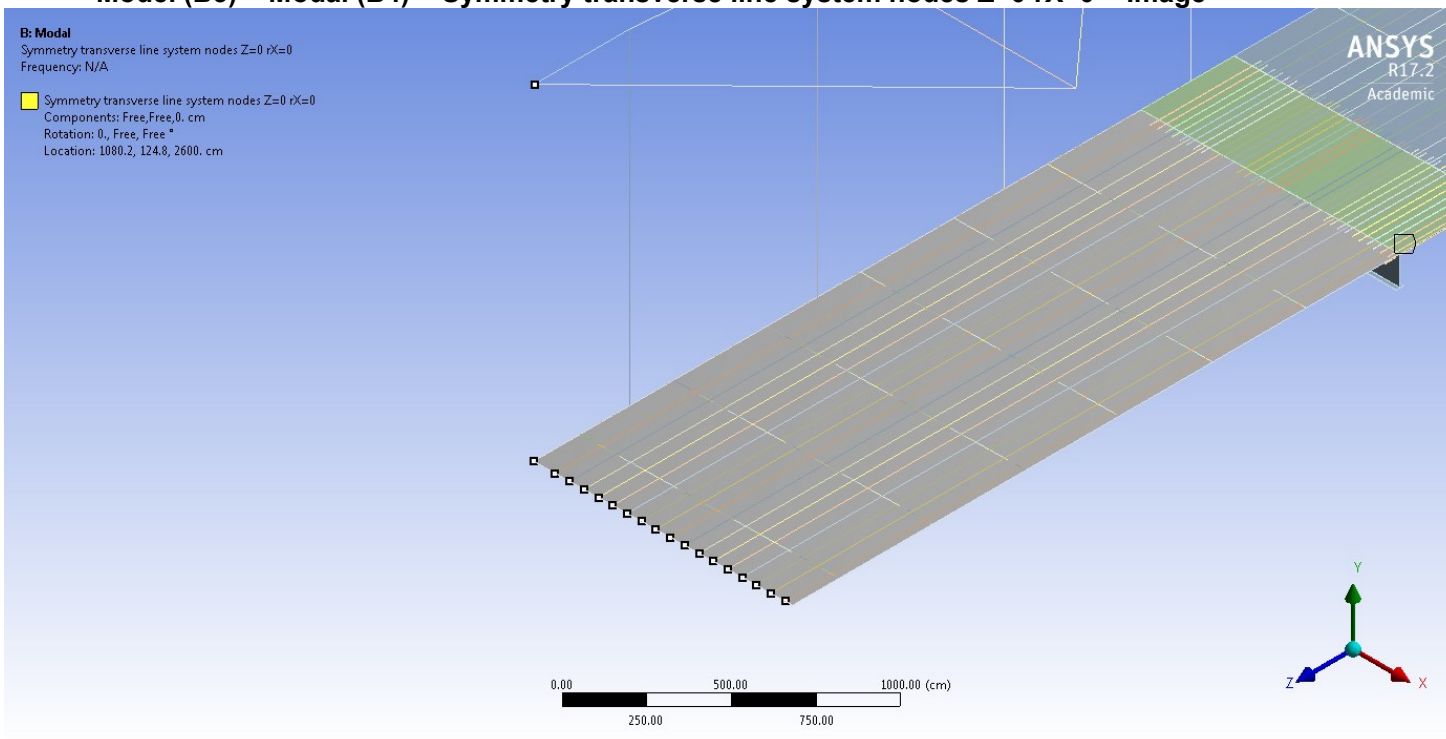
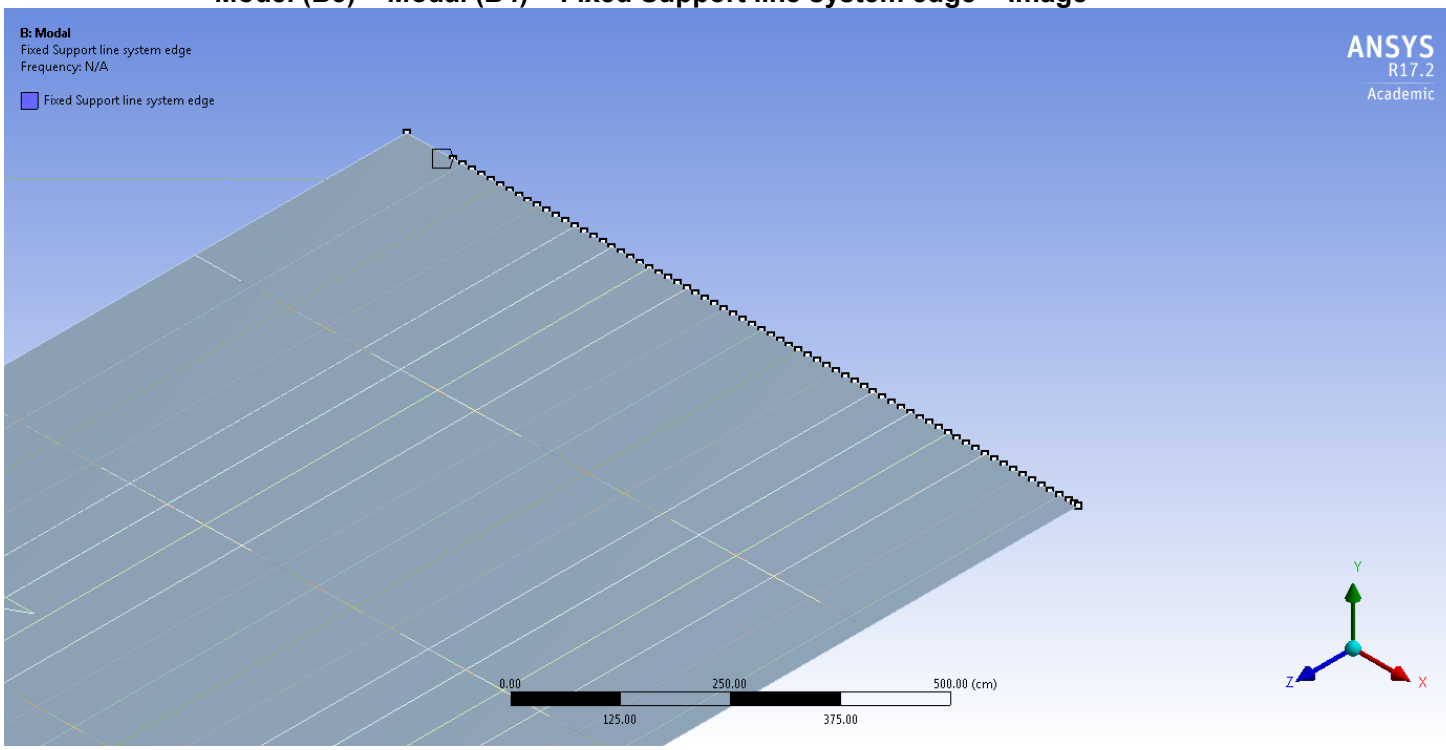


FIGURE 13
Model (B3) > Modal (B4) > Fixed Support line system edge > Image



Solution (B5)

TABLE 122
Model (B3) > Modal (B4) > Solution

Object Name	*Solution (B5)*
State	Solved
Adaptive Mesh Refinement	
Max Refinement Loops	1.
Refinement Depth	2.
Information	
Status	Done
MAPDL Elapsed Time	4 m 22 s
MAPDL Memory Used	7.4443 GB
MAPDL Result File Size	529.56 MB
Post Processing	
Beam Section Results	No

The following bar chart indicates the frequency at each calculated mode.

FIGURE 14
Model (B3) > Modal (B4) > Solution (B5)

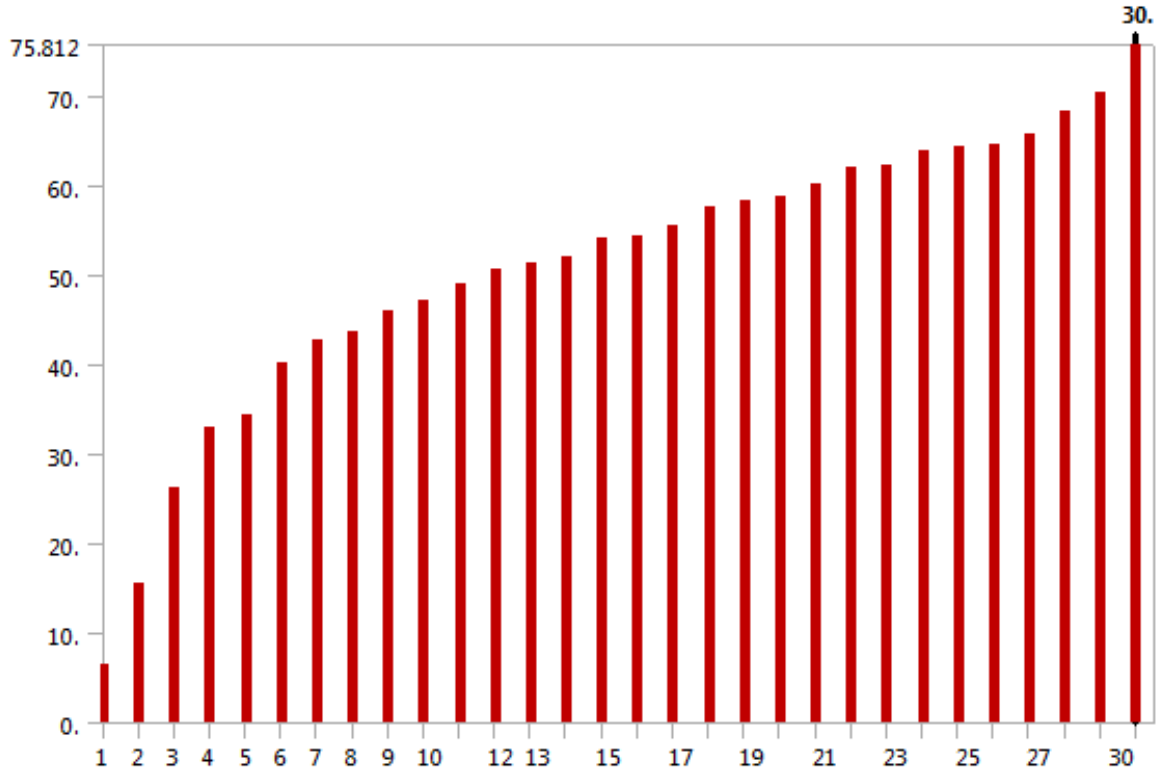


TABLE 123
Model (B3) > Modal (B4) > Solution (B5)

Mode	Frequency [Hz]
1.	6.5236
2.	15.52
3.	26.239
4.	33.081
5.	34.408
6.	40.218
7.	42.756
8.	43.611
9.	45.995
10.	47.129
11.	49.087
12.	50.586
13.	51.342
14.	52.192
15.	54.144
16.	54.447
17.	55.496
18.	57.709
19.	58.348
20.	58.941
21.	60.323
22.	62.139
23.	62.414
24.	63.859
25.	64.402
26.	64.725
27.	65.715
28.	68.353
29.	70.372
30.	75.812

TABLE 124
Model (B3) > Modal (B4) > Solution (B5) > Solution Information

Object Name	*Solution Information*
State	Solved
Solution Information	
Solution Output	Solver Output
Newton-Raphson Residuals	0
Identify Element Violations	0
Update Interval	2.5 s
Display Points	All
FE Connection Visibility	
Activate Visibility	Yes
Display	All FE Connectors
Draw Connections Attached To	All Nodes
Line Color	Connection Type

Visible on Results	No
Line Thickness	Single
Display Type	Lines

0kg

TABLE 125
Model (B3) > Modal (B4) > Solution (B5) > 0kg > Results

Object Name	*0kg total deformation 1*	*0kg total deformation 2*	*0kg total deformation 3*	*0kg total deformation 4*	*0kg total deformation 5*	*0kg total deformation 6*	*0kg total deformation 7*	*0kg total deformation 8*	*0kg total deformation 9*	*0kg total deformation 10*	*0kg total deformation 11*
State	Suppressed										
Scope											
Scoping Method	Geometry Selection										
Geometry	All Bodies										
Definition											
Type	Total Deformation										
Mode	1.	2.	3.	4.	5.	6.	7.	8.	9.	10.	11.
Identifier											
Suppressed	Yes										
Results											
Minimum											
Maximum											
Minimum Occurs On											
Maximum Occurs On											
Information											
Frequency											

FIGURE 15
Model (B3) > Modal (B4) > Solution (B5) > 0kg > 0kg total deformation 1 > Image

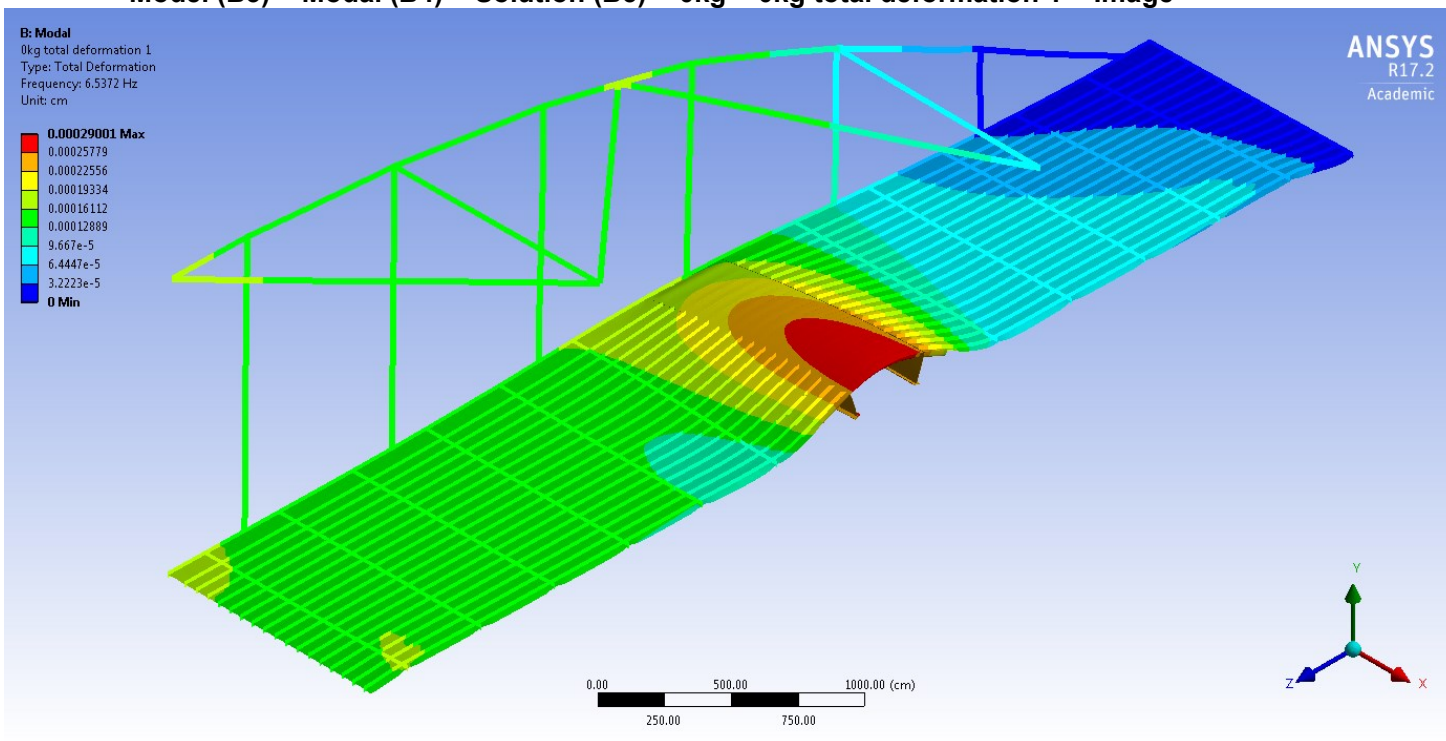


FIGURE 16
Model (B3) > Modal (B4) > Solution (B5) > 0kg > 0kg total deformation 1 > Image

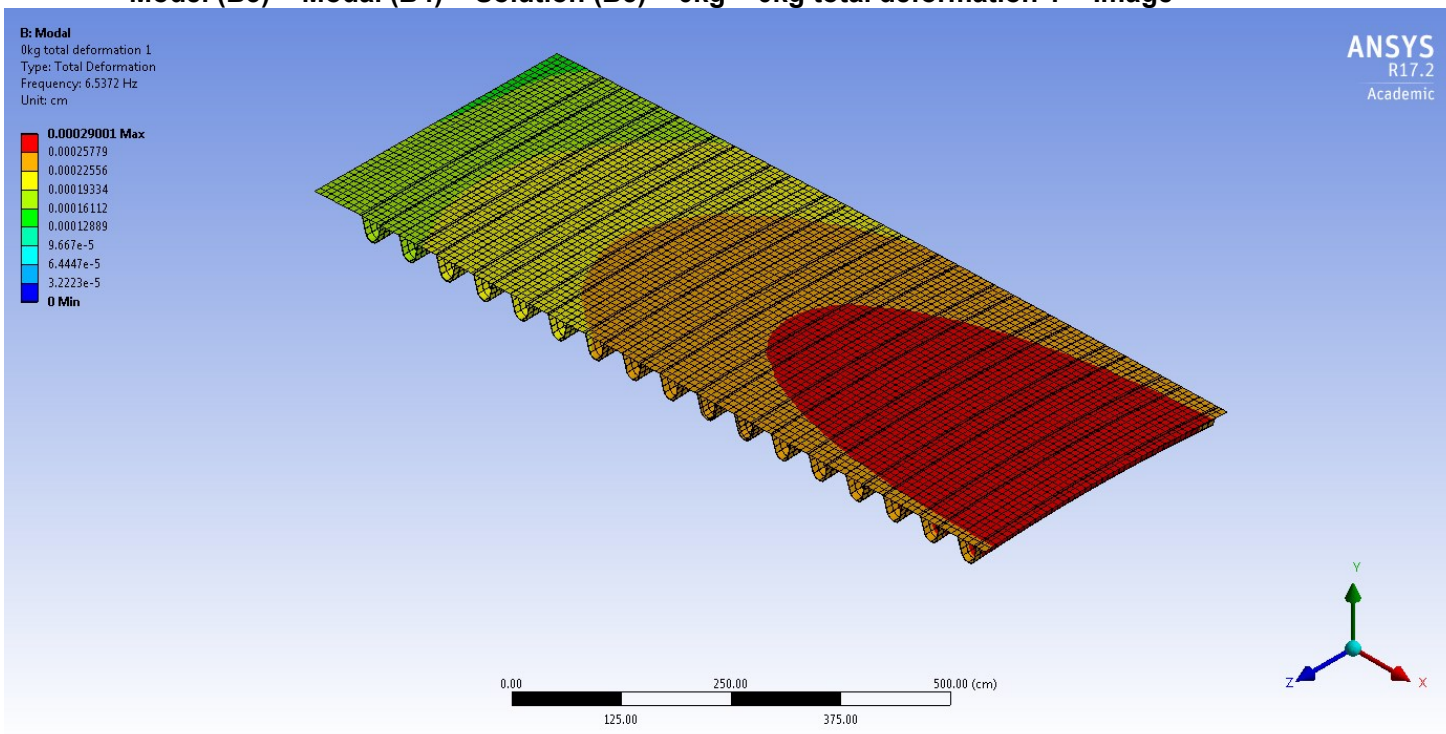


FIGURE 17
Model (B3) > Modal (B4) > Solution (B5) > 0kg > 0kg total deformation 2 > Image

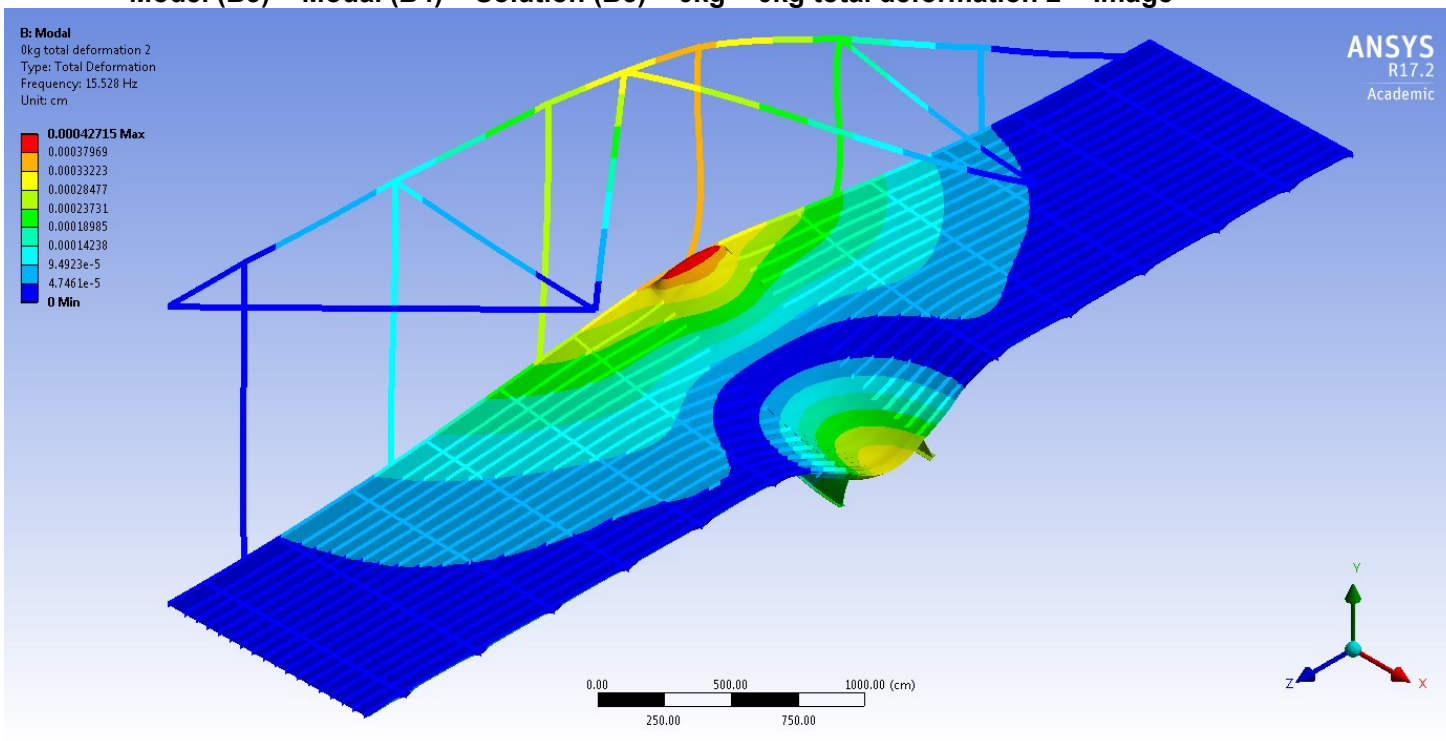


FIGURE 18
Model (B3) > Modal (B4) > Solution (B5) > 0kg > 0kg total deformation 2 > Image

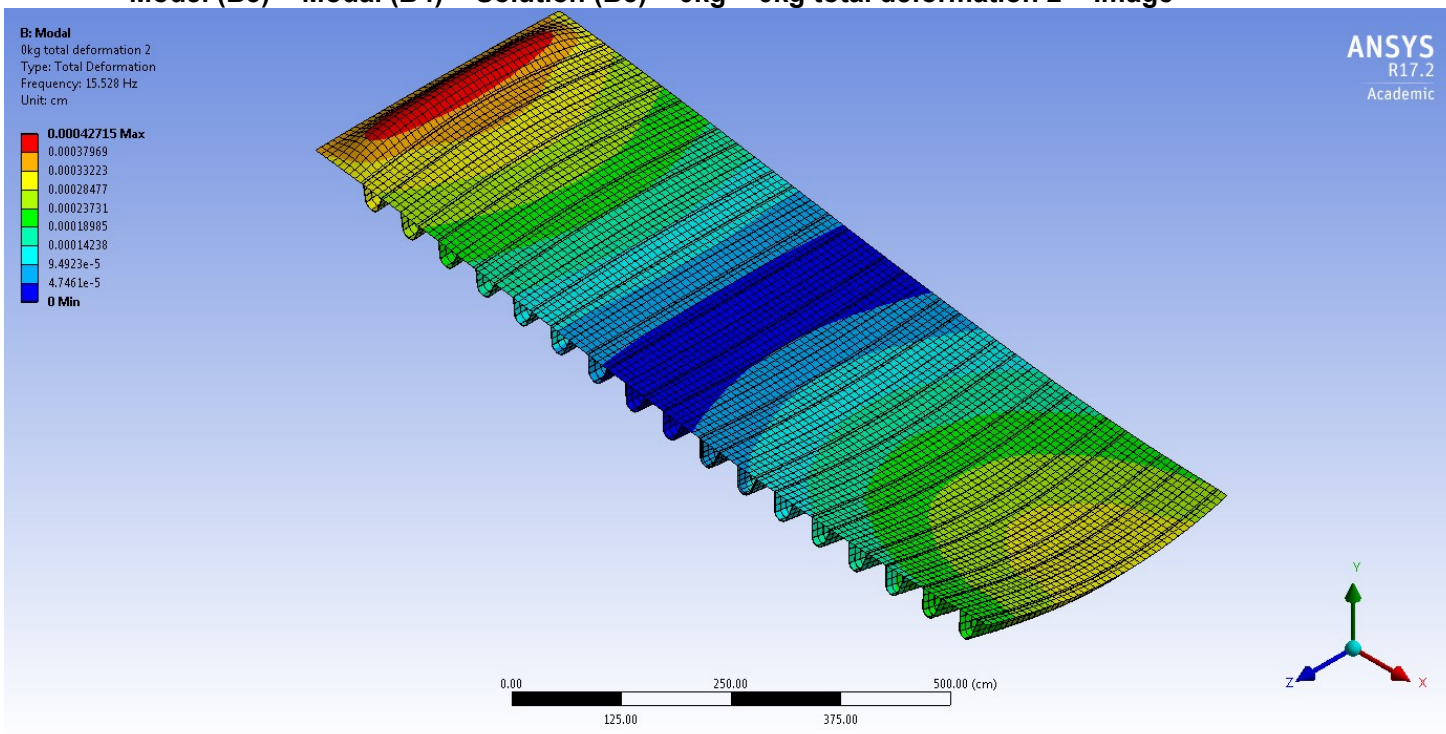


FIGURE 19
Model (B3) > Modal (B4) > Solution (B5) > 0kg > 0kg total deformation 3 > Image

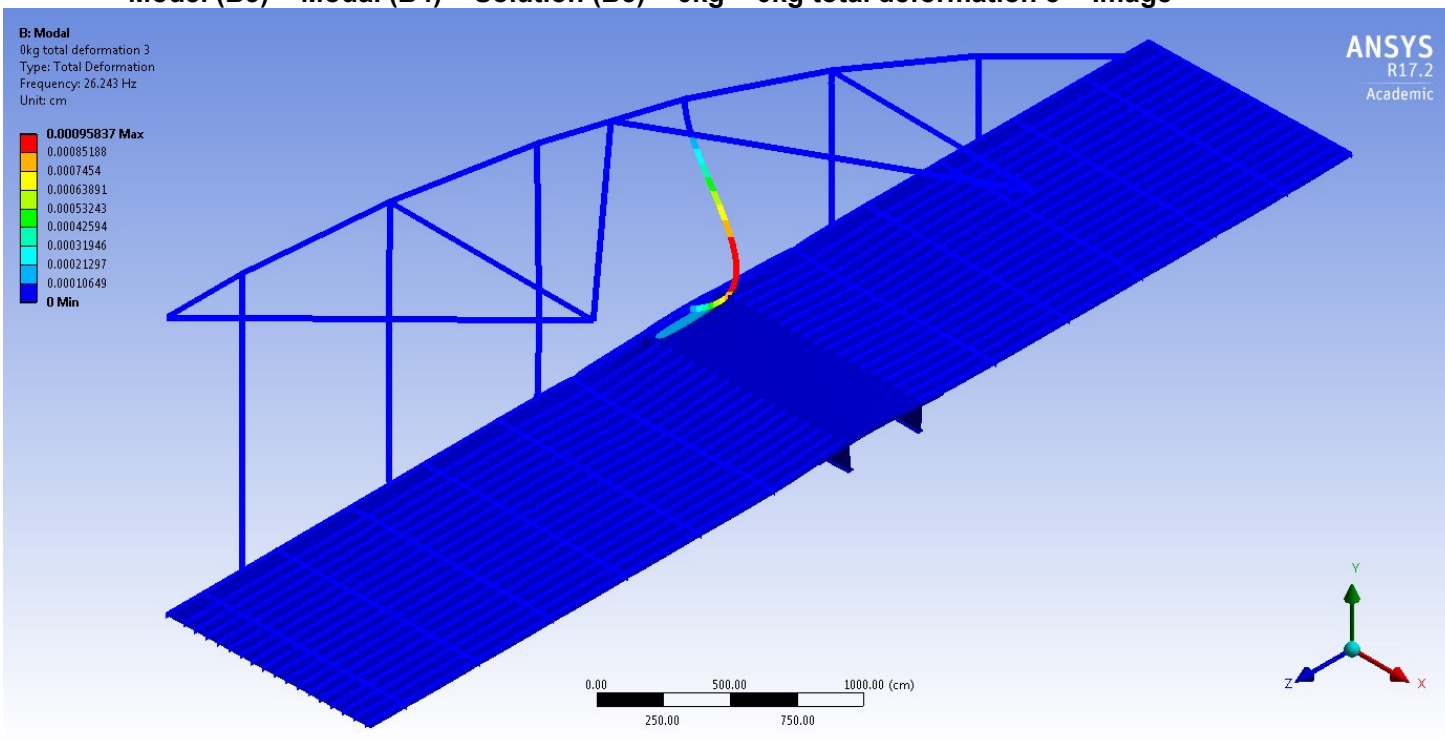


FIGURE 20
Model (B3) > Modal (B4) > Solution (B5) > 0kg > 0kg total deformation 3 > Image

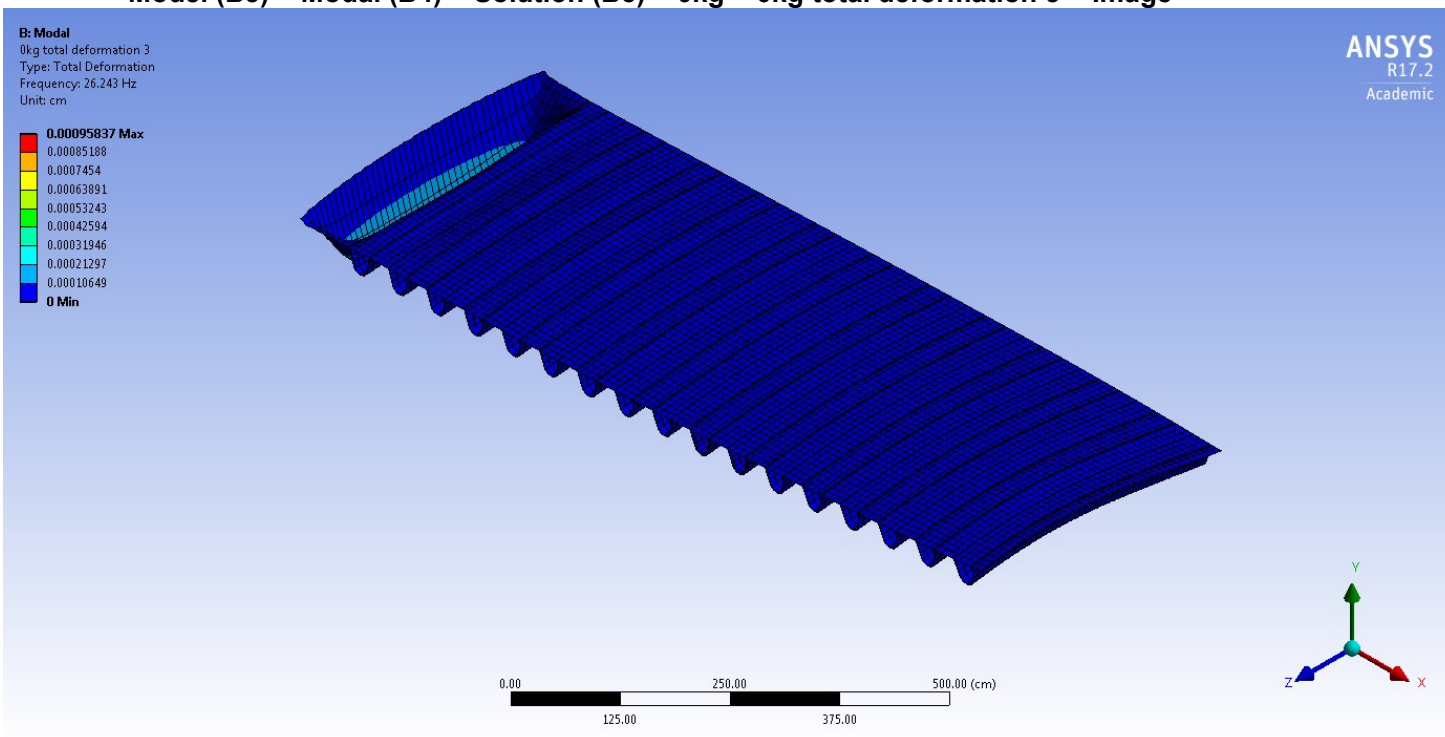


FIGURE 21
Model (B3) > Modal (B4) > Solution (B5) > 0kg > 0kg total deformation 4 > Image

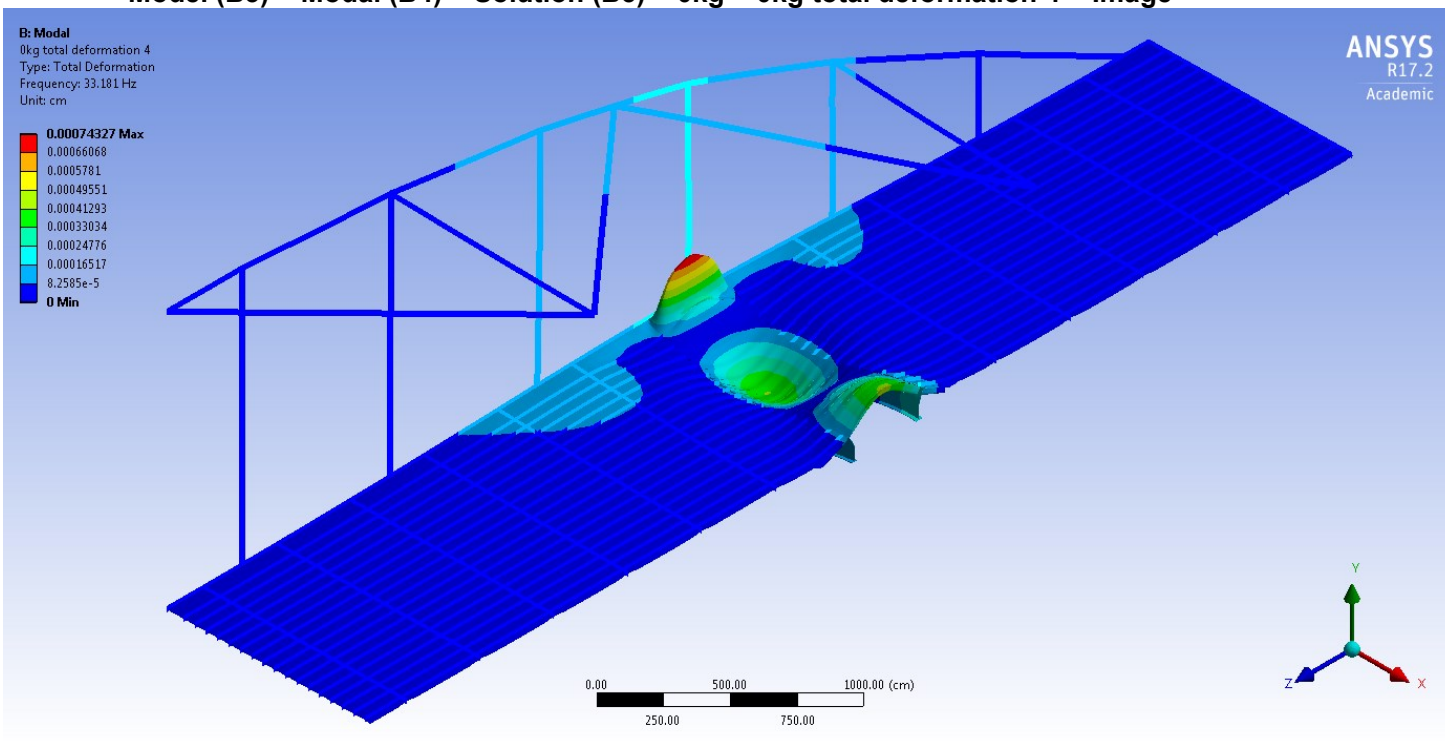


FIGURE 22
Model (B3) > Modal (B4) > Solution (B5) > 0kg > 0kg total deformation 4 > Image

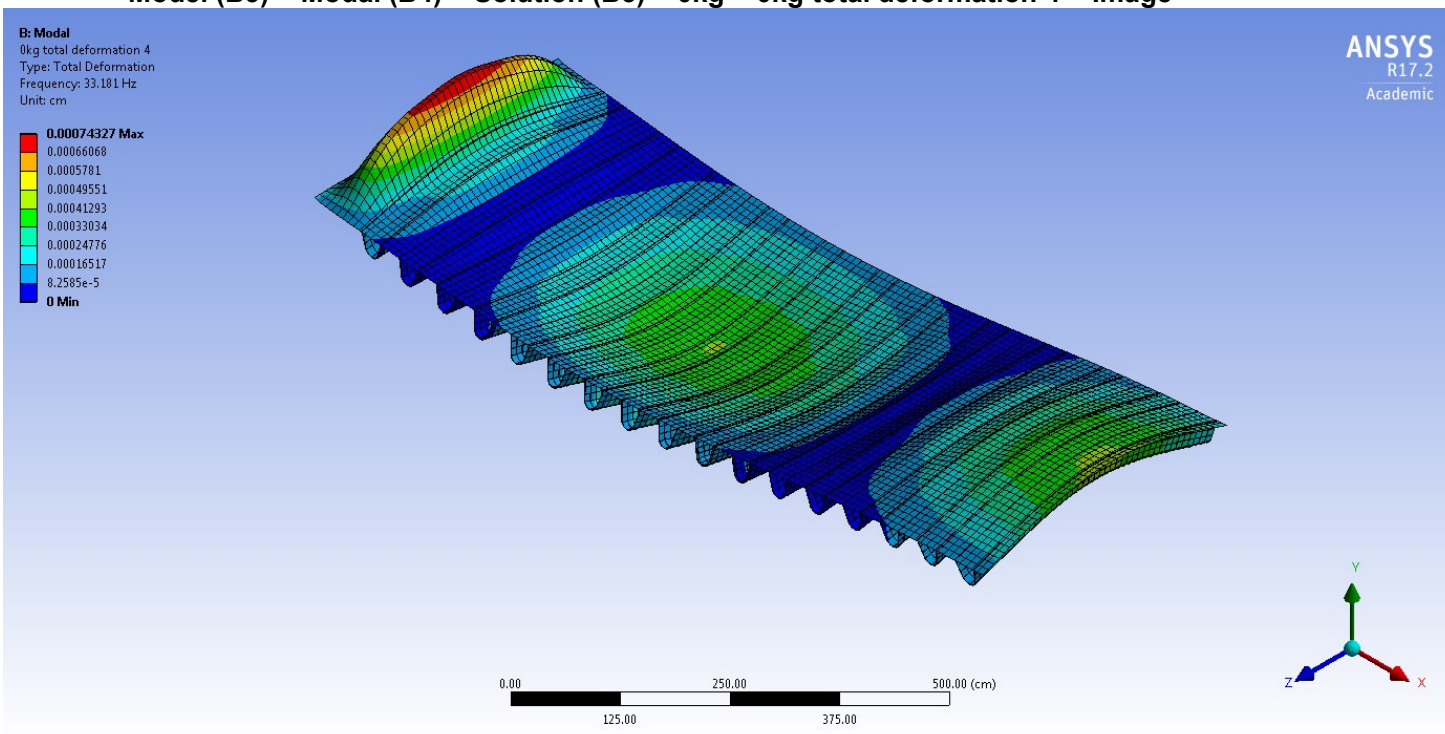


FIGURE 23
Model (B3) > Modal (B4) > Solution (B5) > 0kg > 0kg total deformation 5 > Image

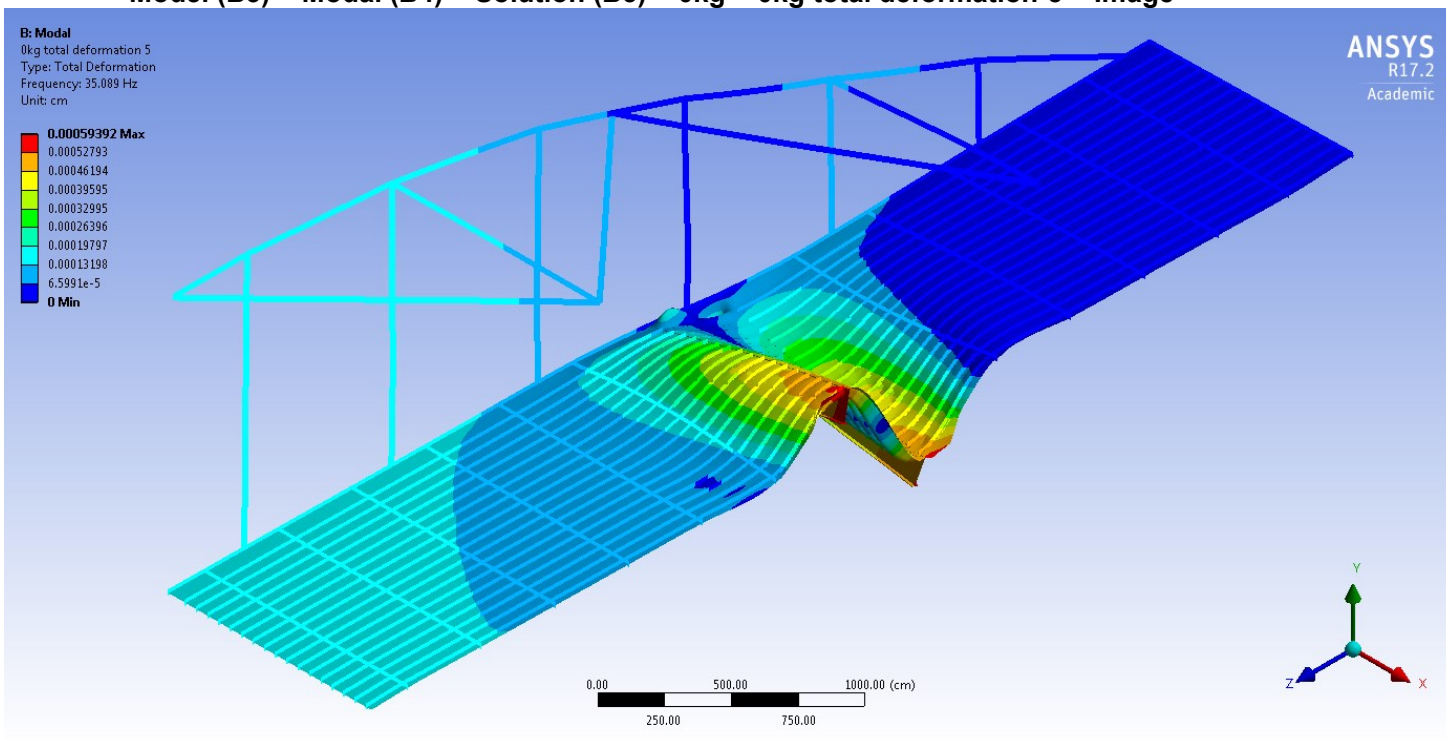


FIGURE 24
Model (B3) > Modal (B4) > Solution (B5) > 0kg > 0kg total deformation 5 > Image

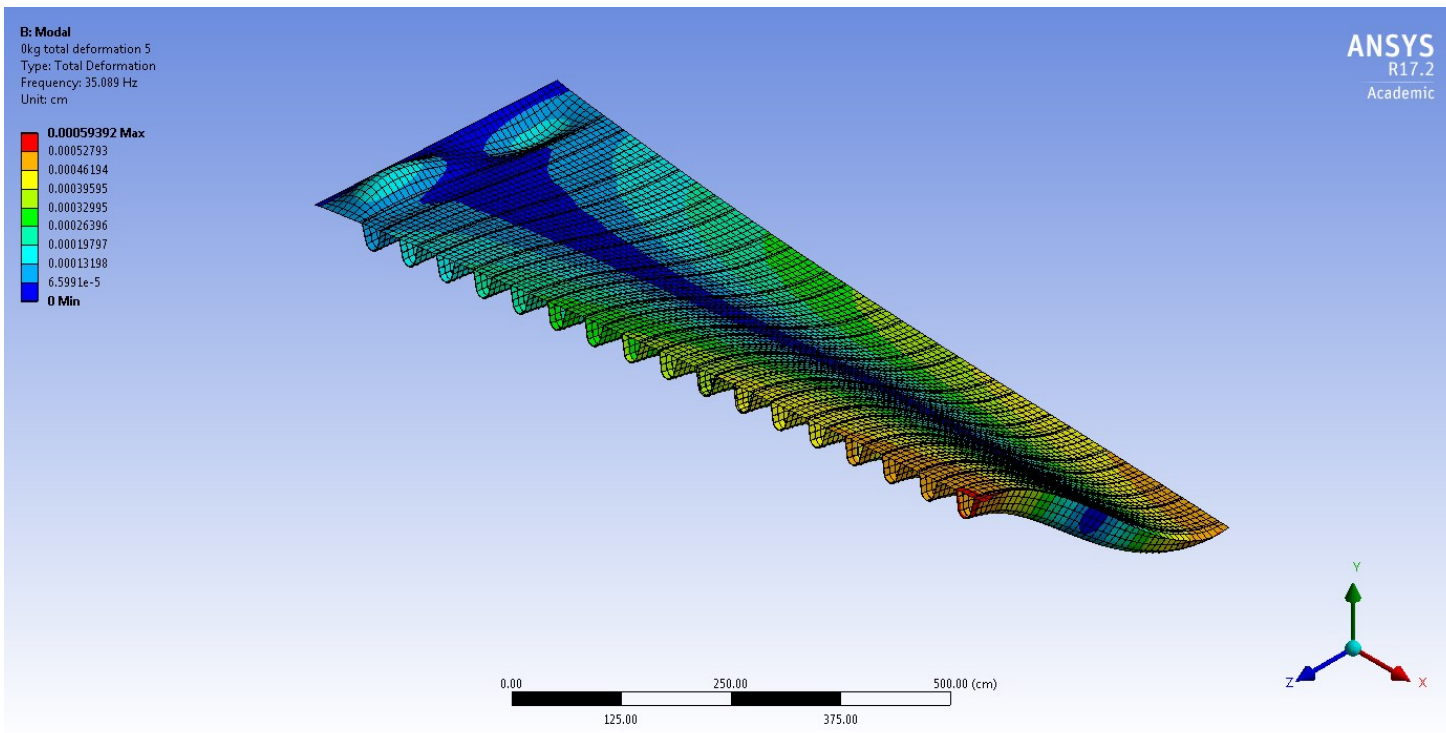


FIGURE 25
Model (B3) > Modal (B4) > Solution (B5) > 0kg > 0kg total deformation 6 > Image

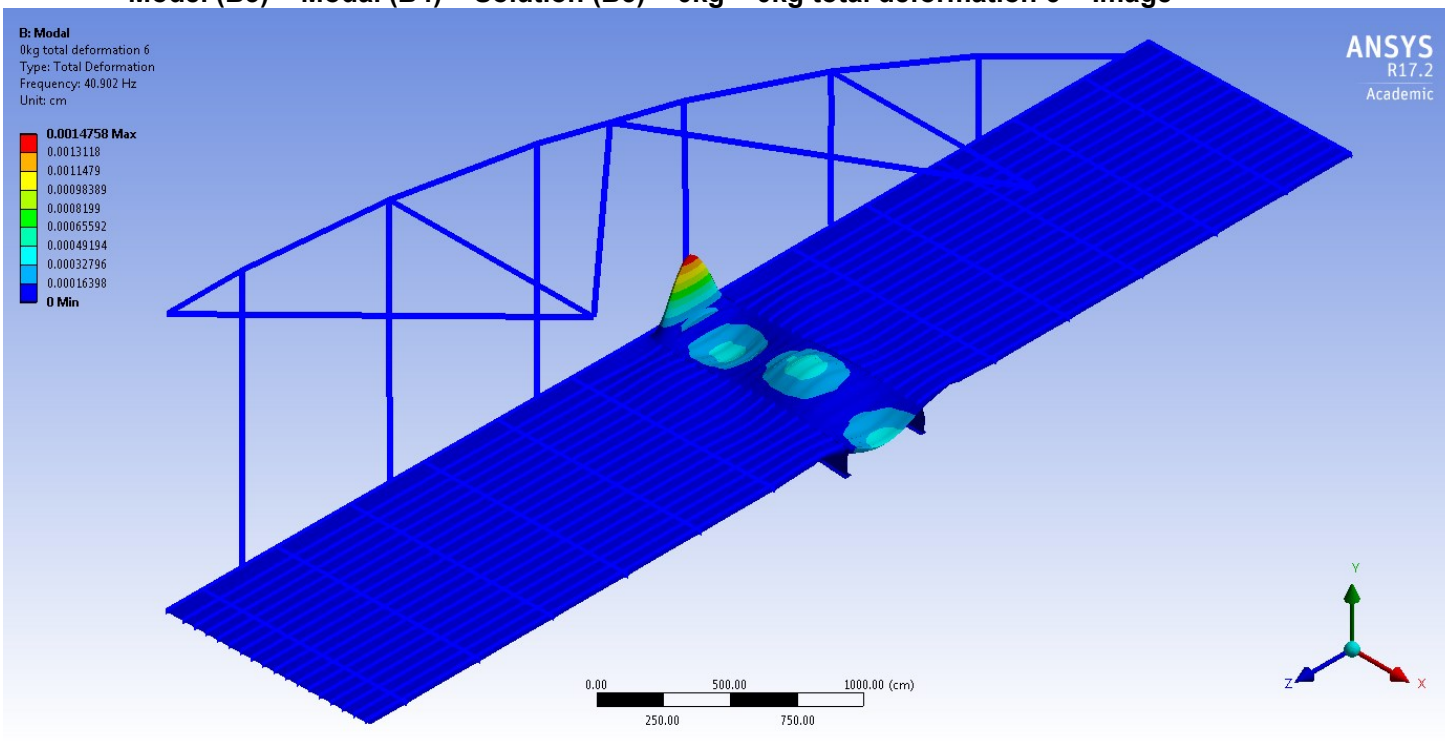


FIGURE 26
Model (B3) > Modal (B4) > Solution (B5) > 0kg > 0kg total deformation 6 > Image

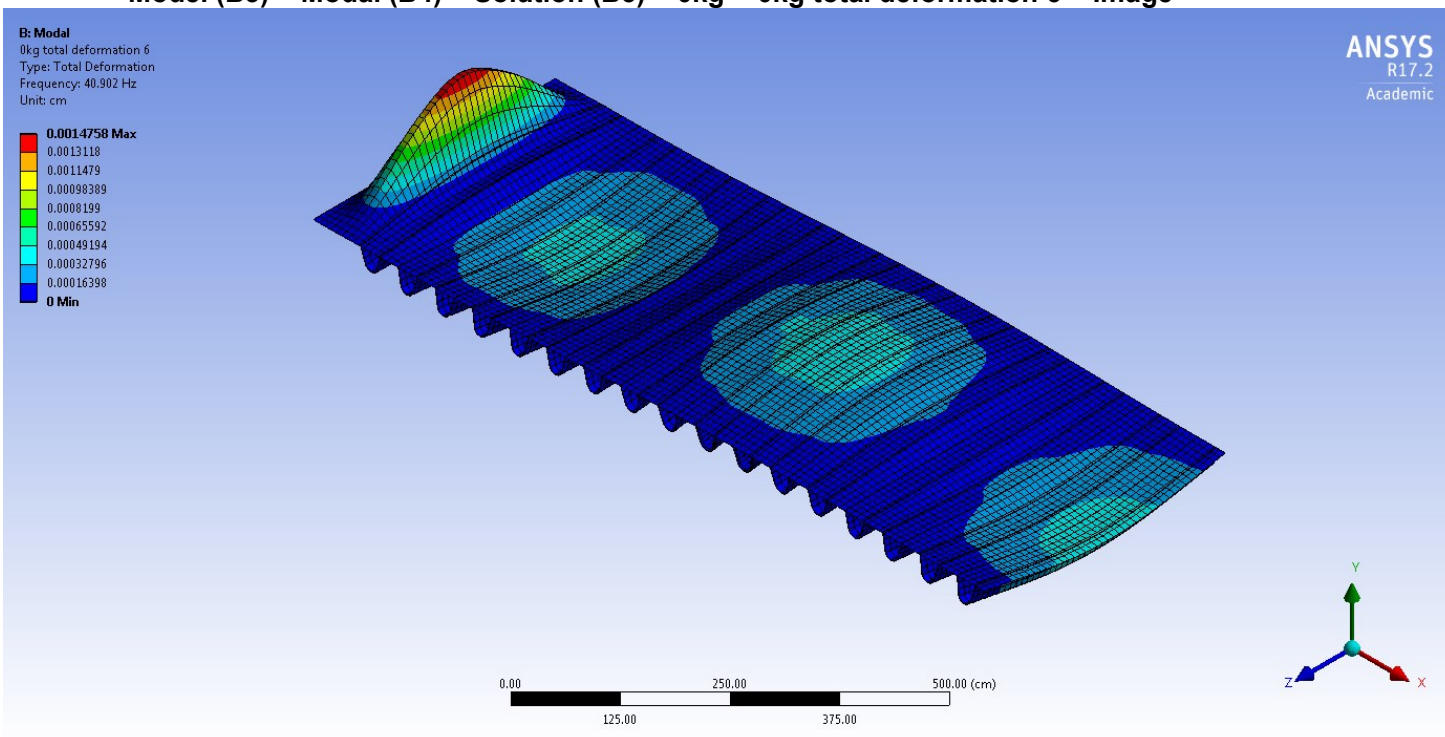


FIGURE 27
Model (B3) > Modal (B4) > Solution (B5) > 0kg > 0kg total deformation 7 > Image

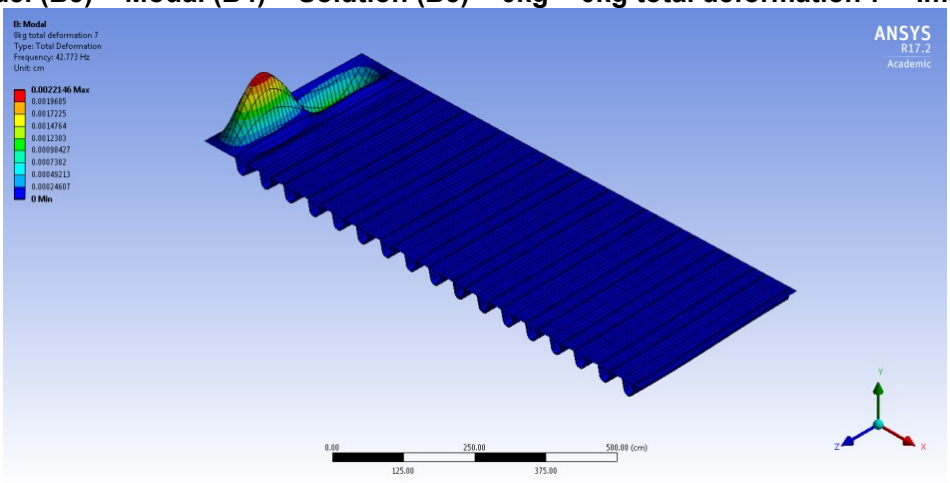


FIGURE 28
Model (B3) > Modal (B4) > Solution (B5) > 0kg > 0kg total deformation 8 > Image

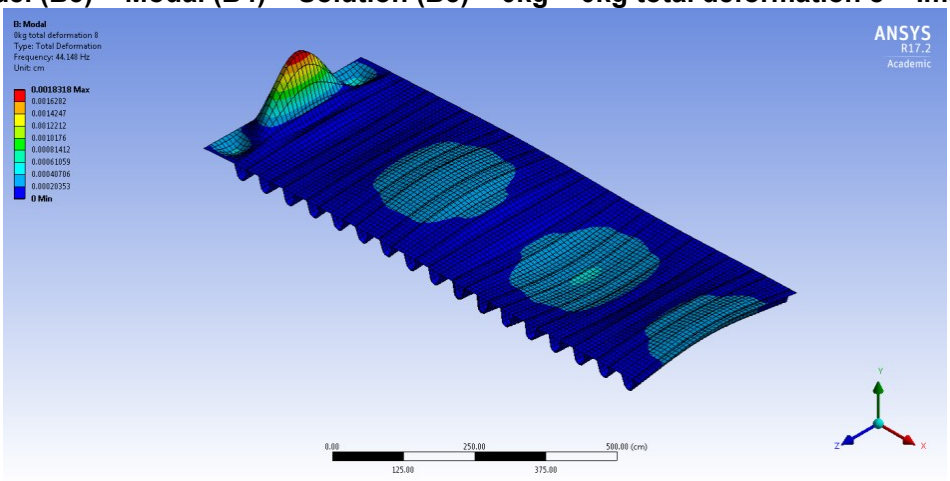


FIGURE 29
Model (B3) > Modal (B4) > Solution (B5) > 0kg > 0kg total deformation 9 > Image

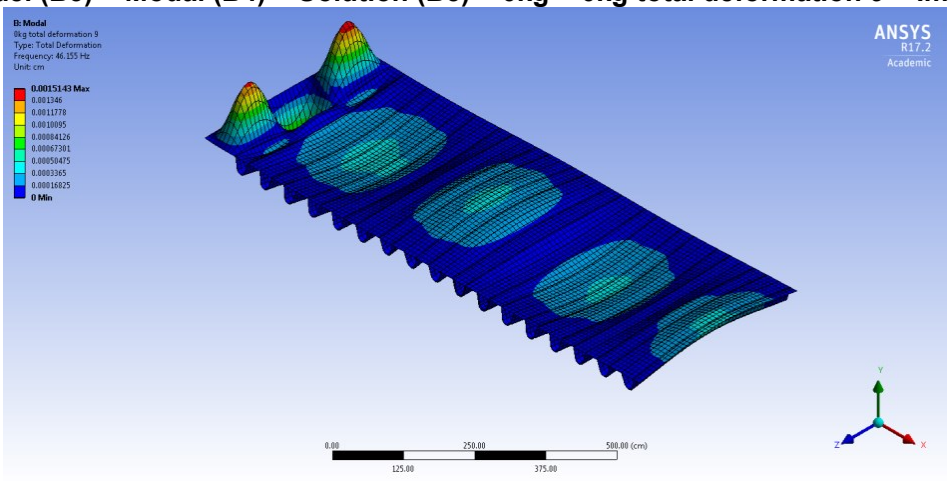


FIGURE 30
Model (B3) > Modal (B4) > Solution (B5) > 0kg > 0kg total deformation 10 > Image

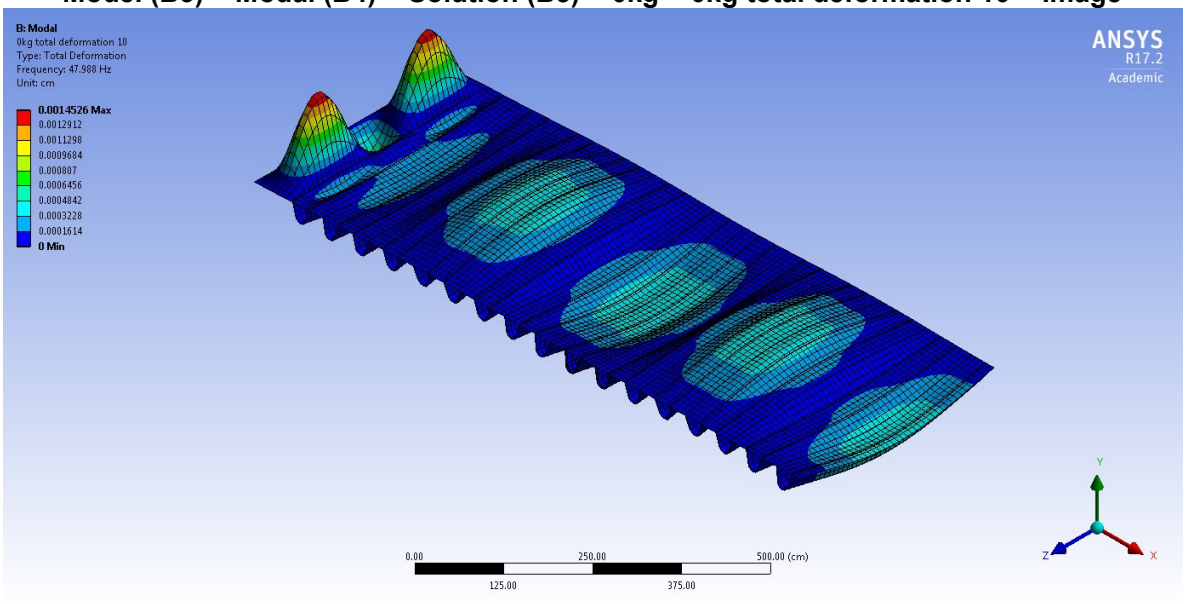


FIGURE 31
Model (B3) > Modal (B4) > Solution (B5) > 0kg > 0kg total deformation 11 > Image

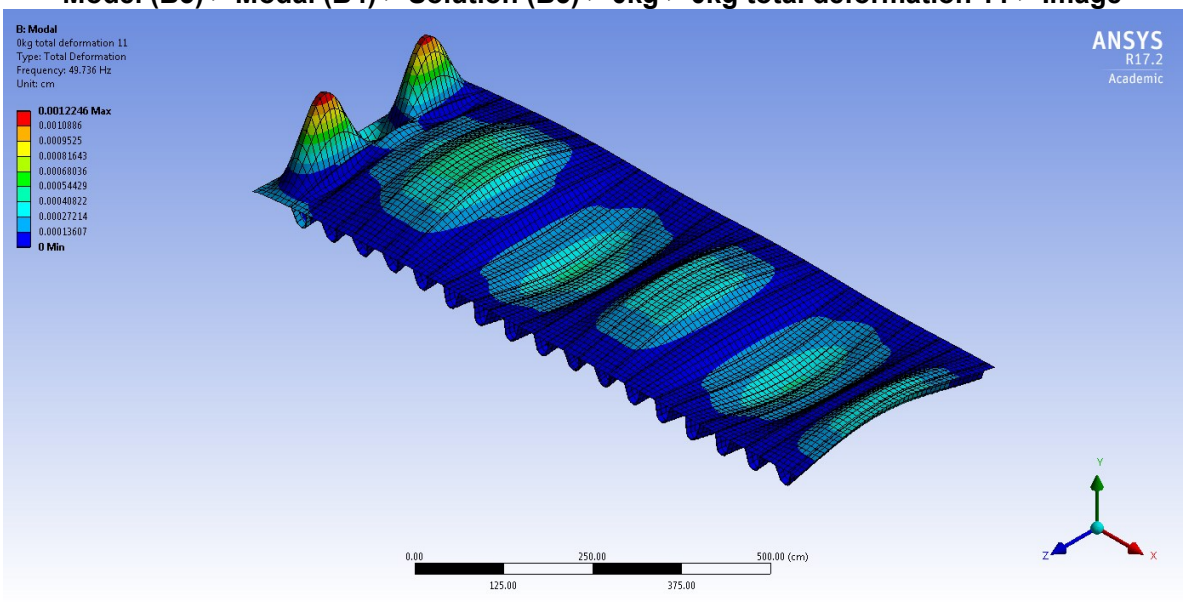


TABLE 126
Model (B3) > Modal (B4) > Solution (B5) > 0kg > Results

Object Name	*0kg total deformation 12*	*0kg total deformation 13*	*0kg total deformation 14*	*0kg total deformation 15*	*0kg total deformation 16*	*0kg total deformation 17*	*0kg total deformation 18*	*0kg total deformation 19*	*0kg total deformation 20*	*0kg total deformation 21*	*0kg total deformation 22*
State	Suppressed										
Scope											

Scoping Method	Geometry Selection										
Geometry	All Bodies										
Definition											
Type	Total Deformation										
Mode	12.	13.	14.	15.	16.	17.	18.	19.	20.	21.	22.
Identifier											
Suppressed	Yes										
Results											
Minimum											
Maximum											
Minimum Occurs On											
Maximum Occurs On											
Information											
Frequency											

FIGURE 32
Model (B3) > Modal (B4) > Solution (B5) > 0kg > 0kg total deformation 12 > Image

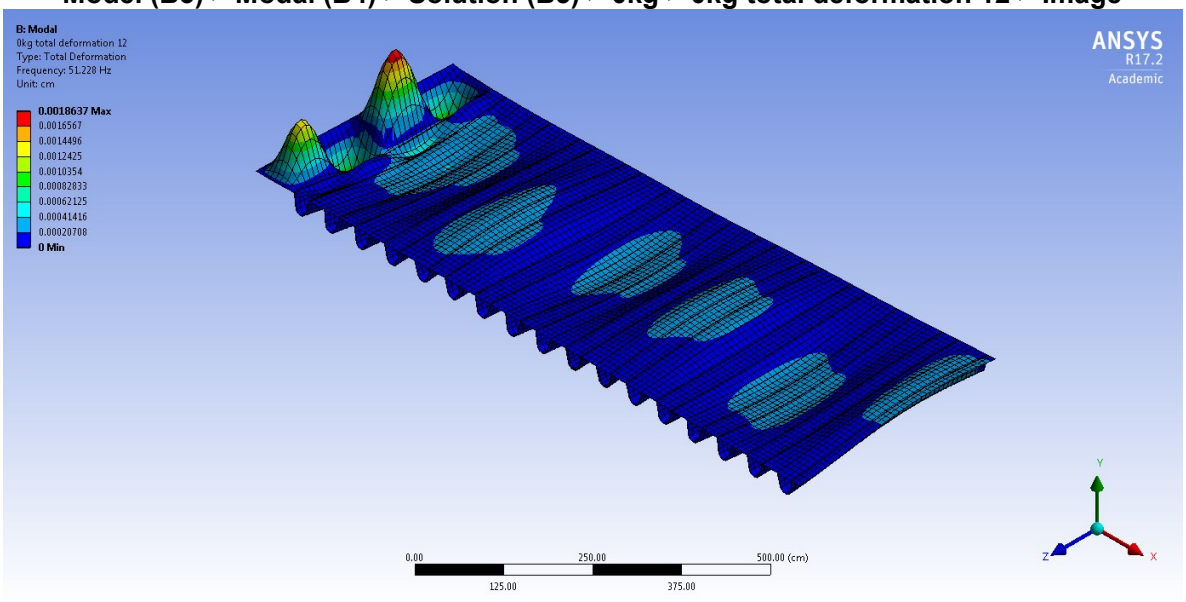


FIGURE 33
Model (B3) > Modal (B4) > Solution (B5) > 0kg > 0kg total deformation 13 > Image

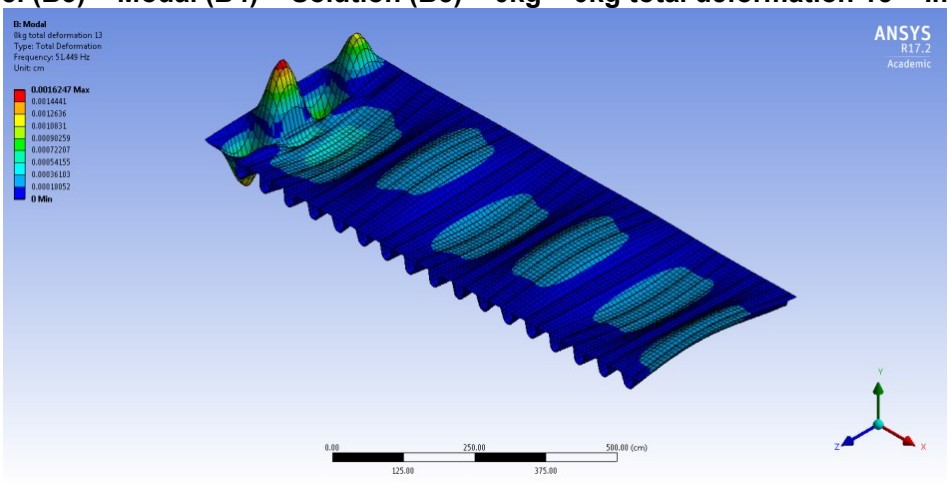


FIGURE 34
Model (B3) > Modal (B4) > Solution (B5) > 0kg > 0kg total deformation 14 > Image

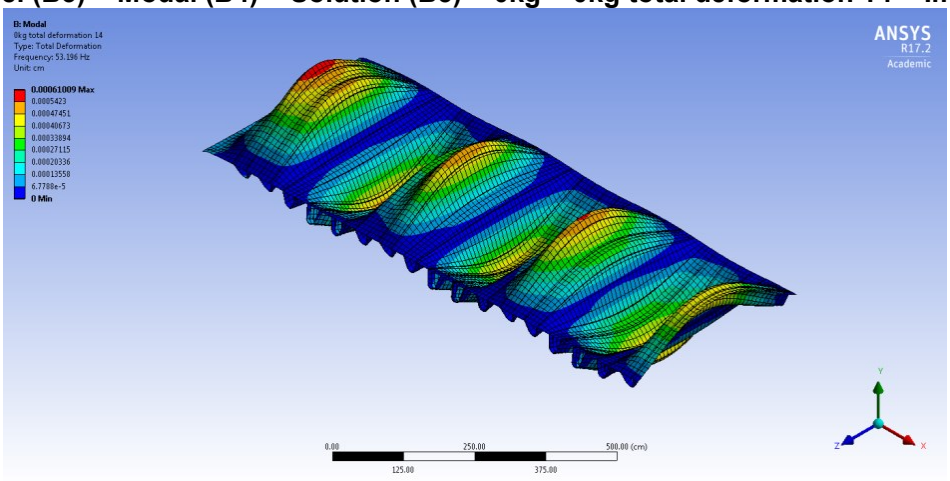


FIGURE 35
Model (B3) > Modal (B4) > Solution (B5) > 0kg > 0kg total deformation 15 > Image

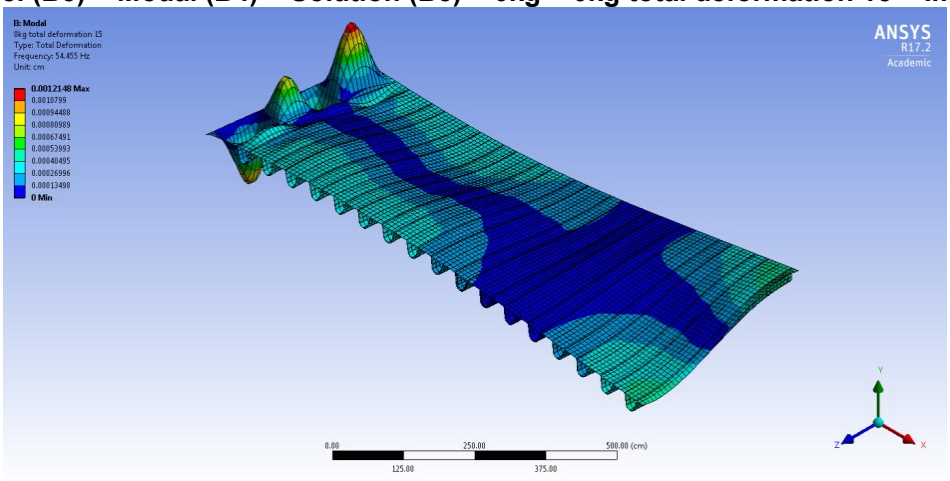


FIGURE 36
Model (B3) > Modal (B4) > Solution (B5) > 0kg > 0kg total deformation 16 > Image

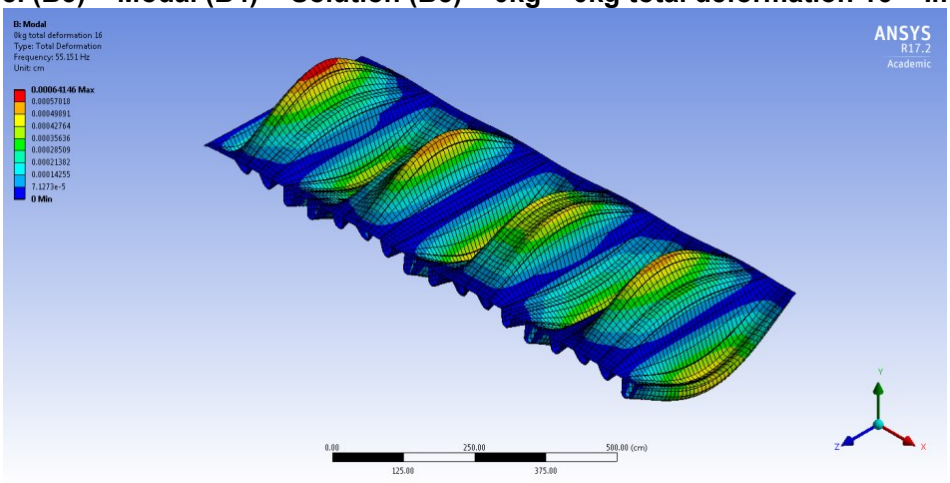


FIGURE 37
Model (B3) > Modal (B4) > Solution (B5) > 0kg > 0kg total deformation 17 > Image

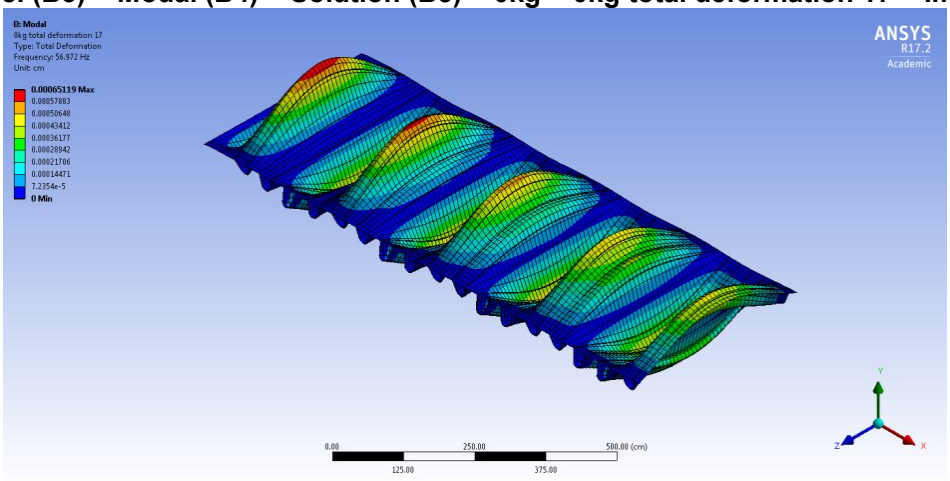


FIGURE 38
Model (B3) > Modal (B4) > Solution (B5) > 0kg > 0kg total deformation 18 > Image

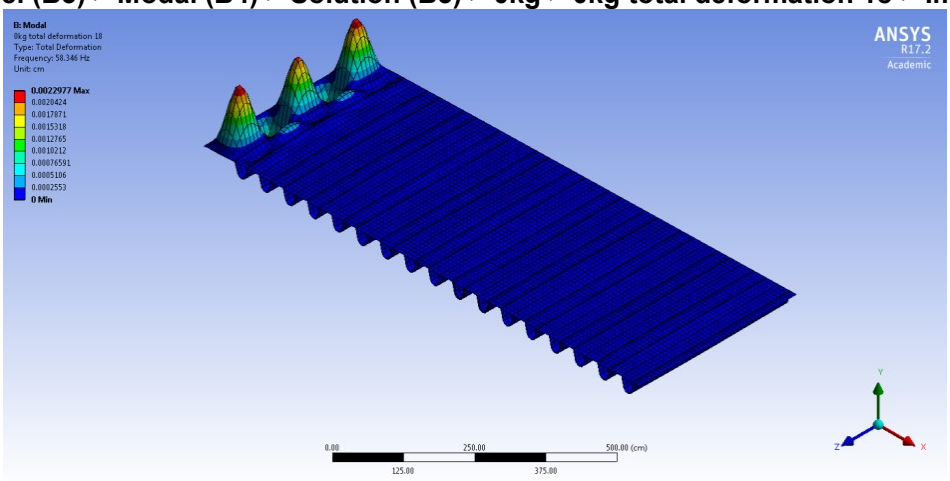


FIGURE 39
Model (B3) > Modal (B4) > Solution (B5) > 0kg > 0kg total deformation 19 > Image

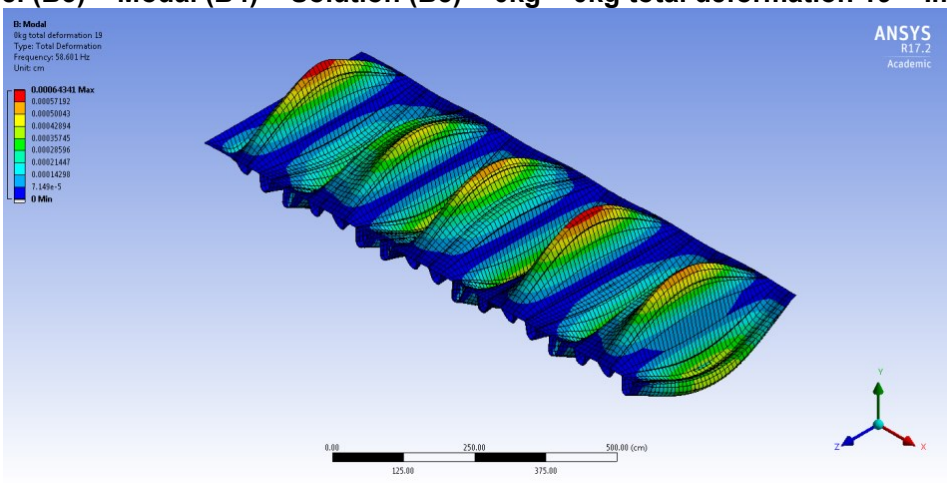


FIGURE 40
Model (B3) > Modal (B4) > Solution (B5) > 0kg > 0kg total deformation 20 > Image

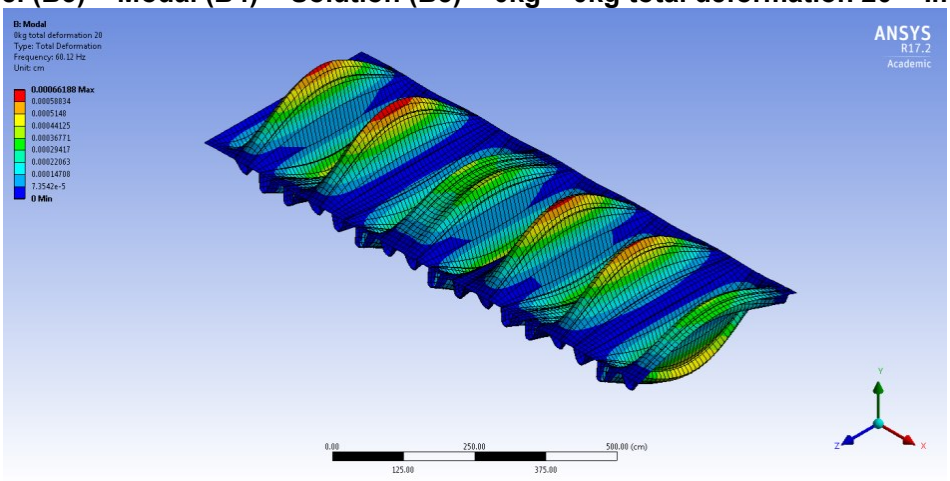


FIGURE 41
Model (B3) > Modal (B4) > Solution (B5) > 0kg > 0kg total deformation 21 > Image

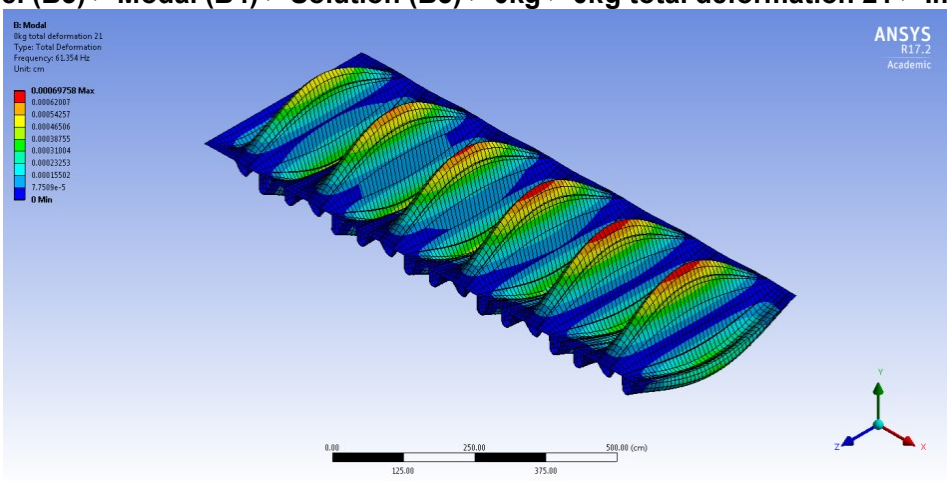


FIGURE 42
Model (B3) > Modal (B4) > Solution (B5) > 0kg > 0kg total deformation 22 > Image

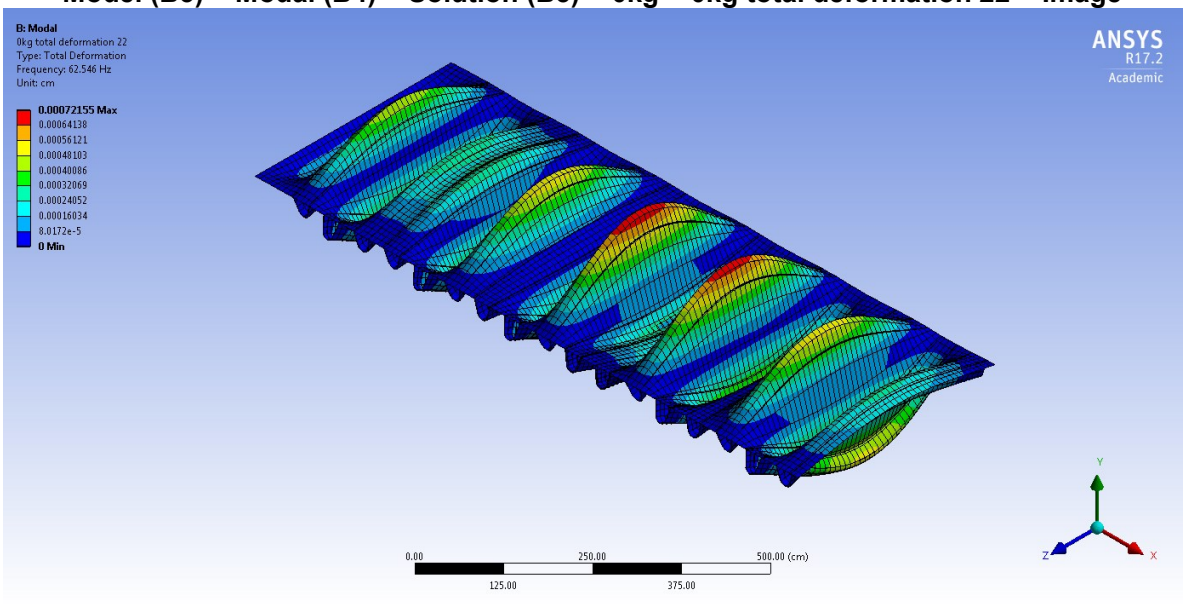


TABLE 127
Model (B3) > Modal (B4) > Solution (B5) > 0kg > Results

Object Name	*0kg total deformation 23*	*0kg total deformation 24*	*0kg total deformation 25*	*0kg total deformation 26*	*0kg total deformation 27*	*0kg total deformation 28*	*0kg total deformation 29*	*0kg total deformation 30*
State	Suppressed							
Scope								
Scoping Method	Geometry Selection							
Geometry	All Bodies							
Definition								
Type	Total Deformation							
Mode	23.	24.	25.	26.	27.	28.	29.	30.
Identifier								
Suppressed	Yes							
Results								
Minimum								
Maximum								
Minimum Occurs On								
Maximum Occurs On								
Information								
Frequency								

FIGURE 43
Model (B3) > Modal (B4) > Solution (B5) > 0kg > 0kg total deformation 23 > Image

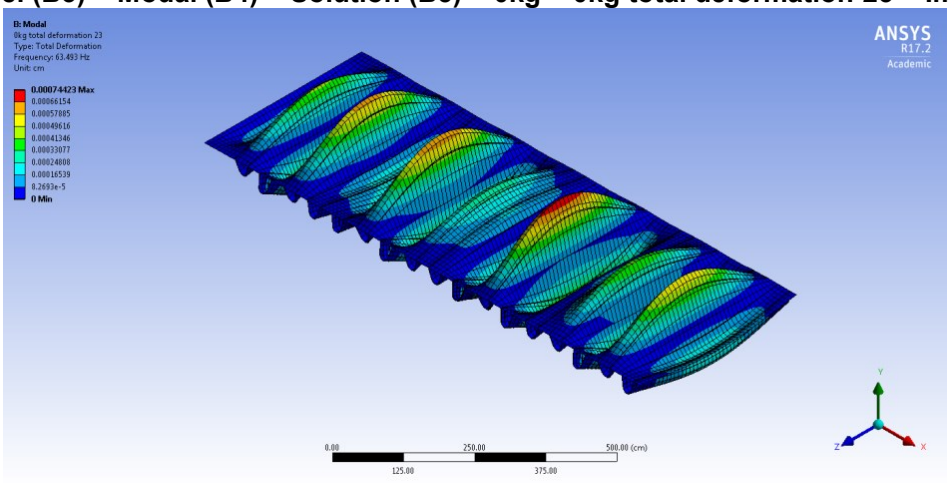


FIGURE 44
Model (B3) > Modal (B4) > Solution (B5) > 0kg > 0kg total deformation 24 > Image

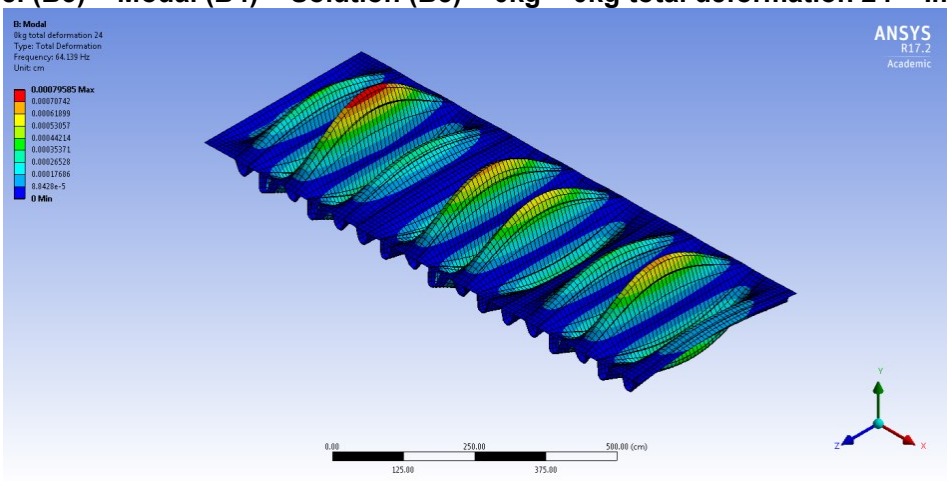


FIGURE 45
Model (B3) > Modal (B4) > Solution (B5) > 0kg > 0kg total deformation 25 > Image

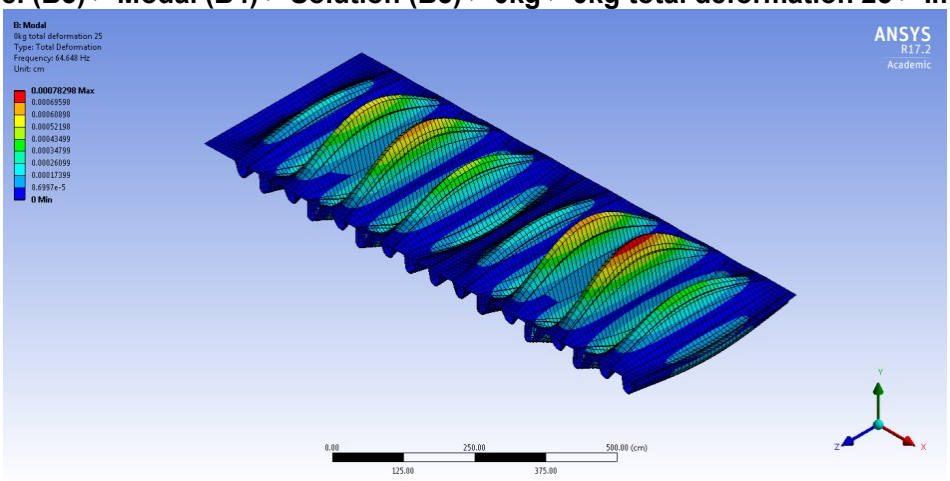


FIGURE 46
Model (B3) > Modal (B4) > Solution (B5) > 0kg > 0kg total deformation 26 > Image

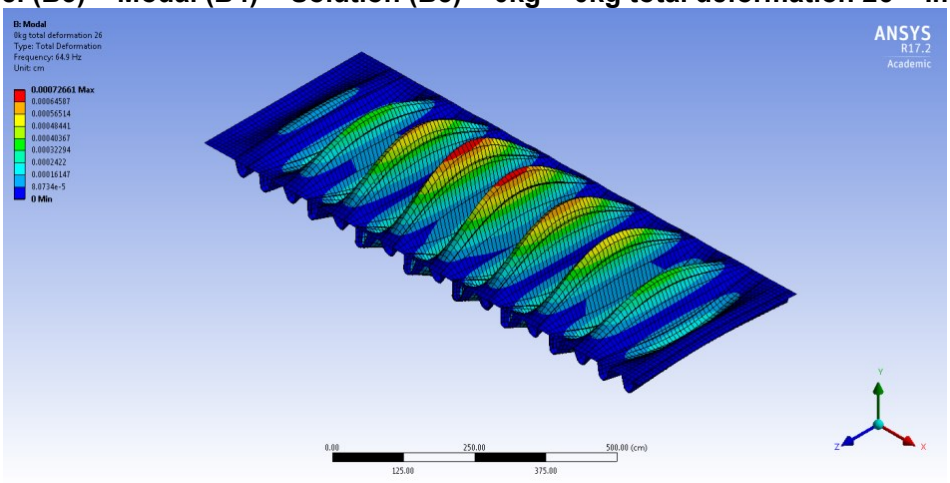


FIGURE 47
Model (B3) > Modal (B4) > Solution (B5) > 0kg > 0kg total deformation 27 > Image

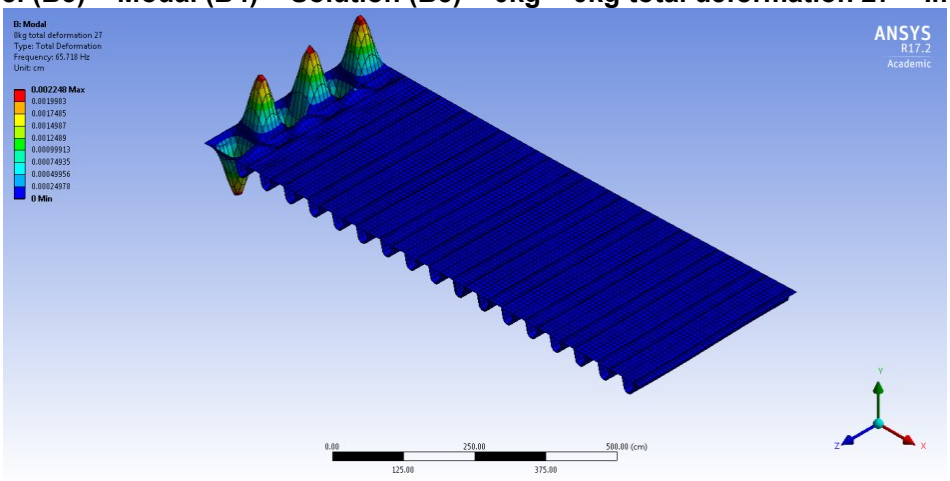


FIGURE 48
Model (B3) > Modal (B4) > Solution (B5) > 0kg > 0kg total deformation 28 > Image

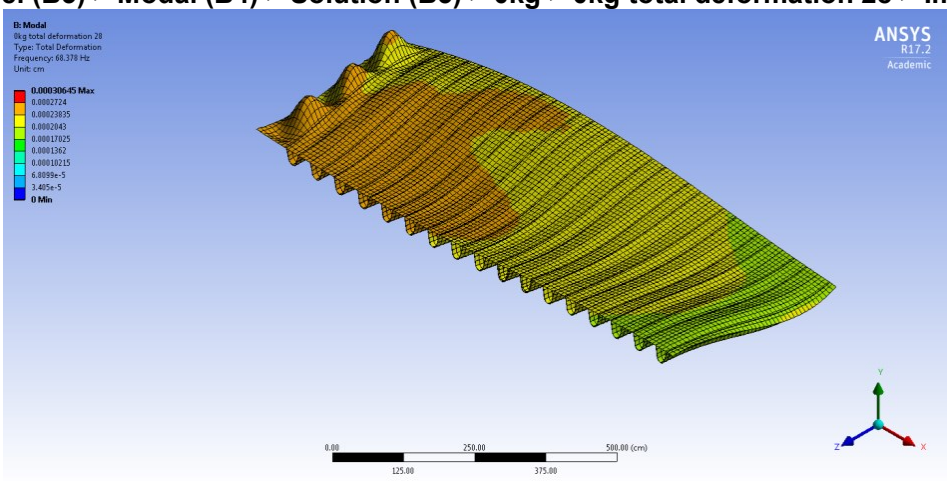


FIGURE 49
Model (B3) > Modal (B4) > Solution (B5) > 0kg > 0kg total deformation 29 > Image

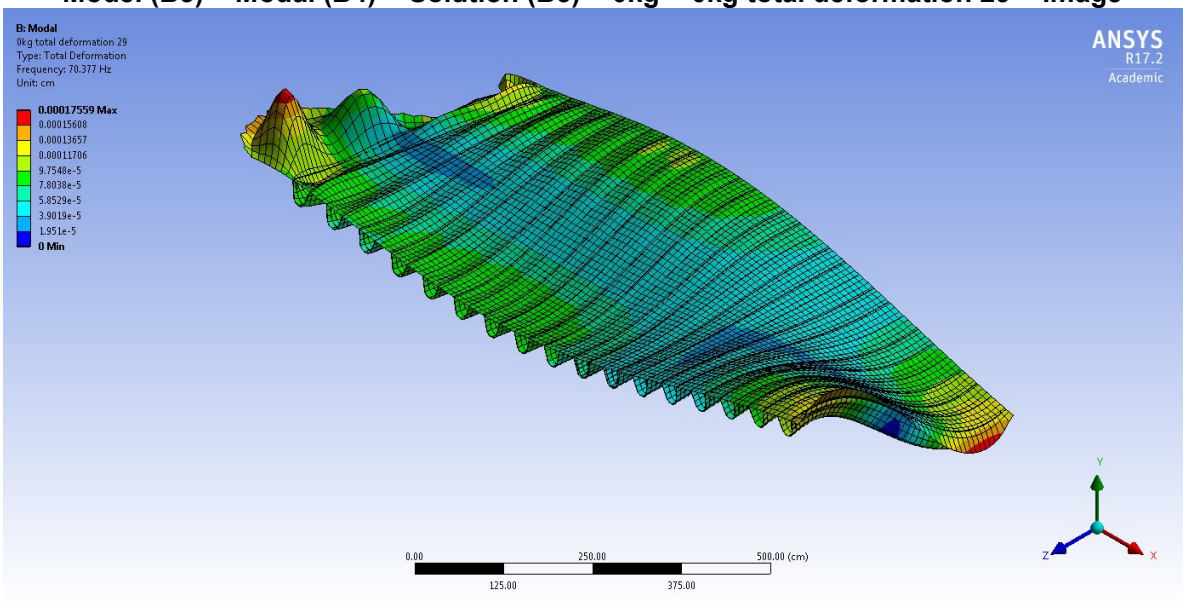
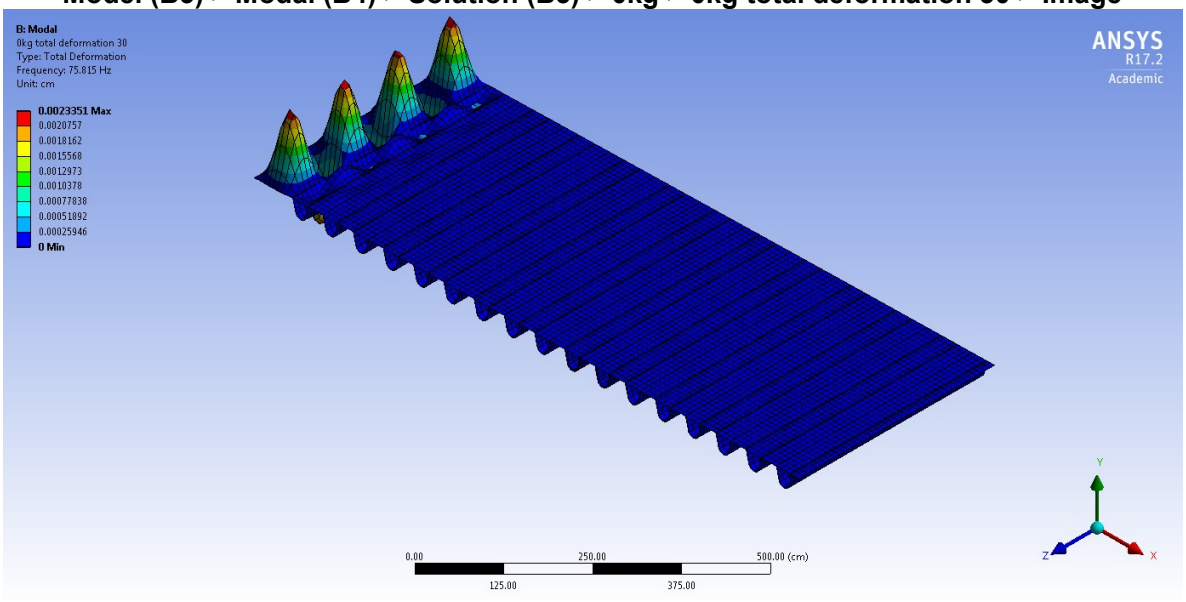


FIGURE 50
Model (B3) > Modal (B4) > Solution (B5) > 0kg > 0kg total deformation 30 > Image



50kg

TABLE 128
Model (B3) > Modal (B4) > Solution (B5) > 50kg > Results

Object Name	*50kg total deformation 1*	*50kg total deformation 2*	*50kg total deformation 3*	*50kg total deformation 4*	*50kg total deformation 5*	*50kg total deformation 6*	*50kg total deformation 7*	*50kg total deformation 8*	*50kg total deformation 9*	*50kg total deformation 10*	*50kg total deformation 11*
State	Suppressed										
Scope											

Scoping Method	Geometry Selection										
Geometry	All Bodies										
Definition											
Type	Total Deformation										
Mode	1.	2.	3.	4.	5.	6.	7.	8.	9.	10.	11.
Identifier											
Suppressed	Yes										
Results											
Minimum											
Maximum											
Minimum Occurs On											
Maximum Occurs On											
Information											
Frequency											

FIGURE 51
Model (B3) > Modal (B4) > Solution (B5) > 50kg > 50kg total deformation 1 > Image

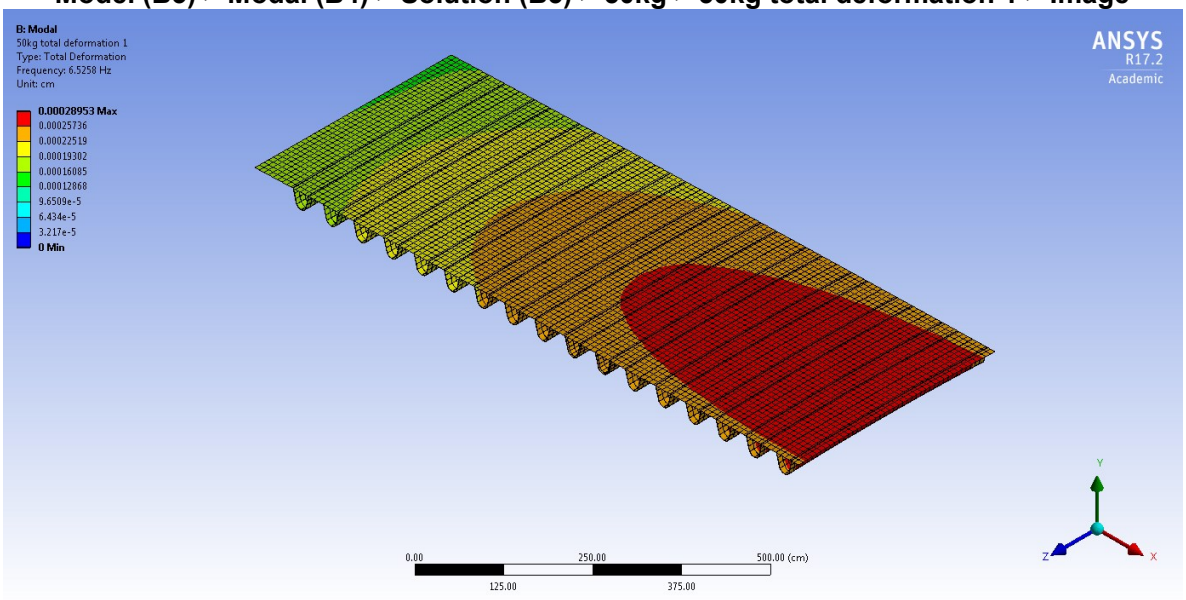


FIGURE 52
Model (B3) > Modal (B4) > Solution (B5) > 50kg > 50kg total deformation 2 > Image

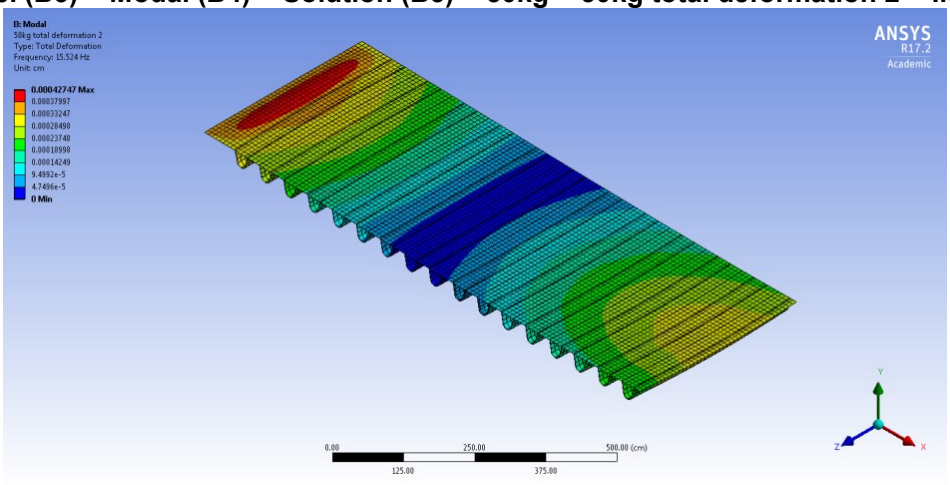


FIGURE 53
Model (B3) > Modal (B4) > Solution (B5) > 50kg > 50kg total deformation 3 > Image

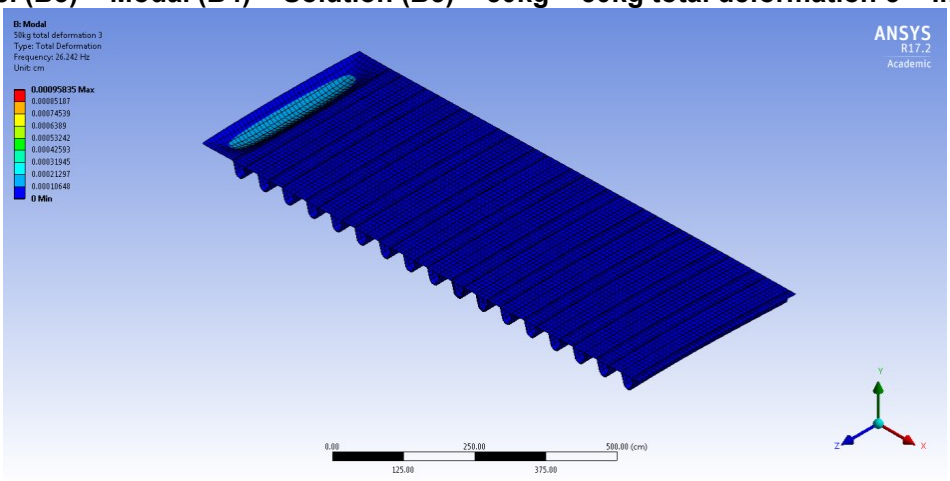


FIGURE 54
Model (B3) > Modal (B4) > Solution (B5) > 50kg > 50kg total deformation 4 > Image

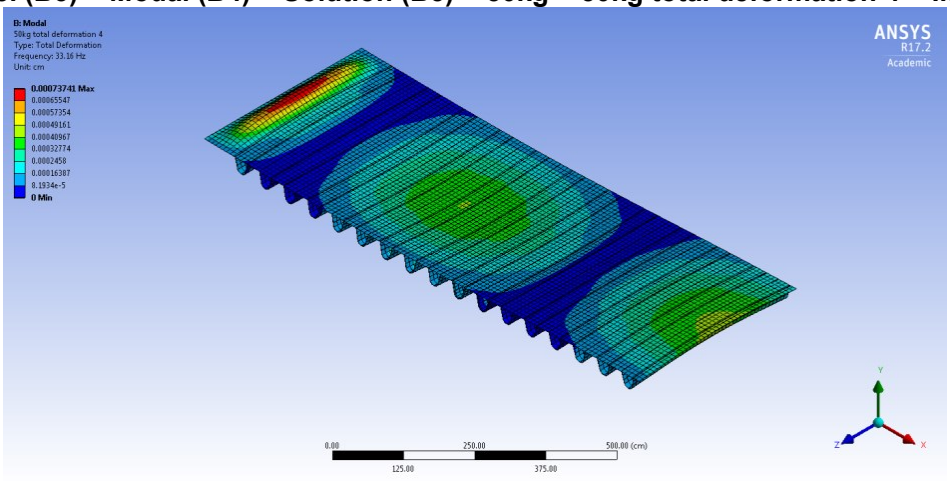


FIGURE 55
Model (B3) > Modal (B4) > Solution (B5) > 50kg > 50kg total deformation 5 > Image

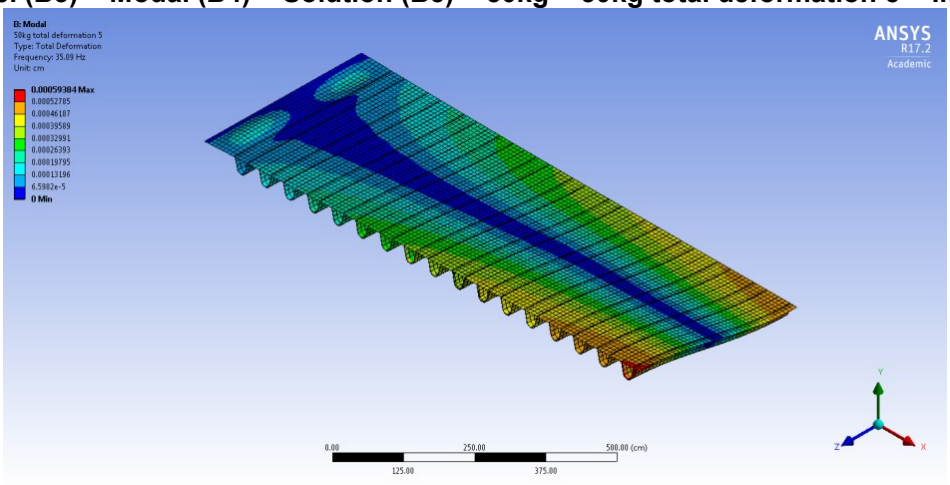


FIGURE 56
Model (B3) > Modal (B4) > Solution (B5) > 50kg > 50kg total deformation 6 > Image

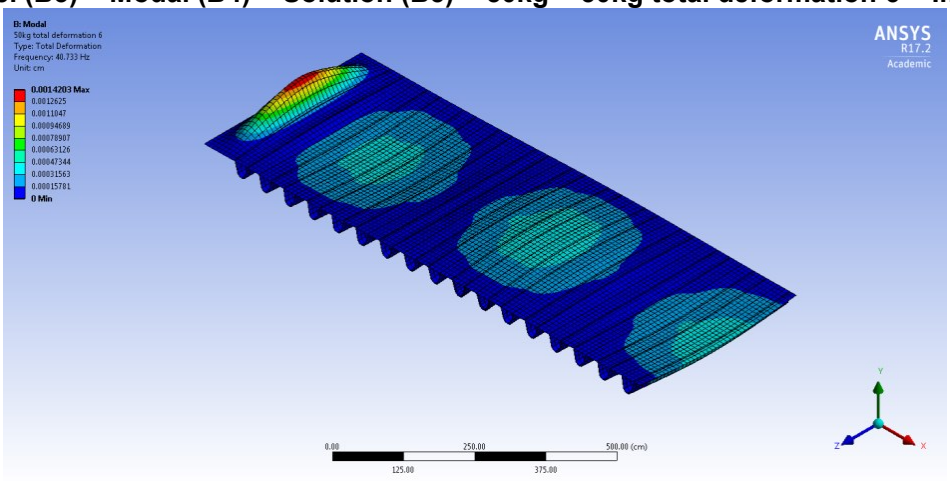


FIGURE 57
Model (B3) > Modal (B4) > Solution (B5) > 50kg > 50kg total deformation 7 > Image

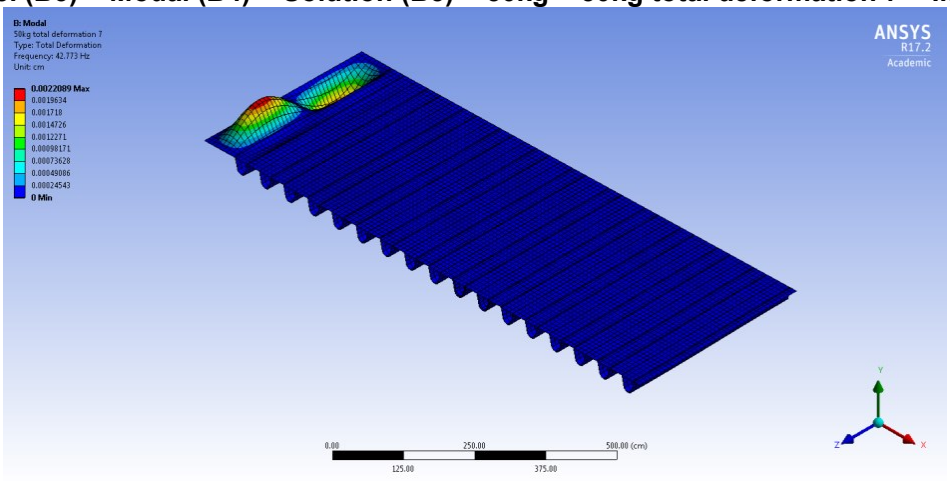


FIGURE 58
Model (B3) > Modal (B4) > Solution (B5) > 50kg > 50kg total deformation 8 > Image

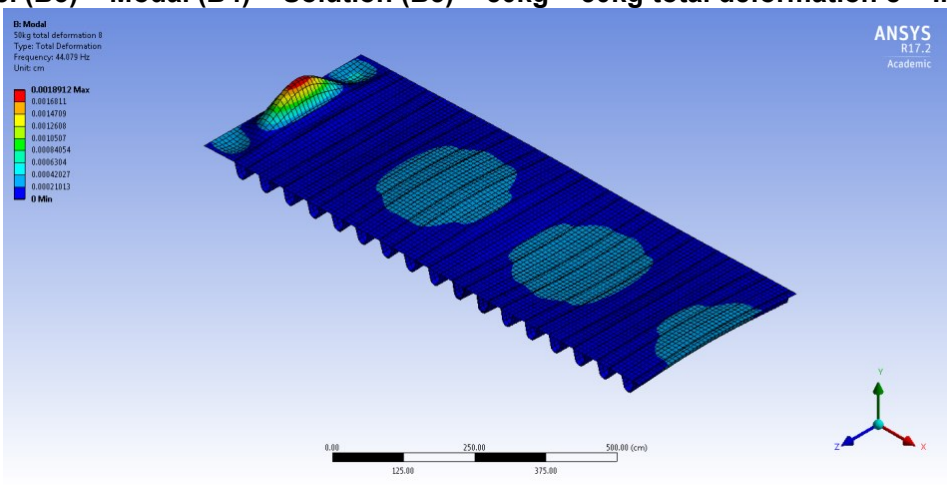


FIGURE 59
Model (B3) > Modal (B4) > Solution (B5) > 50kg > 50kg total deformation 9 > Image

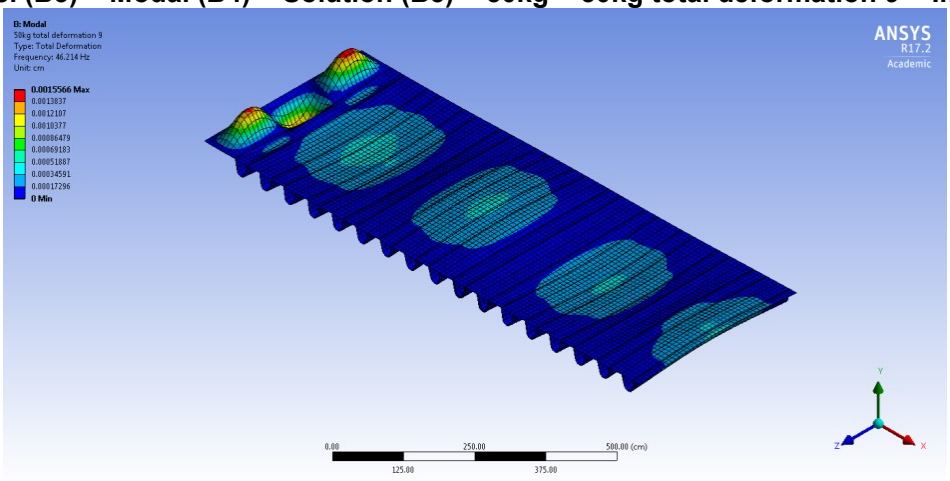


FIGURE 60
Model (B3) > Modal (B4) > Solution (B5) > 50kg > 50kg total deformation 10 > Image

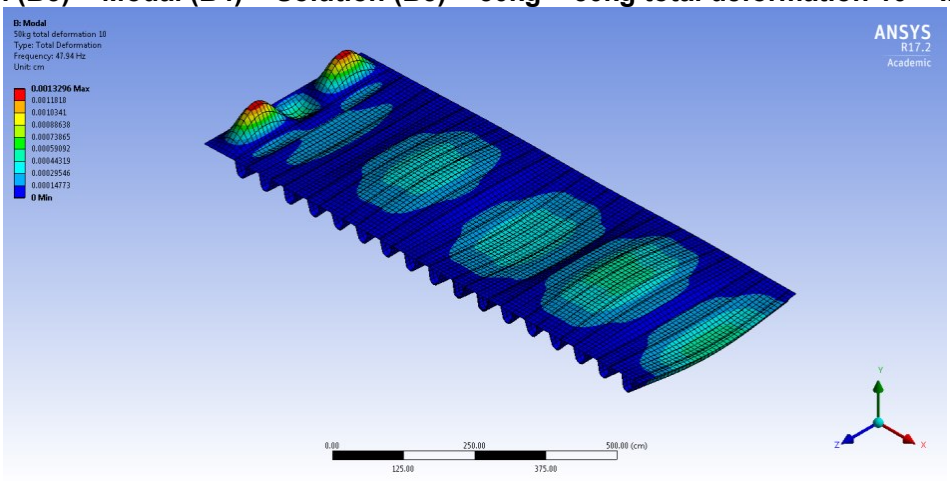


FIGURE 61
Model (B3) > Modal (B4) > Solution (B5) > 50kg > 50kg total deformation 11 > Image

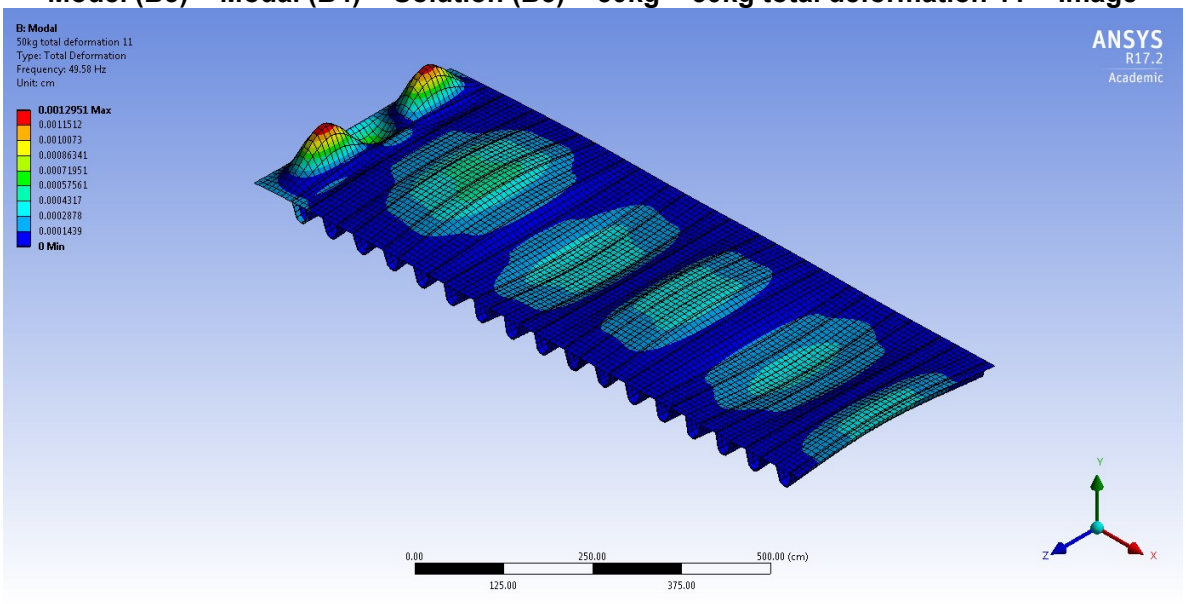


TABLE 129
Model (B3) > Modal (B4) > Solution (B5) > 50kg > Results

Object Name	*50kg total deformation 12*	*50kg total deformation 13*	*50kg total deformation 14*	*50kg total deformation 15*	*50kg total deformation 16*	*50kg total deformation 17*	*50kg total deformation 18*	*50kg total deformation 19*	*50kg total deformation 20*	*50kg total deformation 21*	*50kg total deformation 22*
State	Suppressed										
Scope											
Scoping Method	Geometry Selection										
Geometry	All Bodies										
Definition											
Type	Total Deformation										
Mode	12.	13.	14.	15.	16.	17.	18.	19.	20.	21.	22.
Identifier											
Suppressed	Yes										

FIGURE 62
Model (B3) > Modal (B4) > Solution (B5) > 50kg > 50kg total deformation 12 > Image

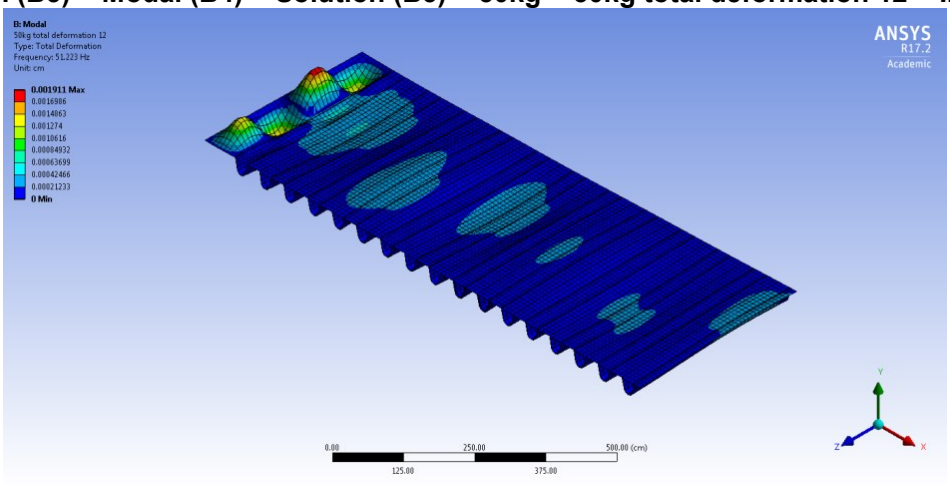


FIGURE 63
Model (B3) > Modal (B4) > Solution (B5) > 50kg > 50kg total deformation 13 > Image

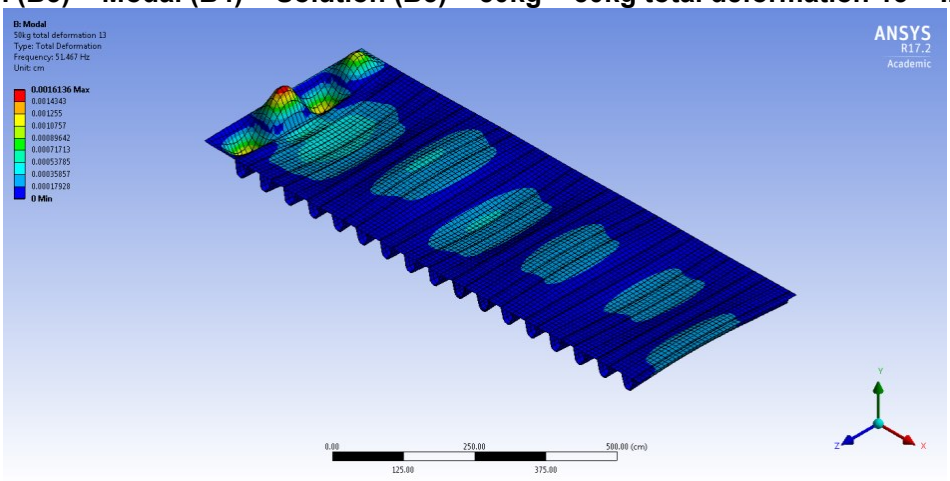


FIGURE 64
Model (B3) > Modal (B4) > Solution (B5) > 50kg > 50kg total deformation 14 > Image

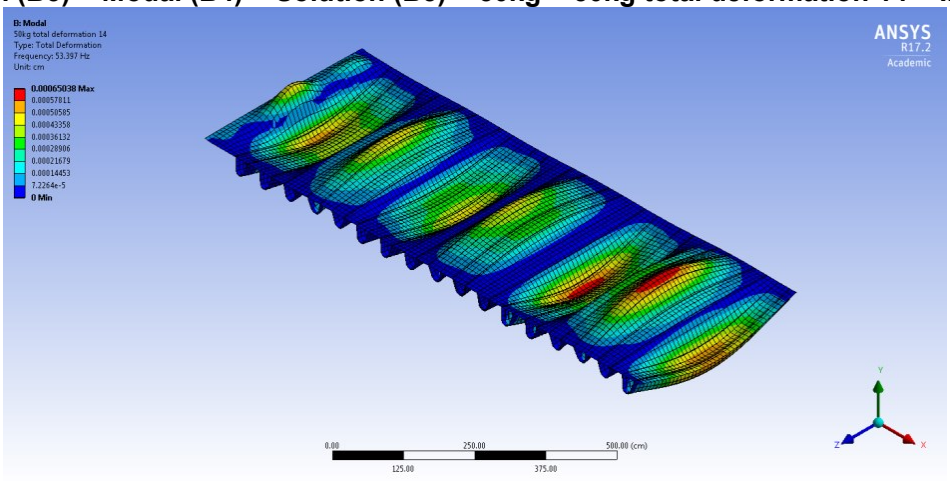


FIGURE 65
Model (B3) > Modal (B4) > Solution (B5) > 50kg > 50kg total deformation 15 > Image

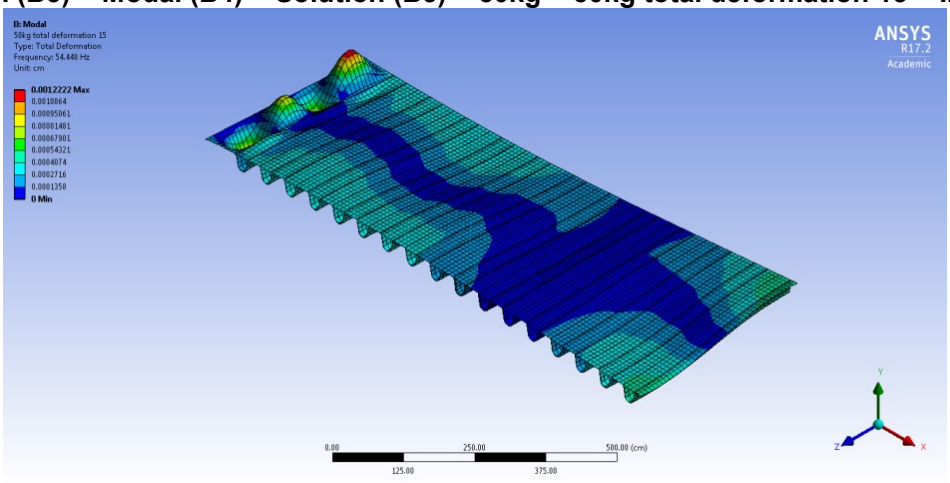


FIGURE 66
Model (B3) > Modal (B4) > Solution (B5) > 50kg > 50kg total deformation 16 > Image

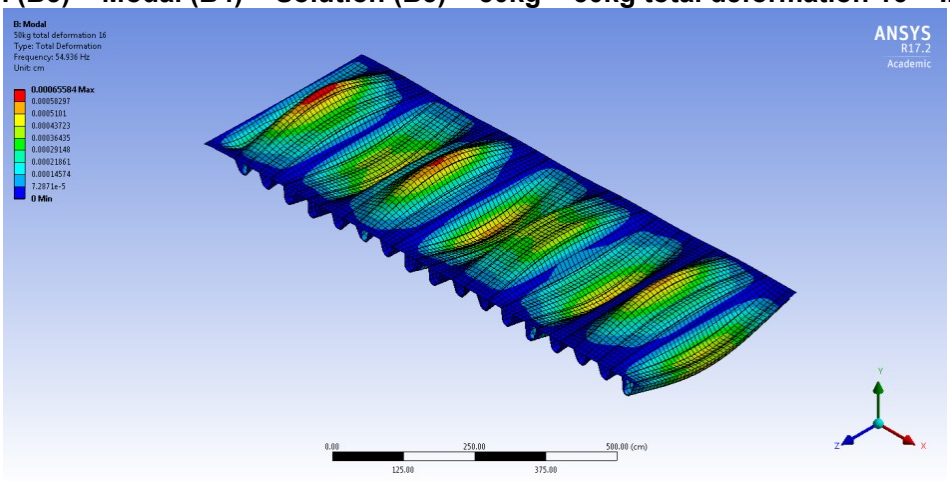


FIGURE 67
Model (B3) > Modal (B4) > Solution (B5) > 50kg > 50kg total deformation 17 > Image

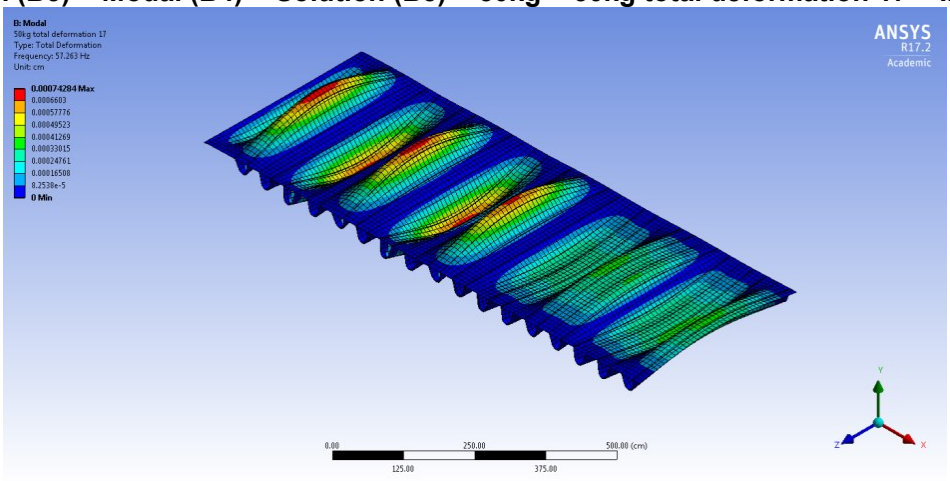


FIGURE 68
Model (B3) > Modal (B4) > Solution (B5) > 50kg > 50kg total deformation 18 > Image

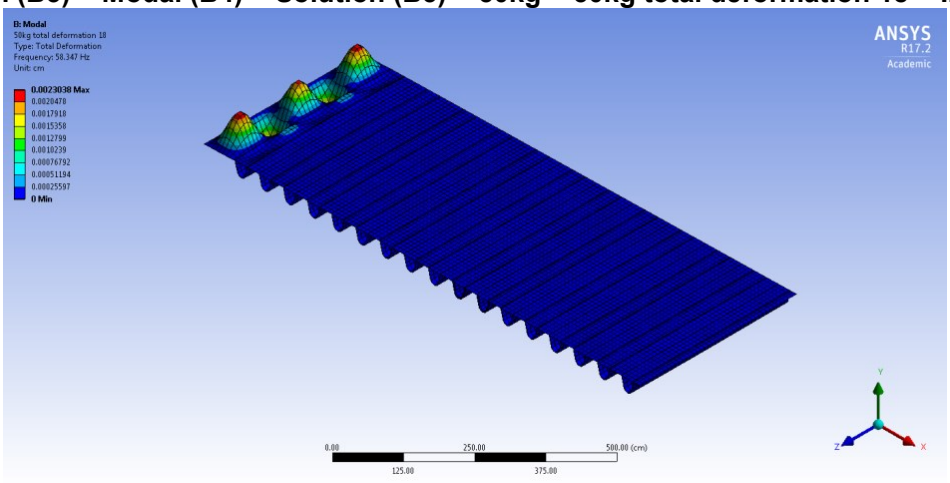


FIGURE 69
Model (B3) > Modal (B4) > Solution (B5) > 50kg > 50kg total deformation 19 > Image

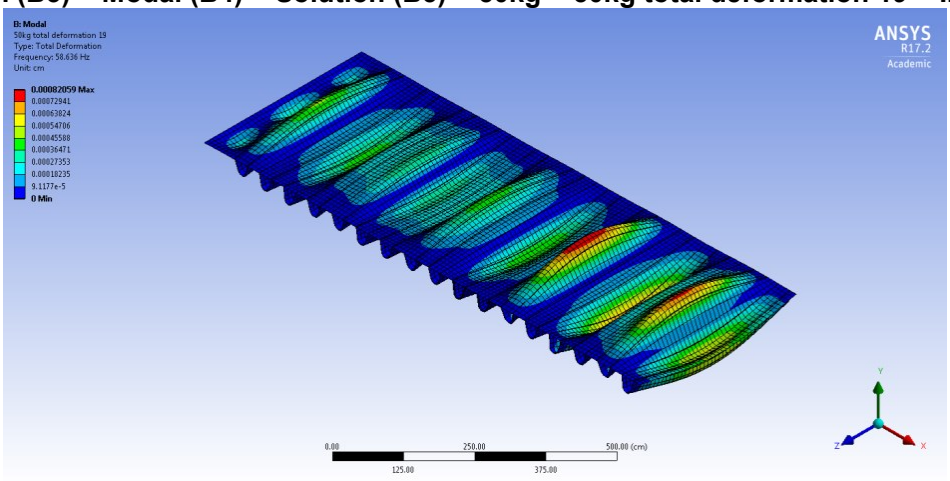


FIGURE 70
Model (B3) > Modal (B4) > Solution (B5) > 50kg > 50kg total deformation 20 > Image

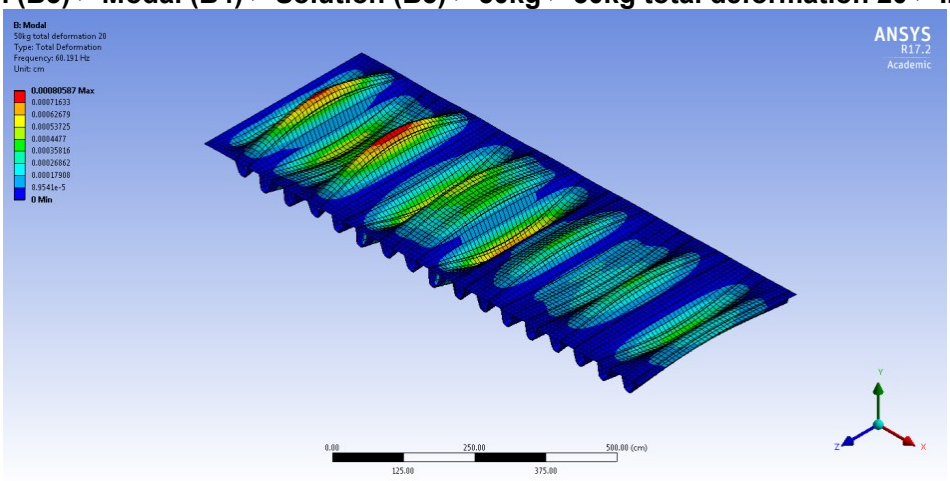


FIGURE 71
Model (B3) > Modal (B4) > Solution (B5) > 50kg > 50kg total deformation 21 > Image

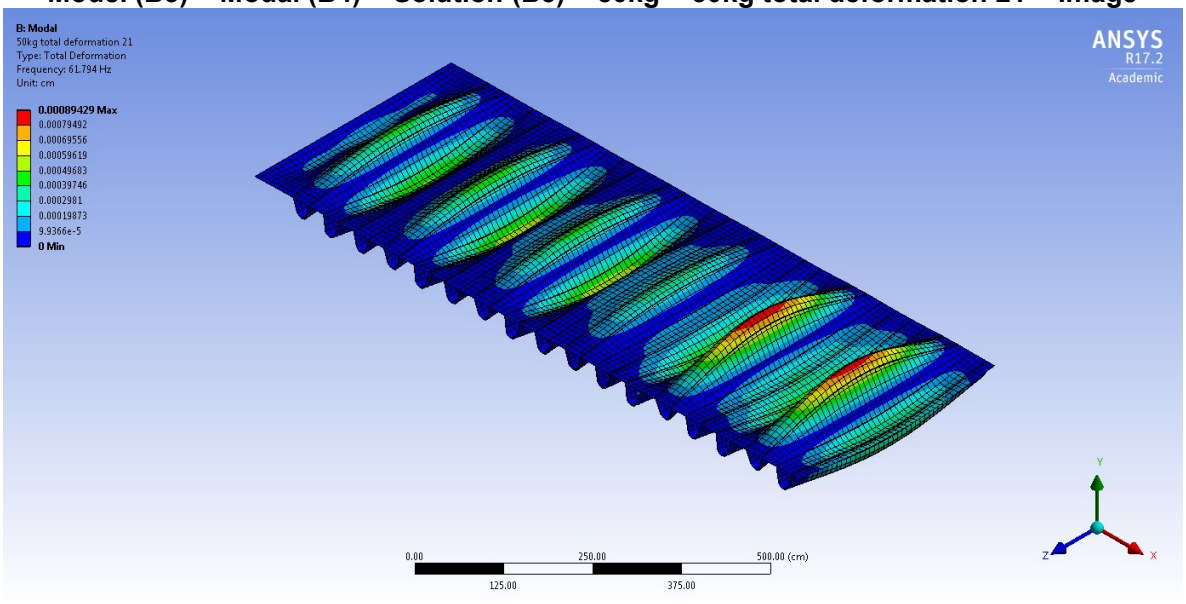


FIGURE 72
Model (B3) > Modal (B4) > Solution (B5) > 50kg > 50kg total deformation 22 > Image

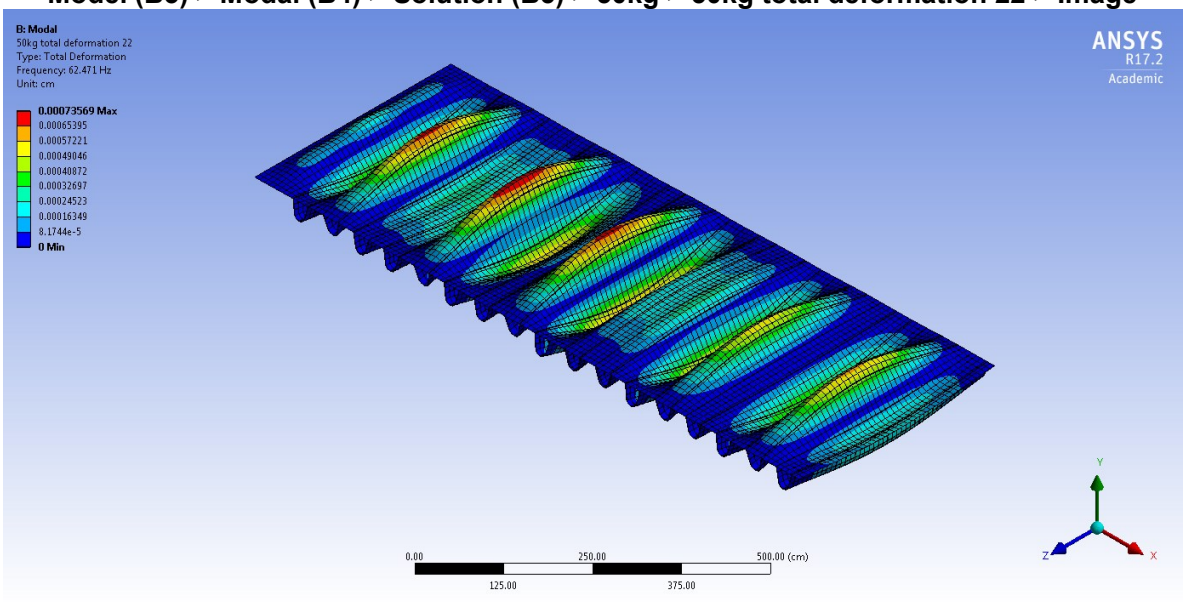


TABLE 130
Model (B3) > Modal (B4) > Solution (B5) > 50kg > Results

Object Name	*50kg total deformation 23*	*50kg total deformation 24*	*50kg total deformation 25*	*50kg total deformation 26*	*50kg total deformation 27*	*50kg total deformation 28*	*50kg total deformation 29*	*50kg total deformation 30*
State	Suppressed							
Scope								
Scoping Method	Geometry Selection							
Geometry	All Bodies							
Definition								

Type	Total Deformation							
Mode	23.	24.	25.	26.	27.	28.	29.	30.
Identifier								
Suppressed	Yes							

FIGURE 73
Model (B3) > Modal (B4) > Solution (B5) > 50kg > 50kg total deformation 23 > Image

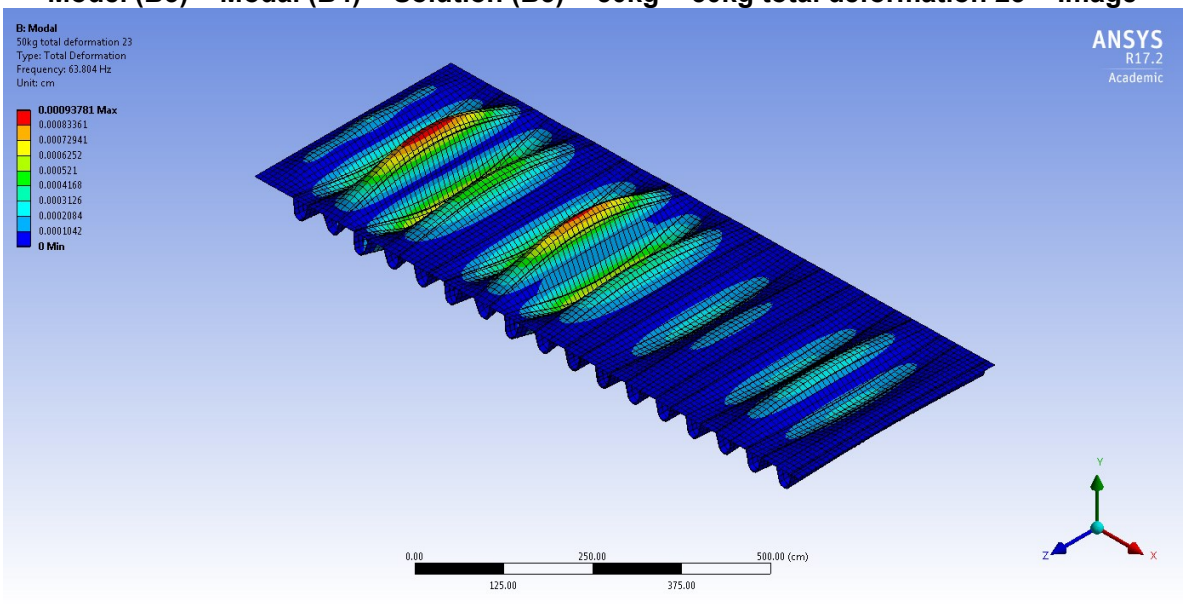


FIGURE 74
Model (B3) > Modal (B4) > Solution (B5) > 50kg > 50kg total deformation 24 > Image

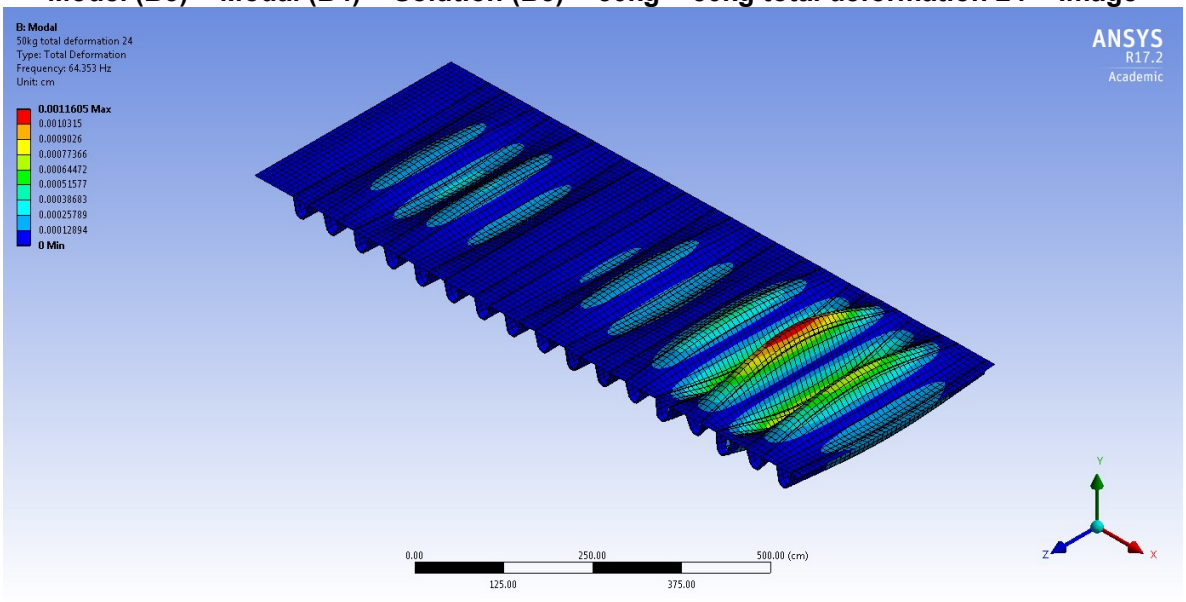


FIGURE 75
Model (B3) > Modal (B4) > Solution (B5) > 50kg > 50kg total deformation 25 > Image

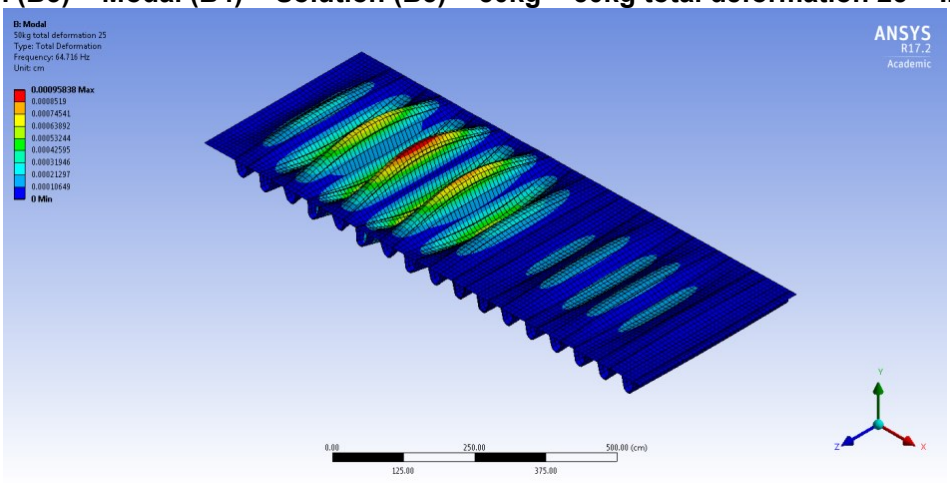


FIGURE 76
Model (B3) > Modal (B4) > Solution (B5) > 50kg > 50kg total deformation 26 > Image

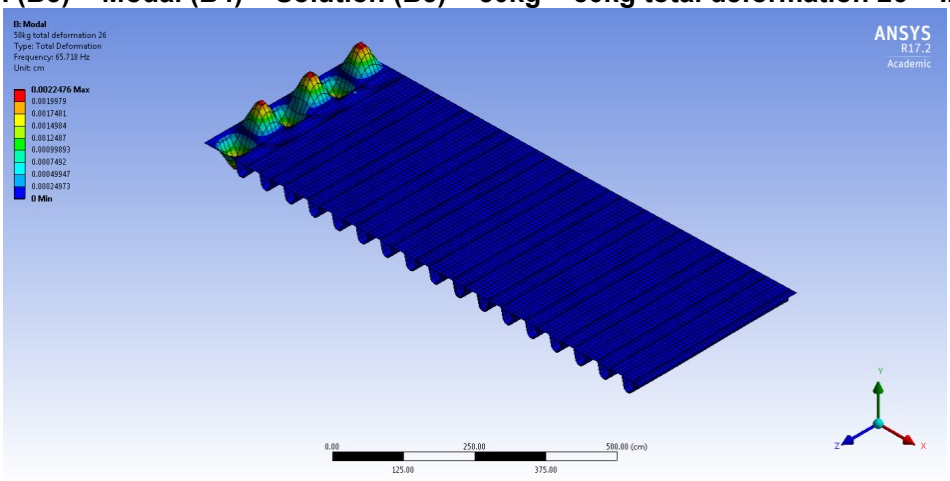


FIGURE 77
Model (B3) > Modal (B4) > Solution (B5) > 50kg > 50kg total deformation 27 > Image

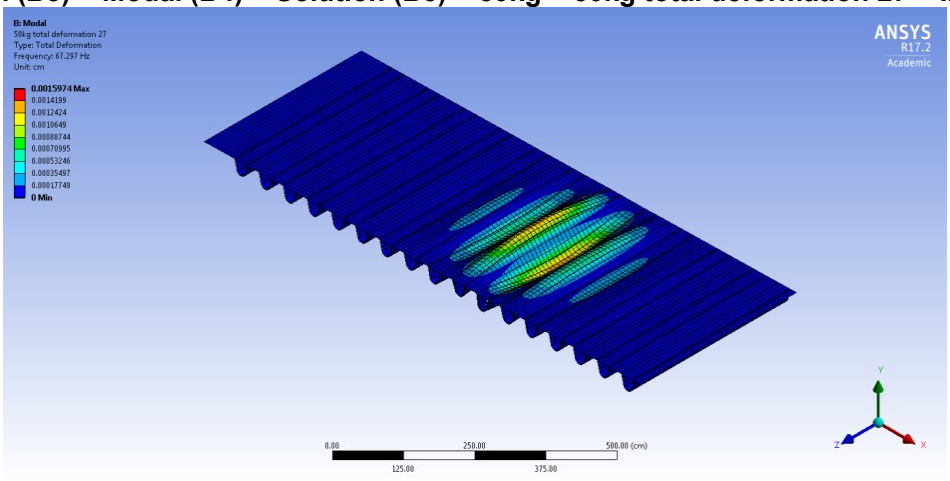


FIGURE 78
Model (B3) > Modal (B4) > Solution (B5) > 50kg > 50kg total deformation 27 > Image

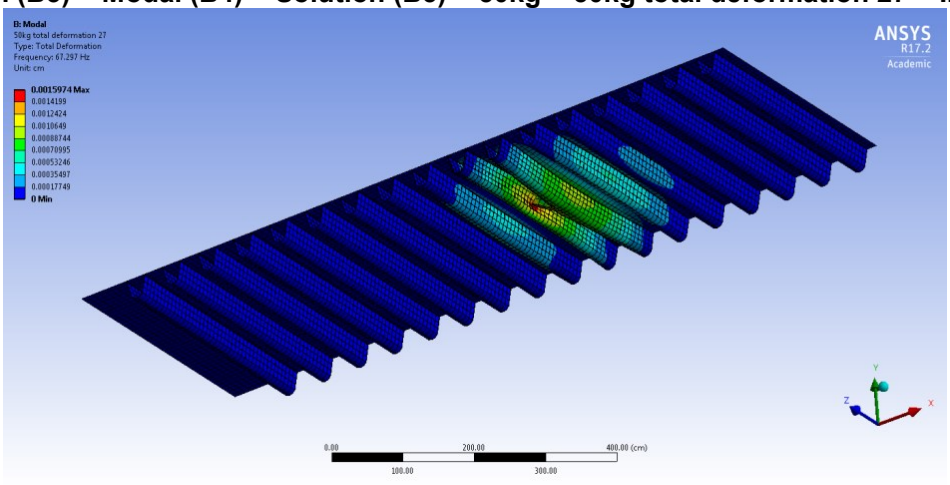


FIGURE 79
Model (B3) > Modal (B4) > Solution (B5) > 50kg > 50kg total deformation 28 > Image

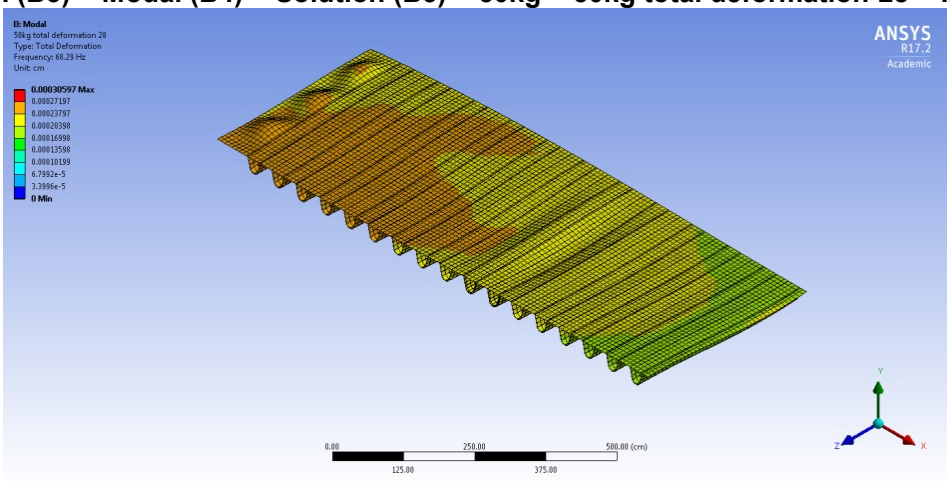


FIGURE 80
Model (B3) > Modal (B4) > Solution (B5) > 50kg > 50kg total deformation 29 > Image

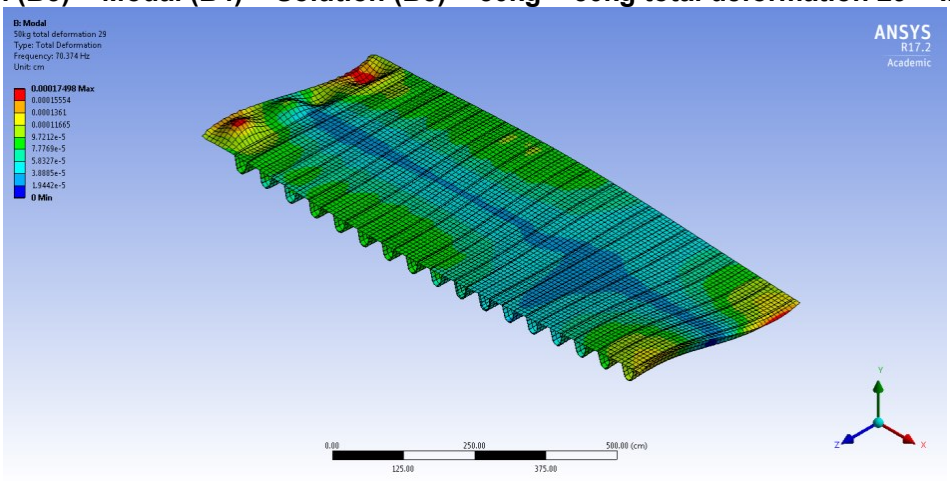
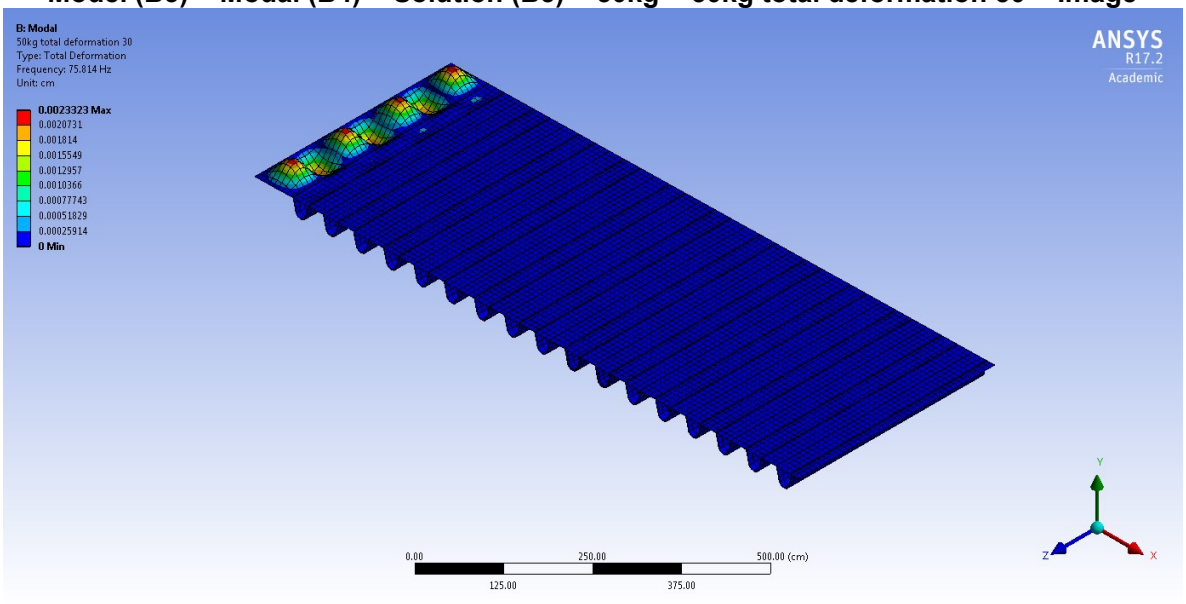


FIGURE 81
Model (B3) > Modal (B4) > Solution (B5) > 50kg > 50kg total deformation 30 > Image



75kg

TABLE 131
Model (B3) > Modal (B4) > Solution (B5) > 75kg > Results

Object Name	*75kg total deformation 1*	*75kg total deformation 2*	*75kg total deformation 3*	*75kg total deformation 4*	*75kg total deformation 5*	*75kg total deformation 6*	*75kg total deformation 7*	*75kg total deformation 8*	*75kg total deformation 9*	*75kg total deformation 10*	*75kg total deformation 11*
State	Suppressed										
Scope											
Scoping Method	Geometry Selection										
Geometry	All Bodies										
Definition											
Type	Total Deformation										
Mode	1.	2.	3.	4.	5.	6.	7.	8.	9.	10.	11.
Identifier											
Suppressed	Yes										

FIGURE 82
Model (B3) > Modal (B4) > Solution (B5) > 75kg > 75kg total deformation 1 > Image

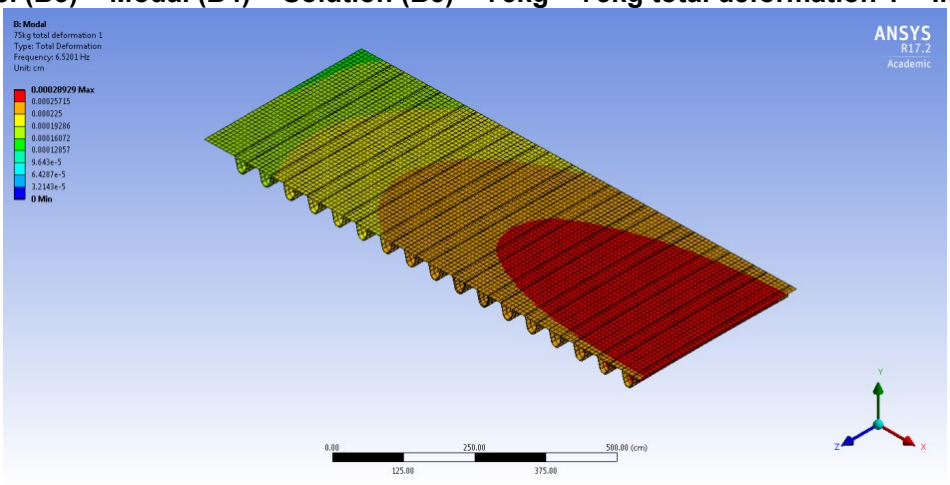


FIGURE 83
Model (B3) > Modal (B4) > Solution (B5) > 75kg > 75kg total deformation 2 > Image

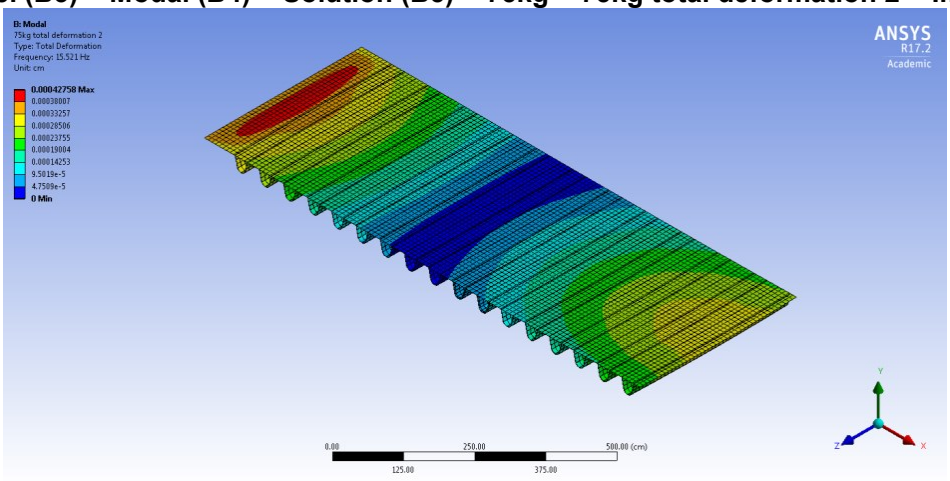


FIGURE 84
Model (B3) > Modal (B4) > Solution (B5) > 75kg > 75kg total deformation 3 > Image

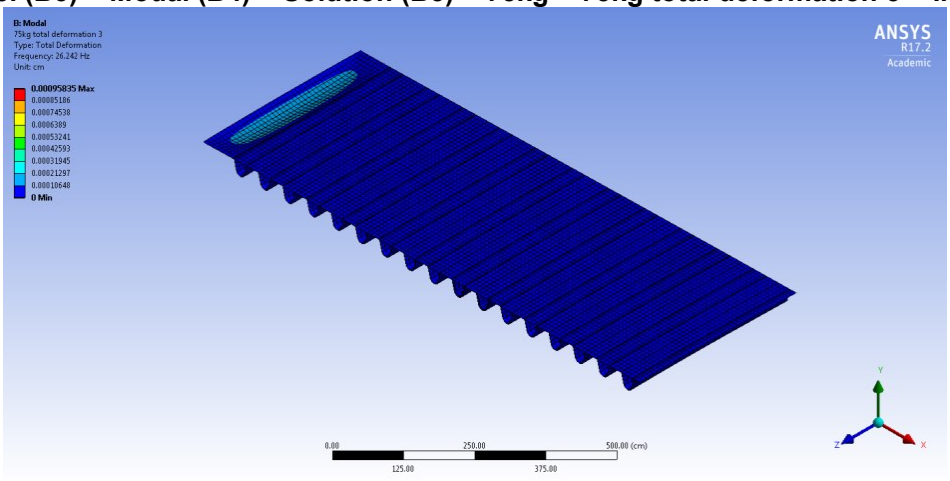


FIGURE 85
Model (B3) > Modal (B4) > Solution (B5) > 75kg > 75kg total deformation 4 > Image

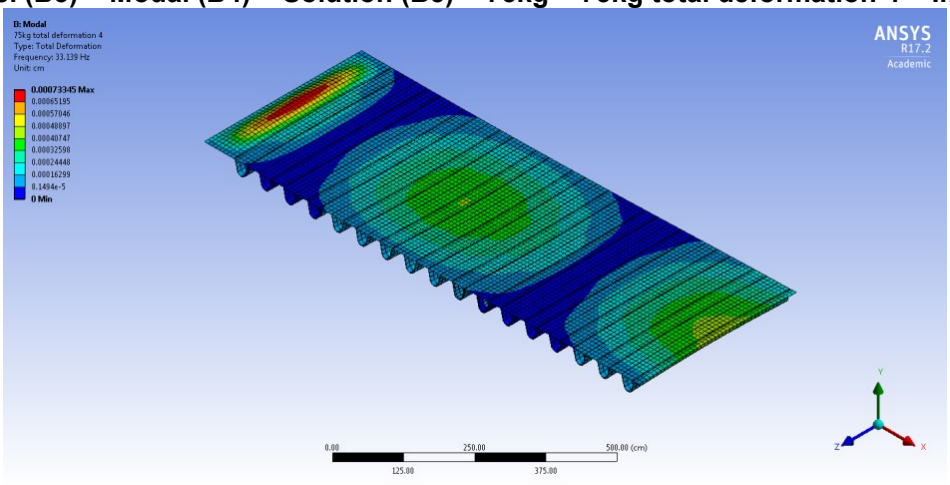


FIGURE 86
Model (B3) > Modal (B4) > Solution (B5) > 75kg > 75kg total deformation 5 > Image

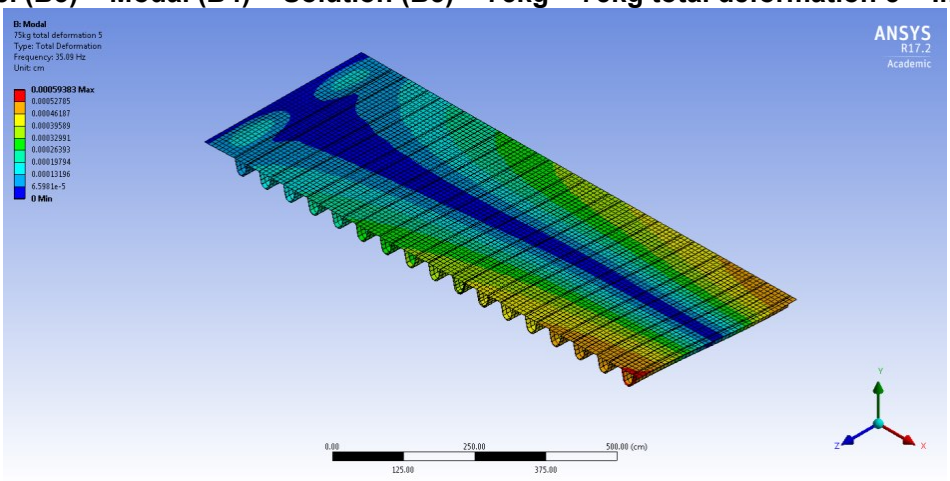


FIGURE 87
Model (B3) > Modal (B4) > Solution (B5) > 75kg > 75kg total deformation 6 > Image

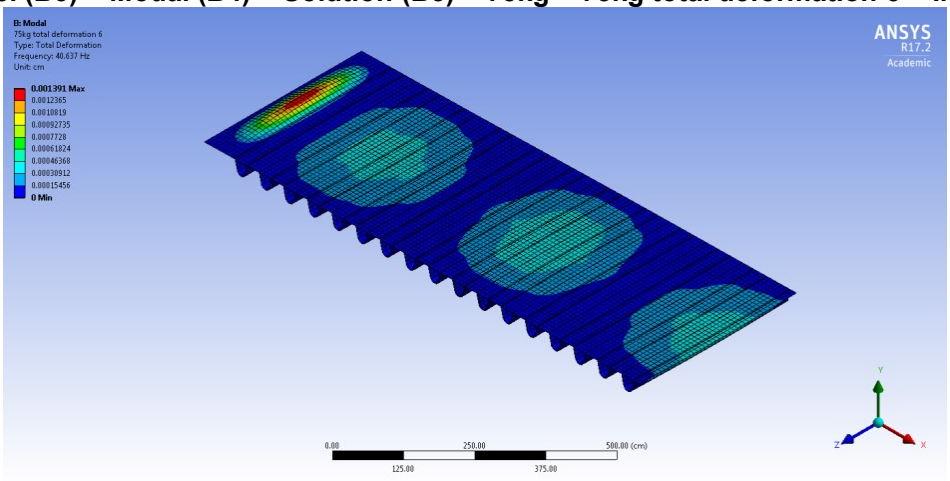


FIGURE 88
Model (B3) > Modal (B4) > Solution (B5) > 75kg > 75kg total deformation 7 > Image

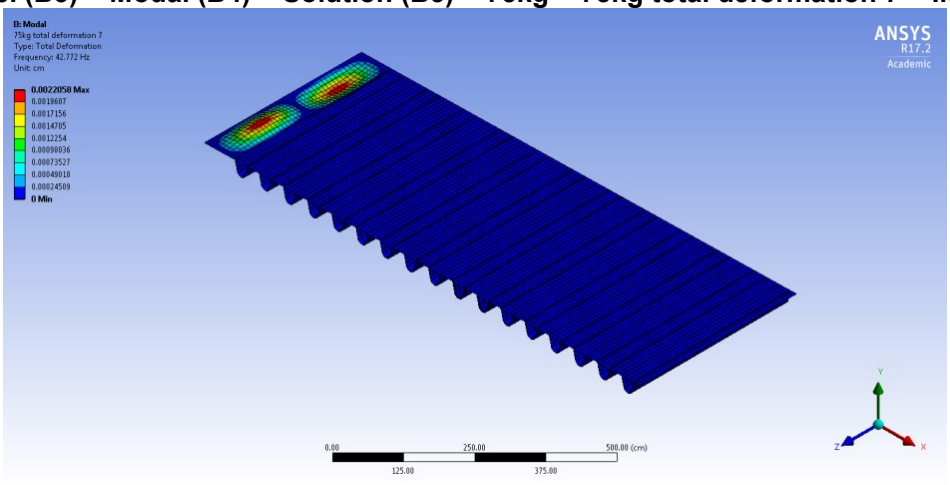


FIGURE 89
Model (B3) > Modal (B4) > Solution (B5) > 75kg > 75kg total deformation 8 > Image

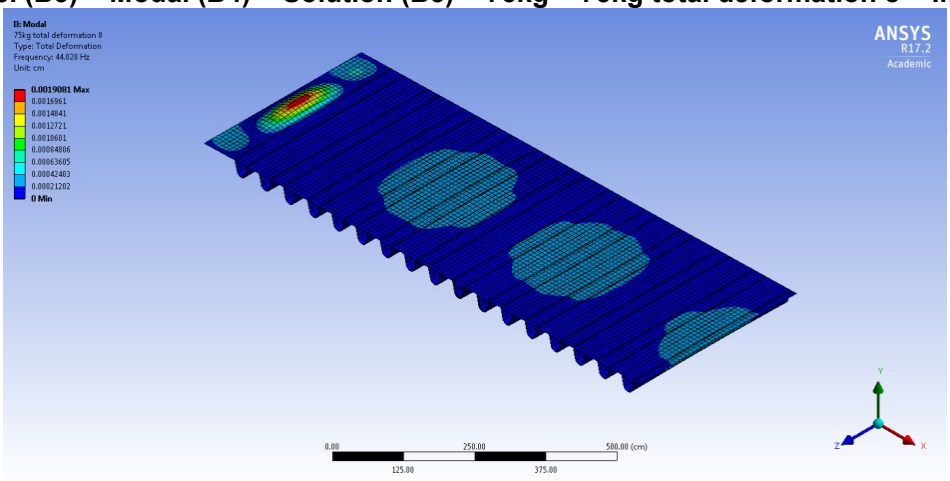


FIGURE 90
Model (B3) > Modal (B4) > Solution (B5) > 75kg > 75kg total deformation 9 > Image

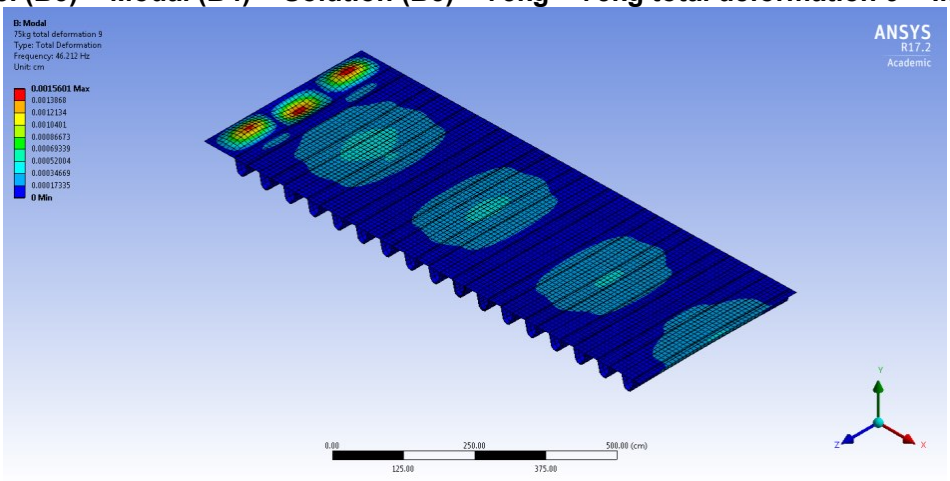


FIGURE 91
Model (B3) > Modal (B4) > Solution (B5) > 75kg > 75kg total deformation 10 > Image

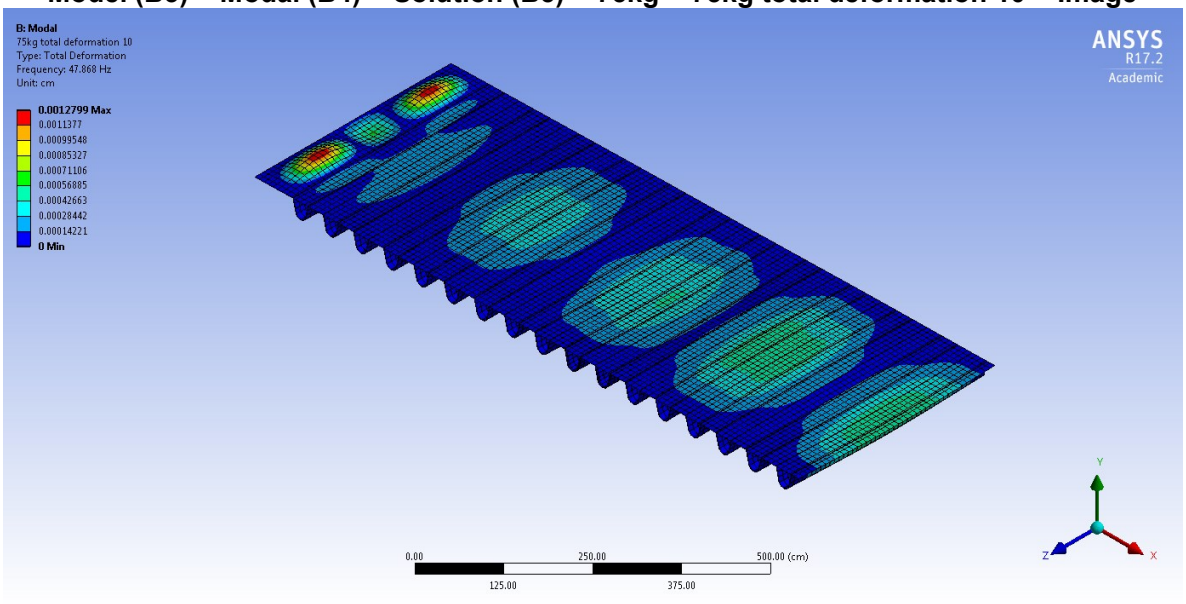


FIGURE 92
Model (B3) > Modal (B4) > Solution (B5) > 75kg > 75kg total deformation 11 > Image

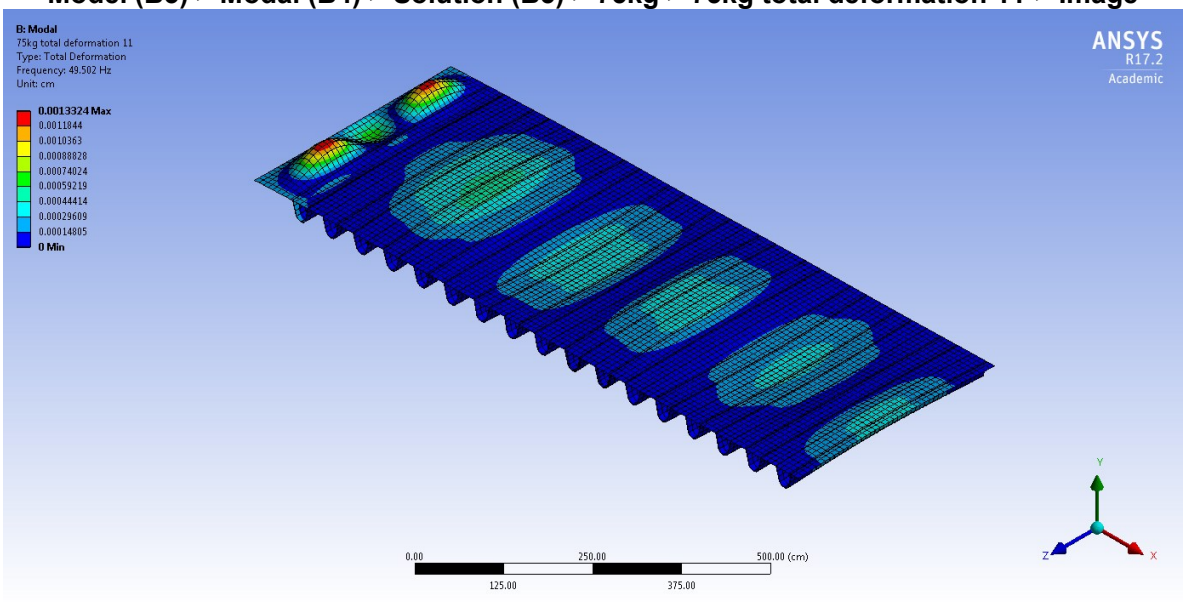


TABLE 132
Model (B3) > Modal (B4) > Solution (B5) > 75kg > Results

Object Name	*75kg total deformation 12*	*75kg total deformation 13*	*75kg total deformation 14*	*75kg total deformation 15*	*75kg total deformation 16*	*75kg total deformation 17*	*75kg total deformation 18*	*75kg total deformation 19*	*75kg total deformation 20*	*75kg total deformation 21*	*75kg total deformation 22*
State	Suppressed										
Scope											

Scoping Method	Geometry Selection										
Geometry	All Bodies										
Definition											
Type	Total Deformation										
Mode	12.	13.	14.	15.	16.	17.	18.	19.	20.	21.	22.
Identifier											
Suppressed	Yes										

FIGURE 93
Model (B3) > Modal (B4) > Solution (B5) > 75kg > 75kg total deformation 12 > Image

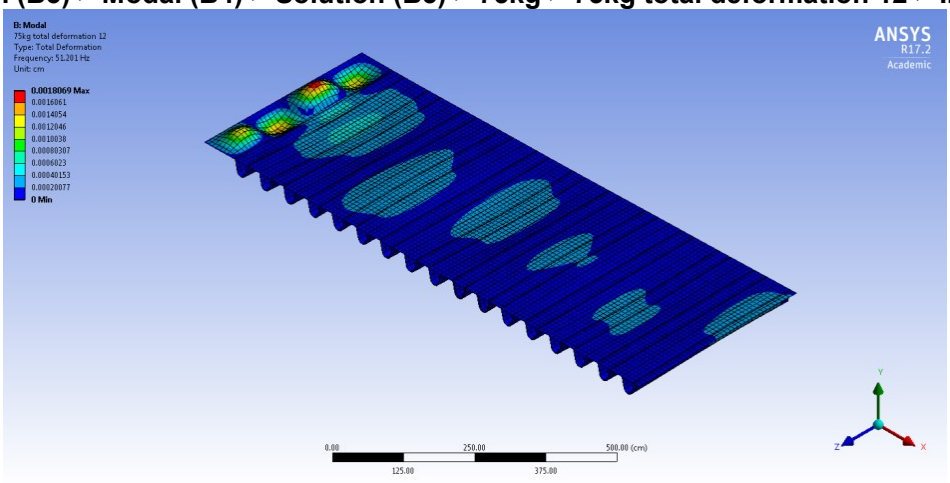


FIGURE 94
Model (B3) > Modal (B4) > Solution (B5) > 75kg > 75kg total deformation 13 > Image

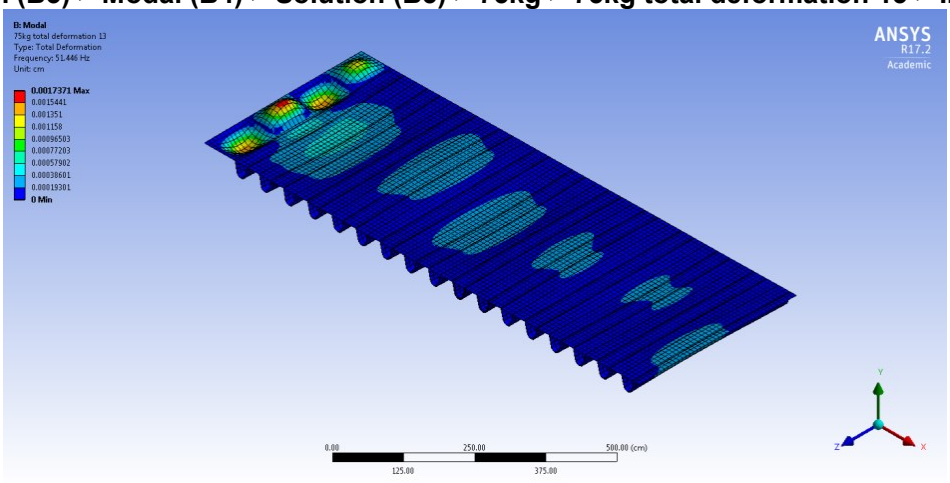


FIGURE 95
Model (B3) > Modal (B4) > Solution (B5) > 75kg > 75kg total deformation 14 > Image

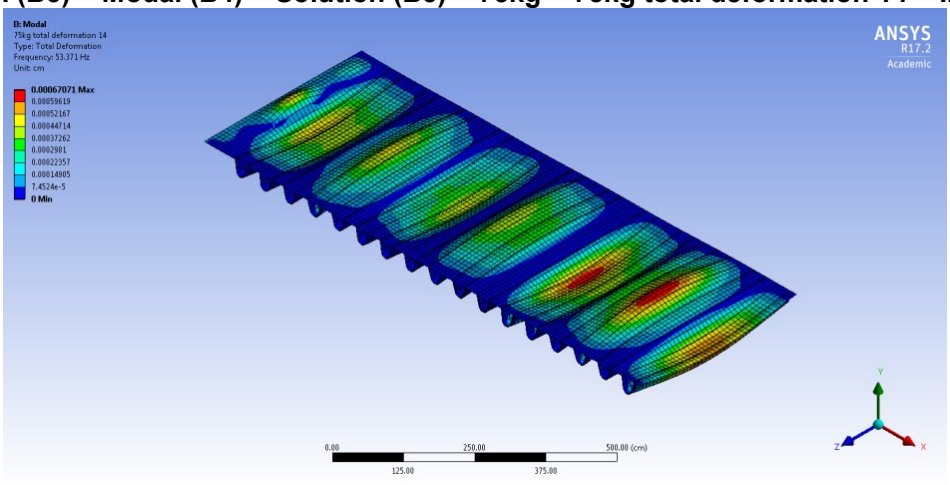


FIGURE 96
Model (B3) > Modal (B4) > Solution (B5) > 75kg > 75kg total deformation 15 > Image

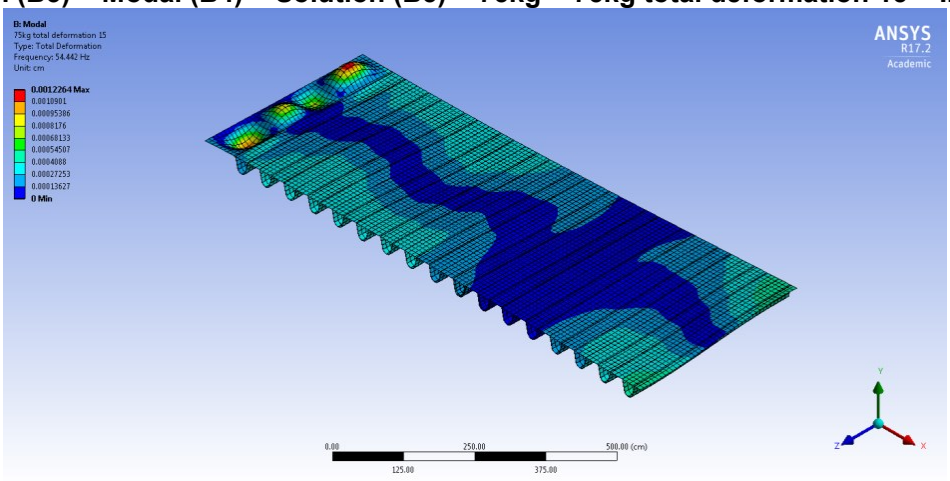


FIGURE 97
Model (B3) > Modal (B4) > Solution (B5) > 75kg > 75kg total deformation 16 > Image

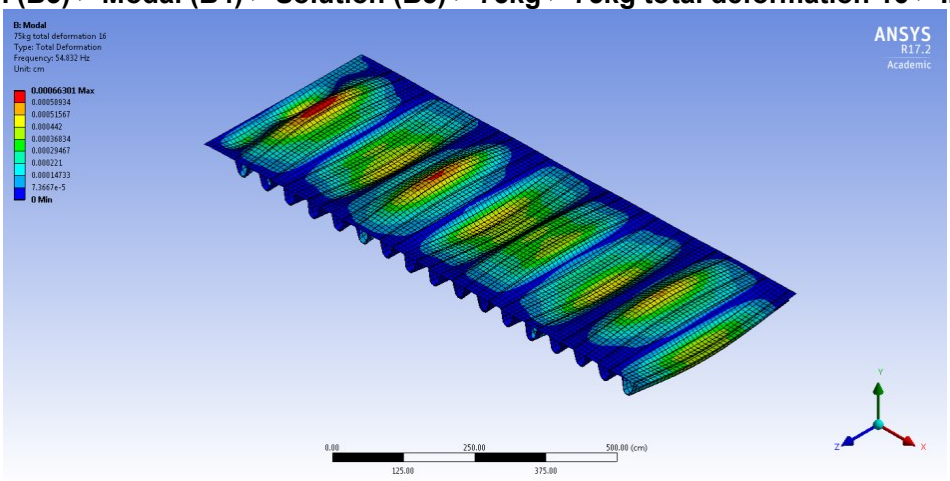


FIGURE 98
Model (B3) > Modal (B4) > Solution (B5) > 75kg > 75kg total deformation 17 > Image

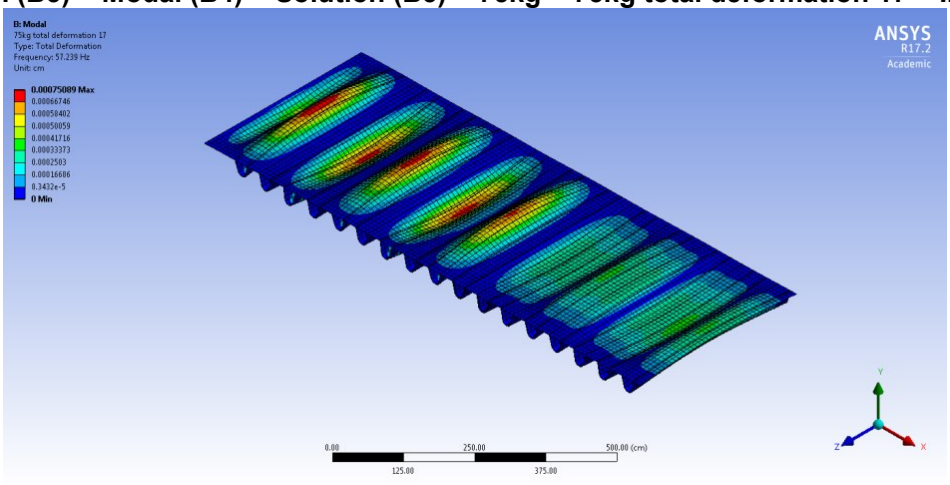


FIGURE 99
Model (B3) > Modal (B4) > Solution (B5) > 75kg > 75kg total deformation 18 > Image

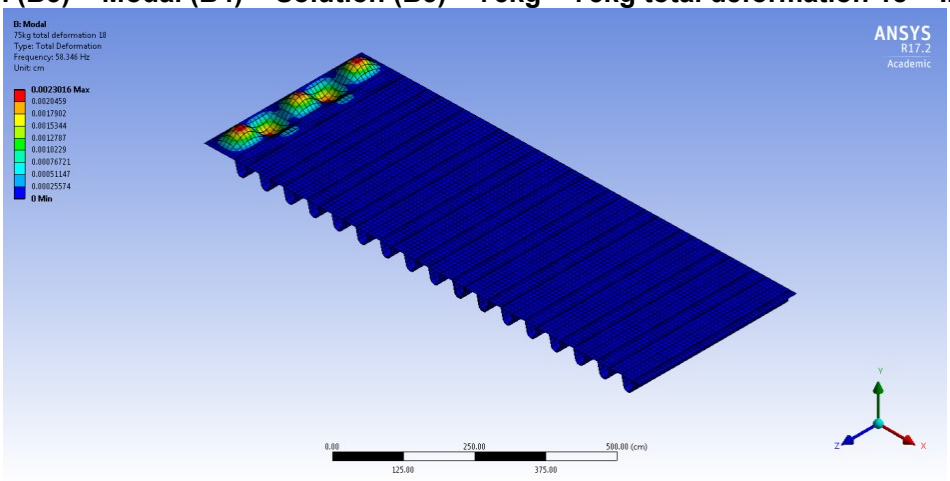


FIGURE 100
Model (B3) > Modal (B4) > Solution (B5) > 75kg > 75kg total deformation 19 > Image

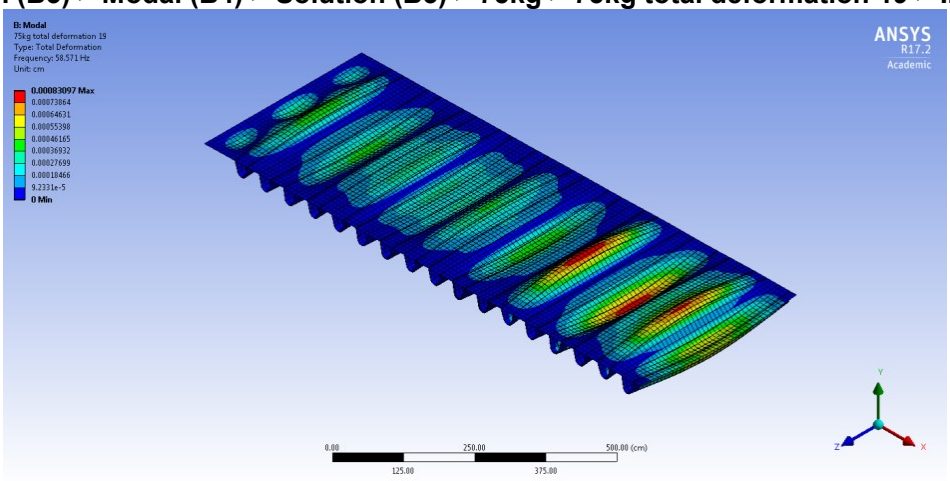


FIGURE 101
Model (B3) > Modal (B4) > Solution (B5) > 75kg > 75kg total deformation 20 > Image

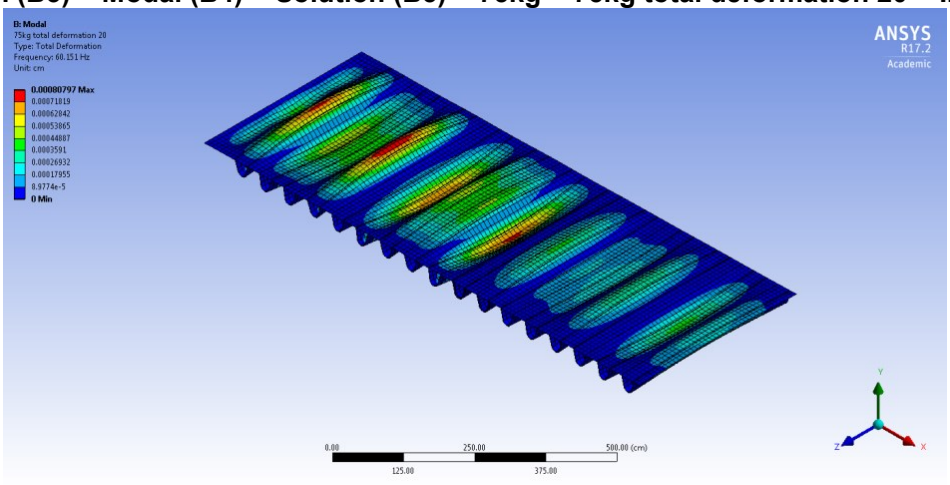


FIGURE 102
Model (B3) > Modal (B4) > Solution (B5) > 75kg > 75kg total deformation 21 > Image

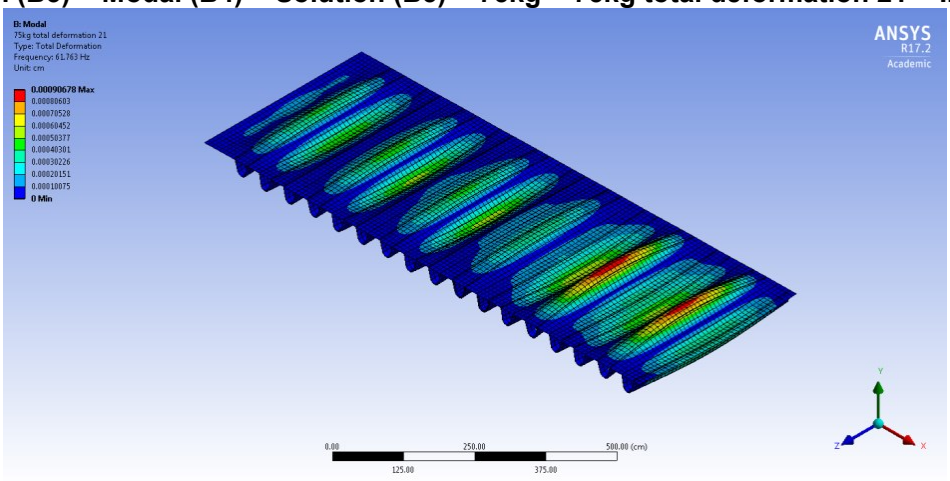


FIGURE 103
Model (B3) > Modal (B4) > Solution (B5) > 75kg > 75kg total deformation 22 > Image

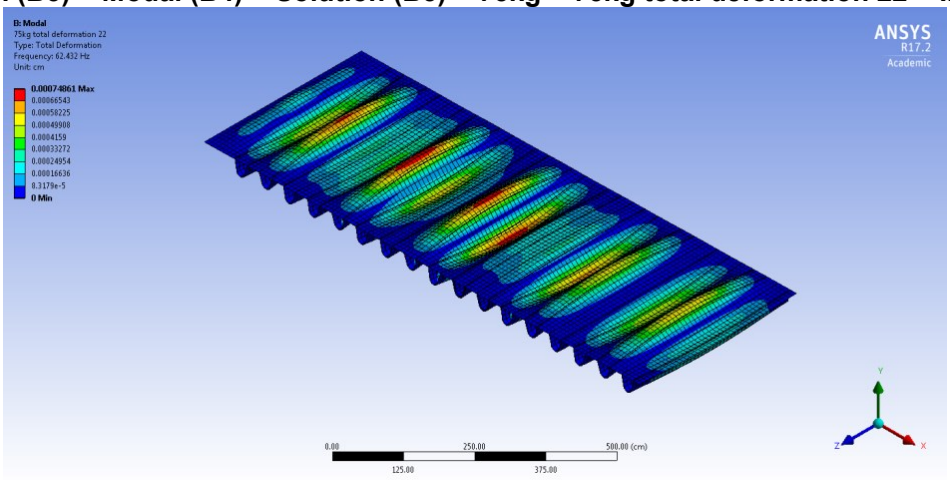


TABLE 133
Model (B3) > Modal (B4) > Solution (B5) > 75kg > Results

Object Name	*75kg total deformation 23*	*75kg total deformation 24*	*75kg total deformation 25*	*75kg total deformation 26*	*75kg total deformation 27*	*75kg total deformation 28*	*75kg total deformation 29*	*75kg total deformation 30*
State	Suppressed							
Scope								
Scoping Method	Geometry Selection							
Geometry	All Bodies							
Definition								
Type	Total Deformation							
Mode	23.	24.	25.	26.	27.	28.	29.	30.
Identifier								
Suppressed	Yes							

FIGURE 104
Model (B3) > Modal (B4) > Solution (B5) > 75kg > 75kg total deformation 23 > Image

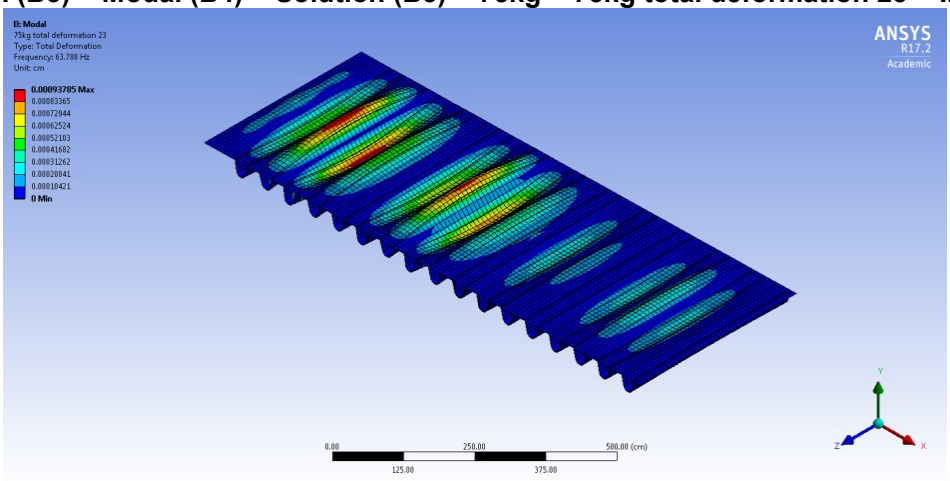


FIGURE 105
Model (B3) > Modal (B4) > Solution (B5) > 75kg > 75kg total deformation 24 > Image

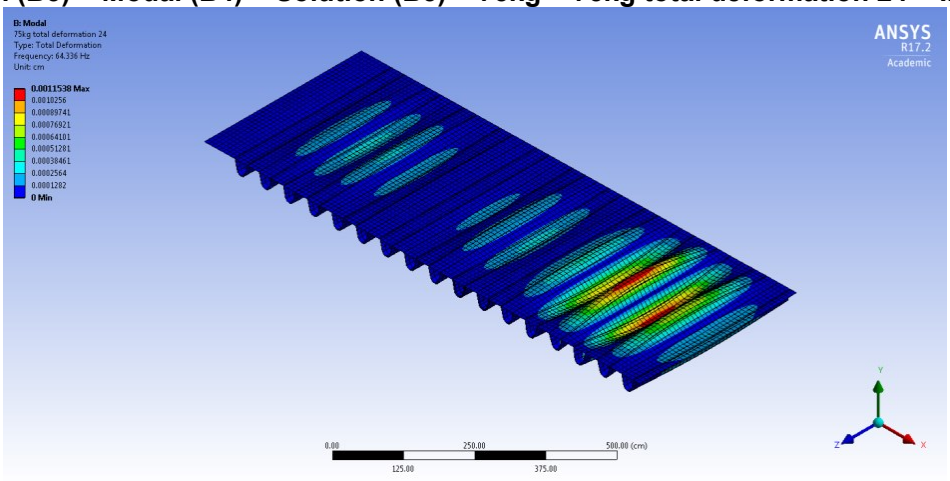


FIGURE 106
Model (B3) > Modal (B4) > Solution (B5) > 75kg > 75kg total deformation 25 > Image

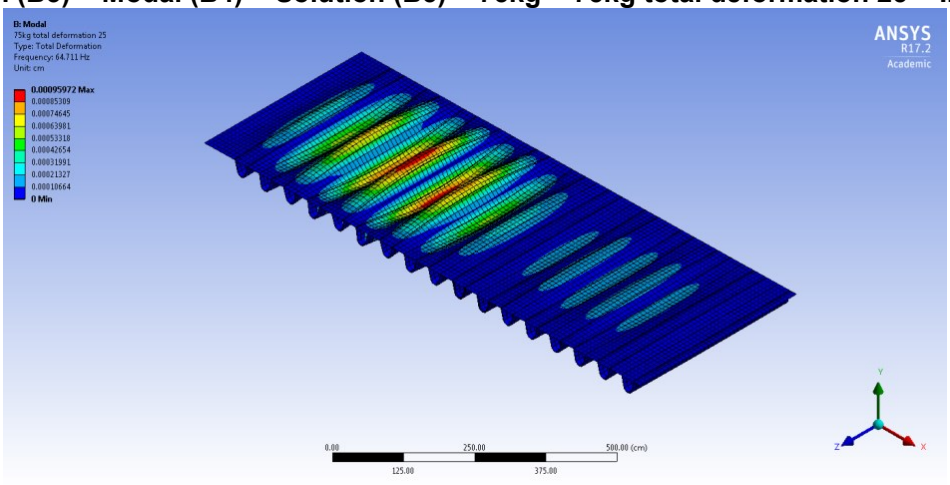


FIGURE 107
Model (B3) > Modal (B4) > Solution (B5) > 75kg > 75kg total deformation 26 > Image

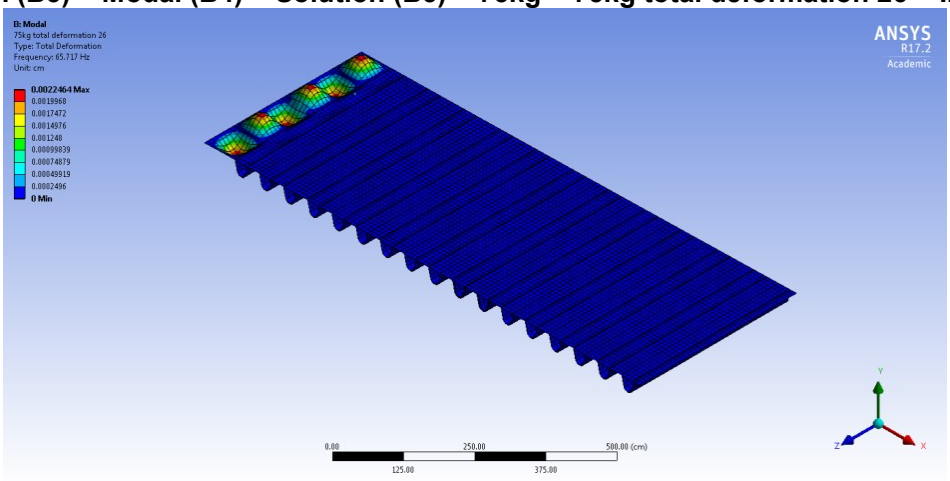


FIGURE 108
Model (B3) > Modal (B4) > Solution (B5) > 75kg > 75kg total deformation 27 > Image

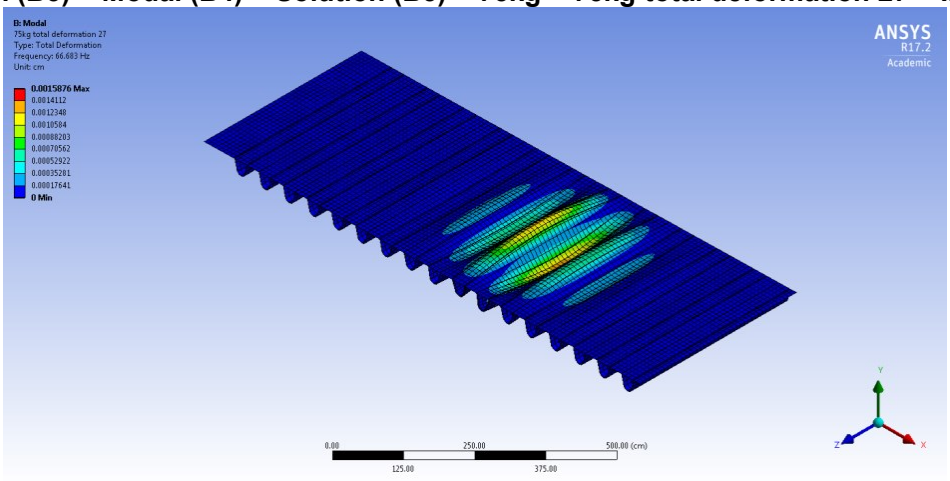


FIGURE 109
Model (B3) > Modal (B4) > Solution (B5) > 75kg > 75kg total deformation 27 > Image

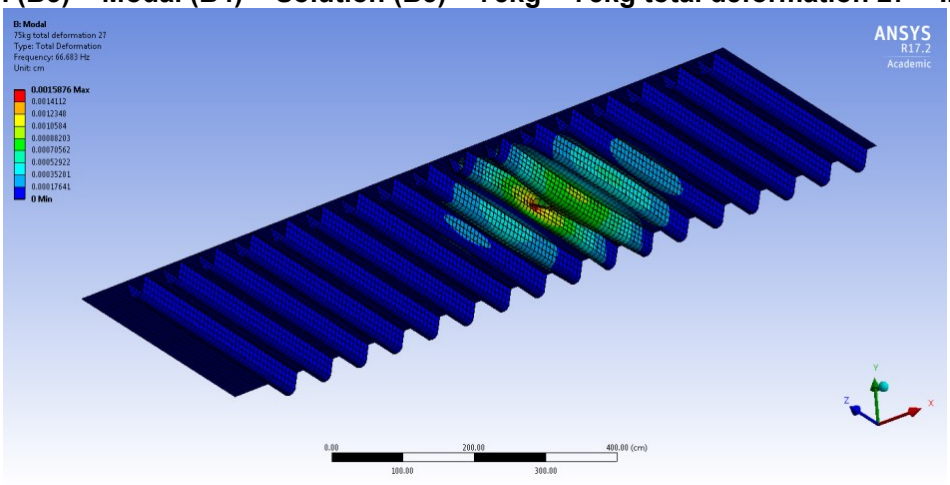


FIGURE 110
Model (B3) > Modal (B4) > Solution (B5) > 75kg > 75kg total deformation 28 > Image

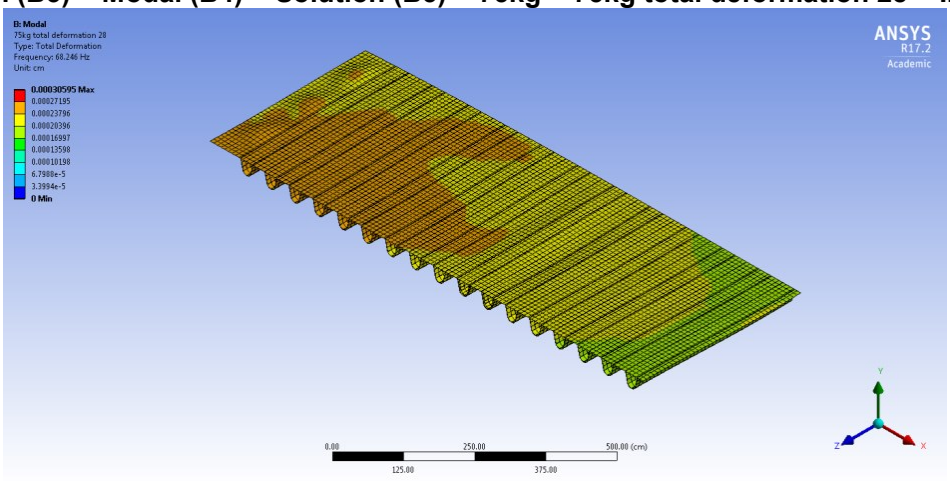


FIGURE 111
Model (B3) > Modal (B4) > Solution (B5) > 75kg > 75kg total deformation 29 > Image

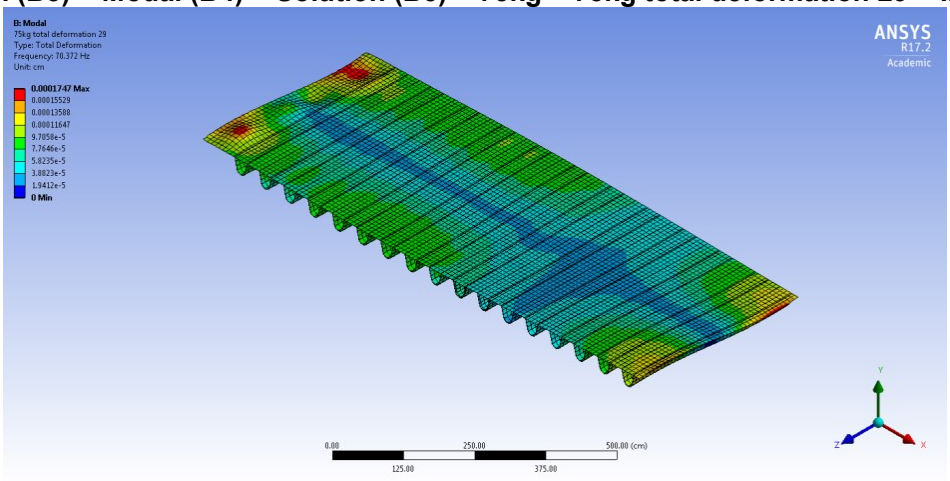
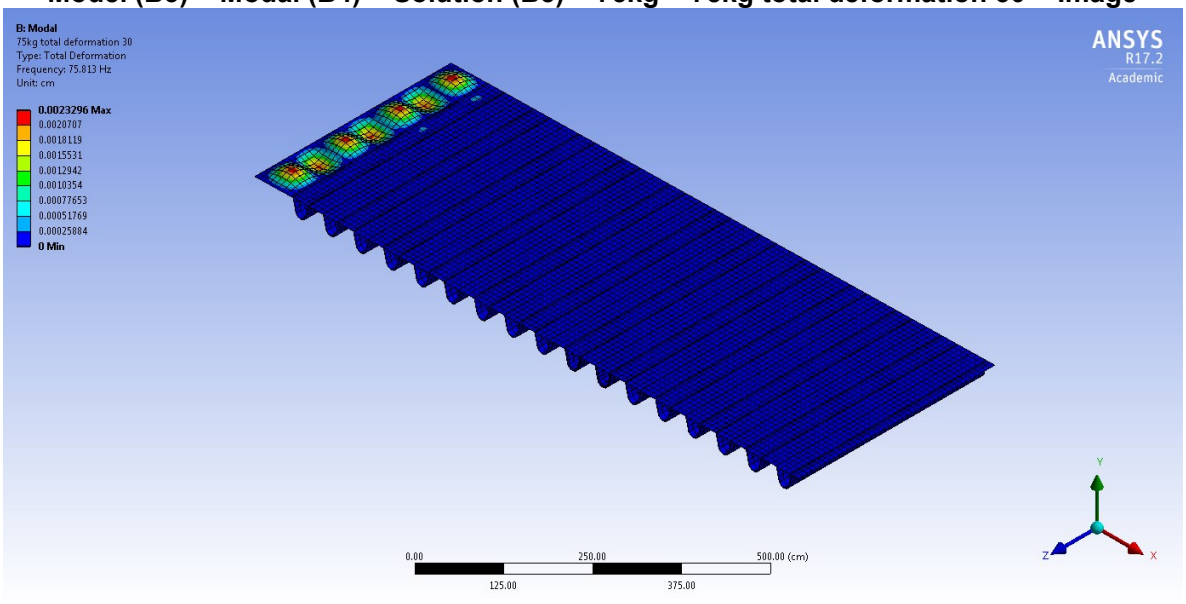


FIGURE 112
Model (B3) > Modal (B4) > Solution (B5) > 75kg > 75kg total deformation 30 > Image



100kg

TABLE 134
Model (B3) > Modal (B4) > Solution (B5) > 100kg > Results

Object Name	*100kg total deformation 1*	*100kg total deformation 2*	*100kg total deformation 3*	*100kg total deformation 4*	*100kg total deformation 5*	*100kg total deformation 6*	*100kg total deformation 7*	*100kg total deformation 8*	*100kg total deformation 9*	*100kg total deformation 10*	*100kg total deformation 11*
State	Suppressed										
Scope											
Scoping Method	Geometry Selection										
Geometry	All Bodies										
Definition											
Type	Total Deformation										
Mode	1.	2.	3.	4.	5.	6.	7.	8.	9.	10.	11.
Identifier											
Suppressed	Yes										

FIGURE 113
Model (B3) > Modal (B4) > Solution (B5) > 100kg > 100kg total deformation 1 > Image

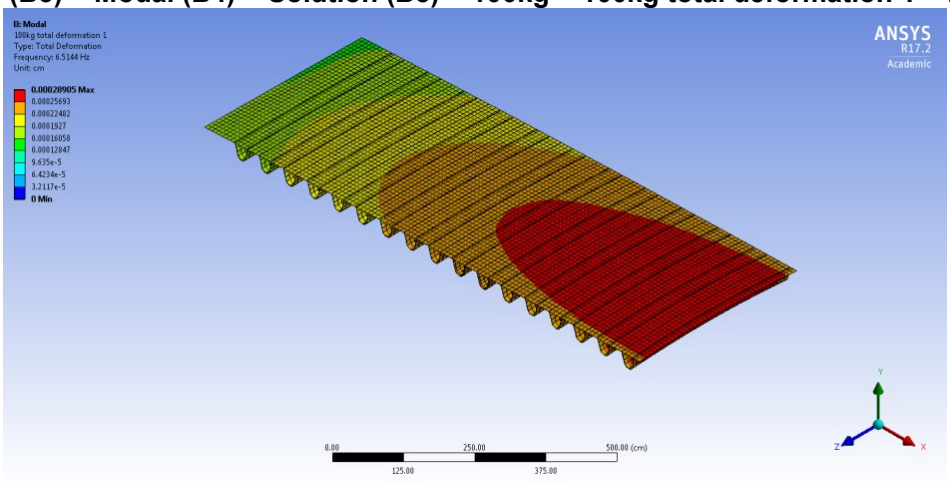


FIGURE 114
Model (B3) > Modal (B4) > Solution (B5) > 100kg > 100kg total deformation 2 > Image

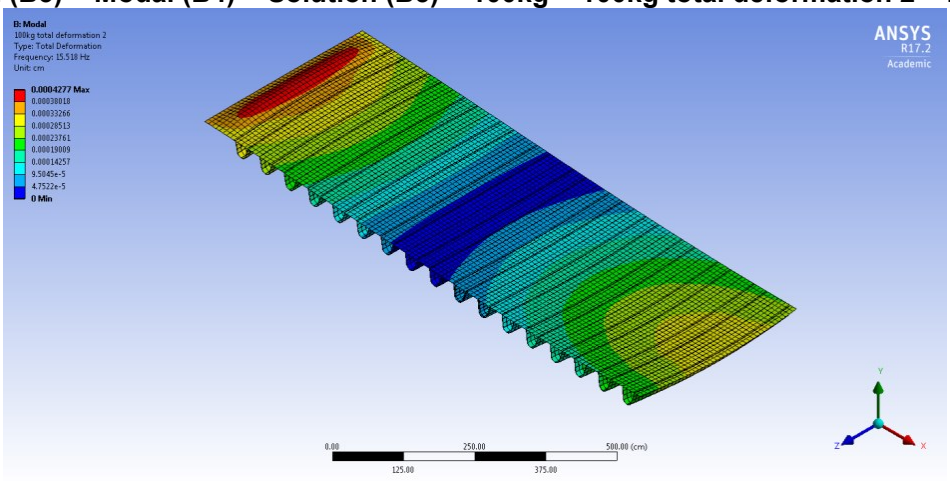


FIGURE 115
Model (B3) > Modal (B4) > Solution (B5) > 100kg > 100kg total deformation 3 > Image

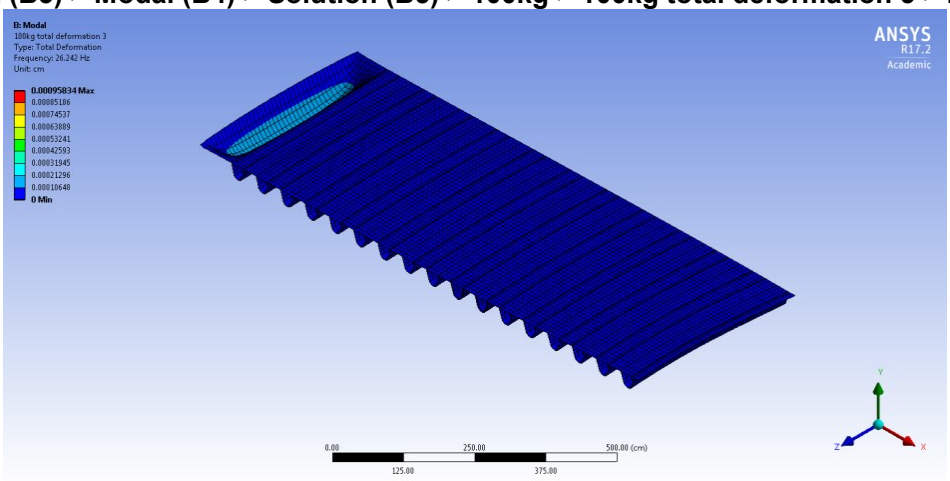


FIGURE 116
Model (B3) > Modal (B4) > Solution (B5) > 100kg > 100kg total deformation 4 > Image

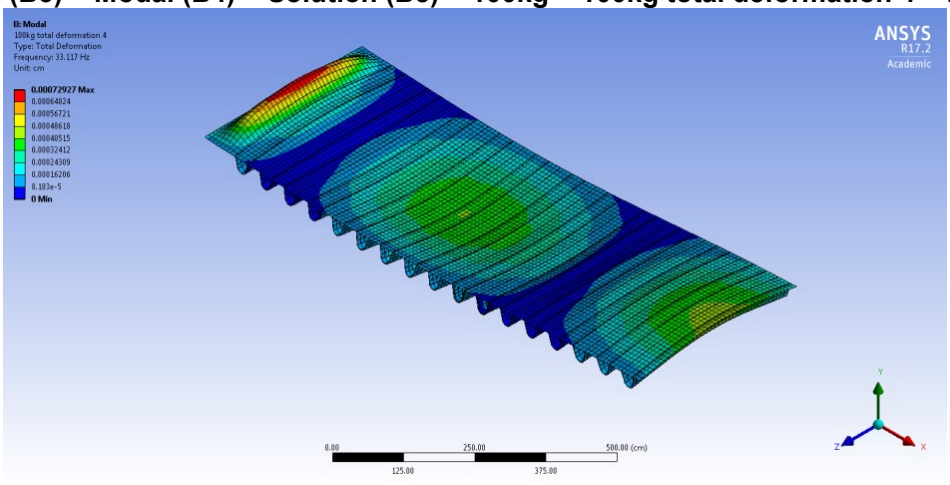


FIGURE 117
Model (B3) > Modal (B4) > Solution (B5) > 100kg > 100kg total deformation 5 > Image

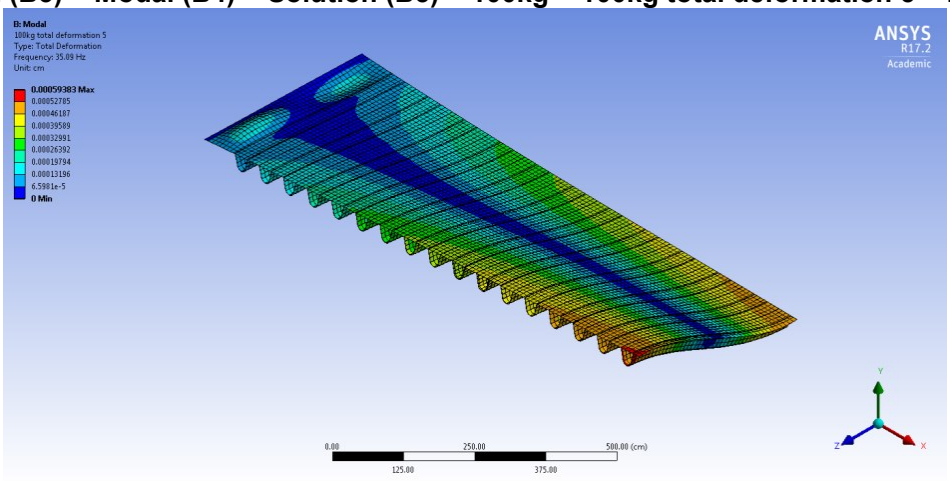


FIGURE 118
Model (B3) > Modal (B4) > Solution (B5) > 100kg > 100kg total deformation 6 > Image

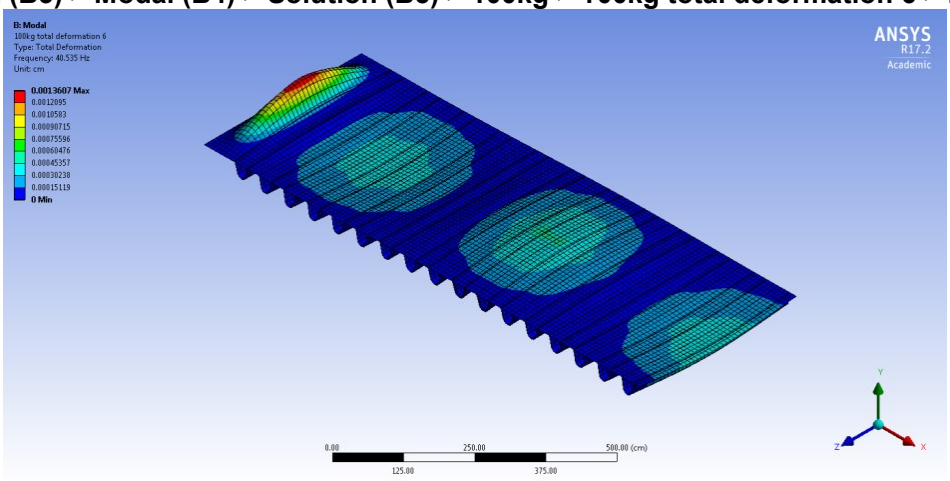


FIGURE 119
Model (B3) > Modal (B4) > Solution (B5) > 100kg > 100kg total deformation 7 > Image

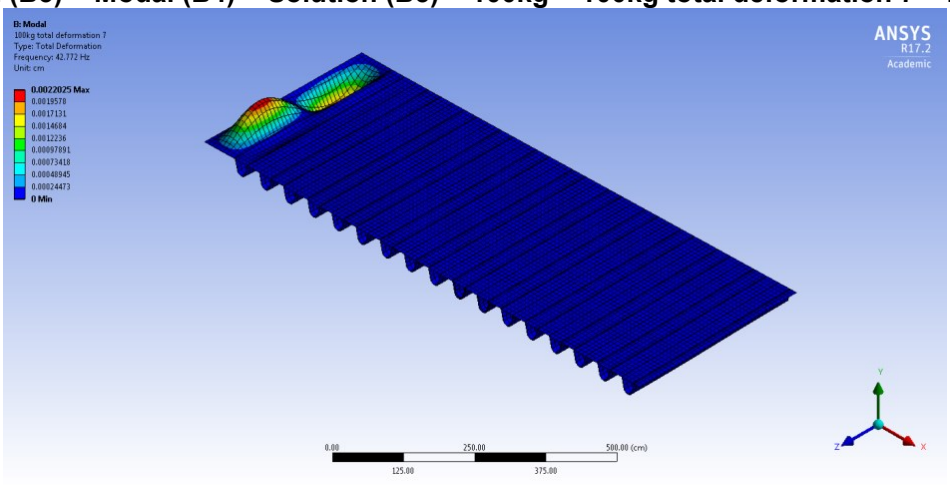


FIGURE 120
Model (B3) > Modal (B4) > Solution (B5) > 100kg > 100kg total deformation 8 > Image

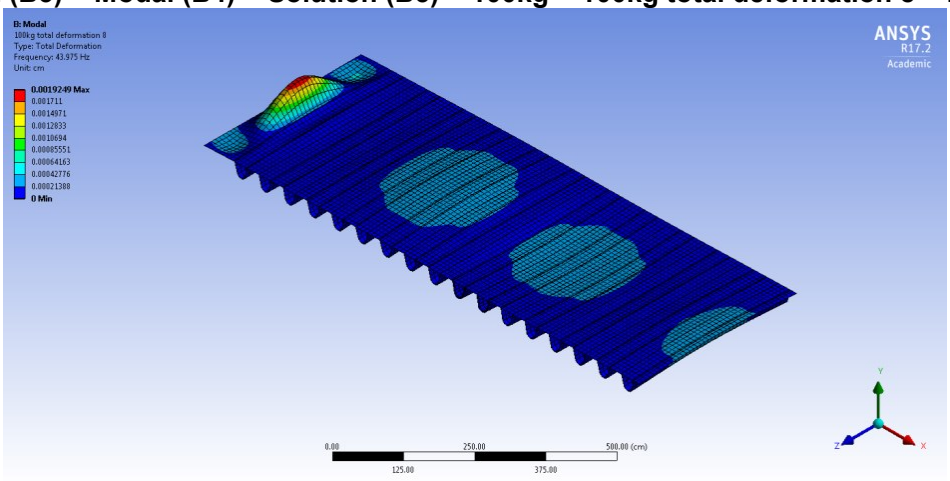


FIGURE 121
Model (B3) > Modal (B4) > Solution (B5) > 100kg > 100kg total deformation 9 > Image

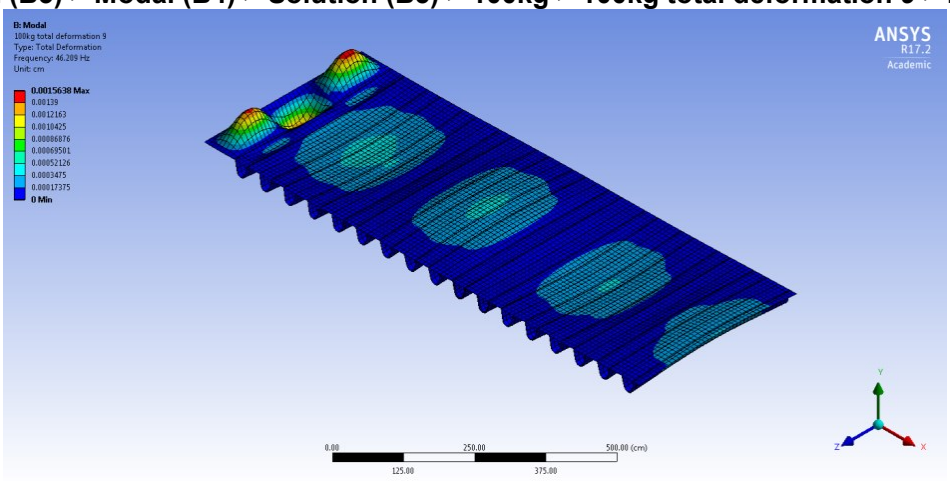


FIGURE 122
Model (B3) > Modal (B4) > Solution (B5) > 100kg > 100kg total deformation 10 > Image

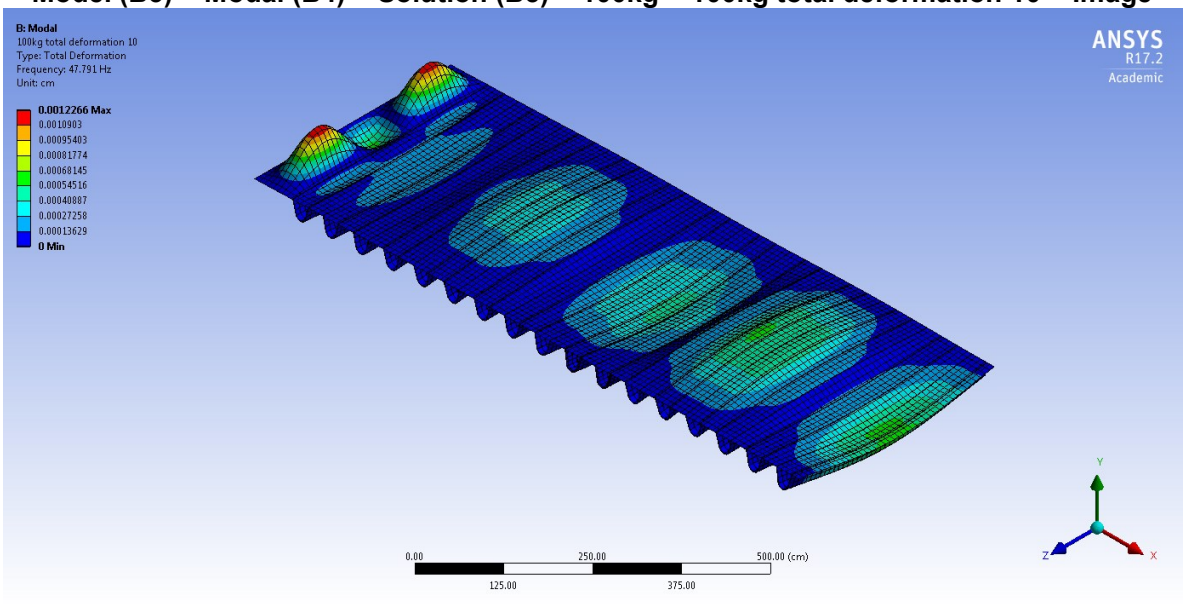


FIGURE 123
Model (B3) > Modal (B4) > Solution (B5) > 100kg > 100kg total deformation 11 > Image

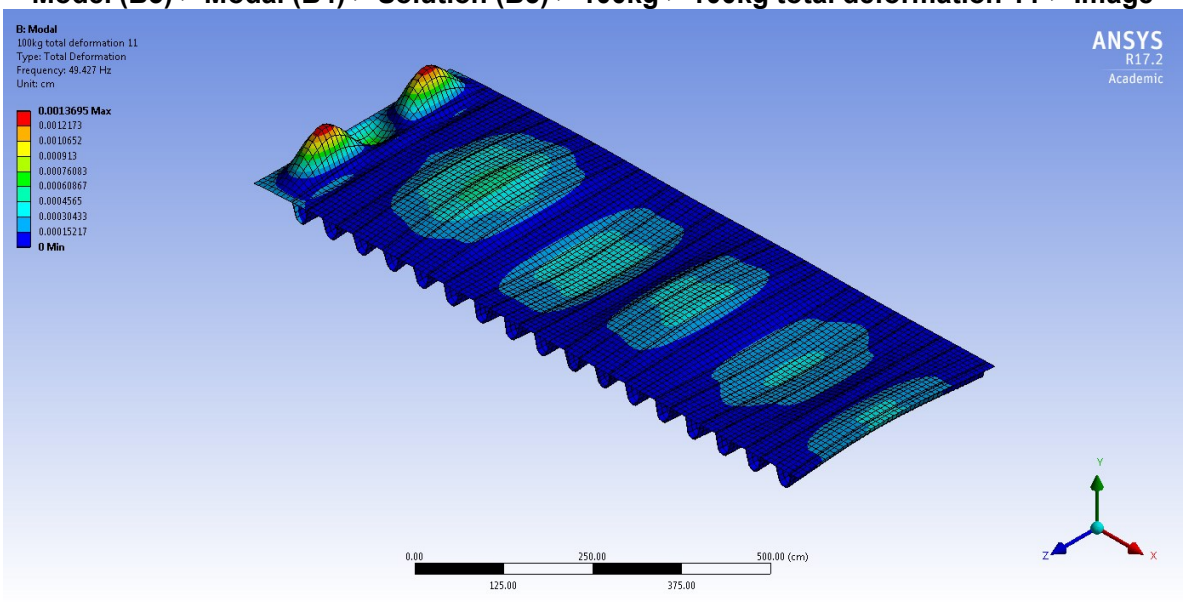


TABLE 135
Model (B3) > Modal (B4) > Solution (B5) > 100kg > Results

Object Name	*100kg total deformation 12*	*100kg total deformation 13*	*100kg total deformation 14*	*100kg total deformation 15*	*100kg total deformation 16*	*100kg total deformation 17*	*100kg total deformation 18*	*100kg total deformation 19*	*100kg total deformation 20*	*100kg total deformation 21*	*100kg total deformation 22*
State	Suppressed										
Scope											

Scoping Method	Geometry Selection										
Geometry	All Bodies										
Definition											
Type	Total Deformation										
Mode	12.	13.	14.	15.	16.	17.	18.	19.	20.	21.	22.
Identifier											
Suppressed	Yes										

FIGURE 124
Model (B3) > Modal (B4) > Solution (B5) > 100kg > 100kg total deformation 12 > Image

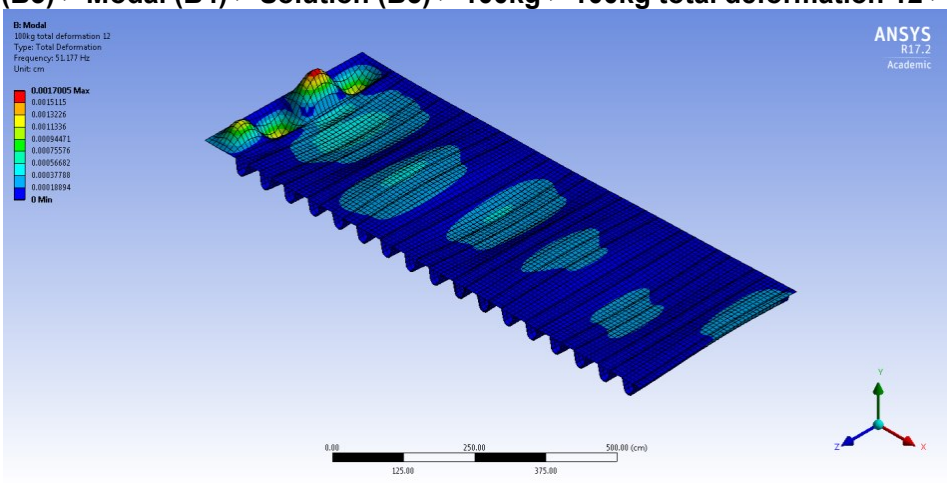


FIGURE 125
Model (B3) > Modal (B4) > Solution (B5) > 100kg > 100kg total deformation 13 > Image

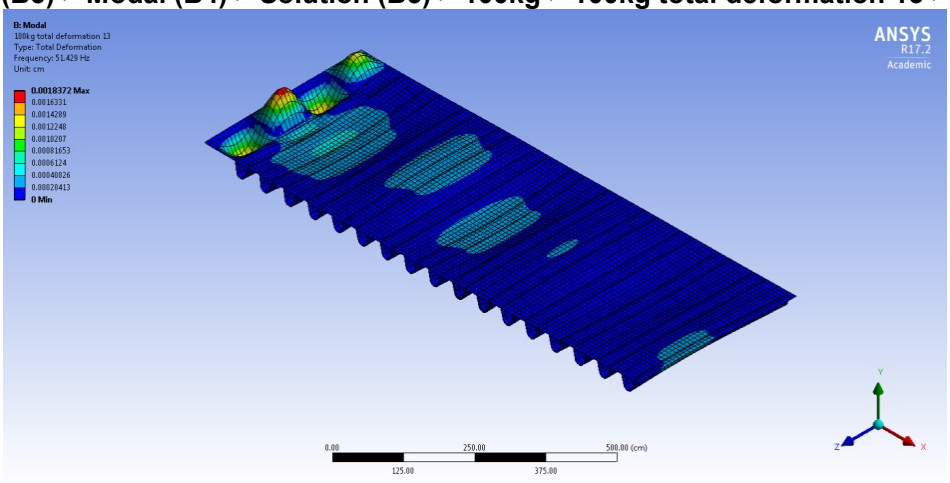


FIGURE 126
Model (B3) > Modal (B4) > Solution (B5) > 100kg > 100kg total deformation 14 > Image

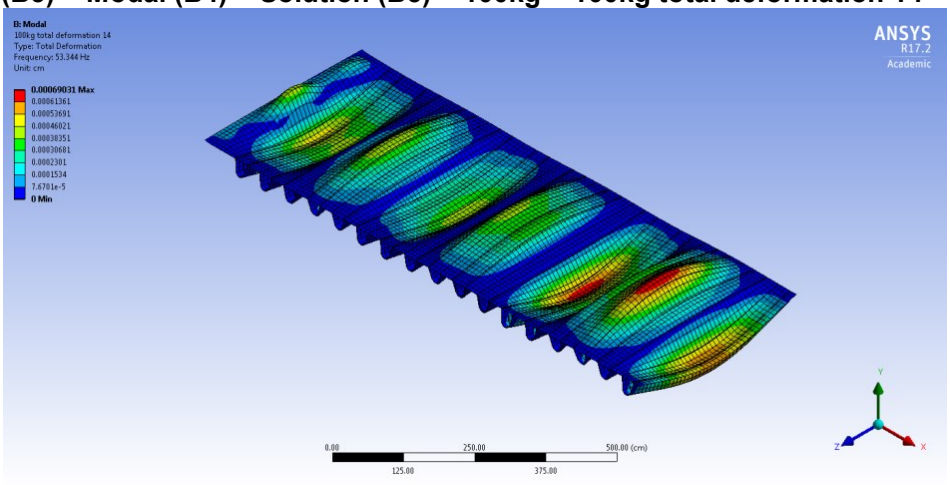


FIGURE 127
Model (B3) > Modal (B4) > Solution (B5) > 100kg > 100kg total deformation 15 > Image

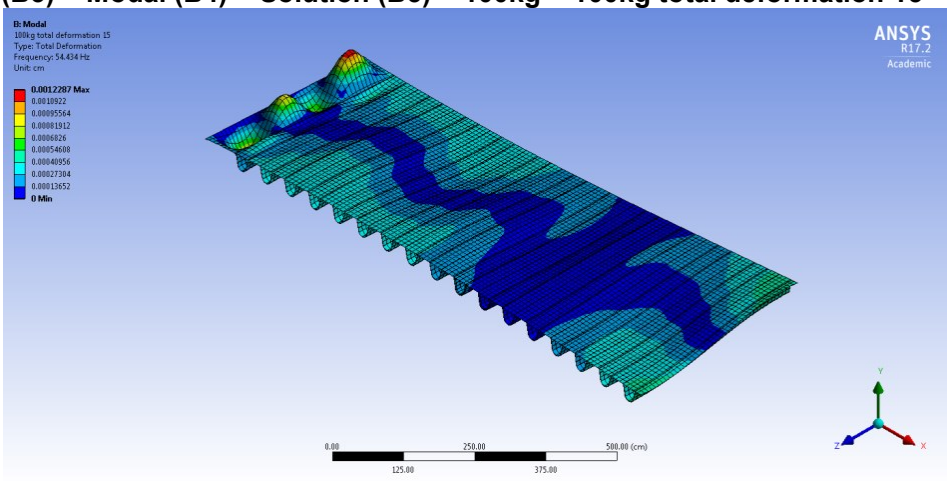


FIGURE 128
Model (B3) > Modal (B4) > Solution (B5) > 100kg > 100kg total deformation 16 > Image

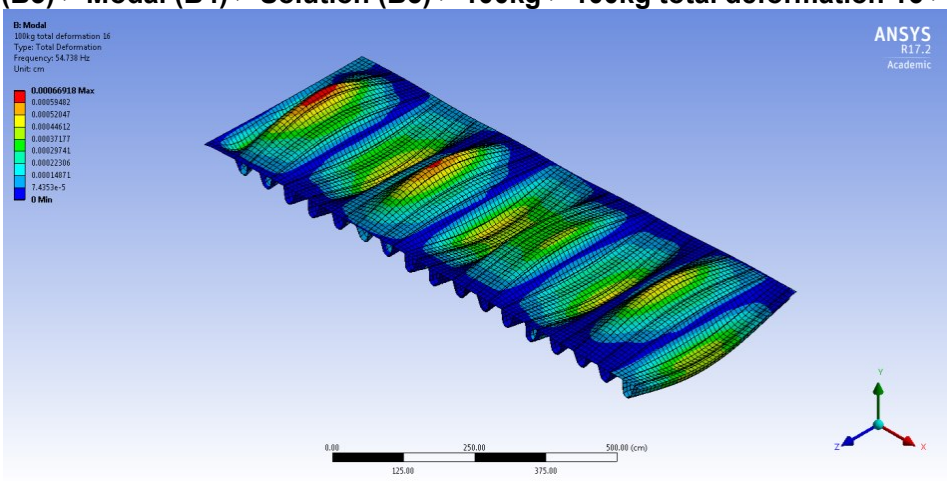


FIGURE 129
Model (B3) > Modal (B4) > Solution (B5) > 100kg > 100kg total deformation 17 > Image

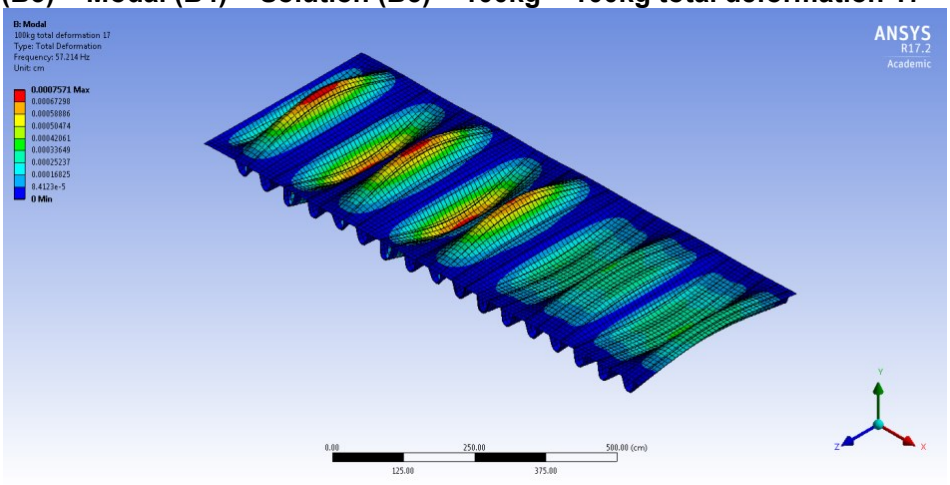


FIGURE 130
Model (B3) > Modal (B4) > Solution (B5) > 100kg > 100kg total deformation 18 > Image

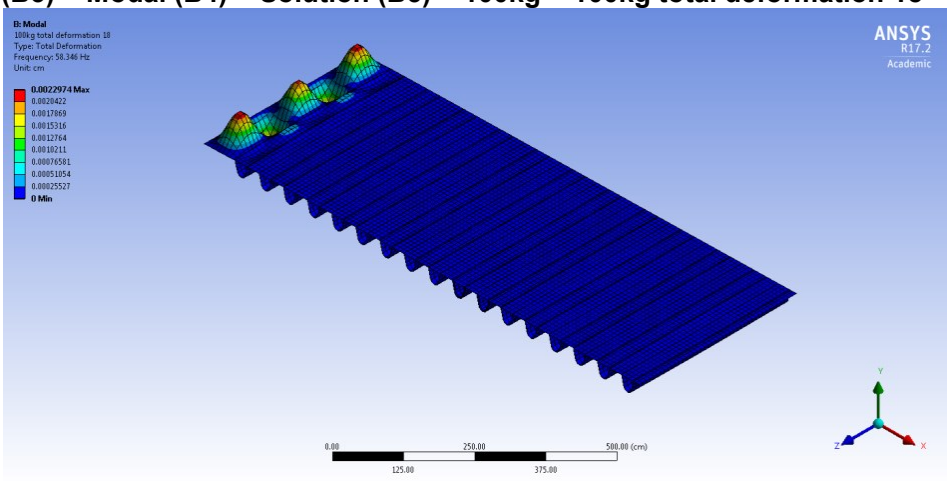


FIGURE 131
Model (B3) > Modal (B4) > Solution (B5) > 100kg > 100kg total deformation 19 > Image

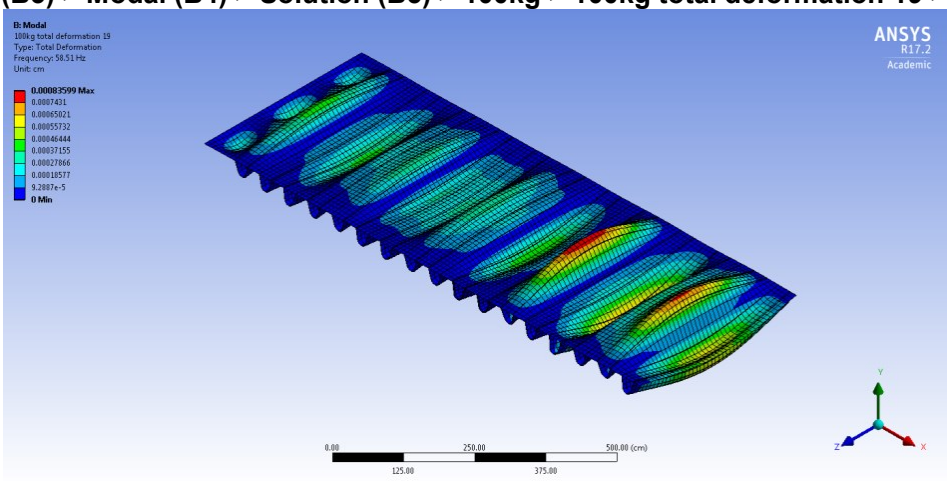


FIGURE 132
Model (B3) > Modal (B4) > Solution (B5) > 100kg > 100kg total deformation 20 > Image

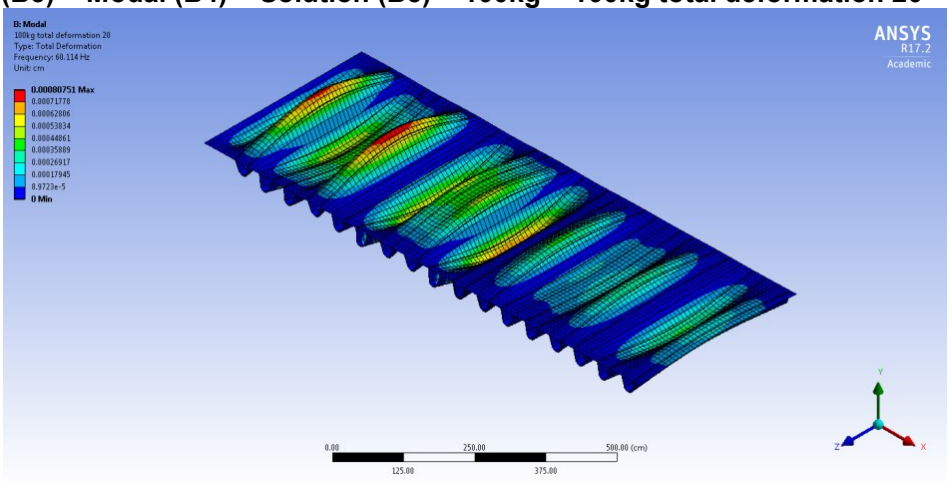


FIGURE 133
Model (B3) > Modal (B4) > Solution (B5) > 100kg > 100kg total deformation 21 > Image

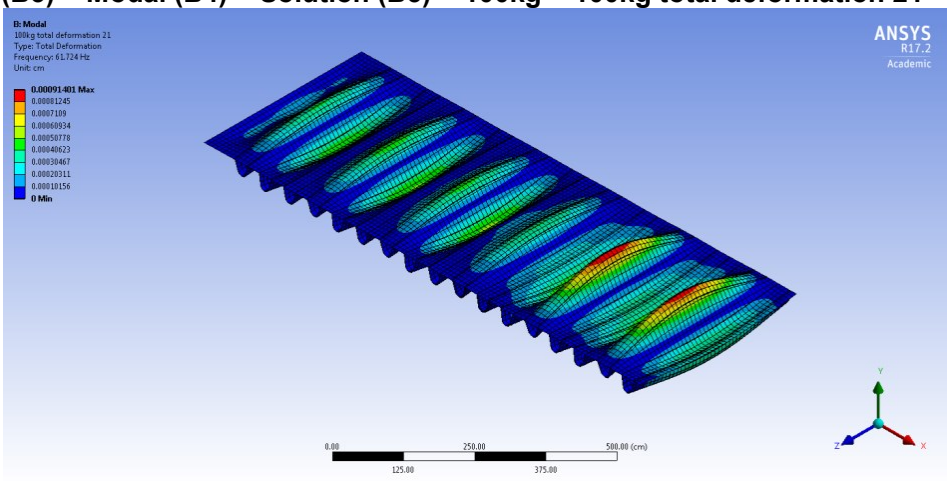


FIGURE 134
Model (B3) > Modal (B4) > Solution (B5) > 100kg > 100kg total deformation 22 > Image

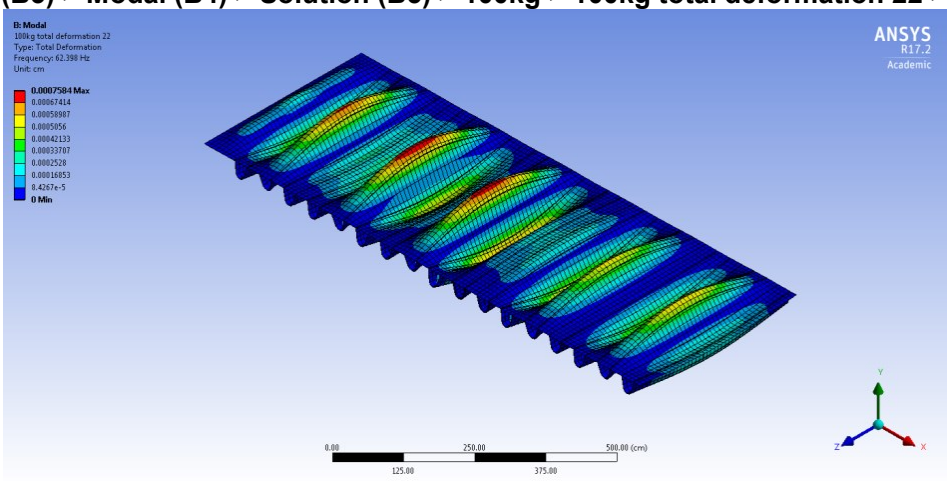


TABLE 136
Model (B3) > Modal (B4) > Solution (B5) > 100kg > Results

Object Name	*100kg total deformation 23*	*100kg total deformation 24*	*100kg total deformation 25*	*100kg total deformation 26*	*100kg total deformation 27*	*100kg total deformation 28*	*100kg total deformation 29*	*100kg total deformation 30*
State	Suppressed							
Scope								
Scoping Method	Geometry Selection							
Geometry	All Bodies							
Definition								
Type	Total Deformation							
Mode	23.	24.	25.	26.	27.	28.	29.	30.
Identifier								
Suppressed	Yes							

FIGURE 135
Model (B3) > Modal (B4) > Solution (B5) > 100kg > 100kg total deformation 23 > Image

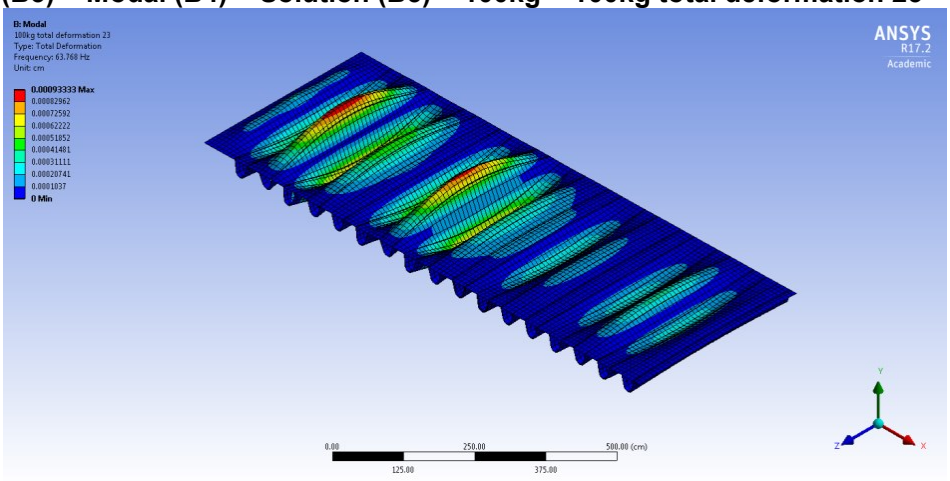


FIGURE 136
Model (B3) > Modal (B4) > Solution (B5) > 100kg > 100kg total deformation 24 > Image

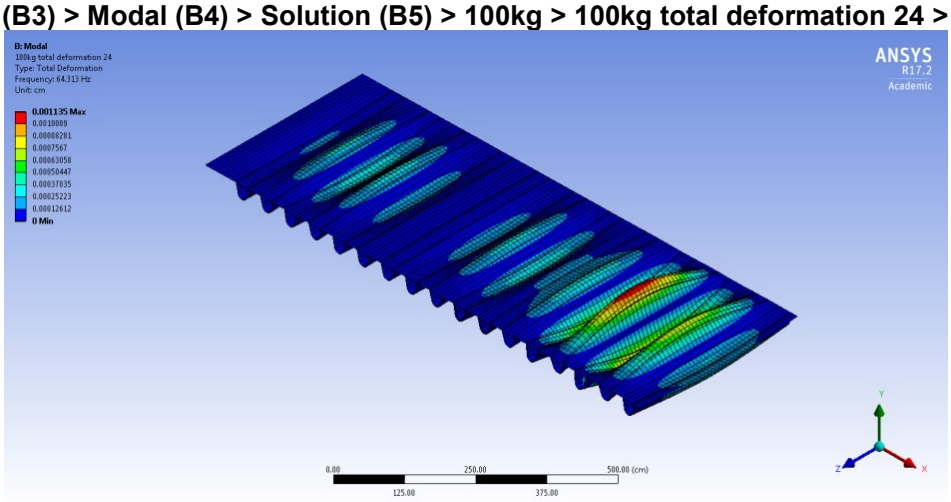


FIGURE 137
Model (B3) > Modal (B4) > Solution (B5) > 100kg > 100kg total deformation 25 > Image

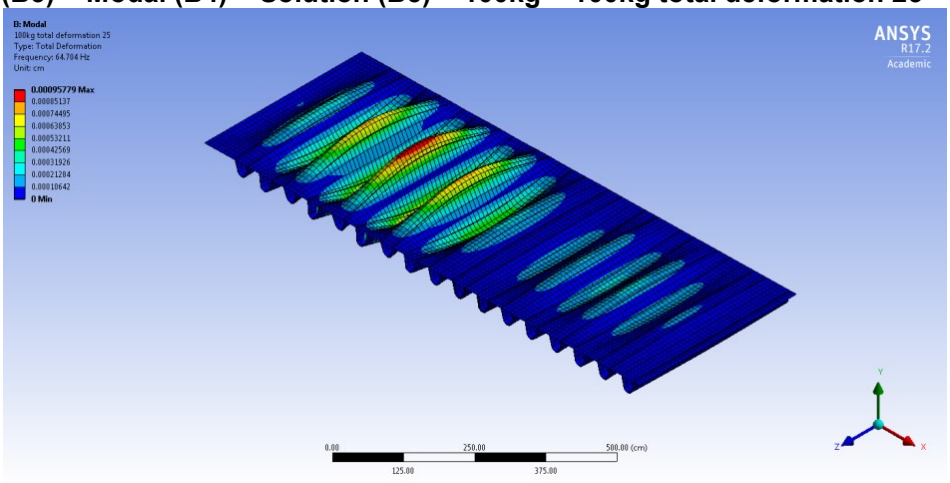


FIGURE 138
Model (B3) > Modal (B4) > Solution (B5) > 100kg > 100kg total deformation 26 > Image

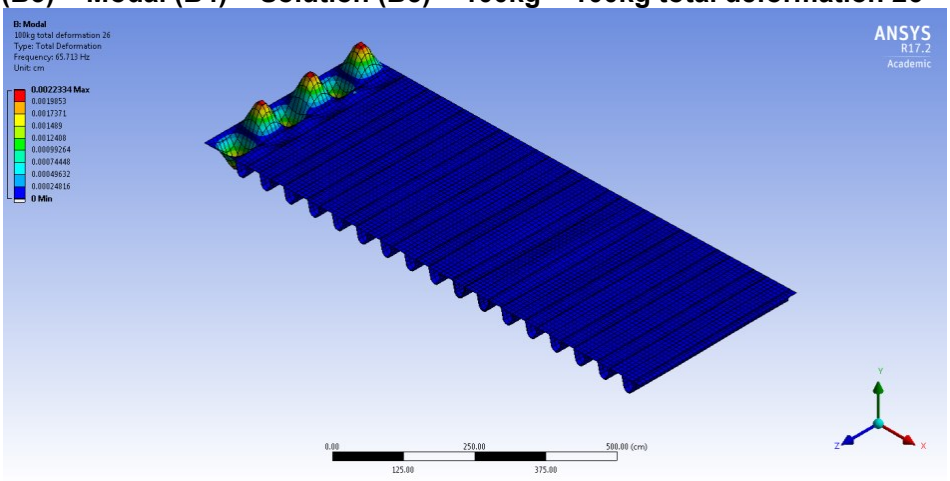


FIGURE 139
Model (B3) > Modal (B4) > Solution (B5) > 100kg > 100kg total deformation 27 > Image

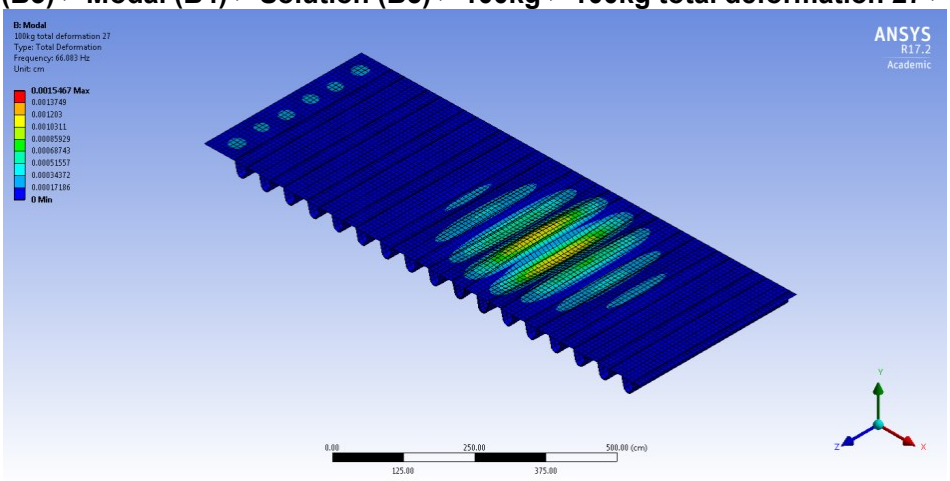


FIGURE 140
Model (B3) > Modal (B4) > Solution (B5) > 100kg > 100kg total deformation 27 > Image

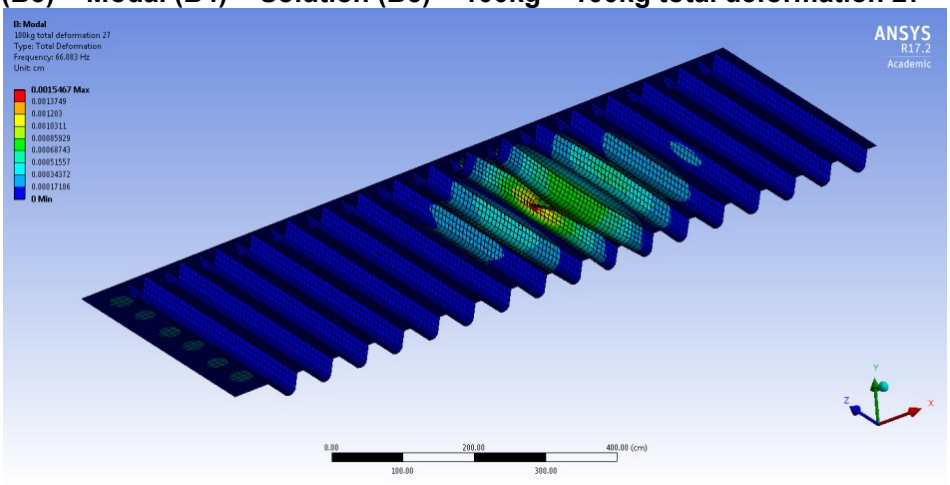


FIGURE 141
Model (B3) > Modal (B4) > Solution (B5) > 100kg > 100kg total deformation 28 > Image

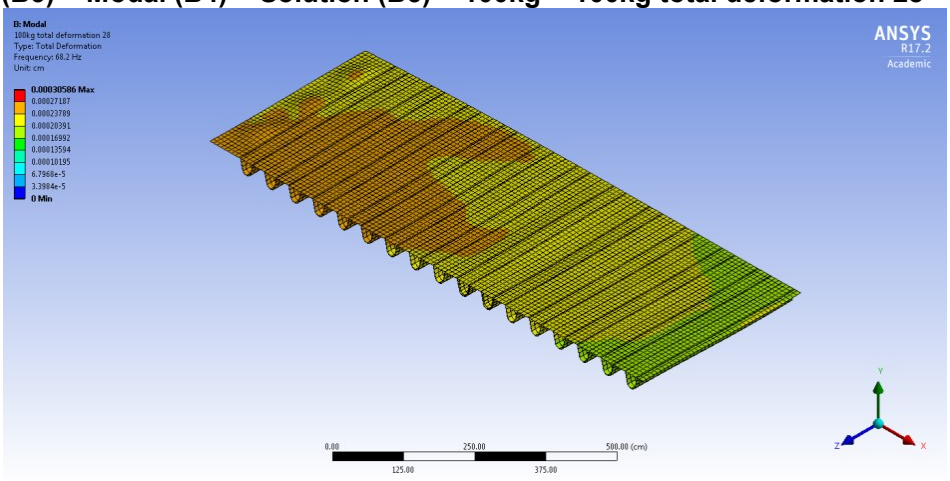


FIGURE 142
Model (B3) > Modal (B4) > Solution (B5) > 100kg > 100kg total deformation 29 > Image

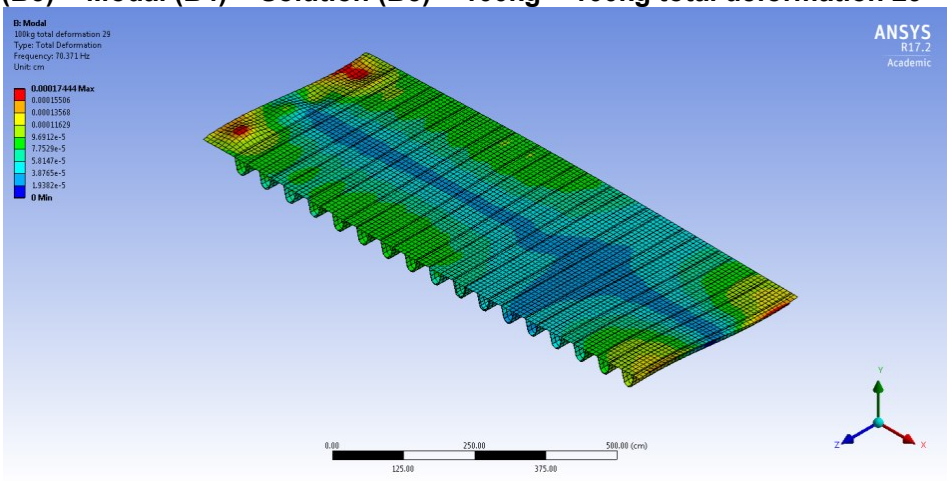
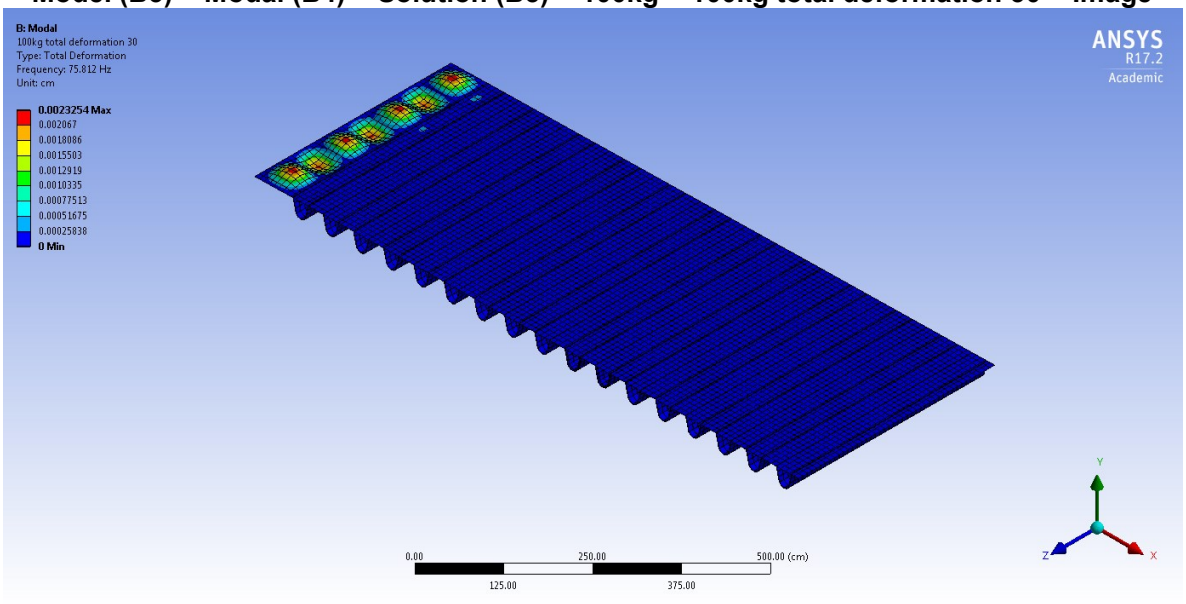


FIGURE 143
Model (B3) > Modal (B4) > Solution (B5) > 100kg > 100kg total deformation 30 > Image



1crack35cm

TABLE 137
Model (B3) > Modal (B4) > Solution (B5) > 1crack35cm > Results

Object Name	*1crack 35cm total deformation 1*	*1crack 35cm total deformation 2*	*1crack 35cm total deformation 3*	*1crack 35cm total deformation 4*	*1crack 35cm total deformation 5*	*1crack 35cm total deformation 6*	*1crack 35cm total deformation 7*	*1crack 35cm total deformation 8*	*1crack 35cm total deformation 9*	*1crack 35cm total deformation 10*	*1crack 35cm total deformation 11*
State	Suppressed										
Scope											
Scoping Method	Geometry Selection										
Geometry	All Bodies										
Definition											
Type	Total Deformation										
Mode	1.	2.	3.	4.	5.	6.	7.	8.	9.	10.	11.
Identifier											
Suppressed	Yes										

FIGURE 144
Model (B3) > Modal (B4) > Solution (B5) > 1crack35cm > 1crack35cm total deformation 1 > Image

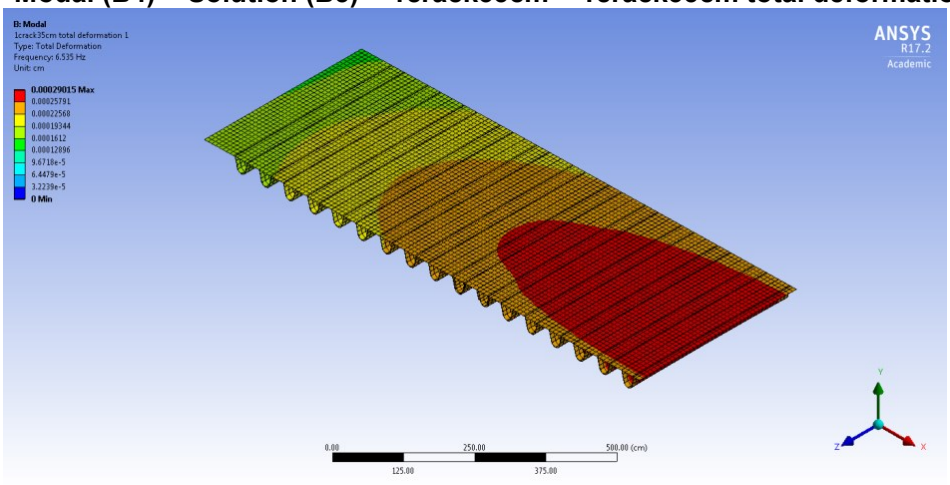


FIGURE 145
Model (B3) > Modal (B4) > Solution (B5) > 1crack35cm > 1crack35cm total deformation 2 > Image

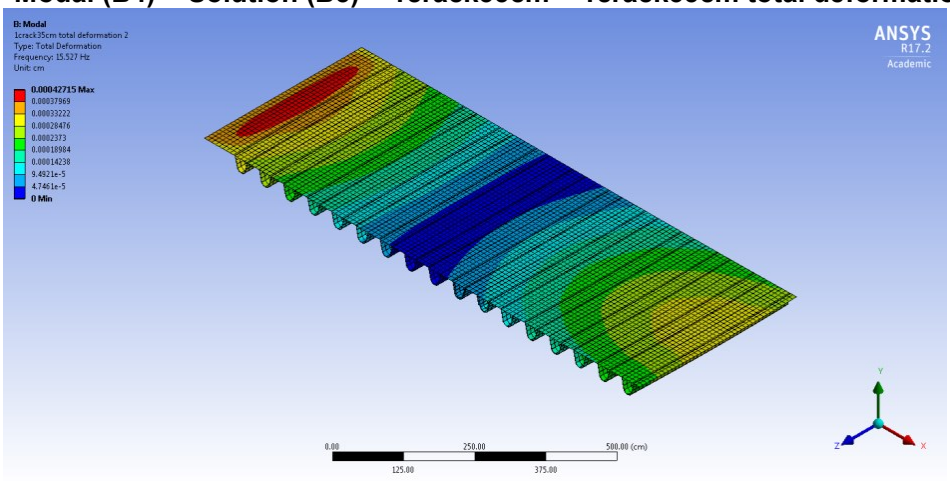


FIGURE 146
Model (B3) > Modal (B4) > Solution (B5) > 1crack35cm > 1crack35cm total deformation 3 > Image

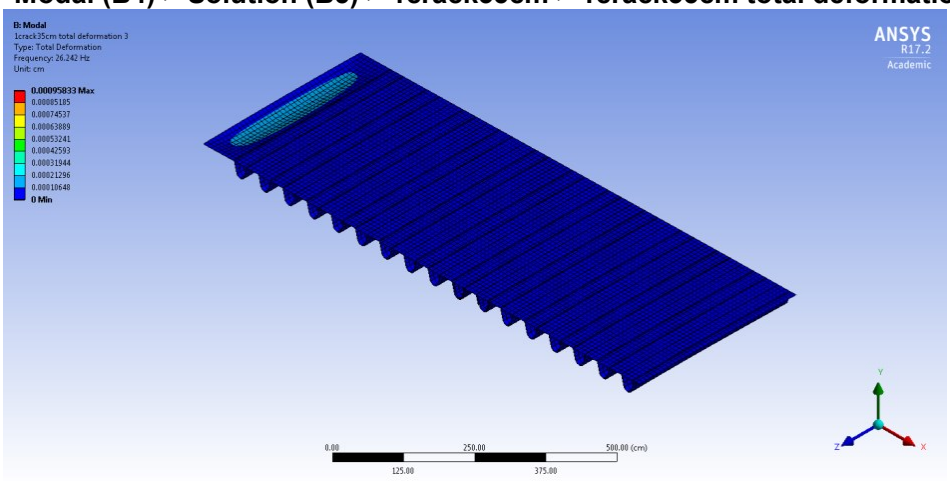


FIGURE 147
Model (B3) > Modal (B4) > Solution (B5) > 1crack35cm > 1crack35cm total deformation 4 > Image

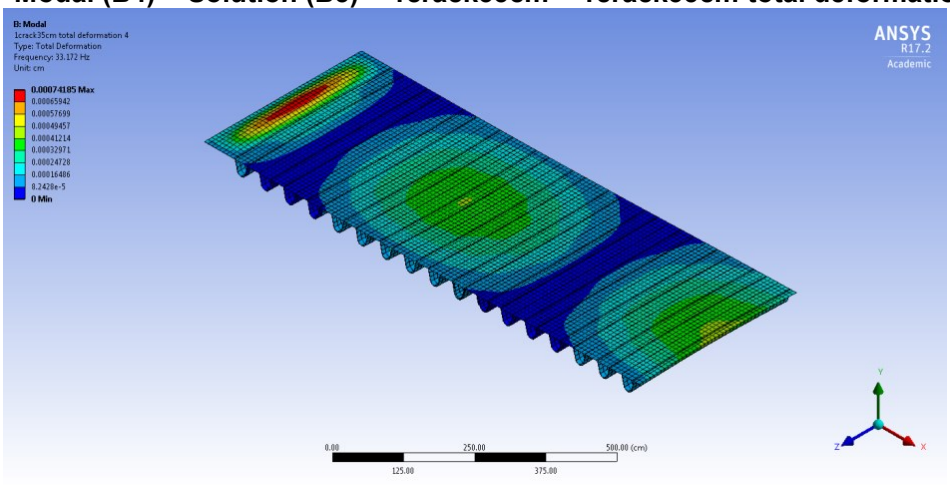


FIGURE 148
Model (B3) > Modal (B4) > Solution (B5) > 1crack35cm > 1crack35cm total deformation 5 > Image

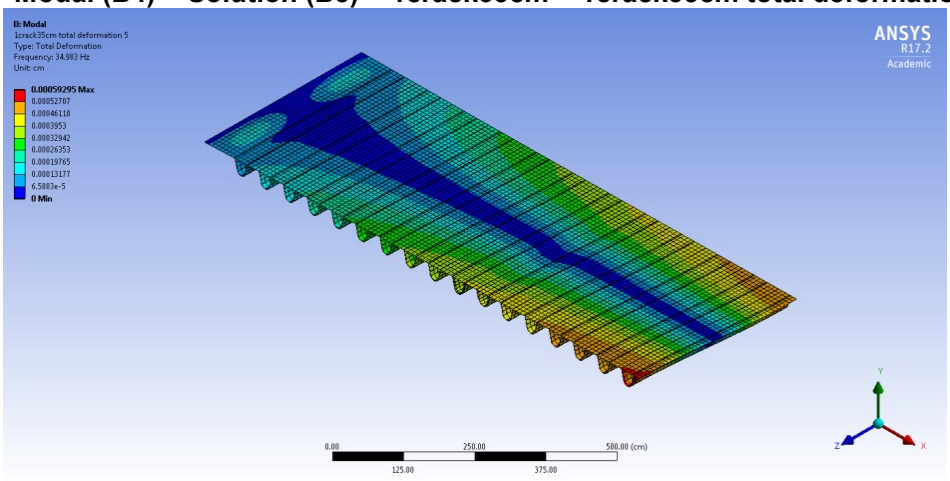


FIGURE 149
Model (B3) > Modal (B4) > Solution (B5) > 1crack35cm > 1crack35cm total deformation 6 > Image

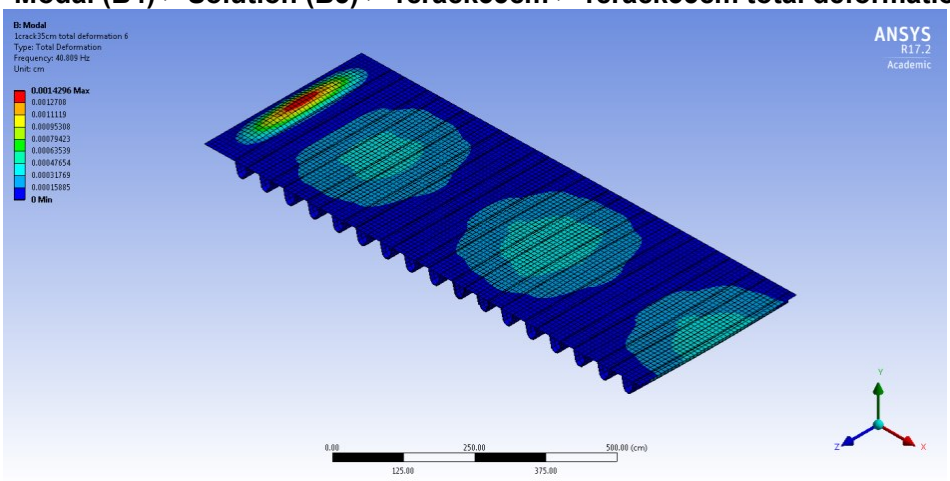


FIGURE 150
Model (B3) > Modal (B4) > Solution (B5) > 1crack35cm > 1crack35cm total deformation 7 > Image

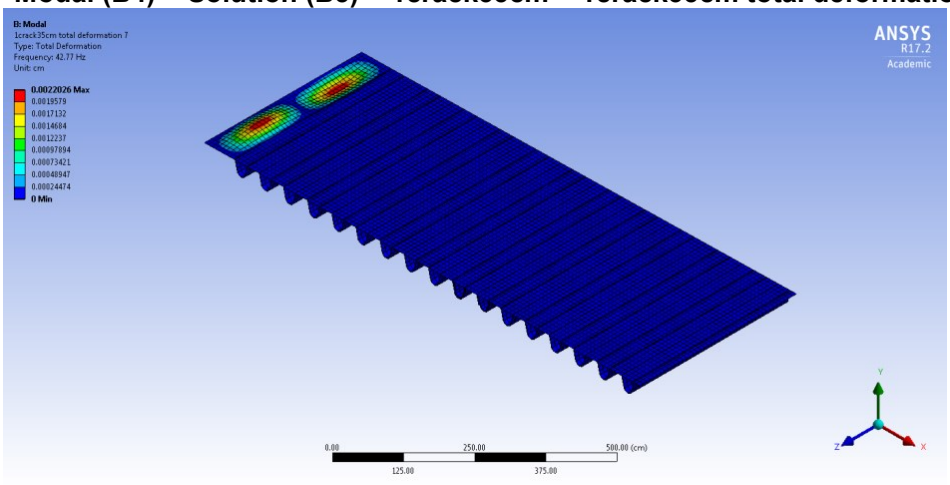


FIGURE 151
Model (B3) > Modal (B4) > Solution (B5) > 1crack35cm > 1crack35cm total deformation 8 > Image

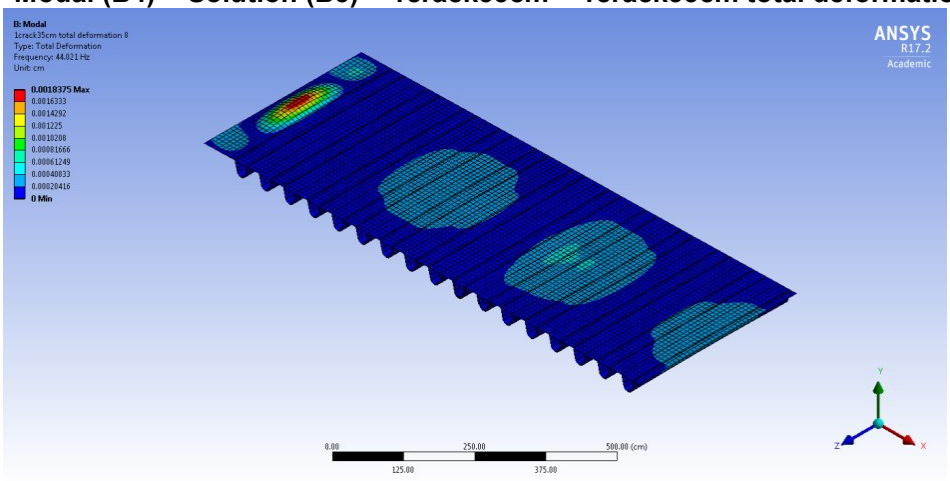


FIGURE 152
Model (B3) > Modal (B4) > Solution (B5) > 1crack35cm > 1crack35cm total deformation 9 > Image

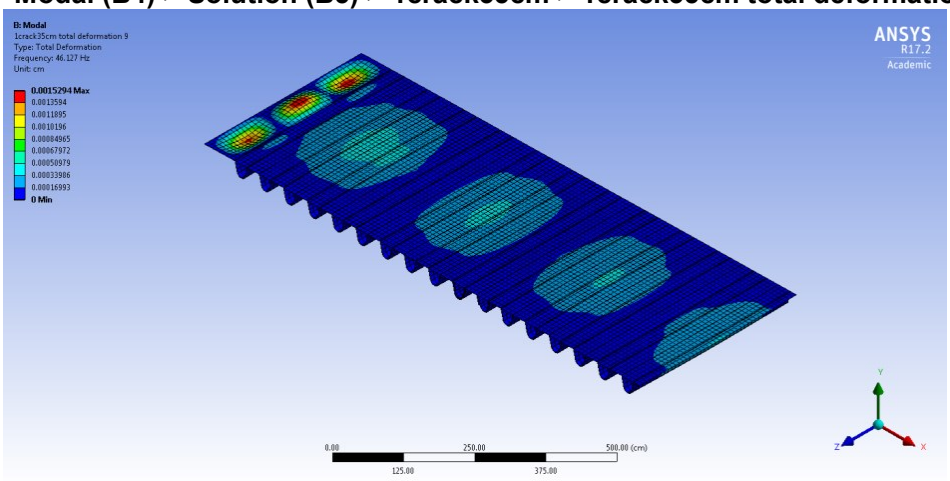


FIGURE 153
Model (B3) > Modal (B4) > Solution (B5) > 1crack35cm > 1crack35cm total deformation 10 > Image

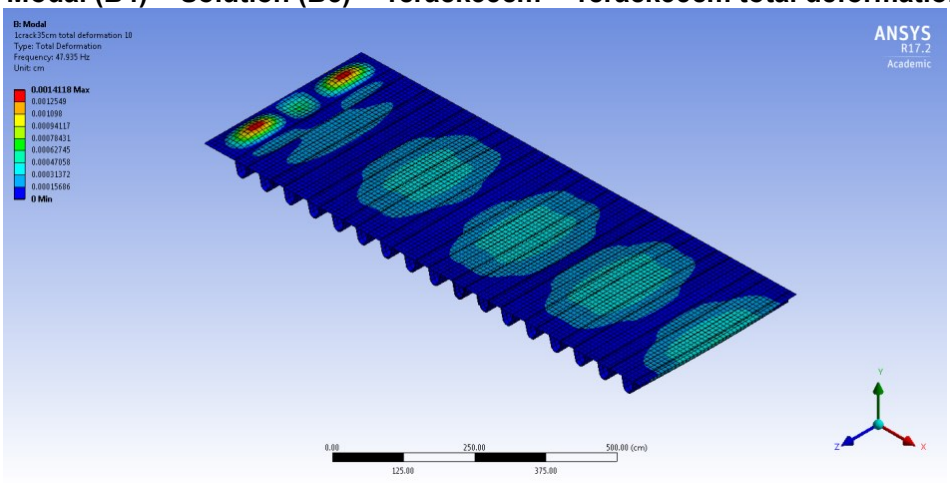


FIGURE 154
Model (B3) > Modal (B4) > Solution (B5) > 1crack35cm > 1crack35cm total deformation 11 > Image

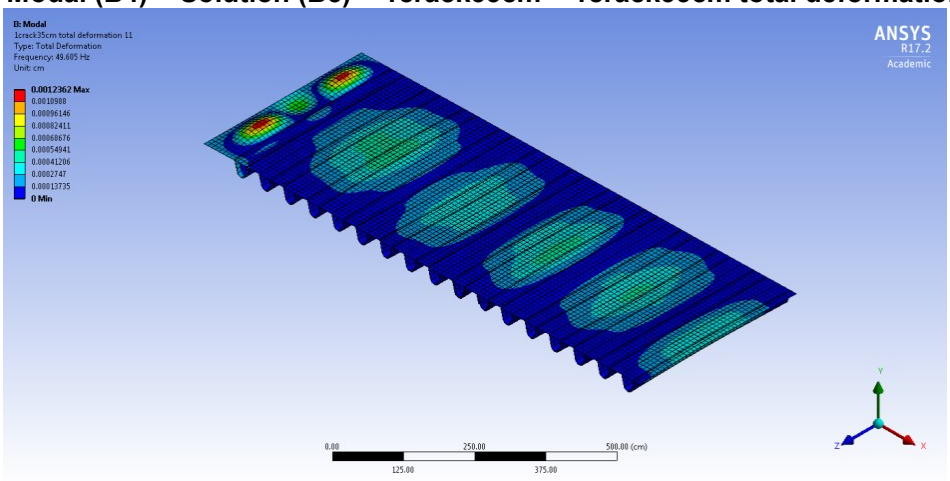


TABLE 138
Model (B3) > Modal (B4) > Solution (B5) > 1crack35cm > Results

Object Name	*1crack 35cm total deformation 12*	*1crack 35cm total deformation 13*	*1crack 35cm total deformation 14*	*1crack 35cm total deformation 15*	*1crack 35cm total deformation 16*	*1crack 35cm total deformation 17*	*1crack 35cm total deformation 18*	*1crack 35cm total deformation 19*	*1crack 35cm total deformation 20*	*1crack 35cm total deformation 21*	*1crack 35cm total deformation 22*
State	Suppressed										
Scope											
Scoping Method	Geometry Selection										
Geometry	All Bodies										
Definition											
Type	Total Deformation										
Mode	12.	13.	14.	15.	16.	17.	18.	19.	20.	21.	22.

Identifier	
Suppressed	Yes

FIGURE 155
Model (B3) > Modal (B4) > Solution (B5) > 1crack35cm > 1crack35cm total deformation 12 > Image

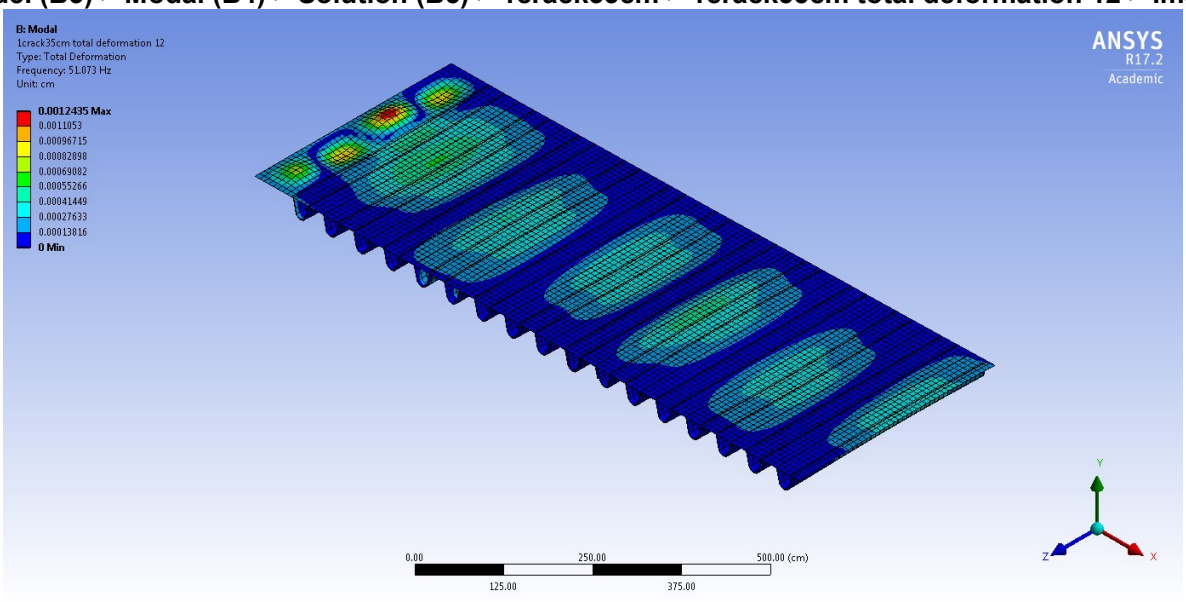


FIGURE 156
Model (B3) > Modal (B4) > Solution (B5) > 1crack35cm > 1crack35cm total deformation 13 > Image

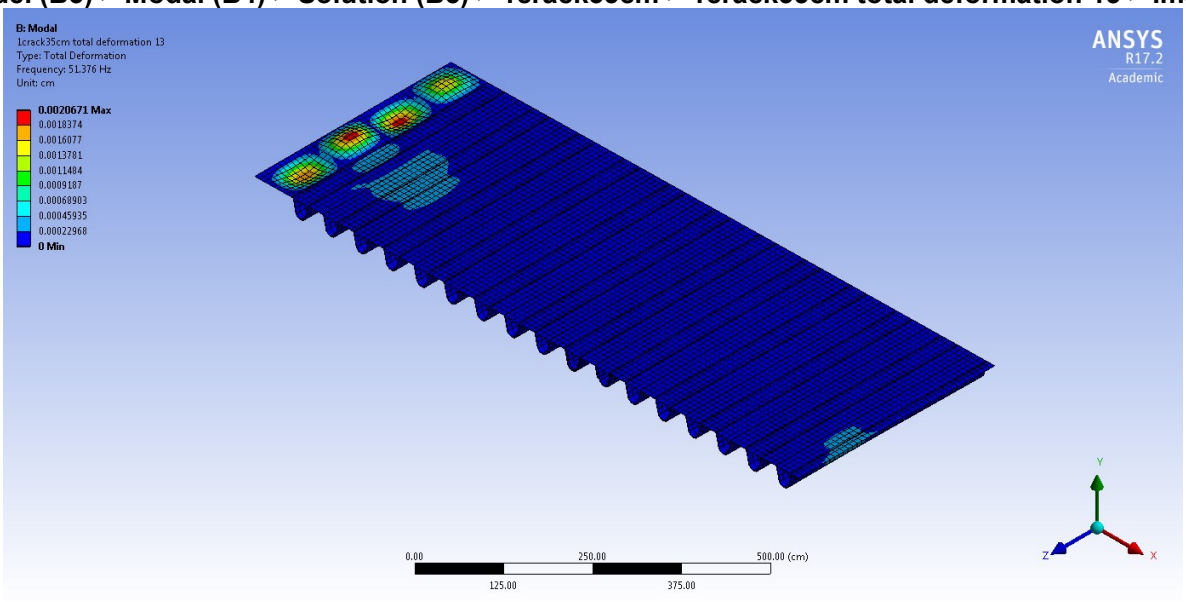


FIGURE 157
Model (B3) > Modal (B4) > Solution (B5) > 1crack35cm > 1crack35cm total deformation 14 > Image

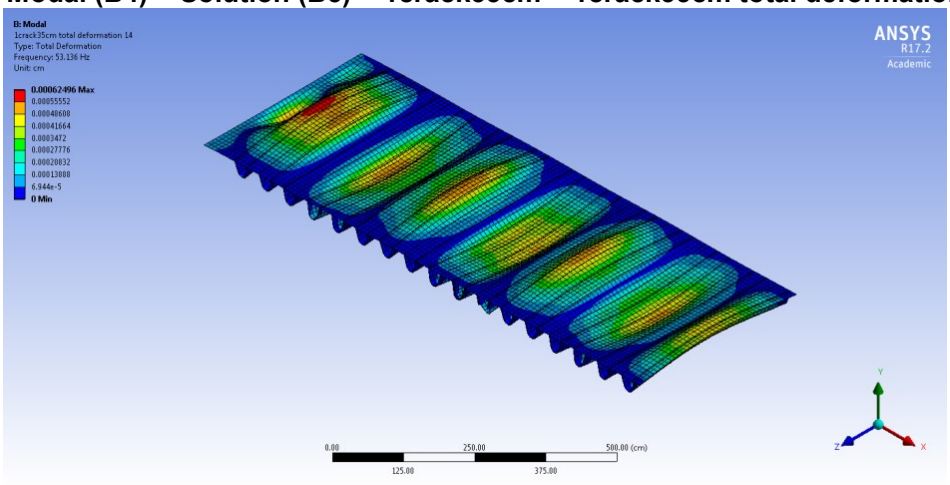


FIGURE 158
Model (B3) > Modal (B4) > Solution (B5) > 1crack35cm > 1crack35cm total deformation 15 > Image

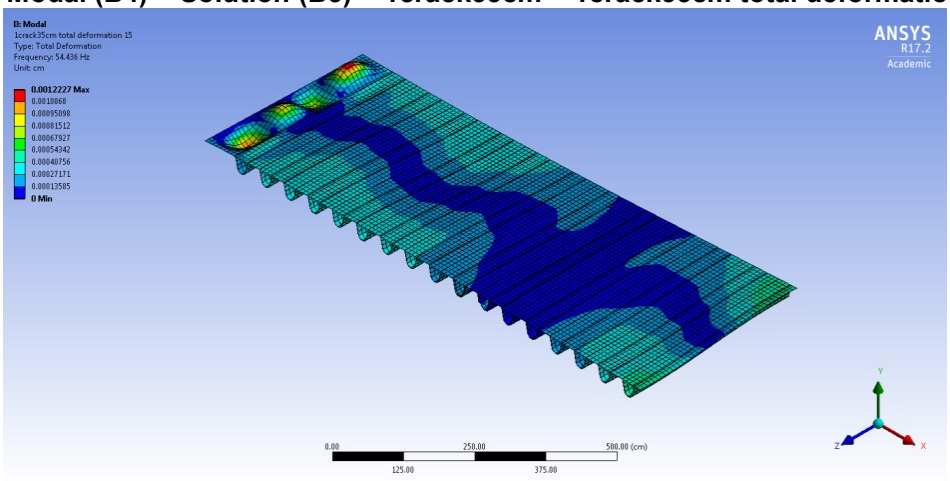


FIGURE 159
Model (B3) > Modal (B4) > Solution (B5) > 1crack35cm > 1crack35cm total deformation 16 > Image

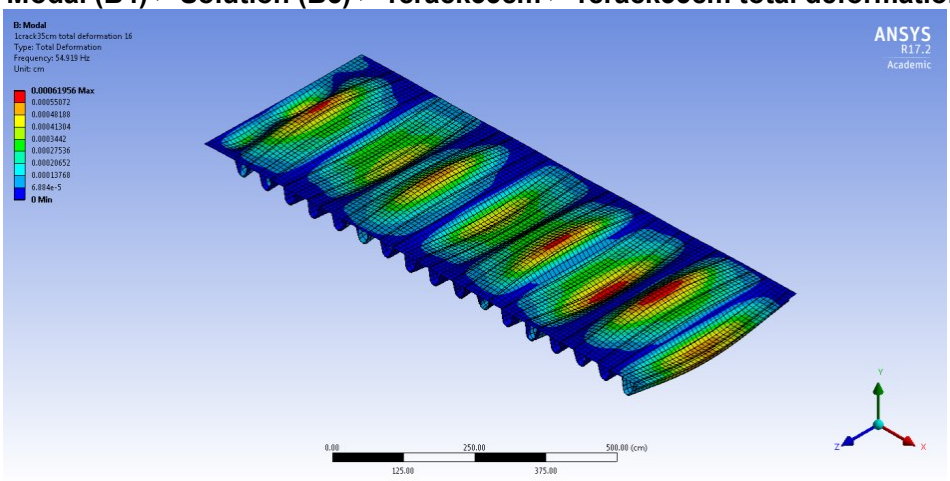


FIGURE 160
Model (B3) > Modal (B4) > Solution (B5) > 1crack35cm > 1crack35cm total deformation 17 > Image

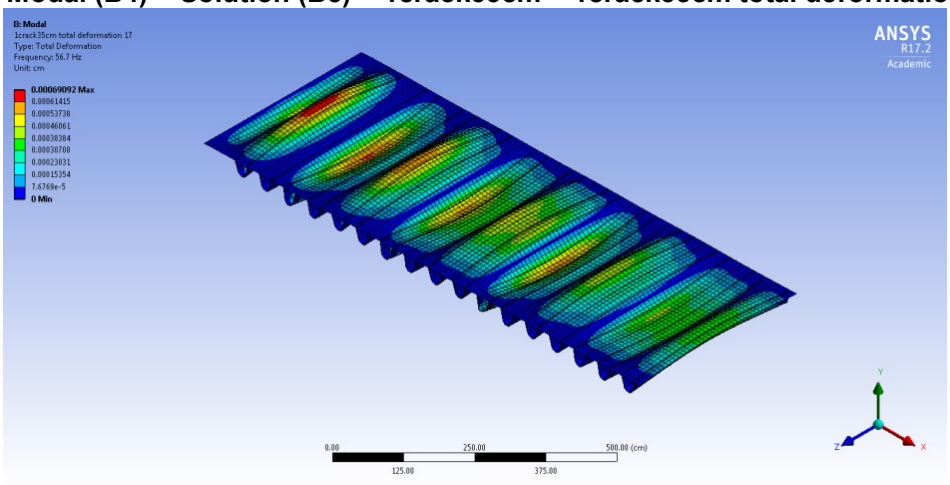


FIGURE 161
Model (B3) > Modal (B4) > Solution (B5) > 1crack35cm > 1crack35cm total deformation 18 > Image

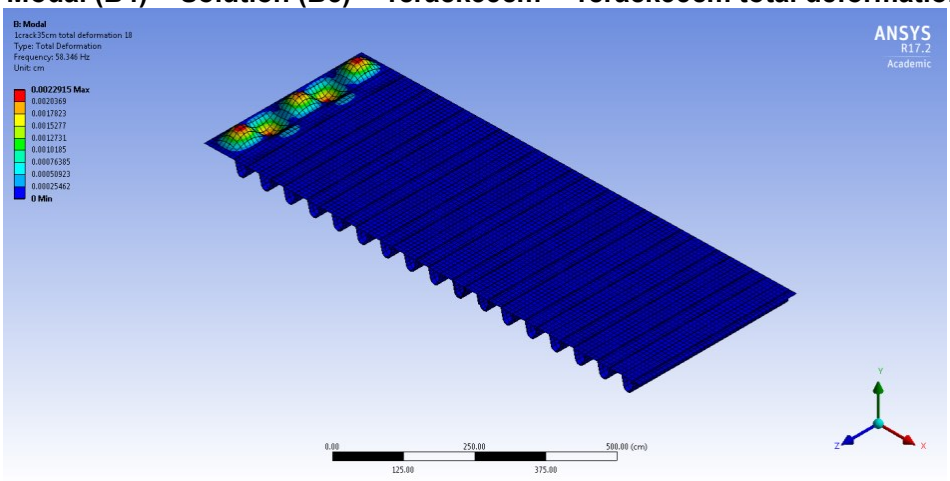


FIGURE 162
Model (B3) > Modal (B4) > Solution (B5) > 1crack35cm > 1crack35cm total deformation 19 > Image

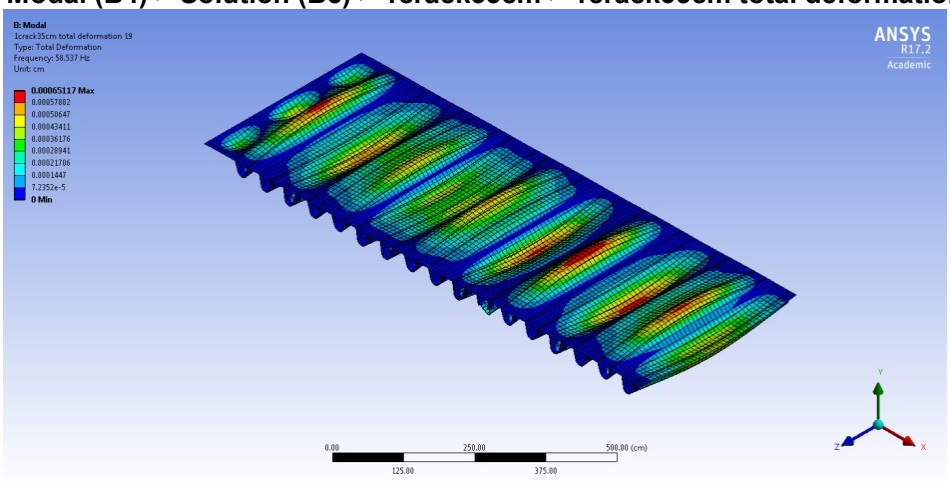


FIGURE 163
Model (B3) > Modal (B4) > Solution (B5) > 1crack35cm > 1crack35cm total deformation 20 > Image

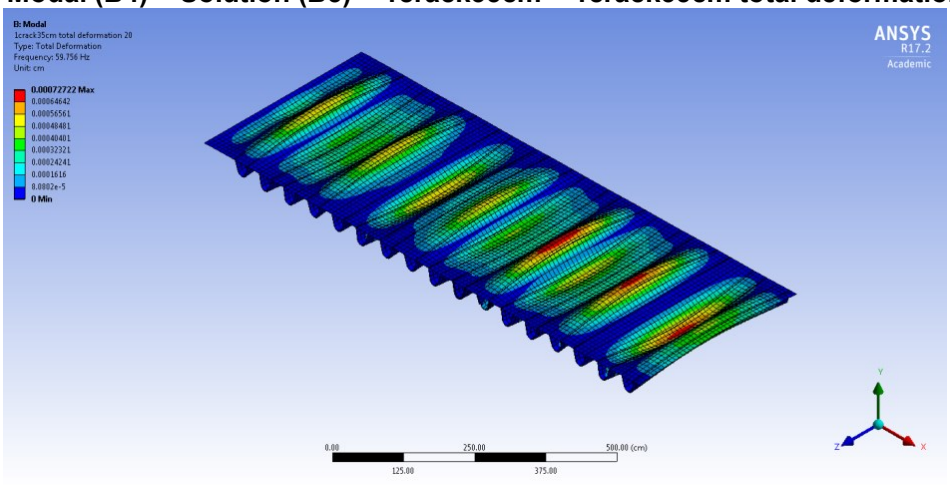


FIGURE 164
Model (B3) > Modal (B4) > Solution (B5) > 1crack35cm > 1crack35cm total deformation 21 > Image

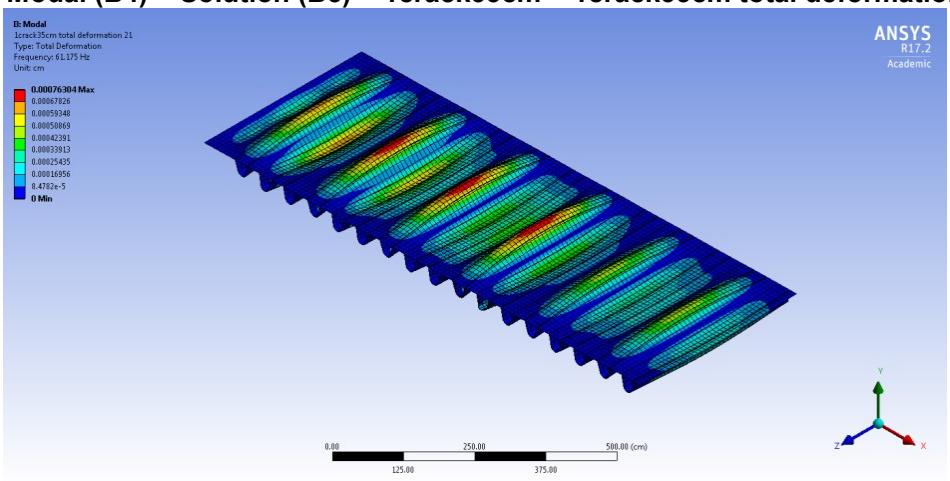


FIGURE 165
Model (B3) > Modal (B4) > Solution (B5) > 1crack35cm > 1crack35cm total deformation 22 > Image

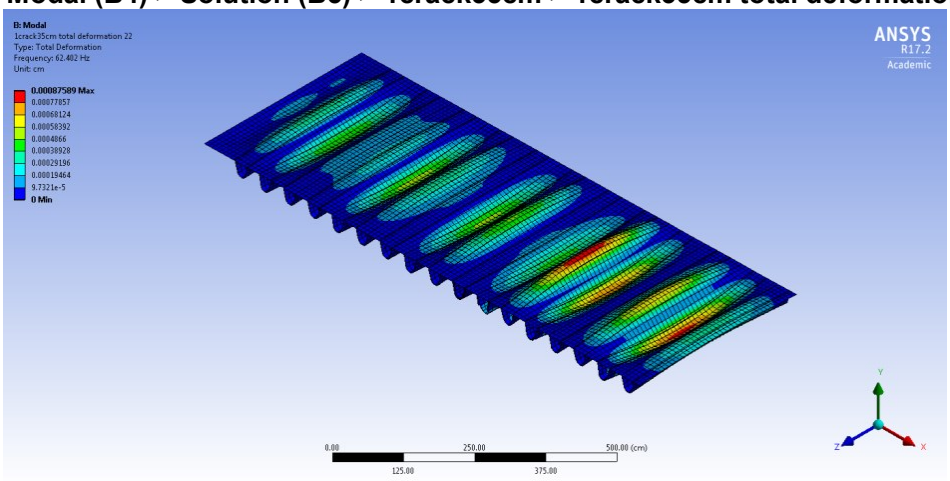


TABLE 139
Model (B3) > Modal (B4) > Solution (B5) > 1crack35cm > Results

Object Name	*1crack35cm total deformation 23*	*1crack35cm total deformation 24*	*1crack35cm total deformation 25*	*1crack35cm total deformation 26*	*1crack35cm total deformation 27*	*1crack35cm total deformation 28*	*1crack35cm total deformation 29*	*1crack35cm total deformation 30*
State	Suppressed							
Scope								
Scoping Method	Geometry Selection							
Geometry	All Bodies							
Definition								
Type	Total Deformation							
Mode	23.	24.	25.	26.	27.	28.	29.	30.
Identifier								
Suppressed	Yes							

FIGURE 166
Model (B3) > Modal (B4) > Solution (B5) > 1crack35cm > 1crack35cm total deformation 23 > Image

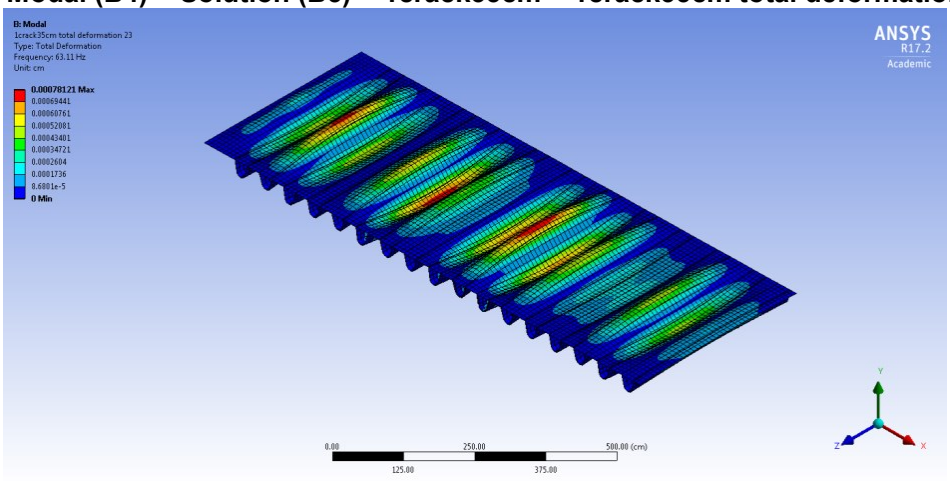


FIGURE 167
Model (B3) > Modal (B4) > Solution (B5) > 1crack35cm > 1crack35cm total deformation 24 > Image

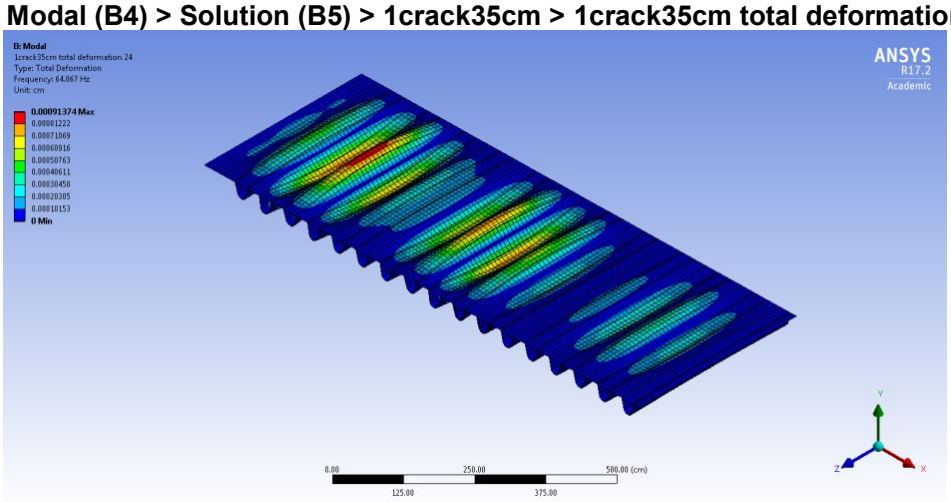


FIGURE 168
Model (B3) > Modal (B4) > Solution (B5) > 1crack35cm > 1crack35cm total deformation 25 > Image

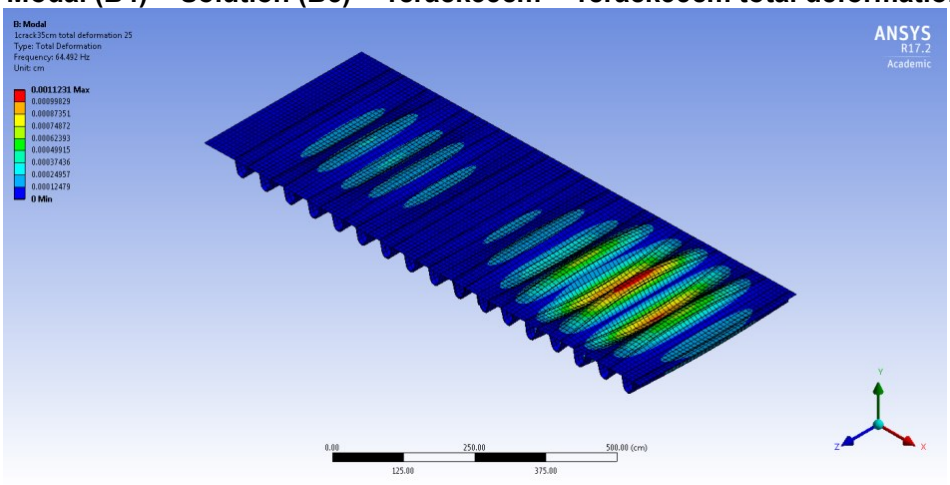


FIGURE 169
Model (B3) > Modal (B4) > Solution (B5) > 1crack35cm > 1crack35cm total deformation 26 > Image

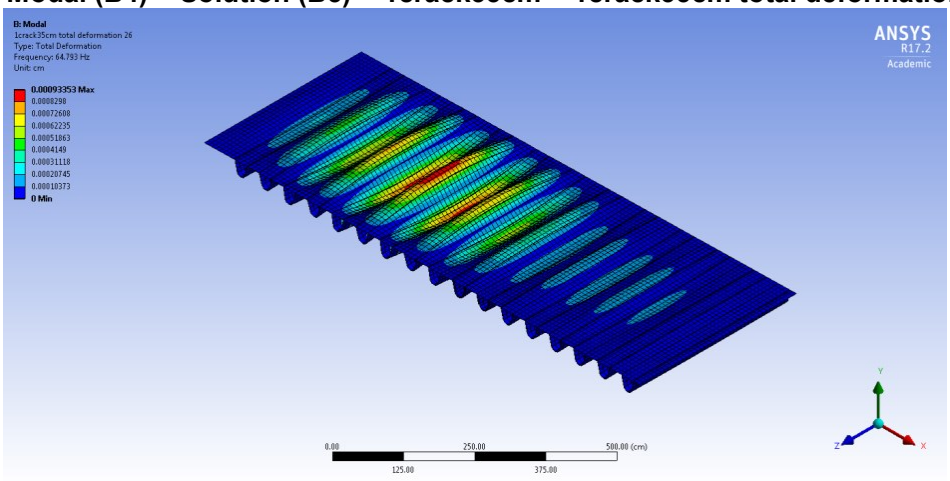


FIGURE 170
Model (B3) > Modal (B4) > Solution (B5) > 1crack35cm > 1crack35cm total deformation 27 > Image

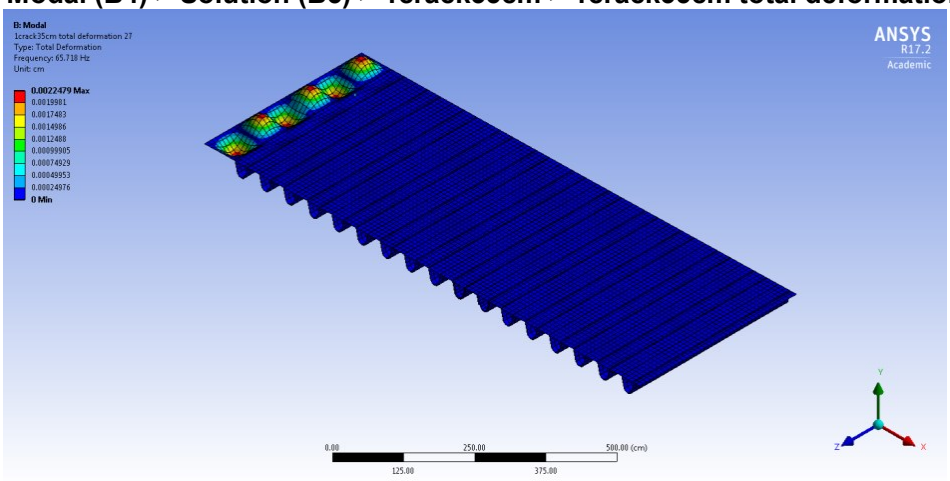


FIGURE 171
Model (B3) > Modal (B4) > Solution (B5) > 1crack35cm > 1crack35cm total deformation 28 > Image

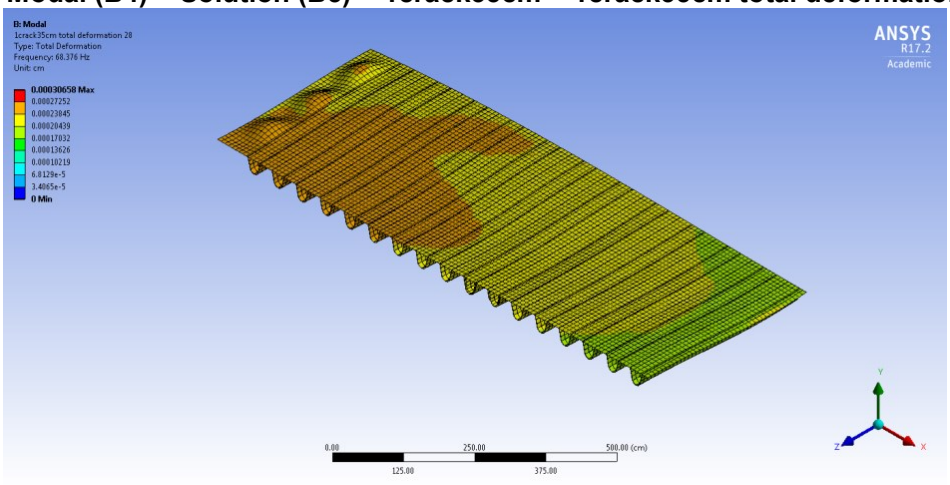


FIGURE 172
Model (B3) > Modal (B4) > Solution (B5) > 1crack35cm > 1crack35cm total deformation 29 > Image

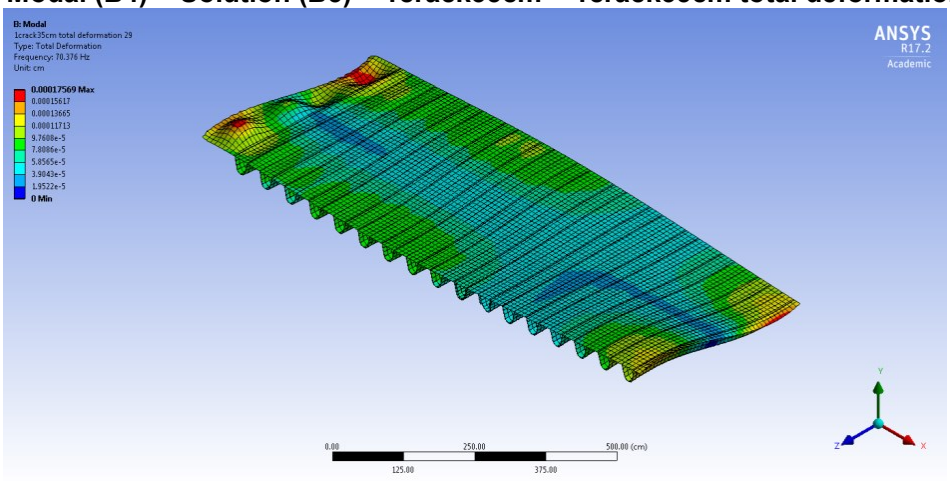
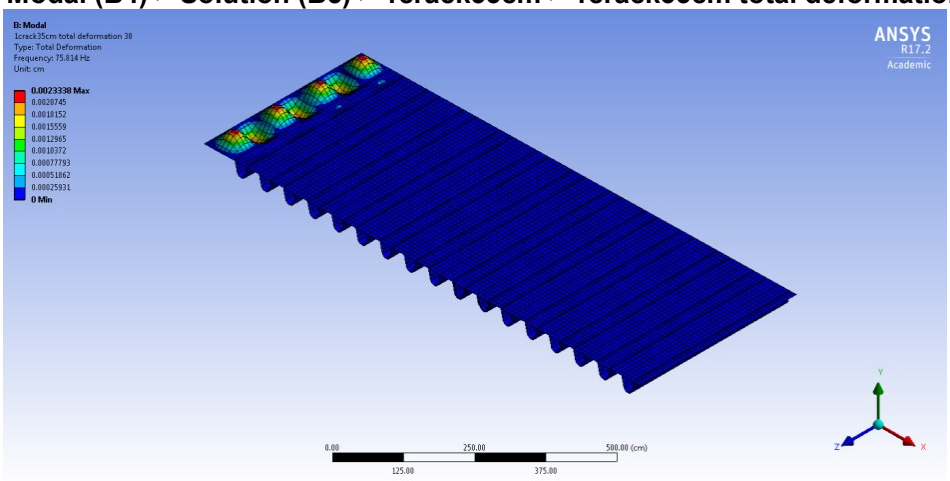


FIGURE 173
Model (B3) > Modal (B4) > Solution (B5) > 1crack35cm > 1crack35cm total deformation 30 > Image



2xcrack35cm

TABLE 140
Model (B3) > Modal (B4) > Solution (B5) > 2xcrack35cm > Results

Object Name	*2xcrack35cm 1*	*2xcrack35cm 2*	*2xcrack35cm 3*	*2xcrack35cm 4*	*2xcrack35cm 5*	*2xcrack35cm 6*	*2xcrack35cm 7*	*2xcrack35cm 8*	*2xcrack35cm 9*	*2xcrack35cm 10*	*2xcrack35cm 11*
State	Suppressed										
Scope											
Scoping Method	Geometry Selection										
Geometry	All Bodies										
Definition											
Type	Total Deformation										
Mode	1.	2.	3.	4.	5.	6.	7.	8.	9.	10.	11.
Identifier											
Suppressed	Yes										

FIGURE 174
Model (B3) > Modal (B4) > Solution (B5) > 2xcrack35cm > 2xcrack35cm 1 > Image

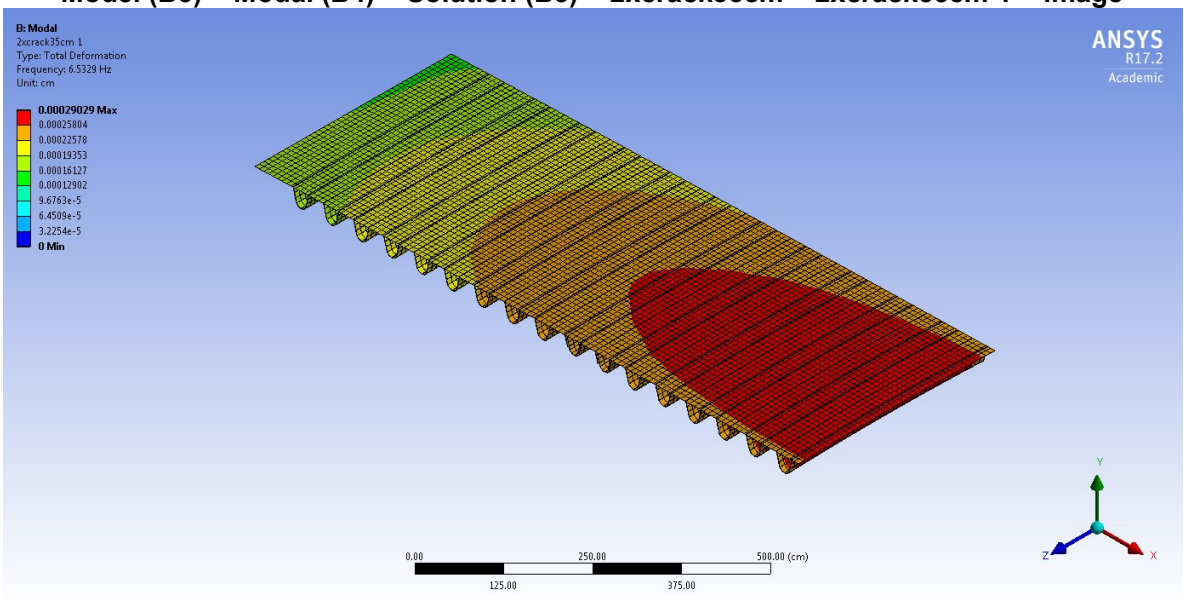


FIGURE 175
Model (B3) > Modal (B4) > Solution (B5) > 2xcrack35cm > 2xcrack35cm 2 > Image

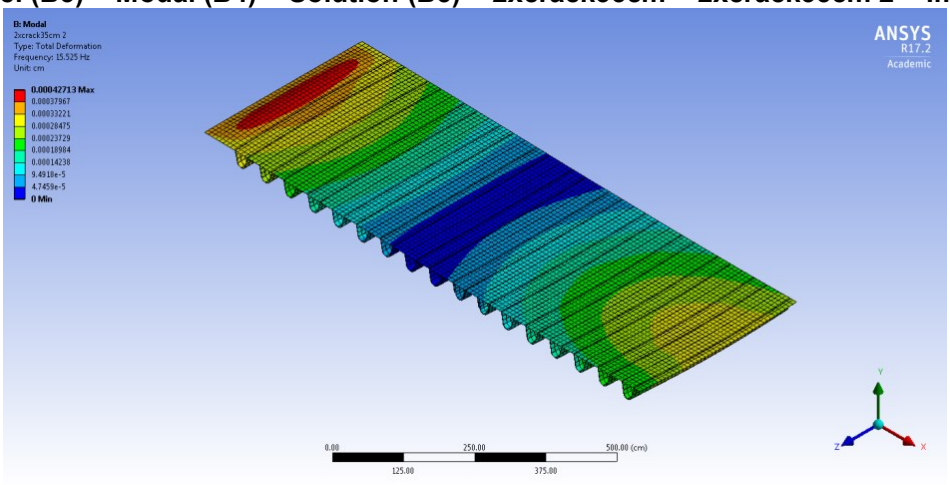


FIGURE 176
Model (B3) > Modal (B4) > Solution (B5) > 2xcrack35cm > 2xcrack35cm 3 > Image

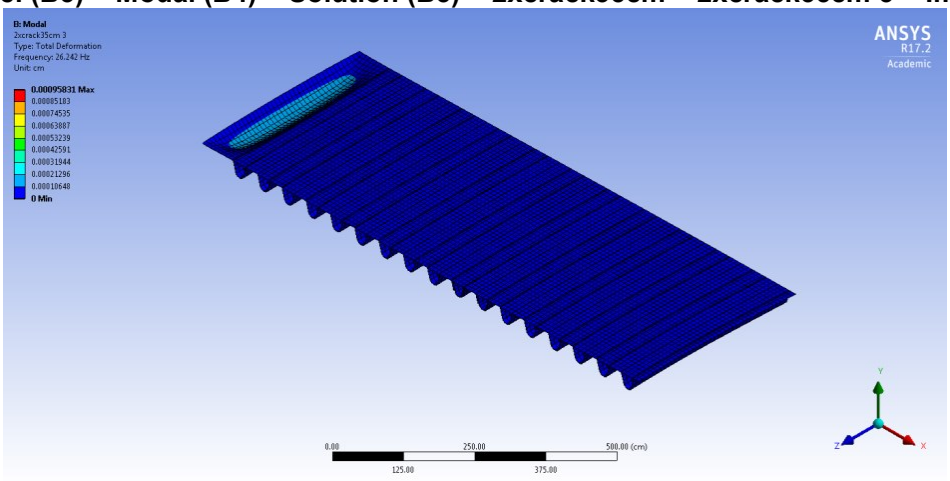


FIGURE 177
Model (B3) > Modal (B4) > Solution (B5) > 2xcrack35cm > 2xcrack35cm 4 > Image

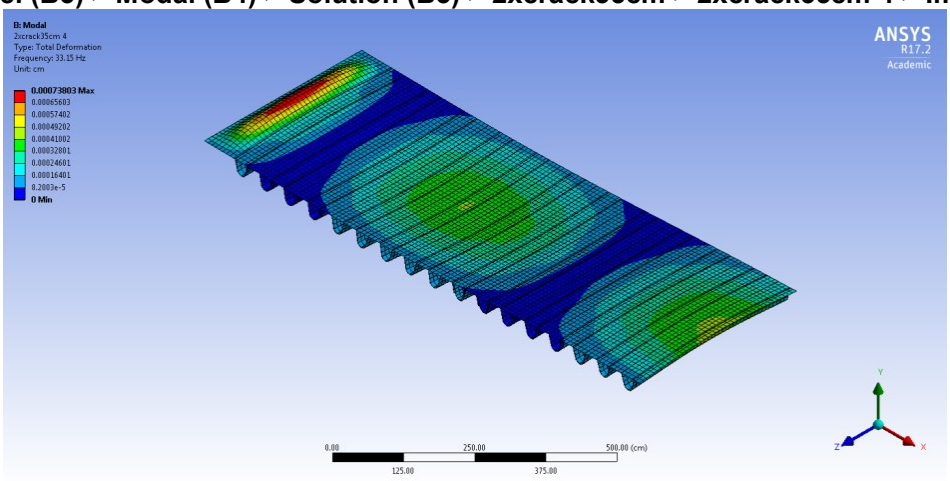


FIGURE 178
Model (B3) > Modal (B4) > Solution (B5) > 2xcrack35cm > 2xcrack35cm 5 > Image

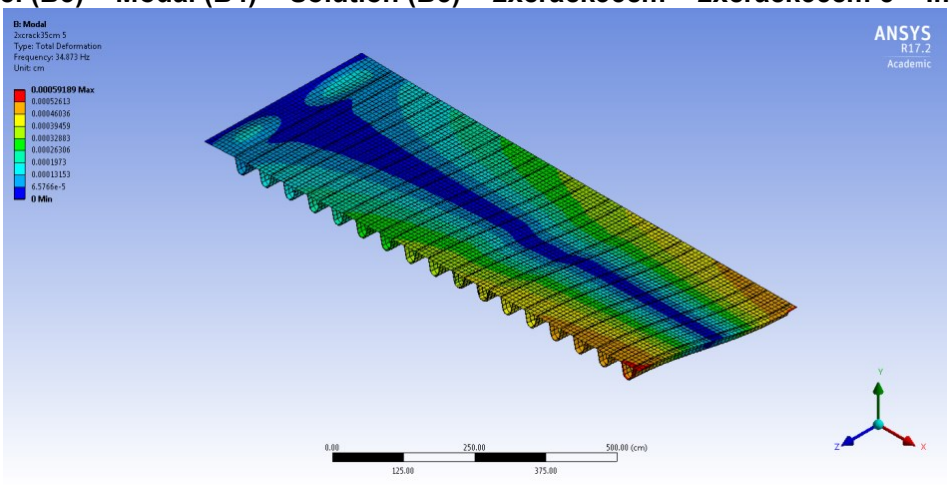


FIGURE 179
Model (B3) > Modal (B4) > Solution (B5) > 2xcrack35cm > 2xcrack35cm 6 > Image

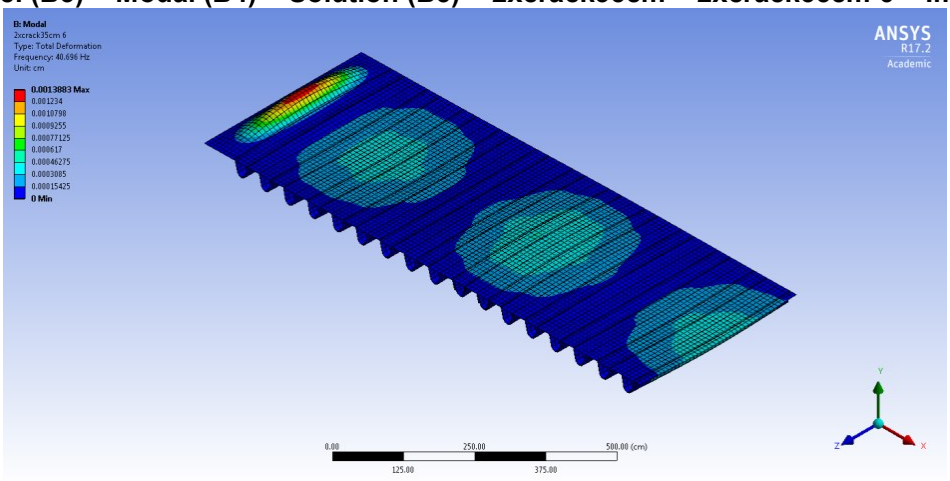


FIGURE 180
Model (B3) > Modal (B4) > Solution (B5) > 2xcrack35cm > 2xcrack35cm 7 > Image

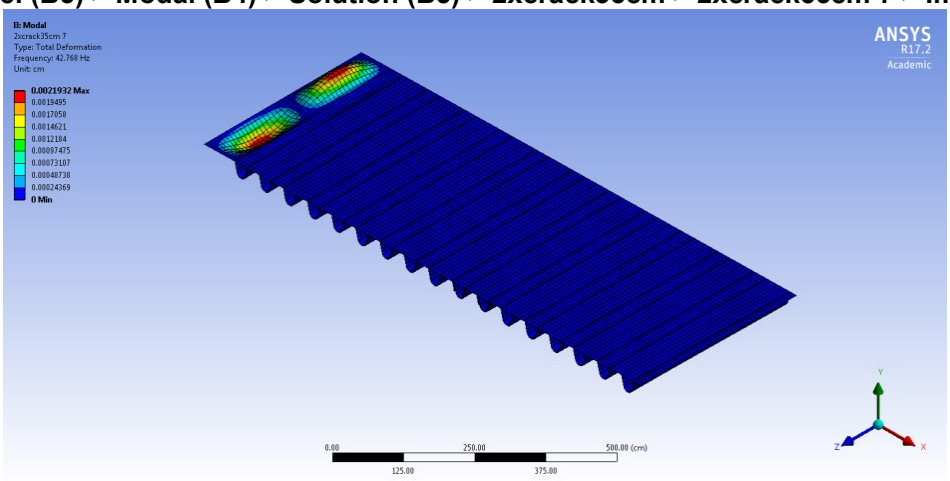


FIGURE 181
Model (B3) > Modal (B4) > Solution (B5) > 2xcrack35cm > 2xcrack35cm 8 > Image

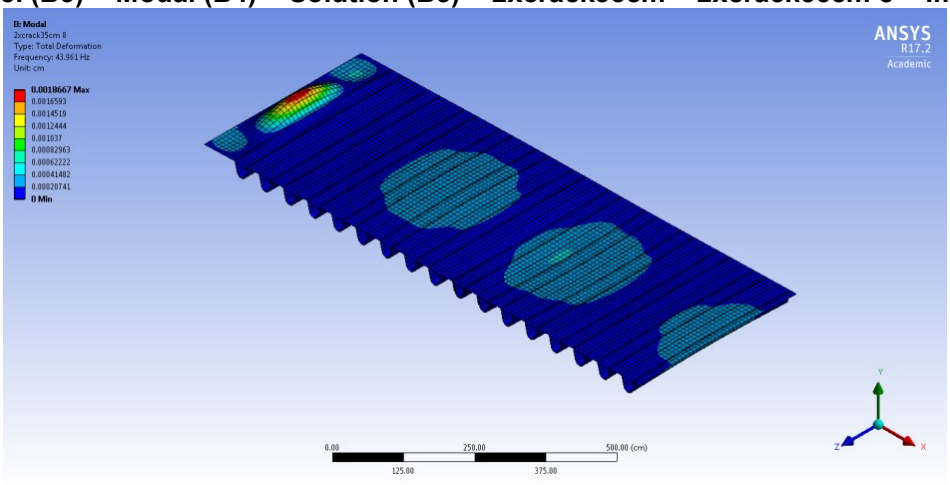


FIGURE 182
Model (B3) > Modal (B4) > Solution (B5) > 2xcrack35cm > 2xcrack35cm 9 > Image

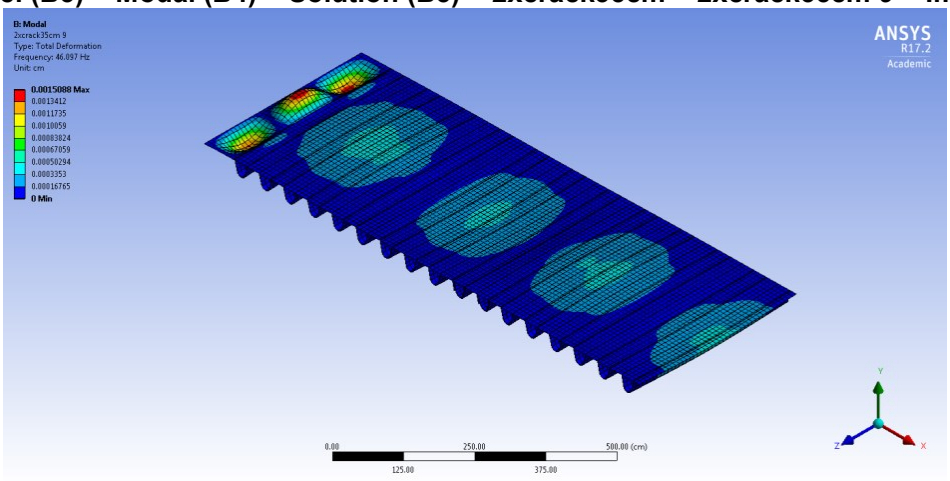


FIGURE 183
Model (B3) > Modal (B4) > Solution (B5) > 2xcrack35cm > 2xcrack35cm 10 > Image

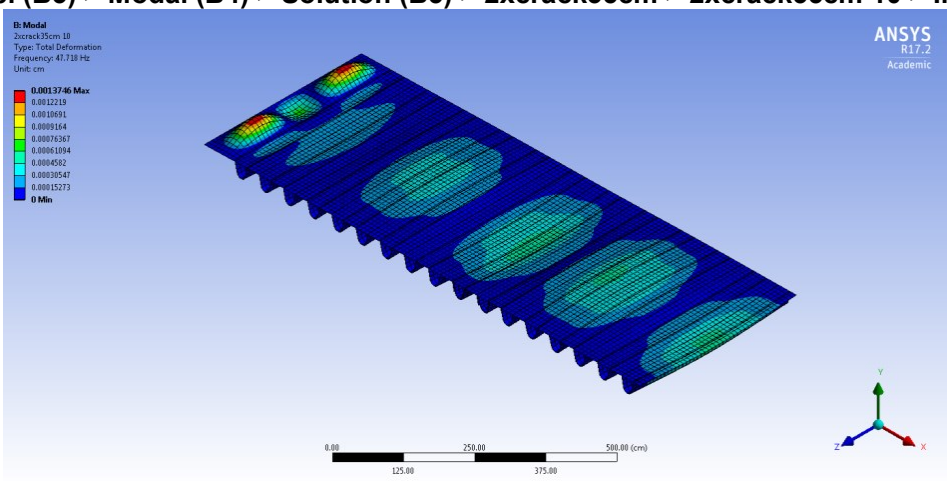


FIGURE 184
Model (B3) > Modal (B4) > Solution (B5) > 2xcrack35cm > 2xcrack35cm 11 > Image

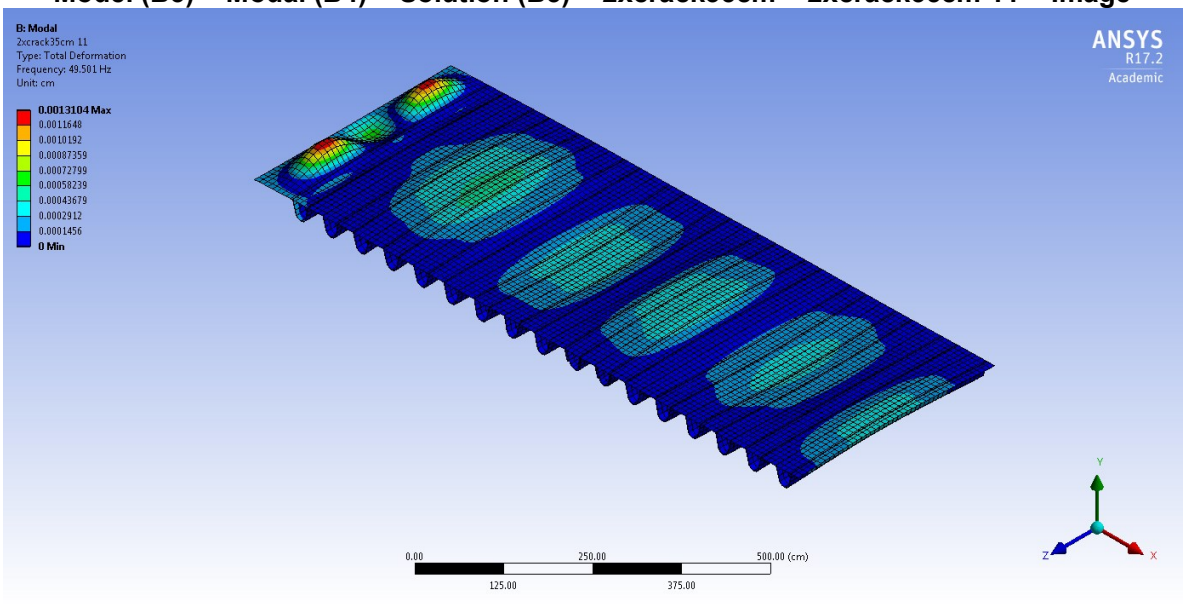


TABLE 141
Model (B3) > Modal (B4) > Solution (B5) > 2xcrack35cm > Results

Object Name	*2xcrack35cm 12*	*2xcrack35cm 13*	*2xcrack35cm 14*	*2xcrack35cm 15*	*2xcrack35cm 16*	*2xcrack35cm 17*	*2xcrack35cm 18*	*2xcrack35cm 19*	*2xcrack35cm 20*	*2xcrack35cm 21*	*2xcrack35cm 22*
State	Suppressed										
Scope											
Scoping Method	Geometry Selection										
Geometry	All Bodies										
Definition											
Type	Total Deformation										
Mode	12.	13.	14.	15.	16.	17.	18.	19.	20.	21.	22.
Identifier											
Suppressed	Yes										

FIGURE 185
Model (B3) > Modal (B4) > Solution (B5) > 2xcrack35cm > 2xcrack35cm 12 > Image

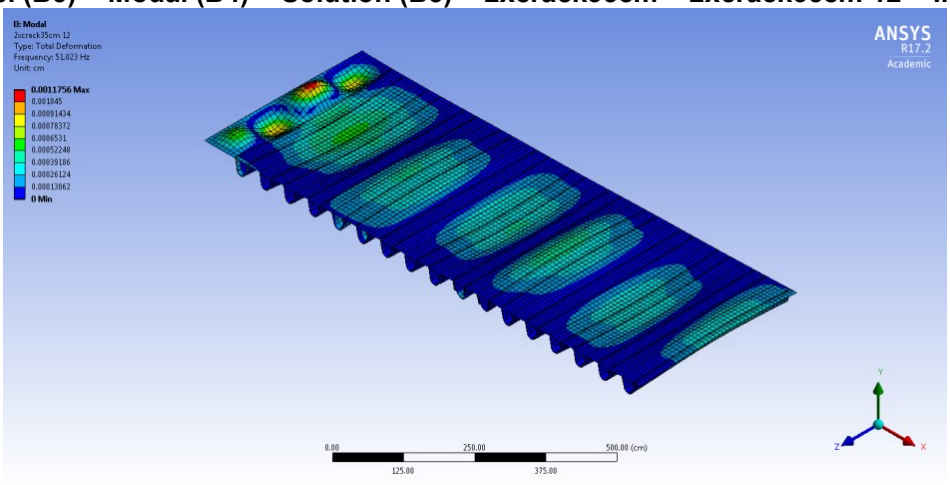


FIGURE 186
Model (B3) > Modal (B4) > Solution (B5) > 2xcrack35cm > 2xcrack35cm 13 > Image

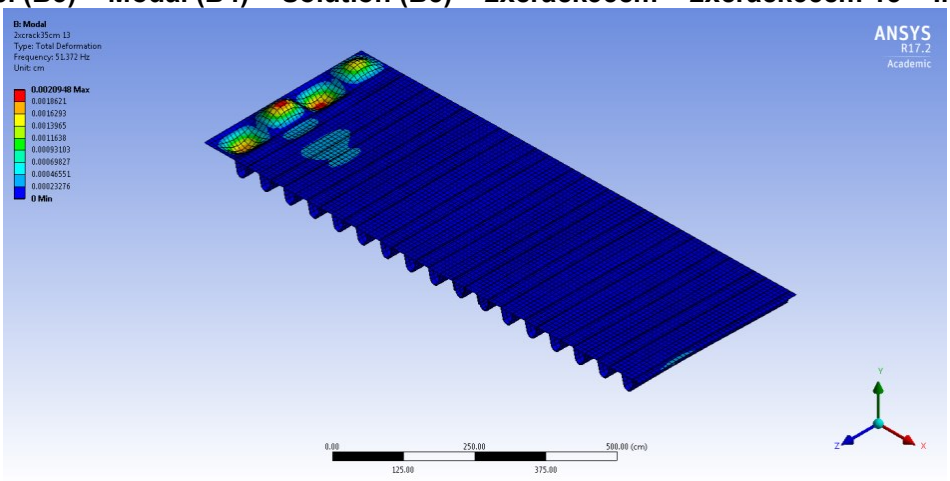


FIGURE 187
Model (B3) > Modal (B4) > Solution (B5) > 2xcrack35cm > 2xcrack35cm 14 > Image

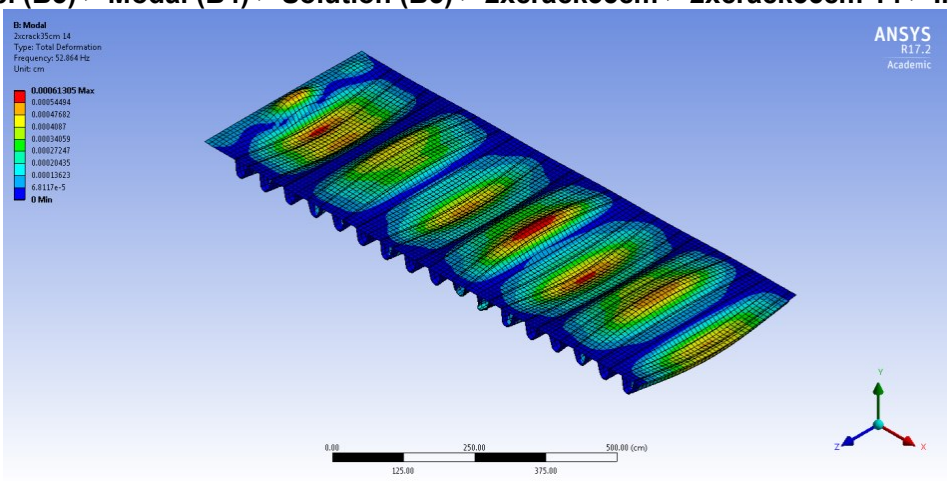


FIGURE 188
Model (B3) > Modal (B4) > Solution (B5) > 2xcrack35cm > 2xcrack35cm 15 > Image

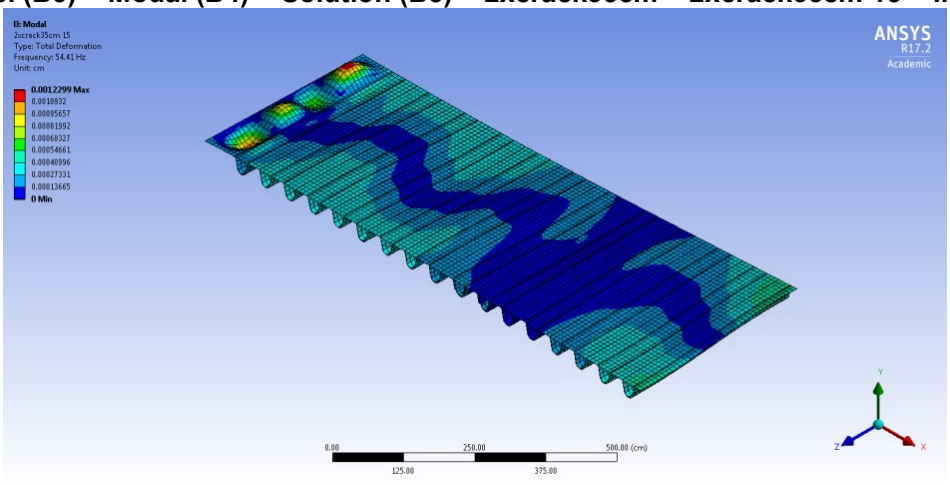


FIGURE 189
Model (B3) > Modal (B4) > Solution (B5) > 2xcrack35cm > 2xcrack35cm 16 > Image

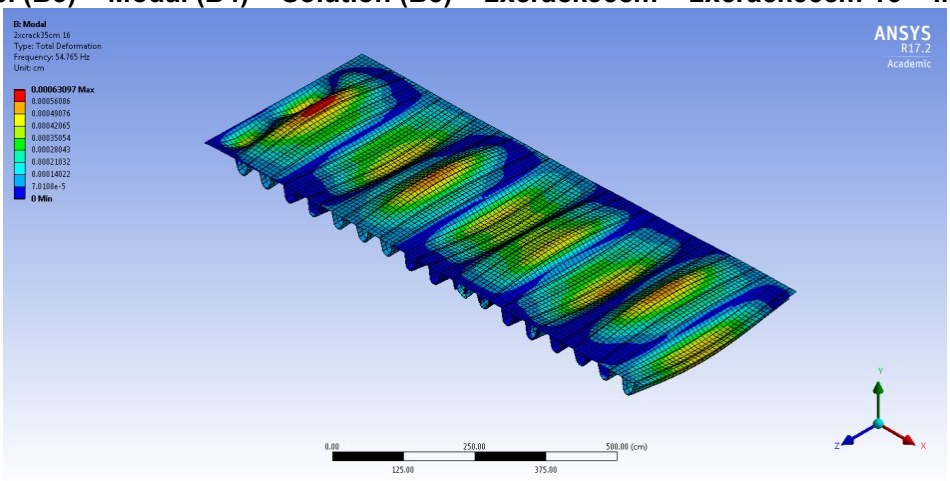


FIGURE 190
Model (B3) > Modal (B4) > Solution (B5) > 2xcrack35cm > 2xcrack35cm 17 > Image

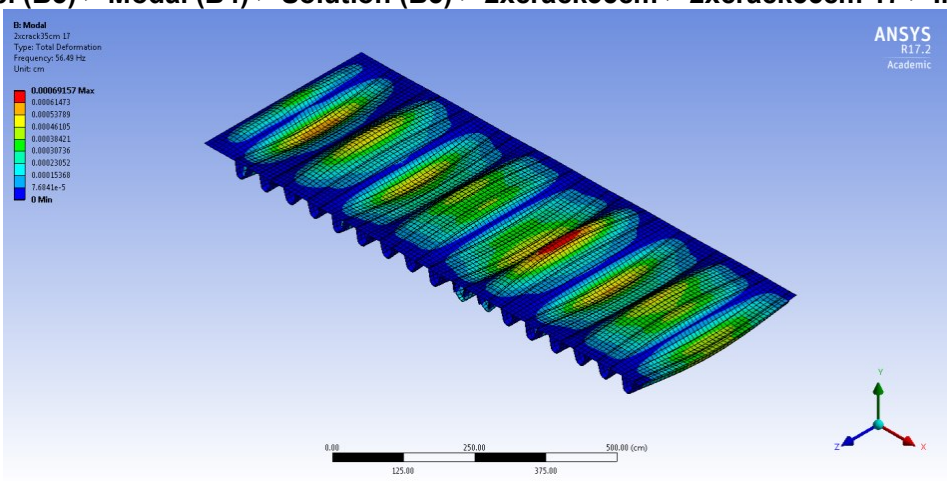


FIGURE 191
Model (B3) > Modal (B4) > Solution (B5) > 2xcrack35cm > 2xcrack35cm 18 > Image

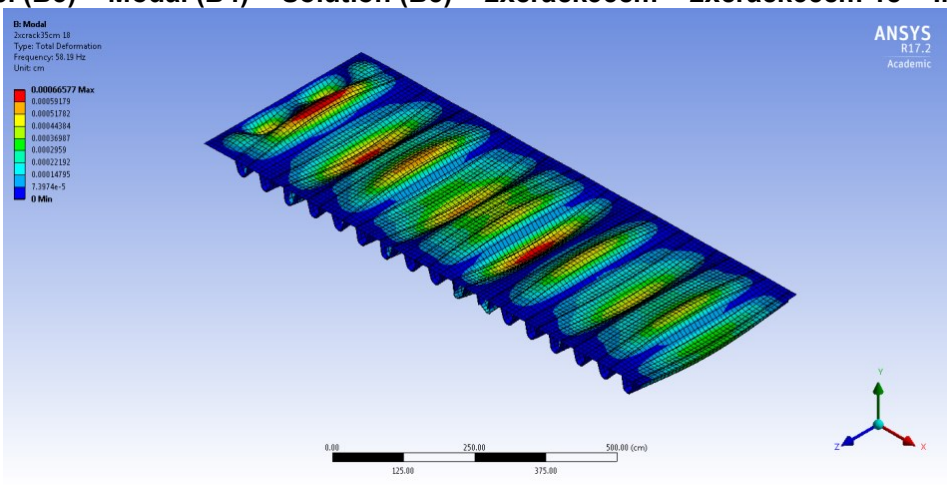


FIGURE 192
Model (B3) > Modal (B4) > Solution (B5) > 2xcrack35cm > 2xcrack35cm 19 > Image

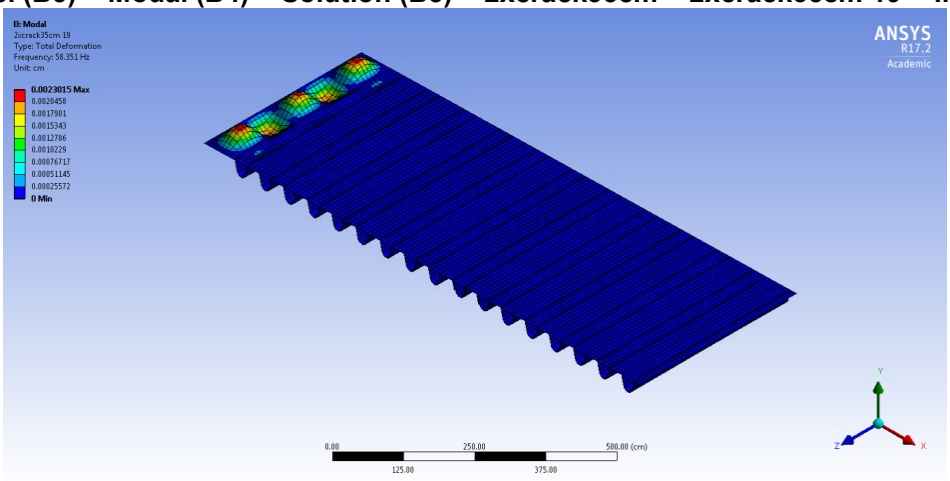


FIGURE 193
Model (B3) > Modal (B4) > Solution (B5) > 2xcrack35cm > 2xcrack35cm 20 > Image

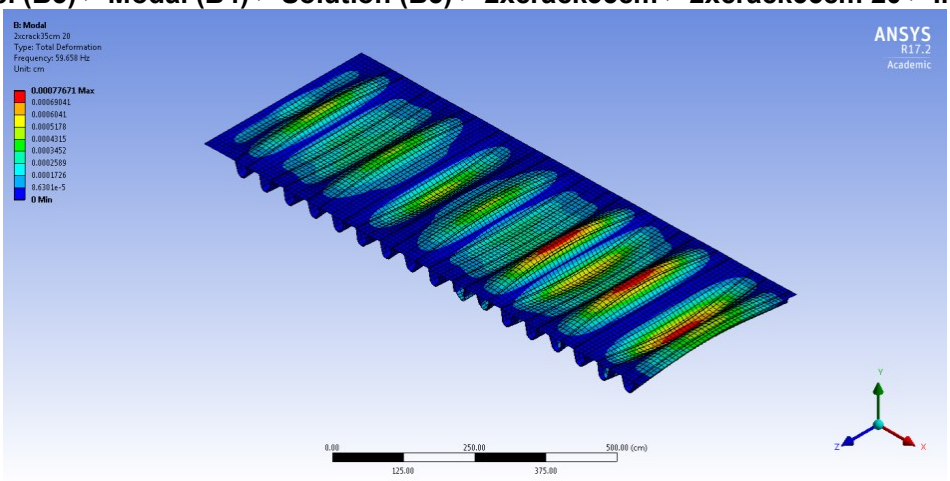


FIGURE 194
Model (B3) > Modal (B4) > Solution (B5) > 2xcrack35cm > 2xcrack35cm 21 > Image

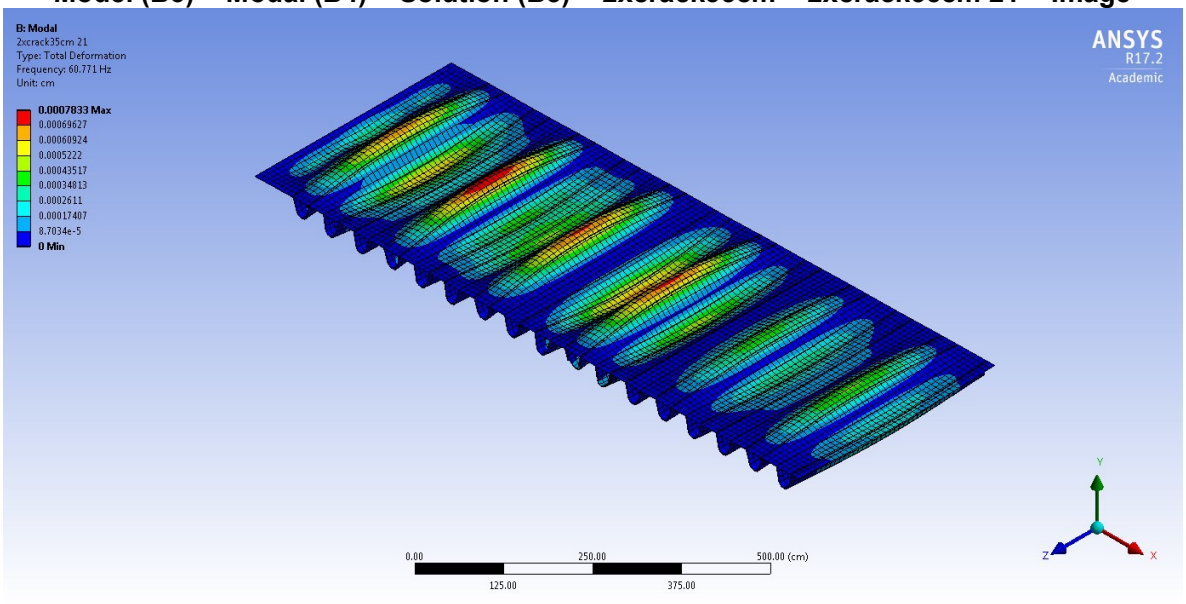


FIGURE 195
Model (B3) > Modal (B4) > Solution (B5) > 2xcrack35cm > 2xcrack35cm 22 > Image

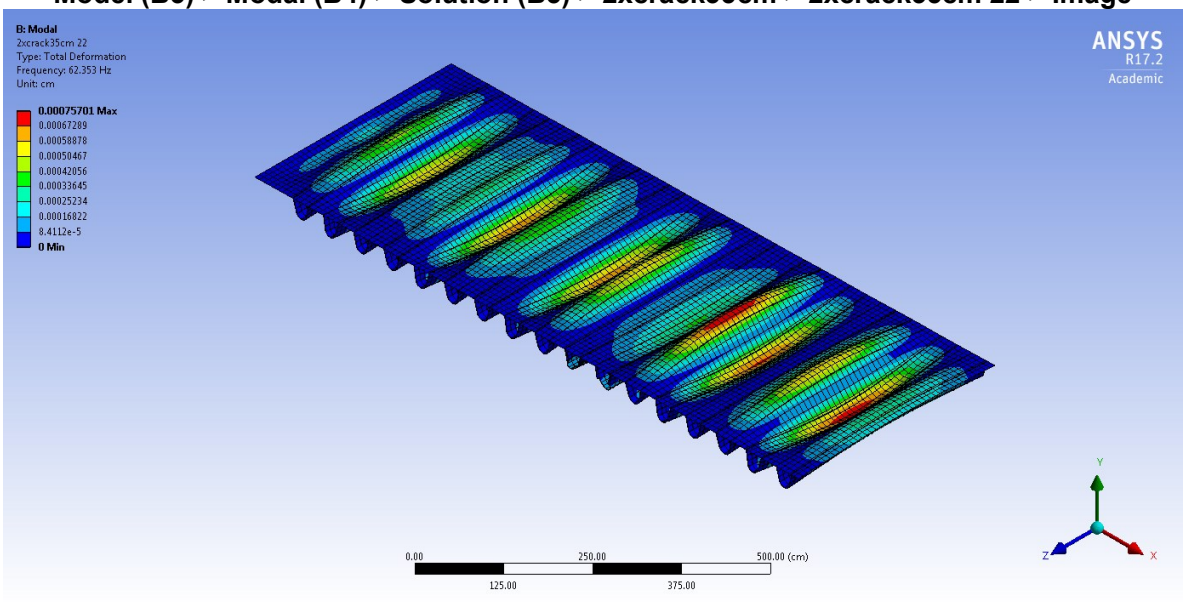


TABLE 142
Model (B3) > Modal (B4) > Solution (B5) > 2xcrack35cm > Results

Object Name	*2xcrack35 cm 23*	*2xcrack35 cm 24*	*2xcrack35 cm 25*	*2xcrack35 cm 26*	*2xcrack35 cm 27*	*2xcrack35 cm 28*	*2xcrack35 cm 29*	*2xcrack35 cm 30*
State	Suppressed							
Scope								
Scoping Method	Geometry Selection							
Geometry	All Bodies							
Definition								

Type	Total Deformation							
Mode	23.	24.	25.	26.	27.	28.	29.	30.
Identifier								
Suppressed	Yes							

FIGURE 196
Model (B3) > Modal (B4) > Solution (B5) > 2xcrack35cm > 2xcrack35cm 23 > Image

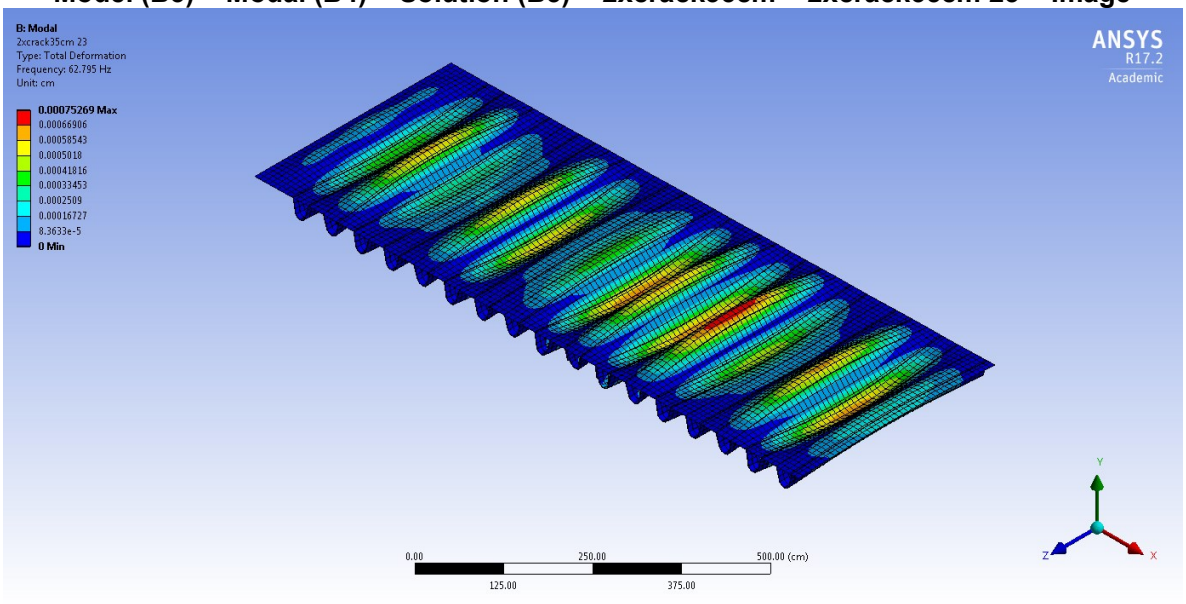


FIGURE 197
Model (B3) > Modal (B4) > Solution (B5) > 2xcrack35cm > 2xcrack35cm 24 > Image

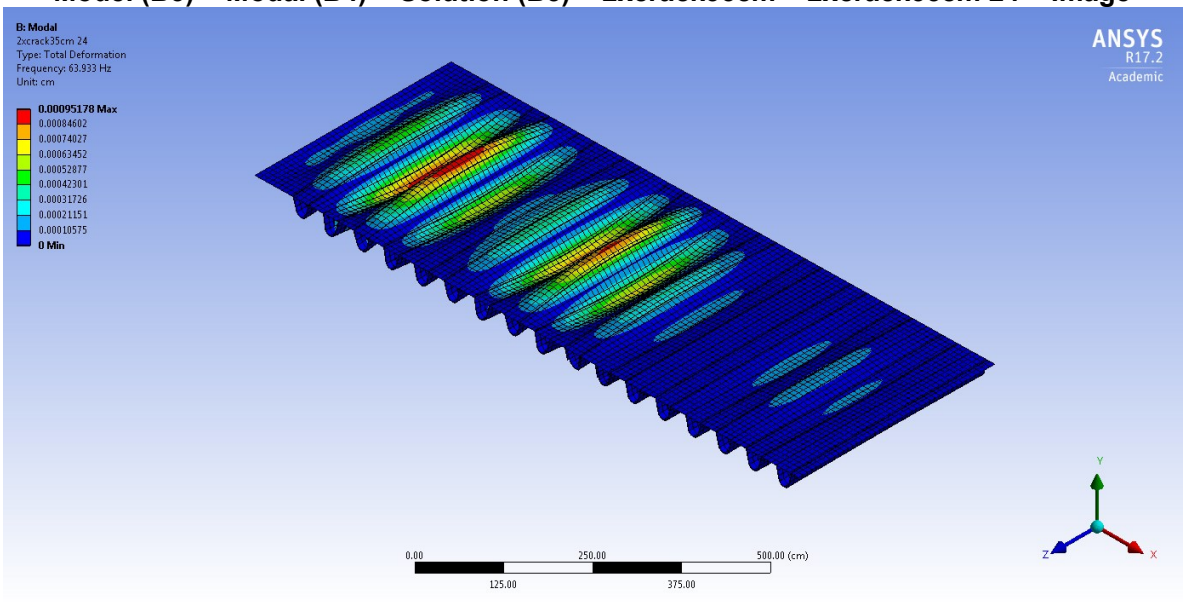


FIGURE 198
Model (B3) > Modal (B4) > Solution (B5) > 2xcrack35cm > 2xcrack35cm 25 > Image

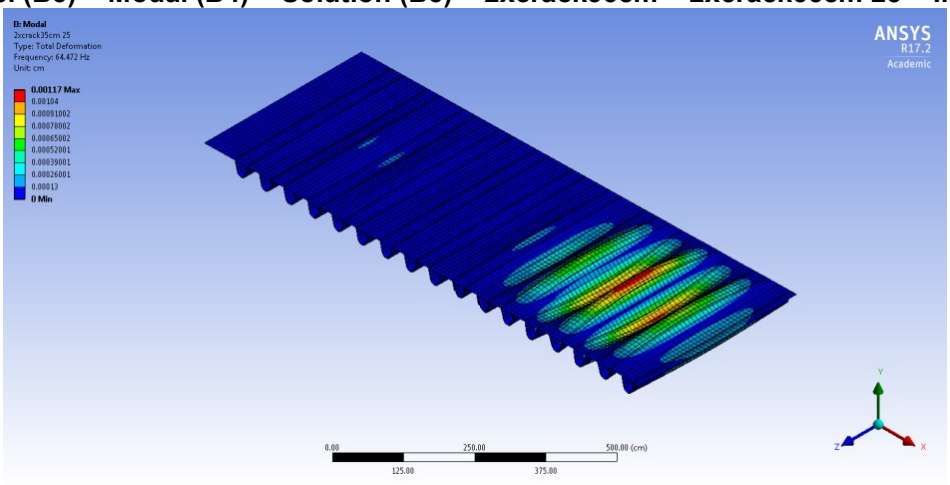


FIGURE 199
Model (B3) > Modal (B4) > Solution (B5) > 2xcrack35cm > 2xcrack35cm 26 > Image

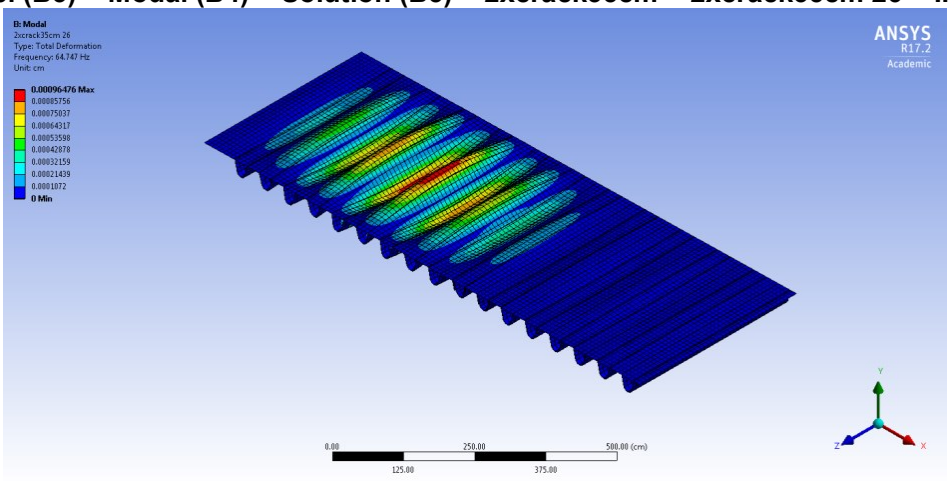


FIGURE 200
Model (B3) > Modal (B4) > Solution (B5) > 2xcrack35cm > 2xcrack35cm 27 > Image

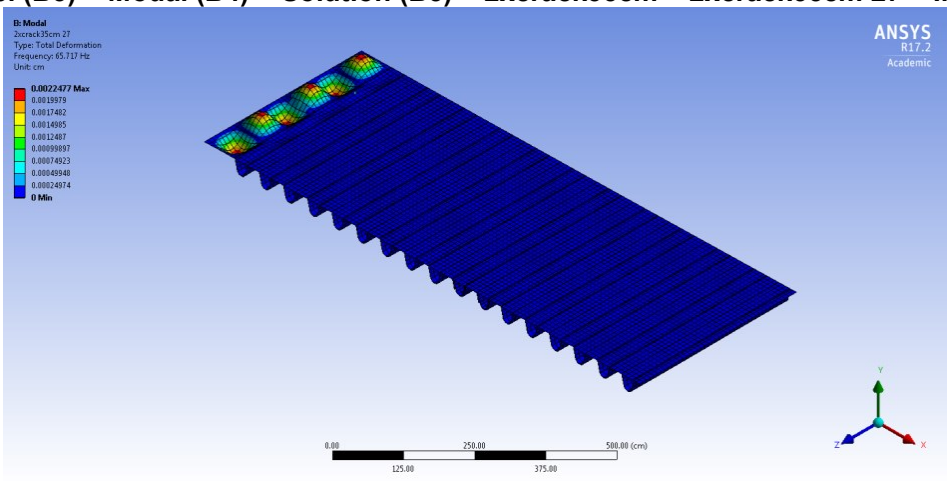


FIGURE 201
Model (B3) > Modal (B4) > Solution (B5) > 2xcrack35cm > 2xcrack35cm 28 > Image

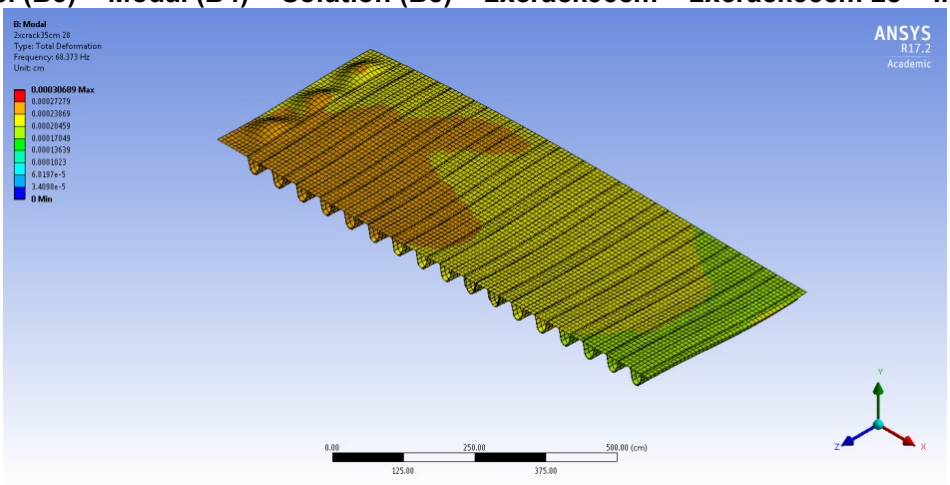


FIGURE 202
Model (B3) > Modal (B4) > Solution (B5) > 2xcrack35cm > 2xcrack35cm 29 > Image

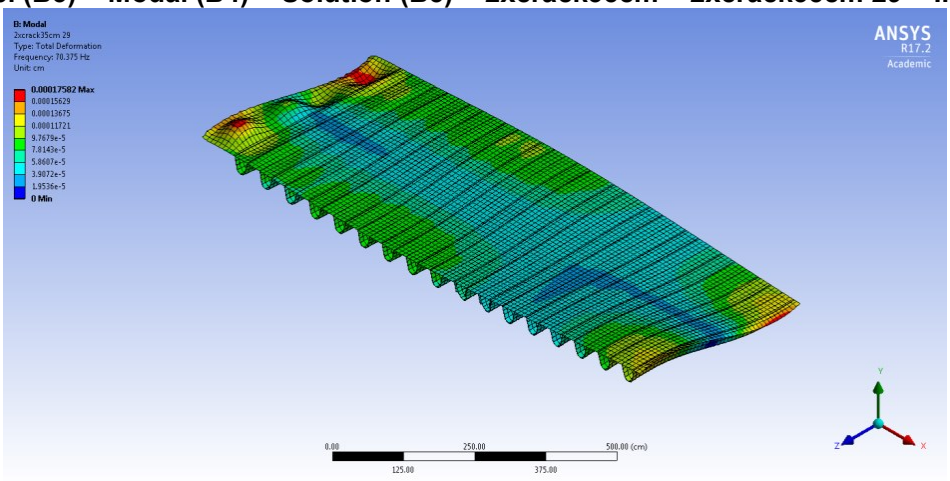
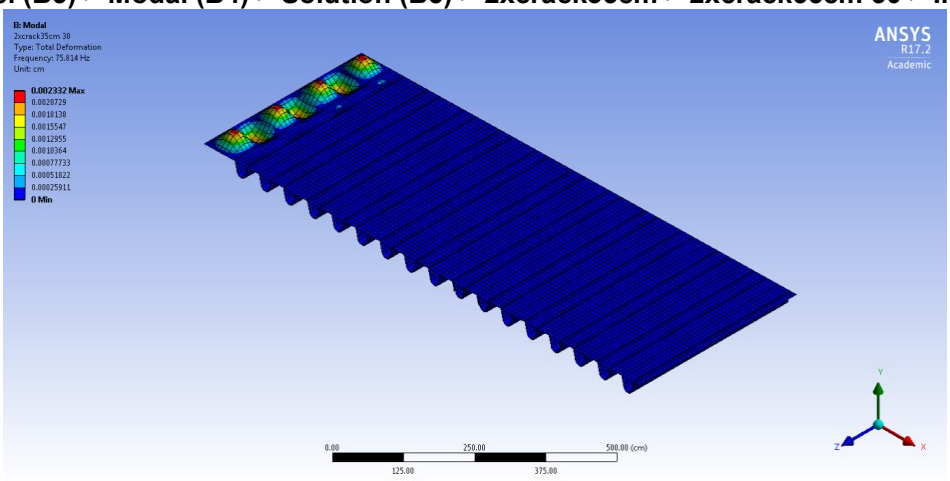


FIGURE 203
Model (B3) > Modal (B4) > Solution (B5) > 2xcrack35cm > 2xcrack35cm 30 > Image



Full 2xU crack

TABLE 143
Model (B3) > Modal (B4) > Solution (B5) > Full 2xU crack > Results

Object Name	*Full 2xU crack 1*	*Full 2xU crack 2*	*Full 2xU crack 3*	*Full 2xU crack 4*	*Full 2xU crack 5*	*Full 2xU crack 6*	*Full 2xU crack 7*	*Full 2xU crack 8*	*Full 2xU crack 9*	*Full 2xU crack 10*	*Full 2xU crack 11*
State	Suppressed										
Scope											
Scoping Method	Geometry Selection										
Geometry	All Bodies										
Definition											
Type	Total Deformation										
Mode	1.	2.	3.	4.	5.	6.	7.	8.	9.	10.	11.
Identifier											
Suppressed	Yes										

FIGURE 204
Model (B3) > Modal (B4) > Solution (B5) > Full 2xU crack > Full 2xU crack 1 > Image

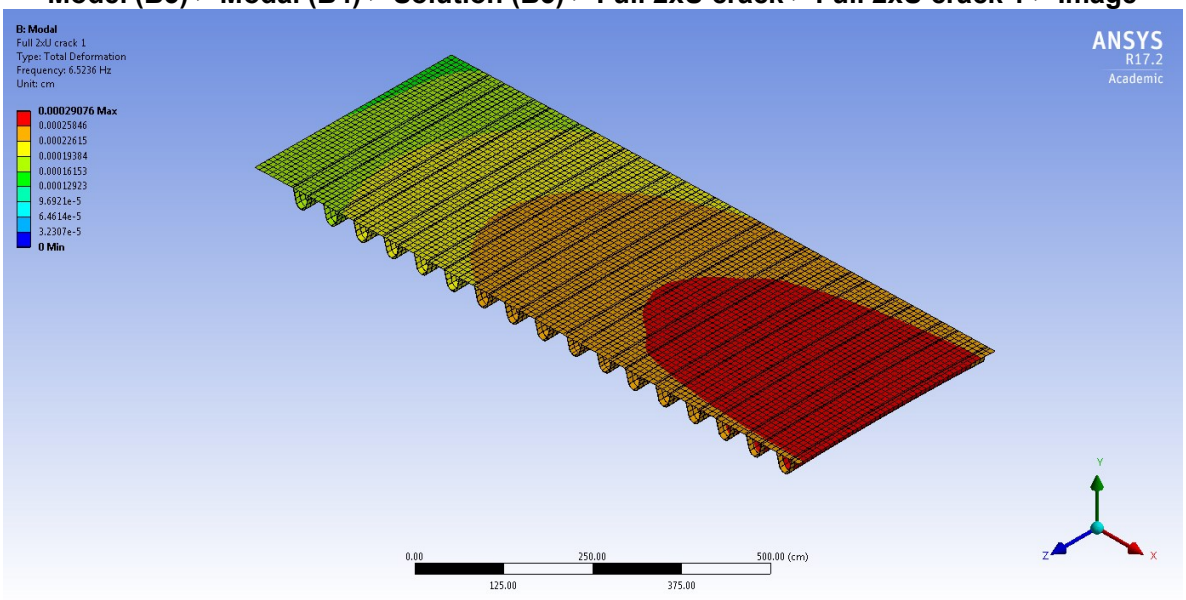


FIGURE 205
Model (B3) > Modal (B4) > Solution (B5) > Full 2xU crack > Full 2xU crack 2 > Image

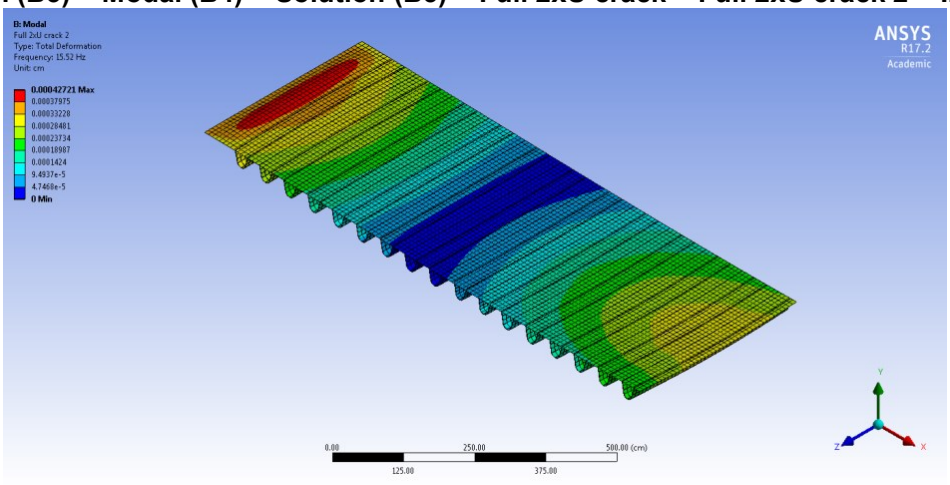


FIGURE 206
Model (B3) > Modal (B4) > Solution (B5) > Full 2xU crack > Full 2xU crack 3 > Image

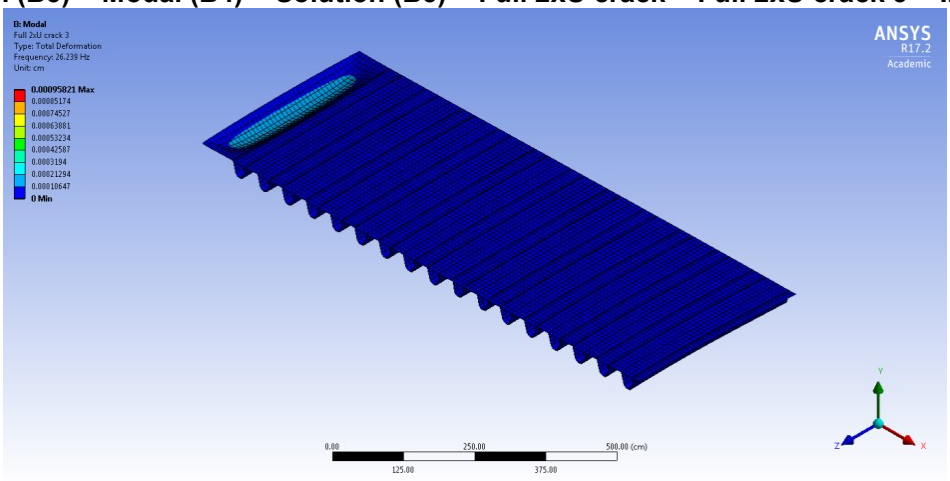


FIGURE 207
Model (B3) > Modal (B4) > Solution (B5) > Full 2xU crack > Full 2xU crack 4 > Image

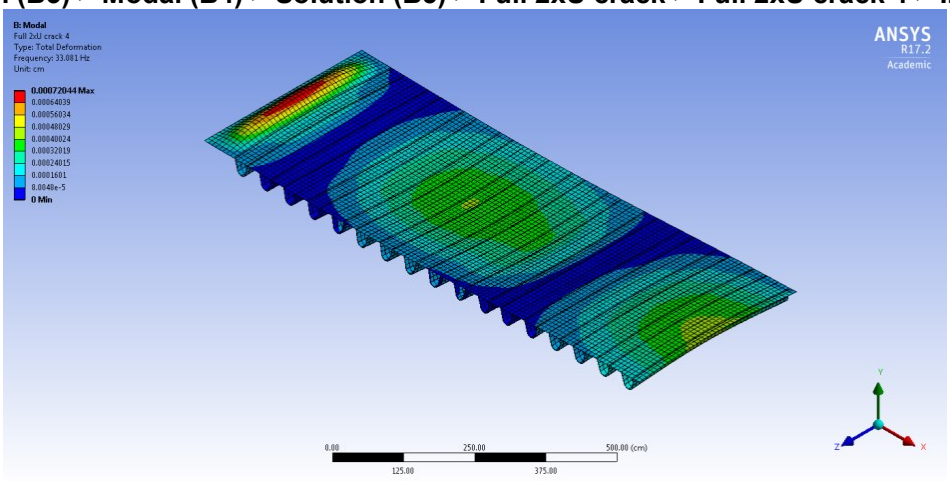


FIGURE 208
Model (B3) > Modal (B4) > Solution (B5) > Full 2xU crack > Full 2xU crack 5 > Image

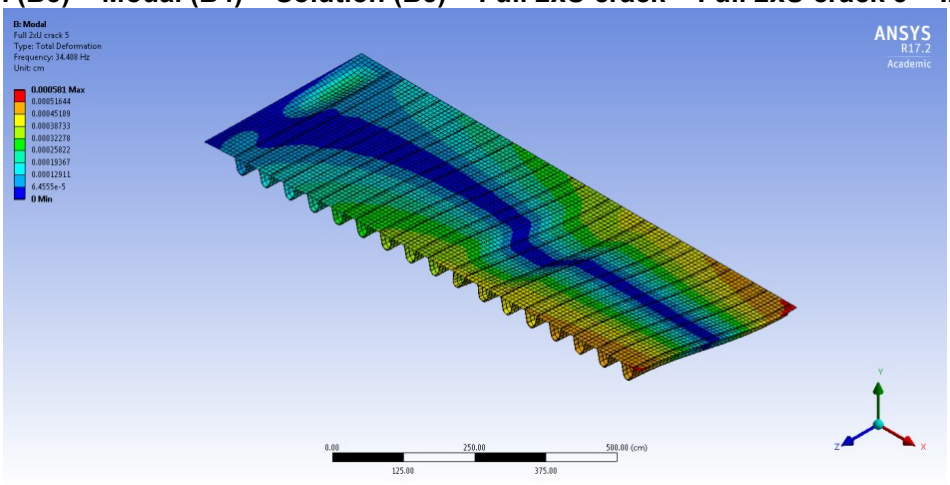


FIGURE 209
Model (B3) > Modal (B4) > Solution (B5) > Full 2xU crack > Full 2xU crack 6 > Image

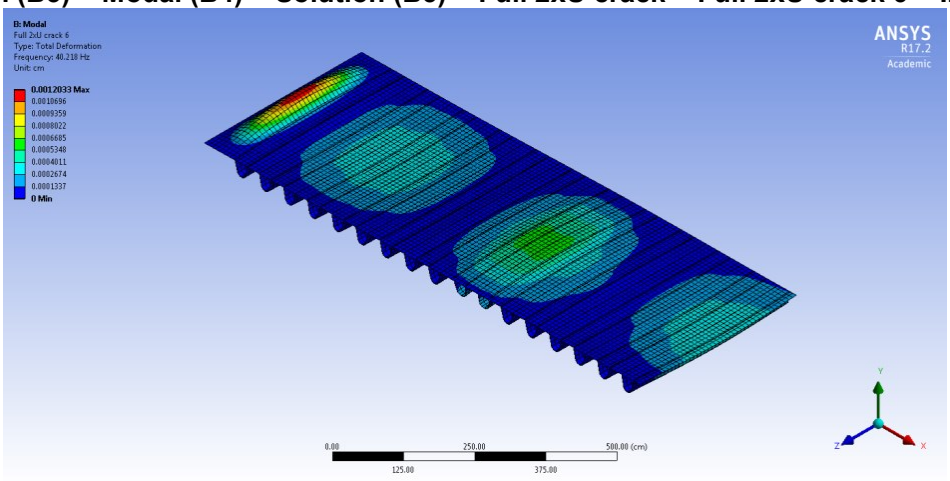


FIGURE 210
Model (B3) > Modal (B4) > Solution (B5) > Full 2xU crack > Full 2xU crack 7 > Image

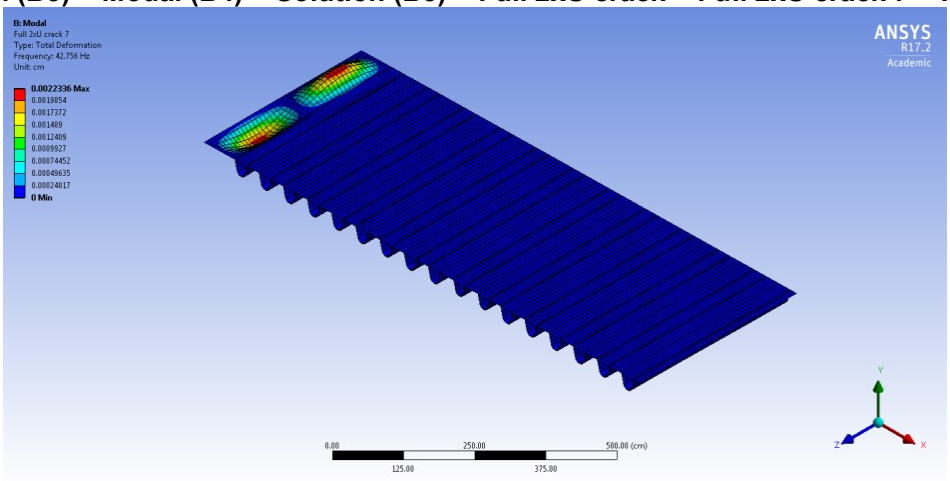


FIGURE 211
Model (B3) > Modal (B4) > Solution (B5) > Full 2xU crack > Full 2xU crack 8 > Image

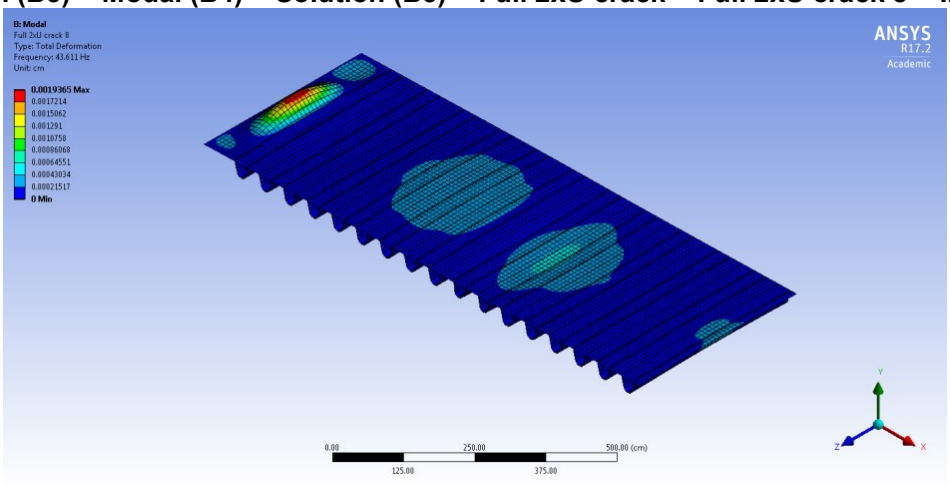


FIGURE 212
Model (B3) > Modal (B4) > Solution (B5) > Full 2xU crack > Full 2xU crack 9 > Image

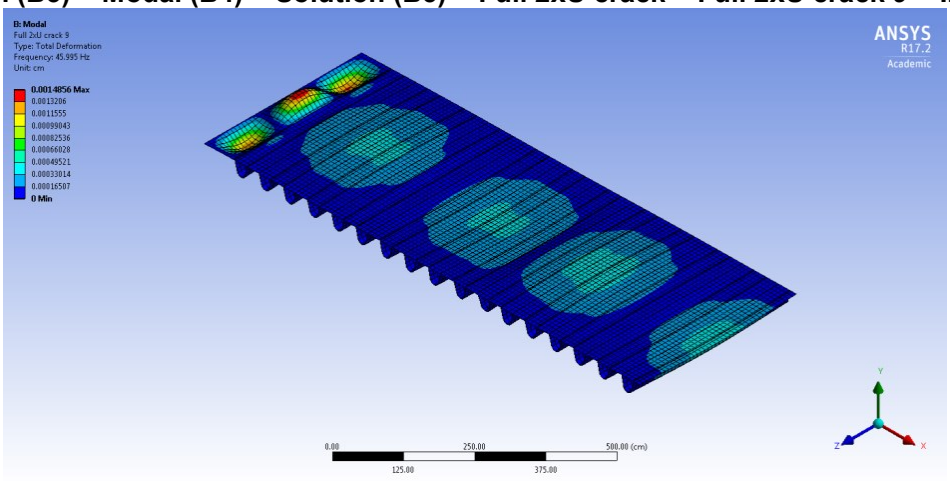


FIGURE 213
Model (B3) > Modal (B4) > Solution (B5) > Full 2xU crack > Full 2xU crack 10 > Image

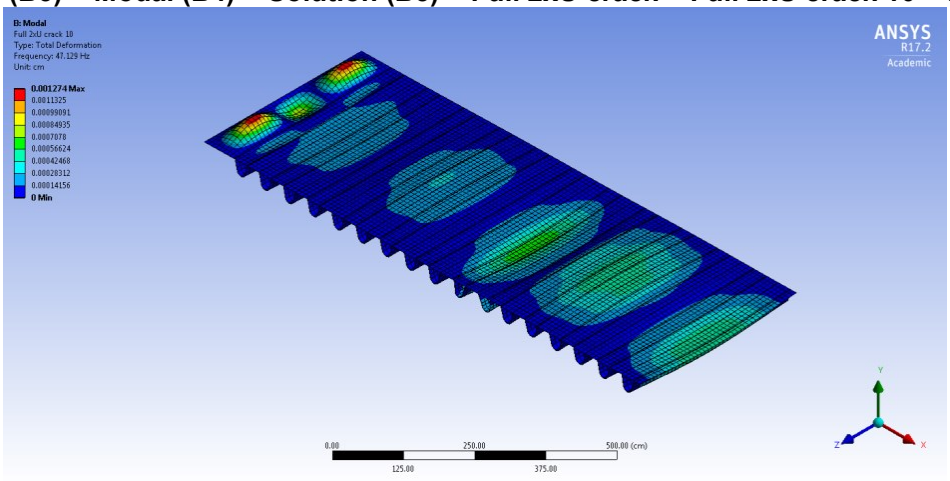


FIGURE 214
Model (B3) > Modal (B4) > Solution (B5) > Full 2xU crack > Full 2xU crack 11 > Image

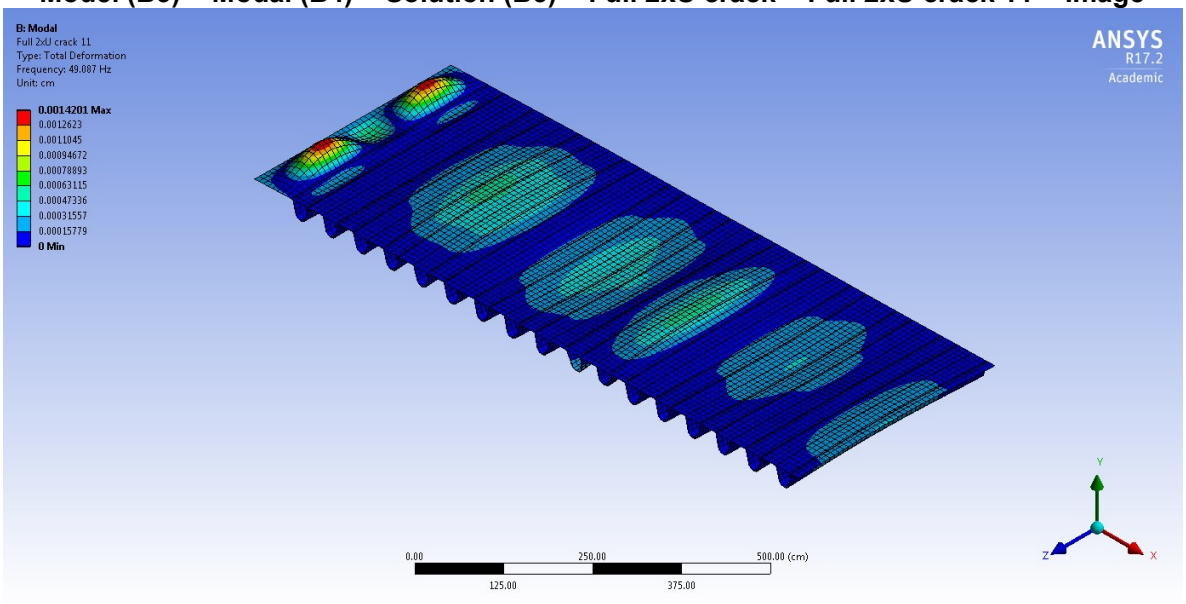


TABLE 144
Model (B3) > Modal (B4) > Solution (B5) > Full 2xU crack > Results

Object Name	*Full 2xU crack 12*	*Full 2xU crack 13*	*Full 2xU crack 14*	*Full 2xU crack 15*	*Full 2xU crack 16*	*Full 2xU crack 17*	*Full 2xU crack 18*	*Full 2xU crack 19*	*Full 2xU crack 20*	*Full 2xU crack 21*	*Full 2xU crack 22*
State	Suppressed										
Scope											
Scoping Method	Geometry Selection										
Geometry	All Bodies										
Definition											
Type	Total Deformation										
Mode	12.	13.	14.	15.	16.	17.	18.	19.	20.	21.	22.
Identifier											
Suppressed	Yes										
Results											
Minimum											
Maximum											
Minimum Occurs On											
Maximum Occurs On											
Information											
Frequency											

FIGURE 215
Model (B3) > Modal (B4) > Solution (B5) > Full 2xU crack > Full 2xU crack 12 > Image

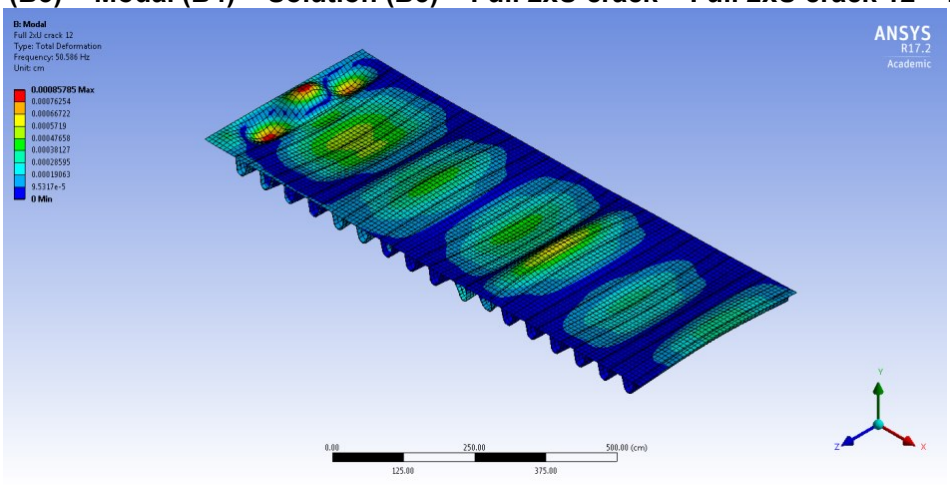


FIGURE 216
Model (B3) > Modal (B4) > Solution (B5) > Full 2xU crack > Full 2xU crack 13 > Image

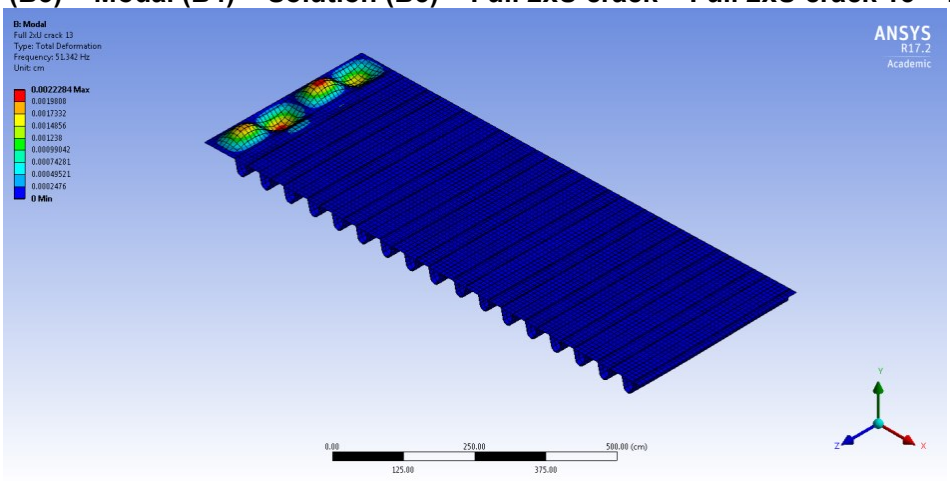


FIGURE 217
Model (B3) > Modal (B4) > Solution (B5) > Full 2xU crack > Full 2xU crack 14 > Image

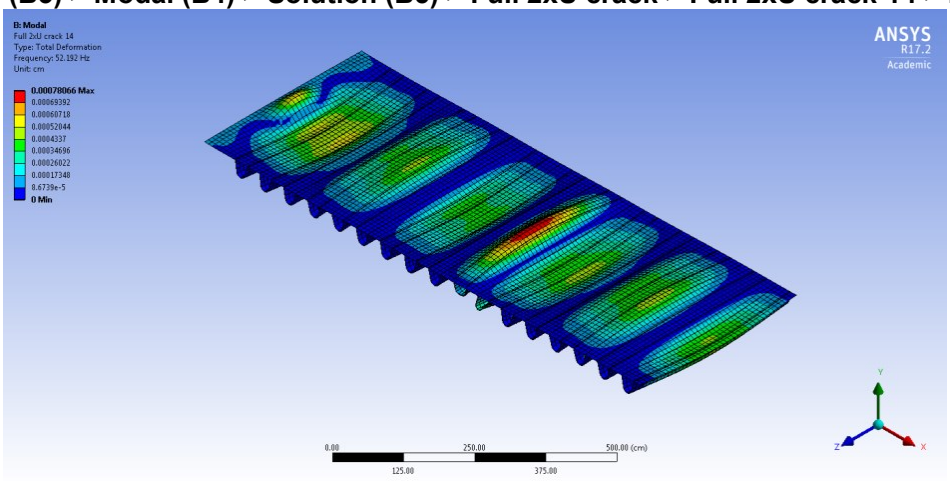


FIGURE 218
Model (B3) > Modal (B4) > Solution (B5) > Full 2xU crack > Full 2xU crack 15 > Image

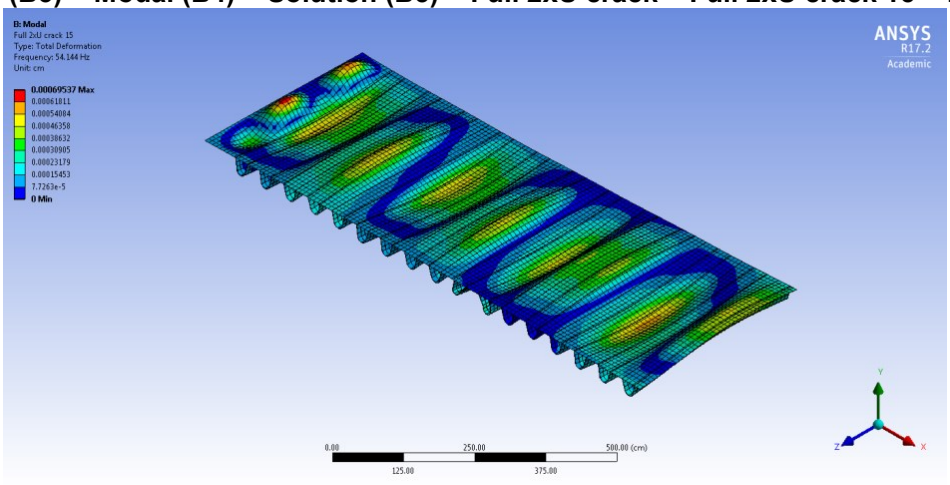


FIGURE 219
Model (B3) > Modal (B4) > Solution (B5) > Full 2xU crack > Full 2xU crack 16 > Image

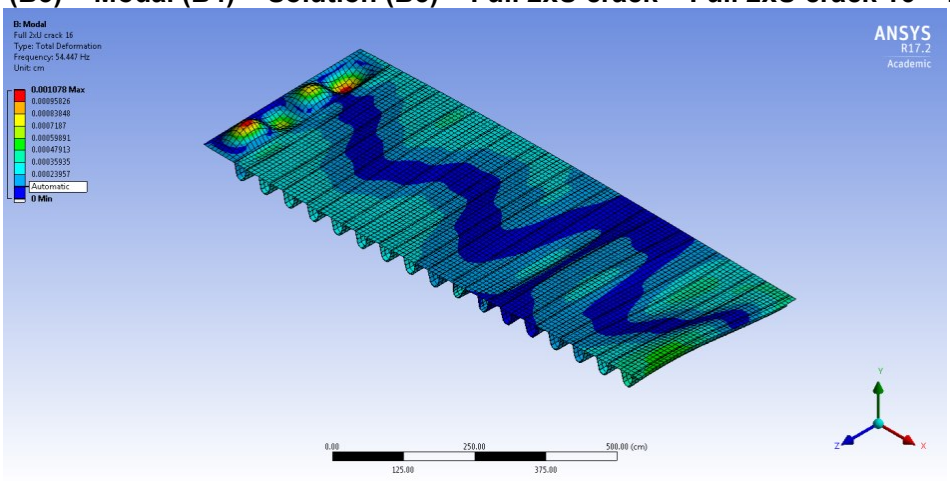


FIGURE 220
Model (B3) > Modal (B4) > Solution (B5) > Full 2xU crack > Full 2xU crack 17 > Image

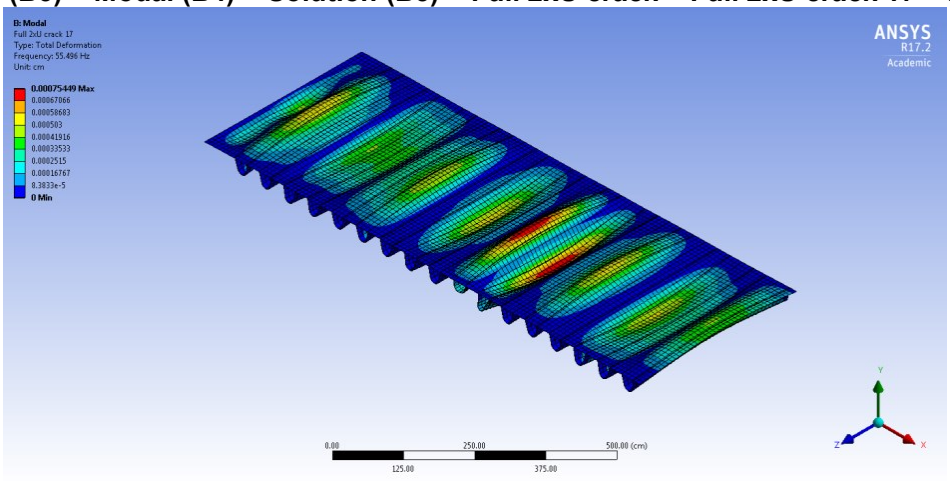


FIGURE 221
Model (B3) > Modal (B4) > Solution (B5) > Full 2xU crack > Full 2xU crack 18 > Image

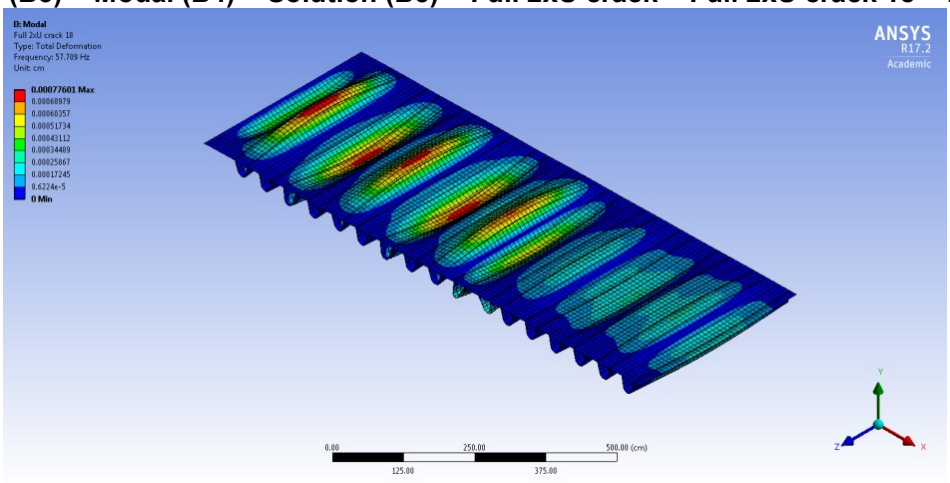


FIGURE 222
Model (B3) > Modal (B4) > Solution (B5) > Full 2xU crack > Full 2xU crack 19 > Image

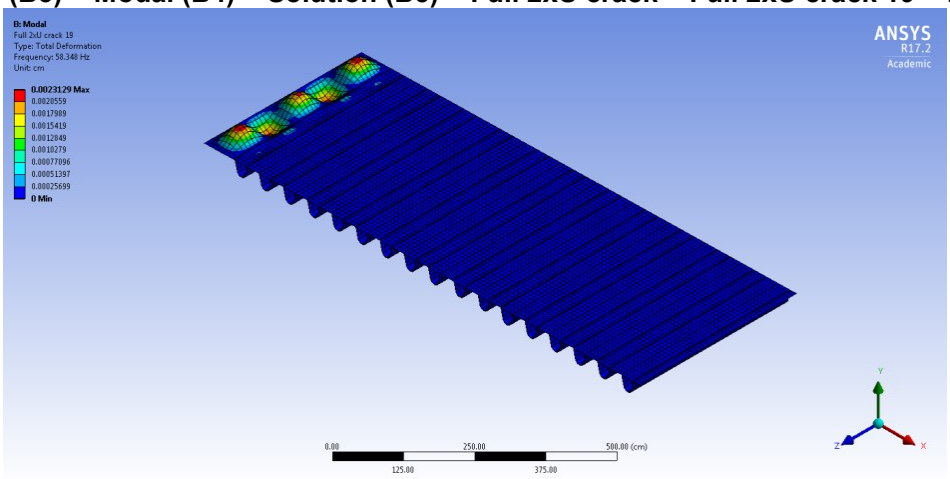


FIGURE 223
Model (B3) > Modal (B4) > Solution (B5) > Full 2xU crack > Full 2xU crack 20 > Image

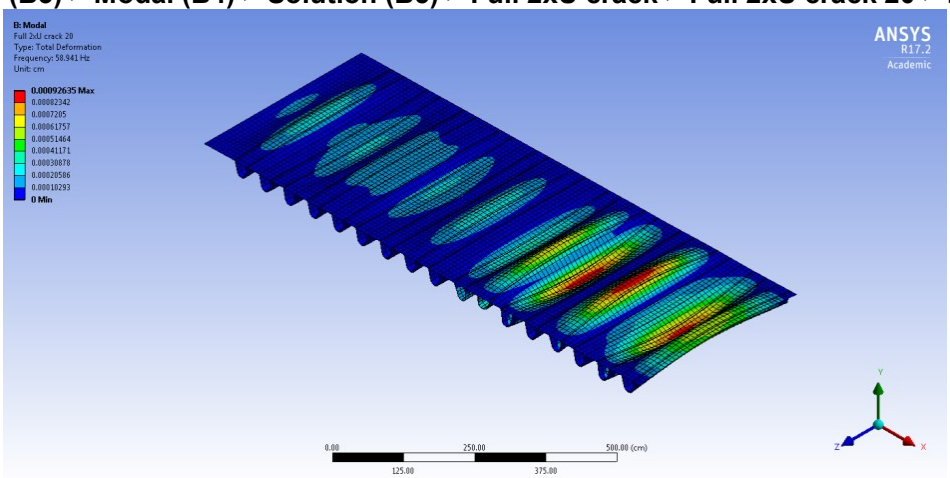


FIGURE 224
Model (B3) > Modal (B4) > Solution (B5) > Full 2xU crack > Full 2xU crack 21 > Image

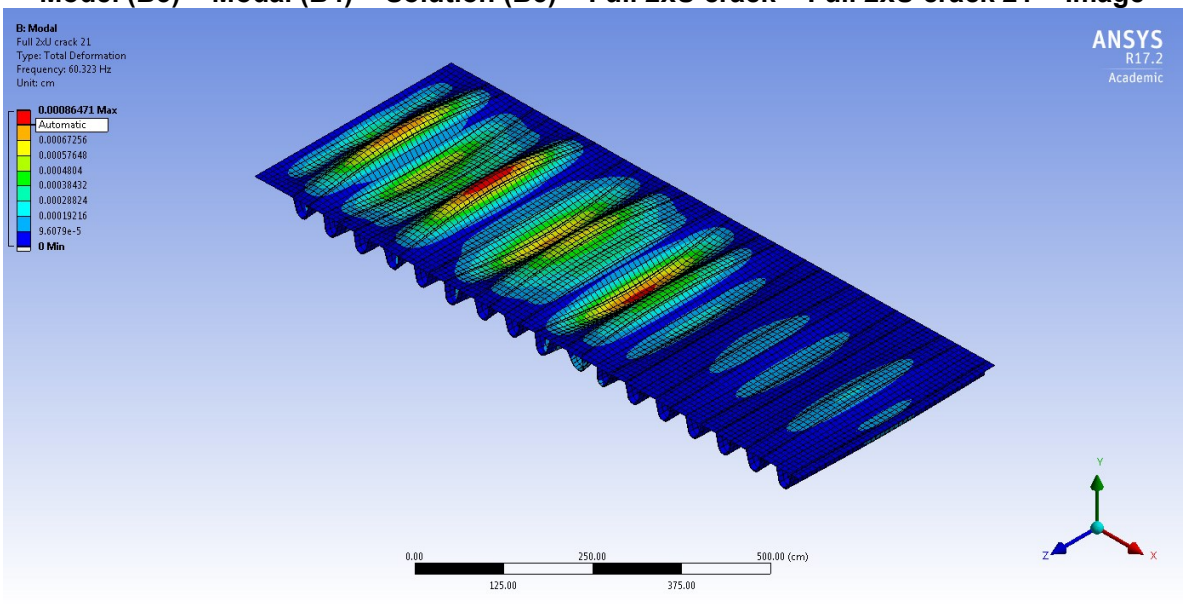


FIGURE 225
Model (B3) > Modal (B4) > Solution (B5) > Full 2xU crack > Full 2xU crack 22 > Image

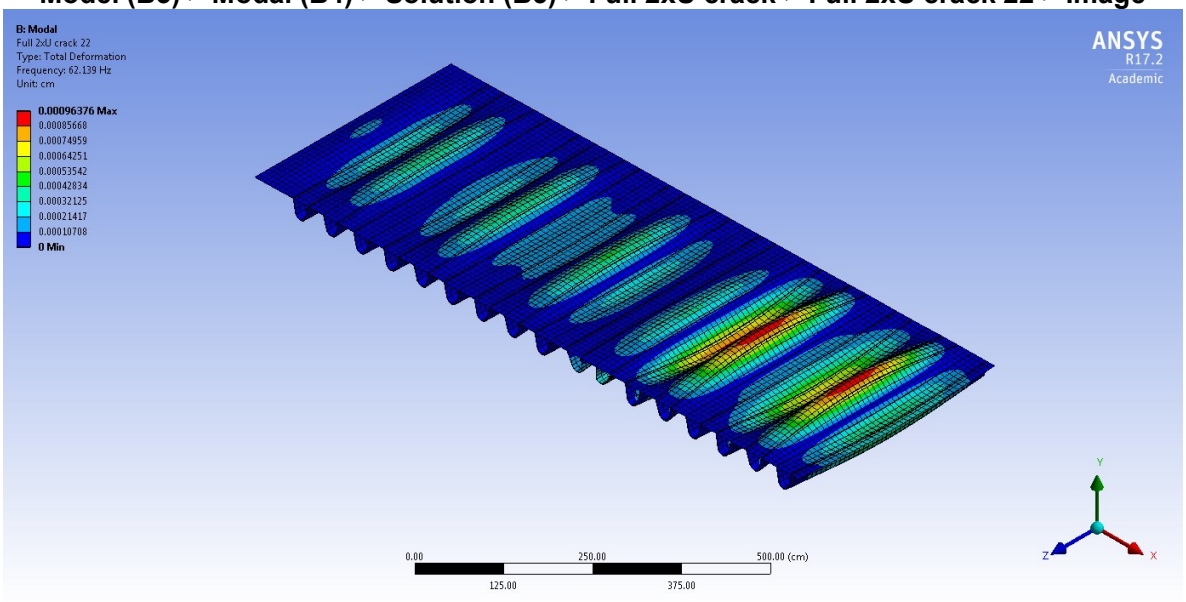


TABLE 145
Model (B3) > Modal (B4) > Solution (B5) > Full 2xU crack > Results

Object Name	*Full 2xU crack 23*	*Full 2xU crack 24*	*Full 2xU crack 25*	*Full 2xU crack 26*	*Full 2xU crack 27*	*Full 2xU crack 28*	*Full 2xU crack 29*	*Full 2xU crack 30*
State	Suppressed							
Scope								
Scoping Method	Geometry Selection							
Geometry	All Bodies							
Definition								
Type	Total Deformation							

Mode	23.	24.	25.	26.	27.	28.	29.	30.
Identifier								
Suppressed	Yes							

FIGURE 226
Model (B3) > Modal (B4) > Solution (B5) > Full 2xU crack > Full 2xU crack 23 > Image

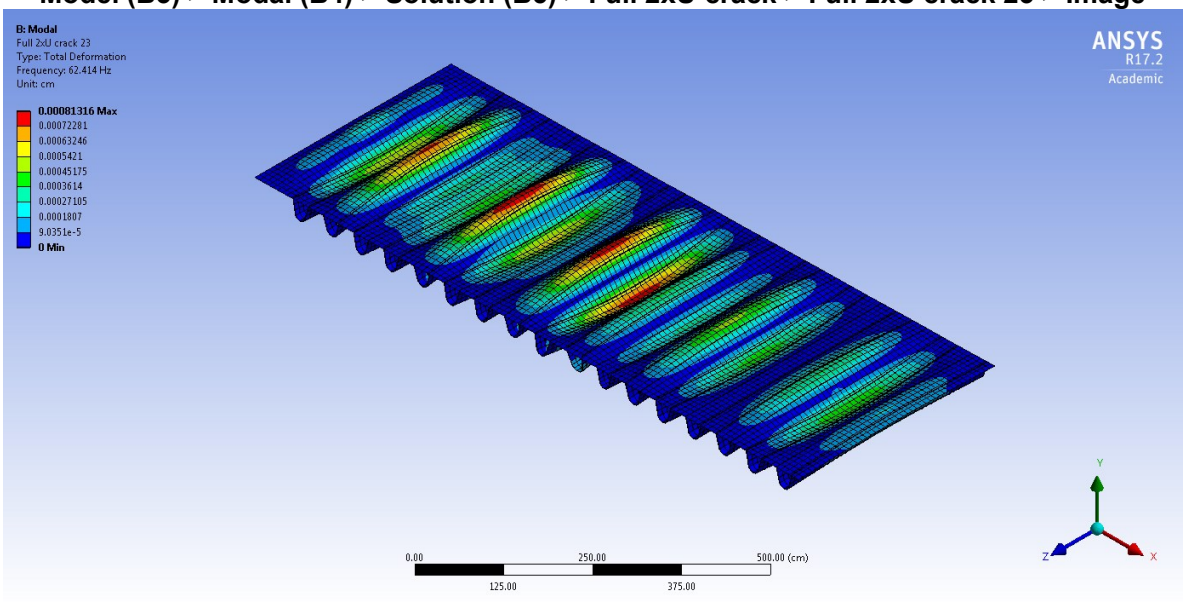


FIGURE 227
Model (B3) > Modal (B4) > Solution (B5) > Full 2xU crack > Full 2xU crack 24 > Image

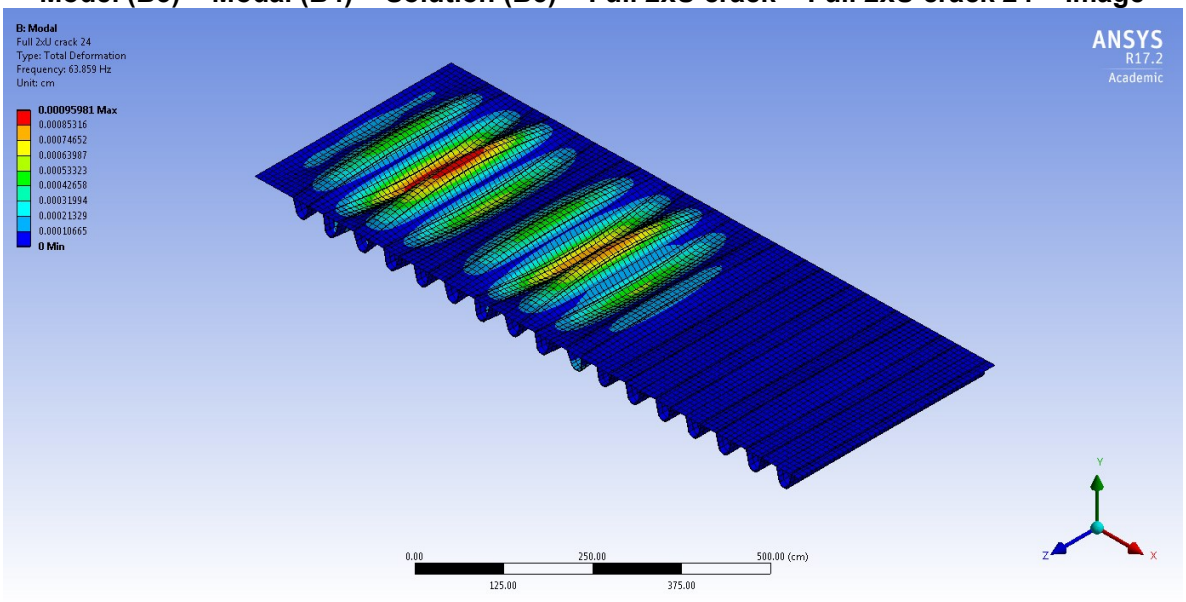


FIGURE 228
Model (B3) > Modal (B4) > Solution (B5) > Full 2xU crack > Full 2xU crack 25 > Image

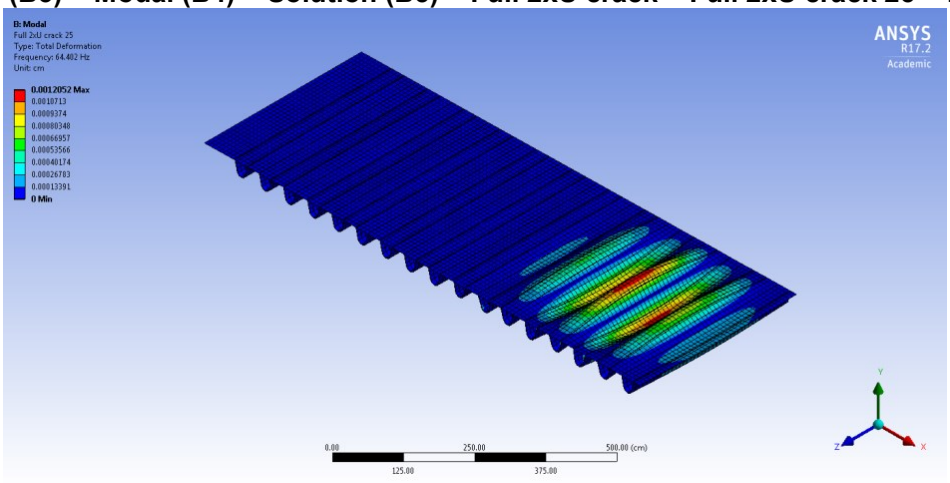


FIGURE 229
Model (B3) > Modal (B4) > Solution (B5) > Full 2xU crack > Full 2xU crack 26 > Image

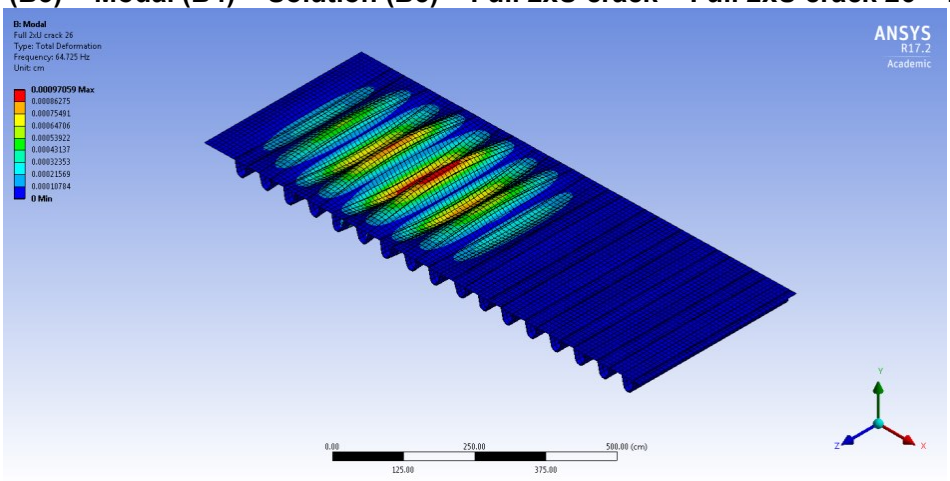


FIGURE 230
Model (B3) > Modal (B4) > Solution (B5) > Full 2xU crack > Full 2xU crack 27 > Image

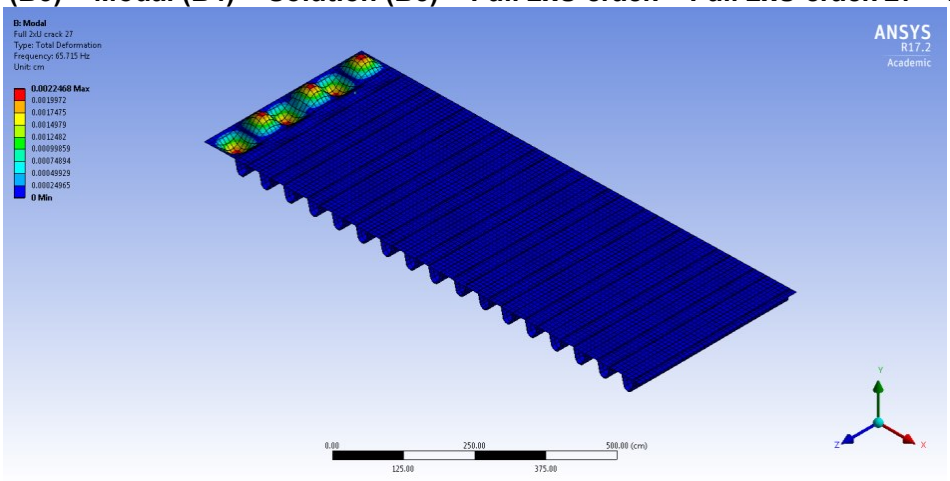


FIGURE 231
Model (B3) > Modal (B4) > Solution (B5) > Full 2xU crack > Full 2xU crack 28 > Image

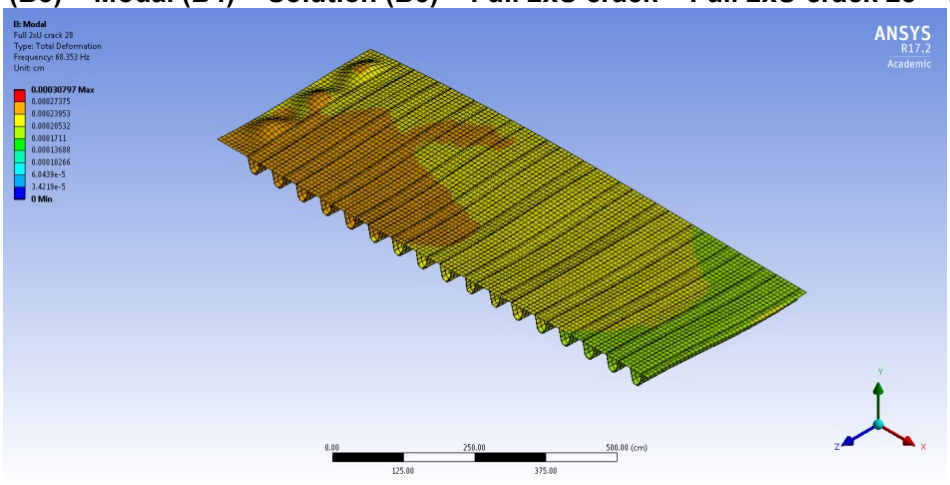


FIGURE 232
Model (B3) > Modal (B4) > Solution (B5) > Full 2xU crack > Full 2xU crack 29 > Image

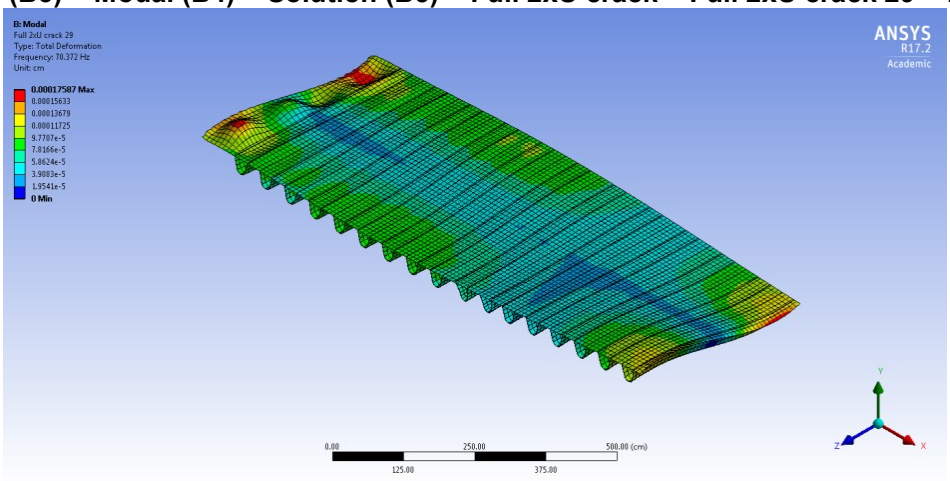
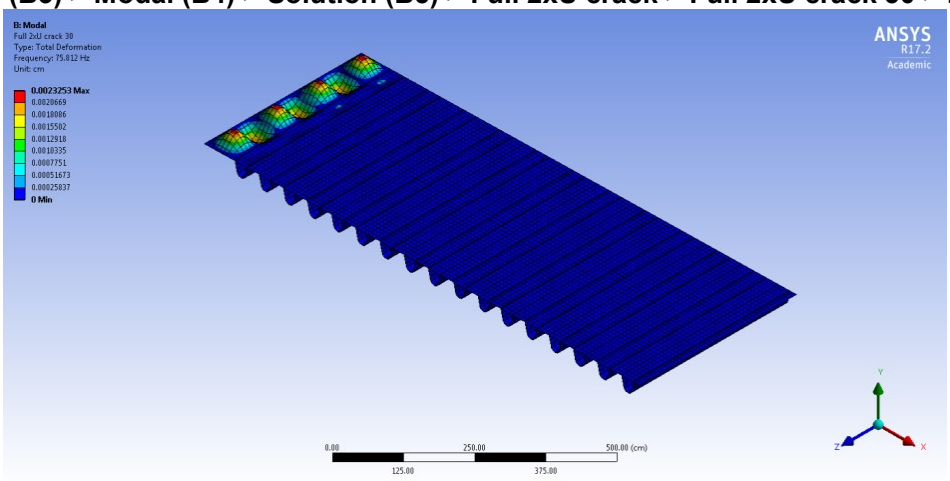


FIGURE 233
Model (B3) > Modal (B4) > Solution (B5) > Full 2xU crack > Full 2xU crack 30 > Image



Material Data

Structural Steel no mass

TABLE 146
Structural Steel no mass > Constants

Density	0 g cm^-3
Coefficient of Thermal Expansion	1.2e-005 C^-1
Specific Heat	4.34e+006 erg g^-1 C^-1
Thermal Conductivity	0.605 W cm^-1 C^-1
Resistivity	1.7e-005 ohm cm

TABLE 147
Structural Steel no mass > Compressive Ultimate Strength

Compressive Ultimate Strength dyne cm^-2
0

TABLE 148
Structural Steel no mass > Compressive Yield Strength

Compressive Yield Strength dyne cm^-2
2.5e+009

TABLE 149
Structural Steel no mass > Tensile Yield Strength

Tensile Yield Strength dyne cm^-2
2.5e+009

TABLE 150
Structural Steel no mass > Tensile Ultimate Strength

Tensile Ultimate Strength dyne cm^-2
4.6e+009

TABLE 151
Structural Steel no mass > Isotropic Secant Coefficient of Thermal Expansion

Zero-Thermal-Strain Reference Temperature C
22

TABLE 152
Structural Steel no mass > Alternating Stress Mean Stress

Alternating Stress dyne cm^-2	Cycles	Mean Stress dyne cm^-2
3.999e+010	10	0
2.827e+010	20	0
1.896e+010	50	0
1.413e+010	100	0
1.069e+010	200	0
4.41e+009	2000	0
2.62e+009	10000	0
2.14e+009	20000	0
1.38e+009	1.e+005	0

1.14e+009	2.e+005	0
8.62e+008	1.e+006	0

TABLE 153
Structural Steel no mass > Strain-Life Parameters

Strength Coefficient dyne cm^-2	Strength Exponent	Ductility Coefficient	Ductility Exponent	Cyclic Strength Coefficient dyne cm^-2	Cyclic Strain Hardening Exponent
9.2e+009	-0.106	0.213	-0.47	1.e+010	0.2

TABLE 154
Structural Steel no mass > Isotropic Elasticity

Temperature C	Young's Modulus dyne cm^-2	Poisson's Ratio	Bulk Modulus dyne cm^-2	Shear Modulus dyne cm^-2
	2.e+012	0.3	1.6667e+012	7.6923e+011

TABLE 155
Structural Steel no mass > Isotropic Relative Permeability

Relative Permeability
10000

TABLE 156
Structural Steel no mass > Color

Red	Green	Blue
-1	-1	-1

Structural Steel

TABLE 157
Structural Steel > Constants

Density	7.85 g cm^-3
Coefficient of Thermal Expansion	1.2e-005 C^-1
Specific Heat	4.34e+006 erg g^-1 C^-1
Thermal Conductivity	0.605 W cm^-1 C^-1
Resistivity	1.7e-005 ohm cm

TABLE 158
Structural Steel > Compressive Ultimate Strength

Compressive Ultimate Strength dyne cm^-2
0

TABLE 159
Structural Steel > Compressive Yield Strength

Compressive Yield Strength dyne cm^-2
2.5e+009

TABLE 160
Structural Steel > Tensile Yield Strength

Tensile Yield Strength dyne cm^-2
2.5e+009

TABLE 161
Structural Steel > Tensile Ultimate Strength

Tensile Ultimate Strength dyne cm^-2
4.6e+009

TABLE 162
Structural Steel > Isotropic Secant Coefficient of Thermal Expansion

Zero-Thermal-Strain Reference Temperature C
22

TABLE 163
Structural Steel > Alternating Stress Mean Stress

Alternating Stress dyne cm^-2	Cycles	Mean Stress dyne cm^-2
3.999e+010	10	0
2.827e+010	20	0
1.896e+010	50	0
1.413e+010	100	0
1.069e+010	200	0
4.41e+009	2000	0
2.62e+009	10000	0
2.14e+009	20000	0
1.38e+009	1.e+005	0
1.14e+009	2.e+005	0
8.62e+008	1.e+006	0

TABLE 164
Structural Steel > Strain-Life Parameters

Strength Coefficient dyne cm^-2	Strength Exponent	Ductility Coefficient	Ductility Exponent	Cyclic Strength Coefficient dyne cm^-2	Cyclic Strain Hardening Exponent
9.2e+009	-0.106	0.213	-0.47	1.e+010	0.2

TABLE 165
Structural Steel > Isotropic Elasticity

Temperature C	Young's Modulus dyne cm^-2	Poisson's Ratio	Bulk Modulus dyne cm^-2	Shear Modulus dyne cm^-2
	2.e+012	0.3	1.6667e+012	7.6923e+011

TABLE 166
Structural Steel > Isotropic Relative Permeability

Relative Permeability
10000

TABLE 167
Structural Steel > Color

Red	Green	Blue
-1	-1	-1

100kg

TABLE 168
100kg > Constants

Density	19.672 g cm^-3

TABLE 169
100kg > Isotropic Elasticity

Temperature C	Young's Modulus dyne cm^-2	Poisson's Ratio	Bulk Modulus dyne cm^-2	Shear Modulus dyne cm^-2
	2.e+012	0.3	1.6667e+012	7.6923e+011

TABLE 170
100kg > Color

Red	Green	Blue
-1	-1	-1